

DTIC
S
D

2

AD-A242 943



PROCEEDINGS OF THE 1990 USAF STRUCTURAL
INTEGRITY PROGRAM CONFERENCE



Editors:

Thomas D. Cooper
Materials Integrity Branch
Systems Support Division
WL/Materials Directorate

John W. Lincoln
ASD/Deputy for Engineering

August 1991

Final Report for Period 11-13 December 1990

Hyatt Regency
San Antonio, Texas

Approved for public release; distribution is unlimited

91-16435

MATERIALS DIRECTORATE
WRIGHT LABORATORY
AIR FORCE SYSTEMS COMMAND
WRIGHT-PATTERSON AFB, OHIO 45433-6533

91 1125 054

NOTICE

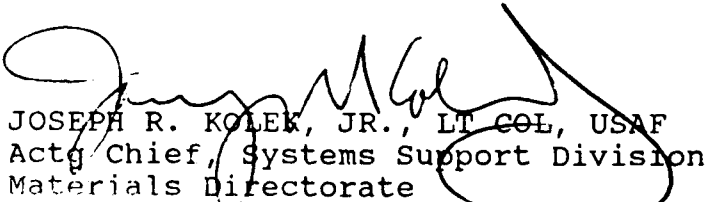
When Government drawings, specifications, or other data are used for any purpose other than in connection with a definitely Government-related procurement, the United States Government incurs no responsibility or any obligation whatsoever. The fact that the government may have formulated or in any way supplied the said drawings, specifications, or other data, is not to be regarded by implication, or otherwise in any manner construed, as licensing the holder, or any other person or corporation; or as conveying any rights or permission to manufacture, use, or sell any patented invention that may in any way be related thereto.

This report is releasable to the National Technical Information Service (NTIS). At NTIS, it will be available to the general public, including foreign nations.

This technical report has been reviewed and is approved for publication.



THOMAS D. COOPER, Chief
Materials Integrity Branch
Systems Support Division
Materials Directorate



JOSEPH R. KULEK, JR., LT COL, USAF
Actg Chief, Systems Support Division
Materials Directorate

If your address has changed, if you wish to be removed from our mailing list, or if the addressee is no longer employed by your organization please notify WL/MLSA, WPAFB, OH 45433-6533 to help us maintain a current mailing list.

Copies of this report should not be returned unless return is required by security considerations, contractual obligations, or notice on a specific document.

UNCLASSIFIED

SECURITY CLASSIFICATION OF THIS PAGE

REPORT DOCUMENTATION PAGE				Form Approved OMB No. 0704-0188	
1a. REPORT SECURITY CLASSIFICATION UNCLASSIFIED			1b. RESTRICTIVE MARKINGS		
2a. SECURITY CLASSIFICATION AUTHORITY			3. DISTRIBUTION/AVAILABILITY OF REPORT Approved for public release; distribution is unlimited.		
2b. DECLASSIFICATION/DOWNGRADING SCHEDULE					
4. PERFORMING ORGANIZATION REPORT NUMBER(S) WL-TR-91-2071			5. MONITORING ORGANIZATION REPORT NUMBER(S)		
6a. NAME OF PERFORMING ORGANIZATION Materials Integrity Branch Systems Support Division		6b. OFFICE SYMBOL (If applicable) WL/MLSA	7a. NAME OF MONITORING ORGANIZATION		
6c. ADDRESS (City, State, and ZIP Code) WL/MLSA Wright-Patterson AFB, Ohio 45433-6533			7b. ADDRESS (City, State, and ZIP Code)		
8a. NAME OF FUNDING/SPONSORING ORGANIZATION Material Directorate		8b. OFFICE SYMBOL (If applicable) WL/MLSA	9. PROCUREMENT INSTRUMENT IDENTIFICATION NUMBER		
8c. ADDRESS (City, State, and ZIP Code) WL/MLSA Wright-Patterson AFB, Ohio 45433-6533			10. SOURCE OF FUNDING NUMBERS		
		PROGRAM ELEMENT NO. 62102F	PROJECT NO. 2418	TASK NO. 07	WORK UNIT ACCESSION NO. 04
11. TITLE (Include Security Classification) Proceedings of the 1990 USAF Structural Integrity Program Conference					
12. PERSONAL AUTHOR(S) Thomas D. Cooper, WL/MLSA; John W. Lincoln, ASD/ENFS, Editors					
13a. TYPE OF REPORT Final		13b. TIME COVERED FROM 11Dec90 TO 13Dec90		14. DATE OF REPORT (Year, Month, Day) August 1991	
15. PAGE COUNT 1064					
16. SUPPLEMENTARY NOTATION					
17. COSATI CODES			18. SUBJECT TERMS (Continue on reverse if necessary and identify by block number)		
FIELD	GROUP	SUB-GROUP			
19. ABSTRACT (Continue on reverse if necessary and identify by block number) This report is a compilation of the papers presented at the 1990 USAF Structural Integrity Program Conference held at the Hyatt Regency, San Antonio, Texas on 11-13 December 1990.					
20. DISTRIBUTION/AVAILABILITY OF ABSTRACT <input checked="" type="checkbox"/> UNCLASSIFIED/UNLIMITED <input type="checkbox"/> SAME AS RPT <input type="checkbox"/> DTIC USERS			21. ABSTRACT SECURITY CLASSIFICATION UNCLASSIFIED		
22a. NAME OF RESPONSIBLE INDIVIDUAL Thomas D. Cooper			22b. TELEPHONE (Include Area Code) (513) 255-3623		22c. OFFICE SYMBOL WL/MLSA

FOREWORD

This report was compiled by the Materials Integrity Branch, Systems Support Division, Materials Directorate, Wright Laboratory, Wright-Patterson Air Force Base, Ohio. It was initiated under Task 24180704 "Corrosion Control & Failure Analysis" with Thomas D. Cooper as the Project Engineer.

This technical report was submitted by the editors.

The purpose of this 1990 Conference was to bring together technical personnel in DOD and the aerospace industry who are involved in the various technologies required to ensure the structural integrity of aircraft gas turbine engines, airframes and other mechanical systems. It provided a forum to exchange ideas and share new information relating to the critical aspects of durability and damage tolerance technology for aircraft systems. The Conference was sponsored by the Aeronautical Systems Division Deputy for Engineering and Materials and Flight Dynamics Directorates of the Wright Laboratory, Wright-Patterson Air Force Base, Ohio. It was hosted by the Air Force Logistics Command's San Antonio Air Logistics Center.

Accession For	
NTIS GRA&I	<input checked="" type="checkbox"/>
DTIC TAB	<input type="checkbox"/>
Unannounced	<input type="checkbox"/>
Justification	
By	
Distribution	
Availability Codes	
Dist	Special
A-1	

TABLE OF CONTENTS

	Page
AGENDA	ix
INTRODUCTION	xiv

SESSION I - OVERVIEWS

Evolution of the Integrity Process for the ATF Engines "Propulsion and Power System Integrity Program"	1
F120 PPSIP - Success Through Supplier Involvement . . .	33
Component Classification and the Product Integrity Programs	48
An Engineering Procedure to Select and Prioritize Component Evaluation Under USAF Structural Integrity Requirements	75
Changes in the General Specification for Aircraft Structures - Air Force Guide Specification - 87221A . .	94
Inspection of Aircraft Structure With Advanced Shearography	103

SESSION II - STRUCTURAL ANALYSIS

Reliability and Quality Control in Fracture Mechanics Analyses Using the P-Version Finite Element Program, MSC/PROBE	117
The Application of Risk Analysis to an Aging Aircraft Fleet	155
A Review of the Effects of Overloads on Fatigue Crack Growth	184
The Zoning Approach to Inspection Intervals for F-5 & T-38 Aircraft	204

The Effects of Runway Surface Roughness on Aircraft Fatigue Life	236
---	-----

A Cost Effective Improvement in Structural Fatigue Life Thru Guaranteed Fastener Hole Quality	263
--	-----

SESSION III - MATERIALS AND NON-DESTRUCTIVE INSPECTION

Fatigue Crack Growth Retardation in Aluminum Alloys	310
---	-----

Quality Nondestructive Evaluation, and the ". . . IP" Process	331
--	-----

Fatigue Life Improvement Through Laser Shock Processing	348
--	-----

Fracture Mechanics Based Assessment of Aluminum Stress Corrosion Durability via the Breaking Load Method	379
--	-----

NDE Productivity Improvements	407
---	-----

Aging Fleet Program	444
-------------------------------	-----

SESSION IV - STRUCTURAL ANALYSIS, TESTING AND FORCE MANAGEMENT

Analysis of Cold Worked Holes for the T-37B Structural Life Extension Program	480
--	-----

Usage Variation and Effects on F-5 Component Life	499
---	-----

Research on Multiple Site Damage	525
--	-----

Status of F-16 Durability Testing	540
---	-----

CF-5 Full Scale Durability and Damage Tolerance Test Preliminary Result	571
--	-----

Application of Damage Tolerance to Helicopter Structure	631
--	-----

OSCAR On Site Collating and Record	681
--	-----

TFE1042/F125 Turbofan Engine Damage Tolerance Verification Program	708
---	-----

Competition in Probabilistic Life Analysis	735
--	-----

Preliminary Damage Tolerance Evaluation of Selected F412-GE-400 Engine Components	754
SPATE (Stress Pattern Analysis by Thermal Emission) and Gas Turbine Engine Structural Integrity	777
Impact of Air Force Damage Tolerance Requirements on the Weight of an Advanced Technology Engine Nozzle . . .	798
Environmental Characterization of External Components for an Advanced Turbofan Engine	837

SESSION VI - FORCE MANAGEMENT

The Results of Using a Micro Processor Based Structural Data Recorder to Support Individual Aircraft Tracking of the B-1B Aircraft	859
"Flight Loads Recorder Installation in Tutor Jet Trainer"	879
From Theory to Practice: Evolution of the Standard Flight Data Recorder	934
A-10A Individual Aircraft Tracking Program (IATP), Validation of Crack Growth Methodology for Changing Flight Spectra	947
Automatic Calculation of an Aircraft's Sink Speed Horizontal Velocity, Pitch angle and Pitch Rate, and Roll Angle and Roll Rate at Touchdown and Their Application to Structural Integrity	990
Health and Usage Monitoring Systems in Airborne Applications	1005
"Shot Peening Can Reduce Effects of Aging on Airframe and Engines"	1029
Model Sensitivity in Stress-Strength Reliability Computations	1039

AGENDA

1990 USAF STRUCTURAL INTEGRITY PROGRAM

11-13 DECEMBER 1990

**Hyatt Regency
San Antonio, Texas**

SPONSORED BY:

**ASD/Deputy for Engineering
WL/Materials Directorate**

HOSTED BY:

**San Antonio Air Logistics Center
Directorate Material Management
Fighter/Tactical/Trainer
Systems Program Management
Division (SA-ALC/MMS)**

AGENDA

TUESDAY, 11 DECEMBER 1990

SESSION I - OVERVIEWS

Chairman - T. Cooper, WRDC/MLSA

- 0830-0900 Computational Schemes for Integrity Analyses of
Fuselage Panels in Aging Airplanes
S. Atluri - Georgia Institute of Technology
- 0900-0930 The Evolution of the Integrity Process for the
ATF Engines (Propulsion and Power System
Integrity Program)
J. Ogg, D. Irwin, and B. Bacon - ASD/YFEP
- 0930-1000 ATF PPSIP Implementation - Success Through
Supplier Involvement
P. Domas and J. McAndrew - General Electric Co
- 1000-1030 REFRESHMENT BREAK
- 1030-1100 Component Classification and the Product
Integrity Programs
H. Wood, ASD/ENF
- 1100-1130 An Engineering Procedure to Select and
Prioritize Component Evaluation Under USAF
Structural Integrity Requirements
B. Brooks - McDonnell Aircraft Co
- 1130-1200 Changes in the General Specification for
Aircraft Structures; Air Force Guide
Specification - 87221A
M. Snead - ASD/ENFS
- 1200-1330 LUNCH AND PRESENTATION
Future Outlook for the Air Force Logistics
Command
Mr. Earl Briesch - Assistant DCS for Material
Management
United States AF Logistics Command Headquarters
- 1330-1400 Advanced Shearography Aviation Applications
John Tyson II - Laser Technology, Inc.

SESSION II - STRUCTURAL ANALYSIS

Chairman - R. Bader, WRDC/FIB

1400-1430 Reliability and Quality Control in Fracture Mechanics Analyses Using the P-Version Finite Element Program, MSC/PROBE
M. Heskitt - MacNeal-Schwendler Corp.

1430-1500 The Application of Risk Analysis to an Aging Aircraft Fleet
A. Berens - UD Research Institute
J. Burns - WRDC/FIBE

1500-1530 REFRESHMENT BREAK

1530-1600 A Review of the Effects of Overloads on Fatigue Crack Growth
R. Carlson, G. Kardomateas, P. Bates - Georgia Institute of Technology

1600-1630 The Zoning Approach to Inspection Intervals for F-5 and T-38 Aircraft
M. Gottier - Eidgenossisches Flugzeugwerk (F+W)
C. Hu - Northrop Aircraft Division
M. Reinke - SA-ALC/LADD

1630-1700 Runway Surface Roughness Effect on Aircraft Fatigue Life
A. Gerardi and Lt D. Krueger - WRDC/FIBEC

1700-1730 A Cost Effective Improvement in Structural Fatigue Life Thru Guaranteed Fastener Hole Quality
W. Lewis - Measurement Systems Incorporated

1730-1930 RECEPTION

WEDNESDAY, 12 DECEMBER 1990

SESSION III - MATERIALS AND NONDESTRUCTIVE INSPECTION

Chairman - W. Wood, ASD/ENF

0830-0900 Successes in Cracked Sheet Metal Problems
L. Rogers - WRDC/FIBG

0900-0930 Fatigue Crack Growth Retardation in Aluminum Alloys
R. Citerley, R. Yee - Anamet Laboratories

0930-1000 Quality Nondestructive Evaluation and the "IP" Process
C. Annis - Pratt & Whitney

1000-1030 REFRESHMENT BREAK

1030-1100 Fatigue Life Improvement Through Laser Shock Processing
A. Clauer - Battelle Memorial Institute
J. Koucky - Wagner Castings

1100-1130 Fracture Mechanics Based Durability Assessment of Aluminum Stress Corrosion via the Breaking Load Test Method
D. Lukasak, R. Bucci, E. Colvin and B. Lifka - Alcoa Laboratories

1130-1200 NDE Productivity Improvements
G. Geier - General Electric Co.

1200-1330 LUNCH AND PRESENTATION
Overview of the FAA Aging Aircraft Program
Mr. Tom McSweeney - Deputy Director, Aircraft Certification Service, FAA Headquarters

SESSION IV - STRUCTURAL ANALYSIS, TESTING AND FORCE MANAGEMENT
Chairman - C. Petrin Jr., ASD/ENFS

1330-1400 Analysis of Cold Worked Holes for the T-37 Structural Life Extension Program
O. Burnside, D. Wieland, J. Cutshall - Southwest Research Institute

1400-1430 Usage Variation and Effects on F-5 Component Life
M. Kaplan and T. Knott - Willis and Kaplan
M. Rienke, C. Massey and D. Ratzer - SA-ALC
R. Welch - Chiapetta Welch & Assoc.

1430-1500 Research Work on the Aging Aircraft Problem
S. Sampath - Transportation Systems Center

1500-1530 REFRESHMENT BREAK

1530-1600 Status of F-16 Durability Testing
Capt S. Perkins - ASD/YPEF

1600-1630 CF5 Full Scale Durability and Damage Tolerance Test Preliminary Results
M. Beaulieu, Y. Beauvais, G. Deziel, E. Van Blaeren and Dr. S. McBride - Bombardier Inc.

- 1630-1700 Application of Damage Tolerance to Helicopter Structure
 D. Tritsch and G. Schneider - Sikorsky Aircraft
 G. Chamberlain - WR-ALC/TILDD
 J. Lincoln - ASD/ENFS
- 1700-1730 On Site Collating and Recording (OSCAR)
 J. Cochran and A. Frese - Lockheed Aeronautical Systems Company
 D. Hammond - WR-ALC/LJL

THURSDAY, 13 DECEMBER 1990

SESSION V - ENSIP
 Chairman - E. Davidson, ASD/YCEF

- 0830-0900 TFE1042/F125 Turbofan Engine Damage Tolerance Verification Program
 K. Buck and J. Hill - Allied Signal Aerospace Co., Garrett Engine Division
- 0900-0930 Competition in Probabilistic Life Analysis
 P. Roth - General Electric Company
- 0930-1000 Preliminary Damage Tolerance Evaluation of Selected F412-GE-400 Engine Components
 R. Kehl - General Electric Company
- 1000-1030 REFRESHMENT BREAK
- 1030-1100 SPATE (Stress Pattern Analysis by Thermal Emission) and Gas Turbine Engine Structural Integrity
 D. Nethaway and T. Purcell - Pratt & Whitney
- 1100-1130 Impact of Air Force Damage Tolerance Requirements on the Weight of an Advanced Technology Engine Nozzle
 J. Long Jr., N. Ducharme Jr., and R. Delaneuville - Pratt & Whitney
- 1130-1200 Environmental Characterization of External Components for an Advanced Turbofan Engine
 J. Hansen, B. Vincent, and E. Smith - Pratt & Whitney
- 1200-1330 LUNCH AND PRESENTATION
 From Canberra to Starship: An Engineering Perspective
 Mr. Ric Abbott - Structural Integrity Manager, Beech Aircraft

SESSION VI - FORCE MANAGEMENT
Chairman - J. Turner, SA-ALC/LADD

- 1330-1400 The Results of Using a Micro Processor Based
 Structural Data Recorder to Support Individual
 Aircraft Tracking of the B-1B Aircraft
 A. Denyer - Rockwell International
- 1400-1430 Flight Loads Recorder Installation in Tutor Jet
 Trainer
 A. Ghannadan and J. Reichel - Esprit Technology
 Inc.
- 1430-1500 From Theory to Practice: Evolution of the
 Standard Flight Data Recorder
 F. Saggio, K. Todoroff - Smiths Industries
- 1500-1530 REFRESHMENT BREAK
- 1530-1600 A-10A Individual Aircraft Tracking Program
 (IATP), Validation of Crack Growth Methodology
 for Changing Flight Spectra
 H. Axelrod and K. Grube - Grumman Aircraft
 Systems
 K. McPhaul - SM-ALC/MMSRC
- 1600-1630 Automatic Calculation of an Aircraft's Sink
 Speed Horizontal Velocity, Pitch Angle and
 Pitch Rate, and Roll Angle and Roll Rate at
 Touchdown and Their Application to Structural
 Integrity
 J. Cicero, J. Mohammadi - Systems &
 Electronics, Inc.
- 1630-1700 Health and Usage Monitoring Systems in Airborne
 Applications
 I. Robertson - Smiths Industries
- 1700 ADJOURN

INTRODUCTION

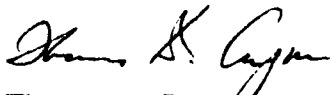
This report contains the proceedings of the 1990 USAF Structural Integrity Program Conference held at the Hyatt Regency Hotel in San Antonio, Texas from 11 - 13 December 1990. The conference, which was sponsored by the ASD Deputy for Engineering and the WRDC Flight Dynamics and Materials Laboratories, was hosted by the San Antonio Air Logistics Center Aircraft Directorate, Aircraft Structural Integrity Branch (SA-ALC/LADD).

This conference, as in previous years, was held to permit experts in the field of structural integrity to communicate with each other and to exchange views on how to improve the structural integrity of military weapon systems. This year, in addition, several of the papers gave the audience a view of the activities relative to the aging commercial aircraft fleet. Most of this work has immediate application to the aging military aircraft. It is anticipated that this conference will include the commercial research and development efforts in the agenda for future meetings.

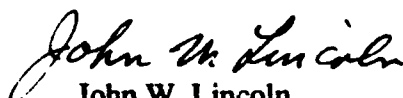
The sponsors are indebted to their hosts for their support of the conference. The sponsors are also indebted to the speakers for their contributions. In particular, thanks are due to the three luncheon speakers for their informative presentations. Mr Earl Briesch from the USAF Logistics Command Headquarters provided an insight into the future of that command. Mr Tom McSweeney, Deputy Director of the Aircraft Certification Service, FAA, presented the results of current activities relating to aging commercial aircraft. Mr Ric Abbott, Structural Integrity Manager, from Beech Aircraft, gave the audience an interesting perspective on the life of an engineer in the aerospace business. Much of the success of the conference is due to the efforts of Jill Jennewine and her staff from the Universal Technology Corporation. Their cooperation is appreciated. We are also grateful to Marianne Ramsey of WRDC/MLSA for compiling the Proceedings and preparing the publication.



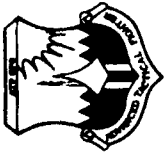
Robert M. Bader
WRDC/FIB



Thomas D. Cooper
WRDC/MLSA



John W. Lincoln
ASD/ENFS



EVOLUTION OF THE INTEGRITY PROCESS FOR THE ATF ENGINES

"PROPULSION & POWER SYSTEMS INTEGRITY PROGRAM"

**BRUCE BACON
PROPULSION DIVISION
ADVANCED TACTICAL FIGHTER SPO**



OVERVIEW

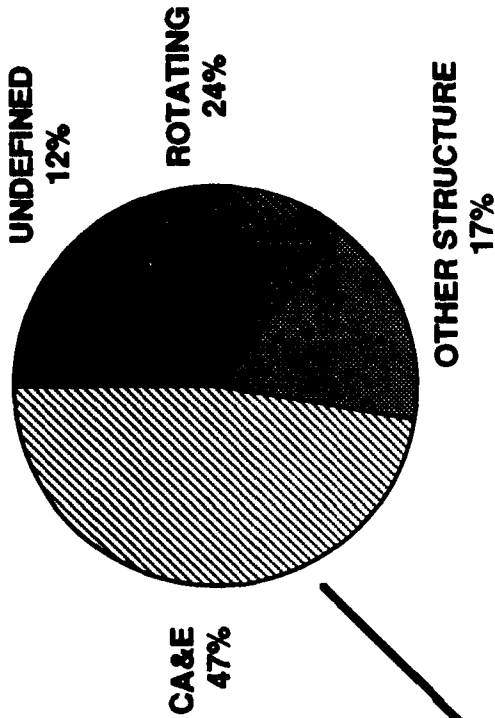
- PPSIP DEVELOPMENT
 - MOTIVATION
 - EVOLUTION
 - CONTENT
- PPSIP IMPLEMENTATION
 - PART CLASSIFICATION METHODOLOGY
 - DAMAGE TOLERANCE CRITERIA
 - PRIME - SUPPLIER INVOLVEMENT
 - INCREASED FOCUS ON MANUFACTURING
 - DEVELOPMENT/QUALIFICATION TESTING IMPROVEMENTS
- PPSIP EXPANSION
 - PERFORMANCE
 - OPERABILITY
 - FUNCTIONALITY
- SUMMARY



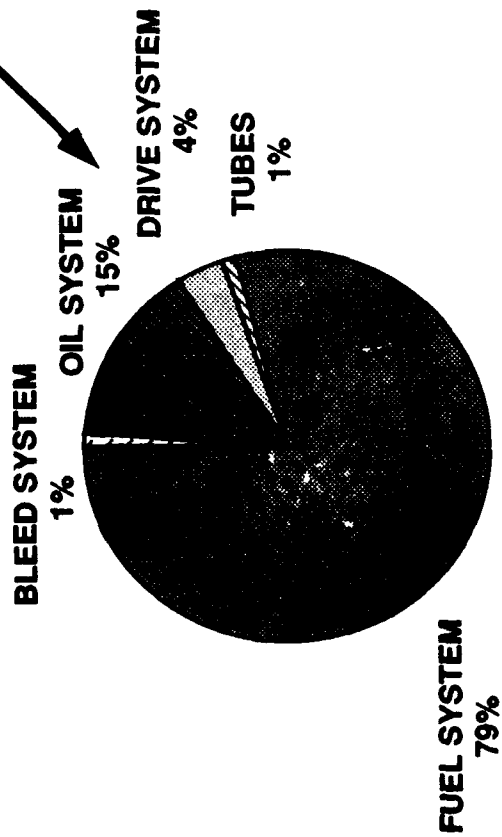
MOTIVATION FOR PPSIP

ENGINE MISHAP EXPERIENCE - CLASS A, B & C MISHAPS

1975 to 1987



CA&E MISHAP DISTRIBUTION CLASS A, B & C MISHAPS



CAUSES FOR CA&E CLASS A MISHAPS

DESIGN	50%
MAINTENANCE	20%
MANUFACTURING	30%
	100%

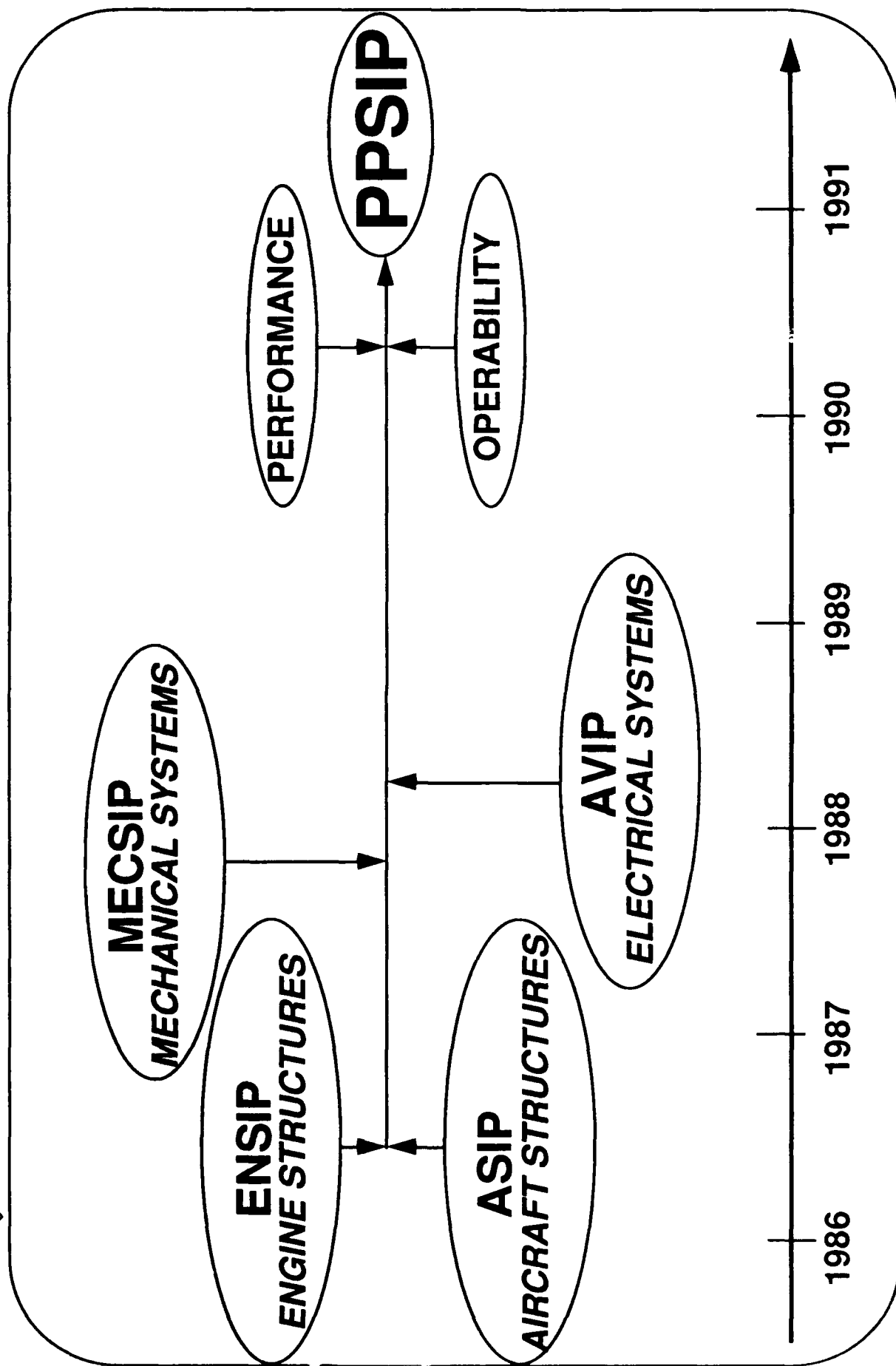


OVERVIEW

- PPSIP DEVELOPMENT
 - MOTIVATION
 - EVOLUTION
 - CONTENT
- PPSIP IMPLEMENTATION
 - PART CLASSIFICATION METHODOLOGY
 - DAMAGE TOLERANCE CRITERIA
 - PRIME - SUPPLIER INVOLVEMENT
 - INCREASED FOCUS ON MANUFACTURING
 - DEVELOPMENT/QUALIFICATION TESTING IMPROVEMENTS
- PPSIP EXPANSION
 - PERFORMANCE
 - OPERABILITY
 - FUNCTIONALITY
- SUMMARY



EVOLUTION OF PPSIP






OVERVIEW

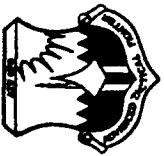
- **PPSIP DEVELOPMENT**
 - **MOTIVATION**
 - **EVOLUTION**
 - **CONTENT**
- **PPSIP IMPLEMENTATION**
 - **PART CLASSIFICATION METHODOLOGY**
 - **DAMAGE TOLERANCE CRITERIA**
 - **PRIME - SUPPLIER INVOLVEMENT**
 - **INCREASED FOCUS ON MANUFACTURING**
 - **DEVELOPMENT/QUALIFICATION TESTING IMPROVEMENTS**
- **PPSIP EXPANSION**
 - **PERFORMANCE**
 - **OPERABILITY**
 - **FUNCTIONALITY**
- **SUMMARY**

PPSIP TASKS -- MECHANICAL INTEGRITY

TASK I	TASK II	TASK III	TASK IV	TASK V
DESIGN INFORMATION	DESIGN ANAL. COMPNT. & MAT. CHARAC.	COMPONENT & RIG TESTING	GROUND & FLIGHT ENGINE TESTS	PROD. QUAL. CONTROL & ENGINE LIFE MGT.
MASTER PLAN	DESIGN DUTY CYCLE	STRENGTH TESTING	ENVIRON. VERIFICATION TESTING	PRODUCTION ENGINE ANALYSIS
DESIGN SERVICE LIFE & USAGE REQUIREMENTS	MAT'L'S & PROCESS DESIGN DATA CHARACTERIZED	DAMAGE TOLERANCE TESTS	<ul style="list-style-type: none"> • THERMAL SURVEY • GROUND VIBE STRAIN & FLUTTER SURVEY • ROTOR DYN. SURVEY • SENSITIVITY TESTS • INSTALLED VIBE SURVEY • INTERNAL COMPONENT RESONANCE SEARCH • CLEARANCE CONTROL • INDIVIDUAL COMPONENT VIBRATION DATA BASE CHARACTERIZATION 	STRUCT. SAFETY & DURAB. SUMMARY
DESIGN CRITERIA	STRUCT./THERMAL ANALYSIS	DURABILITY TESTS		ENGINE STRUCTURAL MAINTENANCE PLAN
<ul style="list-style-type: none"> • DAM. TOL. CRITERIA • DURABILITY CRITERIA • MAINTAINABILITY CRITERIA • RISK ASSESSMENT • INLET/EXHAUST/AIRFRAME COMPATIBILITY CRITERIA • DAM. TOL. & DURABILITY CONTROL PLANS * • DIAGNOSTICS • CONSIDERATIONS • INSTRUMENTATION • CONSIDERATIONS • MAT'L'S. & PROCESS CHARACTERIZATION PLAN • CORROSION CONTROL • PARTS CLASSIFICATION • JOINT INTEGRITY PLAN 	<ul style="list-style-type: none"> • THERM. ENVIRONMENT • COMPONENT STRESS/ ENVIRON. SPECTRA • STRENGTH ANALYSIS • VIBE/FLUTTER ANAL. • DAMAGE TOL. ANAL. • DURABILITY ANAL. • CRITICAL PARTS LIST • SAFETY FAULT ANAL. • FIELD INSP. REQ. ANALYSIS • DIAGNOSTIC ANAL. 	THERMAL SURVEY		LIFE MATURATION PROGRAM *
		VIBRATORY STRAIN & FLUTTER BOUNDARY SURVEY	(AMT) TEST SPECTRUM DERIVATION	INDIVIDUAL COMP. TRACKING
			DURABILITY TESTS	LEAD THE FORCE PROGRAM (USAGE) *
			DAMAGE TOL. TESTS	DUR. & DAMAGE TOL. CONTROL PLAN IMPLEMENTATION
			FLIGHT TEST STRAIN SURVEY	TECHNICAL ORDER UPDATE
			UPDATED DURABILITY & DAM. TOL. CONTROL PLAN *	
			PERFORMANCE DETERIORATION STRUCT. IMPACT ASSESSMENT	
			CRITICAL PART UPDATE	
MFG. & QUALITY CONTROL PLAN				

 -- CONTRACT DELIVERABLES

* -- PLANS EMBEDDED IN OTHER DELIVERABLES



OVERVIEW

- PPSIP DEVELOPMENT
 - MOTIVATION
 - EVOLUTION
 - CONTENT
- PPSIP IMPLEMENTATION
 - PART CLASSIFICATION METHODOLOGY
 - DAMAGE TOLERANCE CRITERIA
 - PRIME - SUPPLIER INVOLVEMENT
 - INCREASED FOCUS ON MANUFACTURING
 - DEVELOPMENT/QUALIFICATION TESTING IMPROVEMENTS
- PPSIP EXPANSION
 - PERFORMANCE
 - OPERABILITY
 - FUNCTIONALITY
- SUMMARY



PART CLASSIFICATION

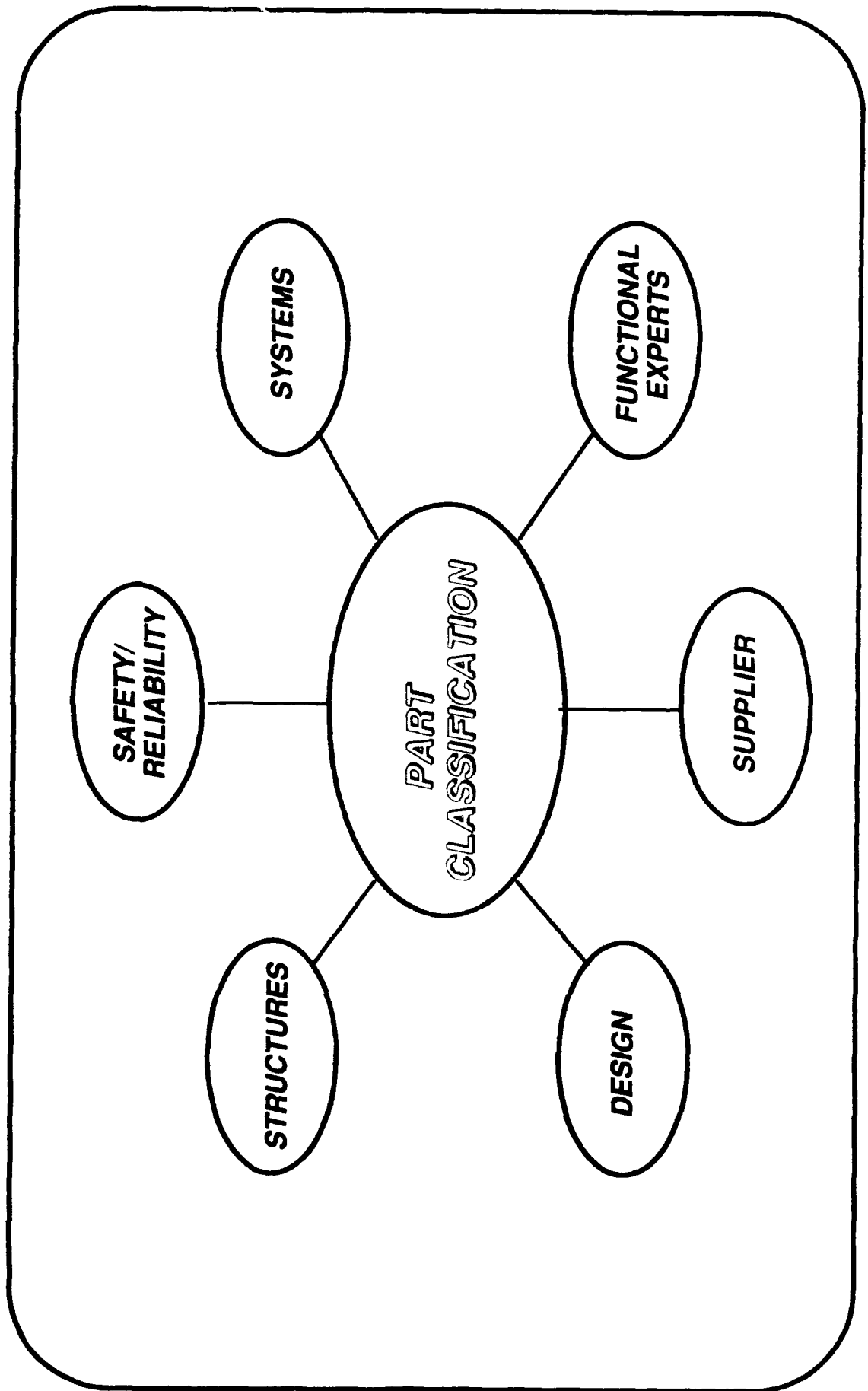
PURPOSE

**CLASSIFY PARTS UP FRONT IN THE DESIGN PROCESS
IN ORDER TO:**

**ENSURE ALL HAZARDS ARE IDENTIFIED AND THE
APPROPRIATE CONTROLS ARE DESIGNED INTO
THE COMPONENT/PROCESSES.**



ATFE PART CLASSIFICATION IS A TEAM EFFORT





CLASSIFICATION DEFINITIONS

SAFETY CRITICAL

- FAILURE WHICH WILL RESULT IN PROBABLE LOSS OF AIRCRAFT OR HAZARD TO PERSONNEL.

MISSION CRITICAL

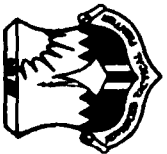
- FAILURE WHICH WILL RESULT IN A SIGNIFICANT OPERATIONAL IMPACT BY DEGRADING MISSION CAPABILITIES OR RESULT IN LESS THAN LEVEL II HANDLING QUALITIES.

DURABILITY CRITICAL

- FAILURE WHICH WILL RESULT IN A SIGNIFICANT ECONOMIC IMPACT.

DURABILITY NONCRITICAL

- FAILURE WHICH WILL RESULT IN A MINOR ECONOMIC IMPACT.



ATFE PART CLASSIFICATION CONSIDERATIONS

1. FUNCTION

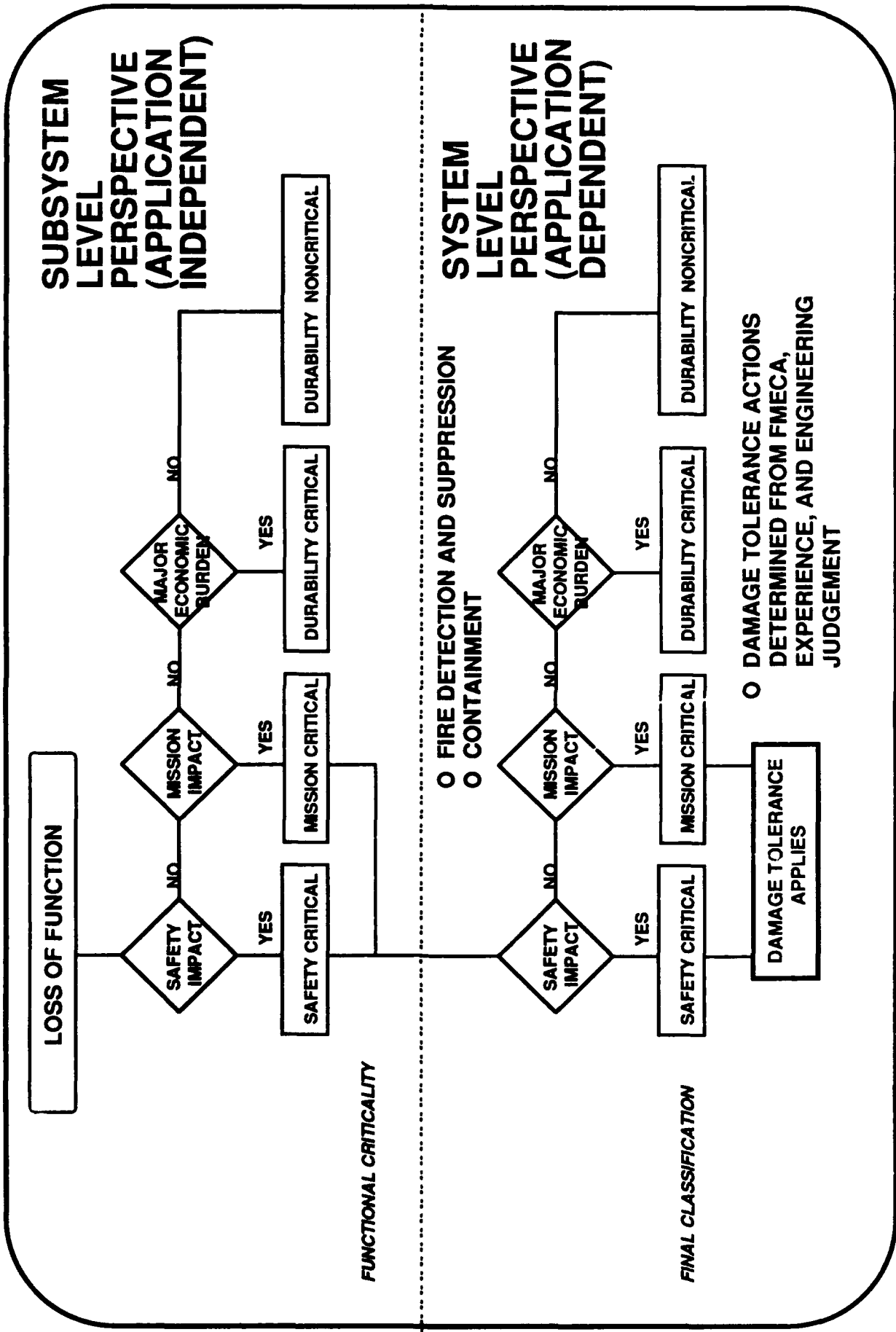
- o *How does the loss of function affect mission capability?*

2. APPLICATION

- o *Will the system configuration affect the consequence of loss of function?*



PART CLASSIFICATION PROCESS





PART CLASSIFICATION EXAMPLES

STEP 1: FUNCTIONAL CLASSIFICATION

<u>COMPONENT</u>	<u>FUNCTION</u>	<u>LOSS OF FUNCTION</u>	<u>FUNCTIONAL CLASSIFICATION</u>
BEARING	PROVIDE SUPPORT FOR FAN, HPC, AND TURBINE	ENGINE SHUTDOWN	SAFETY CRITICAL
FADEC	RECEIVE A/C AND ENGINE DATA, PROVIDE ENGINE CONTROL	ENGINE SHUTDOWN	SAFETY CRITICAL
LOW PRESSURE TURBINE DISK	TRANSMITS WORK FROM TURBINE BLADES TO OPERATE FAN	ENGINE SHUTDOWN UNCONTAINED FAILURE	SAFETY CRITICAL

STEP 2: APPLICATION CLASSIFICATION (DUAL ENGINE)

<u>COMPONENT</u>	<u>FUNCTION</u>	<u>LOSS OF FUNCTION</u>	<u>FINAL CLASSIFICATION</u>
BEARING	PROVIDE SUPPORT FOR FAN, HPC, AND TURBINE	ENGINE SHUTDOWN	MISSION CRITICAL
FADEC	RECEIVE A/C AND ENGINE DATA, PROVIDE ENGINE CONTROL	ENGINE SHUTDOWN	MISSION CRITICAL
LOW PRESSURE TURBINE DISK	TRANSMITS WORK FROM TURBINE BLADES TO OPERATE FAN	ENGINE SHUTDOWN UNCONTAINED FAILURE	SAFETY CRITICAL



OVERVIEW

- PPSIP DEVELOPMENT
 - MOTIVATION
 - EVOLUTION
 - CONTENT
- PPSIP IMPLEMENTATION
 - PART CLASSIFICATION METHODOLOGY
 - DAMAGE TOLERANCE CRITERIA
 - PRIME - SUPPLIER INVOLVEMENT
 - INCREASED FOCUS ON MANUFACTURING
 - DEVELOPMENT/QUALIFICATION TESTING IMPROVEMENTS
- PPSIP EXPANSION
 - PERFORMANCE
 - OPERABILITY
 - FUNCTIONALITY
- SUMMARY



DAMAGE TOLERANCE

PER THE ENGINE SPECIFICATION :

"THE ABILITY OF THE CRITICAL EQUIPMENT TO RESIST FAILURE DUE TO THE PRESENCE OF FLAWS, CRACKS, OR OTHER DAMAGE FOR A SPECIFIED PERIOD OF UNREPAIRED USAGE."

THIS IS NOT A FAIL SAFE CONCEPT.

(I.E., ENGINE SHUTDOWN IS FAIL-SAFE IN A DUAL ENGINE AIRCRAFT, BUT THIS DOES NOT ALLOW CONTINUED MISSION USAGE) - SEE MISSION CRITICAL DEFINITION



DAMAGE TOLERANCE COMPLIANCE

1. FRACTURE MECHANICS
 - A. CONTROLLED CRACK GROWTH (FRACTURE CRITICAL)
 - B. FRACTURE SCREENING (NO GROWTH)
 - C. LEAK BEFORE BURST
2. REDUNDANCY WITH FAULT DETECTION AND ACCOMMODATION
3. OTHER HAZARD CONTROLS (HIGH MARGINS OF SAFETY, LOW PROBABILITY OF FAILURE, ETC) WITH CONCURRENCE OF THE PROCURING ACTIVITY



DAMAGE TOLERANCE EXAMPLES

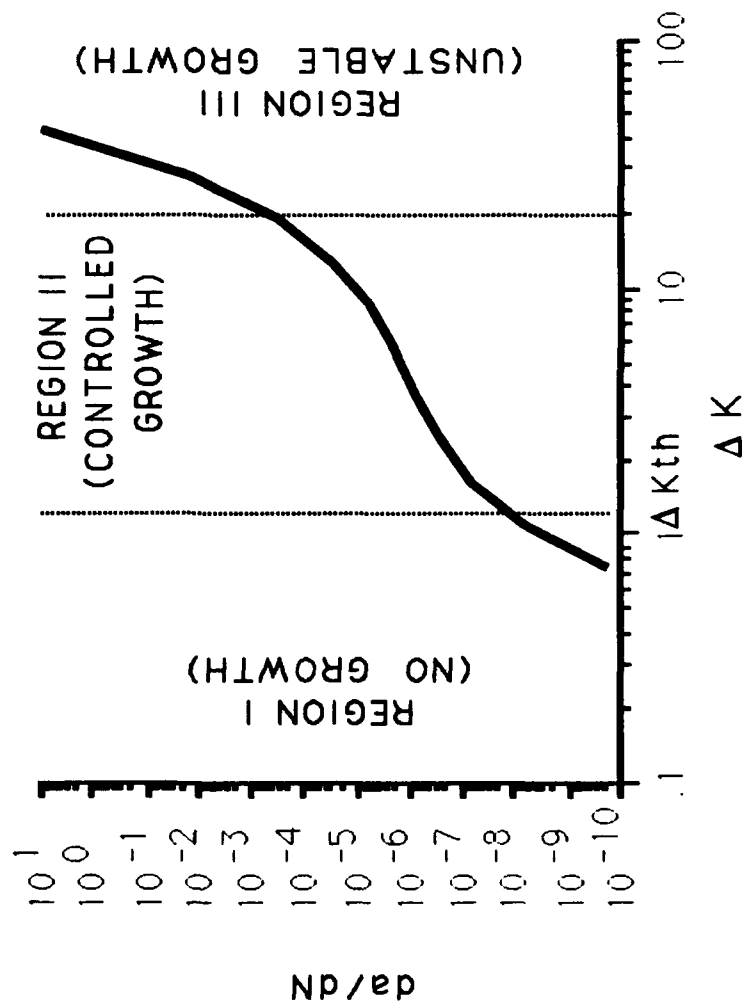
<u>COMPONENT</u>	<u>FAILURE MODE</u>	<u>DAMAGE TOLERANCE COMPLIANCE</u>
1A. LOW PRESSURE TURBINE DISK	MATERIAL SEPARATION	CONTROLLED CRACK GROWTH
1B. FUEL PUMP	FRACTURE OF IMPELLER	FRACTURE SCREENING
1C. ACTUATOR	FRACTURE OF CYLINDER	LEAK BEFORE BURST
2. FADEC	LOSS OF CONTROL PROCESSOR	REDUNDANCY
3. BEARING	SPALLING	OIL SAMPLING, CHIP DETECTORS



FRACTURE SCREENING

**PURPOSE: KEEP STRESS INTENSITY BELOW
THRESHOLD VALUE**

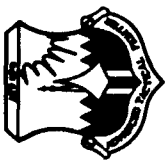
$$\Delta K_{TH} > \Delta \sigma * \beta * (\pi * a)^{0.5}$$





OVERVIEW

- PPSIP DEVELOPMENT
 - MOTIVATION
 - EVOLUTION
 - CONTENT
- *PPSIP IMPLEMENTATION*
 - PART CLASSIFICATION METHODOLOGY
 - DAMAGE TOLERANCE CRITERIA
 - *PRIME - SUPPLIER INVOLVEMENT*
 - INCREASED FOCUS ON MANUFACTURING
 - DEVELOPMENT/QUALIFICATION TESTING IMPROVEMENTS
- PPSIP EXPANSION
 - PERFORMANCE
 - OPERABILITY
 - FUNCTIONALITY
- SUMMARY



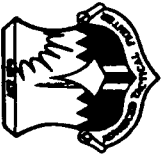
INTEGRITY FLOWDOWN

- **REQUIRES SUBSTANTIAL PARTICIPATION BY ALL STAKEHOLDERS (USAF, PRIMES, SUPPLIERS)**
 - **COMMUNICATION AND ATTENTION TO DETAIL NECESSARY TO IMPLEMENT AN EFFECTIVE INTEGRITY PROGRAM**
- **EXTENSIVE EFFORT TO EDUCATE SUPPLIERS ON THE INTEGRITY PROCESS**
- **NECESSITATES BRINGING SUPPLIERS TECHNOLOGY BASE/ACCESSIBILITY UP TO THAT OF PRIMES**
 - **PRIMES WILL NEED TO TAKE A MORE ACTIVE ROLE IN THE SUPPLIER'S DESIGN & DEVELOPMENT ACTIVITIES**
 - **SUPPLIERS BEING HELD ACCOUNTABLE FOR MEETING SPECIFICATION REQUIREMENTS**



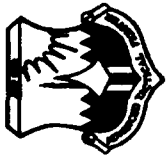
KEY PRIME CONTRACTOR RESPONSIBILITIES

- COMPONENT DUTY CYCLES
- INSTALLED/LOGISTICS ENVIRONMENTS
CHARACTERIZATION
- COMPONENT CLASSIFICATION & RESULTING ACTIONS
- DEFINE LOGISTICS CONSTRAINTS
- ESTABLISH MAINTENANCE CONCEPTS/APPROACHES
- SPECIFICATION REQUIREMENTS/INTEGRITY PROGRAM
TAILORING
- TECHNICAL OVERSIGHT/GUIDANCE



OVERVIEW

- PPSIP DEVELOPMENT
 - MOTIVATION
 - EVOLUTION
 - CONTENT
- *PPSIP IMPLEMENTATION*
 - PART CLASSIFICATION METHODOLOGY
 - DAMAGE TOLERANCE CRITERIA
 - PRIME - SUPPLIER INVOLVEMENT
 - *INCREASED FOCUS ON MANUFACTURING*
 - DEVELOPMENT/QUALIFICATION TESTING IMPROVEMENTS
- PPSIP EXPANSION
 - PERFORMANCE
 - OPERABILITY
 - FUNCTIONALITY
- SUMMARY



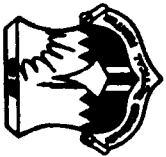
PPSIP EMBODIES INTEGRATED PRODUCT DEVELOPMENT

- CONCURRENT ENGINEERING TEAMS "DESIGN" EVERY COMPONENT
 - DESIGN
 - MANUFACTURING
 - SAFETY
 - MAINTAINABILITY
 - SUPPORTABILITY (INCLUDES REPAIRS)
- CHARACTERIZATION OF ALL MATERIAL & MANUFACTURING PROCESSES
- PERIODIC PRODUCIBILITY REVIEWS BEGINNING AT PDR
- PRODUCTION READINESS REVIEWS PRIOR TO DDR
- PERIODIC REVIEWS AT AND OF SUPPLIERS FACILITIES
- HAZARD ANALYSES OF EACH ASSEMBLY
- USE OF STATISTICAL PROCESS CONTROL TECHNIQUES AT EACH SUPPLIER
- RELIABILITY GROWTH TESTING REQUIRED
- ENVIRONMENTAL STRESS SCREENING (ESS) OF ALL ELECTRICAL AND MOST MECHANICAL DEVICES
- CONTINUOUS IMPROVEMENT OF SUPPLIER PROCESSES REQUIRED AND MONITORED



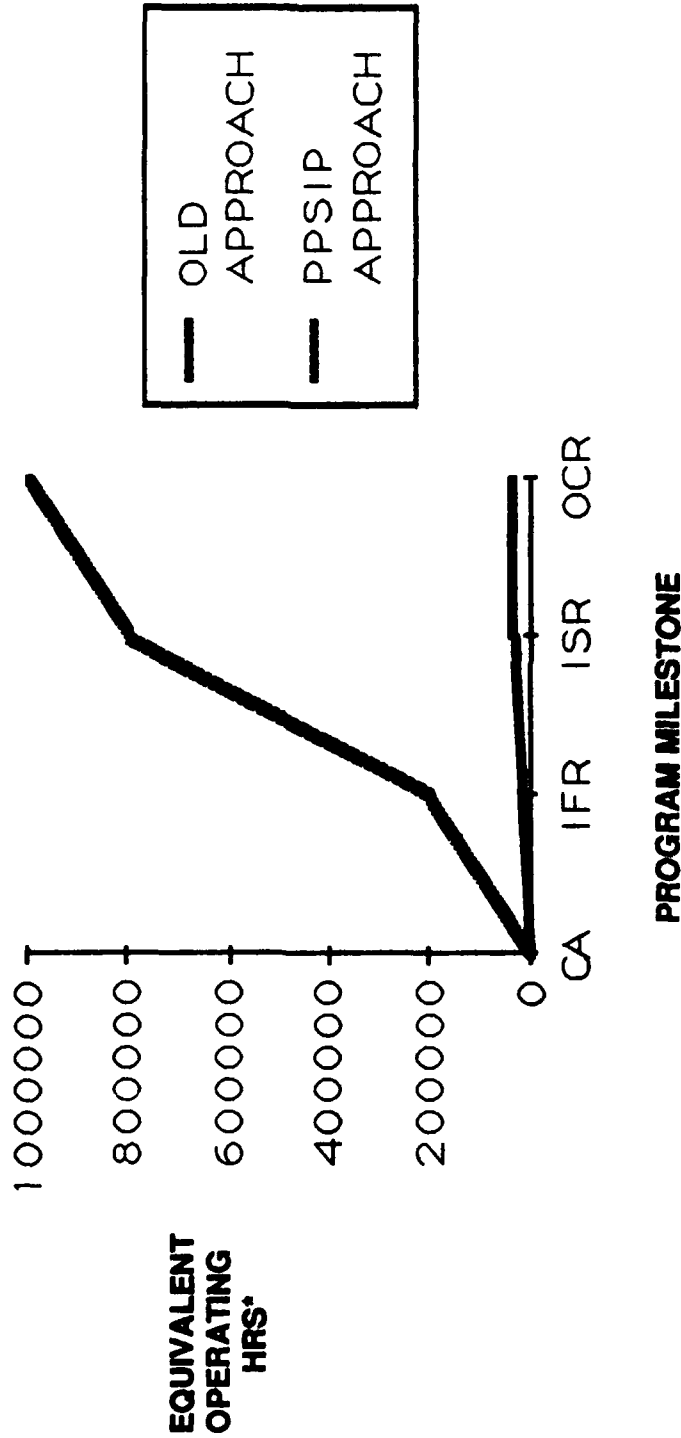
OVERVIEW

- PPSIP DEVELOPMENT
 - MOTIVATION
 - EVOLUTION
 - CONTENT
- PPSIP IMPLEMENTATION
 - PART CLASSIFICATION METHODOLOGY
 - DAMAGE TOLERANCE CRITERIA
 - PRIME - SUPPLIER INVOLVEMENT
 - INCREASED FOCUS ON MANUFACTURING
 - DEVELOPMENT/QUALIFICATION TESTING IMPROVEMENTS
- PPSIP EXPANSION
 - PERFORMANCE
 - OPERABILITY
 - FUNCTIONALITY
- SUMMARY



CA&E DEVELOPMENT/QUALIFICATION TESTING

"AN IMPROVED WAY OF DOING BUSINESS!"



***ESTIMATE BASED ON 40 CA&E COMPONENTS**



OVERVIEW

- PPSIP DEVELOPMENT
 - MOTIVATION
 - EVOLUTION
 - CONTENT
- PPSIP IMPLEMENTATION
 - PART CLASSIFICATION METHODOLOGY
 - DAMAGE TOLERANCE CRITERIA
 - PRIME - SUPPLIER INVOLVEMENT
 - INCREASED FOCUS ON MANUFACTURING
 - DEVELOPMENT/QUALIFICATION TESTING IMPROVEMENTS
- *PPSIP EXPANSION*
 - PERFORMANCE
 - OPERABILITY
 - FUNCTIONALITY
- SUMMARY

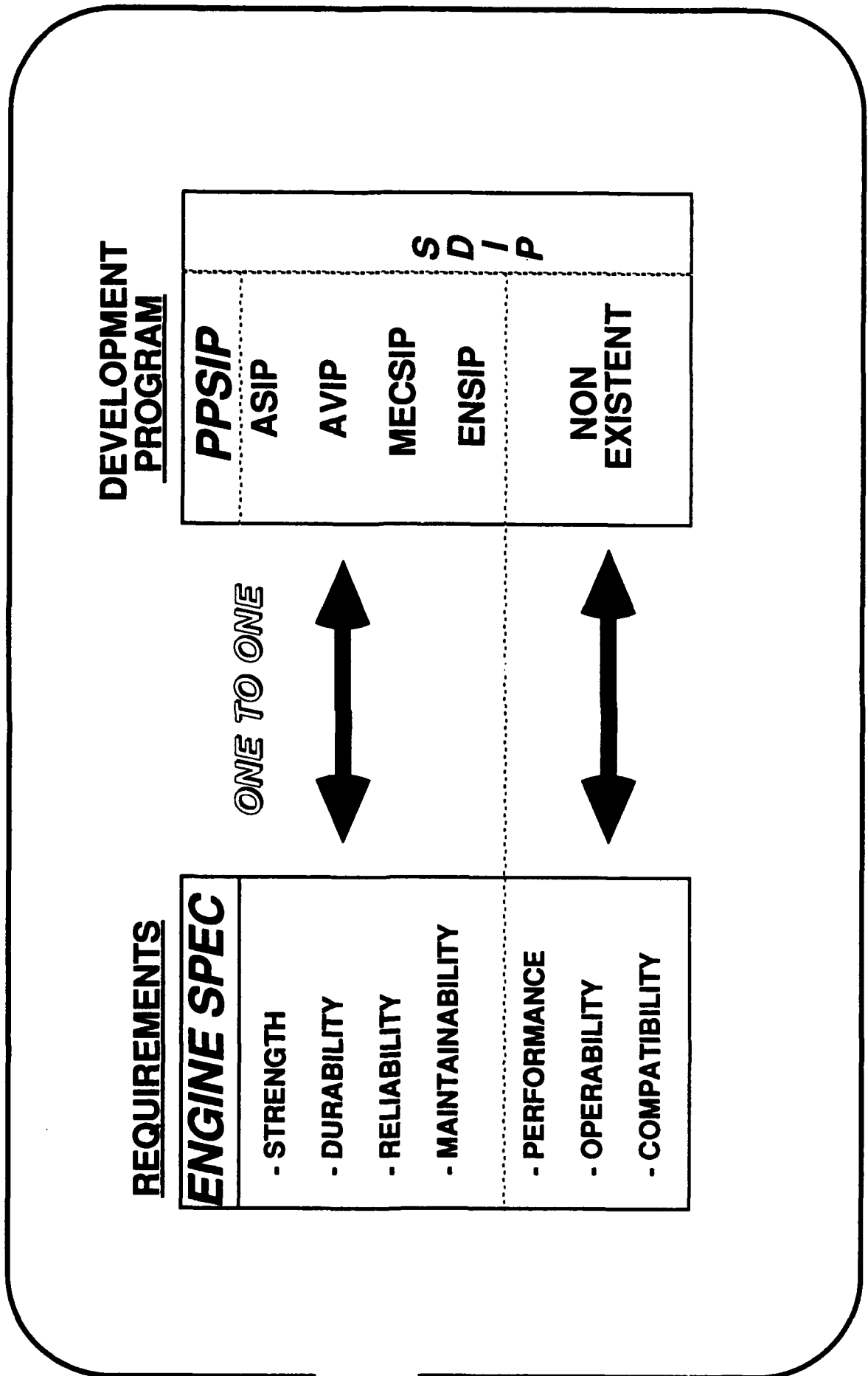


EXPANSION OF THE INTEGRITY EFFORT

- THE MECHANICAL/ELECTRICAL INTEGRITY PROCESS PROVIDES A SOUND STRUCTURE FOR CAPTURING THE EFFORT ASSOCIATED WITH DEVELOPING THE OTHER FUNCTIONAL ELEMENTS OF A SYSTEM.
- APPLICATION TO OTHER FUNCTIONAL DISCIPLINES/REQUIREMENTS (PERFORMANCE, OPERABILITY, FUNCTIONALITY, & COMPATIBILITY) IS A NATURAL EXTENSION OF THIS PROVEN PROCESS.
- EXTENSION PROVIDES ONE -TO - ONE RELATIONSHIP BETWEEN FUNCTIONAL REQUIREMENTS AS CAPTURED IN THE SPECIFICATION TO DEVELOPMENT PROCESS AS DEFINED WITHIN INTEGRITY MASTER PLAN



INTERACTIONS BETWEEN REQUIREMENTS & PROCESSES



PPSIP TASKS -- PERF/OPER/FUNCTIONAL INTEGRITY

TASK I		TASK II		TASK III		TASK IV		TASK V	
DESIGN INFORMATION		DESIGN ANAL COMPNT & AERO/THERMO CHARAC		COMPONENT/RIG & CORE ENGINE TESTING		GROUND & FLIGHT ENGINE TESTING		PROD. QUAL CONTROL & OPERATIONAL VALID.	
MASTER PLAN		OPERATING ENVELOPES - ALPHA, BETA, MACH		COMPONENT AERO/THERMO TESTS		DEVELOPMENT TESTING SEA LEVEL & ALTITUDE		PRODUCTION ENGINE PERFORMANCE ANALYSIS	
FUNCTIONAL/PERF REQUIREMENTS		INSTALLATION SYSTEM CHARACTERIZED		RIG TESTS		STARTING PERFORMANCE - LAPSE RATE - ALTITUDE - CLEARANCE/LEAKAGES - OPERABILITY - TURBOMACHINERY - AUGMENTOR - STABILITY/COMPATIBILITY - DISTORTION - CLEAN STALL LINE DEFN - HOT/COLD ROTOR REBURSTS - FAULT TOLERANCE - SCHEDULE OPTIMIZATION - DETERIORATION VALIDATION - CLEARANCE OPTIMIZATION - AIRFOIL BLENDING AFFECTS - TCLA OPTIMIZATION		PERF/OPER/FUNCTIONAL SUMMARY	
DESIGN CRITERIA		INLET - DISTORTION (PLANAR, TEMP, SPATIAL) - RECOVERY - L/O - DEMANDS - BLD, HPX, APU CHAR, ETC - EXHAUST - COOLING, L/O, VECTORING		CORE TESTS		AERO PERFORMANCE - STABILITY MAPPING - OPERABILITY CHAR. - COMBUSTOR L/O & B/O - VARIABLE GEOMETRY OPTIM. - AEROMECH INTERACTIONS - DISTORTION SENSITIVITY - CLEARANCE EVALUATION - TRANSIENT EVALUATION - AIRFRAME RECTS EVALUATION - BLEED - HPX - ETC - HP FLOW FUNCTIONS		PRODUCTION Q.C. AUDITS OF CRITICAL PERF/OPER CHARACTERISTICS	
		AERO/THERMO DESIGN DATA COMPILED				QUAL DISTORTION (PRESS & TEMP) PATTERN DEFINITIONS		RANDOM OPERABILITY CHECKS ON PRODUCTION ENGINES	
		PERF/OPER/FUNCTIONAL ANALYSES				ALTITUDE AERO-PERF QUALIFICATION TESTS		LEAD - THE - FORCE PROGRAM *	
		THERMODYNAMIC ANALYSES - AERODYNAMIC ANALYSES - STABILITY ANALYSES - STARTING - BLOWOUT - A/B LIGHT/OFF - CONTROL SYSTEM DYNAMIC ANALYSES - COMPATIBILITY ANALYSES - PRESSURE DISTORTION - TEMPERATURE DISTORTION - PLANAR WAVE - STALL/SURGE RECOVERY - SENSITIVITY ANALYSES - DETERIORATION - CONTROL TOLERANCES - HDW QUALITY VARIATIONS - FOD/OO & BLENDING - EFFICIENCY SHORTFALLS - CRITICAL CHARACTERISTIC DETERMINATION - SURFACE FINISH - CONTOURS				FLIGHT TEST VALID.		PERFORMANCE RETENTION TREND PGM	
						INLET RAKE TESTING - MISSILE GAS INGESTION - OPERABILITY - PERFORMANCE - COMPATIBILITY		TECHNICAL ORDER UPDATE	
						FLIGHT MANUAL UPDATE		CONTRACT DELIVERABLES	
						PART II SPECIFICATION ATP DEVELOPMENT		PLANS EMBEDDED IN OTHER DELV.	



OVERVIEW

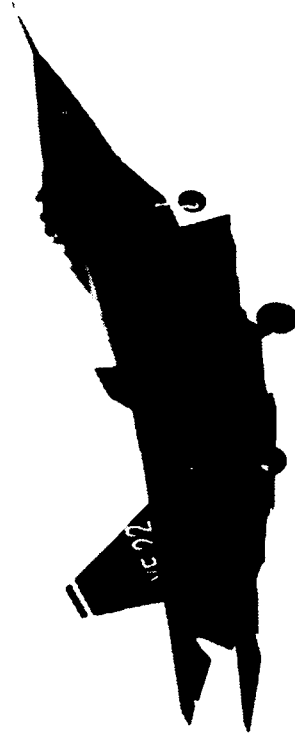
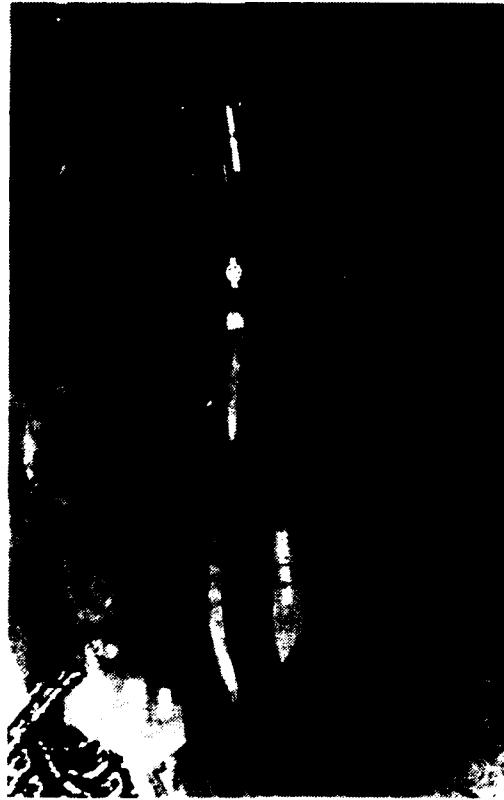
- PPSIP DEVELOPMENT
 - MOTIVATION
 - EVOLUTION
 - CONTENT
- PPSIP IMPLEMENTATION
 - PART CLASSIFICATION METHODOLOGY
 - DAMAGE TOLERANCE CRITERIA
 - PRIME - SUPPLIER INVOLVEMENT
 - INCREASED FOCUS ON MANUFACTURING
 - DEVELOPMENT/QUALIFICATION TESTING IMPROVEMENTS
- PPSIP EXPANSION
 - PERFORMANCE
 - OPERABILITY
 - FUNCTIONALITY
- *SUMMARY*



SUMMARY

- o THE PPSIP PROCESS IS AIMED AT IMPROVING TOTAL ENGINE SYSTEM RELIABILITY THEREBY REDUCING LCC & INCREASING SYSTEM READINESS
- o PPSIP EMBODIES THE CONCURRENT ENGINEERING/INTEGRATED PRODUCT DEVELOPMENT APPROACH TO SYSTEM DEVELOPMENT
- o ATF ENGINE PROGRAM IS TAKING A LEAD IN APPLYING INTEGRITY PROGRAMS ACROSS ALL ENGINE SUBSYSTEMS & FUNCTIONAL DISCIPLINES
- o ALTHOUGH ADDING TO DEVELOPMENT COSTS, THE INSTITUTION OF THE INTEGRITY PROCESS WILL RESULT IN A POSITIVE ROI TO ALL CONCERNED (USER, SPO, INDUSTRY, MAINTAINERS, SUPPORTERS, ETC)
- o PPSIP IS A CULTURAL CHANGE FOR INDUSTRY & USAF ALIKE. IT IS INTENDED TO BE EVOLUTIONARY IN NATURE
- o USAF MUST TAKE THE LEAD IN IMPLEMENTING THE INTEGRITY PROCESS
 - oo EDUCATION AND COMMUNICATION IS ESSENTIAL
 - oo REFERRING TO SPECS AND STANDARDS WILL NOT PRODUCE THE DESIRED RESULTS

F120 PPSIP - Success Through Supplier Involvement



USAF Structural Integrity Conference
December 11-13, 1990
San Antonio, TX

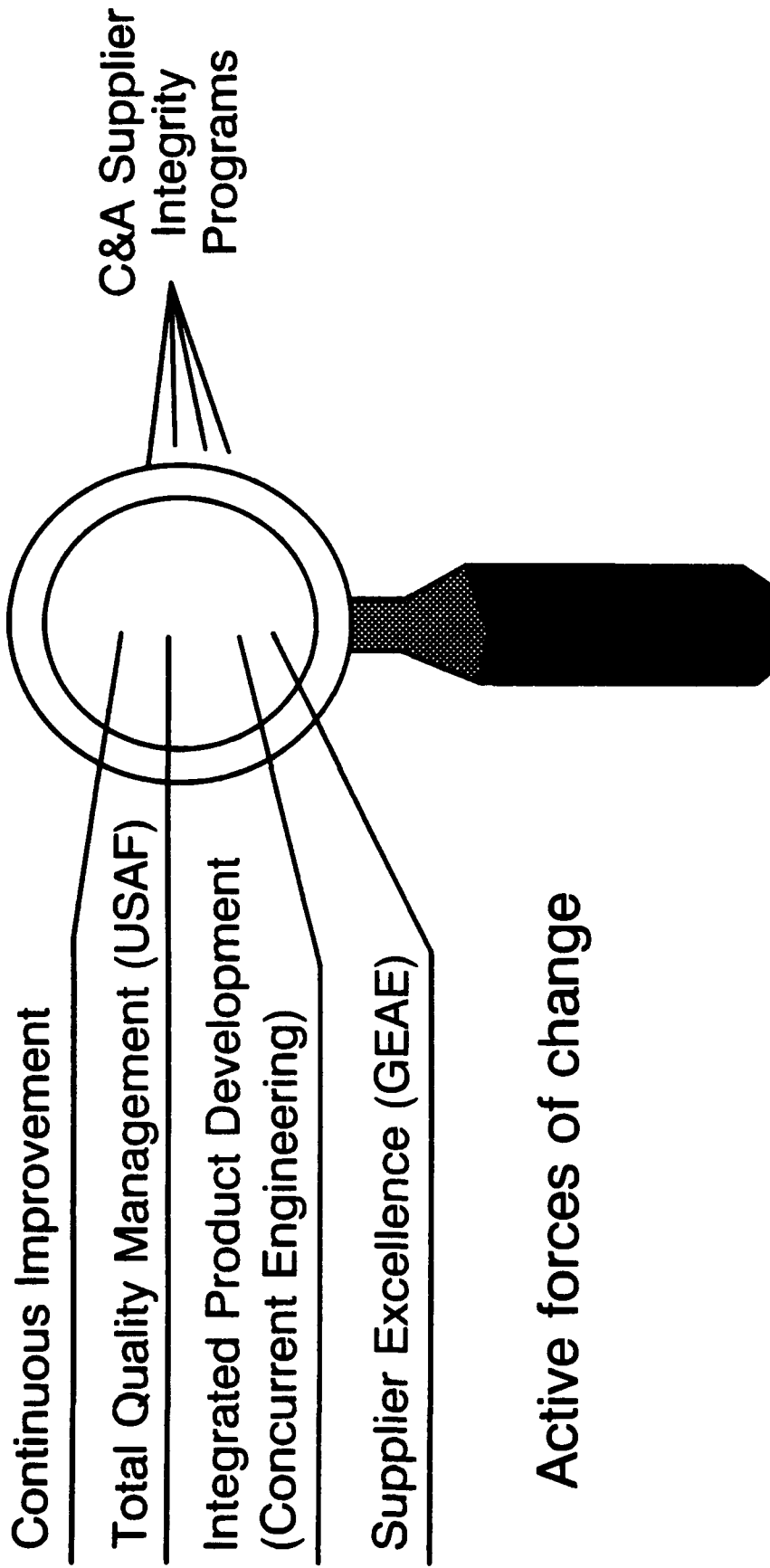
Dr. P. Domas
Life Management Programs
GE Aircraft Engines

Background

- Advanced Tactical Fighter (ATF) propulsion and Power System Integrity Program (PPSIP) includes Engine Controls and Accessories (C&A)
- Approximately 25 GEAE C&A suppliers with multiple sub-tier sources
- Supplier involvement through "Vendor Involvement Plan" is a key ingredient
- 7/24/90, USAF/WRDC sponsored, Dayton, Ohio, Component Integrity Workshop suggests industry is still low on the learning curve, but we've started

Innovation, Hard Work is Showing Progress!

Environment for Change is Present



Active forces of change

F120 PPSIP
focused initiatives

Actions: Specific Major Initiatives

- PPSIP flow down to GEAE functions and suppliers:
 - Standardized requirements
 - Integrated engineering and supportability interfaces
 - GEAE team visits to all C&A suppliers
 - Direct supplier involvement with customer
- Changed C&A testing philosophy
- Supplier selection on "best value" basis
- Improved control over key "Sub-tier" components

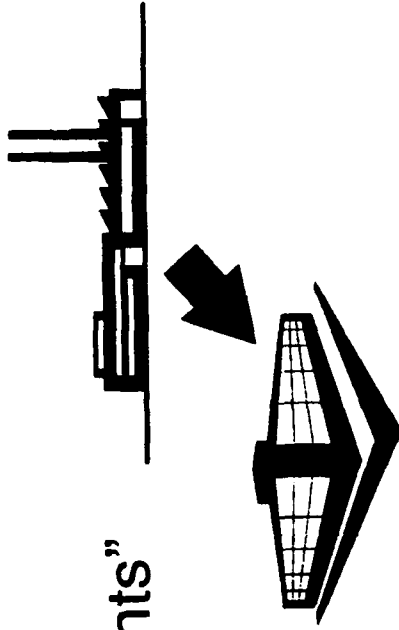
Changed C&A Request for Quote Process

- Consolidated technical requirements from all GEAE functional areas:
 - 27 specific functions integrated including configurations, design, finance, legal, logistic, reliability, support equipment, etc.
- Early definition, early integration
- Total program information provided and quoted (entire engine program)
- Expanded quotation package:
 - Business proposal
 - Technical proposal
 - PPSIP plan (including supportability plan)

Master Plans . . . “Flow Down” (“Flow Up”)

- GEAE issued “guidance documents”

- Clear requirement communication
- Consistency
- Increased supplier buy-in



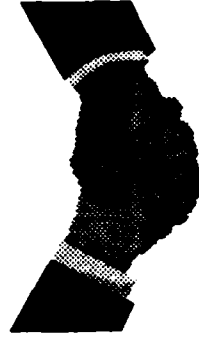
- Supplier PPSIP plans submitted for review

- Direct feedback of supplier strong/weak points
- Integrated business/technical management

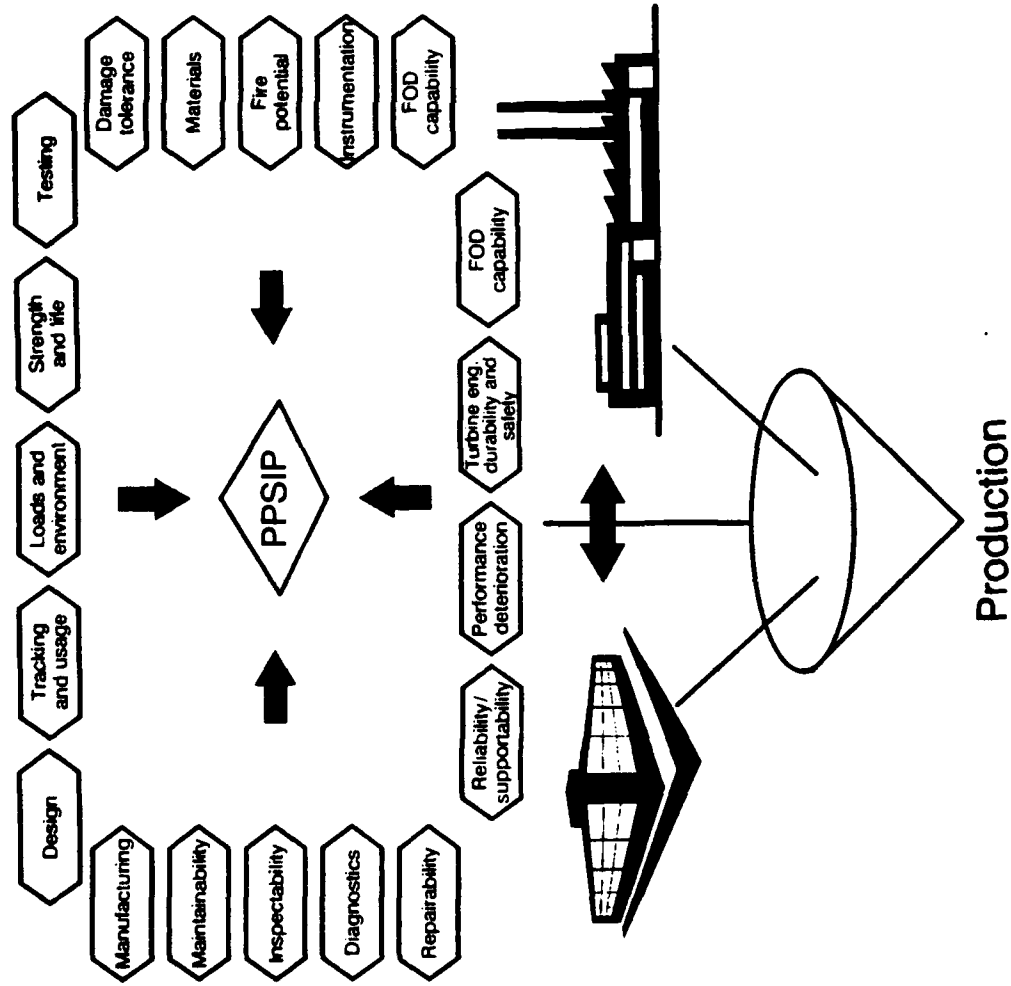


- Up front agreement

- Understanding leading to commitment
- Trust and ownership



Multi-disciplinary Functional Reviews Now Required

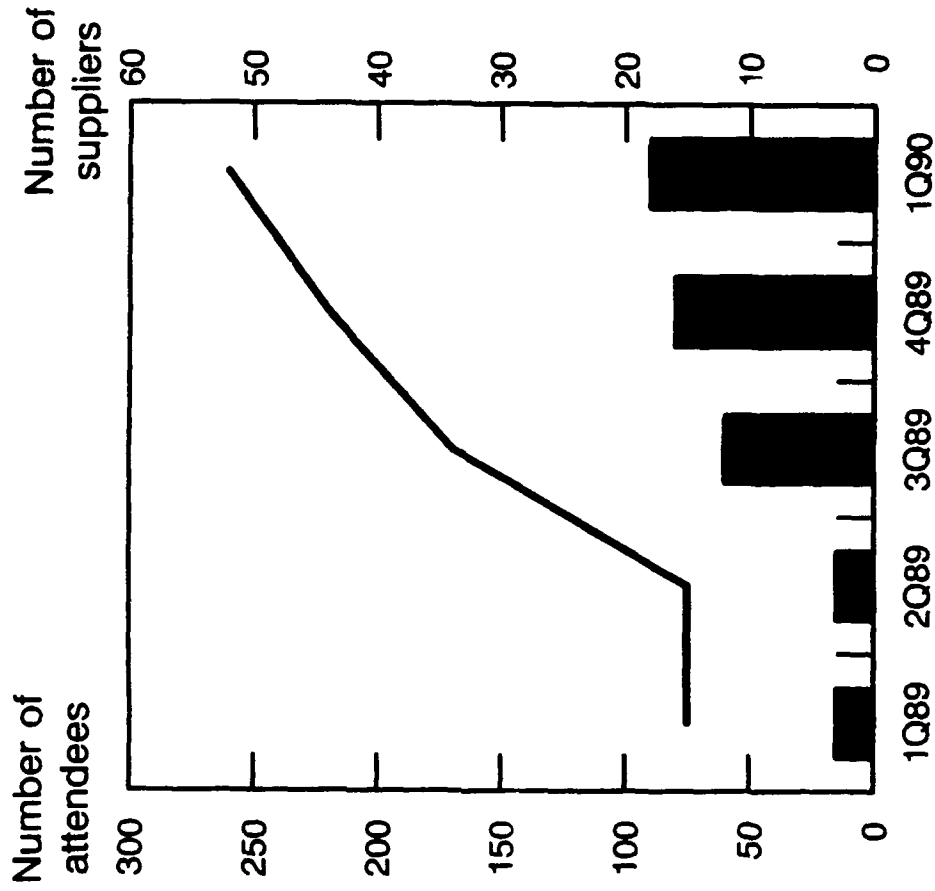


Reviews

- Preliminary functional
- Preliminary design
- Pre-production manufacturing and quality
- Critical design
- Hardware readiness
- Production readiness

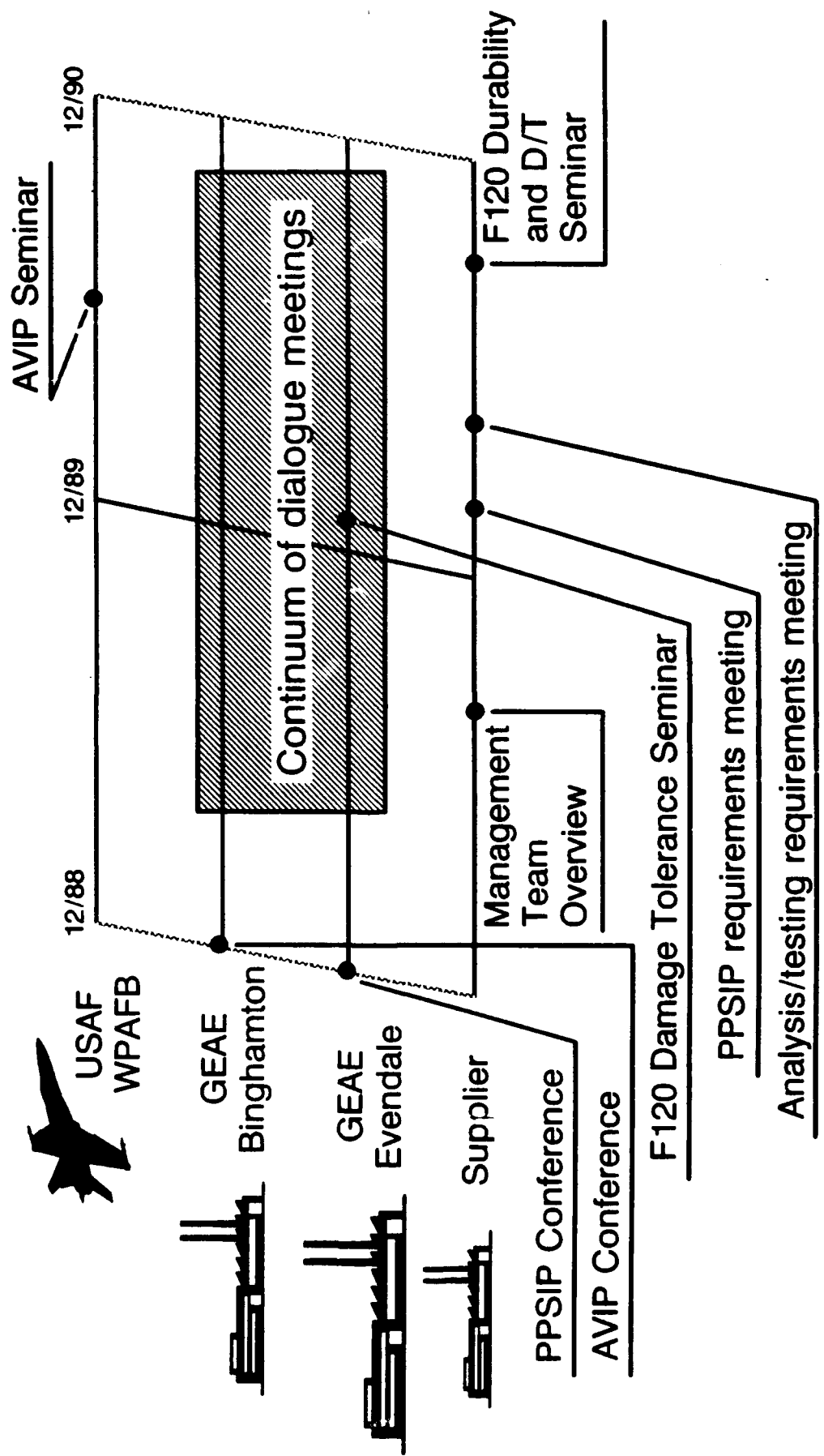
Supplier Visits by GEAE Team

- Multifunctional five manager team
- Topics
 - Total program information
 - Engineering requirements
 - Contract requirements
- Audience
 - Top management through working level
 - Engineering
 - Supportability
 - Manufacturing/Quality
 - Contracts/Sourcing
 - Etc.



Excellent Supplier Response

One Electrical Part Supplier Example

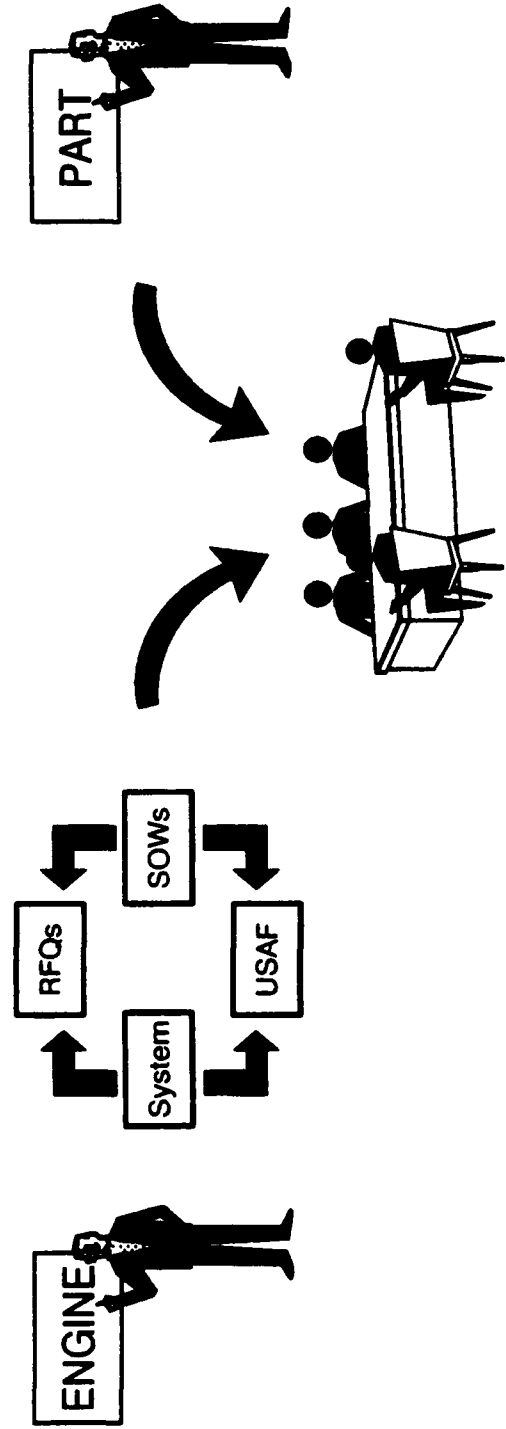


Changed Testing Philosophy

- C&A traditionally tested to “Cookbook” requirements
- New testing follows ASIP/ENSIP philosophy
 - Realistic environments
 - Realistic mission usage
 - Includes life endurance test
- Test hours increased by order of magnitude

Total Value Concept to Supplier Selection

- Suppliers are teammates
 - Input to specifications
 - Interact with GEAE Design and System Engineering
 - Interact with the USAF
- All suppliers selected by multifunction GEAE teams on TOTAL VALUE, not just price



Teaming Approach with Suppliers

- GEAE providing suppliers “tools” to succeed
 - Detailed statements of work
 - January 1990 Damage Tolerance Seminar
 - “Sample” PPSIP Plan given to suppliers
 - Sharing GEAE proprietary information (e.g., Design Practices, materials data)
- Challenging suppliers to challenge us (What do they need?)

Emphasis is on Relationships Not Transactions!

Benefits

- More discipline and organization to program
- More and better information earlier in program
 - Better program planning, managing and control
 - More understandable technical and business requirements
 - Better focus on the higher program risk areas
- More meaningful and efficient dialogue with GEAE personnel

Evidence of Success/Progress

- “Historic” supplier complaints diminished
 - Improved GEAE/Supplier technical interfacing
 - Improved GEAE/Supplier business interfacing
 - Improved internal GEAE consistency
- GEAE has more supplier data on parts/programs than ever before
- Some suppliers have changed their internal systems and procedures to incorporate new approaches
- Successful supplier involvement with USAF design reviews

Summary

- Emphasis is on unified GEAE and supplier program management for optimal system integrity
- Theme is GEAE/Supplier team designing, building quality in
- Process is early, thorough requirement definition and overall communication to build a long-term GEAE/Supplier relationship (trust)
- Process of defining supplier requirements "up front" is much harder but payoffs will continue throughout program
- The F120 customer, GEAE, supplier C&A teams are succeeding in breaking down functional barriers, changing past practice, and implementing PPSIP

**COMPONENT CLASSIFICATION
AND
THE PRODUCT INTEGRITY PROGRAMS**

HOWARD A. WOOD

UNITED STATES AIR FORCE
AERONAUTICAL SYSTEMS DIVISION
WRIGHT PATTERSON AIR FORCE BASE, OHIO

CRITPART 2 10/30/80

OUTLINE

- OVERVIEW OF PROCESS STEPS AND ACTIONS
- TERMINOLOGY
 - ITEMS
 - SIGNIFICANT ITEMS
 - FAILURE IMPACT DEFINITIONS
 - DAMAGE TOLERANCE
 - DURABILITY
 - CRITICAL ITEMS=CONTROLLED ITEMS
 - TRACKED ITEMS
- PROCESS FLOW DIAGRAMS
 - GENERALIZED PRODUCT CONTROL PLAN
 - GENERALIZED APPROACH FOR ESTABLISHING CANDIDATE CONTROLS LIST
 - APPROACH FOR ESTABLISHING CRITICAL ITEMS
- EXAMPLES - DETERMINING WHERE DAMAGE TOLERANCE APPLIES
- TERMINOLOGY DILEMMA
- SUMMARY

CONT PART 2 8/25/90

This material is presented to assist in tailoring the Product Integrity Programs to specific applications. The outline of the presentation is illustrated in this chart.

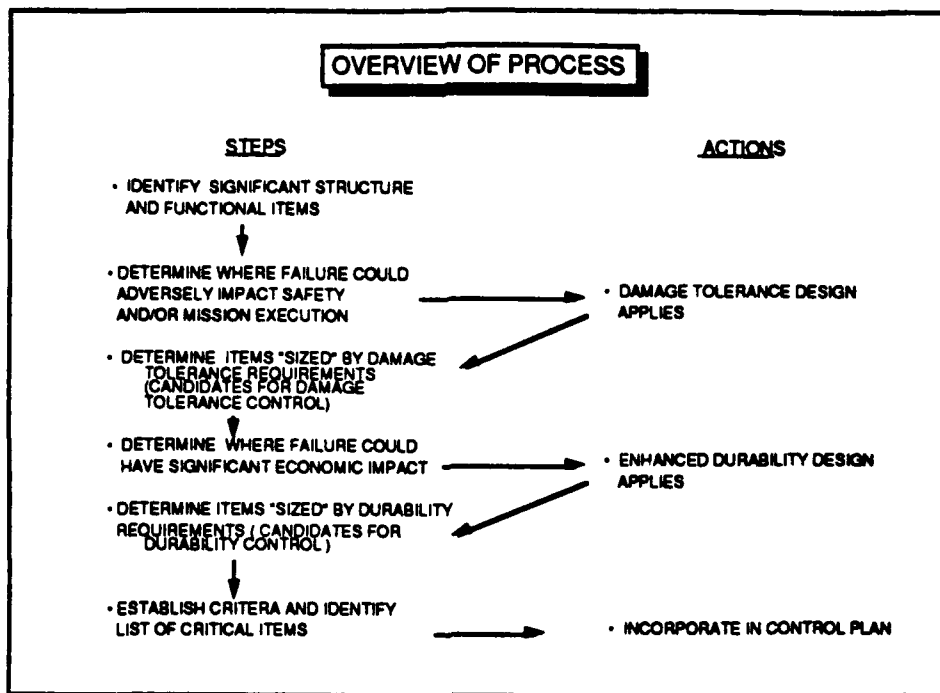
OBJECTIVE OF THIS PRESENTATION MATERIAL

- DESCRIBE THE GENERAL TECHNICAL PROCESS FOR IDENTIFYING THOSE STRUCTURE AND FUNCTIONAL ITEMS WHERE DAMAGE TOLERANCE AND ENHANCED DURABILITY DESIGN IS REQUIRED FOR PRODUCT INTEGRITY PROGRAM APPLICATIONS (e.g., ASIP, AVIP, MECSIP, ENSIP)
- DESCRIBE THE PROCESS FOR DETERMINING WHICH ITEMS ARE CANDIDATES FOR SPECIAL MANUFACTURING AND PROCESS CONTROLS
- DESCRIBE THE PROCESS FOR SELECTING THE FINAL LIST OF ITEMS TO BE CONTROLLED (e.g. CRITICAL ITEMS)
- DISCUSS TERMINOLOGY ISSUES

CRITPART 4 8/28/90

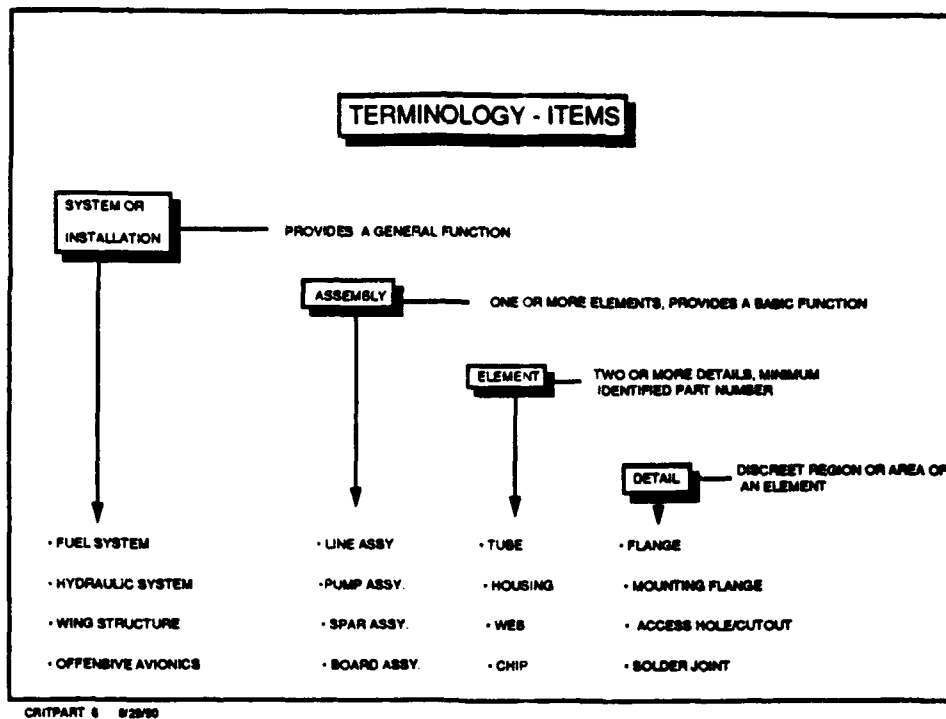
The purpose of this document is to provide guidance and further understanding of the process of identifying those *structure and functional items* where damage tolerance and enhanced durability are required for integrity program applications. A part of the process is to determine where specialized manufacturing and process controls are required to ensure that individual production items will contain the designed- in characteristics to satisfy initial integrity and performance requirements. Critical items are defined as those where specialized controls are needed. Because special controls cost more, the list of items needs to be very carefully reviewed from an economic perspective to avoid overspecification.

A second purpose is to clarify terminology used in the Product Integrity Program documents to better understand the purpose and objectives of the classification process and to propose modifications to existing documentation to be consistent.

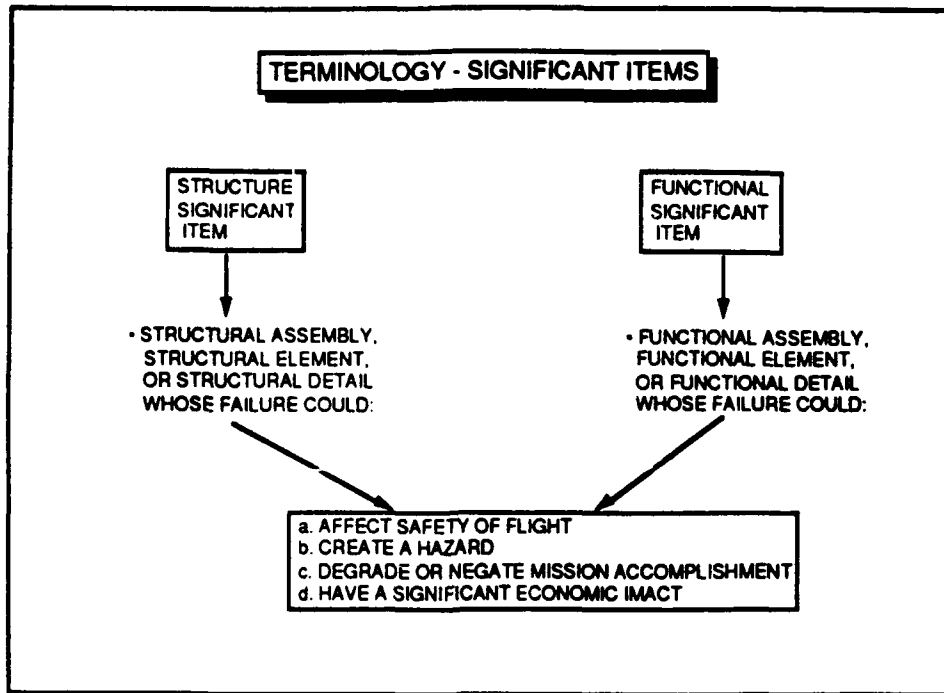


CRITPART 8 8/28/90

As an introduction to the process, the six basic steps and actions are described in this chart. This is the process in the most simple terms. The reason for classifying items is not to make extensive lists or label parts, but to facilitate the actions shown here in a consistent and intelligent manner. The process described herein has been used extensively and with success in ASIP. It is anticipated that the same approach will work with functional hardware as well. Obviously, some differences will result because of the difference in component design, materials and failure modes.



Consistent terminology is important particularly when discussing widely diverse items as structures and electronic components. This chart illustrates a terminology basis which seems logical and will be used throughout this presentation. One issue that often arises is where to begin the examination of items, as for application of damage tolerance requirements (e.g., at the system, assembly, element level). The approach works at any level as will be illustrated in subsequent examples.



CRITPART 7 8/25/90

The initial step in the process is to begin to identify significant items. For illustrative purposes structure is distinguished from functional items. This is consistent with FMECA and Reliability Centered Maintenance documentation. As is shown, the significance of the item is based on the potential impact of loss and is safety, mission and economically based. Although this terminology is presented for hardware items the approach could equally apply to individual functions as well and then to items. Later examples will illustrate where function and hardware are addressed in the same scenario.

ESTABLISHING STRUCTURE AND FUNCTIONAL SIGNIFICANT ITEMS

REVIEW:

- DESIGN INFORMATION AND DESIGN CONCEPT
 - MATERIALS
 - OPERATING STRESSES
 - TESTS AND ANALYSES
 - MAINTENANCE ANALYSES
 - ECONOMIC ASSESSMENTS
- PRIMARY FUNCTIONS
- PRINCIPAL FAILURE MODES POTENTIAL IMPACT OF LOSS OF FUNCTION OR ITEM
- SAFETY ANALYSES
- ETC.

CRITPART 8 8/28/80

This chart illustrates some data that has been used in past evaluations to *establish significant items*. Some of these data may not be available at the time of the assessment and engineering judgement and experience may be called upon. Failure modes effects analyses and safety analyses should be used if available.

TERMINOLOGY - FAILURE IMPACT DEFINITION

- **SAFETY OF FLIGHT** - FAILURE COULD RESULT IN LOSS OF THE AIR VEHICLE OR IF FAILURE REMAINED UNDETECTED COULD RESULT IN LOSS OF THE AIR VEHICLE
- **HAZARD** - FAILURE COULD RESULT IN A HAZARD TO PERSONNEL OR OTHER ITEMS OR IF FAILURE WAS UNDETECTED, COULD LEAD TO FAILURE OF ANOTHER ITEM WITH POTENTIAL SAFETY OF FLIGHT IMPACT
- **MISSION** - FAILURE COULD PROHIBIT THE EXECUTION OF A CRITICAL MISSION OR HAVE SIGNIFICANT OPERATIONAL IMPACT (eg. MISSION CAPABILITY, FLYING QUALITIES, VULNERABILITY, ETC.)
- **ECONOMIC** - FAILURE COULD RESULT IN EXCESSIVE OPERATION, MAINTENANCE OR REPAIR BURDEN OR RESULT IN COSTLY REPLACEMENT

CRITPART 9 8/28/80

Failure impact definitions are generally consistent within the various integrity programs and are shown in this chart. Some items have failure modes that could be potentially hazardous even though the loss of the primary function might be considered to be benign. Pressure vessels are good examples where a rupture could damage surrounding structure or systems or where a leak could be hazardous from a fire potential. The mission category is particularly important for functional items since there are few items that don't contribute to the system mission function. The term critical mission is intended to relate to a wartime or combat scenario. Our experience indicates that specific definitions of mission situations will need to be derived for each specific application. For example, one requirement for a strategic bomber is that it be able to respond to an alert scenario. This means any item that would reduce this capability would be a candidate for the mission category.

FAILURE MODES EFFECTS AND CRITICALITY ANALYSIS

```
graph TD; FMECA[FMECA] --> FMEA[FMEA]; FMEA --> FMECA_RESULTS[FMEA RESULTS - COMPATABLE WITH INTEGRITY PROGRAMS]; FMECA_RESULTS --> FMEA; FMEA --- Plus[+]; Plus --- CA[CA]; FMEA --- FMEA_DESCRIPTION[FAILURE MODES EFFECTS ANALYSIS - EVALUATION OF POTENTIAL FAILURE MODES AND THEIR EFFECTS<br/>• IDENTIFY ALL PROBABLE FAILURE MODES<br/>• EVALUATE EFFECT ON SYSTEM OPERATION<br/>• DETERMINE SINGLE POINT FAILURES]; CA --- CA_DESCRIPTION[CRITICALITY ANALYSIS - ESTABLISHES SEVERITY RANKING USING FAILURE RATE INFORMATION];
```

The diagram illustrates the FMECA process. It begins with a box labeled 'FMECA', which points down to a box labeled 'FMEA'. From 'FMEA', an arrow points down to a box labeled 'FMEA RESULTS - COMPATABLE WITH INTEGRITY PROGRAMS'. A feedback loop arrow points from the bottom of this box back up to the 'FMEA' box. To the right of the 'FMEA' box is a plus sign, followed by a box labeled 'CA'. To the right of the 'FMEA' box is a large bracket containing the text: 'FAILURE MODES EFFECTS ANALYSIS - EVALUATION OF POTENTIAL FAILURE MODES AND THEIR EFFECTS', followed by a bulleted list: '• IDENTIFY ALL PROBABLE FAILURE MODES', '• EVALUATE EFFECT ON SYSTEM OPERATION', and '• DETERMINE SINGLE POINT FAILURES'. To the right of the 'CA' box is another bracket containing the text: 'CRITICALITY ANALYSIS - ESTABLISHES SEVERITY RANKING USING FAILURE RATE INFORMATION'.

REF: MIL - STD - 1689

CRITPART 10 8/20/90

DURABILITY

• THE ABILITY OF AN ITEM TO RESIST DETERIORATION, WEAR, CRACKING, CORROSION, THERMAL DEGRADATION, ETC. FOR A SPECIFIED PERIOD OF SERVICE USAGE

• DURABILITY DESIGN APPLIES TO ALL ITEMS AND FUNCTIONS. ENHANCED DURABILITY (eg. AT LEAST ONE DESIGN LIFE WITHOUT SIGNIFICANT MAINTENANCE) IS REQUIRED FOR ALL SIGNIFICANT ITEMS, I.E. THOSE ITEMS AND FUNCTIONS WHOSE LOSS COULD HAVE SAFETY OF FLIGHT, HAZARD, ADVERSE MISSION EXECUTION IMPACT, AND/OR SIGNIFICANT ECONOMIC IMPACT.

CRITPART 12 8/29/90

It is necessary to discuss durability as well, since part of the process is to identify those items which will benefit from enhanced durability (eg. at least one design lifetime without the need for significant maintenance as a result of the design). Durability design is required for all items, however, trade studies may show that it is more expedient to allow periodic maintenance to be designed into the product. The phrase "as a result of the design" is often confusing particularly to traditional R&M specialists who are accustomed to specifying reliability requirements that can only be measured by field performance after the product has been produced. Under the integrity concept durability design is verified before the product is committed to full production, and an item that cannot be verified in this manner cannot proceed into production until it does. In many cases verification includes the need to conduct some maintenance tasks in service to uphold the durability characteristics designed into the product. When scheduled maintenance is part of the design criteria or when the development program results show the need to perform maintenance, this maintenance is referred to "as a result of the design".

DAMAGE TOLERANCE

• THE ABILITY OF AN ITEM TO RESIST FAILURE DUE TO THE PRESENCE OF FLAWS, CRACKS, OR OTHER DEFECTS RESULTING FROM MANUFACTURE AND/OR OPERATION FOR A SPECIFIED PERIOD OF UNREPAIRED SERVICE USAGE

• DAMAGE TOLERANCE DESIGN APPLIES TO ALL FUNCTIONS AND ITEMS WHOSE LOSS COULD AFFECT SAFETY OF FLIGHT, ADVERSELY AFFECT MISSION EXECUTION OR CREATE A HAZARD TO PERSONNEL OR SURROUNDING SYSTEMS OR EQUIPMENT

CRITPART 11 8/20/00

Since this process is initially used to identify requirements for damage tolerance, the definition and requirement are summarized in this chart. The definition is a literal translation from ASIP and the structures community but applies equally as well to functional items. The term "defects" in the broadest terms can refer to process flaws as well as product flaws. A later chart will illustrate some approaches to satisfy damage tolerance requirements for functional items

TERMINOLOGY- CRITICAL ITEMS

- **CRITICAL ITEMS ARE THOSE SIGNIFICANT ITEMS WHICH AS A RESULT OF THE DESIGN AND/ OR RESULTS OF THE DEVELOPMENT REQUIRE SPECIALIZED CONTROLS ON (a.) SPECIFIC ASPECTS SUCH AS MATERIALS, INSPECTIONS, MANUFACTURING PROCESSES, REPROCUREMENT, ETC., IN ORDER TO ENSURE THAT REQUIRED INTEGRITY CHARACTERISTICS AND MARGINS ARE ACHIEVED IN EACH ITEM DURING PRODUCTION - AND/OR (b) INSERVICE ACTIONS SUCH AS INSPECTIONS OR OTHER PREVENTIVE MAINTENANCE TASKS.**

CRITICAL ITEMS = CONTROLLED ITEMS

CONTROLS MAY BE IMPOSED FOR ECONOMIC AS WELL AS SAFETY OR MISSION IMPACT

CRITPART 13 8/29/90

The use of the term "critical" has not been used consistently within the various Product Integrity documents. For purposes of this discussion , critical items are defined in the manner shown. Critical items refer to those items which require specialized manufacturing and maybe in-service controls to assure and maintain the required level of integrity for each item produced. Controls may be imposed for economic as well as safety reasons. This terminology follows that used in ASIP. Every effort needs to be expended to keep the number of critical items to a minimum since special controls can add cost to the program. Typically, one could expect to review hundreds of significant items, a percentage of which would require damage tolerance and/or enhanced durability design and a few would end up on the critical list.

TERMINOLOGY- TRACKED ITEMS

- SOME CRITICAL ITEMS WILL REQUIRE IN -SERVICE CONTROLS eg. INSPECTIONS AND/OR OTHER PREVENTIVE MAINTENANCE ACTIONS AS "A RESULT OF THE DESIGN".
- WHEN THESE ACTIONS ARE REQUIRED TO BE IMPLEMENTED AT INTERVALS ASSOCIATED WITH TIME AND/ OR USAGE, THEN THESE ITEMS WILL REQUIRE IN -SERVICE TRACKING

SOME CRITICAL ITEMS WILL REQUIRE IN -SERVICE CONTROLS AND USAGE TRACKING OF INDIVIDUAL ITEMS MAY BE REQUIRED

NOT ALL CRITICAL ITEMS WILL REQUIRE TRACKING

CRITPART 14 8/29/90

Another term, tracking, also needs clarification. When, as a result of the design it becomes necessary to implement maintenance actions at prescribed times or intervals which are tied to actual usage, it will be necessary to track or monitor this usage on each fielded item in order to establish schedules. This is the original definition for tracking. Some items tracked may be critical items as previously defined but not all critical items will require tracking. Generally, critical items for production controls will appear in the Product Integrity Control Program (eg. Fracture control program for ASIP). Tracking requirements will appear in the Force Management plan.

CRITICAL ITEM - EXAMPLE FRACTURE CRITICAL STRUCTURE

- **GENERAL CRITERIA:**

SAFETY OF FLIGHT COMPONENTS OR REGIONS OF SAFETY
OF FLIGHT COMPONENTS WHICH ARE EITHER SIZED BY
THE (DAMAGE TOLERANCE) REQUIREMENTS OR WOULD
BE SIZEDIF CONTROLS WERE NOT IMPOSED

- **EXAMPLE - HIGH STRESSED REGION OF STRUCTURAL FORGING**

ITEM WOULD NOT MEET SLOW CRACK GROWTH DAMAGE TOLERANCE
REQUIREMENTS WITHOUT SPECIAL INSPECTIONS IN PRODUCTION TO
MEET INITIAL FLAW SIZE ASSUMPTIONS..... CONTROLS ON DRAWING AND
IN PROCESS REQUIRED

CONTROLS IMPOSED FOR SAFETY OF FLIGHT IMPACT

CNTPART 18 0/23/00

An example of a critical item is illustrated here. The controls would be incorporated into the manufacturing process to assure that specific inspections are conducted.

CRITICAL ITEM - EXAMPLE DURABILITY CRITICAL ITEM

- **GENERAL CRITERIA:**

FUNCTIONAL ITEM WHOSE LOSS WOULD HAVE SIGNIFICANT ECONOMIC IMPACT AND WHICH IS SIZED BY ENHANCED DURABILITY REQUIREMENTS OR WOULD BE SIZED ...IF SPECIALIZED CONTROLS WERE NOT IMPOSED

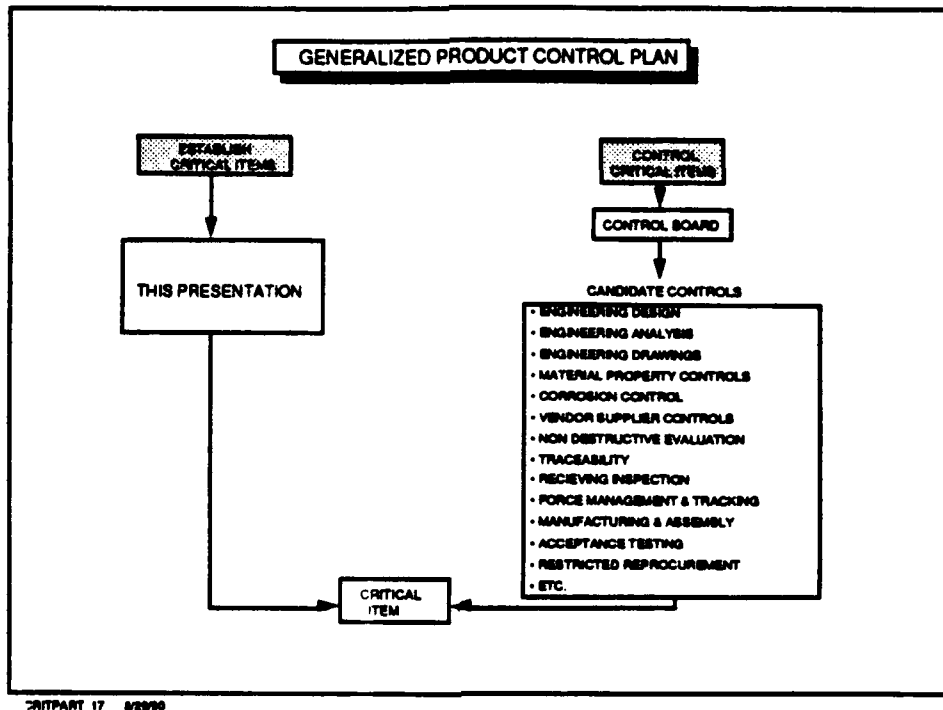
- **EXAMPLE - PUMP**

PREMATURE FAILURE WOULD RESULT IN EXPENSIVE REPLACEMENT AND/OR NEED FOR INCREASED SPARES
....DURABILITY WOULD BE DEGRADED TO AN UNACCEPTABLE LEVEL IF ORIGINAL "DESIGN BASIS" WERE COMPROMISED,
eg. THROUGH UNRESTRICTED REPROCUREMENT...ITEM COULD BE DESIGNATED AS A "DURABILITY CRITICAL ITEM" WITH REPROCUREMENT RESTRICTED TO THE ORIGINAL "QUALIFICATION BASIS"

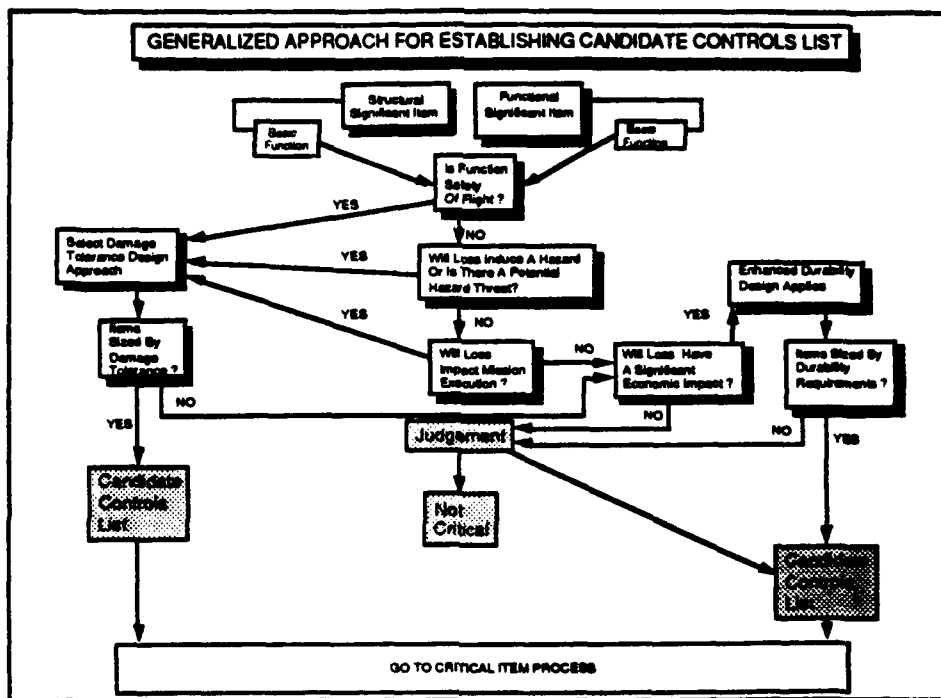
CONTROLS IMPOSED FOR ECONOMIC REASONS

CRITPART 16 8/20/00

Another example for a functional item where controls are imposed on reprocurement. In this situation the *impact of relaxing this requirement* may be economical in nature. This would make the pump a "durability critical item".

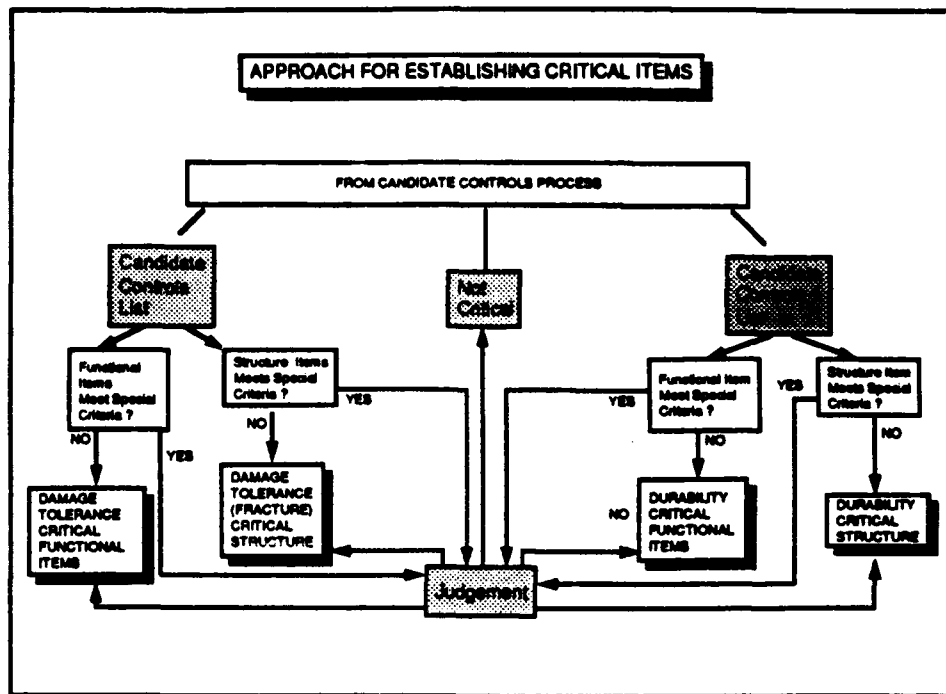


This chart depicts the relationship between selecting critical items and controlling critical items. Some candidate controls are indicated. Further discussion of Product Integrity Controls can be found in the Integrity Program documents.



CRITPART 16 8/29/93

The following two charts illustrate the complete process . This chart depicts the flow paths by which damage tolerance and enhanced durability are applied as a consequence of item or function failure, and these items become candidates for the critical control list if they are sized by the specific requirements. Being sized by the requirements implies that the essential item characteristics (eg. materials, operating stresses, etc.) are selected because of these requirements and either would not be incorporated into the item or to a lesser degree, if the requirements were not specified. It also may refer to situations where an item could be sized by these requirements if controls were not imposed on certain parameters. Both situations would automatically put an item on the candidate list. Note that a judgement box has been included to allow exceptions to remain on the candidate list. The "not critical" category implies that items are clearly not sized by the requirements and/or special controls clearly are not warranted. The process objective is to keep an item as a candidate until all reason not to keep it on has been explored. In other words, an item is kept on the list until it can be justified to not be critical. To be put on the candidate list, an item must go through the entire process. In other words, items cannot be added solely on a judgement basis.



CRTPART 19 8/28/90

The second flow chart depicts the process to arrive at the final list of critical items. Note that there is one step in the path to allow a candidate to be removed and this is if the design satisfies additional criteria developed for the specific product in advance. For structure items, a relatively high margin may be sufficient to allow an item to be removed from the candidate list. These two flow charts have an implied time line associated with them. The special criteria may not have been able to be satisfied at the decision time when candidates were selected. Again, a judgement option is kept to allow exceptions to remain as critical items. These lists usually are kept active during the item development, and items may come and go.

.....MEETS SPECIAL CRITERIA ?

- **DECISION OPTION USED TO DELETE ITEMS FROM CRITICAL LIST**
- **SPECIFIC CRITERIA ESTABLISHED (eg. DAMAGE TOLERANCE MARGIN)**

CRITPART 20 8/29/90

This chart reiterates the special category to allow items to be removed from the critical list.

DAMAGE TOLERANCE SOME EXAMPLES - APPLICATION

• REQUIREMENT

DAMAGE TOLERANCE DESIGN APPLIES TO ALL FUNCTIONS AND ITEMS WHOSE LOSS COULD AFFECT SAFETY OF FLIGHT, ADVERSELY AFFECT MISSION EXECUTION OR CREATE A HAZARD TO PERSONNEL OR SURROUNDING SYSTEMS OR EQUIPMENT

• SOME APPROACHES

- CONTROLLED FLAW GROWTH**
 - SLOW GROWTH**
 - LEAK BEFORE BURST**
 - NO GROWTH**
- REDUNDANCY - FAIL OPERABLE ,FAIL SAFE**
- ROBUST DESIGN**
- READILY DETECTABLE / GRADUAL DEGRADATION WITH MINIMAL LOSS OF FUNCTION**

CRITPART 21 8/20/98

Some examples follow which illustrate how an item and /or function would be evaluated for applicability of damage tolerance design requirements. First, some approaches to damage tolerance design will be discussed. The controlled growth approach follows that used for structures and ensures that initial flaws will not grow to a critical or limiting size within a prescribed service usage period. Several sub-categories fall under this approach. The leak-before -burst category applies to pressure vessels and is imposed to assure that detectable leakage precedes catastrophic loss of the item or function. Redundancy is a common approach for functional systems. This approach implies that the design concept will fail safely and operably , and in some cases with the stipulation that the loss be readily detectable. If loss of a redundant path would not impact safety even if ignored for the life of the system, then it is clearly not safety of flight. On the other hand, a fail safe structure might fail to some safe level of strength but could not operate without imposing stress on adjacent members, the situation would be safety of flight. Robust design refers to an item with extremely low probability of failure. This is usually used as a fall back option with the concurrence of the Air Force. The final approach could be used for components like bearings, where significant degradation can be detected through oil analyses and chip detectors.

EXAMPLE - FUNCTIONAL SIGNIFICANT COMPONENT

ITEM	FUNCTION	LOSS OF FUNCTION	DESIGN APPLICATION
Fuel Line Assembly	Supply Fuel To Engine	Reduced Thrust; Loss Of Thrust; Potential Safety Of Flight; Loss Of Mission Effectiveness	Dual Engine Application ; Single Line To Each Engine
FINAL EVALUATION; LOSS OF FUNCTION PROVIDED BY ITEM		DAMAGE TOLERANCE APPLIES TO ITEM ?	
Loss Of Thrust One engine; Reduced System Thrust; Mission Impact		Yes	

CRITPART 22 9/29/90

The first example considers a fuel line assembly whose principal function is to deliver fuel to the engine. The potential effects of losing a fuel line could be one or all four of the effects shown. The final result depends on the application, and for this example a dual engine application is assumed with a single line assembly to each engine. Loss of the line function, then, would result in the loss of one engine, reduced thrust for the system, and at the minimum, an impact on the mission capability. Accordingly, damage tolerance applies to this item.

EXAMPLE - FUNCTIONAL SIGNIFICANT COMPONENT

ITEM	FUNCTION	LOSS OF FUNCTION	DESIGN APPLICATION
Fuel Line Assembly	Supply Fuel To Engine	Reduced Thrust Loss Of Thrust; Potential Safety Of Flight; Loss Of Mission Effectiveness	Single Line, Single Engine Application

**FINAL EVALUATION;
LOSS OF FUNCTION
PROVIDED BY ITEM**

**DAMAGE
TOLERANCE
APPLIES TO ITEM?**

Loss Of Thrust One Engine;
Loss Of Thrust For System;
Safety Of Flight

Yes

CRITPART 23 8/28/90

In this case, the same item is considered but the application is now a single engine with single fuel line. Based on this application, the loss of function would result in loss of engine and a safety of flight situation. Therefore, damage tolerance applies.

EXAMPLE - FUNCTIONAL SIGNIFICANT COMPONENT

ITEM	FUNCTION	LOSS OF FUNCTION	DESIGN APPLICATION
Hydraulic Pump Assembly	System Pressure To Flight Control Surface	Reduced Power, Loss Of Power To Air Vehicle Systems; Potential Safety Of Flight; Loss Of Mission Effectiveness	Single Pump, Single System
FINAL EVALUATION; LOSS OF FUNCTION PROVIDED BY ITEM		DAMAGE TOLERANCE APPLIES TO ITEM ?	
Loss Of Power; Safety Of Flight,		Yes	

CRITPART 24 8/28/90

Another example considers a hydraulic pump assembly with the primary function of supplying power to a flight control surface. The potential consequences of loss of this function are listed. The design application is considered to be a single line element with the resultant loss being safety of flight. Damage tolerance would apply to the item.

EXAMPLE - FUNCTIONAL SIGNIFICANT COMPONENT

ITEM	FUNCTION	LOSS OF FUNCTION	DESIGN APPLICATION
Hydraulic Pump Assembly	System Pressure To Flight Control Surface	Reduced Power, Loss Of Power Potential Safety Of Flight; Loss Of Mission Effectiveness	Multiple Systems (Multiple Pumps); Redundant System to Control Surface

**FINAL EVALUATION;
LOSS OF FUNCTION
PROVIDED BY ITEM**

**DAMAGE
TOLERANCE
APPLIES TO ITEM ?**

Loss of One Pump, Loss Of One System; Function Retained In Remaining System(s); No Loss Of Power; Not Safety Of Flight; Not Mission Essential

No, Damage Tolerance Satisfied At System Level

CWTPART 25 2/25/90

Same item with a different design application. In this case the system has redundant lines and are fully independent from a functional perspective. If it is assumed that full function can be maintained even with the loss of the pump, then the item is not safety of flight and is not critical to mission execution, and therefore, damage tolerance would not apply to the item. The intent is satisfied at the system level via redundancy. In this example, the redundancy is assumed to be fully independent, in that the system could tolerate the loss for the service life without impact. If this were not the case, each leg of the redundant path would have to meet damage tolerance requirements to assure the remaining functional system could operate safely until detected and repaired.

EXAMPLE - PRIMARY STRUCTURE

ITEM	FUNCTION	LOSS OF FUNCTION	DESIGN APPLICATION
Fuselage Bulkhead	Distribute Wing Loads To Fuselage	No Or Reduced Load Capability; Potential Loss Of Wing; Potential Safety Of Flight; Potential Mission Essential	Multiple Bulkhead Arrangement
FINAL EVALUATION; LOSS OF FUNCTION PROVIDED BY ITEM		DAMAGE TOLERANCE APPLIES TO ITEM ?	
Some Reduction In Overall Load Capability; Increased Stress In Remaining Bulkheads; Loss ,If Not Detected, Would Lead to Eventual Loss Of Remaining Bulkheads; Safety Of Flight; If Detected, Would Curtail Mission		Yes	

CRITPART 26 8/25/90

This example is the classical example of fail safe structure. In this case the structure is safe with a failed bulkhead but the remaining structure has reduced capability and must meet residual strength and remaining life requirements. Since the item is one of several elements it must also satisfy damage tolerance requirements associated with remaining structure.

TERMINOLOGY "DILEMMA"			
* SAFETY OF FLIGHT EXAMPLE ONLY; MISSION IMPACT IS THE SAME; AYP TERMINOLOGY SAME AS MECSIP			
ITEM	ASIP	ENSIP	MECSIP
<ul style="list-style-type: none"> COMPONENTS WHOSE LOSS WOULD PRECIPITATE A SAFETY OF FLIGHT SITUATION PROCESS USED TO IDENTIFY THESE COMPONENTS DESIGNATED COMPONENTS REQUIRING SPECIALIZED CONTROLS IN ORDER TO SATISFY DAMAGE TOLERANCE REQUIREMENTS HOW IDENTIFIED EXTENT OF COMPONENTS WHICH ARE CONTROLLED OTHER COMPONENTS THAT ARE DEFINED AND CONTROLLED IN THE SAME WAY 	<ul style="list-style-type: none"> ALL SAFETY OF FLIGHT STRUCTURE FMECA OR SIMILAR ENGINEERING ANALYSIS FRACTURE CRITICAL PARTS SPECIAL CRITERIA FOR APPLICATION ONLY THOSE WHERE CONTROLS ARE REQUIRED TO MEET DAMAGE TOLERANCE REQUIREMENTS; NOT ALL SAFETY OF FLIGHT STRUCTURE IS FRACTURE CRITICAL. CONTROL PLAN DOES NOT IDENTIFY ALL SAFETY OF FLIGHT COMPONENTS DURABILITY CRITICAL COMPONENTS WHERE CONTROLS ARE REQD TO SATISFY DURABILITY REQUIREMENTS 	<ul style="list-style-type: none"> FRACTURE CRITICAL COMPONENTS FMECA OR SIMILAR ENGINEERING ANALYSIS THOSE FRACTURE CRITICAL COMPONENTS LISTED IN THE DAMAGE TOLERANCE CONTROL PLAN SPECIAL CRITERIA FOR APPLICATION THE DAMAGE TOLERANCE CONTROL PLAN WILL LIST ALL FRACTURE CRITICAL COMPONENTS. SPECIAL CONTROLS RELATE TO A PORTION OF THESE COMPONENTS. THE PLAN WILL DIFFERENTIATE BETWEEN NORMAL AND SPECIAL CONTROLS SAME AS ABOVE FOR DURABILITY CRITICAL COMPONENTS 	<ul style="list-style-type: none"> SAFETY CRITICAL COMPONENTS FMECA OR SIMILAR ENGINEERING ANALYSIS THOSE SAFETY CRITICAL COMPONENTS IDENTIFIED IN THE PRODUCT INTEGRITY CONTROL PLAN SPECIAL CRITERIA FOR APPLICATION SIMILAR TO ENSIP: THE PLAN MAY LIST ALL SAFETY CRITICAL COMPONENTS, HOWEVER THE SPECIAL CONTROLS LIST WILL INCLUDE ONLY A PORTION OF THESE SAME AS ABOVE FOR MISSION CRITICAL AND DURABILITY CRITICAL COMPONENTS

CRITPART 27 82290

This table compares current terminology from ASIP, ENSIP, and MECSIP to illustrate differences in terminology. The most significant difference is the use of the term "critical". There is a need to rectify the situation in Product Integrity document updates.

SUMMARY

- GENERAL PROCESS FOR IDENTIFYING CANDIDATE AND CRITICAL ITEMS IS APPLICABLE TO ALL PRODUCT INTEGRITY PROGRAMS
- PROCESS APPROACH IS TO ESTABLISH LIST OF CANDIDATE CRITICAL ITEMS; ITEMS WHICH MEET SPECIFIC CRITERIA MAY BE REMOVED FROM LIST; FOR ITEMS TO BE PLACED ON LIST, THE PROCESS MUST BE REPEATED
- CRITERIA TO REMOVE AN ITEM FROM CRITICAL LIST WILL VARY WITH PRODUCT TYPE AND APPLICATION AND WILL NEED TO BE DERIVED FOR THAT APPLICATION
- DETERMINATION OF THE APPLICABILITY OF DAMAGE TOLERANCE REQUIREMENTS FOR A SPECIFIC ITEM CAN BE MADE AT ANY LEVEL (eg. ELEMENT, ASSEMBLY SYSTEM OR INSTALLATION)
- USE OF THE TERM "CRITICAL" NOT CONSISTENT IN CURRENT INTEGRITY PROGRAM DOCUMENTATION; HAS CAUSED SOME CONFUSION; DOCUMENTATION CHANGES RECOMMENDED TO BE CONSISTENT WITH ASIP TERMINOLOGY
- CLARIFICATION OF SOME TERMINOLOGY HAS BEEN INCLUDED IN THIS DOCUMENT

CNTPART 25 8/29/96

In summary, this presentation has described the process used to address significant functional and structure items under the Product Integrity Programs. (e.g., ASIP, AVIP, MECSIP, ENSIP). The presumption is that inconsistent terminology can and has led to confusion and misinterpretation of the integrity process requirements. Since the baseline for comparison has been ASIP, this presentation has described the process in ASIP terms as much as possible. A major concern has been for the use and meaning of the term "critical". It appears that the difference is significant enough to warrant revisions to current Integrity Program documentation.

**AN ENGINEERING PROCEDURE TO SELECT AND PRIORITIZE COMPONENT
EVALUATION UNDER USAF STRUCTURAL INTEGRITY REQUIREMENTS**

Presented to:

1990 USAF STRUCTURAL INTEGRITY PROGRAM CONFERENCE

**11-13 December 1990
San Antonio, Texas**

Craig L. Brooks

MC 0341160

**McDonnell Aircraft Company
McDonnell Douglas Corporation
P.O. Box 516
St. Louis, Missouri 63166**

(314) 232-9391

**AN ENGINEERING PROCEDURE TO SELECT AND PRIORITIZE COMPONENT
EVALUATION UNDER USAF STRUCTURAL INTEGRITY REQUIREMENTS**

Craig L. Brooks

**McDonnell Aircraft Company
McDonnell Douglas Corporation
St. Louis, Missouri**

(314) 232-9391

I. Introduction

The Structural Integrity process established by the United States Air Force is an organized and disciplined approach to ensure that each USAF system meets certain structural performance requirements. To simplify the structural integrity process each major system is evaluated separately. Each system evaluation is conducted through a process referred to as a Structural Integrity Program. The intention of this paper is to propose a procedure to address the initial phase in the implementation of a Structural Integrity Program.

The proposed procedure provides a systematic and logical approach for identifying candidate items in a structure or system for specific test, analytical evaluation, or special controls. Specific numerical ranking values are determined for the many durability and damage tolerance aspects of component integrity which allows the analyst to categorize the component's criticality and prioritize subsequent component evaluation. This procedure has been developed for airframe structures to compliment ASIP, and can be readily tailored for application to ENSIP, MECSIP, AVIP, and other integrity programs. The implementation of this procedure as a structural integrity tool will simplify the process of ensuring systems meet USAF requirements.

To illustrate the concept, the details of the procedure as applied to our military fighters was originally intended to be the focus of this paper. However, due to the open nature of this forum a less sensitive airframe was chosen to serve as an example of this procedure, namely, a small high wing turboprop transport.

II. Generation of Significant Items List

The development of a USAF structural integrity program requires a process to identify structural and functional items that may be durability and/or damage tolerance critical. This process starts with the generation of a Significant Items List. Items can be defined as subsystems, assemblies, or regions of structure, as well as elements and details. Compilation of the Significant Items List is best conducted by experienced stress and fracture engineers, with support from design, reliability, NDE, maintenance, and safety engineers.

To begin the selection process, a basic structural review is conducted to select items based upon previous aircraft experience, test experience, design concept, primary functions, and principal failure modes. In addition, items are selected from all major load paths, control surfaces and their attach areas, major splices, complex load paths, access areas, and to represent particular areas or assemblies. The items selected encompass the entire structure and systems.

The structural configuration of the transport aircraft used to demonstrate this procedure was of conventional sheet and stringer construction. The pressurized fuselage and wet wing are primarily constructed of aluminum alloys. The Significant Items List used on this structure contained over one hundred items.

III. Categories for Evaluation

All the items on the Significant Items List are evaluated by the use of a "Category Ranking Guideline". The Category Ranking Guideline is a ranking system that relates significant damage tolerance and durability "categories" to numerical values. The value or maximum rank for each category is weighted relative to the other categories based upon relative level of importance. The summation of the maximum ranks for all categories is 100. Each category is divided into subsets that provide a measure of severity of that particular category to a condition that could exist in the structure or subsystem. Specific values are assigned to each subset in terms of relative severity up to the maximum allocated for the particular category. The analyst is thus able to select the subset from the Category Ranking Guideline sheet that best describes the item being evaluated, and subsequently determine an appropriate numerical value.

In addition to determining the subsets within the category, brief narratives are used with the Category Ranking Guideline to explain the rationale used to develop the ranking. Appendices to the narratives can provide further explanations, technical details, discussions of phenomena, and results of studies used in determining the categories, subsets, and relative ranking. These narratives enhance the analyst's understanding of the ratings and the important aspects of structural integrity.

Nine categories for the small transport aircraft structure are shown with their maximum category ranking in Figure III-1. For the airframe described in this procedure the system results in the accumulation of ratings ranging from a minimum of 8 to a maximum of 100, with 100 representing the maximum possible severity for a item. The Category Ranking Guidelines for each category are described in Figure III-2 through III-10.

IV. Ranking of Significant Items List

To rank each item, the analyst begins by gathering available drawings, material lists, assembly layouts, static stress analysis, and general structural descriptions. Access to a typical structure for physical examination is a significant advantage in this evaluation process.

The analyst then evaluates each candidate item on the Significant Items List. A standardized form is used to provide documentation for each item. On this form brief statements are made as to the justification of the selection, the primary function, a description of the environment, the material used, and a description of the accessibility of the area. The second half of the form contains the worksheet for the ranking to be conducted. The analyst, using the Category Ranking Guidelines, works through each of the categories selecting the subset and ranking score that is applicable. Comments and the selected ranking are then duly recorded, and sketches are assembled for a visual description of the geometry and region being addressed.

A preproduction airframe of the small transport aircraft was available for inspection. An example of the form and the results of the evaluation for a single item from that aircraft is shown in Figure IV-1 and IV-2.

V. Listing, Ranking, and Prioritization

After ranking the significant items, a listing and grouping of the ranking scores is used to prioritize the items. These groupings can be assembled on the total of all categories, on various combinations of categories, or on an individual category. For example, overall priorities can be used to select critical and non-critical items and to establish the order of further evaluations. Low scores indicate the items that are non-critical, and high scores indicate the items that are critical and will require special provisions.

Figure V-1 presents the distribution of the Total Ranking Scores for each of the significant items in the example airframe. A review of the prioritization based upon aircraft structure, as shown on Figure V-2, shows potential "hot spots" or areas of concern. A grouping of the ranking scores obtained by combining

only the 1G stress, the residual strength, and fail-safe aspects is used for determining the priority order of crack growth analysis. To determine how well the ranking of these three categories acted as an indicator of damage tolerance, analyses were conducted at the three mean ranked items. All three analyses showed significant damage tolerance life. As a result, detailed crack growth analyses were conducted on the higher ranked items, thus eliminating detailed crack growth analyses on the less critical items. For another example, the grouping of the two corrosion categories ranking scores can be used to determine areas that might require periodic maintenance. The ranking score of an individual category is also an important indicator. For example, the information and results of the fail safe ranking are direct indicators of safety-of-flight items.

The listing, ranking, and prioritization of items provides a group of useful tools that are beneficial to many disciplines of engineering. The selection and prioritization procedure helps to systematically evaluate the items from this list to determine what analyses, controls, criticality classification, and actions are required for each item. This procedure thus assures that critical areas will not be overlooked and eliminates unnecessary work on relatively non-critical locations.

VI. Summary

This procedure has been successfully applied by MCAIR to a fighter/attack aircraft and a small transport aircraft. For the fighter aircraft, the Category Ranking Guidelines were modified to account for high load factor, results of full scale fatigue tests, and field experience.

By tailoring the "categories", their subsets, and the relative "ranking", this procedure could become a important integrity tool in component selection for application in ENSIP, MECSIP, AVIP, and other integrity programs. The application of this procedure provides many benefits as a structural integrity tool by addressing many of the durability and damage tolerance integrity drivers. The procedure compliments the structural integrity process through a systematic approach to the selection of principal structural components. The selection, ranking, and prioritization process provide valuable information and documentation in support of component classification, subsequent detailed analyses, and potential controls to ensure structural adequacy of critical components.

This procedure could be considered a part of the USAF Structural Integrity Requirements so as to ensure systems meet USAF expectations.

EXPORT AUTHORITY: 22 CFR 125.4 (b) (13)

FIGURE III-1

THE NINE CATEGORIES FOR DURABILITY AND DAMAGE TOLERANCE RANKING

	CATEGORY	RANKING		
		<u>Minimum</u>	to	<u>Maximum</u>
1	1G OPERATIONAL STRESS LEVEL	1	to	20
2	LIMIT STRENGTH AND RESIDUAL STRENGTH	1	to	15
3	FAIL SAFE ASPECTS OF THE STRUCTURE	1	to	15
4	LOAD DISTRIBUTION CHARACTERISTICS	1	to	10
5	SUSCEPTIBILITY TO SUSTAINED STRESS CORROSION CRACKING	0	to	5
6	SUSCEPTIBILITY TO CORROSION	1	to	10
7	STRESS RISER DUE TO GEOMETRY (Kt)	1	to	8
8	SUSCEPTIBILITY TO ACCIDENTAL DAMAGE	1	to	5
9	INSPECTABILITY	1	to	12
TOTAL		8	to	100

FIGURE III-2

CATEGORY RANKING GUIDELINE 1: 1G OPERATIONAL STRESS CONDITION

One of the more important drivers in a structural assessment is the operational stress state. The 1G stress condition is considered to be the typical stress state for a transport aircraft. The number and magnitudes of stress excursions about this condition determine the fatigue capability of the structure. To establish the subsets and their relative ranking for this category, preliminary sensitivity crack growth analyses were conducted using generic spectra for this transport aircraft representing major structural assemblies. These approximations for maneuver load factors, pressurizations, and gust responses provided relative stress severities required to produce equivalent damage for correlation between the assemblies. As a result the subsets for selection are based on the major structural location of the item. The ranking to be selected is to be based on the maximum 1G operational stress of the structure in the area of the item being evaluated.

Subset	Major Structural Assembly Descriptions		Ranking
a	Wing Structure; Wing-Engine and Wing-Fuselage attach Structure	For 1G $\sigma > 9$ ksi	17 to 20
		6 < 1G $\sigma < 9$ ksi	15 to 17
	Stress Level Guidelines for Aluminum Structure	For 1G $\sigma < 6$ ksi	< 15
a*	For other metals; adjust scale by the ratio of yield strength; $\sigma_{\text{alloy}}/\sigma_{\text{aluminum}}$		
b	Fuselage Structure; and Horizontal Stabilizer Structure	For 1G $\sigma > 7.5$ ksi	> 13
		6 < 1G $\sigma < 7.5$ ksi	11 to 13
	Stress Level Guidelines for Aluminum Structure	3 < 1G $\sigma < 6$ ksi	8 to 11
b*	Reference a* above	For 1G $\sigma < 3$ ksi	< 8
c	Systems or Components, such as Hydraulic Systems that operate near limit load for each load excursion.		15
d	Vertical Tail Structure; Control Surfaces; Elevators; Flaps; etc., and their attachments		4 to 8
e	Indirect structural elements and structure not directly responsive to the normal operational flight spectra (e.g. low # of applied cycles)		1 to 4

FIGURE III-3

CATEGORY RANKING GUIDELINE 2: LIMIT STRENGTH AND RESIDUAL STRENGTH

The maximum amount of crack growth damage allowed for a damage tolerant structure is limited by residual strength criteria. The uncracked adjacent structure must have adequate residual strength to sustain the redistributed loads at limit load conditions without loss of performance, loss of stiffness, excessive permanent deformation, loss of control, etc. This category uses static margins-of-safety of the primary structure and of the adjacent secondary structure as indicators of the residual strength. Static margins alone are not adequate, therefore the amount of material available to carry the redistributed loads after the primary load path failure is important. In addition, potential benefits due to crack arrest features should also be included in the evaluation. The definitions and methods of determining low M.S., high M.S., relatively less significant material, and crack arrest features could be given in an Appendix.

Subset	Primary Structure	Adjacent Material and Secondary Structure	Arrest Feature	Ranking
a	Low M.S.	Low M.S. with relatively LESS significant material	NO YES	15 14
b	Low M.S.	High M.S. with relatively LESS significant material	NO YES	13 12
c	High M.S.	Low M.S. with relatively LESS significant material	NO YES	11 10
d	Low M.S.	Low M.S. with relatively Significant material	NO YES	9 8
e	Low M.S.	High M.S. with relatively Significant material	NO YES	7 6
f	High M.S.	High M.S. with relatively LESS significant material	NO YES	5 4
g	High M.S.	Low M.S. with relatively Significant material	NO YES	3 2
h	High M.S.	High M.S. with relatively Significant material	NO YES	1 1

FIGURE III-4

CATEGORY RANKING GUIDELINE 3: FAIL SAFE ASPECTS OF THE STRUCTURE

The Fail Safe aspects of a damaged structural element are intended to ensure that the remaining structure can withstand reasonable loads without failure until damage is detected. This category weights each item according to the anticipated level of evident pre-catastrophic damage and the consequence of failure. The intention is to rank the items based on the criticality and physical chance of avoiding impending failure through early detection. The subsets are determined in accordance with the crew ability to address impending failure or from routine ground inspections.

Subset	Description of Failure Indications	Ranking
a	Damage can only be detected by a scheduled inspection. An in-flight failure would result in the loss of the aircraft WITHOUT warning and/or emergency procedures.	15
b	Damage can only be detected by a scheduled inspection. An in-flight failure WOULD allow the crew to implement immediate emergency landing procedures.	13 to 14
c	Damage can be readily detected by a scheduled inspection. Pre-catastrophic damage would be in-flight evident to crew, thus enabling a safe scheduled landing.	11 to 12
d	Damage would be evident without a scheduled inspection. Pre- or post-flight inspections would indicate incipient damage. Adequate residual strength available to complete a flight prior to catastrophic failure.	6 to 10
e	Damage is obvious to ground crew or flight crew, and inspections are readily performed. Multiple flight capability is available prior to catastrophic failure.	1 to 5

FIGURE III-5

CATEGORY RANKING GUIDELINE 4: LOAD DISTRIBUTION CHARACTERISTICS

A structure with good load path distribution characteristics has the capability to transmit the load that it is carrying to adjacent structural members without generating severe stress states. Global and local design configuration of load path confluences and splices are used for the subsets and ranking of the items for load path distribution characteristics.

Subset	Type of Load Path	Ranking
a	MAJOR LOAD PATH CONFLUENCES <ul style="list-style-type: none"> o Lugs and Primary Fittings o Stringer Runouts with Complex paths o Abrupt area differences in a major load path and/or abrupt changes in direction 	8 to 10
b	SPLICES AND LOAD PATH'S with COMPLEX DISCONTINUITIES <ul style="list-style-type: none"> o Splices where local bending moments are induced through eccentricities o Load paths involving high bearing loads o Complex load path designs; stringer runouts, load transfer thru tension bolts o Limited fasteners available for load transfer, single shear joints 	4 to 8
c	LOAD PATH with MODERATE DISCONTINUITIES <ul style="list-style-type: none"> o Double shear joints o Reinforced splices o Reinforced cutouts 	1 to 4

FIGURE III-6

CATEGORY RANKING GUIDELINE 5: SUSCEPTIBILITY TO SUSTAINED STRESS CORROSION CRACKING

Sustained Stress Corrosion Cracking (SSCC) may be defined as spontaneous cracking resulting from the combined action of corrosion and sustained tension stresses. The subsets used for ranking consider the material's susceptibility to sustained stress corrosion and the potential for a sustained stress condition being induced as a result of the item's geometry and assembly. The material resistance ratings are based on MIL-HDBK-5D ratings. This time dependent and sustained stress dependent phenomena could be further discussed in an appendix along with examples of geometries and sources of induced sustained stress states.

Subset	Material Resistance	Stress State	Ranking
a	Low Resistance to SSCC	Item subject to Process or Assembly Built-in stress or Residual Tension stress	5
b	Low Resistance to SSCC	No Significant Induced Tension Stress	4
c	Intermediate Resistance to SSCC	Item subject to Process or Assembly Built-in stress or Residual Tension stress	3
d	Intermediate Resistance to SSCC	No Significant Induced Tension Stress	2
e	High Resistance to SSCC	Item subject to Process or Assembly Built-in stress or Residual Tension stress	1
f	High Resistance to SSCC	No Significant Induced Tension Stress	0

A Reference List for Material Resistance Rating can be provided to the analyst to expedite the ranking process.

CATEGORY RANKING GUIDELINE 6: SUSCEPTIBILITY TO CORROSION

Maintenance Rating

A: Low probability of maintenance/observation
B: Possibly maintained and/or observed
C: Frequently cleaned and readily observed

Environmental Subset		Environmental & Maintenance Rating		
		A	B	C
a _e	Single Load Path Element; or Corrosion problem area based on experience	5	4	3
b _e	Elements exposed to exhaust gases, excess temperature, heavy salt exposure, sump tank water, anaerobic degradation (e.g.; cargo spillage, tracked in dirt)	4	3	2
c _e	Elements exposed to climatic conditions (e.g.; rain, smog, humidity, condensates)	3	2	1
d _e	Elements contained in closed dry areas, and not exposed to contaminants	2	1	0

Protection Applied to Material		Protection Rating
a _p	Bare Metal	5
b _p	Alodine, Cadmium Plate, or Epoxy Primer only	4
c _p	Chromic Anodizing, or Alclad without chem-mill	3
d _p	Chromic Anodizing plus Polyurethane Fuel Coating	2
e _p	Sulfuric Acid Anodizing	1

86

FIGURE III-8

CATEGORY RANKING GUIDELINE 7: STRESS RISERS DUE TO GEOMETRY (K_T)

Stress risers are irregularities such as holes, screw threads, notches, and shoulders. When present in a beam, shaft, or other member, these irregularities under load produce high localized stresses, referred to as geometrical stress concentrations (K_t 's). The local K_t is particularly important with respect to fatigue crack initiation and thus, at the surface, influential to crack growth. The subsets are grouped by relative severity and the subsequent ranking is proportional to the stress concentration factor.

Subset	Geometric Stress Concentration	Ranking
a	HIGH TENSION K_T 's in descending order <ul style="list-style-type: none"> o Rectangular cut-outs in uniaxial tension o Triangular cut-outs in uniaxial tension o Elliptical cut-outs with major axis perpendicular to the load path o Circular cut-outs in a pressurized shell o Circular/Elliptical holes influenced by other geometric effects (short e/D, etc.) o Diamond fastener hole patterns o Knife Edges (i.e., counter sinks > 70%t) 	8 to 6
b	ADDITIONAL TENSION and BIAxIAL TENSION K_T 'S <ul style="list-style-type: none"> o Fastener holes with thru and bearing o Circular holes in wide sections o Fastener holes with thru only o Reinforced holes and cut-outs o Circular/Elliptical holes influenced by tension-tension loads o Tension bolts 	6 to 5
c	MILD STRESS CONCENTRATIONS <ul style="list-style-type: none"> o Stepped members with shoulder fillets o Reinforced circular holes in biaxial tension-tension loads o Chem-mill fillets o Base radii of U-members 	4 to 2
d	NON-APPRECIABLE K_T <ul style="list-style-type: none"> o Holes or cut-outs in shear loading o Smooth members 	2 1

FIGURE III-9

CATEGORY RANKING GUIDELINE 8: SUSCEPTIBILITY TO ACCIDENTAL DAMAGE

Accidental damage is the physical deterioration of an element caused by contact or impact with an object, or influence which is not part of the aircraft, or through improper manufacturing or maintenance practices. Accidental damage is to include discrete source damage to the item. The subsets for ranking are based on the location, the potential of detection, and load path redundancy.

Damage sources to be considered:

- o Contact with ground or cargo handling equipment
- o Impact of rain, hail, birds, or airborne foreign objects
- o Runway debris or thrown tire treads
- o Improper maintenance or operating procedures
- o Spillage of caustics, acid, or other detrimental chemicals
- o Propeller tip or cast off materials (e.g., ice)

Examples of high probability areas are:

- o Entrance and loading doors
- o Wing and tail leading and trailing edges
- o Frequent maintenance areas and access areas
- o Joints requiring shimming to achieve correct fit
- o Fuselage areas in the vicinity of the propellers
- o Landing gear bays and adjacent structure

Subset	Probability of Damage and Detection	Ranking
a	High probability of damage occurring, generally without timely detection or maintenance; also include structure with low residual strength	5
b	Low probability of damage occurring, generally without timely detection or maintenance; also include structure with low residual strength	4
c	High probability of damage occurring, but area is frequently maintained or inspected with good visibility; also include structure with high residual strength	3
d	Low probability of damage occurring, area is frequently maintained and inspected with good visibility; also include structure with high residual strength	2
e	Negligible probability of accidental damage	1

FIGURE III-10

CATEGORY RANKING GUIDELINE 9: INSPECTABILITY

Detection of damage before it becomes critical is a significant control feature to ensure the damage tolerance characteristics of a structure. The level of difficulty to detect the damage is used for ranking the inspectability aspects of an item. To assess the level of difficulty, a preliminary estimate is required as to the crack definition and of the inspection reliability.

Crack Definition:

- o Crack location/s
- o Probable Initiation site
- o Crack orientation
- o Structural configuration
- o Accessibility

Inspection Reliability:

- o Required Equipment
- o Size of inspection task
- o Technical complexity
- o Extent of damage to be detected

Subset	Inspection Type	Ranking
a	SPECIAL DETAIL INSPECTION: An intensive check of a specific location, detail, assembly, or installation. This check requires some special technique, such as NDE, dye penetrant, high power magnification, etc. Surface cleaning and elaborate access or disassembly procedures may be required. Candidates include obscured items which would otherwise require long crack lengths for detection.	12 to 11
b	DETAIL INSPECTION: An intensive visual check of a specified detail, assembly, or installation. This inspection searches for evidence of structural irregularity using adequate lighting and where necessary, inspection aids such as mirrors. Surface cleaning and elaborate access procedures may be required.	10 to 8
c	INTERNAL SURVEILLANCE: A visual check that will detect obvious unsatisfactory conditions and discrepancies in internal structure. This type of inspection applies to obscured items and installations which require removal of fillets, fairings, access panels, and doors.	7 to 5
d	EXTERNAL SURVEILLANCE: A visual check that will detect obvious unsatisfactory conditions and discrepancies in externally visible structure. Visibility is provided by quick opening access doors or panels. Workstands, ladders, etc., may be required.	4 to 3
e	WALK AROUND CHECK: A visual check conducted from ground level to detect obvious discrepancies.	2 to 1

FIGURE IV-1

EXAMPLE OF THE COMPLETED RANKING FORM FOR A CANDIDATE ITEM

Document# 90-432

Date: 6 Nov. 90

Analyst: C.L. Brooks

ITEM W3Title: CENTER WING, LOWER SURFACE
STRINGER 7, STA. Y= 980

SELECTION:

JUSTIFICATION: The runout of the stringer creates a stress concentration. There is previous aircraft experience of cracking at details with this geometry. Stringer 7 is the highest loaded stringer in this aft plank at this station. The rib at this station redistributes load between the wing and the fuselage.

FUNCTION: This is a primary tension load path for wing up bending from aerodynamic lift and maneuver loads.

ENVIRONMENT: Inb'd of Y= 980 the area is dry normal air.
Outb'd of Y= 980 is a fuel bay, therefore area is subject to aviation fuel and sump tank water. T= -65°F to 120°F

MATERIAL: 2024-T351 Plate Part No: D-12456
Outer Surface: Part is covered with epoxy primer
Inner Surface: Part is chromic anodized with Poly Coating

ACCESSIBILITY: To view the outer surface requires removal of the aerodynamic fairing. Limited access to the inner surface through a upper wing access hole.

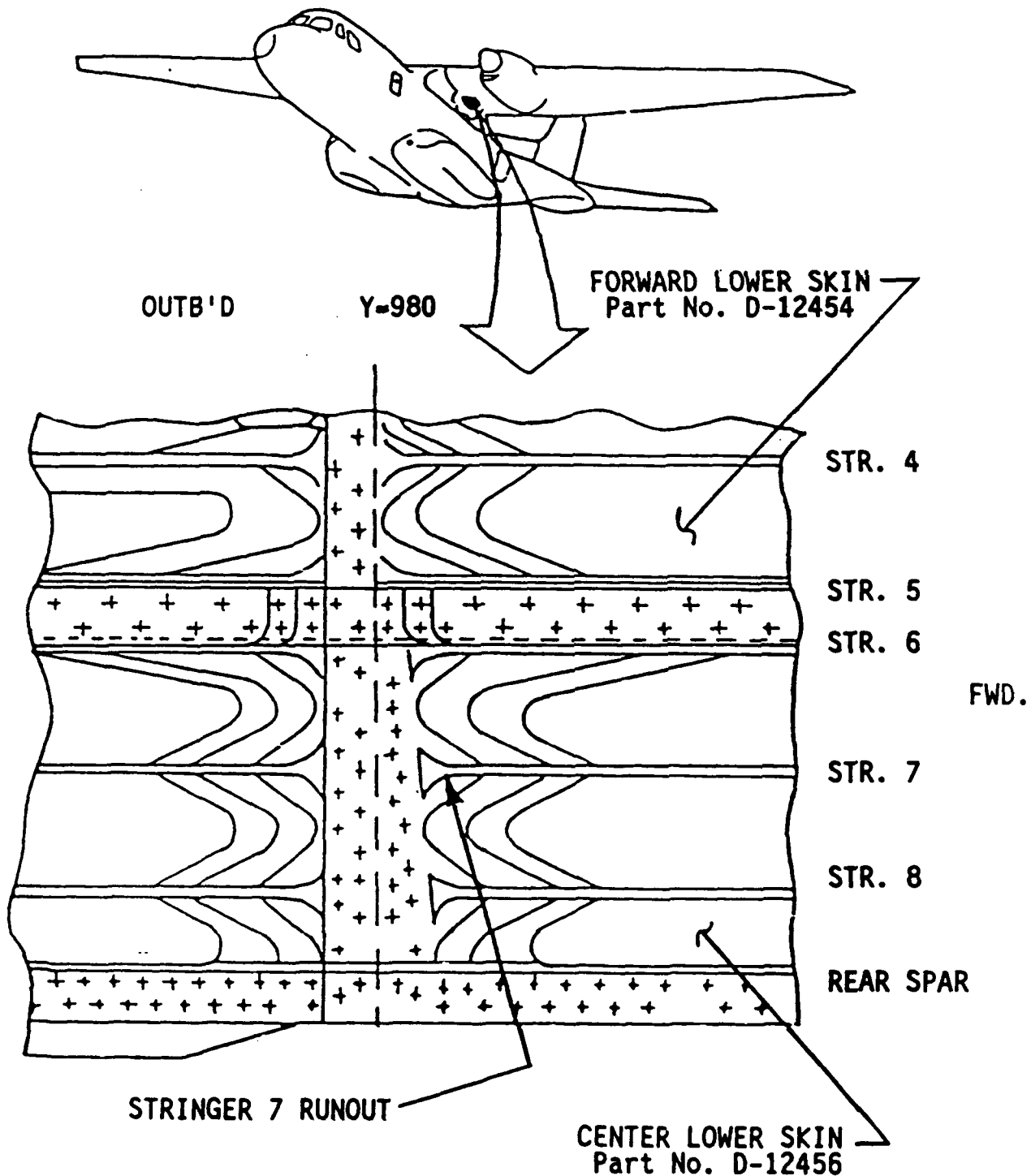
PRIORITIZATION			
Category	Comments	Ref	RANK
1 1G	The local max. 1G stress for the rib attach skin at str.7 runout is 7100 psi.	a	16
2 Lim	The primary member is the skin from the spar to center skin splice with M.S.=.4 ; the secondary members are the rear spar and center skin with M.S.>.5 ; possible arrestment at fastener holes	e	6
3 FS	A crack, hidden by the fairing, could grow undetected to failure resulting in wing & A/C loss	a	15
4 Dis	This is a progressive Stringer runout design, a load confluence near due to wing-fuselage attach	a	8
5 SSC	This is a low resistance alloy. Not considered to have significant residual stresses.	b	4
6 Cor	Item may be in fuel tank environment, surface protection applied.	bea dp	6
7 Kt	A diamond fastener pattern is located at the str. runout attaching the skin to the rib.	a	6
8 Acc	The area is protected by the fairings covering the wing-fuselage attach region. Negligible.	e	1
9 Ins	Elaborate access procedures required for fairing removal to perform a detail inspection.	b	10
TOTAL RANKING SCORE			72

FIGURE IV-2

EXAMPLE OF GEOMETRY AND REGION FOR DOCUMENTATION FOR ITEM W3

Document # 90-432

6 Nov. 90



VIEW LOOKING DOWN ON LOWER WING SKINS AT STA Y-980
ITEM W3 - CENTER WING, LOWER SURFACE, STRINGER 7 RUNOUT

FIGURE V-1

DISTRIBUTION OF TOTAL RANKING SCORE FOR ALL ITEMS
IN EXAMPLE AIRFRAME

102 Total Items

Maximum Ranking 84 out of 100

Minimum Ranking 39

Total Spread = 45

Arithmetic Mean = 62.5

48 Items less than the mean

54 Items greater than the mean

Median = 63

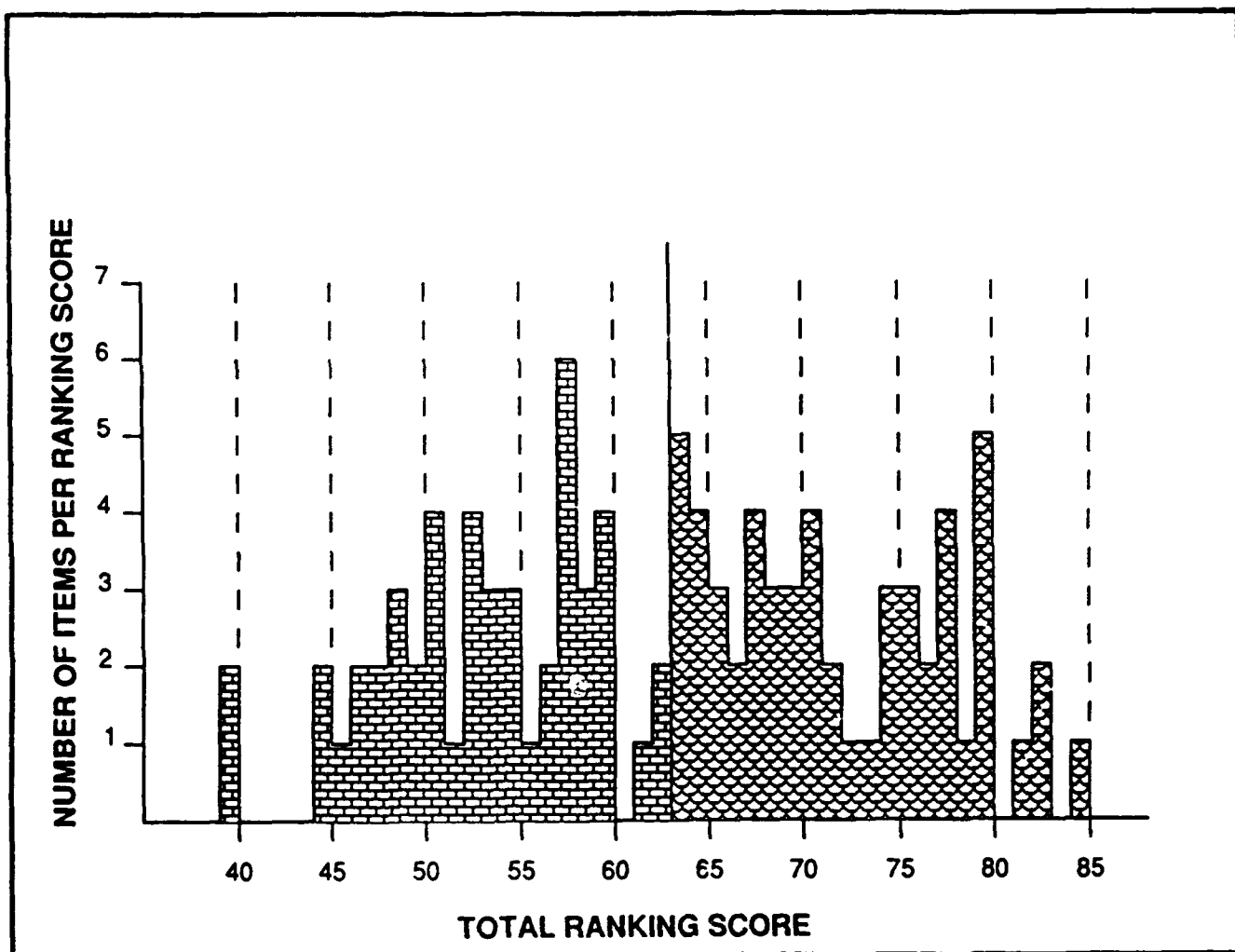
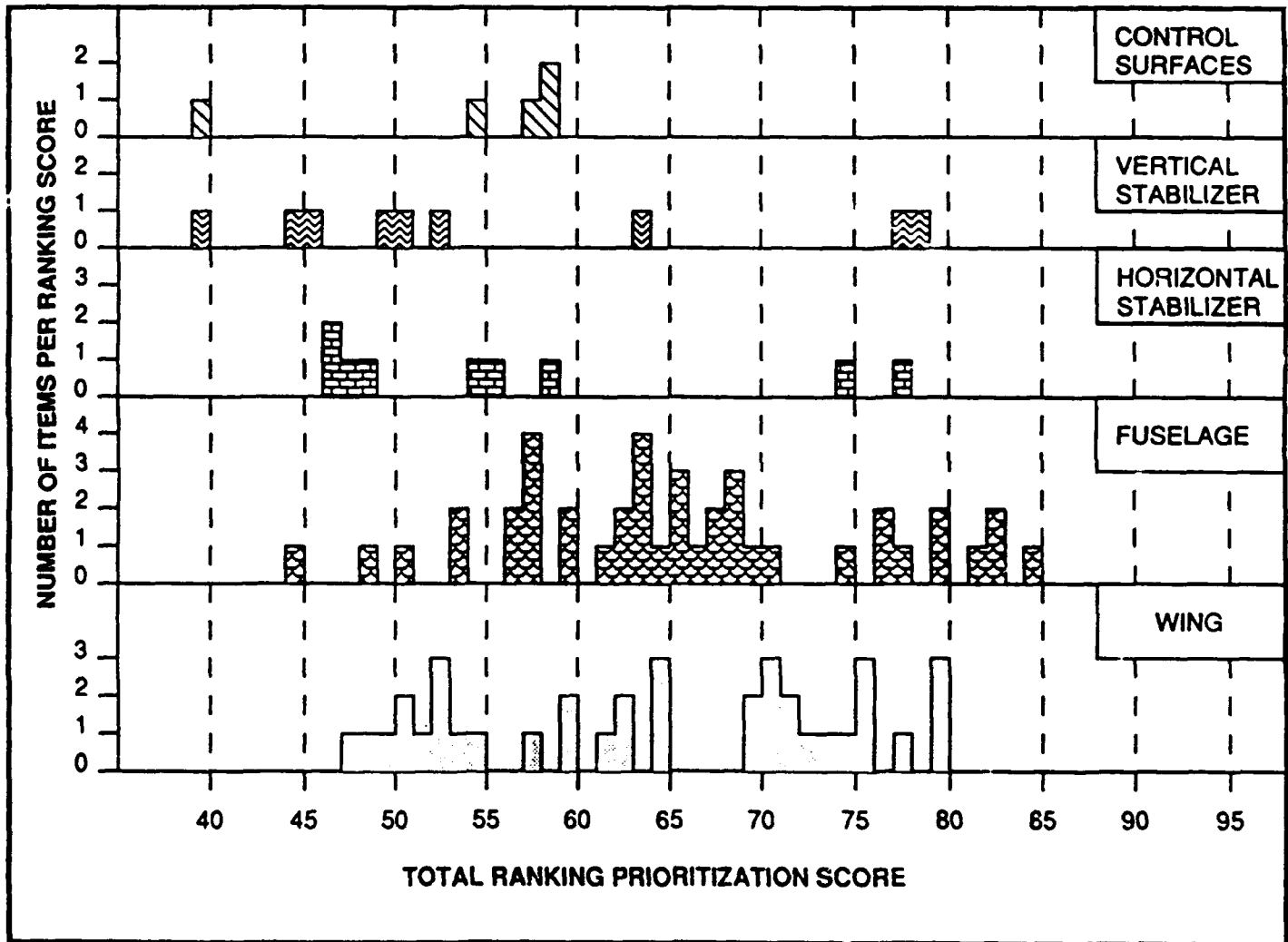


FIGURE V-2
DISTRIBUTION OF TOTAL RANKING SCORE BY AIRFRAME SECTION



**CHANGES IN THE GENERAL SPECIFICATION
FOR AIRCRAFT STRUCTURES
- AIR FORCE GUIDE SPECIFICATION 87221A -**

James M. Snead
Structures Division
Directorate of Flight Systems Engineering
DCS, Integrated Engineering and Technical Management
Aeronautical Systems Division
Air Force Systems Command
USAF, WPAFB OH 45433-6503

11 February 1991

This paper discusses the significant changes incorporated into the revision of the Air Force's Structures Mil-Prime Specification - AFGS-87221A.



EVOLUTION OF REQUIREMENTS

By 1975 there were some 47,000 DoD specifications & standards - of which 43,000 were procurement related:

A 1975 memo from the Deputy Secretary of Defense cited misuse of specs and standards as a major cost driver

A 1977 Defense Science Board report concluded that this misuse represented a bottom-up rather than a top-down approach and dictated design solutions rather than specifying functional needs

A NEW APPROACH WAS MANDATED

In the mid-1970s there was a growing realization that the approach then being used to develop new weapons systems was not yielding the desired results. In particular, it was found that the misuse of specifications and standards, particularly through the imposition of unneeded or incorrect "design solutions", was a major cost driver. It was decided that a new approach should be implemented - one that focused on designing the weapons system to achieve the desired system capabilities.



ACQUISITION OBJECTIVES THAT AFFECT ASIP

Emphasizing cost control by relating requirements to user needs

Sharing of risk and responsibility between the contractor and the government

Streamlining of RFPs and Source Selection process

Encouraging contractor innovation through the tailoring of requirements

Avoiding technical leveling by eliminating government mandated design solutions

This new approach focused on these elements:

- First, to define the performance requirements necessary to enable the user's needs to be met.

- Second, to involve both the government and the contractor in sharing the risk & responsibility of designing a successful product.

- Third, to minimize the bureaucracy and time involved in selecting contractors.

- Fourth, to give the contractor flexibility in developing their preferred solution to meeting the user's needs.



MIL-PRIME PHILOSOPHY ESTABLISHED

Features:

- Emphasis on performance requirements
 - Definitions of performance parameters
 - Leaves specific values blank
- One to one correlation of requirements to verification
- Allows innovative design solutions
- Retains "Lessons Learned" in a non-contractual appendix to assist in tailoring

The resulting philosophy - which the Air Force refers to as the "Mil-Prime" philosophy - has these attributes:

- It emphasizes performance requirements, not design solutions.

- It allows contractors to propose the specific performance values that, in combination, produce the "best" or "preferred" concept.

- It insures that the user's needs are achieved by verifying the ability of the design to meet each performance requirement.

- And, finally, in the appendix, it captures "lessons-learned" - the advantages and disadvantages of different design approaches.



STATUS OF THE MIL-PRIMES

Over 50 of the Aeronautical Systems Division's major acquisition documents have been updated to conform to the Mil-Prime philosophy

The Aircraft Structures MIL-A-87221 was initially released on 28 Feb 1985

A revised version of this Mil-Prime, Version A, was released on 8 Jun 1990

It is now referred to as an Air Force Guide Specification (AFGS) to enhance the understanding that the specific requirements and verification methods are to be tailored to the program requirements

To date, over 50 of the major aircraft acquisition specifications have been rewritten to conform to the Mil-Prime philosophy. For aircraft structures, MIL-A-87221 consolidated all of the structures design, analysis and test requirements into one specification. This Mil-Prime, originally released in 1985, was updated and has been released as AFGS-87221A. The name was changed to "Air Force Guide Specification" to enhance the understanding that this specification serves as a starting point for the development of the final weapons system's structures specification.



SPECIFICATION SCOPE

This specification establishes the structural performance and verification requirements for an airframe. These requirements are derived from operational needs and apply to the airframe structure which is required to function and sustain loads during usage. This usage includes take-off, flight, landing, ground handling, maintenance, and laboratory tests. This specification also establishes certain structural design criteria which, as a minimum, are necessary to enable the airframe to meet these structural performance requirements.

The scope of the specification was expanded to include all test requirements, such as, proof and functional strength tests performed to verify airworthiness in preparation for flight test. The scope was also expanded to clarify that the tailored specification establishes the essential structural design criteria which are necessary to meet the structural performance requirements. This change clarifies the distinction between structural design requirements and structural design criteria - a distinction that was not clear in MIL-A-87221.



ORGANIZATION OF THE AIRCRAFT STRUCTURES SPECIFICATION

- .SECTION 1 - SCOPE
- .SECTION 2 - APPLICABLE DOCUMENTS
- .SECTION 3 - REQUIREMENTS
- .SECTION 4 - VERIFICATION
- .SECTION 6 - NOTES (DEFINITIONS)
- .SECTION 10 - HANDBOOK

The changes incorporated into Sections 1, Scope, Section 3, Requirements, and Section 4, Verification, will be discussed in greater detail.



STRUCTURAL DESIGN REQUIREMENTS

3.1 Detailed structural design requirements. The requirements of this specification reflect operational and maintenance requirements and are stated in terms of parameter values, conditions and discipline (loads, flutter, et cetera) requirements. The air vehicle structure (airframe) shall have sufficient structural integrity to meet these requirements, separately and in attainable combinations.

CLARIFIES THE DISTINCTION BETWEEN STRUCTURAL DESIGN REQUIREMENTS AND STRUCTURAL DESIGN CRITERIA

The basic structural design requirements statement was expanded to clarify that the airframe shall have sufficient structural integrity to meet the requirements of the tailored structures specification.



STRUCTURAL DESIGN CRITERIA

3.1.1 Structural design criteria. The deterministic structural design criteria stated in this specification are, as a minimum, those necessary to ensure that the airframe shall meet the detailed structural design requirements established in this specification. ... Each individual criterion established herein has been selected based upon historical experience with adjustments made to account for new design approaches, new materials, new fabrication methods, unusual aircraft configurations, unusual usage, planned aircraft maintenance activities and _____. The substantiation of the adequacy of these criteria in meeting the specified and inherent design requirements is documented in _____.

A new requirements paragraph was added to address deterministic structural design criteria. This requirement states that the criteria selected must be tailored to the particular design concept, selected materials, fabrication methods, et cetera, used in the air vehicle. This change was made to prevent the repetitive use of inappropriate or historically-used criteria. The change was also made to add the requirement that the selected criteria must be substantiated and this substantiation must be documented. This change will help ensure that a sound set of criteria is selected based upon a good understanding of the circumstances involved in its application.



PROBABILITY OF DETRIMENTAL DEFORMATION & FAILURE

3.1.2 Probability of detrimental deformation and structural failure. (____). A combined load-strength probability analysis shall be conducted to predict the risk of detrimental structural deformation and structural failure. For the design requirements stated in this specification, the airframe shall not experience detrimental structural deformations with a probability of occurrence equal to or greater than _____ per flight. Also, for these design requirements, the airframe shall not experience the loss of adequate structural rigidity or proper structural functioning such that flight safety is affected or suffer structural failure leading to the loss of the air vehicle with a probability of occurrence equal to or greater than _____ per flight.

The specification now provides the option, at the government and contractor's discretion, to use a probabilistic load-strength failure analysis as an alternative to the use of deterministic design criteria for selected structural components. This is done by establishing two probability requirements. The first, similar to the typical strength design requirement at limit load, establishes an unacceptable frequency of occurrence of detrimental structural deformations. The second, similar to the typical ultimate load strength requirement, establishes an

unacceptable frequency of structural failure.



WEIGHTS

3.2.5 Weights. The weights to be used in conducting the design, analysis, and test of the air vehicle are derived combinations of the operating weights, the defined payload, and the fuel configuration. These weights shall be the expected weight at IOC.

3.2.5.1 Operating weight. The operating weight is the weight empty (MIL-STD-1374) plus unusable fuel, oil, crew, and _____.

3.2.5.2 Maximum zero fuel weight. The maximum zero fuel weight shall be the highest required weight of the loaded air vehicle without any usable fuel and is specified as the operating weight plus _____.

The weight requirements have been revised to establish that the expected weights at the Initial Operational Capability (IOC) of the weapons system, not the weights at the beginning of Full Scale Development (FSD), as the weights to be used in the design and analysis process. This was included to address the reduction in mission capability associated with the increase in weight that normally occurs from the start of FSD to IOC.

The weight requirements have also been revised to define design weights in terms of vehicle configurations and not as specific numeric weight values. Again, this was done to prevent the use of out-of-date vehicle weights in the design and analysis process.



LIMIT LOADS

3.2.11 Limit loads. The limit loads, to be used in the design of elements of the airframe subject to a deterministic design criteria, shall be the maximum and most critical combination of loads which can result from authorized ground and flight use of the air vehicle, including maintenance activity, the system failures of 3.2.22 from which recovery is expected, a lifetime of usage of 3.2.14, all loads whose frequency of occurrence is greater than or equal to _____ per flight, and _____. All loads resulting from the requirements of this specification are limit loads unless otherwise specified.

The limit load requirement was updated to ensure that limit loads are the maximum and most critical combination of loads to be experienced during mission use and maintenance activities. The definition of limit loads now includes a requirement to establish a lower bound on the frequency of occurrence of random loads to act as a cutoff for excluding severe but very infrequent loads from the design process. This cutoff frequency is referred to in later sections involving probabilistic

loads. These limit loads are to be used in the design of elements of the airframe subject to a deterministic design criteria.



ULTIMATE LOADS

3.2.12 Ultimate loads. Ultimate loads not derived directly from ultimate load requirements of this specification shall be obtained by multiplying the limit loads by appropriate factors of uncertainty. These ultimate loads shall be used in the design of elements of the airframe subject to a deterministic design criteria. These factors of uncertainty and the circumstances where they are to be used are _____.

There are two changes in the ultimate loads requirements. First, the terminology "Factor of Safety" has been changed to "Factor of Uncertainty." This change was made to better define how this factor is used in the structural design process. The second change states the requirement that the factors of uncertainty and the circumstances where they are to be used are to be incorporated into the tailored specification. This change acknowledges that different factors of uncertainty may be appropriate for different structural concepts in the same vehicle. It also helps to ensure that consideration of the appropriateness of historically-used factors are reviewed before they are incorporated into the tailored specification.



REPEATED LOADS SOURCES

3.2.14.2 Repeated loads sources. All significant sources of repeated loads shall be considered and included in the development of the service loads spectra. The following operational and maintenance conditions shall be included as significant sources of repeated loads.

g. Heat flux. The repeated heat flux time histories are _____.

Heat flux was added to the list of repeated load sources to be considered in the determination of the tailored requirements.



POWER OR THRUST LOADS

3.2.17 Power or thrust loads. The power or thrust of the installed propulsion system shall be commensurate with the ground and flight conditions of intended use, including system failures of 3.2.22, and the capabilities of the propulsion system and crew. The thrust loads attainable shall include all thrust loads up to the maximum. These loads shall include engine transients due to both normal engine operation as well as the engine system failures of 3.2.22 and _____.

The Power or thrust loads requirements were expanded to specify that the thrust loads to be used in the determination of the limit loads shall be all thrust loads up to the maximum. Also, the selection of the critical thrust design loads shall include engine transients due to both normal engine operation as well as engine system failures.



FLIGHT CONTROL & STABILITY AUGMENTATION DEVICES

3.2.18 Flight control and stability augmentation devices. In the generation of loads, flight control and automatic control devices, including load alleviation and ride control devices, shall be in those operative, inoperative and transient modes for which use is required or likely or due to the system failure conditions of 3.2.22 and _____.

The requirement was added that system failures of the flight control system and stability augmentation devices must be considered in the selection of the critical design loads.



MATERIALS & PROCESSES

3.2.19 Materials and processes. Materials and processes shall be selected in consonance with MIL-STD-1587, MIL-STD-1568 and the following requirements so that the airframe meets the operational and maintenance performance requirements.

This and subparagraphs now incorporate all the material and process requirements formerly found in Section 3.10 Strength

Castings, Forgings, Grain Direction,
Environmental Effects, Nonmetallic Materials



MATERIALS

3.2.19.1 Materials. The materials used in the airframe shall be commensurate with the operational and maintenance capability required of the airframe. Whenever materials are proposed for which only a limited amount of data is available, the acquisition activity shall be provided with sufficient background data so that a determination of the suitability of the material can be made. The allowable structural properties shall include all applicable environmental effects, such as exposure to climatic conditions of moisture and temperature; airborne or spilled chemical warfare agents; and maintenance induced environments commensurate with the usage of the airframe. Specific material requirements are:

a. _____



PROCESSES

3.2.19.2 Processes. The processes used to prepare and form the materials for use in the airframe as well as joining methods shall be commensurate with the material application. Further, the processes and joining methods shall not contribute to the degradation of the properties of the materials when the airframe is exposed to operational usage and maintenance environments. Specific material processing requirements are:

a. _____

b. _____

The materials and processes requirements previously found in several different sections of the specification are now consolidate into one section.

One additional change in the area of materials is that "B" basis allowables are now accepted for the design of structures whose strength will be verified by static test. Where appropriate, environmental induced material property degradation must be included.



NON-STRUCTURAL COATINGS, FILMS & LAYERS

3.2.21 Non-structural coatings, films and layers. Coatings, films and layers applied ... Further, methods of nondestructive inspection shall be provided for inspecting the structure behind or beneath the coatings, films and layers for cracks, failures, damage, corrosion and other structural integrity anomalies. In particular, if the inspections of 4.11.1.2.2.d and 4.12.1 are applicable to the structure behind or beneath the coatings, films and layers, the coatings, films and layers shall not preclude or impede the performance of the durability and damage tolerance inspections. If the coatings, films, or layers are attached by adhesive bonding ...

The requirements relating to the non-destructive inspection of non-structural coatings, films and layers were expanded to ensure that such coatings do not unacceptably degrade the ability to maintain the structural integrity of the underlying structure.



SYSTEM FAILURES

3.2.22 System failures. All loads resulting from or following the single or multiple system failures defined below whose frequency of occurrence is greater than or equal to the rate specified in 3.2.11 shall be limit loads. Subsequent to a detectable failure, the air vehicle shall be operated with the flight limits of 3.2.5, 3.2.7.10 and 3.2.9.5.

- Tire failures
- Radome failures
- Hydraulic failures
- Transparency failures
- Propulsion system failures
- Mechanical failures
- Flight control system failures
- Other failures

The specification requirements for establishing the limit loads resulting from single or multiple aircraft system failures has been renamed from "Probable Failures" to "System Failures." The cut-off frequency of occurrence established in the limit loads section is also used here to define which loads resulting from an aircraft system failure - for example, an uncommanded control surface deflection - are to be included in the selection of the limit loads. Other possible system failures to be considered are listed.



FOREIGN OBJECT DAMAGE

3.2.24 Foreign object damage (FOD). () The airframe shall be designed to withstand the FOD environments listed below. These FOD environments shall not result in the loss of the air vehicle or shall not incapacitate the pilot or crew with a frequency equal to or greater than _____ per flight. These FOD environments shall not cause unacceptable damage to the airframe with a frequency equal to or greater than _____ per flight.



PRESSURIZATION

3.4.1.12 Pressurization. The pressure differentials to be used in the design of pressurized portions of the airframe, including fuel tanks, shall be the maximum pressure differentials attainable during flight within the design flight envelope, during ground maintenance, and during ground storage or transportation of the air vehicle. These maximum pressure differentials shall be the maximum attainable with the normal operation of the pressure regulation system (nominal settings plus manufacturing tolerance) or the maximum pressure differentials attainable during or following the system failures of 3.2.22 which occur at a rate greater than or equal to that specified in 3.2.11. ...



BIRD FOD

3.2.24.1 Bird FOD. (). The airframe shall be designed to withstand the impact of _____ pound birds with the corresponding air vehicle speeds of _____ KTAS in a manner consistent with the normal flight without loss of the air vehicle or the incapacitation of the pilot or crew. The airframe shall be designed to withstand the impact of _____ pound birds with the corresponding air vehicle speeds of _____ KTAS with no unacceptable damage. Unacceptable damage is _____.

Also applies to HAIL FOD and RUNWAY, TAXIWAY, AND RAMP DEBRIS FOD



PRESSURIZATION (CONT'D)

These maximum pressure differentials shall include both positive, inside-to-outside, and negative, outside-to-inside pressure differentials as well as pressure differentials across pressure boundaries separating adjacent internal compartments. Where appropriate, these pressures shall be combined with other flight loads to obtain the most critical combination of flight and pressurization loads. The internal stresses and strains arising from the pressurization loads shall not be assumed to be relieving from other flight loads unless the probability of a loss of pressurization is less than the rate specified in 3.2.11. Similarly, structural stabilization derived from pressurization shall not be used to achieve required structural performance capabilities unless the probability of the loss of pressurization is less than the rate specified in 3.2.11.

The foreign object damage (FOD) requirements have been rewritten to establish these requirements on a probabilistic basis. Two cut-off frequencies of occurrence, similar to the approach used for random loads in the limit loads section, were defined. The first establishes an unacceptable frequency of occurrence for the loss of the aircraft or the incapacitation of the pilot or crew due to FOD. The second establishes an unacceptable frequency for the occurrence of unacceptable damage to the airframe.

The specific damage mechanism, such as the size of an impacting bird and the corresponding air vehicle speed, relating to each cut-off frequency as well as the specific definition of what constitutes unacceptable damage is defined in the subparagraphs.

The requirements for pressurization have been rewritten to expand the range of flight and ground operations to be included in the selection of pressurization design loads. The loads resulting from random pressurization system failures are addressed consistent with the previously discussed system failures and the cut-off frequency defined in the limit loads section. Also, the circumstances for the use of pressurization induced stresses and strains to reduce the severity of other flight and ground operations' induced internal loads or for the use of the increased structural stiffness resulting from internal pressurization in achieving limit or ultimate load structural requirements are defined.



FAIL - SAFE STABILITY

3.7.4 Fail-safe stability. For the system failures of 3.2.22, the air vehicle shall be free from flutter, divergence or other aeroelastic or aeroservoelastic instabilities after each failure. In addition, this fail-safe criteria shall include air vehicle augmentation system failures that occur at a rate equal to or more frequent than the rate specified in 3.2.11.

The requirement that the air vehicle be free of aeroelastic or aeroservoelastic instabilities following the defined system failures of 3.2.22 was expanded to ensure that potential augmentation system failures are included in meeting this fail-safe criteria.



STRESSES & STRAINS

3.10.4 Stresses and strains. Stresses and strains in airframe structural members shall be controlled through proper sizing, detail design, and material selections to satisfactorily react all limit and ultimate loads. In laminated composites, the stresses and ply orientation are to be compatible and residual stresses of manufacturing are to be accounted for, particularly if the stacking sequence is not symmetrical.

3.10.4.1 Fitting factor. ...

3.10.4.2 Bearing factor. ...

The general strength requirement relating to stresses was expanded to include strains since strain is the controlling design parameter in some structural materials. These general requirements were also expanded to specifically address laminated composites.



STATIC STRENGTH

3.10.5 Static strength. Sufficient static strength shall be provided in the airframe structure for reacting all loading conditions loads without degrading the structural performance capability of the airframe. Sufficient strength shall be provided for operations, maintenance functions, and any tests that simulate load conditions, such that:

a. Detrimental deformations, including delaminations, shall not occur at or below limit loads, or during the tests required in 4.10.5.3 and 4.10.5.4. The deformation requirements of 3.2.13 apply.

b. Rupture or collapsing failures shall not occur at or below ultimate loads.

The static strength section was modified to include the requirement that the airframe shall have sufficient strength to withstand the loads and load distributions applied to the airframe during ground tests. Specifically, the airframe must have sufficient strength to withstand the functional, strength, and pressurization proof tests. Also, the requirement that no detrimental deformations shall occur at or below limit loads was expanded to include delaminations.



INITIAL & INTERIM STRENGTH FLIGHT RELEASES

3.10.6 Initial and interim strength flight releases. Initial and, as needed, interim strength flight restrictions shall be established to maintain safe flight conditions until all structural validation testing has been successfully completed. The loads resulting from overshoots, upsets and the recovery from overshoots and upsets, and the loads during and following the system failures of 3.2.22 shall be included in the establishment of the flight restrictions.

a. For the initial strength flight release, flight restrictions shall be defined to restrict the air vehicles from experiencing loads greater than _____ percent of limit loads.

b. Prior to the completion of all structural validation testing, interim strength flight releases shall be defined to permit flight up to limit loads or the strength envelope cleared through the strength proof testing of 4.10.5.4, whichever is less.



INITIAL & INTERIM STRENGTH FLIGHT RELEASES (CONT'D)

4.10.6 Initial and interim strength flight releases.

a. Prior to the initial flight release, the airframe shall be satisfactorily strength analyzed for reacting all predicted limit and ultimate loads and this analysis shall be approved by the procuring activity. Also, prior to the initial flight release, the functional proof test requirements of 4.10.5.3 shall be successfully met. Prior to first pressurized flight of all air vehicles, the pressurization proof test requirements of 4.10.5.4 shall be successfully met.



INITIAL & INTERIM STRENGTH FLIGHT RELEASES (CONT'D)

b. Prior to flight beyond the initial strength flight release, the accuracy of the loads predictive methods shall be validated by using an instrumented and calibrated flight test air vehicle to measure actual loads and load distributions during flight within the initial strength flight release envelope. Also, prior to flight beyond the initial strength flight release, the strength proof test requirements of 4.10.5.4 shall be successfully met. Extrapolations of the measured data beyond the initial flight limits shall be used to establish the expected conservatism of the predictive methods for flight up to limit loads. This procedure of loads measurement and data extrapolation shall be used to validate the conservatism of the strength analysis and strength proof tests ...



FINAL STRENGTH FLIGHT RELEASE

3.10.7 Final strength flight release. Prior to final strength flight release for operation up to 100 percent of limit strength for either production air vehicles or flight test air vehicles not proof tested per 4.10.5.4, the airframe shall have exhibited ultimate load static test strength for ultimate loads which reflect verified external limit loads.

The sections defining the initial, interim and final strength flight releases have been reorganized to clarify the limitations to be imposed on the air vehicle as a function of the analyses and tests satisfactorily completed.



DURABILITY

3.11 Durability. The durability of the airframe shall be adequate to resist fatigue cracking, corrosion, thermal degradation, delamination and wear during operational and maintenance use such that the operational and maintenance capability of the airframe is not degraded. These requirements apply to metallic and nonmetallic structures, including composites, with appropriate distinctions and variations as indicated. Durability material properties shall be consistent and congruent with those properties of the same material, in the same component, used by the other structures disciplines. See 3.2.19.1. The economic life of the airframe shall be sufficient to withstand the service life and usage of 3.2.14.



FATIGUE CRACKING / DELAMINATION DAMAGE

3.11.1 Fatigue cracking/delamination damage. Adverse cracking/delamination which would cause functional impairment or require costly maintenance action or both shall not occur within _____ lifetimes when the airframe is subjected to the environment and service usage of 3.2.14, except where it is desired to meet the limited life provisions of 3.11.5. Steady state level flight and ground loading conditions shall not result in sustained growth of cracks/delaminations in the airframe.



DAMAGE TOLERANCE

3.12 Damage tolerance. The damage tolerance capability of the airframe shall be adequate for the service life and usage of 3.2.14 as amplified below. Particular requirements applicable to specific materials are so identified. Safety of flight and other selected structural components of the airframe ... These requirements apply to metallic and nonmetallic structures, including composites, with appropriate distinctions and variations as indicated. Damage tolerance material properties shall be consistent and congruent with those properties of the same material, in the same component, used by the other structure's disciplines. See 3.2.19.1. Damage tolerance requirements shall also be applied to the following special structural components:

The durability and damage tolerance requirements were expanded to better address nonmetallic / composite structures.



FUNCTIONAL PROOF TESTS

4.10.5.3 Functional proof tests prior to first flight. Prior to the first flight of the first flight article, proof tests shall be conducted to demonstrate the functioning of flight-critical structural systems, mechanisms and components whose correct operation is necessary for safe flight. These tests shall demonstrate that the deformation requirements of 3.2.13 have been met. The functional proof tests that will be conducted, the articles on which they will be conducted, and the load level to which the systems, mechanisms and components will be loaded are: _____. Where these tests are not performed on every flight air vehicle, the substantiation that the planned test program is adequate to demonstrate the flight safety of all flight air vehicles is documented in _____.

The functional proof test requirements were rewritten to better clarify the intent of this testing.



STRENGTH & PRESSURIZATION PROOF TESTS

4.10.5.4 Strength and pressurization proof tests. Strength proof tests shall be successfully performed ... Pressurization proof tests shall be successfully performed on every airframe prior to pressurized flight. These proof tests shall demonstrate that the deformation requirements of 3.2.13 have been met at all load levels up to the maximum loads expected to be encountered during flight for flight anywhere within the released flight envelope including the effects of recovery from upsets and the system failures of 3.2.22. These proof tests shall also validate the accuracy of the strength predictive methods through comparisons of measured critical internal loads, strains, stresses, temperatures, and deflections with predicted values. Re-proof tests shall be conducted ...

Conclusion

These changes in the Structures Mil-Prime reflect the experience gained in applying the requirements contained in this Mil-Prime to ASD programs currently in or entering Full Scale Development.

The author, in behalf of the entire Structures Division, extends our appreciation to the Aerospace Industries Association (AIA) for their assistance in developing the Mil-Prime specification's requirements in general and, particularly, the damage tolerance requirements for composites.



STRENGTH & PRESSURIZATION PROOF TESTS (CONT'D)

a. Strength proof test load levels shall be equal to or greater than _____ percent of limit mechanical loads or the maximum mechanical loads to be encountered during flight, whichever is less, and _____ percent of limit thermal loads or the maximum thermal loads to be encountered in flight, whichever is less. The proof load distributions shall be equal to or more severe than the predicted load distributions.



STRENGTH & PRESSURIZATION PROOF TESTS (CONT'D)

b. Prior to the first flight with pressurized compartments, each pressurized compartment of each pressurized flight air vehicle shall be pressure proof tested to _____ percent of the maximum pressure limit loads of 3.4.1.12. Subsequent to the successful completion of ultimate pressurization tests on the static test article, each air vehicle shall be pressure proof tested to the maximum operating pressure differential attainable with normal pressure control system operation multiplied by a factor of _____. Where necessary to demonstrate combined external load and internal pressurization strength, the pressure proof tests shall be combined with the strength proof tests of subparagraph a. above.

The strength and pressurization proof test requirements were combined and rewritten to clarify when these tests are required and what these tests are expected to accomplish.

INSPECTION OF AIRCRAFT STRUCTURE
WITH
ADVANCED SHEAROGRAPHY

By
John W. Newman

Abstract

Electronic shearography has emerged in the last three years as a powerful new tool for the nondestructive inspection of composite and honeycomb structures. Shearography is a laser based interferometer that is sensitive to the out of plane derivative of deformation of a panel due to the nonhomogeneous strain field caused by a flaw. Shearography has been used in the last 12 months to inspect the strain field in riveted lap joints under tensile loads as well as for the NDT of composite and honeycomb repairs. The results indicate that shearography can detect cracks in rivet holes, unbonding of lap joints as well as provide a rapid nondestructive evaluation of aircraft composite and honeycomb repairs and impact damage.

Introduction

Laser Technology, Inc. (LTI) has developed advanced shearography techniques for the detection of debonds, delaminations and impact damage for both the production and repair of composite and honeycomb structures. Recently, LTI was contracted by DOT Transportation Systems Center under the FAA Aging Aircraft Research Program to evaluate the use of shearography for lap joint inspection for cracks, multiple site damage and corrosion unbonding. These tests were conducted on large (10 x 12 ft.) test coupons consisting of fuselage panels manufactured to Boeing 737 drawings and containing a bonded and rivet lap joint. The coupons were fatigue cycled by repeated pressurization, and

shearography was used to examine the changes in the strain field on the joints as the fatigue cracks grew into multiple site damage.

This test and many others have demonstrated that electronic shearography has been developed into a useful tool for nondestructive testing, and that it can be used easily in the hangar environment meeting all laser safety concerns. Additional applications include the nondestructive testing of honeycomb structures such as flaps and control surfaces on-aircraft without removal. The NDT of honeycomb repairs as well as the detection of impact damage and evaluation of repairs in composite panels is fast and effective.

Shearography offers a great increase in the speed of inspection by allowing on-aircraft inspection without removal as well as the inspection of areas up to several sq. ft. in several seconds.

Theory of Shearography NDT

Originally developed for strain measurement, advanced shearography provides a full-field video strain gauge, in real time over a large area. The technique uses a proprietary image shearing optical system to provide two overlapping and laterally sheared images to a CCD camera. These images interfere at paired points over the entire field of vision. The intensity of the laser-illuminated object image at each point is a function of the phase relationship between these paired points over an entire image. If two interferograms representing two different strain states of the test object are image processed, the difference in the strain patterns is displayed. The video processed image yields a fringe which is the locus of surface strains. Subsurface defects induce surface strain anomalies when the test part is properly stressed. Advanced shearography reveals these strain concentrations.

Real time shearography is performed after the operator captures the first image. Each successive image is compared with this first captured image. As the test object is stressed in the course of the NDE test, the strain changes in the object from the first image are displayed as fringes defining the size, shape and location of the defect or amount of plane strain. When the operator decides to "freeze" the real-time test results, the double exposure shearogram is displayed, comparing the first image of the test object with the second "frozen" image.

For on-aircraft inspection, a miniature shearography camera has been developed that weighs only 5 oz. This camera is mounted in a vacuum shell that contains an air seal around the perimeter of the aperture. The inspection head is attached to the panel with a locking vacuum, and the test is accomplished by reducing the pressure further. Debonded areas in a honeycomb panel will expand out of the plane of the panel allowing detection of this localized deformation by the shearography interferometer.

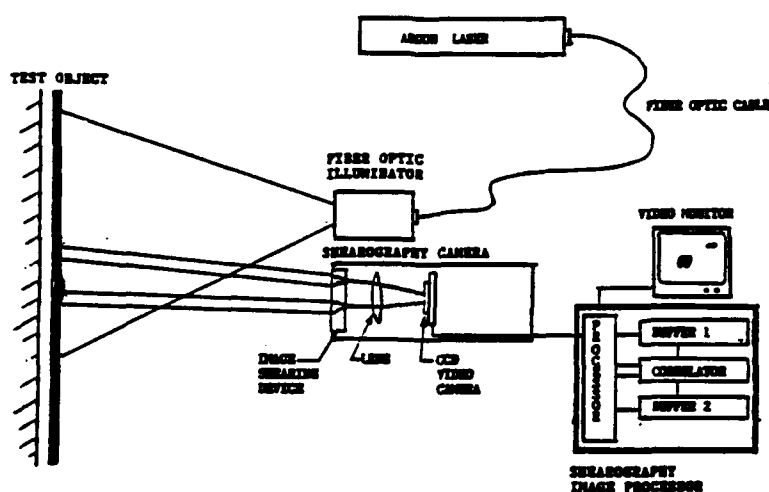


FIGURE 1 Schematic diagram showing the major components of a shearography NDT system. The camera and laser beam illuminator are generally built into a small housing for mounting on a gantry or in a vacuum shell for field testing.

Equipment

A large number of different shearography systems are presently offered by LTI and include laboratory NDT development systems, large production systems and specialized systems for helicopter blades and such components as the F100 engine fan duct assembly. In addition, portable systems for on-aircraft use are being introduced. This equipment has been used successfully to find debonds in honeycomb on-aircraft on the tarmac.

Development Equipment

The ES-9120 uses an air cooled Argon laser and fiber optics to illuminate the test part which is generally placed in a test chamber for pressure reduction stressing. The test chamber controls are mounted on the control console which also contains the shearography image generator and the video monitor. The ES-9120 is excellent for developing NDT test techniques and method development and is the shearography equivalent to a small bench top C-scan system. Using the camera on a tripod allows field inspection with thermal stressing. This has been used on F-14 engine inlet ducts and was used during the LTI tests of the 737 fuselage lap joints, as well as honeycomb engine inlets on C-5A aircraft.

Production Equipment

Production shearography equipment generally consists of a large test chamber with a built-in gantry for scanning the shearography camera. The ES-9150 system has a 1 Watt Argon laser located external to the test chamber with fiber optic delivery of the laser beam to the diffuser mounted on the shearography camera. High definition systems such as the LTI ES-9200 is able to image 1/4 inch debonds in a 36 inch wide field of view.

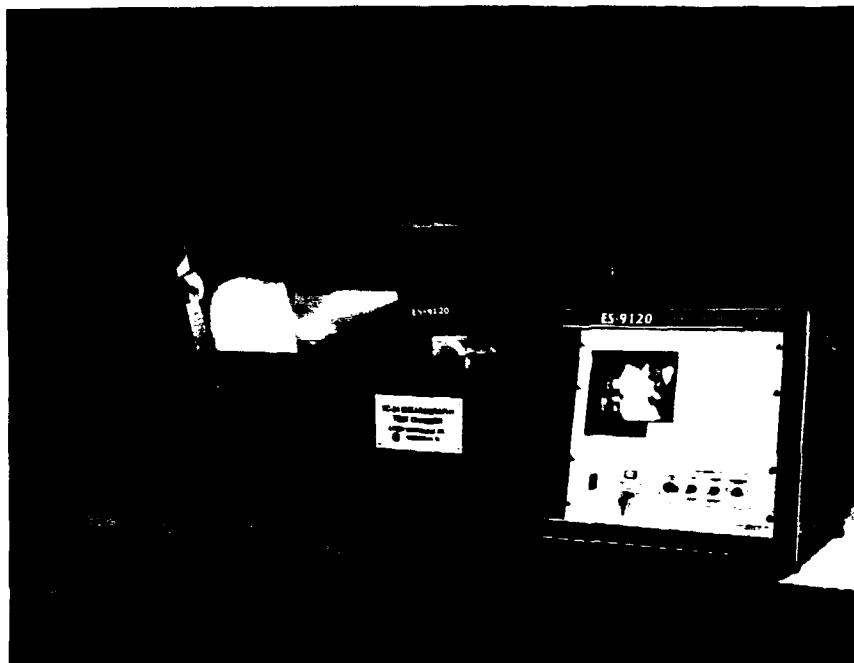


FIGURE 2 ES-9120 Shearography System for NDT Method Development



FIGURE 3 An ES-9150 shearography inspection system showing the test chamber for pressure reduction stressing of honeycomb panels with shearography inspection. Images are presented to the operator in color and stored on disc. Automatic defect analysis and counting is featured on this equipment.

Production shearography systems are configured for numerous aerospace production applications such as helicopter blades, flaps, honeycomb panels, missile fuselages and more. The ES-9200 is used for production inspection of composite honeycomb on the B-2.

On-aircraft Inspection Equipment

The ES-9400 is a portable shearography system for the inspection of aircraft honeycomb structures and can be used for the inspection of lap joints or tear straps for debonding. The vacuum shell of the ES-9400 attaches to the aircraft with a partial vacuum. The operator uses a small hand-held video monitor and control box to perform the tests and operate the system. Typical test times are several seconds.

Key applications for the ES-9400 are honeycomb structures that can be inspected on-aircraft, eliminating the need for removal for C-scan inspection. Repairs to honeycomb are easily evaluated as are repairs to composite panels and the detection of impact damage. Tests have demonstrated the ability to differentiate between dents in aluminum honeycomb and true unbonds.



FIGURE 4 The ES-9400 inspection system head being attached to a lap joint on a 707 for engineering tests.

Aircraft Inspection Applications of Electronic Shearography

Shearography offers the ability to map changes in strains to 0.1 microstrain at video frame rates. Using this strain mapping ability, various crack panels were evaluated using both tension and thermal stressing techniques to observe the presence of cracks at rivet holes. The tension load was applied with the principal stressing being perpendicular to the cracks, simulating the stress that would include this type of crack. Both EDM notches simulating cracks and actual fatigue cracks were examined. Panels were 0.064 inches thick. Cracks as small as 0.2 inches long were easily detected in a large field of view that encompasses a 6 x 8 inch area. Thermal loading produced similar results and is a technique that can be applied easily in the field.

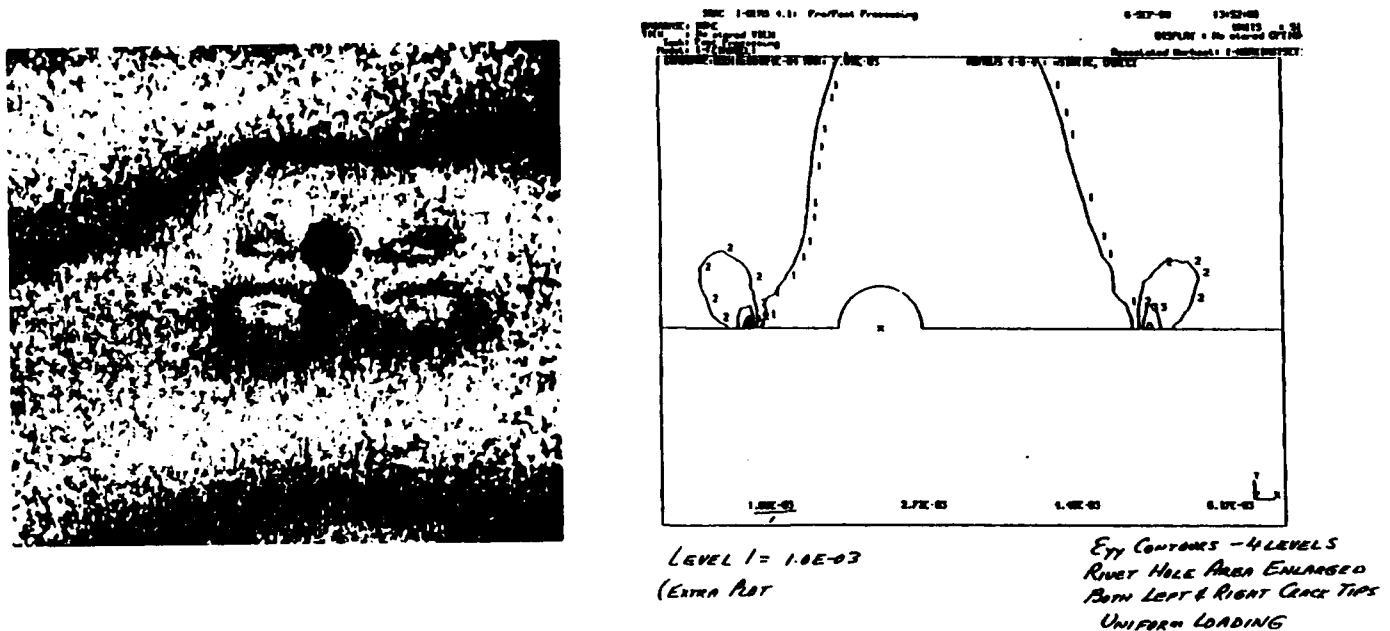
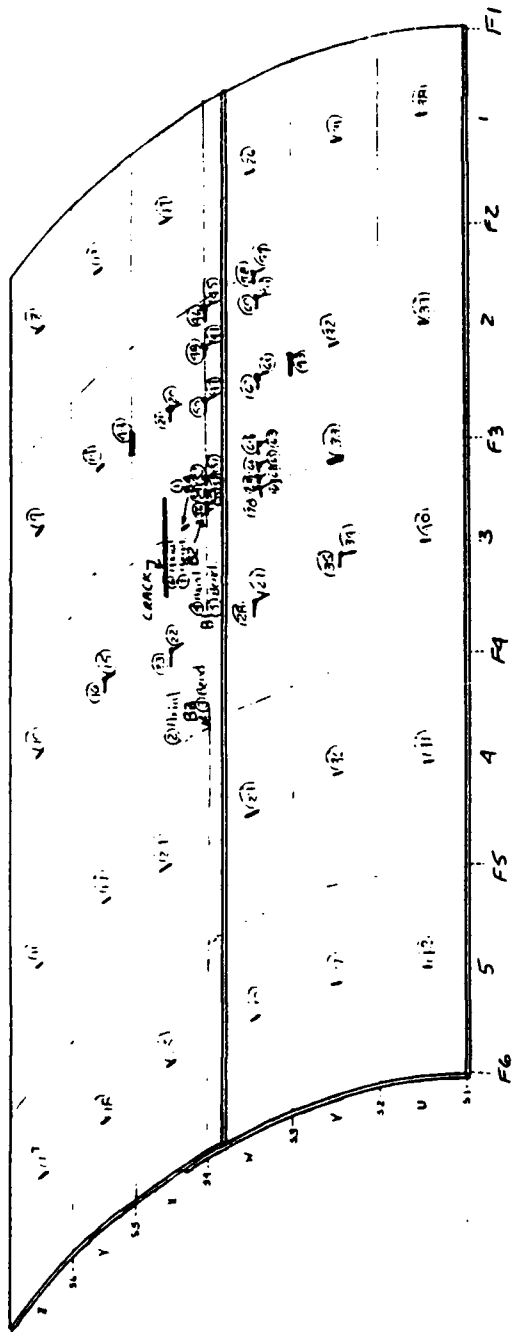


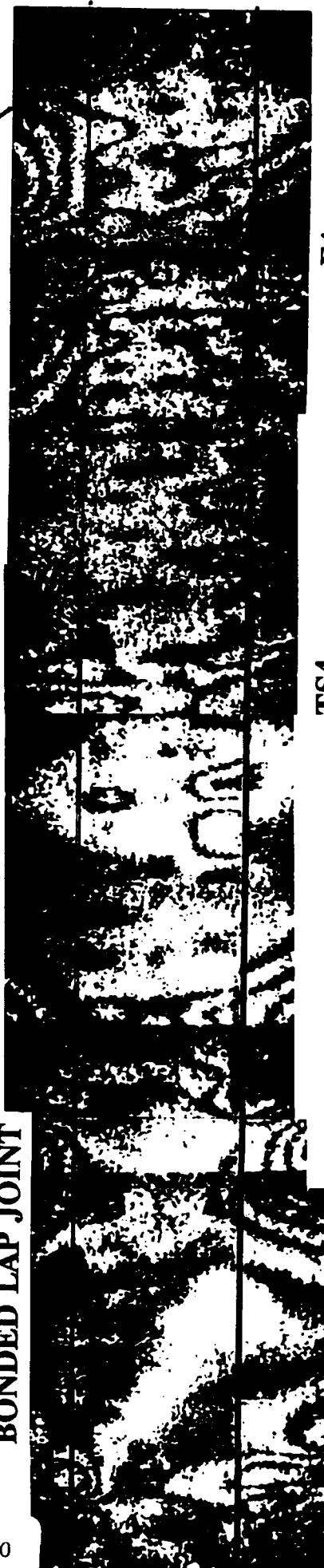
FIGURE 5 An EDM notch on both sides of a rivet hole is seen at left using shearography and at right in a finite element model of a fatigue crack.



BONDED LAP JOINT

UNBONDED LAP JOINT

MSD LINKUP



TS5

TS4

F4

LAP JOINT UNBONDING AND MSD LINKUP

A finite element model of the crack (0.26) and 0.68 in. long) shows the very high strain concentration, value of 5, at the crack tips. While the shearography image shows the strain concentration factor of 2 at the tip, the EDM notch test specimen did not exhibit the large strain concentration at the crack tip due to lack of fatigue sharpening of the crack. EDM notches are more difficult to detect for this reason than a sharpened fatigue crack.

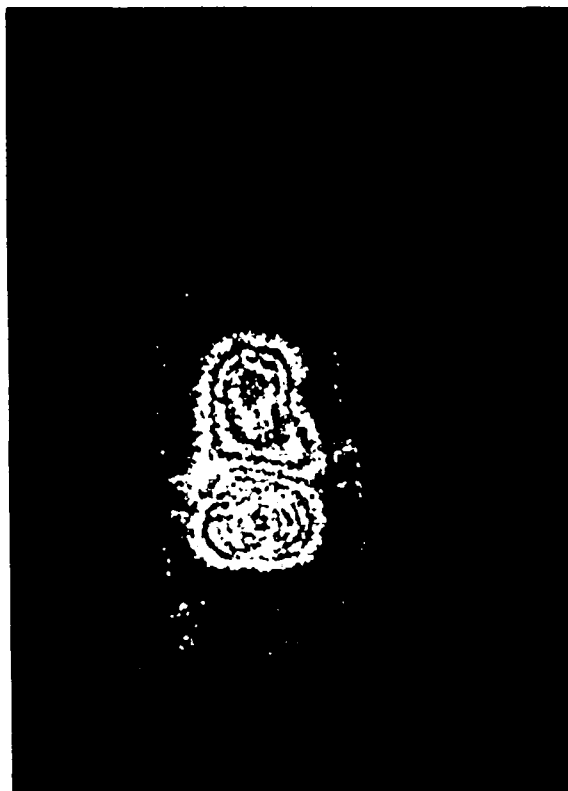
Lap Joint Inspection

In bonded and riveted lap joints, such as found in the fuselage lap joint on the Boeing 737, tensile loading of the joint by pressurization allows the strain concentrations around the rivets and the bonded joint to be observed with shearography. A test fixture, manufactured for the Transportation Systems Center, DOT was used for the pressurization and fatigue cycling of fuselage coupons. Artificial cracks, fatigue damage and unbonded areas could be easily observed with shearography.

At low pressurization differentials, shearography was used to observe the strain concentration factors at rivet holes. It was found that with a differential pressure of only 0.04 psi between the shearography reference image and the final test image, the lap joint showed very low strain concentration factors at the site of well installed rivets and well bonded lap joint skins. Loose rivets or unbonds in the lap joint showed up at strain concentrations. In one test, a single loose rivet in a 36 inch section of the lap joint is easily observed. Figure shows the results of a shearography examination of a 737 lap joint with only 0.04 psid.



A properly installed skin patch on an aluminum honeycomb helicopter panel shows no signs of delamination when tested with the ES-9400.



Defective repair in same panel showing a 1 x 2 inch area is debonded. Test time was 12 seconds.

SHEAROGRAPHY INSPECTION OF BONDED REPAIR TO ALUMINUM HONEYCOMB PANEL



NDT OF COMPOSITE REPAIRS

FIGURE 8

Shearography NDT of Composite Repair Patch in graphite panel with Nomex honeycomb. Repair on the left is free of debonds. Repair on the right has a debond just to the right of center.

Shearography Inspection of Honeycomb and Composite Repairs On-aircraft

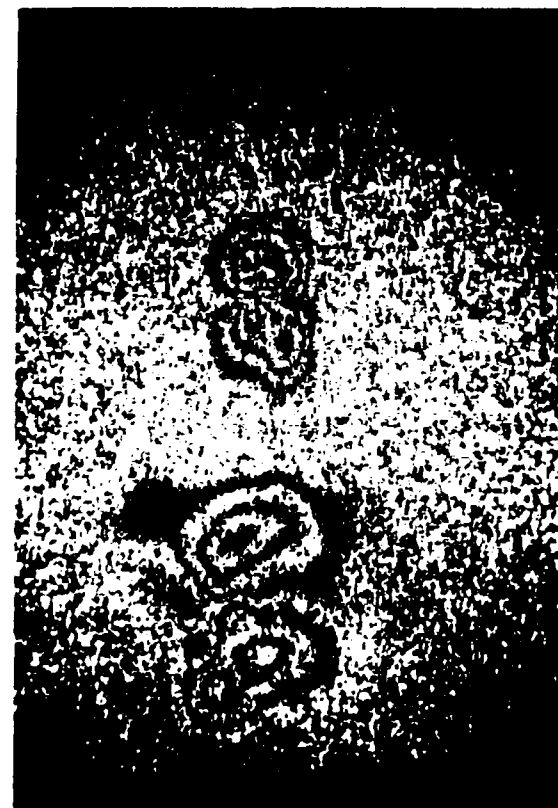
On-aircraft NDT of repairs to honeycomb panels made of aluminum or composites with conventional NDT techniques are very difficult at best due to the nonhomogeneity of the local structure. The local build-up of repair patches make the use of impedance bond testers very questionable. In most cases, the use of through transmission ultrasonics is impossible, while reflection ultrasonics is slow and unreliable. Determination of the far side integrity from a single side is very difficult unless the operator is using shearography with vacuum loading, such as the ES-9400.

By vacuum stressing the skin of the repair, unbonded or weakened areas in the repair as well as far side honeycomb debonds will be detected. Figure 7 shows an aluminum helicopter panel made of 2 1/2 inch thick aluminum honeycomb and doubled skins after two repairs. The defective repair patch is easily detected in seconds and is detectable from the far side of the panel.

Repairs in composite honeycomb and solid laminates are also easily evaluated with vacuum loading shearography. Figure 8 shows a repair in a graphite skin of a honeycomb aircraft panel. Both a good repair and a poor repair with a small skin to core debond are shown.

Shearography Inspection of Impact Damage in Composites

Finally, shearography has been used on-aircraft for the detection of impact damage to composite structures. Recent studies on the Harrier AV-8B have shown that the detection of impact damage to the lower wing skin panels made from graphite epoxy is simple with the ES-9400 using vacuum loading or thermal loading. The equipment fastens to the aircraft with reduced holding vacuum and



COMPOSITE WING PANEL INSPECTION

FIGURE 9 Left photo shows the shearography test result of impact damage on the Harrier AV-8B lower wing skin. Photo at right is a close up showing actual fiber break out. Test time was 2 seconds.

proceeds with the test in seconds. Figure 9 shows an operation impact damage detected with the ES-9400 where no visible damage was detected.

Conclusions

Electronic shearography has been demonstrated to offer significant and unique NDT capability for on-aircraft inspection of the following aircraft maintenance areas:

1. Detection of cracks in skins with pressurization loading to 0.04 psid.
2. Detection of debonds in lap joints.
3. Detection of corroded aluminum honeycomb.
4. Detection of poor or improper repairs to aluminum and composite honeycomb, as well as composite laminates.
5. Detection of impact damage in graphite epoxy or thermoplastic aircraft structures.

Shearography offers identical detection capability both in production as well as in the field on-aircraft. Very high throughputs are obtainable with significant cost savings.

RELIABILITY & QUALITY CONTROL IN FRACTURE MECHANICS ANALYSES
USING THE P-VERSION FINITE ELEMENT PROGRAM, MSC/PROBE

Michael J. Heskitt

28 September 1990

The MacNeal-Schwendler Corporation

St. Louis Office

1600 S. Brentwood Blvd., Suite 840

St. Louis, Mo. 63144

Tel: (314)961-6960 Fax: (314)962-4295

MSC/PROBE Release 4.1

FRACTURE MECHANICS COMPUTATIONS WITH MSC/PROBE

TABLE OF CONTENTS

	<u>Page</u>
1.0 Introduction.....	3
2.0 Quality Control in MSC/PROBE.....	3
2.1 Estimated Error in the Energy Norm.....	4
2.2 Elemental Equilibrium and Stress Continuity Between Elements.	4
2.3 Convergence of Functionals of Interest.....	4
3.0 Planar Fracture Mechanics.....	5
3.1 Extraction Techniques for Planar Models.....	5
3.2 Planar Example Problem:	
Cracked Panel Subjected to Shear and Tension.....	6
3.2.1 Problem Description.....	6
3.2.2 Mesh Design and Boundary Conditions.....	7
3.2.3 Model Checkout and Solution Verification.....	9
3.2.4 Stress Intensity Variation with Crack Length.....	13
3.3 Axisymmetric Example Problem:	
Rod with a Circular Penny Crack.....	14
3.3.1 Problem Description.....	14
3.3.2 Mesh Design and Boundary Conditions.....	15
3.3.3 Model Checkout and Solution Verification.....	16
3.3.4 Stress Intensity Variation with Crack Length.....	18
4.0 Solid Fracture Mechanics.....	19
4.1 Extraction Techniques for Solid Models.....	20
4.2 Solid Example Problem:	
Plate with an Elliptical Surface Crack.....	23
4.2.1 Problem Description.....	23
4.2.2 Mesh Design and Boundary Conditions.....	24
4.2.3 Model Checkout and Solution Verification.....	25
4.2.4 Results.....	28
5.0 Summary and Conclusions.....	31
6.0 References.....	32
7.0 Appendix.....	33

1.0 INTRODUCTION

Methods based on linear elastic fracture mechanics are of great importance in evaluating the strength and durability of structural and mechanical systems. The Finite Element Method (FEM) has become increasingly popular for fracture mechanics computations, and many commercial FEM packages now contain fracture mechanics capabilities. Assessing the quality and reliability of the FEM results has always been a difficult and tedious task. Global energy, local error indicators, and convergence of the appropriate functionals, must all be checked to determine the accuracy of the FEM solution. These procedures are often neglected in production environments due to time constraints, and thus the quality of the finite element solution is often dependent on the experience of the analyst.

MSC/PROBE contains fracture mechanics extraction procedures developed specifically for the p-version of the finite element method. These techniques are extremely efficient and easy to use. This, along with the explicit quality control features, provides an excellent tool for performing fracture mechanics analyses and verifying the accuracy of the results. This report discusses the quality control procedures in MSC/PROBE and demonstrates both planar and solid fracture mechanics computations through examples.

2.0 QUALITY CONTROL IN MSC/PROBE

To be complete, quality control procedures in the FEM must contain some form of an evaluation of the error in the overall strain energy, the local contribution of errors by elements, and the convergence of the data of interest. Proper evaluation of these conditions is very laborious and hence impractical with conventional h-version FEM programs. MSC/PROBE includes features which make these tests easy and straightforward to perform. Each of the quality control procedures are discussed in the following sections, and selected tests are demonstrated in the example problems.

2.1 ESTIMATED ERROR IN THE ENERGY NORM

MSC/PROBE automatically provides a sequence of solutions, corresponding to increasing polynomial degree (p-level) shape functions, from which an estimate of the exact strain energy can be obtained. This estimated exact strain energy is then compared to the strain energy of the current p-level solution and the error in the energy norm is computed. The estimated relative error in the energy norm provides feedback to the overall convergence of the model. It does not, however, reflect the solution quality on a local level. Therefore, this is a necessary but not sufficient check that must be augmented by the local quality control procedures described next.

2.2 ELEMENTAL EQUILIBRIUM AND STRESS CONTINUITY BETWEEN ELEMENTS

Tabulated data displaying elemental freebody information is provided by MSC/PROBE. The freebody data is not the nodal force balance h-version programs customarily provide (which will trivially balance), but rather the integral of the stress vector components computed from the finite element solution along the element boundaries. The relative imbalance in equilibrium for each element, and the continuity of the force resultants along common edges or faces of elements are indicators of the quality of the mesh. If these values are approximately the same for each element, (with respect to each interelement boundary), then the mesh is well designed. This type of feedback is not generally provided from h-version programs.

2.3 CONVERGENCE OF FUNCTIONALS OF INTEREST

To increase the accuracy of the solution in the FEM, whether using h-version, p-version or a combination of the two, the number of Degrees of Freedom (DOF) of the model must be increased in what is called an extension process. Without performing an extension process, no estimate can be made as to how close the data of interest, (i.e. δ , σ , ϵ , K_I , K_{II} , etc.), computed from the finite element solution is to the same data computed from the exact solution. Local error indicators may help guide decisions on where to refine a mesh or where to increase the p-level, but they cannot provide quantitative information on the accuracy of the data computed from the finite element

FRACTURE MECHANICS COMPUTATIONS WITH MSC/PROBE

solution. Because MSC/PROBE automatically provides a sequence of solutions, where the number of DOF increase with the p-level of each element, convergence through the p-extension process can be examined. As such, the convergence of any functional can be shown. This provides the most powerful method for evaluating the solution accuracy available.

3.0 PLANAR FRACTURE MECHANICS

MSC/PROBE-PLANAR consists of modules that allow the analysis of plane stress, plane strain, or axisymmetric problems. In each case, a crack configuration can be modeled and automatic extraction procedures can be used to obtain the stress intensity factors, the strength of the singularity, and the energy release rates. Special superconvergent extraction techniques are used. No special "crack tip" elements are needed in the vicinity of the crack tip. Rather, meshing guidelines, including grading in geometric progression towards the crack tip, are used. A discussion of the extraction techniques follows, and the meshing guidelines are discussed in connection with the example problems.

3.1 EXTRACTION TECHNIQUES FOR PLANAR MODELS

Two new algorithms, called The Contour Integral Method (CIM) and The Cutoff Function Method (CFM), have been implemented in MSC/PROBE. The familiar Energy Release Rate Method (ERRM) is also provided..

The CIM and the CFM are extremely efficient extraction techniques that will separate the Mode I and Mode II stress intensity factors. The methods employ contour and area integrals to extract K_I and K_{II} . A complete description of these methods is beyond the scope of this report but can be found in [1]. The present implementation restricts their use to models with constant thickness (inside the integral path only), with isotropic materials, and where no thermal loading or body forces are present.

The ERRM, as implemented in MSC/PROBE, uses the Parks Stiffness Derivative Method [2]. The crack length is increased by a small amount and the change in the local elemental stiffnesses are used to estimate the change in the strain

FRACTURE MECHANICS COMPUTATIONS WITH MSC/PROBE

energy, ΔU . This is then divided by the change in crack area, ΔA , for the Energy Release Rate (\mathcal{G}):

$$\mathcal{G} = \Delta U / \Delta A \quad (1)$$

The magnitude of the stress intensity vector is then calculated from \mathcal{G} using the relation [3],

$$|\vec{K}| = \sqrt{K_I^2 + K_{II}^2} = \sqrt{\frac{\mathcal{G} E}{(1-\nu^2)}} \quad (\text{psi } \sqrt{\text{in}}) \quad \text{for Plane Strain,} \quad (2.a)$$

or

$$|\vec{K}| = \sqrt{K_I^2 + K_{II}^2} = \sqrt{\mathcal{G} E} \quad (\text{psi } \sqrt{\text{in}}) \quad \text{for Plane Stress,} \quad (2.b)$$

where E is the Modulus of Elasticity and ν is Poisson's ratio for the material.

Computationally, the ERRM is somewhat less efficient than either the CIM and the CFM, and it does not separate K_I and K_{II} , but it can be used for almost any crack/model configuration without restrictions on the thickness, materials, or loading conditions. All three methods will converge to the same results, although the CFM has been shown to converge more rapidly than the other two methods [1].

3.2 PLANAR EXAMPLE PROBLEM: CRACKED PANEL SUBJECTED TO SHEAR AND TENSION

3.2.1 PROBLEM DESCRIPTION

The first fracture mechanics example discussed in this paper is a large flat panel with a crack located near one edge. The panel is loaded in tension (normal to the crack) as well as in shear. The panel configuration, material properties, and loading are shown in Figure 3.1.

This problem contains both Mode I and Mode II excitations of the crack. The crack half-length, (a) , will be varied from .2 inches to .8 inches to illustrate the convenient procedures provided within MSC/PROBE for investigating the stress intensity variation with crack length.

FRACTURE MECHANICS COMPUTATIONS WITH MSC/PROBE

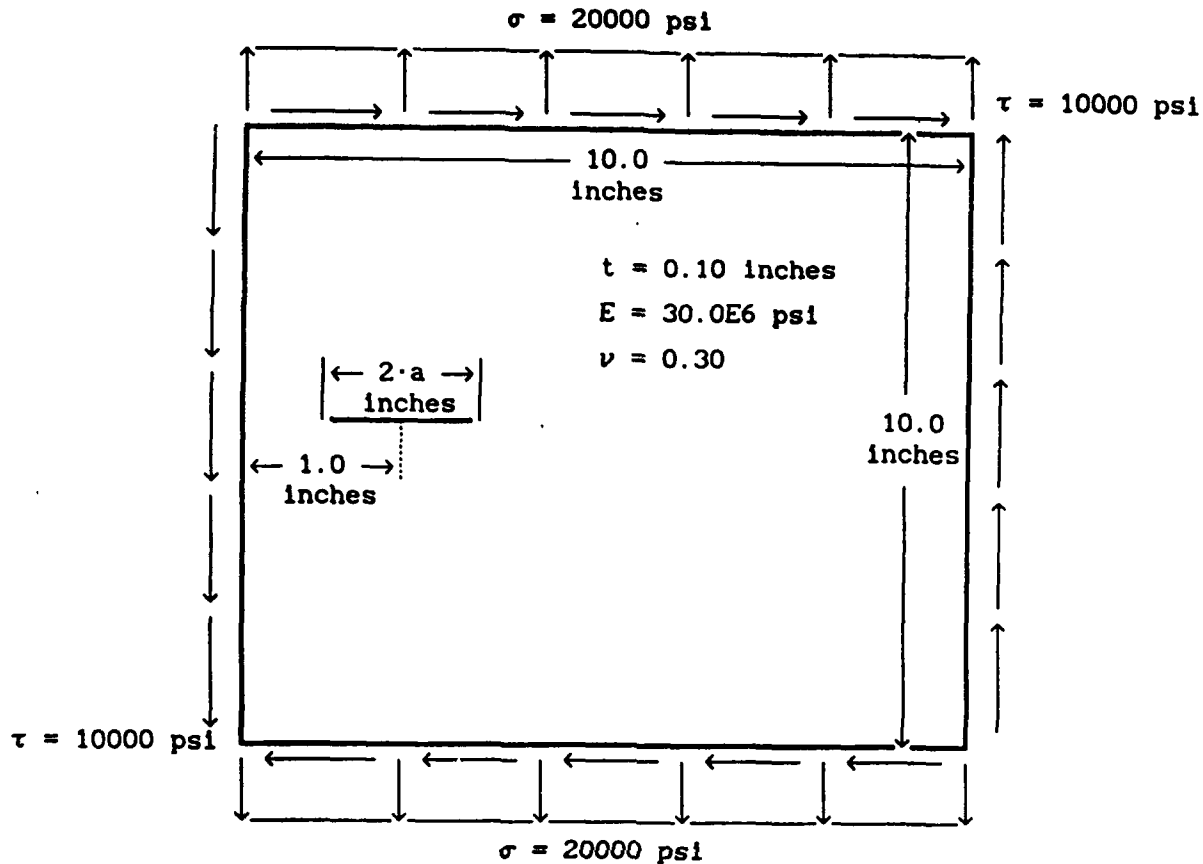


FIGURE 3.1: CRACKED PLATED SUBJECTED TO SHEAR AND TENSION

3.2.2 MESH DESIGN AND BOUNDARY CONDITIONS

Meshing fracture mechanics problems with traditional h-version programs is inherently cumbersome due to the stringent restrictions that are placed on the size and shape of an h-version element. This makes transitions from important areas with high stress gradients (i.e. in the locale of a crack tip or stress concentration) to the surrounding regions difficult, with many elements (and DOF) "wasted" in the transition zones. At the crack tip, special quarter point, or singular, elements are often employed to improve the approximation.

By employing the p extension process on properly designed meshes, the rate of convergence is much faster than in the case of the h-version. An important added benefit is that the elements may have much higher aspect ratios. In fracture mechanics applications, this allows far simpler meshes with fewer

FRACTURE MECHANICS COMPUTATIONS WITH MSC/PROBE

elements to be used. Also, no special elements are necessary at the crack tip.

The mesh for this example is shown in Figure 3.2. The complete mesh required only 42 elements. Figure 3.3 shows the areas surrounding the two crack tips magnified. Geometric grading ratios were used to focus the DOF at the crack tips. Grading ratios of 7:1 to 10:1 were used in the two rings of elements surrounding the tip. Two rings, used in this manner, will be sufficient in most cases to assure exponential convergence of the strain energy, and quality results from the fracture mechanics extraction techniques. Many cases will require only one ring of elements.

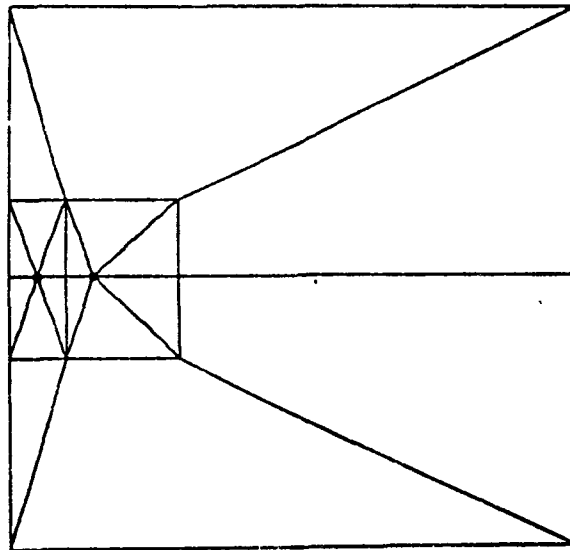


FIGURE 3.2: MSC/PROBE MESH FOR THE CRACKED PLATE

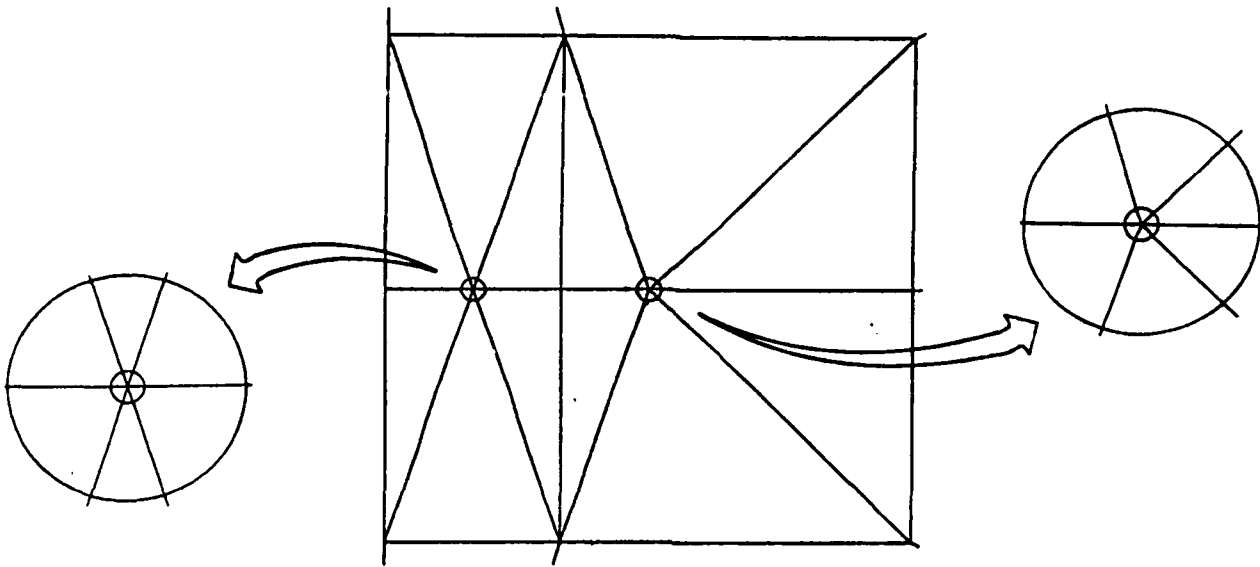


FIGURE 3.3: DETAILS OF THE CRACK TIP REGION

The tension and shear loading were applied as tractions along the outer element boundaries. In this case, only constant tractions were required, but MSC/PROBE allows traction inputs of CONSTANT, FORMULA, or INTERPOLATION, so a great deal of flexibility is provided for load inputs. The loading for this problem is self equilibrating, so constraints are needed only to restrict rigid body motion. These were applied at two of the corner nodes.

3.2.3 MODEL CHECKOUT AND SOLUTION VERIFICATION

The tests performed to establish that the discretization errors were reasonably small are described in this section.

The first check is for the convergence of the strain energy. Figure 3.4 shows a plot of the strain energy and the estimated percent error in the energy norm provided in MSC/PROBE. The estimated percent error in the energy norm at a p-level of 8 is 0.29%. This indicates that the overall accuracy of the finite element solution is well within the range normally expected in engineering computations. This strong convergence in the strain energy is typical for p-extensions on geometrically graded meshes.

FRACTURE MECHANICS COMPUTATIONS WITH MSC/PROBE

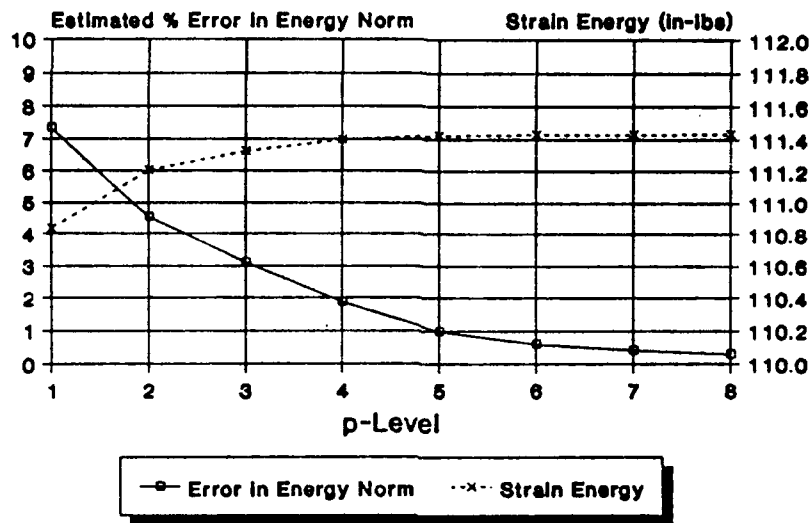


FIGURE 3.4: ENERGY CONVERGENCE FOR THE CRACKED PANEL

The next global check is simply to view the deformed shape to assure that the loads were applied in the proper directions and positions. Figure 3.5 shows the deformed shape of the model. The deformed shape is as would be expected for this type of loading.

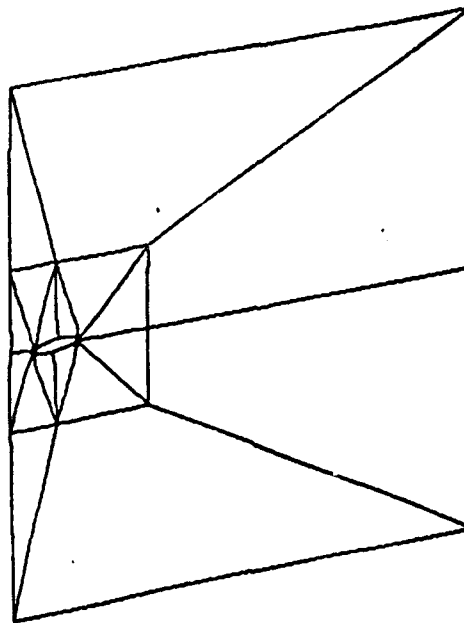


FIGURE 3.5: DEFLECTED SHAPE FOR THE CRACKED PANEL

FRACTURE MECHANICS COMPUTATIONS WITH MSC/PROBE

Several local quality checks were performed before accepting the results. The first was to investigate the continuity of the stresses along the element boundaries. This was done using the *Elemental Stress Report* provided in MSC/PROBE. Another method of visualizing this effect is by using stress contour plots. MSC/PROBE does not average the stress results along elemental boundaries. The results, shown in Figure 3.6, show that, at element boundaries, several small discontinuities occur. A "perfect" solution would display no discontinuities in the contour plots. The contour plot shown in Figure 3.6 is close to this ideal case. Note that the contour was limited to exclude the gradients in the local vicinity of the crack tips for a better display of the contours remote from this region. The contour plot also serves to verify that no reactions are generated at the rigid body constraints. If the applied loads were not in equilibrium, and reactions were generated at the points where the rigid body constraints were applied, we would see local stress concentrations at the constrained points because the nodal constraints would be singular points.

Another local check of the solution quality is the elemental equilibrium. This was investigated via the *Element Freebody Report* provided by MSC/PROBE. All the elements not directly connected to the singular points were found to have less than 1% error in the equilibrium.

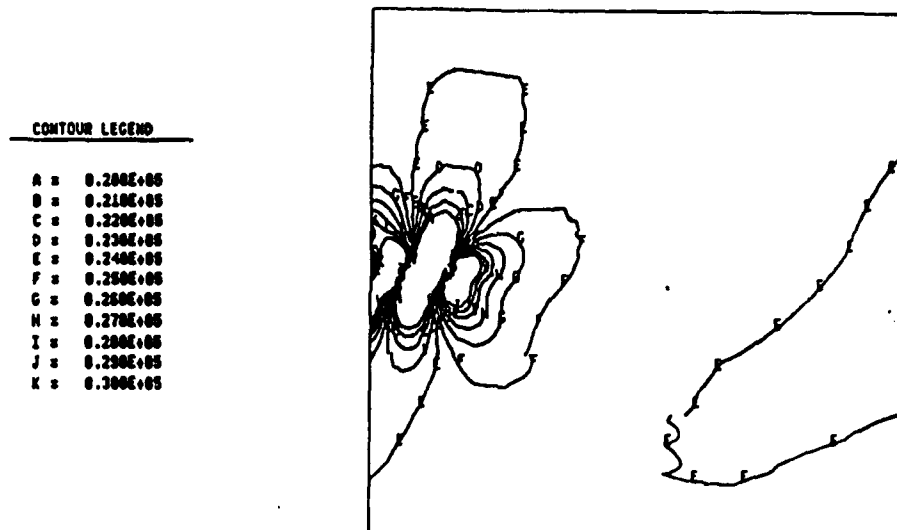


FIGURE 3.6: MAXIMUM PRINCIPAL STRESS CONTOUR PLOT FOR THE CRACKED PANEL

FRACTURE MECHANICS COMPUTATIONS WITH MSC/PROBE

The last and most definitive check of the local solution quality, is to investigate the convergence of the functional of interest. Here we are interested in the Mode I and Mode II stress intensity factors at the end of the crack nearest to the panel edge. All three extraction methods available in MSC/PROBE were used to compare the results for the 1.0 inch crack length. These are shown in Table 3.1 and a graph of $|\vec{K}|$ for the three methods is included in Figure 3.7. The solutions from all three methods at a p-level of 8 agree to within 0.1%. These results are much more accurate than the results from [3] where $K_I = 27300$ (psi $\sqrt{\text{in}}$) and $K_{II} = 13700$ (psi $\sqrt{\text{in}}$).

	CIM			CFM			ERRM
PLEVEL	K_I	K_{II}	$ \vec{K} $	K_I	K_{II}	$ \vec{K} $	$ \vec{K} $
1	36334	12455	38409	29082	9787	30684	32172
2	27012	12322	28690	29761	13782	32797	32748
3	29228	14383	32575	28036	13890	31288	31368
4	27867	13627	31020	28290	13889	31515	31433
5	28414	13820	31596	28217	13724	31377	31311
6	28056	13655	31202	28140	13704	31299	31253
7	28197	13736	31364	28157	13715	31319	31286
8	28127	13704	31287	28145	13713	31307	31281

(Units in psi $\sqrt{\text{in}}$)

TABLE 3.1: CONVERGENCE OF STRESS INTENSITY FACTORS FOR THE CRACKED PANEL WITH A 1.0" CRACK

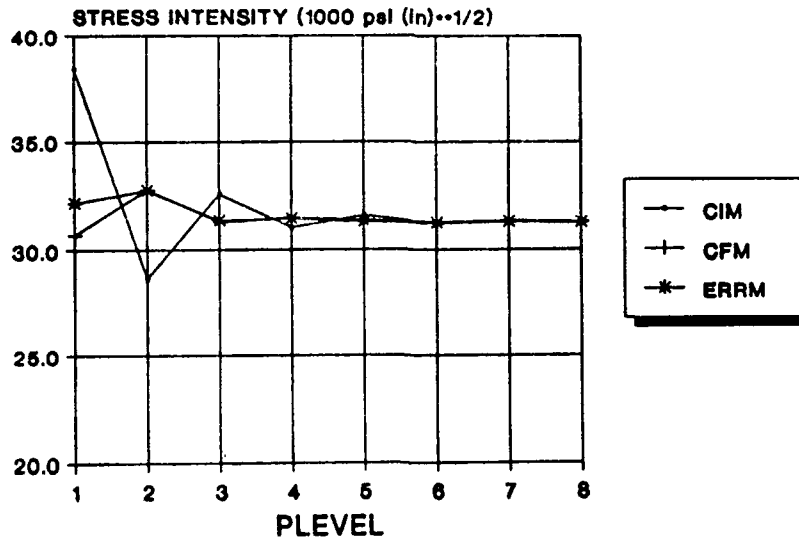


FIGURE 3.7: CONVERGENCE OF THE STRESS INTENSITY VECTOR FOR THE CRACKED PANEL

3.2.4 STRESS INTENSITY VARIATION WITH CRACK LENGTH

A study of the change in the stress intensity factors as the crack grows is greatly facilitated by some of the features in MSC/PROBE. If the circles enclosing the two rings of elements at each crack tip (See Figure 3.3) are defined relative to local coordinate systems at each crack tip, then the cracks can be "grown" by simply changing the location of the two local coordinate systems. The nodes and elements around the crack tip are associated with these circles, so they will move along with the new tip locations. No new mesh is required because the p-version elements are tolerant of large aspect ratios and skew.

The crack length was varied from 0.2 inches to 0.8 inches, and was centered at 1.0 inch from the panel edge. Details of the resulting mesh for the two extreme cases are shown in Figure 3.8. The results for the Mode I and Mode II stress intensity factors vs. the crack length are shown in Figure 3.9. Also shown are the results from [3] for comparison.

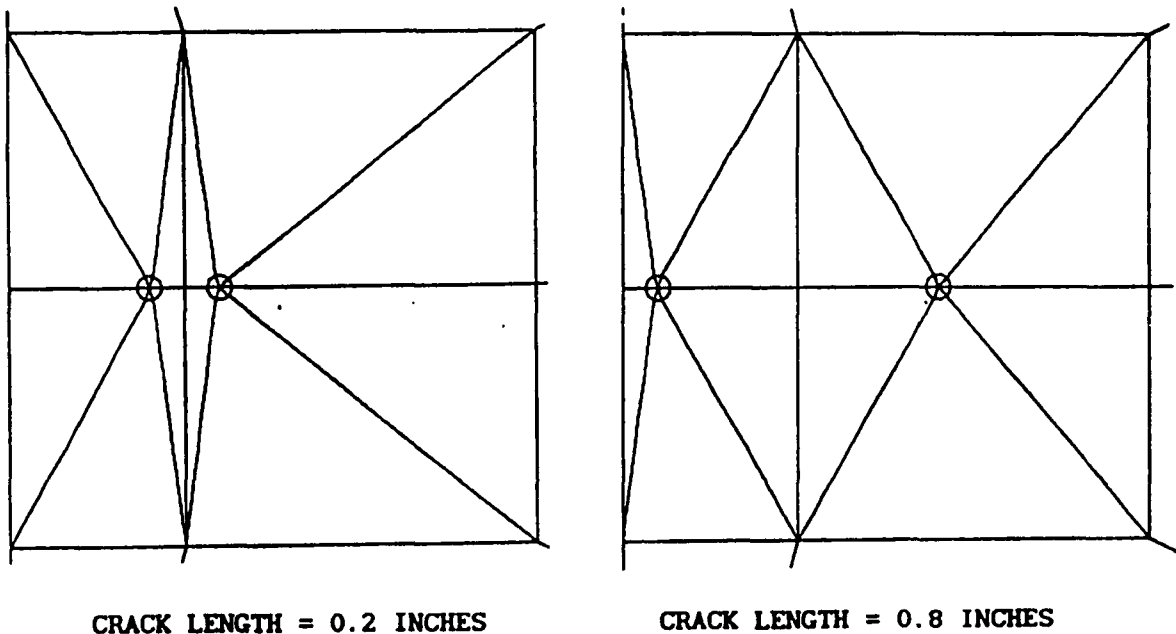


FIGURE 3.8: CRACK TIP MESH DETAILS FOR THE SMALLEST AND LARGEST CRACK SIZES IN THE CRACK GROWTH ANALYSIS

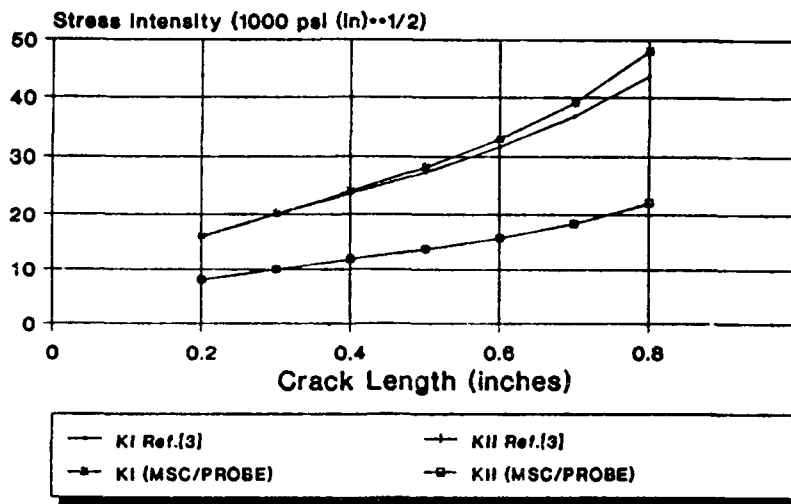


FIGURE 3.9: STRESS INTENSITY RESULTS VS. CRACK LENGTH

3.3 AXISYMMETRIC EXAMPLE PROBLEM: ROD WITH A CIRCULAR PENNY CRACK

3.3.1 PROBLEM DESCRIPTION

The next fracture mechanics example is a circular bar with an imbedded penny shaped crack. The crack is normal to the centerline of the bar. The bar is loaded in uniaxial tension so only Mode I excitation will occur. A cross section of the bar is shown in Figure 3.10. The applied traction at the upper and lower surface is 20000 psi. The material is steel.

This is actually a solid fracture mechanics problem, but the **AXISYMMETRIC** module in **MSC/PROBE-PLANAR** was used. This allows problems of this nature to be solved quickly, with far simpler meshes and less man-time and computer resources than would be needed with a fully solid model. General solid fracture mechanics problems are addressed in Chapter 4.

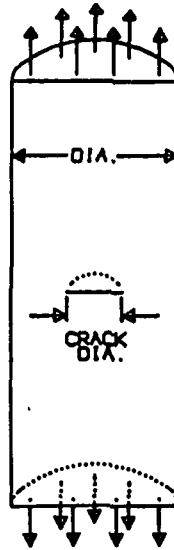


FIGURE 3.10: CIRCULAR BAR WITH PENNY SHAPED CRACK

3.3.2 MESH DESIGN AND BOUNDARY CONDITIONS

The **AXISYMMETRIC** module in **MSC/PROBE-PLANAR** was used for this problem. The model is constructed as the cross section or generating surface that would be swept through 360° to generate the complete solid volume. **MSC/PROBE** then uses a one radian slice of the solid model for the analysis. Therefore, for example, if a 1 psi traction (p) were applied to the upper surface of a cylinder with an outside radius, r_o , the total force that acts on the cylinder is

$$F_{\text{Total}} = p\pi r_o^2 \text{ (lbf)} \quad (3)$$

and the resulting force that will be reported for that "edge" of the model (actually the 1 radian face) is

$$F_{\text{Radian}} = \frac{F_{\text{Total}}}{2\pi} = \frac{pr_o^2}{2} \text{ (lbf/radian)} \quad (4)$$

Meshing guidelines similar to the previous example were used, but in this case, symmetry conditions were employed to reduce the model size. A typical mesh is shown in Figure 3.11 along with a magnification of the crack tip detail. For this problem symmetric boundary conditions are used along the lower face outside the crack front. The left edge is the axis centerline for the bar.

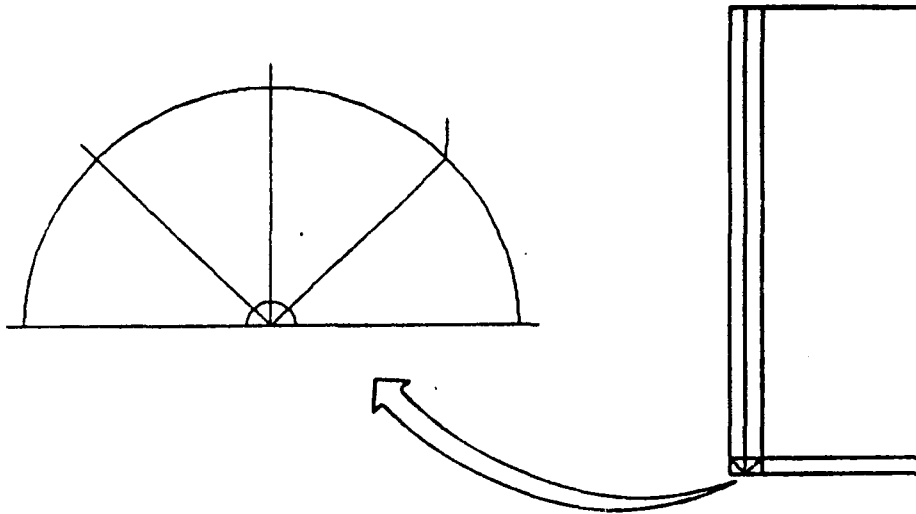


FIGURE 3.11: MSC/PROBE MESH FOR THE CRACKED BAR

3.3.3 MODEL CHECKOUT AND SOLUTION VERIFICATION

Essentially the same procedures as in the first example were used for model checkout and solution verification. The results for the case with a rod diameter of 10 inches and an imbedded crack diameter of 0.2 inch ($a/r = 0.02$) will be shown here. Other cases with increasing crack-size/rod-diameter ratios are presented in the next section.

The strain energy convergence and estimated error in the energy norm are shown in Figure 3.12. Again, excellent convergence was obtained with the percent relative error estimated at 0.05% for the p-level of 8. We should note that it is not necessary to obtain the entire sequence of solutions, to $p=8$, allowed by MSC/PROBE. Good engineering accuracy is obtained in this case by $p=5$ or $p=6$. The entire sequence is shown here for purposes of illustration.

FRACTURE MECHANICS COMPUTATIONS WITH MSC/PROBE

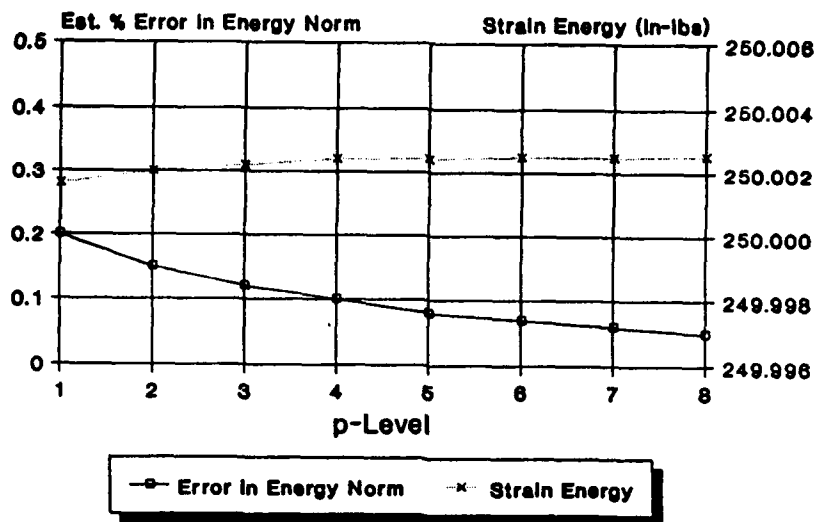


FIGURE 3.12: ENERGY CONVERGENCE FOR THE CRACKED ROD

The deflected shape of the local area around the crack tip is shown in Figure 3.13. The Mode I displacements are apparent in this figure.

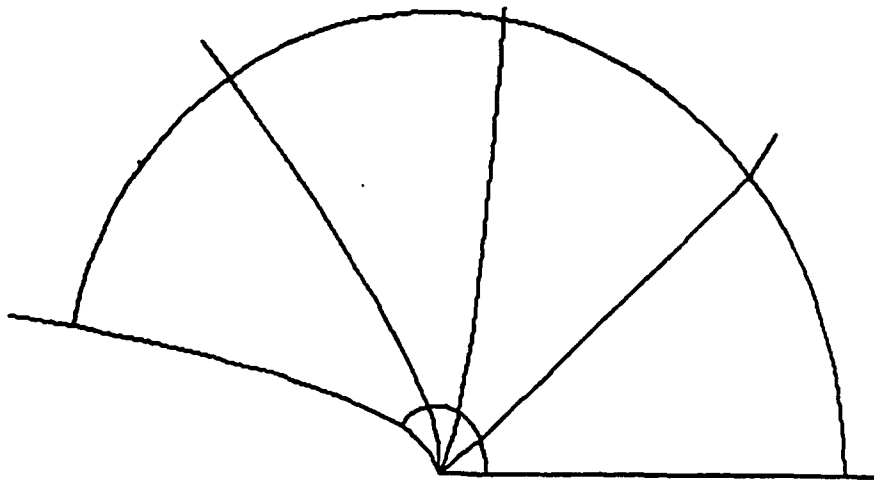


FIGURE 3.13: DEFLECTED SHAPE OF THE CRACK FACE

Again, other local indicators were checked to assure the validity of the local solution. These included elemental equilibrium from the *Element Freebody*

FRACTURE MECHANICS COMPUTATIONS WITH MSC/PROBE

Report and continuity of stresses between elements using the *Element Stress Report* and contour plots. Lastly, the convergence of the stress intensity vector magnitude, $|\vec{K}|$, was checked and is shown in Figure 3.14. In this case, since $K_{II} = 0.0$, $K_I = |\vec{K}|$, and the ERRM was used to extract the results (The CIM and CFM are not available in the AXISYMMETRIC Module). The ERRM uses the plane strain assumption for calculating $|\vec{K}|$ from the energy release rate in the AXISYMMETRIC Module.

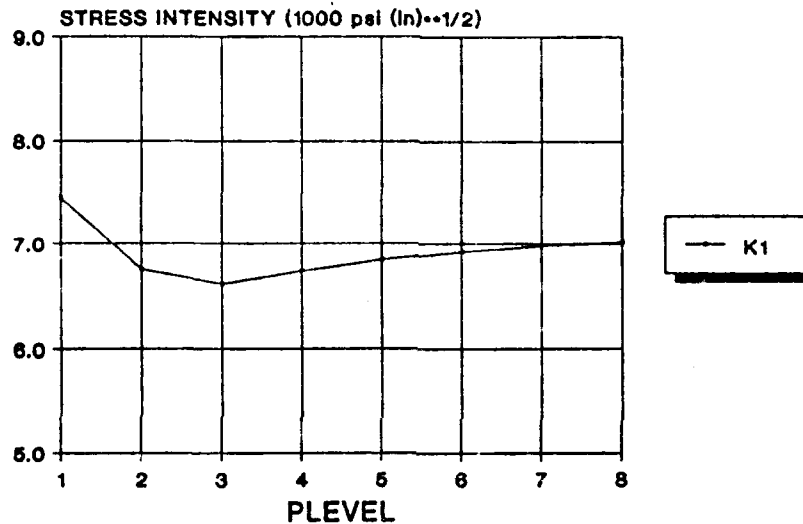


FIGURE 3.14: K_I CONVERGENCE FOR A 10" DIA ROD WITH A 0.1" DIA CENTER CRACK

3.3.4 STRESS INTENSITY VARIATION WITH CRACK LENGTH

To study the effect of the crack diameter to rod diameter ratio (a/r) on the stress intensity factor, several MSC/PROBE models were run. In the previous example, the crack was grown by simply moving a local coordinate system located at the crack tip. In this case, the outer diameter of the rod, which was defined as a line, is moved towards the centerline, while keeping the crack tip constant, to increase the ratio of the crack size to the rod diameter. The resulting mesh for the two extreme cases and one intermediate case are shown in Figure 3.15. The results from the crack length variation are shown in Figure 3.16 and are compared with results from [3]. Once again, the results obtained from MSC/PROBE are more accurate than those presented in [3].

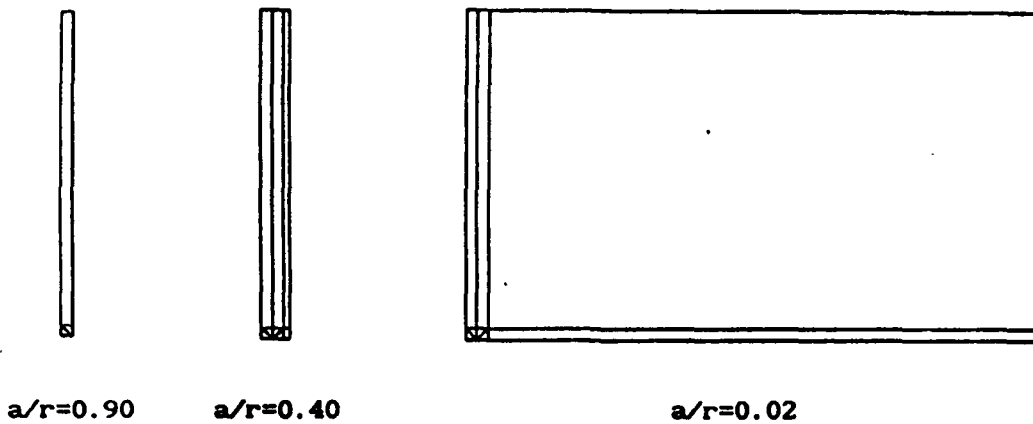


FIGURE 3.15: MSC/PROBE MESHES FOR CRACK GROWTH STUDY OF ROD MODELS

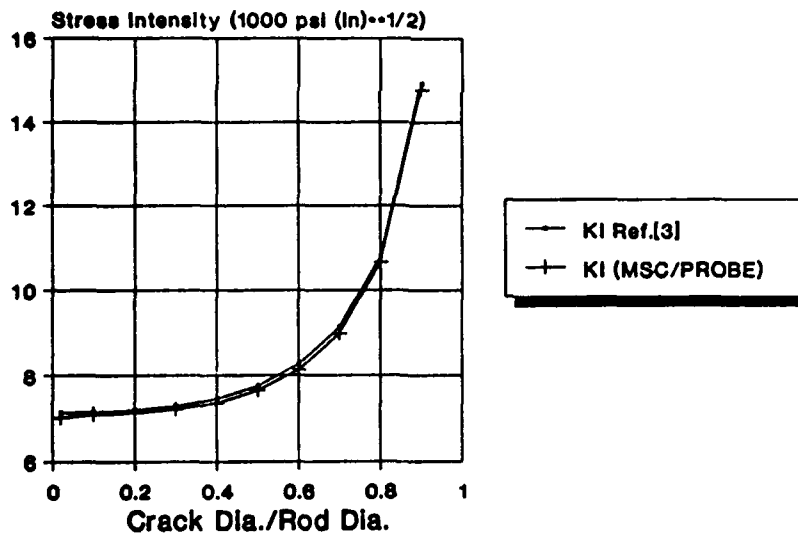


FIGURE 3.16: STRESS INTENSITY RESULTS VS. CRACK LENGTH FOR THE ROD

4.0 SOLID FRACTURE MECHANICS

MSC/PROBE can also be used for fracture mechanics analysis of solids. One case, the axisymmetric problem, although analyzed using the AXISYMMETRIC module in MSC/PROBE-PLANAR, represents a solid fracture mechanics problem.

FRACTURE MECHANICS COMPUTATIONS WITH MSC/PROBE

More general solid problems can be analyzed using MSC/PROBE-SOLID. Although in the current release there are no automatic extraction capabilities for stress intensity factors for solid problems, several methods may be used to extract fracture mechanics results reliably with a reasonable amount of effort. One method is discussed in the next section, and demonstrated with an example.

4.1 EXTRACTION TECHNIQUES FOR SOLID MODELS

Several aspects of the p-version, and features in MSC/PROBE make possible the construction of simple meshes for solid crack problems. The robust nature of the p-version allows larger aspect ratios and skew angles which greatly facilitate transitioning from the area around a crack tip to the surrounding regions. This is especially important in three dimensions. Also, the smooth nature of the solution and the ability to examine the convergence of the displacement and stress data at any point within the model allows reliable use of the extraction methods. In general, complete quality control tests are extremely difficult to perform with traditional h-version programs and are rarely used in professional practice.

Equations of the stress and displacement distributions in the region around a crack were developed by Irwin (1957) based on the method of Westergaard (1939) and are repeated in [3] and [4]. Specifically, the displacement field along the crack face can be used to calculate the Mode I, Mode II, and Mode III stress intensity factors using the equations [3],

$$v = \frac{K_I}{G} \sqrt{\frac{r}{2\pi}} \sin \frac{\theta}{2} \left[2-2\nu - \cos^2 \frac{\theta}{2} \right] + \text{Higher Order Terms} \quad (5a)$$

$$u = \frac{K_{II}}{G} \sqrt{\frac{r}{2\pi}} \sin \frac{\theta}{2} \left[2-2\nu + \cos^2 \frac{\theta}{2} \right] + \text{Higher Order Terms} \quad (5b)$$

$$w = \frac{K_{III}}{G} \sqrt{\frac{r}{2\pi}} \sin \frac{\theta}{2} + \text{Higher Order Terms} \quad (5c)$$

where G is the material Shear Modulus, θ is the angle measured from the

FRACTURE MECHANICS COMPUTATIONS WITH MSC/PROBE

extension of the crack face into the material (i.e. the x-axis), r is the distance from the crack tip, and the u , v , and w displacements follow the conventions of the x , y , and z axes, respectively, as shown in Figure 4.1. Equations (5a) and (5b) assume plane strain in the x - y plane and Equation (5c) assumes plane strain in the x - z plane. We note that the plane strain assumption is only an approximation to the fully three-dimensional case, however, since fracture mechanics data are generated in essentially two-dimensional experiments, such approximations are generally accepted.

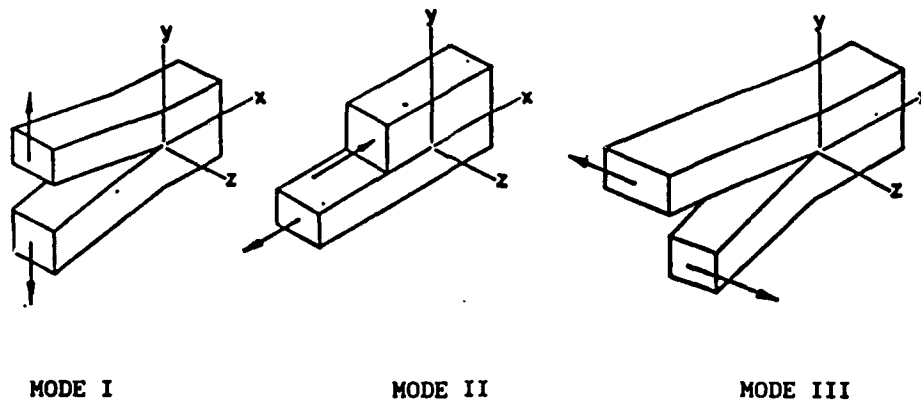


FIGURE 4.1: BASIC MODES OF CRACK SURFACE DISPLACEMENTS

If the limit of equations (5) is taken as $r \rightarrow 0$, the higher order terms can be neglected. Equations (5) can then be rearranged to solve for K_I . Doing this and recognizing that on the crack face $\theta = 180^\circ$, so $\cos(\theta/2) = 0.0$ and $\sin(\theta/2) = 1.0$, gives

$$K_I = \lim_{r \rightarrow 0} \left\{ \frac{vG}{(2-2\nu)} \sqrt{\frac{2\pi}{r}} \right\} \quad (6a)$$

$$K_{II} = \lim_{r \rightarrow 0} \left\{ \frac{uG}{(2-2\nu)} \sqrt{\frac{2\pi}{r}} \right\} \quad (6b)$$

$$K_{III} = \lim_{r \rightarrow 0} \left\{ wG \sqrt{\frac{2\pi}{r}} \right\} \quad (6c)$$

FRACTURE MECHANICS COMPUTATIONS WITH MSC/PROBE

For plane stress (used where the crack front reaches a free surface) equations (5) and (6) are modified by replacing Poisson's ratio, ν , with $\nu/(1+\nu)$.

In the finite element method, one can only expect accurate results some finite distance away from the crack tip, which is a singularity. Therefore, to use this method, the analyst must be able to determine the zones where the finite element solution is inaccurate ("close" to the crack tip), and where the higher order terms become dominant ("far" from the crack tip). The region between these zones should be linear with respect to r , and can be used to extrapolate to $r \rightarrow 0$ for the stress intensities. This limiting process is displayed graphically in Figure 4.2.

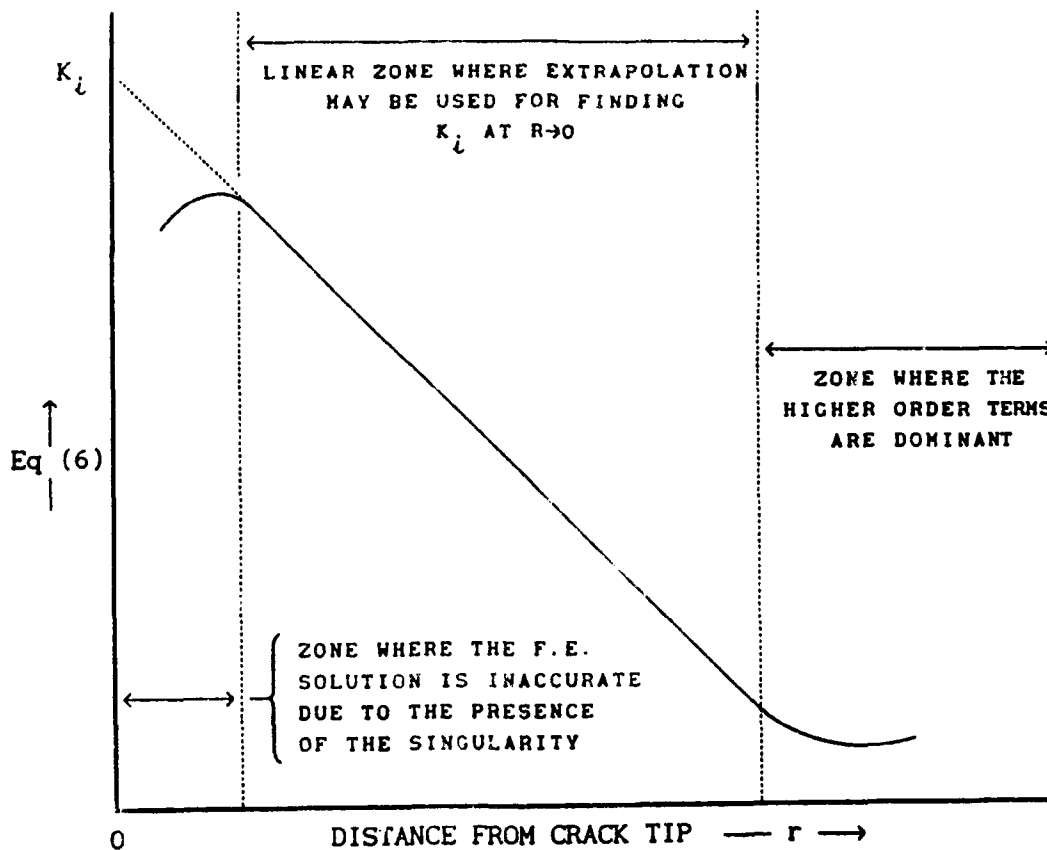


FIGURE 4.2: SCHEMATIC VIEW OF THE DISPLACEMENT METHOD FOR STRESS INTENSITY COMPUTATIONS

In MSC/PROBE, the displacements can be output along any line using any local coordinate system (in this case; in the crack plane starting at the point of

FRACTURE MECHANICS COMPUTATIONS WITH MSC/PROBE

interest on the crack tip and normal to the crack front). The results can then be multiplied by the appropriate factors in Eq. (6), and plotted as in Figure 4.2. The extrapolation can then be performed for the stress intensity factor. One very important feature is that the zone where the displacements are inaccurate can be readily identified by examining the convergence of the displacements as the p-level is increased. This procedure is demonstrated in the following example.

4.2 SOLID EXAMPLE PROBLEM: PLATE WITH AN ELLIPTICAL SURFACE CRACK

4.2.1 PROBLEM DESCRIPTION

The solid fracture mechanics example problem consists of a large rectangular plate with a semi-elliptical surface crack. The plate is loaded in bi-axial tension and in-plane shear. The plate is 10.0 inches on each side and 0.40 inches thick. The crack is located on the centerline with a minor half-axis (into the plate thickness) of 0.10 inches and a major half-axis (on the plate surface) of 0.30 inches. See Figure 4.3 for the problem geometry. The applied tensile traction is 20000 psi and the applied shear traction is 10000 psi. The material is steel.

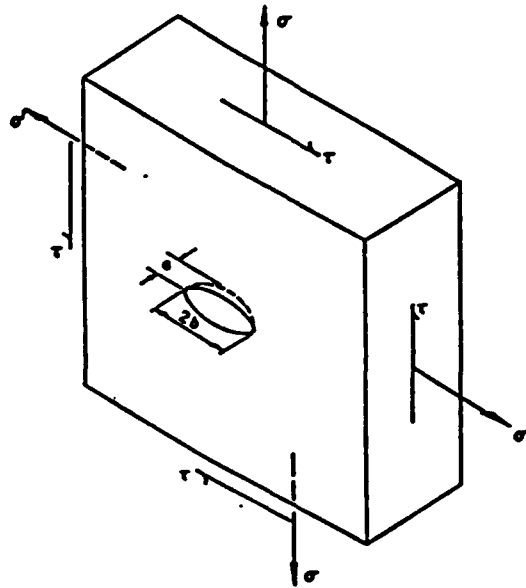


FIGURE 4.3: PLATE WITH A SEMI-ELLIPTICAL SURFACE CRACK

4.2.2 MESH DESIGN AND BOUNDARY CONDITIONS

To allow only one quarter of the plate to be discretized, symmetric boundary conditions were used for the tension loading, and anti-symmetric conditions were used for the shear loading. The tension load parallel to the crack face does not excite any of the three modes, so it is ignored. The finite element mesh consists of 287 elements. The model is shown in Figure 4.4 with a magnification of the area around the crack tip. Figure 4.5 shows the bottom layer of elements along the crack face for more clarity.

Characteristic of p-version meshes, this model shows how rapid transitions can be made from a fine to a coarse mesh. This is especially important in solid models to reduce the number of DOF necessary for the analysis. Another method used to limit the number of DOF was to restrict the polynomial order of the elements in non-critical regions, while increasing the p-level in only the critical areas. MSC/PROBE allows predefined sets of elements to be assigned a fixed p-level. Here, elements removed from the crack zone were limited to a p-level of 2, while the p-level of the elements in the crack zone were increased from 1 to 6 to provide information on convergence. This kept the number of DOF for the model below 27,500 for the p-level of 6 solution. The higher p-levels of 7 and 8 were not necessary in this analysis, but if the error estimates and quality control procedures had indicated that greater accuracy was needed, then the higher p-levels could have been run without any changes to the mesh. Only if this last step proved inadequate would the analyst need to make mesh refinements.

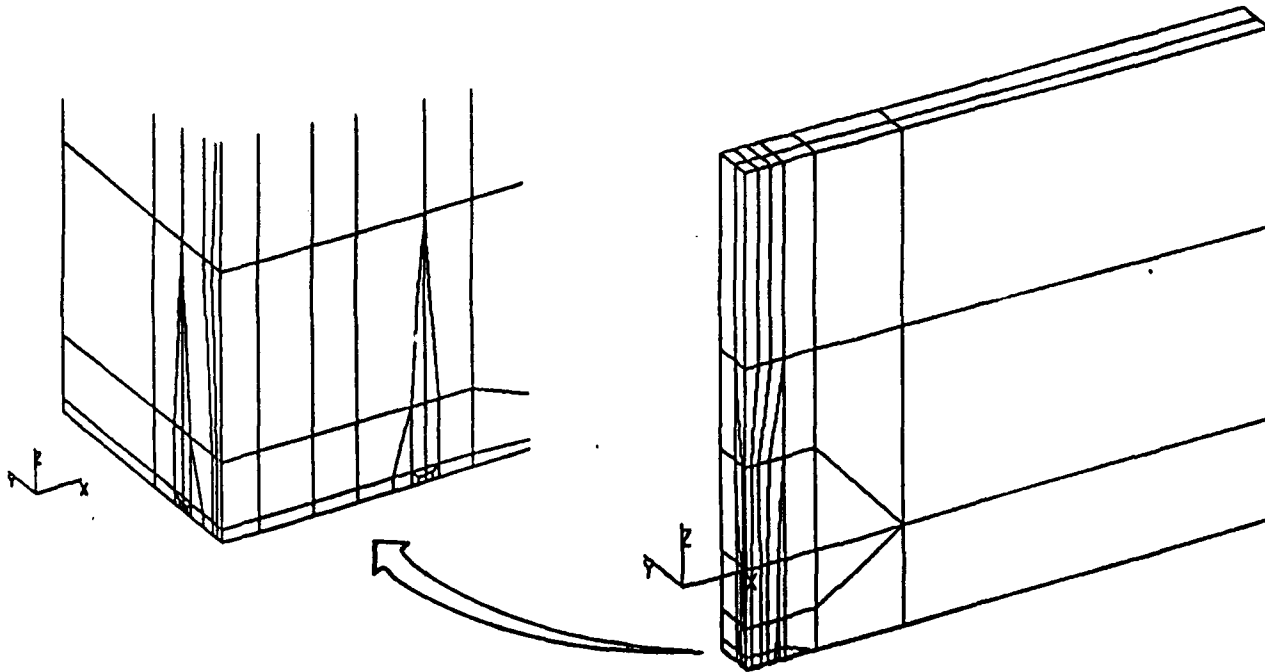


FIGURE 4.4: QUARTER MODEL OF THE PLATE WITH A SURFACE CRACK

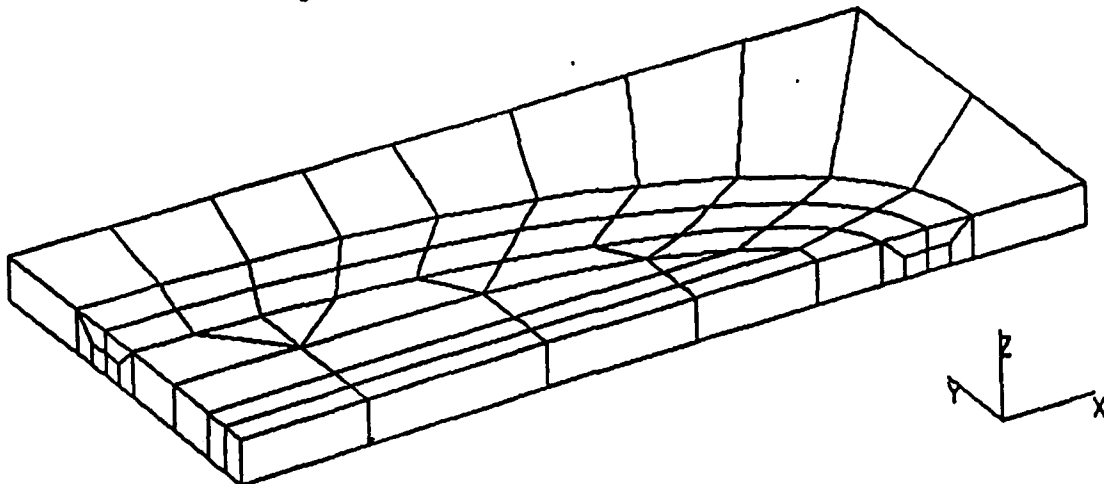


FIGURE 4.5: ELEMENTS ALONG THE CRACK FRONT

4.2.3 MODEL CHECKOUT AND SOLUTION VERIFICATION

As in the planar examples, the first step in verifying the model is to look at the convergence of the strain energy. The estimated error in the energy norm is shown in Figure 4.6 for both the tension and shear load cases.

FRACTURE MECHANICS COMPUTATIONS WITH MSC/PROBE

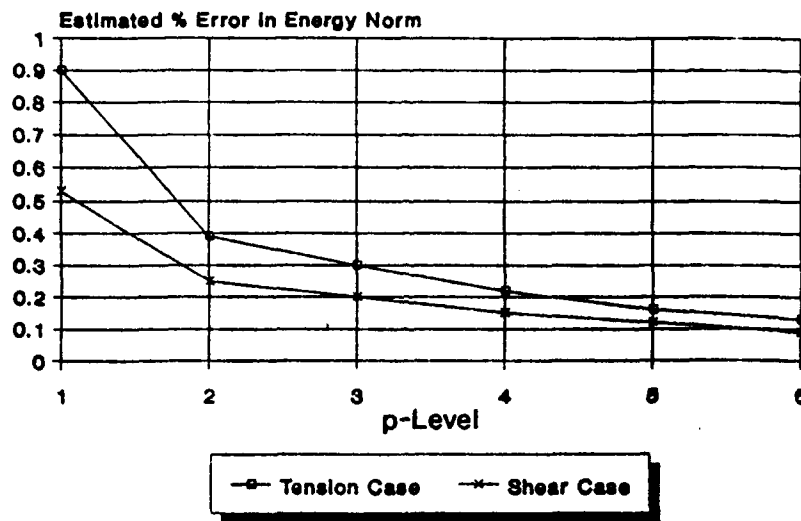


FIGURE 4.6: PERCENT ERROR IN THE ENERGY NORM FOR THE CRACKED PLATE

Another global check of the model is to view the displacements. The overall model displacements were as expected for each load case. Local displacements around the crack tip were also displayed to check proper constraints in the region. Figure 4.7 shows the bottom layer of elements around the crack tip under the tension loading. A refined "data recovery" grid is overlaid on the original p-version elements to allow better displacement visualization from the post-processing program. This is done automatically from the plotting options in MSC/PROBE. The original p-version elements are shown in Figure 4.5.

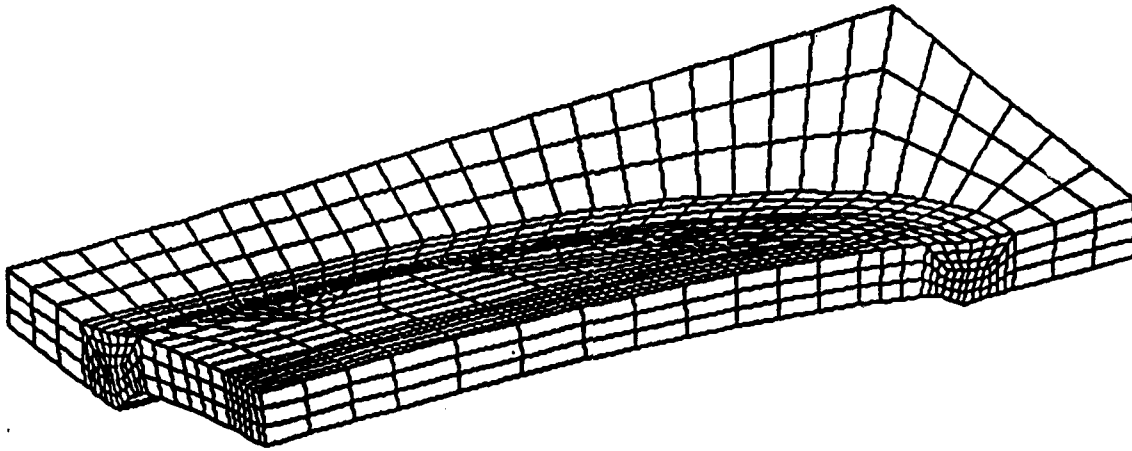


FIGURE 4.7: CRACK FACE DISPLACEMENTS UNDER TENSION LOAD

The elemental equilibrium and stress continuity between the elements were also investigated to assess the quality of the solution. The elements showing the highest percent force imbalance are near the crack front. This can be expected since the crack front is a strong singularity. The proper interpretation of this information is that if greater accuracy is needed in the data of interest, and this accuracy cannot be realized by p-extension, then these elements should be refined. For this particular analysis, the displacements in the region of the crack are the functionals of interest, since these will be used with Eq.(6) to determine the stress intensity factors. Therefore, establishing confidence in the displacement results near the crack tip is necessary.

To evaluate the displacements close to the crack tip, local coordinate systems were used and the displacements relative to the crack face were obtained in the local systems. The convergence of the displacements with respect to increasing p-level is shown in Figure 4.8 for the position along the centerline of the minor axis of the ellipse. Each line in Figure 4.8 represents the displacement convergence at a point of radius, R , from the crack tip, as the p-level is increased from 1 to 6. As can be seen, for the points closest to the tip (i.e. $R=0.003$ inches) the displacements have not converged. They continue to increase with the p-level. Further away from the

FRACTURE MECHANICS COMPUTATIONS WITH MSC/PROBE

crack (i.e. $R > 0.020$ inches) the displacements have leveled off very well by a p-level of 6. This then establishes the quality of the converged displacements, and the regions within the domain where they have converged. This information is available for a single mesh and additional user interaction is not required.

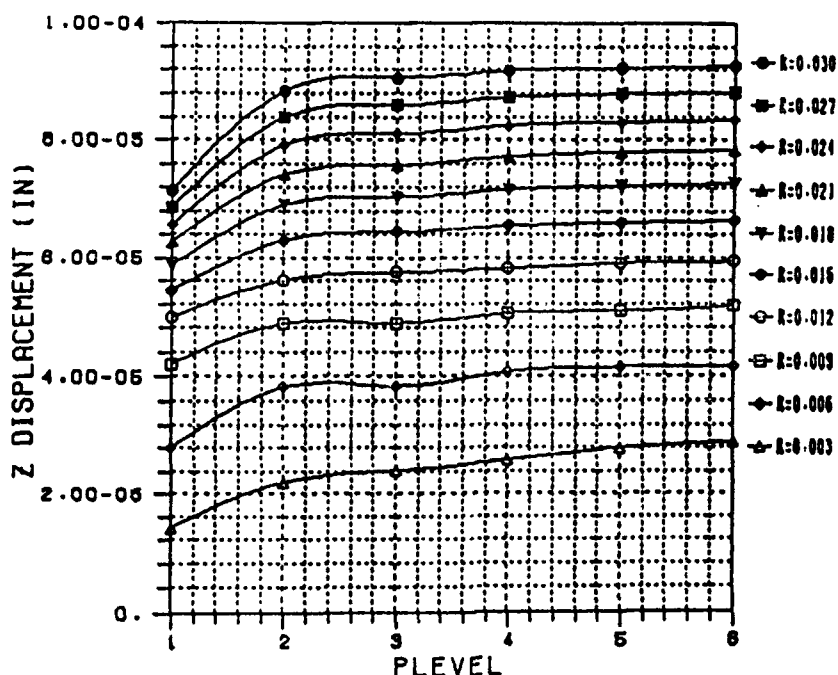


FIGURE 4.8: CONVERGENCE OF DISPLACEMENTS FOR POINTS ALONG THE CRACK CENTERLINE

4.2.4 RESULTS

Once the displacements have been verified, plots similar to Figure 4.2 can be generated at any position for which the stress intensity factors are desired. The plot of Eq.(6) versus the distance from the crack tip, R , is shown in Figure 4.9 for the crack centerline. Here the limiting process is displayed graphically as an extension of the linear portion of the curve to $R=0.00$ inches. The results for K_I and K_{III} at the crack centerline are compared to References [4] and [5] in Table 4.1.

FRACTURE MECHANICS COMPUTATIONS WITH MSC/PROBE

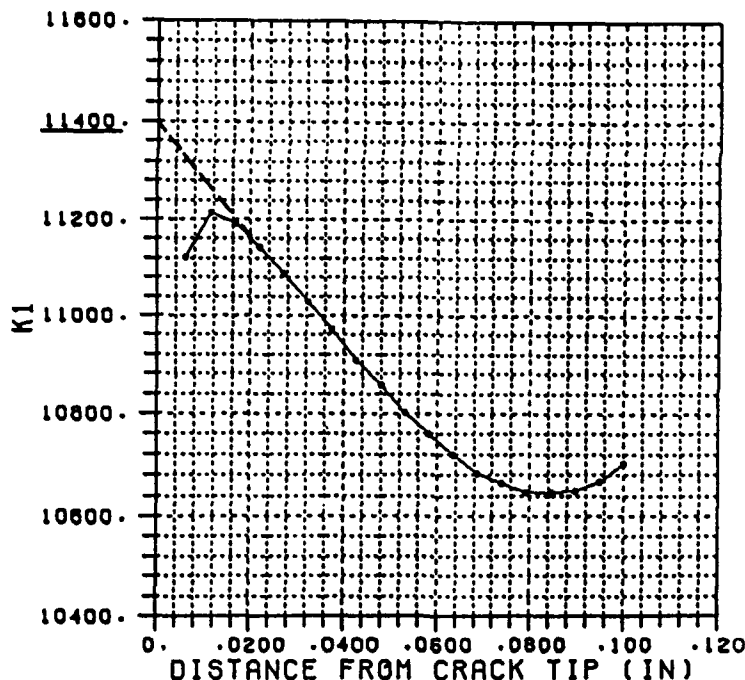


FIGURE 4.9: EQUATION 6 PLOT ALONG CRACK CENTERLINE

	MSC/PROBE	REF [4]	REF [5]
K_I	11400	11120	11840
K_{III}	5740	5150	N/A

TABLE 4.1: MODE I AND MODE III COMPARISONS AT CRACK CENTERLINE

This procedure was continued at various other points around the crack face for the Mode I Intensity Factors. The plot of Eq. (6) for each position along the crack front is included in the Appendix. It should be noted that the plane stress approximation that was used to develop Eq. (5), and (6) becomes less accurate as the free surface is approached. The behavior in this region becomes more three dimensional due to the gradients parallel to the crack front. As such, some of the plots of Eq. (6) from the region close to the free surface were not as well defined as those closer to the crack centerline (i.e. Figure 4.9). Reasonable extrapolations were obtained, though, and the results are shown in Figure 4.10 with Reference [5] as a comparison. The X axis coordinates are relative to the angle from the free face (ie. $\phi=0$ at the

FRACTURE MECHANICS COMPUTATIONS WITH MSC/PROBE

free face, $\phi=\pi/2$ at the centerline). The results from MSC/PROBE are generally less than 5% below those from Reference [5] except at the free surface. Subsequent studies by some of the authors of [5], found in [6], showed behavior more similar to the results from MSC/PROBE in the region close to the free surface. Again, though, the behavior in this region is three dimensional in nature, and the limitations of the plane stress and plane strain assumptions should be recognized.

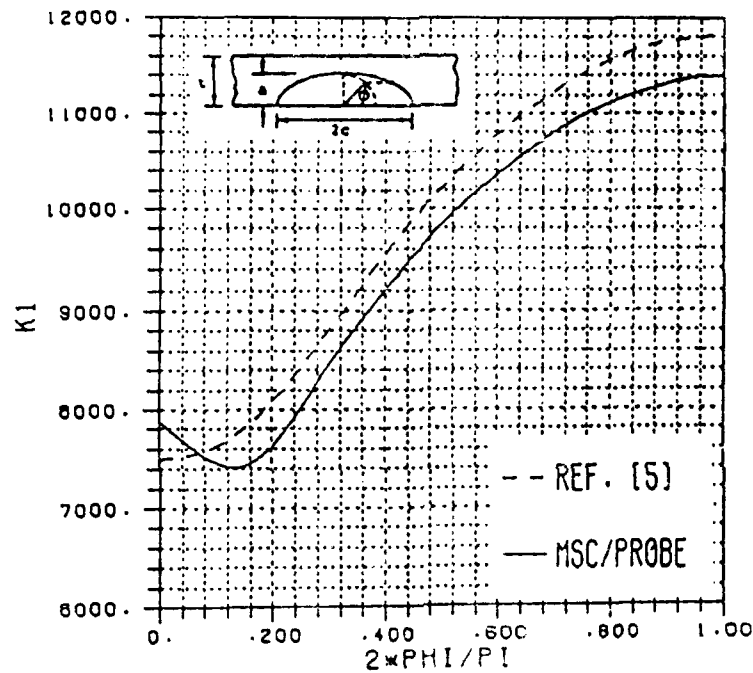


FIGURE 4.10: K_I RESULTS ALONG THE CRACK FRONT

5.0 SUMMARY AND CONCLUSIONS

This paper has discussed the application of the Finite Element Method to fracture mechanics computations. Particular emphasis was placed on proper evaluation of the quality of the numerical solution. The p-version finite element program, MSC/PROBE, which has extensive quality control features, was used for this purpose.

Several examples were provided to demonstrate the use of MSC/PROBE for fracture mechanics computations. The examples included a cracked panel with tension and shear loading, an axisymmetric solid rod with an imbedded penny shaped crack loaded in tension, and a solid plate with a semi-elliptical surface crack loaded in shear and tension. The quality control procedures were outlined for each example, and the fracture mechanics results were provided.

The p-version of the finite element method, as implemented in MSC/PROBE, has been demonstrated to be particularly well suited for fracture mechanics computations. The automatic fracture mechanics extraction methods used in the planar and axisymmetric modules are extremely efficient and accurate. The quality control features that are provided, namely the global error in the energy norm, the elemental equilibrium, the inter-element stress continuity, and the convergence of the data of interest, all combine to provide the most powerful solution verification that can be found in finite elements today.

6.0 REFERENCES

- [1] Szabó, B. and Babuška, I., "Computation of the Amplitude of Stress Singular Terms for Cracks and Reentrant Corners.", ASTM STP 969, pp. 101-124, 1988

- [2] Parks, D., "A Stiffness Derivative Finite Element Technique for Determination of Crack Tip Stress Intensity Factors.", Int. J. of Fracture, Vol. 10. No. 4, (1974)

- [3] Tada, H., Paris, P., Irwin, G., "The Stress Analysis of Cracks Handbook", Missouri: Paris Productions Inc., 1985.

- [4] Paris, P., Sih, G., "Stress Analysis of Cracks", American Society for Testing and Materials, Special Technical Publication 381, 1970.

- [5] Raju, I. S., Newman, J. C. Jr., "Stress Intensity Factors for a Wide Range of Semi-Elliptical Surface Cracks in Finite Thickness Plates.", Engineering Fracture Mechanics, Vol. II, pp. 817-829, 1979.

- [6] Tan, P. W., Raju, I. S., Shivakumar, K. N., Newman, J. C. Jr., "A Re-evaluation of Finite Element Models and Stress-Intensity Factors for Surface Cracks Emanating from Stress Concentrations.", NASA Technical Memorandum 101527, 1988.

7.0 APPENDIX

The following pages contain the plots of Eq. (6) for various points around the elliptical crack for the sample problem from Chapter 4. Each plot is along a line perpendicular to the crack front, as shown in Figure A.1. The extrapolation to the limit of $R=0.0$ is also displayed on each plot.

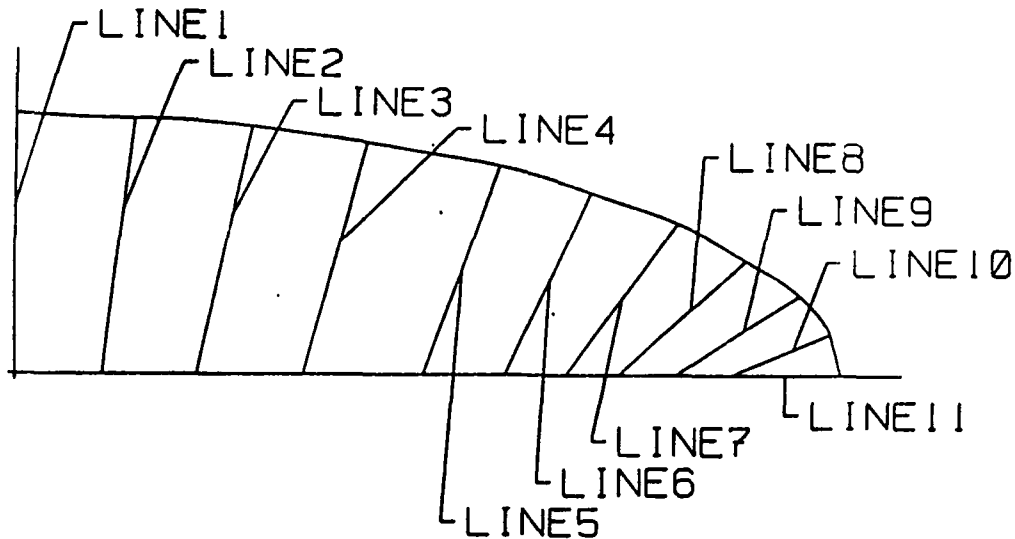


FIGURE A.1: VIEW OF EXTRACTION LINES ON THE CRACK FACE

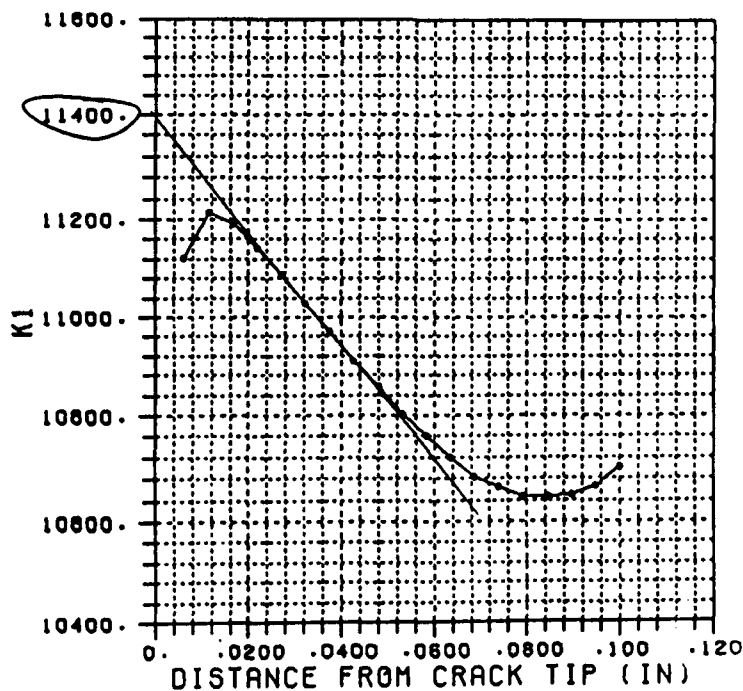


FIGURE A.2: EQUATION 6 PLOT ALONG LINE 1

FRACTURE MECHANICS COMPUTATIONS WITH MSC/PROBE

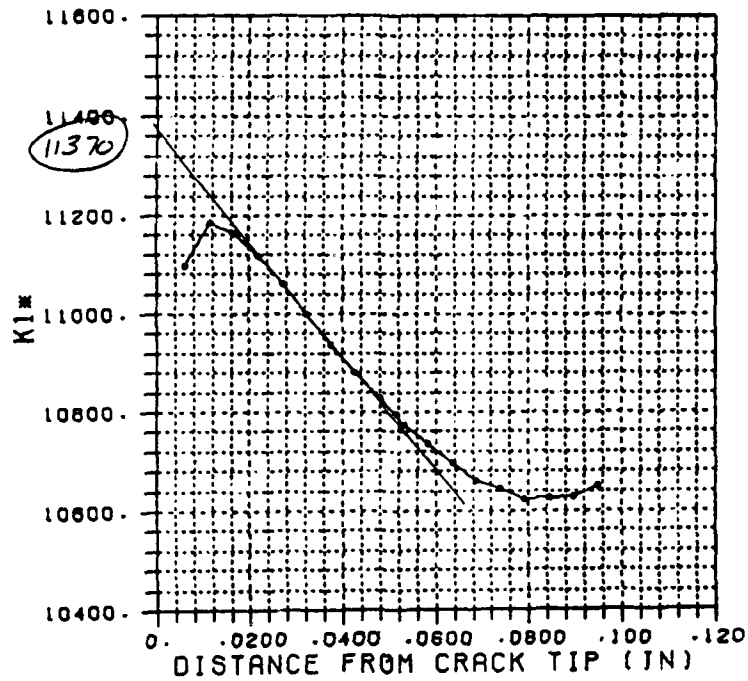


FIGURE A.3: EQUATION 6 PLOT ALONG LINE 2

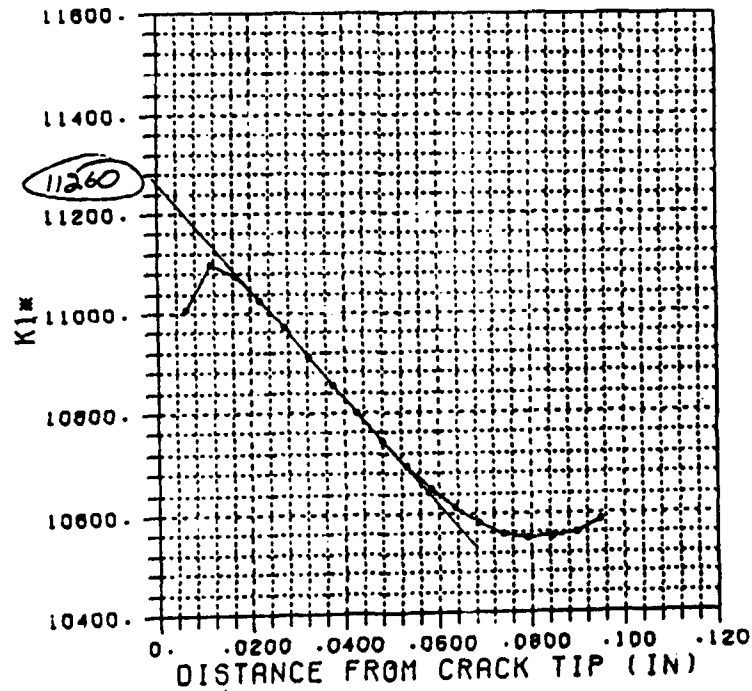


FIGURE A.4: EQUATION 6 PLOT ALONG LINE 3

FRACTURE MECHANICS COMPUTATIONS WITH MSC/PROBE

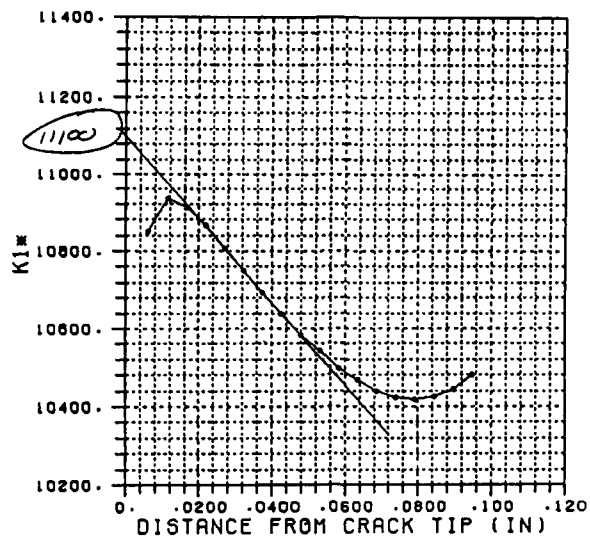


FIGURE A.5: EQUATION 6 PLOT ALONG LINE 4

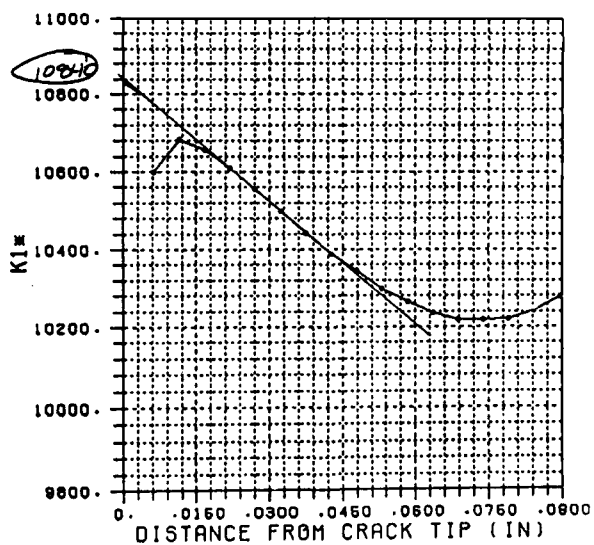


FIGURE A.6: EQUATION 6 PLOT ALONG LINE 5

FRACTURE MECHANICS COMPUTATIONS WITH MSC/PROBE

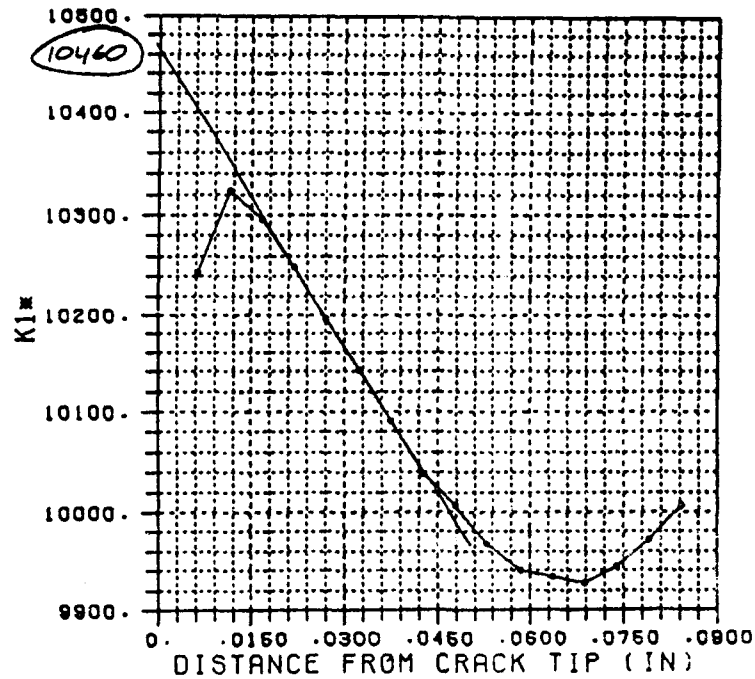


FIGURE A.7: EQUATION 6 PLOT ALONG LINE 6

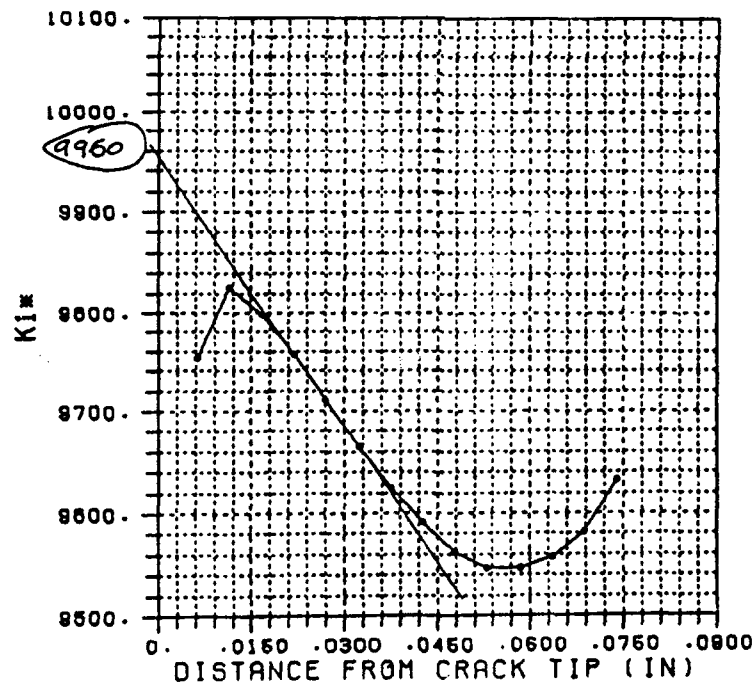


FIGURE A.8: EQUATION 6 PLOT ALONG LINE 7

FRACTURE MECHANICS COMPUTATIONS WITH MSC/PROBE

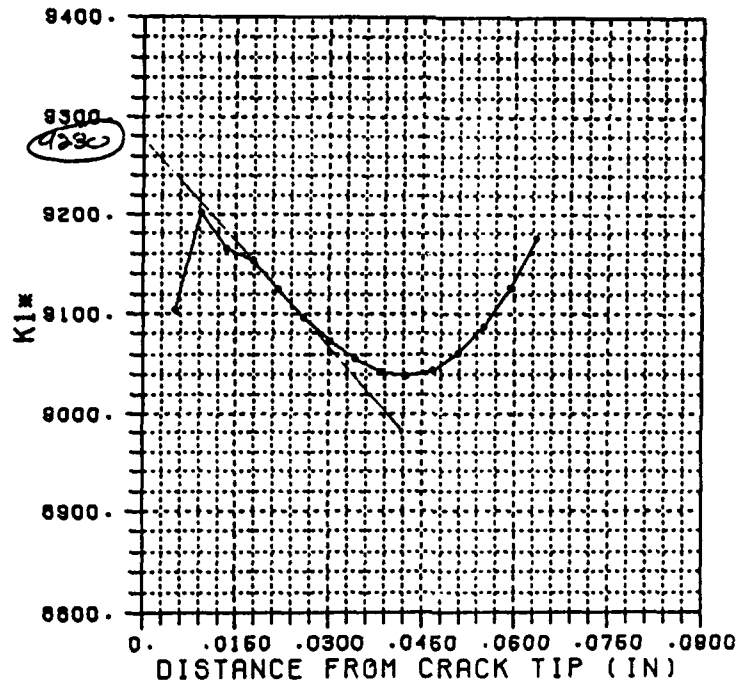


FIGURE A.9: EQUATION 6 PLOT ALONG LINE 8

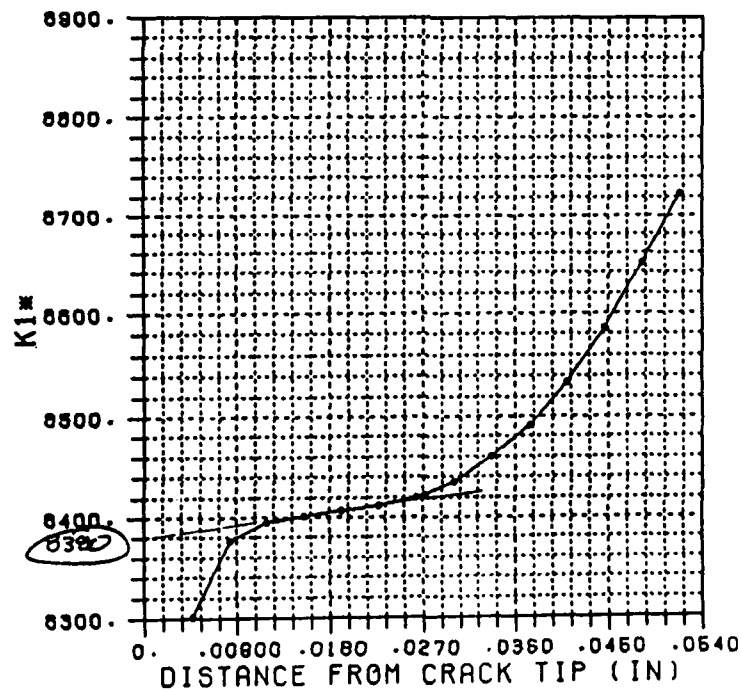


FIGURE A.10: EQUATION 6 PLOT ALONG LINE 9

FRACTURE MECHANICS COMPUTATIONS WITH MSC/PROBE

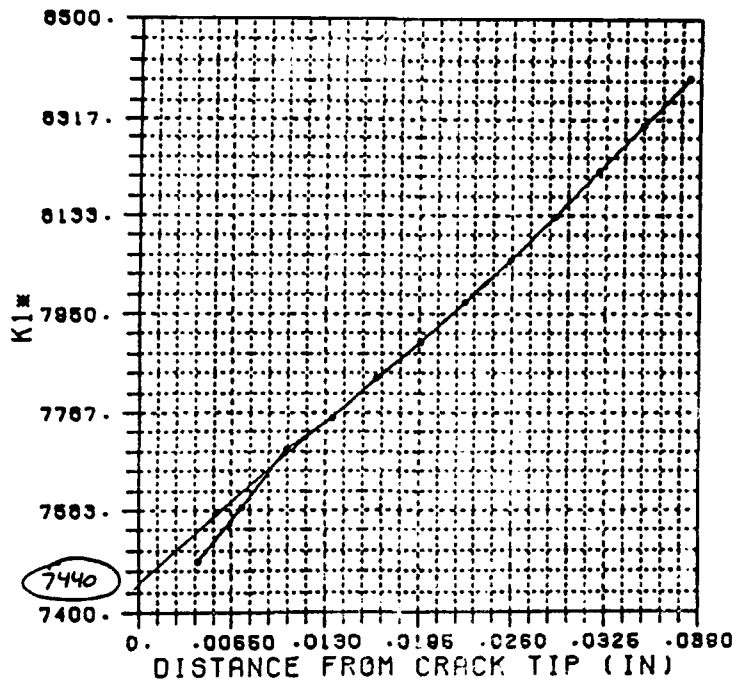


FIGURE A.11: EQUATION 6 PLOT ALONG LINE 10

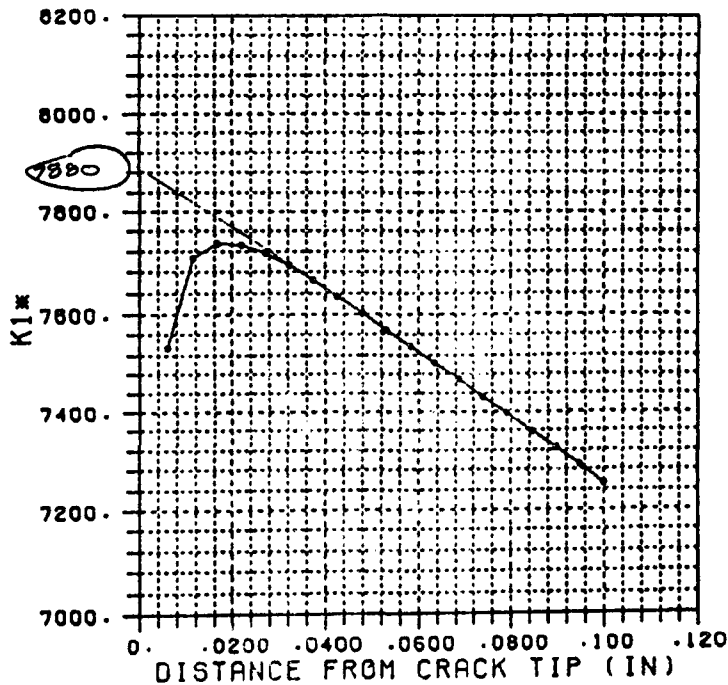


FIGURE A.12: EQUATION 6 PLOT ALONG LINE 11

**THE APPLICATION OF RISK ANALYSIS
TO AN AGING AIRCRAFT FLEET**

**A. BERENS
UDRI**

**J. BURNS
WRDC/FIBEC**

**1990 USAF STRUCTURAL INTEGRITY
PROGRAM CONFERENCE**

SAN ANTONIO, TEXAS

ASD90-3146

STRUCTURAL RISK ANALYSIS

- **ASSESSMENT OF STRUCTURAL INTEGRITY**

- **Safety**
 - probability of fracture
- **Durability**
 - economic repair
 - functional impairment

- **MANAGEMENT OF STRUCTURAL INTEGRITY**

- **Maintenance Policies**
 - inspection/repair costs
 - safety

STRUCTURAL RISK ANALYSIS

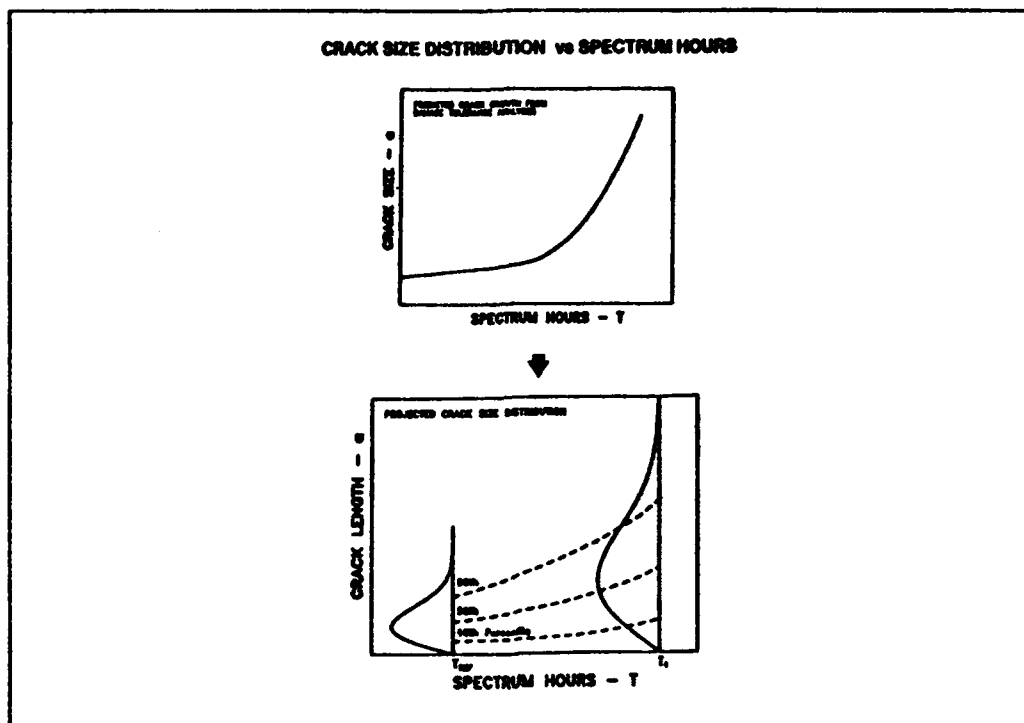
The objectives of the Air Force program on structural risk analysis are to stochastically assess structural integrity in terms of both safety (as quantified by the probability of fracture of a population of structural details) and durability (as quantified by the expected number and sizes of cracks that will be detected at an inspection). This characterization of structural integrity can then be applied as an additional tool in making decisions concerning the timing of maintenance actions.

AIR FORCE DATA BASE

- **AIRCRAFT STRUCTURAL INTEGRITY PROGRAM (ASIP)**
 - **Damage Tolerance Analyses**
 - **Durability Analyses**
 - **Force Management**
 - **Individual aircraft tracking**
 - **Inspection feedback**
 - **loads/environment spectra survey**

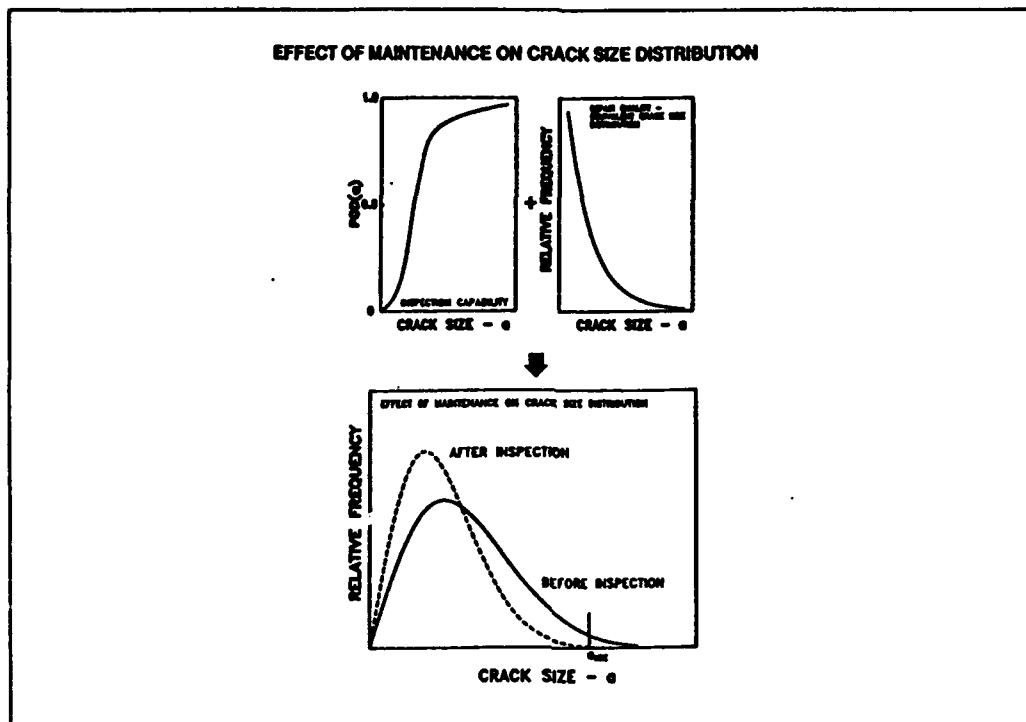
AIR FORCE DATA BASE

Because of the Aircraft Structural Integrity Program (ASIP) requirements of MIL-STD-1530A, the Air Force has an extensive data base for the evaluation of structural integrity. Of particular application to risk analysis are the data associated with the damage tolerance and durability analyses that are performed for all potential airframe cracking sites and the data associated with the force management tasks of ASIP. These data provided the basis of the risk analysis methodology both from the viewpoint of data that would be available and that which would not be available.



CRACK SIZE DISTRIBUTION VS SPECTRUM HOURS

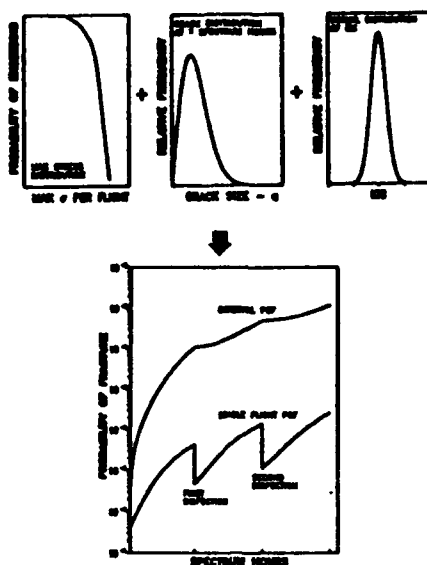
Because of the available data, the risk analysis methodology was constructed around the growth of a distribution of cracks. The initial distribution would be estimated from the best available data. This data may result from routine or teardown inspection or may be estimated from equivalent initial crack size distributions derived during durability analyses. Given an initial distribution at some reference time, the program estimates the distribution at a later time by projecting the percentiles using the crack growth versus time curve from the damage tolerance analyses.



EFFECT OF MAINTENANCE ON CRACK SIZE DISTRIBUTION

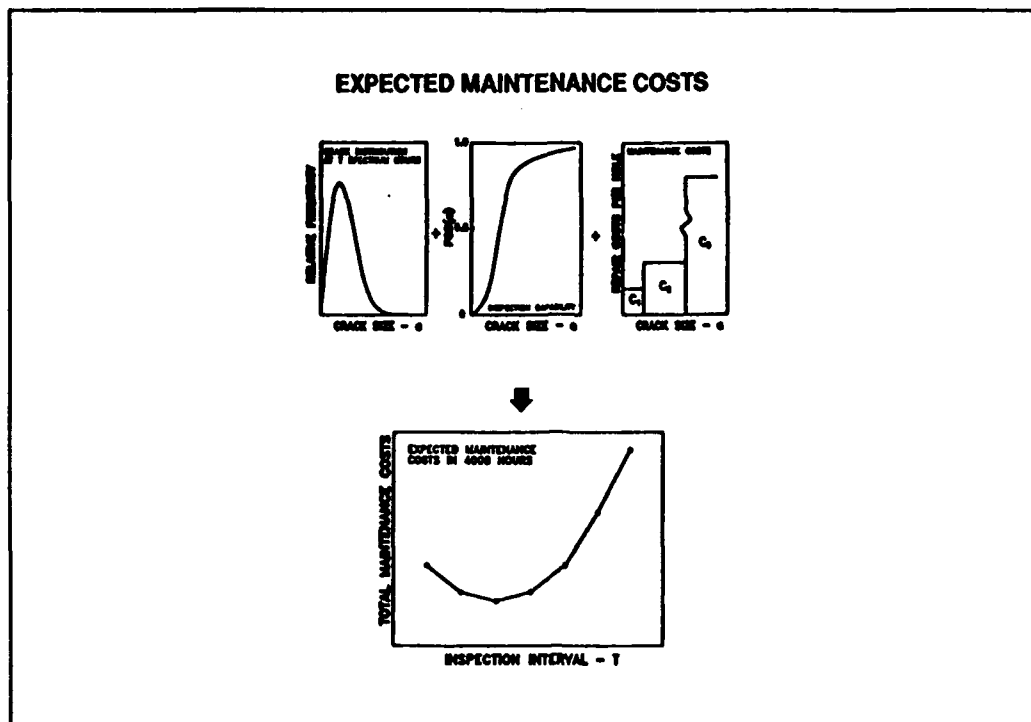
At a maintenance action, the population of details are inspected and all detected cracks are repaired. This maintenance action changes the crack size distribution and the change is a function of the inspection capability and the quality of repair. Repair quality is expressed in terms of an equivalent repair crack size distribution, i.e., in a manner similar to the equivalent initial flaw size distribution which can be used to characterize durability. The post maintenance crack size distribution is then projected forward for the next interval of uninspected usage. The process is continued for as many inspection intervals as desired.

SAFETY - PROBABILITY OF FRACTURE



SAFETY - PROBABILITY OF FRACTURE

Safety is quantified in terms of the thprobability of fracture (POF). POF is calculated as the probability that the maximum stress encountered in a flight will produce a stress intensity factor that exceeds the critical stress intensity factor for a structural detail. This calculation is performed in two contexts. The single flight POF is the probability of fracture in the flight given that the detail has not fractured previously. This number can be compared to other single event types of risks such as the risk of an automobile accident in an hour or the risk of death per year due to home accidents. The interval probability is the probability of fracture at any time between the start of the analysis (reference time of zero) and the number of spectrum hours. This POF is useful in predicting the expected fractures in a fleet of aircraft.



EXPECTED MAINTENANCE COSTS

Given the predicted crack size distribution at the time of an inspect/repair maintenance action and the POD function, the expected number and sizes of the cracks that will be detected can be calculated. This information can be interpreted as it stands or it can be combined with the costs of repairing the cracks (which may vary with size) to produce expected maintenance costs in pre-defined intervals. Such data can then be used to evaluate maintenance strategies to determine in the scheduling can be optimized.

INPUT

	NATURE	FORMAT
• MATERIAL/GEOMETRY		
K_I vs a	DETERMINISTIC	DATA FILE
K_{II}	STOCHASTIC	PARAMETERS (NORMAL)
• AIRCRAFT/USAGE		
ANALYSIS LOCATIONS		CONSTANTS
a vs T	DETERMINISTIC	DATA FILE
MAX a PER FLT.	STOCHASTIC	PARAMETERS (GUMBEL)
INITIAL CRACK SIZES	STOCHASTIC	DATA FILE
• INSPECTION/REPAIR		
TIMES		CONSTANTS
INSPECTION CAPABILITY	STOCHASTIC	PARAMETERS (LOGNORMAL)
REPAIR QUALITY	STOCHASTIC	DATA FILE

INPUT

Nine types of data are required to perform a risk analysis run. This table summarizes the type of information required, its nature, and the format of the data as input to the computer program.

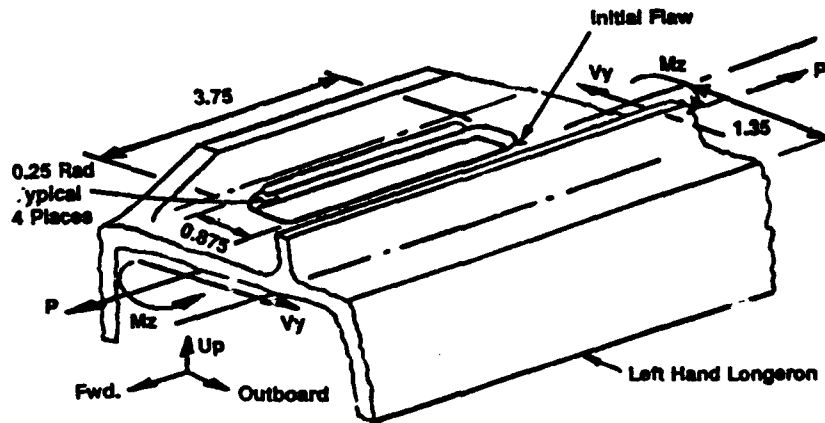
EXAMPLE

- **AGING A/F/T/ AIRCRAFT**
- **CRACKS DETECTED IN AFT, OUTBOARD CORNER OF UPPER COCKPIT LONGERON CUTOUT**
- **EDDY CURRENT INSPECTION - $a_{NDE} = 0.100$ in.**
- **TWO USAGE SEVERITIES**
- **INSPECTION INTERVALS?**

EXAMPLE

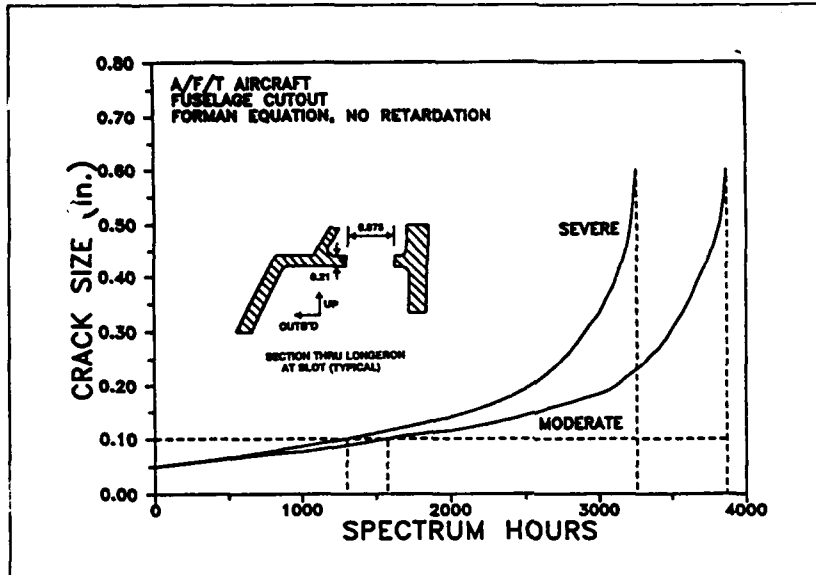
As an example application of the risk analysis program, representative data from an attack/fighter/trainer (A/F/T) aircraft will be used to evaluate inspection intervals and as a basis of comparison of the effects of the input data. Cracks greater than 0.100 in. were detected during scheduled inspections and the inspection interval was shortened. The need for the shortened inspection interval must be determined. The aircraft experiences two usage severities which will be denoted moderate and severe. The analyses will be started at a reference number of spectrum hours. An inspection capability was assumed for which the probability of detecting a 0.050 in. crack was 0.5 and the probability of detecting a 0.100 in. crack was 0.90 (reset crack size after an inspection is 0.100 in.). The baseline equivalent repair flaw size distribution was assumed to be a uniform distribution on the interval of 0 to 0.050 in.

UPPER COCKPIT LONGERON CUTOUT



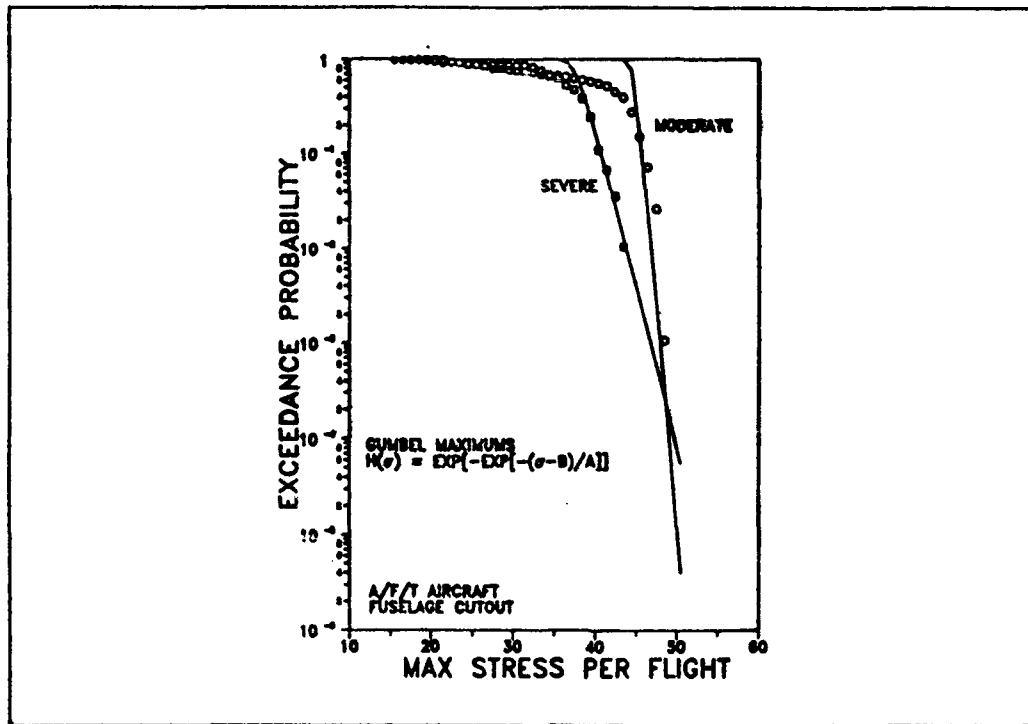
SCHEMATIC OF DETAIL

The population of details of interest comprise fatigue cracks growing from slots for canopy attach hooks in the horizontal flange of the upper cockpit longeron. There are five such cutouts on each side of the fuselage and, for the rear cutout of concern, the highest stress levels occur at the aft outboard corner and are due to fuselage bending. For the population of 7075-T6 aluminum details, it was assumed that the critical stress intensity factors (K_{IC}) were normally distributed with a mean of 27.5 and a standard deviation of 1.5.



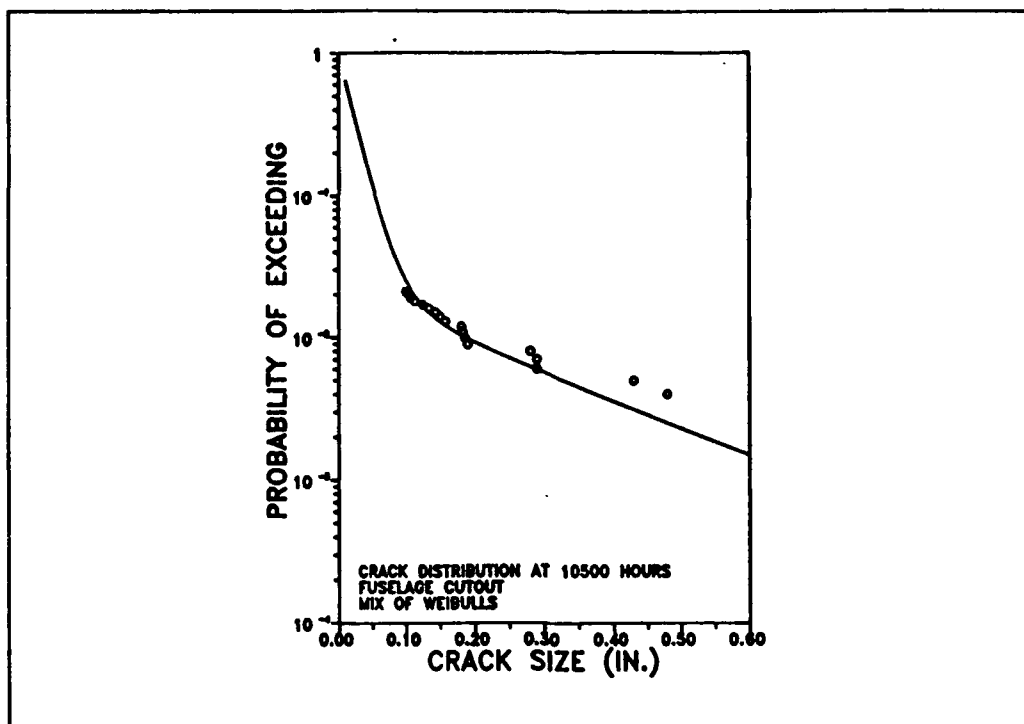
PREDICTED CRACK GROWTH

The crack size versus spectrum hours curves were calculated using the flight-by-flight moderate and severe spectra. The detail of a growing crack is schematically shown in the figure. For these crack growth curves, DTA inspection intervals were 1150 and 975 spectrum hours for the moderate and severe spectra, respectively.



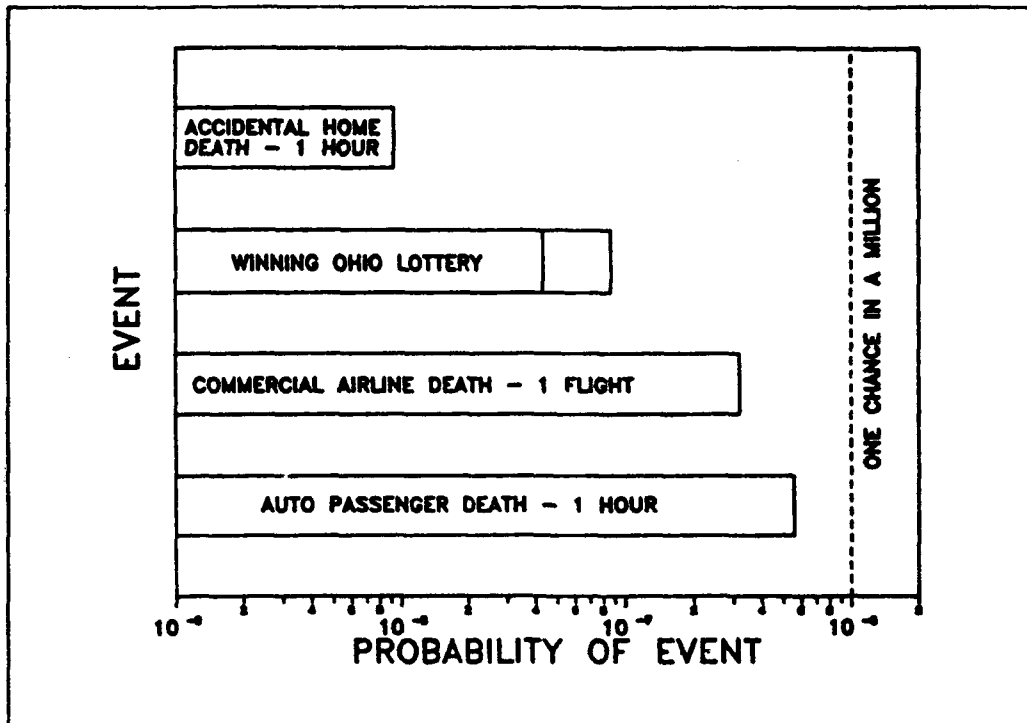
MAXIMUM STRESS PER FLIGHT

A Gumbel extreme value model was fit to the distribution of maximum stresses in each flight of the respective spectra. The Gumbel model provides an acceptable fit to the highest levels of the max stress per flight distribution. The differences at lower stress levels are believed to result from the mixture of mission severities that are represented in the composite spectrum. At the time of the analysis, mission data were not available. It should be noted that only the high stress levels have a significant contribution to the probability of fracture.



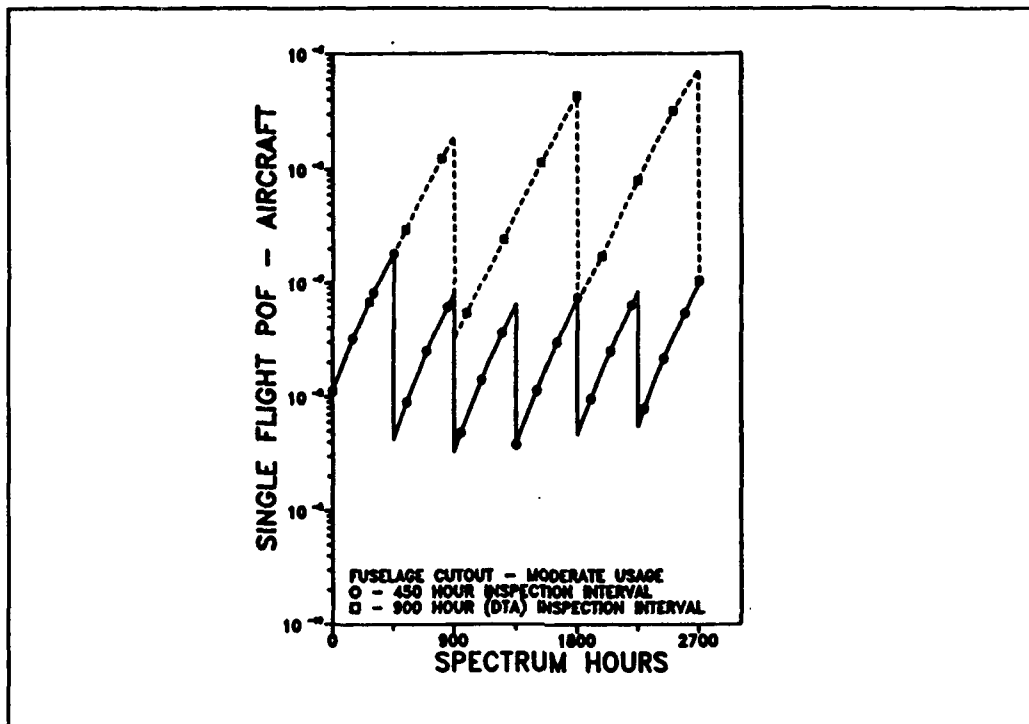
INITIAL CRACK SIZE DISTRIBUTION

Every airframe in the moderate use population was inspected and, after adjusting for differences in experienced flight hours, two percent of the subject cutouts had cracks greater than 0.100 in. at the reference number of spectrum hours. A Weibull distribution was fit to the cracks greater than 0.100 in. It was assumed that crack sizes in the other details were exponentially distributed. At the reference time, the sizes of the cracks in the population of cutouts was a mixture of the two distributions with a mixing percentage of 2 percent.



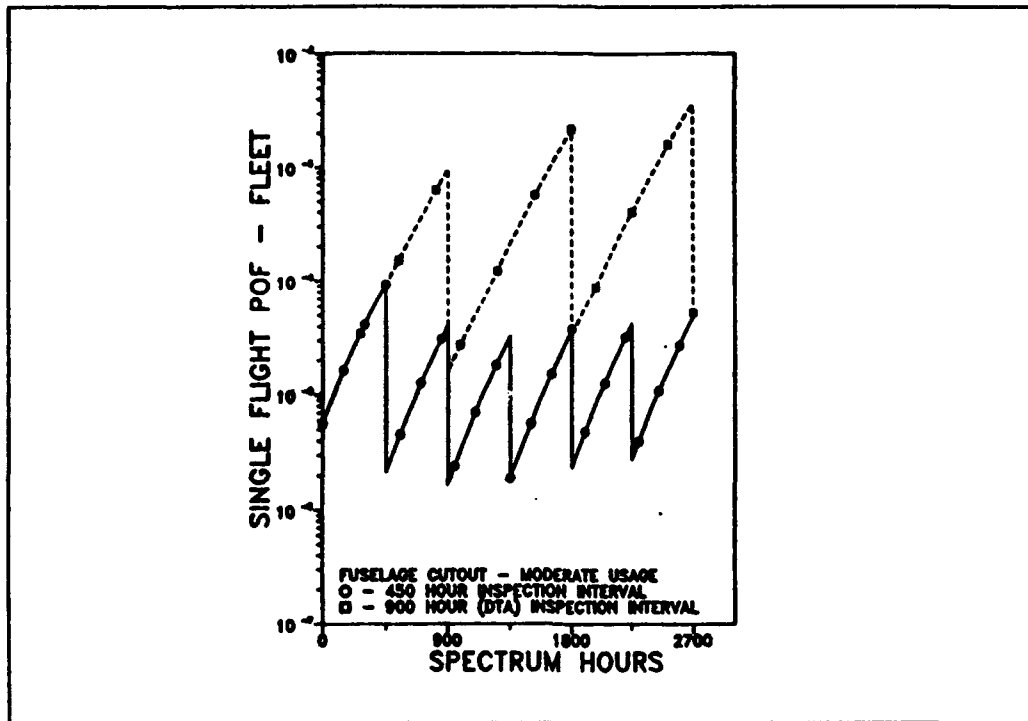
COMPARATIVE RISKS

To put fracture probabilities in perspective, this slide shows the probability of more familiar events.



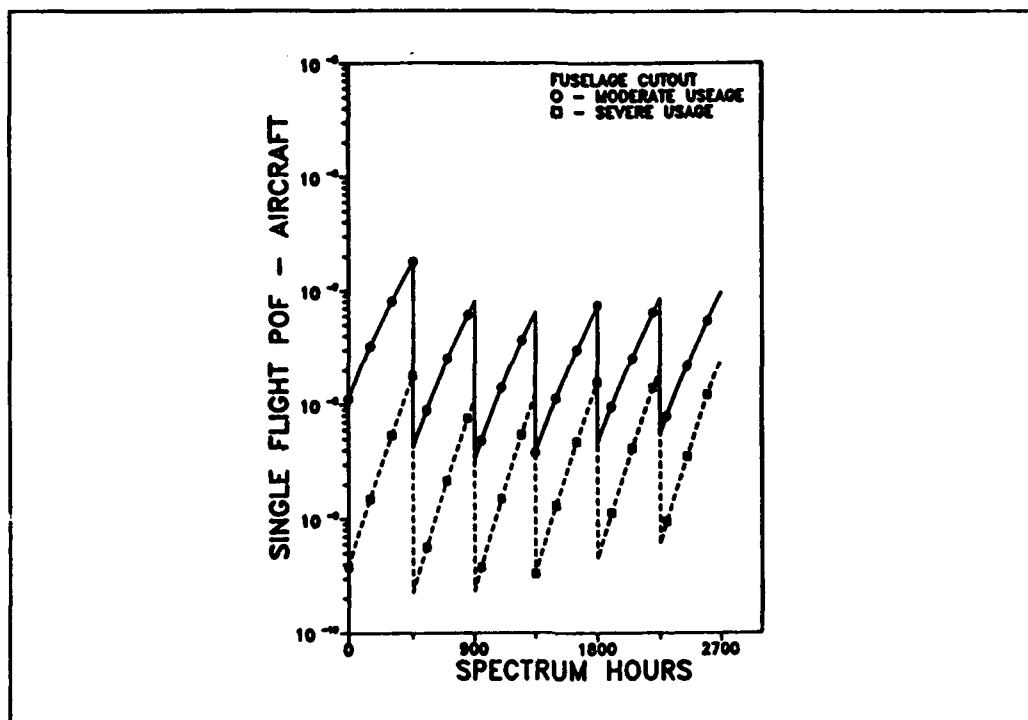
POF COMPARISON OF INSPECTION INTERVALS - SINGLE AIRFRAME

This chart presents the moderate usage probability of fracture (POF) as function of spectrum hours during a single flight at either of the two cutouts on the fuselage of an airframe. All analyses assume an inspection at the reference time ($T=0$). Single flight POF less than 10^{-6} has been suggested as an acceptable risk for military flights. Because of other maintenance activities, the fuselage inspections are scheduled in multiples of 450 hours. The 900 hour inspection interval does not keep the POF below 10^{-6} and has about 1.5 orders of magnitude higher risks than the 450 hour inspection interval. It is apparent that the large cracks are being repaired at the inspections.



POF COMPARISON OF INSPECTION INTERVALS - FLEET

This chart shows the single flight POF for the entire fleet of approximately 500 airframes. The fleet POF values are about 500 times larger than the single airframe POF values. The relatively high POF values for the 900 hour inspection interval indicate the potential for a fracture in the fleet if this inspection is maintained.



POF COMPARISON OF USAGE SEVERITIES

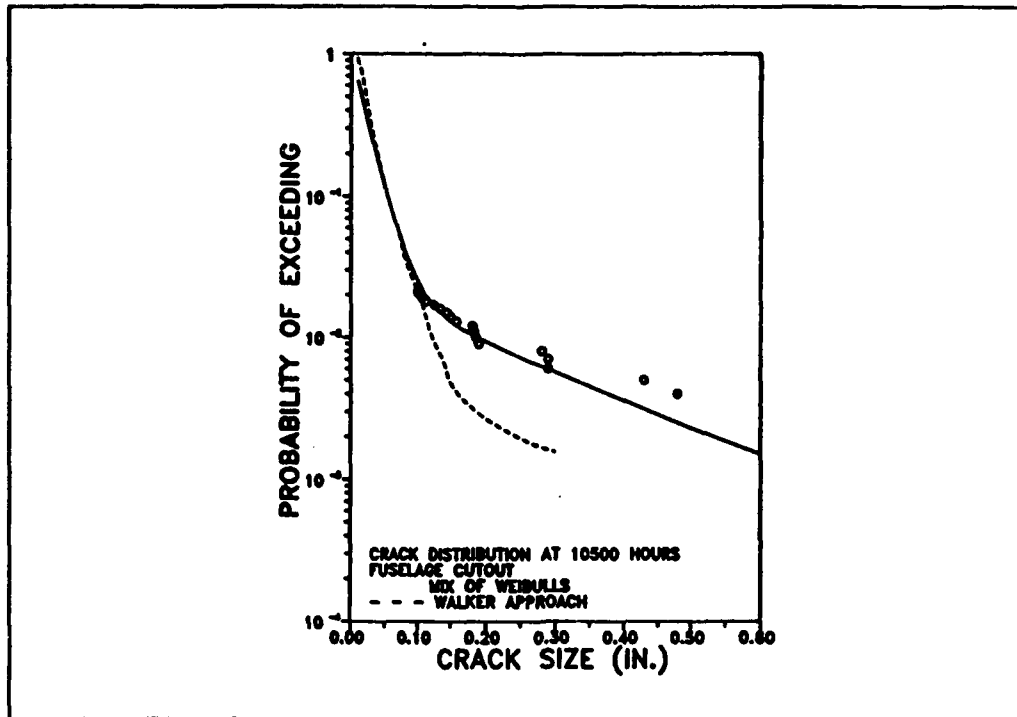
This chart shows the interesting result that the severe usage has lower POF than the moderate. The cracks grow faster under the severe spectrum but the moderate spectrum contains higher maximum stresses. It should be noted that the crack size data came from the moderate use airframes. No cracks have been detected in the severe use airframes. Since the severe spectrum resulted in smaller POF values and the sensitivity to input parameters were equivalent, only the moderate spectrum is considered in the remaining analyses.

SENSITIVITY TO INPUT

- **INITIAL CRACK SIZE DISTRIBUTION**
- **K_{Ic} DISTRIBUTION**
- **INSPECTION CAPABILITY**
- **PEAK STRESS DISTRIBUTION**

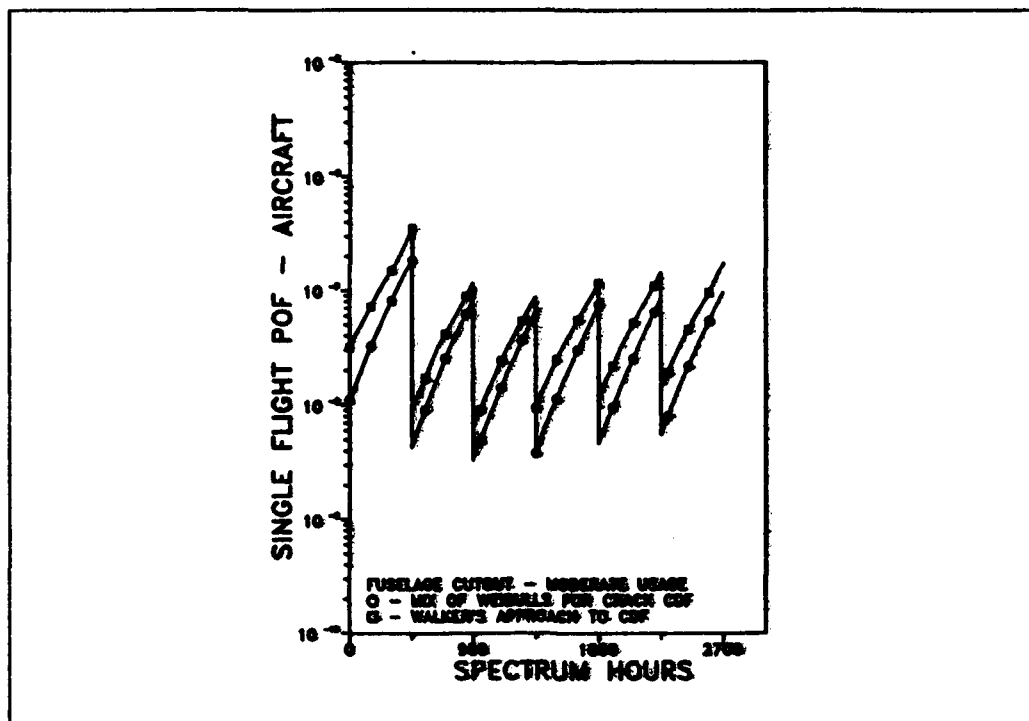
SENSITIVITY TO INPUT

To test the sensitivity of the risk calculations to input data quality, selected variations were introduced to determine the magnitude of the resulting changes in the fracture probabilities.



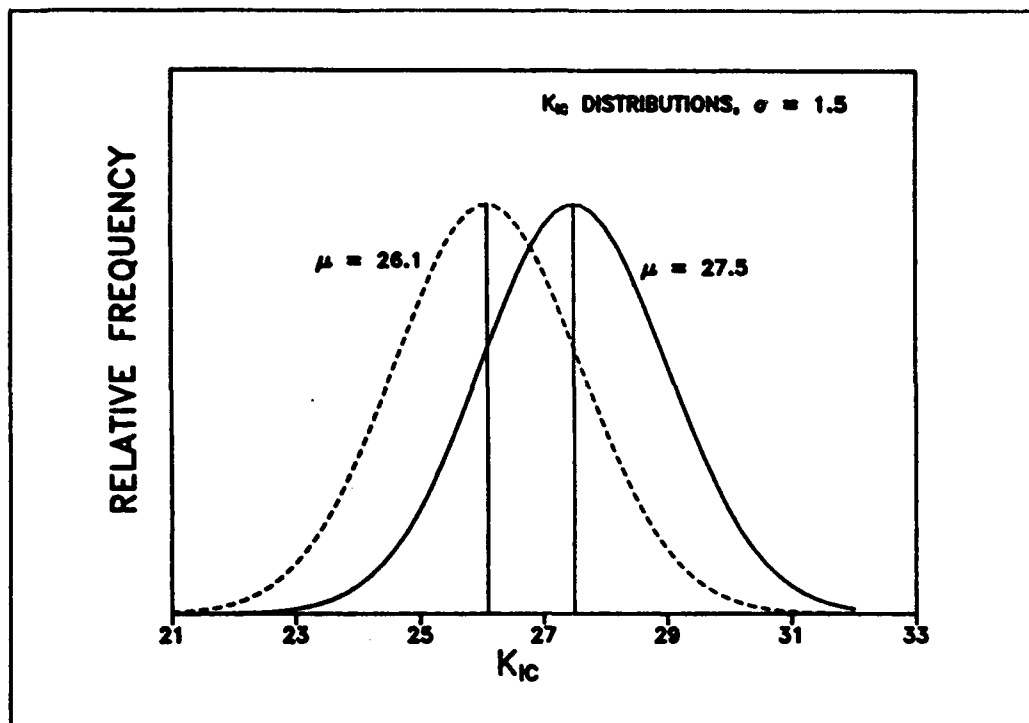
INITIAL CRACK SIZE DISTRIBUTION

Walker's approach to estimating the crack size distribution at a reference time was adapted to estimate the initial crack size distribution. This approach assumes that the time to initiate a crack to 0.100 in. has a log normal distribution with $\sigma=0.14$. The a versus T curve is assumed to model the mean of the time to crack initiation distribution. The two percent of the sites that were determined to have 0.100 in. cracks at the reference time located the a versus T curve and the distribution of the crack sizes at the reference time was calculated. This model underestimated the probability of the large cracks but agreed reasonable well with the previous model at cracks less than 0.100 in.



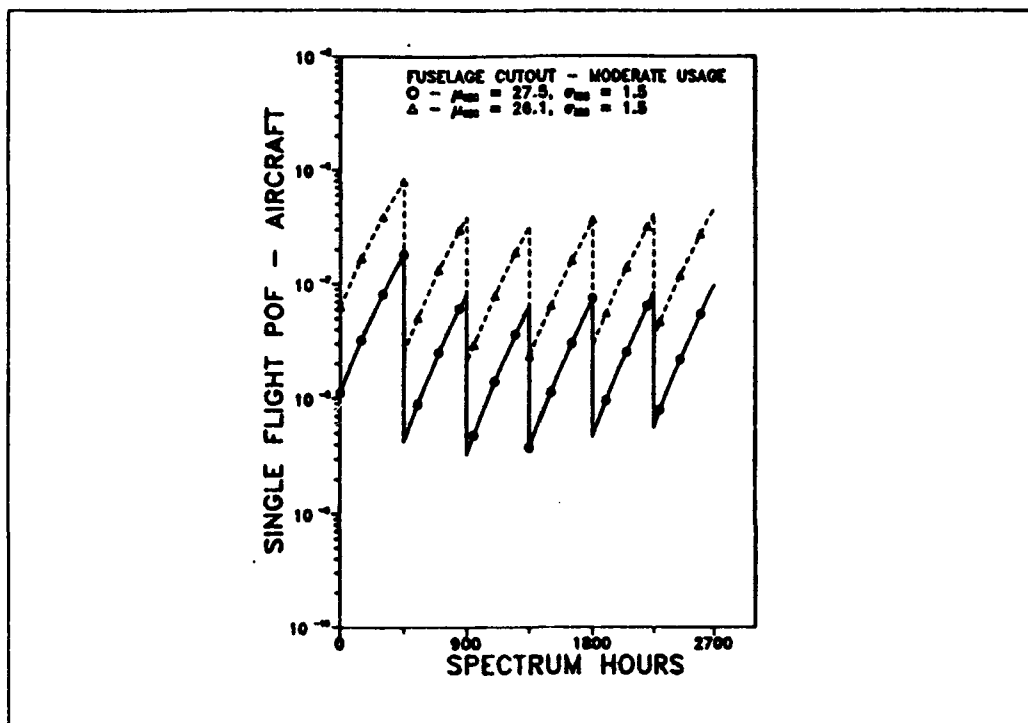
POF FOR DIFFERENT INITIAL CRACK SIZE DISTRIBUTIONS

The POF values from the Walker crack size model are higher than those of the previously assumed mix of Weibulls. Apparently, large cracks are immediately detected and repaired (i.e., removed from the analysis) while the intermediate sized cracks dominate the risk calculation. Both models may have larger cracks than are actually in the structure. The calculations indicate the detection of cracks at too many sites as compared to actual inspection results. While this effect could also be the result of assuming a much better inspection capability than is actually being used, the uncertainty in the crack size data is judged to be greater than the uncertainty in the characterization of the inspection capability.



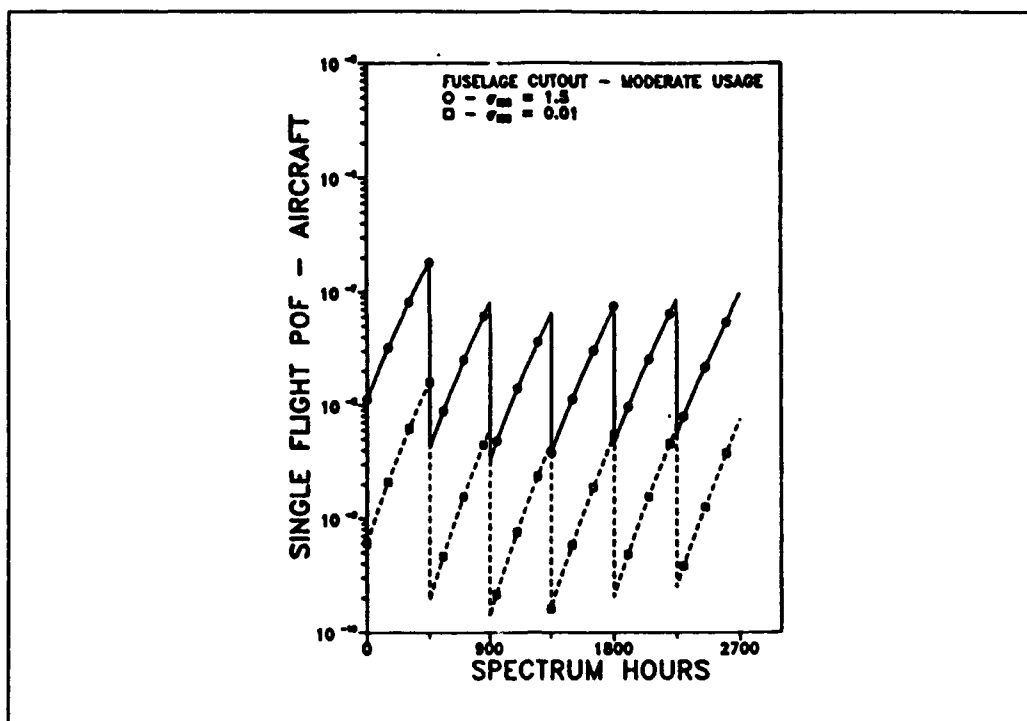
SENSITIVITY TO VARIATION IN K_{IC}

To test the sensitivity to fracture toughness, the mean K_{IC} was arbitrarily reduced by five percent. A second comparison was made in which fracture toughness was essentially made constant by greatly reducing the standard deviation.



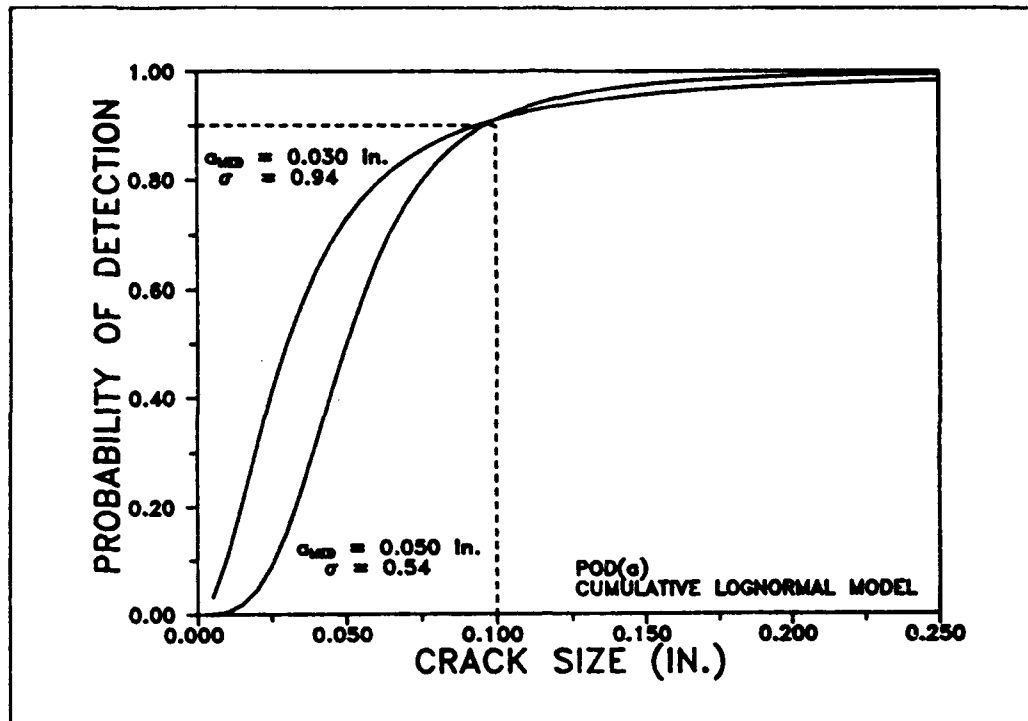
POF FOR SHIFT IN AVERAGE FRACTURE TOUGHNESS

The fracture probabilities display a strong dependence on the mean of the distribution of K_{IC} values of the material. This figure compares a five percent shift in the mean of the K_{IC} distribution. Decreasing the mean by five percent changed the POF values by a factor of about 4.5 to 5. While this result is applicable only for the conditions of this analysis, similar changes have been noted in other A/F/T application.



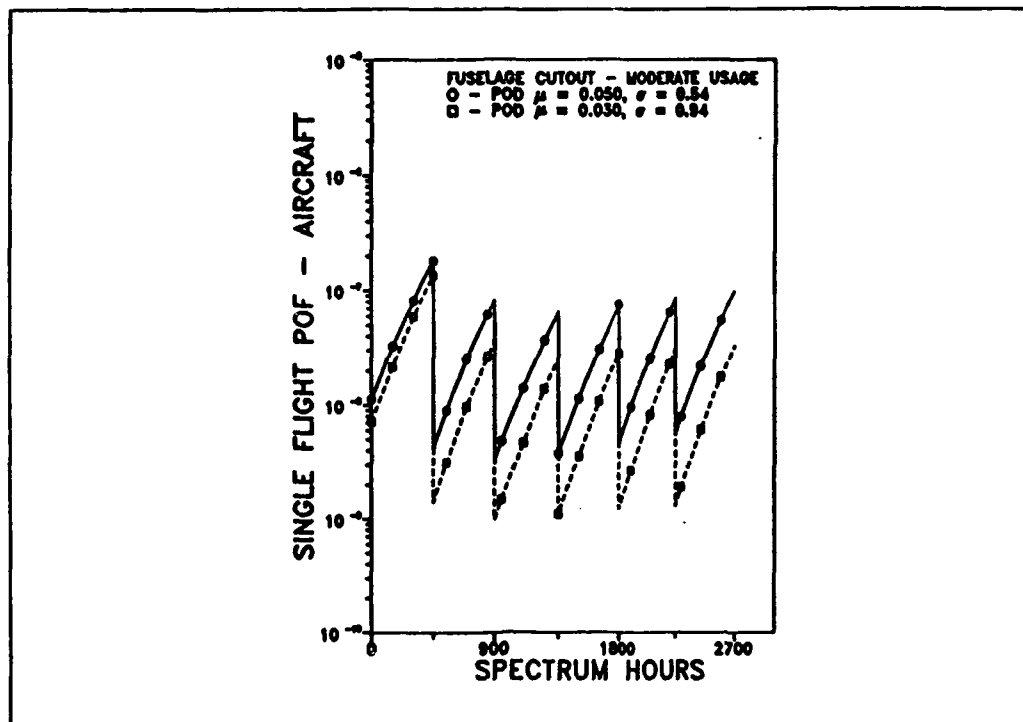
POF FOR A CONSTANT FRACTURE TOUGHNESS

Making K_{IC} essentially a constant ($\sigma = 0.01$) reduced the POF values from the baseline by more than an order of magnitude. These results on fracture toughness indicate the necessity of careful characterization of the fracture toughness properties of the materials when critical crack sizes are relatively small.



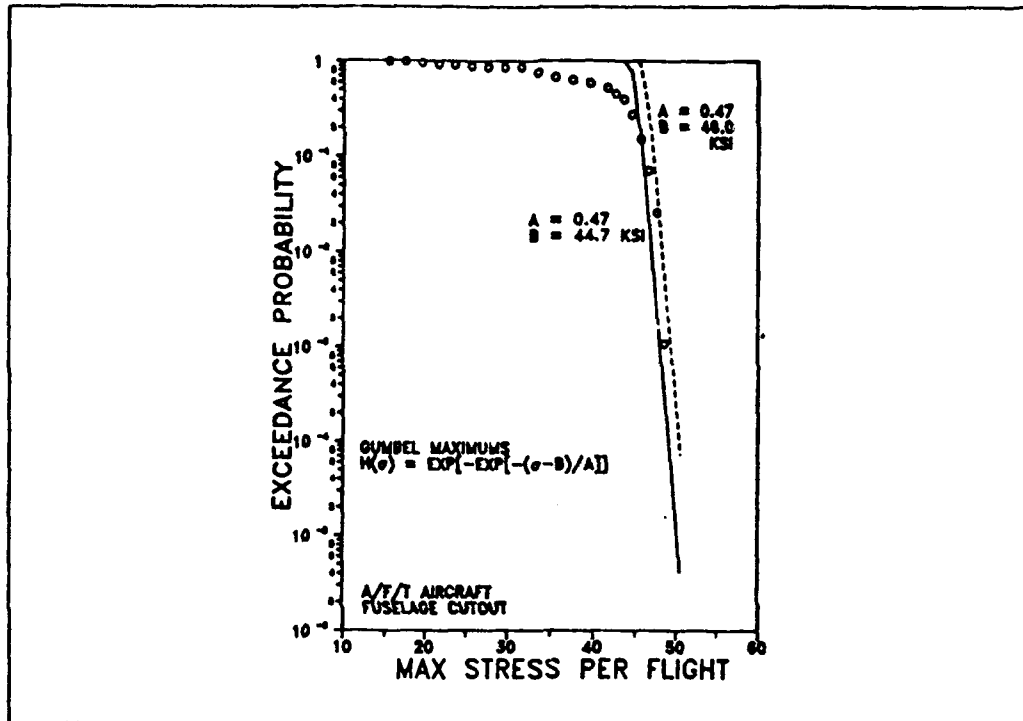
SENSITIVITY TO INSPECTION CAPABILITY

A change in inspection capability was arbitrarily introduced by reducing the median detectability (the crack size which is detected half the time) but keeping the 90 percent detectability at 0.100 (increasing σ). This change produces a larger chance of missing big cracks but increased the probability of detecting small cracks. Higher values of σ may be more representative of field inspections.



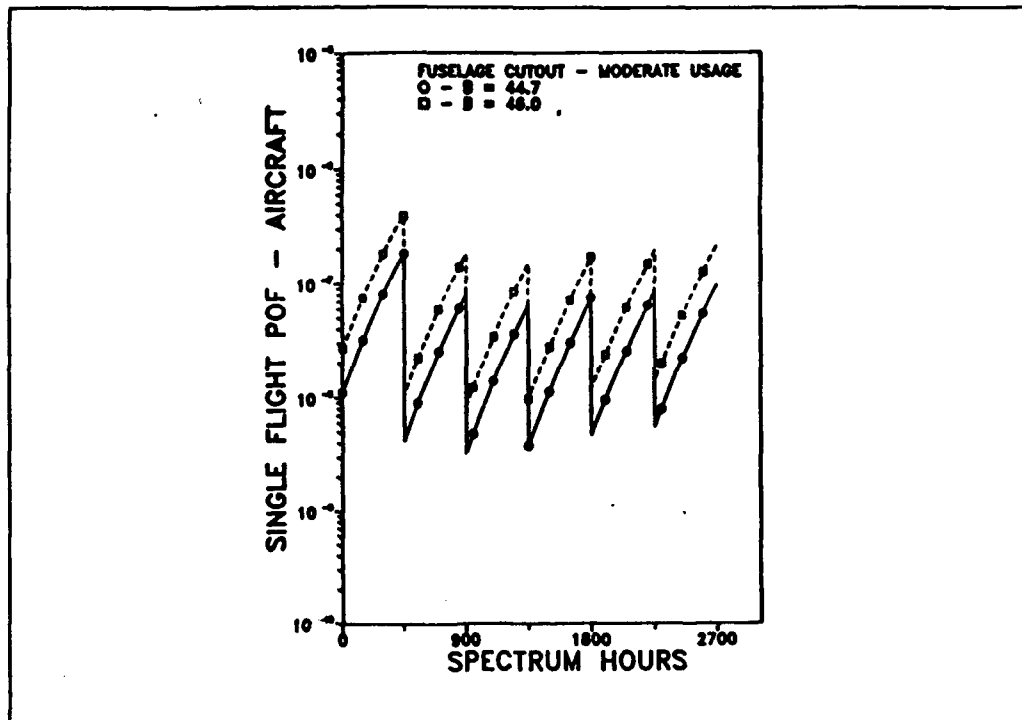
POF FOR DIFFERENT INSPECTION CAPABILITIES

Reducing the median inspection capability has greater effect than the increased chance of missing the large cracks.



SENSITIVITY TO PEAK STRESS DISTRIBUTION FIT

A Gumbel distribution of maximum values of a distribution is used as the basis for extrapolating the distribution of the maximum stresses encountered in an operational flight. Due to the mixture of usages that are often represented in the data, the parameters of the Gumbel distribution should only be obtained from a "few" of the highest stress levels. Since this process is subjective, the sensitivity to the Gumbel parameters was tested by fitting a function that bounded the "observed" max stress per flight values.



POF FOR SHIFT IN MAX STRESS PER FLIGHT DISTRIBUTION

The 3 percent shift in the location (B) of the peak stress per flight distribution produced a factor of two change in the POF. Similar effects were noted for changes in slope (A). Since these effects could be significant, care will be required in judging the goodness of fit of any particular Gumbel fit to the data of the peak stress distribution.

GENERALIZATIONS

- **CRACK GEOMETRY**
- **MISSION STRESS SPECTRA**
- **CHANGE IN STRESS LEVEL**
 - **REPAIR**
 - **MULTI SITE DAMAGE**

GENERALIZATIONS

The computer code calculates probabilities of fracture and distributions of crack sizes for each individual run. However, more complex scenarios can be addressed through the combination of results from multiple runs. For example, if several crack initiation sites give rise to different geometry factors (and different σ versus T curves), fracture probabilities can be calculated for each geometry. A weighted average of the fracture probabilities, with the weights being the proportion of cracks initiating at each site, provides an overall estimate of the detail POF. (In the example of this paper, the most critical initiation site was assumed. If cracks initiate at less severe locations, their fracture probabilities would be smaller.) Similarly, if max stress per flight data are available for different mission types, POF can be calculated for each mission type and combined using the appropriate mission mix. In the example, essentially every flight is assumed to be from the missions that produce the highest stresses.

Changes in stress levels can be accommodated by stopping the analysis at an inspection and starting a new analysis with the crack size distribution at the stopping time. Similarly, the statistical characterization of the sites for which cracks were detected and repaired can be kept segregated from the remainder of the population and analyzed separately. For example, if repair comprises oversizing of hole, stress levels are increased for the repaired details and they are a different population.

Although the program does not currently address the multi-site damage or continuing damage problems, it is believed that the computer code could be generalized to address these problems.

SUMMARY

- **POF DETERMINED BY TAILS OF DISTRIBUTIONS**
 - **Comparisons More Sensible Than Absolutes**
- **DESIGN STAGE EFFECTS**
 - **Material Characterization**
 - **Stress Levels**
 - **Geometry**
- **FORCE MANAGEMENT EFFECTS**
 - **Usage**
 - **Inspection Intervals**
 - **Inspection Method**
 - **Repair**
- **NEED GOOD MAINTENANCE FEEDBACK**

SUMMARY

Practical POF values are determined by the tails of the crack size, K_{IC} , and peak stress distributions. Since there are seldom sufficient data to precisely characterize the tail behavior of these parameters, absolute interpretations of the estimated POF values should be treated with caution. Relative POF magnitudes, however, can provide a basis for choice of actions. Design consideration, as always, are important as the material characterization, stress levels at the critical location and crack geometry all have a significant effect on the fracture probabilities. Force management actions in terms of shortening inspection intervals and using better inspection and repair methods can also significantly reduce fracture probabilities.

Finally, risk analyses are no better than the data available to describe the initial conditions and use. A critical need exists good feedback on the size of the cracks that are being found at the inspections. The crack size data are the most nebulous in the model and crack size information on real cracks is most helpful for initiating or updating risk calculations.

A Review of the Effects of Overloads on Fatigue Crack Growth

by

R. CARLSON, G. KARDOMATEAS and P. BATES

School of Aerospace Engineering, Georgia Institute of Technology

Atlanta, Georgia 30332-0150

Abstract

Several theories have been proposed to explain the transient fatigue crack growth decelerations and accelerations which follow overloads. The mechanisms that have been proposed to explain retardation after a tensile overload, for example, include residual stress, crack deflection, crack closure, strain hardening, and plastic blunting/resharpening. These mechanisms are reviewed in the light of recent experimental results and implications with regard to their applicability are examined. Also, the possible extension of the proposed theories to represent compressive overloads is considered. It is suggested that no single mechanism can be expected to represent observed effects over the entire range of da/dN versus ΔK ; e.g., behavior ranging from the near threshold region to the Paris region.

The applicability and limitations of proposed methods of analysis for the development of fatigue crack growth codes for general, variable amplitude loading are discussed. Recommendations for possible analytical procedures are offered.

Introduction

The loading conditions developed in structural components in aircraft are aptly described as variable amplitude loading. A comprehensive treatment of the causes and the effects of these conditions includes an integrated consideration of flight load spectra, component load spectra, crack tip stress analysis, and a crack growth law. Some of the difficulties of the problems involved have been clearly identified recently by Partl and Schijve [1] who reconstructed crack growth from fractographic observations for two flight simulation loadings. The incentive for initiating their research was their conclusion that a basic correlation between crack growth and load history must be developed. Previously, Schijve [2] had concluded that "it can not be said that a generally applicable and reliable crack

growth prediction model is now available".

The difficulties encountered in developing a crack growth prediction model can be recognized by isolating attention to the transient effects which have been observed after a single overload. The mechanisms that have been proposed to explain the transient retardation after a single overload, for example, include residual stress [3], crack deflection [4], crack closure [5], strain hardening [6] and plastic blunting/resharpening [7]. Of these mechanisms, two have been the subjects of the most intensive examination and application. These are the effects of residual stress and crack closure. Willenborg et al [8] and Wheeler [9] proposed models which account for the effect of residual stress. Modifications of these models have been adopted for use in a number of fatigue crack growth programs. Crack closure, which involves the development of obstructions to crack closure upon unloading, is manifested in different forms. Research studies for developing an understanding of these complex mechanisms are still being conducted.

If, during load cycling, the minimum load is large enough, the crack faces will not come in contact with one another, so then crack closure mechanisms need not be considered. It is then reasonable to expect that a Willenborg type model describes crack growth. In the near threshold region, however, conditions for crack closure are often encountered, so they cannot be ignored. The relative roles of these two mechanisms in fatigue crack growth, therefore, need to be examined. The objective of this paper is to present the results of analyses of recent experimental results which contribute to an understanding of roles of these two mechanisms.

Recent Experimental Results

Experimental results on the features of crack closure behavior following tensile overloads have been presented by Ward-Close and Ritchie [10]. They conducted experiments in which variations of the effective stress intensity factor ranges before and after overloads were determined. Near-tip closure was measured by the use of strain gages mounted above the crack plane, and the values of the effective stress intensity ranges were determined. Their tests were performed on compact tension specimens which were machined from IMI 550 titanium alloy plate, and all tests were performed under predominantly plane-strain

conditions.

A variety of variable load experiments were conducted. The results used here were obtained from tests on specimens with a fine grained α/β microstructure. In their experiments the stress intensity factor range $\Delta K = 15 \text{ MPa}\sqrt{\text{m}}$ with $R = 0.1$ was maintained constant. Single 100% and 150% overloads for which $K_{OL} = 2K_{\max}$ and $2.5K_{\max}$, respectively, were applied. Test data points for the variation of the opening stress intensity factor, K_{OP} , with crack length are shown in Fig. 1. The data in Fig. 1a are for an overload of 100%. Those of Fig. 1b are for an overload of 150%. As plotted, the overloads occurred at the origins. During the interval between the origin and the first data point, a transient crack growth acceleration rather than a retardation was observed. This behavior had also been observed previously by Nowack et al [11] and by Paris and Hermann [12]. This immediate, post-overload behavior was attributed to a crack tip stretching which reduced closure contact pressures and, by effectively increasing the stress intensity factor range, resulted in a brief crack growth acceleration period. Ultimately, the crack extended through the stretched ligament and formed an asperity which resulted in the K_{OP} data points shown in Fig. 1. It should be noted that the immediate post-overload transient cannot be rationalized by use of residual stress models of the Willenborg type. The solid curves and the parameters C_0 and L shown in Fig. 1 will be discussed in the section on Application of the Model..

Obstruction to closure has been observed to occur in different forms. In sheets the obstruction is formed at the specimen faces at the free ends of the crack tip front. For dominantly plane strain conditions obstructions on the interior crack surfaces in the form of surface roughness can be developed [13].

Recently, McEvily and Yang [14] presented results of experiments designed to examine the form of closure obstruction after an overload. They presented evidence which indicated that even though crack closure obstruction prior to an overload was of the plane strain form, obstruction after an overload occurred at the specimen faces; i.e., under plane stress conditions. Data points for K_{OP} obtained by McEvily and Yang [14] for a 100% overload on an aluminum alloy 6061-T6 compact tension specimen are presented in Fig. 2. For this test the constant value of $\Delta K = 8.0 \text{ MPa}\sqrt{\text{m}}$, $R = 0.05$ and the overload ΔK

= $16.0 \text{ MPa}\sqrt{\text{m}}$ with K_{\min} unchanged. The trend of the data points is similar to that observed by Ward-Close and Ritchie [10]. To examine the character of the obstruction form resulting from the overload, McEvily and Yang [14] repeated their experiment, but after the overload, they removed surface layers from the specimen by machining. Upon resumption of testing, no retardation transient was observed. They suggest that the results of Ward-Close and Ritchie [10] are subject to the same interpretation; i.e., the obstructions to closure after the overloads occur at the side faces of the specimens.

McEvily and Yang [14] also conducted experiments on the closure behavior developed for multiple overloads. From their results they concluded that during the transient period following the start of overloading, there was a transition from a surface obstruction to a through-the-thickness obstruction. These results clearly indicate that the form of closure obstruction is subject to a number of variables.

Closure Models

The generation of crack growth programs which include the effects of closure obstruction requires the development of closure models. Several models have been developed. Newman [15] has provided a good description of the features of a modified Dugdale strip model which has been applied by a number of researchers. This model has been used by Ward-Close et al [16] to analyze results from the paper by Ward-Close and Ritchie [10].

An alternative, discrete asperities model has also been proposed [17-19]. The features of this model can be described by reference to Fig. 3. Obstruction to closure is developed by the discrete asperities on the fracture surface. The geometric features of the asperities and their distances from the crack tip at the right are model parameters. These should be considered as effective values. It will be shown that the primary values can be determined from experiments.

The features of the model are used in conjunction with the elasticity solution for concentrated forces acting on a crack face. This problem is illustrated in Fig. 4. The stress intensity factor, K , developed and the displacement, u , at the load point are also given. The solution for multiple asperities has been developed by use of superposition [18].

The equation for the opening stress intensity factor for a single asperity is

$$K_{OP} = \frac{LG}{2(1-\nu)} \left(\frac{2\pi}{C} \right)^{0.5} \quad (1)$$

where G is the elastic modulus of rigidity and ν is the Poisson's ratio.

The features of the model can be illustrated by reference to the plot of stress intensity factor versus external load in Fig. 5. For no obstruction to closure, or no asperities, the loading cycle passes along the straight line from A to B. The corresponding stress intensity range is then measured between A and E. For a single asperity loading proceeds along D-C-B, and clearly, the range of the stress intensity factor is reduced, being measured from D to E. Additional features of the model can be illustrated by reference to the dashed lines. For two asperities, loading proceeds along G-F-C-B. If asperities weld to one another, then loading is extended from D-C to the dashed line to the right. This corresponds to the development of a tensile force in the asperities to the right of point C. This results in a further reduction in the range of stress intensity factor and properly describes the difference in crack growth rates between tests in an inert atmosphere, where welding can occur, and an active atmosphere where welding does not occur [20].

The model can also be extended to the left of the origin; i.e., for cases in which the external loading contains a compressive overload. If the compressive overload is sufficiently large, it may be anticipated that the asperities will undergo inelastic deformation. This is illustrated by the downward curve of the extended dashed line. Reloading would then occur along the lower straight line returning to the right. The subsequent loading cycle would then exhibit an increased stress intensity range which would result in the increased crack growth rate which has been observed after a compressive overload.

In the next section the discrete asperities model will be used to analyze the data by Ward-Close and Ritchie [10] and that of McEvily and Yang [14].

Application of the Model

When closure conditions are developed, the crack growth rate is determined by the range of the stress intensity factor. Thus, the equation $\Delta K_{eff} = K_{max} - K_{OP}$ indicates that K_{OP} must be determined. The discrete asperities model will be used to demonstrate

the correlation between Eq. 1 and the data of Ward-Close and Ritchie [10] and McEvily and Yang [14].

The variable C in Eq. (1) represents the distance between an asperity and the crack tip. This corresponds to the abscissa variable of Fig. 1. From [10], Young's modulus $E = 107$ GPa. Assuming material isotropy and a Poisson's ratio of 0.3, an estimate of the rigidity modulus $G = 41.2$ GPa. Using these property values and an asperity misfit value of $L = 1.1 \mu\text{m}$ in Eq. 1 yields the curve shown in Fig. 1a for an overload of 100%. An obstruction misfit value of $L = 4.3 \mu\text{m}$ gives the curve of Fig. 1b for an overload of 150%. These curves describe how K_{OP} decreases as the distance increases between the tip of the growing crack and the asperity which results from the overload. An examination of these plots reveals that the data points are well correlated by the use of Eq. 1.

In the experiments analyzed, retardation did not begin until values of C of about 0.04 mm and 0.65 mm after the overloads were achieved. This immediate, post-overload behavior was attributed to a crack tip stretching which relieved the contact pressure on asperities developed prior to the overload. Ultimately, the crack extended through the stretched ligament, and the asperity causing retardation was formed. The values of C_0 in Fig. 1 represent initial, effective distances from the crack tips.

The data of McEvily and Yang [14] for K_{OP} have also been analyzed. For their aluminum alloy 6061-T6 specimen $G = 26.5$ GPa for a value of Poisson's ratio of 0.3. For a value of $L = 1.26 \mu\text{m}$ in Eq. 1, the solid curve of Fig. 2 is obtained. Again, Eq. 1 provides a good correlation with the data. A value for $C_0 = 0.075$ mm represents the initial, effective distance of the asperity from the crack tip at the beginning of retardation.

Discussion

The experimental results of Ward-Close and Ritchie [10] and McEvily and Yang [14] demonstrate that the retardation transient observed after a tensile overload can be attributed to the obstruction to closure developed by the overload. The discrete asperity model can describe the opening stress intensity variation after the overload. The primary parameter in the model is the obstruction misfit, L , which can be determined from experimental data.

It should be noted that the determination of the obstruction dimension is also the goal of the modified Dugdale strip model [15]. For this model the determination is, however, based on an analysis of the production of the obstruction layer.

The discrete asperity model is two dimensional and therefore may be considered to be more applicable to through-the-thickness closure. The correlation with the McEvily and Yang [14] data, however, suggest that L can be considered the "effective" value of obstruction which props the crack open. It would appear that it represents an experimentally integrated measure of closure obstruction.

The results which have been presented here are limited in scope and represent an exploratory examination of the use of a relatively simple method for describing the effect of an overload on asperity induced closure. It would, in future work, be of interest to examine possible correlations of the parameters L and C_0 with such basic quantities as crack tip opening displacement. An examination of the limited data of Ward-Close and Ritchie [10] indicate that it may be possible to develop a simple relationship between L and C_0 with K^2 , which is proportional to crack opening displacement, for overloads up to 100% [19]. A marked nonlinearity which is observed for K^2 above 100% overloads may be related to the details of the crack extension mechanism. Ward-Close and Ritchie [10] observed that for the higher loads, there was, in addition to crack tip stretching and blunting, tearing or crack extension during the overload cycle. This added complication of incremental crack advance during the overload cycle must, therefore, be considered.

As the asperity produced by the overload recedes from the crack tip and loading at a lower, constant ΔK resumes, additional asperities are produced. If L_1 represents the overload asperity height and L_2 a subsequent asperity height, a condition in which L_1 is much greater than L_2 would develop. Then near tip contact would occur, but it would not be on the asperity closest to the crack tip. Nearest crack tip asperity contact would not develop until K_{OP} for the most recently produced asperity was larger than the current K_{OP} for the overload asperity. In the process of asperity production under variable amplitude loading, a sequence of scalloped curve segments derived from curves of the type shown in Fig. 1 can be visualized. The operative K_{OP} curve would be the highest one for the current crack length.

The retardation behavior observed for the data considered can also be analyzed by use of the modified Willenborg model. Since this model uses the crack tip plastic zone as a measure of the reduction of the stress intensity factors, it proves revealing to examine its size. The distance the crack extends during the retardation transient has been described as the delay distance [10]. It may be shown that the delay distance for the modified Willenborg model is less than the plastic zone size. The delay distances for the data considered here are presented in Table 1.

Table 1
Delay Distances

Material	Measured delay	Plastic zone*	Willenborg delay**
	mm	mm	mm
Titan. alloy	0.88	0.14	0.07
Alum. alloy	0.35	0.51	0.23

$$* \frac{1}{2\pi} \left(\frac{K_{OP}}{\sigma_y} \right)^2$$

** Based on the requirement that the retardation stress intensity factor must be greater than zero.

An examination of the results in Table 1 indicates that the modified Willenborg model underestimates the delay distance substantially for the titanium alloy and slightly for the aluminum alloy. It could be inferred from these results that both surface roughness, which is related to microstructural features, and hardness or yield strength are important variables in the retardation behavior.

The ultimate interest in the use of the models discussed focuses on their predictive capability. The data of Ward-Close and Ritchie [10] for the 100% overload can be used to examine this issue. The modified Willenborg model is based on the use of a retardation stress intensity factor K_R which is used to compute the effective values of stress intensity factor and the effective stress ratio R [21]:

$$K_R = \Phi \left[K_{OL} \left(1 - \frac{a}{\rho_{OL}} \right) - K_{max} \right] , \quad (2)$$

where

$$\Phi = \frac{1 - K_{th}/K_{max}}{S - 1} .$$

For the given application the overload stress intensity factor is $K_{OL} = 33.4 \text{ MPa}\sqrt{\text{m}}$, the overload plastic zone is $\rho_{OL} = 0.14 \text{ mm}$, $K_{max} = 16.7 \text{ MPa}\sqrt{\text{m}}$ and the threshold stress intensity factor is $K_{th} = 5 \text{ MPa}\sqrt{\text{m}}$. A shut-off ratio of $S=2$ has been used.

A da/dN versus ΔK curve for a value of $R = 0.1$ was available, so data were fitted to the Forman equation. The crack growth equation used was

$$\frac{da}{dN} = \frac{4 \times 10^{-7} (\Delta K)^{3.5}}{[(1 - R)K_c - \Delta K]} . \quad (3)$$

A comparison of the crack growth rates predicted by the use of Eqs. 2 and 3 with the measured rates obtained by Ward-Close and Ritchie [10] is presented in Fig. 6. The ranges of crack growth rates for the two curves are the same. Since the measured values extend over a larger delay distance, however, it can be expected that the conservatism of the Wilienborg crack extension prediction should be significant.

The transient behavior following a tensile overload can rationally be attributed to either a residual stress effect or to closure obstruction. It is not, however, necessary to choose one model at the exclusion of the other. Certainly, both surface roughness obstructions to closure and residual stresses in front of the crack tip due to the overload can be expected to be present in the near threshold region. A combined procedure for determining effective stress intensity factors is possible. Thus, let

$$_{eff}K_{max} = K_{max} - K_R , \quad (4)$$

$$_{eff}K_{min} = K_{OP} - K_R , \quad (5)$$

for $K_{OP} - K_R > 0$,

and

$$_{eff}K_{min} = 0 , \quad (6)$$

for $K_{OP} - K_R < 0$.

It also follows that

$$_{eff}R = \frac{_{eff}K_{min}}{_{eff}K_{max}} . \quad (7)$$

The K_R in this formulation would not be determined by use of the modified Willenborg model which is not based on an actual determination of the residual stress state in front of the crack tip. The K_R in Eqs 4 and 5 should be based on the actual state developed by the overload.

In the near threshold region in which closure obstruction is clearly present, K_{OP} may dominate. When the crack faces do not impinge upon one another during a cycle, K_R probably dominates. A proper partitioning of K_{OP} and K_R should be the subject of future research. It should, however, be noted that the interaction between K_{OP} and K_R may well be complex. Suppose that both closure obstruction and residual compressive stresses in front of the crack tip are present. Then, if the local compressive stresses were relieved, the pressure across the asperities would be increased. This, in turn, would signify an increase in K_{OP} . The two effects are not, therefore, uncoupled. The extent of this coupling probably varies with the level of loading, but at present, it is unknown.

Conclusions

A review of the available crack growth prediction methods was performed to assess their limits and regions of validity. Plastic deformation occurring around the tip of a fatigue crack following an overload induces residual stresses and causes crack closure. Although current fatigue life estimation procedures make use of one model at the exclusion of the other, both mechanisms need be considered especially in the near threshold region. An examination of the results of the modified Willenborg model was also performed to obtain insight into its degree of conservatism. The following conclusions can be specifically drawn:

1. Available crack growth prediction models do not properly account for all of the mechanisms which are operative under variable amplitude loading.
2. A discrete asperities model can be used to describe the variation in the opening stress intensity factor after a tensile overload which results in an obstruction to closure. Crack tip closure measurements of the type made by Ward-Close and Ritchie [10] and by McEvily and Yang [14] can be used to determine the two parameters of the discrete asperities model.
3. The discrete asperities model has features which can rationalize the acceleration tran-

sient after a compressive overload, and the difference in crack growth rates observed in inert and active atmospheres.

4. When obstruction to closure develops after a tensile overload, retardation continues beyond the crack tip plastic zone. This indicates that retardation models based on residual stress effects alone cannot describe the transient behavior observed. Fracture surface features, which are microstructure dependent, must also be considered.
5. Ultimately, a model which incorporates both residual stress effects and closure obstruction effects may be required to describe the full range of possibilities under variable amplitude loading.

Acknowledgement

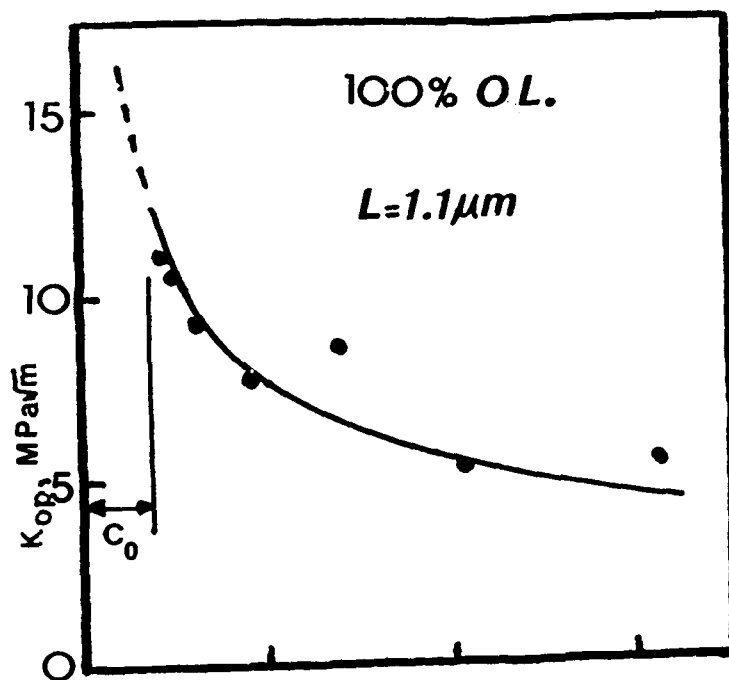
The authors acknowledge the support provided by the Warner Robins Air Logistics Center, Robins AFB under Contract No: F09603-85-G-3104-0034. They are also grateful for the interest and encouragement provided by Dr. T. Christian.

References

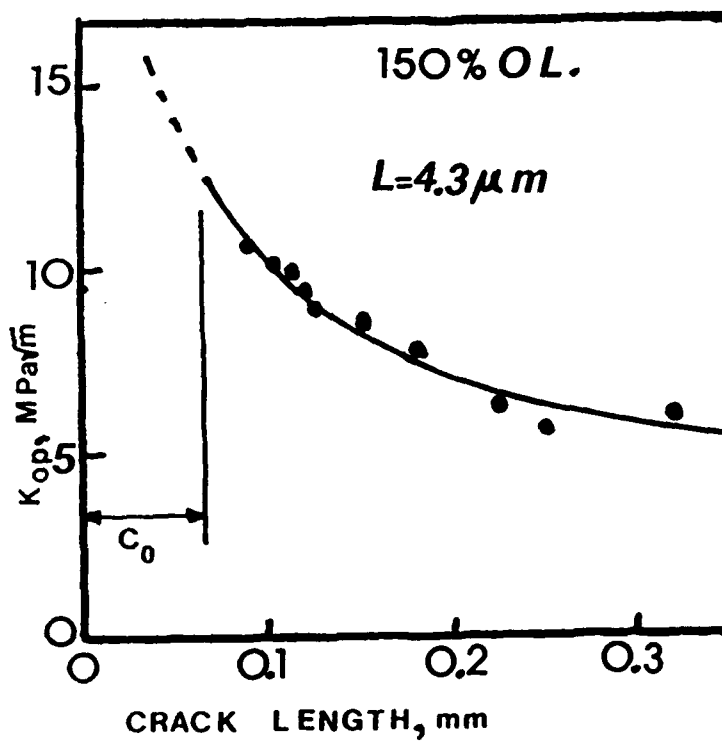
1. O. Partl and J. Schijve, "Reconstruction of crack growth from fractographic observations after flight simulation loading", *Int. J. Fatigue*, 12, 175-183 (1990).
2. J. Schijve, "Fatigue crack growth predictions for variable amplitude and spectrum loading", *Proc. Int. Conf. Fatigue 87*, EMAS, Warley, UK, vol III, 1685-1721 (1987).
3. J. Schijve, "Fatigue crack propagation in light alloy sheet materials and structures", *NRL Report MP 195*, National Aeronautical and Astronautical Research Institute, Amsterdam, Holland (1960).
4. J. Lankford and D.L. Davidson, "The effect of overloads upon fatigue crack tip opening displacement and crack tip opening/closing loads in aluminum alloys", *Advances in Fracture Research* (Ed. by D. Francois), vol. 2, Pergamon Press, 899-906 (1982).
5. W. Elber, "The significance of fatigue crack closure", *Damage Tolerance in Aircraft Structures*, *ASTM STP 486*, 230-242 (1971).
6. R.E. Jones, "Fatigue crack growth retardation after single cycle peak overload Ti-6Al-4V Titanium alloy", *Engineering Fracture Mechanics*, 5, 585-604 (1973).
7. R.H. Christensen, *Metal Fatigue*, McGraw-Hill, New York (1959).

8. J. Willenborg, R. Engle and H. Wood, "A crack growth retardation model using an effective stress concept", AFFDL-TM-71-1 (1971).
9. O.E. Wheeler, "Spectrum loading and crack growth", *Journal of Basic Engineering*, Trans. of Amer. Soc. of Mech. Eng., 94, 181-187 (1972).
10. C.M. Ward-Close and R.O. Ritchie, "On the role of crack closure mechanisms in influencing fatigue crack growth following tensile overloads in titanium alloys", *Mechanisms of Fatigue Crack Closure* (Ed. J.C. Newman and W. Elber), *ASTM STP 982*, Amer. Soc. for Testing and Materials, 93-111 (1988).
11. H. Nowack, K.H. Trautmann, K. Schulte and G. Lutjering, *Fracture Mechanics* (Ed. C.W. Smith), *ASTM STP 677*, Amer. Soc. for Testing and Materials, 36-53 (1979).
12. P.C. Paris and L. Hermann, "Twenty years of reflection on questions involving fatigue crack growth, Part II: Some observations on crack closure", *Proc. 1st Intl. Conf. on Fatigue Thresholds* (Ed. J. Backlund, A.F. Blom and C.J. Beevers), vol. I, EMAS Ltd, Vorley, U.K., 11-33 (1982).
13. J.L. Robinson and C.J. Beevers, "The effects of load ratio, interstitial content and grain size on low-stress fatigue crack propagation in α titanium" *Met. Sci.*, 7, 153-159 (1973).
14. A.J. McEvily and Z. Yang, "Fatigue crack growth retardation mechanisms of single and multiple overloads" *Proc. Fourth Intl. Conf. on Fatigue and Fatigue Thresholds* (Ed. H. Kitagawa and T. Tanaka), vol. I, MCEP Ltd., Birmingham, UK, 23-36 (1990).
15. J.C. Newman, Jr., "A crack closure model for predicting fatigue crack growth under aircraft spectrum loading", *Methods and Models for Predicting Fatigue Crack Growth under Random Loading* (Ed. J.B. Chang and C.M. Hudson), *ASTM STP 748*, Amer. Soc. for Testing and Materials, 53-84 (1981).
16. C.M. Ward-Close, A.F. Blom and R.O. Ritchie, "Mechanisms associated with transient fatigue crack growth under variable amplitude loading: An experimental and numerical study", *Engineering Fracture Mechanics*, 32, 4, 613-638 (1989).
17. C.J. Beevers, K. Bell, R.L. Carlson and E.A. Starke, "A model for fatigue crack closure", *Engineering Fracture Mechanics*, 19, 93-100 (1984).

18. R.L. Carlson and C.J. Beevers, "A multiple asperity crack closure model", *Engineering Fracture Mechanics*, 20, 687-690 (1984).
19. R.L. Carlson and C.J. Beevers, "A discrete asperities model for fatigue crack growth after an overload", *Proc. Fourth Intl. Conf. on Fatigue and Fatigue Thresholds* (Ed. H. Kitagawa and T. Tanaka), vol. III, MCEP Ltd., Birmingham, UK, 1511-1516 (1990).
20. C.J. Beevers and R.L. Carlson, "A consideration of the significant factors controlling fatigue thresholds", *Fatigue Crack Growth - 30 Years of Progress* (Ed. R.A. Smith), Pergamon Press, 89-101 (1986).
21. J.P. Gallagher and I.F. Hughes, "Influence of yield strength on overload affected fatigue crack growth behavior in 4340 steel", AFFDL-TR-74-27. Air Force Flight Dynamics Lab., Wright-Patterson Air Force Base, Ohio (1974).



(a)



(b)

Fig. 1. Opening stress intensity factor versus crack extension (a) after 100% overload and (b) after 150% overload for Ref. 10 data.

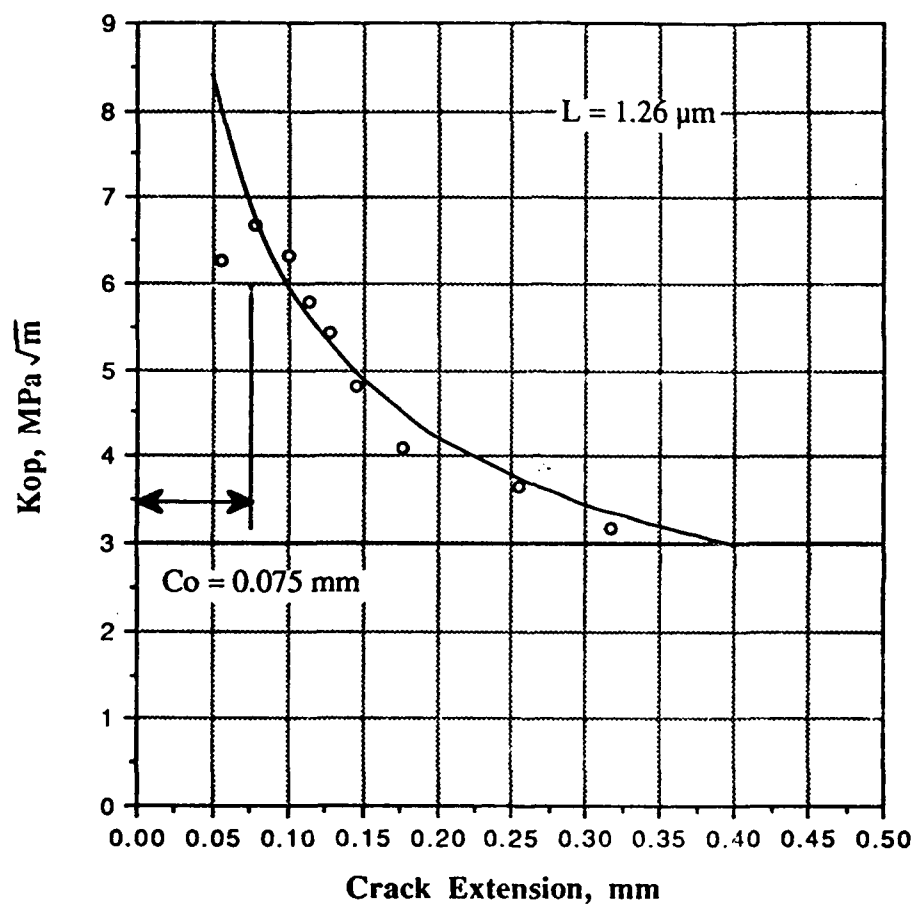


Fig. 2. Opening stress intensity factor versus crack extension for Ref. 14 data.

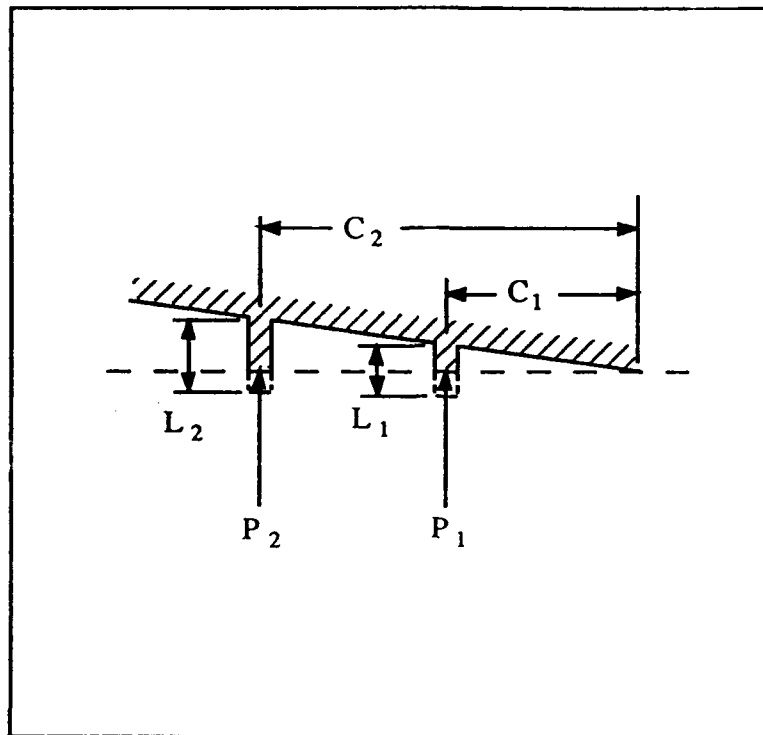
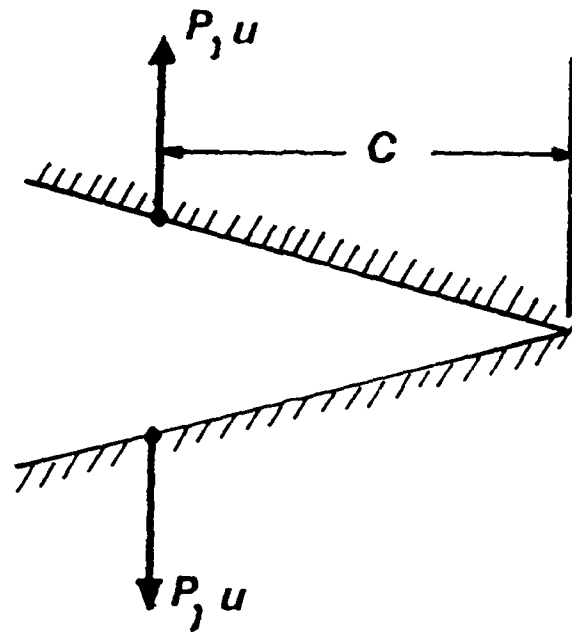


Fig. 3. Discrete asperities model.



$$K = \left(\frac{2}{\pi C} \right)^{0.5} \frac{P}{B}$$

$$u = \frac{2}{\pi G} (1 - \nu) \frac{P}{B}$$

Fig. 4. Concentrated forces on crack faces problem.

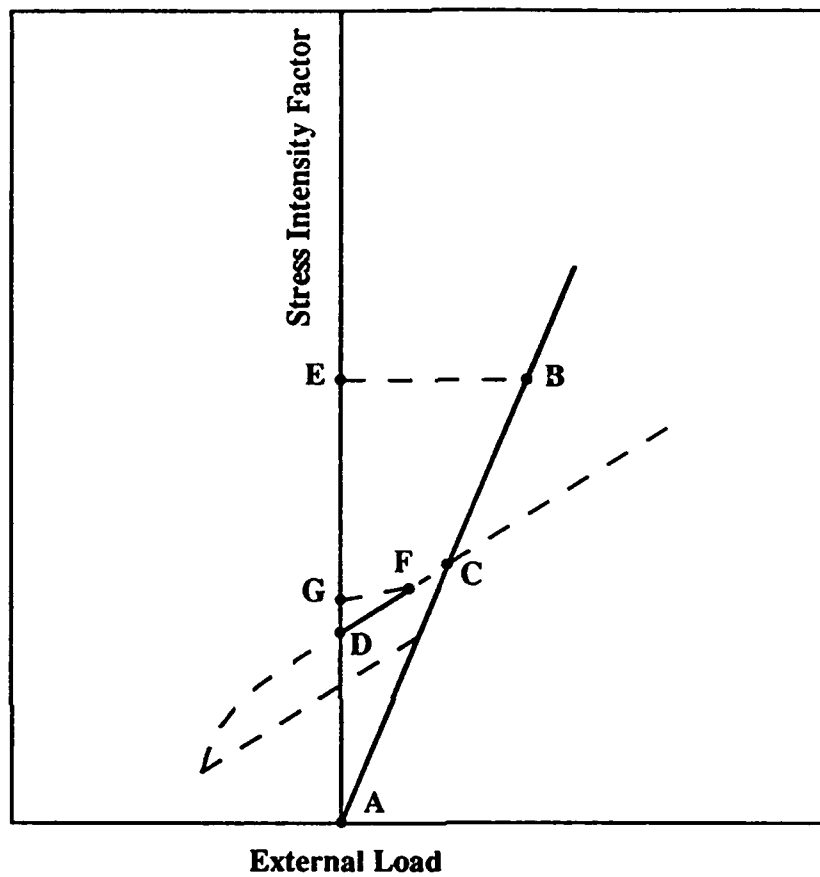


Fig. 5. Closure model for stress intensity factor versus external load.

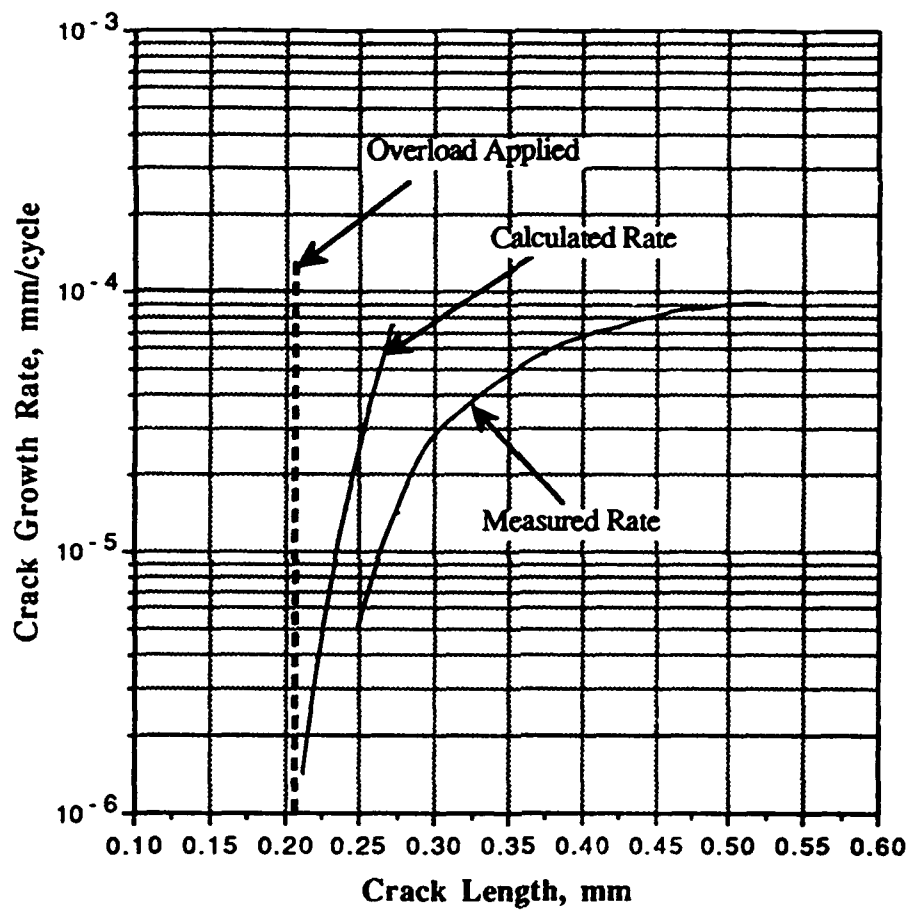


Fig. 6. Comparison of crack growth rates after tensile overload.



NORTHROP

Aircraft Division

Northrop Corporation

One Northrop Avenue
Hawthorne, CA 90250-3277
Telephone 213-332-1000



DEPARTMENT OF THE AIR FORCE
HEADQUARTERS SAN ANTONIO AIR LOGISTICS CENTER (AFLC)
KELLY AIR FORCE BASE, TEXAS 78141-9000

THE ZONING APPROACH TO INSPECTION INTERVALS FOR F-5 AND T-38 AIRCRAFT

M. Gottier, Swiss Federal Aircraft Factory (F + W)
Emmen, Switzerland

-and-

C. Hu, Northrop Corporation, Aircraft Division
Hawthorne, California

M. Reinke, SA-ALC/MMEOD Kelly AFB, Texas

1990 USAF STRUCTURAL INTEGRITY
PROGRAM CONFERENCE

SYNOPSIS

"THE ZONING APPROACH TO INSPECTION INTERVALS FOR F-5 & T-38 AIRCRAFT"

by

M. Gottier, Eidgenossisches Flugzeugwerk (F+W),
Emmen, Switzerland

-and-

C. Hu, Northrop Aircraft Division, Hawthorne, CA

M. Reinke, SA-ALC/MMEOD Kelly AFB, TX

The increased severity of usage for both F-5 and T-38 aircraft have led to requirements to develop new inspection intervals for individualized spectrum for Swiss AF usage of their F-5 aircraft, and USAF advanced training in air combat maneuvering using T-38's. Based on an extensive analytical and experimental program performed by F+W, Switzerland, with technical support from Northrop, the requirements for new inspection intervals for Swiss Air Force usage were established. The concept of structural zoning of the F-5 was developed, and applied to all critical structure for both inspection times and NDI procedure, and a usage peculiar document was prepared for both maintenance and inspection personnel.

Under USAF/SA-ALC contract the T-38 aircraft was analyzed to current Lead-in-Fighter usage. The zoning concept was employed to determine inspection intervals for the T.O.-6. The determination and selection process for those zones will be presented.

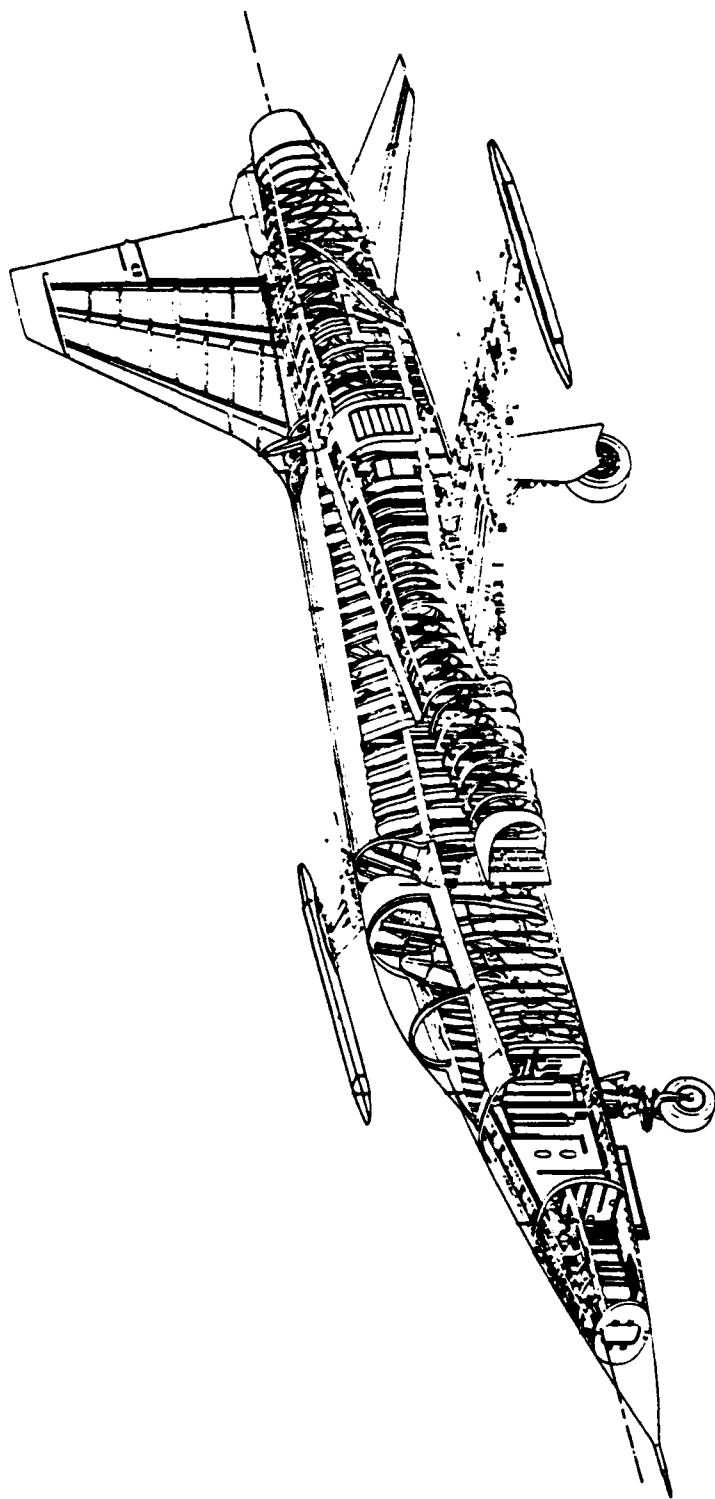
Both F-5 and T-38 programs have made extensive use of confirmatory damage tolerance testing, improved stress intensity factors, and retardation data, which will be presented. The final inspection intervals and use of the zoning concept will be detailed so that others may consider using it for supplemental data to better understand the T.O.-6.

Objectives:

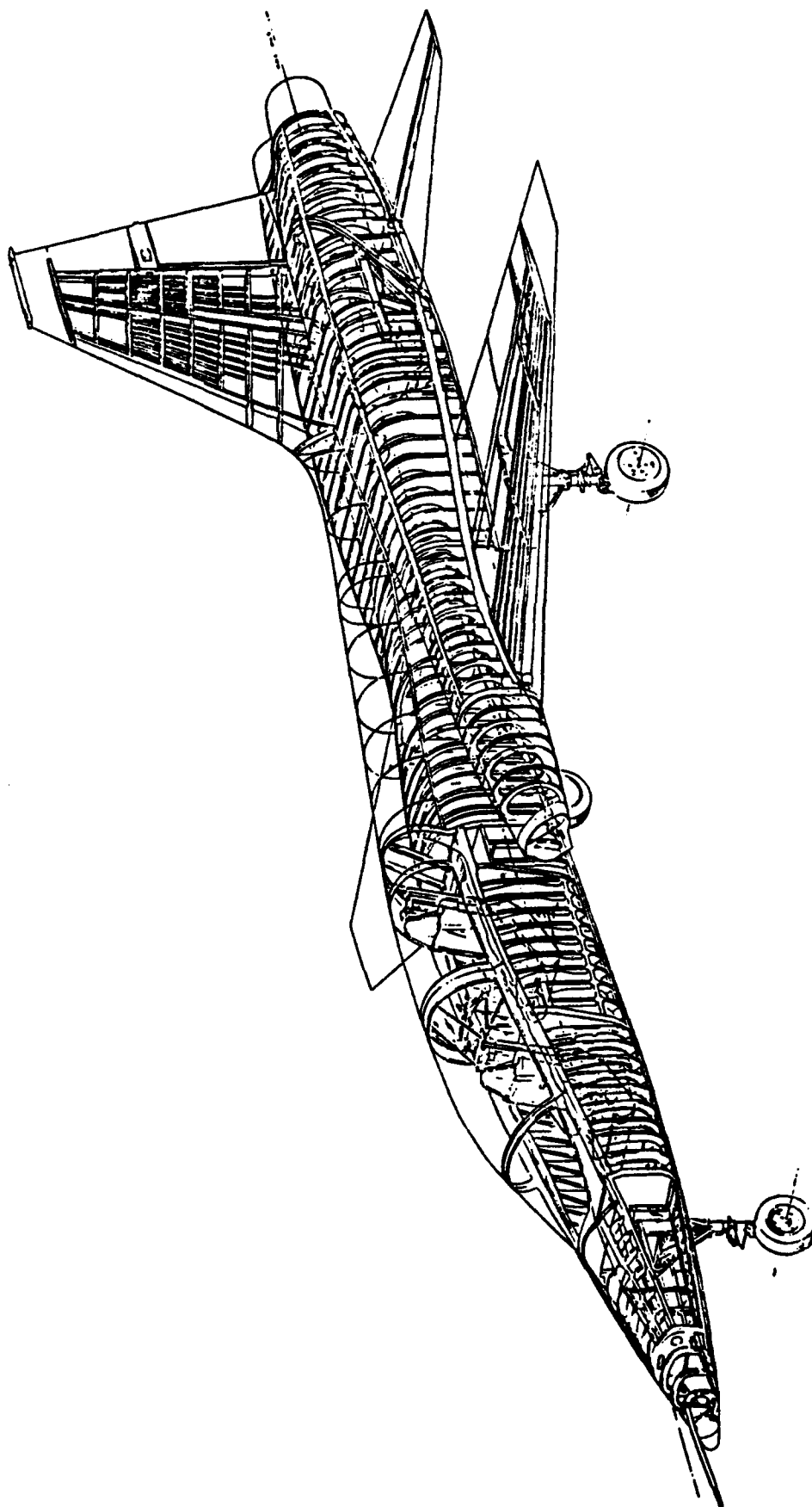
- Adjust the inspection intervals to new usage spectrum
- Enhance the efficiency of NDI procedure
- ↑ Minimize the cost of structural NDI while maintaining aircraft safety and integrity

F-5 AND T-38 STRUCTURES

**DIAGRAMS OF F-5 AND T-38 STRUCTURES TO SHOW THE
OVERALL STRUCTURE AND THE WING PLANFORM
OF EACH AIRCRAFT**



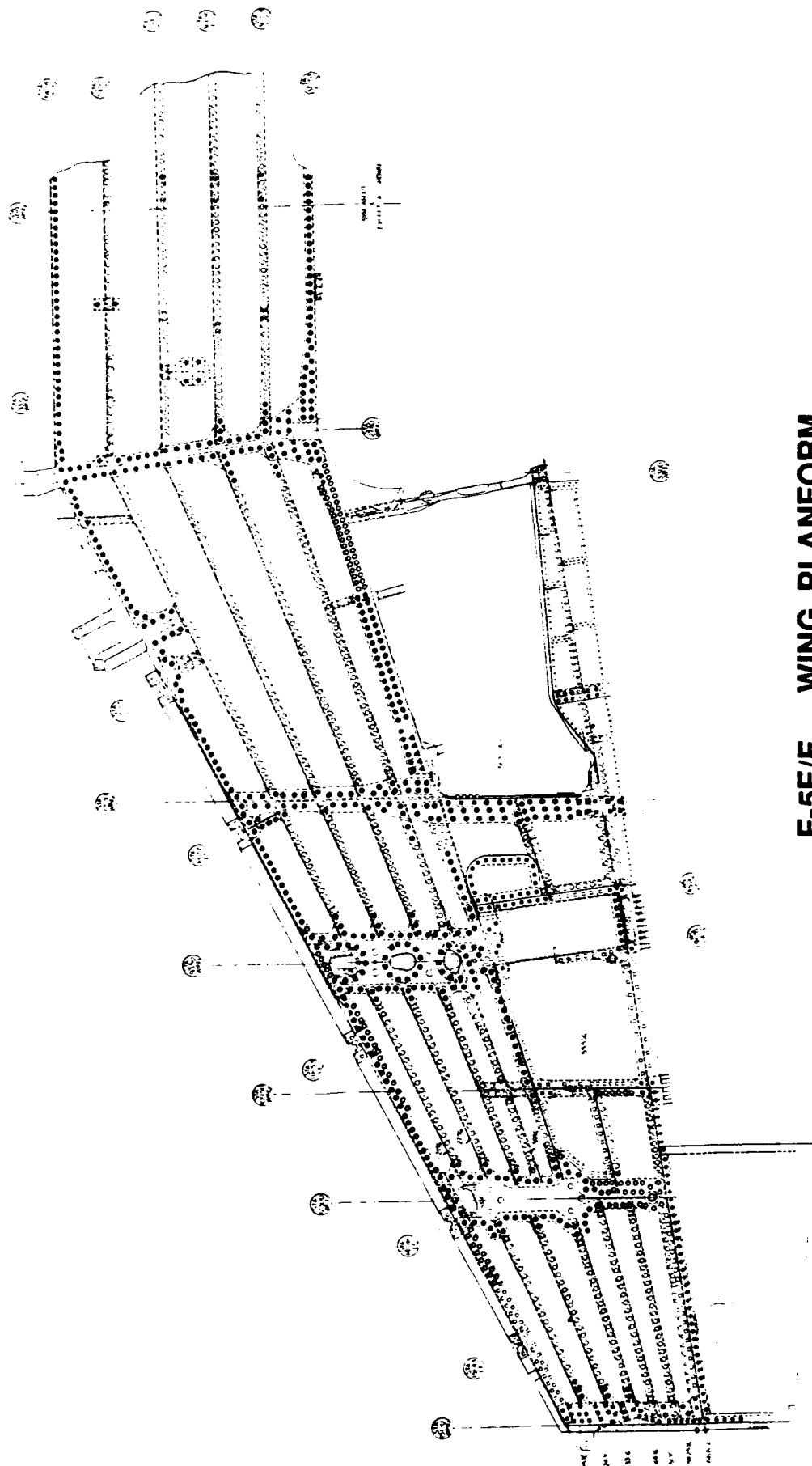
F-5E AIRFRAME STRUCTURAL DIAGRAM



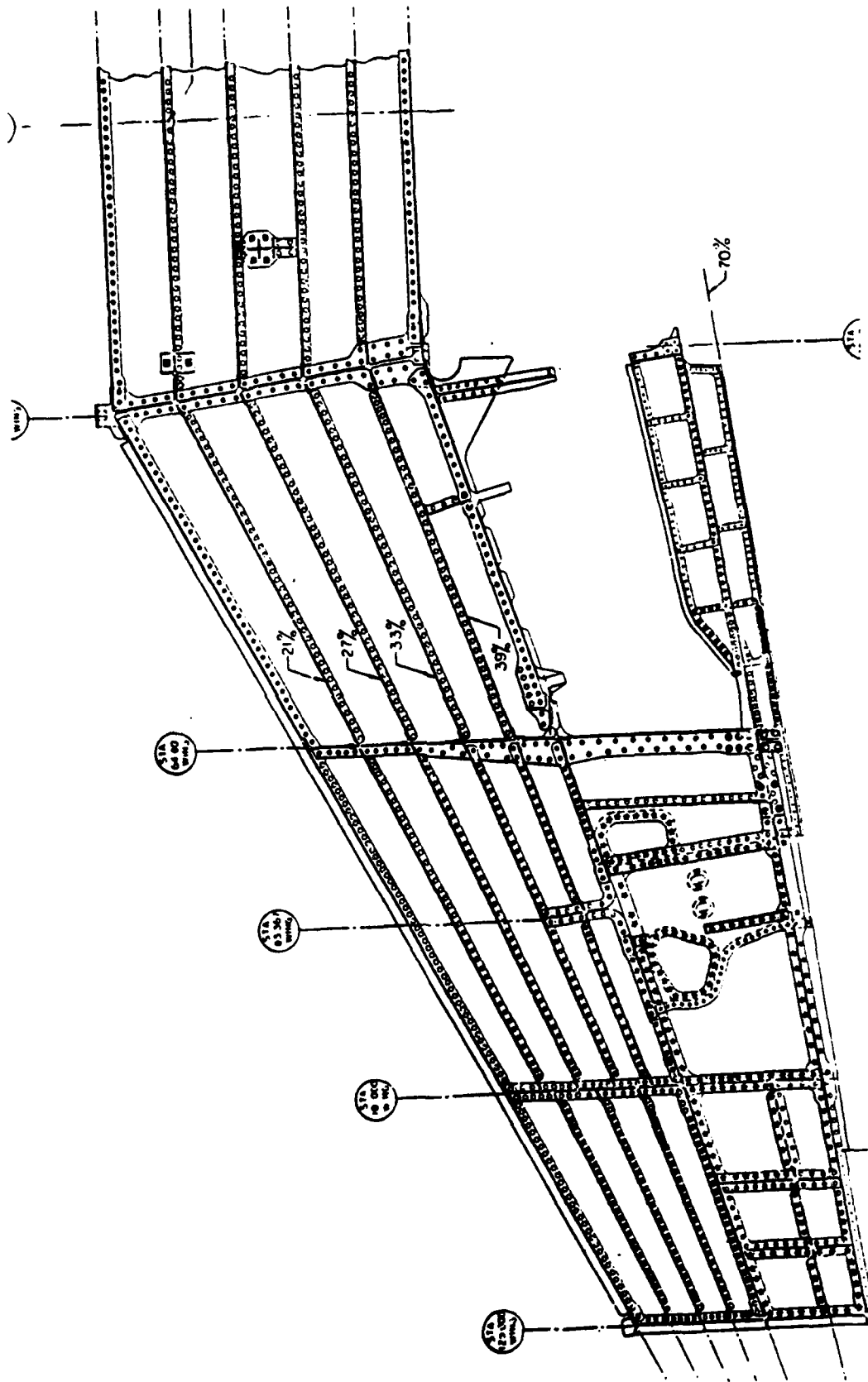
T-38 AIRFRAME STRUCTURAL DIAGRAM

COMPARISON OF F-5E/F AND T-38 WINGS

- **WING PLANFORMS OF F-5E/F WING AND T-38 -29 WING**



F-5E/F WING PLATFORM



T-38 -29 WING PLANFORM

WING ZONING

SCOPE

**F-5: DETERMINE INSPECTION INTERVALS FOR THE F-5 WING FOR
SWISS AF USAGE OF THE F-5 AIRCRAFT IN COMPLIANCE WITH
USAF DAMAGE TOLERANCE PHILOSOPHY**

**T-38: DETERMINE INSPECTION INTERVALS FOR THE T-38 WING FOR
THE CURRENT USAF LEAD-IN-FIGHTER USAGE IN COMPLIANCE
WITH USAF DAMAGE TOLERANCE PHILOSOPHY.**

WING ZONING FOR F-5 AIRCRAFT

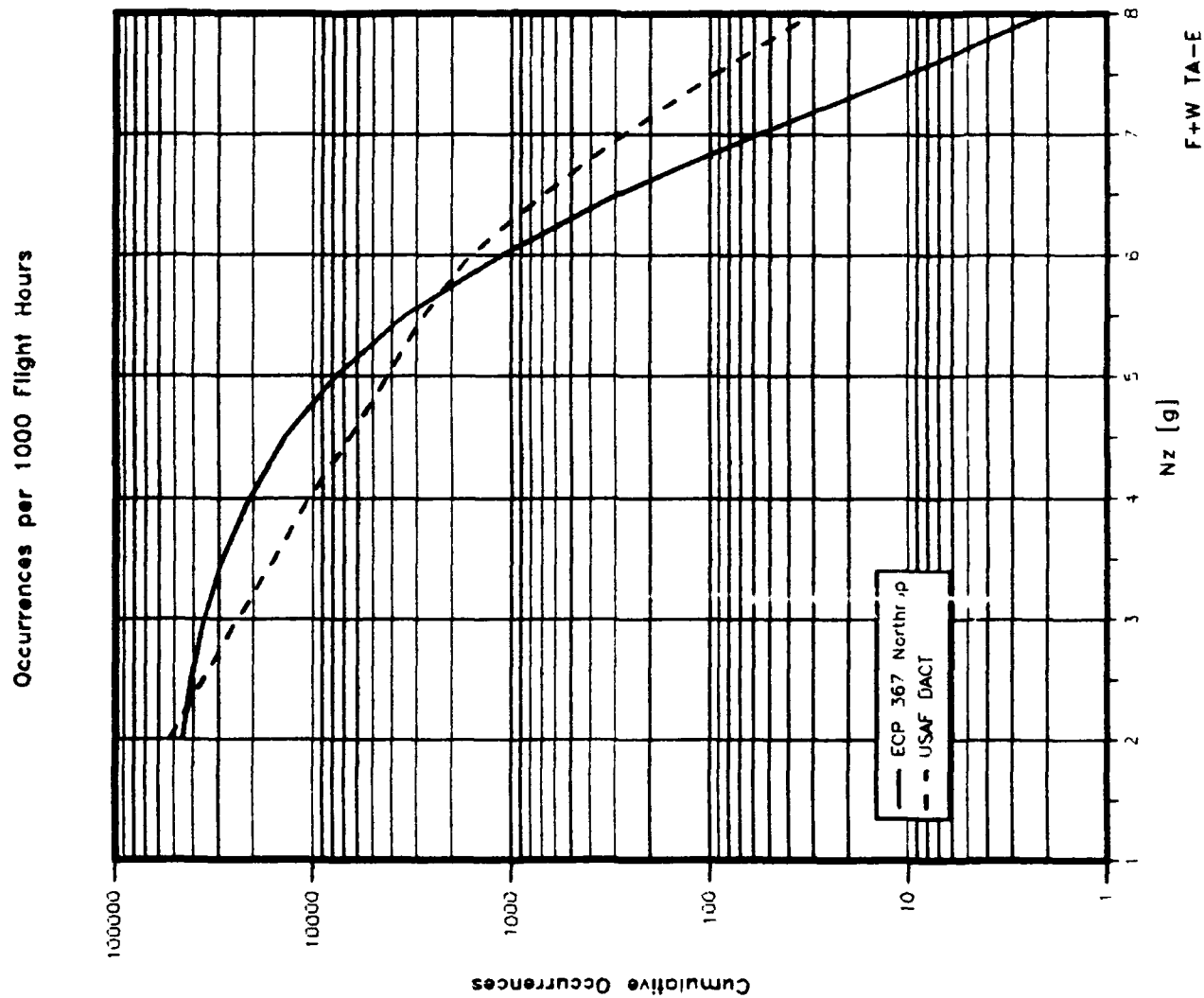
Basic Documents for Structural Maintenance of Swiss F-5 Fleet in 1985:

- T.O. 1F-5E/F-6**
- T.O. 1F-5E-6 WC-3**
- NOR Report, "Swiss F-5E/F Damage
Tolerance Assessment"**

The damage tolerance analysis, carried out in 1983 by Northrop, was based on:

- 152 flight hours of measured n_z -data
- 22 flight hours of measured maneuver type data (n_z , roll acceleration, flap setting)
- mission mix based on 10 missions

F-5E Maneuver Load Spectra, Fleet Average

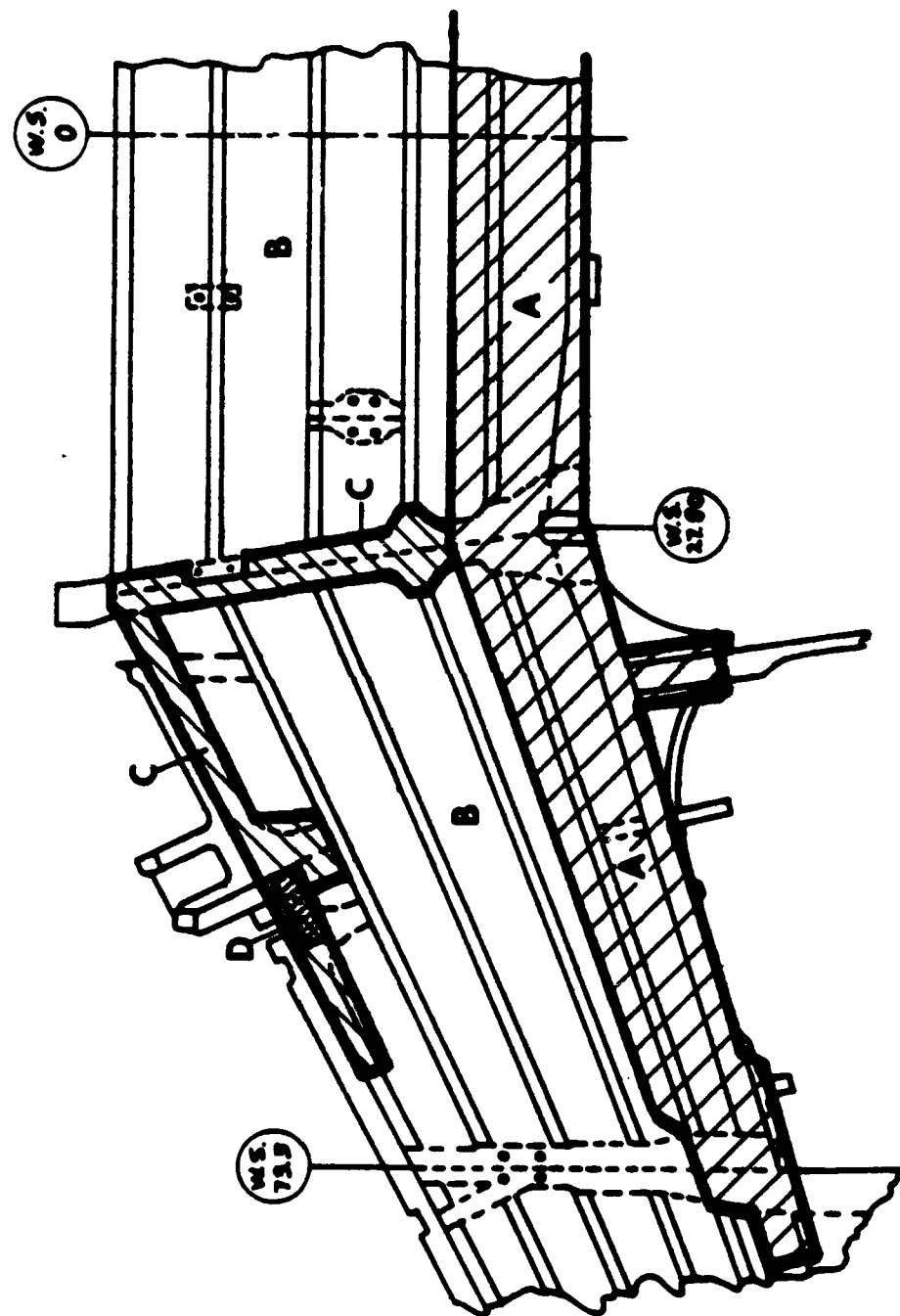


Comparison of Wing Zone Inspection Intervals DACT Spectrum vs Swiss Spectrum

Zone	F-5E		F-5F	
	DACT	Swiss	DACT	Swiss
A	4800 600	900 300	4500 300	900 not def.
B	3600 1200	900 300	3000 900	1500 not def.
C	6000 1200	2400 600	5700 900	3600 300
D	6000 600	3600 300	5400 300	not def.

xxxx	← initial inspection
xxxx	← subsequent inspection

Inspection Zones of F-5E/F Lower Wing Skin T.O. 1F-5E/F-6



**Using inspection zones in
in T.O. 1F-5E/F-6 means:**

- A need of great inspection effort**
- Big part of F-5E/F fleet is not available**
- Operational readiness is not guaranteed**

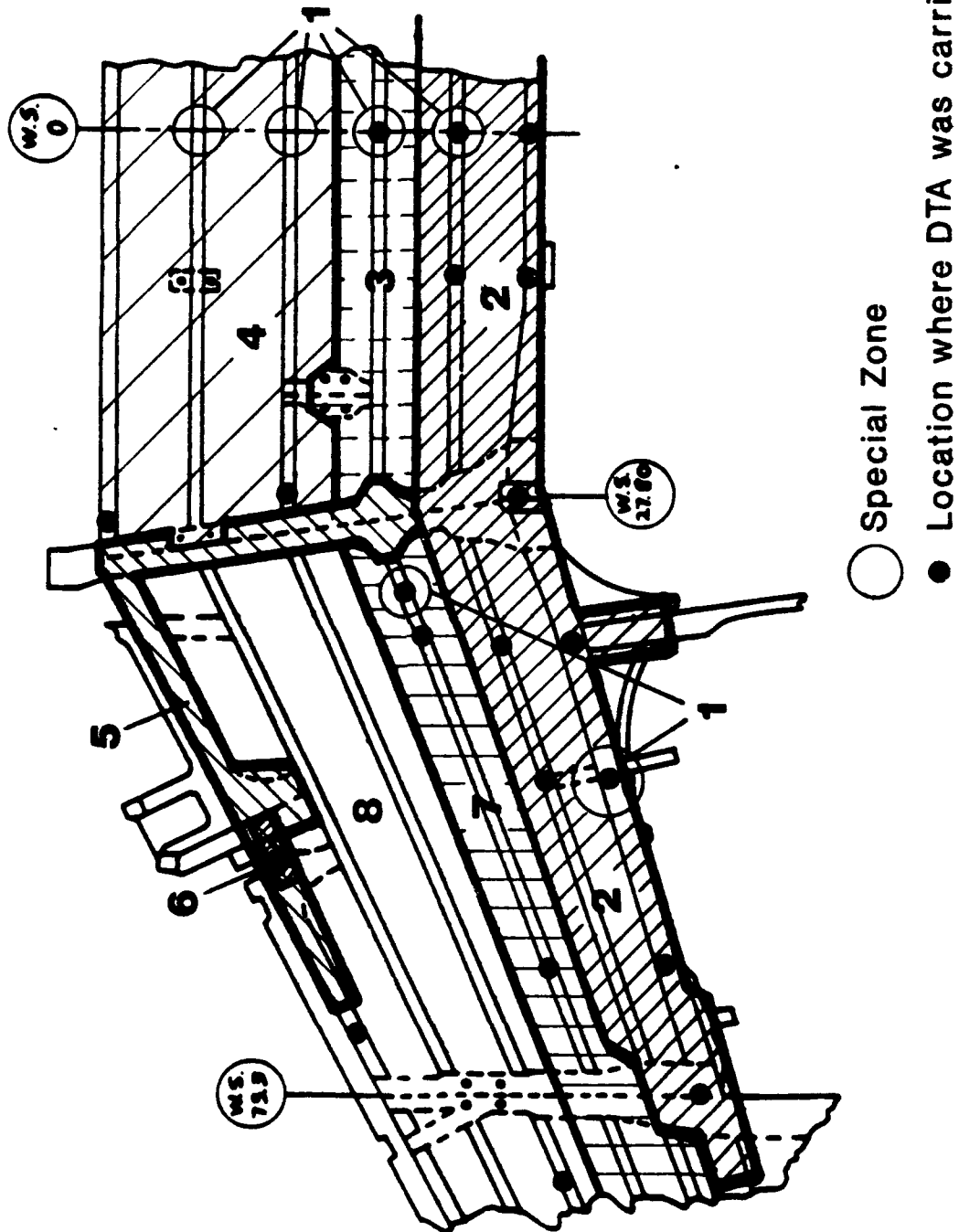
**New zoning of lower F-5E/F
wing skin will result in:**

- Drastic reduction of inspection effort**
- Enhancement of probability for detection
of possible cracks**
- Guarantee of airworthiness of F-5E/F fleet**

Procedure to Define New Zones in F-5E/F Lower Wing Skin:

- FEM results to determine highly stressed locations**
- Fatigue equivalent stresses to take in account of skin thicknesses and fastener hole diameters**
- Areas with fatigue improvements**
- Areas with specific structure geometry**
- Data from maintenance and service experiences**

Inspection Zones of F-5E/F Lower Wing Skin New Zones



**The inspection intervals of the
8 zones were defined using:**

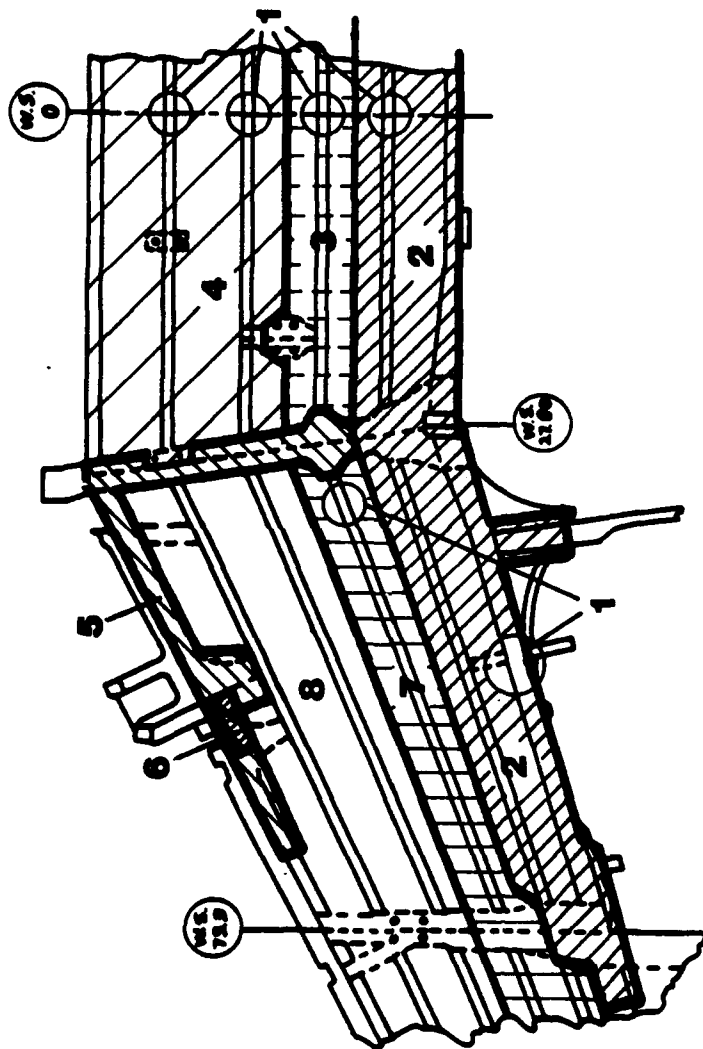
- Crack growth analysis data
from 20 locations**
- In service experience data**

Crack growth analysis has been carried out with SWISCRAK computer program.

Following parameters were used for crack growth analysis:

- Usage Spectrum
- Material Properties (DA/DN, K_{app})
- Stress Environment (Loads and Nastran Analysis)
- Crack Growth Retardation Parameters for Willenborg Model (Damage tolerance testing under spectrum usage)
- Cold-working or Non Cold-working
- Geometry
 - Flaw at Fastener Hold or Edge Flaw
 - Fastener Hole Size, if Flaw at Fastener Hole
 - Edge Distance, if Flaw at Fastener Hole
 - Material Thickness

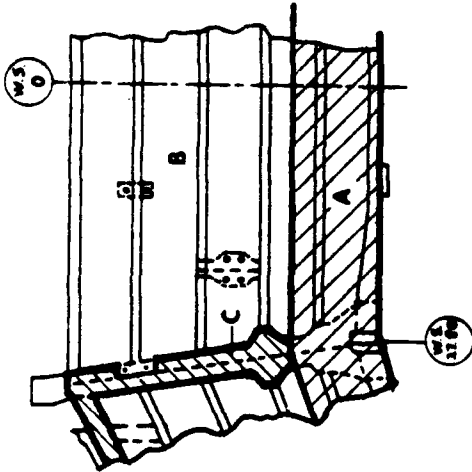
New Wing Zone Inspection Intervals for F-5E/F a/c



	1	2	3	4	5	6	7	8
F-5E	900 600	1800 600	1800 600	3600 1800	3000 600	3000 300	1800 600	2400 1800
F-5F	1800 900	2700 900	2700 900	6300 900	4500 1800	4500 900	3600 900	8100 3600

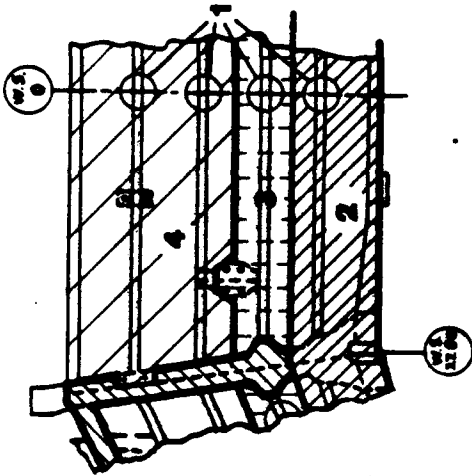
Comparison of Inspection Intervals in the Center Part of the Lower Wing Skin: Zone B vs. Zone 1, 3, 4

Old Zones



B
900/300

New Zones



1	2	3
900/600	1800/600	3600/1800

Conclusions

- Based on our experience, the new wing zoning concept allows us to reduce the inspection effort by more than 50%.
- Despite the drastic reduction of inspection effort, the Swiss Air Force is confident in the ability to maintain the F-5E/F fleet in a safe manner and to guarantee the airworthiness of these aircraft at any time.
- The new zoning concept is part of the Swiss F-5E/F inspection concept, which is the basic document for the structural maintenance of the F-5 a/c since 1988.
- The inspection concept is updated from time to time. These updates are due to feedback from service and maintenance experiences and new collected flight data monitored with the 4 channel tracking system. This system is installed in 30% of the Swiss F-5 fleet.

WING ZONING FOR T-38 AIRCRAFT

WING ZONING FOR T-38

**CRITERIA FOR CHOOSING CRITICAL LOCATIONS ON WING LOWER SKIN
FOR DAMAGE TOLERANCE ANALYSIS**

- WING WAS DIVIDED INTO SECTIONS ACCORDING TO RIB STATIONS
- NASTRAN FEM RESULTS UTILIZED TO IDENTIFY HIGH STRESS LOCATIONS WITHIN EACH SECTION
- STRESS CONCENTRATIONS AND STRESS GRADIENTS TAKEN INTO CONSIDERATION
- HOLE DIAMETERS, EDGE DISTANCES, AND COLD-WORKING TAKEN INTO CONSIDERATION FOR FASTENER HOLES
- IN-SERVICE EXPERIENCE AND FATIGUE TESTING EXPERIENCE ALSO CONSIDERED

ANALYSIS LOCATIONS CHOSEN BASED ON ABOVE CRITERIA

- 52 LOCATIONS CHOSEN FOR ANALYSIS

WING ZONING FOR T-38

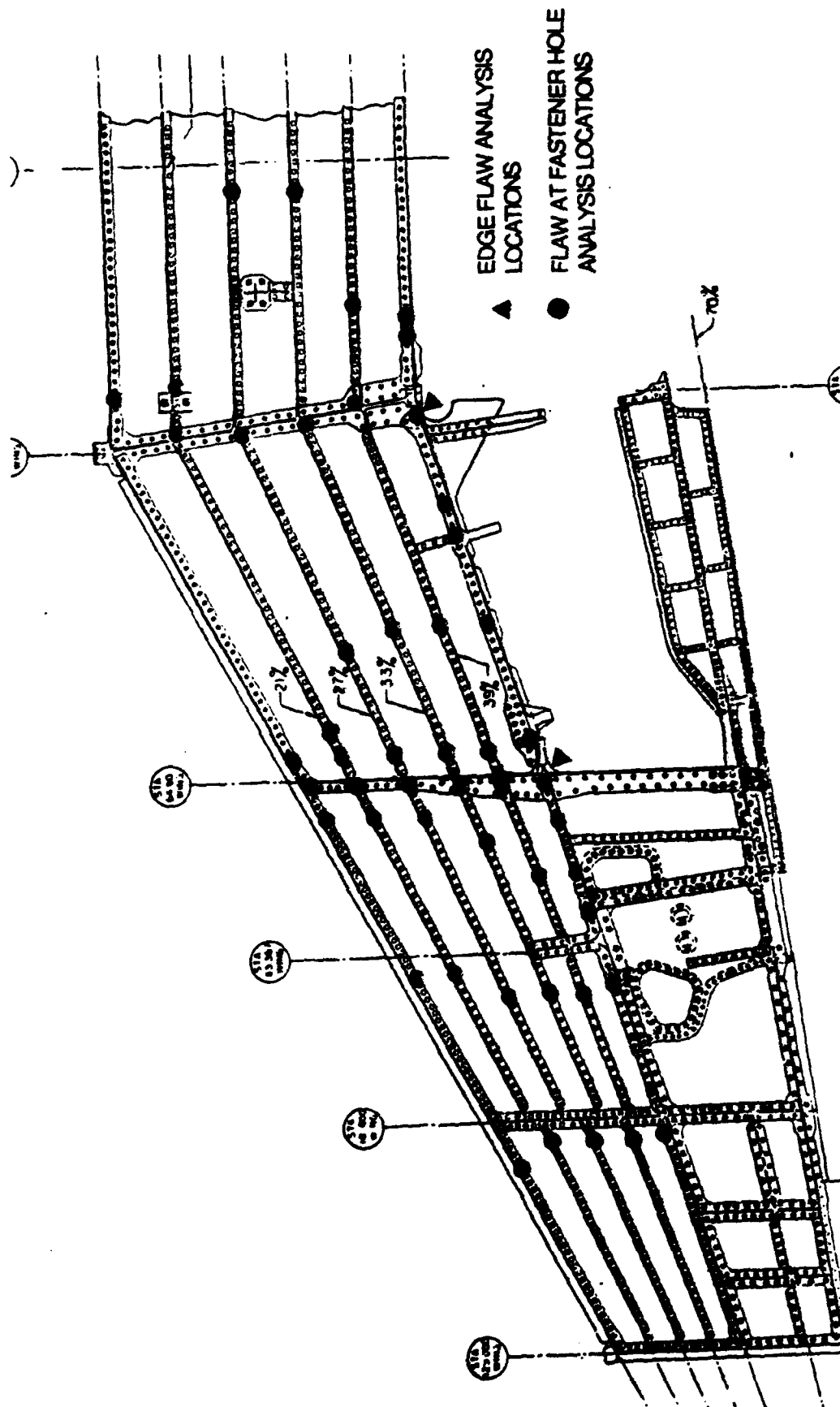


DIAGRAM SHOWING ANALYSIS LOCATIONS
ON WING LOWER SKIN

WING ZONING FOR T-38

DAMAGE TOLERANCE ANALYSIS

- USAGE SPECTRUM BASED ON T-38 USAF LEAD-IN-FIGHTER (LIF) USAGE
- NORCRACK CRACK GROWTH PROGRAM
- MODIFIED WILLENBORG RETARDATION MODEL
- DA/DN DATA FOR 7075-T73511 PLATE
- RESIDUAL STRENGTH CALCULATION BASED ON K_{Ic} AND K_{Ic} FOR 7075-T73511 PLATE

DAMAGE TOLERANCE TESTING

- VERIFY DA/DN DATA CRACK GROWTH DATA FOR 7075-T73511 PLATE
- VERIFY RETARDATION PARAMETERS FOR MODIFIED WILLENBORG RETARDATION MODEL FOR CURRENT LIF USAGE

WING ZONING FOR T-38

**STRESS INTENSITY FACTORS UTILIZED FOR CRACK GROWTH
AND RESIDUAL STRENGTH ANALYSIS**

- FLAW AT A FASTENER HOLE

**NEWMAN-RAJU 1984 CORNER CRACK AT A
FASTENER HOLE STRESS INTENSITY FACTOR**



COUNTERSUNK FASTENER CORRECTION FACTOR

- EDGE FLAW

**NEWMAN-RAJU 1984 CORNER CRACK AT
AN EDGE STRESS INTENSITY FACTOR**



WING ZONING FOR T-38

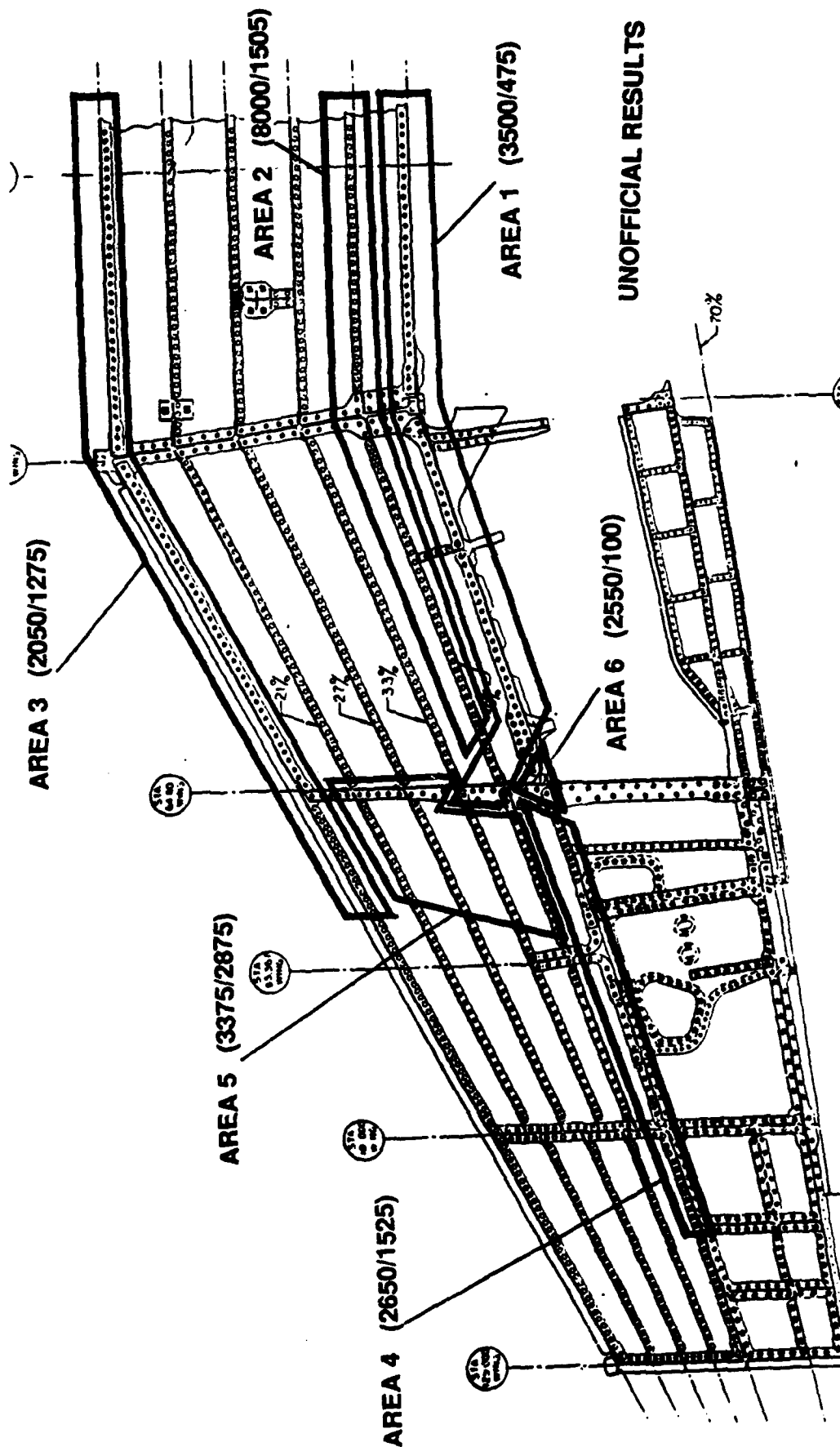
WING ZONING RESULTS FOR T-38

**REVISED INSPECTION INTERVALS FOR T-38 -29 WING FASTENER HOLES
(BASED ON PRELIMINARY RESULTS OF DADTA UPDATE, JAN 90)**

AREA	WING LOCATION	NO. OF HOLES	CURRENT INSPECTION INTERVALS FOR LIF INITIAL/RECURRING	REVISED INSPECTION INTERVALS FOR LIF INITIAL/RECURRING
1	44% SPAR W.S. 63 - W.S. 63	146	3600/900	3500/475
2	39% SPAR W.S. 65 - W.S. 65	144	3600/900	8000/1505
3	15% SPAR W.S. 70 - W.S. 70	170	N/A	2050/1275
4	44% SPAR W.S. 66 - W.S. 110	94	N/A	2650/1525
5	21% - 39% SPAR W.S. 64 - W.S. 80	136	N/A	3375/2875
6	44% SPAR W.S. 64 - W.S. 66	12	3600/900	2550/100
TOTAL NO OF FASTENERS		702		

UNOFFICIAL RESULTS

T-38 WING ZONING



UNOFFICIAL RESULTS

REVISED INSPECTION INTERVALS FOR T-38 -29 WING FASTENER HOLES
(BASED ON PRELIMINARY RESULTS OF DADTA UPDATE, JAN 90)

**THE EFFECTS OF RUNWAY SURFACE ROUGHNESS
ON AIRCRAFT FATIGUE LIFE**

by

**LT David J. Krueger
Mr. Anthony G. Gerardi**

**WRIGHT RESEARCH AND DEVELOPMENT CENTER
FLIGHT DYNAMICS LABORATORY
STRUCTURAL INTEGRITY BRANCH
WRIGHT-PATTERSON AFB, OH**

**1990 USAF STRUCTURAL INTEGRITY
PROGRAM CONFERENCE**

SAN ANTONIO, TEXAS

INTRODUCTION

Recently, the Structures Division of the Flight Dynamics Laboratory at Wright-Patterson Air Force Base, Ohio was asked to take a look at the surface of runway 16/34 at Dyess AFB TX. Pilots using this runway have complained about experiencing an unusual amount of discomfort during ground operations. Several pilots have made claims of being temporarily incapacitated while operating on portions of this rough runway. This particular runway is about 35 years old and has never been overlayed, although small repairs have been made.

Due to the significant accelerations experienced by pilots on the Dyess runway, it was postulated that fatigue damage would be a likely consequence. The next question posed was by what percent would the fatigue life of an aircraft be reduced if it spent its whole life operating on a "rough" as opposed to a "smooth" runway?

The objective of this paper is to present the method and results on the work performed on examining the effects of runway surface roughness on aircraft fatigue life.

The appropriate military specification applicable to ground loads is MIL-A-87221, "General Specification for Aircraft Structures". [1] This specification states that runway roughness for ground operations will be stated in terms of power spectral density levels or discrete (1-COS) bumps and (COS-1) dips. PSD have the distinct advantage of reducing large quantities of data to a few power spectra in the frequency domain. Since PSD techniques have been successfully applied in the area of flight turbulence, similar techniques were also investigated for runway surface effects. The thought was that runways with similar roughness power spectra would provide similar aircraft responses. Reference 2 describes an attempt to apply PSD techniques in comparing roughness effects on aircraft for two different runways. Although both runways had similar roughness power

spectra, in practice one runway was found to be quite smooth while the other produced numerous complaints from flight crews. The failure of this method is because it is only valid for a linear system [3]. This linear assumption is reasonable for flight loads, but not for ground loads. The landing gear are so strongly non-linear that loads derived from PSD analysis can be grossly misleading.

Power spectral density profiles were not used in the present analysis. Instead discretized runway data, along with aircraft model data, was used as input to a computer code to predict accelerations at the aircraft center of gravity. MIL-A-87221 states that dynamic taxi analyses must account for pitch, translation, and roll rigid body modes, and all significant flexible modes. The aircraft gear's complete nonlinear air spring and hydraulic damping of the oleo and tire must be included. Aerodynamic lift and engine thrust shall also be included.

The only criteria from MIL-A-87221 applicable to this analysis is found in Table XII. This table is reproduced in the results section of this paper. It contains occurrences of load factors experienced at the aircraft center of gravity.

Discretized data for three different runways were used in this analysis. The three runways examined were (1) Dyess AFB TX, (2) Palmdale CA and (3) King Kamehameha Air Base, Saudi Arabia. Each of these runways represent various levels of surface roughness. Two different aircraft models were also used. The first aircraft model used in this study was the Boeing KC-135. The second aircraft analyzed was the Rockwell International B-1B.

The aircraft c.g. accelerations obtained from the dynamic taxi analysis were converted to stresses at various locations on the aircraft. These taxi stresses were used with the corresponding flight stresses for each aircraft to make a complete stress spectrum. This full stress spectrum was used as input to a PC based fatigue crack growth analysis code to

study the effect of each runway on the fatigue crack growth at each of the structural locations chosen for analysis.

Dynamic Taxi Analysis

The general mathematical model (TAXI) is represented as an asymmetrical body with a nose, and a right and left main landing gear. [4] For this study, however, symmetry was assumed. Each landing gear strut is assumed to have point contact with the runway profile. The model has aerodynamic lift and drag, and thrust applied at the aircraft's center of gravity.

The airplane is free to pitch, plunge and translate horizontally down the runway and each landing gear unsprung mass is free to translate vertically. To these rigid body degrees of freedom, up to 30 airframe modes of vibration are included. This airplane motion is controlled by the landing gear strut forces, lift, drag, thrust and the resisting parameters of aircraft mass and inertia. The landing gear struts are nonlinear, single or double acting oleo pneumatic energy absorbing devices and are represented in the model as the sum of the three nonlinear forces; pneumatic, hydraulic and strut bearing friction. The tire force is represented as a linear spring constant times an instantaneous deflection.

The runway elevation profile data provides the forcing function for the mathematical model. The profile data is input on two foot intervals and is then made continuous by fitting a polynomial curve through three elevation data points and the slope from the end of the previous profile segment. This polynomial fit technique simulates the engulfing effect that a tire exhibits on step bumps.

The differential equations of motion for the mathematical model (figure 1) were derived by application of the method of Lagrange. These coupled nonlinear differential

equations that describe the simulated aircraft response are solved using a direct three term Taylor series with a time step increment of 0.001 second.

The computed results are displayed as time history printouts or plotted time histories of either gear forces or fuselage vertical accelerations.

TAXI was originally developed in 1970 and has been validated with actual aircraft test data on many occasions. Figure 2 shows a comparison of simulated versus measured aircraft dynamic response for the B-52 aircraft operating out of U-TAPAO AB Thailand during the Vietnam War. Since then, many fighter, cargo, and bomber aircraft have been simulated with TAXI and validated with measured test data. Consequently, a great deal of confidence exists in using TAXI to predict aircraft dynamic response.

The runway profile data used to represent the Dyess runway was measured by Dyess civil engineers using a rod and level. Measurements were taken every two feet for the entire length of the runway. Figure 3 shows a plot of a section of the Dyess profile compared to a known smooth runway at Palmdale CA.

Figures 4 and 5 show the plotted response generated by TAXI of the B-1B aircraft taking off of the Palmdale runway and the Dyess runway, respectively. The difference in load factor level is significant.

The change in dynamic response for the KC-135 was also significant, but not as severe as the B-1B. One reason for this increase response is that the B-1B flexible wing and fuselage structure resonated with the rigid body modes of vibration.

Structurally Critical Locations

The locations on the aircraft structure examined in this analysis were chosen by the aircraft contractors. The selection of these so-called structurally critical locations was based on the respective contractor's experience with the KC-135 and the B-1B and the sensitivity of these aircraft to ground loads.

Two structural locations were chosen for the KC-135 analysis, and four locations for the B-1B analysis. The two structural locations chosen for the KC-135 analysis are an upper wing skin section and a fuselage crown station. The wing detail is an upper wing skin section located at a fuel filler cap cutout between stiffener S-10 and S-11 at wing station 295. The material used at this station is 7178-T6 aluminum. The body detail is a stiffener located at body station 960. The material used at this location is 7075-T6 aluminum. The four locations chosen for analysis of the B-1B are an upper and lower wing station and an upper and lower fuselage station. The upper wing station is located at stringer number 7 at $X_n = 240.6$. The material used is 2124-T851 aluminum. The lower wing station is a rib land fastener hole located at $X_n = 314$ and $Y_n = -23.3$. The material used is 2219 - T851 aluminum. The upper fuselage station is a dorsal longeron located at fastener holes from $Y_t = 820$ to $Y_t = 875$. The material used is PH 13-8Mo, H100 extract. The lower fuselage station is a longeron located at $Y_t = 639.5$. The material used is 7075-T6511 aluminum.

An eight mission composite stress spectrum for the two KC-135 structural locations was also included in the data package. Included with the spectrum for each location was a factor used to convert the accelerations at the aircraft center of gravity to stresses at the location of interest. Stress spectra were also obtained for each of the four structural locations analyzed on the B-1B. A load factor spectrum for the wing and one for the fuselage was also obtained. The load factor spectrum for the taxi loads was correlated with the corresponding stress spectra to obtain a ratio of σ/n_z at each of the four structural locations. This ratio was then used to convert the accelerations at the aircraft center of gravity obtained from the TAXI program, to stresses at the location of interest.

The stresses resulting from the taxi analysis were added to the beginning of the flight spectra obtained from the aircraft contractors. This resulting stress spectra was used in the

analytical fatigue crack growth analysis. Table 5 shows the maximum, minimum, and average values for each of the taxi and flight stress spectra used in the analysis.

Since the objective of this analysis was to obtain general trends for fatigue crack growth occurring from various runway surfaces, the damage that occurs at the actual geometry is not important. To simplify the analytical predictions and to allow for experimental verification of the analytical predictions, the same geometry was used for each structural location analyzed.

The geometry used in the analysis is shown in Figure 6. It consists of a 7075-T6511 aluminum plate that is 4.0 inch wide, 16.0 inch long and 0.25 inch thick. A 0.25 diameter hole is located in the center of the plate. For the purpose of this analysis, the hole used was open and unloaded. In any aircraft structure, initial flaws are assumed to exist as a result of material and structure manufacturing and processing operations. MIL-A-87221 was used to determine the initial flaw size for the test specimen. According to this military specification at a hole where the material thickness is greater than 0.05 inch, the assumed initial flaw shall be a 0.05 inch radius corner flaw at one side of the hole. This is also shown in Figure 6.

Analytical Fatigue Crack Growth Prediction Methodology

The crack growth analysis methodology is based on linear elastic fracture mechanics (LEFM) principles, where it is assumed that at the initiation of fracture, any localized plastic deformation is small and contained within the surrounding elastic stress field. The plastic zone is considered small with respect to the features of the structural geometry and to the physical length of the crack.

The analytical method used in this analysis to predict fatigue crack growth rate is based on tabular data and the Walker equation [5,6]. The Walker equation is a

modification of the Paris equation in that it accounts for the shift in crack growth data due to stress ratio effects. The Walker equation is given below in equation 1.

$$\frac{da}{dN} = C [\Delta K (1-R)^{(m-1)}]^n, \quad (1)$$

where C and n are the fatigue crack growth rate constants, ΔK is the stress intensity factor range, R is the stress ratio, and m is the Walker stress ratio layer "collapsing" factor. When plotted using a logarithmic scale for da/dN vs. ΔK , this equation describes a straight line. Experimental test data shows that crack growth data is usually linear over a limited range of crack growth rates [7]. It takes several Walker lines to account for this change in shape. A problem arises when using the Walker equation in this manner. The shift that occurs due to the stress ratio is parallel for each Walker line when a logarithmic scale is used. This can be a source of error since the shift in the crack growth rate data as a function of the stress ratio is usually not parallel throughout the entire crack growth range. This is particularly true near the threshold stress intensity factor and critical stress intensity factor ranges.

To account for the non-uniformity in spacing between the curves with variations in the stress ratio, Mr James Harter developed the Point-by-Point Walker Shift Method. [6] This method is used in the fatigue crack growth prediction program called MODGRO.

At a given crack growth rate, the crack growth rate constants C and n, may be eliminated from the Walker equation by the relationship shown below.

$$\Delta K_1 (1-R_1)^{m-1} = \Delta K_i (1-R_i)^{m-1} \quad (2)$$

Both R and ΔK are known during a crack growth rate test. Therefore, only one equation is needed to determine the value of m for a given crack growth rate. MODGRO uses 25 pairs of tabular da/dN vs. ΔK data. This requires experimental data for two different stress ratios to determine the 25 associated m values.

The stress intensity factor solution used in this analysis for a single corner crack at a hole is based on the work accomplished by Newman and Raju and is documented in Reference 8.

Since this case deals with a part-through flaw, the analysis transitions to the case for a single through crack at a hole when the depth of the crack has grown through 95 percent of the specimen thickness.

Since a variable amplitude spectrum loading is being used in this analysis, it is important to consider the effects of load interactions on the crack growth behavior. Results from experimental fatigue crack growth tests have shown that tensile overloads cause a retardation in the crack growth rate. The amount of retardation depends on the ratio between the magnitude of the overload and the subsequent cycles. Hold periods, where the stress is maintained at a positive load, increase the retardation effect. Multiple overloads can significantly enhance retardation [9]. The fundamental assumption of yield zone models used in crack growth predictions is that there is retardation as long as the current plastic zone is contained within a previously generated plastic zone.

The retardation model used in MODGRO is the Generalized Willenborg model [10]. This model relates the magnitude of a retardation factor to the overload plastic zone size. The magnitude of this retardation factor is determined by using an effective stress intensity factor that senses the differences in the compressive residual stress state caused by differences in the load levels. The effective stress intensity factor, $K_{I,eff}$, is equal to the remote intensity factor, K_I , for the i_{th} cycle minus the residual stress intensity factor, K_R .

$$K_{leff} = K_i - K_R \quad (3)$$

The residual stress intensity factor, the real meat of the Generalized Willenborg model is given by equation 4.

$$K_R = \Phi \left[K_{max_{OL}} \left(1 - \frac{a_i - a_{OL}}{Z_{OL}} \right)^{1/2} - K_{max_i} \right], \quad (4)$$

where K_{max_i} is the maximum stress intensity factor corresponding to the remotely applied stress of the current cycle in the crack growth calculation. The incremental crack growth immediately following the overload cycle is $\Delta a = a_i - a_{OL}$. The overload plastic yield zone size is given by Z_{OL} . The multiplier Φ is determined from

$$\Phi = \left[\frac{1 - \left(\frac{K_{max_{TH}}}{K_{max_i}} \right)}{R_{SO} - 1} \right], \quad (5)$$

where $K_{max_{th}}$ is taken to be the lowest value of K that will cause a crack to grow for $R=0$. It is determined from the relation of $K_{max_{th}} = \Delta K / (1-R)$. R_{SO} is the overload shut-off ratio, and is defined as the ratio of the overload maximum stress to the subsequent minimum stress required to stop further crack growth.

$$R_{SO} = \frac{K_{max_{OL}}}{K_{max_i}} \quad (6)$$

This ratio is determined by experimental testing and is affected by the type of underload/overload cycle, as well as the frequency of the overload occurrence. Equation 3

indicates the complete stress intensity cycle is reduced by the same amount. This means that the retardation effect is sensed by the change in the effective stress ratio calculated by

$$R_{eff} = \frac{K_{min}|_{eff}}{K_{max}|_{eff}} = \frac{K_{min} - K_R}{K_{max} - K_R} \quad (7)$$

Another load interaction effect that must be considered when using variable amplitude spectra is the crack growth acceleration effect due to compressive underloads. A compressive underload will annihilate some of the residual compressive stresses left by a tensile overload and reduce the crack retardation benefit caused by a tensile overload. MODGRO incorporates a method to handle compressive load effects. When a compressive stress is encountered, the overload yield zone size is reduced by the ratio of the minimum stress to the most recent overload stress. An effective crack is also determined by adding the current yield zone to the calculated crack length. If this effective crack length extends beyond the overload yield zone, then the previous overload is no longer assumed to retard crack growth.

All of the stress spectra used in this analysis contained blocks of cycles. The numerical method used to accumulate the growth of a crack is a modification of the Vroman linear approximation technique. This method assumes that the crack growth rate is constant throughout a block of cycles. A limit of 3 percent was used as the maximum allowed crack growth increment. This crack growth increment is divided by the current crack growth rate to determine a value for δN . If the number of cycles in the current block is greater than δN , the crack length is incremented by $\delta N \cdot \frac{Da}{DN}$. If, however, the value of δN is greater than the number of cycles in the current block, the crack length is incremented by $N \cdot \frac{Da}{DN}$, where N is the number of cycles in the current

block. After the crack length has been increased, a new crack growth rate is determined and the integration procedure continues.

RESULTS

MIL-A-87221 contains criteria for aircraft taxi ground loads. The criteria is based on load factor occurrences experienced at the aircraft center of gravity. A summary of the load factor occurrences predicted for each aircraft model during the taxi analysis is shown in Tables 1 through 3. Also shown, as a reference, are the guidelines presented in the military specifications. The results listed in these tables include the load factors experienced during both takeoff and landing. For this study, the ground loads experienced during taxi were assumed equivalent to those experienced during landing. The results presented in these three tables for the two aircraft and three runways show that the Dyess runway is the roughest of the three runways. This conclusion is based on the larger number of load factor occurrences experienced by each aircraft operating on this runway compared with the results obtained by operating on the other two runways. The smoothest runway is the King Kamehameha runway in Saudi Arabia. Notice that the fewest number of load factor occurrences are obtained using this runway, and also the smallest acceleration peaks occur on this runway.

The analytical fatigue crack growth predictions are shown in Figures 7 through 10. A summary of these results are shown in Table 4. The fatigue life of the KC-135 fuselage location is reduced by 4.7% when operated on a rough (Dyess) versus a smooth (KKAB) runway. This is shown graphically in Figure 7. This is an insignificant reduction in life, especially since it occurs over a period of more than 20,000 flights. A summary of the stress spectra used for all the analyses is presented in Table 5. The reason the change in taxi spectra for the KC-135 fuselage locations produces insignificant results is that the flight stresses are more severe than the taxi stresses. These flight stresses dominate in the

analytical fatigue crack analyses. Most of the overload zones are produced from the flight stresses.

Figure 8 shows the fatigue crack analyses for the upper wing location on the KC-135. For this case, operation on the rough runway at Dyess reduces the life by 47.5% over operation on the KKAB runway, certainly a significant reduction. However, when one considers that this reduction occurs over a period of more than 93,000 flights, these results become less significant. These results are reasonable when considering the stress spectrum used in the analysis. The flight stress are all in compression, which is expected since the wing experiences a vertical force in flight due to the force of lift. This will put the upper surface of the wing in a state of compression. Therefore, since the opposite trend occurs while the aircraft is on the ground, the only tensile stresses on the upper wing occur as a result of the ground loads. The long life predicted seems reasonable when one considers that the ground loads are relatively small. The average stress from the taxi loads used in the analysis is roughly 6 ksi. The stress ranges used at this location are also very small. This means that the stress intensity factor range will also be quite small. Since this is the driving parameter for the fatigue crack growth, the long life prediction is reasonable.

The fatigue crack analysis results on the upper fuselage location for the B-1B are shown graphically in Figure 9. Notice that the stresses occurring during taxi operations on different runway have no effect on the fatigue crack growth surface roughness conditions at this structural location. The stresses experienced at this location are very high, as Table 5 shows. This is why a material with a strong resistance to fatigue crack propagation must be used at this location. Table 5 shows that the average stress range for the flight loads are more than 10 times as large as that for the ground loads. In fact, the stress range for the ground loads is only about 1 ksi. Since the critical crack size for this location is very small (0.16 in), the ΔK for the ground loads is probably not above the threshold level.

If the critical crack size were larger, this small ΔK value may be above the threshold value and hence would have an effect on the fatigue crack growth rate.

Table 5 shows that all the stresses occurring at the lower fuselage location are in compression for both the taxi and flight spectra. Since a crack does not open under compression, and hence $\Delta K < 0$ is undefined in the analytical fatigue crack predictions, there is no fatigue crack growth at this structural location.

The analytical fatigue crack growth predictions, for the B-1B lower wing location is shown in Figure 10. Once again the various taxi stress spectra do not have any effect on the fatigue life at this structural location. All of the taxi stresses are compressive for the lower wing. The only effect that the compressive stresses have is to accelerate the crack growth rate. The manner in which compressive stresses are accounted for in the analytical code were discussed earlier. If the current plastic yield zone has grown out of the overload zone before a compressive stress is encountered, that compressive stress has no effect on the fatigue crack growth. *There are some compressive stresses contained within the flight stress spectrum itself.* These loads may account for acceleration effects before the taxi stresses are reached. Since there are quite a few tensile cycles encountered before and after each taxi spectra, the crack has probably grown out of the current yield zone and a new overload zone is created.

CONCLUSIONS AND RECOMMENDATIONS

The objective of this study was to determine what effect, if any, runway surface roughness has on aircraft fatigue life. Based on the initial results obtained for the KC-135 and B-1B analyses, it appears that runway roughness has a minimal effect on the aircraft fatigue during the life of the aircraft. This conclusion is, however, speculative because of questionable stress levels used in the analysis and therefore requires further analysis or testing for verification. Other airframe structural locations should be analyzed, particularly the landing gear. Verification of the fatigue crack growth predictions should be made with experimental testing using the same stress spectra, material, and geometry. Validation of the taxi analysis computer code could be accomplished with an aircraft flight test program. This would also produce actual stress data which would remove any errors involved in transferring aircraft c.g. acceleration data to stress data at the location of interest.

Several conclusions can be made with a high level of confidence, based on the results obtained from this study. The first is that the *Dyess runway is indeed a rough runway*. This conclusion is based on aircraft pilot station and c.g. acceleration data obtained from the taxi analysis computer code. The second conclusion is that the KC-135 seems to be more sensitive to fatigue crack growth than the B-1B, even though higher load factors were obtained at the c.g. on the B-1B. This is probably due to design and structural considerations. The third and final conclusion is that the B-1B is more sensitive to runway roughness than the KC-135.

REFERENCES

1. "General Specification for Aircraft Structures" MIL-A-87221, Air Force Aeronautical Systems Division, Wright-Patterson Air Force Base, Ohio, February 1985.
2. Implications of Recent Investigations on Runway Roughness Criteria, AGARD Report 416, January 1963.
3. Hacklinger, Max, "The Problem of Design Criteria for Aircraft Loads Due to Rough Runway Operation," Aircraft Dynamic Response to Damaged and Repaired Runways, AGARD-CP-326, August 1982, pp. 15.1-15.3.
4. Gerardi, Anthony G., "Digital Simulation of Flexible Aircraft Response to Symmetrical and Asymmetrical Runway Roughness," AFFDL-TR-77-37, August 1977.
5. Walker, K. in Effects of Environmental and Complex Load History on Fatigue Life, ASTM STP 462, American Society for Testing and Materials, 1970, pp. 1-14.
6. Harter, James A., "MODGRO User's Manual," AFWAL-TM-88-157, February 1988.
7. "Damage Tolerant Design Handbook," Part 2, Metallics and Ceramics Information Center, Columbus Ohio, January 1975.
8. Newman, J.C., and Raju, I.S., "Stress Intensity Factor Equations for Cracks in Three Dimensional Finite Bodies," NASA TM 83200, Langley Research Center, Hampton VA, 1981.
9. Gallagher, J.P., Giessler, F.J., Berens, A.P., "USAF Damage Tolerant Design Handbook: Guidelines for the Analysis and Design of Damage Tolerant Aircraft Structures," AFWAL-TR-82-3073, May 1984.
10. Chang, J.B., Szamossi M. and Liu, K-W, "A User's Manual for a Detailed Level Fatigue Crack Growth Analysis Computer Code, Volume I - The CRKGRO Program," AFWAL-TR-81-3093, November 1991.
11. Chang, J.B., Szamassi, M., and Liu, K-W, "Random Spectrum Fatigue Crack Life Predictions With or Without Considering Load Interactions," Methods and Models for Predicting Fatigue Crack Growth Under Random Loading, ASTM STP 748, 1981, pp. 115-132.

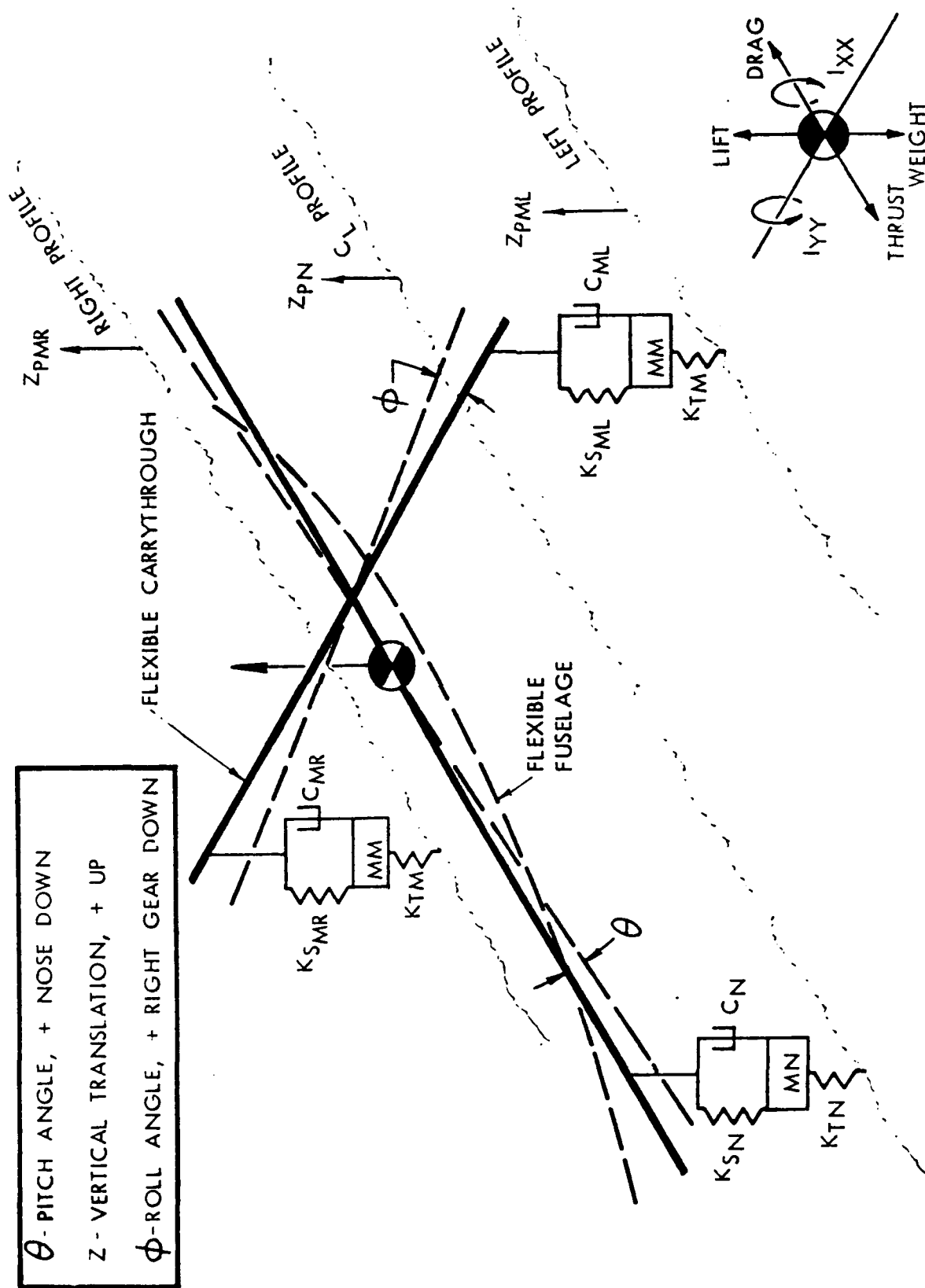
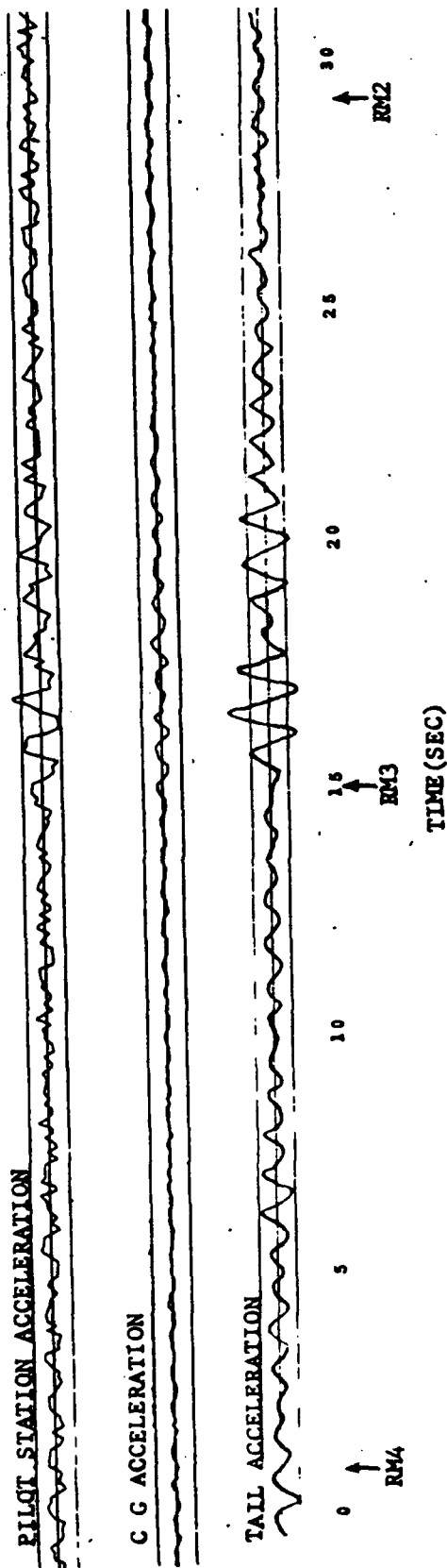


FIGURE 1 Free Body Diagram Used to Develop the Mathematical Model

B-52 40 KNOT TAXI AT U-TAPAO

SIMULATED



EXPERIMENTAL

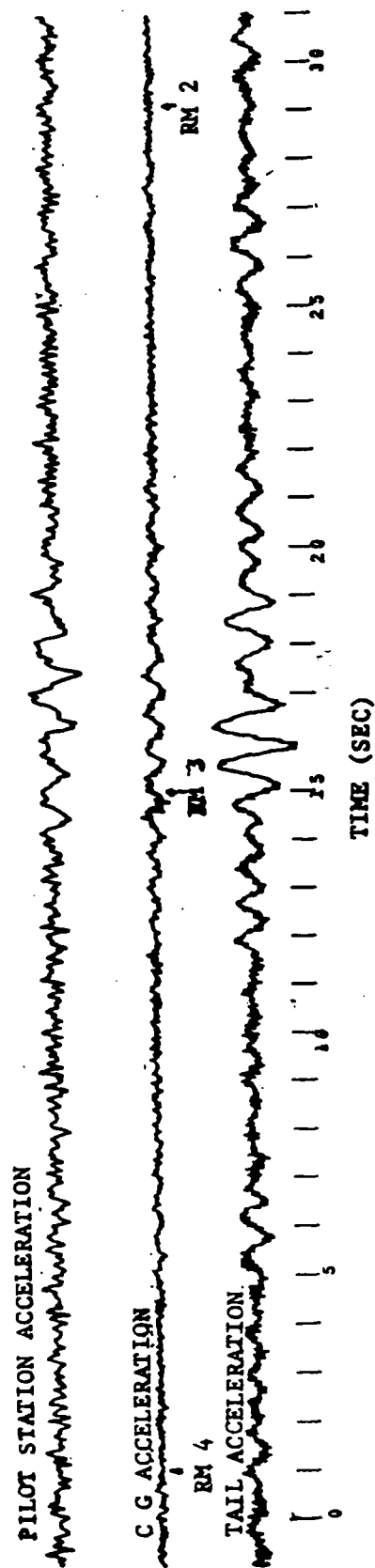


FIGURE 2 Simulated and Experimental Taxi Results

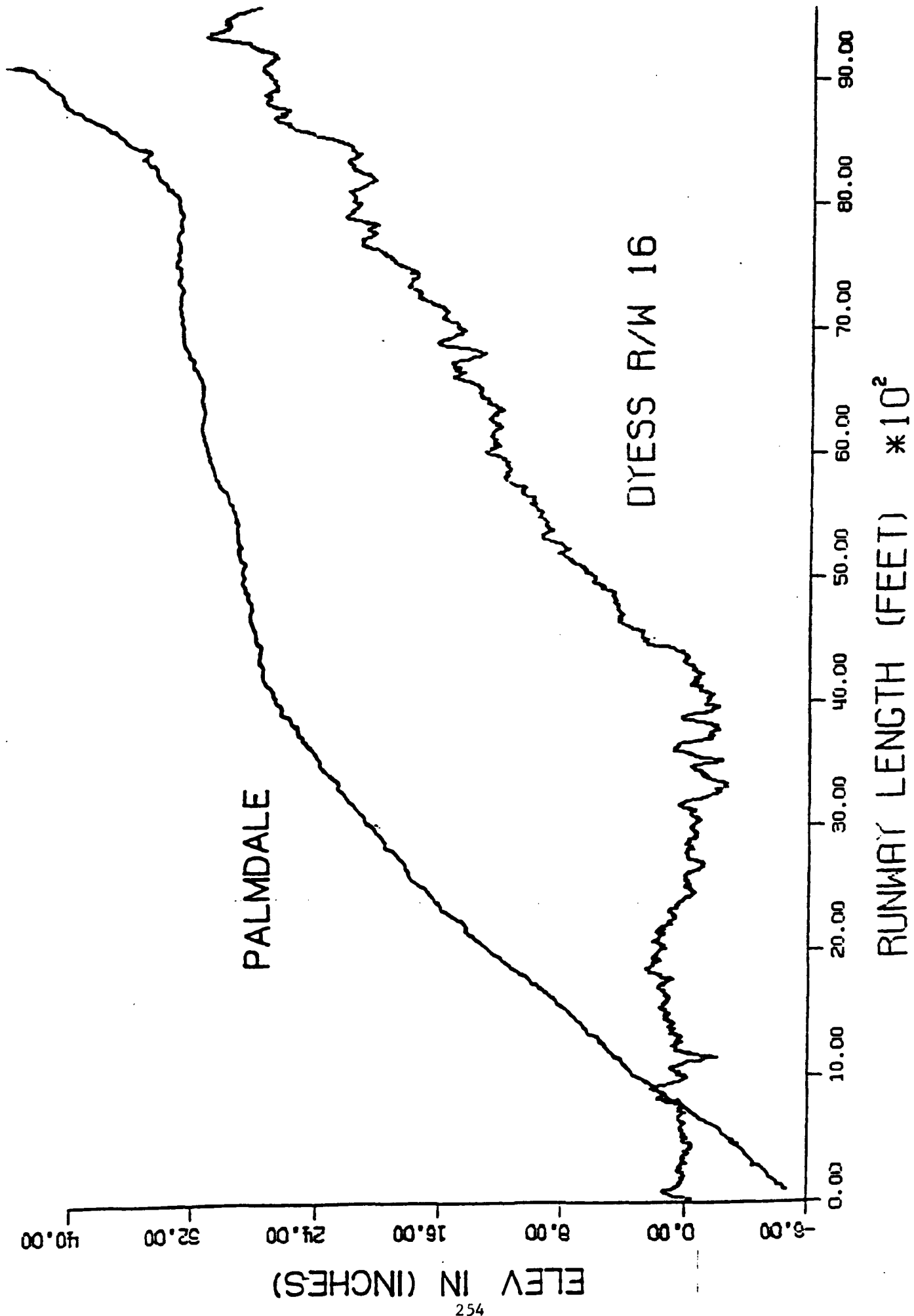


FIGURE 3 Runway Profile Data

B1B 346,500 lbs. 20 deg wing sweep. ful
PALMDALE CA RWY 7/25 centerline from 70

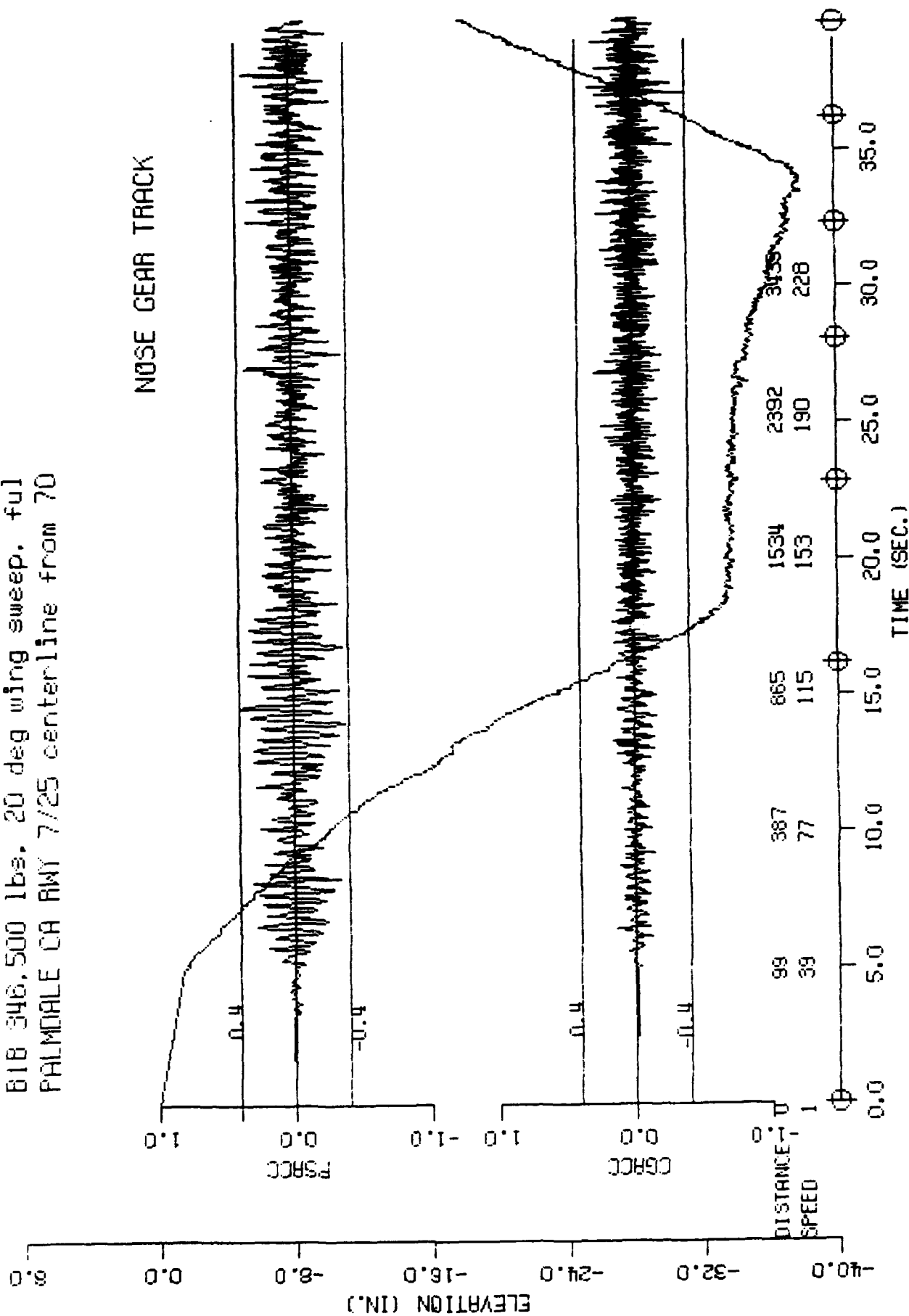


FIGURE 4 Dynamic Taxi Analysis Results on Palmdale Runway

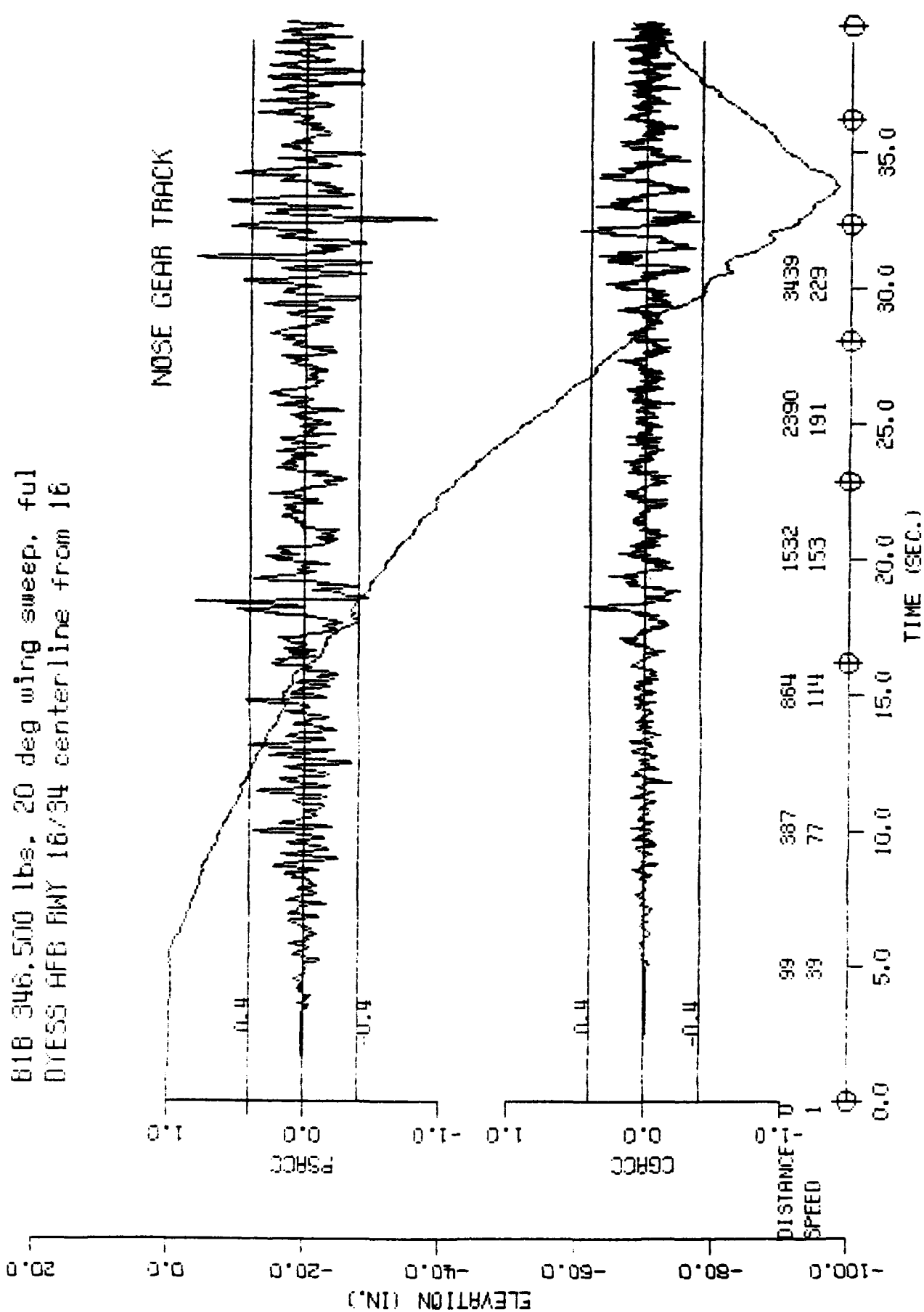


FIGURE 5 Dynamic Taxi Analysis Results on Dyess Runway

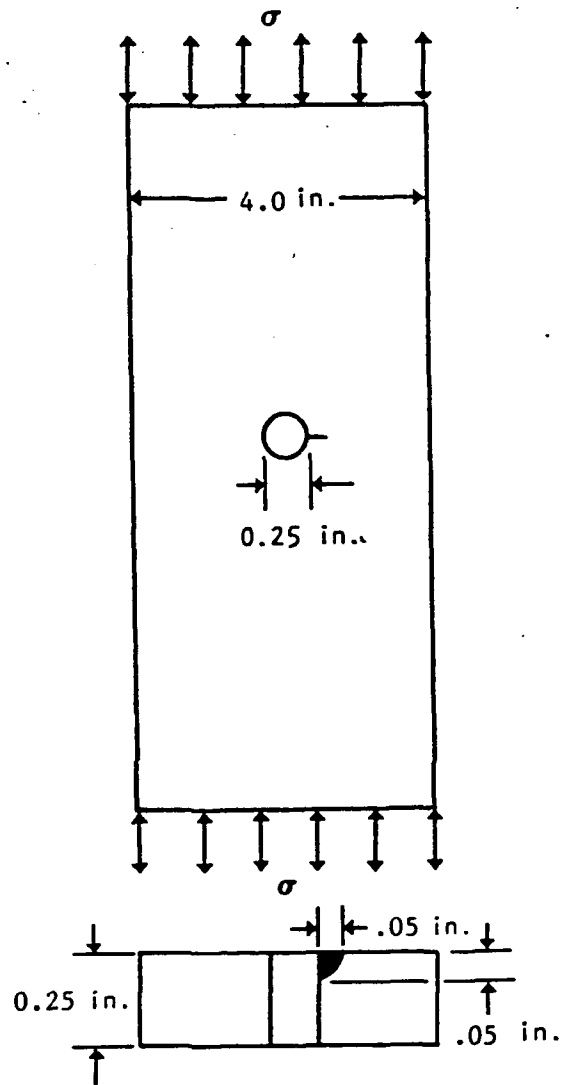


FIGURE 6 A 7075-T6511 Aluminum Plate Containing a Hole With a Corner Crack

KC-135 FUSELAGE SPECTRUM

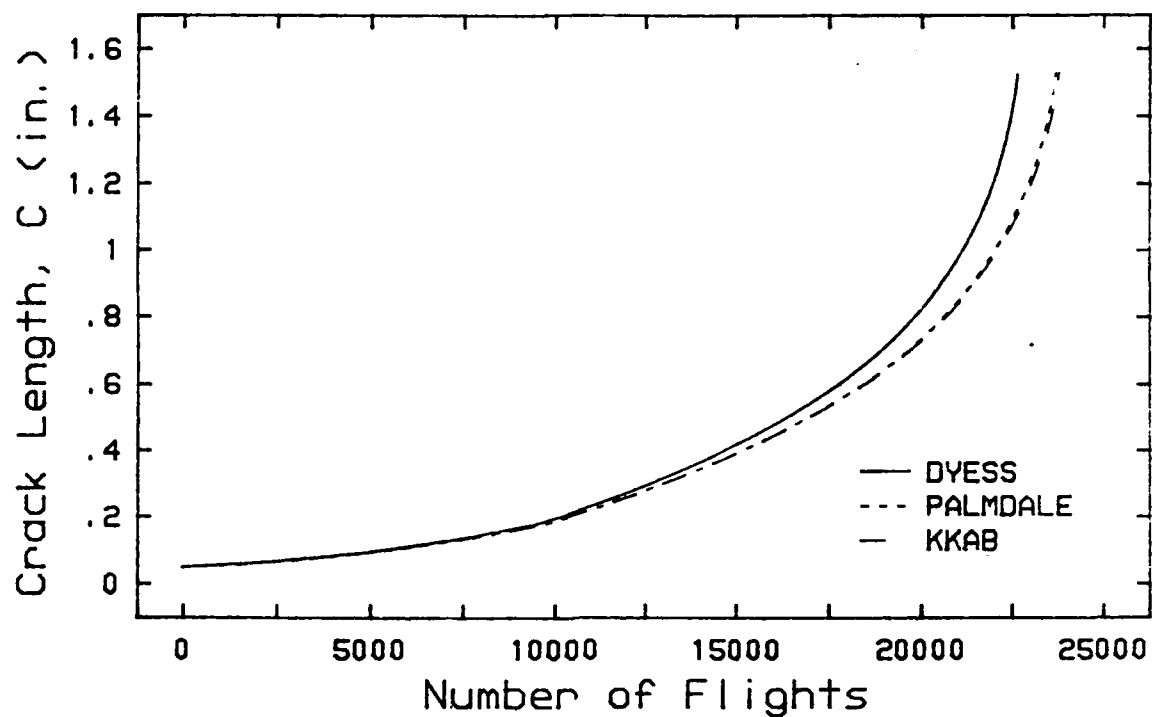


FIGURE 7 Crack Growth Results

KC-135 UPPER WING SPECTRUM

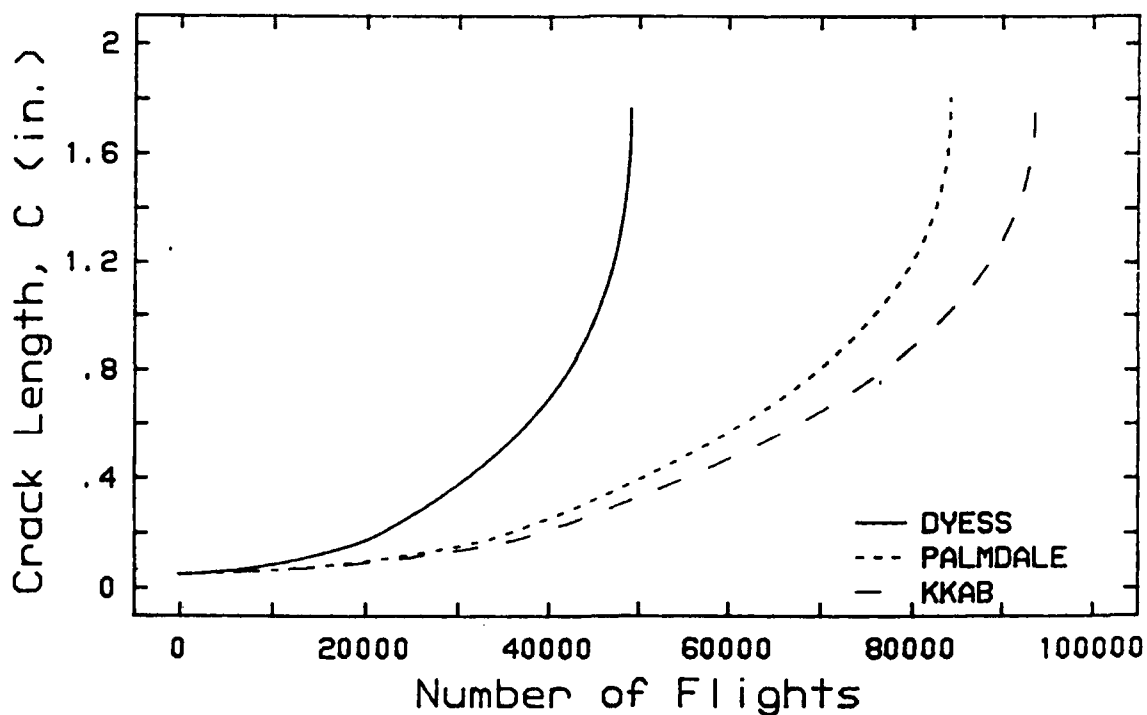


FIGURE 8 Crack Growth Results

B-1B UPPER FUSELAGE SPECTRUM

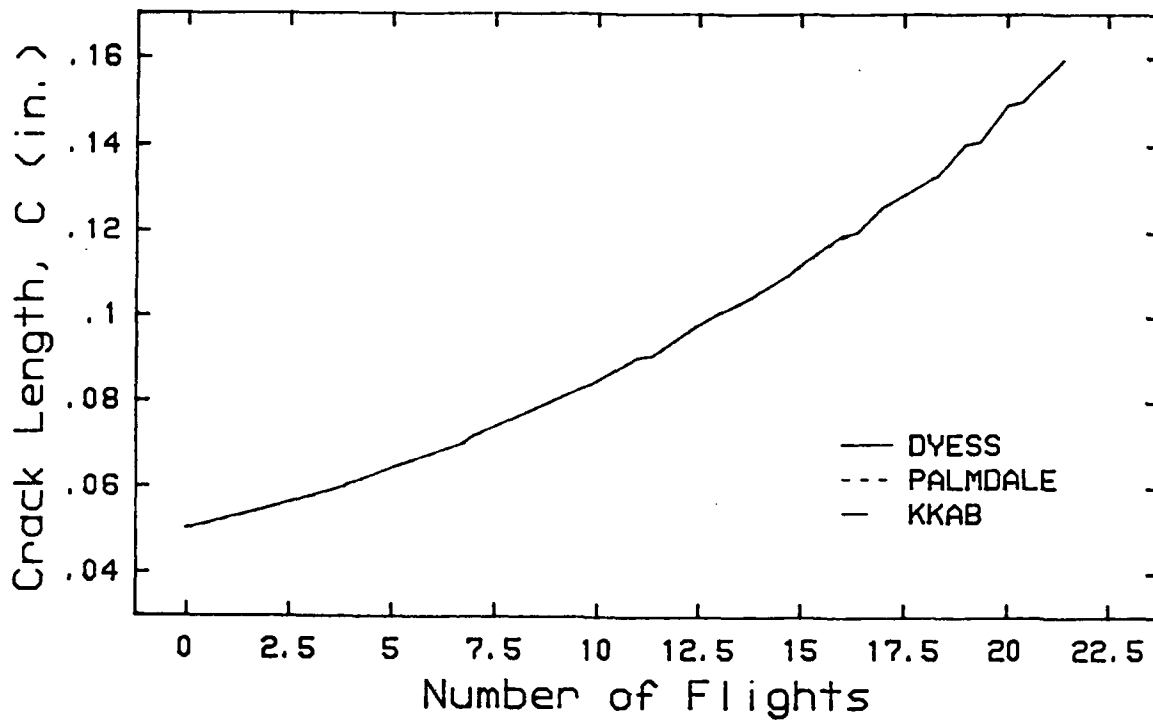


FIGURE 9 Crack Growth Results

B-1B LOWER WING SPECTRUM

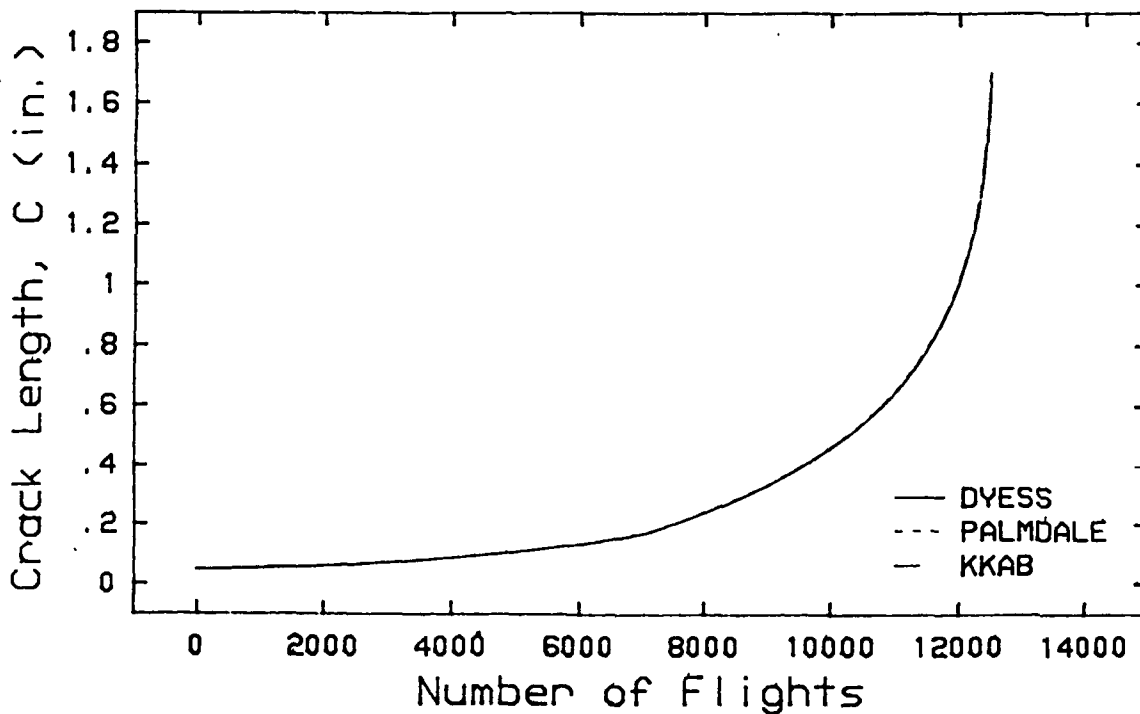


FIGURE 10 Crack Growth Results

**CUMULATIVE OCCURRENCES/1000 RUNWAY LANDINGS
THAT LOAD FACTOR (N_z) IS EXPERIENCED AT THE C.G.**

LOAD FACTOR	OCCURRENCES (KC-135)	OCCURRENCES (B-1B)	OCCURRENCES (MIL-A-87221)
1 +/- 0.0	972000	4480000	988000
1 +/- 0.1	1702000	2716000	388000
1 +/- 0.2	404000	516000	58000
1 +/- 0.3	74000	200000	4200
1 +/- 0.4	0	32000	188
1 +/- 0.5	0	0	8
1 +/- 0.6	0	0	0.31
1 +/- 0.7	0	0	0.01
1 +/- 0.8	0	0	0

TABLE 1 DYESS RUNWAY

**CUMULATIVE OCCURRENCES/1000 RUNWAY LANDINGS
THAT LOAD FACTOR (N_z) IS EXPERIENCED AT THE C.G.**

LOAD FACTOR	OCCURRENCES (KC-135)	OCCURRENCES (B-1B)	OCCURRENCES (MIL-A-87221)
1 +/- 0.0	1428000	4490000	988000
1 +/- 0.1	1572000	3150000	388000
1 +/- 0.2	142000	302000	58000
1 +/- 0.3	4000	22000	4200
1 +/- 0.4	0	4000	188
1 +/- 0.5	0	0	8
1 +/- 0.6	0	0	0.31
1 +/- 0.7	0	0	0.01
1 +/- 0.8	0	0	0

TABLE 2 PALMDALE RUNWAY

**CUMULATIVE OCCURRENCES/1000 RUNWAY LANDINGS
THAT LOAD FACTOR (N_z) IS EXPERIENCED AT THE C.G.**

LOAD FACTOR	OCCURRENCES (KC-135)	OCCURRENCES (B-1B)	OCCURRENCES (MIL-A-87221)
1 +/- 0.0	2820000	6240000	988000
1 +/- 0.1	322000	1690000	388000
1 +/- 0.2	0	8000	58000
1 +/- 0.3	0	0	4200
1 +/- 0.4	0	0	188
1 +/- 0.5	0	0	8
1 +/- 0.6	0	0	0.31
1 +/- 0.7	0	0	0.01
1 +/- 0.8	0	0	0

TABLE 3 KING KAMEHAMEHA RUNWAY

STRUCTURAL LOCATION	CRITICAL CRACK LENGTH (IN.)	NUMBER OF FLIGHTS
<hr/>		
KC-135 FUSELAGE		
1. DYESS	1.525	22659.9
2. PALMDALE	1.531	23679.9
3. KKAB	1.531	23788.9
KC-135 UPPER WING		
1. DYESS	1.767	49150.0
2. PALMDALE	1.807	84206.0
3. KKAB	1.768	93670.0
B-1B UPPER FUSELAGE		
1. DYESS	0.160	21.4
2. PALMDALE	0.160	21.4
3. KKAB	0.160	21.4
B-1B LOWER WING		
1. DYESS	1.705	12485.0
2. PALMDALE	1.705	12485.0
3. KKAB	1.705	12485.0
<hr/>		

TABLE 4 FATIGUE CRACK GROWTH ANALYSIS SUMMARY

STRUCTURAL LOCATION	TAXI STRESS SPECTRUM (KSI)				FLIGHT STRESS SPECTRUM (KSI)			
	MAX.	AVE.	MIN.	AVE.	MAX.	AVE.	MIN.	AVE.
KC-135 FUSELAGE								
1. DYESS	8.35	6.36	3.90	5.77	14.99	10.48	2.70	6.82
2. PALMDALE	7.56	6.29	4.69	5.91	14.99	10.48	2.70	6.82
3. KKAB	6.88	6.17	5.60	6.05	14.99	10.48	2.70	6.82
KC-135 UPPER WING								
1. DYESS	8.23	6.28	3.86	5.70	8.82	-5.07	-13.40	-9.17
2. PALMDALE	7.46	6.21	4.63	5.84	8.82	-5.07	-13.40	-9.17
3. KKAB	6.79	6.09	5.53	5.97	8.82	-5.07	-13.40	-9.17
B-1B UPPER FUSELAGE								
1. DYESS	19.29	13.46	8.19	12.50	56.69	31.27	-1.42	16.57
2. PALMDALE	17.02	13.68	7.87	12.25	56.69	31.27	-1.42	16.57
3. KKAB	15.78	13.32	10.52	12.62	56.69	31.27	-1.42	16.57
B-1B LOWER FUSELAGE								
1. DYESS	-2.45	-3.73	-5.76	-4.02	-0.91	-7.93	-31.83	-13.96
2. PALMDALE	-2.35	-3.66	-5.08	-4.08	-0.91	-7.93	-31.83	-13.96
3. KKAB	-3.14	-3.77	-4.71	-3.98	-0.91	-7.93	-31.83	-13.96
B-1B UPPER WING								
1. DYESS	3.45	2.41	1.46	2.23	2.41	-4.64	-17.39	-10.16
2. PALMDALE	3.04	2.44	1.41	2.19	2.44	-4.64	-17.39	-10.16
3. KKAB	2.82	2.38	1.88	2.26	2.38	-4.64	-17.39	-10.16
B-1B LOWER WING								
1. DYESS	-0.99	-1.51	-2.33	-1.62	12.48	7.38	-1.71	3.14
2. PALMDALE	-0.95	-1.48	-2.05	-1.65	12.48	7.38	-1.71	3.14
3. KKAB	-1.40	-1.61	-1.73	-1.52	12.48	7.38	-1.71	3.14

TABLE 5 STRESS SPECTRA SUMMARY

**A COST EFFECTIVE IMPROVEMENT
IN STRUCTURAL FATIGUE LIFE
THRU GUARANTEED FASTENER HOLE
QUALITY**

by

William H. Lewis, President
Measurement Systems Incorporated
Marietta, Georgia

A COST EFFECTIVE IMPROVEMENT IN STRUCTURAL FATIGUE LIFE THRU GUARANTEED FASTENER HOLE QUALITY

INTRODUCTION

A prime concern in aircraft design and fabrication is the techniques used for joining structural members and components. The method most commonly used is some type of mechanical fastening system. But, whenever holes are placed in components for the purpose of joining them together with bolts or fasteners, the stress concentration resulting from these holes significantly reduces the dynamic load which the components can safely carry. It is sometimes possible to reduce the importance of these stress concentrations by locating the holes in areas which are not critically stressed. As a practical matter however, the requirements for fasteners are so numerous and their placement so widespread that other means must be used to mitigate the fatigue strength degradation due to the stress concentrations caused by many holes.

As a consequence, many varieties of "joint fatigue life enhancement" fastener systems have been developed. One of the most widely used approaches to enhancing the fatigue life of structural joints is through the use of interference fit fasteners. Fasteners designed to produce a controlled interference with their hole preload the region around the hole in such a way that the range of cyclic stress will be reduced, thereby improving the joint fatigue life.

Experience has shown that the joint fatigue performance of interference fit fasteners is highly dependent upon the preparation of the holes into which the fasteners are placed. This presentation (Figure 1) discusses the effects of fastener hole quality on structural fatigue life, the methods currently used to inspect and evaluate holes and their limitations, and a new cost effective method which has been developed that assures hole quality.

EFFECTS OF HOLE QUALITY ON FATIGUE LIFE

Although it may be assumed that fastener hole quality may have an effect on joint fatigue life, a belief has existed that by placing an interference fit fastener in the hole, any effects of poor hole quality are mitigated. In actuality however, very little experimental data exists to verify this belief. About the only comprehensive test results available on the effects of hole quality on fatigue life of interference fit structural joints is contained in a report issued by the U. S. Air Force

Materials Laboratory in 1977. This report, AFML-TR-77-185, "Verification of Production Hole Quality", concluded that a variety of hole quality factors (listed in Figure 2) will adversely affect joint fatigue life. The results of this study are summarized in Figure 3 and further discussed below.

Hole Size/Interference The amount of interference between the fastener and hole must be within specification limits to achieve desired joint life performance. Variations within specification limits have little effect, but low interference fits produce larger data scatter.

Bearing Barrelling Figure 4) and bellmouthing (Figure 5) of the hole have serious effects on joint fatigue life. At higher interference fits, bellmouthing has a less detrimental effect. Hole ovality (Figure 6) has a highly detrimental effect on joint fatigue life. Hole ovality is more serious than any other single condition evaluated.

Surface Condition Holes with a surface finish greater than 125 RMS have a detrimental effect on joint fatigue life. Rifling (Figure 7), axial scratches (Figure 8), and chatter all have a detrimental effect on fatigue life. Surface tears and tool marks also have a detrimental effect but to a lesser degree.

Angularity/Perpendicularity Test results indicate that there is no reduction in joint fatigue life for up to 3 degrees misalignment from the centerline of the hole relative to perpendicularity of the surface (Figure 9).

Another factor considered detrimental to joint fatigue life, although not included in the above program, are gaps between faying surfaces (Figure 10). When a joint with gaps between the faying surfaces is pulled together by the fastener, stresses are induced into the members which are pulled together which may have adverse effects on fatigue life.

In summary, any requirement to insure the fabrication of a quality structural joint must include inspection methods to guarantee these quality factors.

STANDARD HOLE INSPECTION METHODS

No single conventional inspection method is available which will measure and evaluate all of the quality factors necessary for an interference fastener hole. In fact, as shown in Figure 11, a number of separate inspections must be accomplished to evaluate all the quality factors. These are briefly discussed below.

Air Gauge Air gauging (Figure 12) is widely used throughout industry for quantitative dimensional measurement of holes. A controlled air flow is metered thru a hollow spindle of known diameter which is inserted into the hole to be measured. The air escapes through opposing orifices and the corresponding pressure change is proportionate to the distance between the spindle and the hole, thereby providing a measure of hole diameter. Accuracies of modern air gauging equipment are generally adequate for fastener hole requirements.

Unfortunately, measurement is only made inside the hole at the location of the orifices on the spindle. Therefore, unless time and great care are taken to record corresponding dimensional measurements all around the hole circumference at incremental depths along the hole bore, nothing regarding the hole shape (ovality, barrelling or bellmouthing) can be learned. In most industrial environments today with the pressures of workload and schedule however, detailed profiling of fastener holes is simply not accomplished even though it has been shown that improperly shaped holes (which provide poor bearing between the hole and fastener) severely effect fatigue life.

Plug Gauge Plug gauging is simply two master male pins, one which is sized for the minimum acceptable diameter and the other sized just in excess of the maximum acceptable diameter for a particular hole. If the first pin cannot be inserted, the hole is too small. If the second pin can be inserted, the hole is too large. This inspection is quick, takes little operator training, and requires minimum cost. However, it again tells nothing about the actual size or shape of the hole, only whether the overall diameter at the hole entrance is within specification allowables.

Protrusion Measurement Protrusion measurements (Figure 13) of the extension of the fastener head above the hole surface are sometimes required for tapered fastener holes. The proper amount of head protrusion is an indirect indication of proper hole taper and interference fit and therefore, to some degree, proper bearing between the hole and fastener. This measurement is usually made with feeler gauges or a depth gauge, is reasonably quick, dependant upon the inspectors feel and judgement, and is rarely recorded as a quantitative number.

Blue Pin Sometimes known as a Bluing Dye Pin Check, (Figure 14) this inspection is usually required for tapered fastener holes. A tapered pin similar in size to the hole is covered with machinists bluing dye (Prussian blue) and "tapped" into the hole with a mallet. The pin is then

knocked out of the hole in such a way as not to smear the dye and rolled onto a sheet of coordinate paper to provide a permanent record of the results. The object is that wherever the pin made contact with the hole, the dye was rubbed off and where dye remains, there was no contact, hence no bearing at that location. This method, while antiquated and time consuming and requiring proper interpretation, will provide an indication of the shape of the hole (oval, bellmouthed, barrelled, etc.). Most engineering specifications require a minimum amount of bearing between the fastener and the hole usually spelled out as a percentage. This inspection does not provide any quantitative measurement, only a pictorial of the hole shape. This method can only be used for tapered holes and cannot be applied to straight holes. Air gauging is the only conventional method of providing any data regarding the shape and subsequent bearing for a straight shank interference fastener hole.

Profilometer A Profilometer (Figure 15) and a Surfindicator are both stylus type surface roughness measurement instruments designed to provide a measure of roughness (or smoothness). Both are difficult and very time consuming to use particularly in holes on built-up structure, and are impractical for small fastener holes. It does provide a quantitative measure of surface roughness however.

Visual The most common method of inspecting fastener holes, visual inspection (Figure 16) is sometimes supplemented with the aid of a flashlight, mirror or Borescope. Usually, a comparative standard is provided the inspector, either as a series of opened half holes or photographs of holes depicting acceptable and non-acceptable hole conditions. This method is very quick but also very subjective and highly dependent on inspector skill level.

Angularity/Perpendicularity Although several aerospace manufacturers have developed their own proprietary methods for measuring hole perpendicularity (Figure 17), they all involve some form of physical measurement. Normally, for tapered fastener holes, the head protrusion measurement discussed above is made at 90 degree intervals around the head and the hole perpendicularity calculated.

In summary, most of the conventional methods used today for interference fastener hole inspection are either subjective, depending upon the operators skill and interpretation, or are time consuming and costly, or both. In almost all cases when an inspection is completed, there is no quantitative data available on the quality of fatigue critical fastener holes, only the inspectors initials or stamp to verify that the holes in question were actually inspected and met drawing requirements.

CAPACITANCE HOLE INSPECTION METHOD

Basically, in order to assure the quality (and fatigue life) of interference fastener holes, the diameter of the hole must be known at many locations in order to ascertain the true size, shape, roundness and straightness of the hole. Using only conventional inspection and measurement methods, this task is prohibitively expensive and impractical.

However, now there is a practical and inexpensive method available to achieve this purpose which uses the principle that electrical capacitance varies inversely with the distance between two opposing plates (Figure 18). By using a capacitance measuring probe with many tiny capacitor plates and the hole wall as an opposing plate, discrete changes in the hole condition can be quickly and accurately measured as shown in Figure 19. By placing capacitor sensors around the circumference of the probe, the circular shape of the hole can be readily determined as illustrated in Figures 20 and 21. Accordingly, with capacitor sensors placed along the length of the probe, the entire bore of the hole (See Figures 22 and 23) can be measured and evaluated for straightness and other factors relating to correct interference and bearing.

A high speed microcomputer converts capacitance data into dimensional values for true hole size, and highly sophisticated algorithms then determine the hole shape, roundness, straightness, etc. This information is then compared with specification tolerances already loaded into memory to provide a simple go-no-go signal to the operator.

This method, known as the Capacitance Measurement System, or simply CMS and shown in Figure 24, is finding widespread usage throughout the aerospace industry for inspection of interference fastener holes. It is extremely accurate, requires a minimum of operator training, and inspects a fastener hole in just a little over one second, and records all the data from each inspection for future reference. Now, for the first time, each and every critical fastener hole can be economically inspected to guarantee its quality is acceptable for maximum fatigue life performance.

The CMS is basically comprised of four major components. These are 1) the capacitor probe which is inserted into the hole, 2) an electronics assembly which contains all the circuitry necessary for measuring extremely accurate capacitance values, 3) a microcomputer which processes, analyzes and stores the data

as well as displaying graphic and pictorial representations of the hole, and 4) a hand held device with which the operator can remotely control the system's operation (see Figure 25).

All the operator requires at the workpiece to perform hole inspections is the capacitor probe and the hand held control device. Each hole requiring inspection has its own number and the specification requirements for that hole are contained in computer memory. The operator simply calls up the hole number to be inspected by increasing or decreasing the increment switches (see Figure 26). After inserting the probe into the fastener hole, the operator simply presses the test button located on the hand control device and all three of the lights go out while the CMS makes its capacitance measurements. In about two-tenths of a second, all three lights will come back on while the computer is analyzing and processing the data. After about a second, two of the lights will go out and one light will remain on. If the light which remains on is green, the hole is acceptable, that is, it has met the specification requirements for that particular hole. A red light indicates that the hole is unacceptable, and a yellow light signals that a retest is necessary. Usually a retest is the result of the operator not completely inserting the probe into the hole.

The complete system is housed in a convenient pushcart, shown in Figure 27, which is easily transported around a shop floor. The cart contains storage drawers for extra probes, cables, etc. The capacitor probes are available in many sizes and shapes (as seen in Figure 28) to accommodate almost any conventional size fastener hole. The system operation is user friendly (Figure 29) and training usually takes less than a half day. The microcomputer used with the CMS is a Hewlett-Packard R/332 controller shown in Figure 30 which is operated by a touch screen. Each and every hole inspected can be displayed on the microcomputer screen in several different ways. Figure 31 shows what is called circular plots (or horizontal slices) of the hole. The upper left plot represents the top of the hole, and the lower right represents the bottom of the hole. Each of the remaining plots is a corresponding slice down the hole bore. For each plot, the larger dotted circle represents the maximum hole diameter established by the drawing specification, and the smaller dotted circle represents the minimum hole specification diameter. The solid line shows the actual hole diameter and shape at each of the locations down the length of the hole.

Each hole can also be displayed in vertical cross-section as shown in Figure 32. These are four vertical slices of the hole taken at 45 degree intervals. The two sets of dotted lines represent the minimum and maximum requirements for the hole, the dashed line represents the hole center, and the solid line is

the actual hole shape at that location. You can see at the top of this Figure that the actual hole measurements are displayed (minimum, maximum and average) along with the specification requirements. These measurements can be printed on hard copy for each and every inspection by hole number, all in about one second per hole and to an accuracy of ± 0.0001 inches.

APPLICATIONS

Figure 33 illustrates the time required to perform all the conventional inspections that are usually required in order to insure maximum fatigue life performance for a critical interference fit fastener hole. A conservative estimate is about 5 minutes per hole assuming all the equipment and documentation is available at the work site. At an average production manhour rate of \$50.00 per hour, each fastener hole cost approximately \$4.16 to inspect if done correctly (Figure 34). For an aircraft that may have as many as 10,000 fatigue critical fastener holes, that computes to a fastener hole inspection total cost of \$41,650.

By using the Capacitance Measurement System which performs all the required inspections with a single probe insertion in just a little over one second, a conservative assumption would be an average hole inspection time of about 3 seconds. This equates (see Figure 35) to a cost of less than \$0.05 per hole, or less than \$500 for the same aircraft with 10,000 fastener holes. The savings on just one such aircraft would almost pay for the cost of the entire capacitance system. And the accuracy and consistency of the inspection results assures hole quality. Maximum fastener hole fatigue life can be guaranteed.

This is why so many aerospace manufacturers are now using the CMS for inspection of all interference fastener holes, straight or tapered. Figure 36 shows a growing list of applications where the CMS is being used in either initial manufacture of new holes, or in modification/rework programs where either new holes are drilled or old holes are reamed prior to reuse.

The Capacitance Measurement System (Figure 37) is a unique and innovative approach to an old and troublesome inspection problem. One which uses the established principle of electrical capacitance coupled with the latest computer and electronic technology to provide a better, cheaper, and faster way of guaranteeing hole quality (Figure 38). Further information on the Capacitance Measurement System may be obtained from Measurement Systems Incorporated (Figure 38), 2262 Northwest Parkway, Marietta, Georgia USA.

- Why Hole Quality Is Important
 - Fatigue Life Impact
 - Typical Hole Defects
- Standard Hole Inspection Methods
 - Advantages
 - Disadvantages
- New Capacitance Inspection Method
 - Advantages
 - Disadvantages
 - Current Applications

FIGURE 1

HOLE QUALITY FACTORS AFFECTING FATIGUE LIFE

- Hole Size
 - Interference
 - Taper
- Bearing
 - Barrelling
 - Bellmouthing
 - Ovality
- Surface Condition
 - Rifling
 - Scratches
 - Laps/Tears
 - Chatter/Tool Marks
- Angularity/Perpendicularity
- Faying Surface Gaps

FIGURE 2

EFFECTS OF FASTENER HOLE QUALITY ON FATIGUE LIFE PERFORMANCE*

- Hole-Size/Interference - Must Be Within Limits To Achieve Fatigue Life Performance

- Bearing

- Barrelling
 - Bellmouthing
 - Ovality
- < Serious Detrimental Effect On Fatigue Life
- High Detrimental - Most Serious Single Condition On Fatigue Life

- Surface Condition

- Finish
 - Rifling, Scratches
 - Tears, Tool Marks
- Rougher Than 125 RMS Has Severe Effect On Fatigue Life
- Serious Detrimental Effect On Fatigue Life
- Moderate Detrimental Effect On Fatigue Life
- Angularity/Perpendicularity No Effect Within $\pm 3^\circ$

* AFML-TR-77-106

FIGURE 3

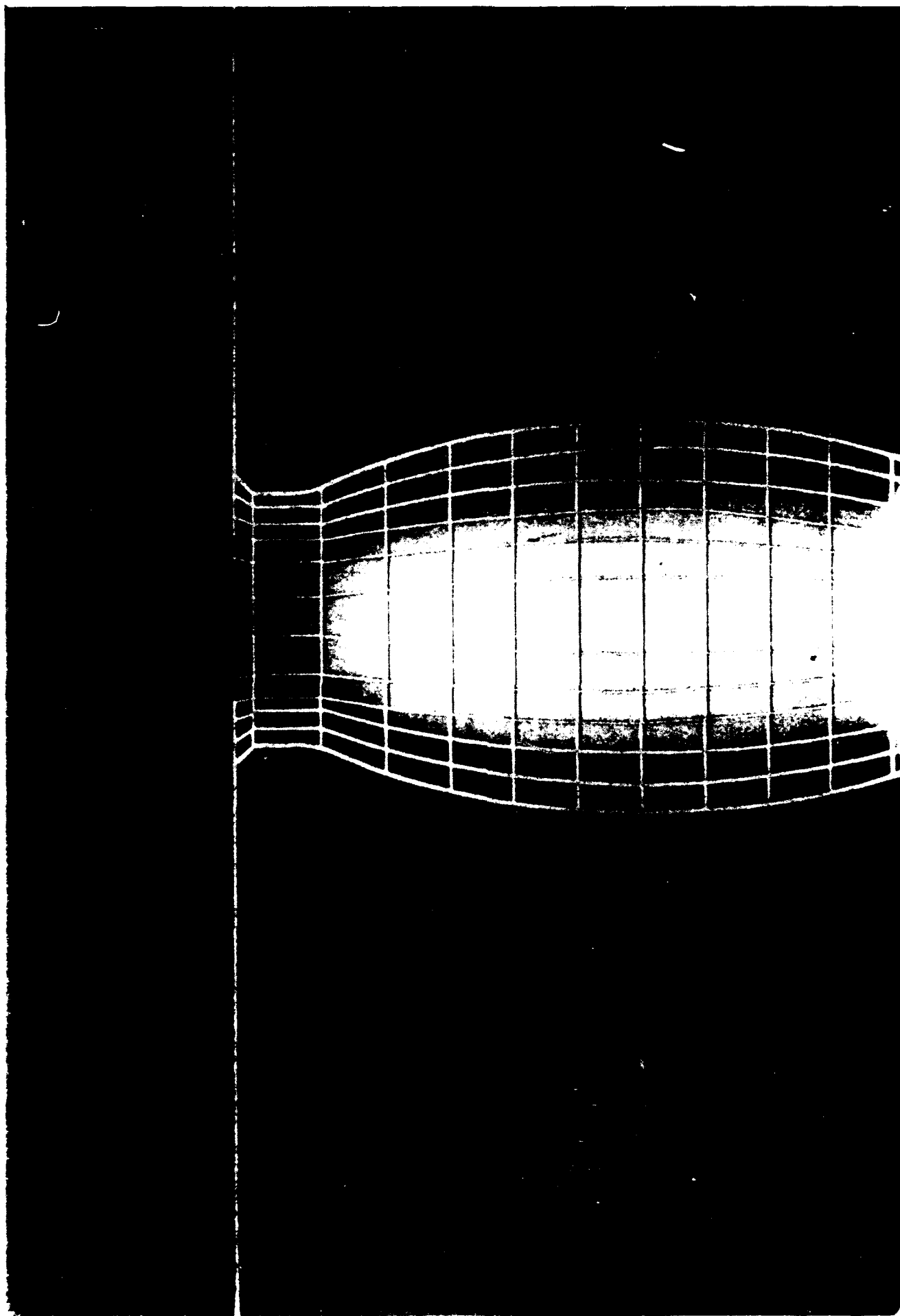
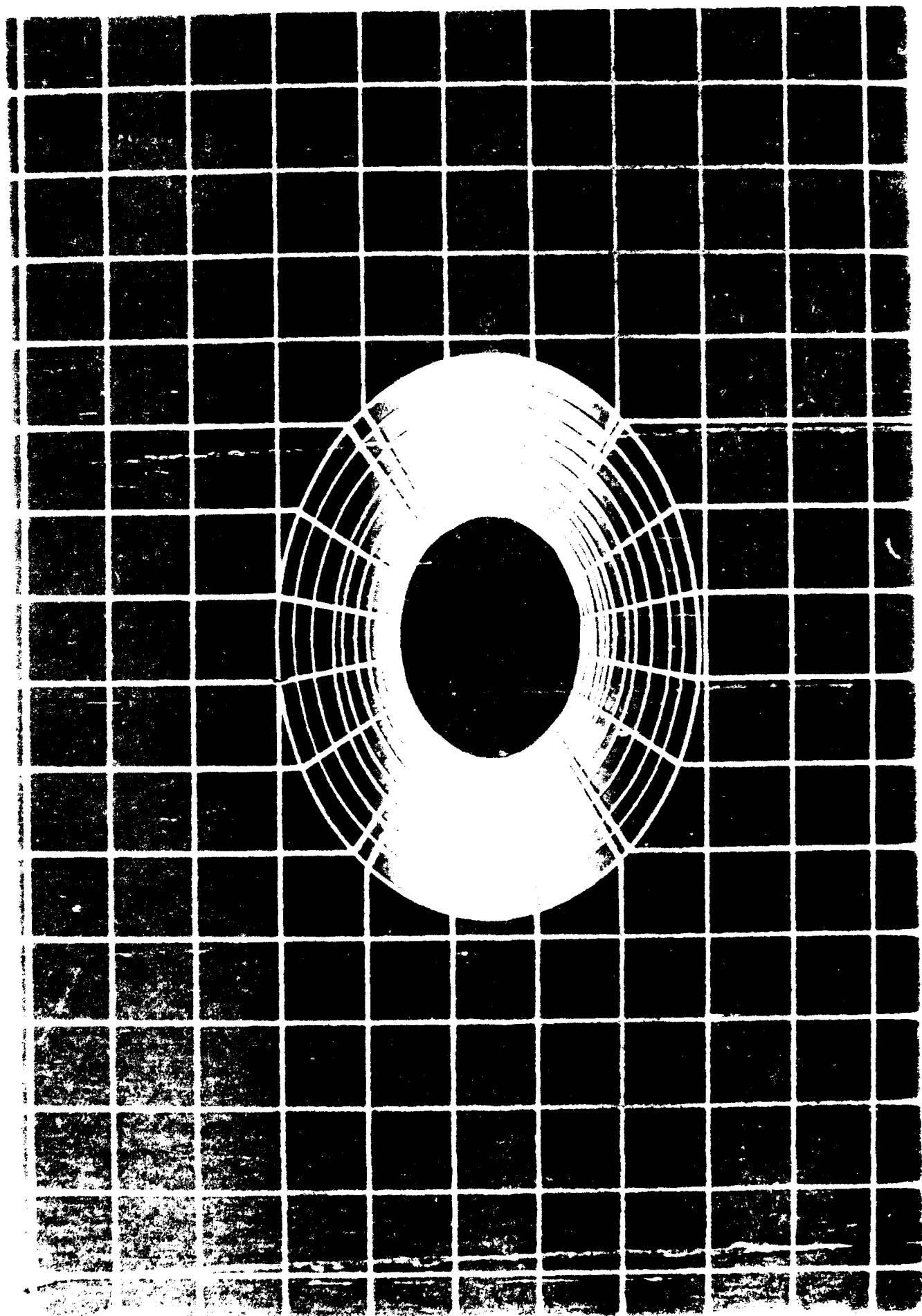
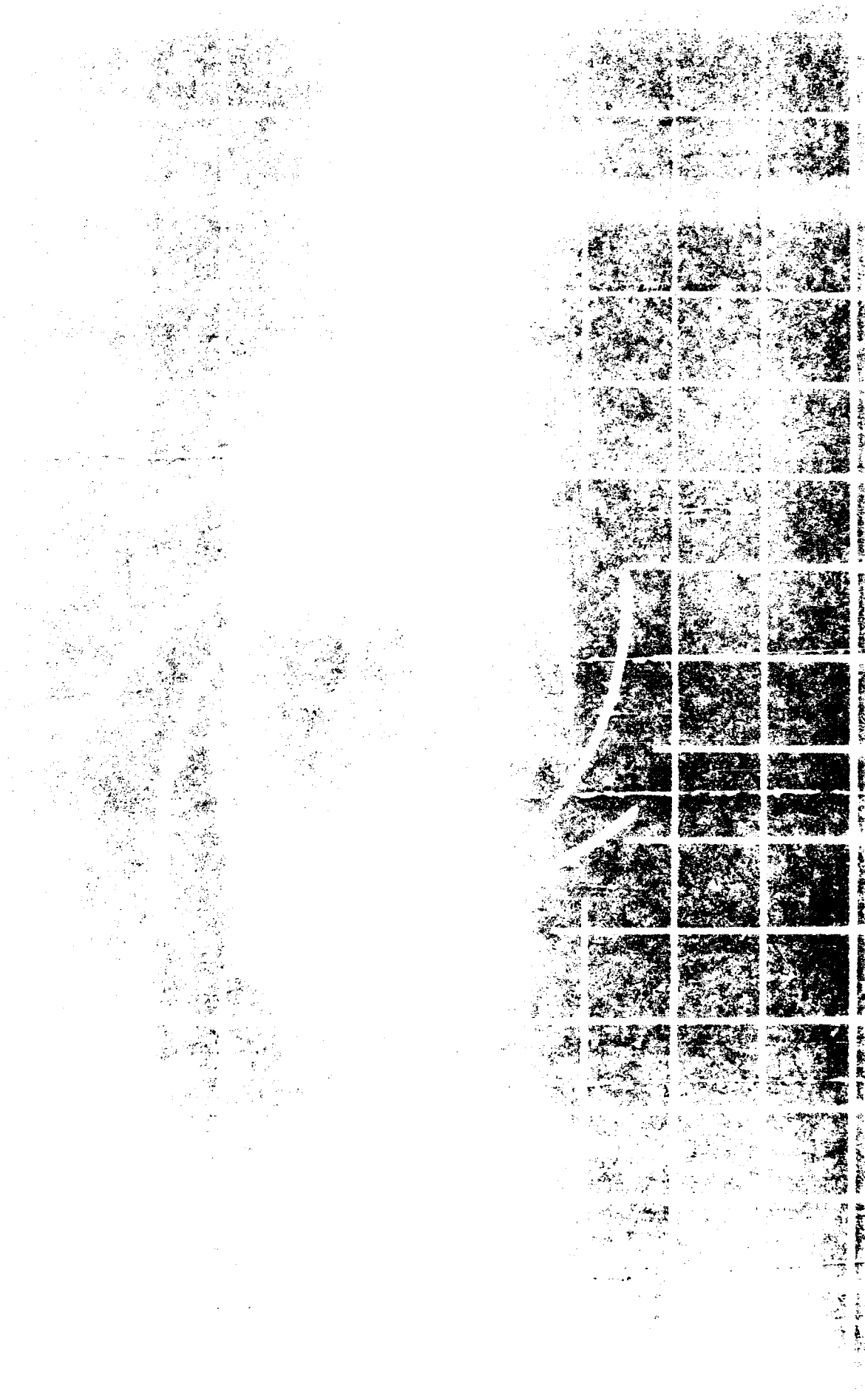
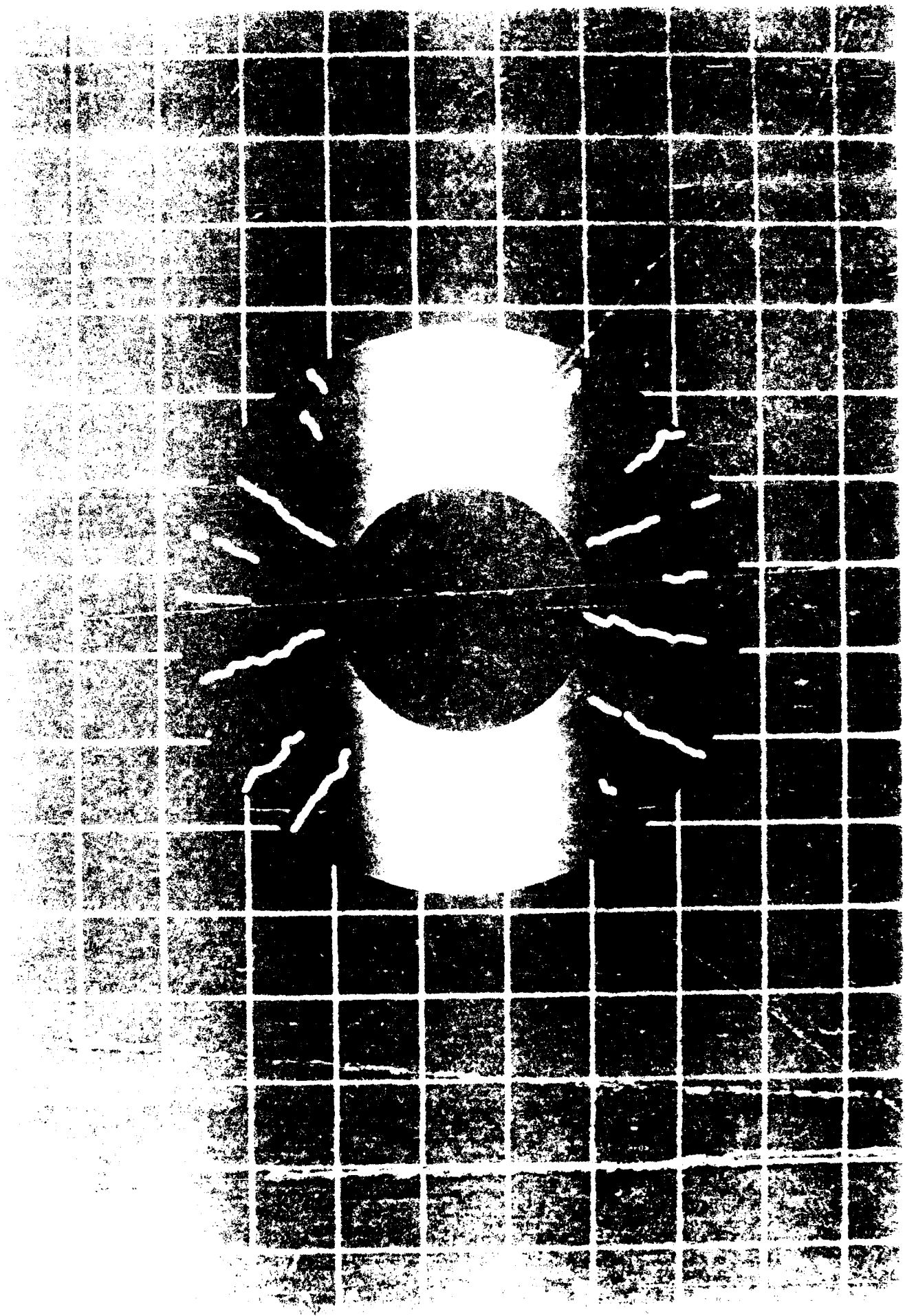


FIGURE 4









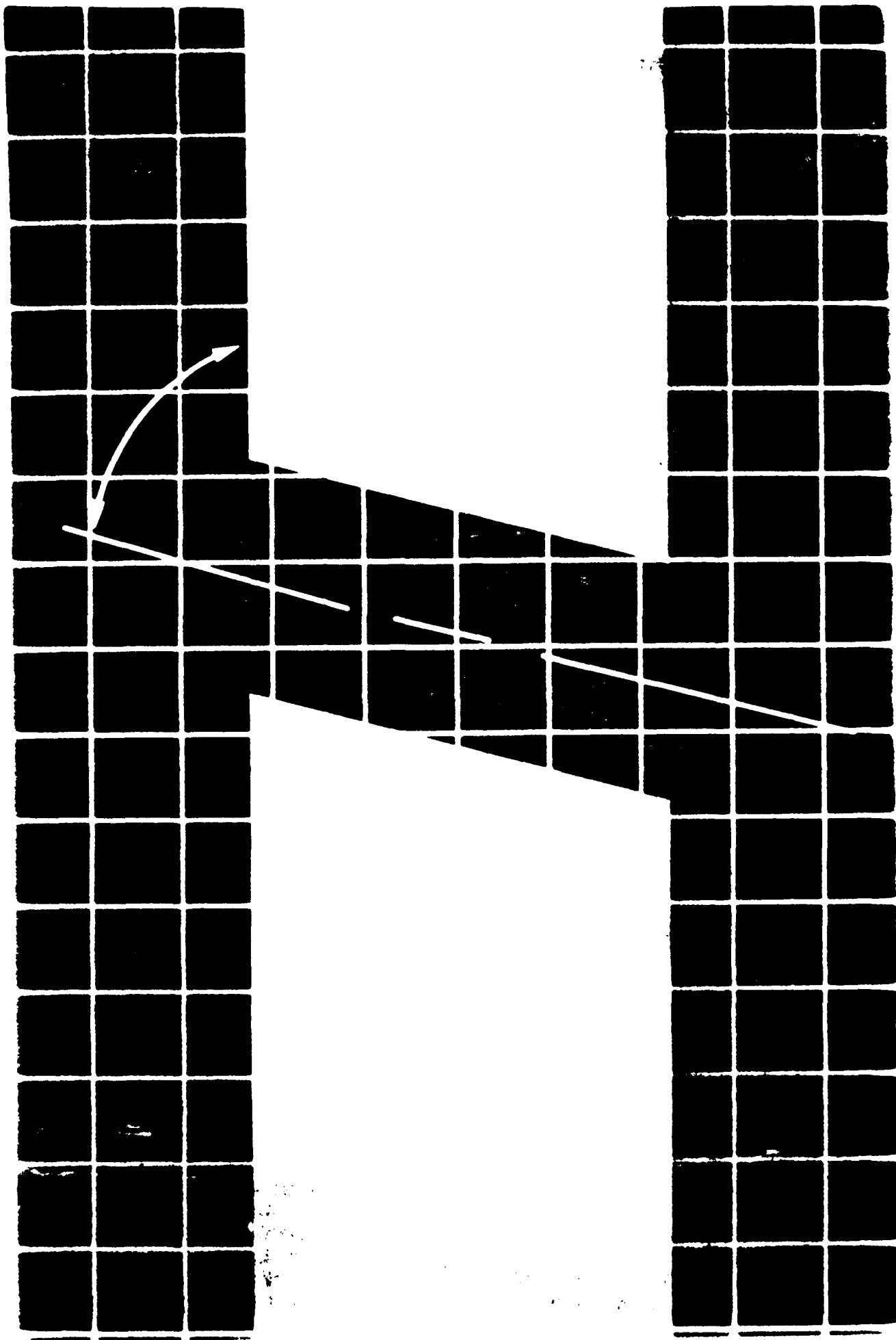


FIGURE 9

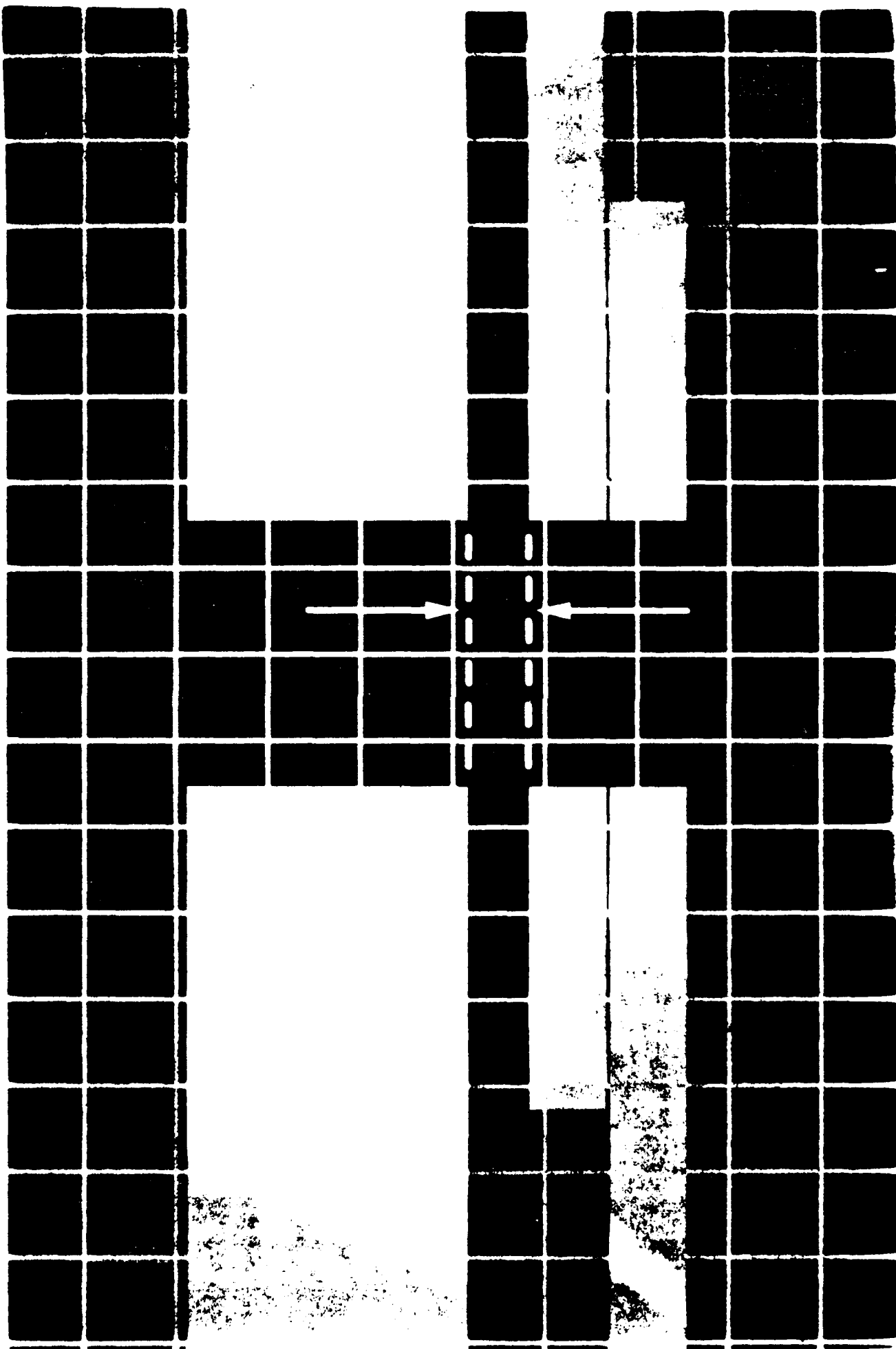


FIGURE 10

STANDARD METHODS FOR ASSURING HOLE QUALITY

Inspection Requirement	Inspection Method
<ul style="list-style-type: none"> • Hole Size <ul style="list-style-type: none"> - Interference - Taper • Bearing <ul style="list-style-type: none"> - Barrelling - Bellmouthing - Ovality • Surface Condition <ul style="list-style-type: none"> - Rifling - Scratches - Laps/Tears - Chatter/Tool Marks • Angularity/Perpendicularity • Faying Surface Gaps 	<ul style="list-style-type: none"> Air Gauge, Plug Gauge Protrusion Measurement* Protrusion Measurement* Blue Dye Check Pin* Air Gauge, Dye Check* Air Gauge, Dye Check* Air Gauge, Dye Check* Profilometer Visual, Borescope Visual, Borescope Visual, Borescope Visual, Borescope Physical Measurement Visual, Borescope

* Threaded Hole Only

FIGURE 11

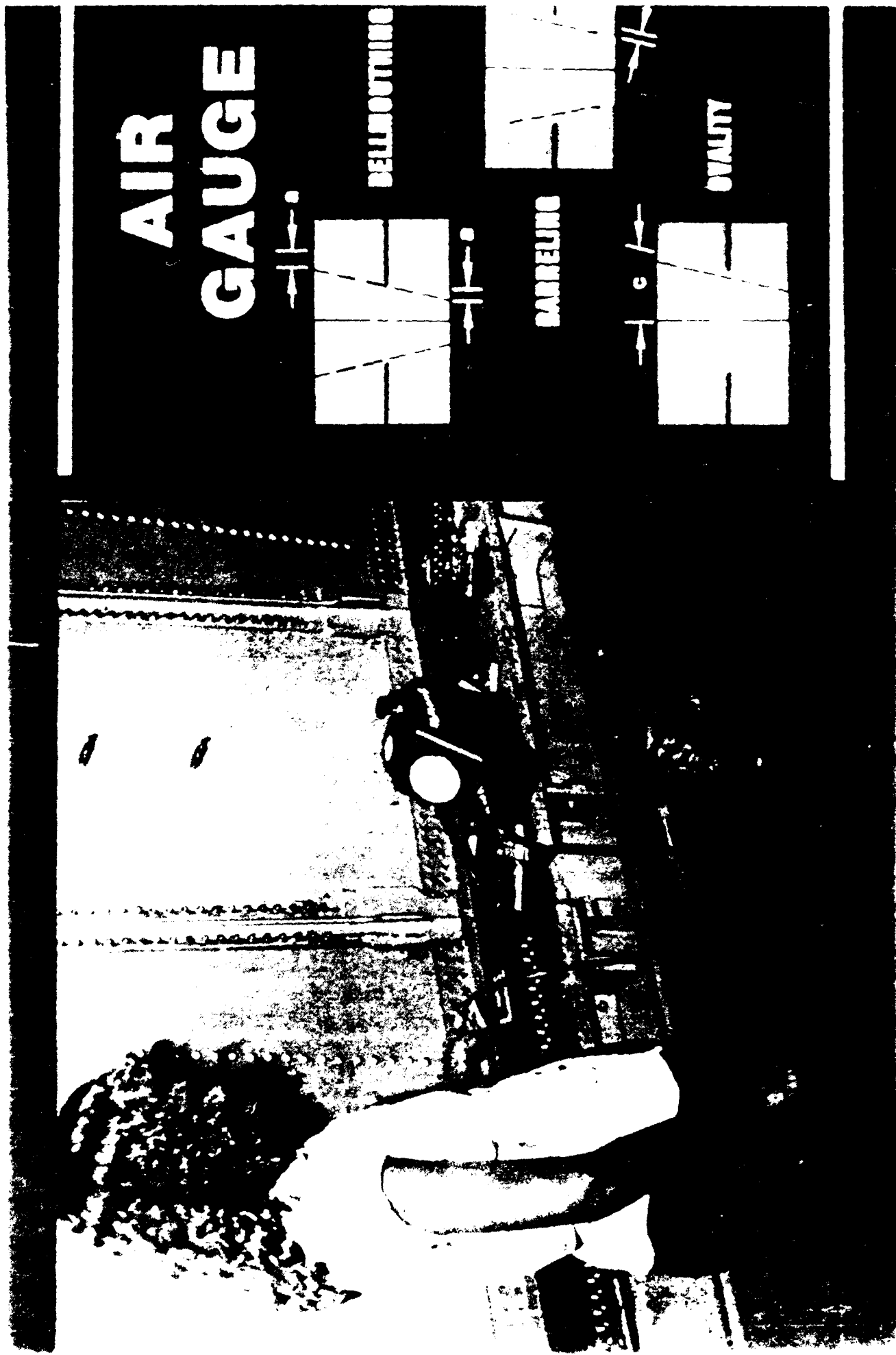


FIGURE 12

PROTRUSION MEASUREMENT

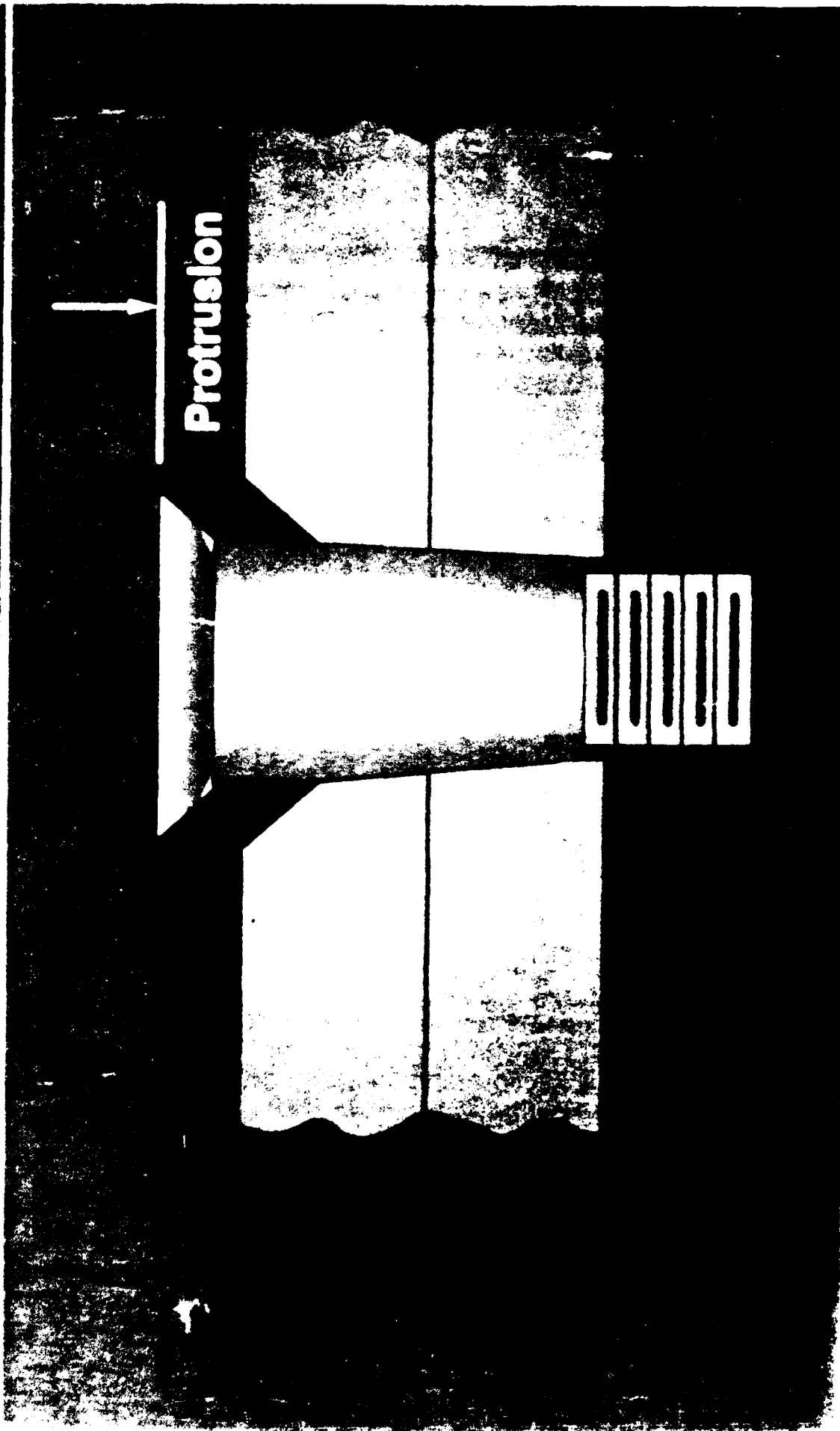
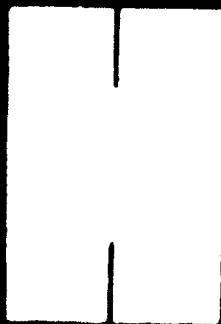


FIGURE 13

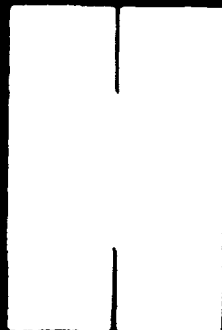


FIGURE 14

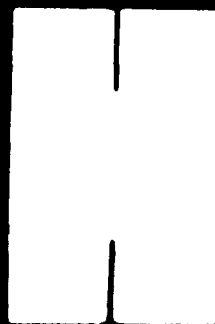
PROFILOMETER



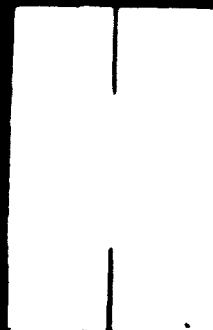
PLASTIC DEF.



LATEX/PLASTIC DEF.



PLASTIC



TOOL MARKS

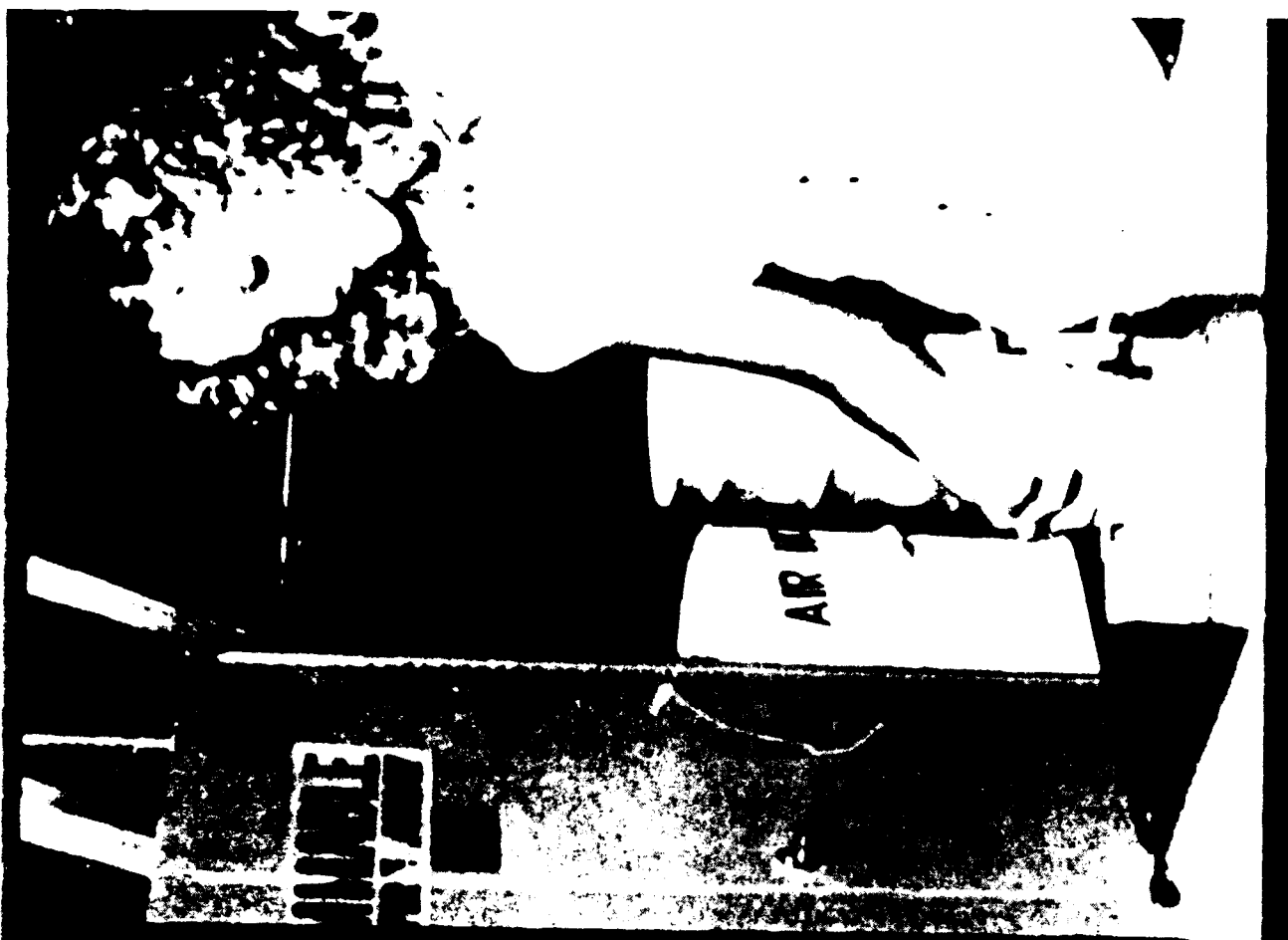


FIGURE 15



VISUAL COMPARATOR



Finish



Vertical Scratch



Rimling

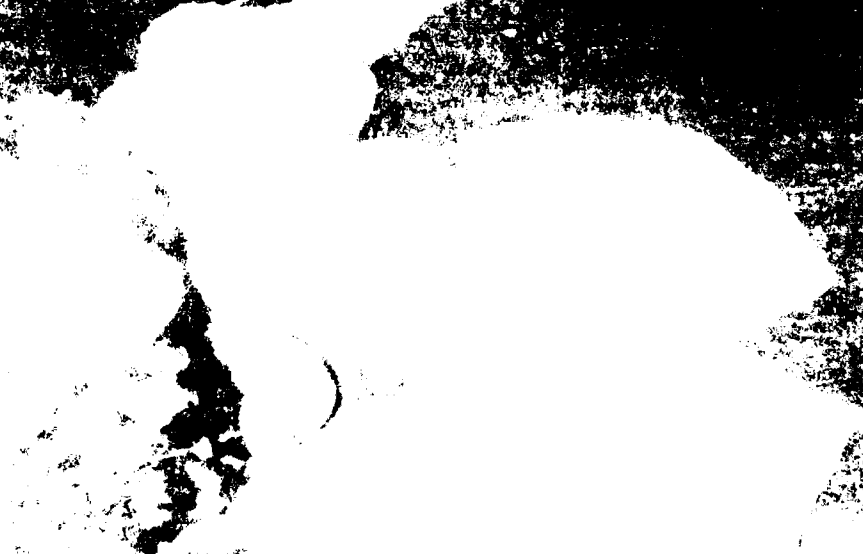
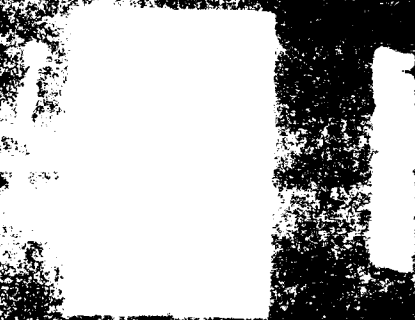


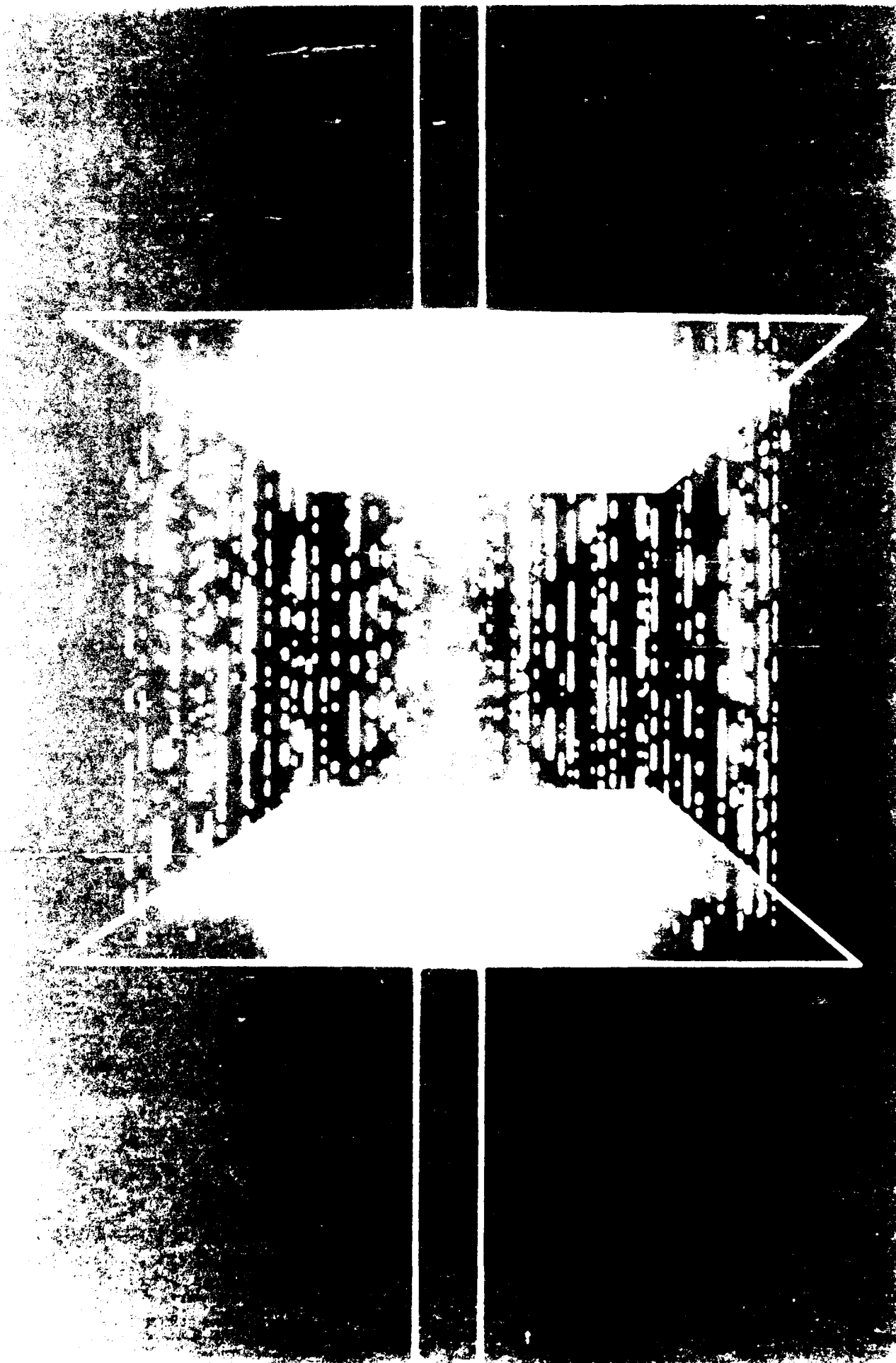
Tool Marks



Chatter

ANGULAR GAUGE





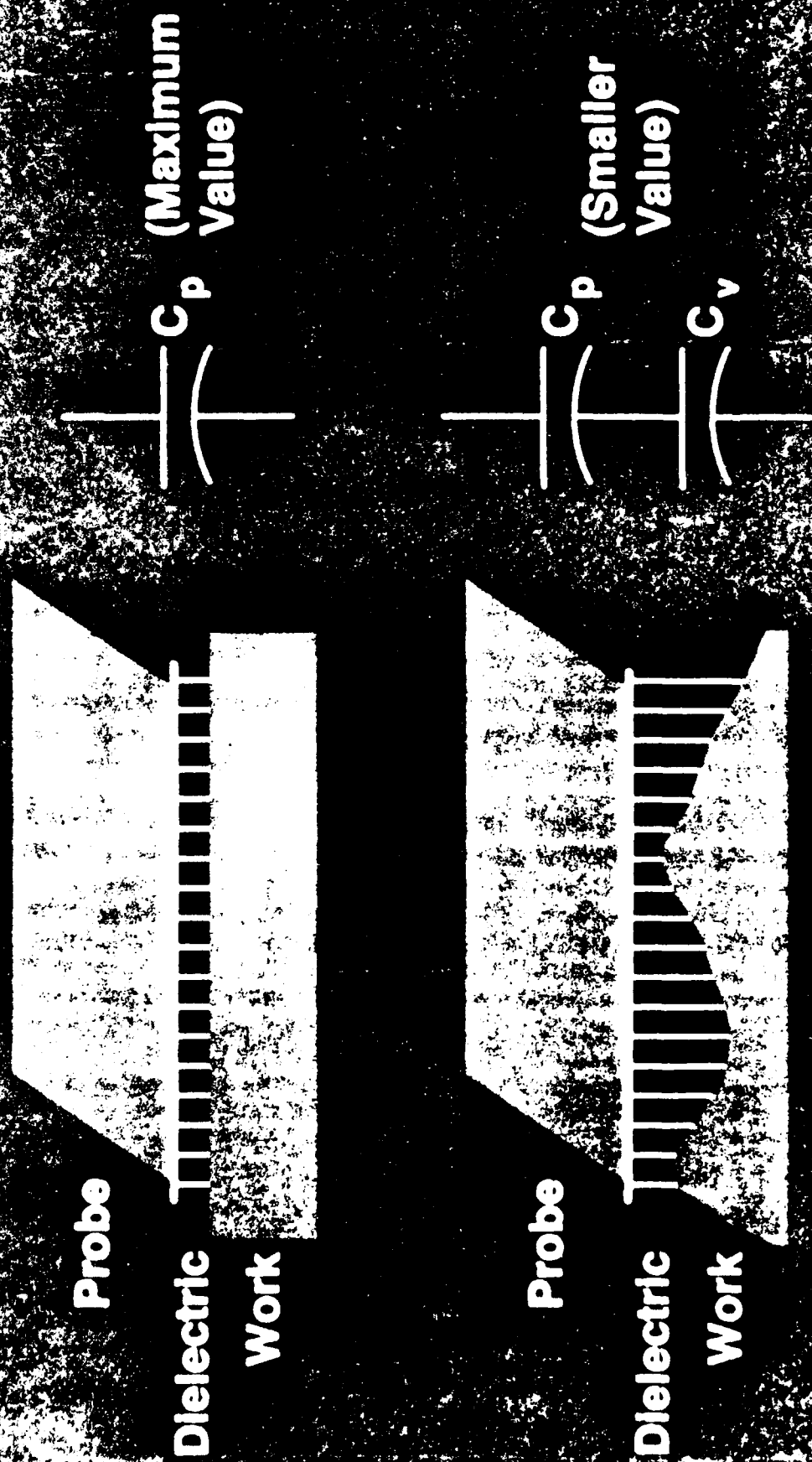
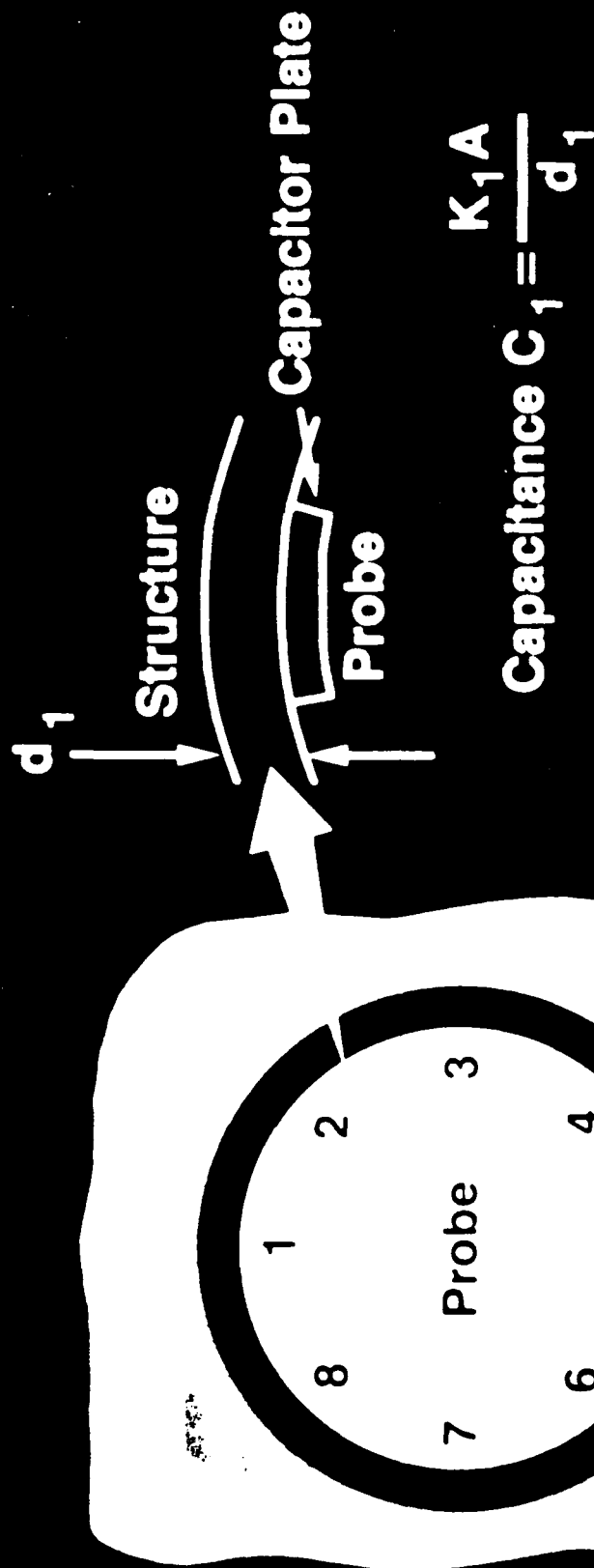


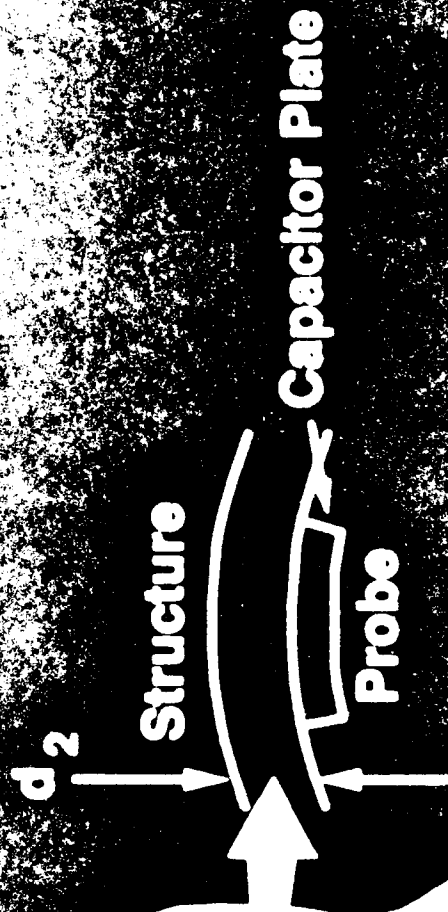
FIGURE 19

PERFECT HOLE



All 8 Elements Show Perfect Hole

FIGURE 20



$$K_2 < K_1$$

$$K_2 A \quad d_2 > d_1$$

$$\text{Capacitance } C_2 = \frac{C_1}{d_2}$$

Elements 1 And 5 Show Good Hole
 Elements 2, 4, 6 And 8 Show Marginal Hole
 Elements 3 And 7 Reject Hole

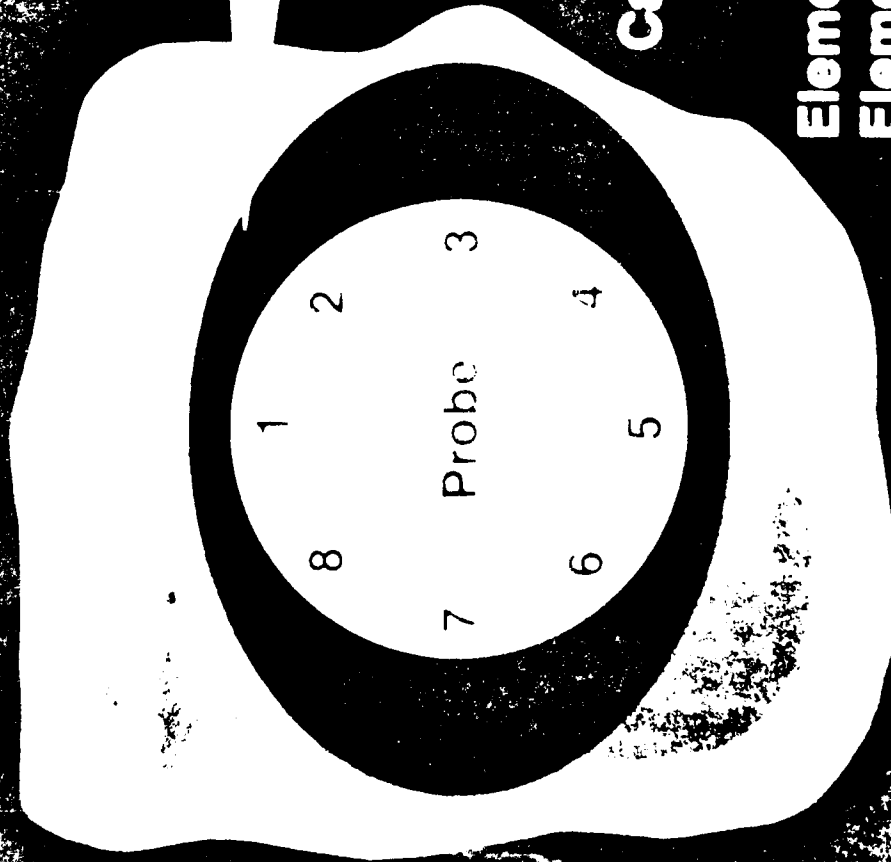


FIGURE 21

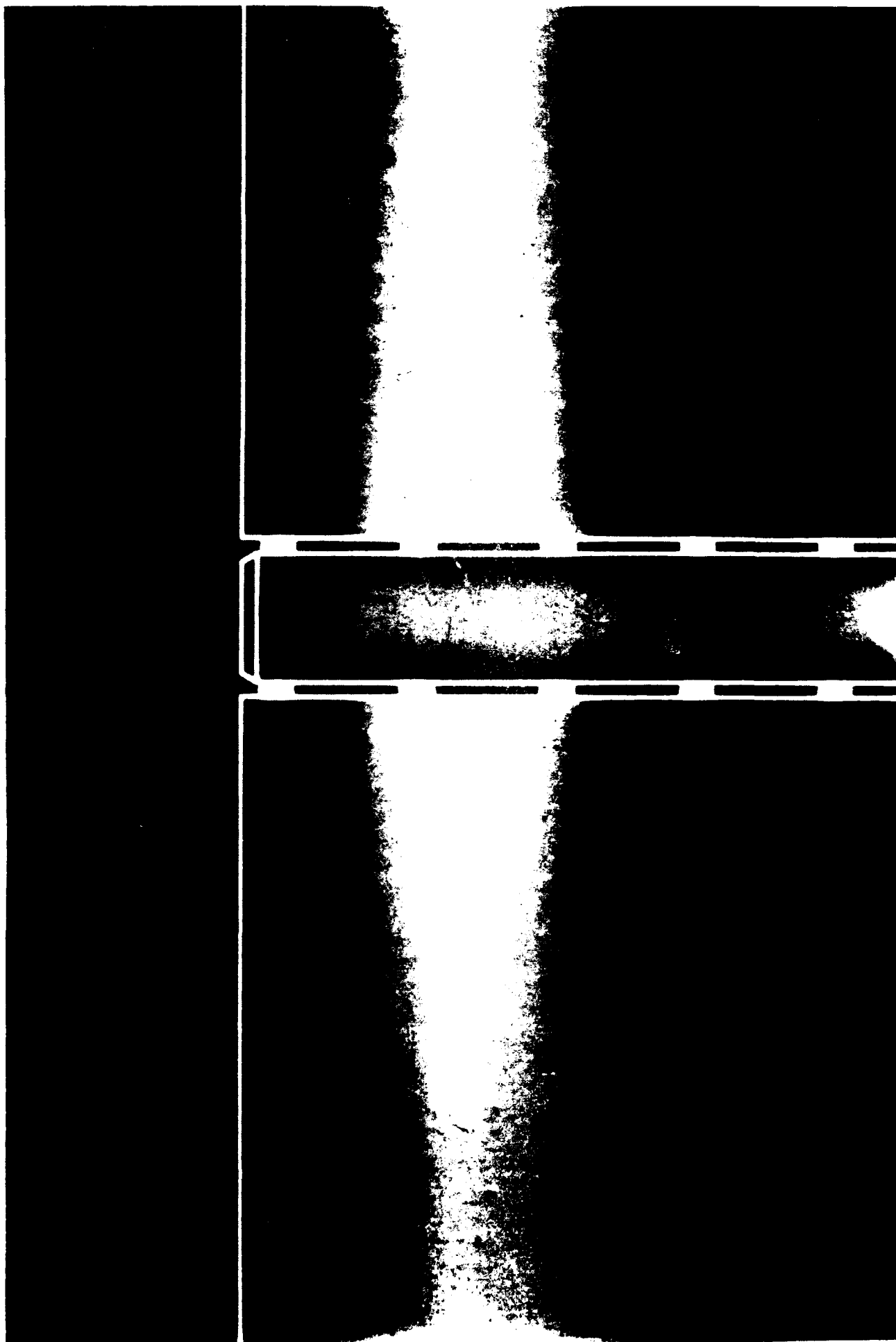


FIGURE 22

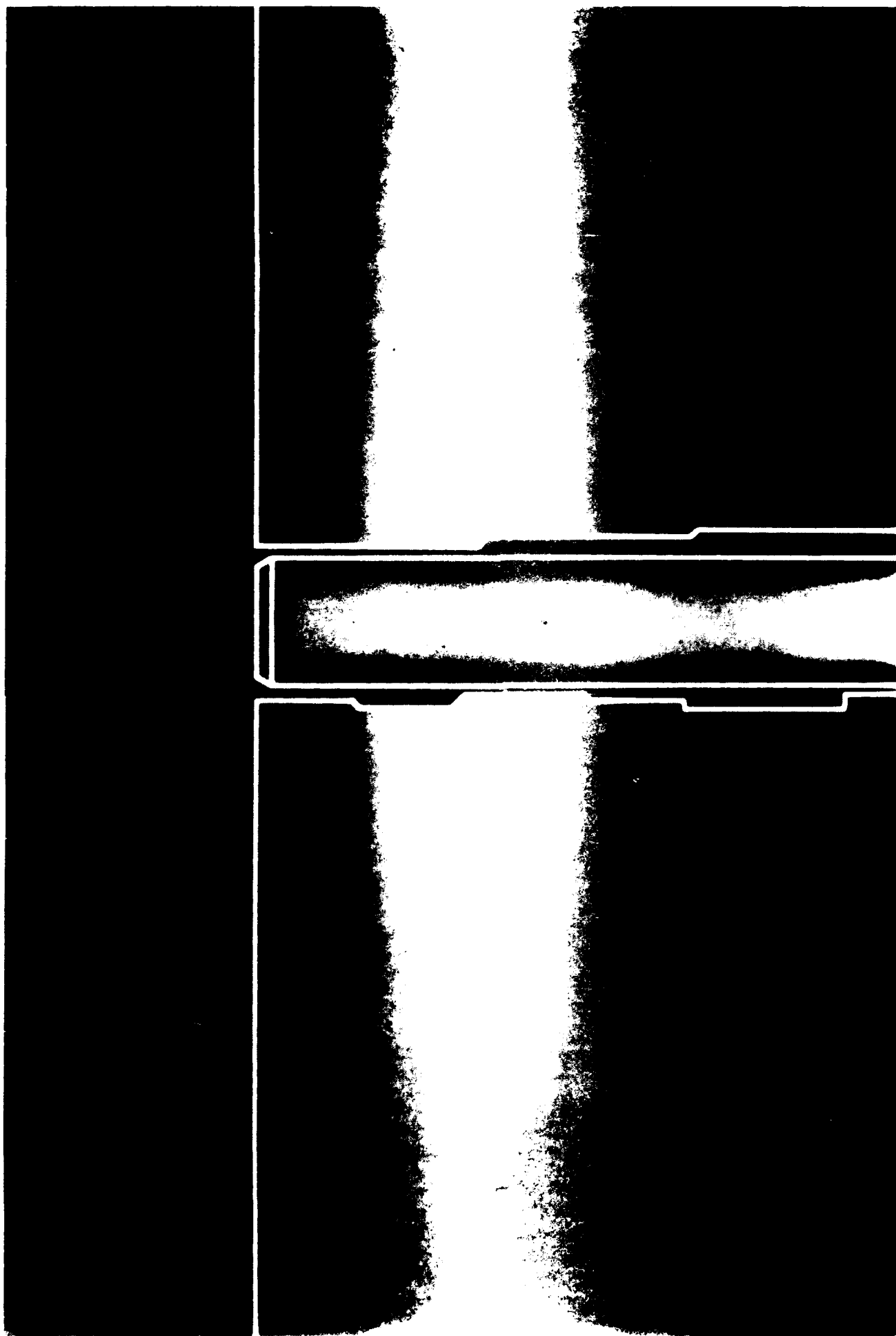


FIGURE 23





FIGURE 25



FIGURE 26



FIGURE 27



FIGURE 208



FIGURE 29

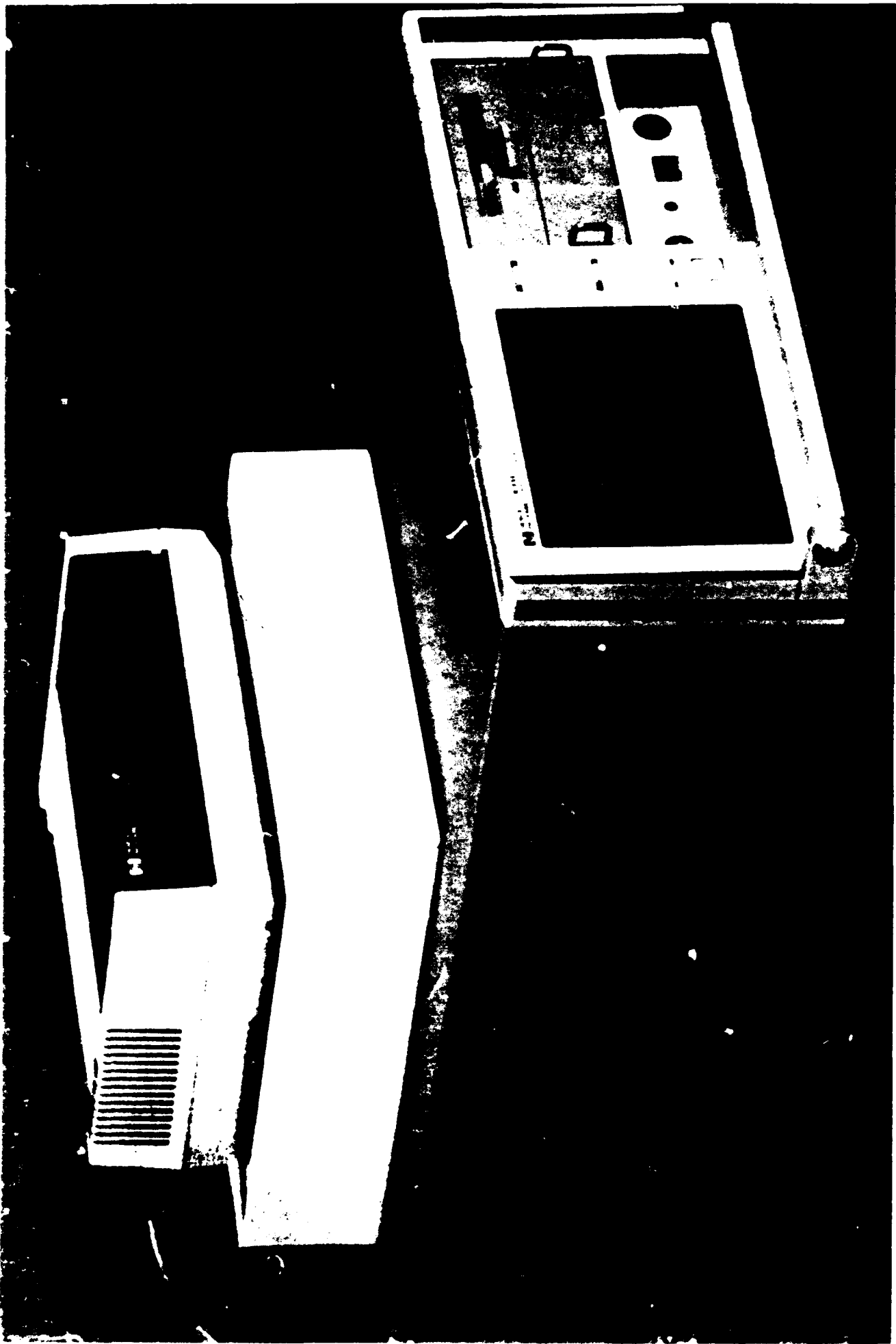
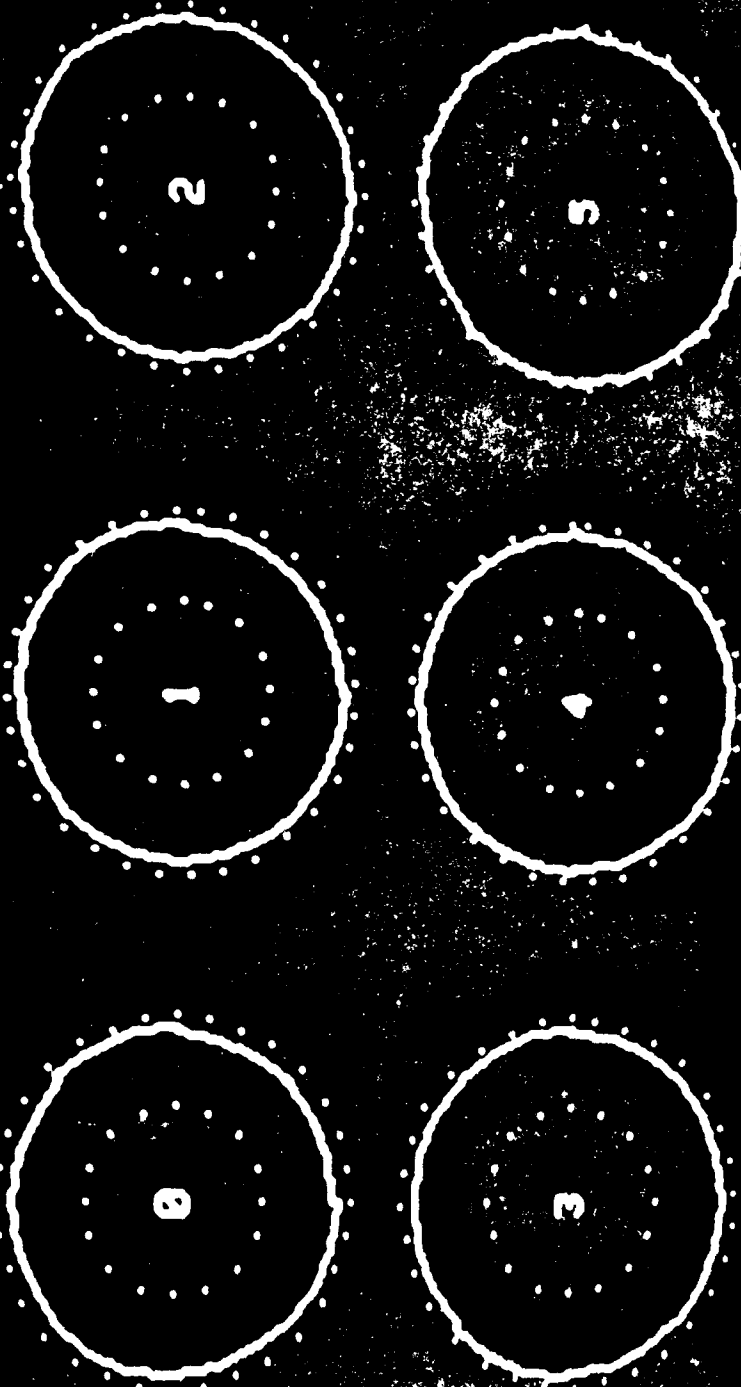


FIGURE 30

Reay # 35 Drawing # - Hole # 8899
 Hole: Min dia .289004 Max dia .31034
 Avg dia .310074 Tip: 137H010
 Spec: Min dia .3075 Max dia .3105



APPROVAL: _____
 LITHO: _____
 DATE: _____
 TIME: _____

FIGURE 31

[illegible]

302

TIME REQUIRED FOR STANDARD INSPECTION METHODS

<u>Method</u>	<u>Minutes Per Hole</u>
Air Guage	1.50
Profilometer	1.25
Borescope/Visual	0.25
Protrusion	0.50
Angularity	0.50
Bluing Dye Check	<u>1.00</u>
Total	<u><u>5.00</u></u>

FIGURE 33

HOLE INSPECTION COST CONVENTION INSPECTION METHODS

5 Min/Hole @ \$50.00/Hr

= \$4.16/Hole

10,000 Holes/Aircraft

= \$41,650/Aircraft

FIGURE 34

**HOLE INSPECTION COST
CAPACITANCE INSPECTION METHOD**

**0.05 Min/Hole @ \$50.00/Hr
= \$0.0416/Hole**

**10,000 Holes/Aircraft
= \$416.65/Aircraft**

FIGURE 35

CURRENT APPLICATIONS CAPACITANCE INSPECTION METHOD

F/A - 18

C - 141

F - 15

B - 2

C - 5

F - 117

B - 1

FIGURE 36

The Capacitance Measurement System

FIGURE 37



FIGURE 38

AMS

MEASUREMENT SYSTEMS INCORPORATED

FIGURE 39

**FATIGUE CRACK
GROWTH RETARDATION IN
ALUMINUM ALLOYS**

By

**Raymond K. Yee
Richard L. Citerley**

**Anamet Laboratories, Inc.
3400 Investment Blvd.
Hayward, California 94545**

Presented at

**1990 USAF Structural Integrity
Program Conference
San Antonio, Texas**

December 11-13, 1990

ABSTRACT

A unique method is examined for reducing the growth rate of fatigue cracks in aluminum alloy sheet materials. This is accomplished by thermally inducing a tensile residual stress in front of the crack.

2024-T3 and 7075-T6 aluminum alloys center-cracked tension specimens were made for fatigue testing. The crack growth rates of the specimens with localized heating to 200°C and global cooling by liquid nitrogen are compared with those with no treatment. Based on these preliminary results, 7075-T6 aluminum sheet specimens show a reduction of crack growth rate by 50% while 2024-T3 aluminum specimens show a reduction of 33%. At this stage, the conclusion may be premature but yet these results indicate that extending fatigue life is possible.

1.0 INTRODUCTION

Aircraft safety has always been of paramount importance, for both the military and commercial aircraft industry. For example, the B-52 has long been designated as the primary aircraft for long range delivery system. Many of the present-day pilots of these aircraft were not even born when their planes were first put into service. To keep these planes flying for so many years, a great deal of maintenance, inspections and even several complete refurbishments have taken place. The basis and issues discussed at this conference clearly illustrate the concerns DoD has on the subject. The commercial air transport industry is faced with a similar but slightly different problem than those encountered in the military. The aging aircraft issue presents a major economic challenge to both military, as well as commercial air carriers. The average age of commercial airline airplanes is 12.9 years. By 1993, over 1,350 Boeing 727, 737 and 747 aircraft will exceed their economic design life.

Several studies have been performed by a variety of Government agencies to insure the safety of the older fleet of commercial aircraft. The concerns of the Federal Aviation Administration (FAA), aircraft manufacturers, NASA and the airlines have recently begun a general review of aircraft maintenance, inspection and design. Even so, recent DC-10 and 737 failures have dramatized the need for more control on inspection procedures, and new methods have to be employed if the aircraft life is to be extended.

The two choices for the original operators are: 1) retire the older aircraft from service and replace these with new ones or 2) perform the required inspection and maintenance operations until the aircraft reaches its economic life. If the first option is selected, then the responsibility of aircraft certification is relegated to the new owner.

It has been estimated that approximately \$600,000 to \$800,000 will be required per aircraft to replace the fuselage rivets and sheet material in the early Boeing 737 [1] (the primary cause of the Aloha 737 failure). Since the replacement cost of an aircraft is on the order of \$28 million plus, and the buying cycle and supply of aircraft requires a minimum of three years lead time, extension of aircraft life is essential. To reduce the economic impact of this dilemma, engineering studies have been used to define ways to extend aircraft life. In 1975, Yang [2] demonstrated that the cumulative cost of maintenance, inspection and repair was well within acceptable economic limits for two and perhaps four service lifetimes of the aircraft. These same conclusions can be drawn today, but probably with less optimistic forecasts. The accepted reliance on fracture mechanics methods has proven to be an efficient tool for the industry.

The effects of an overload or underload on subsequent crack propagation are understood qualitatively; however, obtaining a quantitative estimate for structure life requires a fracture mechanics approach that models the basic physics at the crack tip without being burdened with excessive computations. Vlieger [3] has presented a discussion on how to determine a Safe Inspection Period (SIP) for damage-tolerant (Fail-safe) and fatigue (Safe-life) composite metal structures. For various load path and structural designs, a Safe Inspection Interval (SII) is established. The FAA recommends [4]:

for single load path damage tolerant structures (slow crack growth structures):

$$SII = SIP/3$$

and for multi-site fail-safe structures:

$$SII = SIP/2$$

Thus, the examination of a new and unique method that uses these principles for reducing the rate at which fatigue cracks propagate is in order.

Prof. Earl R. Parker, formerly with the University of California, has filed a patent disclosure entitled "A Method For Greatly Retarding The Rate At Which Fatigue Cracks Will Grow In Aluminum Alloy Sheet Materials Used In Aircraft", dated May 9, 1989 [5]. Prof. Parker's patent disclosure is principally based upon the metallurgical aspects of the material properties and their extension to crack growth rates. The proposed method provides a relatively simple and inexpensive means for greatly retarding crack growth rates, and in some cases, for actually stopping a crack in an aluminum alloy sheet material. Preliminary results of an investigation by Anamet are presented herein to provide a technical basis for the procedure. The examination of the behavior of the stress intensity factor is used to demonstrate the feasibility of the proposed method. If the stress intensity at the tip of a crack is reduced by a factor of two, the growth rate of the crack can be reduced by a factor as much as one tenth. In this way, the proposed method can be applied to aircraft during the regular inspection procedures now set forth, and can therefore add years of service life with the assurance of safety. The delineated approach will provide a logical and assured solution, as well as the theoretical basis for this life extension concept.

2.0 TECHNICAL DISCUSSION

The overall simplicity of linear elastic fracture mechanics (LEFM) is an inherent advantage when using a computational proce-

ture that must account for millions of cycles of behavior; unfortunately, many crack-related phenomena are not captured within the framework of LEFM. That these phenomena are not predictable in a linear sense is irrefutable evidence that the proper and complete mechanics of the fracture process are not properly modeled. To develop a methodology that will permit the suppression of growth of cracks, this modeling must be adequately represented in the evaluation. Preliminary investigation of the crack suppression process from both a structural mechanics and metallurgical point of view provides the justification of the proposed approach. This paper initially examines the overall first order effects of local behavior.

2.1 CLASSES OF FAILURE

It is the consensus of most air transport, commercial carrier and military system managers that older aircraft will continue to be in service despite the added maintenance costs resulting from the inspection and repair requirements imposed by the FAA and the military Logistic Centers. Because of the economic environment, it will be cheaper to operate and maintain these aircraft than to purchase new ones. As the age of the fleet increases, so does the likelihood of fatigue crack existence. Several Service Bulletins and Airworthiness Directives have been issued by the FAA that pertain to investigative procedures designed to detect and repair cracks found in aging aircraft. Interestingly, the size or extent of the crack length is never specified in these directives, although the airframe manufacturer has specific limits set for the inspection teams to monitor. The location and extent of the cracks found within a specific aircraft differ considerably with aircraft class and type and their components. Significant numbers of cracks which have been attributed to pressurization have been discovered in the skin of aircraft.

When commercial aircraft are flown, a pressurization cycle is encountered for each landing and takeoff -- known as Ground-Air-Ground (GAG) cycle. From nominal dimensions of typical commercial aircraft used today, it is estimated that the hoop stress due to pressurization in the skin is in the order of 15 ksi. Experience of the operators has shown that significant crack extensions have been observed adjacent to the lap joints along the rivet line of mating skin surfaces in the range of 30,000 to 40,000 cycles. In addition to normal crack growth due to pressurization-depressurization cycles, some additional growth of these cracks has also been attributed to the corrosion process in a hostile atmosphere.

Fatigue cracks have been observed in other parts of the aircraft, such as in the horizontal and vertical stabilizers. These service loads are entirely different than those encountered in the pressurization problem, but the same proposed methodology to reduce the extension of the cracks can be employed.

2.2 CRACK GROWTH

The rate of crack growth is specified by the change in crack length per load cycle (da/dn). The range in stress intensity factor is specified by either ΔK for LEFM or ΔJ for an inelastic path-independent process. The linear elastic fracture mechanics definition for the stress intensity factor, K , is given by Irwin [6]:

$$K = Y \sigma_{\infty} \sqrt{(\pi a)}$$

where σ_{∞} is the remote boundary stress, $2a$ is the crack length and Y is a shape correction factor that accounts not only for the shape of the crack, but the method of loading, adjacency to near

boundaries, etc. Note, for an apparent critical stress intensity factor of $100\text{ksi}\sqrt{\text{in.}}$ (plane stress), the critical crack length is in excess of 20 inches for the pressurization problem.

The J-integral is given by the expression

$$J = \int (W dy - \sigma_{ij} n_j \partial u_i / \partial x ds)$$

where, W is the strain-energy density of the material under consideration, σ_{ij} is the stress tensor, u_i is the displacement field, n is the outward normal of the contour encircling the crack tip. The J-integral can be shown to reduce to the stress intensity factor, K , for linear states of stress. It has been observed [6] for many aluminum materials that the relationship between the rate of crack growth with increasing ΔK (ΔJ) follows the Paris type [7], i.e.,

$$da/dn = C_f (\Delta J)^{M_f}$$

For all aluminum alloy sheet materials, this relationship falls into a relatively narrow band, as illustrated in Figure 1 [8].

The significance of Figure 1 for this problem is that it provides a measure of crack growth retardation: a decrease in stress intensity factor by two corresponds to a decrease in crack growth rate by a factor of ten. Therefore, a process must be considered to change the state of stress adjacent to the crack tip in such a way as to reduce the stress intensity factor.

Beyond the tip of the crack there is a region in the metal that has undergone plastic flow. This region results from the high state of stress of the crack tip. The stress level at the outer boundary of the plastic flow is at the yield strength of the material. Ideally, if a local residual stress equal and opposite to the longitudinal stress could be introduced, the net

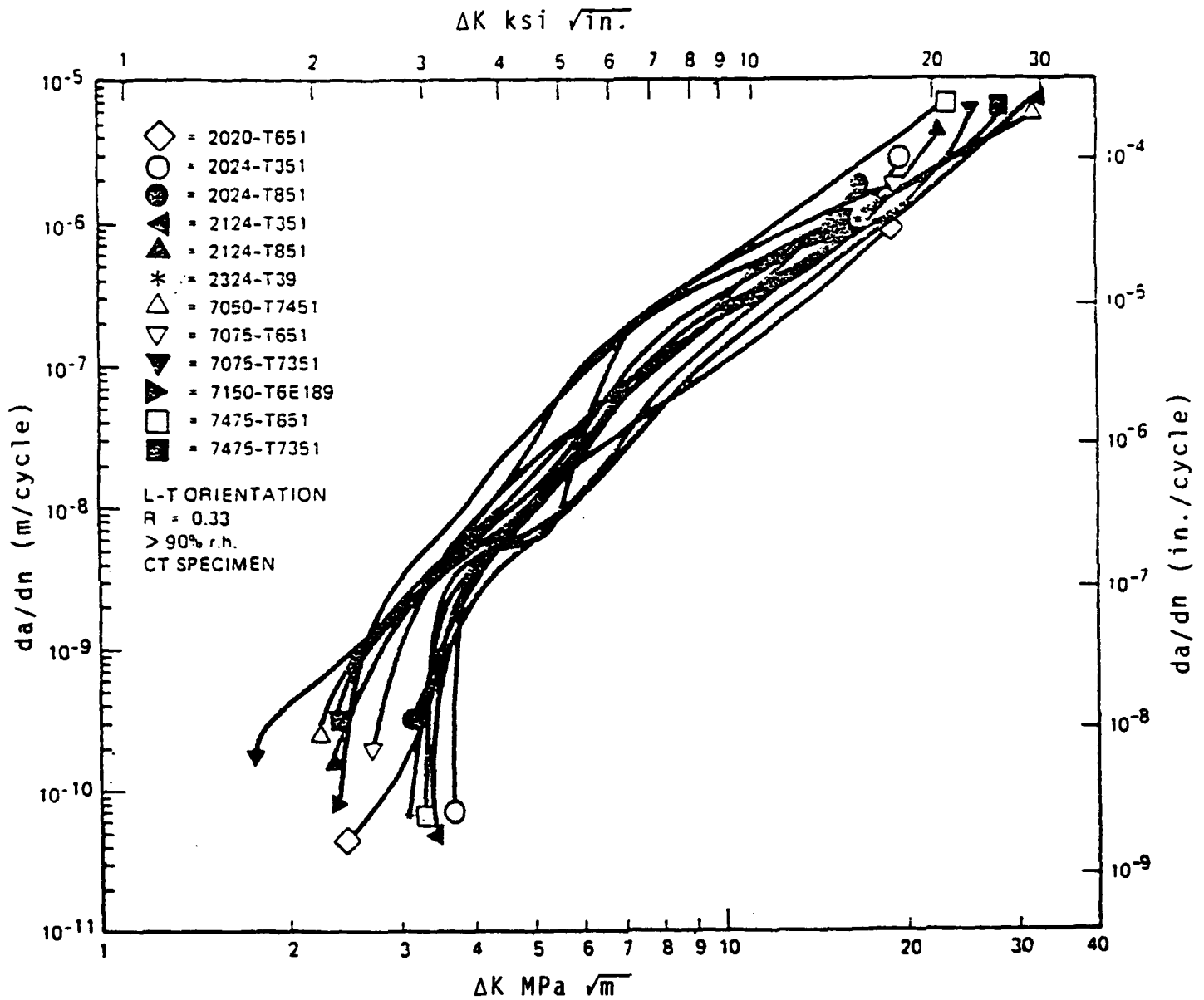


Figure 1 Constant-Amplitude fatigue crack growth curves.

stress would be zero and the crack would cease to grow. There seems to be no simple way to introduce such a residual stress, so the solution to the problem of retarding crack growth must come from a different approach.

The successful solution proposed by Prof. Parker is based on the knowledge of the microscopic nature of the crack growth process in aluminum and its alloys. Such materials do not fracture on the plane of maximum tensile stress. Rather, the local microscopic fracture path is on slip planes of the individual crystals that have slip planes on or near the macroscopic plane of maximum shear stress (at 45° angles to the direction of the load producing stresses). The reduction in the shear stress can be accomplished by introducing a tensile stress acting in the direction that is 90° to the line of the load stress. If a residual tensile stress in a direction parallel to the crack could be introduced in the aluminum alloy sheet at and near the crack, and extending a significant distance in the uncracked sheet ahead of the crack, and if the magnitude of this stress were equal to the magnitude of the longitudinal stress, the shear stress on the 45° plane would be zero -- further crack growth could not occur.

The method employed for producing the required stress in the transverse direction with respect to the load and the device used in the process comprise the basic elements of the disclosure. The method consists of first cooling the base temperature of the material to a sufficiently low temperature (-196°C). Next, a strategically located strip of the sheet material is heated to a high enough temperature (200°C) to produce a region of plastic flow. When the base temperature of the sheet is again normal, a residual tensile stress in the transverse direction develops. The consistency of the residual stress around the boundary of the plastic flow will dictate the effectiveness of the procedure. Further, the extent of the induced plastic zone will be dictated

by the change in material properties at the extreme temperature limits. In this way, the properties and residual stress states of the base material in the remaining sheet at normal ambient temperatures will not be affected.

2.3 PRELIMINARY ANALYTICAL STUDIES

One of the primary concerns of an initial study is to assure that the proposed process is technically feasible. It would be prohibitively expensive only to experiment and test the proposed procedure on different structural configurations. For each one studied, the size and shape of the affected area and the establishment of the equipment to produce the desired effect would have to be examined. Further, since the process is known to require the study of nonlinear effects, a means to separate these parameters should be provided. This can be accomplished through computational methods. Before these studies are even pursued, practical considerations need to be established. To gain some insight in this proposed procedure, two methods were examined. The first stems from a simplified analysis technique to predict the residual stress in the direction parallel to the direction of crack growth. The second stems from a LEFM model to determine if extension of the initial crack is possible during the cool down cycle.

A procedure to calculate the residual transverse direction stress is enumerated below:

1. Calculate the elastic strain ϵ_y at the 24°C yield stress (see Figure 2).
2. Calculate the elastic strain, ϵ_{YT} at a selected temperature, T.
3. Calculate the thermal expansion strain, ϵ_p at T.
4. Equate thermal expansion strain to $\epsilon_{YT} + \epsilon_{PT}$ and solve for ϵ_{PT} .

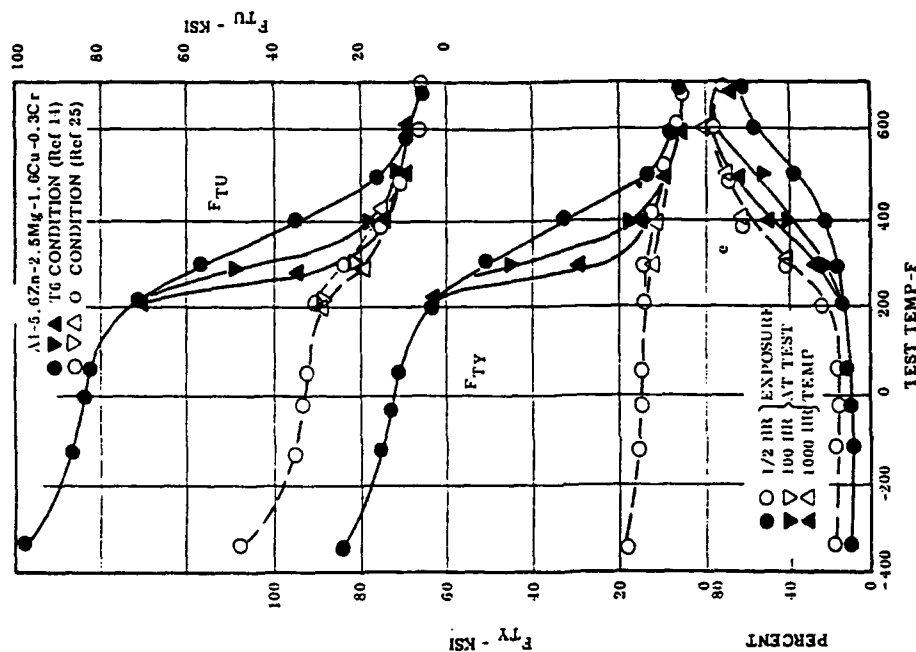


FIG. 3.0314 EFFECT OF EXPOSURE AND TEST TEMPERATURE ON TENSILE PROPERTIES OF ALLOY IN O AND T6 CONDITIONS.

(24)(25)

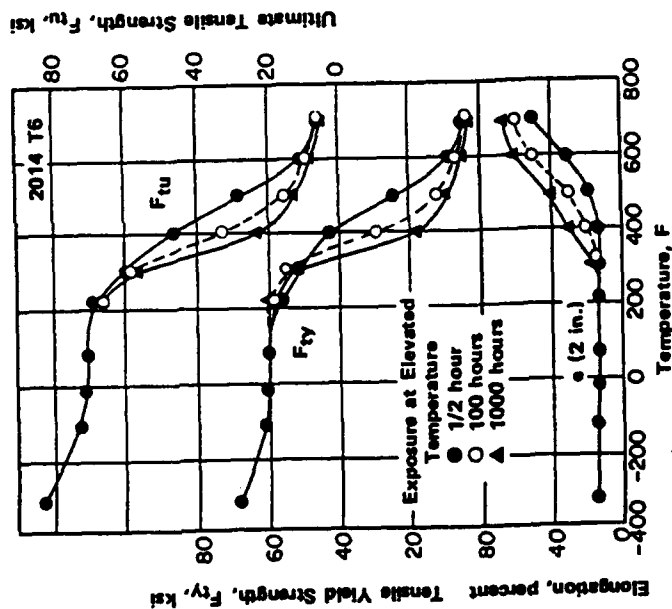


FIGURE 3.0313. EFFECT OF EXPOSURE AND TEST TEMPERATURE ON TENSILE PROPERTIES OF ALLOY IN T6 CONDITION (6)

Figure 2 The effect of temperature on material properties for 2014T6 and 7075T6.

5. Calculate the residual stress in the transverse direction, σ_v , at 24°C that is produced by ϵ_{PT} .
6. Equate shear stress τ_{lv} to $(\sigma_l - \sigma_v)/2$, where σ_l is the stress in the longitudinal crack direction.

The reduction of the maximum shear stress, $\sigma_v/2$ by a transverse direction tensile stress equal to 50% of σ_l would reduce the crack growth rate, da/dn by a factor of 10. Similarly, a value of $\tau_w = 75\%$ of $\sigma_l/2$ would reduce the crack growth by a factor of at least 50. These rates are based on data presented in Figures 1 and 2 [9].

To establish the possibility of crack growth during the cool down cycle, LEFM was employed. A specimen as shown in Figure 3 was selected. The dimensions of the original length of the crack and the dimensions of the specimen were selected for analysis convenience only. The material is assumed to be an aluminum alloy. A selected zone of heating is assumed to be approximately 0.2 in. long. The temperature distribution as a function of time was calculated. An initial temperature of -196°C was imposed along this strip. At approximately 150 milliseconds (ms) in the thermal cycle, a reversing temperature of 200°C was imposed. The temperature distribution resulting from a two-dimensional finite element solution was determined at all of the nodal points of the model throughout the specimen, and these transient temperatures were saved for further processing.

From the thermal distributions at specific times along the thermal cycle, the states of stress were calculated. The crack element used in Version 66 of MSC/NASTRAN, which was developed by Anamet, was used to determine both the stress state and stress intensities [10,11]. The results of this study are given in Table 1.

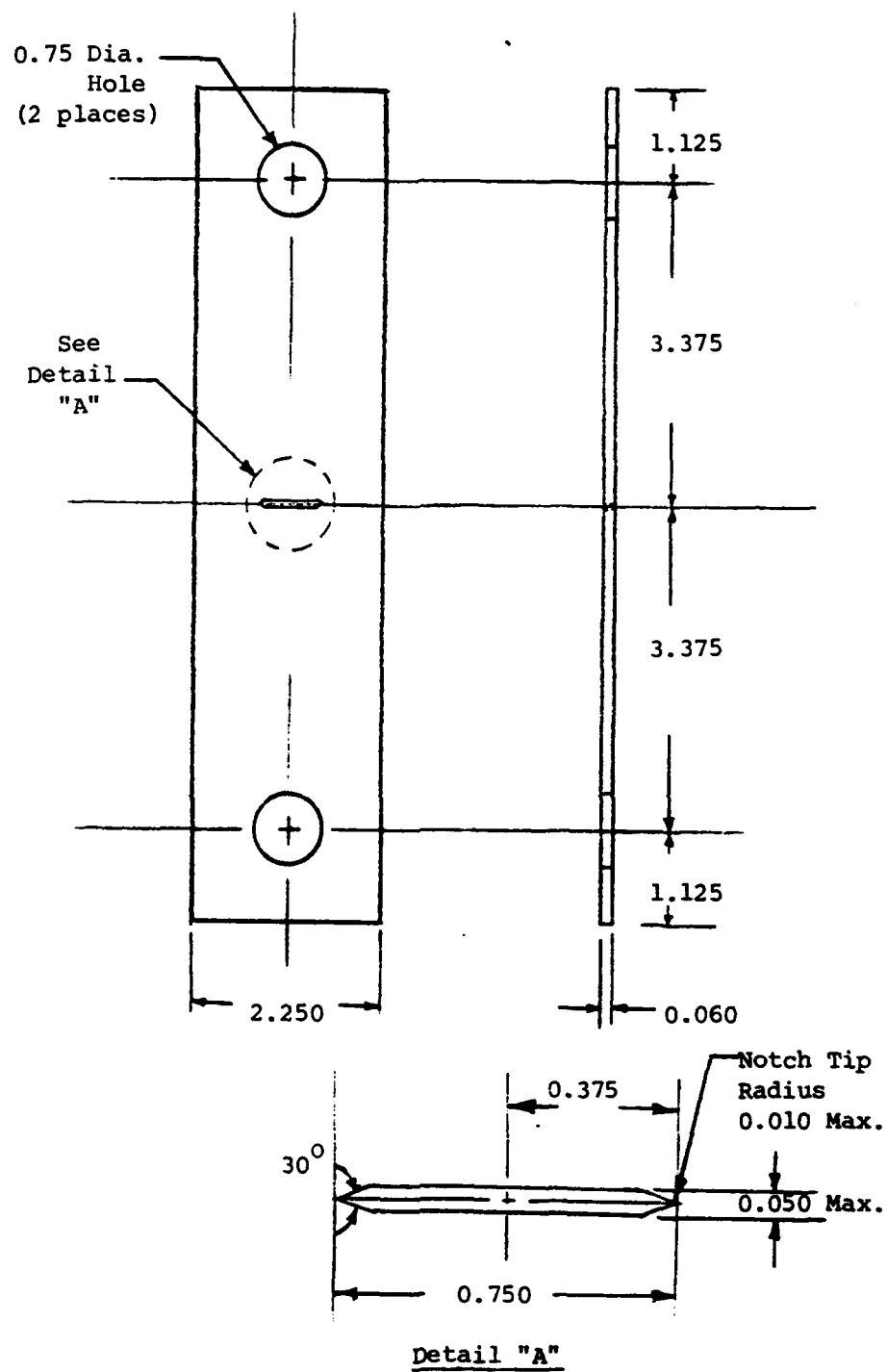


Figure 3 Test specimen (all dimensions are in inches).

TABLE 1
STRESS INTENSITY FACTORS AT DIFFERENT APPLICATION TIMES

Time (ms)	K_I psi $\sqrt{\text{in.}}$	K_{II} psi $\sqrt{\text{in.}}$
10	17,872	786
20	28,315	1,253
50	45,753	2,011
100	59,583	2,605
150	65,468	2,858
160	36,597	1,587
170	19,729	834
200	-8,441	-391
250	-30,783	-1,351
300	-40,289	-1,759

The maximum allowable stress intensity factor (K_{app}) for thin sheet aluminum at the coolest temperature (-196°C) is estimated to be in excess of 100,000 psi $\sqrt{\text{in.}}$. Thus, the crack will not extend during the initial cool down phase. The reversal of the stress intensity at the higher temperatures indicate that Prof. Parker's hypothesis is valid, and the process is feasible.

2.4 PRELIMINARY EXPERIMENTAL STUDIES

Sample 2024-T3 and 7075-T6 specimens were constructed. Typically, a fatigue specimen per ASTM E 647-88a [12], center-cracked-tension (CCT) was used. The baseline applied stress level was taken to be approximately 10% of the yield strength for each material. The minimum load is 0.10 of the maximum tension load. Initial cracks were induced by imposing up to approximately 45,000 load cycles. Crack growths were measured on virgin material and heat/cooled affected specimens.

The test method to determine the crack growth rate (da/dn) is described in ASTM E 647-88a. The constant-load-amplitude test procedure described in this method was used to plot da/dn as a function of the stress-intensity factor range (ΔK). The crack length was measured periodically at high magnification using an optical microscope.

The test is only valid when the specimen ligaments in the plane of the crack are predominantly elastic at all values of applied load; i.e., the net section stress based on the physical crack size must be less than the yield strength of the material.

For test specimens with a constant width of 2 inches, the value of $\frac{K_{max}}{\sigma_y}$ should be less than $0.63 \sqrt{\text{in.}}$ to avoid too large a plastic zone relative to the specimen width. Without *a priori* knowledge of the K values for these materials across the temperature range of interest, or even of the yield stress, the acceptability of the specimen geometry cannot be absolutely known for all cases anticipated in the test. Specimen sizes must be adjusted within these constraints to acquire acceptable data. However, for the preliminary study, the specimen in Figure 3 was used for both materials.

Several specimens were prepared and different heat sources were used to develop a residual stress adjacent to the crack tip. This study was performed to determine if life enhancement could be achieved even though less than optimum sources were used. The sources were:

- 1) A 600 Watt laser source.
- 2) A free flame from an acetylene torch with an 00 tip.
- 3) A restricted torch with flame over an insulated mask.
- 4) A liquid nitrogen source.

For each of the above sources, the flux and/or film coefficients at the specimen surface could not be measured. The conduct of these preliminary tests were executed in such a way as to minimize the fixturing costs. Temperature-sensitive patches were used to determine when the backside of the specimen reached approximately 200°C. When the laser source was used, only the heating cycle was considered. The reflectivity of the aluminum was so high that localized heating of the specific zone around the crack could not be attained. When a black spot was used adjacent to the crack, some control of the local heating could be attained. However, consistent results could not be obtained, since the spot density was not controlled. For the tests conducted with a torch, temperature sensitive patches were again used to indicate when the desired temperature had been reached. When cold temperatures were needed, liquid nitrogen was allowed to pass over the specimen. The backside temperature was monitored with a thermocouple. When the temperature at the backside reached approximately -196°C, an acetylene torch was passed over a predefined slot of the insulating pad. The slot conformed to a predetermined footprint aspect ratio. The heat source was removed when the patch changed color. After each of the above techniques were employed, the specimens were then ready for re-testing.

2.5 RESULTS

In this experiment, 2024-T3 and 7075-T6 aluminum alloys were chosen for this study. A total of 18 center-cracked-tension specimens were used for the fatigue crack growth rate test. Two

specimens of each material were tested without heating to establish a reference value of crack growth rate (da/dn). Four 2024-T3 aluminum specimens were tested after laser heat treatment, and another five 2024-T3 aluminum specimens were tested after heating with a restricted torch flame. For 7075-T6 aluminum, five specimens were tested after heat treatment by a restricted torch flame and cooling. The initial crack length (a) in the specimen is 0.425 in., and the crack is extended by fatigue to approximately 0.625 in. The results of these tests are listed in Table 2.

TABLE 2
TEST RESULTS

<u>Heat Source</u>	<u>Material</u>	<u>Reference</u> (μ in/cycle)	<u>da/dn</u> (μ in/cycle)	<u>% Life</u> <u>Enhancement</u>
Laser	2024-T3	3.16	0.9	251
			3.17	0
			3.2	0
			3.15	0
Torch	2024-T3	3.16	2.23	29.4
			2.10	33.5
			2.30	27.2
			2.31	26.9
			2.29	27.5
Torch with cooling	7075-T6	5.8	2.81	52
			3.02	48
			3.74	35.5
			4.07	30
			3.64	37.2

2.6 DISCUSSION OF RESULTS

The results of the tests show that life enhancements are ranging from 30% to 52% for the 7075-T6 aluminum specimens and 27% to 33% for the 2024-T3 aluminum specimens, with one exception which reaches over 250%.

When the laser was used as a heat source, one of the 2024-T3 specimens approached the theoretical life enhancement prediction, while the others showed no observable improvement on crack growth retardation. This discrepancy was probably caused by the control of the black ink spot density on the specimens. The emissivity (reflectivity) has a strong influence on the amount of heat absorption into the sheet aluminum. Although no life improvement was observed in these specimens, there was no sign of detrimental effect on crack growth by the heating process. When the acetylene torch was used, a consistent 27% to 33% improvement on crack growth retardation was observed in the 2024-T3 specimens. For the 7075-T6 aluminum, a liquid nitrogen cooling was imposed on the test specimens to induce a desirable tensile residual stress in the crack growth direction. When the heat flux was applied to these specimens, it was observed that the heating time to the observed temperature took longer than uncooled specimens. This is partly because the localized heating region of the specimen has to be raised from -196°C to 200°C . It was also noticed that liquid nitrogen vapor formed a film on the specimen which delayed the heat transfer to the metal. Thus, this also contributed to the longer heating time. Even with this experimental difficulty, the 7075-T6 specimens achieved a 30% to 52% life enhancement by this localized heating and global cooling process. The limited life enhancement is not caused by the process but rather caused by the lack of precision of the experiment. The feasibility of the process is validated by the result of the laser heating on the 2024-T3 specimen. This life enhancement concept on aluminum alloy was also supported by the heat treatment process called

Retrogression and Reaging [13]. This process was applied to 7075-T6 aluminum and involved a short time exposure at a high temperature, followed by a long time low temperature reaging. The tempering and reaging process gives high resistance to stress corrosion cracking. For the present case, the room temperature properties of the base material were not changed.

3.0 CONCLUSIONS

Only a limited number of specimens and heat/cooling sources were used in this experiment, so general conclusions for universal applications to all aircraft structural components cannot be obtained. However, it may be concluded from the present results that laser treatment to sheet aluminum may provide the desired life enhancement characteristics needed for the industry. The following conclusions can be drawn from this limited investigation:

1. The process suggested by Prof. Parker to extend the life of sheet aluminum alloys has been demonstrated -- the preliminary results are encouraging.
2. Although the majority of the results of this investigation show a limited improvement (30% to 50% increase in life expectancy), we attribute the results to technique and not the process.
3. It has been demonstrated that the process does not have a derogatory effect on virgin or fatigued components.
4. With careful construction and application of the heat and cooling source, it is possible to approach the theoretical limits of life enhancement.
5. Research is need to more accurately document the total effects of the process and determine its limitations.

4.0 REFERENCES

1. De Meis, R., "Aging Aircraft," Aerospace/America, July 1989.
2. Yang, J.-N. "Statistical Estimation of Service Cracks and Maintenance Cost for Aircraft Structures", AIAA Paper No. 75-767, 1975.
3. Vlieger, Henk, "Damage Tolerance of Stiffened-Skin Structures: Prediction and Experimental Verification," Fracture Mechanics: 19th Symposium, ASTM STP 969, T. A. Cruse, Ed., ASTM, Philadelphia, 1988, pp. 169-219.
4. Swift, T. "Verification of Methods for Damage Tolerance Evaluation of Aircraft Structures to FAA Requirements," 12th ICAF Symposium, International Committee on Aeronautical Fatigue, Toulouse, France, 1983.
5. Parker, E. R., "A Method for Greatly Retarding the Rate at Which Fatigue Cracks Will Grow in Aluminum Alloy Sheet Materials Used in Aircraft," May 9, 1989.
6. Irwin, G. R., Journal of Applied Mechanics, Vol. 2, p. 361, 1957.
7. Paris, P. C., Journal of Basic Engineering, Vol. 85, p. 528, 1963.
8. Antolovich, S. D., Ritchie, R. O. and Gerberich, W. W., "Mechanical Properties and Phase Transformation in Engineering Materials," Earl R. Parker Symposium on Structure Property Relationships, The Metallurgical Society, 1986.
9. Aerospace Structural Metals Handbook, Vol. 3, 1989 Ed.
10. Woytowitz, P. J. and Citerley, R. L., "Crack Elements for COSMIC/NASTRAN," Thirteenth NASTRAN Users' Colloquium, 1985.
11. Parekh, J. C., Arnold, R. R. and Woytowitz, P. J., "A Modern Family of Crack Tip Elements for MSC/NASTRAN," MSC/NASTRAN Users' Conference, 1986.
12. ASTM E 647-88a, "Standard Test Method for Measurement of Fatigue Crack Growth Rates."
13. Beddoes, J. C., deMalherbe, M. C., and Wallace, W., "A New Approach to the Problem of Stress Corrosion Cracking in 7075-T6 Aluminum", Canadian Aeronautics and Space Journal, Vol. 27, No. 3, Third Quarter 1981.

1p\062

**Quality,
NonDestructive Evaluation,
and the
" . . . I P " Process**

Charles Annis
Pratt & Whitney
P.O. Box 109600
West Palm Beach, Florida 33410-9600

-- Abstract --

The " . . . I P " process is a design and maintenance philosophy which insists on structural integrity as an integral part of any component design. Successful in airframes, ASIP (Aircraft Structural Integrity Program), and gas turbine engines (ENGINE Structural Integrity Program), it is now being applied to their ancillary equipment through PPSIP and MECSIP (Propulsion and Power Systems Integrity Program and MECHANICAL equipment and subSystem Integrity Program) and other-SIPs. These new programs are focusing attention on the changing role of NDE in the ... IP process.

In manufacturing, NDE has long been regarded as akin to radical surgery: non-conforming parts were culled (then reworked or scrapped). NDE wasn't thought of as being part of the fabrication process itself but rather something to be applied to the finished product. But that approach is inefficient and costly, and this fact is now recognized by American industry. To continue the medical analogy, NDE is now viewed as preventative medicine: monitoring the process itself to maintain statistical control and thus insure healthy parts.

This paper discusses the changing requirements of NDE in the context of Quality initiatives and maintenance requirements and their contributions to the . . . IP process.

**QUALITY,
NON DESTRUCTIVE EVALUATION,
and
the " . . . IP " PROCESS**



**Chuck Annis
(407) 796-6565**

Examples of the " ... IP " Process

- **ASIP Aircraft Structural Integrity Program**
- **ENSIP *EN*gine Structural Integrity Program**
- **PPSIP Propulsion and Power System *I. P.***
- **MECSIP *ME*chanical and Subsystem *I. P.***

What IS the " ... IP " Process?

**The process of assuring a component's
(structural / mechanical / functional)
integrity, throughout its service lifetime.**

Service Lifetime

can be thought of as consisting of two distinct phases:

- 1. Manufacturing to first overhaul,**
- 2. First overhaul, thereon.**

NON DESTRUCTIVE EVALUATION:

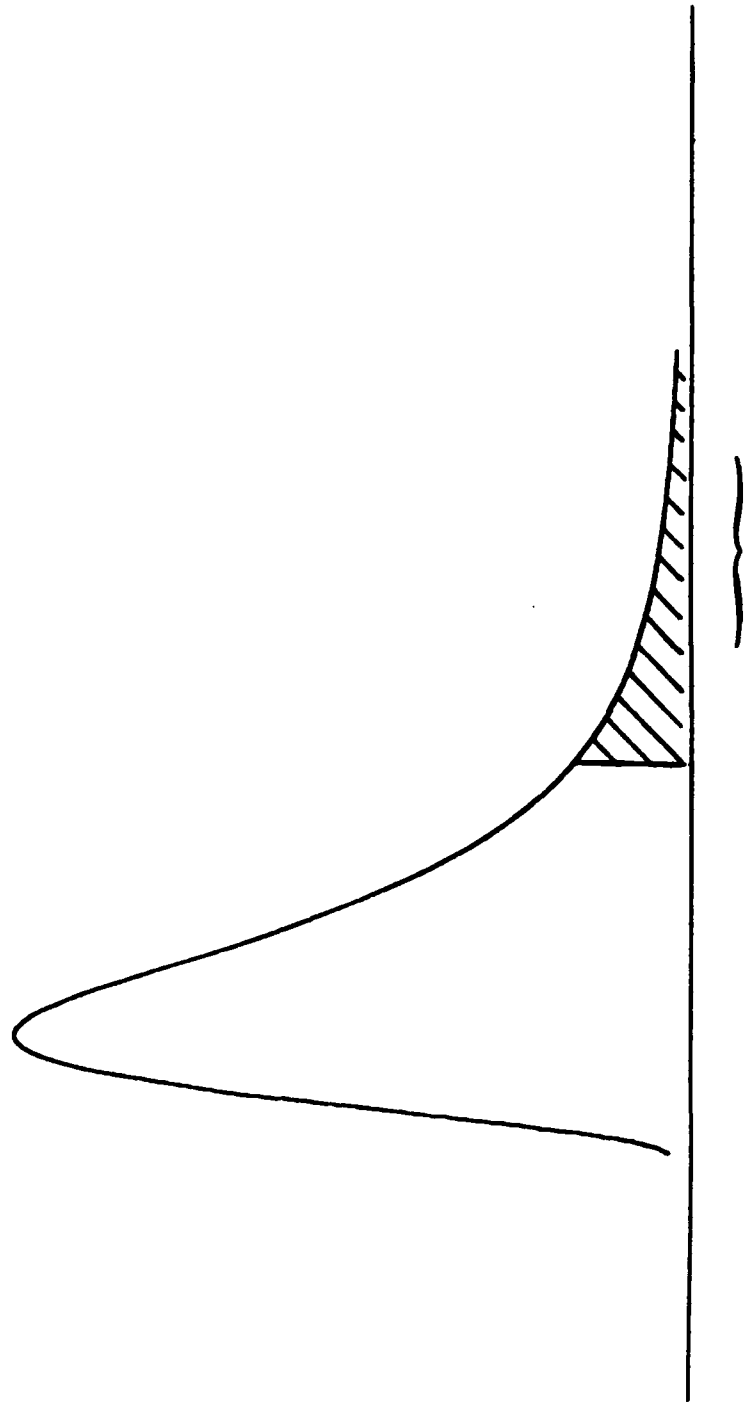
Preventative Medicine

VS

Radical Surgery

Inspection / Rejection ...

CAN be improved upon in MANUFACTURING.



"removed" by NDE / Rejection

NON DESTRUCTIVE EVALUATION:

can only be a passive contributor to component integrity.

**Relying on Inspection to produce a quality product
would be like relying on a stethoscope and
inflatable cuff to control high blood pressure.**

N D E Fanaticism ,

to borrow from the American philosopher George Santanya,

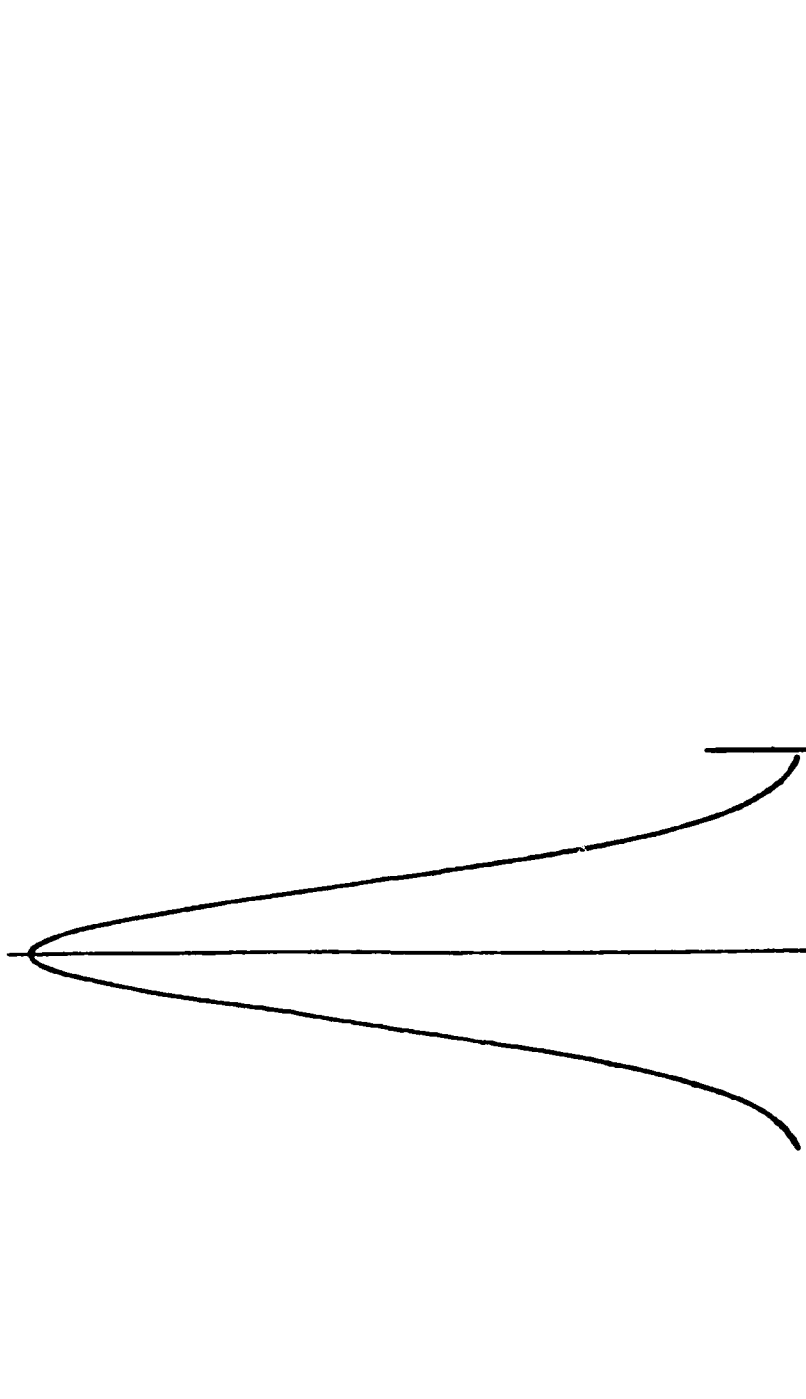
**consists in redoubling your effort
when you have forgotten your aim.**

Remember: the " . . . IP " Process . . .

**is intended to provide a component so
reliable that the damage inspected for
at overhaul is service-induced only.**

Quality Must Be Built - In

because it CANNOT be inspected - in.



<----- Good

P O O P C

pronounced: "poopsie"

Point - Of - Origin

Process Control

S P C , Statistical Process Control

**can only maintain CONTROL
of a process already IN Control.**

STATISTICAL EXPERIMENTATION

Beyond Taguchi ...

1. Screening Designs
 - a. factorial
 - b. fractional factorial
 - c. saturated (Taguchi) designs
2. Response Surface Designs
 - a. regular polyhedral
 - b. central composite
 - c. Box-Behnken
 - d. hybrid, and others

Inspection / Rejection . . .

IS appropriate in the MAINTENANCE situation.

NDE at Overhaul

must be able to count upon an inspectable component.

The " . . . IP " process is intended to assure this.

RECOMMENDATIONS:

- NDE can be more effective in furthering " . . . IP "

Process goals if its use in Manufacturing is in monitoring
process integrity.

- Active NDE is more appropriate at Overhaul in assessing
component integrity.

Fatigue Life Improvement Through Laser Shock Processing

**1990 USAF Structural Integrity
Program Conference**

**December 12, 1990
San Antonio, Texas**

Allan H. Clauer, Battelle Memorial Institute

John Koucky, Wagner Laser Technologies

Outline

- **Background**
- **Benefits**
- **How process works**
- **Effects on properties**
- **Types of applications**
- **Laser equipment**
- **Status**

High Intensity Pulsed Laser

- Mechanical working effect
- Not a thermal effect

**High Surface
Compressive
Stresses** —————→ **Increased
Fatigue Strength**

Property Improvements

- **Fatigue life**
- **Fatigue strength**
- **Fretting fatigue resistance**
- **Surface hardness**
- **Thin section strength**
- **Relieve residual weld stresses**

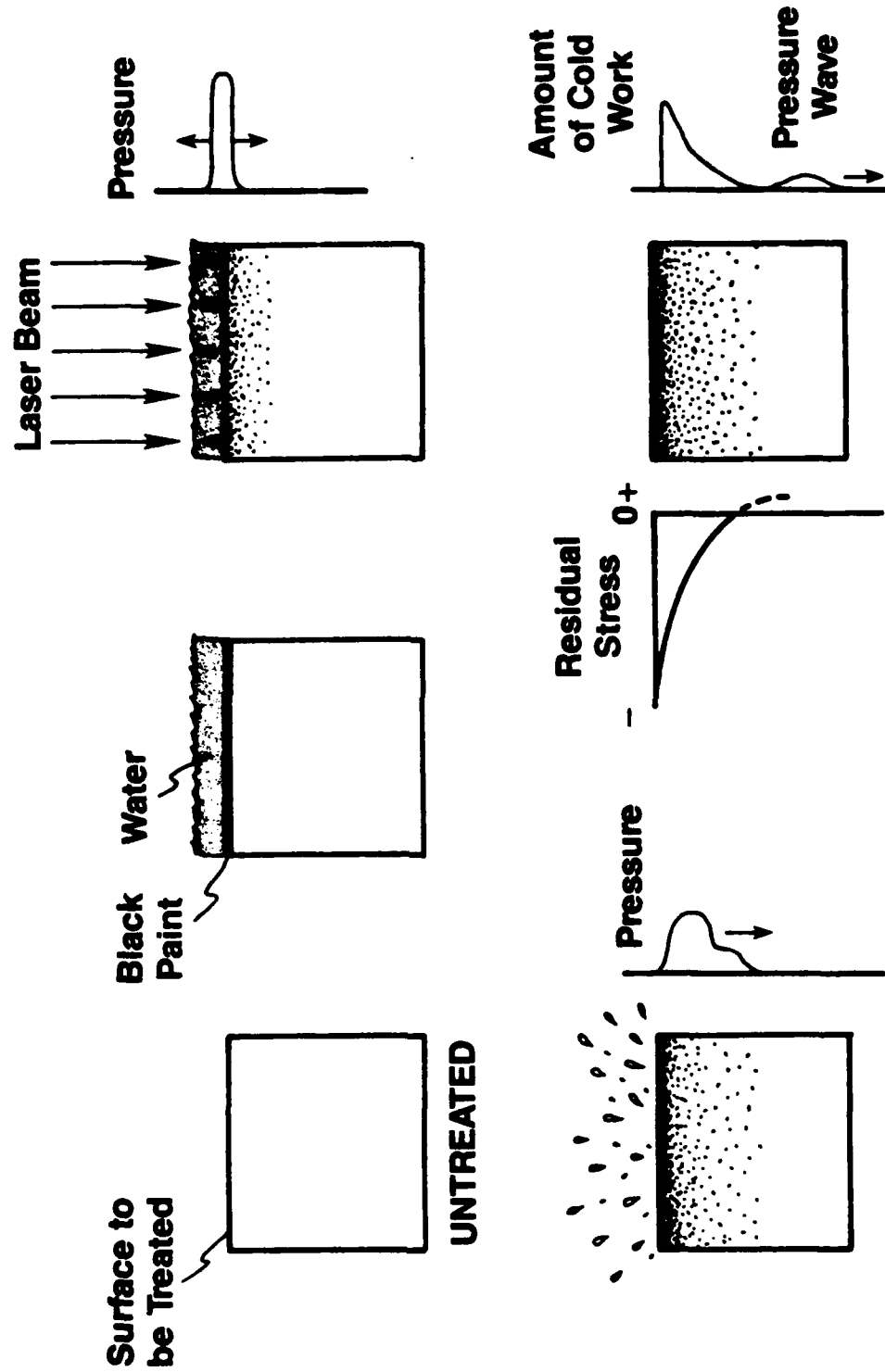
Benefits of LSP

- **Broad application to fatigue critical parts**
- **Can treat machined surfaces**
- **Need treat only the fatigue-critical areas**
- **High potential for reproducible, consistent treatment**

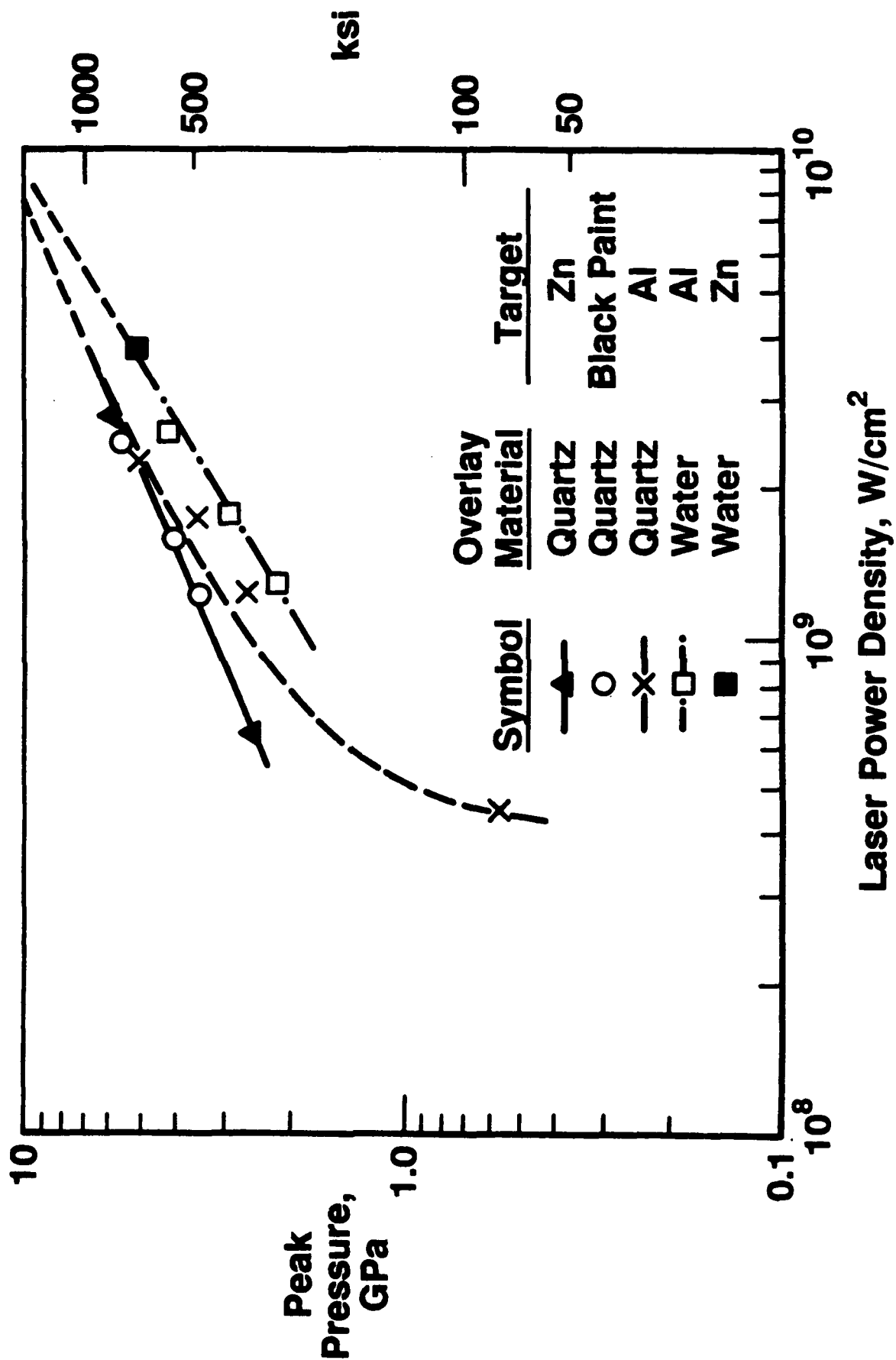
Materials Evaluated After LSP

- Aluminum alloys
- Steels
- Cast irons
- Ferrous powder metallurgy alloy
- Stainless steel

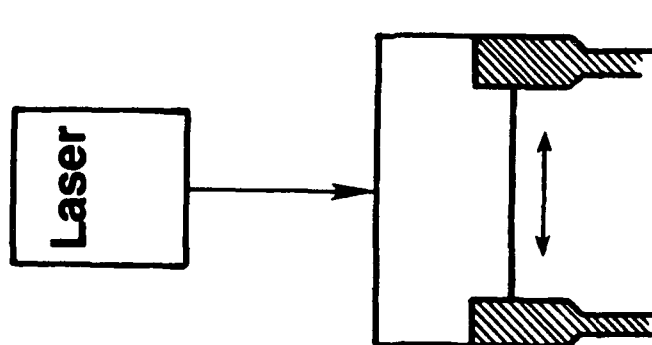
What Happens in LSP



Peak Pressures for Different Surface Conditions

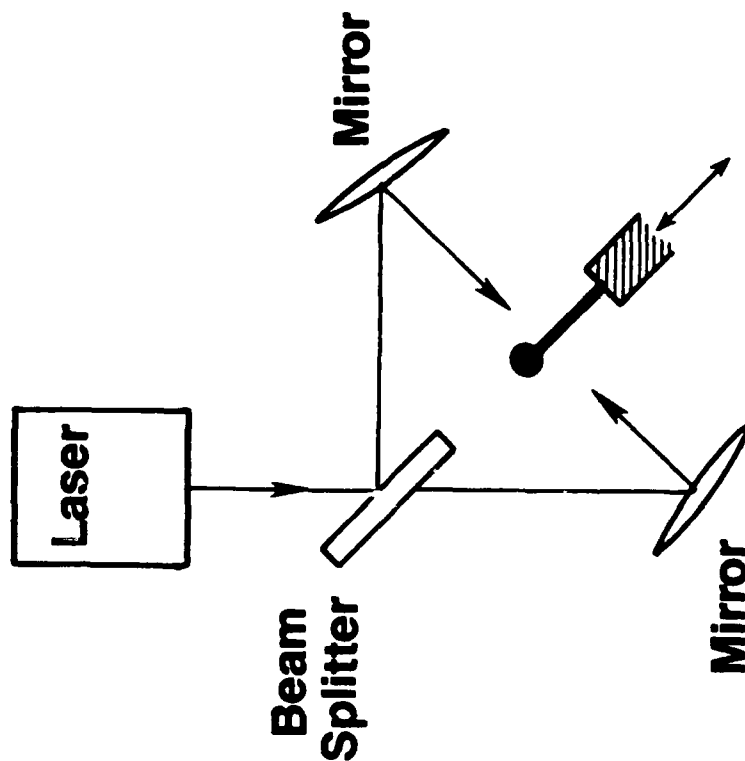


Treat One Side or Two Sides at Same Time



- Large Parts
- Thick Sections

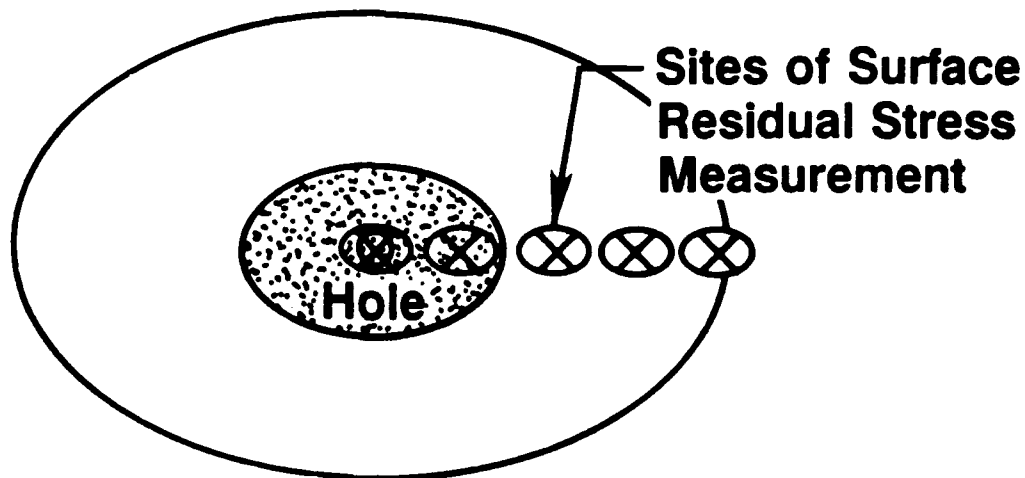
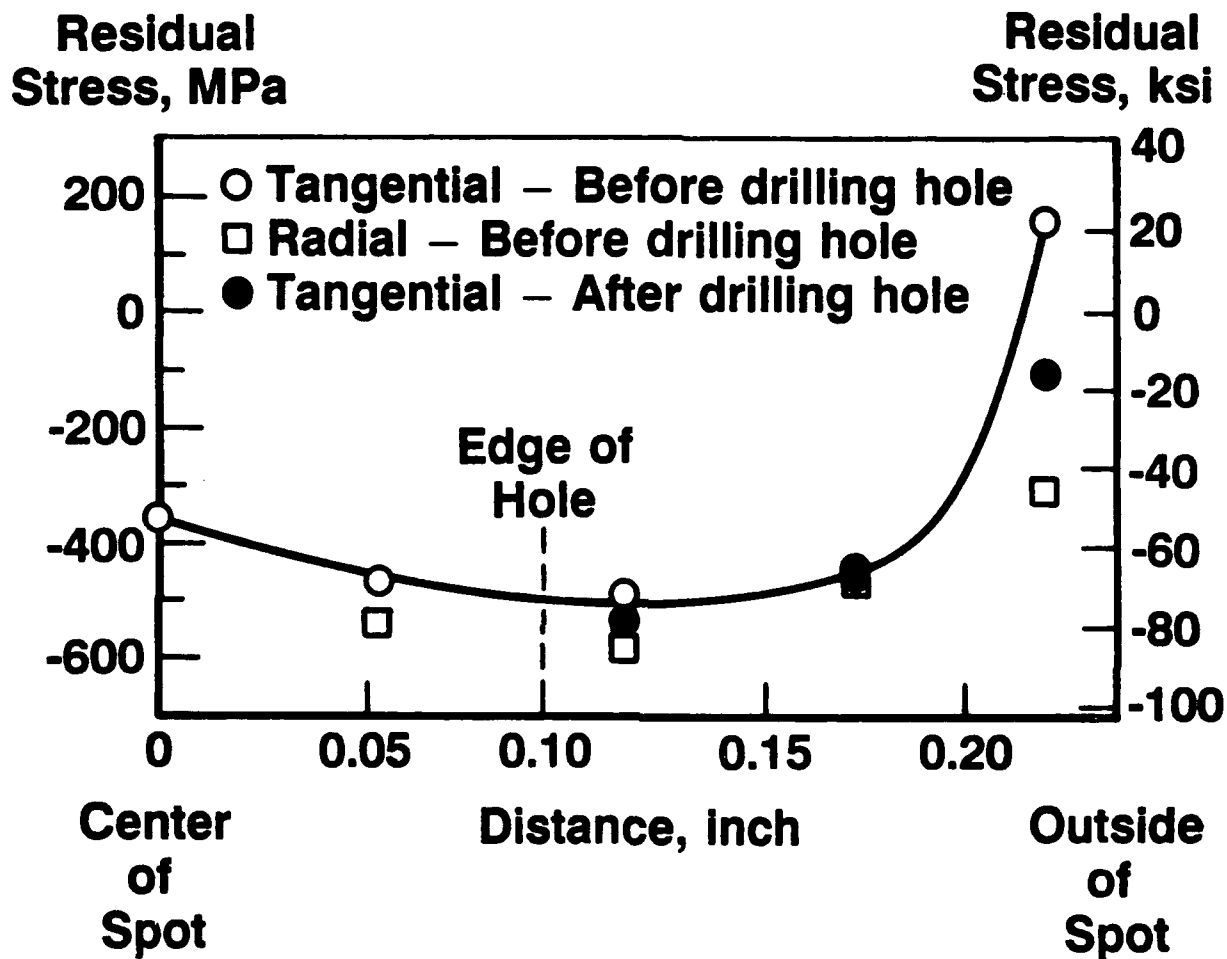
ONE SIDE



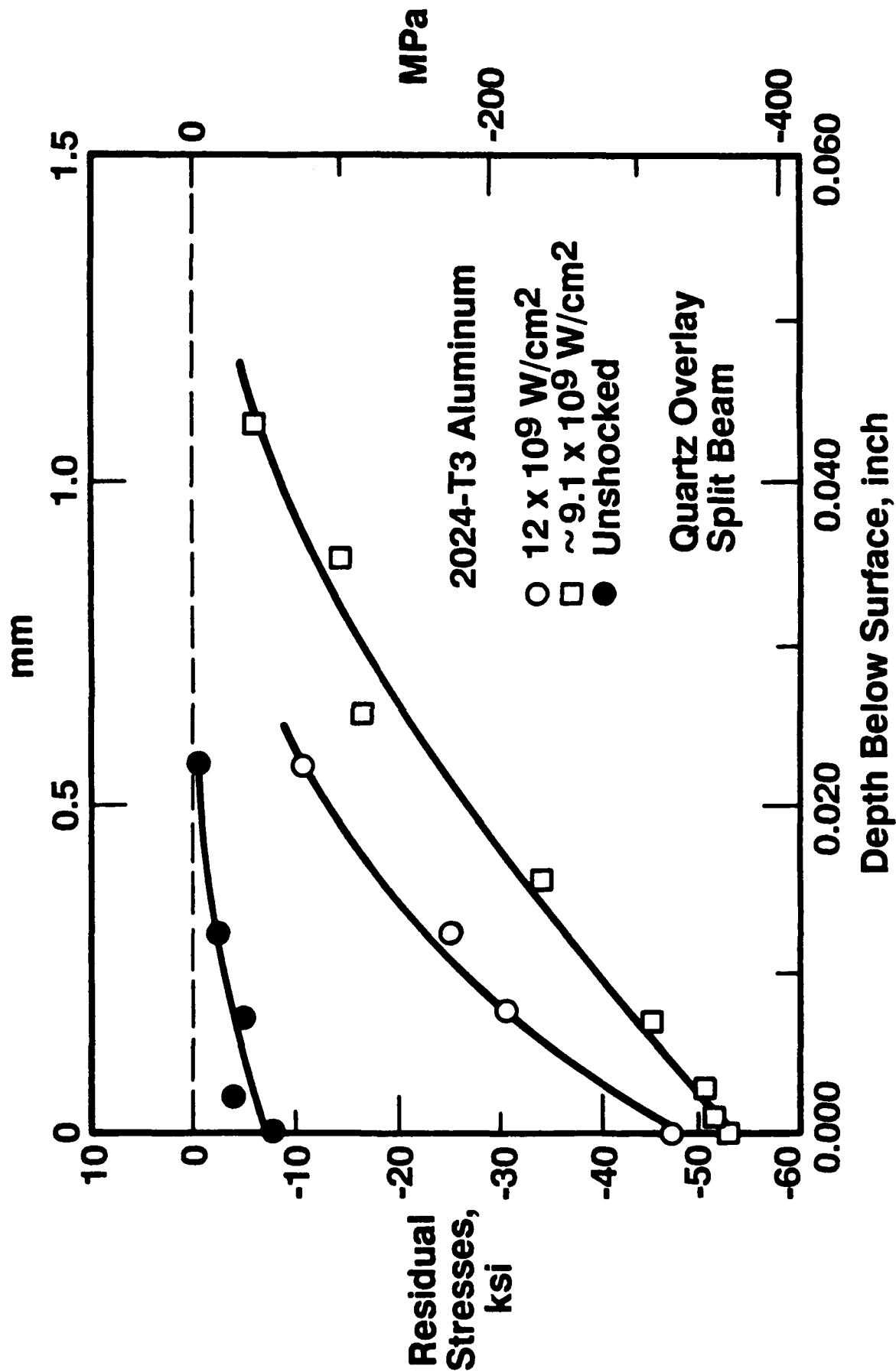
- Small Parts
- Thin Sections

TWO SIDES

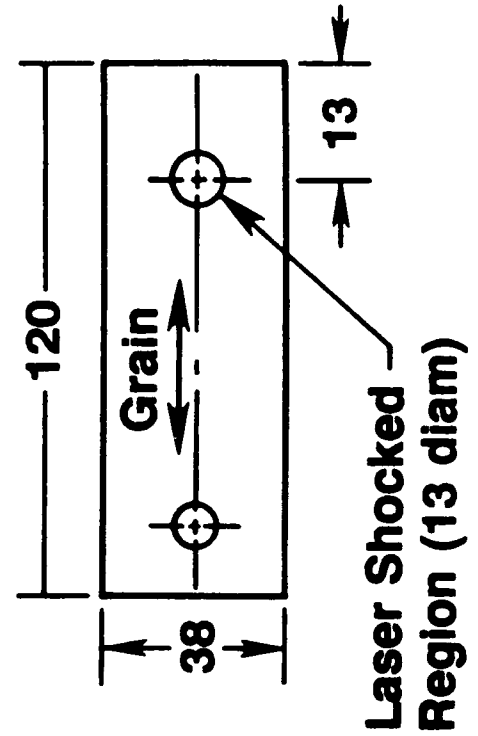
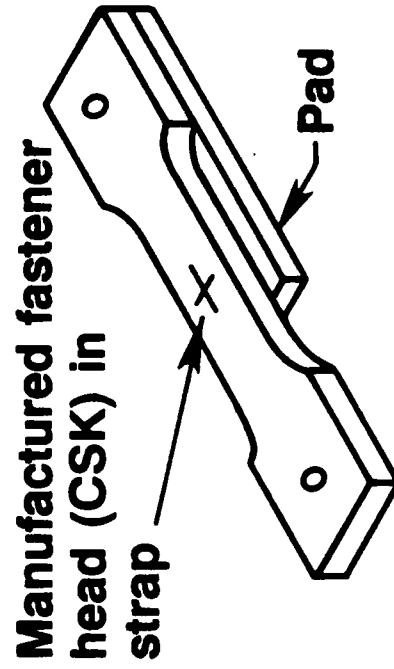
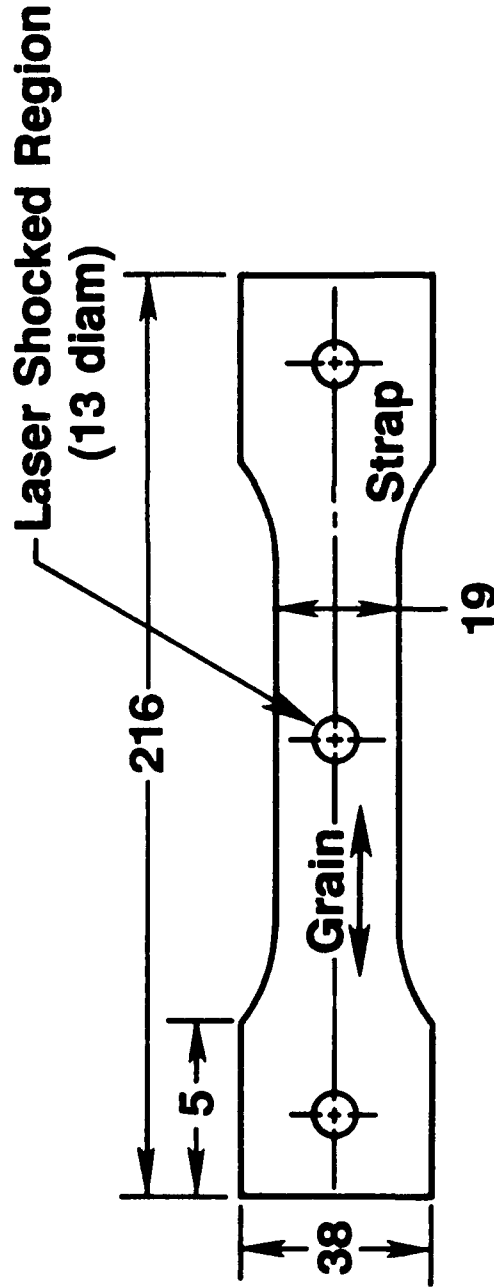
Surface Residual Stress Distribution



Depth of Residual Stress



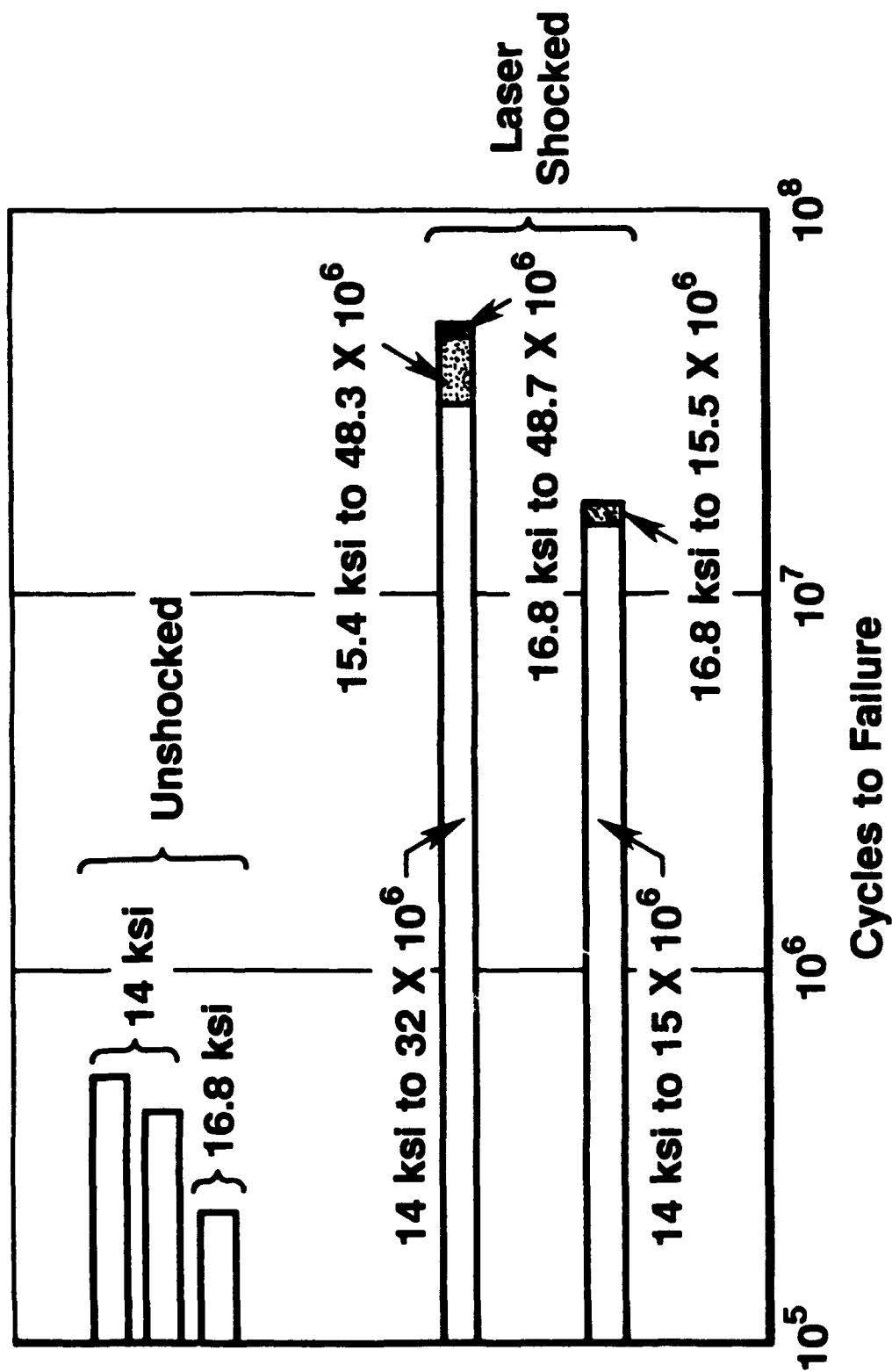
Fastened Joint Fretting Fatigue Specimen



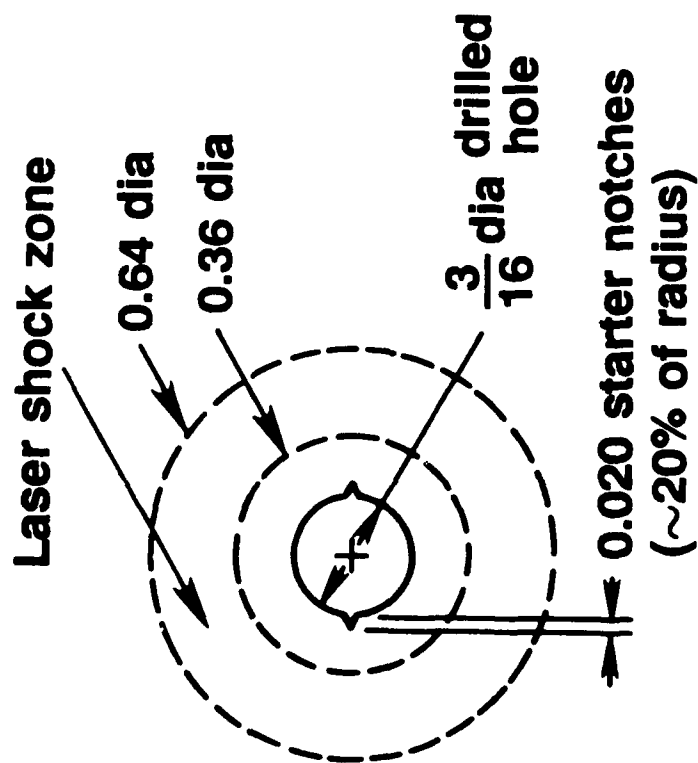
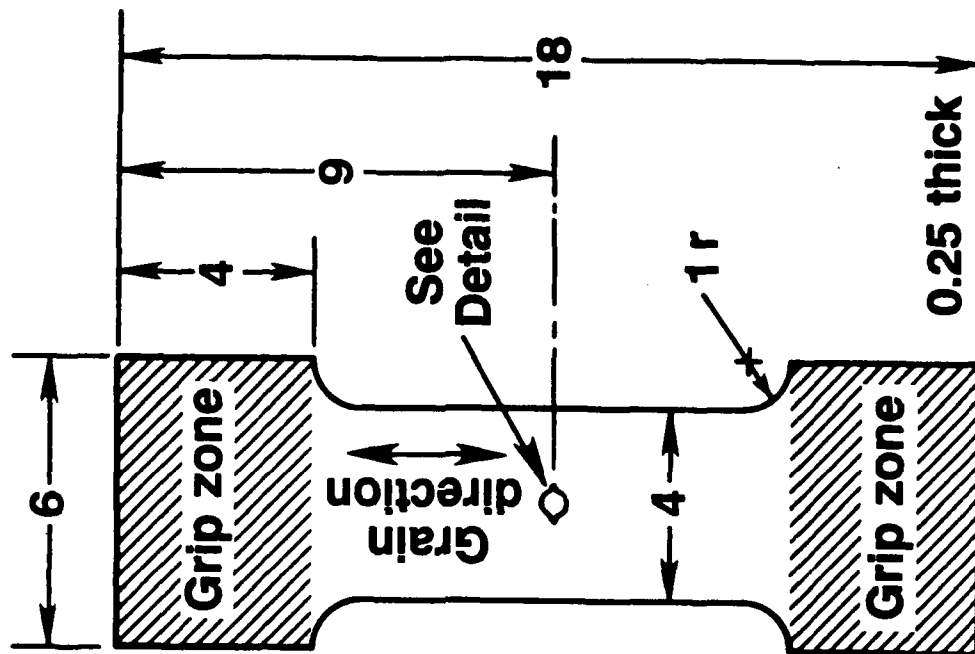
Dimensions in mm

Effect of Laser Shock Processing

**Fretting Fatigue Failure of Fastened Joints in
7075-T6 Aluminum (Stress Ratio = 0.1)**

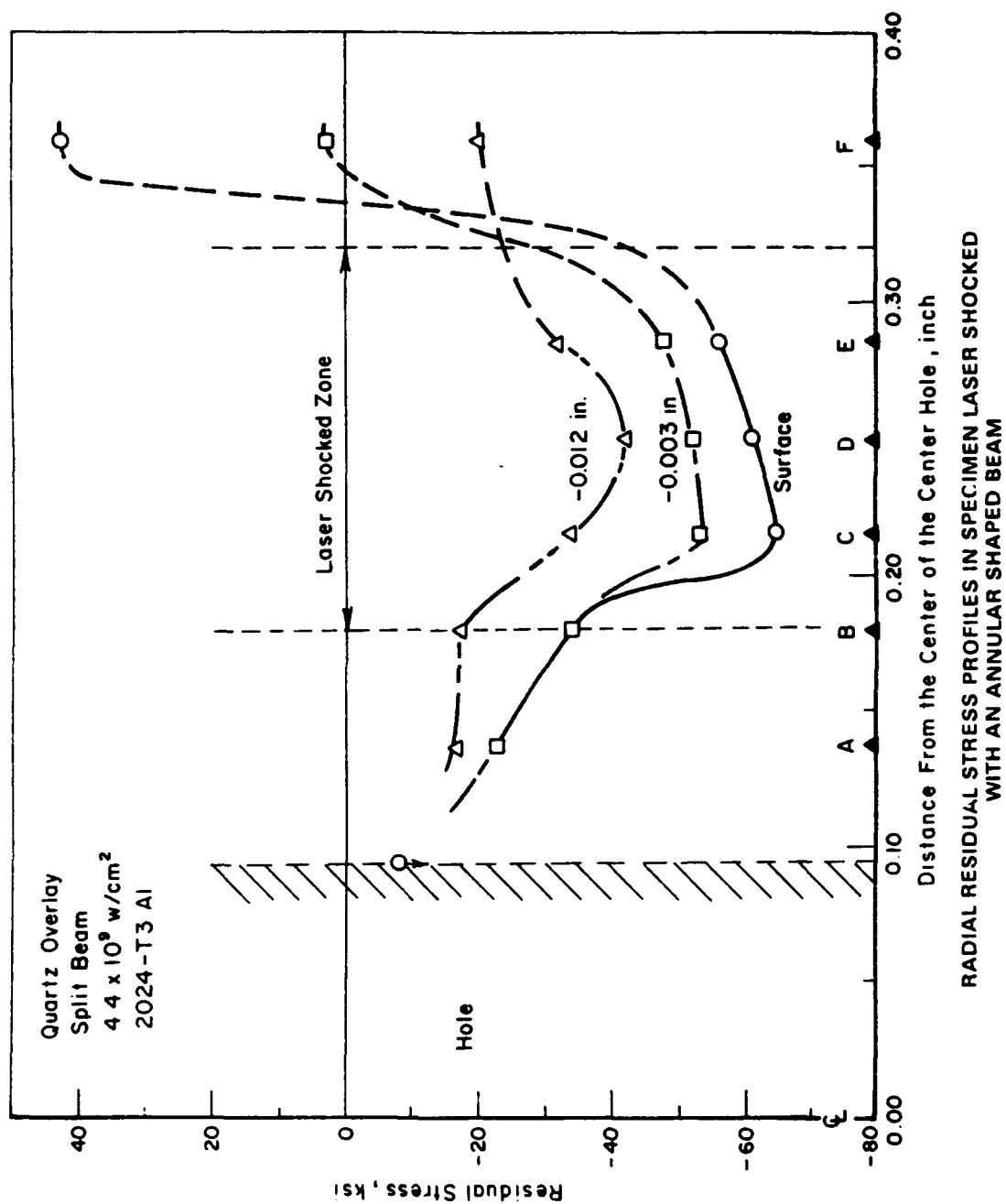


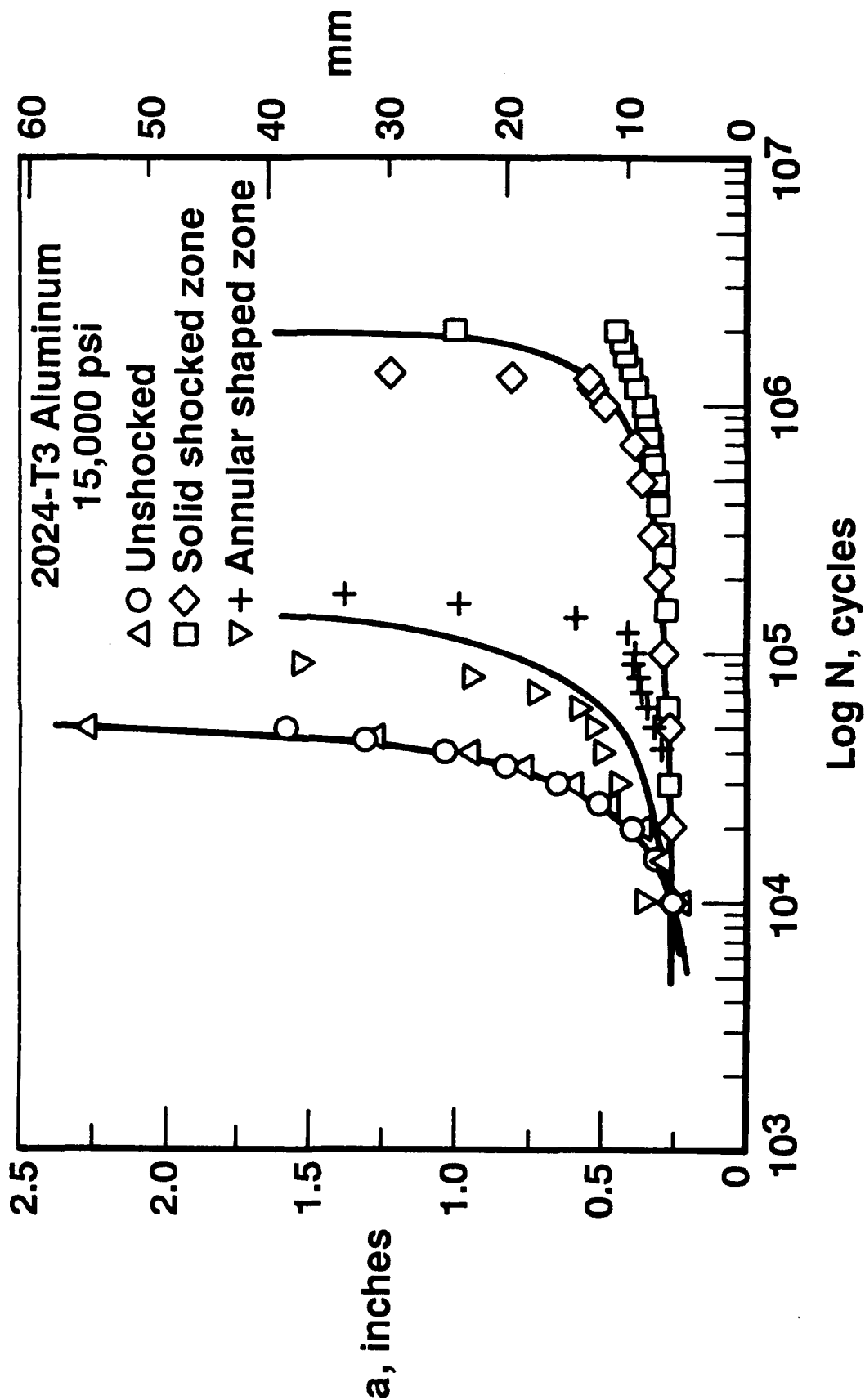
2024-T351 Aluminum Fatigue Specimen



Laser shocked regions

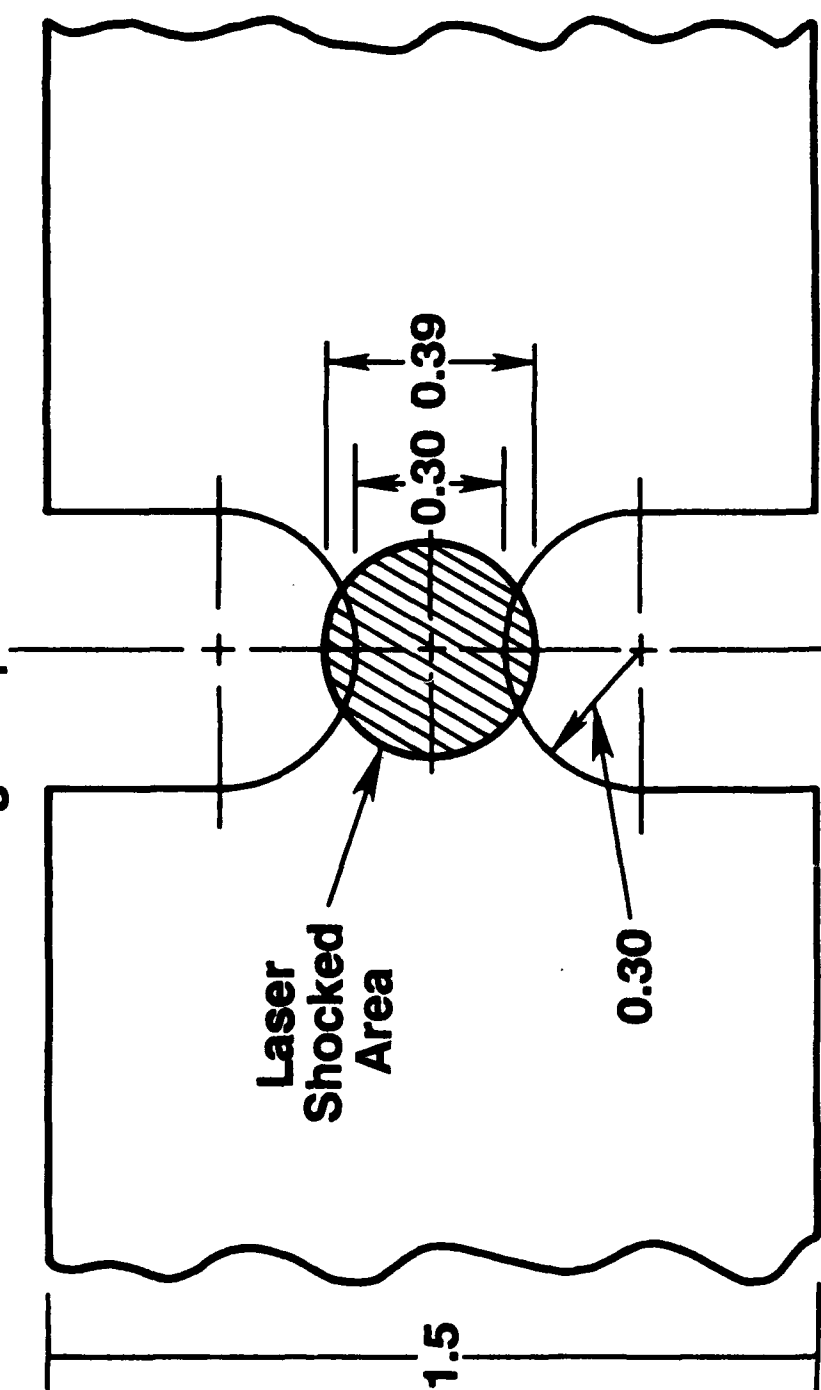
Dimensions in inches





4340 Steel Fatigue Specimen

Laser Shocked Region in Notched
Sheet Fatigue Specimens

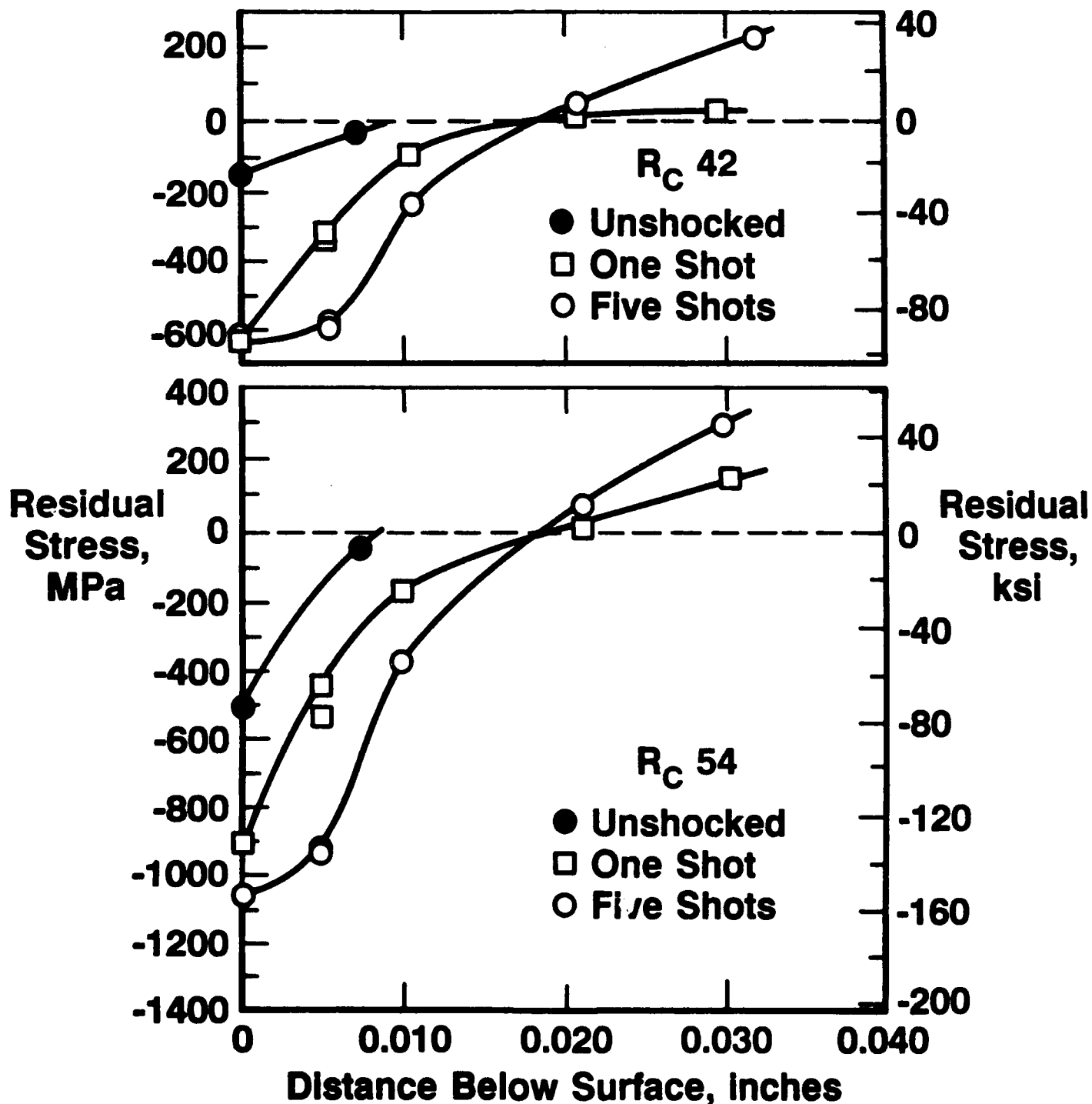


All dimensions in inches

Residual Stress Profiles



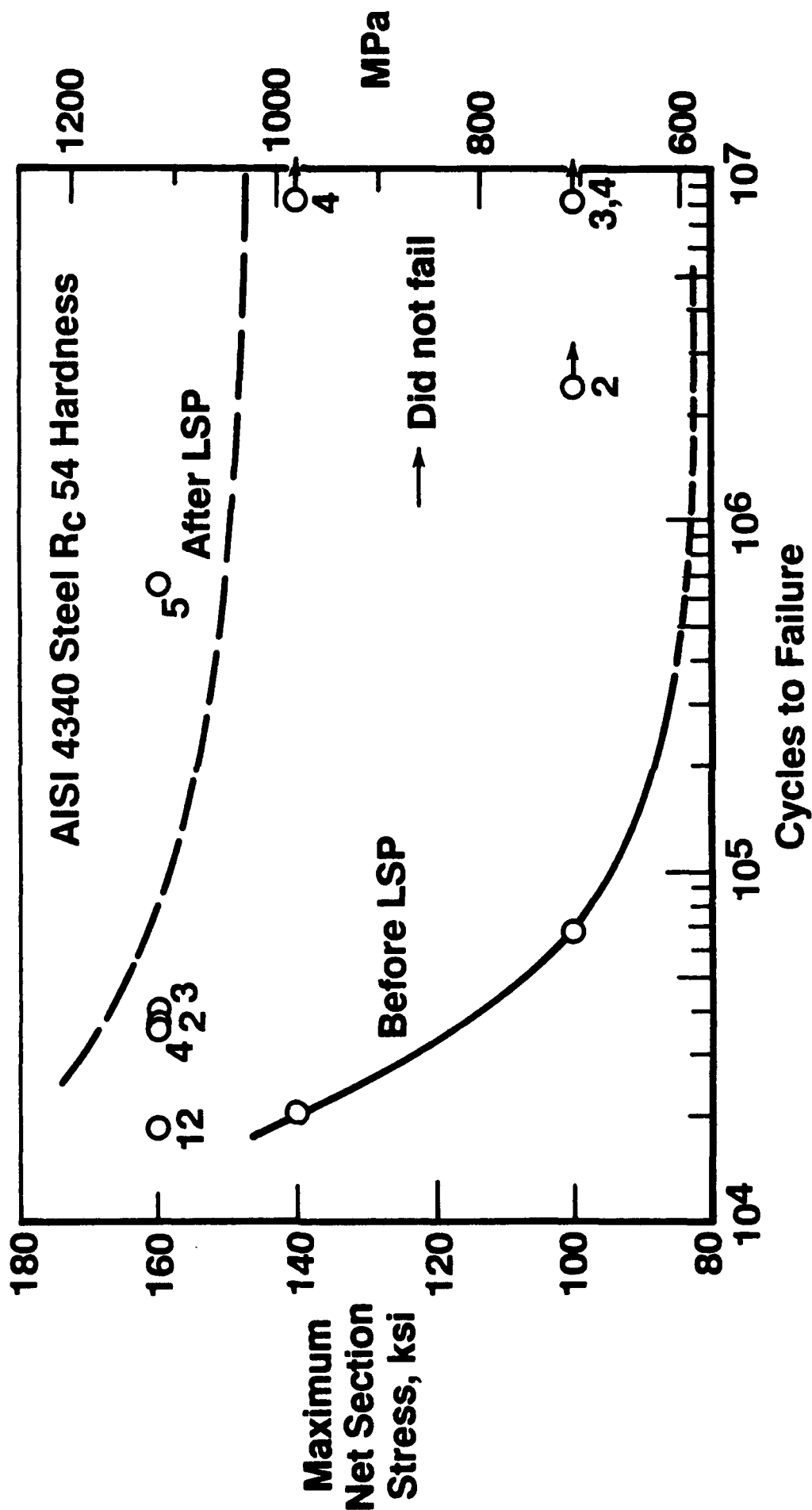
AISI 4340 Steel Sheet 0.060 Inches Thick Split Beam Shocked



Increased Fatigue Strength

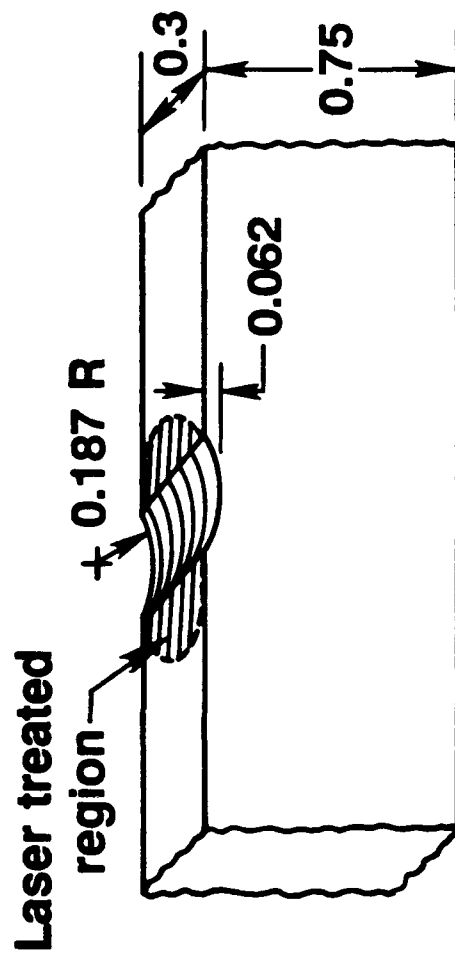


... Putting Technology To Work

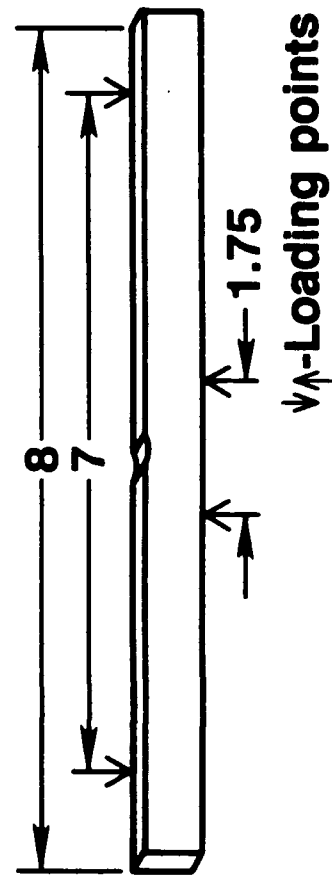


One-Sided Laser Treatment

**Configuration of the
notched zone showing
the laser treated region**



Loading configuration



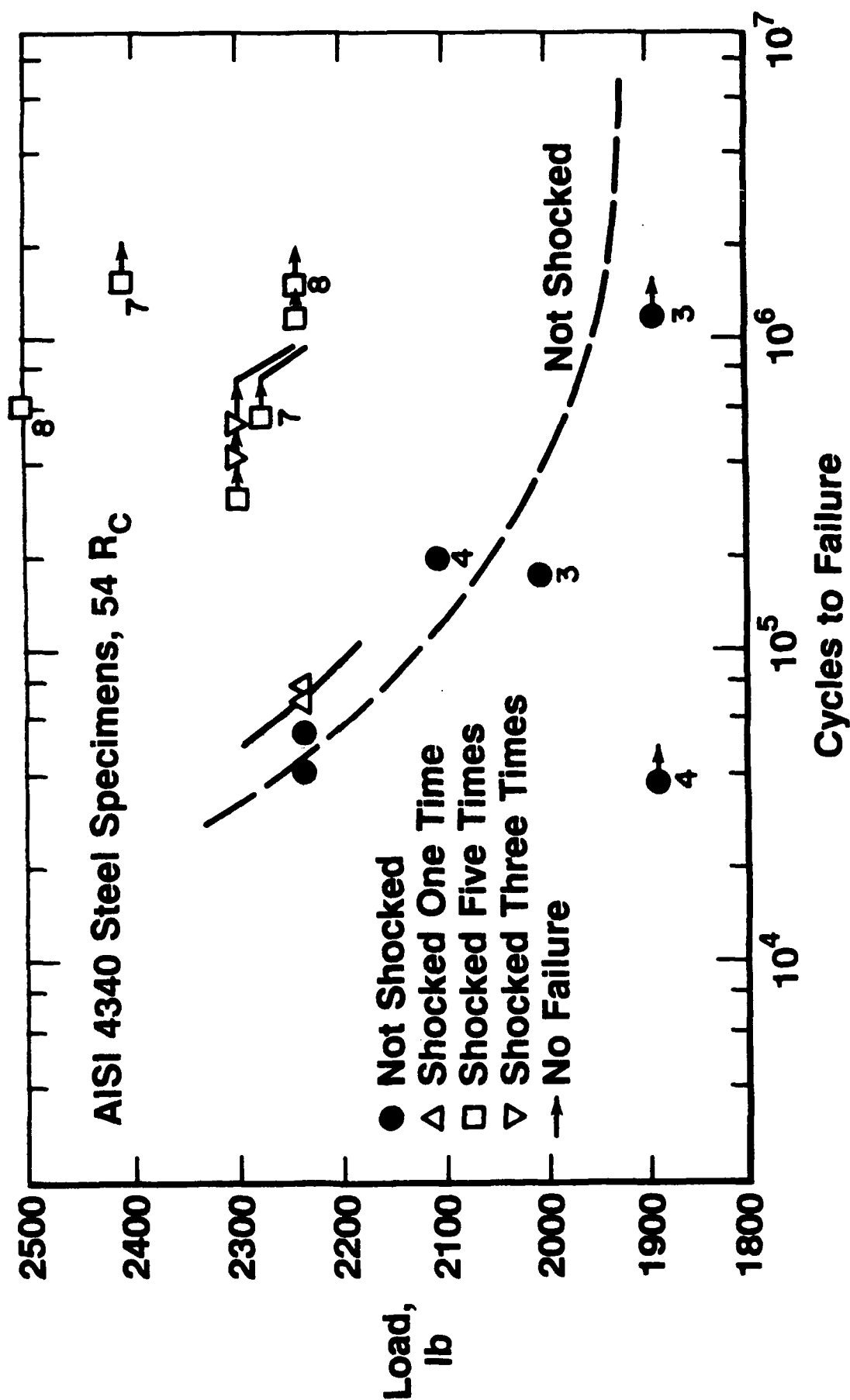
↕ Loading points

Dimensions in inches

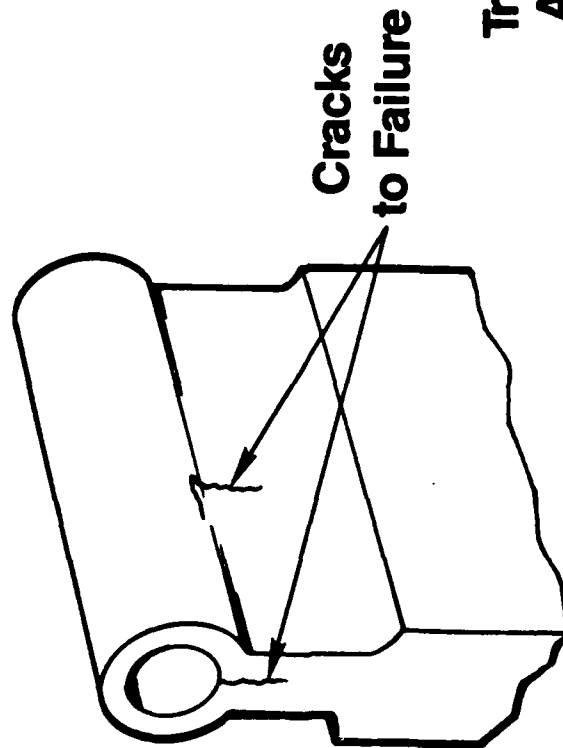
One-Sided Treatment of 4-Point Bend Specimen



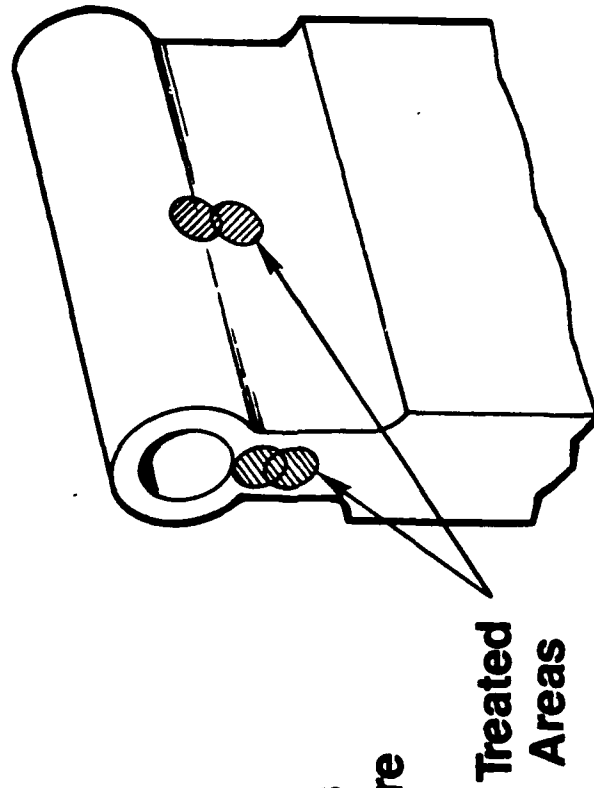
... Putting Technology To Work



Steering Rod Treatment



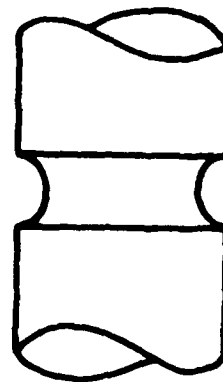
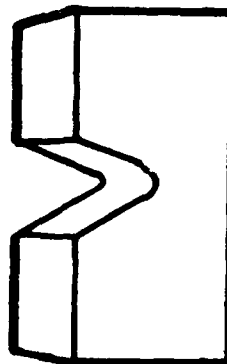
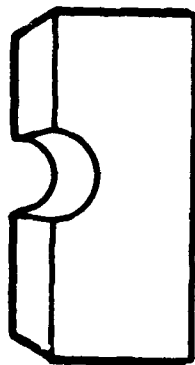
UNTREATED
33,000 Cycles
to Failure



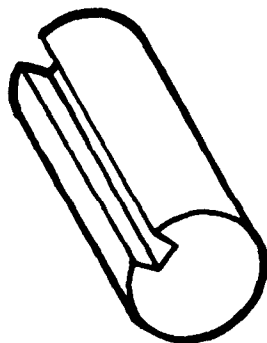
LSP-ZAP
92,000 Cycles
to Failure

Treatable Configurations, Examples

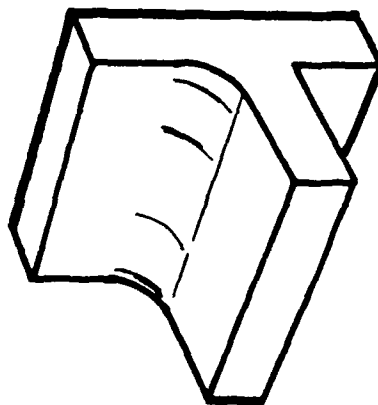
Notches



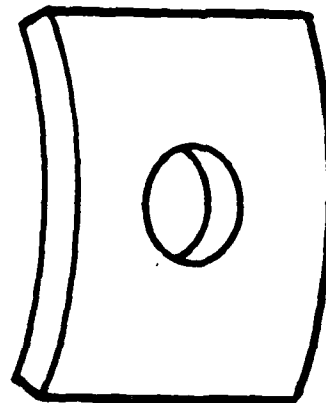
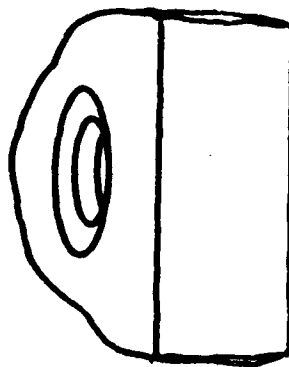
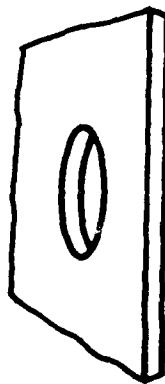
Keyways



Fillets



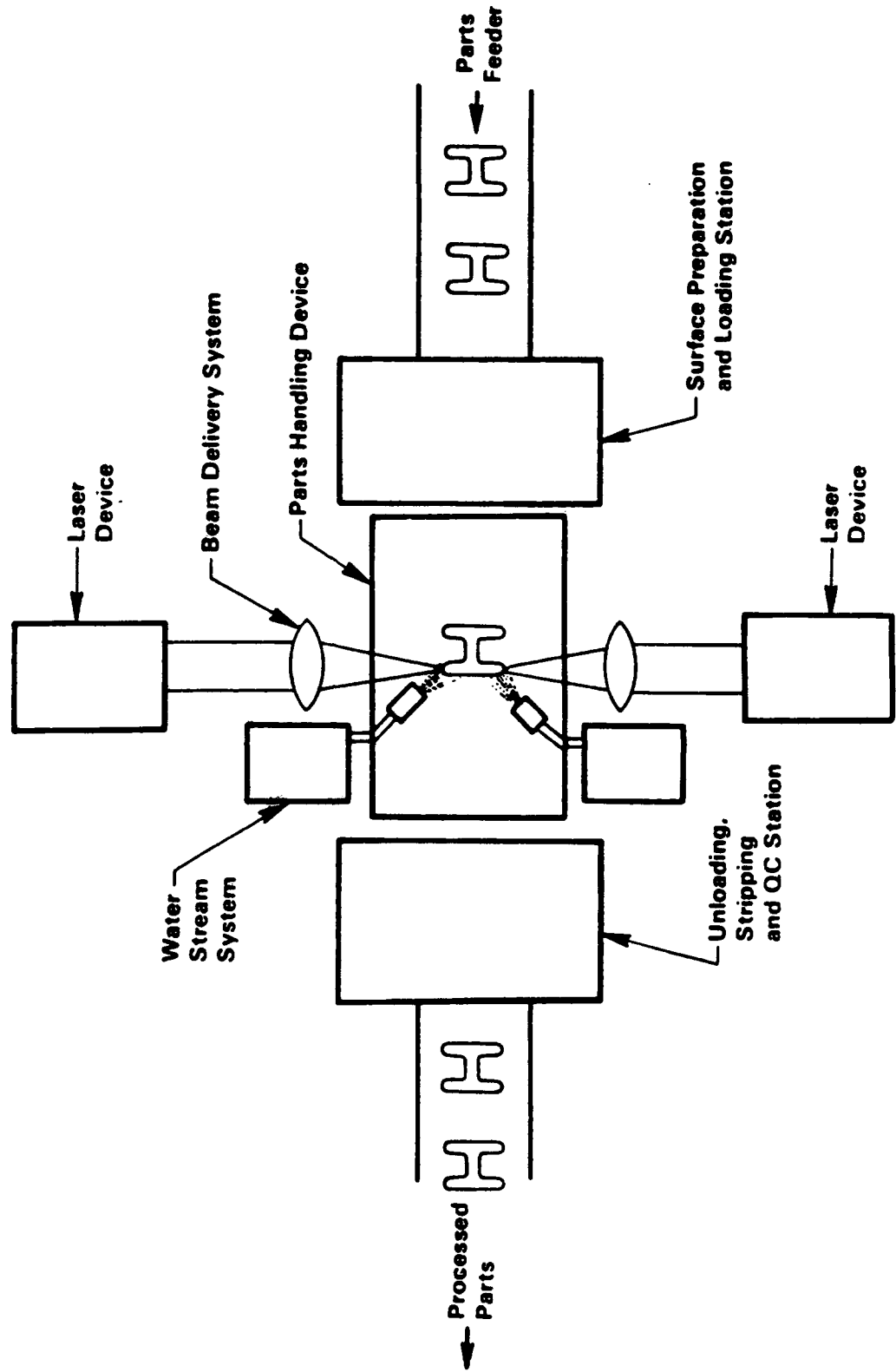
Holes

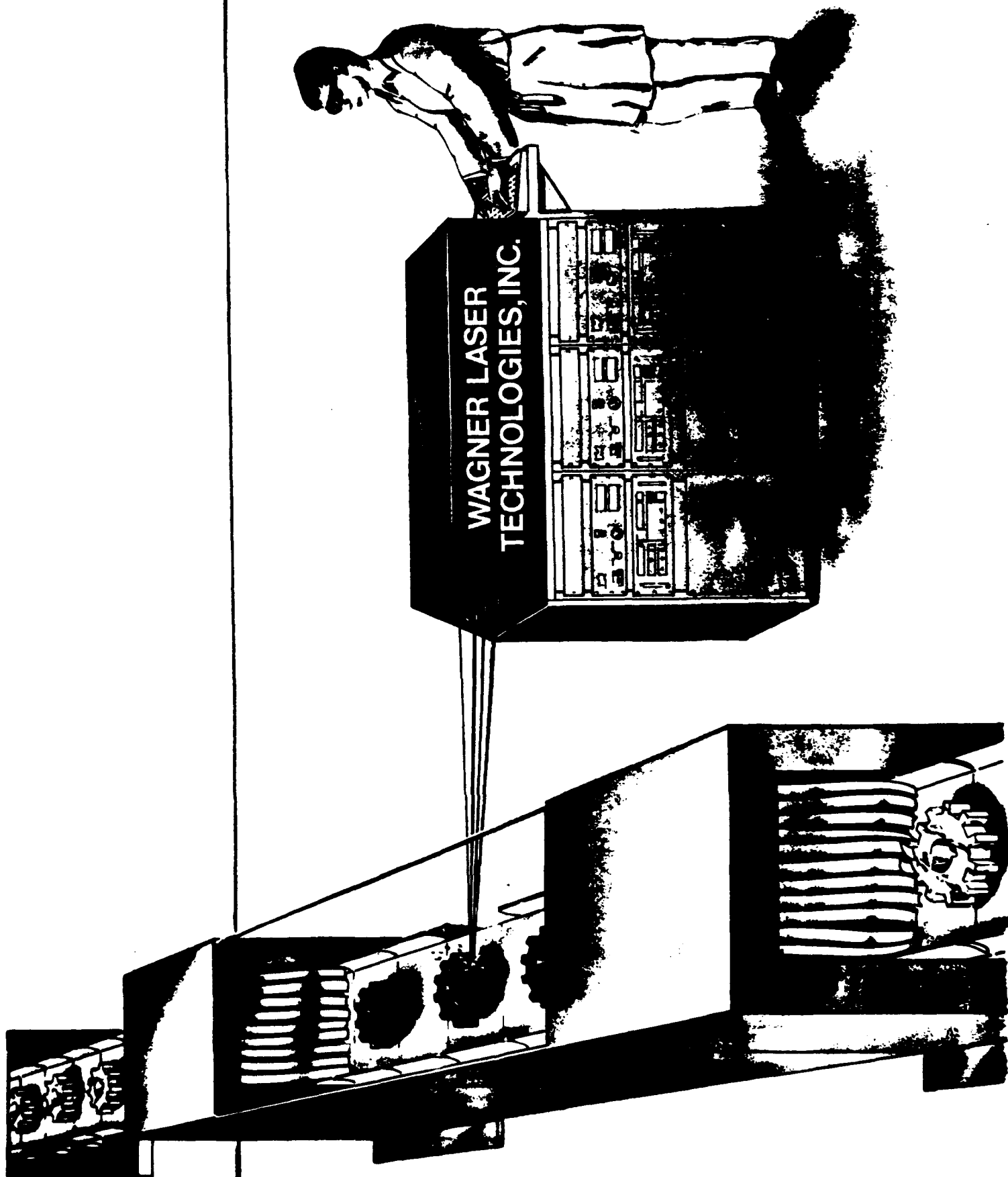


Laser Equipment

- **Designed to occupy small space**
- **Laboratory prototype operating**
- **Can be engineered to be safe on factory floor**

SCHEMATIC ARRANGEMENT OF LSP FACILITY





Processing Features



... Putting Technology To Work

- Can be set-up in automated manufacturing line
- Area coverage
 - Flexible: depends on laser power and material processing requirements
 - Typically spot of 0.4 inch diameter
 - Larger areas
 - Spot overlap
 - Larger laser = larger spot
 - Beam shape can be changed
- One shot/second design
- Expanding overlay system options

Quality Control

Primary

- Monitor beam energy of each shot
- Monitor beam shape of each shot
- Monitor mechanical impulse to part holder

Secondary on Random Samples

- Surface residual stresses (X-Ray)
- Condition of paint film
- Surface depression if any
- Property tests

Application of LSP



- Where current fatigue resistance treatments are unsatisfactory
- Where fatigue resistance treatments are desired but can not be used
 - Machined surfaces
 - Deep notches
 - Other
- In design of new parts or components where LSP can enable
 - Use of alternate materials
 - Lighter weight design
 - Fabrication benefits

Potential Applications



Aerospace Industry

Engines: Compressor blades, disks, shafts, and gears
Airframe and Structures: Fastener holes, wheel housings, and landing gear

Automotive Industry

Crankshafts, camshafts, connecting rods, gears, rocker arms, and shafts

Electric Utilities

Turbine blades, disks, and gears

Tool Industry

Small tool inserts and tool holders

Medical Industry

Hip implants and knee implants

Status of LSP

- **Demonstrated improvement in fatigue life of metals and alloys**
- **Operating laboratory prototype laser**
- **Treating commercial parts for feasibility**
- **Pursuing development of commercial laser**

Fracture Mechanics Based Assessment of Aluminum Stress Corrosion Durability via the Breaking Load Method

R. J. Bucci, D. A. Lukasak, E. L. Colvin, and B. W. Lifka

**Alcoa Laboratories
Alcoa Center, PA 15069**

at

**1990 USAF Structural Integrity Program Conference
San Antonio, TX
1990 December 11-13**



**Fracture Mechanics Based Assessment of Aluminum
Stress Corrosion Durability via the Breaking Load Method**

by

R. J. Bucci, D. A. Lukasak, E. L. Colvin, and B. W. Lifka
Alcoa Laboratories
Alcoa Center, PA 15069

at

1990 USAF Structural Integrity Program Conference
San Antonio, TX
1990 December 11-13

Abstract

At Alcoa Laboratories the breaking load test procedure was developed to provide an efficient and more discriminating accelerated laboratory practice for rating stress corrosion cracking (SCC) performances of relatively resistant aluminum materials. The method involves residual strength determinations from smooth tensile bars previously subjected to static loading within a corrosive medium. The post-exposure tension test seeks out the specimen location most weakened by the prior exposure history.

One measure of SCC degradation from the breaking load test is to compare the specimen post-exposure strength to the original tensile strength (no exposure); the greater the strength loss the more severe the attack. A more damage oriented interpretation of the test exploits fracture mechanics concepts to quantify extent of SCC in terms of an "effective flaw size" calculated from the specimen breaking strength. The effective flaw estimates maximum damage penetration from the specimen surface, and predicted penetrations are shown to agree quite well with fractographic evidence of actual SCC. The good agreement between prediction and experiment facilitates mathematical representation of natural SCC flaws, and their statistical size variation with time can be approximated from tension test results on specimens precracked under progressively increasing exposure durations. Thus, expression of SCC ratings in terms of both flaw size exceedance probabilities and growth rates can be accommodated by a simple smooth specimen testing approach. Further, it is shown that fracture mechanics analysis of residual strength data provides a unifying bridge for contrasting SCC test performances from specimens of differing geometry and materials of differing strength - toughness property combinations.

The above interpretive features of the breaking load test provide a significant improvement over more traditional smooth specimen pass/fail or precracked specimen (KISCC type) evaluations. Moreover, because of its simplicity, the breaking load method is ideally suited for material development and selection oriented to corrosion durability performance objectives. Standardization of the breaking load test method is ongoing within ASTM Committee G1, and work has been initiated to develop experience after long term, natural exposures. The progress made is encouraging, and the breaking load approach offers promise as a framework for incorporating damage quantification into material specifications and design for corrosion integrity assurance. An analogy is drawn between the proposed SCC test framework and emerging fatigue durability assessment methodology.

References

1. D. O. Sprowls, R. J. Bucci, B. M. Ponchel, R. L. Brazill, and P. E. Bretz, "A Study of Environmental Characterization of Conventional and Advanced Aluminum Alloys for Selection and Design, Phase II - The Breaking Load Method," NASA Contractor Report 172387, 1984 August 31.
2. "Alcoa develops new stress corrosion cracking test method...", Alcoa Technology Report, No. 3, 1985 June.
3. R. J. Bucci, R. L. Brazill, D. O. Sprowls, B. M. Ponchel, and P. E. Bretz, "The Breaking Load Method: A New Approach for Assessing Resistance to Growth of Early Stage Stress Corrosion Cracks," Proceedings ASM International Conference and Exposition on Fatigue, Corrosion Cracking, Fracture Mechanics and Failure Analysis - Corrosion Cracking, ASM, 1986, pp. 267-277.
4. R. J. Bucci, R. L. Brazill, and J. R. Brockenbrough, "Assessing Growth of Small Flaws from Residual Strength Data," Small Fatigue Cracks, Proceedings of the Second International Conference/Workshop, The Metallurgical Society of AIME, 1986, pp. 541-556.
5. E. L. Colvin and M. R. Emptage, "The Breaking Load Method: Results and Statistical Modifications from the ASTM Inter-Laboratory Test Program," presented ASTM International Symposium on Corrosion Testing of Aluminum Alloys, San Francisco, CA, 1990 May 21-22.
6. D. A. Lukasak, R. J. Bucci, E. L. Colvin, and B. W. Lifka, "Damage Based Assessment of Stress Corrosion Performances Among Aluminum Alloys," presented ASTM International Symposium on Corrosion Testing of Aluminum Alloys, San Francisco, CA, 1990 May 21-22.
7. ASTM Working Document - Test Method for Determining the Stress-Corrosion Cracking Resistance of High Strength Aluminum Alloy Products Using the Breaking Load Method, Draft 2, ASTM Committee G01.06, 1990 July.



Structural Integrity

- | | |
|--------------------|---|
| • Strength | How strong is it |
| • Damage tolerance | Is it safe |
| • Durability | How long will it last |
| • Reliability | Are you sure |
| • Supportability | How efficient to inspect,
maintain, and repair |

Aluminum Aerospace Products The Next Frontier?

**Extend/guarantee life capability through novel material
designs and process controls**

- **Fatigue**
- **Corrosion**
- **Elevated temperature**

The Future...

- **Rapid analytical tradeoffs to get best mix of performance, reliability, supportability, and cost.**
- **Material qualification through defect distribution.**
- **New material parameters and data bases.**

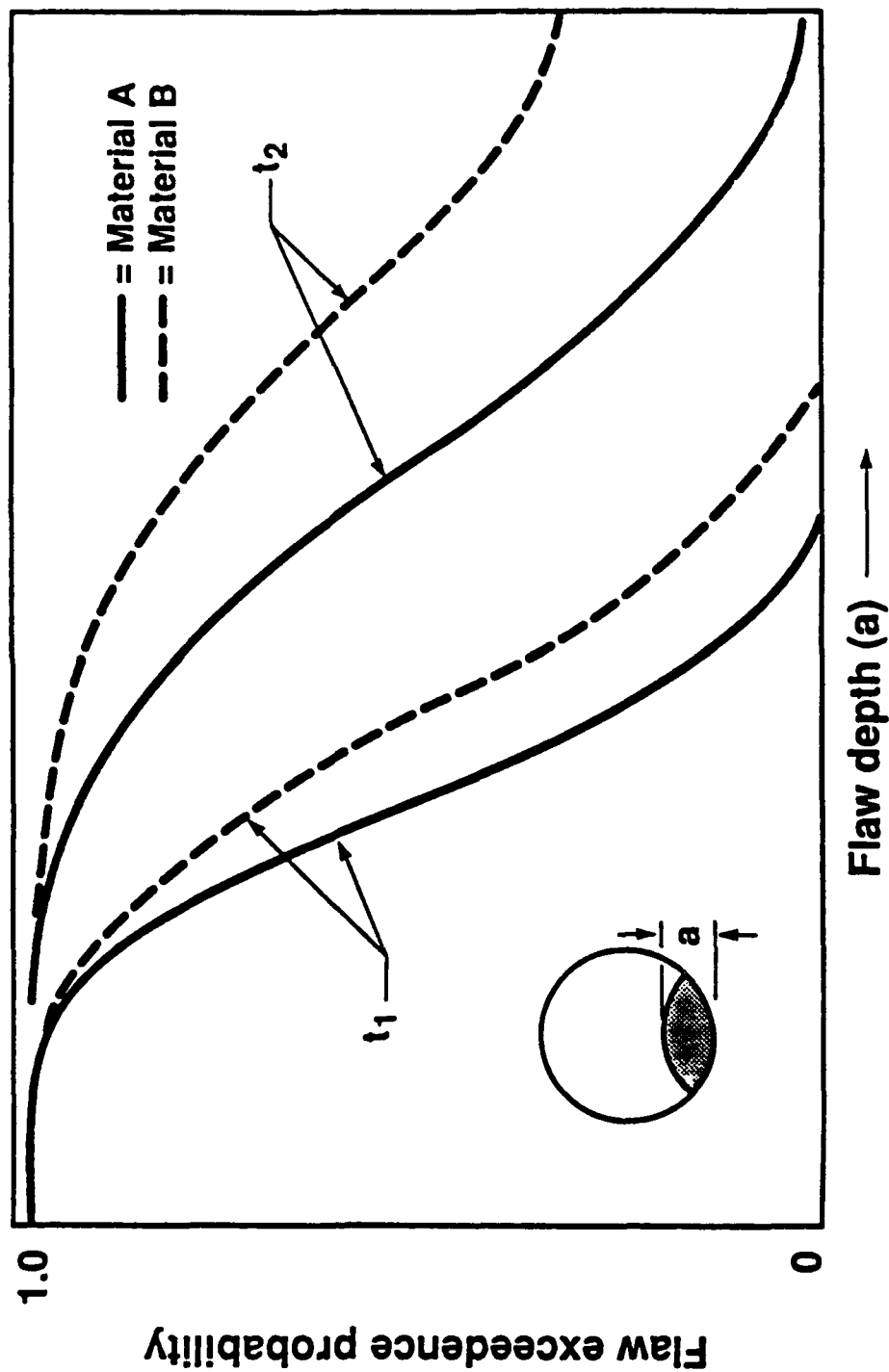
Probability at Time (t) That Unit Surface Area of Material Will Develop Damage Penetration Greater Than Depth (a)

GA-28142.1



ALCOA

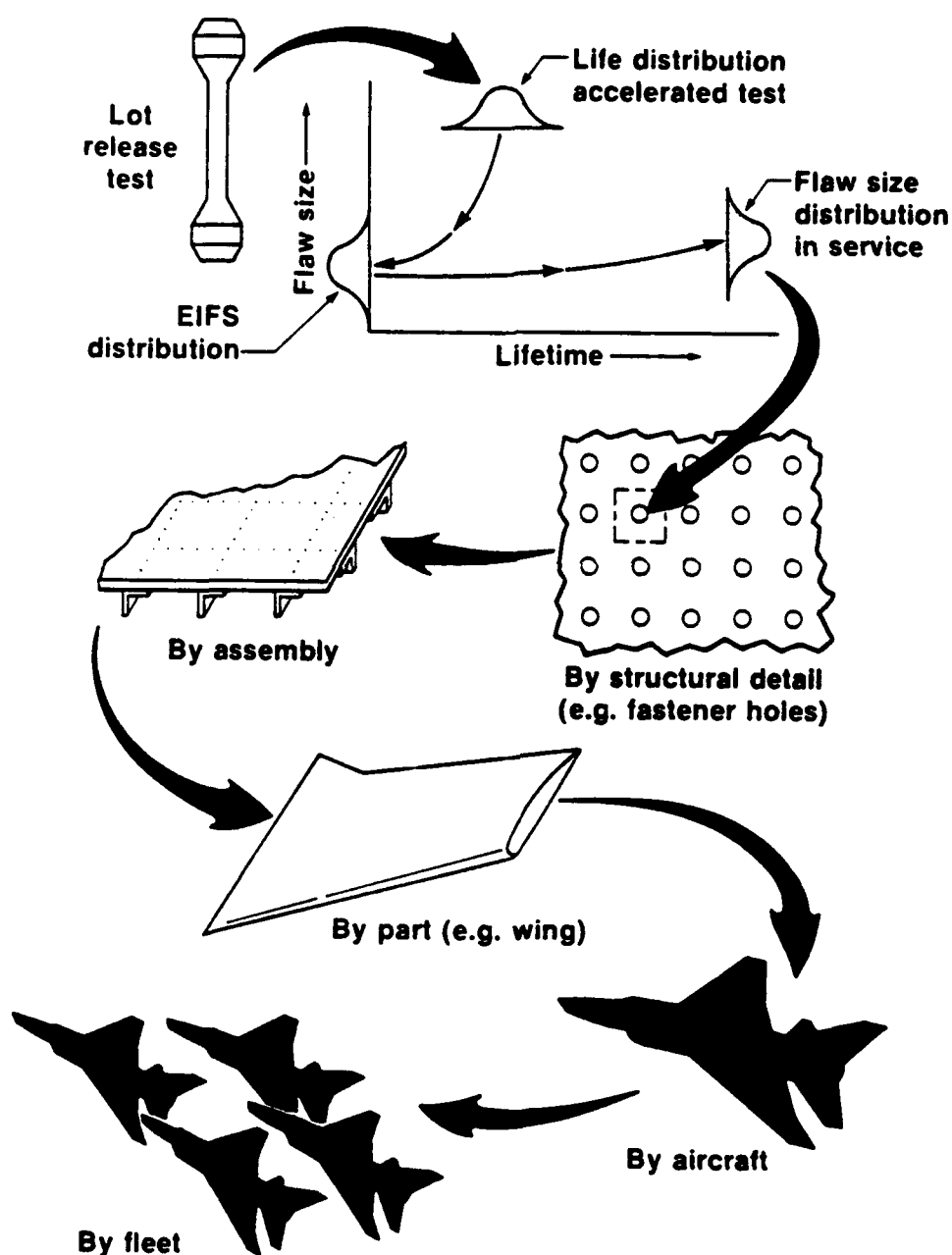
Material Reliability



The EIFS Distribution

Starting Point for Life Management

at Various Structural Levels



Hypothetical Durability Analysis

7050-T7451 Thick Plate

Calculated crack growth potential out of F-16 lower wing skin fastener holes (M.E. Artley, USAF, 88-04-15)

Number of flaw size exceedances per 1000 holes

Flaw size (in.)	<u>1 service lifetime (8000 flt. hrs.)</u>		<u>2 service lifetimes (16000 flt. hrs.)</u>	
	Old quality material	New quality material	Old quality material	New quality material
0.03	196	3	-	-
0.05	2	0	-	-
0.10	0	0	195	3
0.20	0	0	3	0

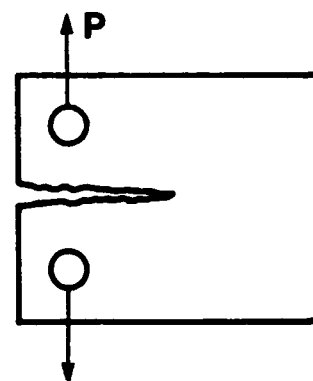
SCC Test/Evaluation - Traditional Approaches

Specimen Type

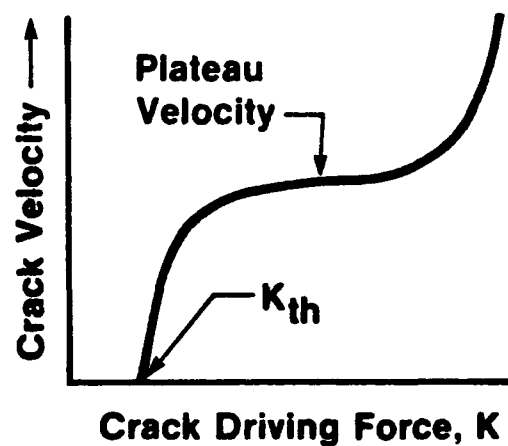
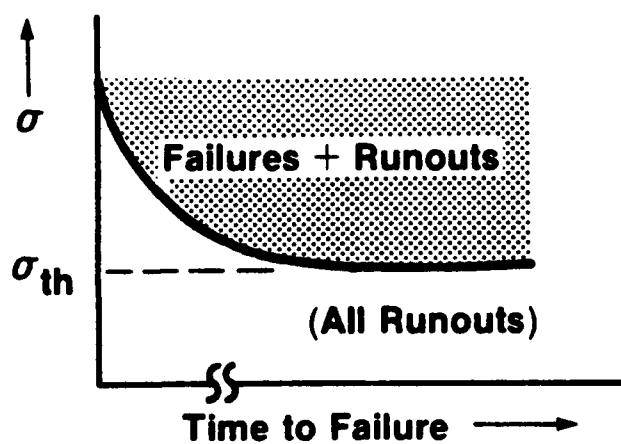
Smooth

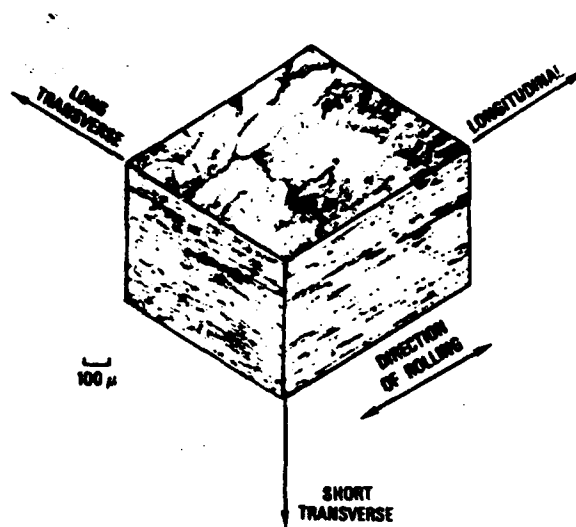


Precracked (LEFM)

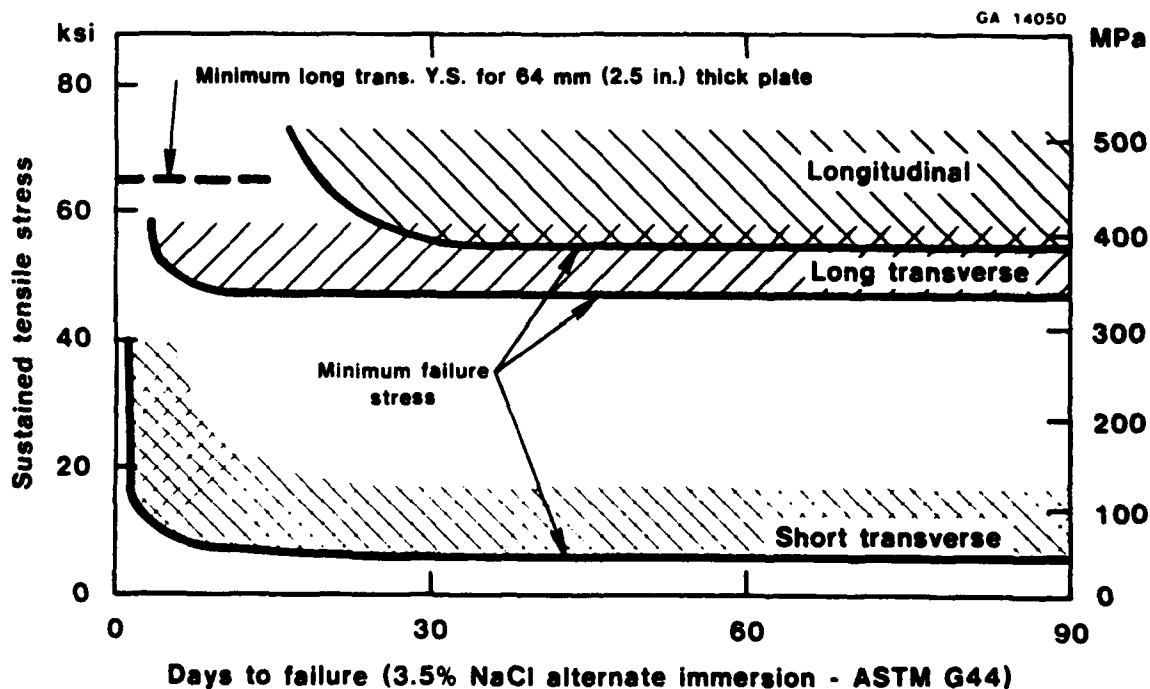


Basic Material Data





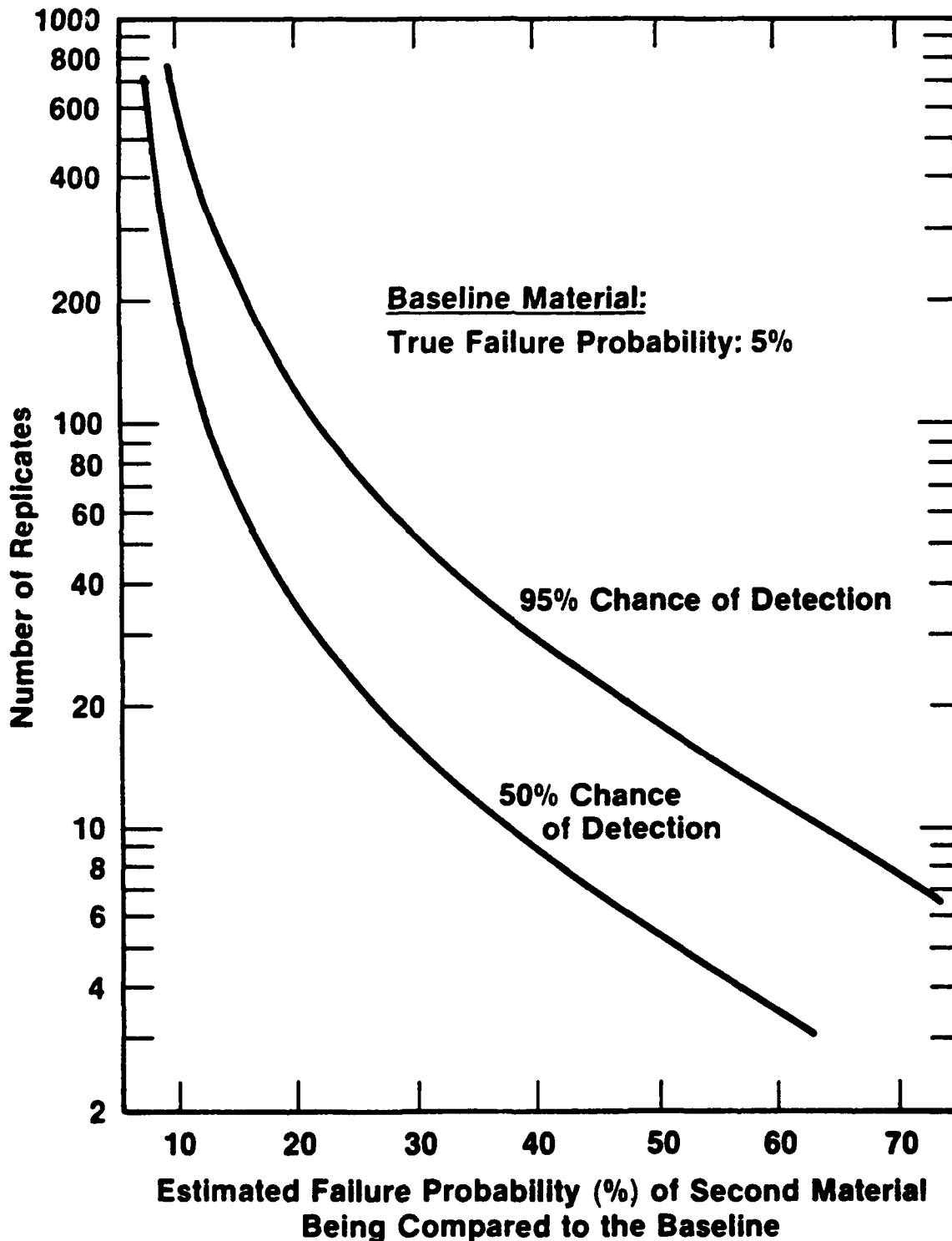
Directional Grain Structure of 7075-T651 Hot Rolled Plate



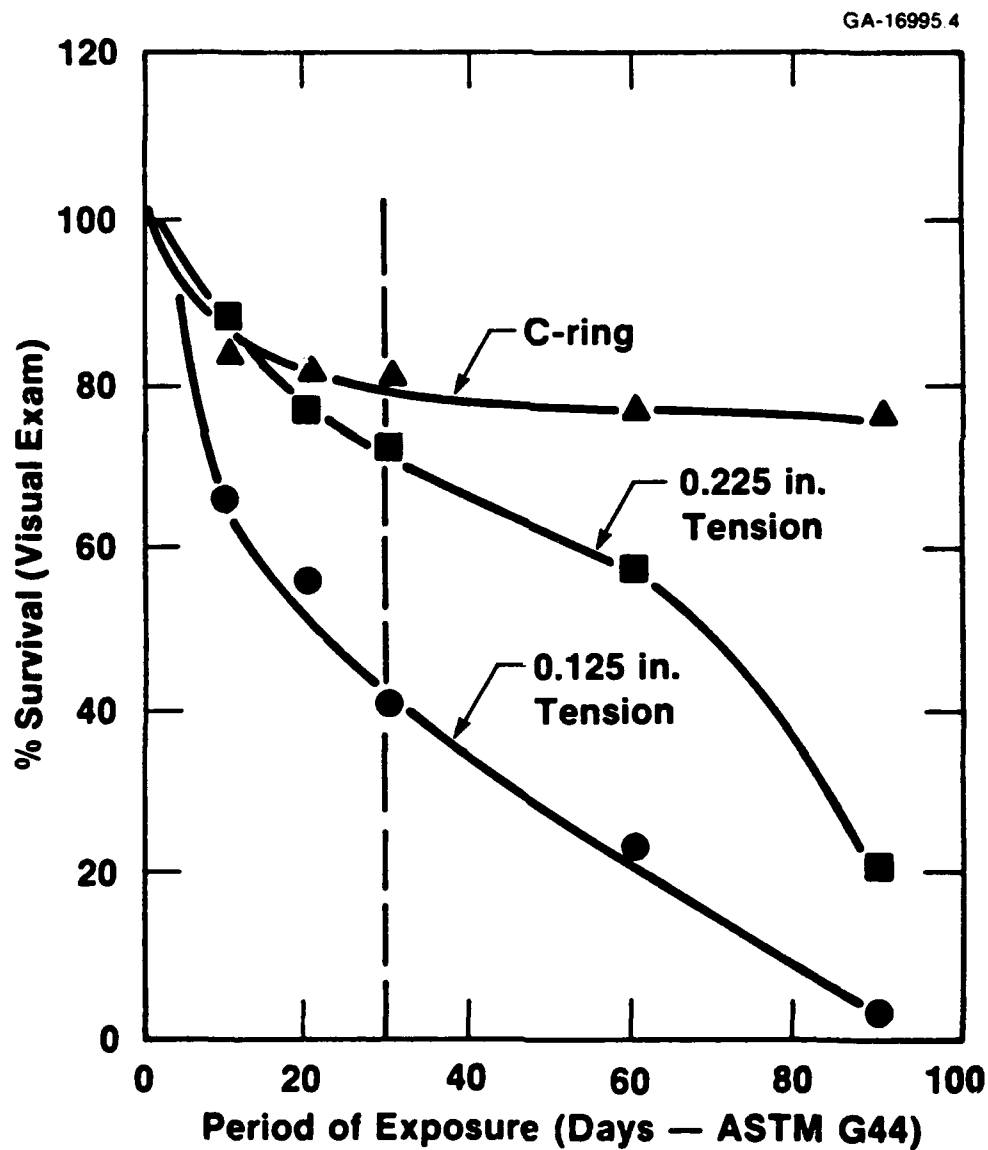
Tests were made on 3.18 mm (0.125 in.) diameter tension specimens machined from the mid-plane of 7075-T651 plates of various thicknesses. The solid line, lower bound defines the SCC performance of test specimens with different orientation to the grain structure. Note the relatively low stress levels at which short transverse specimens failed compared to the long transverse and longitudinal specimens.

Effects of the Magnitude of Sustained Tensile Stress and Its Orientation Relative to the Grain Structure on the SCC Resistance of a Metallurgically Susceptible Material

**Number of Replicate Tests Required
to Distinguish Performance Difference Between
Materials - the Baseline Having a True Failure Probability
of 5%, and the Second Having the Estimated Failure
Probability Indicated**

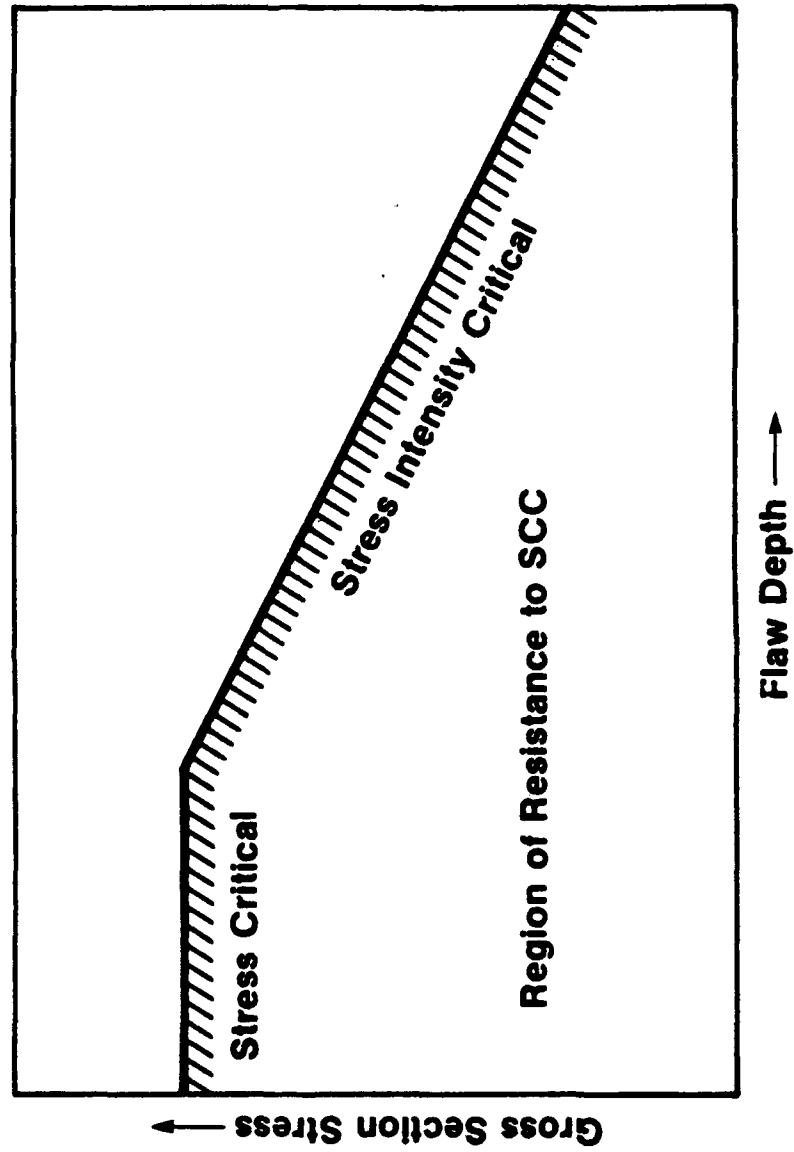


Influence of Specimen Configuration on Short Transverse SCC Performance of 7075-T7X51 (Stressed 45 ksi)



Composite Stress-Stress Intensity SCC Threshold Characterization for Aluminum Alloys

GA-16995-24

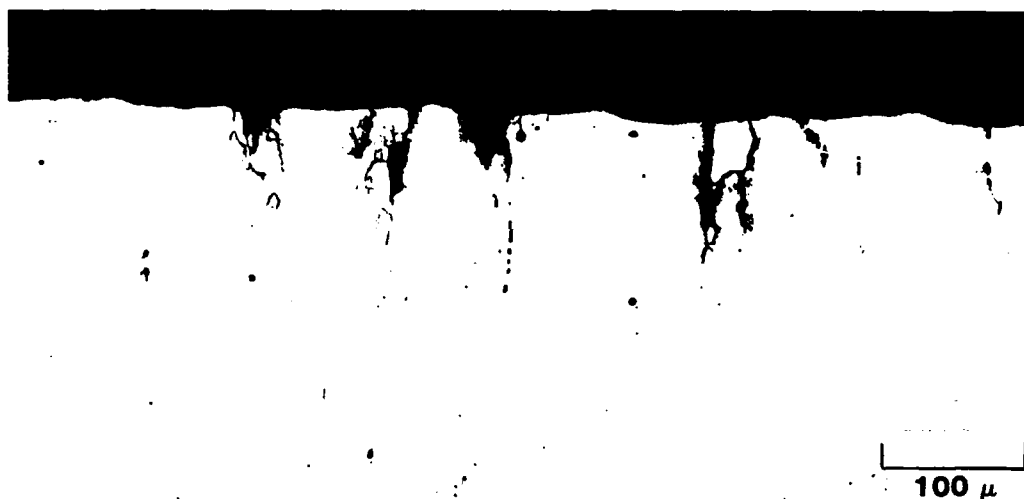


**Typical Surface Attack in Short-Transverse Tensile Bars of Three
7075 Alloy Plate Temper Variants Exposed 6 Days in 3.5% NaCl Solution
by Alternate Immersion and Then Tension Tested**

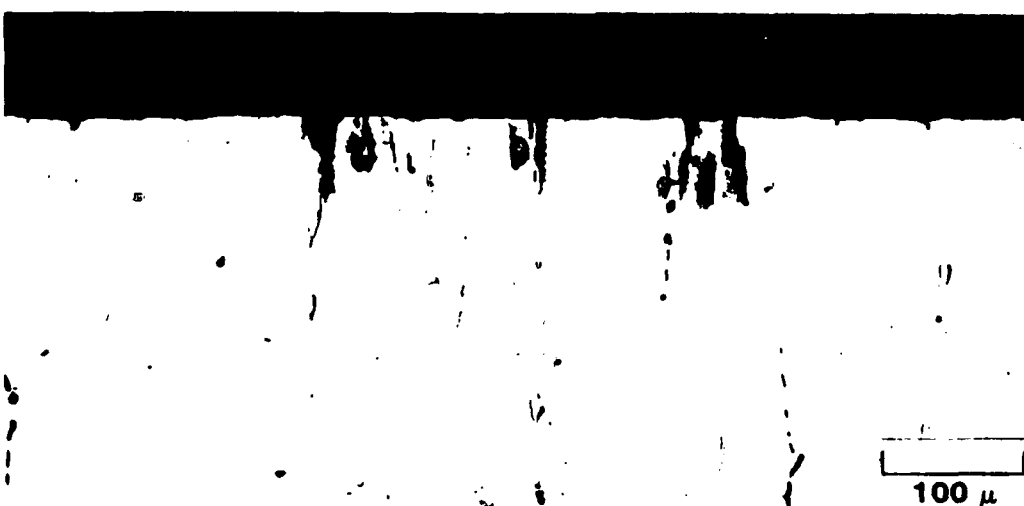
GA-28770.2



(a) T651



(b) T7651

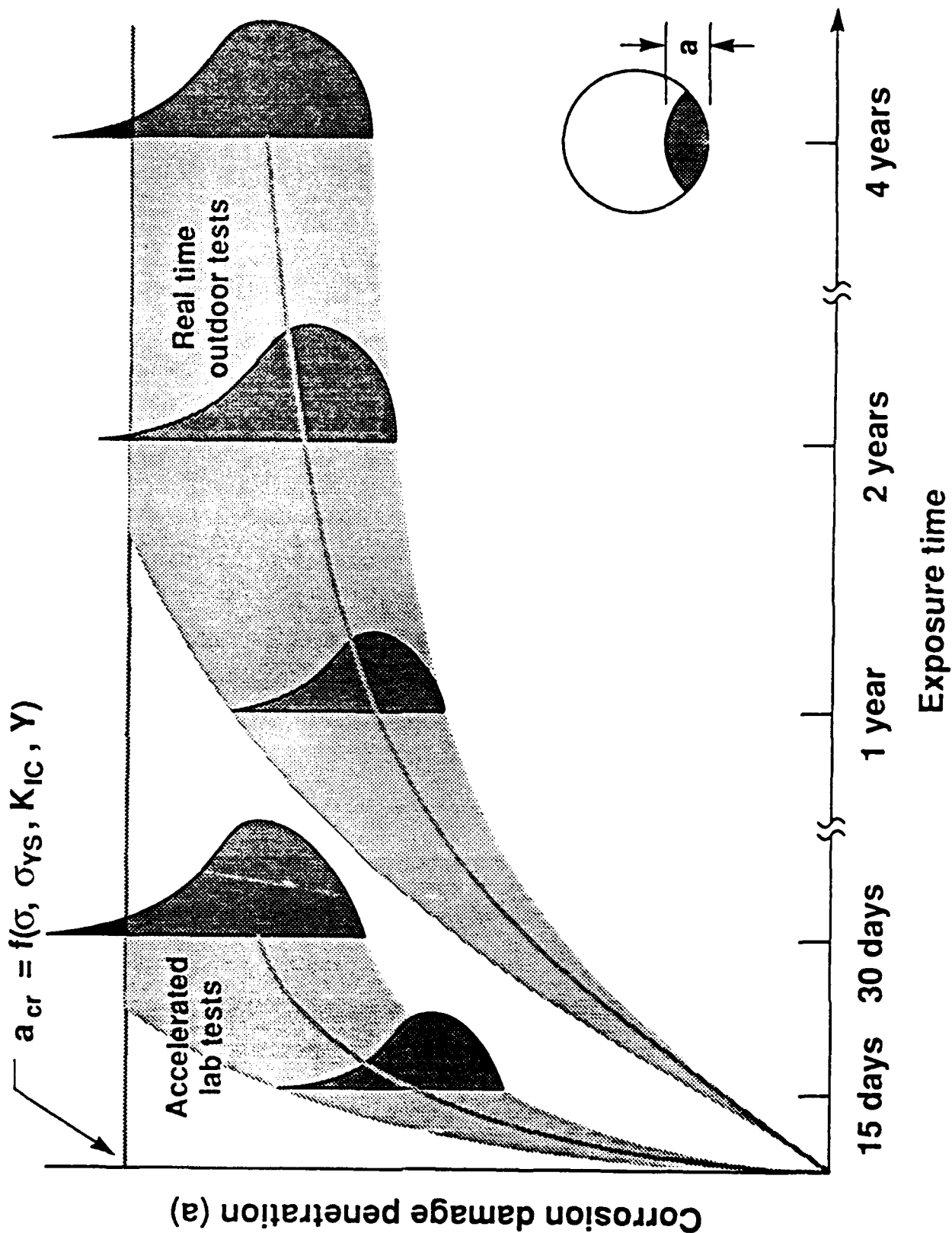


(c) T7351

As polished sections from failed specimen half

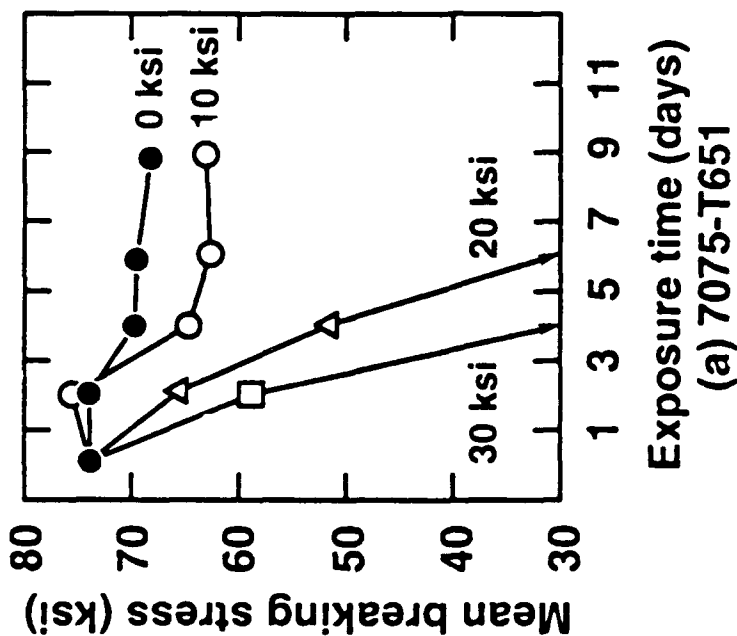
↔ Short transverse plate direction, ↑ Plate rolling plane

Statistical Damage Correlation in Accelerated and Real Time Corrosion Tests

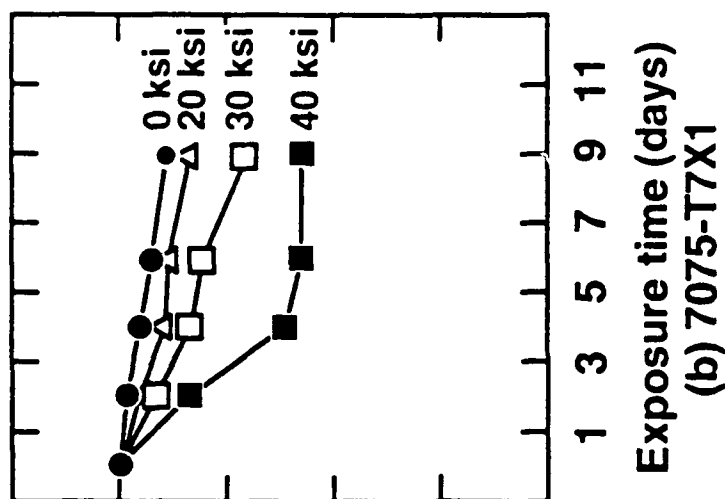


Effect of Temper on Alloy 7075 Short Transverse Tension Specimen (0.125 in. dia.) Residual Strength after Exposure to 3.5% NaCl by Alternate Immersion (ASTM G-44) at Various Stress Levels

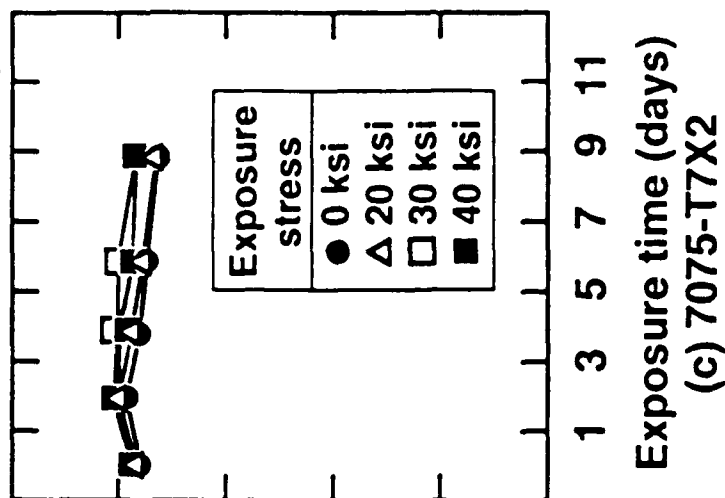
QA 28770 6



(a) 7075-T651



(b) 7075-T7X1



(c) 7075-T7X2

- (1) The T7X1 and T7X2 temper materials were obtained by progressive overaging of T651 plate material to establish controlled test samples of low (T651), medium (T7X1) and high (T7X2) resistance to stress corrosion cracking. Aging practices for the T7X1 and T7X2 temper conditions were respectively chosen to be comparable to those of the T7651 and T7351 commercial product temper conditions.
- (2) Each data point represents the averaged breaking strength of five replicate specimens subjected to identical exposure conditions. The exposure stress was taken as the breaking stress for those specimens failing in the environment, prior to tension testing.

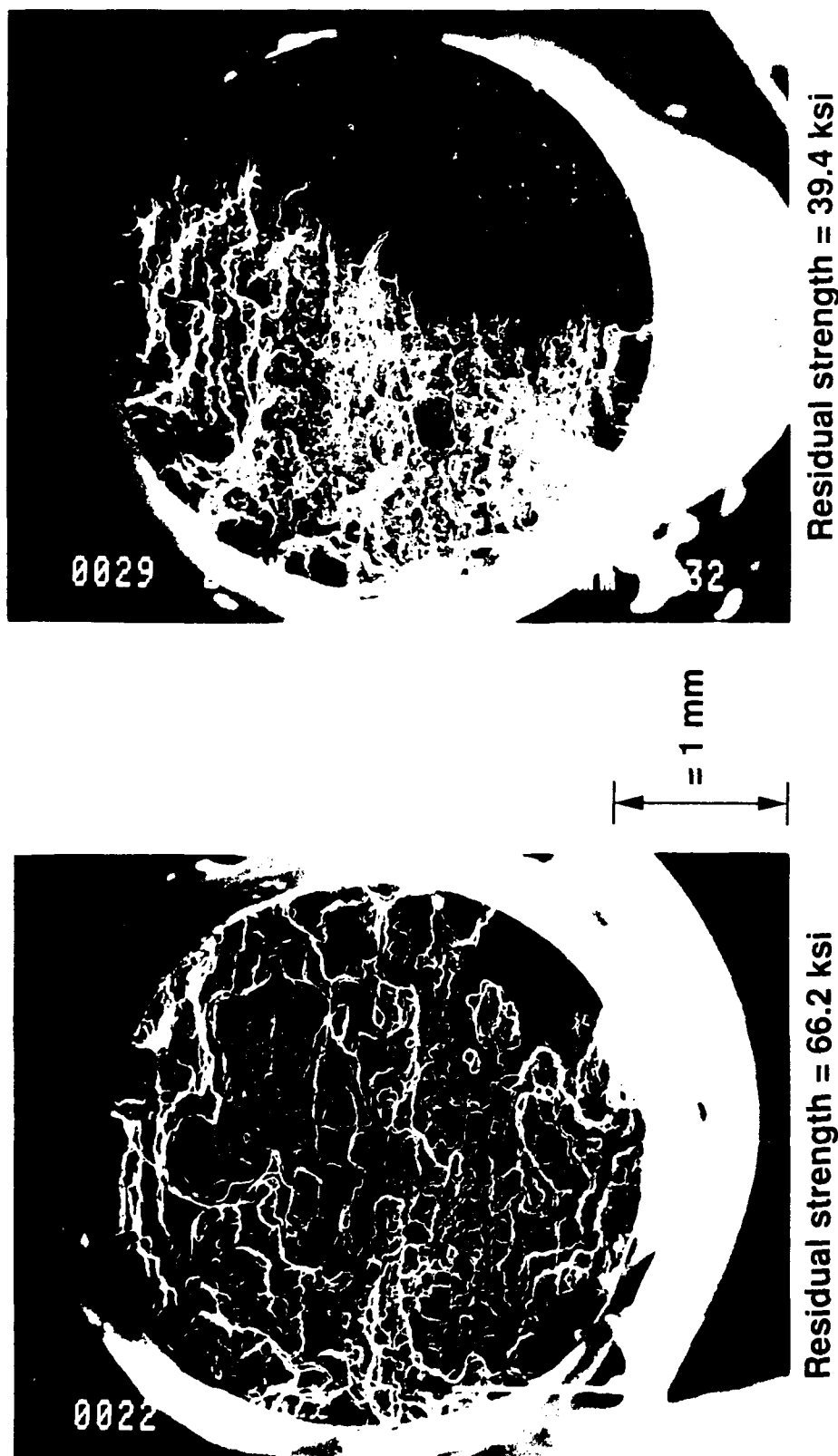
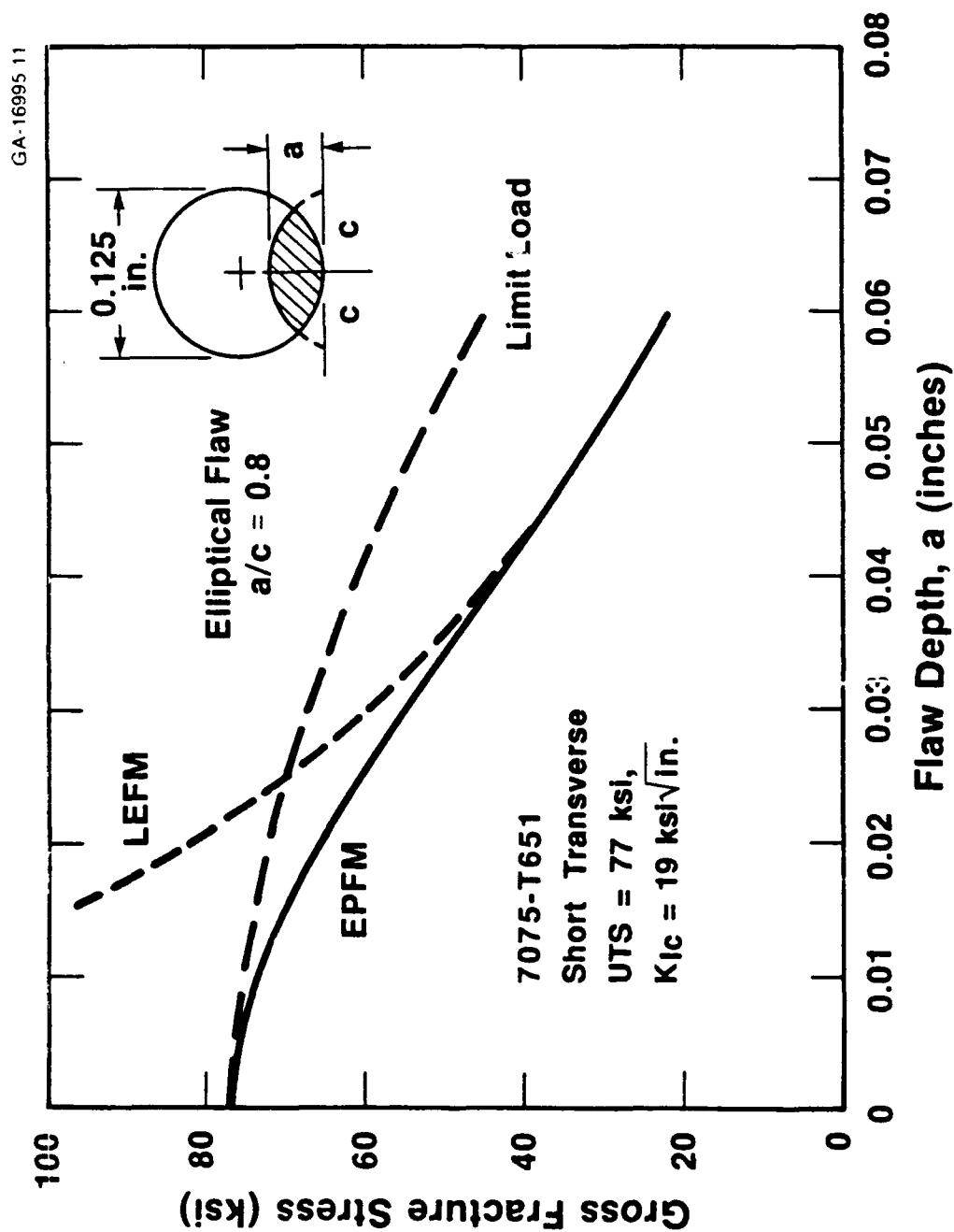


Figure 2. SEM Micrographs Showing Two 7075-T7X1 Specimens with Different SCC Flaw Sizes. The Dark Areas of the Fracture Surfaces are Corrosion Sites. The Measured Residual Strength Values Clearly Reflect the Larger Flaw in the Right Hand Specimen.

Analytical Approach used to Relate Residual Strength and Flaw Size for the Breaking Load Specimen Configuration



EPFM Estimate

$$\sigma_{\text{EPFM}} = \sigma_{\text{L}} \left[1 - \left(\frac{a}{R} \right)^q \right] + \sigma_{\text{LEFM}} \left(\frac{a}{R} \right)^s$$

Where:

σ_{EPFM} = The EPFM Breaking Stress

σ_{L} = The Breaking Stress Predicted by the
Limit Load Failure Criterion

σ_{LEFM} = The Breaking Stress Predicted by the
LEFM Failure Criterion

a = Flaw Depth

R = The Specimen Radius

q, s = Weighting Exponents



(a) Fatigue Precracked Specimen

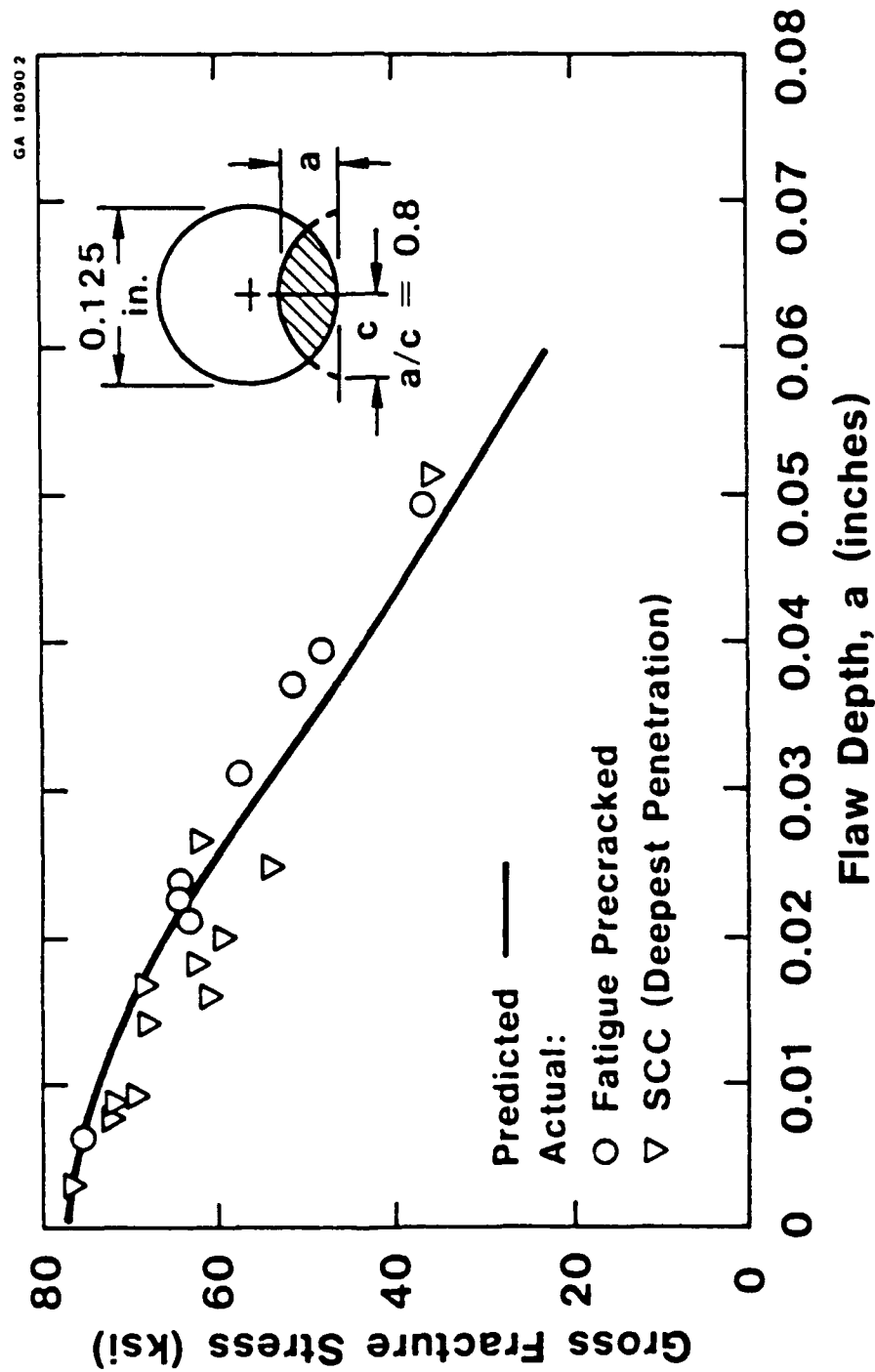


(b) Stress Corroded Specimen
(Border of SCC flaw outlined
for clarity)

Typical Appearance of 7X75 Alloy Fatigue Precracked and Stress Corroded Tensile Bar Fractures

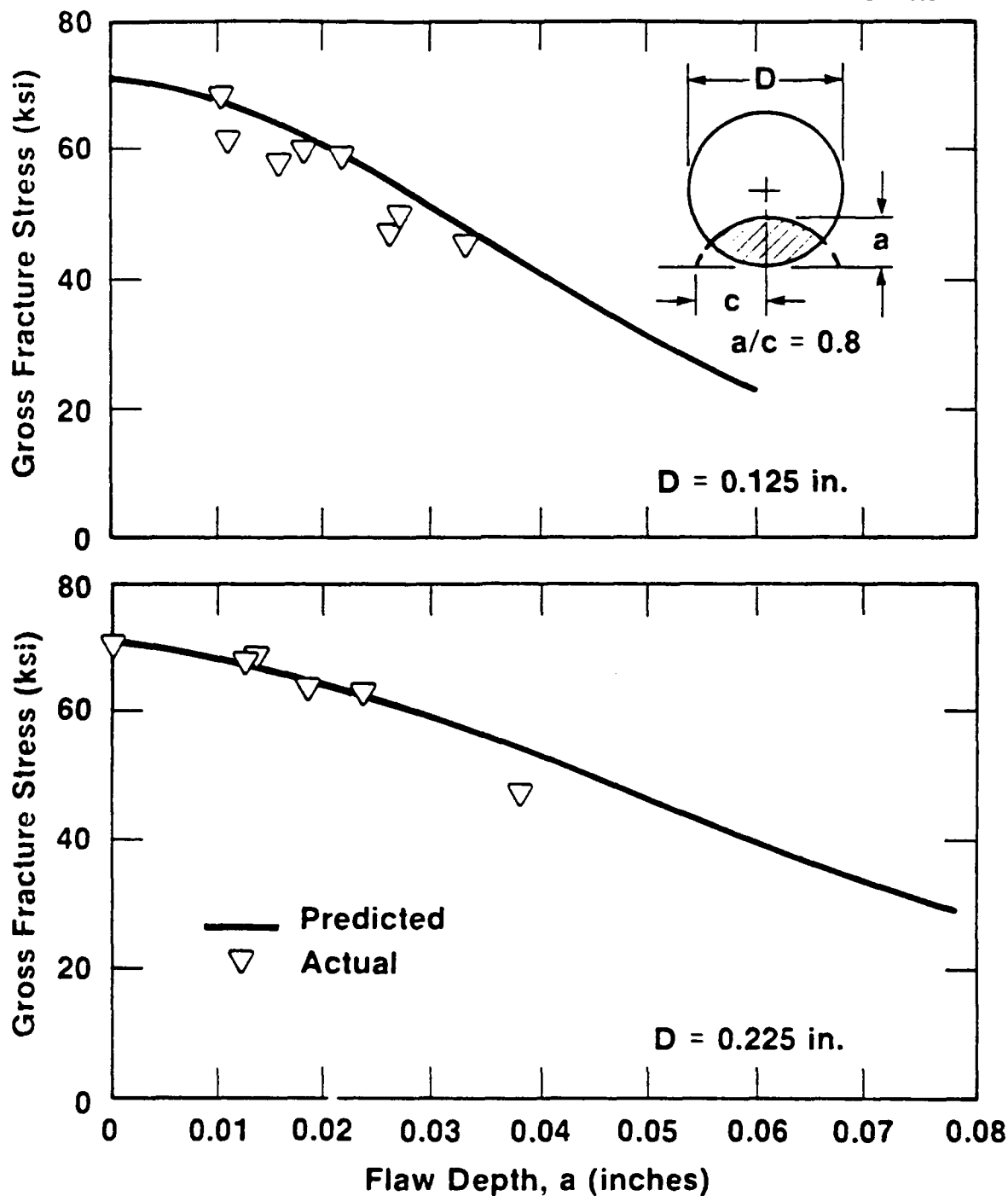
Figure 3

Fracture Stress vs. Maximum Flaw Depth in Fatigue Precracked and Stress Corroded, Short Transverse Tensile Bars of Alloy 7075-T651

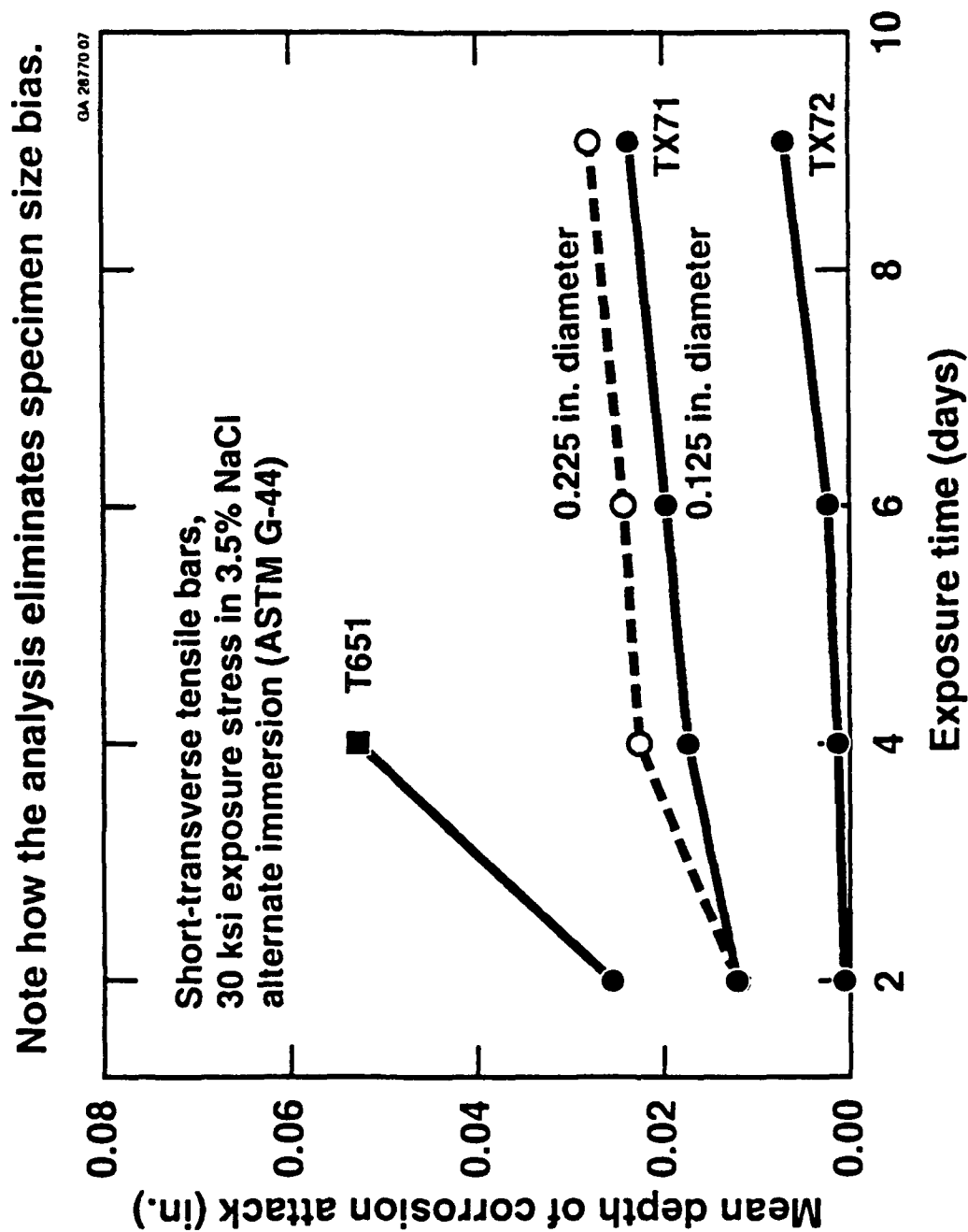


Fracture Stress vs. Maximum Flaw Depth in Stress Corroded Alloy 7075-T7X1 Tensile Bars of Different Diameters

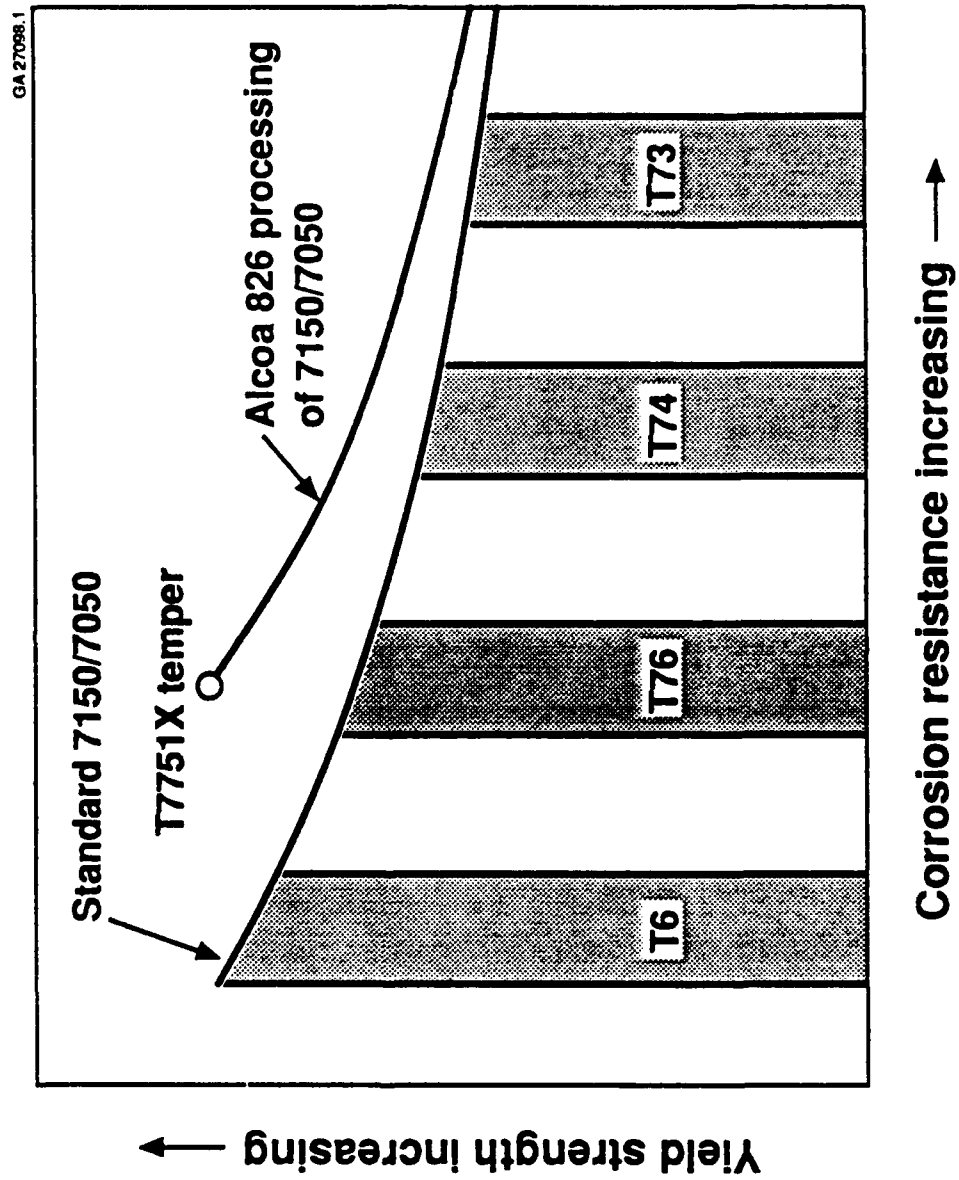
GA-16995 15



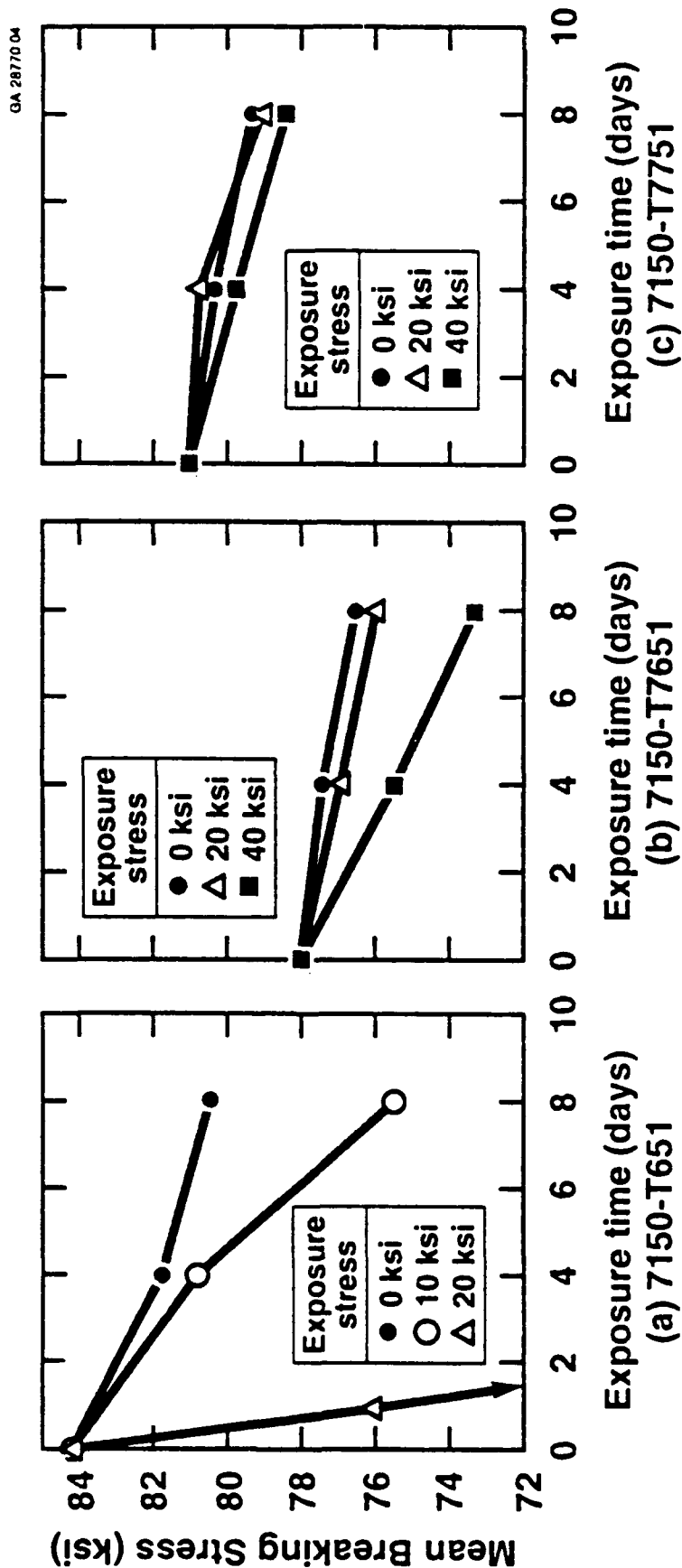
Breaking Load Test Data Transformed Using the Fracture Mechanics Analysis to Illustrate Effect of Temper on 7075 Aluminum Plate SCC Performance



Schematic Illustration of Improvements in Combination of Strength/Corrosion Resistance by New Processes

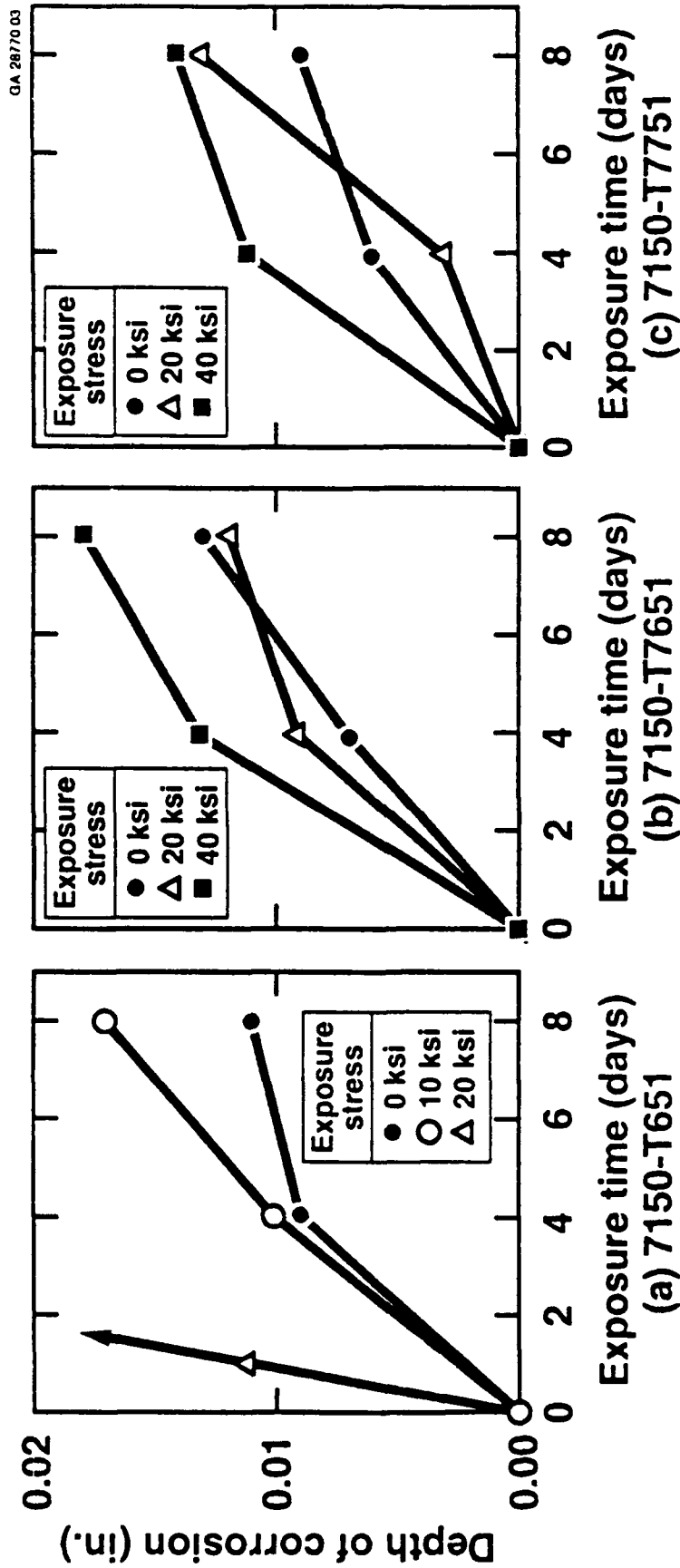


Effect of Temper on Alloy 7150 Short Transverse Tension Specimen (0.125 in. dia.) Residual Strength after Exposure to 3.5% NaCl Solution by Alternate Immersion (ASTM G-44) at Various Stress Levels



Each data point represents five specimen average.

SCC Propagation with Time in Various Tempers of Aluminum Alloy 7150



Depth of SCC penetration calculated from residual strength data of short-transverse tensile coupons (0.125 in. dia.) exposed to 3.5% NaCl by alternate immersion (ASTM G-44) at indicated stress levels. Each data point represents a five specimen average.

The Breaking Load Method:

- Promising new SCC test approach
- Advantages:
 - Quantitative
 - Gives more information in shorter time with fewer tests
 - Facilitates comparison of resistant materials
 - Amenable to fracture mechanics interpretation
 - Results meaningful in engineering sense
- Status:
 - Concept verified on several aluminum alloy systems
 - ASTM standardization ongoing
 - Work initiated in seacoast environment
- Potential for generalization to other types of behavior



GE Aircraft Engines

NDE Productivity Improvements

NDE for Engine Structural Integrity Program

1990 USAF Structural Integrity Conference
San Antonio, Texas
December 11-12, 1990

G.W. Geier

Outline

- Background
- Productivity improvement status
 - Dovetail imaging
 - Waveform analysis
 - Standard inspection
- Alternate inspection method

Background

- Engine Field Management under the USAF Engine Structural Integrity Programs (ENSIP) relies heavily on eddy current inspection to detect small cracks
- The same inspections used in the factory are to be implemented in the field to:
 - Assure part inspectability
 - Assure that there are no pre-existing cracks or stress risers that will cause premature crack initiation/growth

Background (Continued)

- Currently we are using image analysis and waveform pattern recognition to inspect production hardware in addition to standard eddy current techniques:
 - Waveform separates indications by frequency:
 - Stress risers
 - Cracks
 - Nicks
 - Gouges
 - Pits
 - Scratches
 - Geometry
 - Out-of-round holes (minor)
 - Non-concentric break edge

Background (Continued)

- Image analysis is used to inspect complex geometries:
 - Axial dovetails
 - Lock-and-load slots
 - Oil drain holes

Axial Dovetails



Lock-and-Load Slot

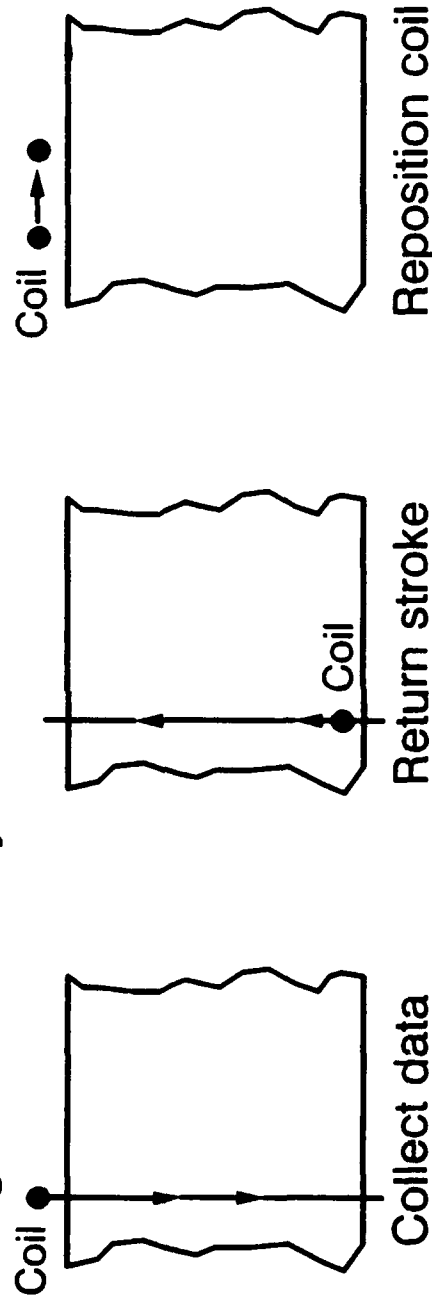


Oil Drain



Background (Continued)

- Our approach to imaging requires a raster type scan of dovetail geometry in small increments while taking data in only one direction

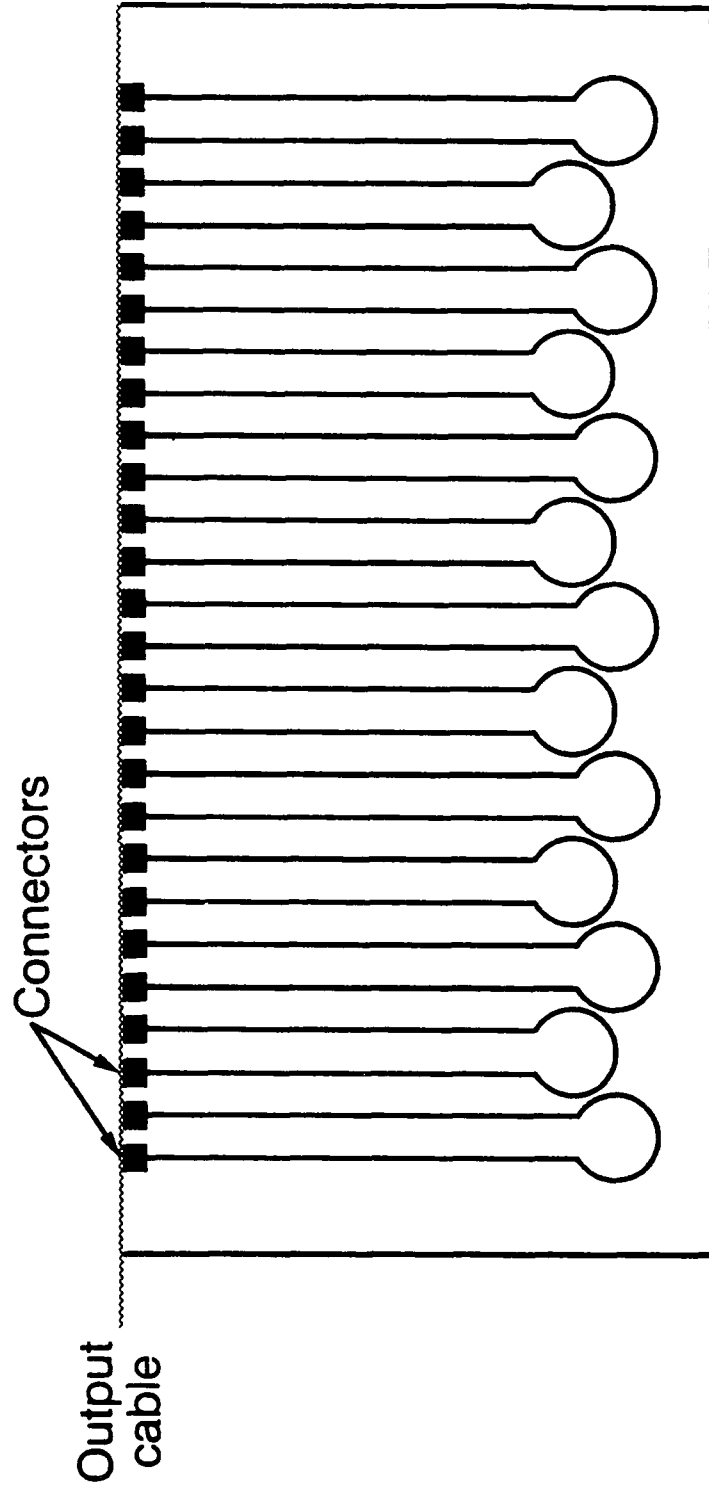


- This data collection method is very time consuming and requires large amounts of labor and equipment
- Each of 30 to 108 dovetail slots may require 100 passes or more to achieve total coverage

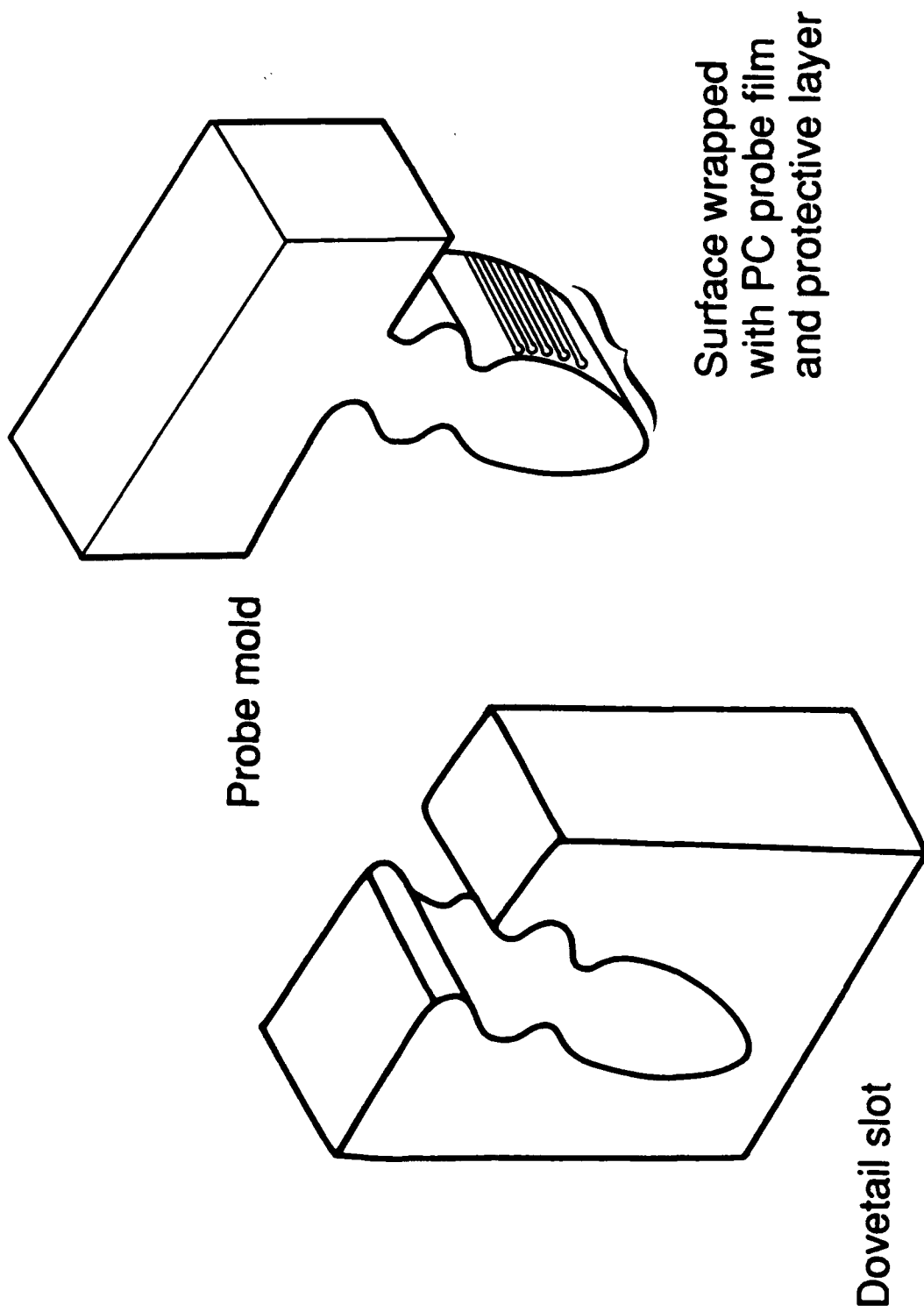
Productivity Improvement Status

Dovetail Imaging Improvement

- General Electric is developing the use of flexible substrate or thin film which contains 50 to 100 eddy current coils



Mold with Coils

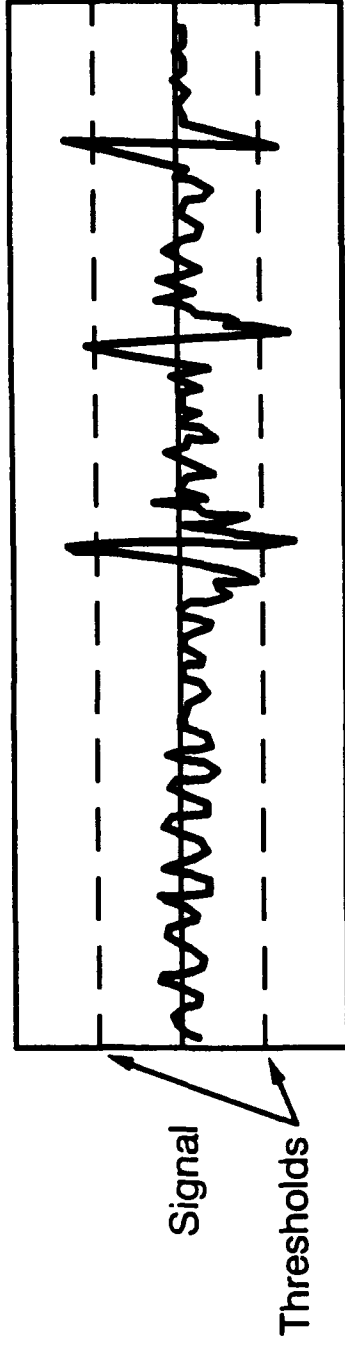


Dovetail Imaging Improvement (Continued)

- Substrate bonded to a model of the part feature to be inspected
- Allows inspection of all dovetails and other unique features with only one pass of the probe per slot
- Should reduce inspection time by approximately 100 hours per engine set

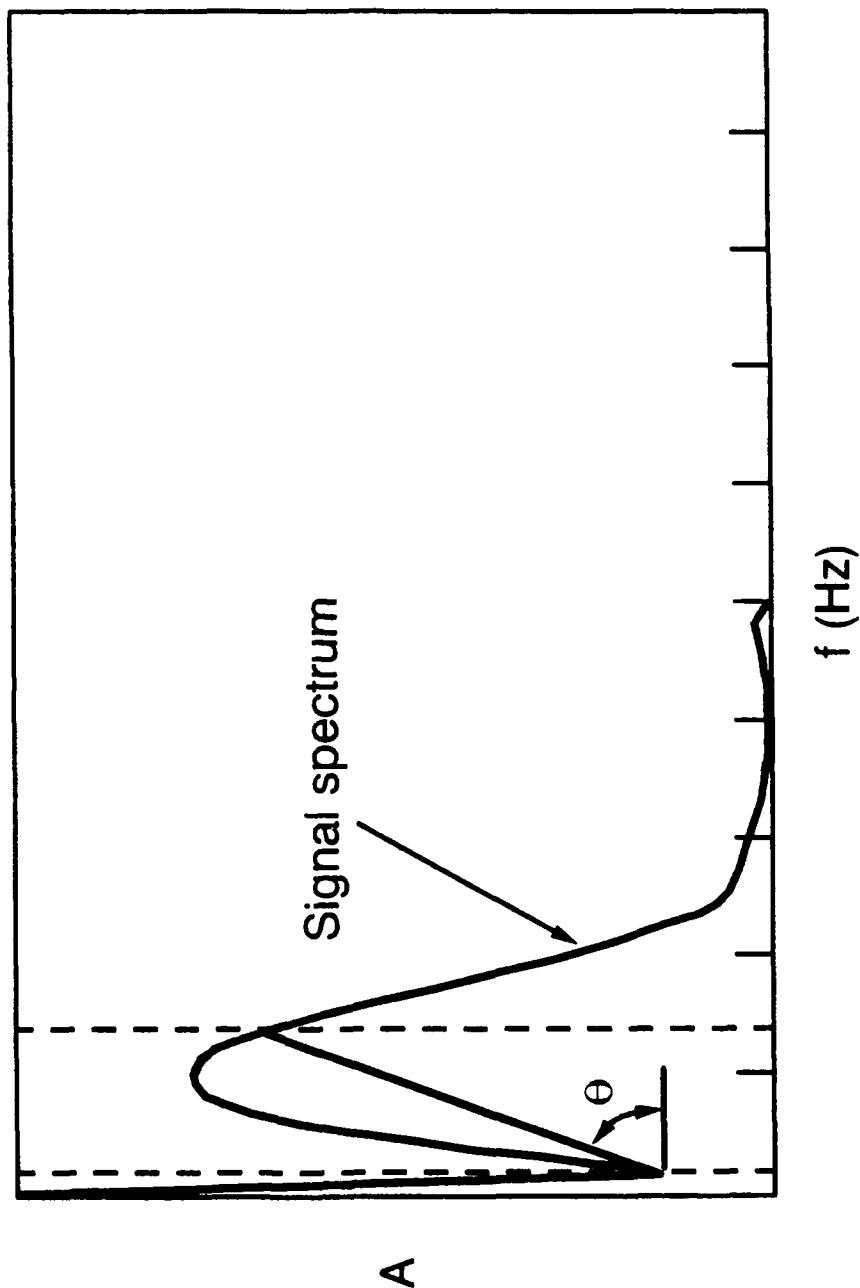
Waveform Analysis

- Examines each separate indication above the standard millivolt threshold:



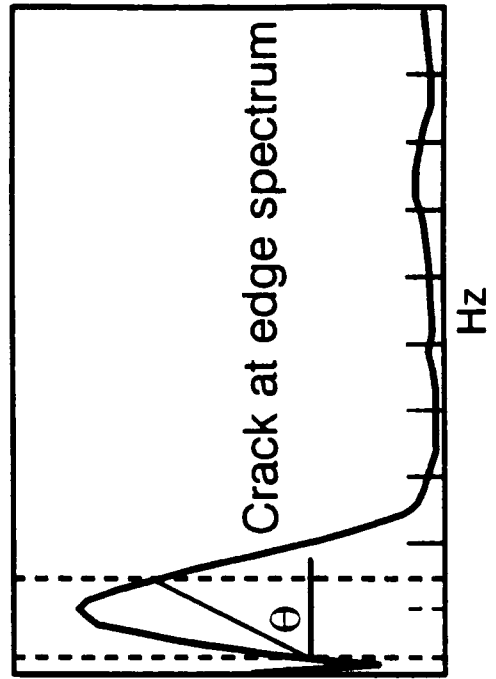
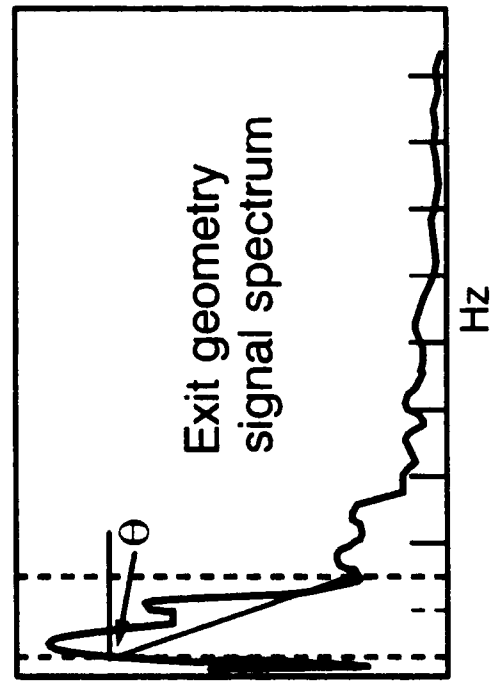
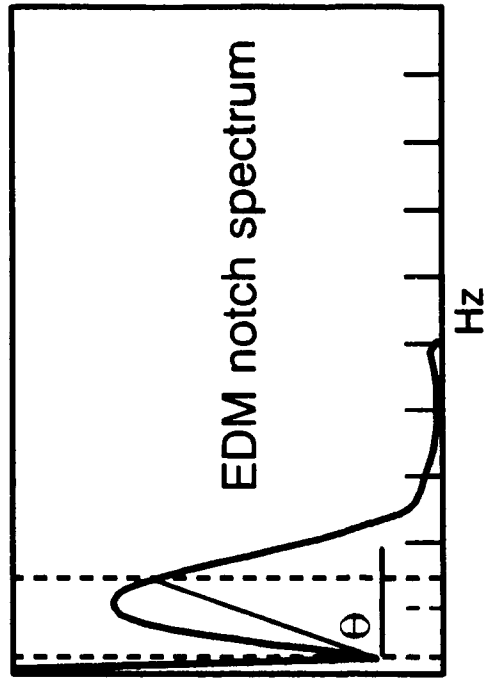
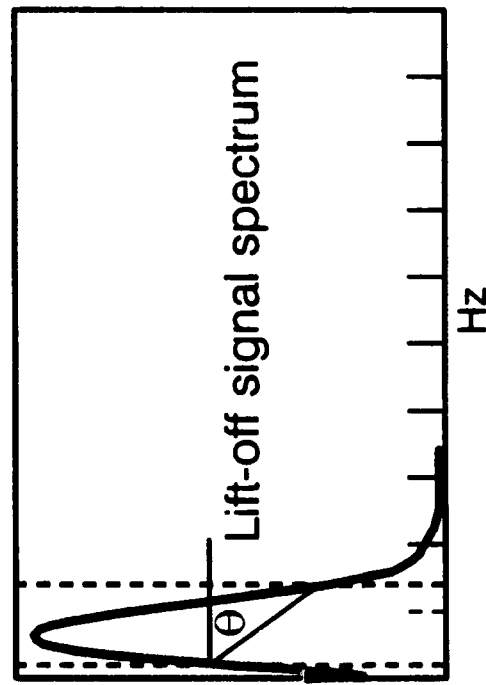
- Each waveform is individually considered in the frequency domain

This Waveform Analysis is Based on the Bandwidth of the Signal Frequency Spectrum



Bandwidth angle of a frequency spectrum

Discriminate Geometry Signals from Discrete Signals (Entry and Exit Geometry from Defect)



Waveform Analysis

- Currently each area is inspected
 - If area fails the feature is polished
- Future systems
 - Signal evaluation circuit (black box) will be incorporated
 - Real-time evaluation of bandwidth
 - Signals discrete indication for polish/rework

Standard Inspection

Improvements

- Single material calibration standard
- 5 inches/second contact bolthole inspection
- Shimless bolthole probe
- Extended wear tape
- Coated pencil probes

Standard Inspection

Single Material Standard

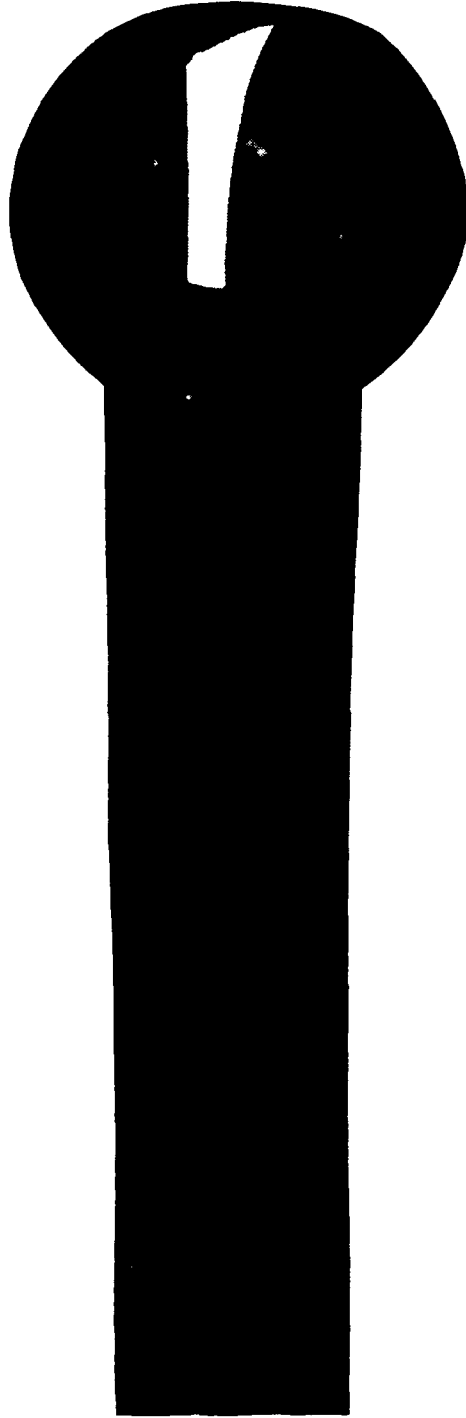
- Prior to each part inspection a calibration is performed on a standard of like material (R95, Inco 718, Ti-6-4) to adjust for conductivity differences
- Single material Inco 718 standard replaces all others
 - Correction factor introduced to adjust for conductivity differences
- Savings in both time and calibration standard cost
 - Calibrations standards cost reduced from approximately \$36,000 to \$7,000

Standard Inspection

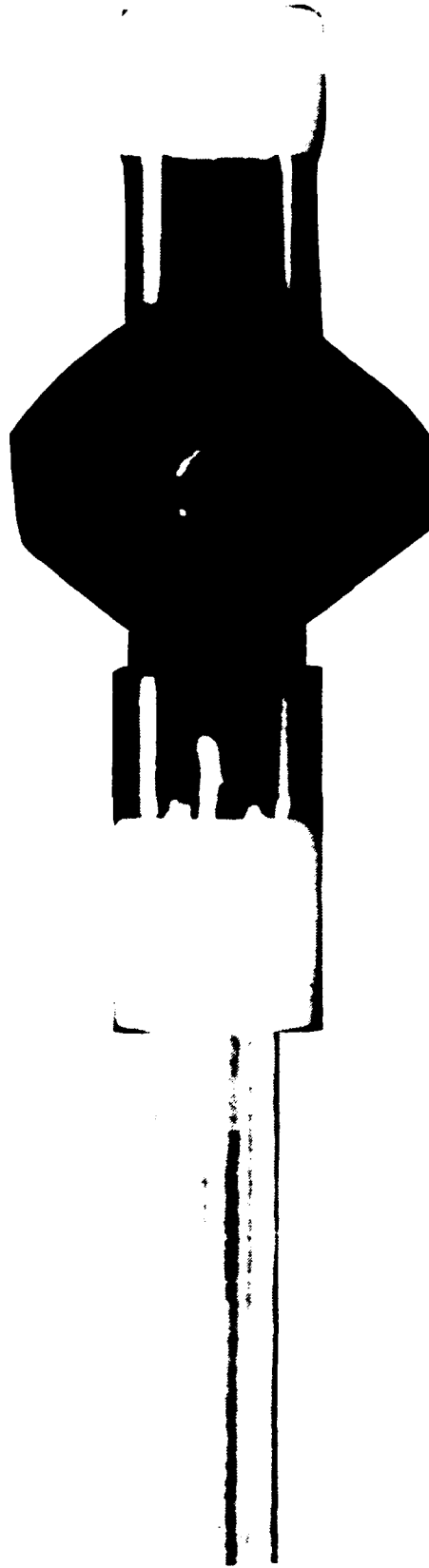
Bolthole Inspection

- Increasing inspection speed to 5 inches/second
 - Reduced inspection time per hole by approximately 40%
- Use of the PS4 scanner with SCR recessed coil contact probes
- A shim is used to adjust for fit on a set of boltholes
 - Requires extra operator involvement
 - Development is underway to eliminate shimming which would yield more uniform results and time savings

SCR Probe



Shimless Probe



Standard Inspection

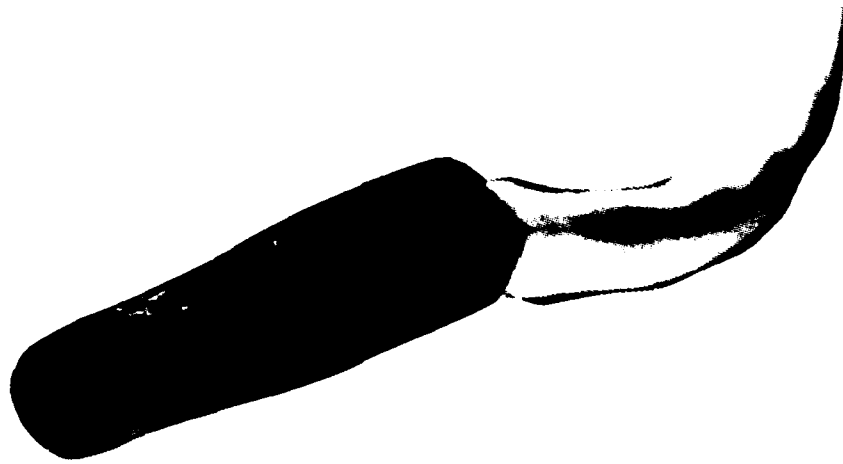
Contact Pencil Probes

- Early 1990 a 0.003 inch thick Teflon tape was used to protect the coil from damage with approximate life 15-30 minutes per application
- Two improvements have been made to protect coils
 - Kapton tape
 - Replaces the Teflon tape
 - Yields a 16X improvement in wear characteristics
 - Coated pencil probes
 - A 0.003 inch coating is bonded to the coil for protection
 - Tests show no wear in 200 hours running at 5 inches/second

Side-Mount Coil



Coated Absolute Coil



Alternate Inspection Method

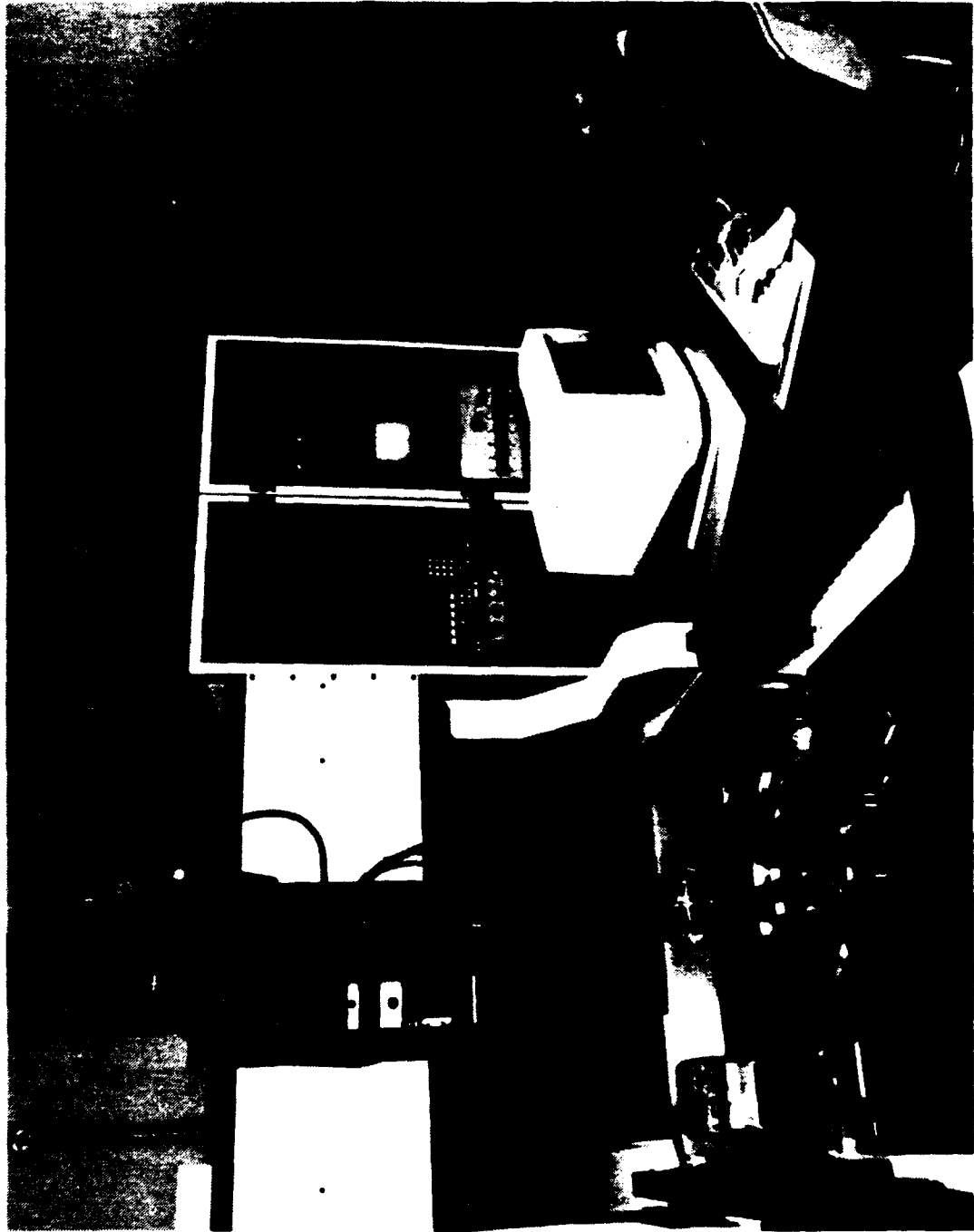
Automated FPI (Fluorescent Penetrant Inspection)

- This system has been developed by GE to replace existing eddy current inspections on rotating hardware for the F110-GE-129 and to be incorporated into future engine initial inspection requirements

Why the System is Being Developed

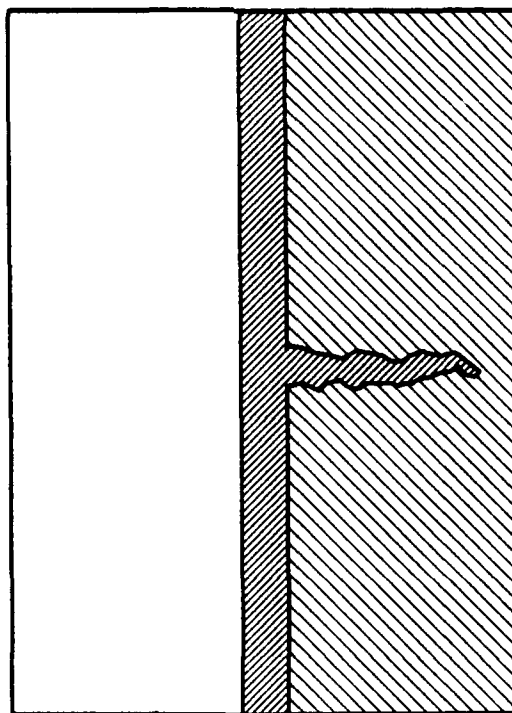
- Eddy current inspection is sensitive but slow
- Auto FPI can cover large areas rapidly
- Many critical areas would not meet inspection interval requirement with manual FPI (0.070 inch at 90/95 POD)
- An in-between area of 0.020 inch up to 0.070 inch POD can be inspected by Auto FPI instead of eddy current
- The technology is needed to improve FPI POD
- Future engines will count on Auto FPI

Automated FPI System

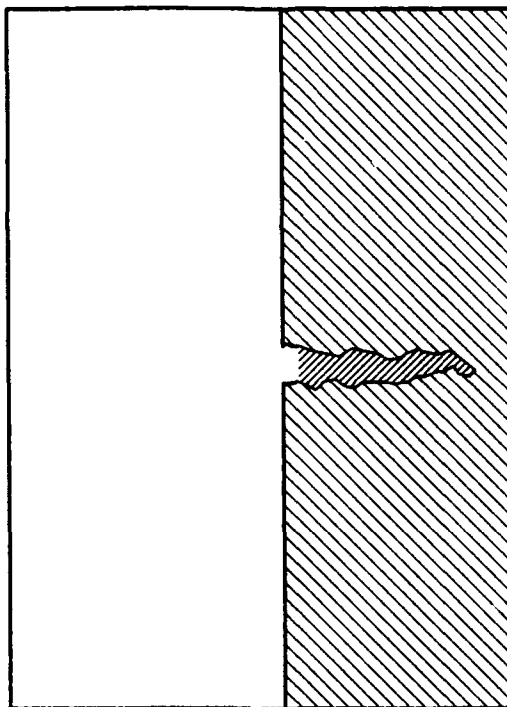


Fluorescent Penetrant Inspection Process

1. Application of a dye penetrant solution to the part



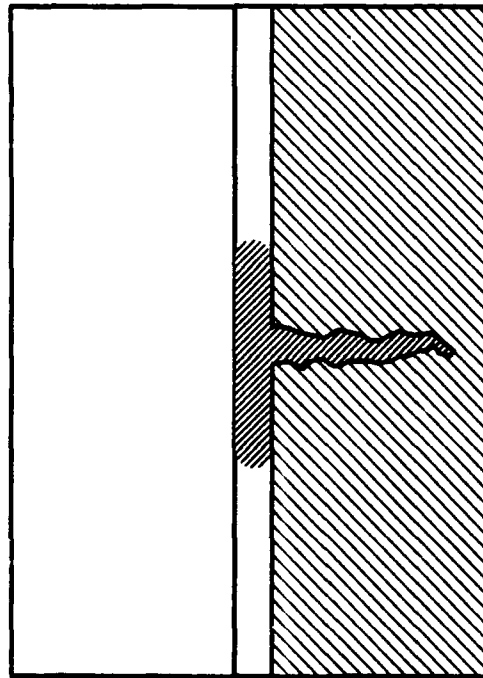
2. A series of rinses removes excess penetrant



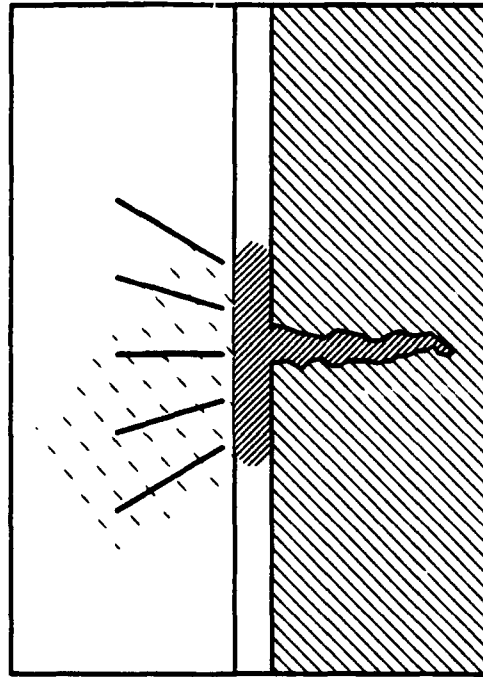
3. A dwell in heated air allows the part surface to dry

Fluorescent Penetrant Inspection Process

4. Application of a developer



5. Inspection under UV light



6. Evaluation of indications/bleedback

Fluorescent Penetrant Process Variables

Material properties	Remover application	Developer application
- Part geometry	- Type	- Dust
- Surface condition	- Spray	- Mist spray
- Material	- Bath	- Spray
- Cleaning method	- Agitated bath	- Hand spray
	- Contact time	- Brush
Penetrant type	- Temperature	
- Water washable	- Pressure	Reading
- Lipophilic	- Concentration	- Operator expertise
- Hydrophyllic		- Operator reliability
- Sensitivity	Post rinse	- Bleedback
	- Pressure	- UV light intensity
Penetrant application	- Time	- UV light spectrum
- Spray	- Temperature	- Room light level
- Electrostatic spray		- Light reflections
- Brush	Drying cycle	- Surface accessibility
- Dip	- Time	
	- Temperature	
Penetrant dwell	Developer cycle	
- Time	- Dry powder	
- Temperature	- Nonaqueous wet	
Pre-rinse cycle	- Water suspendible	
- Pressure	- Water soluble	
- Time		
- Temperature		

Probability of Detection

- Use LCF plate with 6 cracks of known length
- Batch-run 10 plates
- Clean them thoroughly
- Run through fluorescent penetrant process line
- Inspect plates with automatic system
- Enter results (hits/misses) and crack lengths into UDRI "Pass/Fail" program
- Results in 90/50 and 90/95 POD

*Once You Can Quantify the Process It Is Then
Possible to Minimize the Variables*

Implementation Lessons Learned

- Parts must be CLEAN before processing
- Processing must be automatic and tightly controlled
- Cleaning through inspection must be a continuous process
- Inspection system must discriminate and quantify
- Part overcall rate will be less than 25%

ENSIP Disk FPI System

- Target parts (accessible webs/bores)
 - Ti-6-4
 - Stage 3 fan disk
 - Stage 2 fan disk
 - R88DT
 - HPT CDP seal
 - HPT forward shaft
 - Forward outer seal
 - HPT disk
 - LPT stage 1 disk
 - DA718
 - LPT stage 2 disk
 - Ti-17B
 - Compressor spool stages 1-2

Conclusions

- The automatic FPI has a scan rate of 50 times existing eddy current inspection
- 90/50 POD for surface crack lengths range from 10 to 20 mils
- Capability has been demonstrated to Air Force
 - Multiple runs, multiple operators
 - Consistent

Summary

General Electric will continue to develop and use new techniques and technologies to improve productivity without sacrificing detection capability



AGING FLEET PROGRAM

AIRCRAFT CERTIFICATION SERVICE
FEDERAL AVIATION ADMINISTRATION

PROBLEM



- * ALOHA AIRPLANE N73711
- * RUPTURE OF FORWARD FUSELAGE CROWN, APRIL 28, 1988
- * NTSB FINAL REPORT PUBLISHED JULY 21, 1989
- * APPEARS TO HAVE RESULTED FROM A COMBINATION OF FACTORS - DESIGN, MAINTENANCE, AND INSPECTION
- * MANUFACTURER RECOGNIZED DESIGN PROBLEM AND CORRECTED
- * THE FAA RECOGNIZED PROBLEM AND ISSUED AD
- * ALOHA INSPECTED
- * THE ACCIDENT STILL HAPPENED

CONFERENCE ON OLDER AIRPLANES



* FAA SPONSORED A "CONFERENCE ON OLDER AIRPLANES,"
JUNE 1 TO 3, 1988, THAT DISCUSSED FOUR TOPICS

- AIRFRAMES
- ENGINES
- NON-DESTRUCTIVE INSPECTION
- HUMAN FACTORS OF INSPECTION



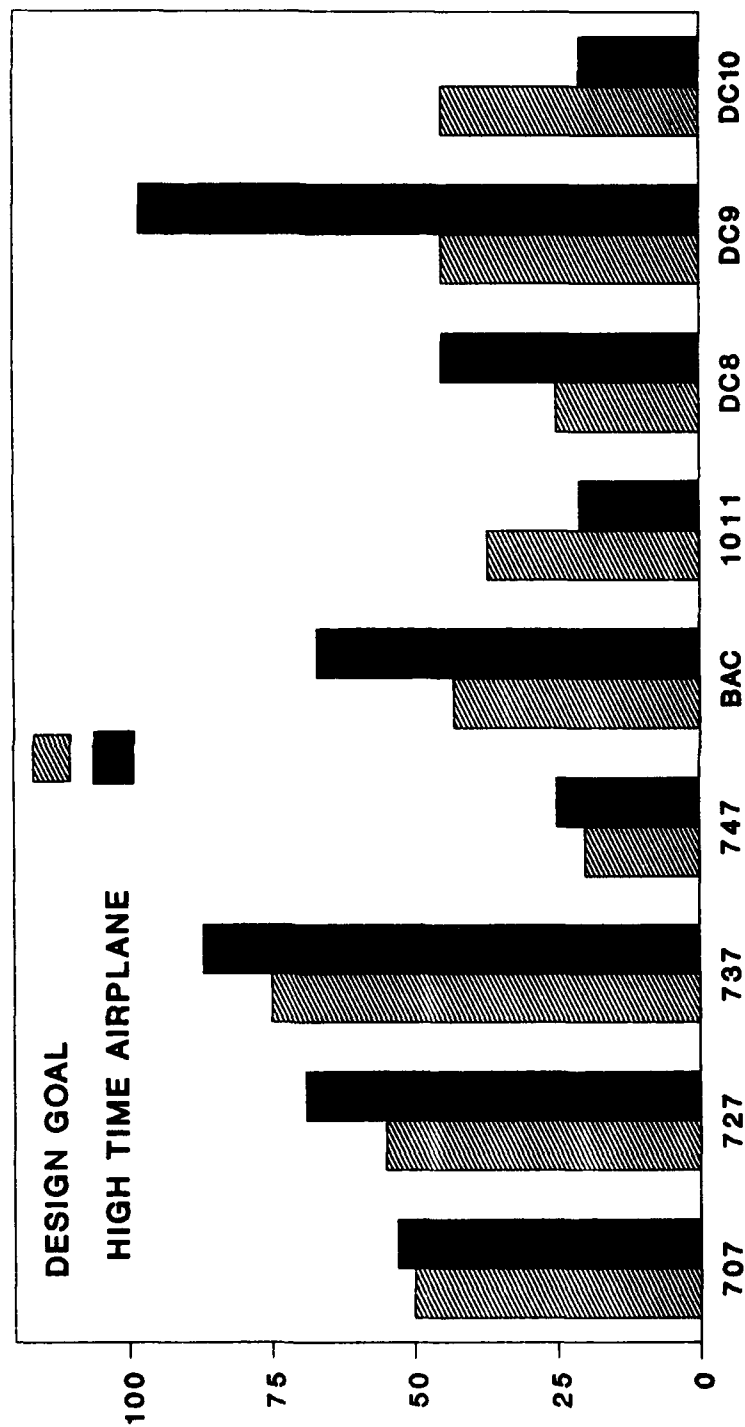
CONCERN

- * AS AIRCRAFT AGE
 - INCIDENCE OF FATIGUE INCREASES
 - CORROSION CAN BECOME MORE WIDESPREAD
- * ARE ASSUMPTIONS CORRECT
 - DESIGN PROCEDURES
 - INSPECTION AND MAINTENANCE PROCEDURES
- * RESEARCH AND DEVELOPMENT NEEDS FOR HUMAN FACTORS
- * RESEARCH AND DEVELOPMENT NEEDS FOR INSPECTION

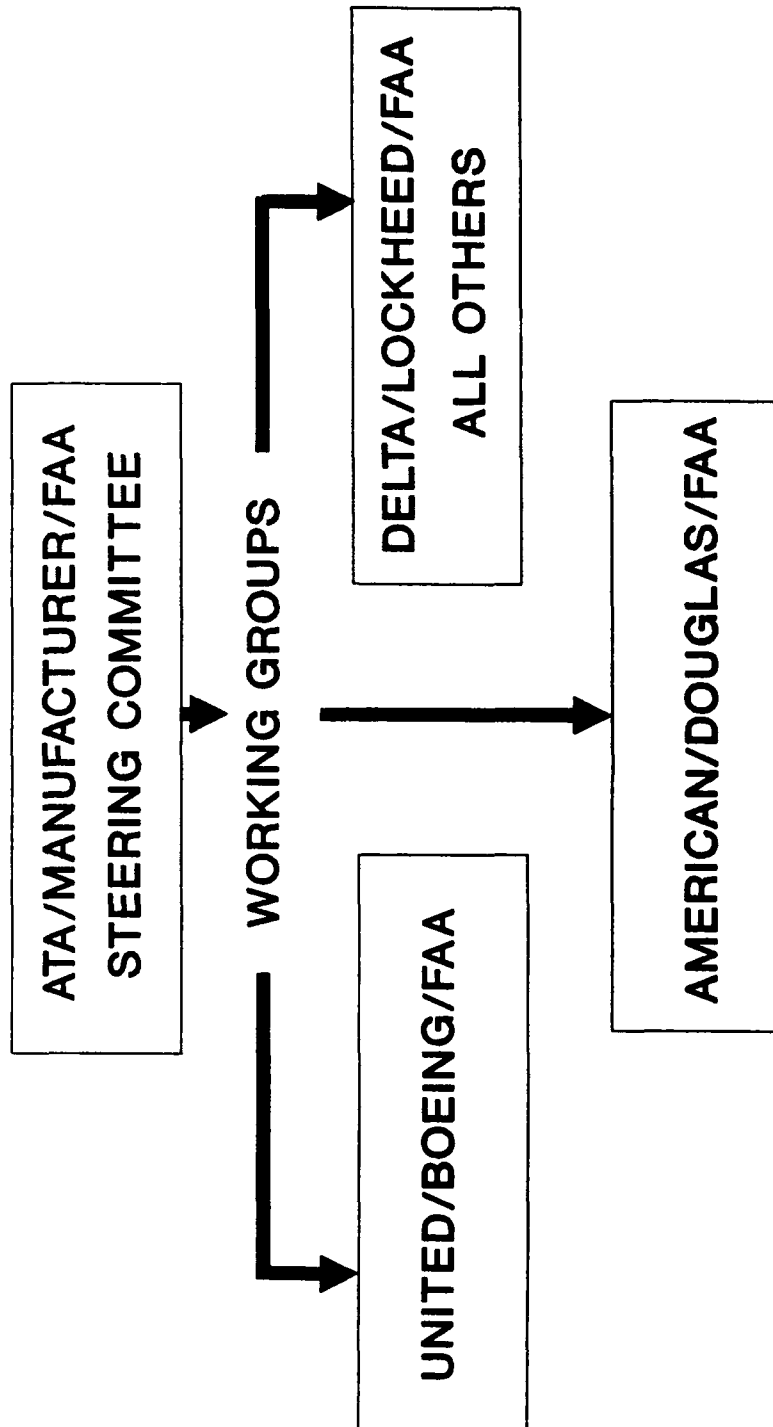
FLEET STATUS



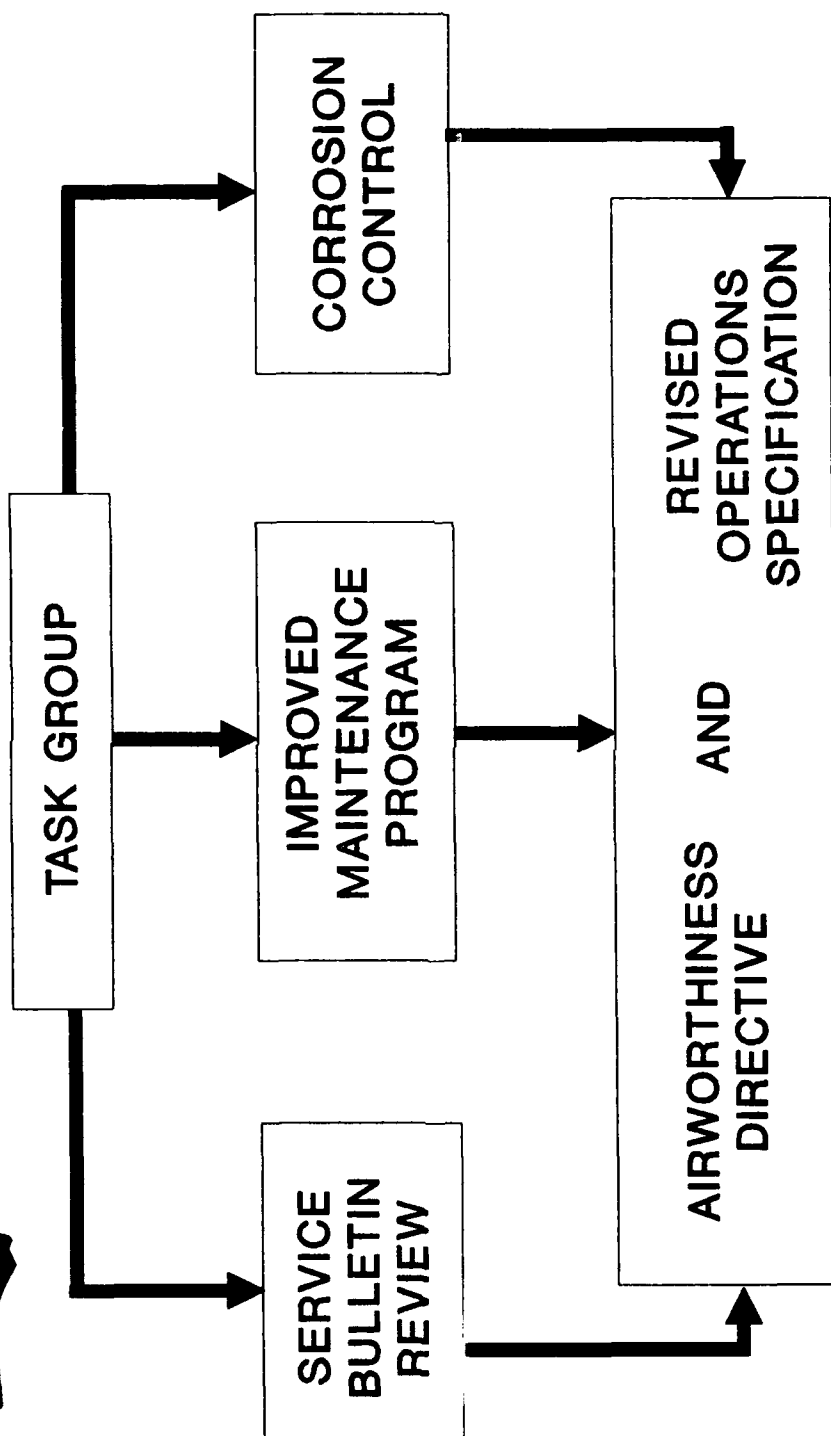
ESTIMATED NUMBER OF LANDING CYCLES (THOUSANDS OF CYCLES)



ATA AGING AIRCRAFT TASK FORCE



ATA AGING AIRCRAFT TASK FORCE



FAA POLICY CHANGE



CONTINUED INSPECTION OF AN AIRPLANE FOR EVIDENCE OF OCCURRENCE OF A KNOWN PROBLEM FOR THAT MODEL AIRPLANE, IS AN UNACCEPTABLE PROCEDURE TO ASSURE SAFETY. MODIFICATION OR REPLACEMENT OF PARTS MUST BE ACCOMPLISHED TO PRECLUDE THE OCCURRENCE OF THE PROBLEM.

FINAL AGING AIRCRAFT AD ACTION

BOEING 727



* 76 SERVICE BULLETINS

- WING 12
- FUSELAGE 47
- DOORS 8
- EMPENNAGE 7
- LANDING GEAR 1
- PROPULSION 1

* 1,710 AIRPLANES WORLDWIDE

* 67 U.S. AIRPLANES IN FIRST FOUR YEARS

* \$1,057,000/AIRPLANE



FINAL AGING AIRCRAFT AD ACTION

BOEING 737

- * 58 SERVICE BULLETINS
 - WING 15
 - FUSELAGE 25
 - DOORS 8
 - EMPENNAGE 8
 - LANDING GEAR 2

- * 1,500 AIRPLANES WORLDWIDE

- * 28 U.S. AIRPLANES IN FIRST FOUR YEARS

- * \$898,000/AIRPLANE



FINAL AGING AIRCRAFT AD ACTION BOEING 747

- * 31 SERVICE BULLETINS
 - WING 8
 - FUSELAGE 13
 - EMPENNAGE 1
 - LANDING GEAR 4
 - PROPULSION 5
- * 680 AIRPLANES WORLDWIDE
- * 20 U.S. AIRPLANES IN FIRST FOUR YEARS
- * \$2,300,000/AIRPLANE

PROPOSED AGING AIRCRAFT AD ACTION
MCDONNELL DOUGLAS DC-8 & DC-9



*** DC-8**

- 52 SERVICE BULLETINS
- 339 AIRPLANES WORLDWIDE
- \$245,800/AIRPLANE
- EXPECT FINAL RULE MID 1990

*** DC-9**

- 52 SERVICE BULLETINS
- 919 AIRPLANES WORLDWIDE
- \$554,950/AIRPLANE
- EXPECT FINAL RULE MID 1990



PROPOSED AGING AIRCRAFT AD ACTION MCDONNELL DOUGLAS MD-80 & DC-10

* MD-80

- 22 SERVICE BULLETINS
- 683 AIRPLANES WORLDWIDE
- \$57,100/AIRPLANE
- EXPECT FINAL RULE MID 1990

* DC-10

- 33 SERVICE BULLETINS
- 427 AIRPLANES WORLDWIDE
- \$142,900/AIRPLANE
- EXPECT FINAL RULE MID 1990



FUTURE AD ACTIONS LOCKHEED L1011

*** 243 AIRPLANES WORLDWIDE**

- 39 SERVICE BULLETINS RECOMMENDED FOR TERMINATION**
- 7 SERVICE BULLETINS RECOMMENDED FOR MANDATORY INSPECTION**



FUTURE ACTIONS

- * RECOMMENDATIONS FROM OTHER ATA WORKING GROUPS WILL FOLLOW IN THE NEXT FEW MONTHS AS THEY COMPLETE THEIR SERVICE BULLETIN REVIEWS
 - FOKKER F-28, BAC 1-11, AIRBUS A300 AND CONVAIR 580
- * ADDITIONAL TASK ITEMS MAY ALSO GENERATE FAA ACTION
 - SSID UPDATE, REPAIRS, MAINTENANCE

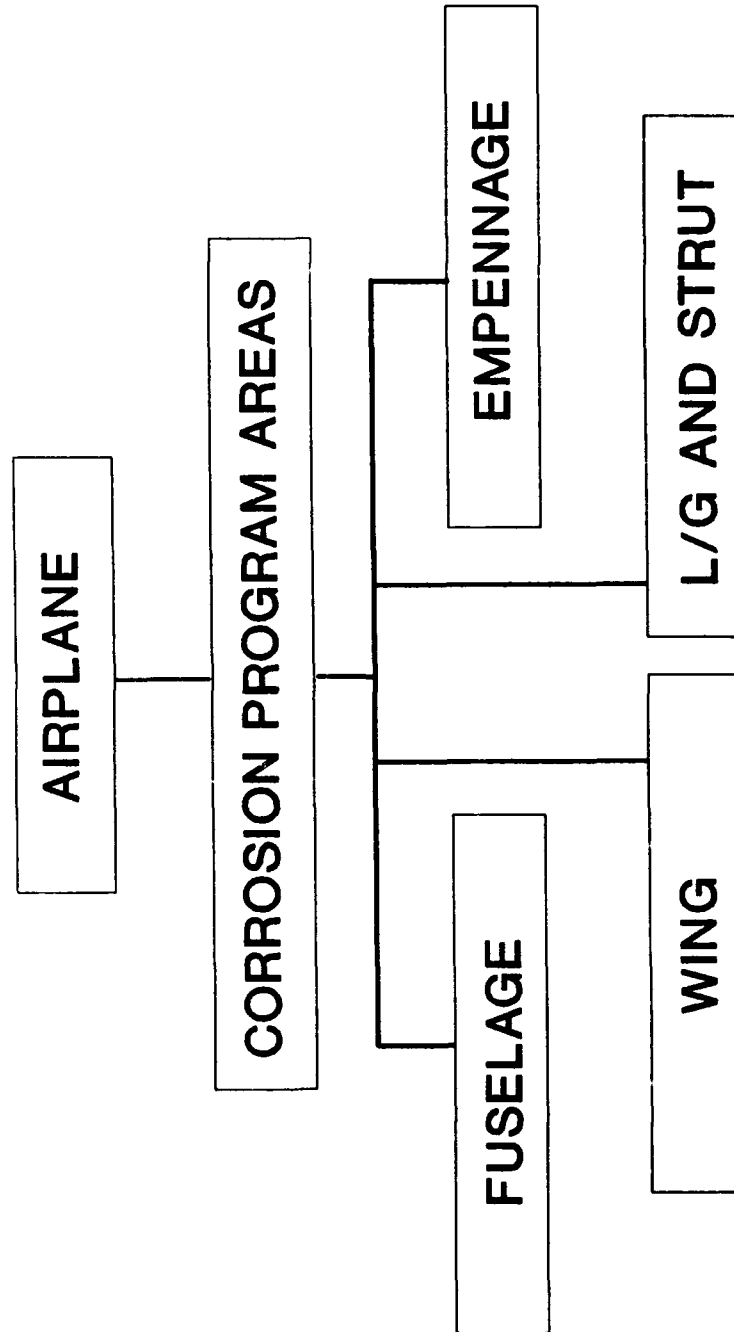
CORROSION PREVENTION/CONTROL PROGRAM



* PROGRAM OBJECTIVE

TO ESTABLISH MINIMUM PROCEDURES FOR PREVENTING
OR CONTROLLING CORROSION THAT MAY JEOPARDIZE
CONTINUING AIRWORTHINESS IN AGING AIRPLANES

CORROSION PROGRAM AREAS



WORKING GROUP ACTIVITY



- * ANY CORROSION PROBLEM AREAS IDENTIFIED BY THE AIRLINES WERE INCLUDED IN THE REVIEW
- * CURRENT CORROSION CONTROL PROCEDURES BEING USED BY OPERATORS WERE REVIEWED
- * THE MANUFACTURERS PROPOSAL WAS COMBINED WITH THE OPERATOR INPUTS AND USED BY THE WORKING GROUP TO DEVELOP A BASELINE CORROSION PREVENTION AND CONTROL PROGRAM FOR EACH AIRPLANE AREA



BASELINE PROGRAM

- * THE BASELINE PROGRAM FOR EACH AIRPLANE MODEL ESTABLISHES MINIMUM REQUIREMENTS FOR OPERATORS WHO DO NOT HAVE A PROVEN EFFECTIVE CORROSION PREVENTION AND CONTROL PROGRAM
- * THE PROGRAMS INCLUDE THE FOLLOWING:
 - CORROSION LEVEL DEFINITIONS
 - A BASIC TASK
 - PROGRAM IMPLEMENTATION } AIRPLANE MODEL AND REQUIREMENTS } AREA/ZONE DEPENDENT
 - REPEAT INTERVALS
 - A MANDATORY REPORTING SYSTEM
- * PROGRAM REQUIREMENTS APPLY TO ALL AIRPLANES THAT REACH OR HAVE ALREADY EXCEEDED THE IMPLEMENTATION AGE FOR EACH AIRPLANE AREA

CORROSION LEVEL DEFINITIONS



* THE FOLLOWING CORROSION LEVEL DEFINITIONS ARE
IN THE PROGRAM

- LEVEL 1 CORROSION
 - CORROSION DAMAGE OCCURRING BETWEEN
SUCCESSIVE INSPECTIONS THAT IS LOCAL
AND CAN BE REWORKED/ BLENDED-OUT
WITHIN ALLOWABLE LIMITS AS DEFINED BY
THE MANUFACTURER (E.G., SRM, SB, ETC.)

CORROSION LEVEL DEFINITIONS

Continued



* THE FOLLOWING CORROSION LEVEL DEFINITIONS ARE
IN THE PROGRAM

- LEVEL 1 CORROSION
- CORROSION DAMAGE THAT IS LOCAL AND
EXCEEDS ALLOWABLE LIMITS BUT CAN BE
ATTRIBUTED TO AN EVENT NOT TYPICAL OF
THE OPERATOR'S USAGE OF OTHER AIRPLANES
IN THE SAME FLEET (E.G., MERCURY SPILL)



CORROSION LEVEL DEFINITIONS

Continued

* THE FOLLOWING CORROSION LEVEL DEFINITIONS ARE
IN THE PROGRAM

- LEVEL 1 CORROSION

- OPERATOR EXPERIENCE OVER SEVERAL YEARS
HAS DEMONSTRATED ONLY LIGHT CORROSION
BETWEEN SUCCESSIVE INSPECTIONS BUT
LATEST INSPECTION AND CUMULATIVE BLEND-
OUT NOW EXCEEDS ALLOWABLE LIMIT

CORROSION LEVEL DEFINITIONS

Continued



* THE FOLLOWING CORROSION LEVEL DEFINITIONS ARE
IN THE PROGRAM

- LEVEL 2 CORROSION

- CORROSION OCCURRING BETWEEN SUCCESSIVE INSPECTIONS THAT REQUIRES REWORK/BLEND-OUT THAT EXCEEDS ALLOWABLE LIMITS, REQUIRING A REPAIR OR COMPLETE OR PARTIAL REPLACEMENT OF A PRINCIPAL STRUCTURAL ELEMENT (PSE) AS DEFINED BY THE ORIGINAL EQUIPMENT MANUFACTURER'S STRUCTURAL REPAIR MANUAL

CORROSION LEVEL DEFINITIONS



Continued

* THE FOLLOWING CORROSION LEVEL DEFINITIONS ARE
IN THE PROGRAM

- LEVEL 2 CORROSION

- CORROSION OCCURRING BETWEEN SUCCESSIVE
INSPECTIONS THAT IS WIDESPREAD AND
REQUIRES BLEND-OUT APPROACHING THE
ALLOWABLE REWORK LIMITS

CORROSION LEVEL DEFINITIONS



Continued

* THE FOLLOWING CORROSION LEVEL DEFINITIONS ARE
IN THE PROGRAM

- LEVEL 3 CORROSION

- CORROSION FOUND DURING THE FIRST OR
SUBSEQUENT INSPECTIONS THAT IS DETERMINED
(NORMALLY BY THE OPERATOR) TO BE A
POTENTIAL URGENT AIRWORTHINESS CONCERN
REQUIRING EXPEDITIOUS ACTION

* AN EFFECTIVE PROGRAM IS ONE THAT CONTROLS CORROSION
OF ALL PRIMARY STRUCTURE TO LEVEL 1 OR BETTER



PROGRAM IMPLEMENTATION

- * PRIMARY CONCERN IS FOR AIRPLANES THAT HAVE ALREADY REACHED OR EXCEEDED AGES WHERE SIGNIFICANT CORROSION IS OCCURRING
- * FOR THESE AIRPLANES THE MAXIMUM PERIOD FOR IMPLEMENTING THE PROGRAM IN A GIVEN AIRPLANE AREA CORRESPONDS TO THE REPEAT INTERVAL FOR THAT AREA
- * FOR AIRPLANES EXCEEDING 20 YEARS THE IMPLEMENTATION PERIOD IS 6 YEARS OR THE REPEAT INTERVAL, WHICHEVER IS LESS
- * A MINIMUM IMPLEMENTATION RATE EQUIVALENT TO ONE AIRPLANE PER YEAR IS REQUIRED FOR EACH AREA

PROGRAM IMPLEMENTATION

Continued



- * FOR YOUNGER AIRPLANES AN IMPLEMENTATION AGE WAS DETERMINED ON THE BASIS OF CONTINUING AIRWORTHINESS REQUIREMENTS:
 - PREVENTION OF WIDESPREAD/SEVERE CORROSION
 - MINIMIZING THE LIKELIHOOD OF SIGNIFICANT CORROSION COMBINING WITH OTHER FORMS OF DAMAGE SUCH AS FATIGUE
- * TO MEET THE SECOND REQUIREMENT THE CORROSION PROGRAMS MUST BE IMPLEMENTED EARLIER THAN WOULD BE REQUIRED TO ADDRESS CORROSION PROBLEMS IN ISOLATION

PROGRAM IMPLEMENTATION

Continued



- * IMPLEMENTATION AGES ARE BASED ON ENGINEERING ASSESSMENTS BY THE WORKING GROUPS OF:**
 - REPORTED SERVICE DATA**
 - INFORMATION DERIVED FROM AIRPLANE SURVEY VISITS**
 - DATA SUPPLIED BY WORKING GROUP OPERATORS**

REPEAT INTERVALS



- * REPEAT INTERVALS WERE ESTABLISHED BY THE WORKING GROUPS FROM EVALUATIONS OF THE MANUFACTURER'S RECOMMENDATIONS AND DATA FROM CURRENT OPERATOR PROGRAMS
- * TO ACCOMMODATE AIRLINE SCHEDULING, REPEAT INTERVALS CAN OCCASIONALLY BE INCREASED BY UP TO 10%
- * ADJUSTMENTS TO SOME REPEAT INTERVALS ARE LIKELY TO BE REQUIRED FOR AIRPLANES OPERATING IN SEVERE ENVIRONMENTS OR CARRYING CORROSIVE CARGO. THESE ADJUSTMENTS WILL BE BASED ON INDIVIDUAL OPERATOR EXPERIENCE

REPORTING SYSTEM



- * THE AGING AIRPLANE CORROSION PROGRAMS INCLUDE A MANDATORY SYSTEM FOR REPORTING LEVELS 2 AND 3 FINDINGS TO THE MANUFACTURERS
- * REPORTED DATA WILL BE USED BY THE MANUFACTURER TO SUMMARIZE PROGRAM PROGRESS AND FINDINGS, SUPPORT PROGRAM REVIEWS, AND DETERMINE ANY ADDITIONAL ACTION REQUIRED TO ASSURE CONTINUING AIRWORTHINESS AND/OR ECONOMIC OPERATION
- * THERE IS NO REQUIREMENT TO REPORT INSPECTION COMPLETIONS OR LEVEL 1 CORROSION FINDINGS TO THE MANUFACTURER

ALTERNATE MEANS OF COMPLIANCE



- * ANY REQUEST TO A REGULATORY AUTHORITY FOR ALTERNATIVE MEANS OF COMPLIANCE FOR THIS PROGRAM MUST INCLUDE JUSTIFICATION OF THE EFFECTIVENESS OF THE ALTERNATIVE PROGRAM
- * THIS WILL NORMALLY INCLUDE VISUAL EXAMINATION OF A SUFFICIENT NUMBER OF AIRPLANES TO SHOW THAT CORROSION IS NOT EXCEEDING LEVEL 1 IN THE OPERATOR'S FLEET
- * SUCH REQUEST WILL BE HANDLED ON AN AREA-BY-AREA BASIS FOR A GIVEN AIRPLANE MODEL IN THE OPERATOR'S FLEET
- * OPERATORS, HAVING ADEQUATE MAINTENANCE EXPERIENCE AND SUPPORTING DATA FROM PREVIOUS INSPECTIONS, MAY APPLY FOR AN EXTENSION TO THE PERIOD FOR COMPLETING THE INITIAL VISUAL EXAMINATIONS



ANNUAL REVIEW

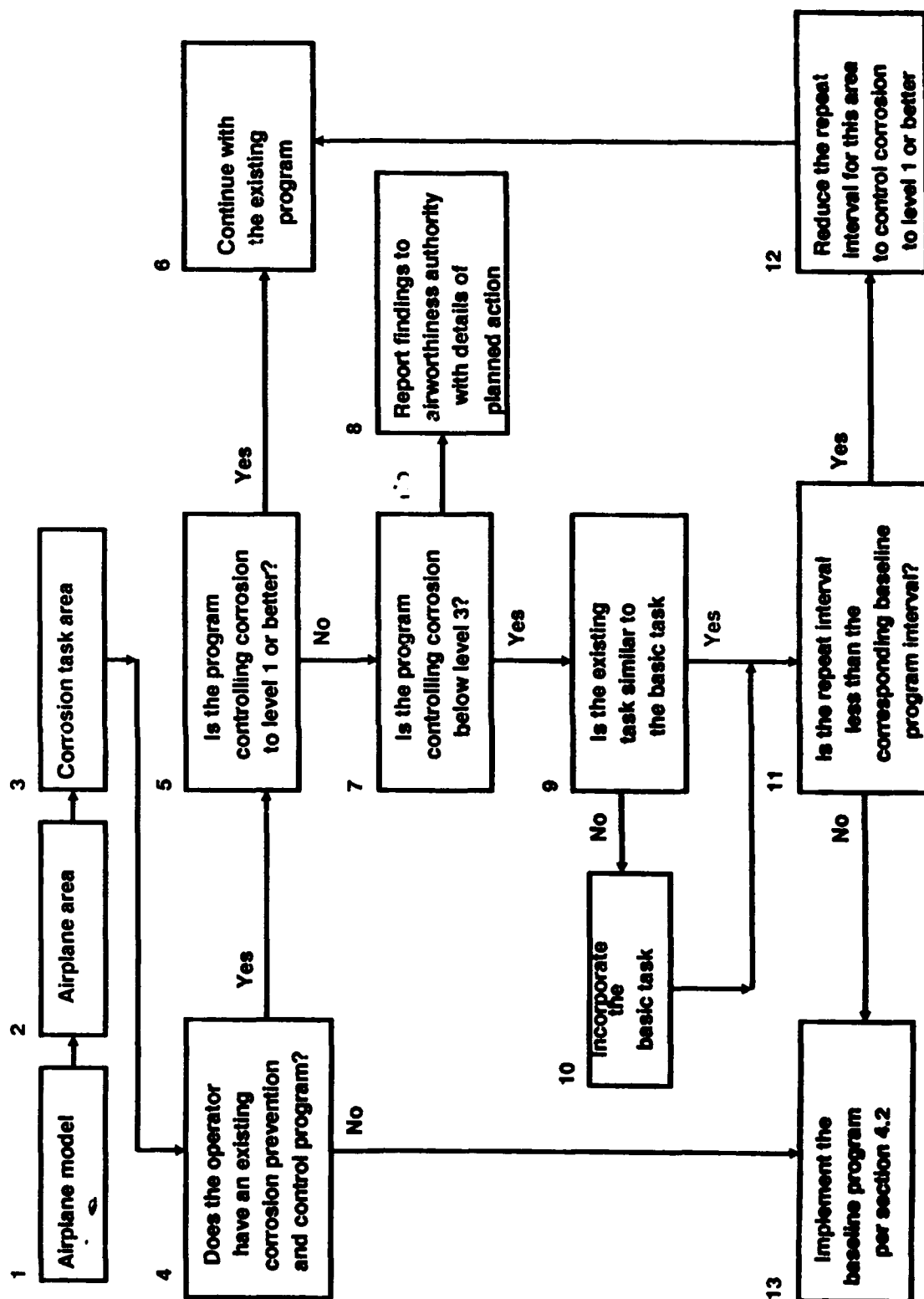
- * THE AGING AIRPLANE CORROSION PROGRAMS WILL BE REVIEWED ANNUALLY TO:
 - REVIEW REPORTED DATA
 - MAKE FURTHER SERVICE BULLETIN RECOMMENDATIONS, AS REQUIRED
 - ASSESS EFFECTIVENESS OF THE BASELINE PROGRAMS AND DETERMINE ANY NECESSARY CHANGES
- * WORKING GROUP MEMBERSHIP WILL BE UPDATED AS REQUIRED TO REFLECT CHANGES IN THE FLEET



MODEL 737

CORROSION TASK NO.	DESC. OF AREA TO BE INSPECTED	ZONES	EFFEC-		I	R
			TIVITY	YRS		
C5370102	HORIZONTAL STABILIZER	7-01	ALL	6	2	
	LUGS ON THE FRONT	7-09				
	AND REAR SPAR-TO- CENTER SECTION ATTACH FITTINGS. (SB 55-1028)	7-10				
C5370103	HORIZONTAL STABILIZER	7-01	ALL	8	2	
	CENTER SECTION	7-09				
	JACKSCREW TRUSS, HINGE PINS AND NUTS.	7-10				
C5370104	HORIZONTAL STABILIZER	7-09	ALL	10	8	
	CENTER SECTION STRUCTURE INCLUDING THE FRONT AND REAR SPARS.	7-10				

PROGRAM APPLICATION





PROPOSED CORROSION AD ACTION BOEING 707/720/727

* 707/720

- 126 AREAS
- 400 AIRPLANES WORLD WIDE
- 74 U.S. AIRPLANES
- \$80,640/AIRPLANE

* 727

- 125 AREAS
- 1,710 AIRPLANES WORLDWIDE
- 1,143 U.S. AIRPLANES
- \$80,000/AIRPLANE



PROPOSED CORROSION AD ACTION

BOEING 737/747

* 737

- 121 AREAS
- 595 AIRPLANES WORLDWIDE
- 232 U.S. AIRPLANES
- \$38,720/AIRPLANE

* 747

- 118 AREAS
- 284 AIRPLANES WORLDWIDE
- 65 U.S. AIRPLANES
- \$188,800/AIRPLANE



**ANALYSIS OF COLD WORKED HOLES
FOR THE T-37B STRUCTURAL LIFE EXTENSION PROGRAM**

David Wieland

*Division of Engineering and Material Sciences
Southwest Research Institute
San Antonio, Texas*

*Presented at the 1990 USAF Structural Integrity Program Conference
San Antonio, Texas
December 11-13, 1990*



***T-37B Service Life Extension Program
Program Objective***

***To Design, Analyze, Test and Manufacture
Structural Life Extension Kits to
Extend the Life of the T-37B by an
Additional 8,000 Flight Hours***



***T-37B Service Life Extension Program
SWRI Areas Of Responsibility***

Structural Design

Structural Analysis

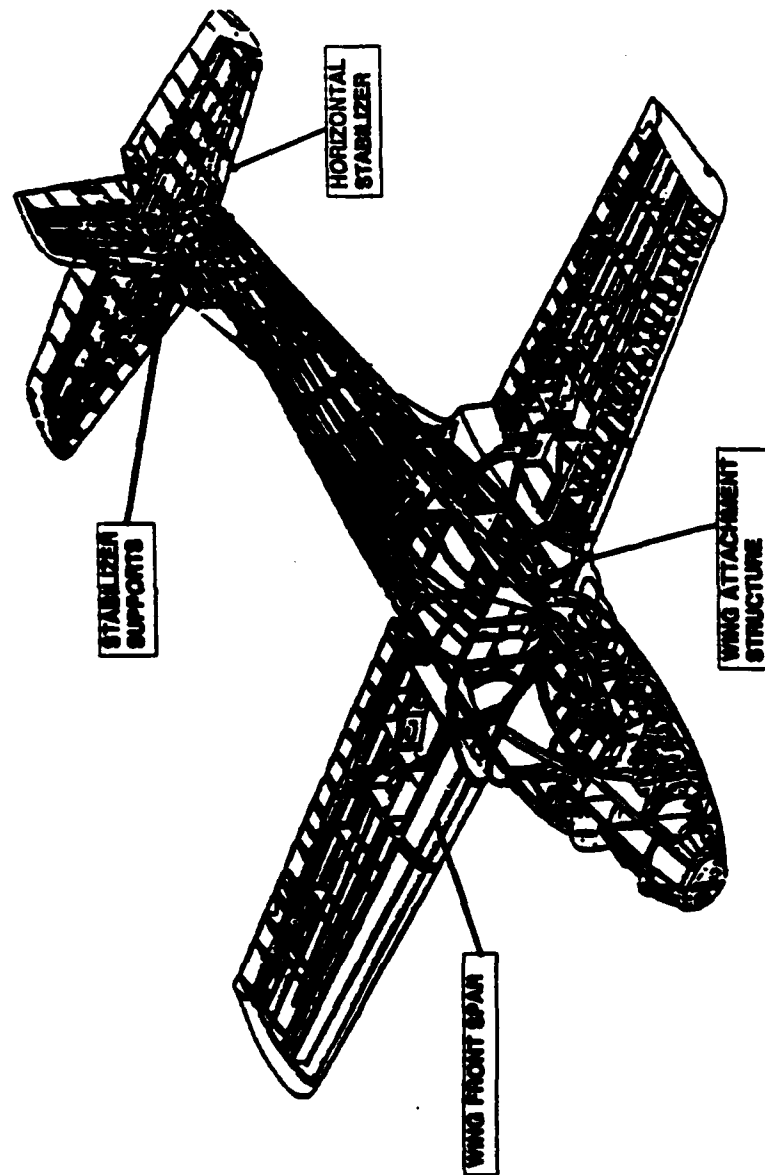
Material Component Testing

Full-Scale Testing

Structural Flight Demonstration



T-37B Service Life Extension Program





Analysis of Cold Worked Holes For the T-37 Structural Life Extension Program

- ***Introduction***
- ***Stress Analysis of Cold Worked Holes***
 - ***Plasticity Model Used***
 - ***Model Validation***
 - ***Stress Analysis Results***
- ***DTA of Cold Worked Holes Using Superposition***
 - ***Stress Intensity Factor (SIF) Development***
 - ***DTA Compared to Test Data***
 - ***DTA Compared to 0.005 Initial Flaw***
- ***Conclusions***

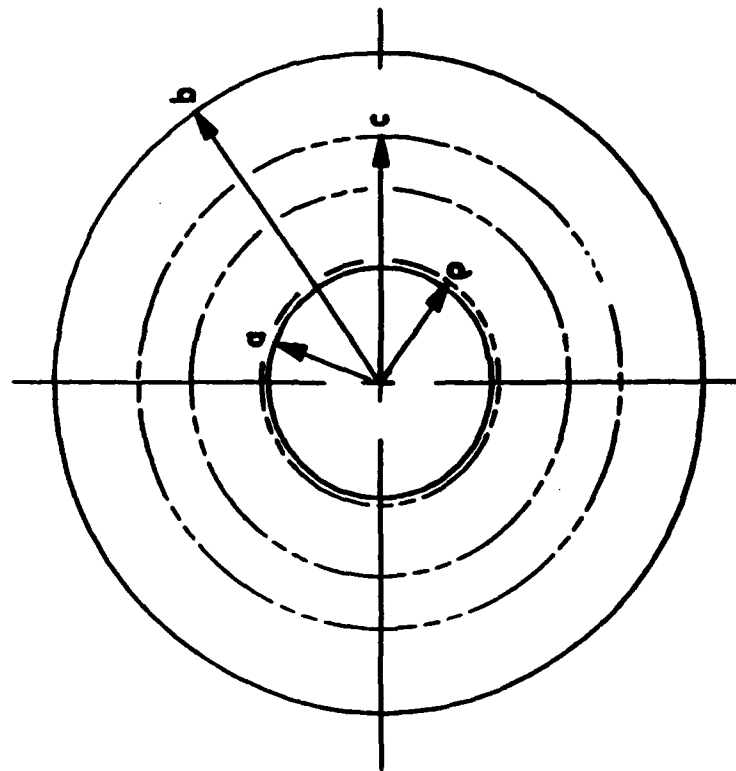


***Purpose
of Stress Analysis of Cold Worked Holes***

- ***Determine Stresses Induced by Cold Working (C.W.)***
 - ***Insure Parts Would Not Fail During C.W.***
- ***Determine Residual Stress Field***
 - ***Determine Free Edge Stresses***
 - ***Residual Stress Field Used In DTA***



**Plasticity Model
Geometric Configuration**

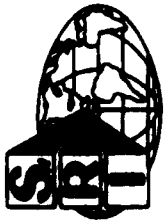


a = hole radius

b = distance to free edge

c = plastic zone radius

p = reverse yield radius



**Elastic/Plastic Induced Stresses
in a Thick Walled Tube**

for $a \leq r \leq c$

$$\sigma_r = -k \left(1 - \frac{c^2}{b^2} + \ln \frac{c^2}{r^2} \right)$$

$$\sigma_\theta = k \left(1 + \frac{c^2}{b^2} - \ln \frac{c^2}{r^2} \right)$$

for $c \leq r \leq b$

$$\sigma_r = -\frac{kc^2}{b^2} \left(\frac{b^2}{r^2} - 1 \right)$$

$$\sigma_\theta = \frac{kc^2}{b^2} \left(\frac{b^2}{r^2} + 1 \right)$$



**Elastic/Plastic Residual Stresses
in a Thick Walled Tube**

$$a \leq r \leq \rho$$

$$\sigma_r^i = 2k \left(1 - \frac{\rho^2}{b^2} + \ln \frac{\rho^2}{r^2} \right)$$

$$\sigma_\theta^i = -2k \left(1 + \frac{\rho^2}{b^2} - \ln \frac{\rho^2}{r^2} \right)$$

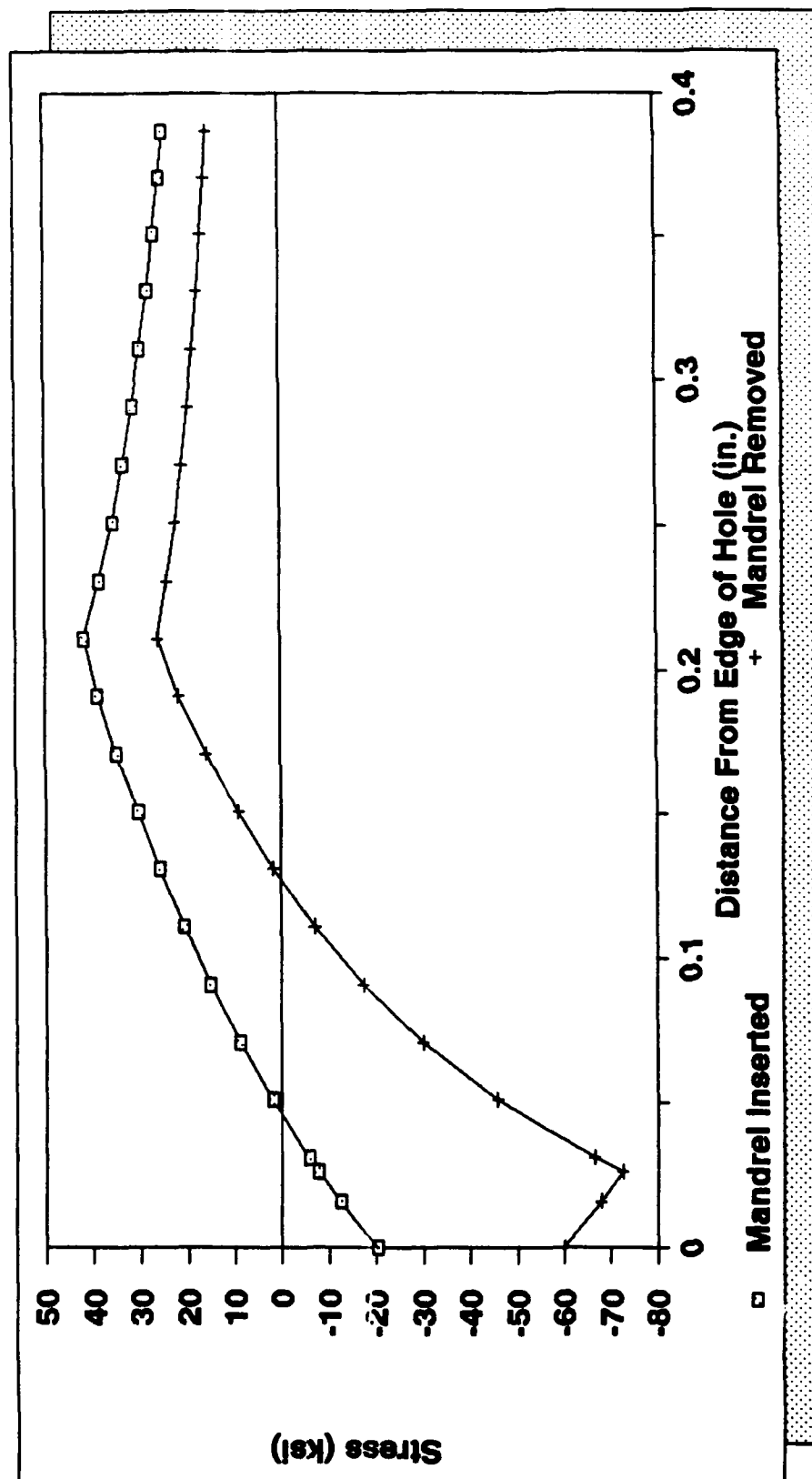
$$\rho \leq r \leq b$$

$$\sigma_r^i = 2k \frac{\rho^2}{b^2} \left(\frac{b^2}{r^2} - 1 \right)$$

$$\sigma_\theta^i = -2k \frac{\rho^2}{b^2} \left(\frac{b^2}{r^2} + 1 \right)$$

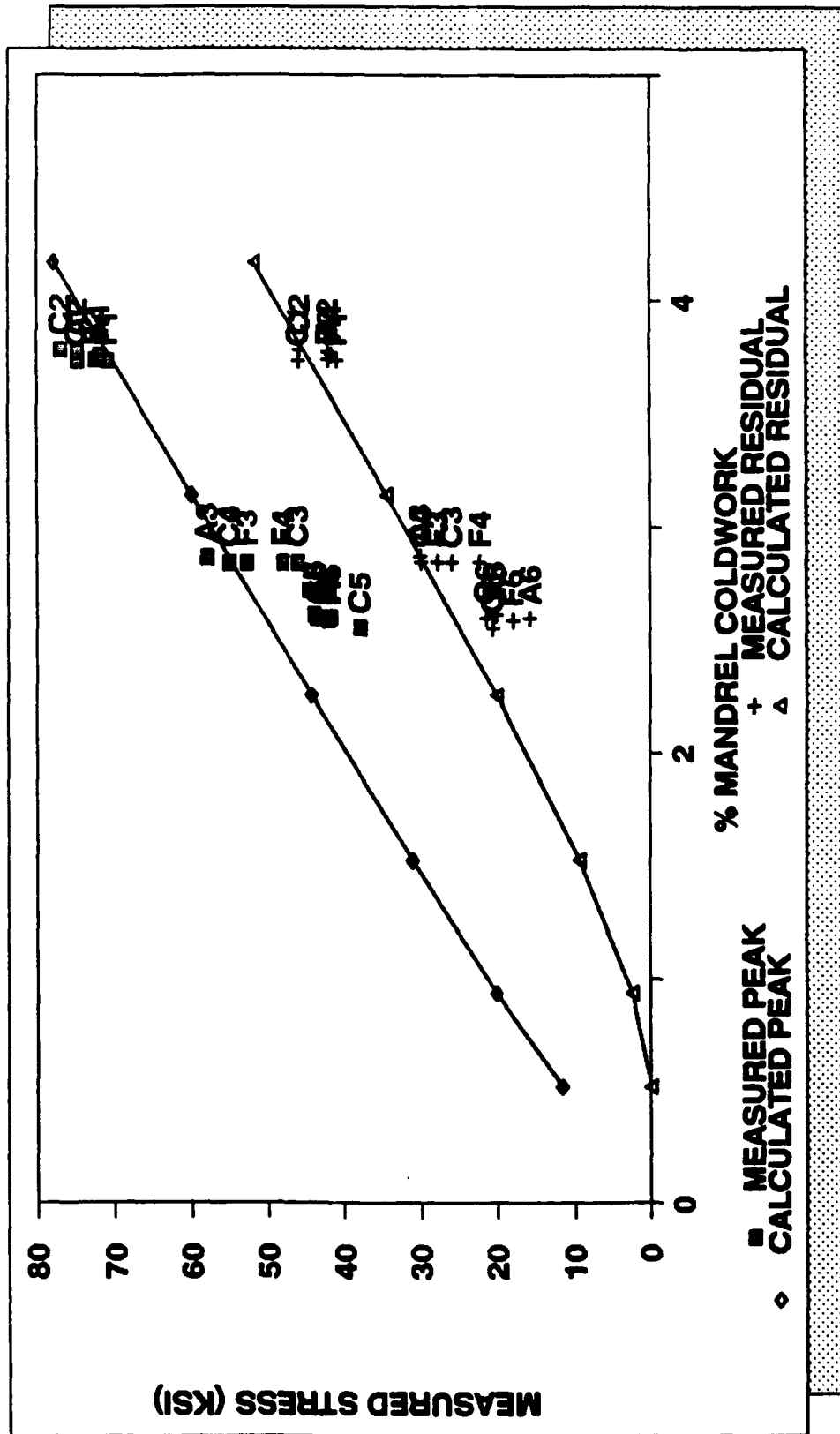


**Typical Hoop Stress in an Elastic/Plastic Thick
Walled Tube With Mandrel Inserted
and Mandrel Removed**



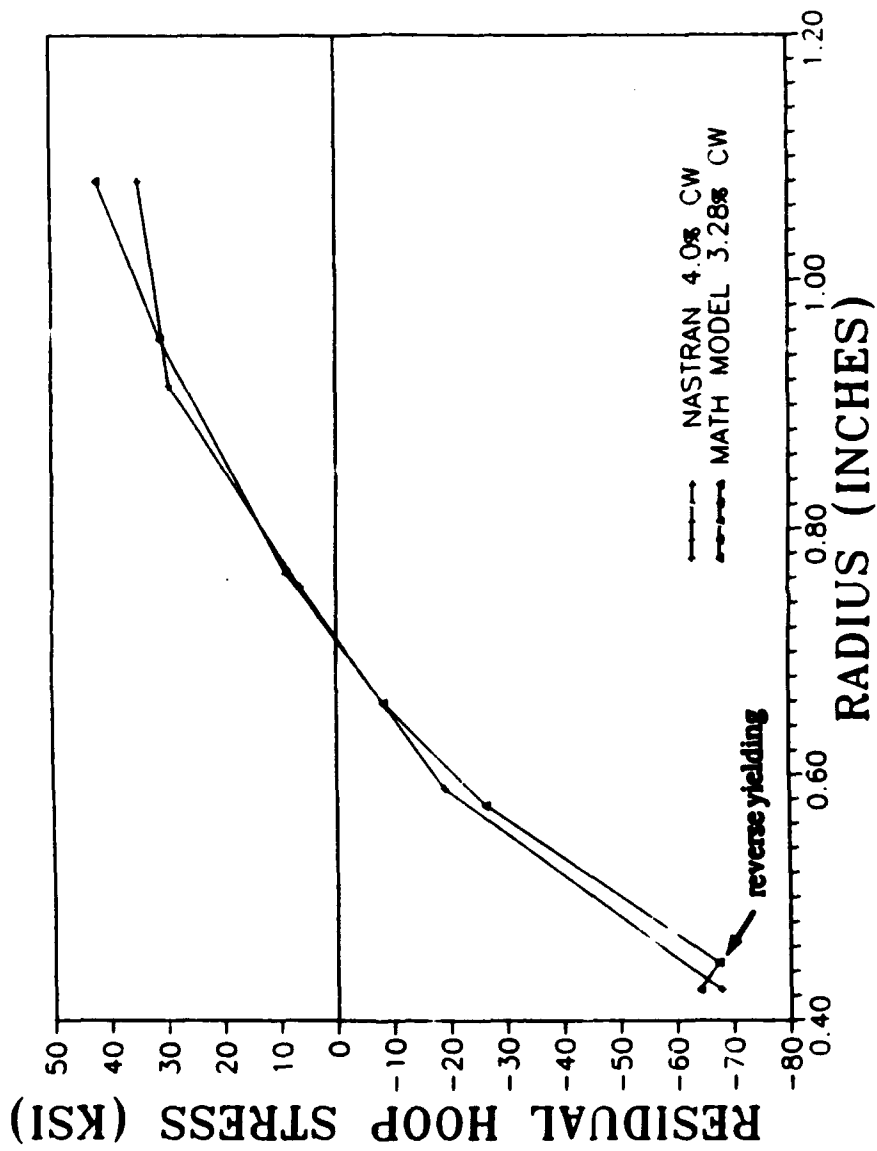


**Cold Working in 302 Lug
Measurements at RA/FB**





**Comparison of Elastic/Plastic Analysis
and USAF NASTRAN Model of "302" Lug**





Elastic/Plastic Stress Analysis Results

- *Unique Cold Worked Geomtries Analyzed*
- *Over Half Had Standard Tools Changed to:*
 - *Insure The Ligament Did Not Fail*
 - *Reduce The Residual Tension Stress
On the Free Edge*

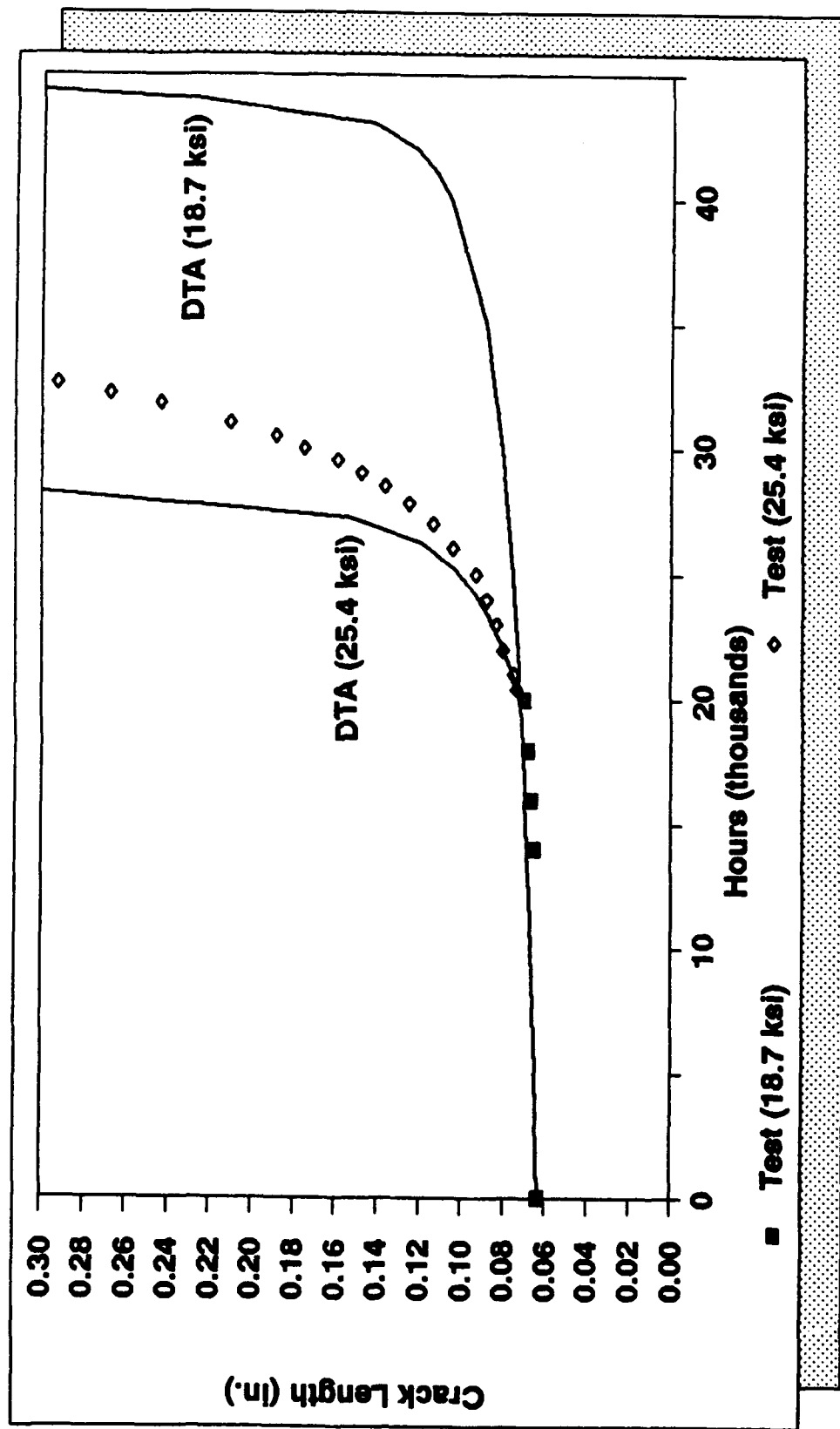


*Damage Tolerance Analysis of Cold Worked Holes
Using Superposition*

- *SIF Determined by Superposition*
 - *Elastic/Plastic Residual Stresses*
 - *Shah's Green Function for a Radial Crack from a Hole*
 - *Flaw Shape Factor (Q)*
- *Modified Cracks III to Perform Superposition*

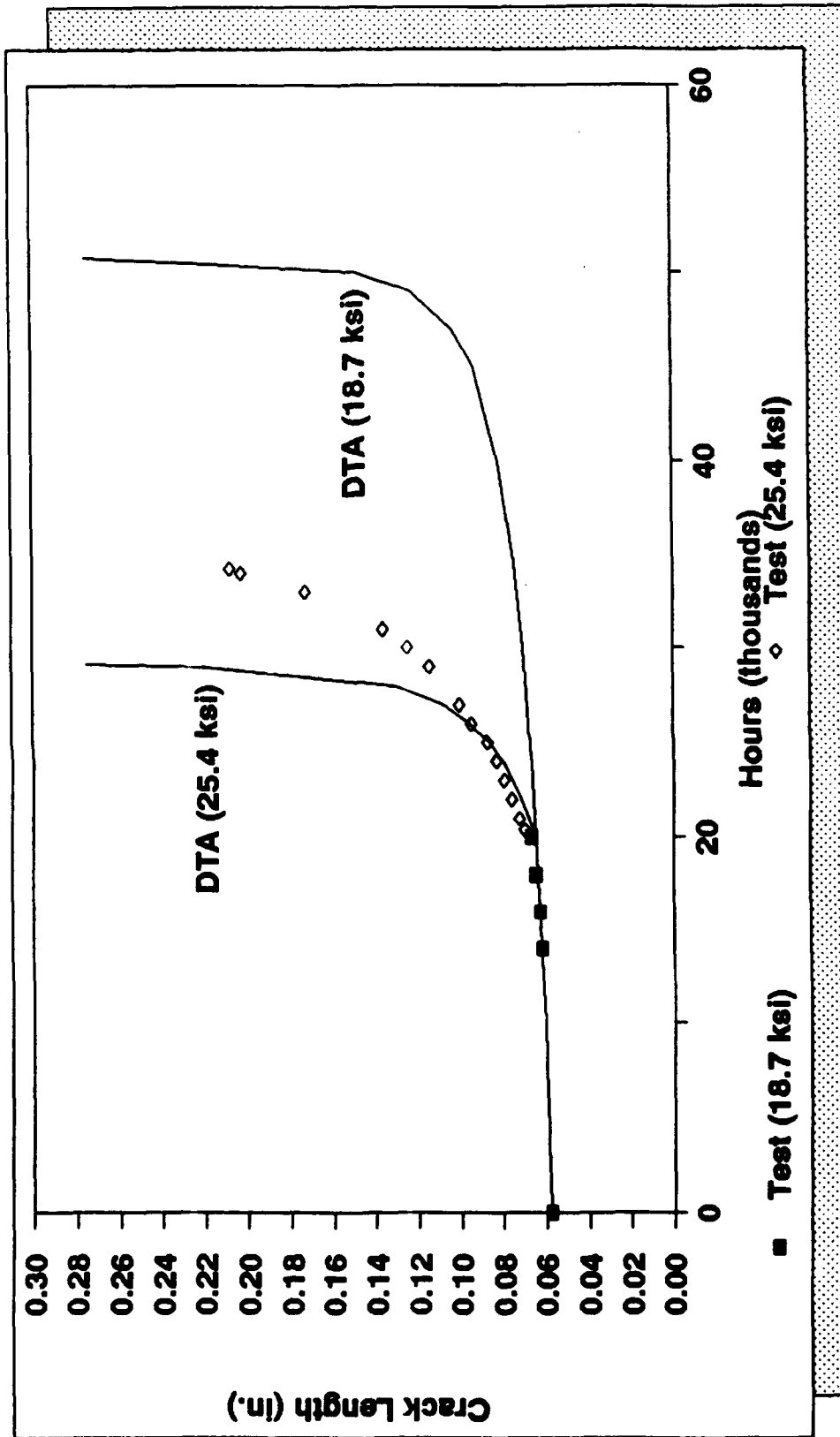


**Wing Spar 2.8% Cold Worked Hole
Test Data and DTA Comparison**



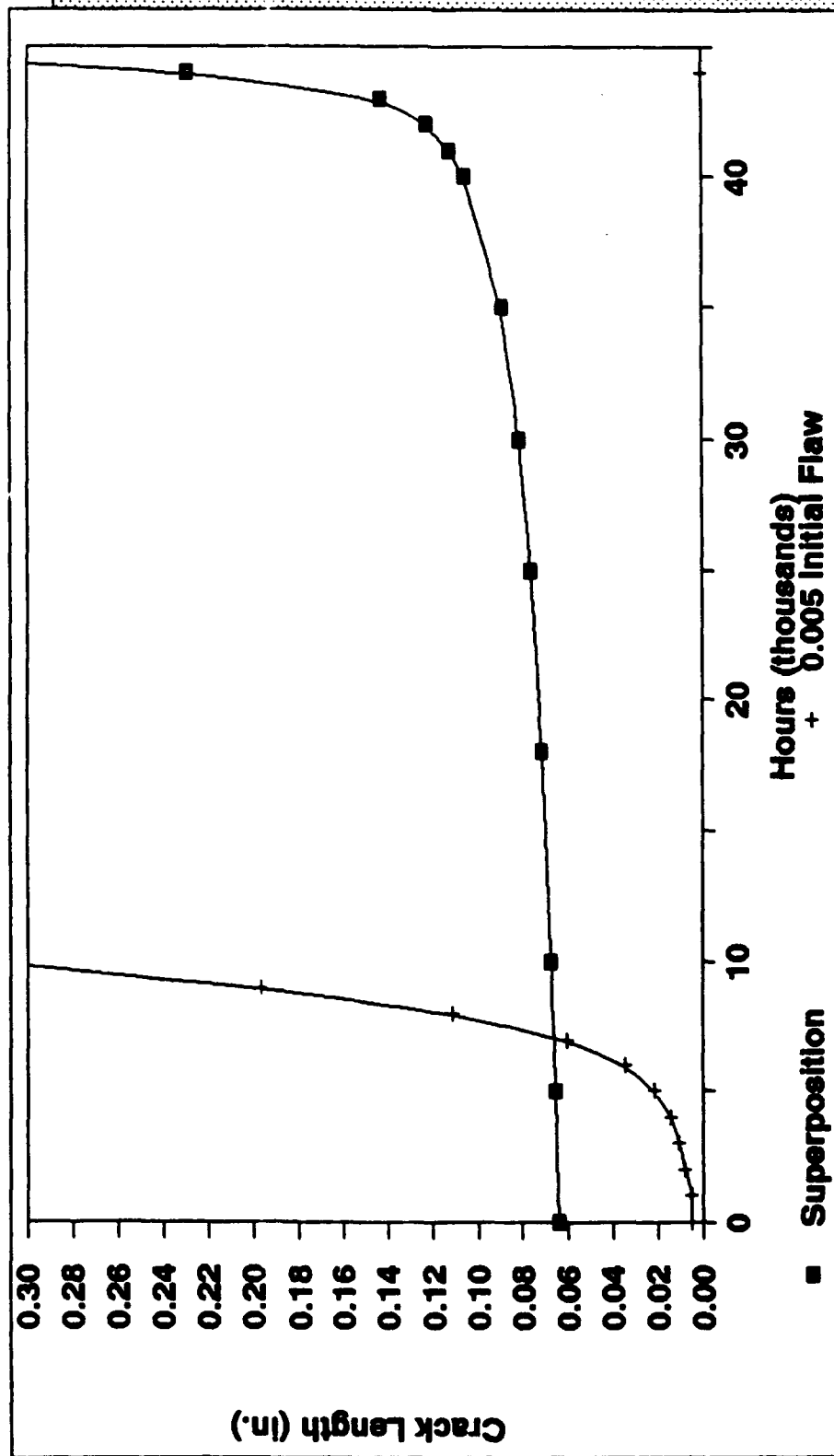


**Wing Spar 3.8% Cold Worked Hole
Test Data and DTA Comparison**



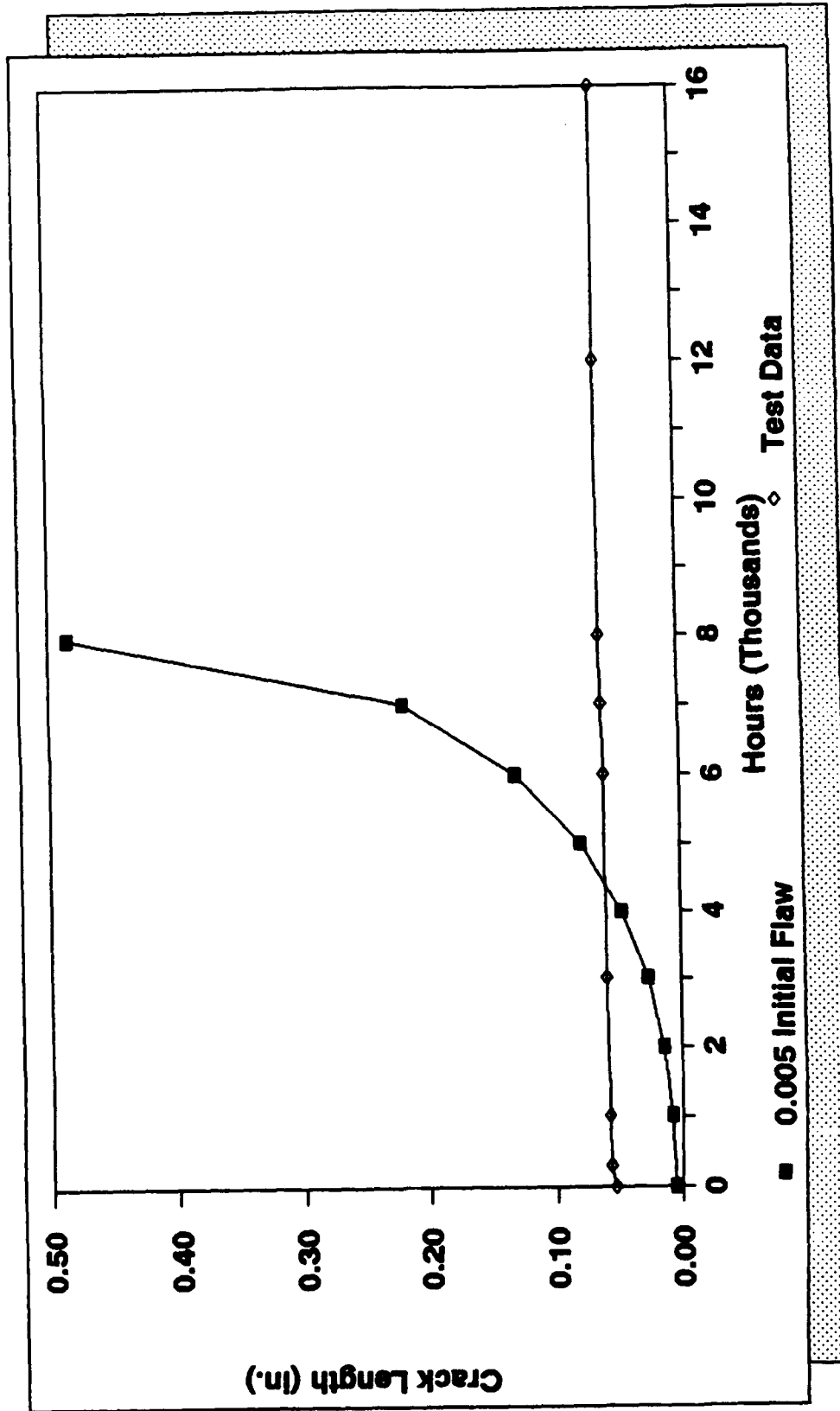


*Wing Spar 2.8% Cold Worked Hole
Superposition Compared to 0.005 Flaw*





***Banjo Fitting Cold Worked Hole
Test Results Compared to a 0.005 Initial Flaw***





Analysis of Cold Worked Holes Conclusions

- *Elastic/Plastic Analysis*
 - *Valid for Design Evaluation of Cold Working*
 - * *Ligament Stresses During Cold Working*
 - * *Residual Stress Field in Ligament*
- *DTA of Cold Worked Holes Using Superposition*
 - *Compares Well With Test Data*
 - * *Crack Growth Curve*
 - * *Prediction of No Crack Growth*

Usage Variation Analysis and Effects on F-5 Component Life

Prepared by: M.P. Kaplan
T.A. Knott
R.E. Welch*
M. Reinke**
D. Ratzer**
C. Massey***

Willis & Kaplan, Inc.
720 Armstrong Drive
Buffalo Grove, IL 60089

*Chiapetta, Welch, & Associates, Ltd.
9748 Roberts Road
Palos Hills, IL 60465

**SA-ALC/LADD
Kelly AFB, TX 78241

***SA-ALC/LAVE
Kelly AFB, TX 78241

1.0 Overview of the F-5 DTA

The recently completed F-5 Usage Assessment and Damage Tolerance Assessment Update was a project intended to determine the current usage severity of the F-5 fleet, and determine appropriate inspection intervals based on that usage.

The project was broken down into ten tasks. Task 1 was the F-5 Usage Assessment, which involved data analysis, statistical analysis, and spectrum development for the SAP usage. The other nine tasks included five analytical and four test tasks to determine inspection intervals for both the F-5E and F-5F aircraft in both the DACT and SAP usages.

The analytical tasks used stress spectra that were developed at Willis & Kaplan, Inc. to determine safety limits and inspection intervals for the fuselage, wing, and empennage of the F-5E and F-5F aircraft. Loads analysis and stress analysis were used in the development of these spectra. To determine the safety limits and inspection intervals, the Forman crack growth model (1) was used, with crack growth data obtained in the test tasks. The Modified Willenborg retardation model (2) was used, with shutoff ratios determined by coupon testing.

A unique aspect of this project which will be discussed in this paper was the development of a technique and a computer program (FLTGEN) which takes statistical data of usage patterns and generates a random sequence representative of that usage.

2.0 Task 1 Overview

The first task of the contract was the processing of recorded SAP flight data, and developing spectra representative of that usage. There were three sub-tasks in Task 1: analysis of data from MXU-553 recorders, statistical analysis, and spectrum development.

Approximately 960 hours of data were examined, and each valid flight was categorized into one of four mission types. Each flight was also segmented into phases, such as climb, cruise, and primary. The flight data was viewed and segmented using the EPRE (Edit/Pre-Analysis) program written by Alamo Technology, Inc. (3). Figure 1 shows an example of a segmented flight using

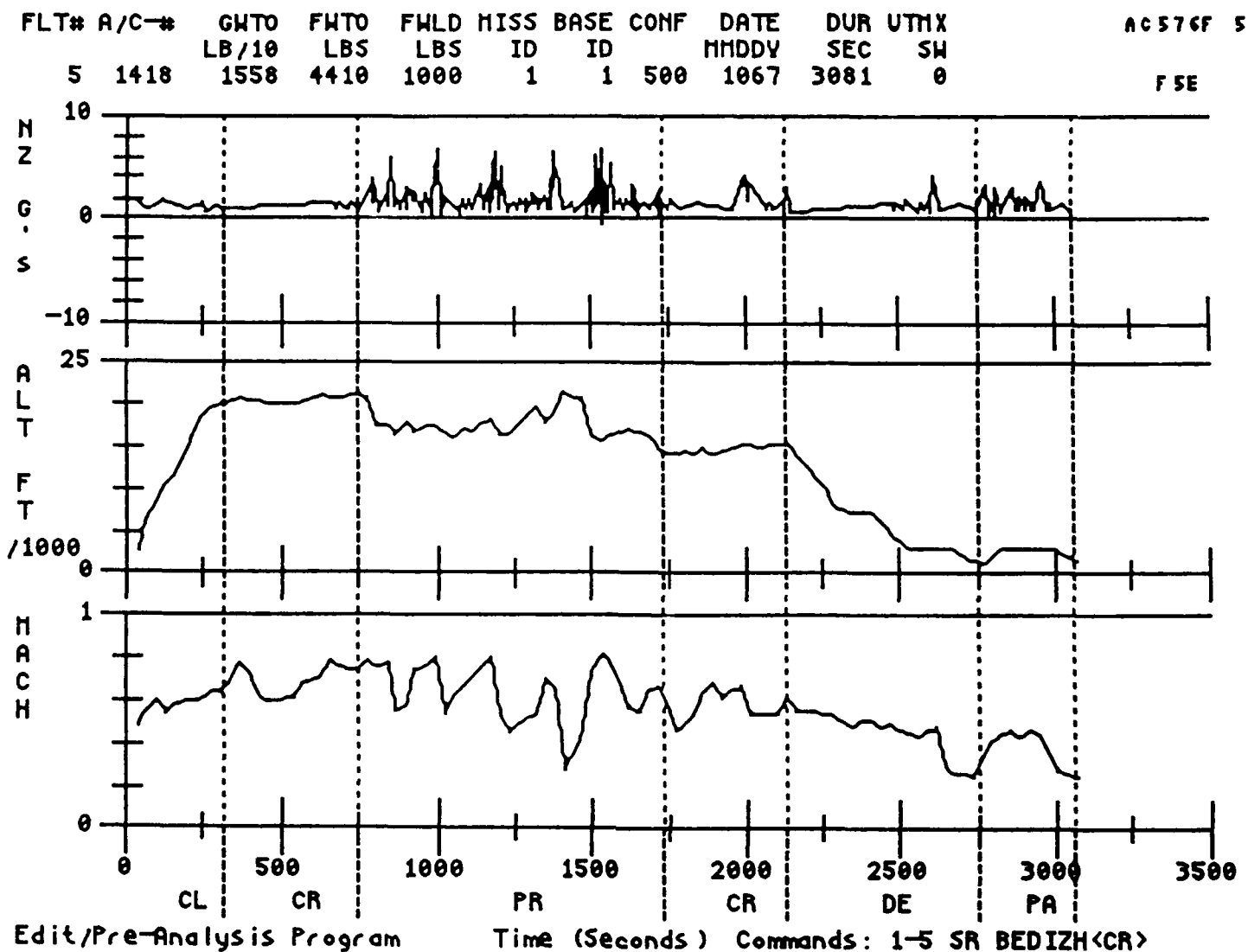


Figure 1
Example of Flight Data Edited with EPRE

EPRE. This example is categorized as High Altitude Combat.

The next step was to obtain statistical information on the flights just processed. This was done using the SOUP (Spectra and Operational Usage Profiles) written by Southwest Research Institute under subcontract to Alamo Technology (4). Output from the SOL P program is in the form of Nz and VTMX occurrences normalized to a 1000 flight, mission, or phase hour basis. Counts are also given for each "point in the sky" flight condition. Also, statistical information is given on the time percentage breakdown of missions and phases.

The last sub-task of Task 1 was the development of spectra for the SAP usage. These spectra were to represent 1000 hours of simulated usage. Because of the enormity of the counts, numerical procedures were necessary. The remainder of this paper will discuss the program that was written for this purpose.

3.0 SAP Spectra Development

This section describes the methods used to create the bending moment and stress sequence files.

The bending moment and stress sequence files represent 1000 hours of simulated DACT or SAP usage. The bending moment and stress sequence files were generated with the FLTGEN computer program. Briefly, this computer program takes statistical output data from the SOUP program and uses it to shape the generation of a random occurrence-time history. These occurrences are then converted to bending moments or stresses at the appropriate location by means of tabular data and/or factors.

The bending moment and stress sequences generated for the following locations were required by Task 1 of the contract:

- W.S. 29.5 Streamwise Bending Moment
- W.S. 57 Swept Bending Moment
- W.S. 0.0/33% Spar Stress
- W.S. 50/44% Spar Stress
- F.S. 405.5 Bending Moment
- Vertical Tail Root Bending Moment (VTMX)

Corresponding sequences generated by Alamo Technology in their previous analysis of DACT usage were provided as government furnished data.

In addition, bending moment and stress sequences were generated for other locations for both DACT and SAP usages as required for other tasks of the contract. These sequences include:

- W.S. 73 swept bending moments
- W.S. 123 swept bending moments
- W.S. 29.5 bending moments in the root rib axis
- B.L. 25.07 (F-5E only) (horizontal tail bending moment)
- B.L. 26.26 (horizontal tail bending moment)
- B.L. 28.6 (horizontal tail bending moment)
- F.S. 194 original design (F-5E only)
- F.S. 194 redesign (ECP145) (F-5E only)
- F.S. 205 (F-5F only)
- F.S. 233.7 (F-5E only)
- F.S. 257 original design (F-5E only)
- F.S. 257 redesign (ECP145) (F-5E only)
- F.S. 267 (F-5F only)
- F.S. 284 forward
- F.S. 284 bolt
- F.S. 284 aft
- Nz sequence

3.1 Stress Sequence Tape Generation

The FLTGEN computer program was developed in support of the Damage Tolerance Assessment Update of the F-5E/F aircraft. The principal purpose of the program is to generate random flight stress sequence data based on operational usage profile data produced by the SOUP program from MXU flight data files. A secondary purpose of the program is to provide access to the MXU flight data independently of the EPRE and SOUP programs for review and summary purposes.

The relationship of the FLTGEN program to other phases of the data processing activities involved in this study is illustrated in Figure 2. The MXU flight data base, one each for both F-5E and F-5F aircraft, contains digital images of R-tape data arranged flight-by-flight with one sub-directory for each

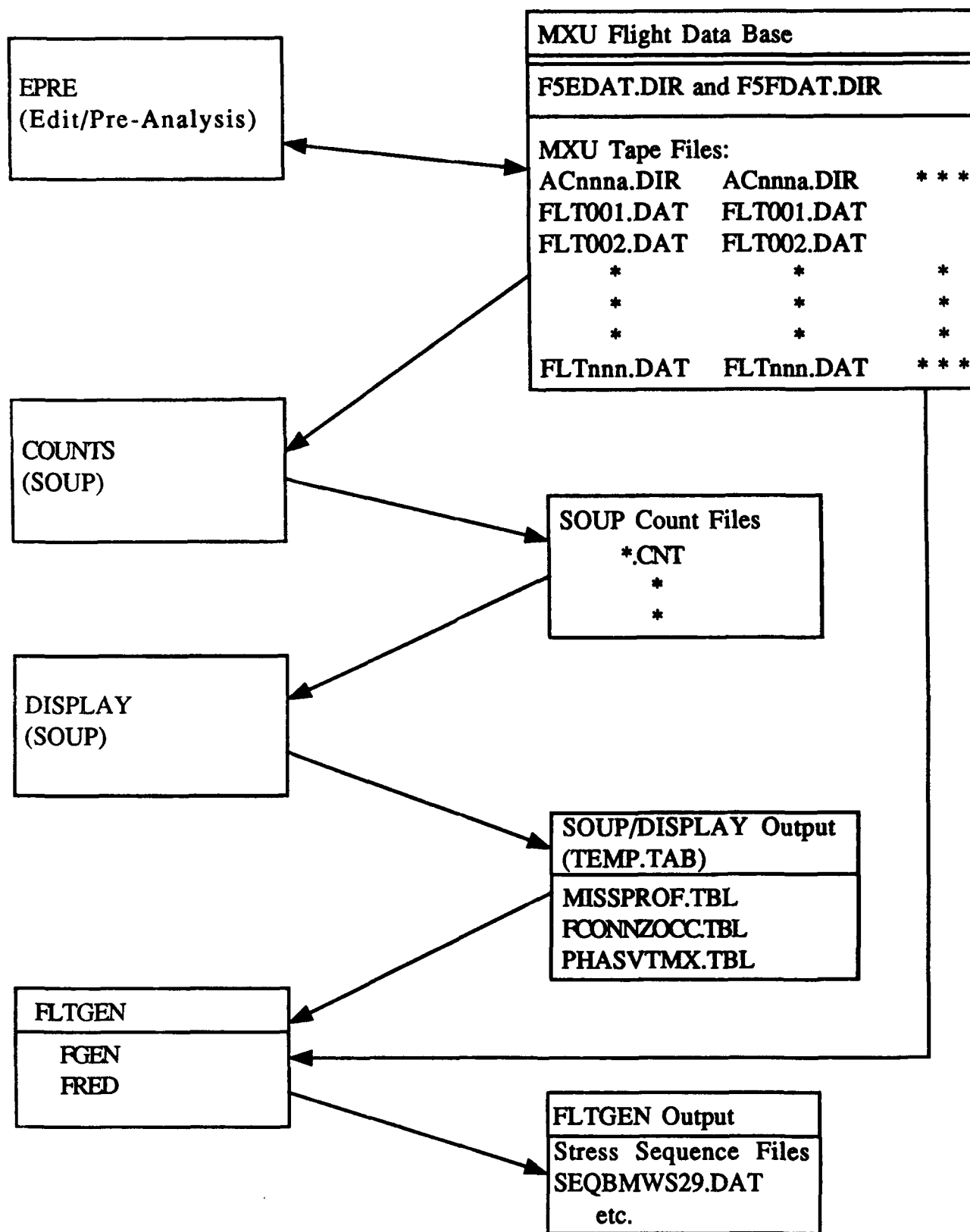


Figure 2
DTA Data Processing

R-tape. This data base is reviewed, edited, and phase marked using the EPRE (Edit/Pre-Analysis) programs. Subsequently, the COUNTS/SOUP program is used to develop a statistical data base of load occurrences and other flight parameters. This data is then interrogated by the DISPLAY/SOUP process to provide data summaries and tabulations of various types. For purposes of the current study, certain DISPLAY print files are intercepted to provide a data base for the FLTGEN program. Specifically, this data consists of tables of mission and phase duration data (Missprof.tbl), and occurrence table of normal load, Nz, and vertical tail moment, VTMX, arranged by missions and mission phases. The FLTGEN program is then used to access this data and generate various type of random flight stress sequence data files.

The following sections present an overview of the program, a detailed discussion of program operation, a description of the algorithms employed in the flight sequence generation, and a discussion of program data requirements.

3.1.1 Outline of FLTGEN program

This section presents an overall summary of the principal modules and operations which make up the FLTGEN program. It will be noted that while the program has been designed in a modular form for fairly general application, it is limited, in its present form, to the specific data structures and operation required in support of the present F-5E/F DTA. The program may be easily modified to accommodate the development of spectra for other aircraft and structures.

The FLTGEN program is command driven and offers the user a selection of operations. At present, four operations are defined (MENU, MODE, FRED, and FGEN) as illustrated in Figure 3. The principal features of each of these operations are given below. Detailed discussions of program operation and the principal modules are given in subsequent sections.

FLTGEN (Main Program)

The main program is a simple skeleton which inquires for commands from the terminal and passes control to various operating modules as discussed below.

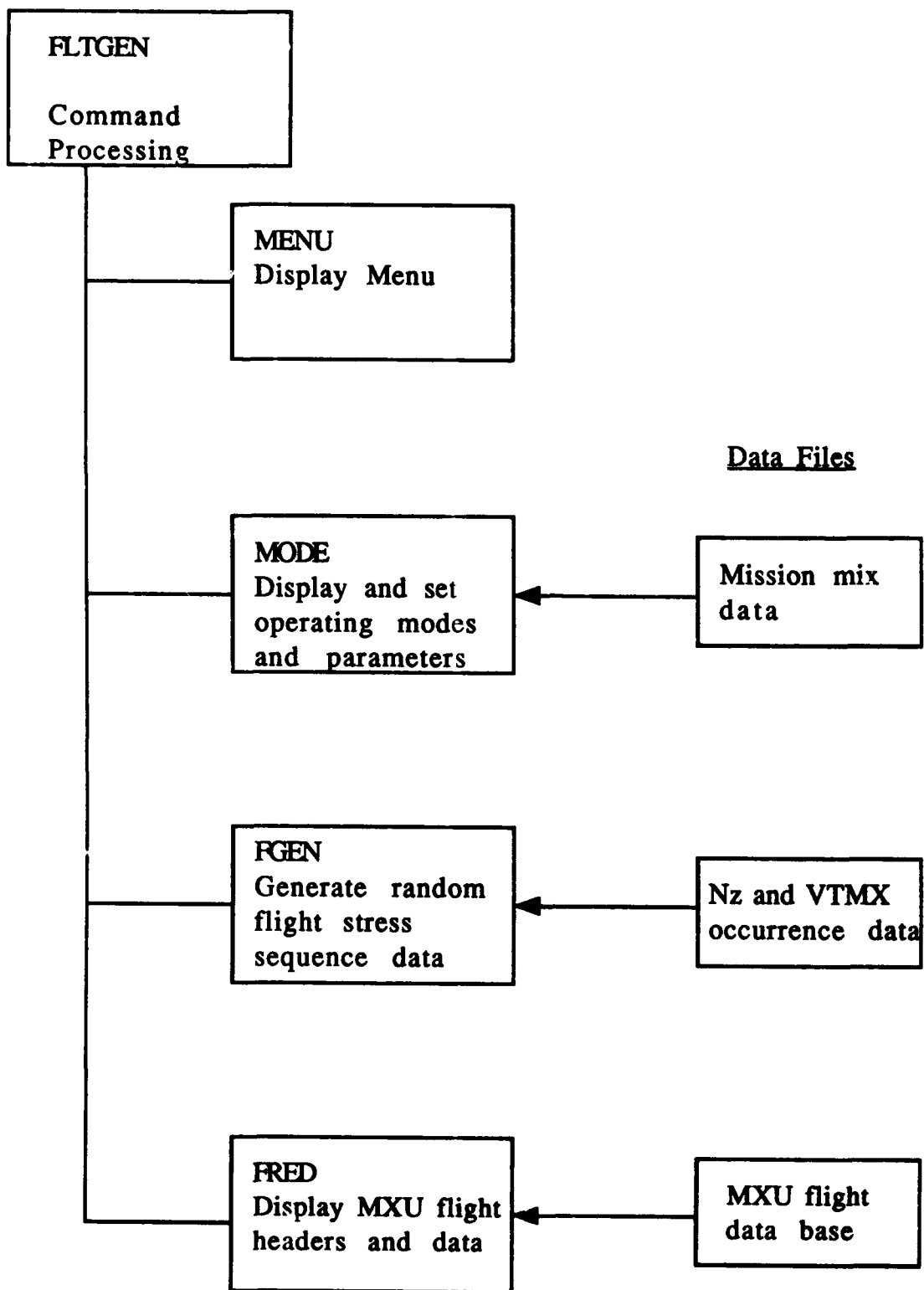


Figure 3
Principal FLTGEN Modules

MENU

This is a simple program which displays the current selection of program operations at the terminal.

MODE

This routine controls the selection and setting of overall program options and parameter values. The items which are presently displayed and controlled by this routine are:

Terminal: The program displays a list of terminal types and prompts for a selection. This selection then governs subsequent terminal operations.

Echo Mode: Allows the user to set a flag which enables/disables the output to an ASCII file of certain types of selected supplementary data not normally displayed or generated by the program. At present this flag generates ASCII copies of MXU flight data during the FRED operation.

Hours: This option allows to reset the total number of flight hours of random flight stress sequence data to be generated by the FGEN module.

Sequence Type: The program displays the current specification for the generation of stress sequence data and prompts the user for changes in the selection of the stress sequence specification and subordinate parameters.

FRED

This auxiliary routine is used to access the MXU flight data files directly (i.e., without use of the Edit/Pre-Analysis and SOUP programs). The user is prompted for a choice of flight data directory and range of flight data files. The program reads each flight data file and reports the flight header information to the screen and to a summary output file. In addition, if the echo mode is enabled, the program generates a file containing the flight data in ASCII format.

FGEN

This routine is the principal operation of the FLTGEN program and deals with the generation of random stress sequence data from operational usage profiles generated by the SOUP program. The program generates a sequence of simulated flights amounting to a pre-specified total number of flight hours. For each generated flight the mission type is obtained by a random choice

weighted from the pre-specified mission mix tables on the basis of percentage of total flight time attributable to each mission type. Subsequently, for each flight the program generates a random sequence of Nz (or VTMX) occurrences scaled according to the 1000 hour occurrence tables organized by mission, phase and flight condition. This data is then converted to the appropriate bending moment (with the tables of moments by Nz and flight condition number) and stress values (as appropriate to the particular stress sequence specification), arranges the data in peak-valley sequence and writes the data to a flight-by-flight stress sequence data file.

3.1.2 Program Operation

The FLTGEN program is menu and command driven from the terminal with commands and terminal level input intended to be reasonably self-explanatory. In addition to screen level input the program seeks data input in the local operating directory from the following three files:

- * missprof.tbl : A mission profile table which provides flight weight, airspeed, and time duration by mission and mission phase. If this table is loaded during program initialization and, if not found during this step, the program defaults to internal data for F-5E DACT usage, from Alamo Technology (5).
- * fconnzocc.tbl : A table of Nz occurrence counts organized by mission, phase and flight condition and obtained from the SOUP program. This data is loaded by the FGEN routine.
- * phasvtmx.tbl : A table of VTMX occurrence counts organized by mission and phase and obtained from the SOUP program. This data is loaded by the FGEN routine.

A detailed description of these data files is given in a subsequent section dealing with the FGEN program.

All commands, mode settings, and parameters are entered at the terminal in response to prompts from the program. Initially the program displays the main menu of program operations which gives the name and function of the main program modules at the command level. This menu can subsequently be recalled from the command level with the MENU command. The current menu

is as follows:

FLTGEN Vers. 2.0 Nov. 1989

Op Commd Description

1 MENU Display this Menu
3 END Wrap up and quit run
5 FRED Read the Flight Data

Op Commd Description

2 MODE Display/Set Operating Modes
4 FGEN Generate Flight Sequences

Command:

The remainder of this section provides details of the screen prompts arising in response to the MODE command, which is the major program control module. The FRED module has numerous screen interaction commands which are not presented here, and the FGEN module has no terminal level input requirement. The response:

Command: MODE

displays the program status screen and a prompt line giving a list of accessible items:

FLTGEN Program Status
Flight Read Echo is: OFF
Aircraft type: F-5E
Required Mission Mix for: 1000.0 Total Hours
No. Type Pct. Mission Flights Hours
1 HAC 61.9 High Altitude Combat 0 .0
2 LAC 10.5 Low Altitude Combat 0 .0
3 OTH 6.5 Other 0 .0
4 X-C 21.1 Cross Country 0 .0

Current Stress Sequence ID: 3 BMUS29

Open Items are:

TERMinal,ECHO,SEQ,HOURS,NONE or <CR> Enter Item to be changed:

This screen displays the following information relative to the status of the program:

***Echo mode status:** This item refers to operations during subsequent direct flight read operations (FRED) during which a simple ASCII copy of each complete flight data set will be deposited in a local file for examination if the echo mode is ON. See the description of the FRED module for additional information relating to the flight read operation.

***Aircraft Type:** This item identifies the aircraft type (F-5E/F) as established by the data in the mission profile file during program initialization. This item cannot be reset.

***Required Mission Hours:** This item displays the total number of combined flight hours which will be generated by the next execution of the FGEN module.

***Mission mix:** This table summarizes the mission mix in terms of mission type, percentage of total hours for a specific mission, a brief description of each mission type, and the actual number of flights in the latest generated set of flight stress sequence data. The four missions shown (i.e., HAC, LAC, OTH, and X-C) correlate numerically with the first four missions in the SOUP program mission sequence (transition, formation, air combat maneuver, and basic flight).

***Stress sequence ID:** This item identifies the type of stress sequence data to be generated on the next pass through the FGEN module.

Finally, those items which can be reset at this level are identified as terminal, echo, sequence, and hours. Subsequent prompt sequences for each of these responses are as follows:

***TERM (Reset terminal type):**

Terminal Types are: TUI U603 U241
Enter Terminal Type: U603

The three terminal type specifically supported are:

TVI : Televideo 925

V603: Visual 603 (VT100 and VT200 emulations)

V241: Visual 241 (VT241 emulation)

***ECHO (Reset FRED echo mode):**

Flight Read Echo is: OFF
Set Echo Mode (<OFF>,ON): off

The flight read echo mode as described above can be set OFF (default) and ON.

***SEQ (Reset stress sequence specification):**

Available Stress Sequence Definitions:

ID: 1	NZ	ID: 2	UTM
ID: 3	BMUS29	ID: 4	BMUS57
ID: 5	BMUS73	ID: 6	BMUS123
ID: 7	STRESSA	ID: 8	STRESSB
ID: 9	FS1940	ID: 10	FS194R
ID: 11	FS205	ID: 12	FS233
ID: 13	FS2570	ID: 14	FS257R
ID: 15	FS267	ID: 16	FS284F
ID: 17	FS284B	ID: 18	FS284A
ID: 19	BMF405	ID: 20	BMBL25
ID: 21	BMBL26	ID: 22	BMBL28
ID: 23	BM29RR	ID: 24	OTHER

Current Stress Sequence ID: 3 BMUS29

Change Current Seq. I.D.(Y,<N>)?Y
Enter new Sequence I.D: 3

Current Stress Sequence ID: 3 BMUS29
Basic Data : NZ Bend Mom. Table : US29
Stress Factor: .1000E+01 File Pack Factor: 100.0
File Name : SEQBMUS29.DAT
File Header:
F-SeqMom. Seq. Data for US29 (Mom/100)

The response SEQ provides a display of available stress sequence definitions and a prompt for a request to reset the stress sequence ID, which is then followed by a display of the current parameters for the stress sequence requested and a subsequent set of prompts to reset any of the subordinate parameters involved in the stress sequence definition. This last series of prompts is terminated with a response of NONE of <CR>. A typical sequence of such prompts which, as a demonstration, reset the original parameter values for the BMWS29 wing bending moment sequence, are as follows:

```
-----
Change:<NONE>, NAME, BASE data, BMTABLE, STR fac, PACK fac, FILE, HEADER:NAME
Enter Sequence ID Name(8a):BMWS29
```

```
-----
Change:<NONE>, NAME, BASE data, BMTABLE, STR fac, PACK fac, FILE, HEADER:BASE
Enter Data Type (<NZ>,UTMX):NZ
```

```
-----
Change:<NONE>, NAME, BASE data, BMTABLE, STR fac, PACK fac, FILE, HEADER:BMT
Enter BMT Name: ,NONE ,WS29 ,WS50 ,F405 :WS29
```

```
-----
Change:<NONE>, NAME, BASE data, BMTABLE, STR fac, PACK fac, FILE, HEADER:STR
Enter Stress Factor:1.
```

```
-----
Change:<NONE>, NAME, BASE data, BMTABLE, STR fac, PACK fac, FILE, HEADER:100
Enter File Packing Factor(data/n):100.
```

```
-----
Change:<NONE>, NAME, BASE data, BMTABLE, STR fac, PACK fac, FILE, HEADER:FILE
Enter File Name (20a):SEQBMWS29.DAT
```

```
-----
Change:<NONE>, NAME, BASE data, BMTABLE, STR fac, PACK fac, FILE, HEADER:HEAD
Enter Seq. File Header:F-SE Mom. Seq. Data for WS29 (mom/100)
```

```
-----
Change:<NONE>, NAME, BASE data, BMTABLE, STR fac, PACK fac, FILE, HEADER:<cr>
Change Current Seq. I.D.(Y,<N>)?<cr>
-----
```

***HOURS (flight hours specification):**

```
Enter Required Flight Hours: 1000.
```

The response to the reset hours option is a prompt for a new value of total generated flight hours.

***NONE or <CR>**

This response terminates the prompt sequence for mode resetting and returns control to the Command level:

FLTGEN Vers. 2.0 Nov. 1989

Op Commd Description

1 MENU Display this Menu
3 END Wrap up and quit run
5 FRED Read the Flight Data

Op Commd Description

2 MODE Display/Set Operating Modes
4 FGEN Generate Flight Sequences

Command:

3.1.3 Flight Read Module (FRED)

This auxiliary module is used to access the MXU flight data files directly (i.e., without use of the Edit/Pre-Analysis and SOUP programs). The user is prompted for a choice of flight data directory and range of flight data files. The program reads each flight data file and reports the flight header information to the screen and to a summary output file. In addition, if the echo mode is enabled, the program generates a file containing the flight data in ASCII format. Additional details regarding the operation of this module and prompt sequences follow.

The routine prompts at three levels after being invoked at the command level with the response: FRED.

***Aircraft Type: The initial prompt, which occurs only at entry to the module, asks for a specification of aircraft type (F-5E or F-5F) independently of the aircraft type specified in MODE in connection with the FGEN module. The default value is F-5E. This value sets the top level of the flight data sub-directory reference as [...F5EDAT...] or [...F5FDAT...]**

***The second level of prompts deals with the specification of an MXU R-tape designator corresponding to the next lowest data directory in the flight data tables. These designators have the**

form ACnnna where nnn is a three digit number (327, for instance) and a is a single alphabetic character (typically A through I in the current data). Note that the user must have the three digit tape serial numbers in hand (from a directory listing, for example) before execution the FLTGEN program. The program will search through the alphabetic descriptor, however, if it given as an asterisk (*). The tape designator then forms the directory name of the flight data of interest, [...F5EDAT.AC327C] for instance.

The third level of prompts deals with the specification of specific flight data files within the specific directory established above. Specific flight data files are specified as a three digit number, (005, for instance) or by an asterisk () indicating all data files. Thus a particular flight data file reference is established as: [...F5EDAT.AC327C]FLT005.DAT for the examples given above.

For each flight data specification for which data is requested the program will read through the data and report the file header information to the terminal and to the program output file (FGEN.OUT), and, if ECHO mode is ON (see MODE description) will also form an ASCII version of the complete file in a separate auxiliary file, named typically for this example as FLTAC327A005.

3.1.4 Stress Sequence Generation Module (FGEN)

The FGEN module contains the principal operations of the FLTGEN program and deals with the generation of random stress sequence data from operational usage profiles and load occurrence data generated by the SOUP program. The program generates a random sequence of simulated flights amounting to a pre-specified total number of flight hours based on the percentage mission distribution obtained from the SOUP mission profile data. For each mission the program generates a random sequence of loads (either Nz or VTMX, depending on the specified type of sequence) with a total number determined by the length of mission and and total occurrences per 1000 hours as determined by the SOUP tabulations. Load sequence generation proceeds phase by phase throughout each mission and, for Nz load sequences, by flight condition occurrences within each phase based on the SOUP output occurrence totals. As each load pair is generated, the result is transformed to bending moment (with the tables of bending moments by Nz and flight condition number) or stress values based on the stress

sequence definition table and entered into an array of peak-valley pairs of data. As each set of flight data is concluded this array is written to the stress sequence output file. A schematic diagram of the FGEN module logic is given in Figure 4 and more detailed description of the major sub-operations in this module are given in below.

3.1.4.1 Random Occurrence Generation

The FGEN module makes extensive use of the selection of random parameter values based on cumulative occurrence weighting tables and a utility subroutine, RANMIX, has been developed as part of this project to implement these procedures in a somewhat general manner. Given a table of occurrence counts, N_i , at parameter value levels, V_i , for values of i up to some final level, K , a cumulative occurrence table (C_j) giving the total number of occurrences up to some level, j , is obtained as:

$$C_j = \sum_{i=1,j} N_i$$

with the total number of occurrences at all levels obtained as

$$C_K = N_{tot}$$

A general table of this type is illustrated in Figure 5. A random choice from this table is made by generating a random number in the range

$$0 < x < 1$$

which forms a choice among all occurrences

$$y = x * N_{tot} \quad 0 < y < N_{tot}$$

and in turn a choice of parameter level, i , by a simple table look-up operation in the stepwise distribution table illustrated in Figure 5. This procedure is used at various points in the FGEN module for random choices of mission type, flight condition type, and load values.

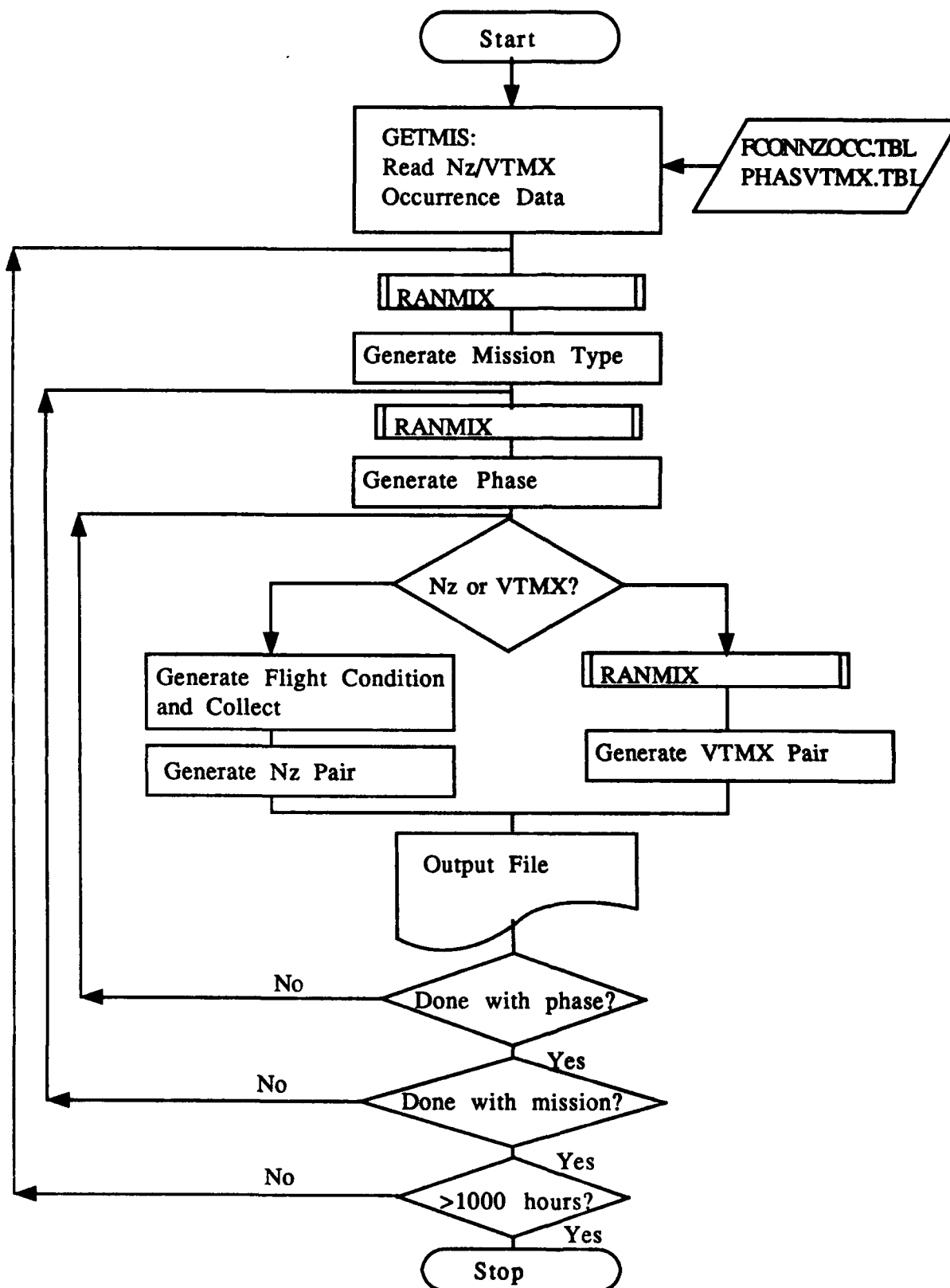


Figure 4
FGEN Module Schematic

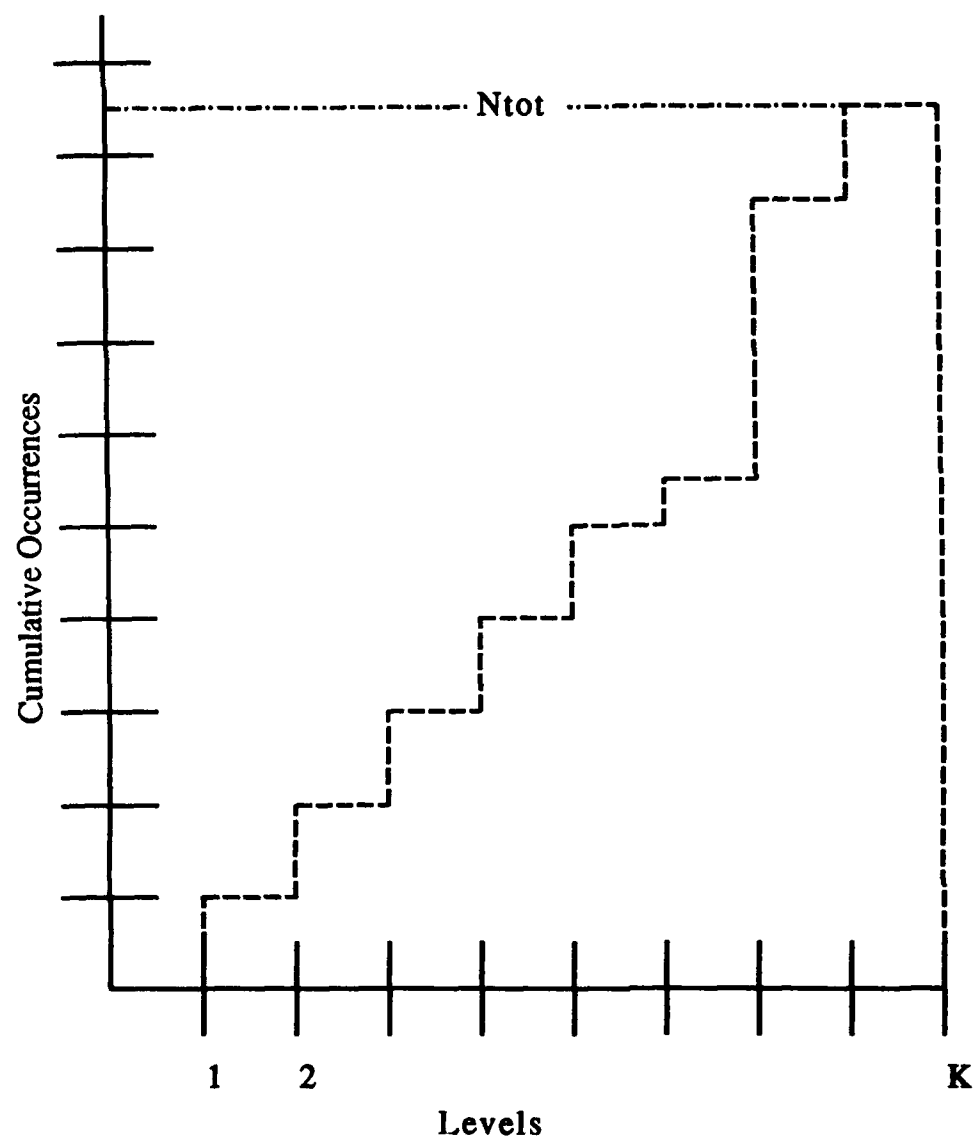


Figure 5
Cumulative Occurrence Table (Schematic)

3.1.4.2 Flight Sequencing

Flights are selected continuously until the total number of flight hours equals or exceeds the requested total flight hours. Each flight is assigned a mission type based on a random choice of flight weighted according to the percentage of each type of flight and average duration given in mission profile tables extracted from the SOUP data. For a given mission type, m , with an average duration of T_m and an hourly percentage, P_m , the number of total hours and flights for this type of mission for a total flight time of H_t for all flights and missions will be:

$$\text{Hours: } H_m = P_m * H_t$$

$$\text{Flights: } N_m = H_m / T_m = P_m * H_t / T_m$$

Thus N_m constitutes a flight occurrence table and a cumulative flight occurrence table (C_m) can be formed for the four types of missions considered (namely; High Altitude Combat, Low Altitude Combat, Other, and Cross-Country) by a summation of the form:

$$C_m = \sum_{i=1,m} P_m * H_t / T_m \quad (m=1,2,3,4)$$

The table formed from the values C_m ($m=1,2,3,4$) constitutes a cumulative flight occurrence table and the mission type for each flight is selected based on a random generated number in the range 1 through the total number of flights. A random choice of mission type for each flight is made using this table and the RANMIX program as described above. In terms of mission selection there are four parameter levels (1 through 4) corresponding to the four mission types and the four corresponding cumulative occurrence levels are the flight occurrence totals as given above.

3.1.4.3 Load Occurrence Tables

The SOUP program provides occurrence tables for load (N_z and $VTMX$) organized by mission type, phase, and flight condition (for N_z only) which form the database for FGEN stress sequence generation operations. These are loaded into computer memory by the GETMIS subroutine at the first entry into the

FGEN module. The organization of these tables for the two types of loads (Nz and VTMX) are as follows:

Nz Data: These data consist of occurrence counts per 1000 mission hours for each mission type at 22 levels from -2.5 G to 9.0 G at 0.5 G increments with the 1.0 and 1.5 G levels omitted. The data is organized by phase within each mission and by flight condition within each phase. Up to 19 flight conditions are identified for F-5E aircraft and up to 24 conditions for F-5F aircraft. All Nz occurrence data tables are converted to cumulative occurrence tables as they are read into the FGEN program.

VTMX Data: These data consist of occurrence counts per 1000 phase hours for each mission type at 18 levels of Mx/1000 from -400 through 400 at increments of 50 with an additional level at -0.1 included. The data is organized by phase within each mission type. Each VTMX occurrence data table is converted to two separate cumulative occurrence tables over the ranges -400 through -0.1 and 0 through 400 respectively, as they are read into the FGEN program.

3.1.4.4 Load Sequence Generation

For each flight the program generates a sequence of random load occurrences for each phase sequentially through a particular mission type. The total number of occurrences in each phase is determined by scaling from the duration of each phase and the total number of load occurrences recorded in the load occurrence tables for that phase. The generating sequences are somewhat different for Nz and VTMX as outlined separately below:

Nz occurrences: For each load occurrence within a phase of a flight a particular flight condition is selected at random from the cumulative occurrences of flight conditions within that phase. Having selected a flight condition, the program selects on a random basis an Nz level from the cumulative occurrence table for that particular flight condition and phase. The value of Nz corresponding to that selected level is then paired with an Nz value of 1.0, representing 1 g level flight, to form a load sequence pair, which is then arranged in valley-peak order. Thus every occurrence

in the Nz tables is taken to represent a single valley-peak load sequence.

VTMX occurrences: For each two VTMX load occurrences within a phase, two VTMX occurrences are drawn randomly from the mission-phase occurrence totals; one each from the lower and upper halves of the cumulative occurrence tables formed from the SOUP program data tabulations. Thus, unlike the Nz data counts, a VTMX occurrence is taken to mean a single load level rather than an implied pair.

3.1.4.5 Load Data Transformation

After each random load sequence data value is selected as outlined above, it is transformed to appropriate bending moment or stress values depending on the stress sequence specification selected in the MODES program. These specifications follow a consistent format in which each particular specification consists of a data basis (Nz or VTMX), a bending moment table (W.S. 29.5, W.S. 57, F.S. 405.5, or other), a stress multiplying factor (to convert bending moment to stress), and a file packing factor (to normalize the output data to a particular file format). The bending moment specifications consist of three-point piece-wise linear tables giving bending moment as a function of Nz value for a given flight condition number. This is depicted in Figure 6. Linear interpolation is used for Nz values between the three data points on a bi-linear curve. Bending moment tables, which allow transference from Nz to bending moments, were obtained from Reference 5 or 6 for F-5E aircraft and from Reference 7 for F-5F aircraft. These bending moments for symmetric maneuvers only.

3.1.4.6 Data Sequencing and Output

As each simulated flight is completed, the data is passed to a routine (FLTOUT) which enforces valley-peak sequence throughout the complete flight stress sequence record, divides the individual data values by the packing factor to conform to the required data format, and writes the data to the stress sequence data output file.

The stress sequence data output files have an 80 column width format. The first line is an A80 character format for a title line. The remaining lines

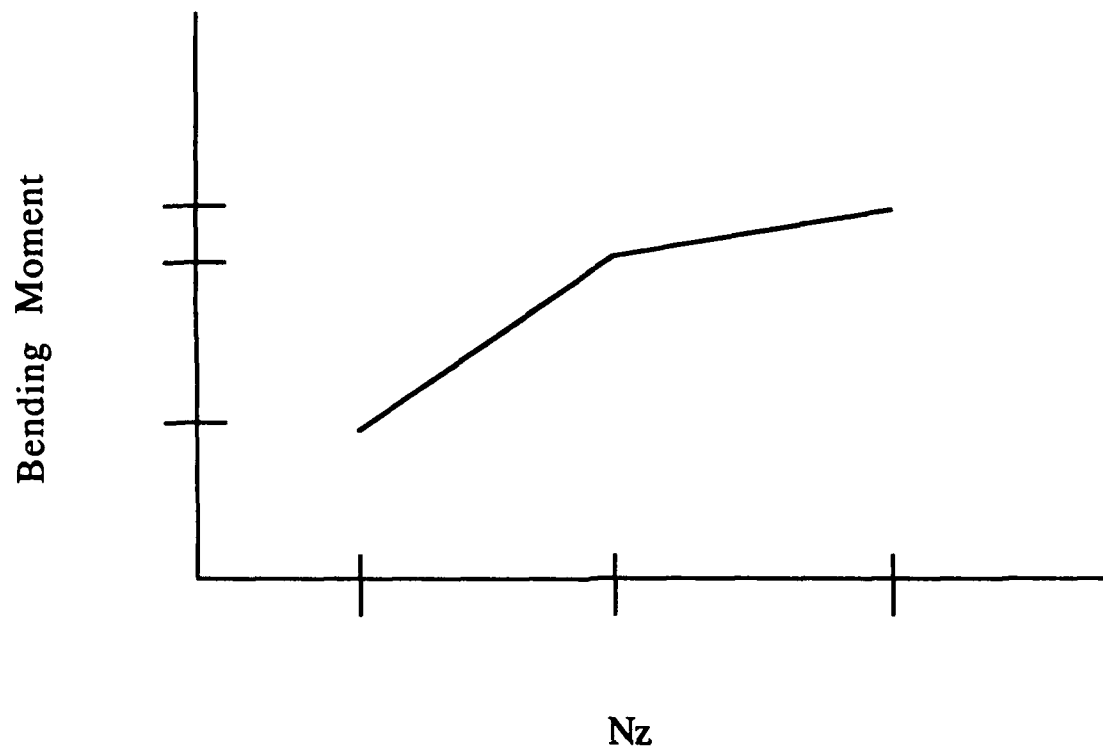


Figure 6
Bi-Linear Bending Moment versus N_z Curve

are 1615 numerical format. The first I5 in the second line (first numerical line) is for the "flight" number, in this case 1. The next I5 gives the number of stresses in the "flight," which fill the remaining 14 I5 slots of the first line and for as many I5 slots in the following lines as necessary. When all the stresses for the first flight have been listed, the flight number for the second "flight" (2) is placed in the first I5 slot of the next line. The number of stresses in the second "flight" are listed in the next I5 slot, followed by 14 stresses on the same line. The remaining stresses fill the I5 slots on the following lines as necessary. This process repeats itself until all of the stresses for all of flights have been listed.

3.1.5 FLTGEN Data Files

The FLTGEN program requires three basic data files for operation. These files are:

MISSPROF.TBL - Tables of mission profile data consisting of altitude, gross weight, and phase duration broken down by mission type and phase.

FCONNZOCC.TBL - Tables of Nz occurrences broken down by mission, phase, and flight condition.

PHASVTMX.TBL - Tables of VTMX occurrences broken down by mission and phase.

Two types of table format have been used with this program depending on the source of data. One set of data (prefixed with the line /FREE) were transcribed from the data given in Reference 5 and entered in Fortran list-directed format. The other two sets of data (corresponding to F-5E and F-5F aircraft) were developed during the present investigation from the SOUP programs and are basically the SOUP formatted print output files prefixed by a data line of /FIXED.

Initially, the program inquires for the missprof.tbl file and if this file is not found the program defaults to internal data comprising the mission profile data given in Reference 5. Otherwise the program reads the contents of this file and establishes the aircraft type and the mission profile tables. Subsequently, load occurrence tables are loaded from the appropriate files of either format in the

GETMIS program when called initially by the FGEN program.

4.0 Summary

Task 1 of the F-5 DTA was to analyze SAP flight data, and produce spectra representative of that usage. Other tasks of the F-5 DTA required spectra to be developed at other locations, for both DACT and SAP usages. A computer program (FLTGEN) was written to take the statistical output from SOUP and generate random stress sequences. This computer program, along with SOUP, allows the analyst to try "what if" scenarios, such as changing the amount of time in the primary phase (where most of the severe exceedances occur), or changing the relative percentages of the mission types. It is now possible to predict the effects of changes in the training syllabus, or to determine the effect of structural life when the aircraft is exposed to an operational theatre. The results of the complete effort by WKI has resulted in a change of the -6 T.O. inspection intervals for the F-5E and F-5F aircraft by the Air Force.

References

- (1) R.G. Forman, V.E. Kearney, and R.M. Engle, Jr., "Numerical Analysis of Crack Propagation in Cyclic Loaded Structures," Transactions of ASME, Journal of Basic Engineering, Vol. 89, No. 3, September, 1967, pp. 459-464.
- (2) J. Willenborg, R.M. Engle, Jr., and H.A. Wood, "A Crack Growth Retardation Model Using an Effective Stress Concept," AFFDL-TM-71-1 (FRP), January, 1971.
- (3) Alamo Technology, Inc., "Edit/Pre-Analysis V3.0, Volume I, User's Manual," ATI-87-0061, March, 1987. Also presented at the 1987 ASIP Conference; AFWAL-TR-88-4128 pp. 845-866.
- (4) Alamo Technology, Inc., "Spectra Operational Usage Profiles, Volume I, Display Program User's Manual," ATI-87-0743, and "Spectra Operational Usage Profiles, Volume II, Opts & Counts Program User's Manual," ATI-87-0273, February, 1988. Also presented at the 1987 ASIP Conference; AFWAL-TR-88-4128 pp. 793-818.
- (5) Alamo Technology Inc., "Analysis of F-5E MXU-553 Data," Contract No. F41608-86-C-C261, CDRL Sequence No. A027, Document No. ATI-87-0373, May 1987. (F-5E DACT usage)

(6) Northrop Corporation, "F-5E/F Fatigue Loads for the Damage Tolerance Assessment, Appendix A," Report No. NOR 76-164, March 1977.

(7) Northrop Corporation, "F-5E/F Fatigue Loads for the Damage Tolerance Assessment, Appendix B," Report No. NOR 76-164, March 1977.

RESEARCH ON MULTIPLE SITE DAMAGE

SAMPATH, S. G.
U.S. Department of Transportation
Federal Aviation Administration Technical Center
Atlantic City International Airport, NJ 08405

VIOLETTE, Melanie and TONG, Pin
U.S. Department of Transportation
Volpe National Transportation Systems Center
Cambridge, MA 02142

ABSTRACT

Multiple Site Damage (MSD) is a type of cracking that may be found in aging airplanes. The primary focus of the research presented in this paper is the effect of MSD on an airplane's structural integrity. This research includes investigations of the causes of MSD, the threshold at which MSD may first occur, crack growth and material behavior in the presence of MSD, and the potential interactions between MSD and repairs and corrosion. Nondestructive inspection techniques appropriate to MSD, and the frequency with which they are to be used, are also considered.

1. INTRODUCTION

The occurrence of Multiple Site Damage (MSD) in older aircraft was highlighted by the in-flight loss of a portion of the fuselage of an Aloha Airlines Boeing 737 in April, 1988. MSD is defined as a group of small cracks that appear in an airframe at about the same time and that originate from similar structural details close together. One example of a location in which MSD has been observed is the rivets in fuselage joints. MSD has been detected in aging aircraft of different makes and models, and has raised concern about the effect of MSD on the continuing airworthiness of older aircraft.

At the International Conference on Aging Airplanes in June, 1988, several interrelated technical areas were identified as key to a proper understanding of the aging airplane problem [1]. The Industry and the Federal Aviation Administration (FAA) have formulated an integrated plan to act on the specific recommendations emerging from the conference.

The FAA has developed a National Aging Airplanes Research Program (NAARP) to determine if current rules for design, inspection, and maintenance are sufficient to ensure the safety of the aging airplane fleet [2]. The Volpe National Transportation Systems Center (VNTSC) is assisting the FAA in conducting research pertinent to MSD and structural integrity. This paper contains an overview of the FAA/VNTSC program.

2. EARLY WARNING

The objective of this task is to determine the current and future compositions of the aging fleet in the U.S., and the current status of such airplanes in regard to requirements that have been especially mandated for aging airplanes, and to identify, through analysis, sites where increasing fatigue and corrosion-related incidences have occurred. The basis for the analysis will be technical data that is resident within the FAA and Industry. The principal output of this work will be a report which will enable the FAA to evaluate, monitor, and predict the structural integrity status of the commercial aircraft fleet.

The report will contain projections for the profiles of the fleet composition three, five and ten years from now, based on analysis of currently available fleet data (calendar age and utilization history, including flight cycles and flight hours). The report will contain a summary of airlines schedule data, currently being collected by FAA's Principal Maintenance Inspectors (PMIs).

The history of structural degradation, repairs, and operating environment will be examined, as well as the structurally significant Airworthiness Directives (ADs) and Service Bulletins (SBs). The structurally significant ADs applicable to each model will be assembled into a list, which will include the AD number and amendment number, and whether it requires repetitive inspections, terminating action or both. The area(s) of the airplane to which each structural AD applies will be identified on a diagram of the airplane. The extent of operators' compliance with each AD will also be determined.

The structural service difficulties that have been reported (SDR and other available data) will be analyzed, resulting in a series of charts separately depicting the reported instances of cracks, corrosion, and delamination or disbonding. The charts shall include a plot of all skin cracks reported on the model for the past five years and during the past six months. The plot should be depicted on a diagram or diagrams of the airplane, and on a graph where the ordinate will be the number of cracks and the abscissa, the number of cycles. Separate graphs will be made for specific areas of the airplane. Similar plots will be made for corrosion and for delamination or disbonding. An estimate of the accuracy of the data will be included for each chart.

3. EFFECT OF MSD ON DAMAGE TOLERANCE

Typical design of aeronautical structures, fuselages in particular, include the use of frame members and, in certain instances, tear straps, which act with other stiffening elements to allow the fuselage to withstand an isolated longitudinal crack up to two bays long. Fail-safety is preserved even if the crack is longer because the stiffening members will cause the longitudinal crack to change direction and run along the circumference, resulting in a "flap" and controlled decompression.

The objective of the current research is to determine if frames and tear straps can arrest a fracture in the presence of MSD. The general scenario assumes a fracture resulting from linkup of a group of MSD cracks. The fracture in this case lies along a skin splice, rather than in the mid-bay position usually assumed in present design and test practices. Also, the fracture may be advancing toward adjacent bays which contain additional (but as yet unlinked) MSD cracks.

To investigate the effectiveness of frames and tear straps in arresting a longitudinal fracture when MSD is present, a special loading fixture, which is shown in Figure 1, has been constructed to accommodate curved panels 66 inches on the circumference by 120 inches axially, with allowance for a range of 70 to 75 inches in radius [3]. The fixture is a shallow pressure box which accommodates the test article by means of floating seals. Pressure can be applied to the panel hydraulically or pneumatically. The pressure produces hoop stress in the skin, which is reacted through lateral turnbuckles. Hydraulic cylinders and turnbuckles at the ends of the panel produce an axial stress proportional to and in phase with the hoop

stress, thereby simulating the biaxial stress state found in a fuselage. The loading is controlled through an Instron Universal Testing Machine in conjunction with a hydraulic pressure unit, providing coordinated hoop and longitudinal loading of the test panel.

The structural elements of the test panel are shown in Figure 2. The dimensions, construction details, and materials were chosen to simulate configurations similar to those found in aging airplanes. The test panels do not precisely match the design of any actual aircraft model, and, therefore, the test results are intended to have only semi-quantitative significance. However, the panels will provide stress levels and structural flexibilities which do lie in the range of existing designs, and the test results will thus be sufficiently realistic for the purposes of drawing general conclusions about MSD behavior and calibrating damage tolerance estimation procedures.

The first panel which was tested was extensively instrumented, and used to demonstrate the successful operation of the test rig and to compare the strain fields in the panel to those calculated for a full fuselage. Figure 3 shows a comparison of the top skin stress, which combines the membrane and bending components, in a mid-bay position, both for the uncracked panel and with a crack present. The initial checks were successful. Subsequently, tests of fatigue, MSD crack growth, and residual strength have been conducted.

The first phase of testing, which has been completed, consisted of fracture resistance tests of single long cracks, to calibrate the analytical model and develop a predictive capability. Subsequent tests will focus on panel tolerance of two situations: small MSD cracks approaching linkup size, and a long lead crack with adjacent MSD.

Concurrent with the testing, detailed finite element analyses have been performed. The analysis has determined the rivet loads and stress distribution in the curved test panel and has predicted the internal pressure required to fracture the panel for a given crack length.

4. CAUSES AND LIKELIHOOD OF MSD

To identify and counter MSD as it appears in the current fleet, and to avoid MSD in future designs, it is important to understand which design features have an increased susceptibility to develop MSD, and to be able to predict how likely MSD is to occur in a given design.

Several flat coupon configurations have been analyzed to design a fatigue test coupon with a stress distribution equivalent to that of a fuselage. Four coupons are shown in Figure 4. Coupon A is a section of an unstiffened lap joint. Each of the other three coupons has three stiffeners, of about the same thickness as the skin, simulating tear straps. The stiffeners in Coupon B are full-length, while those in Coupons C and D are shorter. In addition, the stiffeners in Coupon D are wider at the lap joint and tapered at the ends.

Figure 5 compares the calculated stress distribution of each coupon with the stress distribution calculated for a full fuselage. Coupon C is considered adequate for fatigue testing, but Coupon D most closely simulates the fuselage stress distribution.

A test program is underway to identify design features which have higher MSD potential [4]. The basic test specimen is a 12 inch wide flat panel, with two short, straight tear straps, corresponding to one side of Coupon C of Figure 4. A large number of panels are being tested, in a test matrix that includes parameters such as stress level, skin thickness, rivet type, and rivet spacing. The loading in most of the tests is uniaxial tension, but some tests apply combined tension and shear, to determine the effect of mixed-mode loading on fatigue crack growth. Table 1 shows data from initial baseline testing, including the number of cycles required to initiate a 0.1 inch crack, cycles for a 0.25 inch crack, and the number of rivets at which cracks were present when the first crack reached 0.25 inches. The test panels listed in this table were 2024-T3 aluminum, with countersunk (flush) rivets, skin thickness 0.04 inches, and a maximum nominal stress of 16 ksi. Figure 6 gives a typical profile for the distribution of MSD cracks at 64,820 cycles.

Tests are also being conducted to determine the long-term effect of the terminating action which has been mandated by the FAA for certain MSD-prone lap joints. The terminating action replaces the upper-row countersunk rivets with larger, button-head rivets. In particular, these tests investigate the concern that, following the terminating action, MSD may recur in the inner skin, lower rivet row, where it is not easily detectable.

The fatigue test data will be used to calibrate a conceptual model [5] which ranks the MSD potential of alternative design details. The model combines fatigue and damage tolerance analyses in a practical engineering tool which yields a quantitative risk parameter. The analytical model is based on an assumed Weibull distribution for fatigue life.

5. INSPECTION INTERVAL

One key element of a successful inspection program is the interval between inspections. Too short an interval becomes economically burdensome, while too long an interval increases the possibility that a critical crack will go undetected.

A numerical model for predicting MSD crack growth and detection has been developed, based on conventional nondestructive inspection (NDI) techniques [7]. This model has been used to generate data on cumulative probability of detection, which is the probability that a crack will be detected at some time between initiation and failure. The results of this analysis indicate that the currently mandated inspection interval may need to be revised.

However, the model had to rely on NDI reliability data generated by measurements using flaw samples that were devoid of MSD. A program is being initiated to collect data on the probability of detection of MSD by NDI techniques currently used in the industry. The data will be used in an updated model, with which the requirement for the inspection interval will be reevaluated.

6. ALTERNATIVE CRACK MEASUREMENT TECHNIQUES

Established methods, such as optical and DC potential drop, for measuring crack length in fatigue and fracture experiments are suitable for measuring a single, identified crack of substantial length. However, these methods do not give accurate results when applied to much smaller cracks and potential crack sites in a MSD situation.

Alternating current potential drop (ACPD) equipment and procedures are being evaluated for use in measuring small cracks typical of MSD. Controlled laboratory experiments have been conducted, in which the ACPD method was used to measure crack length. The test specimens were subsequently fractured, and the actual crack lengths were verified fractographically. Initial tests indicate that the ACPD technique can be successfully used to measure MSD crack growth.

7. MATERIAL BEHAVIOR CHARACTERIZATION

A better understanding of material behavior in the presence of MSD will enable more accurate analysis techniques. Although several crack-tip parameters are widely recognized as growth criteria for the case of long, isolated cracks, no such parameter has been clearly identified for MSD. Both conventional and advanced fractographic techniques have been used to characterize material behavior in the presence of MSD.

The fracture features of riveted lap joint specimens tested in fatigue have been analyzed fractographically [8]. The investigation included a count of fatigue striation, spacing and density, assessment of the fracture mode in the cladding near the surface, and review of the mode of failure (plane stress versus plane strain). The crack growth rates were determined from the striation spacing and reported as a function of maximum stress values. The plastic zone size was correlated with the stress intensity factor calculated for the assembly being tested.

MSD crack growth has also been investigated using an advanced quantitative fractographic technique known as FRASTA (Fracture Reconstruction Applying Surface Topographic Analysis) [9]. A three-hole specimen with crack-starter notches at the center hole was tested, first under fatigue cycling, then by applying a monotonically increasing load until the specimen failed.

Analysis of the fracture surfaces produced crack profiles and fractured area projection plots for both fatigue and stable crack growth. The results revealed significant tunneling of the crack front during the early stages of fatigue cycling, and that the crack grew at a constant opening angle during stable crack growth under monotonic loading. A finite element analysis was used to confirm the fractographic results, and to calculate two crack-tip parameters: the stress intensity factor (K) and the J-Integral.

8. DYNAMIC EFFECTS DURING MSD LINKUP

Dynamic fracture behavior may differ substantially from static test failure conditions, and neglect of dynamic effects during linkup of MSD may be unconservative because the inertial forces during linkup will amplify the crack driving force. A combined experimental and analytical approach will result in an estimate of the magnitude of these dynamic effects.

Preliminary analysis was performed to select a specimen configuration likely to produce dynamic linkup of MSD cracks. The configuration is now undergoing testing, during which the crack lengths, applied load, far-field stress levels, and overall specimen displacement are measured using high-speed instrumentation. The data is used as input to the analysis, which will re-create the MSD linkup, and extract the material's dynamic fracture toughness. This value will then be used to predict analytically the results of future tests, and to estimate the significance of the dynamic effects.

9. DAMAGE TOLERANCE OF REPAIRS

Despite the fact that modern transport airplanes are designed to damage tolerance requirements, most repairs to aircraft structures have hitherto been designed on the basis of static strength equivalency. Improper repairs, or several repairs in close proximity, can degrade the fatigue life and damage tolerance of the original structure.

One objective of this work is to develop repair analysis tools, such as load spectra and stress analysis methods, which will aid repair stations in designing repairs [10]. A second objective is to identify risks of MSD, decreased damage tolerance, or reduced inspectability associated with modifications covered by Supplemental Type Certificates (STCs).

A computer program based on a two-dimensional compatible displacement method has been developed, to analyze different repair types and configurations. A computer program based on the hybrid finite element method is also being developed for stress analysis of repair doublers [11]. The programs are being validated by comparison with test data and previous analytical results.

General fatigue load spectra have been derived for stress levels in fuselages, for use in testing and analysis of repair patches. Tests using wide flat panels are being conducted to assess the fatigue resistance and structural integrity of a few basic repair configurations.

The use of bonded composite repair patches is also being investigated. Composite patches are desirable because of their light weight and high strength, stiffness, and resistance to fatigue and corrosion. The advantages of bonded repairs include the gradual load transfer through the bond and the absence of fastener holes, thus eliminating much of the stress concentration problems associated with conventional, mechanically fastened repairs.

This research effort will examine different bonding methods and materials, and their relative advantages and disadvantages. A data base will be developed to assist in the selection of appropriate composite materials, adhesives, application techniques, and crack inspection methodology. Procedures for analyzing load characteristics of bonded repairs will be developed and incorporated in a general-purpose computer program. The program will be used to analyze a number of test cases, and the results will be compared with experimental data. Bonded repair methodology for a typical fuselage lap joint containing MSD will be developed and tested.

10. CORROSION AND STRUCTURAL INTEGRITY

Evidence of corrosion in the airplane fleet is abundant, but its effect on structural integrity and fatigue life is inadequately understood. The objective of this effort is to develop a quantitative understanding of the synergistic relationship between mechanical fatigue and corrosion.

Procedures are being developed for reproducing the important forms of corrosion, and for accelerated testing of corrosion. A series of environmentally-assisted fatigue tests for long hold times will be performed, and the stress distribution and fatigue performance of corroded joints will be evaluated analytically and experimentally.

11. COMMUTER FLEET ASSESSMENT

Many commuter airplanes currently operating in the United States were designed under the "safe-life" philosophy, which has since been superseded by the "damage tolerance" philosophy. The objectives in this work are to assess the effects of aging on the structural integrity of commuter airplanes, and to determine the practicality of retroactive application of damage tolerance methodology.

The commuter fleet assessment is being conducted with the assistance of a team of industry and government experts in the areas of damage tolerance analysis and small plane design and maintenance. The team has visited several commuter airplane manufacturers, to obtain information about their design practices and to determine which models would benefit from development of a Supplemental Structural Inspection Document (SSID) program. This effort includes a review of the applicable Airworthiness Directives and Service Bulletins, and an assessment of the current repair and corrosion control programs. Simplified methods for performing damage tolerance analysis of commuter planes are being developed.

REFERENCES

- [1] "Proceedings of the International Conference on Aging Airplanes," Federal Aviation Administration, U.S. Department of Transportation, DOT-TSC-FA890-88-26, August, 1988.
- [2] "Program Plan, National Aging Aircraft Research Program," Federal Aviation Administration Technical Center, U.S. Department of Transportation, DOT/FAA/CT-88/32-1, Draft Plan, September, 1990.
- [3] Samavedam, G., Hoadley, D. and Davin, J., "Test Facility for Evaluation of Structural Integrity of Stiffened and Jointed Aircraft Curved Panels," Proceedings of the International Symposium on Structural Integrity of Aging Airplanes, Atlanta, GA, March, 1990.
- [4] Mayville, R., Hilton, P. and Samavedam, G., "A Laboratory Study of Fracture in the Presence of MSD," Proceedings of the International Symposium on Structural Integrity of Aging Airplanes, Atlanta, GA, March, 1990.
- [5] Orringer, O., "How Likely is Multiple Site Damage?" Proceedings of the International Symposium on Structural Integrity of Aging Airplanes, Atlanta, GA, March, 1990.
- [6] Tyson, J. and Feferman, B., Contractor Technical Report on Shearography and Aging Aircraft, VNTSC contract DTRSS7-90-P-80922.
- [7] Sampath, S. and Broek, D., "Estimation of Requirements of Inspection Intervals for Panels Susceptible to Multiple Site Damage," Proceedings of the International Symposium on Structural Integrity of Aging Airplanes, Atlanta, GA, March, 1990.
- [8] Pelloux, R., "Macro and Microfractographic Analyses of Initiation and Growth of Fatigue Cracks at Rivet Holes," Proceedings of the International Symposium on Structural Integrity of Aging Airplanes, Atlanta, GA, March, 1990.
- [9] Kobayashi, T., Shockey, D. and Giovanola, J., "Reconstruction of Fatigue Crack Behavior and Determination of Toughness Parameters from Fracture Surfaces," Proceedings of the International Symposium on Structural Integrity of Aging Airplanes, Atlanta, GA, March, 1990.
- [10] Rice, R., Smith, S. and Sampath, S., "Issues Related to Repairs of Aging Aircraft," Presented at the International Symposium on Structural Integrity of Aging Airplanes, Atlanta, GA, March, 1990.

- [11] Tong, P., Greif, R. and Chen, L., "Application of Hybrid Finite Element Method to Aircraft Repairs," XXII National Congress on Fracture Mechanics, Atlanta, GA, June 1990.

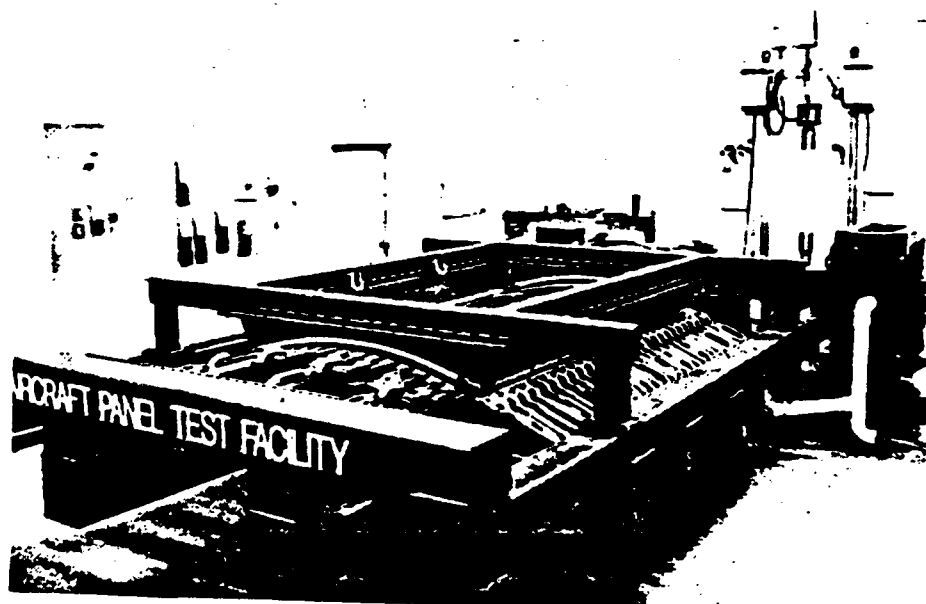
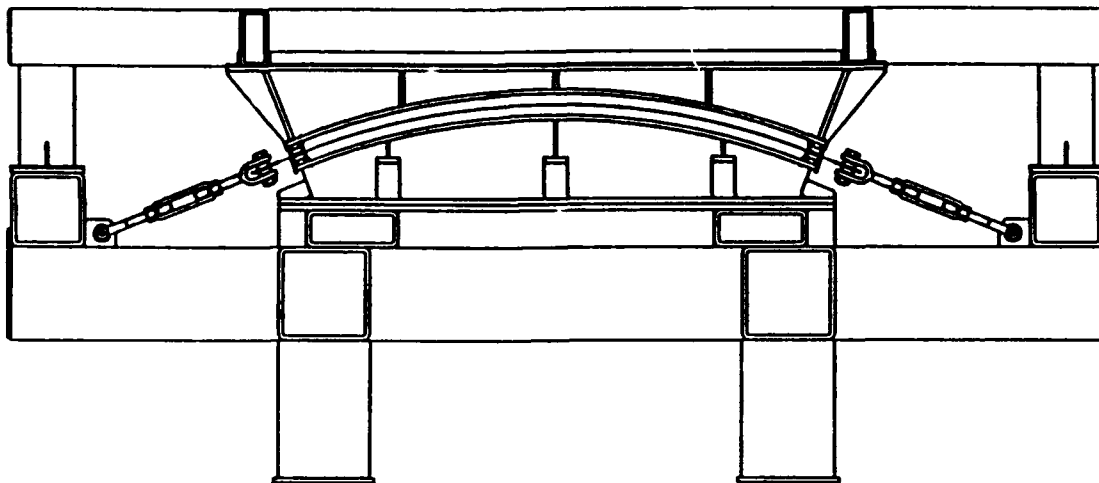


FIGURE 1. TEST FIXTURE

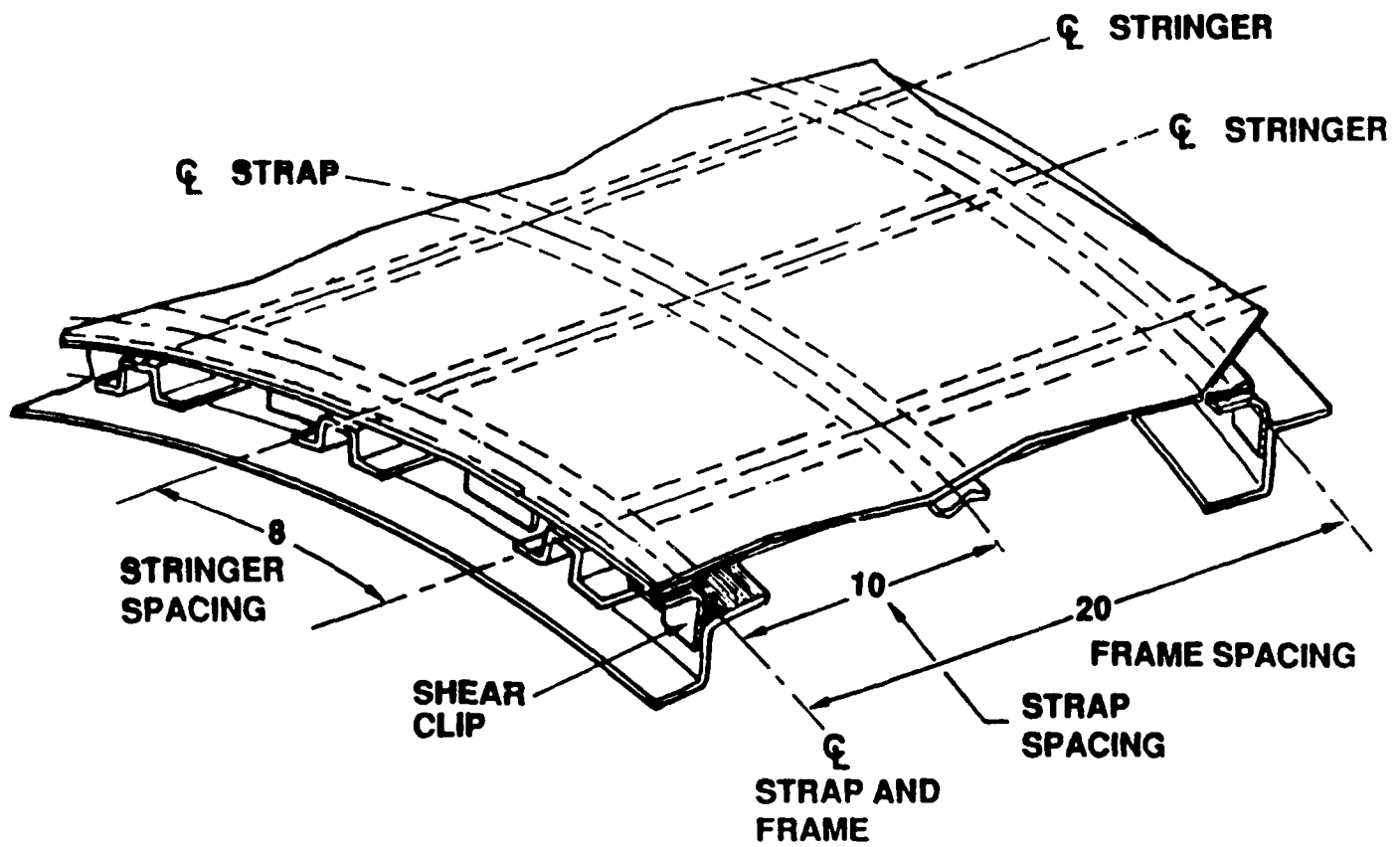
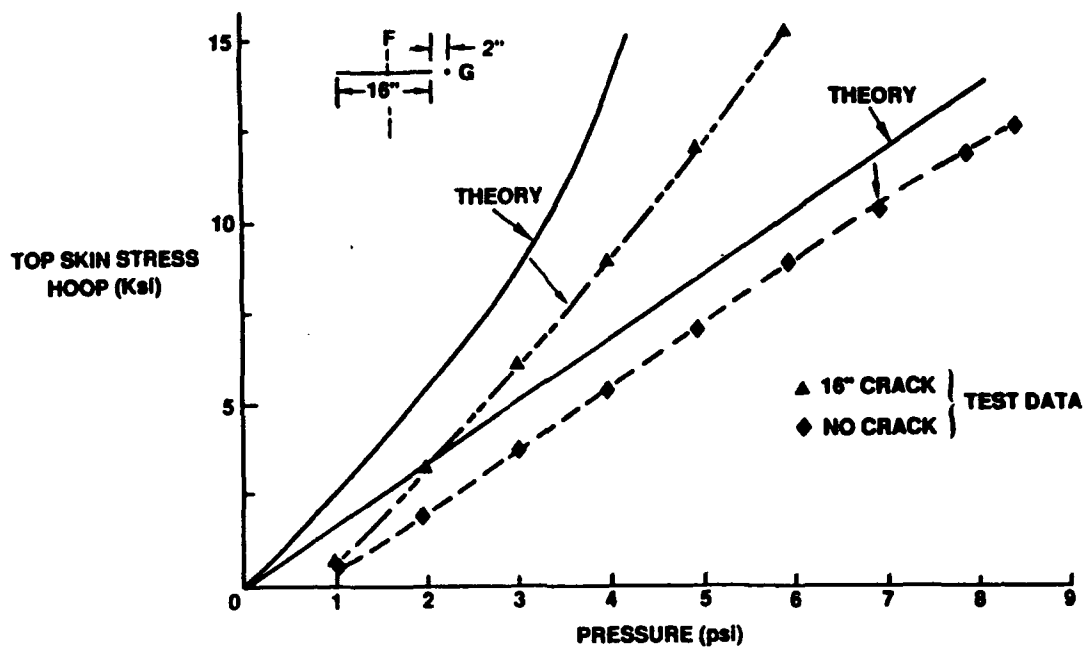
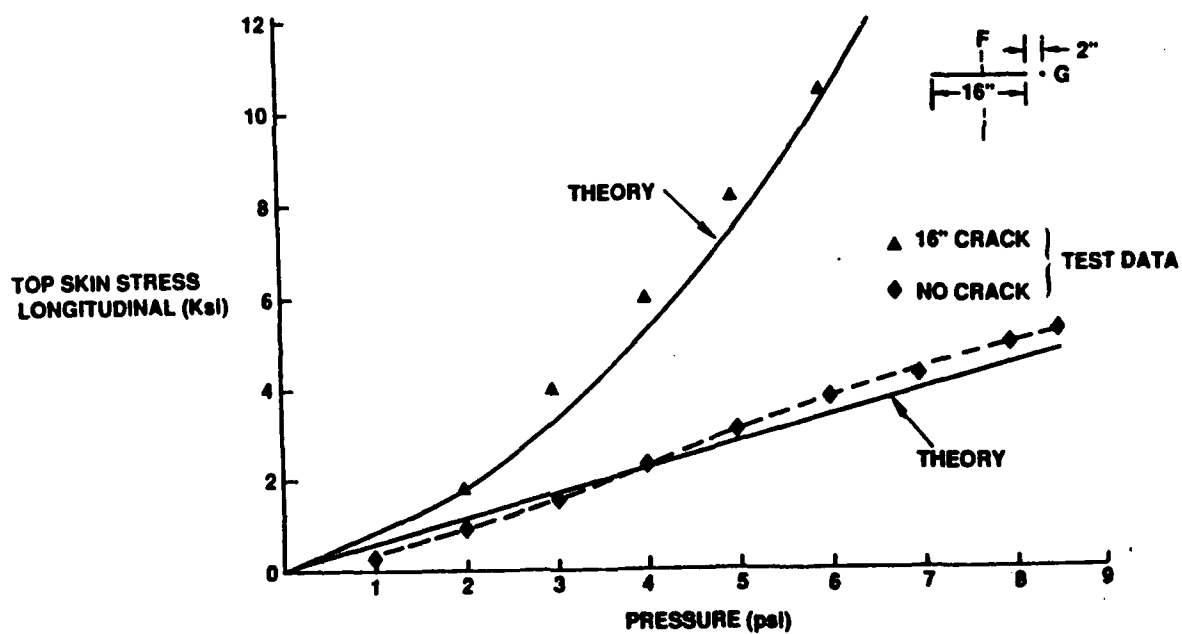


FIGURE 2. TEST PANEL



A. HOOP DIRECTION



B. LONGITUDINAL DIRECTION

FIGURE 3. COMPARISON OF STRAIN GAGE MEASUREMENTS WITH CALCULATED VALUES OF TOP SKIN STRESS (MEMBRANE + BENDING).

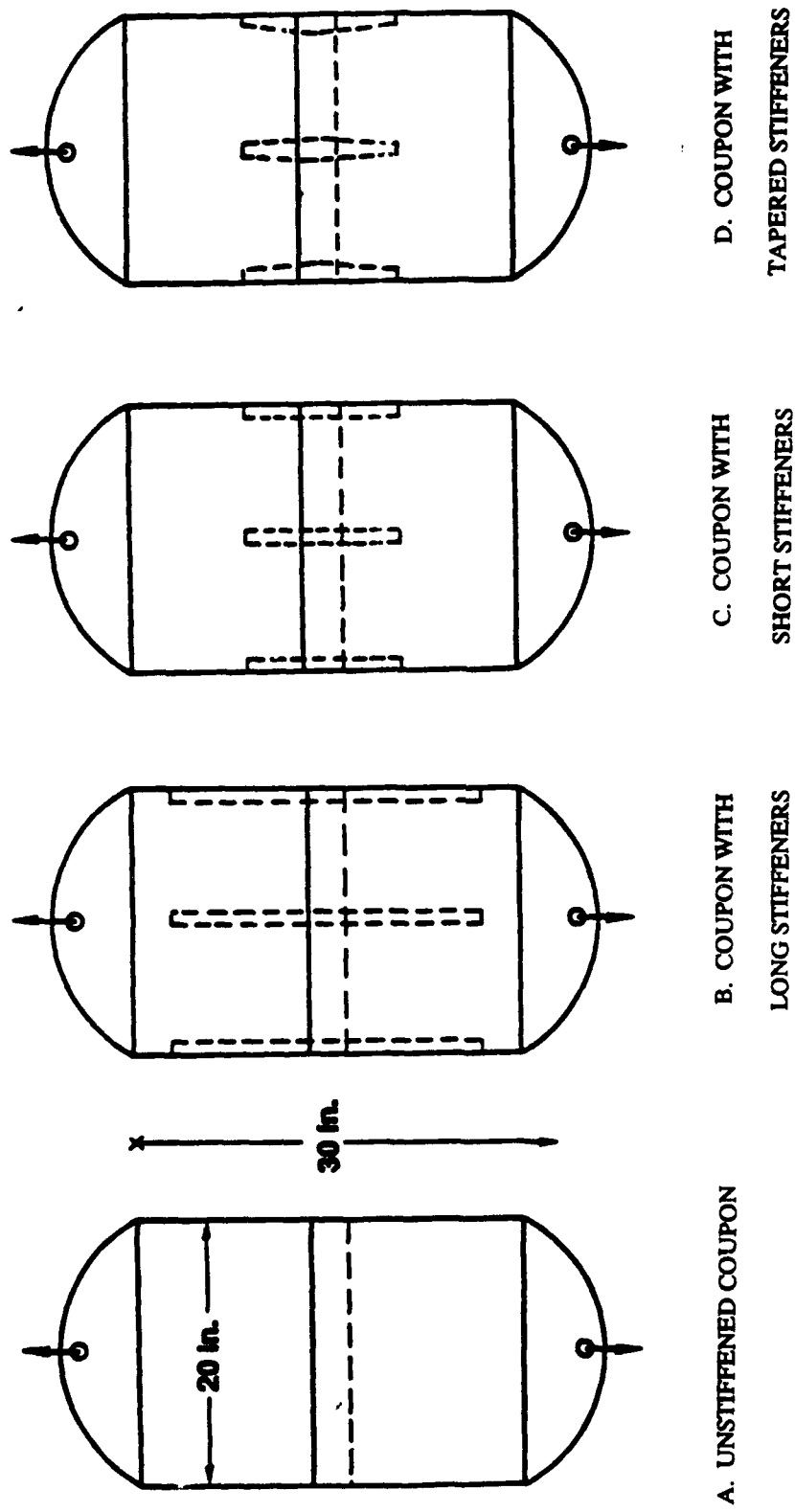
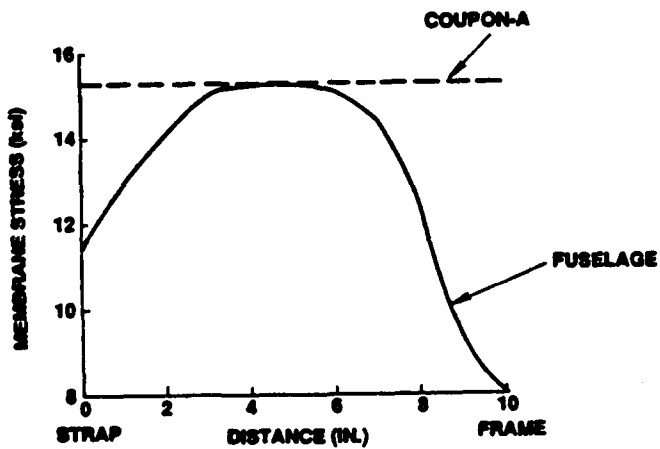
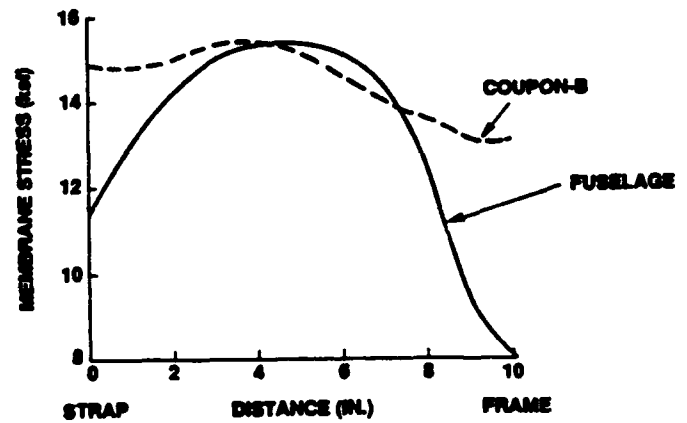


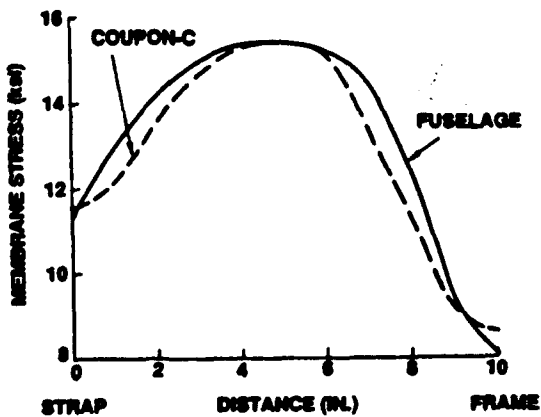
FIGURE 4. COUPON CONFIGURATIONS



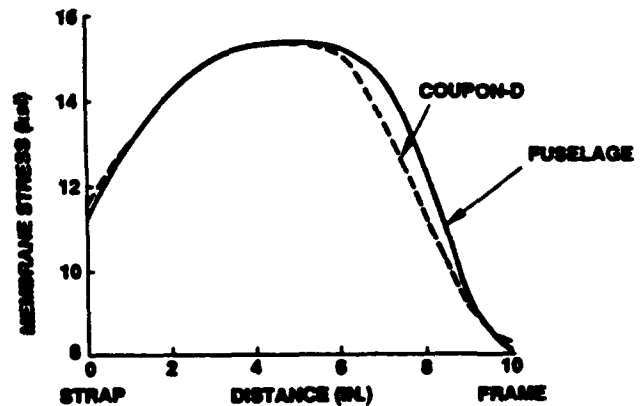
A. UNSTIFFENED COUPON



B. COUPON WITH LONG STIFFENERS



C. COUPON WITH SHORT STIFFENERS



D. COUPON WITH TAPERED STIFFENERS

FIGURE 5. COMPARISON OF FUSELAGE STRESS DISTRIBUTION WITH COUPON STRESS DISTRIBUTIONS.

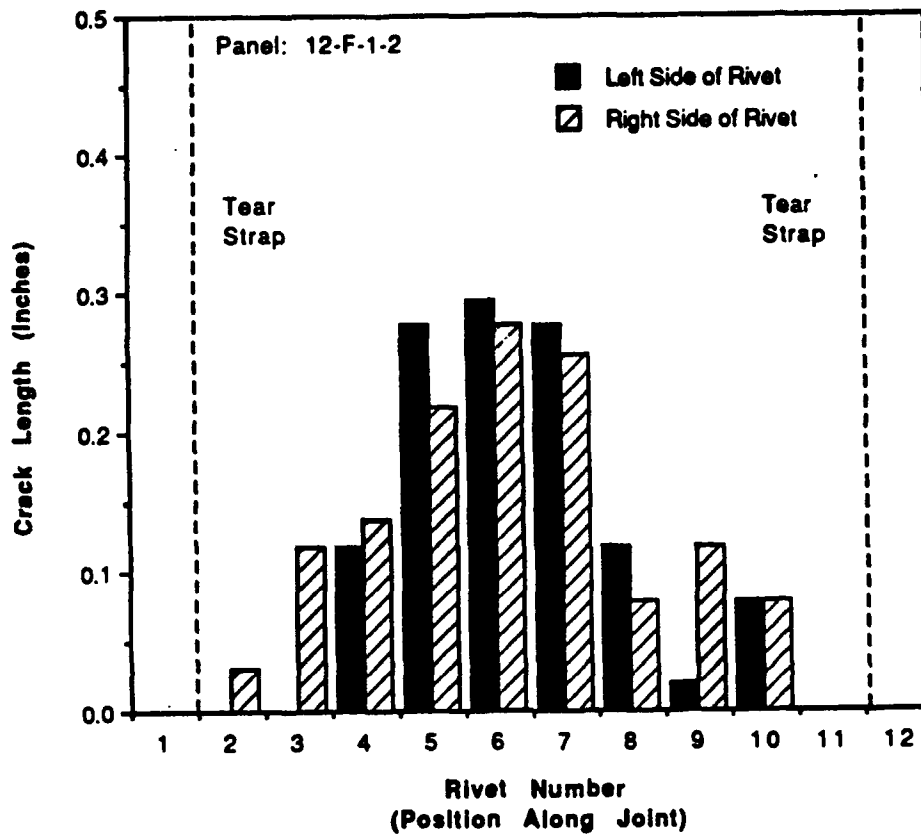


FIGURE 6. PROFILE OF CRACK LENGTH VS. POSITION FOR TYPICAL TEST PANEL AT 64,820 CYCLES.

Top Row Rivet Type	Panel Width (inches)	Number of Cycles to First 0.1 inch Crack	Number of Cycles to First 0.25 inch Crack	% of Cracked Rivet Holes
Flush	20	54,330	67,300	50%
Flush	12	30,000	44,450	50%
Flush	12	50,930	63,319	70%
Flush	12	40,667	49,455	92%
Flush	12	40,000	56,500	42%
Flush	12	82,000	100,000	42%
Flush	12	53,000	71,000	58%
Flush*	12	28,215	33,686	67%

*Test was performed in tension/shear configuration

MATERIAL: 2024-T3 ALUMINUM

SKIN THICKNESS: 0.040 INCHES

MAX. NOMINAL STRESS: 16 KSI (R = 0.05 - 0.1)

TABLE 1. FATIGUE TEST DATA FOR 12 INCH TEAR STRAP REINFORCED TEST
PANELS.

Status of F-16
Durability Testing

Capt Sid Perkins *S* 12 Dec 1990
ASD/YPEF
Wright-Patterson AFB

Outline

- Background
- Types of Testing
- Problems Identified/Actions Being Taken
- Summary

Background

- F-16 is one of the most successful airplanes ever
 - Developed by US and four European Participating Air Forces (EPAF): Belgium, Denmark, Norway, Netherlands
 - Almost 15 years since first introduced
 - Well over 2000 built
 - Serves in 17 air forces worldwide
- "Blocks"
 - First aircraft built were "A/B" aircraft
 - Block 1, 5, 10, and 15
 - Subsequent aircraft are "C/D" aircraft
 - Block 25, 30/32, and 40/42
 - Block 50/52 aircraft due to deliver Oct '91

Type of Testing

- Block 30 Full-Scale Durability Test
 - First full-scale durability test since FSD
 - Currently at 7330 hours
 - Have spent last year replacing test article center fuselage with a Block 15 center fuselage
- Block 40 Aft Fuselage Durability Test
 - Currently at 10,355 hours
 - Down for repairs in the transition structure
- "Heavyweight" Landing Gear Fatigue Tests
- Various Coupon, Subcomponent Tests
- Field Operations

"Heavyweight" Landing Gear Fatigue Tests

- Developed for use in the F-16XL program of early '80s
- First installed on Block 40/42 aircraft
- Will undergo six full lifetimes of fatigue testing
 - Four lifetimes of ground loads
 - Six lifetimes of airloads
 - Final two lifetimes of ground loads

Problems Discovered/Actions Being Taken

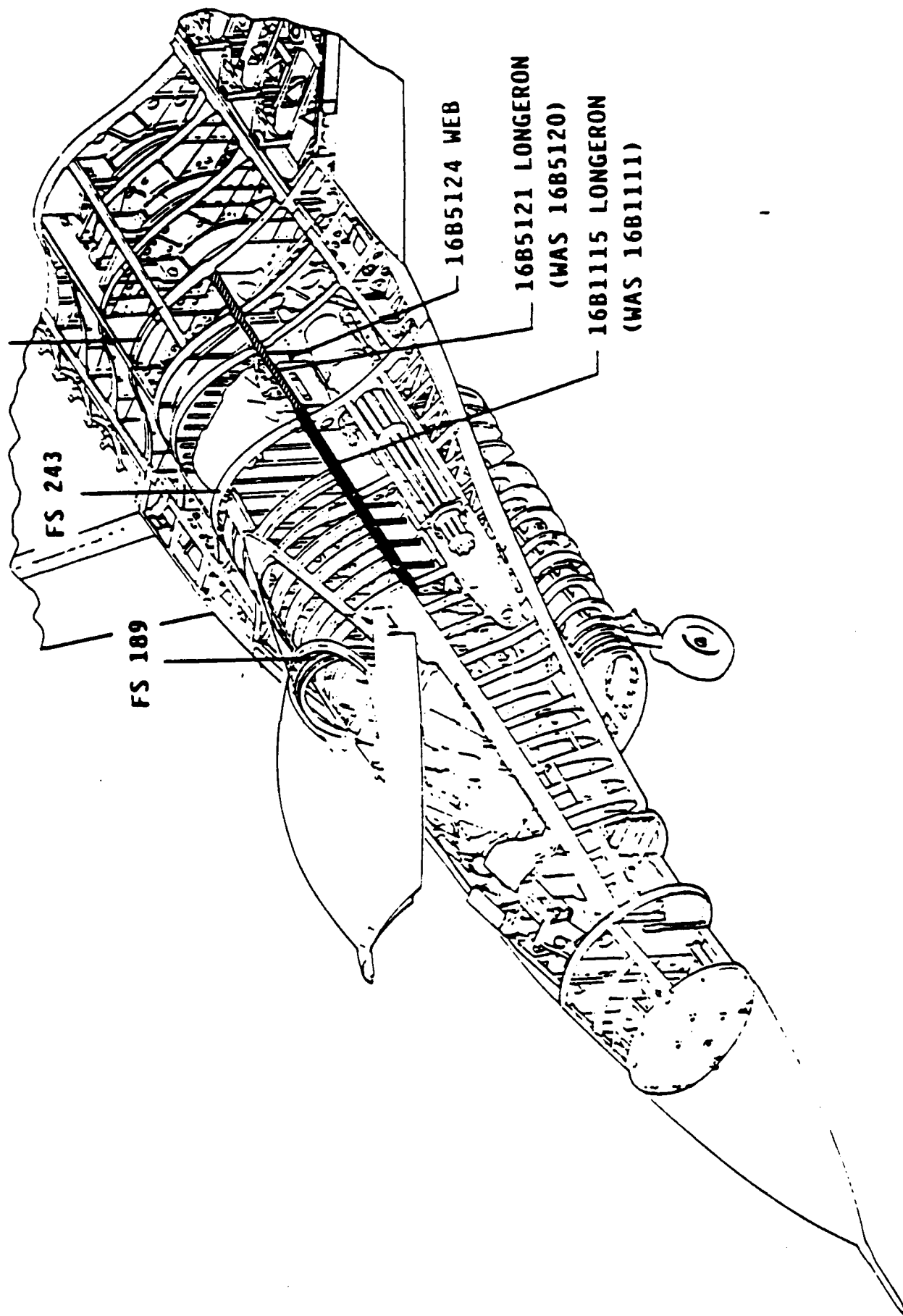
- Discussion of Problem
 - Method of discovery
 - Pictures/Sketches (where available)
- Aircraft Affected
- Actions Being Taken

Forward/Center Fuselage Longerons (P/N 16B1111/5120)
and Web (P/N 16B5124)

- Where Discovered:
 - Block 30 Full-Scale Durability Test (multiple failures)
- Actions
 - Block 40
 - ECP 1840: Service life extension; new materials and new geometry
 - ECP 1871: Full retrofit with Block 50 configuration
 - Block 30
 - New designs/materials being placed on Block 30 test
 - Block 15
 - Improvement ECP has been initiated for new EPG and FMS production Block 15s

F-16C MODEL

FS 293.8



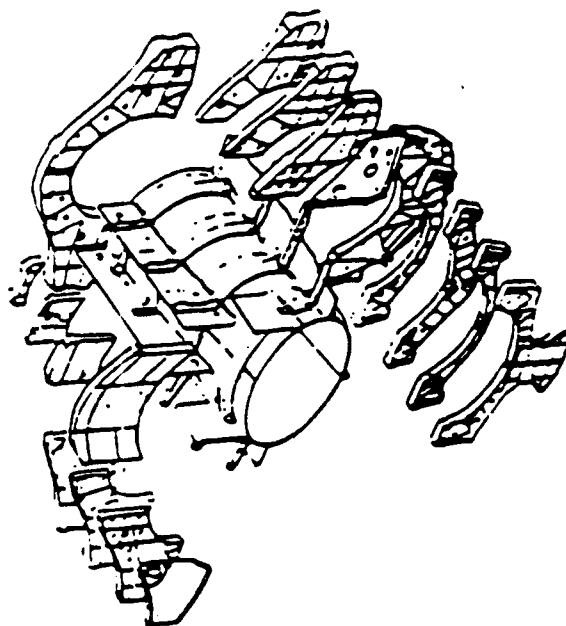
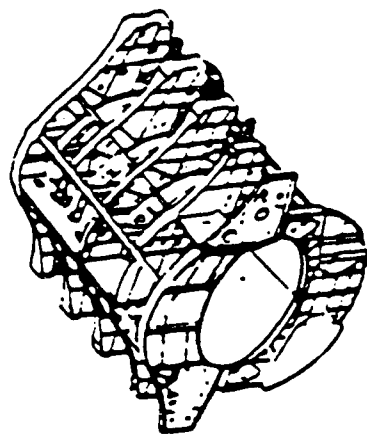
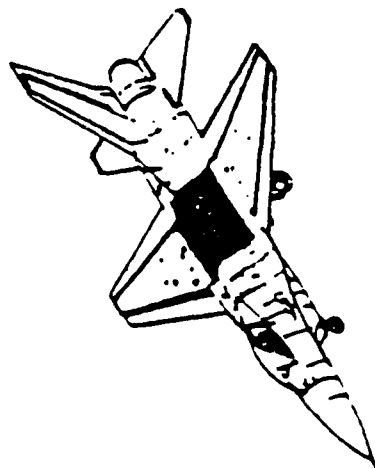
Center Fuselage Bulkheads and Fuel Shelf
(@ FS 309, 325, 341, 357)

- Where Discovered:
 - Block 30 Full-Scale Durability Test (multiple locations)
- Actions
 - Block 40
 - ECP 1910 will coldwork center fuselage bulkheads in production
 - Will also address coldworking in retrofit
 - Block 30
 - Addressed by retrofit under ECP 1607R1
 - Block 15
 - OO-ALC has initiated an enhancement study to identify tooling requirements for retrofit



ECP 1607 - WING SUPPORT BULKHEADS

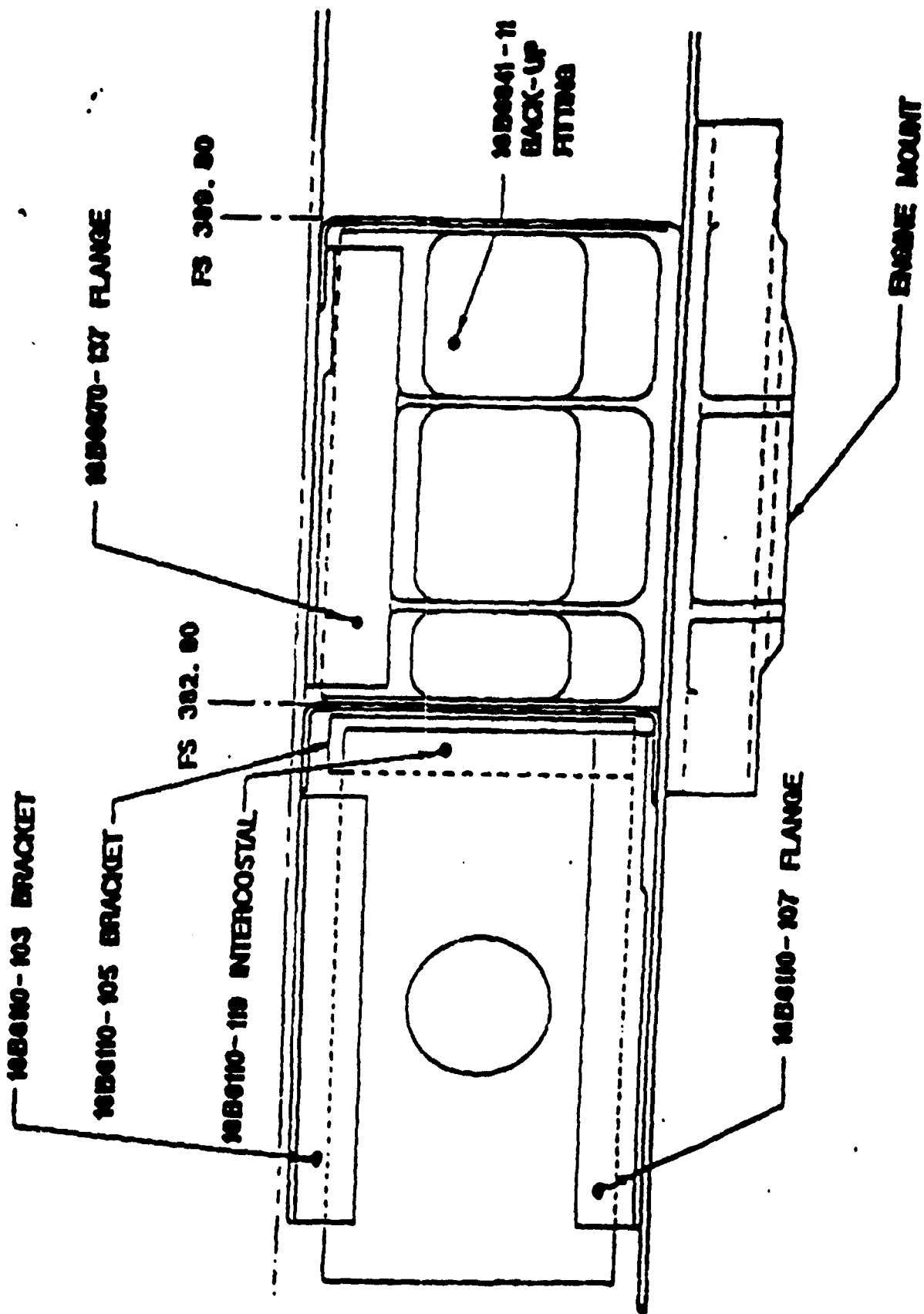
SERVICE LIFE ESTIMATE: 2500 - 4000 HOURS



P&W Forward Engine Mount Backup Fitting

- Where Discovered:
 - Block 40 component testing program
- Actions
 - Block 40
 - Change to new material (titanium)
 - Will retrofit all Block 42s with new titanium fitting
 - Block 25/32
 - Will require retrofit with new titanium fitting
 - Block 15
 - Will receive new titanium fitting in production
 - Other A/Bs may only require brace for retrofit

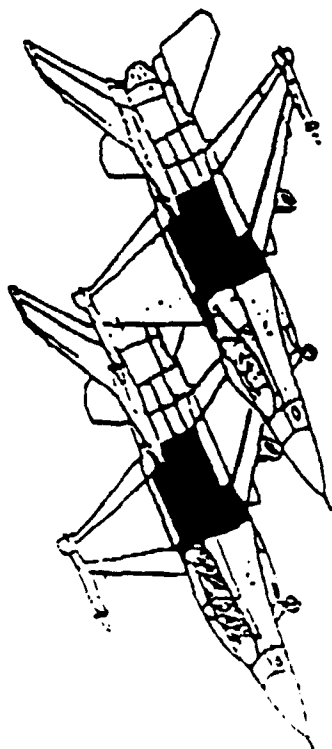
27



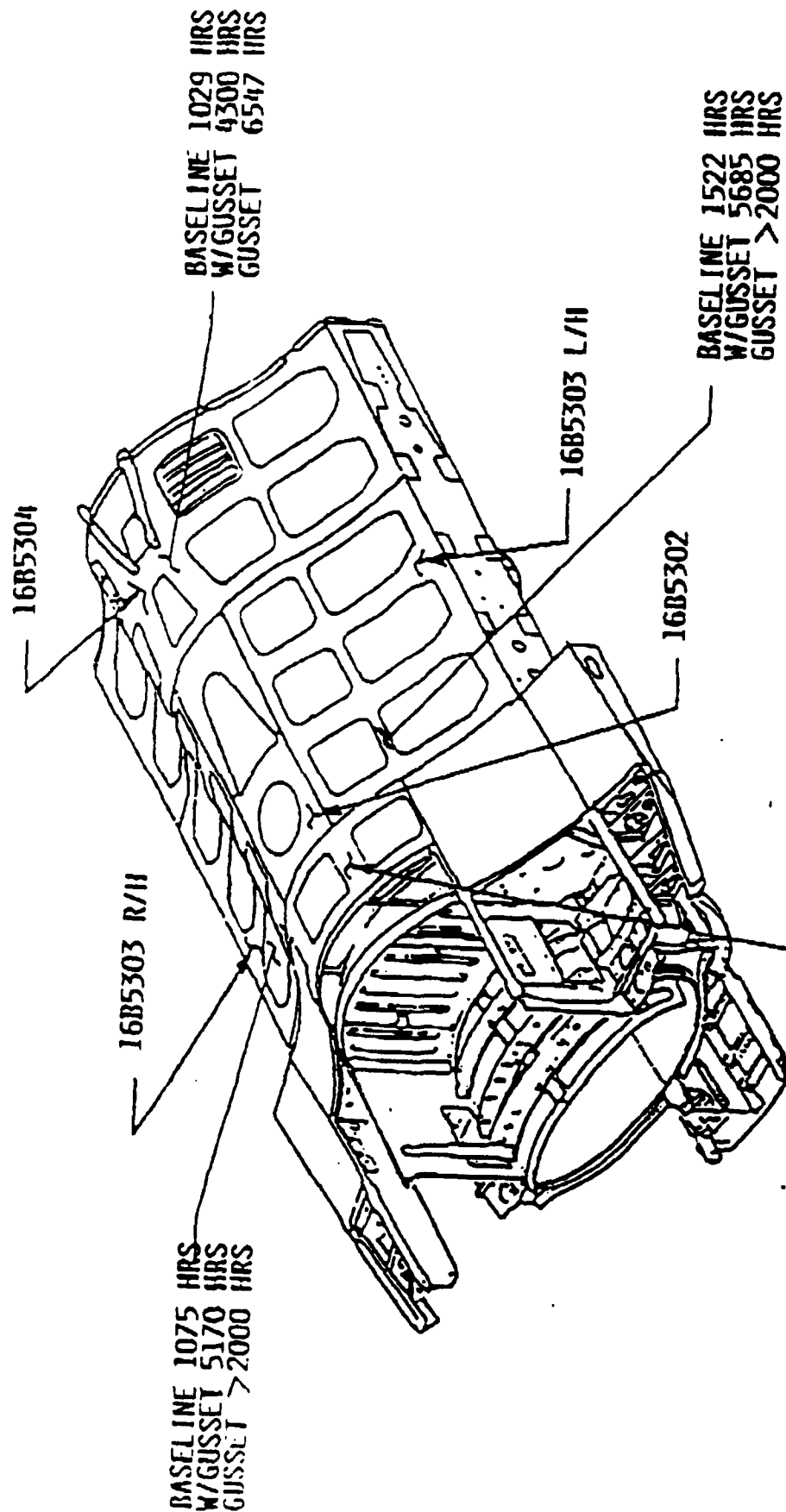
TITANIUM FITTING

Upper Center Fuselage Skins
(P/N 16B5301/5303/5304)

- Where Discovered:
 - Block 30 and Block 40 durability testing
- Actions
 - Block 40
 - Final production fix is production breakin of Block 50 upper skins
 - Interim production fix and interim retrofit will extend service life to approximately 2000 hours
 - Full retrofit will allow skins to meet the 8000-hour service life requirement
 - Block 30
 - Retrofit concept similar to Block 40 final retrofit



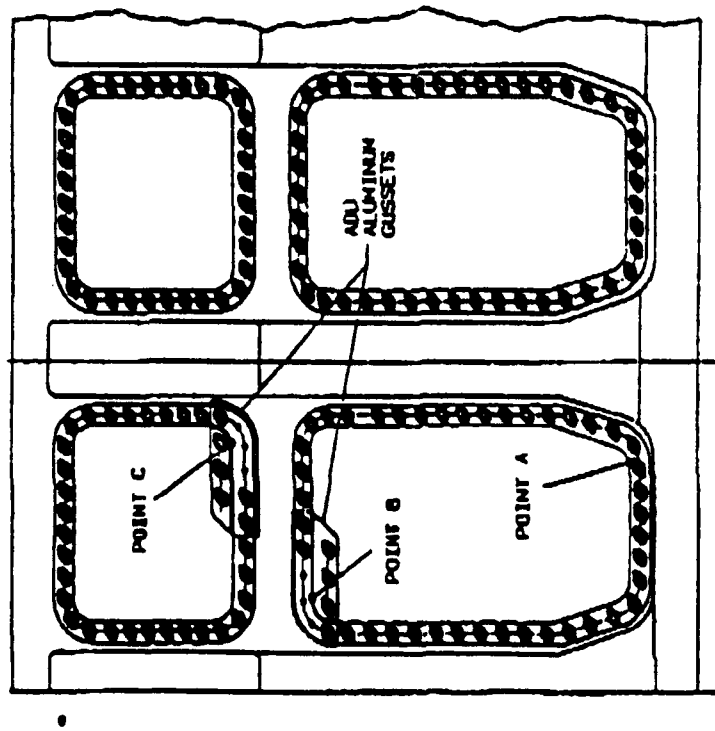
CENTER FUSELAGE DURABILITY DATA



will be replaced
at final retrofit (Falcon step)

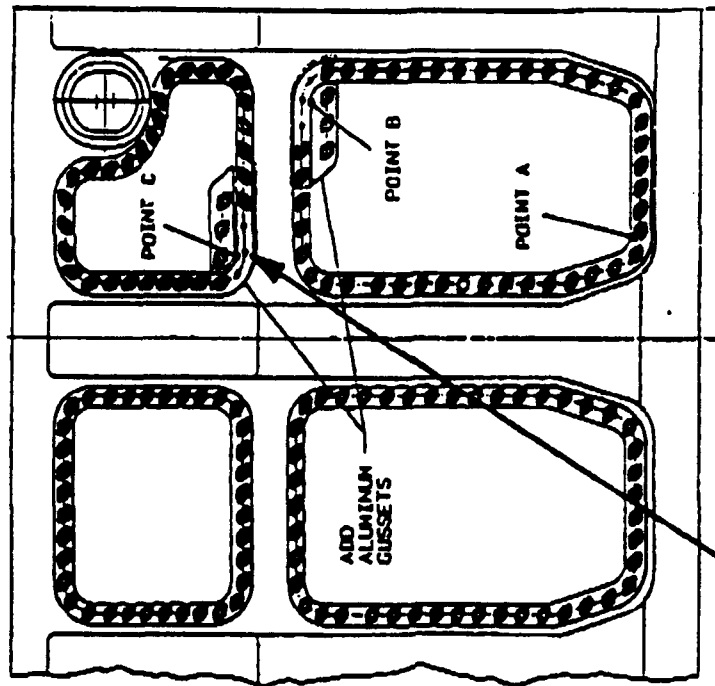
(7)

16B5303 UPPER FUSELAGE SKIN
INTERIM IMPROVEMENT (LWS)



FS 309.8
LH SIDE
VIEW LOOKING DOWN
BLOCK 40

16B5303 UPPER FUSELAGE SKIN
INTERIM IMPROVEMENT (RWS)

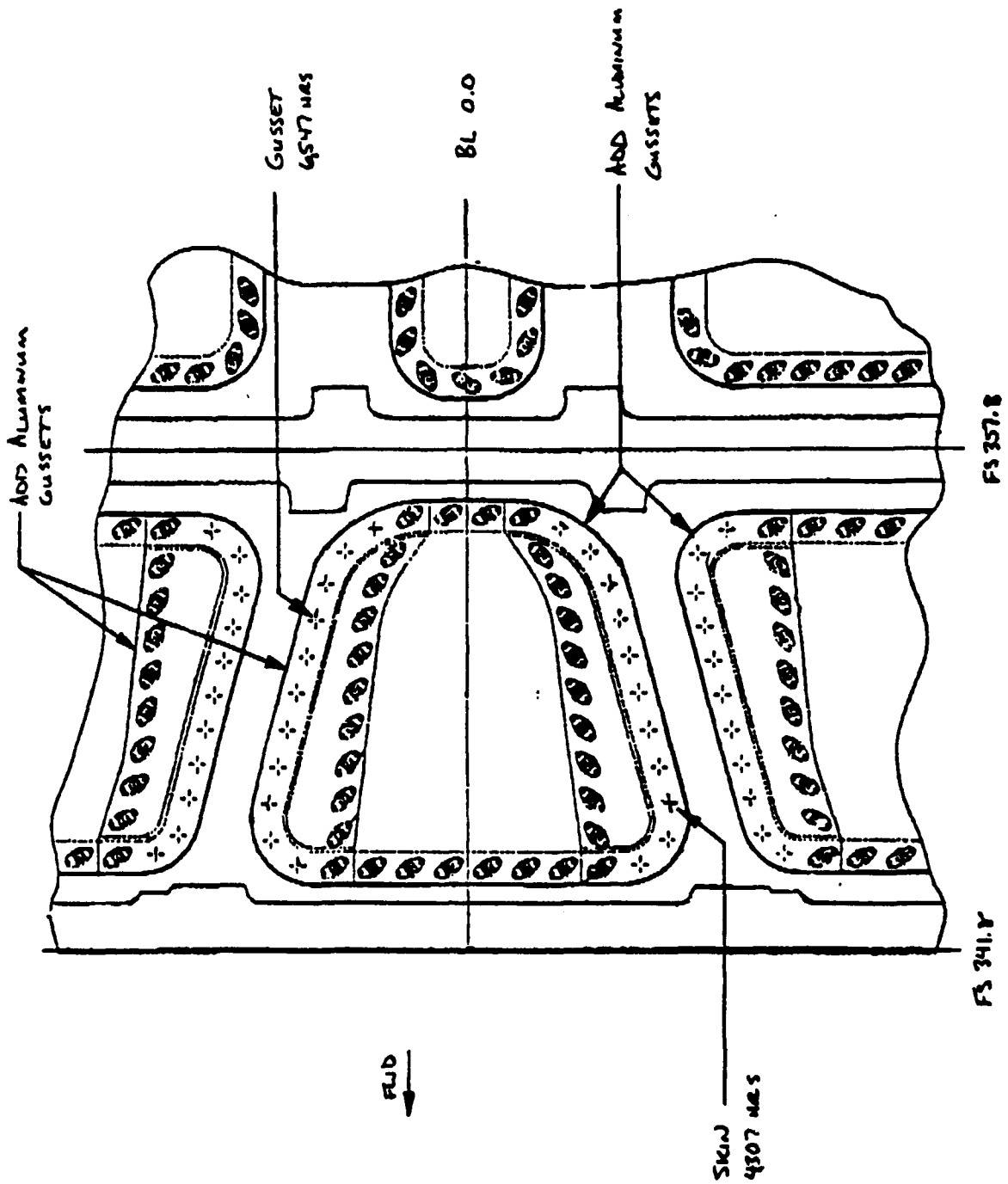


FS 309.8
RH SIDE
VIEW LOOKING DOWN
BLOCK 40

SKIN CORRECTION
POINT : 5170 WS
DURABILITY

9

465304 UPPER FUSelage SKIN
INTERNAL IMPROVEMENT



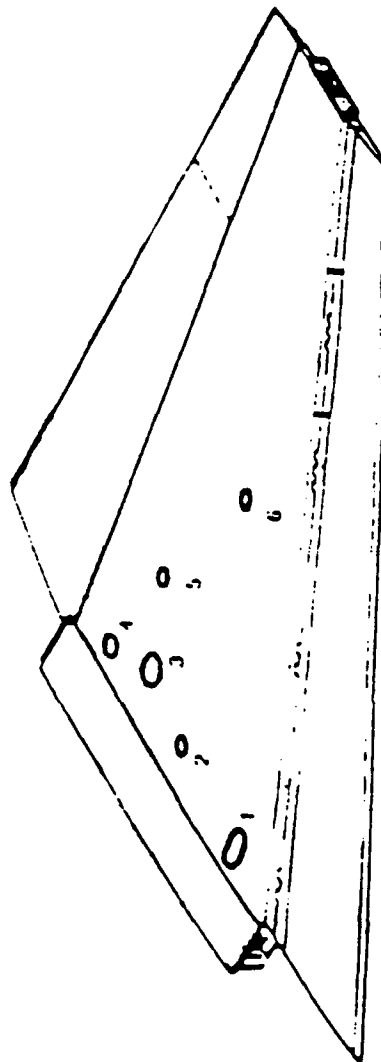
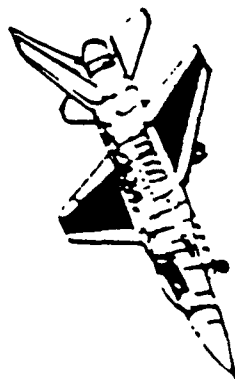
Upper Wing Skin Access Holes #2, 5, and 6

- Where Discovered:
 - Block 40 Component Testing
- Actions
 - Block 40
 - Final production fix is production breakin of Block 50 upper wing skins
 - Interim production fix is Block 40 upper wing skins with doublers
 - Final retrofit: probably some form of split doublers



ECP 1637 - UPPER WING SKIN ACCESS HOLES

SERVICE LIFE ESTIMATE: 2000 - 3000 HOURS



ADD INTERNAL
DOUBLER ON
RHS ONLY

CL SPAR 6

CL SPAR 7

CL SPAR 8

ADD INTERNAL
DOUBLERS

2

- Where Discovered:
 - Block 30 full-scale durability test
- Actions
 - Block 40
 - New design for first Block 40 aircraft
 - Under analysis due to Block 30 test failures
 - Block 30
 - Test article being fitted with strake support similar to Block 40 design

Bulkhead Web at FS 293

- Where Discovered:
 - Field Failures
- Actions
 - Block 40
 - Thicker webs were broken in during Block 40 production
 - Block 30, Block 15
 - Probable retrofit fix: bonded doublers

Leading Edge Flap Nosecap Rivets

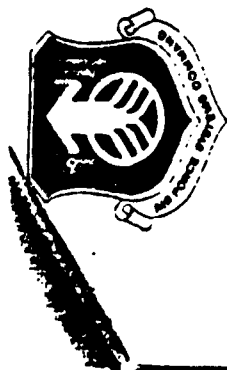
- Where Discovered:
 - Block 30 Full-scale durability testing
- Actions
 - Block 40
 - All have "rivetless" leading edge flap nosecap
 - Block 30
 - Will modify flap to "rivetless" design

Upper Wing Skin Access Holes #2, 3, and 4

- Where Discovered:
 - Block 30 Static Testing
- Actions
 - Block 30
 - ECP 1637 is providing plates/plugs to give needed strength
 - Kitproofing in work at OO-ALC
 - Retrofit to begin in Jan/Feb '91

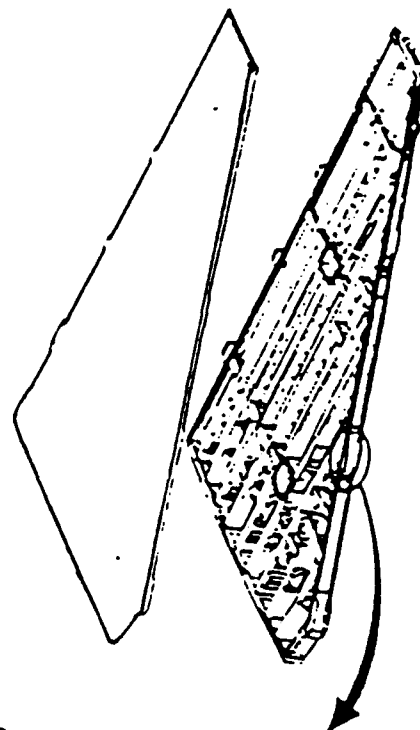
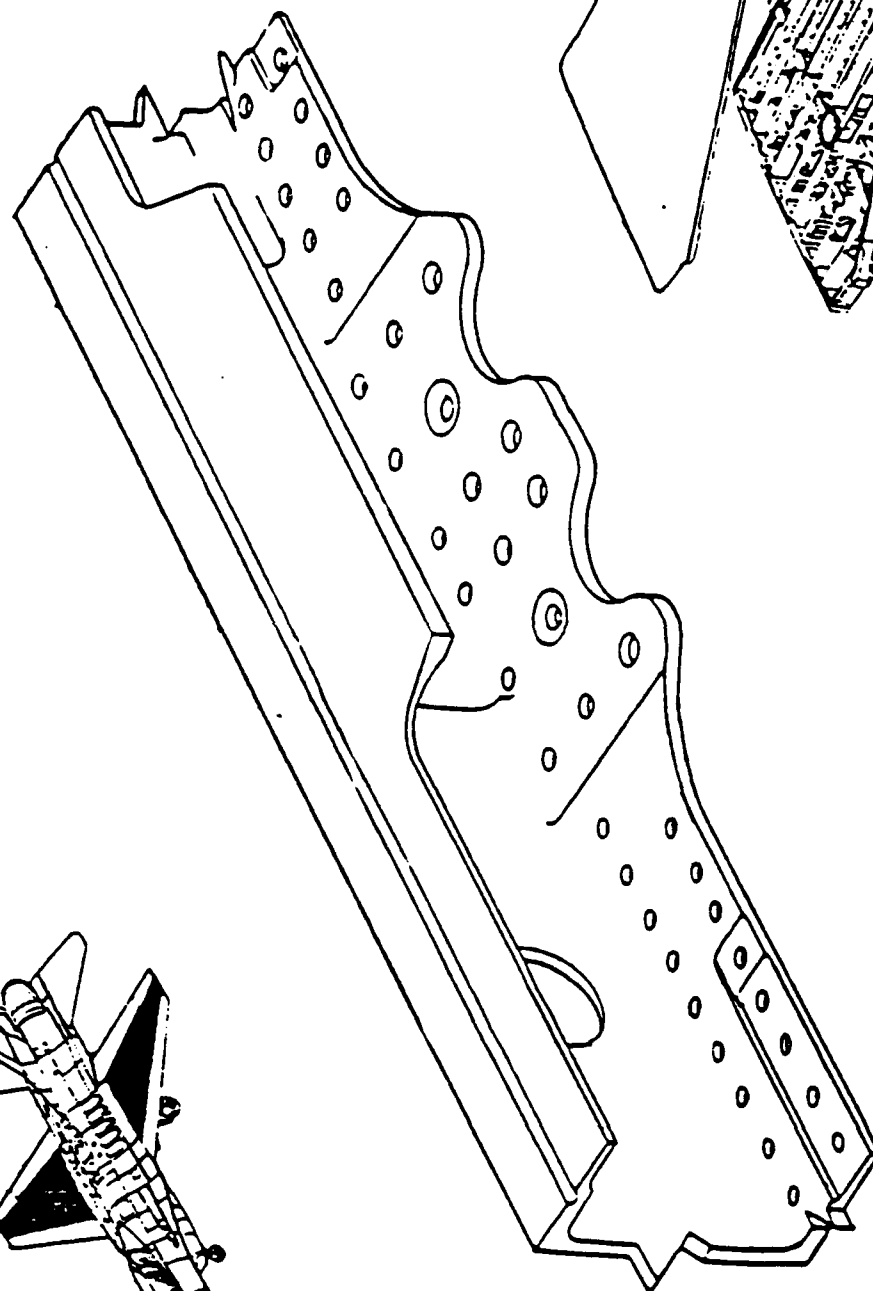
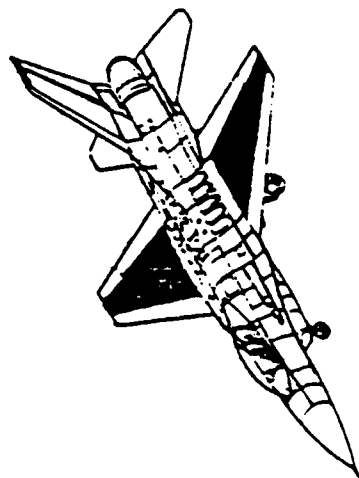
Wing Skin and Spar at
Leading Edge Flap Rotary Actuator
(LEFRA) #2

- Where Discovered:
 - Block 30 Full-scale durability testing
- Actions
 - Block 30
 - Reinforcement fitting designed for installation on Block 30 test article
 - Block 15
 - Reinforcement also applicable for cracked Block 15 aircraft



LOWER WING SKIN/SPAR AT LEFRA #2

SERVICE LIFE ESTIMATE: 6000 - 8000 HOURS

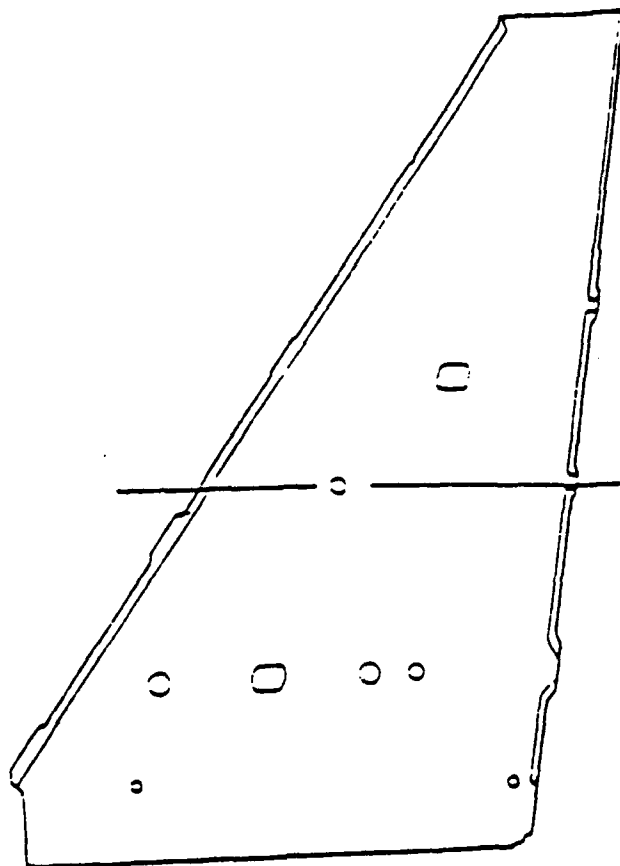
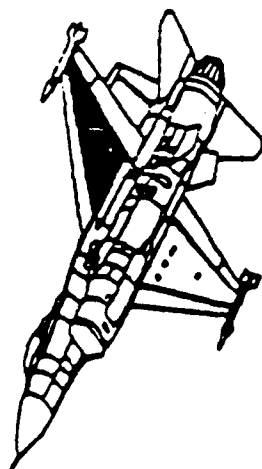


BL 102 Fuel Vent Hole

- Where Discovered:
 - Fleet Failures in A/B aircraft
- Actions
 - Block 15, Block 30, Block 40
 - Interference fit fasteners used in patterns around fuel vent hole
 - Repair under development for this area
 - Doubler and/or coldworking



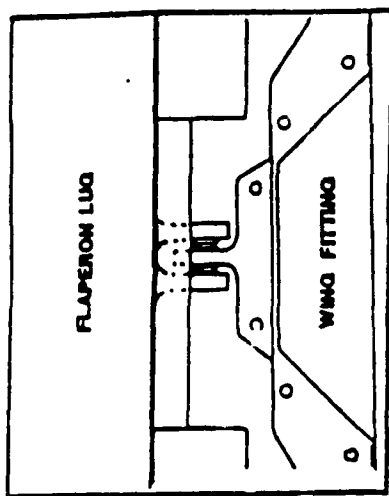
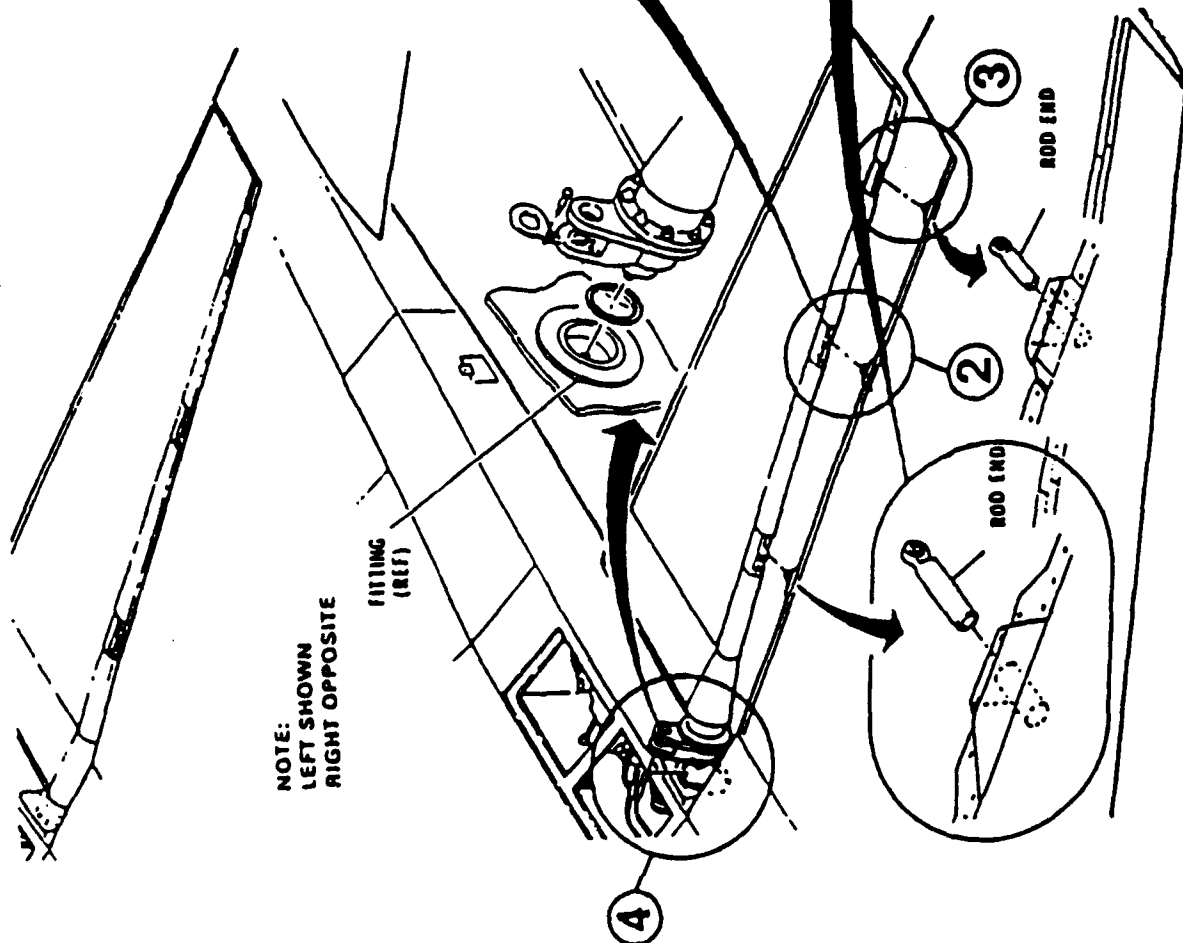
LOWER WING SKIN FUEL VENT HOLE SERVICE LIFE ESTIMATE: 4000 - 6000 HOURS



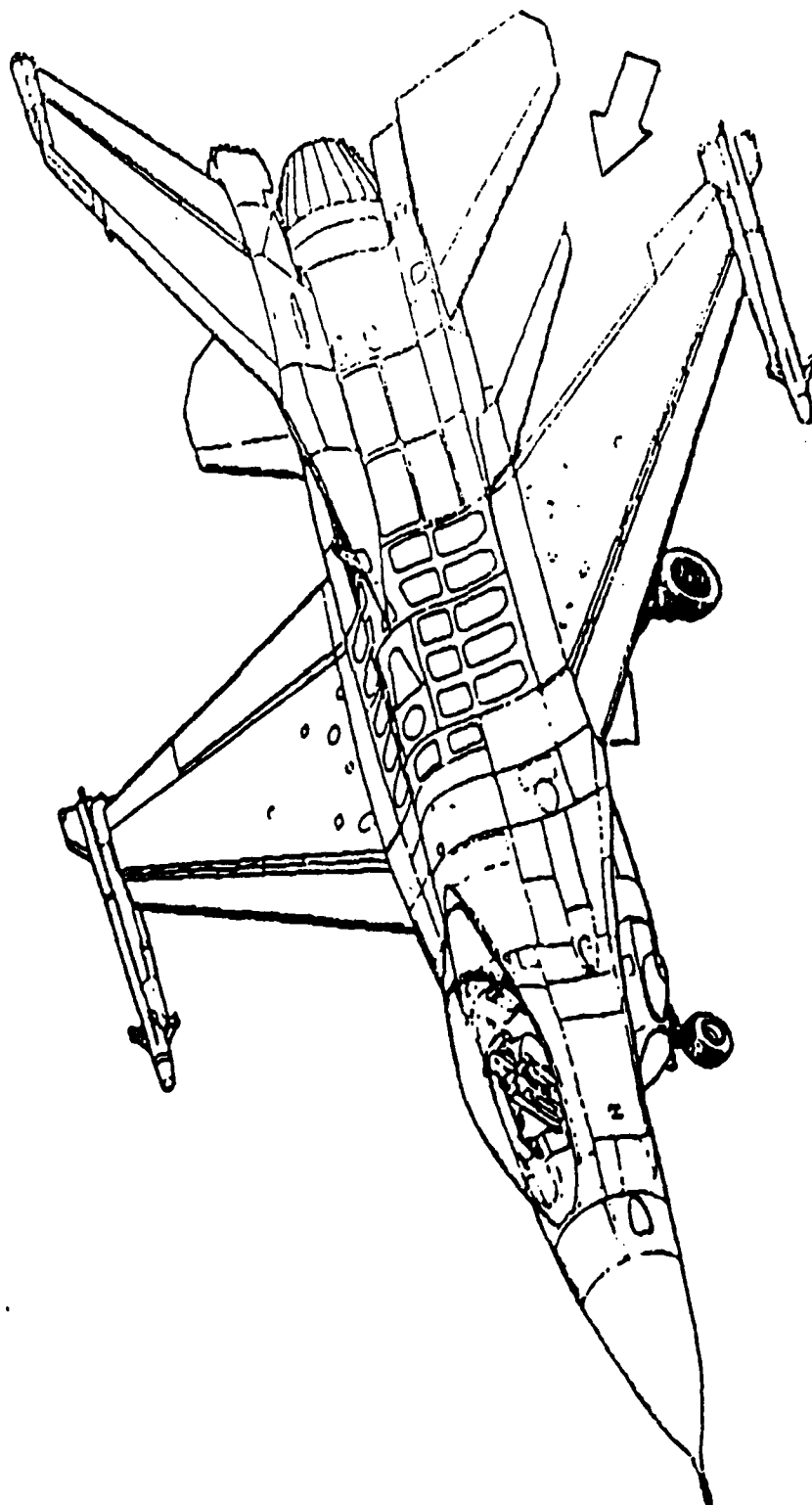
Flaperon Slider Pins

- Where Discovered:
 - Fleet Failures
- Actions
 - Block 40
 - ECP 1751: Production breakin of new design with thicker lugs
 - Will also address retrofit into Block 40 aircraft
 - All other F-16 aircraft
 - New design has been released as a "preferred spare"
 - OO-ALC is planning a buy of 6000 slider pins of new design

PROBABLE FLAPERON FAILURE SEQUENCE ① ② ③ ④



FLAPERON FAILURE



Summary

- Durability testing is doing its job
 - Allows for timely retrofit actions
 - Prevents damage to aircraft systems
 - Maintains fleet safety

CF-5 Full Scale Durability and
Damage Tolerance Test
Preliminary Result

G. Deziel

Department of National Defence, Canada

M. Beaulieu

Bombardier Inc., Canadair Group

Presented at

USAF Aircraft Structural Integrity Program

Conference, San Antonio, Texas

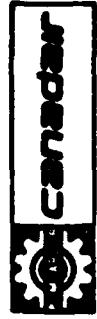
11 - 13 December, 1990

CF-5 FSDADTT PRELIMINARY RESULTS



CF-5 FSDADTT AGENDA

- **INTRODUCTION**
- **TEST RESULTS**
- **FRACTOGRAPHY/MARKER BLOCKS**
- **ACOUSTIC EMISSION RESULTS**



CF-5 FSDADTT

AGENDA

- INTRODUCTION
- TEST RESULTS
- FRACTOGRAPHY/MARKER BLOCKS
- ACOUSTIC EMISSION RESULTS



CF-5 FSDADTT

INTRODUCTION

- **BACKGROUND**

- CF-5 WAS DESIGNED IN 60'S USING SAFE-LIFE APPROACH.
INITIAL LIFE ESTIMATE : 4000 HOURS
- S.L.E.P. IN THE LATE 70'S USING DAMAGE TOLERANCE APPROACH.
ANALYTICAL LIFE ESTIMATE : 6000 HOURS
- FATIGUE TESTS:
 - T-38 & F-5A/B COMPONENTS
 - F-5E FULL SCALE TEST
- APPLICABILITY AND DIFFERENCES:
 - STRUCTURAL
 - CF LOAD SPECTRA



CF-5 FSDADTT

INTRODUCTION

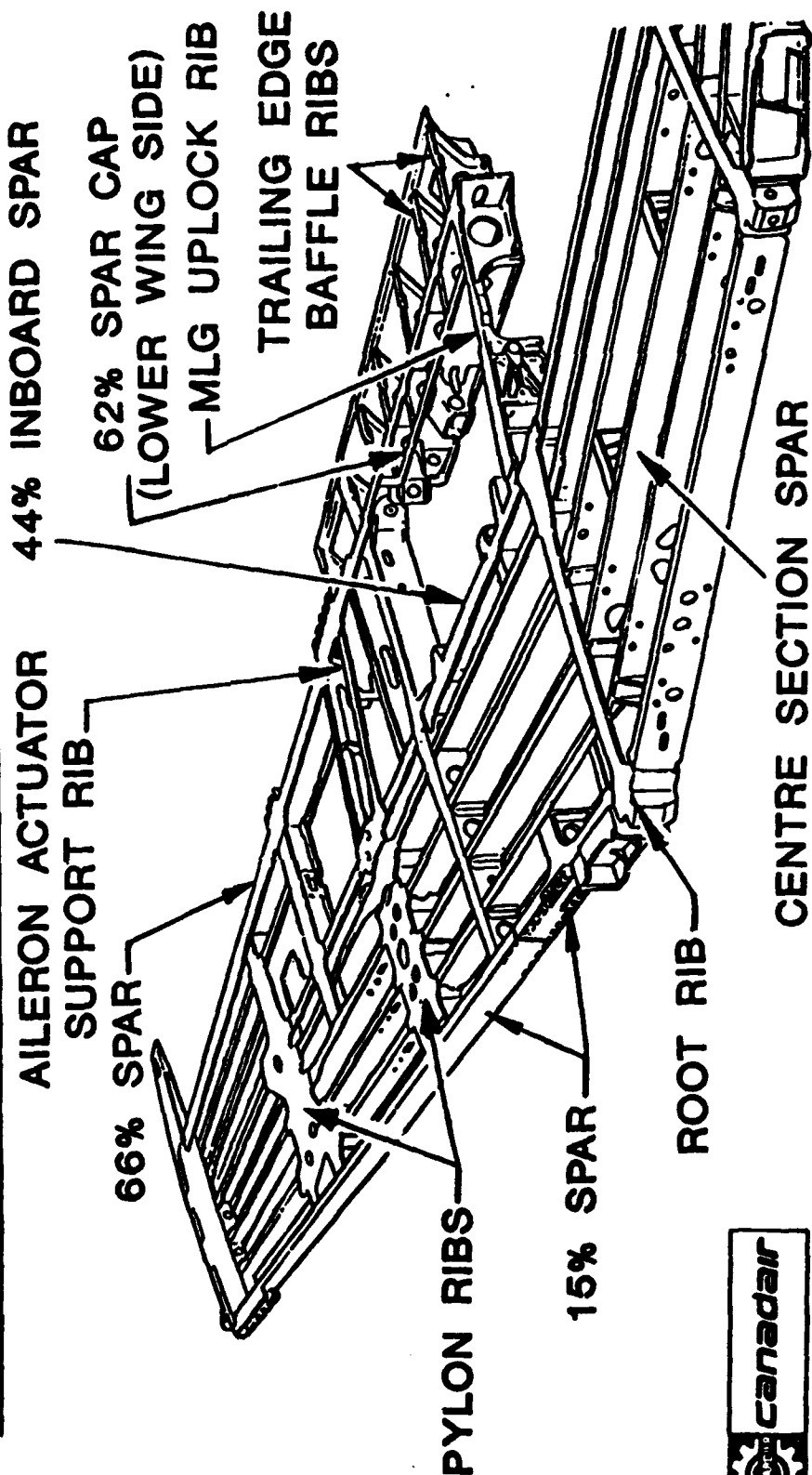
- BACKGROUND :
 - STRUCTURAL DIFFERENCES :
 - WING COMPONENTS REDESIGN
NEW LOWER SKIN
NEW REDESIGNED SPARS & RIBS
 - NEW STEEL DORSAL LONGERON
 - NEW REDESIGNED AFT FORMERS



CF-5 FSDADTT

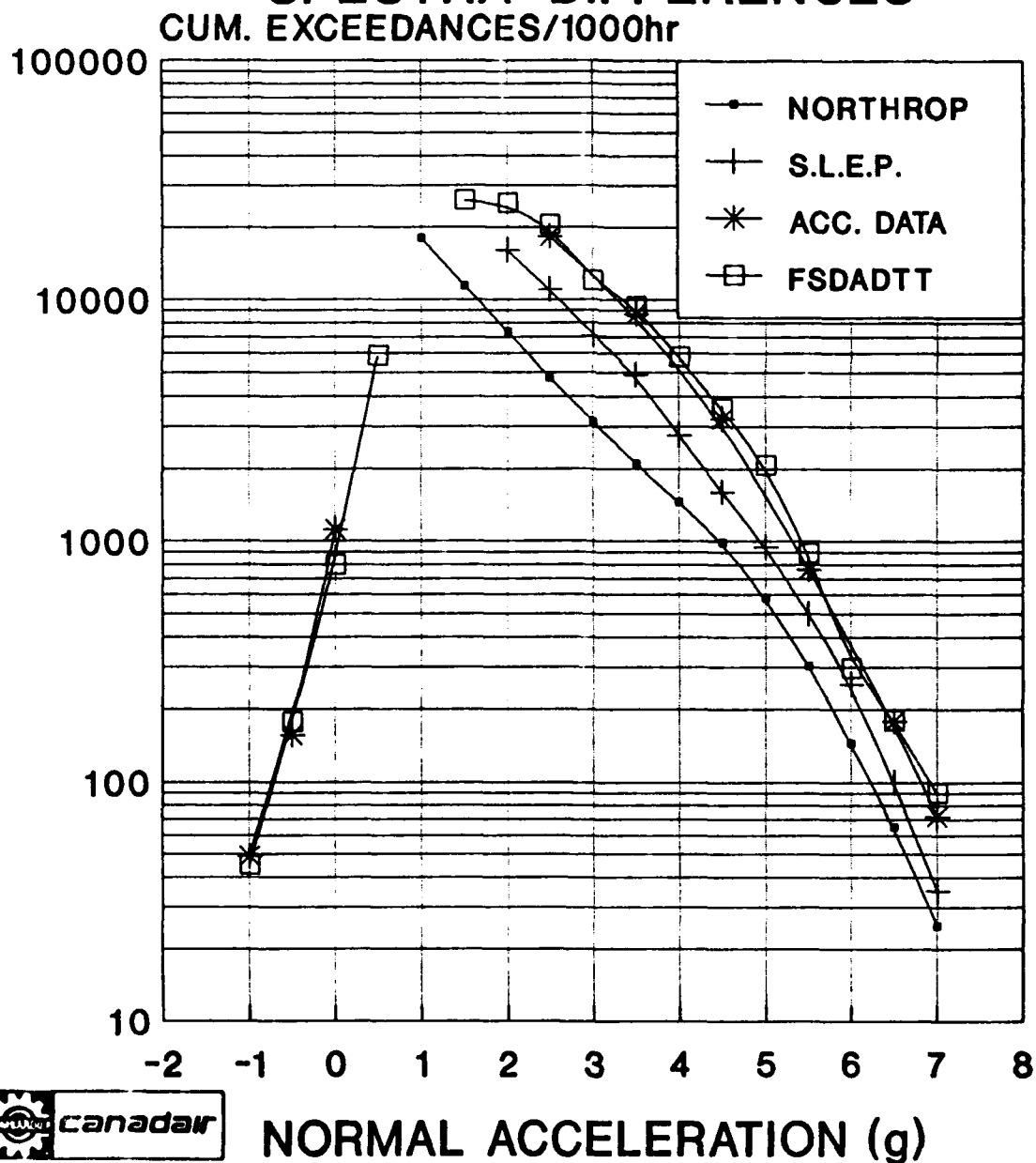
INTRODUCTION

- WING COMPONENTS REDESIGN



CF-5 FSDADTT INTRODUCTION

- BACKGROUND :
 - SPECTRA DIFFERENCES





CF-5 FSDADTT

INTRODUCTION

- TEST GOALS:

- VALIDATE THE 6000 HOURS LIFE CALCULATED DURING THE S.I.E.P.
- DETERMINE THE STRUCTURAL ECONOMIC LIFE
- SUBSTANTIATE THEORETICAL ANALYSES (DDTA AND NASTRAN FEM)
- IDENTIFY PROBLEMS AREA
- EVALUATE REPAIR SCHEMES
- VALIDATE INSPECTION TECHNIQUES
- ESTABLISH SPARE PART REQUIREMENTS



CF-5 FSDADTT

INTRODUCTION

- **MILESTONES:**

- CONTRACT ISSUED APRIL 1987
- SELECTION OF A REPRESENTATIVE TEST AIRCRAFT
- TEST RIG FACILITIES DESIGN (COMPLETED JAN. 1989)
- LOAD SPECTRUM DEV. (COMPLETED DEC. 1988)
- FIRST DURABILITY TESTING (8000 HOURS)
(COMPLETED NOV. 1989)
- SECOND DURABILITY TESTING (8000 HOURS)
(IN PROGRESS)
- DAMAGE TOLERANCE TESTING (8000 HOURS)
- TEARDOWN INSPECTION + FINAL REPORT

CF-5 FSDADTT

INTRODUCTION

- TEST STATUS:

- TEST WAS COMMISSIONED IN MAY 1989
- FIRST DURABILITY LIFETIME TEST WAS COMPLETED IN NOV. 1989
- SECOND DURABILITY LIFETIME TEST WAS HALTED IN JUNE 1990 AT 9755 HOURS AFTER NUMEROUS CRACKS WERE DETECTED ON THE WING LOWER SKIN
- WING IS BEING REPAIRED. TESTING SHOULD RESUME BY DEC. 1990



CF-5 FSDADTT

AGENDA

- INTRODUCTION
- TEST RESULTS
- FRACTOGRAPHY/MARKER BLOCKS
- ACOUSTIC EMISSION RESULTS



CF-5 FSDADTT

TEST RESULTS

- MAIN ENGINE MOUNT - BOLT FAILURES
- TRAILING EDGE BAFFLES CRACKING
- 15% INBOARD SPAR CRACKING
- ENGINE MOUNT FORWARD LINK FAILURE
- F.S. 325 FRAME STRESS CORROSION CRACKING
- LOWER WING SKIN CRACKING
- WING ROOT RIB UPPER FLANGE CRACKING
- VERTICAL STABILIZER SKIN - ABSENCE OF DAMAGE



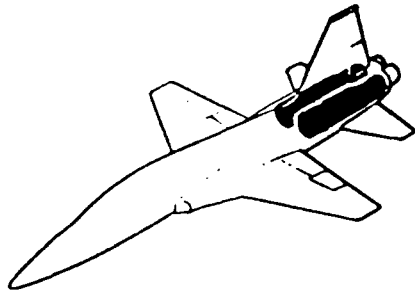
CF-5 FSDADTT

MAIN ENGINE MOUNT - BOLT FAILURES

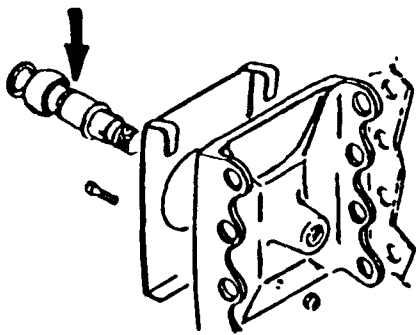
- INBOARD AND OUTBOARD BOLTS FAILED AT 2800 HOURS
- ANALYTICAL RESULTS:
 - DURABILITY: 1420 HOURS (SCATTER=3.0)
 - DAMAGE TOLERANCE: 144 HOURS
(initial crack 0.005")
- RECOMMENDATION: REPLACE BOLTS EVERY 400 HOURS.
(IMPLEMENTED IN THE FLEET)



CF-5 FSDADTT MAIN ENGINE MOUNT BOLTS

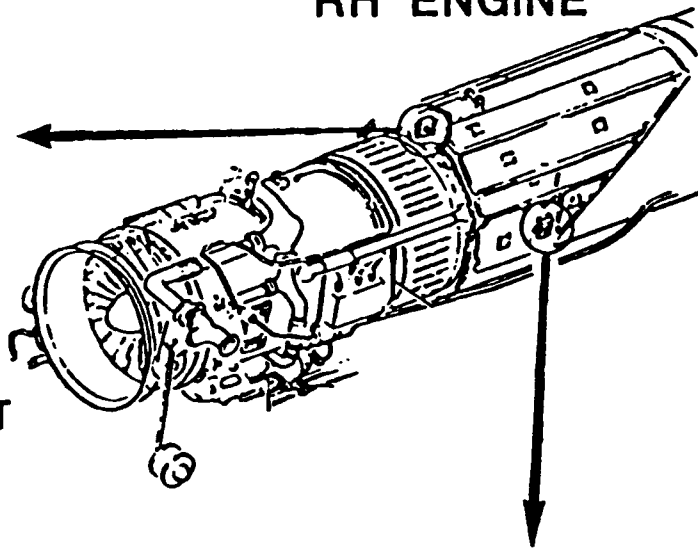


BOLT

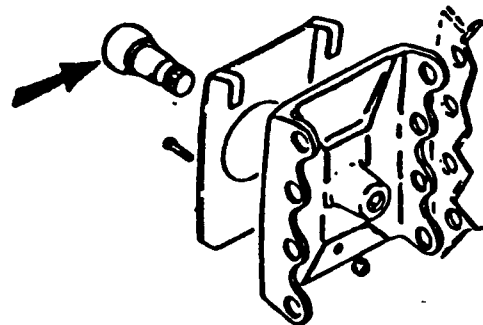


MAIN OUTBOARD MOUNT

RH ENGINE

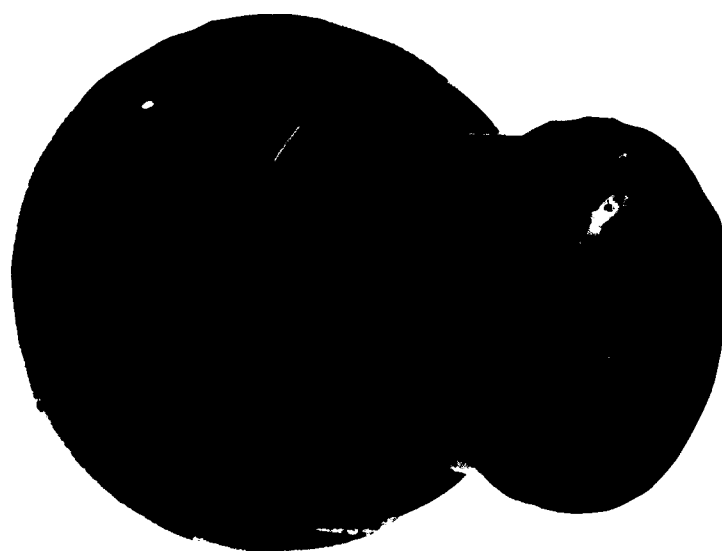


BOLT



MAIN INBOARD MOUNT



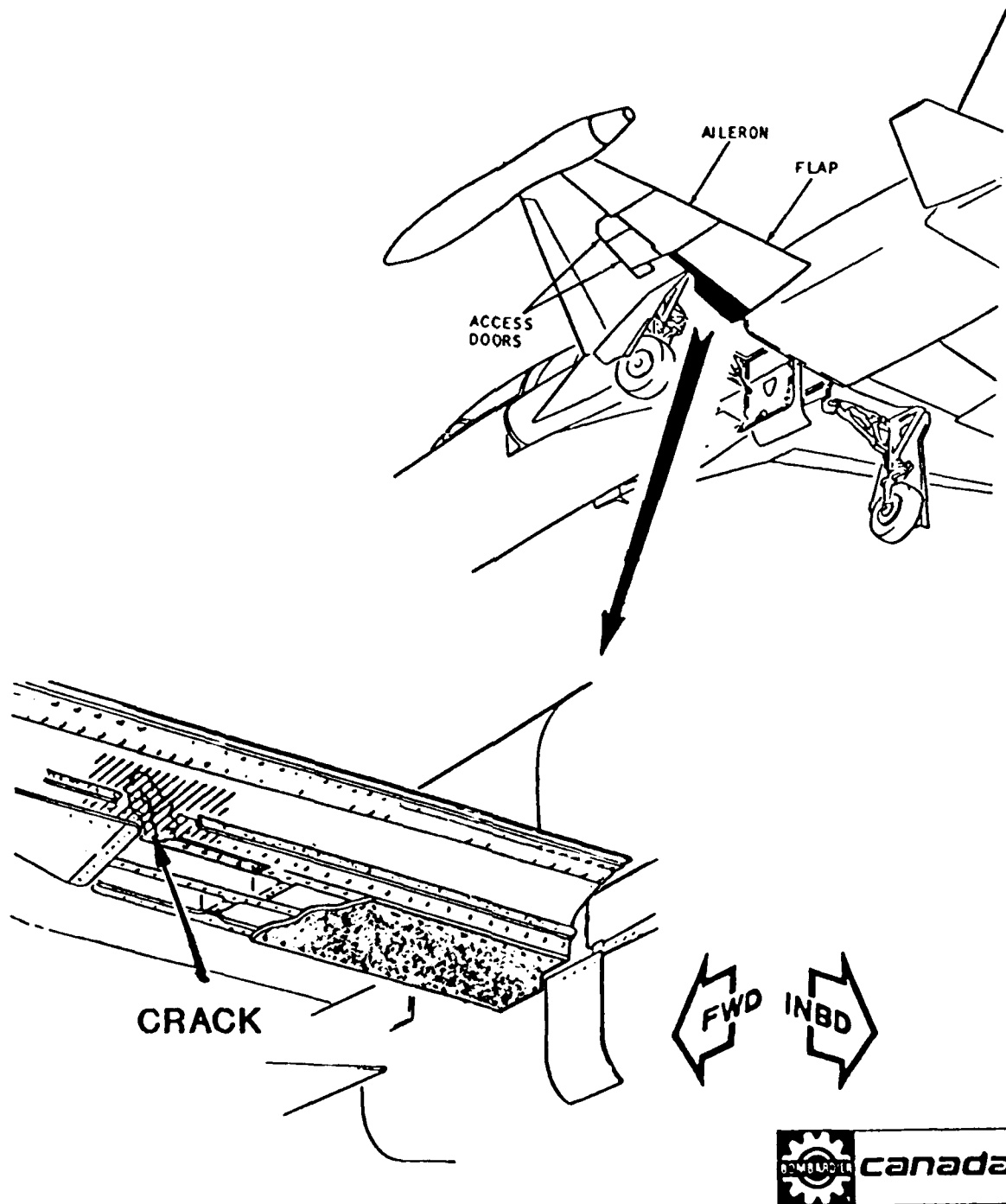


CF-5 FSDADTT TRAILING EDGE BAFFLE

- CRACK WAS DISCOVERED AT 4900 HOURS
- THIS PART IS SECONDARY STRUCTURE
 - NO ANALYSIS WAS PERFORMED
 - DAMAGE IS CONSISTANT WITH FIELD EXPERIENCE
- REPAIR ALREADY EXISTS AND WAS PERFORMED ON TEST ARTICLE
- REPAIR CRACKED AFTER 3700 HOURS OF TESTING
 - STOP DRILL CRACK AND COLD-WORK



CF-5 FSDADTT TRAILING EDGE BAFFLE







CF-5 FSDADTT

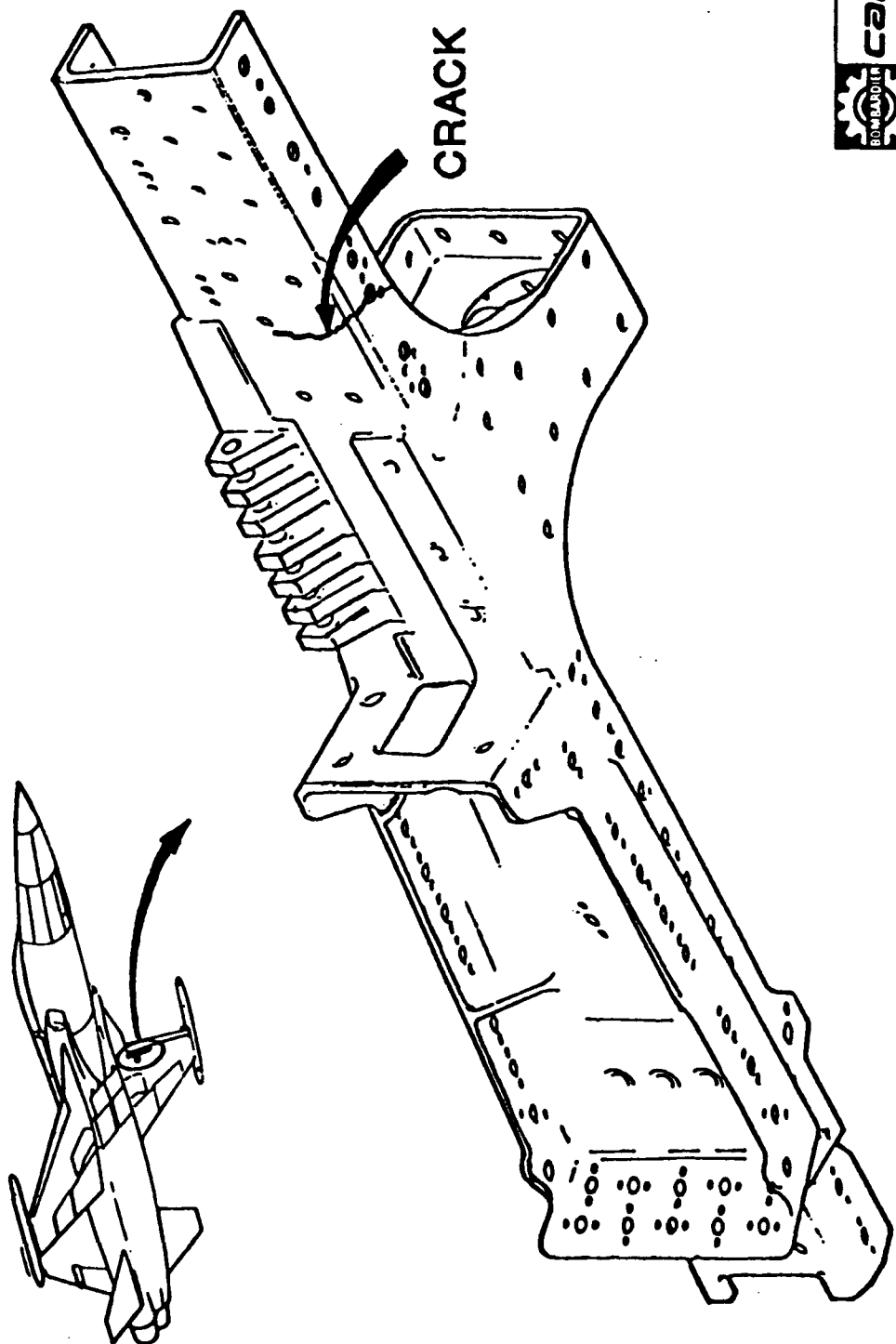
15% INBOARD SPAR CRACKING

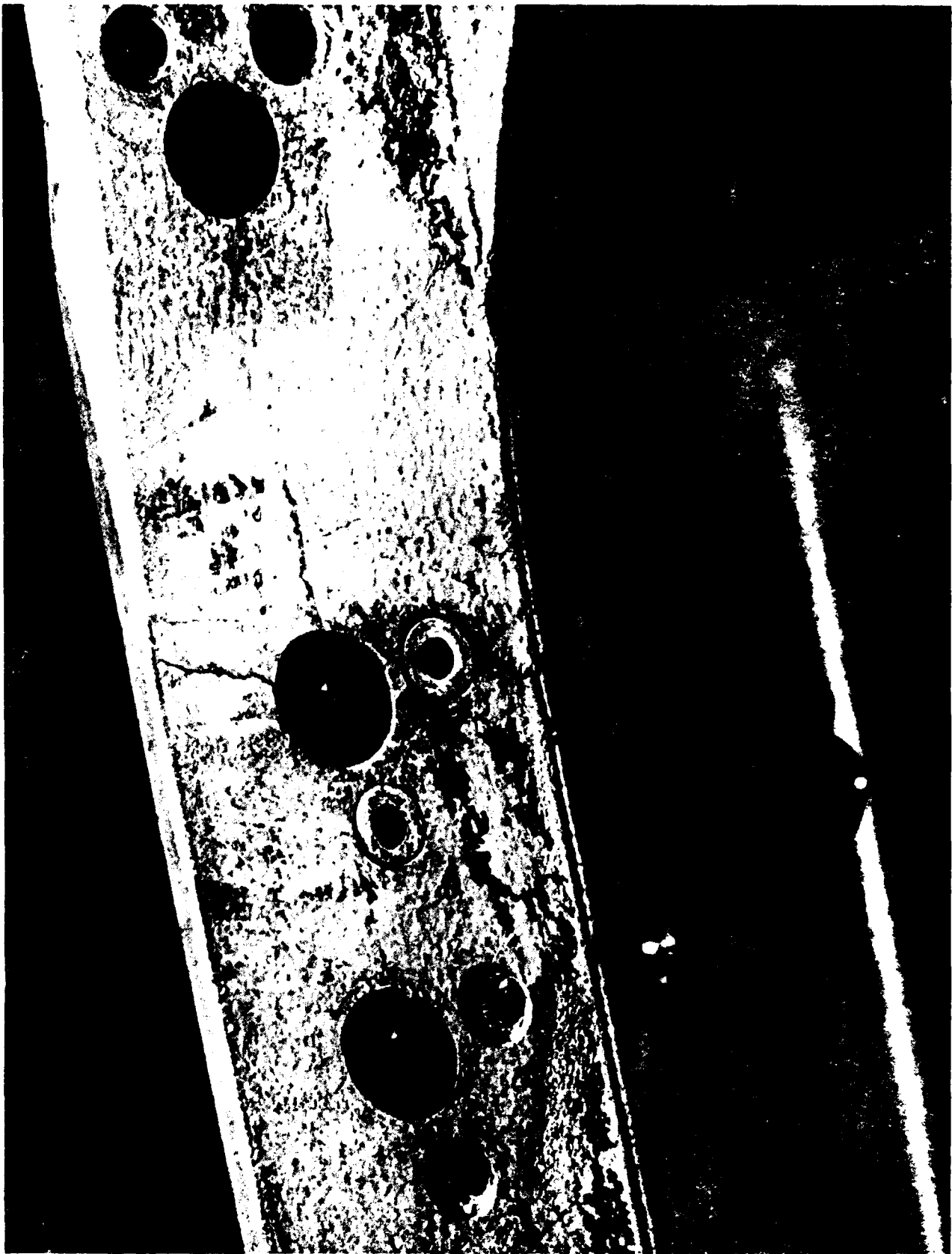
- CRACK WAS DISCOVERED AT 6000 HOURS
STARTED FROM NUT-PLATE HOLE
- ANALYTICAL RESULTS:
 - SPECTRUM BASED ON STRAIN GAUGE INSTALLED
ON SKIN
 - DURABILITY: 21464 HOURS(SCATTER=3.0)
 - DAMAGE TOLERANCE: 19300 HOURS ($A_0=0.050"$)
- RECOMMENDATIONS:
 - VERIFY THAT NEW SPARS DO NOT
HAVE NUT-PLATE IN THAT AREA
 - INSTALL REPAIR ANGLE ON TEST
ARTICLE AND CONTINUE TESTING

NOTE: -RIGHT SPAR WAS LATER REPLACED WITH A STRAIN
GAUGE ON THE SPAR FLANGE
-STRAIN SIGNIFICANTLY HIGHER ON SPAR FLANGE
THAN ON SKIN



CF-5 FSDADTT 15% INBOARD SPAR







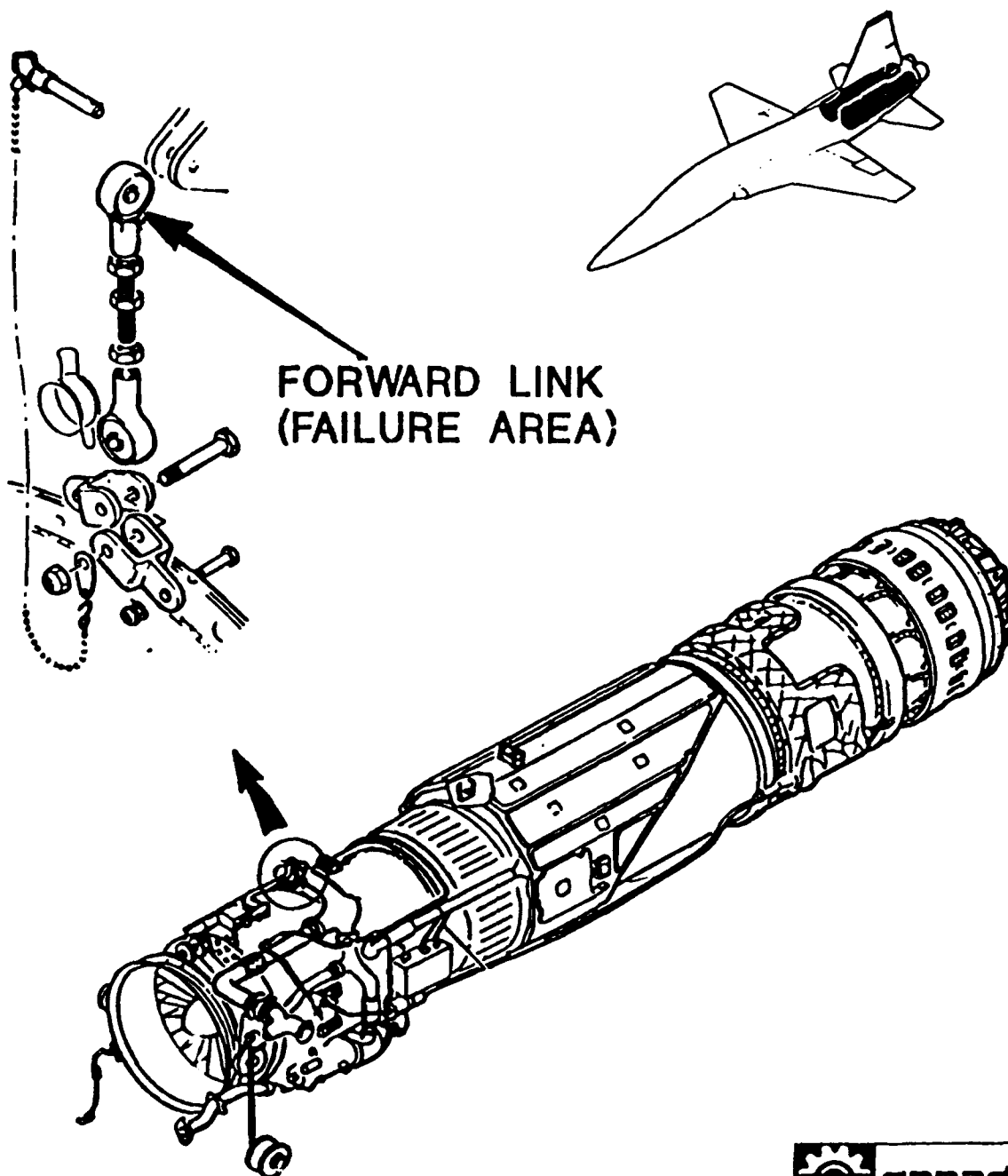
CF-5 FSDADTT

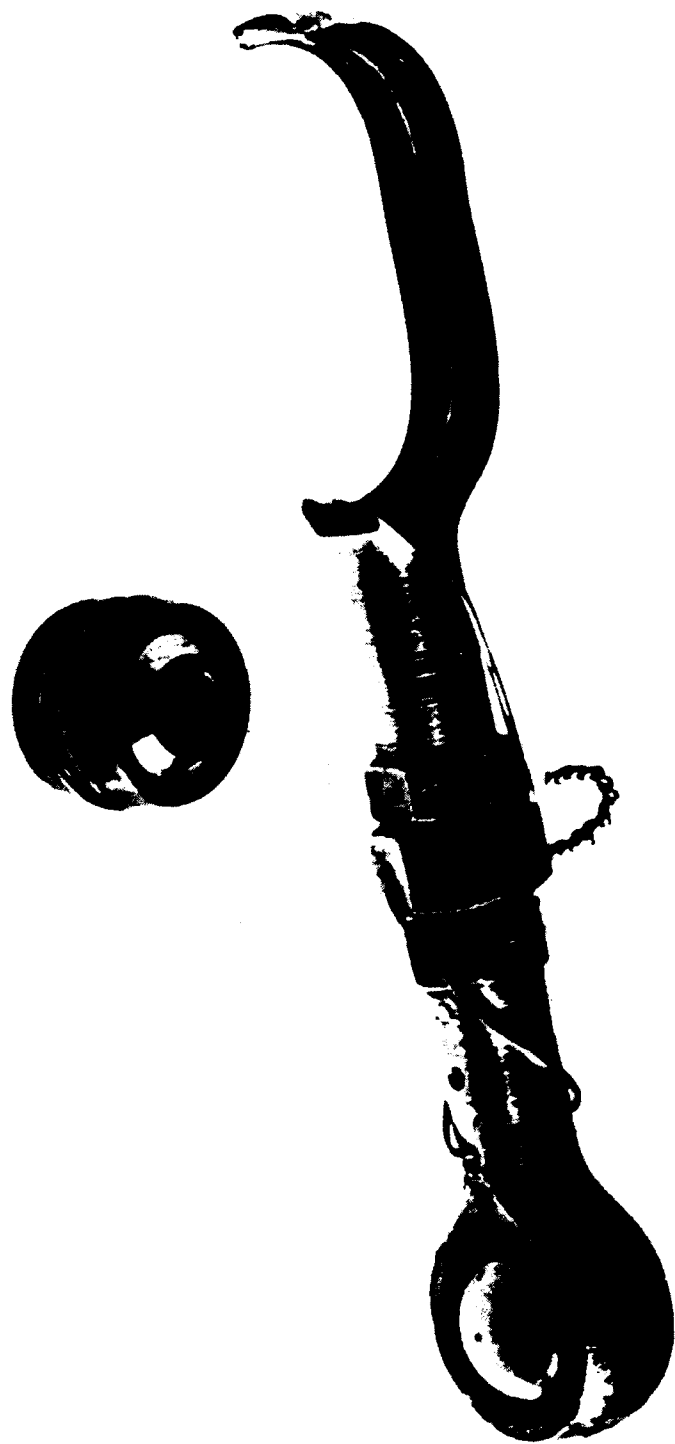
ENGINE MOUNT FORWARD LINK

- LINK FAILED AT 6400 HOURS
- RECOMMENDATIONS:
 - INSPECT FORWARD MOUNT EVERY 400 HOURS
 - REPLACE ROD END EVERY 2000 HOURS (IMPLEMENTED ON THE FLEET)



CF-5 FSDADTT ENGINE MOUNT FORWARD LINK





CF-5 FSDADTT

FRAME F.S. 325

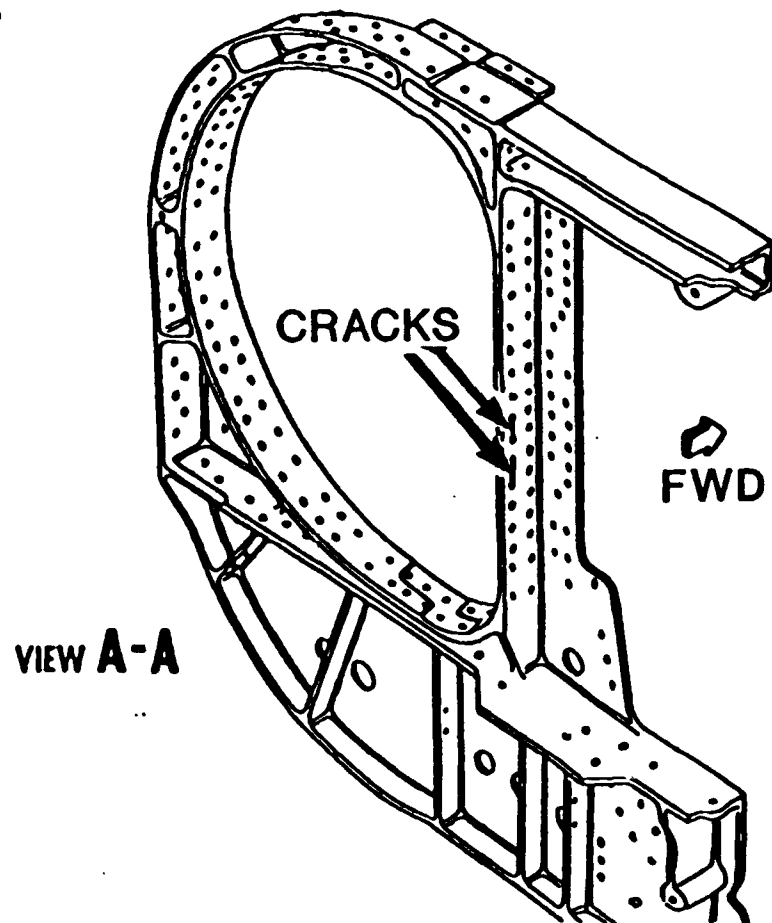
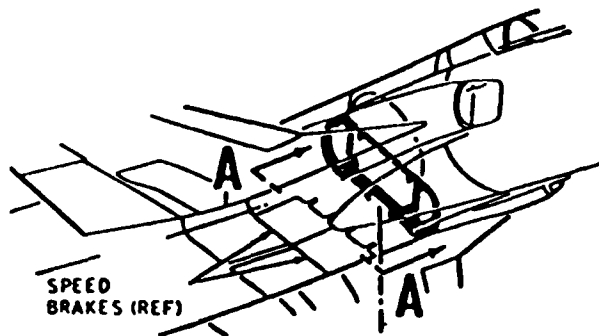
- STRESS CORROSION CRACKS IN THE FLEET.
- TEST ARTICLE CRACK LENGTHS :
 - RH SIDE 1 CRACK 2.25"
 - LH SIDE 2 CRACKS 0.75" EACH
- THE AREA WAS STRAIN-GAUGED AND IS CLOSELY MONITORED. AT CRITICAL LOCATION (CROSS-SECTION 118) STRESS IS 3.3 TIMES LOWER THAN ORIGINAL DESIGN STRESS.



CF-5 FSDADTT

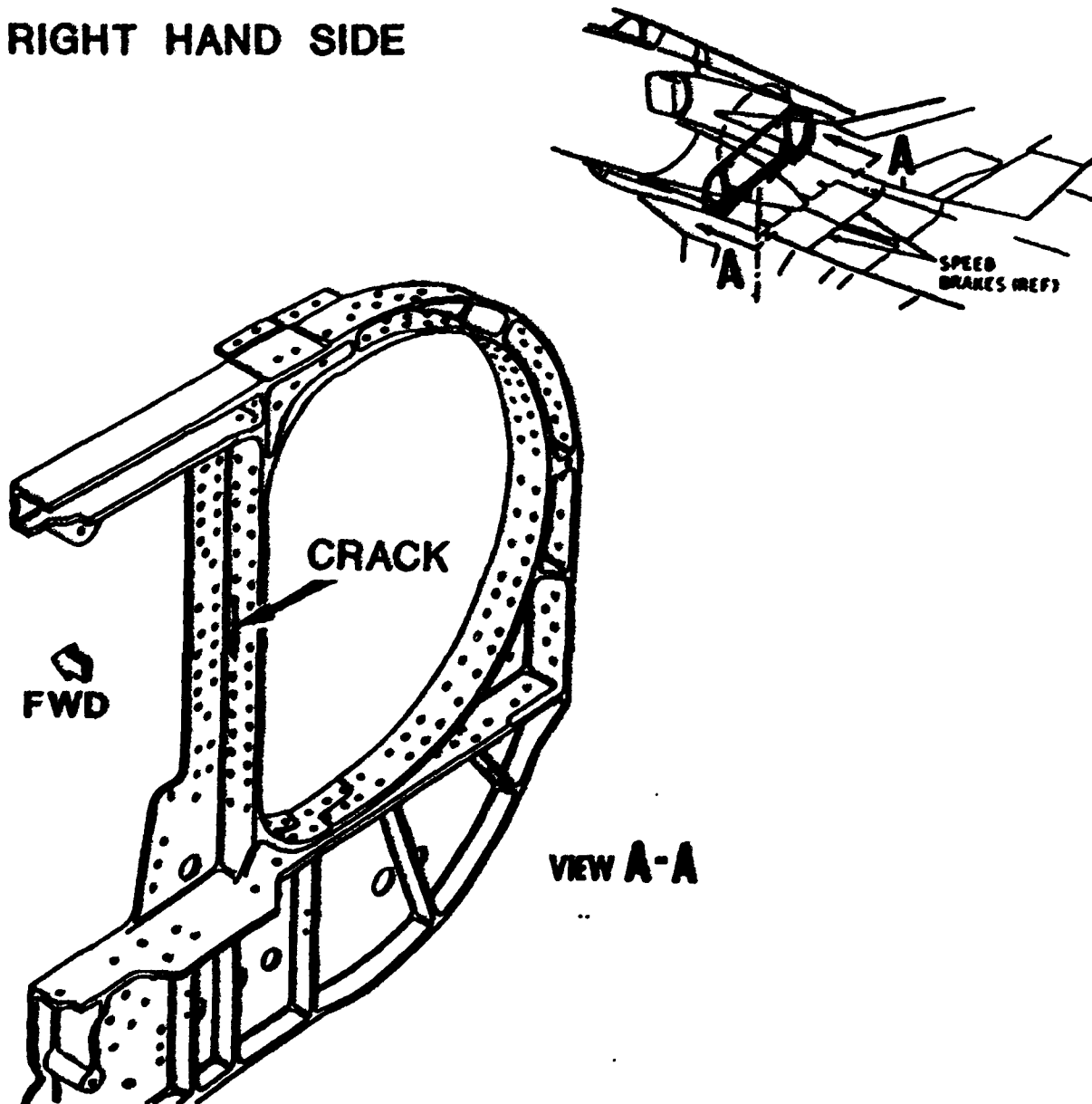
FRAME F.S. 325

LEFT HAND SIDE



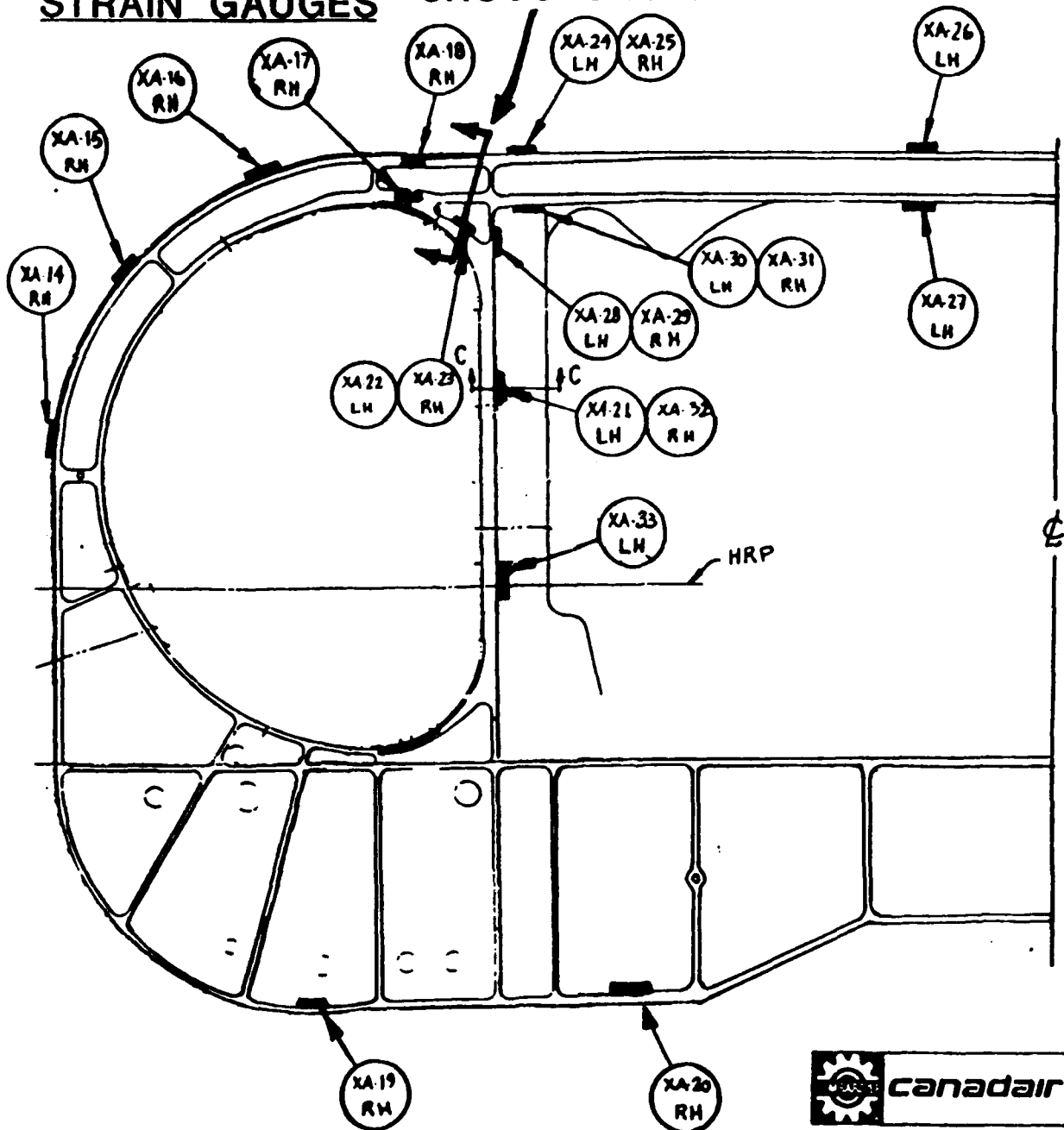
CF-5 FSDADTT FRAME F.S. 325

RIGHT HAND SIDE



CF-5 FSDADTT FRAME F.S. 325

STRAIN GAUGES CRITICAL AREA
CROSS SECTION 118



CF-5 FSDADTT

LOWER WING SKIN

- CRACKS WERE DISCOVERED DURING 8000 HOURS INSPECTION. CRACKS STARTED AT FASTENER HOLES.
- AT 9755 HOURS, TEST WAS STOPPED AFTER CRACKS WERE DISCOVERED.
- THE INSPECTION CARRIED OUT AT 9755 HOURS REVEALED CRACKS AT:
 - 42 FASTENER HOLES
 - 2 DRAIN HOLES (1 ON EACH SIDE)
 - THE LOWER SKIN CRITICAL RADIUS



CF-5 FSDADTT

LOWER WING SKIN

- CRACKS AT FASTENER HOLES :
 - RANGE FROM 0.006" TO 0.075"
 - ANALYTICAL RESULTS (AT MOST CRITICAL HOLE):
 - SPECTRUM BASED ON STRAIN GAUGES IN THE AREA
 - DURABILITY: (NO SCATTER)
 - FOR 7075-T651 SKIN: 6300 HOURS
 - FOR 7475-T651 SKIN: 6300 HOURS
 - DAMAGE TOLERANCE:
 - FOR 7075-T651 SKIN: 1617 HOURS
(A₀ = 0.005" , A_c = 0.060")
 - FOR 7475-T651 SKIN: 4887 HOURS
(A₀ = 0.005" , A_c = 0.350")



CF-5 FSDADTT

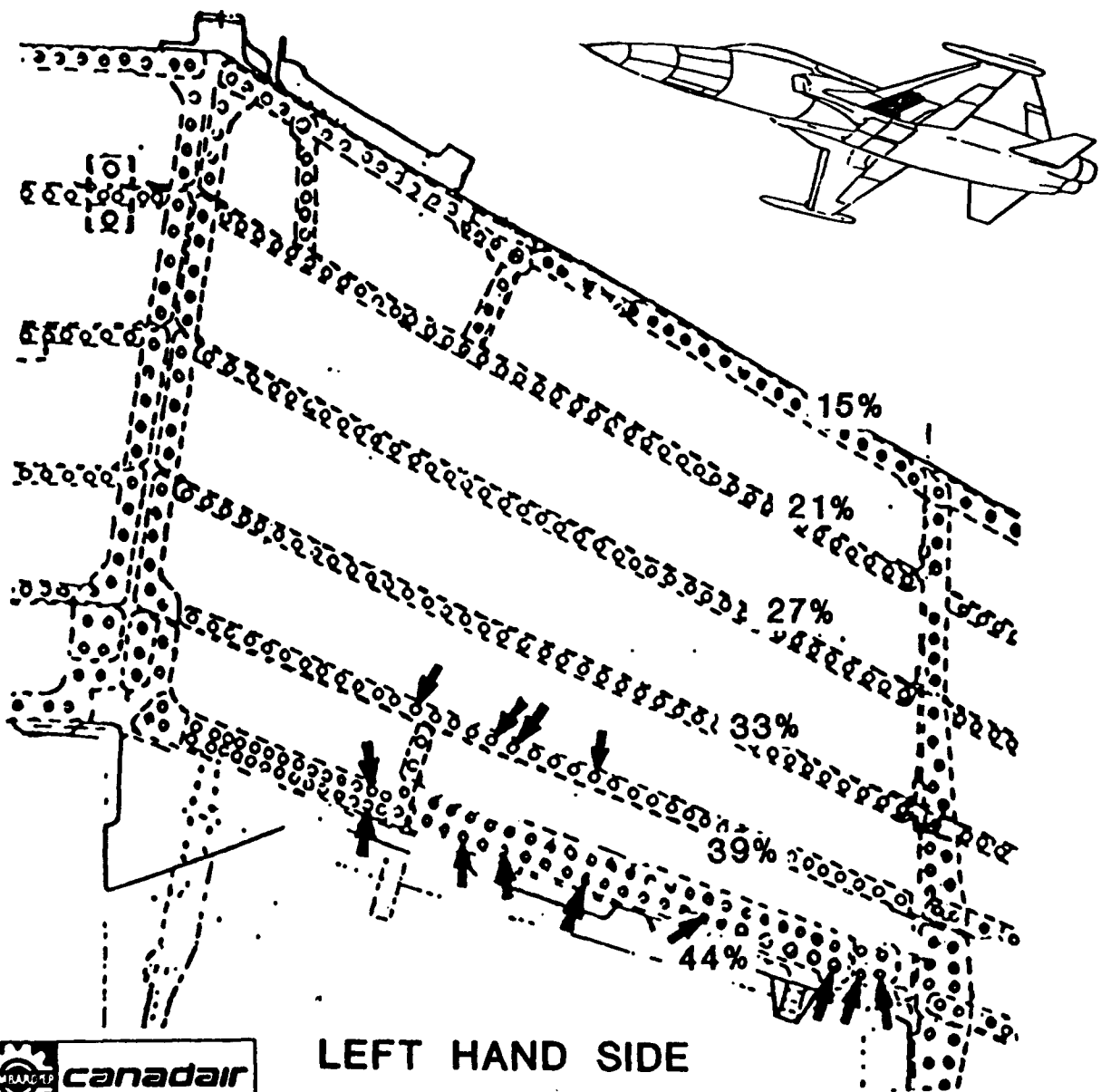
LOWER WING SKIN

- CRACKS AT FASTENER HOLES :
 - TEST ARTICLE REPAIR:
 - REAM HOLES TO REMOVE CRACKS AND PLASTIC ZONES
 - COLD-WORK ALL HOLES IN THE AREA SHOWN
 - FLEET RECOMMENDATIONS:
 - COLD-WORK SAME AREA AS TEST ARTICLE (IMPLEMENTED)
 - 7075-T651 SKIN NOT DAMAGE TOLERANT
SAFE LIFE - 3000 HOURS
 - 7475-T651 SKIN DAMAGE TOLERANT
INSPECTION INTERVAL - 200 HOURS



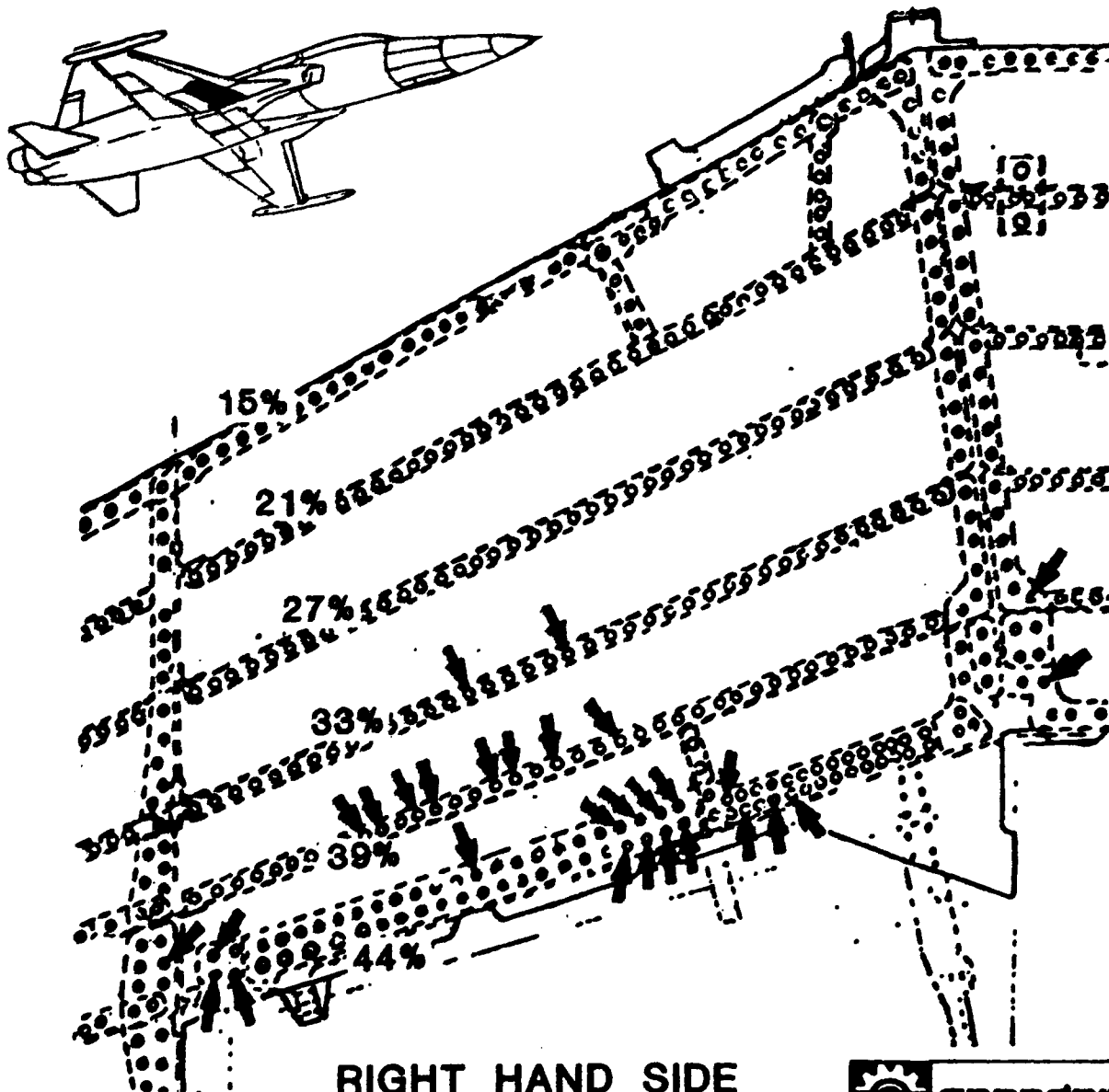
CF-5 FSDADTT LOWER WING SKIN

- FASTENER HOLES



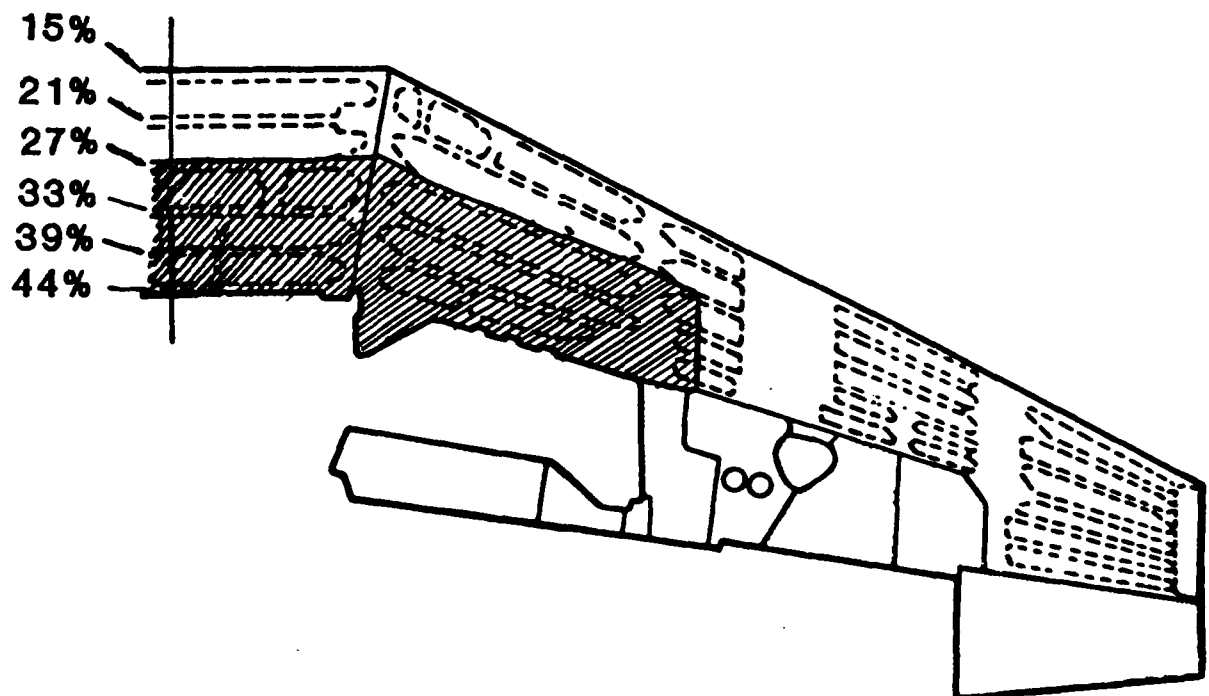
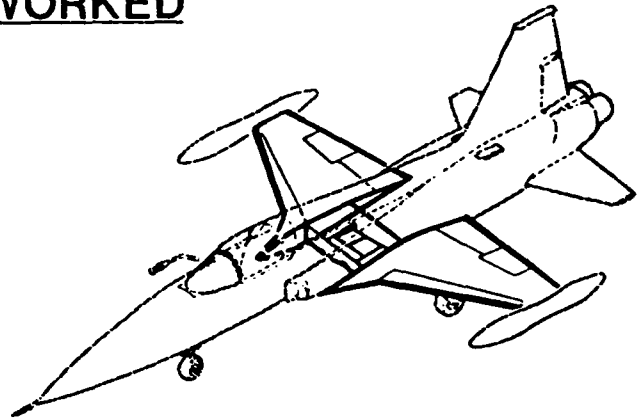
CF-5 FSDADTT LOWER WING SKIN

- FASTENER HOLES



CF-5 FSDADTT LOWER WING SKIN

- AREA TO BE COLD-WORKED



CF-5 FSDADTT

LOWER WING SKIN

- DRAIN HOLES :

- CRACKS ARE APPROX. 0.070"

- ANALYTICAL RESULTS:

- SPECTRUM BASED ON STRAIN GAUGE
 - DURABILITY: 36400 HOURS
 - DAMAGE TOLERANCE: 11890 HOURS
(A₀ = 0.005")

- TEST ARTICLE REPAIR:

- REAM HOLES TO REMOVE
CRACK AND COLD-WORK

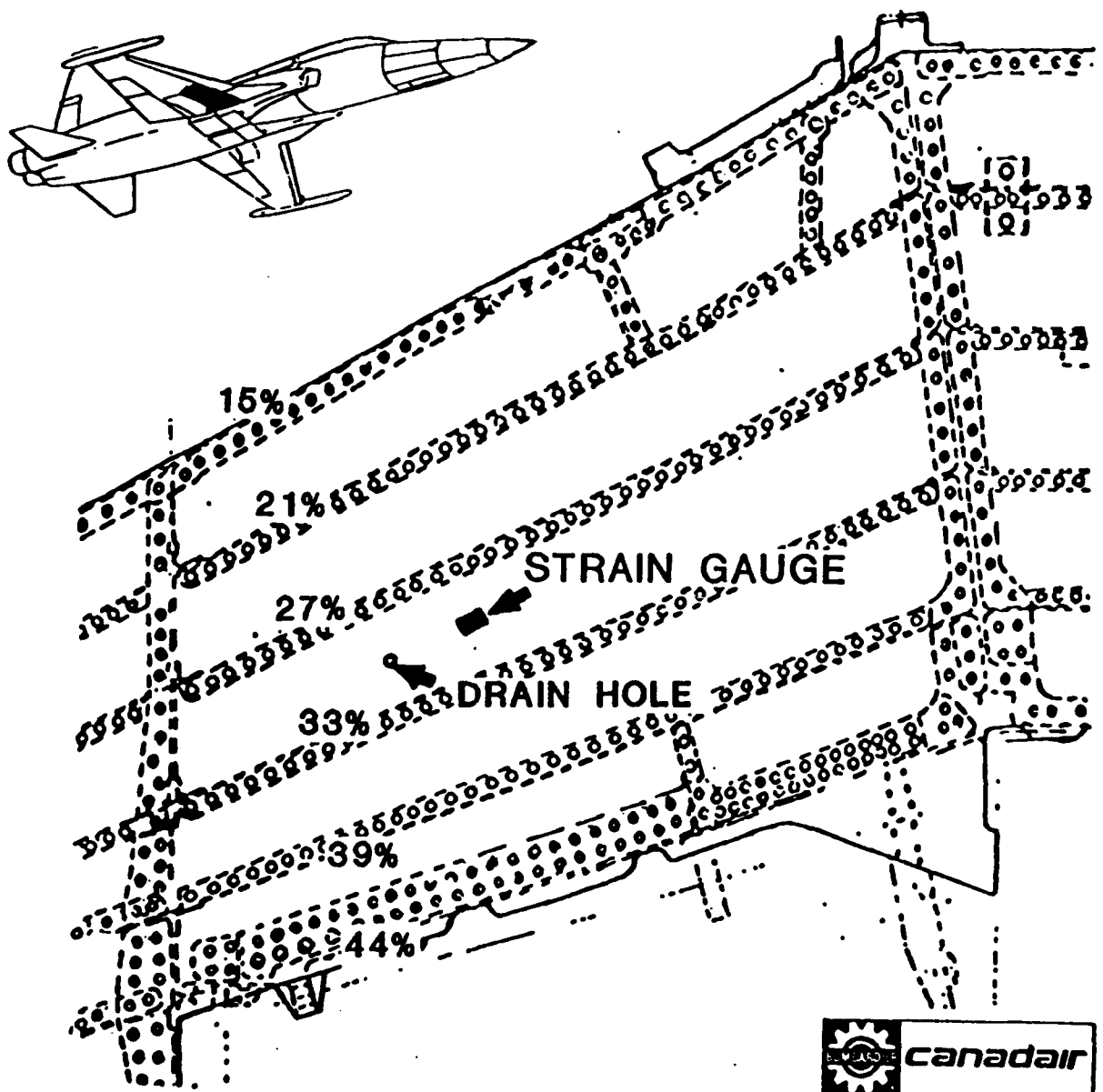
- FLEET RECOMMENDATION:

- INSPECT EVERY 250 HOURS
(IMPLEMENTED)



CF-5 FSDADTT LOWER WING SKIN

- DRAIN HOLES





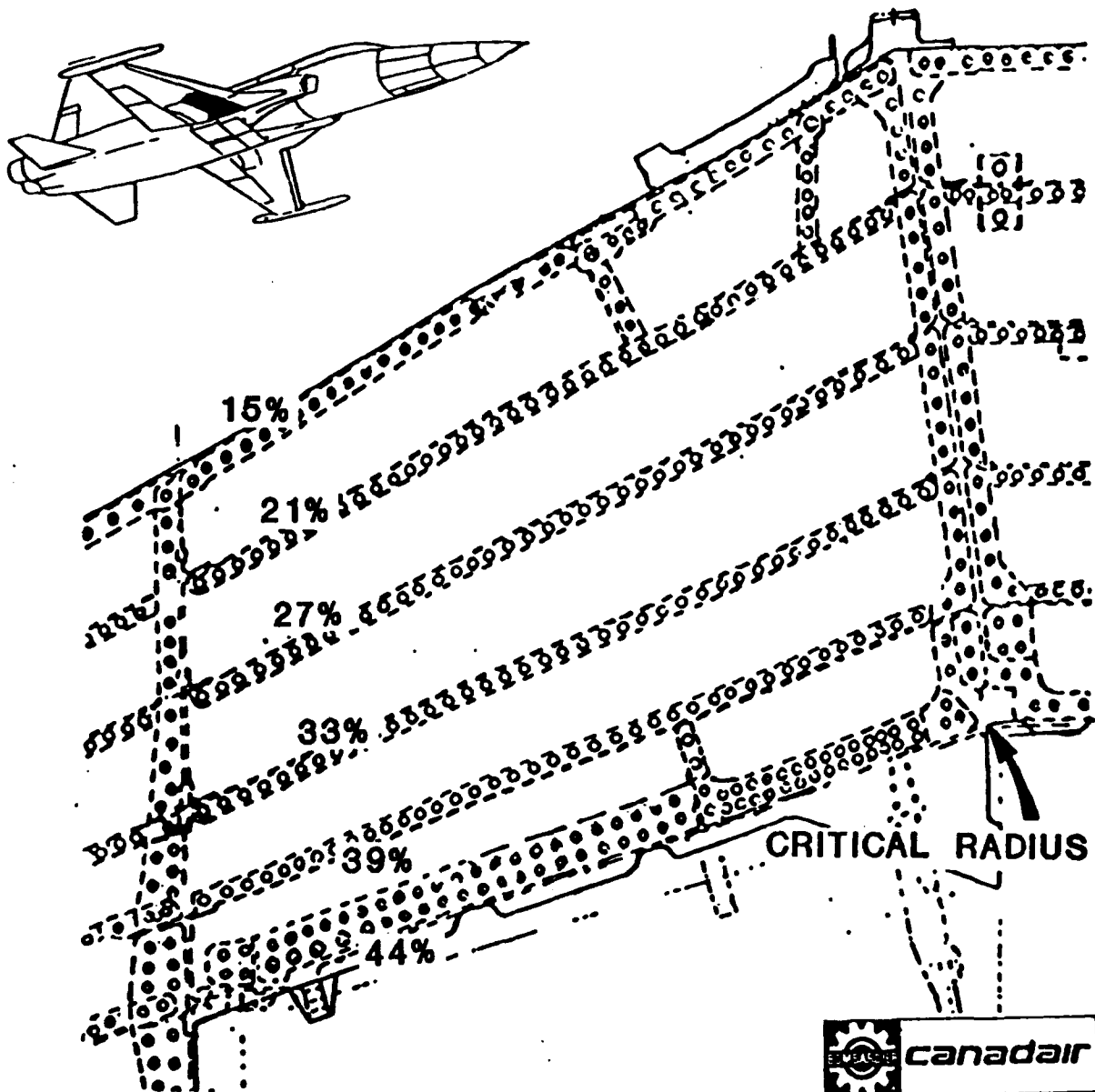
CF-5 FSDADTT

LOWER WING SKIN

- CRITICAL RADIUS :
 - CRACK IS 0.083" LONG AND 0.354" DEEP
 - ANALYTICAL RESULTS:
 - DURABILITY: 5140 HOURS (SCATTER=3)
 - DAMAGE TOLERANCE: 4541 HOURS (FOR CORNER CRACK, $A_0 = 0.050"$)
 - TEST ARTICLE REPAIR:
 - BLEND THE CRACK AWAY (INCREASE RADIUS FROM 0.5" TO 0.76") AND SHOT PEEN
 - INSTALL TITANIUM PATCH OVER RADIUS AREA TO REDUCE STRESS LEVEL
 - TEST PROGRAM PROVIDES OPPORTUNITY TO EVALUATE THIS REPAIR FOR THE FLEET
 - FLEET RECOMMENDATION:
 - KEEP EXISTING INSPECTION INTERVAL (200 HOURS)

CF-5 FSDADTT LOWER WING SKIN

- CRITICAL RADIUS



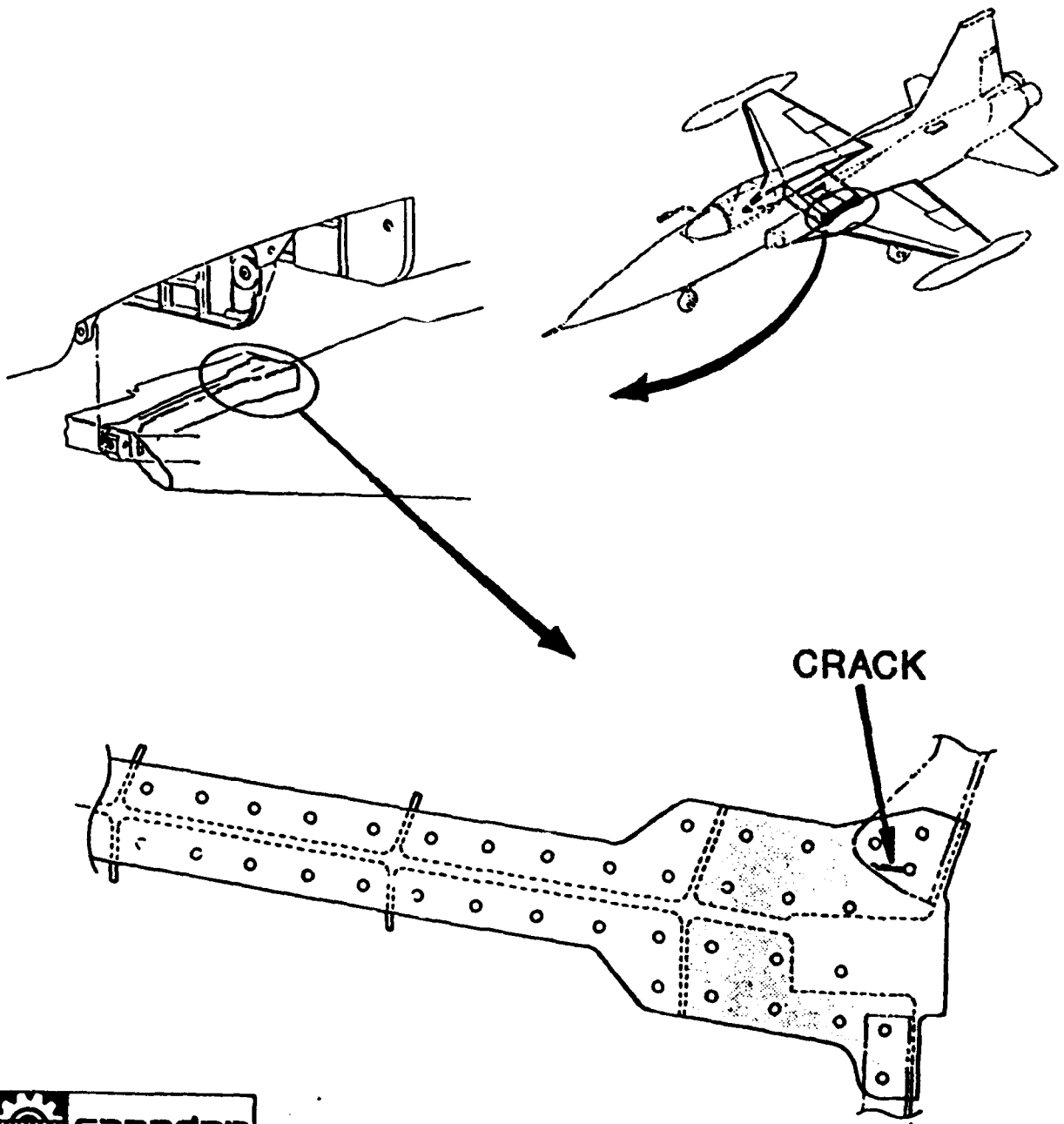
CF-5 FSDADTT

WING ROOT RIB UPPER FLANGE

- CRACK WAS DETECTED DURING THE INSPECTION AT 9755 HOURS
- CRACK RUNS FORWARD FROM FASTENER HOLE AT THE 44% SPAR ATTACHMENT
- AREA IS LOADED PRINCIPALLY IN COMPRESSION. TENSILE RESIDUAL STRESS DUE TO LARGE COMPRESSIVE LOADS AROUND FASTENER HOLE IS THE LIKELY CAUSE OF CRACKING IN THIS AREA.
- TEST WILL RESUME WITH THE CRACK STILL PRESENT. THE AREA WILL BE CLOSELY MONITORED.



CF-5 FSDADTT WING ROOT RIB



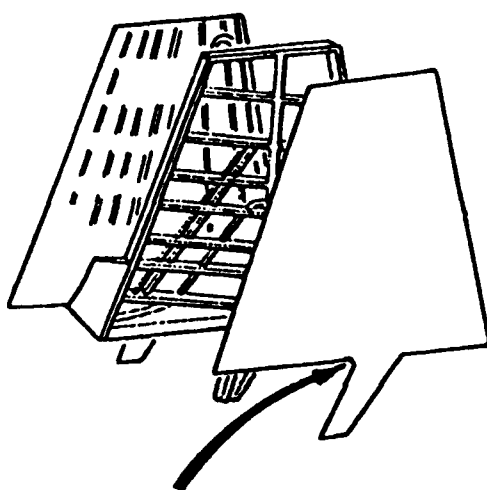
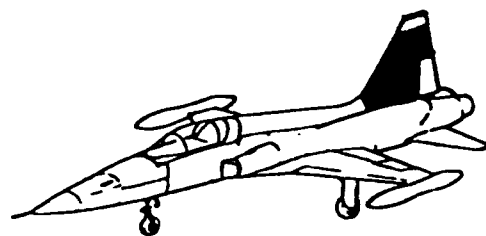
CF-5 FSDADTT

VERTICAL STABILIZER SKIN

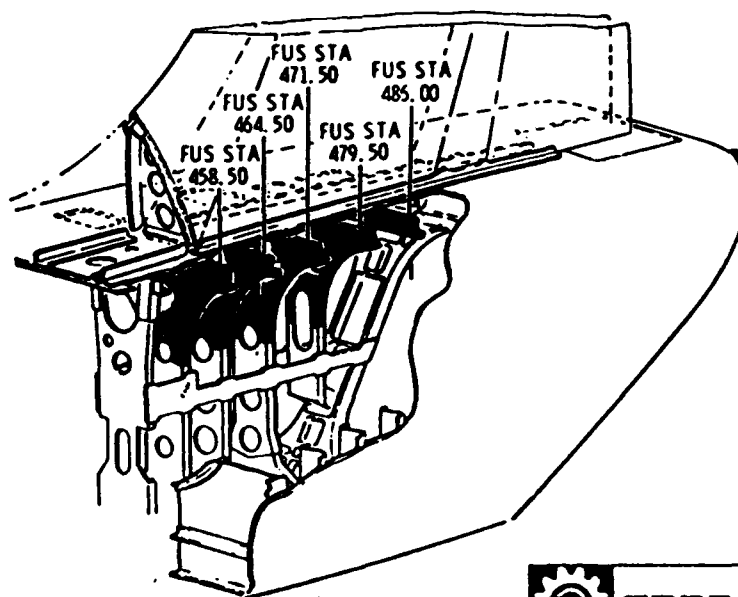
- CRACKS HAVE BEEN DISCOVERED ON MANY AIRCRAFT IN THE FIELD (70 SKINS CRACKED, AVERAGE 2500 HOURS)
- NO CRACKS WERE DETECTED ON THE TEST AIRCRAFT AT THE CRITICAL RADIUS OF THE V. STAB.
- MODIFICATIONS OF THE FUSELAGE FORMERS UNDER THE V. STAB. HAVE CHANGED THE LOAD PATH IN THE AREA.



CF-5 FSDADTT VERTICAL STABILIZER



**SKIN CRITICAL
RADIUS**



CF-5 FSDADTT

AGENDA

- INTRODUCTION
- TEST RESULTS
- FRACTOGRAPHY/MARKER BLOCKS
- ACOUSTIC EMISSION RESULTS



CF-5 FSDADTT

FRACTOGRAPHY/MARKER BLOCK

- CRACKED CRITICAL RADIUS WAS CUT OFF THE WING FOR FRACTOGRAPHIC ANALYSIS.
- SEVERAL MICROCRACKS WERE FOUND ON THE SHOT PEENED SURFACE.
- EXAMINATION OF FRACTURE SURFACE REVEALED THAT MAIN CRACK IS COMPOSED OF 7 THUMB NAIL FATIGUE CRACKS.
THESE CRACKS INITIATED FROM THE SHOT PEENED EDGE SURFACE AND PROPAGATED IN THE MATERIAL.
- EXAMINATION OF THE 7 THUMB NAIL CRACKS REVEALED THE PRESENCE OF 1 MARKER BAND IN CRACKS 5 AND 7.



CF-5 FSDADTT

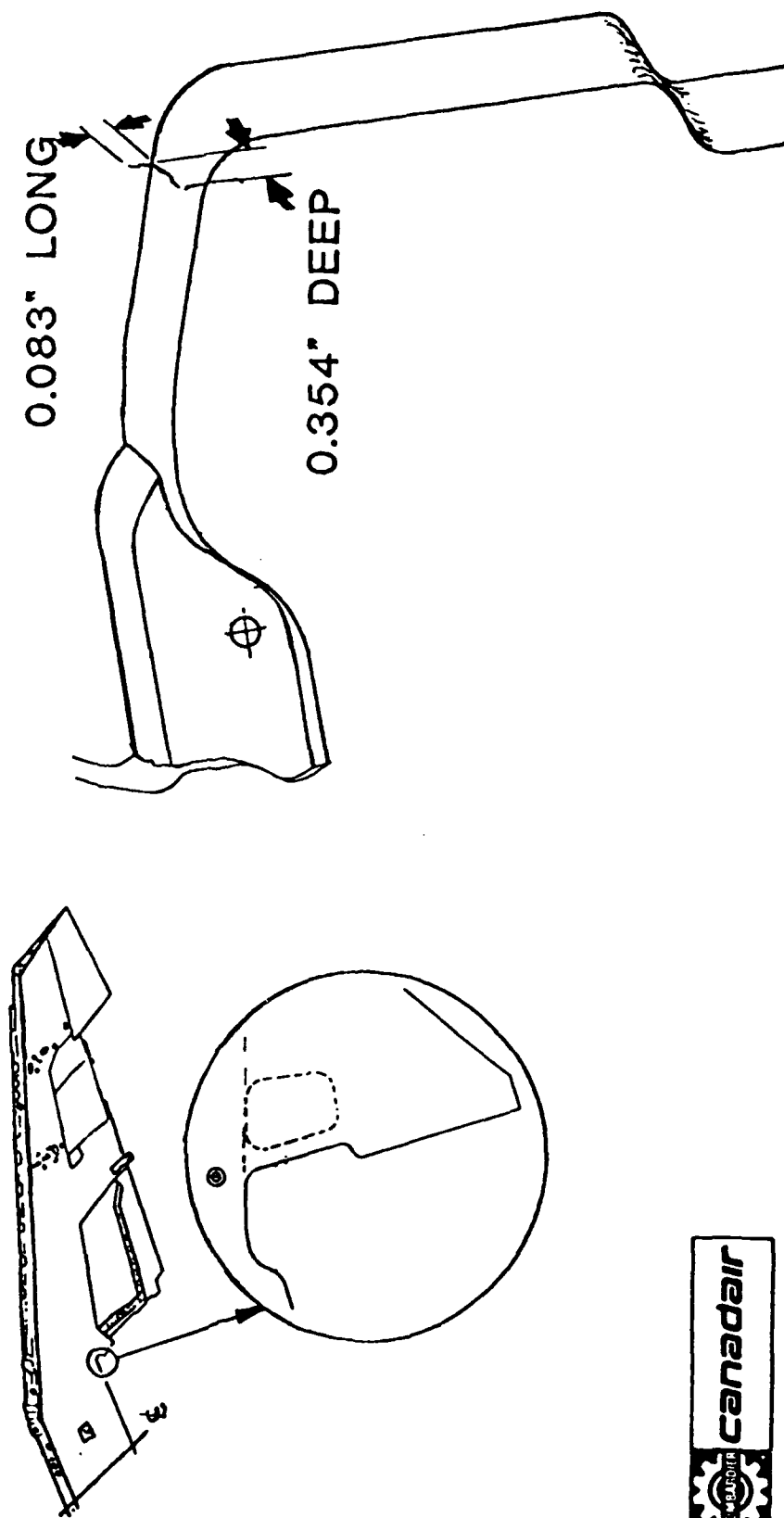
FRACTOGRAPHY/MARKER BLOCK

- ANALYTICAL DURABILITY LIFE : 5140 HOURS (SCATTER= 3.0)
- ANALYTICAL DAMAGE TOLERANCE LIFE : 4541 HOURS (FOR CORNER CRACK, $A_0 = 0.050"$)
- MARKER BLOCKS INCLUDE 20 MEDIUM-AMPLITUDE AND 200 LOW-AMPLITUDE CYCLES. MAXIMUM STRESS IN ALL THESE CYCLES IS AROUND 70% OF MAXIMUM STRESS IN THE SPECTRUM.
- 2 MARKER BLOCKS PER 1000 HOURS.
- THE PRESENCE OF 1 MARKER BAND ONLY ON THE FRACTURE SURFACE SEEMS TO INDICATE THAT THE CRACKS PROPAGATED IN A SHORT PERIOD OF TIME (LESS THAN 1000 HOURS).

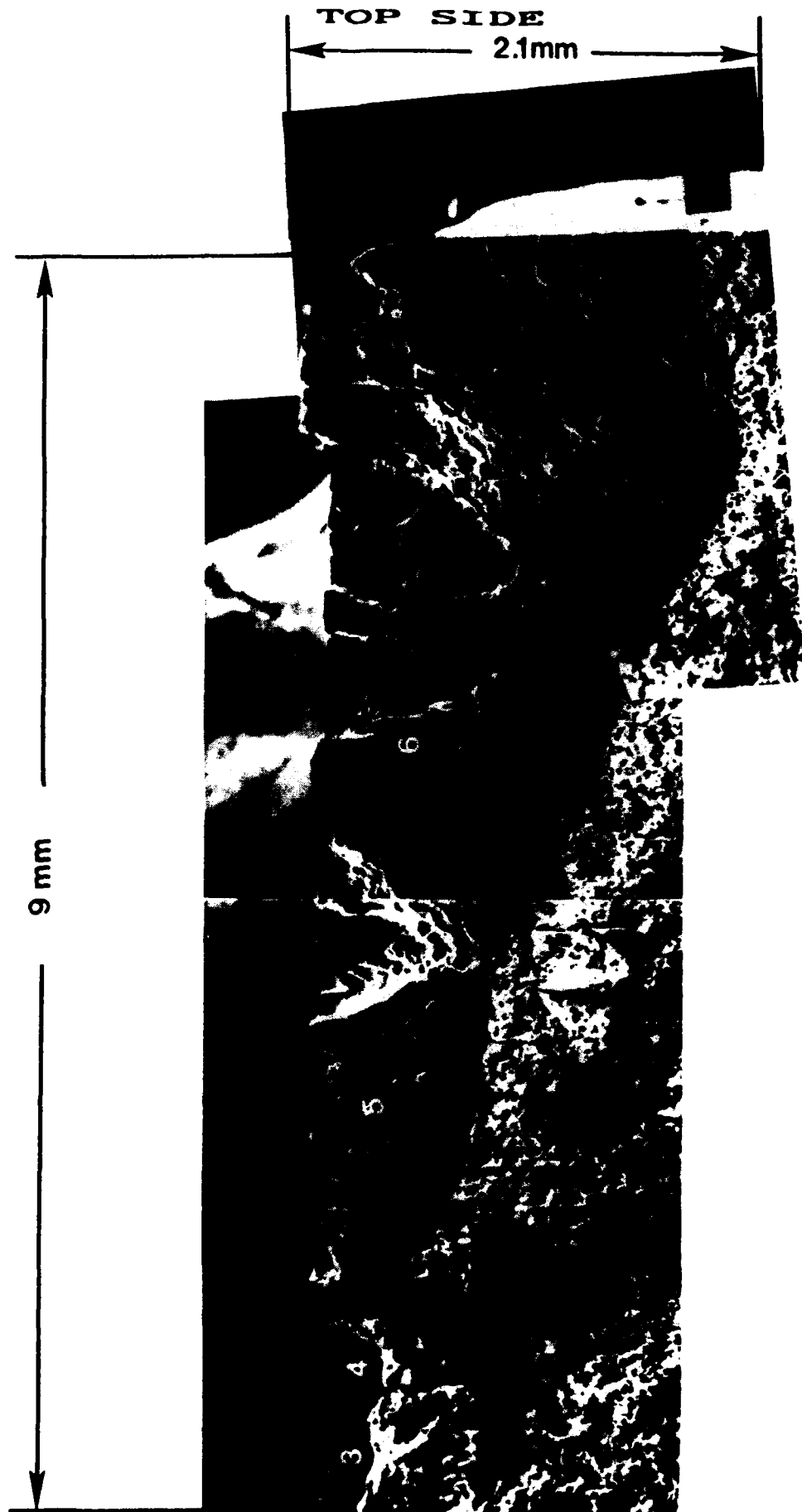


CF-5 FSDADTT FRACTOGRAPHY/MARKER BLOCK

CRACK AT WING CRITICAL RADIUS



SHOT PEENED SURFACE



Prepared by P. Leblanc

Date 1990 September 28

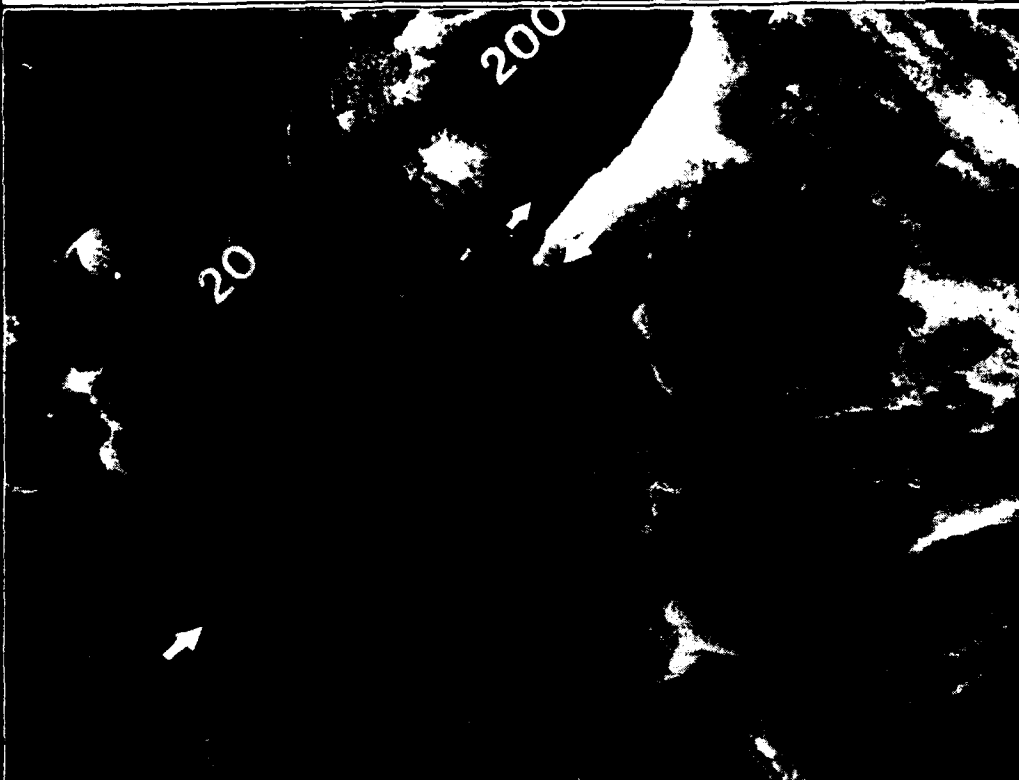


Photo #8

SEM Micrograph
Magnification: 2375x

Marker block found on
the surface of the
crack labeled #7.

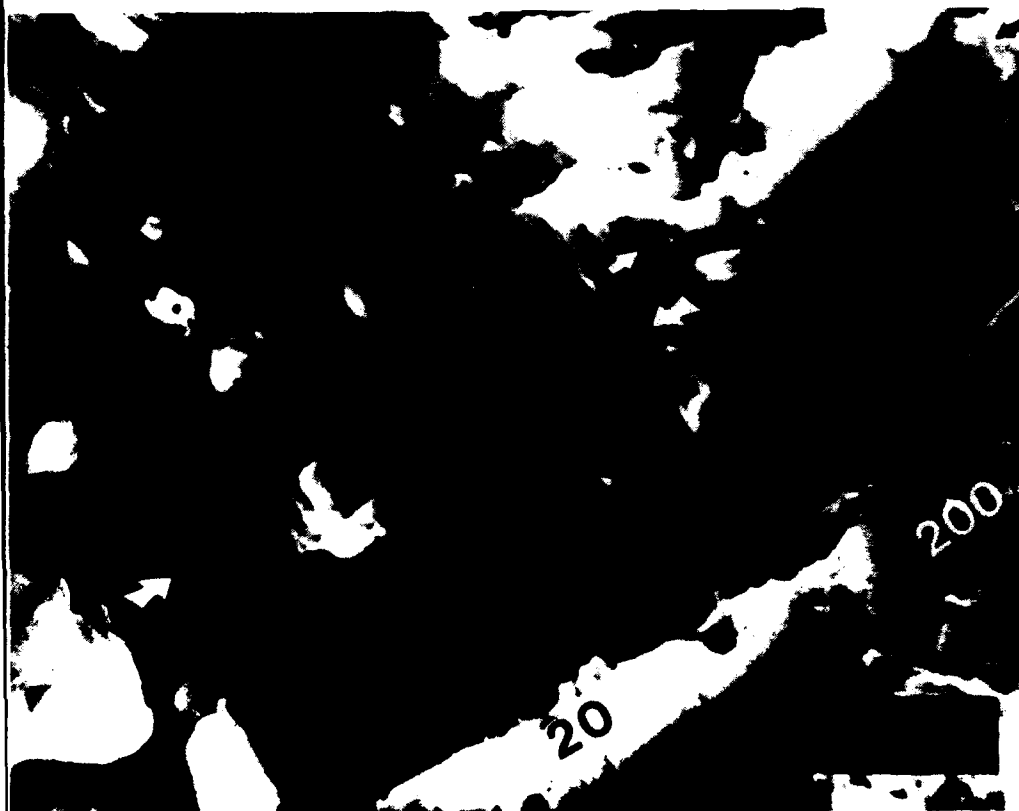


Photo #9

SEM Micrograph
Magnification: 225x

Marker block found on
the surface of crack
labeled #5.

CF-5 FSDADTT

AGENDA

- INTRODUCTION
- TEST RESULTS
- FRACTOGRAPHY/MARKER BLOCKS
- ACOUSTIC EMISSION RESULTS



CF-5 FSDADTT

ACOUSTIC EMISSION RESULTS

- BACKGROUND
- AIMS
- INITIAL MONITORING TRIAL
AT 15% SPAR LOCATION
- CONTINUOUS MONITORING OF LARGE
AREA OF LOWER WING SKIN
- CONCLUSIONS
- FUTURE MONITORING WORK

CF-5 FSDADTT

ACOUSTIC EMISSION RESULTS

- BACKGROUND:

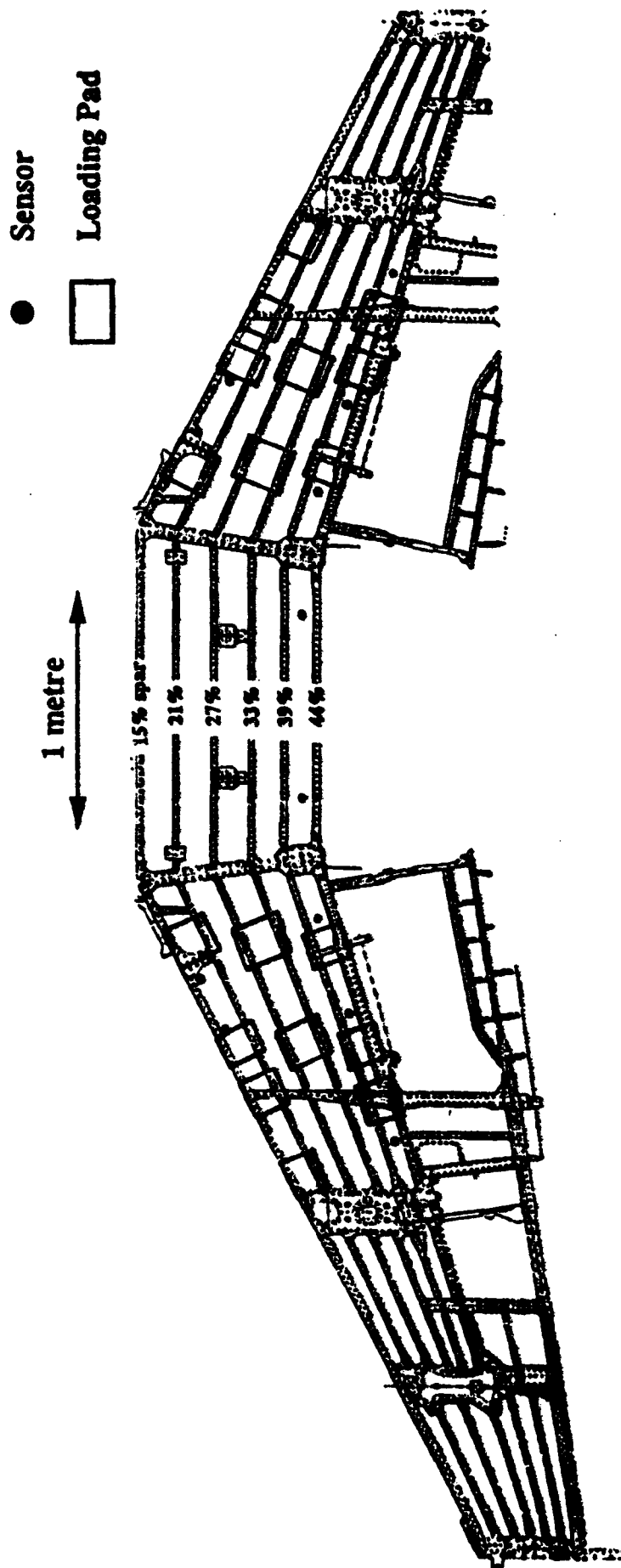
- DEFENCE RESEARCH PROGRAM WITH ROYAL MILITARY COLLEGE, KINGSTON SINCE 1976.
- PROGRAM GOAL WAS THE DETECTION OF CRACK ADVANCE IN AIRCRAFT STRUCTURE IN FLIGHT.
- EXPERIENCE GAINED WITH IN-FLIGHT MEASUREMENTS ON:
 - CF100
 - CT114
 - CC130
 - CC115
 - CF-5
 - TORNADO (UK)

CF-5 FSDADTT

ACOUSTIC EMISSION RESULTS

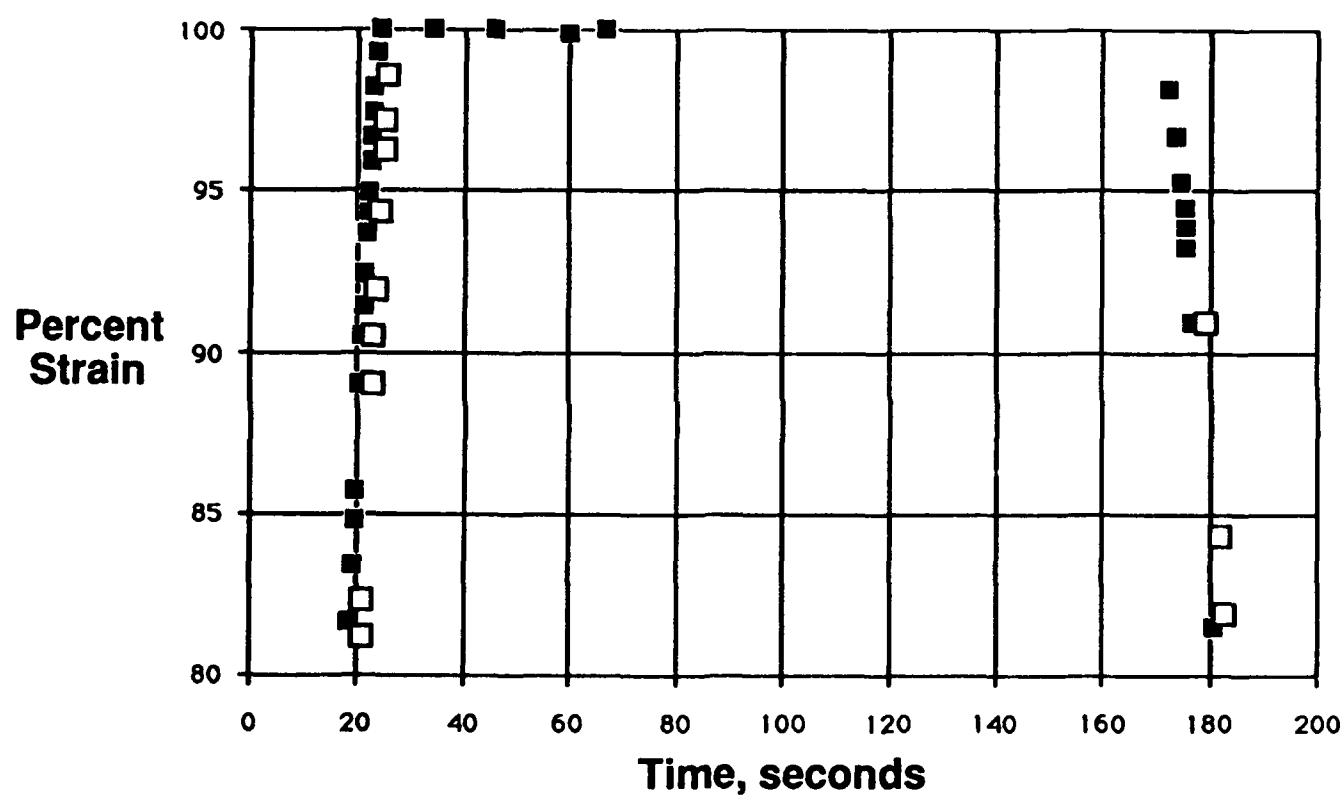
- AIMS:

1. TO CONTINUOUSLY MONITOR AN AIRCRAFT STRUCTURE DURING A GROUND DURABILITY AND DAMAGE TOLERANCE TEST.
2. TO ASSESS ACOUSTIC EMISSION AS A PREDICTOR OF CRACK PRESENCE AND CRACK ADVANCE IN A STRUCTURE WHICH IS SUBJECT TO EXTENSIVE NDT INSPECTION.
3. TO EXTEND THE RESULTS TO IN-FLIGHT MONITORING IN A FLEET ENVIRONMENT.

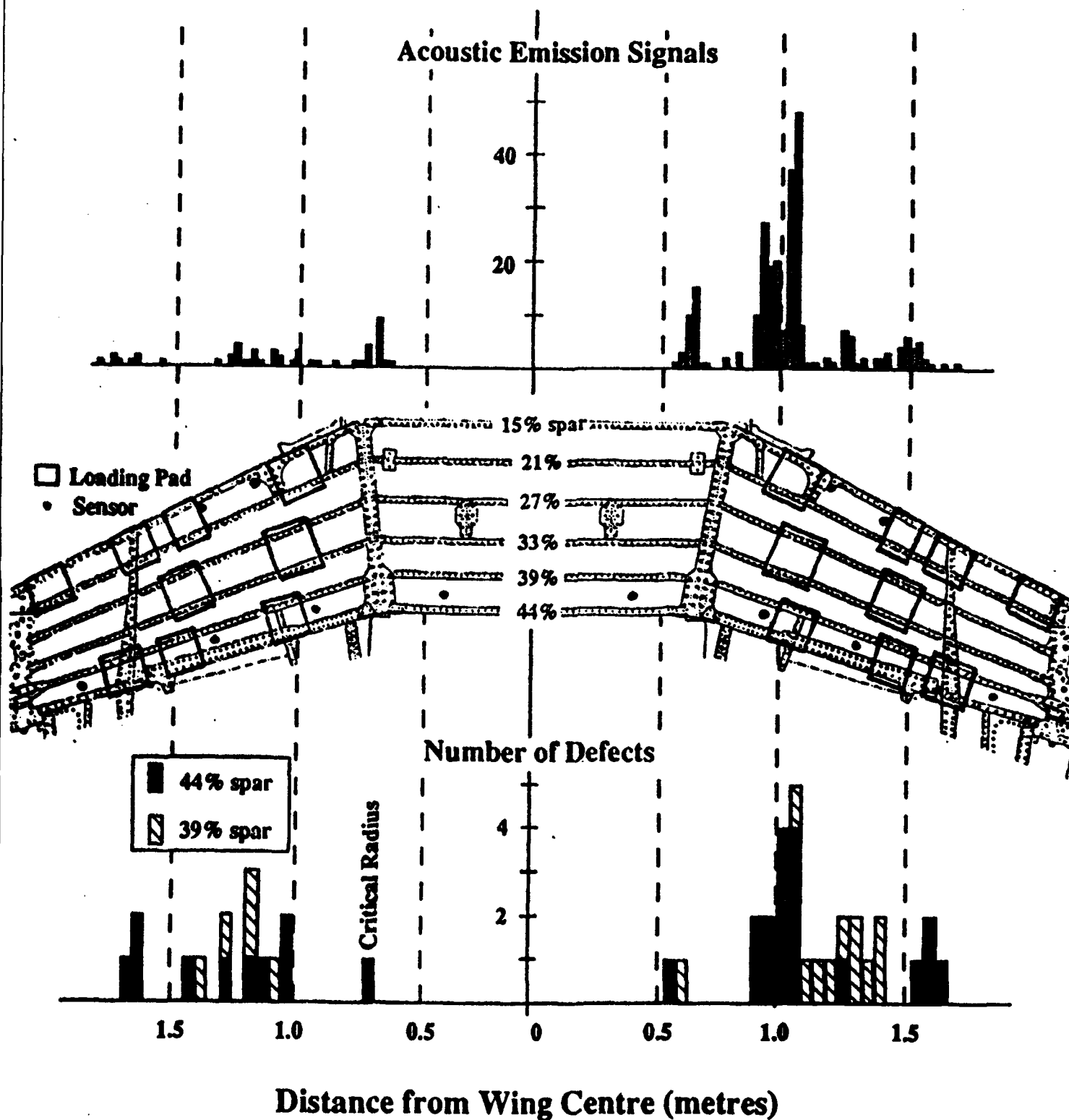


GROUND FATIGUE TEST ARTICLE (WING)

AE Comparison of Cracked (■) and Uncracked (□) Locations During Static Loading Test



Comparison of Acoustic Emission Results with 44 Defects Detected by Eddy Current (Canadair 31Aug90) [Before Reaming]



Dr. S.L. McBride
Royal Military College
Kingston, Ontario, Canada

CF-5 FSDADTT

ACOUSTIC EMISSION RESULTS

- CONCLUSIONS:

1. LARGE AREA OF THE LOWER WING SKIN OF A MILITARY AIRCRAFT WAS MONITORED DURING A GROUND DURABILITY AND DAMAGE TOLERANCE TEST.
2. CRACKS IN THE LOWER WING SKIN AND INNER SPAR STRUCTURE WERE PREDICTED BY ACOUSTIC EMISSION DETECTION.
3. ALL ACOUSTIC EMISSION PREDICTIONS OF CRACK LOCATIONS WERE LATER CONFIRMED (ROTOSCAN, EDDY CURRENT AND LPI).
4. NO CRACKS WERE FOUND BY CONVENTIONAL NDT TECHNIQUES WHICH WERE NOT PREDICTED BY ACOUSTIC EMISSION.
5. NDT CONFIRMATION OF SOME CRACKS PREDICTED BY ACOUSTIC EMISSION REQUIRED STATIC LOADING OF THE STRUCTURE TO "OPEN" THE CRACKS.

CF-5 FSDADTT

ACOUSTIC EMISSION RESULTS

- FUTURE MONITORING WORK:
 - ADDITION OF MORE SENSORS TO PROVIDE FOR TRIANGULATION ON FSDADTT.
 - IN-FLIGHT CALIBRATION TRIAL ON THE CF-5 WING HAS BEEN DONE.
 - EVALUATION OF THE IN-FLIGHT DATA IN PROGRESS.
 - MONITORING APPLICATION IN CF-5 FLEET.

APPLICATION OF DAMAGE TOLERANCE TO HELICOPTER STRUCTURE

GEORGE J. SCHNEIDER SIKORSKY AIRCRAFT
DOUGLAS TRITSCH SIKORSKY AIRCRAFT
JOHN W. LINCLON WRIGHT PATTERSON
GARY CHAMBERLAIN WARNER ROBINS ALC

1990 USAF AIRCRAFT STRUCTURAL INTEGRITY
PROGRAM CONFERENCE

APPLICATION OF DAMAGE TOLERANCE TO HELICOPTER STRUCTURE

George J. Schneider
Douglas Tritsch
Structures Research, Sikorsky Aircraft

Gary Chamberlain
Engineer, Structural Analysis Team, Warner Robins ALC

John W. Lincoln
Engineering Specialist, Aeronautical Systems Division,
Wright Patterson AFB

INTRODUCTION\BACKGROUND

The design and management of helicopter structure throughout the world is still primarily based on a "safe life" approach to define component replacement times. These replacement times are based on conservative fatigue life assessments. For example, reference 1 indicates that a part with a mean life of around 200,000 flight hours has a replacement time around 5000 flight hours. The disadvantages of a safe life approach is then that, in order to provide a high level of safety, the average part is replaced with very little of its life having been used; and although the conservative replacement times may provide considerable damage tolerance, this capability is unquantified. Damage tolerance management has the problems of introducing additional inspections, but this cost may be traded off against improved or similar safety with extended replacement times.

The application of damage tolerance to helicopter structure at Sikorsky (Figure 1) initiated in the 1970's out of a need to quantify inspection intervals for specific problems in which cracks were identified in service, and the basic technology was developed in this decade. Around 1983 Sikorsky entered a contract with Warner Robins Air Logistics Center (WR-ALC) to evaluate the applicability of damage tolerance for broad based force management of the H-53 helicopter (Figure 2) rotor and dynamic structure. Since WR-ALC manages their large inventory of fixed wing C130's C141's and F15's on a damage tolerance basis, it was logical to evaluate this approach for helicopter rotor and airframe structure. Sikorsky is also now under contract to WR-ALC to develop a flight data recorder for the H-53.

The results of these efforts have indicated that damage tolerance design and management is feasible for helicopter airframes and some if not all rotor structure. While significant progress has been made, problems still exist in the basic technology which needs to be addressed before safe damage tolerance management can be realized. One significant problem at Sikorsky arises as a legacy of safe life

management in which a high degree of conservatism has been used in defining usage data and fatigue loading. This conservatism is not appropriate in damage tolerance assessments.

The purpose of this presentation is to review the results of the H-53 damage tolerance evaluations, the current state of the technology, and the rationale and requirements for improvement in the technology.

DAMAGE TOLERANCE EVALUATION RESULTS

As part of the H-53 Damage Tolerance Assessment Program Sikorsky Aircraft has developed and delivered to WR-ALC a general computer processor for damage tolerance assessment of helicopter structure (Figure 3). Basically this processor provides the data bases and management software to generate usage load, and stress spectra; a crack model, and perform the crack propagation analysis. For the H-53 program the data bases were constructed for this aircraft, but they can be readily replaced with those for any other aircraft. It is planned that this processor will eventually be modified to interface with flight data recorder usage data and with improved flight test data.

A majority of the structures for which damage tolerance assessments were conducted in the H-53 Air Force contract are illustrated in Figure 4. Figure 5 shows details of crack locations on the main rotor structures, and indicates that many cracks are inaccessible except at a complete rotor tear down. Even at teardown problems exist in that bonded and press fit sleeves cover potential crack sites. At the current time, main and tail rotor tear downs for Sikorsky helicopters range between 800 and 1500 flight hours. Phase inspections performed on the aircraft are typically every 100 flight hours, but special inspections can be as short as 10 flight hours for areas where cracks have been experienced in service.

The crack growth results for the H-53 Air Force contract are presented in Figures 6 through 8. Also presented in these figures are approximate teardown and phase inspection intervals. These crack growth results are mean times based on the defined usage of these aircraft. They are also based on an analysis with no retardation effects, and on conservative evaluation of flight loads. The main and tail rotor structure are considered to be fairly typical, whereas the airframe structure tend to be biased toward "hot spots".

Assuming that in general for rotor parts .005 inch cracks can be detected in tear down inspections (as has been demonstrated in engine retirement for cause programs, references 2 and 3), and .030 inch cracks can be detected at phase inspections, the current crack growth results indicate

that 4 out of the 8 H-53 rotor parts might be managed on a damage tolerance basis. At first glance the airframe results look discouraging, but it must be remembered that all these structures except the transmission beams were selected based on service problem history. The transmission structure is considered to be representative of the majority of airframe structure, and it is clearly damage tolerance manageable.

Based on the results presented here, it seems reasonable to continue to improve the technology for helicopter damage tolerance assessment in order to remove uncertainty and conservatism. The remainder of this paper discusses the status of this technology in several key areas, and the recommendations and rationale for improvement. These key areas include usage data, loads data and data processing, stress analysis, and crack propagation data.

USAGE AND LOADS DATA

At the current time usage and loads data are obtained from pilot surveys and flight test strain surveys, respectively (Figure 9). For example, for the H-53 Damage Tolerance Assessment Contract, usage data was obtained from surveys of Air Force pilots conducted by WR-ALC using a basic questionnaire. This was supplemented by information from Sikorsky test pilots on aircraft behavior and performance. As a result an approximate and probably conservative usage spectrum was developed in terms of time and occurrences of various flight regimes (Figure 10). Loads data was obtained from a 1983 PAVELOW III flight strain survey sponsored by the Air Force. The processing of this data was preformed in a conservative manner in accordance with practices for safe life evaluations.

Flight Data Recorders

In order to remove uncertainty and probably conservatism from usage data, Sikorsky Aircraft is now under contract to WR-ALC to develop a flight data recorder (FDR) for the MH-53J aircraft. In addition this FDR will also have the capability of loads monitoring. A flow diagram of the flight data recorder and the interface with the Damage Tolerance Computer Program is presented in Figure 11. A prototype FDR has now been assembled and delivered to Sikorsky, and the software for regime recognition has been developed. The software is now being introduced into the recorder which will then be bench tested. Flight test is planned for 1991.

Figure 12 presents the parameters which will be used for usage monitoring and the sampling rates for these parameters. Algorithms within the FDR will interpret these parameters to define flight regimes (Figure 10). The usage data output from the flight data recorder will be in terms of total time and numbers of occurrence of each flight regime for each

flight as shown in Figure 13. This FDR usage data will be combined with flight log data which provides mission, cg, and gw information.

The FDR will also have the capability to monitor key loads (strain) information, and in general the data will be stored in terms of load histograms as a function of flight regime as shown in Figure 14. The trend at this time in helicopter loads monitoring is to identify strains which can be measured on the airframe and fixed system rotor servos which can be used to understand both fixed and rotating system key loads. Army contracts are now in progress to evaluate this technology which will eventually be applied to the Air Force FDR. Initial fatigue and damage tolerance evaluations will likely rely primarily on the flight test loads data base verified through FDR loads measurements.

Flight Testing and Data Processing

Examples of the load parameters measured in a flight test program are presented in Figure 15. The flight test is conducted by flying several repeats of each flight regime (Figure 10), cg, and gw combination. For each flight regime a 10 to 20 second data burst is recorded for each of the Figure 15 "load" parameters. In some maneuvers (e.g. longitudinal reversal) this data burst may represent the entire maneuver, but in other maneuvers (e.g. level flight) it represents only a sampling of time in the maneuver.

Figure 16 shows the flight test data processing used to obtain the crack propagation analysis results presented in Figures 6 through 8. In this data processing the 95% or maximum vibratory load in the data burst is used to represent the entire data burst at the dominate frequency of the data burst. In other words the actual data burst is approximated by a single vibratory load with the same number of cycles as in the data burst. This is definitely conservative for the transient maneuvers itemized in Figure 10.

Since a maneuver is repeated several times in a flight test program a distribution of 95% and max loads for each flight regime is obtained (e.g. Figure 17). These distributions indicate that the same 95% or max load is not realized each time a flight regime is flown. These distributions are incorporated in the current crack propagation analyses.

Requests for funding have now been submitted to WR-ALC to improve the flight test data processing, and to have this processing available for the upcoming MH-53J flight tests. This would include evaluation of the effects on crack growth times of rainflow counting of data bursts. It is expected that significant increases in crack propagation times would result. Figure 18 shows the process of using fully cycled counted loads and flight data recorder usage data to develop

improved load spectra.

STRESS ANALYSIS

In order to determine the relationship between loads and the stresses along a potential crack path, detailed stress analyses are required. Finite element and boundary element models are often used to perform these analyses. Figures 19 through 21 show typical examples of finite element models. Figure 19 shows a combined model of the H-53 vertical hinge and upper and lower hub plate as well as a separate model of the spindle. The combined model hub plate/vertical hinge was made to gain some understanding of the complex load paths between the vertical pin and the hub plates which includes bearing surfaces. Figure 19 gives some idea of the detail in these models at potential crack locations. Figure 21 is a finite element model of a portion of a main rotor spindle made to determine thread root stresses. Analysis on thread stresses is a difficult problem and finite element models such as that shown in Figure 21 are expensive to build. Therefore, alternate solutions to thread analysis have been investigated using published thread load distribution analyses and boundary element models to obtain thread root stresses.

Figure 22 shows the excellent agreement between finite element and boundary element thread root stress distribution predictions. The boundary element programs used to date can not model both threaded parts (i.e. rod and nut), and therefore the thread load distribution had to be calculated by separate analysis. Although the thread load distribution analyses have given reasonable correlation with finite element results, improvements in the analysis are considered necessary. One possibility involves the use of a new boundary element analysis available in UTC in which both threaded parts can be modeled.

Figure 22 shows the correlation between the results of an H-53 rotor finite element model shown in Figure 19, and some strain measurements at the lug crack location shown in Figure 20. The nonlinearity in the strain with load is evident from the measurements, but the analysis is quite good. Strain surveys to verify the finite element results for rotor head components are, however generally not available, and some of the analytical predictions are in conflict with available fatigue test results. In order to develop high confidence in the stress analyses, Sikorsky is proposing to conduct detail strain surveys on H-53 rotor heads in the head and shaft facility shown in Figure 24. The head and shaft facility allows simulation of complex combinations of centrifugal load, damper load, flapping angle, and lag angle. Accurate and verified stress analyses are considered critical to reliable crack propagation analysis.

CRACK PROPAGATION DATA

Small specimen crack propagation tests have been conducted to obtain basic crack propagation rate data, evaluate prediction capabilities for small cracks in nonuniform stress fields, and evaluate spectrum effects. The test specimens used in this testing consisted of compact tension specimens and edge notch specimens shown in Figure 25. In the notched specimens a .01 inch EDM corner flaw was introduced at the root of the notch, and valid crack propagation data was generally obtained from initial cracks of .02 to .04 inches.

The testing conducted to obtain basic crack propagation rate data is presented in Figure 26. A primary goal of this testing was to obtain data near the crack growth threshold at two R (S_{min}/S_{max}) values typical of those in helicopter structure. Problems were encountered in testing the Al-6061 and Al 7075-T73 materials and valid data was not obtained. For these materials data in the literature had to be used.

The spectrum and notched specimen testing programs are presented in figure 27. Tests consisted of compact tension spectrum tests; and notched specimen constant amplitude and spectrum tests. As shown in the figure the AK values for the initial crack sizes were large enough such that the testing was primarily in the midrange crack growth rate region. The spectrum used in these tests was based on flight test data for an airframe structure. An airframe structure was chosen since its spectrum had more variation in the maximum stress than is typical of rotor parts (Figure 28), and could therefore be expected to upper bound spectrum retardation effects for helicopter structure.

Figures 29a and b show typical material sources and grain structure for the test specimens. Figures 30a and b show typical fracture surfaces on the notched specimens. One interesting point is that the critical crack sizes were usually around 0.25 inches, and the test stresses were generally below probable limit load levels.

Figure 31 shows typical crack propagation rate test data obtained from the constant amplitude compact tension specimen testing. Also shown in this plot is the range of data available from the Air Force design guide. As shown the Sikorsky test data extends much closer to the crack propagation threshold which is a critical area for helicopter structure.

Figure 32 shows a comparison of crack growth analysis versus test data for constant amplitude notched specimen tests in two materials. Correlation is very good for the Al 7075-T73, but only fair for 4340 steel.

Figure 33a,b show some of the results for compact tension and

notched specimen spectrum tests. As shown spectrum effects are small in the Al 7075-T73. In the 4340 steel the comparison of no retardation model analysis ($SOR = \infty$) and compact tension constant amplitude and spectrum test results are similar. Therefore retardation effects appear minimal at this crack size. However, at the smaller crack sizes of the notched specimen, spectrum effects appear to provide a increase in crack propagation times of about 2. As previously noted the spectrum used in these tests was based on an airframe part; and less variation in max stress, and therefore less retardation effect, would be expected in rotor parts.

The retardation effects seen in the testing to date are based on testing with both large (0.5 inch) and fairly small (.02 - .04 inch) initial cracks, but with stress intensities always at "midrange" levels. Analysis of small cracks at near threshold stress intensity levels indicates much greater retardation effects as shown in Figure 34. Figure 34 also shows the high sensitivity of crack growth predictions to small variations in stress. Both of these sensitivities are the result of propagating cracks near the threshold.

The retardation effect is illustrated in Figure 35. As shown from the equation a Willenborg retardation model effectively lowers the effective R ratio. In the "midrange" this simply results in a lower crack growth rate; however near threshold a very small change in R can result in essentially "dropping through" the threshold resulting in a mathematical prediction of total crack arrest. Although there is some data (i.e. reference 4) on the effects of spectrum overloads on threshold stress intensity, in general the necessary data and verified retardation models are not available. Therefore the crack propagation results reported in Figures 6 through 8 are currently based on no retardation models.

The sensitivity shown in Figure 34 to stress variation is the result of having a large number of cycles in the spectrum near the threshold. Therefore small changes in stress result in moving large numbers of cycles above and below the threshold resulting in large changes in predicted crack propagation time. This sensitivity to stress is similar to that encountered near the endurance limit in S-N curves when performing "safe life" analysis. As a result Sikorsky uses both a factor of safety on stress and life when determining safe life component replacement times. The stress factor of safety dominates near the endurance limit and the life factor dominates in the low cycle S-N area. A similar process is recommended in determining inspection intervals from crack growth analysis results. In this case the stress factor of safety would dominate when initial stress intensities are in the threshold region, and the life factor would dominate when initial stress intensities are in the "midrange".

A final observation related to damage tolerance of helicopter structure is presented in Figure 36. This figure shows the threshold crack sizes for several materials assuming the vibratory stress at 100%, 75%, and 50% of the working endurance limit used in safe life design. The values for R ratio and stress concentration are 0.7 and 3.0, respectively, which are typical of the high cycle loads found in rotor structure. This figure indicates that damage tolerance management of mature helicopter rotor parts will depend on showing that a majority of high cycle stresses are less than 50% of the safe life working endurance stress. In order to do this the information from service usage monitoring and from improved flight test data processing is essential. This figure also suggests that steel parts present the most difficulty for damage tolerance management.

SUMMARY

In summary, the work that has been conducted to date at Sikorsky Aircraft, particularly under Air Force contract has ~~was~~ pointed out the key technical issues which must addressed (Figure 37). This work has also led to some general recommendations for damage tolerance assessment of helicopter structure (Figure 38).

For most of the technology issues presented in Figure 37 proposals have been submitted to WR-ALC, and the flight data recorder work is, as mentioned, under contract. The recommendation in Figure 38 to not use retardation models may be eliminated if reliable retardation models can be established near the threshold.

REFERENCES

1. Thompson, A. E., and D. O. Adams, "A Computational Method For The Determination of Helicopter Dynamic Components", 46th Annual AHS Forum Proceedings, May 1990.
2. Lincoln, J. W., "Damage Tolerance For Helicopters" 1990 ICAF Conference.
3. Hoppe, W. C., "A General Discussion of the Retirement For Cause Inspection System", 1987 Aircraft/Engine Structural Integrity Program (ASIP/ENSIP) Conference, AFWAL-TR-4128.
4. Hopkins, S. W., et. al., "Effect of Various Programmed Overloads on the Threshold for High-Frequency Fatigue Crack Growth", ASTM STP 595, 1976.

APPLICATION OF DAMAGE TOLERANCE TO HELICOPTER STRUCTURE

- **DAMAGE TOLERANCE ASSESSMENT - SPECIFIC SERVICE PROBLEMS**

- 1970 - Present

- **H-53 DAMAGE TOLERANCE ASSESSMENT PROGRAM**

- Phases I - IV

- 1983 - 1989 Air Force Contract

FIG. 1

H-53 HELICOPTER



FIG.2

DAMAGE TOLERANCE ASSESSMENT COMPUTER PROGRAM

```
graph TD
    US[USAGE STATISTICS] --> USG[USAGE SPECTRUM TIME HISTORY GENERATION]
    USG --> LSG[LOAD SPECTRUM GENERATION]
    USG --> FLT[FLIGHT TEST LOAD DATA STATISTICS]
    LSG --> LSG_BOX[LOAD SPECTRUM GENERATION  
FLIGHT DATA BASED  
AIRFRAME MANEUVER]
    FLT --> HFD[HELIPTER FLIGHT DYNAMICS PROGRAM (GEN-HEL)]
    HFD --> AAL[APPLIED AIRFRAME LOADS ARRAY]
    AAL --> ILIF[INTERNAL LOADS INFLUENCE FUNCTIONS]
    ILIF --> NAF[NASTRAN AIRFRAME FINITE ELEMENT MODEL]
    NAF --> SSG[STRESS SPECTRUM GENERATION]
    LSR[LOAD/STRESS RELATIONS] --> SSG
    LSR --> SIM[STRESS INTENSITY MODEL]
    SIM --> SD[STRESS DISTRIBUTION]
    SD --> GSAM[GENERAL STRESS ANALYSIS OR COMPONENT F.E. MODELS]
    GSAM --> SD
    SSG --> MG[MODEL GENERATION]
    MD[MATERIALS DATA] --> MG
    MG --> CG[CRACK GROWTH]
    MG --> CI[CRACK INITIATION]
    CG --> AN[ANALYSIS]
    AN --> II[INSPECTION INTERVAL]
    AN --> RT[REPLACEMENT TIME]
```

FIG. 3

FIG. 3

AIR FORCE H-53 DAMAGE TOLERANCE ASSESSMENT STRUCTURE ANALYZED

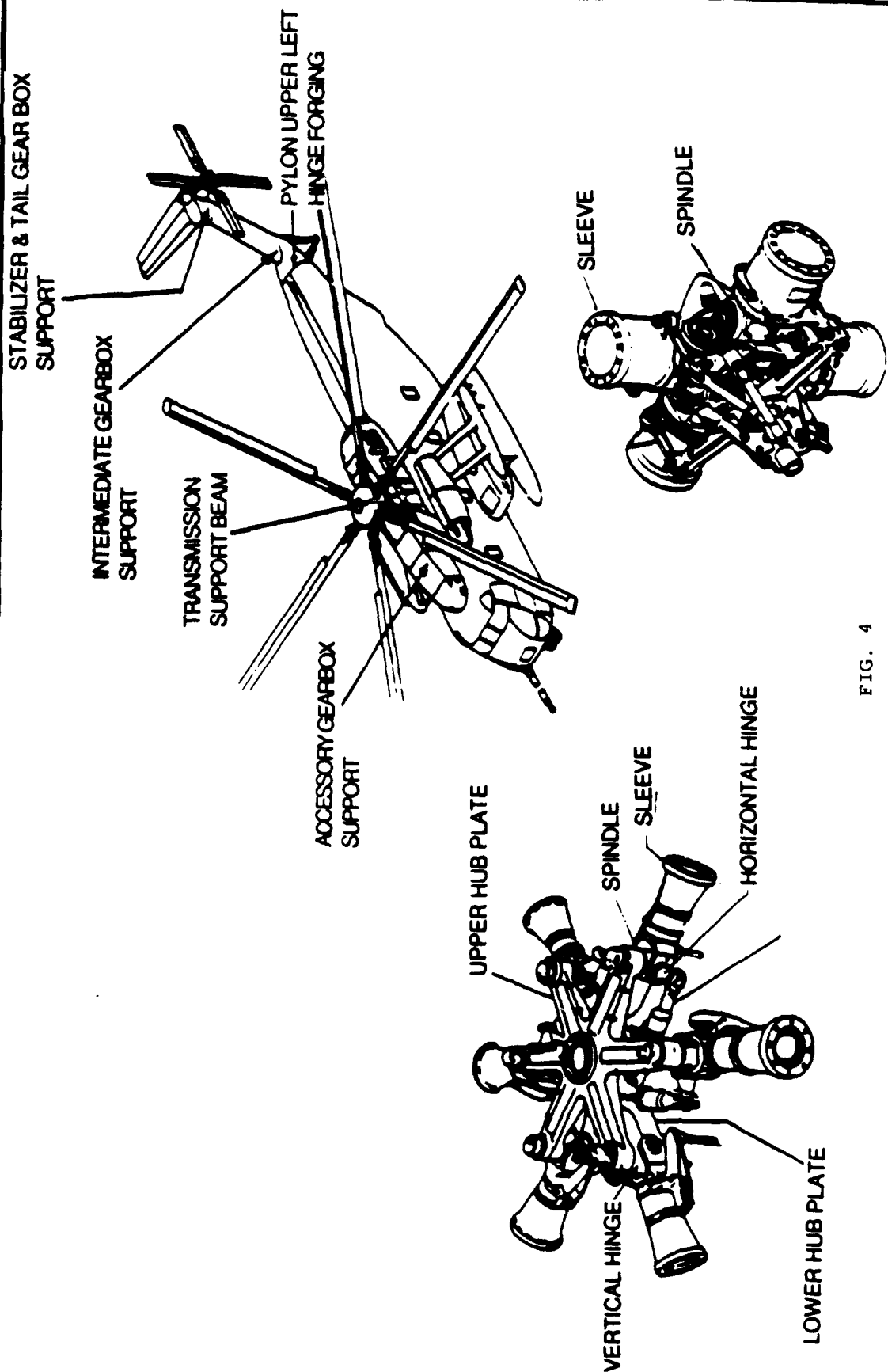


FIG. 4

SOME POTENTIAL MAIN ROTOR CRACK LOCATIONS

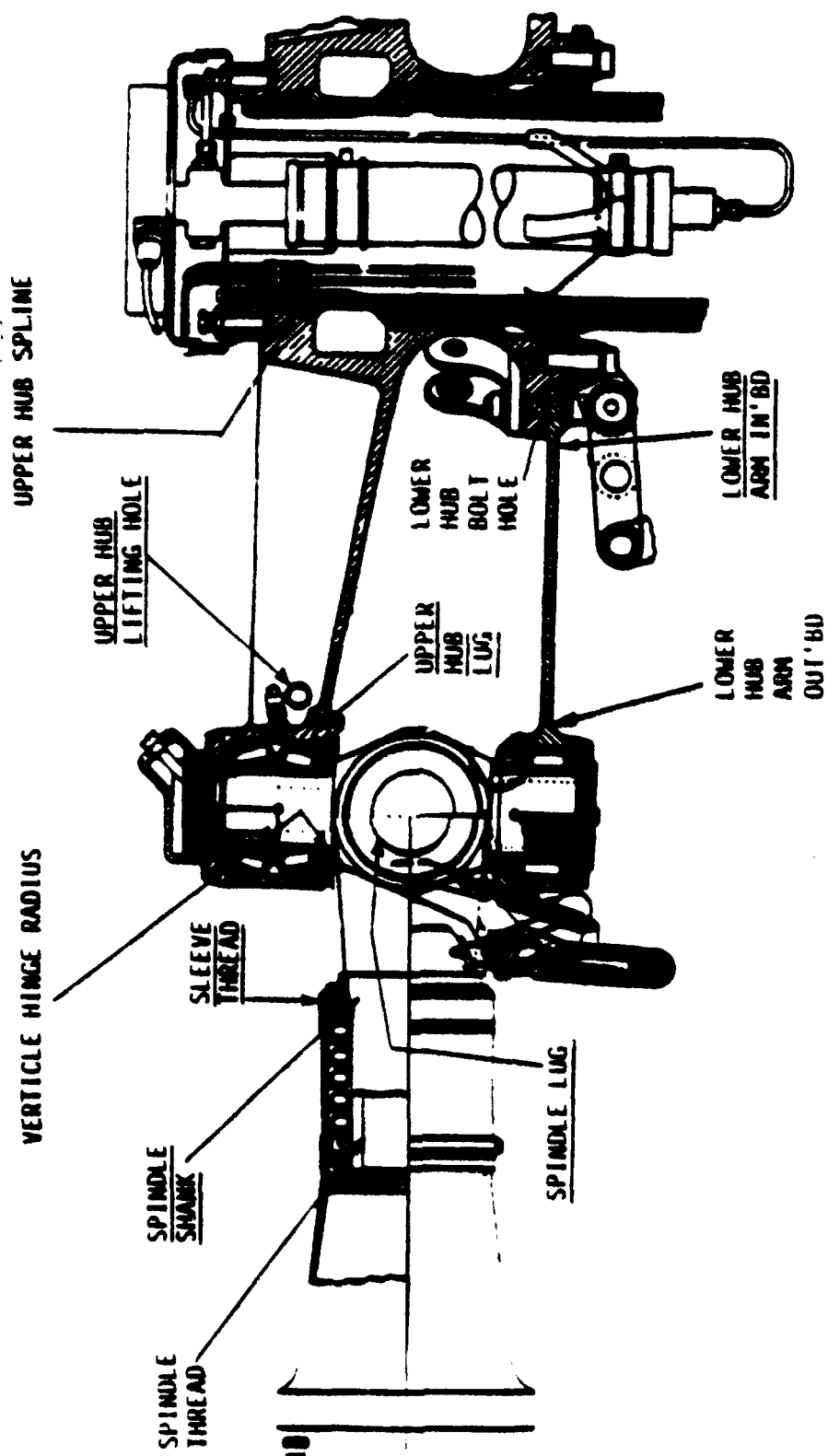


FIG. 5

DAMAGE TOLERANCE ASSESSMENT PERFORMED FOR UNDERLINED LOCATIONS

MAIN ROTOR CRACK GROWTH RESULTS

Phase Inspection is 100 Flt. Hours (Typical)
Time Between Overhaul (TBO) is 1000 Flt. Hours (Typical)

Structure - Crack Location	Material	High Cycle Threshold Crack Depth (inches)	Crack Propagation Time* (Flight Hours) From Initial Crack Depths of: 0.005" 0.010" 0.030"
H-53			
Upper Hub Plate	Ti-6Al-4V		
- Lifting Hole	Alpha-Beta	0.003	50
- Lug		0.003+	High
Lower Hub Plate	Ti-6Al-4V		
- Inboard Arm	Alpha-Beta	0.008	558
Horizontal Hinge	4340 Steel		
- Damper Radius		0.003	212
Spindle			
- Lug	Ti-6Al-4V	0.022	--
- Shank Radius	Alpha-Beta	0.012	--
Sleeve			
- Threads	Ti-6Al-4V	0.002	150
Blade Spar	Al 6061-T6	0.030	--

FIG. 6

TAIL ROTOR CRACK GROWTH RESULTS

Phase Inspection is 100 Flt. Hours (Typical)
Time Between Overhaul (TBO) is 1000 Flt. Hours (Typical)

Structure - Crack Location	Material	High Cycle Threshold Crack Depth (inches)	Crack Propagation Time* (Flight Hours) From Initial Crack Depths of: 0.005" 0.010" 0.030"
H-53			
Spindle	Ti-AL-4V		
- Shank Radius		0.023	56
- Threads		0.007	10
Sleeve			
- Threads	Ti-6AL-4V	0.002	>2000
			475

FIG. 7

AIRFRAME CRACK GROWTH RESULTS

Phase Inspection is 100 Flt. Hours (Typical)
Time Between Overhaul (TBO) is 1000 Flt. Hours (Typical)

Structure - Crack Location	Material	High Cycle Threshold Crack Depth (inches)	Crack Propagation Time* (Flight Hours) From Initial Crack Depths of: 0.005" 0.010" 0.030"
H-53			
Upper Left Pylon	Al7075-T73		
Fold Hinge Ftg.			
- Rivet Hole		0.005	410 170 45
Acc. Gear Box	Al7075-T73		
Support Fitting			
- Bolt Hole		0.002	50 29 7
Stabilizer Support	Al7075-T73		
Fitting			
- Hole		0.004	40 21 6
Transmission	Al7075-T73		
Support Frame			
- Holes		0.050 0.100 1.000	-- -- -- >2000 >2000 >2000

FIG. 8

USAGE AND LOADS DATA - SUMMARY

CURRENT

USAGE - AIR FORCE PILOT SURVEYS

LOADS - SIKORSKY FLIGHT TEST PROGRAM

FUTURE

USAGE - FLIGHT DATA RECORDER - INDIVIDUAL HELICOPTER TRACKING
PROGRAM (IHIP)

LOADS - FLIGHT TEST DATA

- FLIGHT DATA RECORDER - LOADS AND ENVIRONMENTAL
SPECTRA SURVEY (LESS)

FIG. 9

HELICOPTER USAGE SPECTRUM - FLIGHT REGIMES

<u>Regime</u>	Occur. Per 100 Flt Hrs	Percent Time	<u>Regime</u>	Occur. Per 100 Flt Hrs	Percent Time
Ground			Fwd Flt & Related		
rotor Engagement*	49	2.04	Climb	98	7.64
rotor Stop*	49	2.04	Lt Turn (Climb)	98	0.55
Taxi (Inc. turns)*	49	2.45	Rt. Turn (Climb)	98	0.55
			Auto	19	0.53
Hover			Auto Turns	37	0.05
IGE	49	6.56	Auto Entry/Recovery*	19	0.04
OGE	49	6.56	Lt Turn*	351	1.27
Side Flt	0	0.0	Rt. Turn*	351	1.27
Rear Flt	0	0.0	Long Rev.*	196	0.08
Left Turn*	98	0.55	Lat. Rev.*	253	0.1
Right Turn*	98	0.55	Rud. Rev.*	98	0.04
Long. Rev.*	294	0.12	Coll. Rev.*	258	0.11
Lat. Rev.*	294	0.12	Pullout*	253	0.7
Rud. Rev.*	294	0.12	Pushover*	253	0.7
Coll. Rev.*	294	0.12	0.5 Vmax		2.74
			0.6		12.98
Takeoff & Landing			0.7		23.23
Vert. T/O*	78	0.13	0.8		14.77
Running T/O*	20	0.03	0.9		3.32
Hover Approach*	98	0.2	1.0		0.27
Vert. Landing*	88	0.07	1.1 Vmax Dive	23	0.77
Running Landing*	10	0.02	P.P.D.		
			(.6-.8 Vmax)	56	6.23
Gusts					
Vertical Gust*	897	0.37			

FIG. 10

* Indicates Transient Manuevers - Others Are Stesdy State

FLIGHT DATA RECORDER/DAMAGE TOLERANCE FLOW CHART

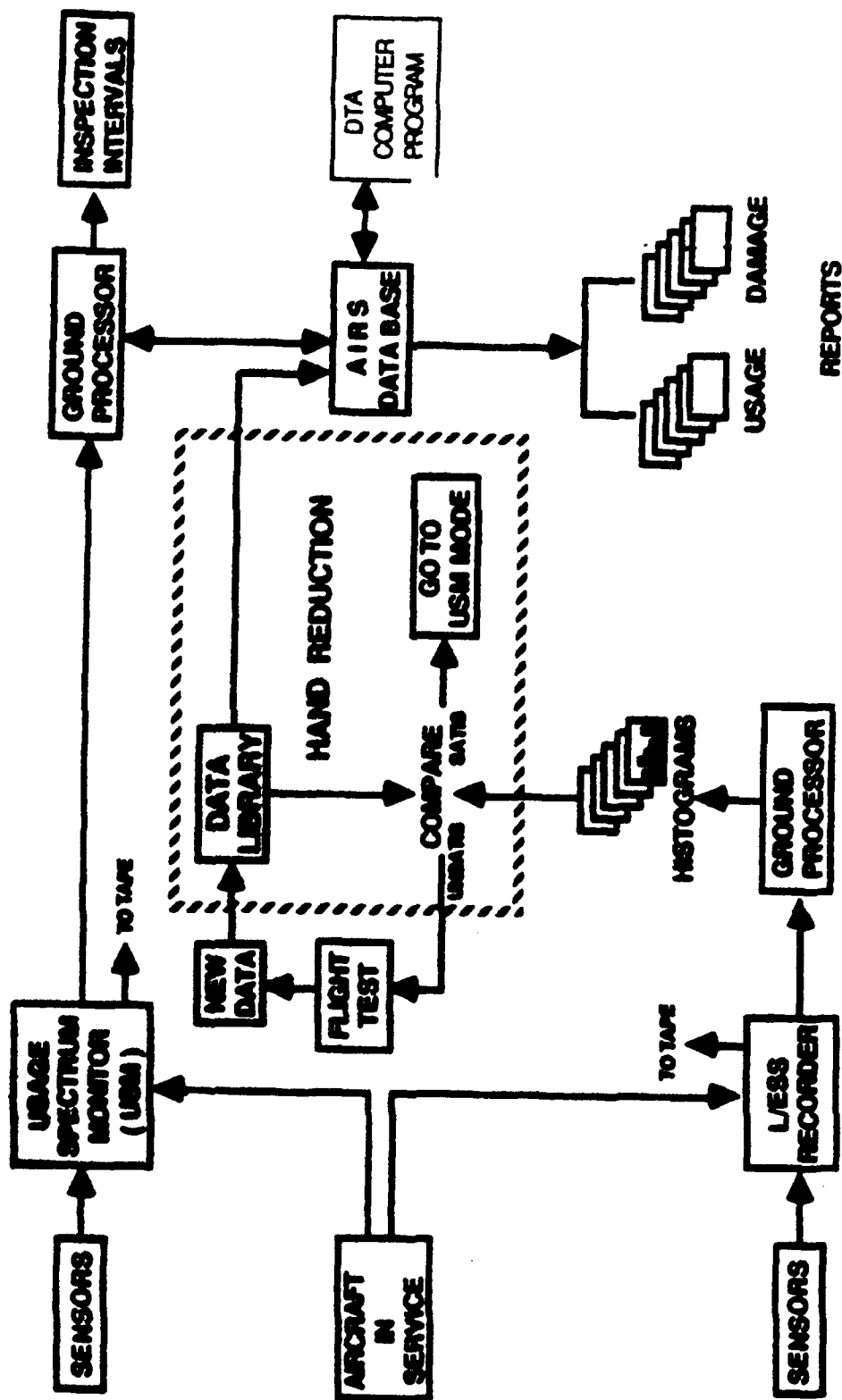


FIG. 11

USAGE PARAMETERS MONITORED ON FLIGHT DATA RECORDER

SIGNAL	RANGE	SAMPLE RATE
PITCH/ROLL ATTITUDE	±90 deg	4 HZ
YAW ATTITUDE	0-360 deg	4 HZ
ROLL/YAW/PITCH RATE	±40 deg/sec	4 HZ
LONG./LAT. STICK POS.	±50%	16 HZ
COLL. STICK POS.	0 -100%	16 HZ
PEDAL POS.	±50%	16 HZ
LOAD FACTOR	64.4 ft/sec**2	4 HZ
TORQUE, ENGINE	0-130%	4 HZ
OUTSIDE AIR TEMP	±60 deg C	4 HZ
ENGINE GAS TURBINE SPEED	0%=0 HZ 120%=84 HZ	±2% BET. 40-120%
ROTOR SPEED	0%=0 HZ 130%=91 HZ	±2% BET. 40-130%

FIG. 12

FLIGHT DATA RECORDER USAGE DATA

```
graph LR; AR[Aircraft Recorder] --> FFF[1 File / Flight]; FFF --> CF[Combine Files]; FL[Flight Log] --> CF; CF --> DBE[Data Base Entry]
```

The diagram illustrates the workflow for flight data recorder usage data. It begins with an **Aircraft Recorder**, which outputs **1 File / Flight**. This file is then processed by the **Combine Files** step, which also receives input from a **Flight Log**. The final output is **Data Base Entry**.

Flight Log

AC #	Date	Time	Mission	Wt	CG

Combine Files

AC # ☐ **PR #** ☐ **Rec #** ☐
Mission ☐ **Wt** ☐ **CG** ☐

Startup	Date	Time
Shutdown		

Recdme. **Time** **Occurrences**

15	50	4
21	207	12
22	91	3
30	710	7
...
...
...

Data_Alt **Time**

1	2000
3	750
2	300

Data Base Entry

FIG. 13

Data Base Entry

TYPICAL L/ESS DATA HISTOGRAM

Parameter: Stationary Schedulers Load (MRSTASC)
Regime: Right Turn 40 - 50 Deg. AoB

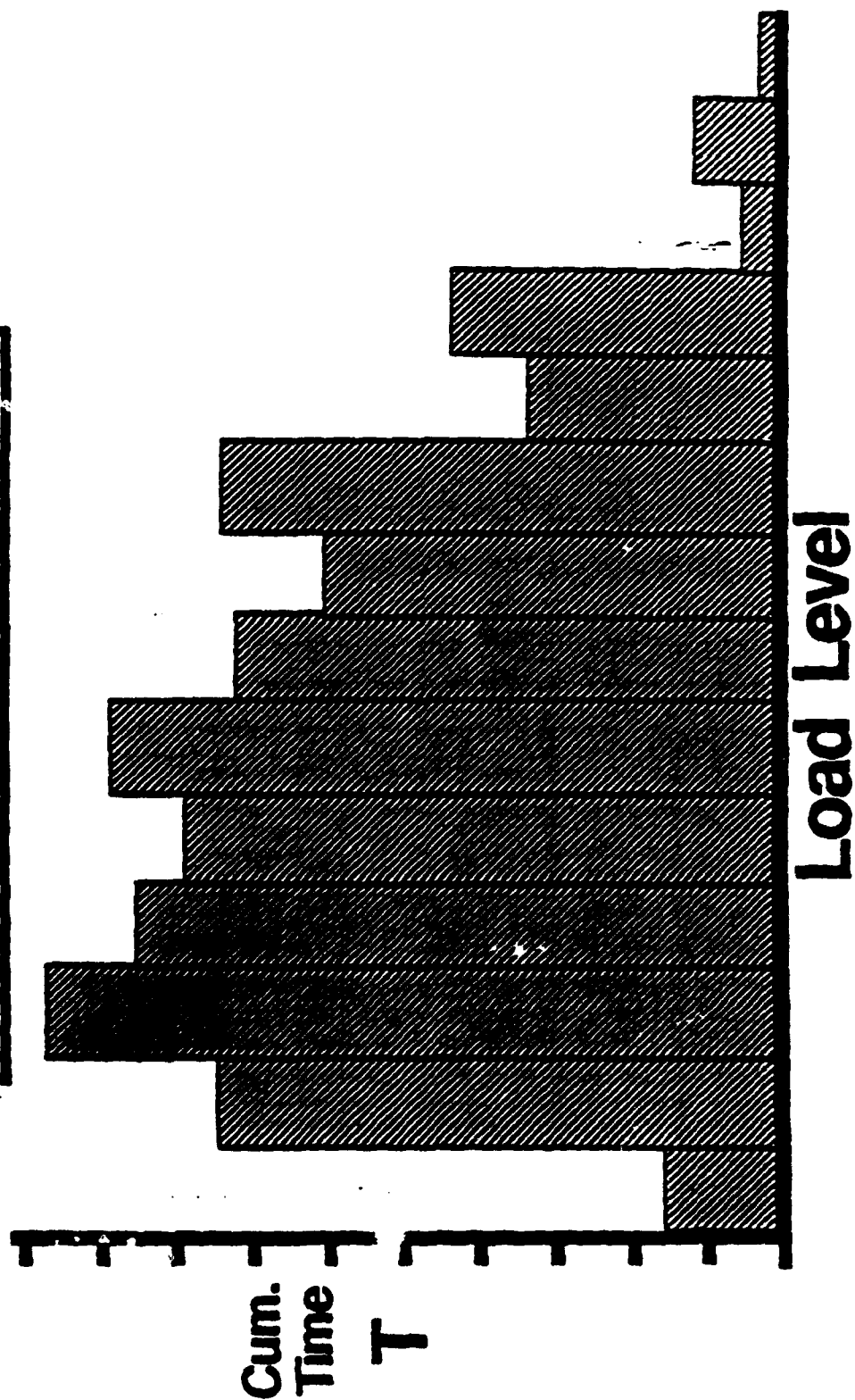


FIG. 14

FLIGHT TEST LOAD PARAMETERS

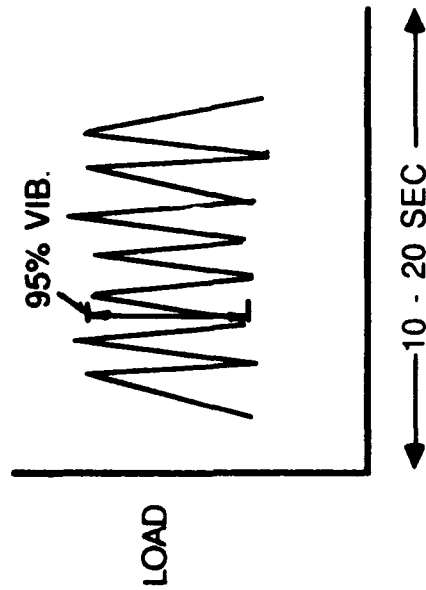
Structure	Main Rotor Structural Load (or Parameter)	Method of Load Determination	Airframe Structure	Structural Load (or Parameter)	Method of Load Determ.
Upper Hub Plate	Centrifugal	Calculated	Upper Lt.Pylon Fold Fitting	Stress Gage	Flight Test
	Flapping Angle	Flight Test			
	Lag Angle	Flight Test			
	Damper Moment	Flight Test			
Lower Hub Plate	Centrifugal	Calculated	Accessory Gearbox Support Fitting	Stress Gage	Flight Test
	Lag Angle	Flight Test			
	Damper Moment	Flight Test			
Vertical Hinge Pin	Centrifugal	Calculated	Inter. Gearbox Support Fitting	Stress Gage	Flight Test
	Damper Moment	Flight Test			
Horizontal Hinge Pin	Centrifugal	Calculated	Stabilizer & Tail Gearbox Support Fitting	Stress Gage	Flight Test
	Damper Moment	Flight Test			
Spindle	Centrifugal	Calculated	Main Transmission Support Structure	Transmission Load Stress Gage	Calculated
Sleeve	Damper Moment	Flight Test			
Push Rod	Push Rod Load	Flight Test			
Blade Spar-Out'd	Axial Gage Stress	Flight Test			
Blade Spar-Inb'd	Centrifugal	Calculated			
	Edgewise B.Stress	Flight Test			
	Flatwise B.Stress	Flight Test			
Blade Cuff	Centrifugal	Calculated			
	Edgewise B.Stress	Flight Test			
	Flatwise B.Stress	Flight Test			
Control Servo	Servo Load	Flight Test			

FIG . 15

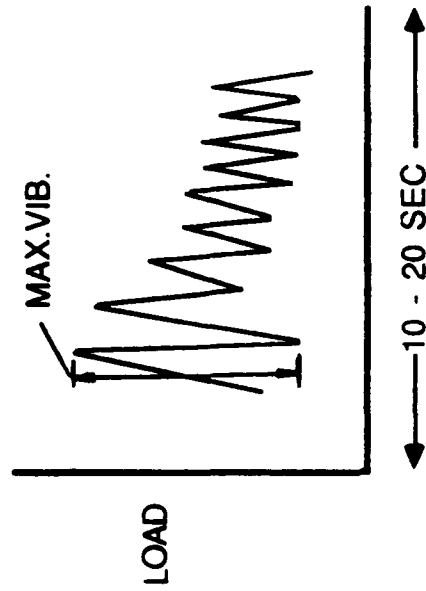
FIG. 15

CURRENT FLIGHT TEST DATA PROCESSING

STEADY STATE: e.g. level flt. 0.9 Vh



TRANSIENT: e.g. pull up



- EACH REGIME FLOWN SEVERAL TIMES AT VARIOUS CG's AND GW's

- STEADY STATE REGIMES : 95% VIBRATORY USED

- TRANSIENT REGIMES : MAX. VIBRATORY USED

FIG. 16

TYPICAL WEIBULL PLOT OF FLIGHT LOADS

AIRCRAFT : UH-60A ESSS

REGIME : HOVER - LOW ALTITUDE - ALL CG'S, 95 % LOADS

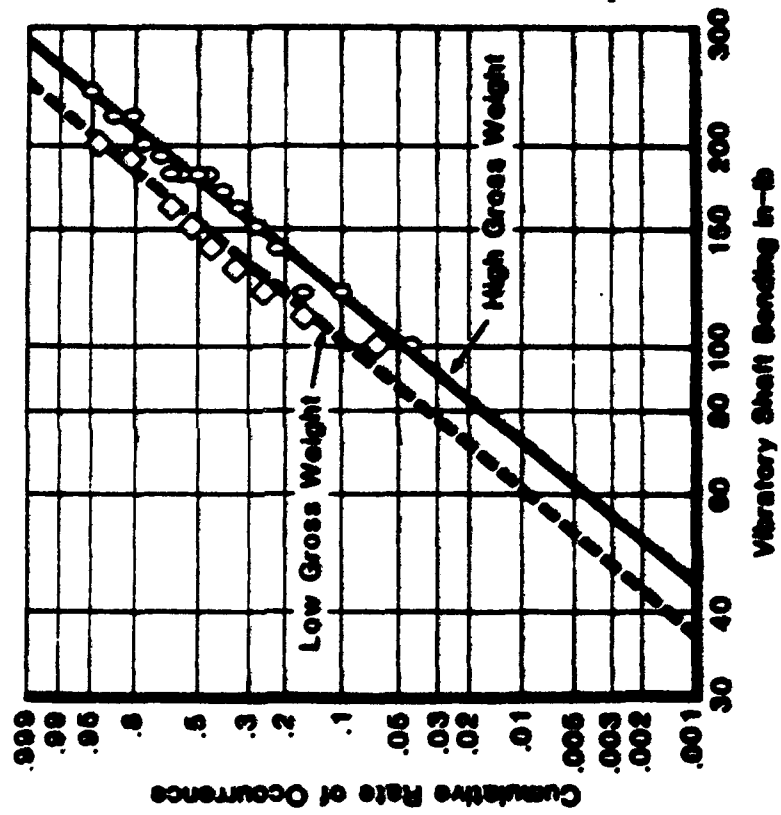


FIG. 17

APPLICATION OF CYCLE COUNTED LOADS DATA

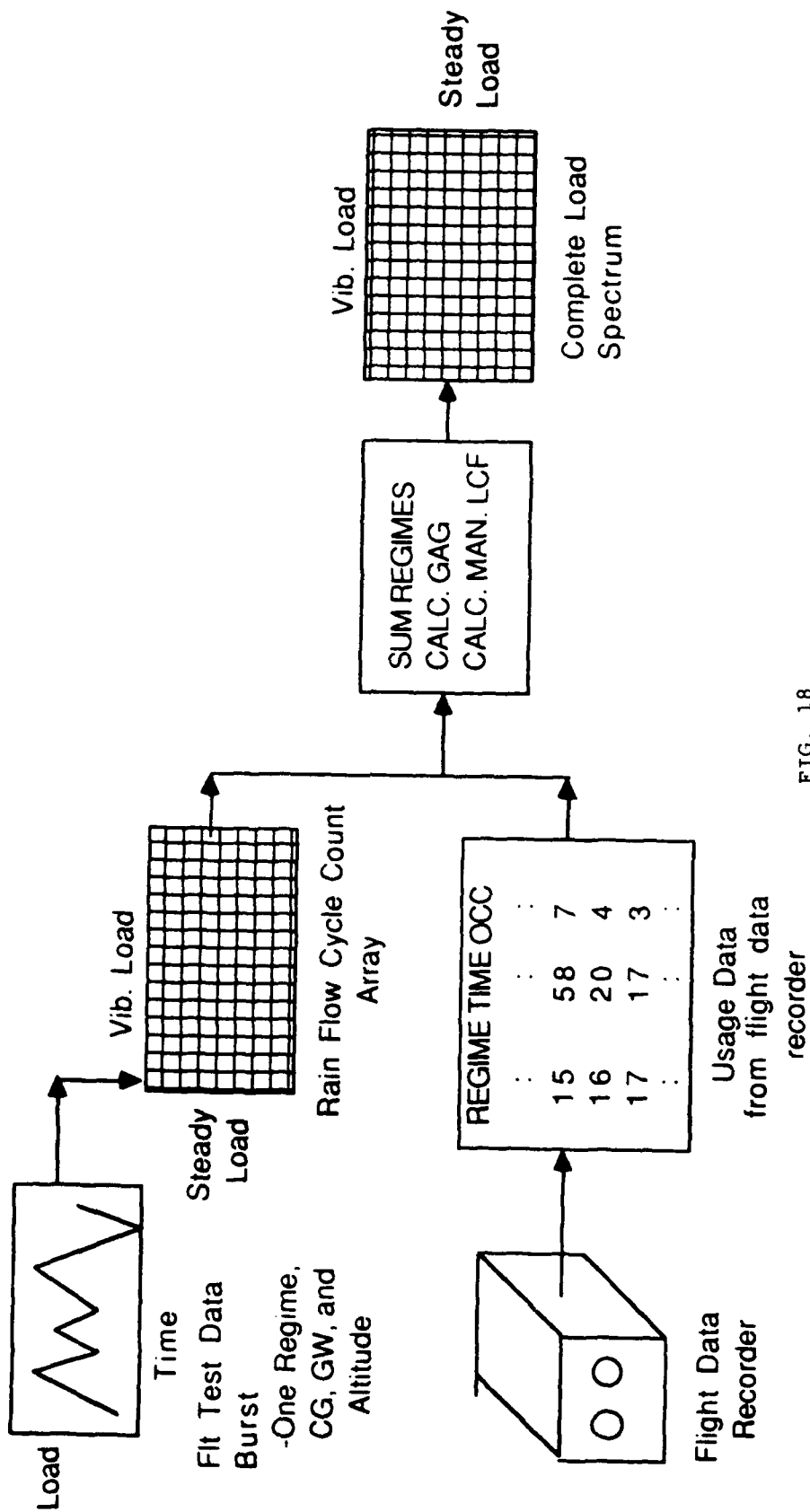
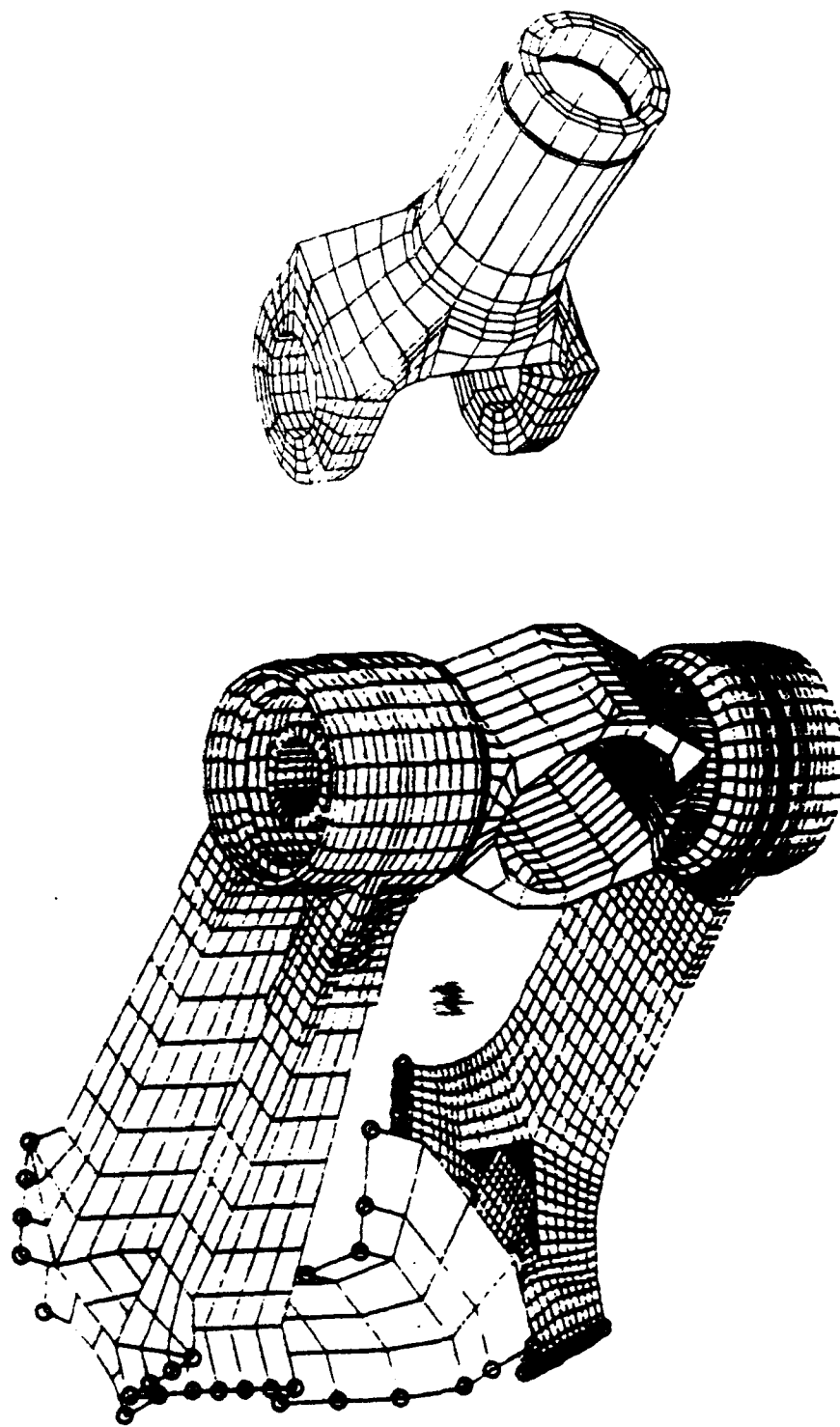


FIG. 18

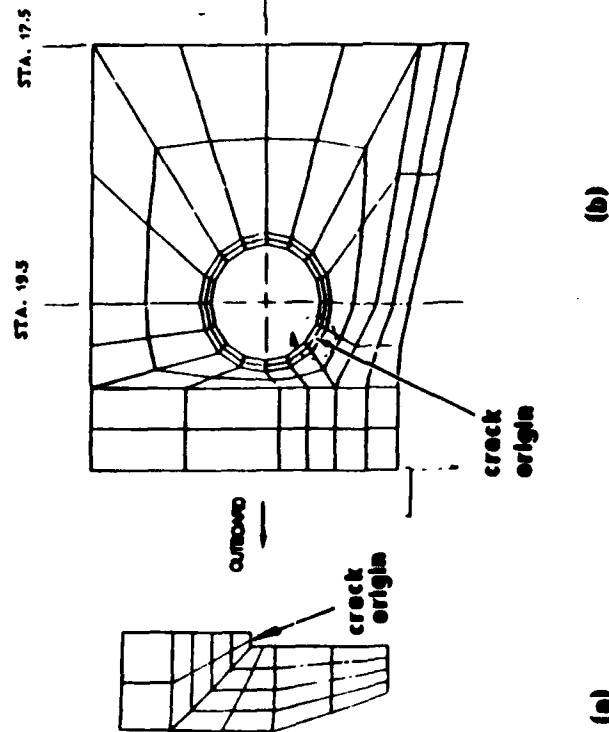
H-53 MAIN ROTOR FINITE ELEMENT MODELS



O All Degrees of Freedom Fixed

FIG. 19

H-53 MAIN ROTOR STRUCTURE CRACK LOCATIONS



1. main rotor upper hub plate
- a. cross section at lug crack location
- b. lifting hole crack location

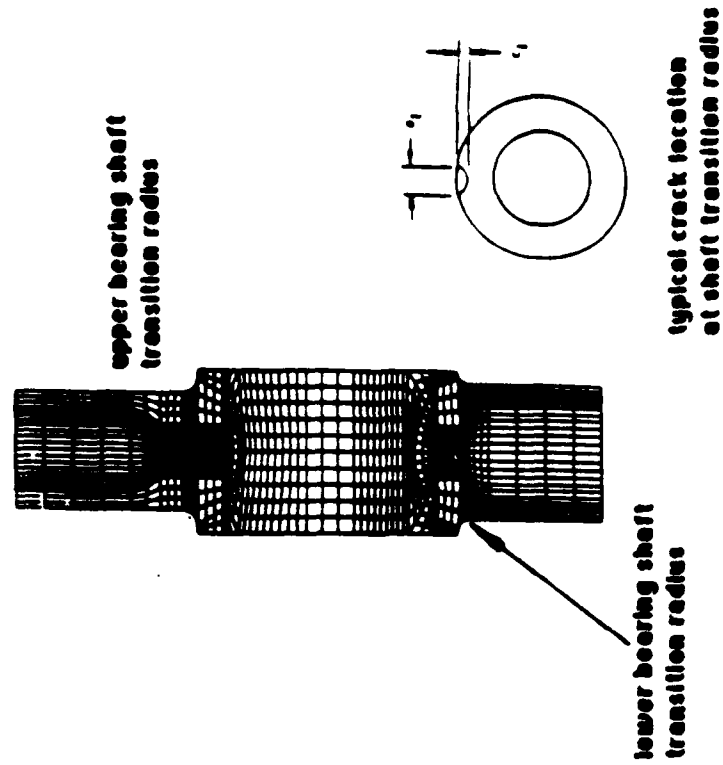


FIG. 20

NASTRAN MODEL - MAIN ROTOR SPINDLE - THREAD AREA

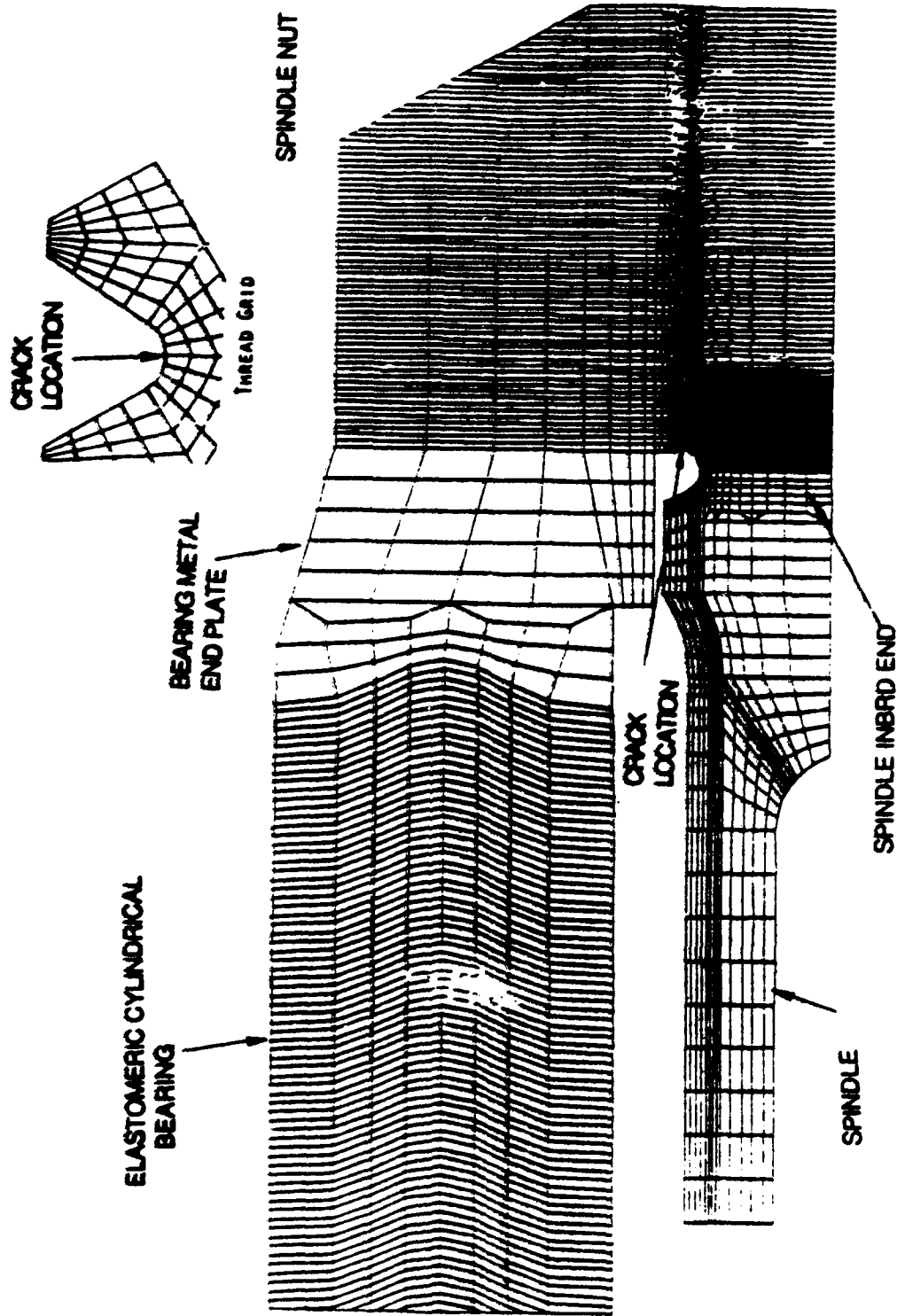


FIG. 21

FINITE ELEMENT & BOUNDARY ELEMENT THREAD STRESS ANALYSIS

• STRESS CONCENTRATION FACTOR - 1ST THREAD ROOT

Finite Elements -- 3.58
Boundary Elements -- 3.55

• TENSILE STRESS DISTRIBUTION IN RADIAL DIRECTION

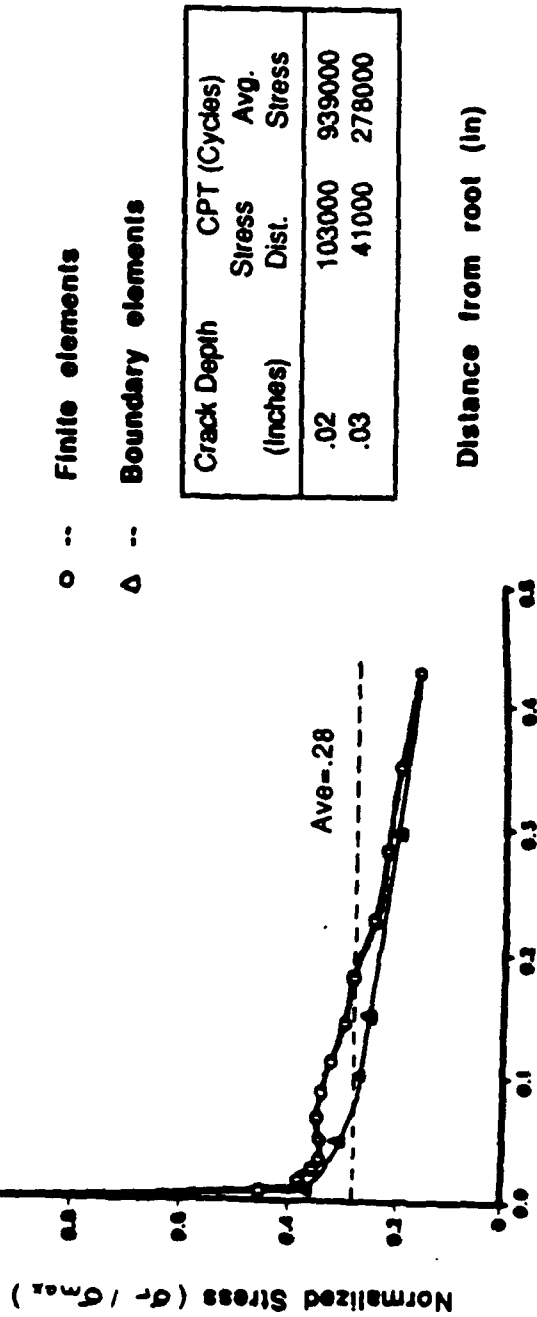
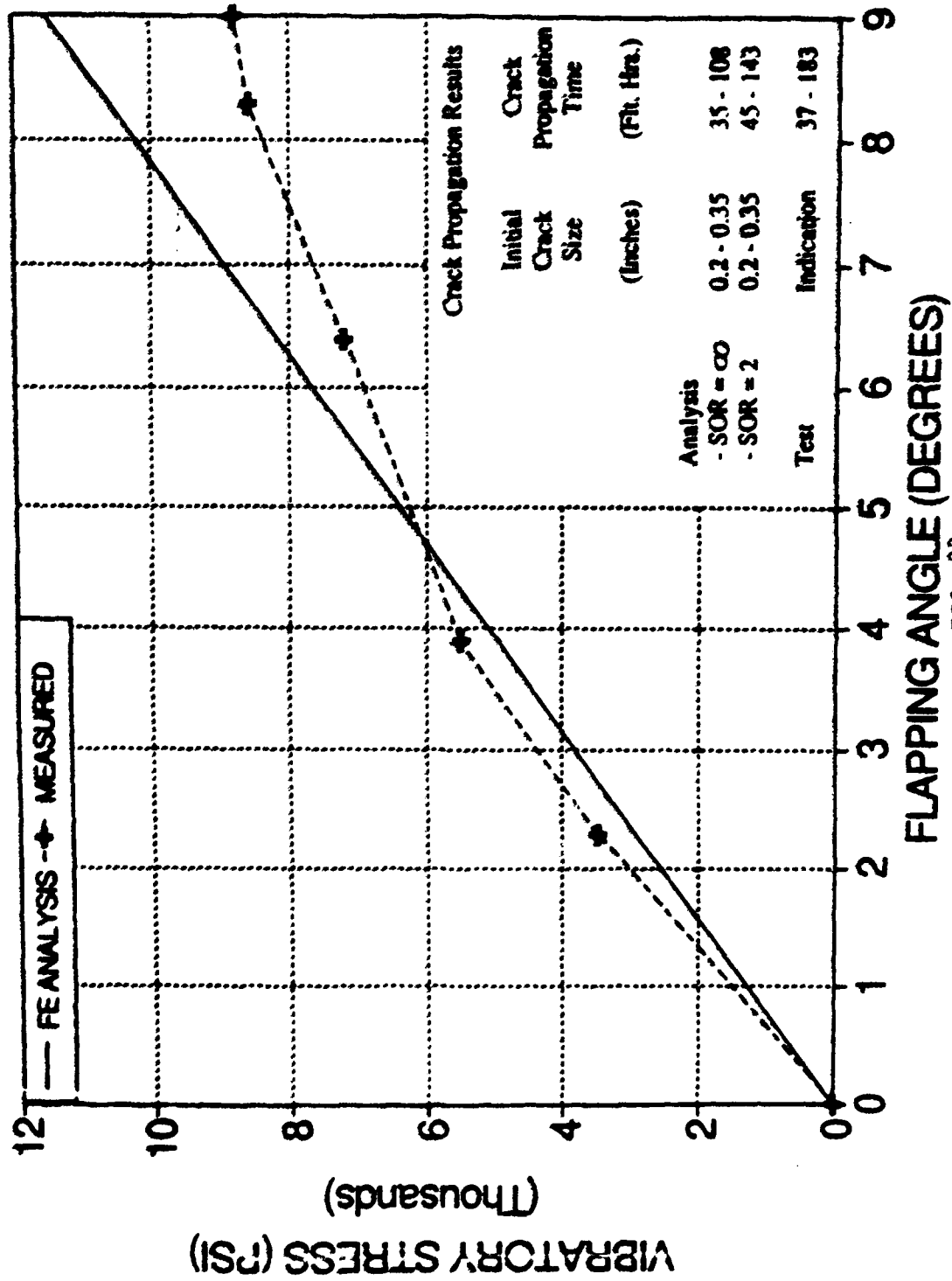


FIG. 22

H-53 UPPER HUB LUG ANALYSIS/ TEST CORRELATION



MAIN ROTOR HUB & SHAFT TEST FACILITY

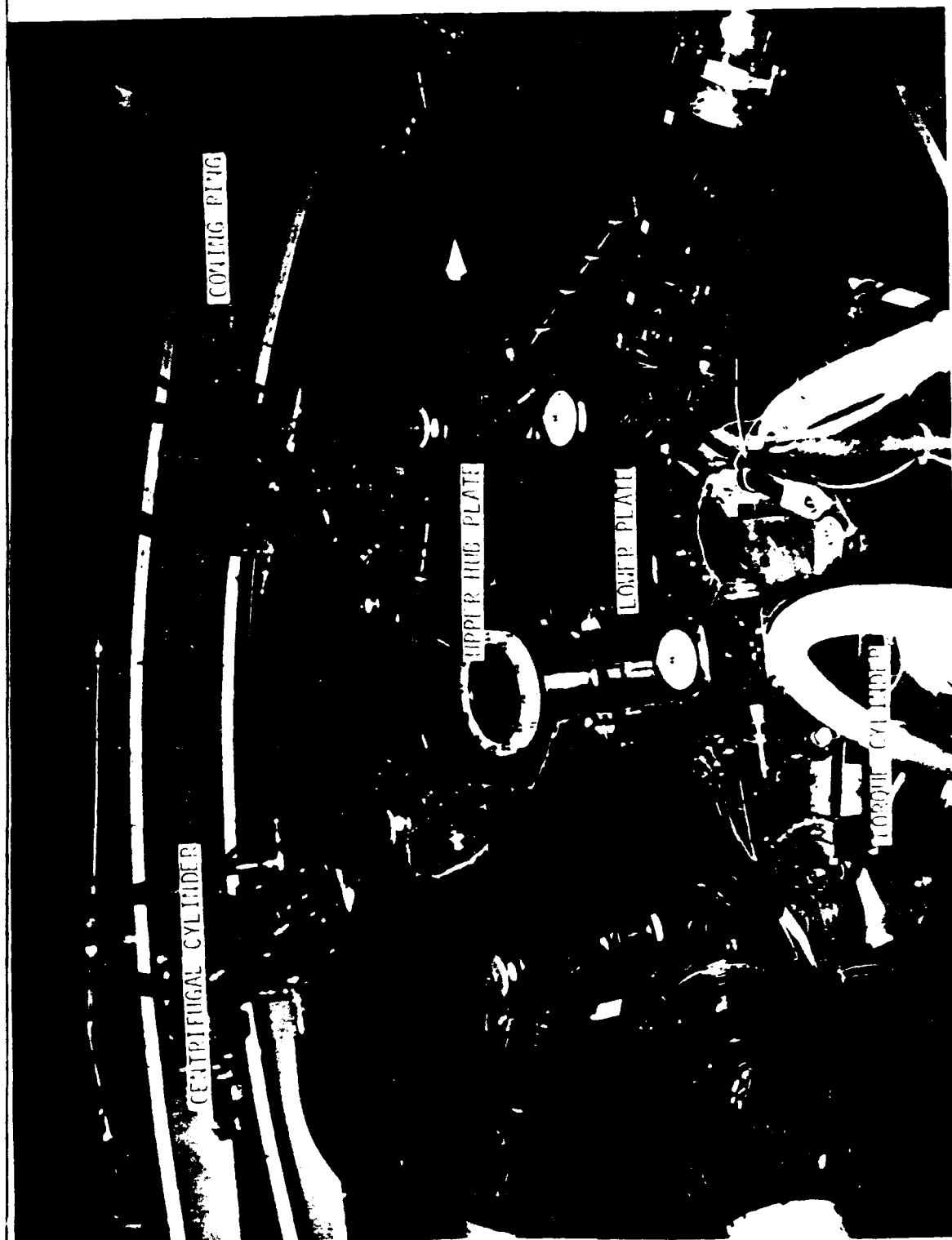
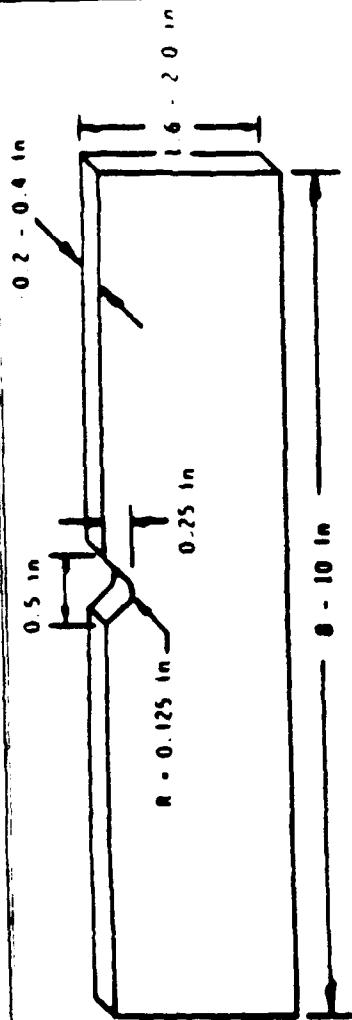
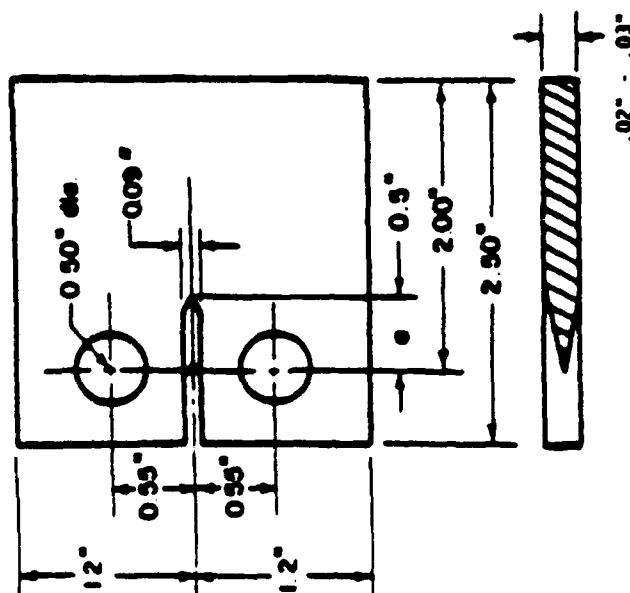
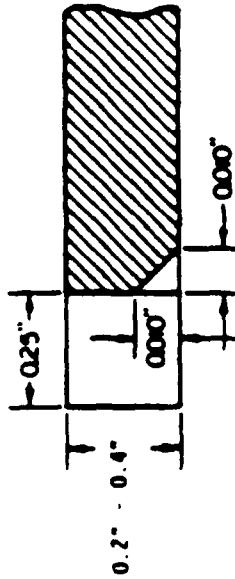


FIG. 24

MATERIAL AND VERIFICATION TESTS



(a) Notched Specimen



(b) (On Flow Detail)

Notched Specimens

- Const. Amp. Tests - Stress Intensity
- Spectrum Tests - Stress Intensity
- Spectrum Effects

FIG. 25

Compact Tension Specimens

- Constant Amp. Tests - Material Data
- Spectrum Tests - Spectrum Effects

MATERIAL TEST PROGRAMS CONSTANT AMPLITUDE COMPACT TENSION SPECIMENS

MATERIAL	APPLICATION	NEAR THRESHOLD		MIDRANGE		TOTAL
		R VALUE	# SPECIMEN	R VALUE	# SPECIMEN	
AL6061 Ext	MAIN & TAIL BLADE	0.1, 0.5	4	0.1, 0.5	2	6 *
TI-6AL-4V α - β Forged	ROTOR & CONTROL	0.1	2	---	---	2
TI-6AL-4V β -STOA Forged	ROTOR & CONTROL	0.1, 0.7	4	---	---	4
STEEL 4340 FORGED 150 KSI 180 KSI	ROTOR & CONTROL	0.1	2	0.1	1	3
AL 7075-T73 FORGED	ROTOR, CONTROL & AIRFRAME	0.1, 0.5	4	0.1, 0.5	2	6 *
AL 7075-T65 FORGED	AIRFRAME	0.1, 0.5	4	---	---	4

FIG. 26

* ONLY 2 TESTS PERFORMED PROBLEM - NO VALID DATA OBTAINED

SPECTRUM AND NOTCHED SPECIMEN TEST PROGRAMS

MATERIAL	COMPACT TENSION SPECTRUM			NOTCHED SPECIMEN CONST. AMP. SPECTRUM			
	ao	GAG ΔK_o	HCF ΔK_o	ao	ΔK_o	ao	GAG ΔK_o HCF ΔK_o
AL 7075-T6511 EXTRUSION	.5	10.1	4.0	-	-	-	-
AL 7075-T73 FORGED	.5	13.4	7.5	0.035	6.7	.027	6.9 5.0
STEEL 4340 FORGED 180	.5	35.4	18.0	0.016	10.1	.0176	11.2 9.0
TI-6AL-4V α - β FORGED	.5	17.6	10.0	-	-	-	-
TI-6AL-4V β STOA FORGED							

FIG. 27

TYPICAL HELICOPTER LOAD SPECTRUM

HELIX Training Flight - 90 Seconds

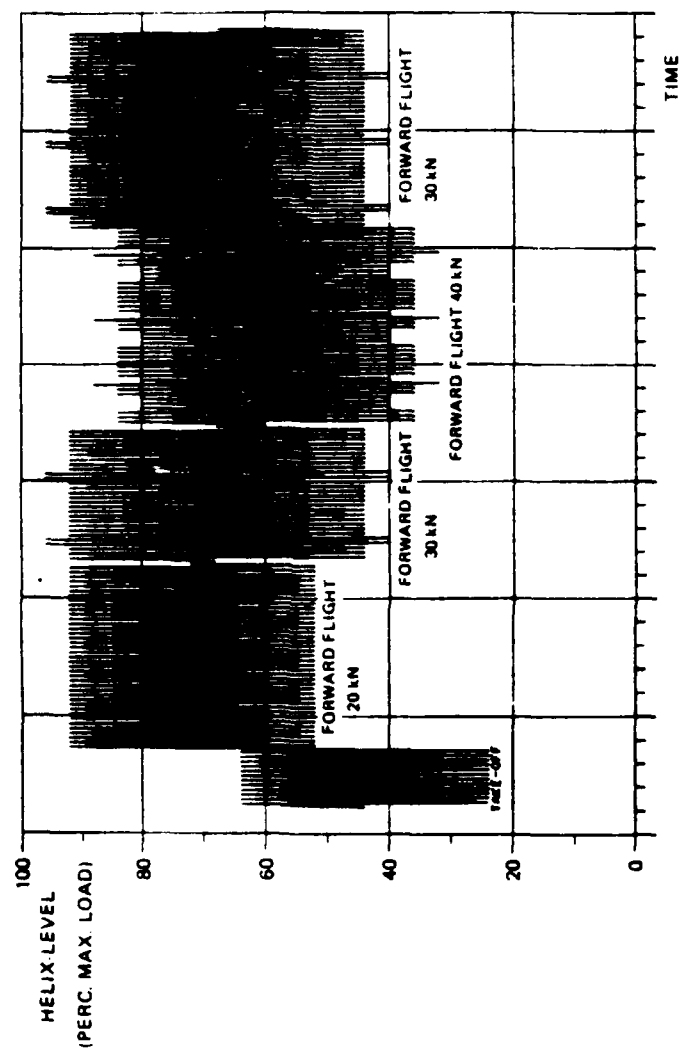


FIG. 28

TEST SPECIMEN MATERIAL SOURCES

4340 Steel Forging
Horizontal Hinge



Ti-6Al-4V α - β Forged
H-53 MR Upper Hub Plate



FIG. 29a

TEST SPECIMEN MATERIAL SOURCES

AL 7075-T73 FORGING
H-53E MAIN CABIN FRAME

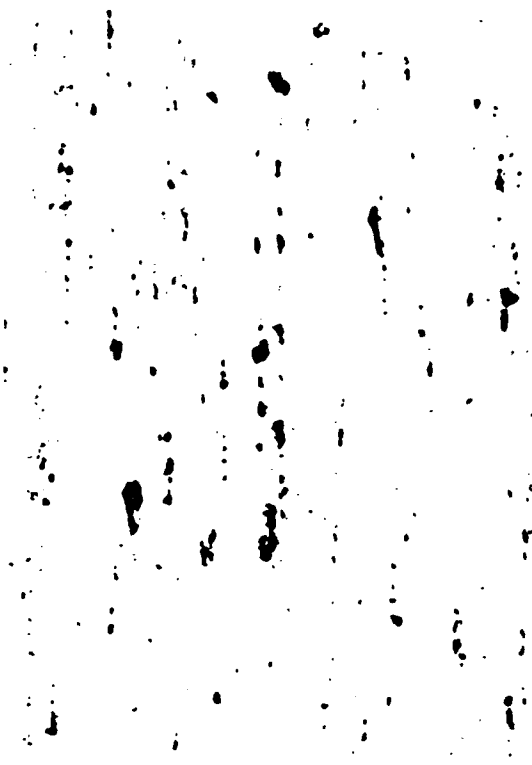
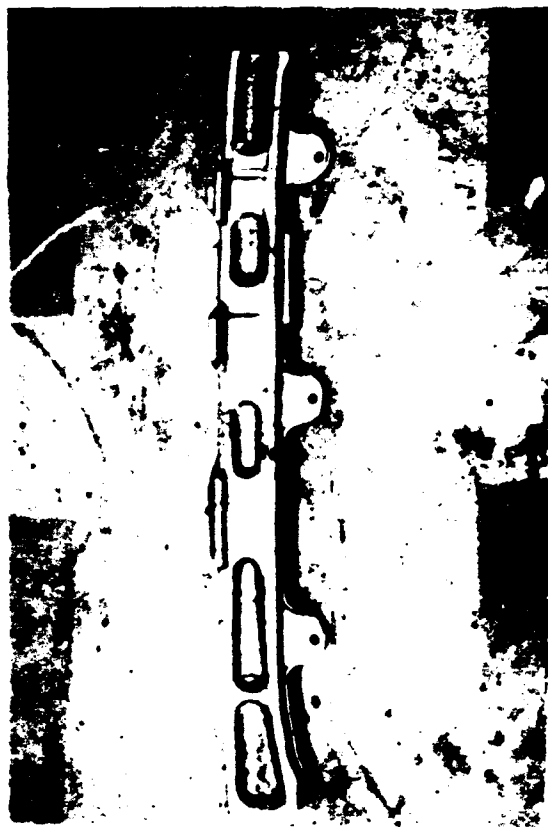


FIG. 29b

AL 7075-T73 CONSTANT AMPLITUDE FRACTURE SURFACES

Notched Test Specimen

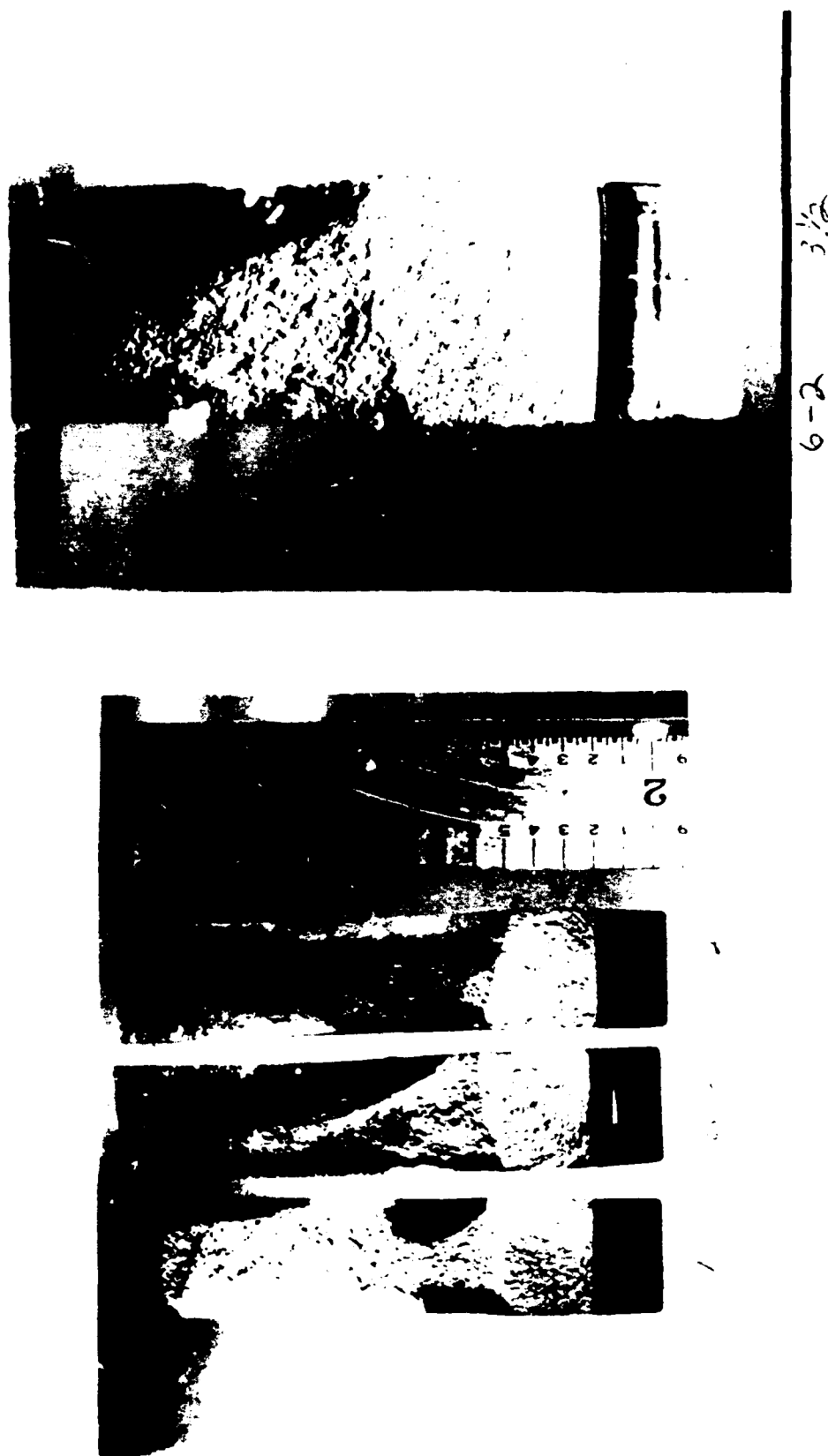


FIG. 30a

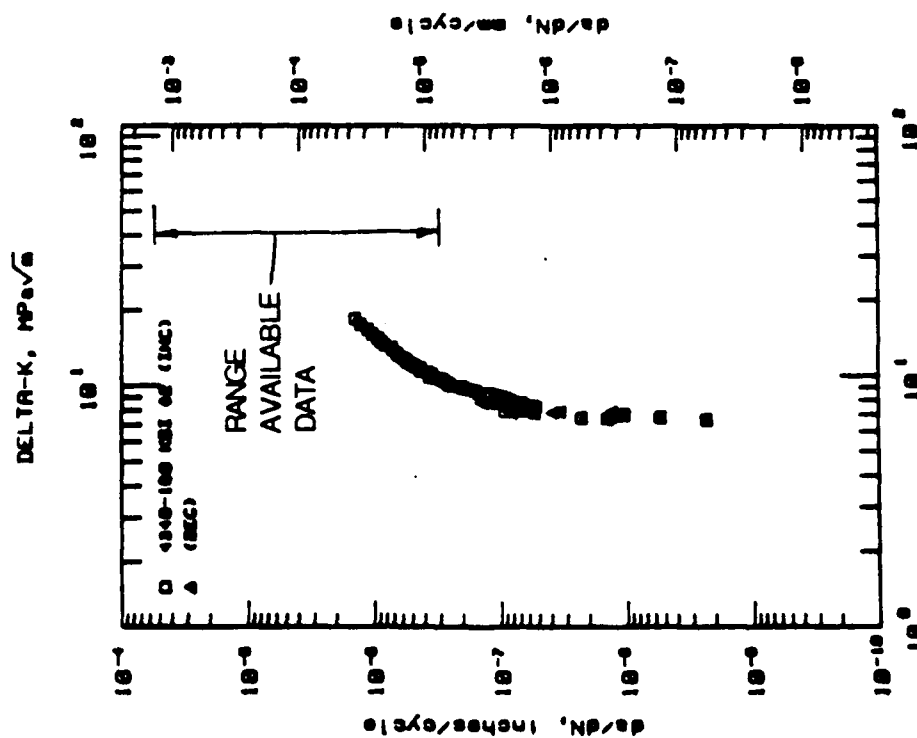
AL 7075-T73 SPECTRUM FRACTURE SURFACES

Notched Test Specimen

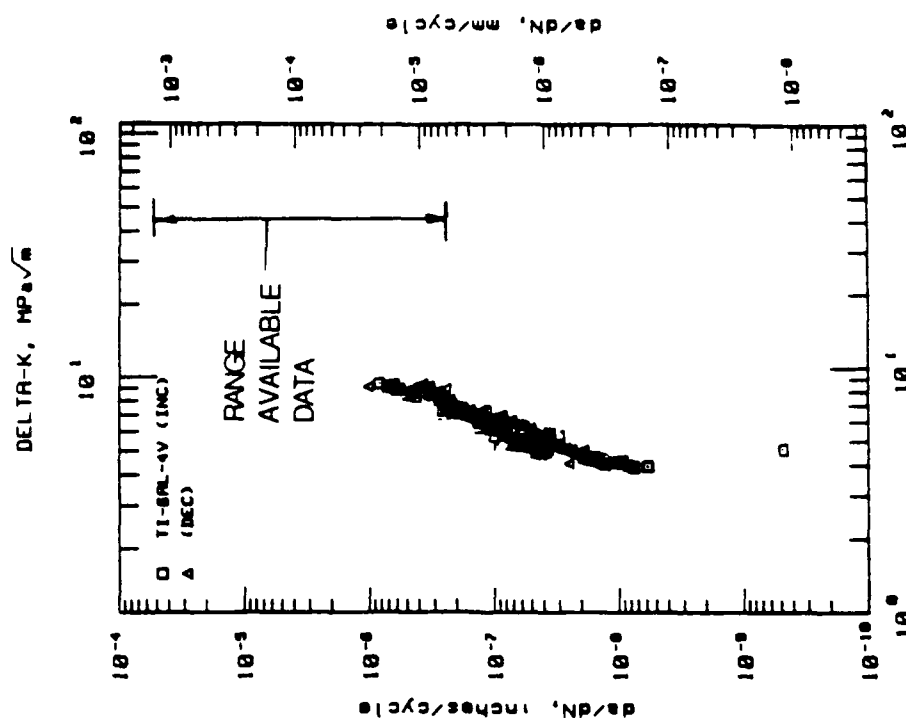


FIG. 30b

TYPICAL CRACK PROPAGATION RATE DATA



NEAR-THRESHOLD FATIGUE-CRACK-GROWTH BEHAVIOR OF 180 KSI YIELD STRENGTH 4340 STEEL AT $R = 0.1$

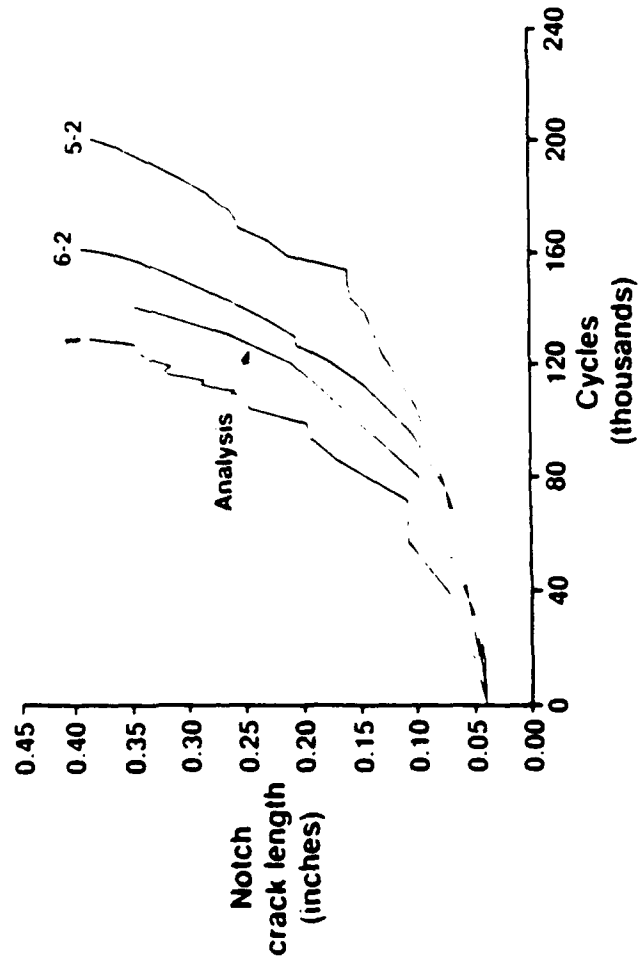


NEAR-THRESHOLD FATIGUE-CRACK-GROWTH BEHAVIOR IN TWO SPECIMENS OF FORGE-ANNEALED TI-6AL-4V ALLOY TESTED AT $R = 0.1$

FIG. 31

NOTCHED SPECIMEN CONSTANT AMPLITUDE TESTS

Al 7075 - T73 Forging



Steel 4340 (180 Ksi) Forging

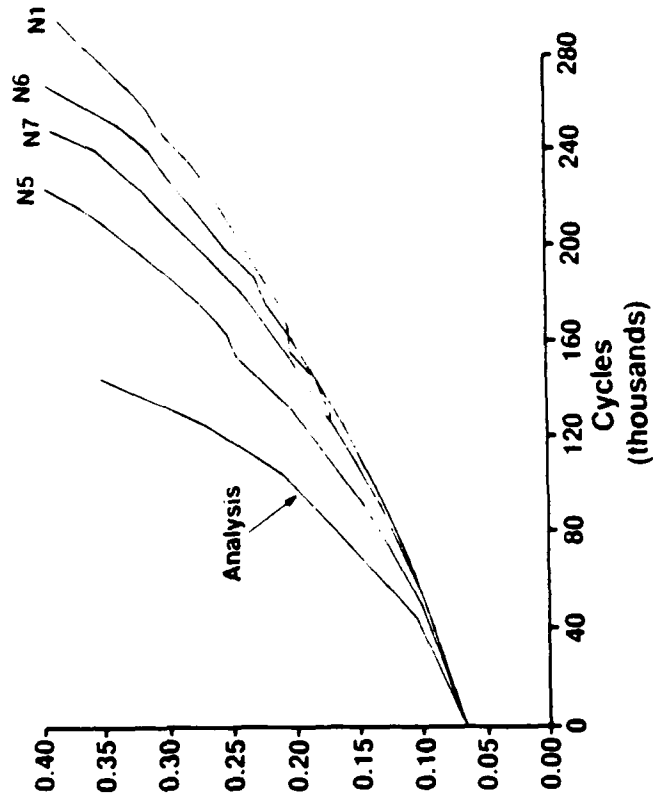
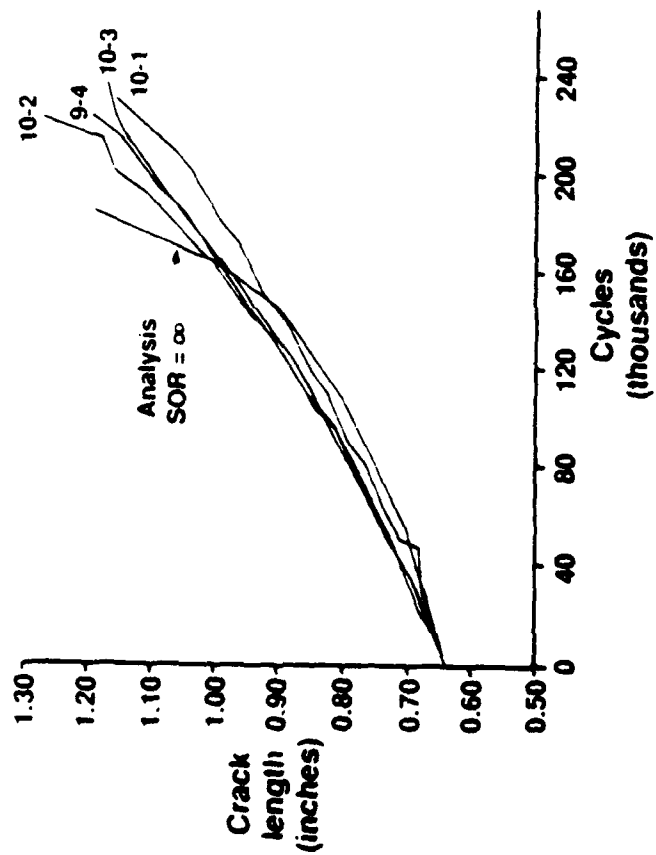


FIG. 32

AL7075-T73 SPECTRUM TEST RESULTS

Compact Tension Specimen



Notched Specimen

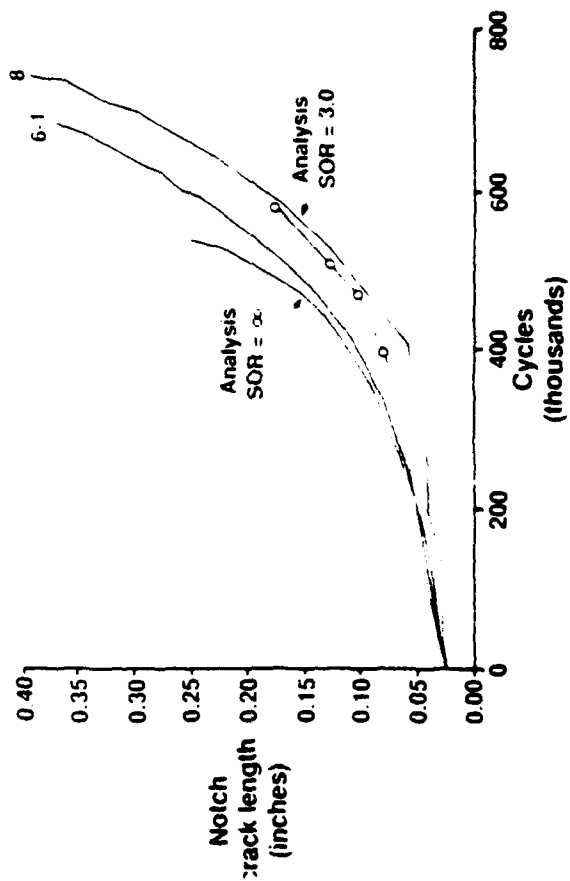
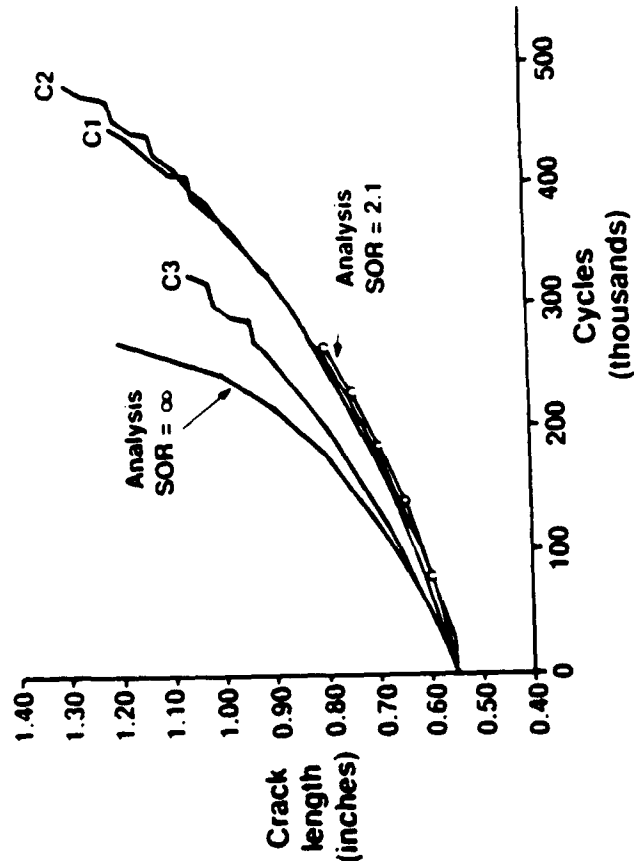


FIG. 33a

STEEL 4340 (180 KSI) SPECTRUM TEST RESULTS

COMPACT TENSION SPECIMEN



NOTCHED SPECIMEN

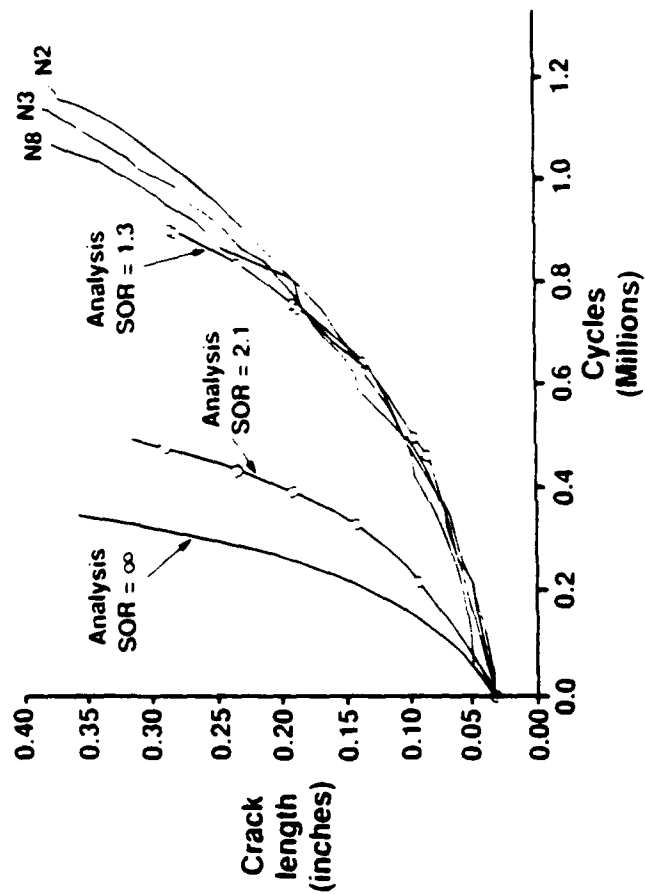


FIG. 33b

CRACK PROPAGATION TIME SENSITIVITY

CRACK LOCATION	HCF THRESHOLD CRACK DEPTH (Inches)	INITIAL CRACK DEPTH (Inches)	SPECTRUM STRESS FACTOR	CRACK PROPAGATION TIME (Flt Hours)	
				without retardation	with retardation
MR Spindle Lug	.022	.030	1.0	270	5320
		.020	1.0	2650	-
		.020	1.1	450	-
		.020	0.9	21400	-
MR Sleeve Thread	.002	.005	1.0	145	1120
		.005	1.1	71	-
		.005	0.9	2000 +	-

FIG. 34

MIDRANGE AND NEAR THRESHOLD RETARDATION BEHAVIOR

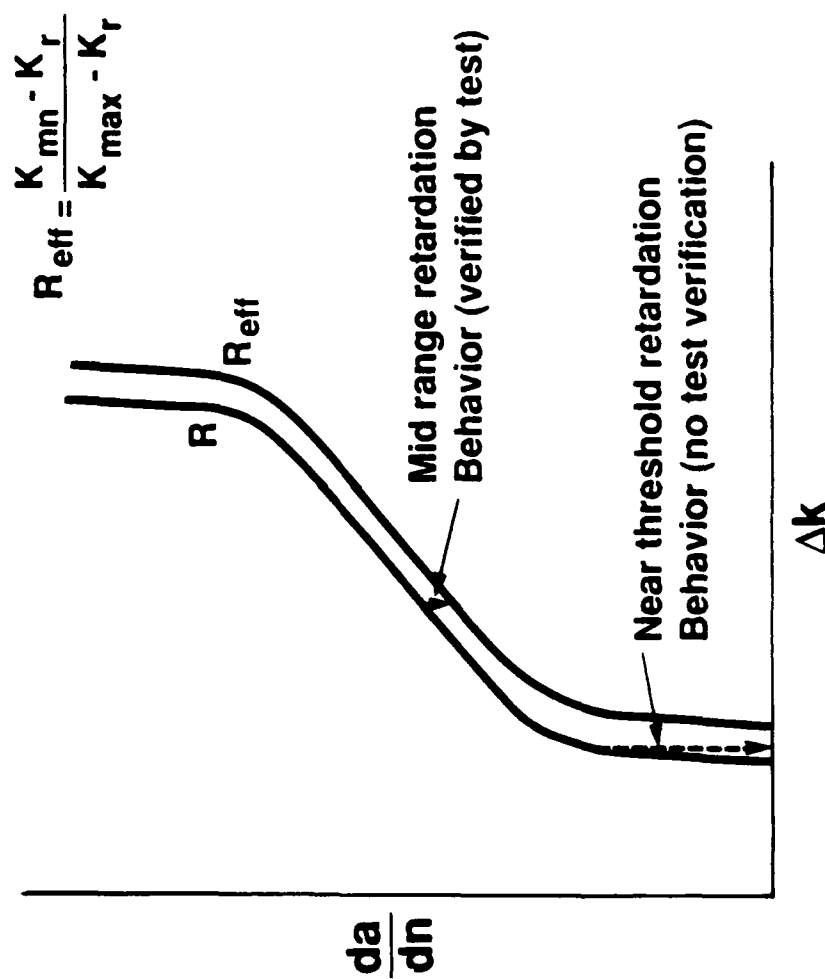


FIG. 35

SAFE LIFE VS. DAMAGE TOLERANT DESIGN

Threshold Crack Sizes for Stress Ratio, $R = 0.7$ and Stress Concentration, $K_t = 3.0$

Material	Working Endurance Limit, S_e (KSI)	Mean K_{th} (KSI in.)	Threshold Crack Sizes (inches)		
			@ S_e	@ 0.75 S_e	@ 0.50 S_e
Steel 4340(150)	12	1.5	0.0003	0.0005	0.0011
Steel 4340(180)	13	2.2	0.0005	0.0009	0.0020
Al6061-T6	1.6	0.8	0.0040	0.0070	0.0150
Al7075-T73	2.1	1.3	0.0070	0.0120	0.0260
Ti-6Al-4V	3.5	2.0	0.0060	0.0110	0.0248

FIG. 36

REQUIRED TECHNOLOGY DEVELOPMENT

- Flight Test Data Processing - Complete Cycle Counting
- Flight Data Recorder - Improved Usage and Loads Data
- Crack Propagation - Small Cracks Data (.005 - .020 inches)
 - Propagation Models
 - Threshold scatter and Retardation Data
- NDI - Applicability of Engine NDI to Helicopters
- Stress Analysis Verification - Strain Surveys on Full Scale Parts (e.g. Main Rotor Head)
- Threaded Parts - Improved Stress Analysis and Stress Intensity Models
 - Crack Propagation Verification Data
- Regime Sensitivity - Critical Flight Regimes

FIG. 37

GENERAL RECOMMENDATIONS FOR HELICOPTER DAMAGE TOLERANCE ASSESSMENT

INITIAL SCREENING OF ROTOR PARTS

All Parts Are Critical (same as safe life)
Identify Potential Crack Locations and Inspection Feasibility

INITIAL SCREENING OF AIRFRAME PARTS

Identify Critical Parts
Identify Potential Crack Locations and Inspection Feasibility

CRACK PROPAGATION ANALYSIS

Retardation Models Can Not Be Used At This Time
Factors of Safety On Both Life and Stress Should Be Used

NDI

Combined Overall and Detail NDI May Be Required

FIG. 38

OSCAR

On-Site Collating And Recording

**1990 USAF ASIP CONFERENCE
DECEMBER 11-13, 1990
SAN ANTONIO, TEXAS**

**J.B. COCHRAN, LASC-GA
A.G. FRESE, LASC-GA
D.O. HAMMOND, WR-ALC/LJLEA**

AGENDA

This presentation will cover the application of a portable data collection computer known as OSCAR. Some background of how OSCAR came into being, description of exactly what OSCAR is, some of its features, capabilities, and how it has been applied to the data collection process will be discussed. The advantages of OSCAR are many and will also be covered.

AGENDA

- Introduction
- Background
- Description
- Features
- Input / Output
- Software
- Capabilities
- Applications
- Advantages

INTRODUCTION

OSCAR is an idea born out of the need for responsive, accurate data feedback on structural inspections. LASC-GA initiated a study under IRAD project 950 to determine the feasibility of a voice recognition hand held unit that would provide a means of rapid, accurate feedback data.

OSCAR represents the latest in portable, voice recognition / synthesis technology. It is felt that through application of OSCAR, the data collection process can be dramatically improved over the current paper form method.

Introduction

OSCAR

- Initiated through IRAD project 950 @ LASC-GA as an inspection data feedback system.
- OSCAR is a hand-held, IBM PC-XT compatible, voice recognition/synthesis computer.
- A data collection method via electronics (miniature microprocessor unit) that eliminates use of paper forms, OPSCAN or otherwise.

BACKGROUND

Current tracking programs require use of OPSCAN forms to transfer inspection data to ASIP manager. Reliability of forms input and accuracy varies between 70 and 80%.

The Condition Assessment / Improvement Program (CA/IP) required the collection of large amounts of data. This was accomplished by having Lockheed engineers enter the data into laptop personal computers.

Future programs like the Functional Systems Integrity Program (FSIP) dictate that more and more military personnel will be used in lieu of engineers to collect the necessary data. In addition, people involved in other programs, such as the corrosion tracking program, have desires to improve data quality and quantity.

With these programs providing impetus, the idea to apply hand-held computer technology to the problem of data collection was born.

OSCAR represents the latest in computer technology through miniaturization and voice recognition/synthesis capability.

Background

OSCAR

- ASIP data collection currently by OPSCAN forms.
- CA/IP data collected by Lockheed Engineers using laptop PC's.
- Future programs dictate eventual use of military personnel to collect data with minimum training.
- Overall, an easy and efficient method of ASIP and FSIP data collection was sought.
- OSCAR takes advantage of latest computer technology to provide efficient and easy data collection.

DESCRIPTION

The voice recognition and synthesis hardware and associated algorithms were developed by The Voice Connexion in Irvine, California. This technology was initially developed for use in an add-in PC board for desktop PC's. This board is known as the InterVoice VI. Miniaturization technology allowed development of hardware that could fit into a hand-held PC.

The hand-held PC selected to house the Voice Connexion hardware was the PTVC-750 computer manufactured by Tebxon Corporation. This unit is marketed as the PTVC-756 and has won the prestigious Design News Award for design excellence. For Lockheed applications this computer is known as OSCAR.

Since OSCAR contains the same technology that was originally developed for the InterVoice VI, they operate identically. This allows applications to be developed on a desk top PC and downloaded to work on OSCAR.

Description

OSCAR

- The OSCAR computer was developed by The Voice Connexion in Irvine, California.
- Manufactured by Telxon Corporation, maker of several hand-held computer models.
- Evolved from desktop PC add-in board already in production by The Voice Connexion.
 - Utilized surface-mount technology for miniaturization.
 - Both PC board and OSCAR operate identically.

FEATURES

The following are a list of features and specifications about OSCAR. Notice that it is quite portable at a little over 2 pounds.

Battery life is adequate for even all day applications. An automatic display blanking routine helps save battery life.

The unit being tested contains 1 MB of RAM. This must be used for both program memory space and virtual hard disk. A model that contains up to 4 MB of RAM is possible, but was not in production at the time of purchase.

A 5 volt backup battery is located in the computer that will preserve the data that is resident in RAM in case of main battery pack failure.

Features

OSCAR

- Approx. 9.5" long by 3.25" wide by 2.0" deep.
- Weighs 2.1 pounds.
- Utilizes 80C88 microprocessor
- Uses 6 AA batteries
 - 8 hours on alkaline batteries
 - 4 hours on nicad batteries
- Up to 4 Mb of static RAM.
 - Partitioned for disk and program memory
- 5 volt lithium battery to assure data security.

FEATURES (Cont.)

Input into OSCAR is controlled by three methods; a keypad, barcode reader and a microphone. These can all operate concurrently and independent of each other. This allows a variety of data input methods. Applications can be tailored to use the most appropriate input method. Of course, the voice input is the most novel of the three and has far reaching applications.

Output from OSCAR is accomplished by three methods. A speaker allows audio output in the form of a synthesized voice. The LCD display provides visual output. And a RS-232 serial interface allows uploading and downloading to a desktop PC, serial printer or modem.

Features

OSCAR

- INPUT

- 50 Key Alphanumeric Keypad
- Bar Code Reader
- Voice Microphone

- OUTPUT

- Voice Speaker
- 16 line by 21 character backlit LCD display
- RS-232 Serial Interface

SOFTWARE

Since OSCAR uses the 80C88 microprocessor, it utilizes the MS-DOS operating system found on most desktop PC's. This means that software that runs on a desktop PC should run on OSCAR. Memory limitations and nonconformance to the smaller display screen will prevent some "off the shelf" software from running on OSCAR.

The Voice Connexion provides all software utilities and drivers that are needed to control voice and barcode input / output. These utilities run transparent to the application software in use.

Software

OSCAR

- Runs any MS-DOS software.
- All software must be tolerant of non-standard screen.
- Voice Connexion includes all text-to-speech and voice recognition software.

CAPABILITIES

Each input method into OSCAR runs simultaneously and transparently to the applications software. This means that data normally entered by the keyboard can just as easily be entered via the microphone or barcode reader. This does not require any special programming by the user.

Data input verification is accomplished by either voice or visual prompts on the screen. For instance, when the user says "C-130" and OSCAR recognizes the input, it will respond by outputting C-130 on the screen and/or saying "See One Thirty" over the speaker. This is especially useful when data collection must be done in poorly lit areas.

OSCAR can recognize up to 500 words or phrases that are preprogrammed into it before use. These words or phrases are known as the vocabulary. OSCAR must be "trained" by every person that uses it. This training consists of saying each word in the vocabulary about 7 times. After training, OSCAR is ready for use. Each "trained" vocabulary is stored in a separate file under the users initials. The use of a vocabulary that was not trained by that particular user will not work.

Each word or phrase can invoke up to 1,000 characters or keystrokes. This is a nice short cut when, say, you want the definition of a code instead of the code itself to be substituted into a database.

The voice synthesizer chip is capable of pronouncing all text. The ability to alter the way that words are pronounced (i.e. tone, pitch, rate, etc.) is also available.

Data can be uploaded and downloaded to desktop PC's via serial port. Serial printers and modems are also available to provide hardcopies and communications with other PC's.

Capabilities

OSCAR

- Data input via keyboard, bar code reader, or voice.
 - Each method operates concurrently
 - Operates transparently with application software
- Input verification via verbal and/or visual prompts.
- Voice recognition of 500 words or phrases.
- Up to 1,000 characters or keystrokes can be invoked by one spoken word or phrase.
- Unlimited text-to-speech synthesis.
- Data upload/download via RS-232 serial interface.
- Serial printer and modem available.

APPLICATIONS

There are many uses of OSCAR in the area of data collection on structural and functional systems.

Four major areas for which OSCAR is currently being developed are 1) PDM, 2) Inspections, 3) Repairs, and 4) Parts replacements.

Applications

OSCAR

- PDM Performance
- Inspections
 - Structural (ASIP)
 - Functional (FSIP, MECSIP, AVIP, ENSIP)
- Repairs
- Part Replacements

APPLICATIONS

Basically, the OSCAR unit is preprogrammed and coded depending upon which application is desired (PDM functions, inspections, repairs, etc.)

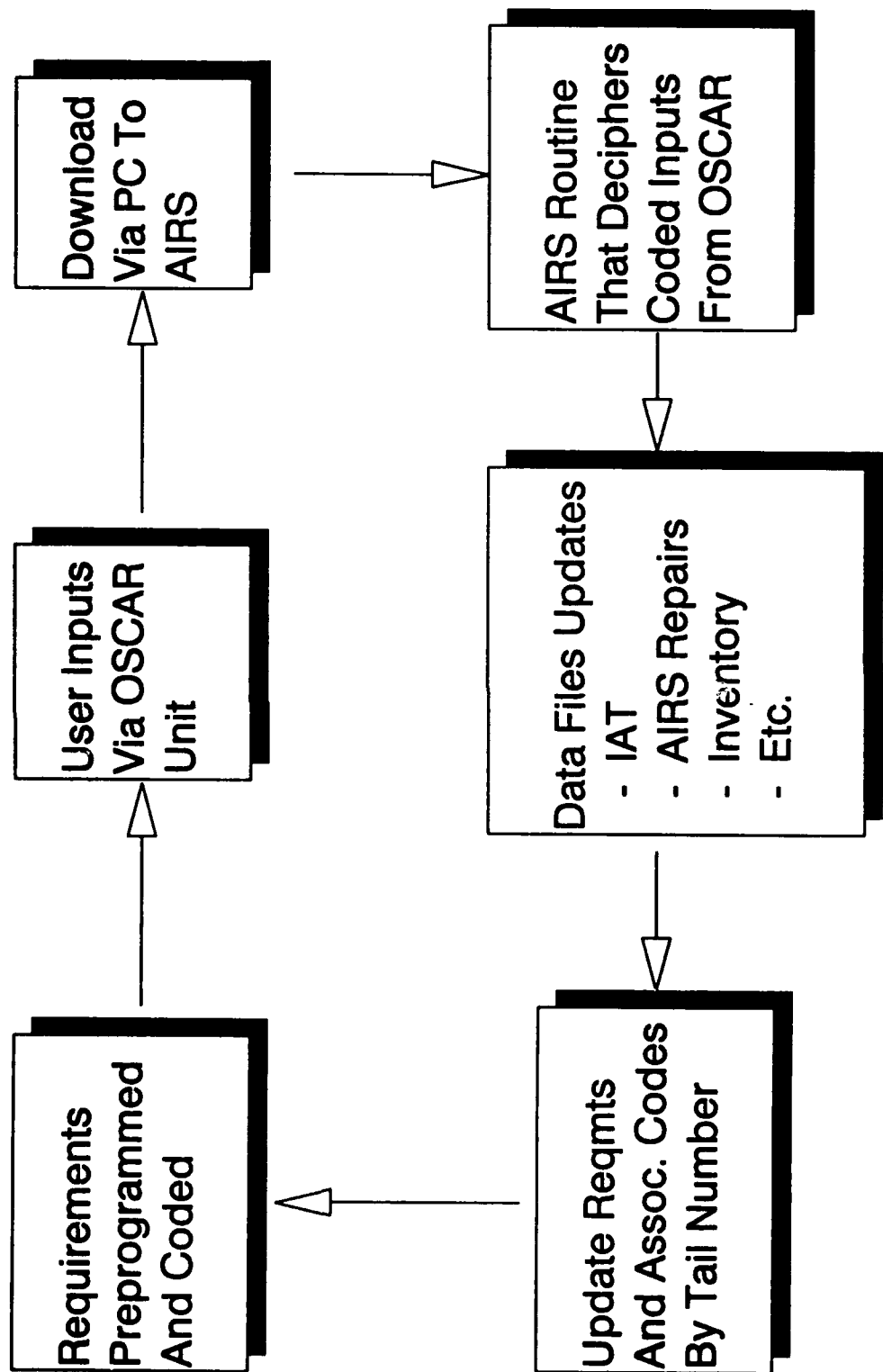
The user inputs data to OSCAR via voice and at the appropriate time downloads to a PC which interfaces with the Aircraft Information Retrieval System (AIRS).

AIRS routines decipher coded inputs and provides update information for tracking programs, repairs data, inventory, etc.

The OSCAR unit is updated with latest data requirements before next use.

Applications

OSCAR



APPLICATIONS

Three applications are in development. Two deal with the CA/IP and another deals with corrosion tracking. One goal is to use OSCAR to collect CA/IP component data. A similar application that involves collecting CA/IP landing gear data has been tested at Hill AFB, Ogden Utah. A program was developed to collect condition information on landing gear components. Instead of an engineer collecting the data a technician was trained and started inputting test data within 30 minutes. The reception to OSCAR was quite favorable during testing.

An application that collects corrosion tracking information has been developed and is in testing. This involves the partial automation of the AFTO Form 58 used to collect corrosion data. This program has been demonstrated several times with over a 90% voice recognition reliability rate.

Since OSCAR runs MS-DOS software, many applications running on desktop PC's can be run on OSCAR with minimum modification.

Applications

OSCAR

- Three initial applications in development
 - CA/IP Component Bench Test and Teardown
 - CA/IP Landing Gear Study
 - Corrosion Tracking Program (AFTO Form 58)
- Many applications running on desktop PC can run on OSCAR.

ADVANTAGES

The advantages of OSCAR are many. It provides a means of data collection that is quick, efficient and paperless.

Data can be input without the need to remove hands or sight from the work area.

Help to the user is readily available on the same unit that is used to collect the data. Help with data collection procedures or proper collection codes could come in the form of visual prompts on the screen or verbal prompts from the speaker. Help can be invoked, for example, when the users says the command "Help" into the microphone.

Since OSCAR monitors all data input it can help verify that complete and proper inputs are made and notify the user when incorrect inputs have been attempted. This will help assure data quality and completeness.

Since the data is in digital form right from the start, it is readily available for processing. After uploading to a "base" PC the data can then be sent anywhere over a modem. This will provide much quicker response times, prevent data loss, and allow for data backup.

Advantages

OSCAR

- Paperless data collection.
- Hands and Sight free data collection.
- Verbal and/or Visual Real-Time Help
 - Help with proper data collection procedures
 - Help with proper selection of How Mal & Work Unit Codes.
- Real-Time data verification and audit.
- Faster post-processing of data.

SUMMARY

OSCAR through hands off (or on), voice recognition synthesis will provide a system of data feedback that virtually eliminates the need for forms such as AFTO 178, 58 and 451 currently in use on the C-141.

ALC ASIP/FSIP managers will benefit from up-to-date, accurate feedback data that will give them a better base from which "next" actions can be projected or required.

The IRAD work @ LASC-GA will continue in 1991, and in cooperation with WR-ALC will develop and put into place a prototype system on the C-141 by the end of 1991.

Summary

OSCAR

- OSCAR has potential of significant improvement in current methods of data feedback.
- ASIP/FSIP managers will benefit in terms of accurate data bases upon which projections and requirements can be identified.
- IRAD investigation at LASC-G in cooperation with WR-ALC will continue in 1991, with full prototype system in place by year's end.

TFE1042/F125 TURBOFAN ENGINE DAMAGE TOLERANCE VERIFICATION PROGRAM

**K.D. BUCK, J.E. HILL
GARRETT ENGINE DIVISION
STRUCTURAL INTEGRITY PROGRAM CONFERENCE
SAN ANTONIO, TEXAS
DECEMBER 11-12 1990**

21-7762

Allied-Signal Aerospace Company

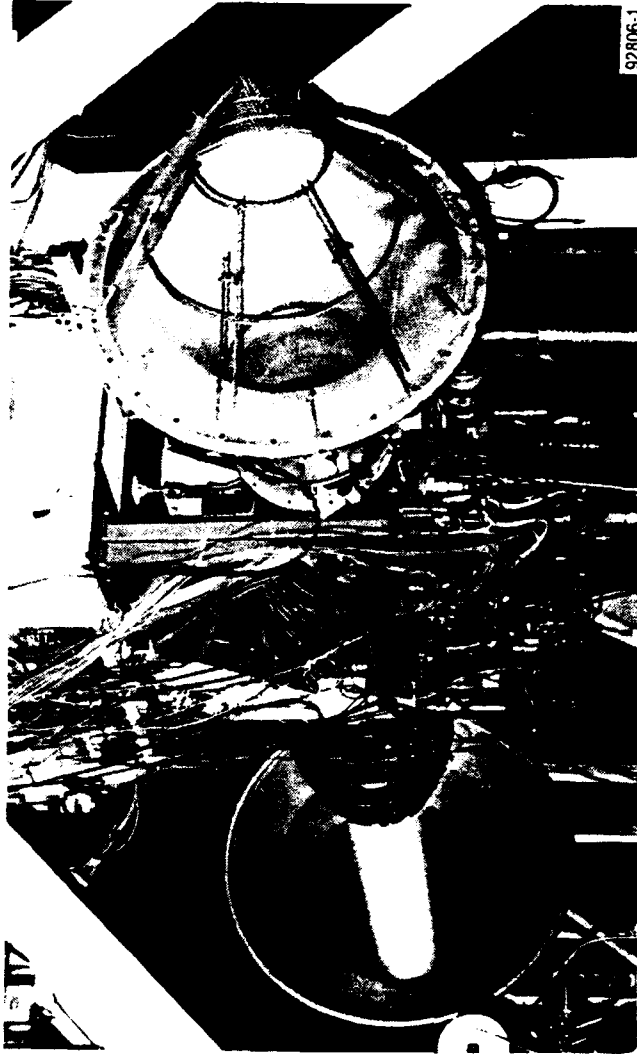
Garrett Engine Division



AGENDA

- **TFE1042/F125 PROGRAM BACKGROUND**
- **TFE1042 DAMAGE TOLERANCE AND LOW CYCLE FATIGUE VERIFICATION**
- **SECOND-STAGE COMPRESSOR DISK DAMAGE TOLERANCE RESULTS**
- **HIGH PRESSURE TURBINE DISK DAMAGE TOLERANCE RESULTS**
- **COMBUSTOR CASE DAMAGE TOLERANCE RESULTS**
- **CONCLUSIONS**

THE TFE1042 FAMILY OF ENGINES HAS BEEN UNDER DEVELOPMENT SINCE 1983



- DRY ENGINE DESIGNATOR: F124-GA-100 (6300 LB THRUST)
- AFTERBURNING ENGINE DESIGNATOR: F125-GA-100 (6213/9338 LB INTERMEDIATE/AUGMENTED THRUST)

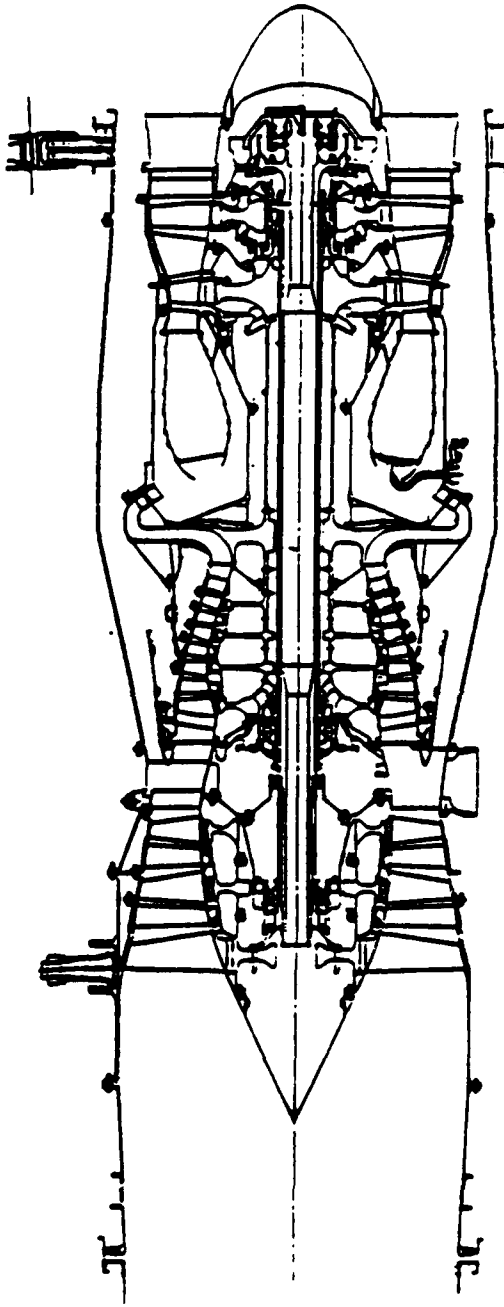
4G0457-3 A

Allied-Signal Aerospace Company

Garrett Engine Division



THE F124/F125 ENGINE DESIGN MEETS MILITARY SPECIFICATION STANDARDS



- BASED ON U.S. MILITARY SPECIFICATION MIL-E-87231 AND THE ENGINE STRUCTURAL INTEGRITY PROGRAM (ENSIP) REQUIREMENTS (MIL-STD-1783)
- ALL HIGH TEMPERATURE GAS PATH ENGINE COMPONENTS 2000 MISSION FLIGHT HOURS/> 4400 TOTAL EQUIVALENT CYCLES
- ALL OTHER ENGINE COMPONENTS 4000 MISSION FLIGHT HOURS/>8800 TOTAL EQUIVALENT CYCLES

•G0457-4 A

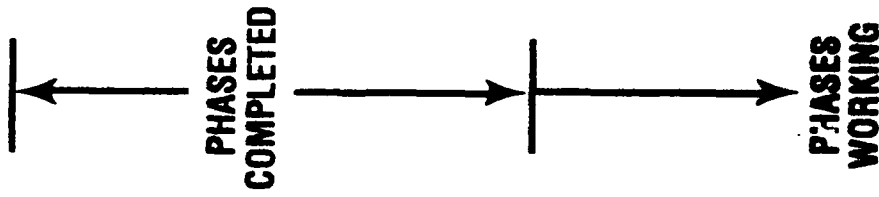
Allied-Signal Aerospace Company

Garrett Engine Division



F125 DEVELOPMENT/QUALIFICATION PROGRAM CONSISTS OF FIVE PHASES

- DEVELOPMENT TESTING
- PRELIMINARY EVALUATION OF THE ENGINE MECHANICAL DESIGN
- INITIAL FLIGHT RELEASE (IFR)
- ASSURES THE SAFETY OF THE ENGINE FOR FLIGHT TEST
- FULL FLIGHT RELEASE (FFR)
- CLEARS THE ENGINE FOR LOW RATE PRODUCTION
- INITIAL SERVICE RELEASE (ISR)
- CLEARS THE ENGINE FOR HIGH RATE PRODUCTION
- CONTINUOUS ENGINEERING PROGRAM (CEP)
- INCORPORATION OF PRODUCT IMPROVEMENTS



400457-5 A

Allied-Signal Aerospace Company
Garrett Engine Division



F125 FFR COMPLETED, VALIDATED ANALYSES AND VERIFIED ENGINE DURABILITY THROUGH FSD ENGINE TESTS

- **ENGINE TESTS INCLUDED**
- **THERMAL SURVEY: TRANSIENT AND STEADY STATE**
- **DYNAMIC STRAIN RESPONSE: BLADES, VANES, AND DISKS AND RESONANT DWELL TESTS**
- **EXTERNAL COMPONENT RESONANCE SURVEY AND ENDURANCE TESTS**
- **ROTOR DYNAMIC SURVEY**
- **FLUTTER BOUNDARY DYNAMIC SURVEY**
- **1000 FLIGHT MISSION HOUR ACCELERATED MISSION TEST (AMT)**
- **OVERSPEED/OVER TEMPERATURE TESTS**

F125 FFR COMPLETED, VALIDATED ANALYSES AND VERIFIED ENGINE DURABILITY THROUGH COMPONENT TESTS

- **COMPONENTS TESTS INCLUDED**
- **STRUCTURAL LOAD TESTS**
- **OVERPRESSURE TESTS**
- **BENCH DYNAMIC VERIFICATION**
- **LOW CYCLE FATIGUE TESTS: DEFINED BLADE AND DISKS**
- **DAMAGE TOLERANCE TESTS: DEFINED FRACTURE CRITICAL COMPONENTS**

460457-7 A

Allied-Signal Aerospace Company

Garrett Engine Division



AGENDA

- TFE1042/F125 PROGRAM BACKGROUND
- TFE1042 DAMAGE TOLERANCE AND LOW CYCLE FATIGUE VERIFICATION
- SECOND-STAGE COMPRESSOR DISK DAMAGE TOLERANCE RESULTS
- HIGH PRESSURE TURBINE DISK DAMAGE TOLERANCE RESULTS
- COMBUSTOR CASE DAMAGE TOLERANCE RESULTS
- CONCLUSIONS

PARAMETERS CONSIDERED FOR COMPONENT DAMAGE TOLERANCE AND LCF VERIFICATION

- DAMAGE TOLERANT SELECTION PARAMETERS
 - FRACTURE CRITICAL COMPONENTS*
 - UNIQUE MATERIAL COMPONENTS
 - UNIQUE GEOMETRIC CONSIDERATIONS
 - MOST LIFE LIMITED DAMAGE TOLERANT COMPONENTS IN THE COLD AND HOT ENGINE SECTIONS
- LCF SELECTION PARAMETERS
 - FRACTURE CRITICAL COMPONENTS
 - UNIQUE MATERIAL COMPONENTS*
 - MOST LIFE LIMITING COMPONENT IN THE COLD AND HOT ENGINE SECTIONS

* RELATIVE TO GED EXPERIENCE

460457-9

Allied-Signal Aerospace Company

Garrett Engine Division



DAMAGE TOLERANCE AND LOW CYCLE FATIGUE TESTS EVALUATED AGAINST THE F125 DESIGN DUTY CYCLE

SUMMARY OF LOW CYCLE FATIGUE DESIGN DUTY CYCLE:
(BASED UPON 4000 FLIGHT MISSION HOURS)

<u>TYPE OF CYCLES</u>	<u>NUMBER OF CYCLES</u>
0-MAXIMUM-0	> 3200
IDLE-MAXIMUM-IDLE	> 20,000
TAC COUNT	> 8800
$TAC = (0-MAX-0) + (I-MAX-I)/4 + (CRUISE-MAX-CRUISE)/40$	

SPIN PIT LOW CYCLE FATIGUE TESTS WERE SUCCESSFULLY COMPLETED

- **SECOND-STAGE COMPRESSOR (HPC) DISK**
- **IMPELLER DISK**
- **HIGH PRESSURE TURBINE DISK**

**LCF SPINPIT TESTING, ENGINE ENDURANCE TESTING
AND ANALYSES WERE USED TO ESTABLISH PART LIFE**

LCF FATIGUE TESTS WERE DESIGNED TO DEMONSTRATE A -3 SIGMA 4000 MISSION FLIGHT HOUR LIFE

TYPICAL DAMAGE SUSTAINED RELATIVE TO THE MISSION LIFE

<u>MATERIAL PROPERTIES</u>	<u>ENGINE CONDITIONS NORMALIZED LCF DAMAGE FRACTION</u>	<u>SPIN PIT CONDITIONS NORMALIZED LCF DAMAGE FRACTION</u>
AVERAGE	0.25	1.0
-3 SIGMA	1.0	4.0

SPINPIT TESTS WERE CONDUCTED CONSERVATIVELY

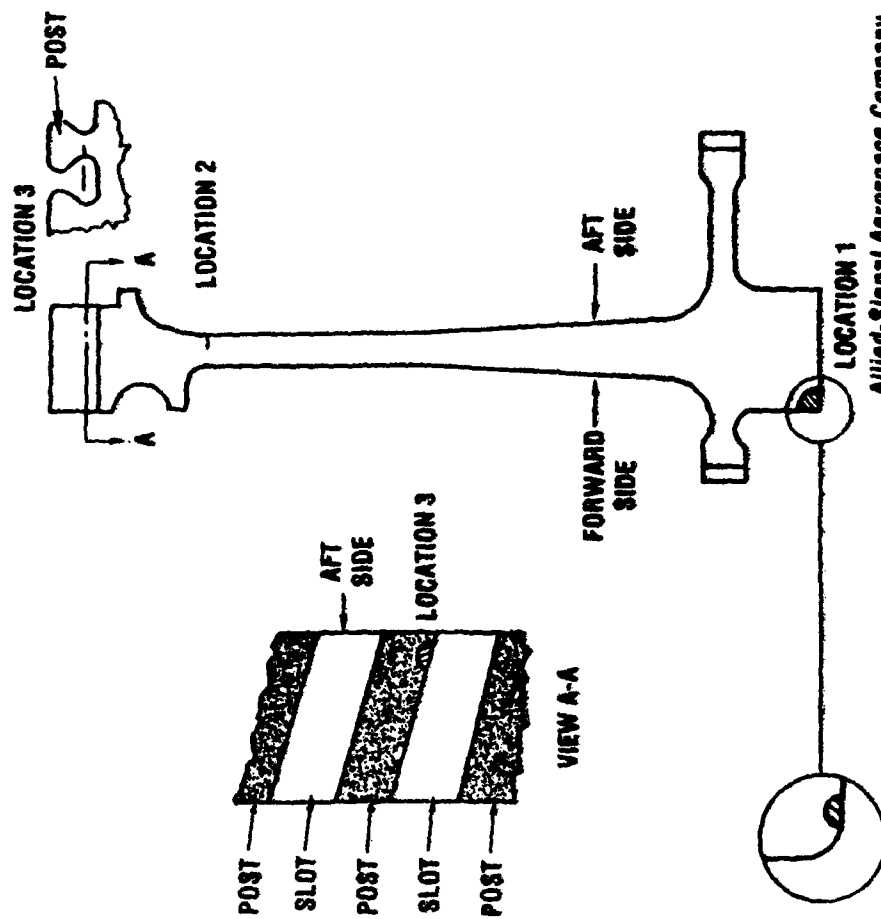
DAMAGE TOLERANCE TESTS WERE SUCCESSFULLY COMPLETED

- **SECOND STAGE COMPRESSOR DISK**
- **IMPELLER**
- **COMBUSTOR CASE**
- **HIGH PRESSURE TURBINE DISK**
- **HIGH PRESSURE TURBINE SEAL PLATE**

AGENDA

- TFE1042/F125 PROGRAM BACKGROUND
- TFE1042 DAMAGE TOLERANCE AND LOW CYCLE FATIGUE VERIFICATION
- **SECOND-STAGE COMPRESSOR DISK DAMAGE TOLERANCE RESULTS**
- HIGH PRESSURE TURBINE DISK DAMAGE TOLERANCE RESULTS
- COMBUSTOR CASE DAMAGE TOLERANCE RESULTS
- CONCLUSIONS

SECOND-STAGE HP COMPRESSOR DISK FLAW LOCATIONS

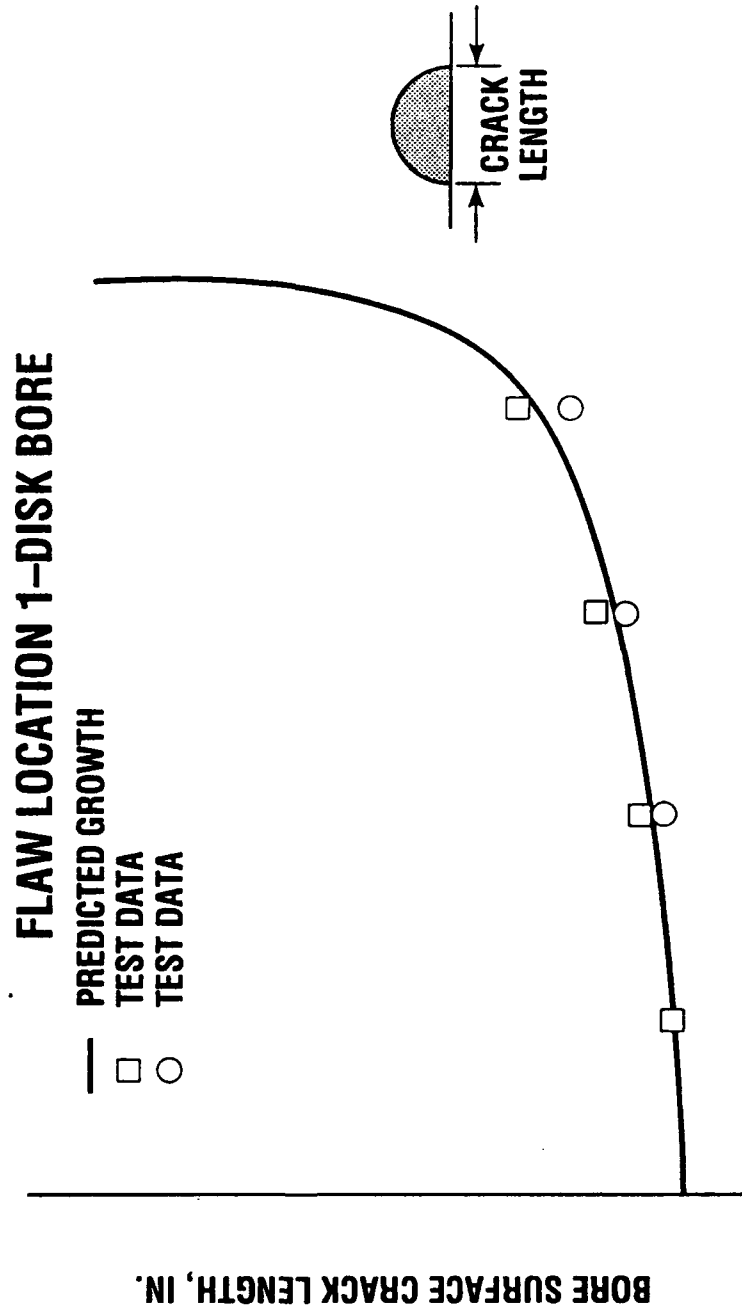


460457-19

Allied-Signal Aerospace Company
Garrett Engine Division



SECOND-STAGE HP COMPRESSOR DISK BORE CRACK GROWTH HAS DIRECT CORRELATION TO ANALYSIS



4G0457-20A

CYCLES

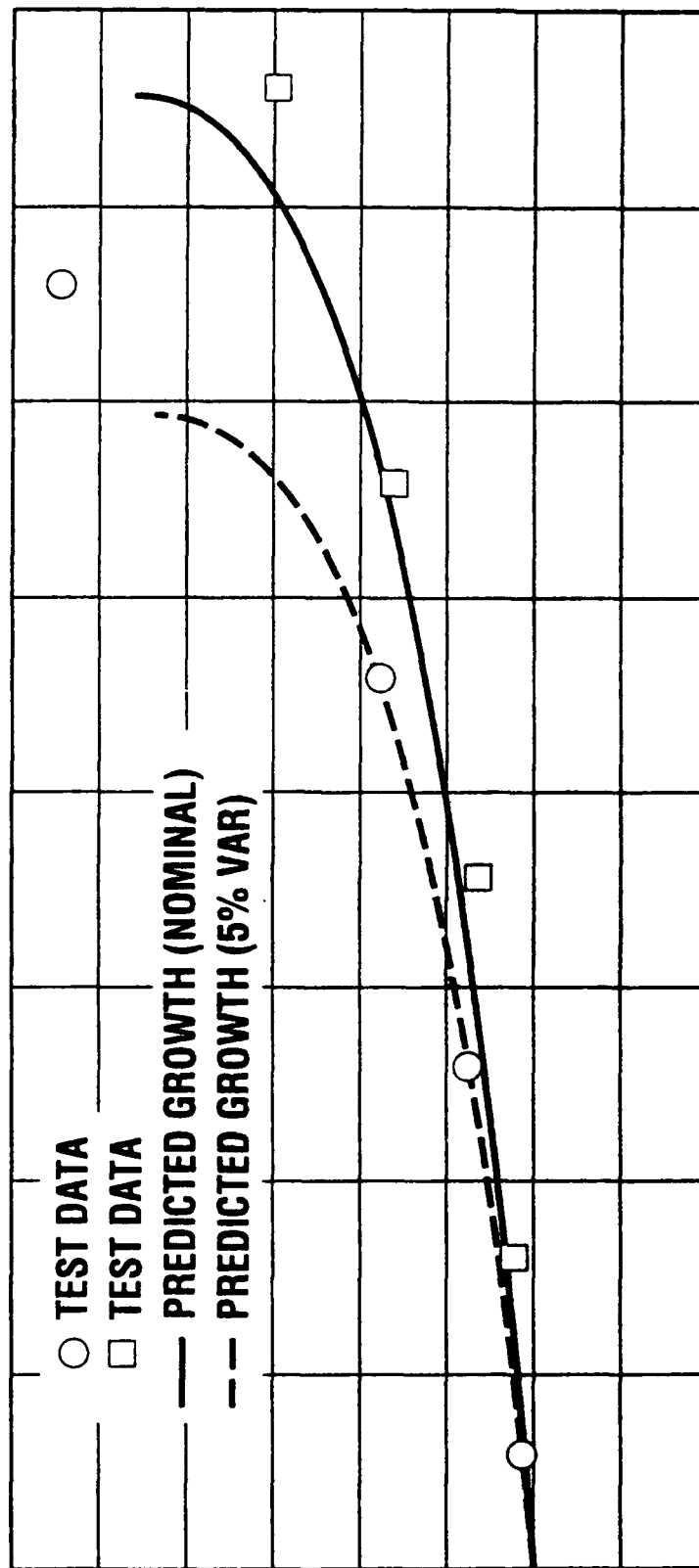
Allied-Signal Aerospace Company

Garrett Engine Division



SECOND-STAGE HP COMPRESSOR DISK WEB CRACK HAS DIRECT CORRELATION ONCE THICKNESS TOLERANCES WERE CONSIDERED

FLAW LOCATION 2--DISK WEB



WEB SURFACE CRACK LENGTH, IN.

CYCLES

Allied-Signal Aerospace Company

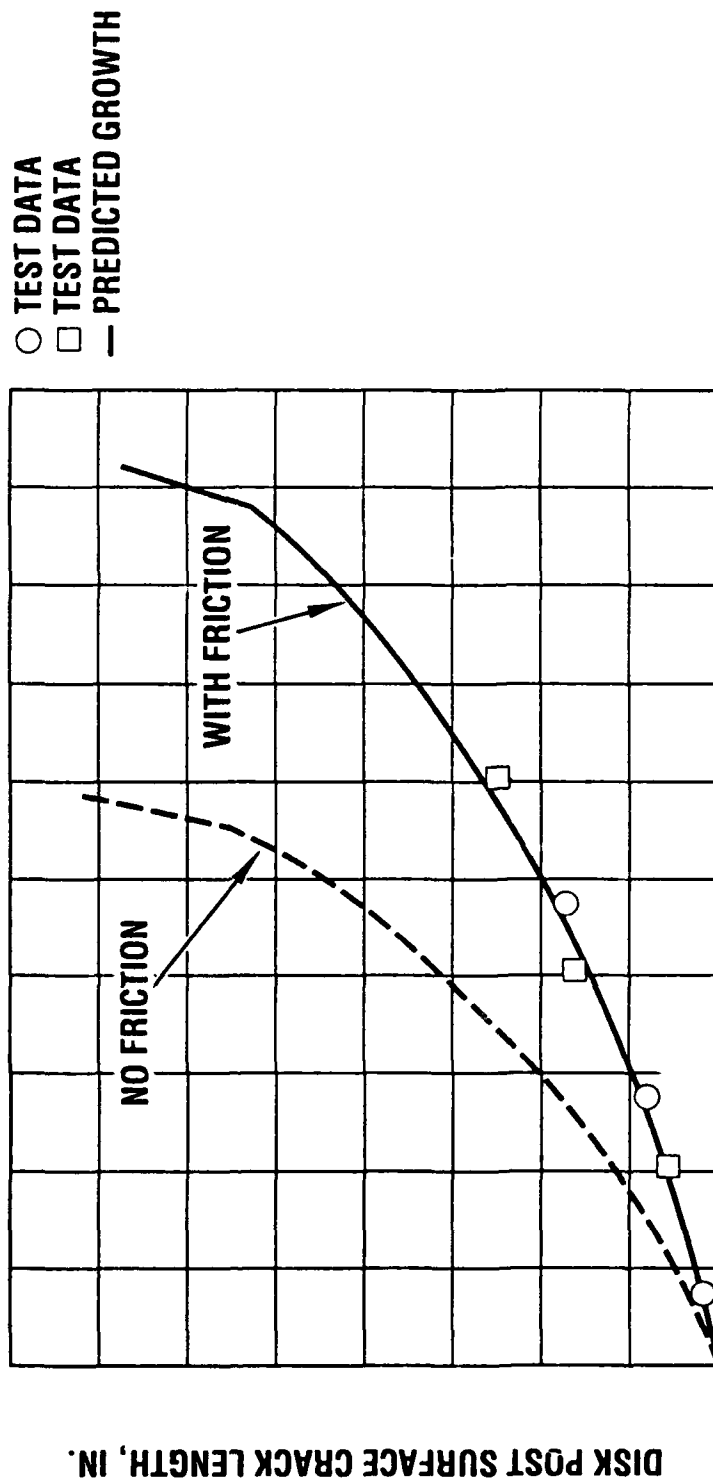
Garrett Engine Division

460457-21A



SECOND-STAGE HP COMPRESSOR DISK POST CRACK GROWTH HAS DIRECT CORRELATION ONCE ATTACHMENT FRICTION EFFECTS WERE INCLUDED

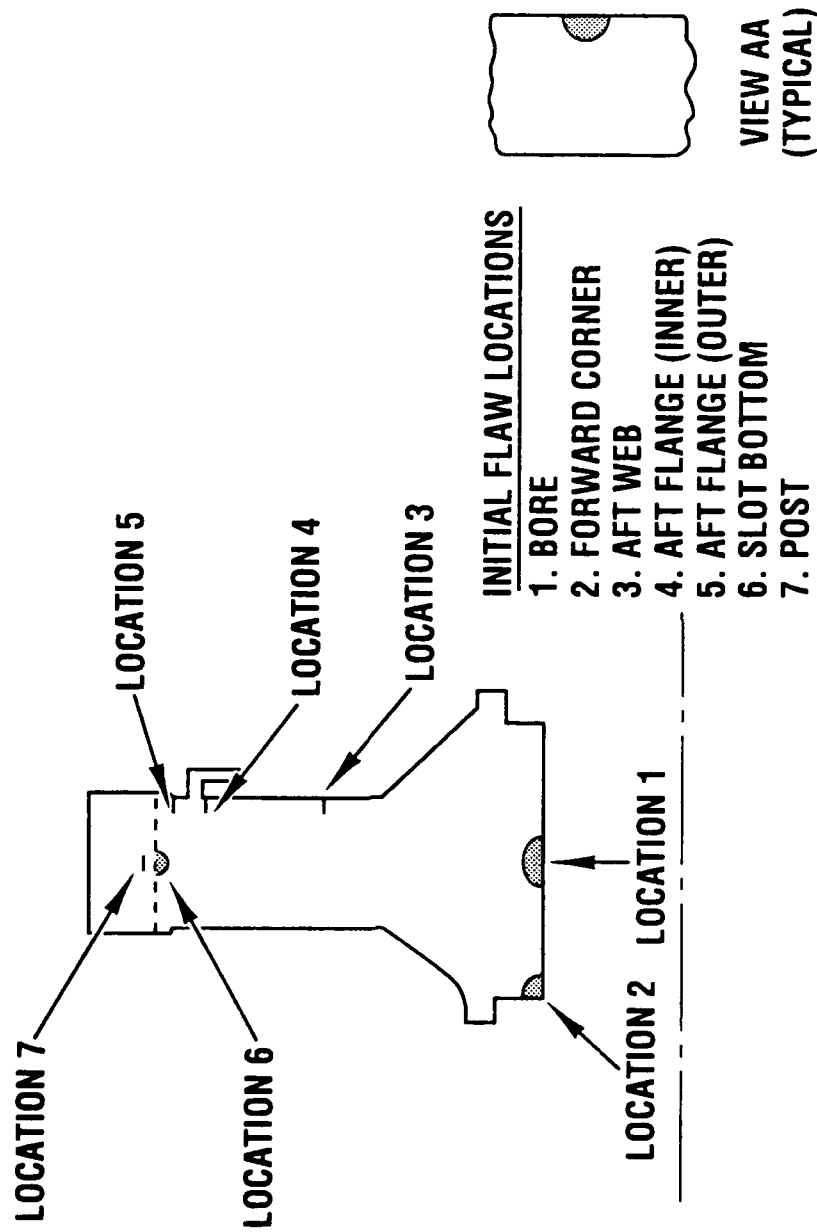
FLAW LOCATION 3--DISK POST



AGENDA

- TFE1042/F125 PROGRAM BACKGROUND
- TFE1042 DAMAGE TOLERANCE AND LOW CYCLE FATIGUE VERIFICATION
- SECOND-STAGE COMPRESSOR DISK DAMAGE TOLERANCE RESULTS
- HIGH PRESSURE TURBINE DISK DAMAGE TOLERANCE RESULTS
- COMBUSTOR CASE DAMAGE TOLERANCE RESULTS
- CONCLUSIONS

HIGH PRESSURE TURBINE DISK FLAW LOCATIONS

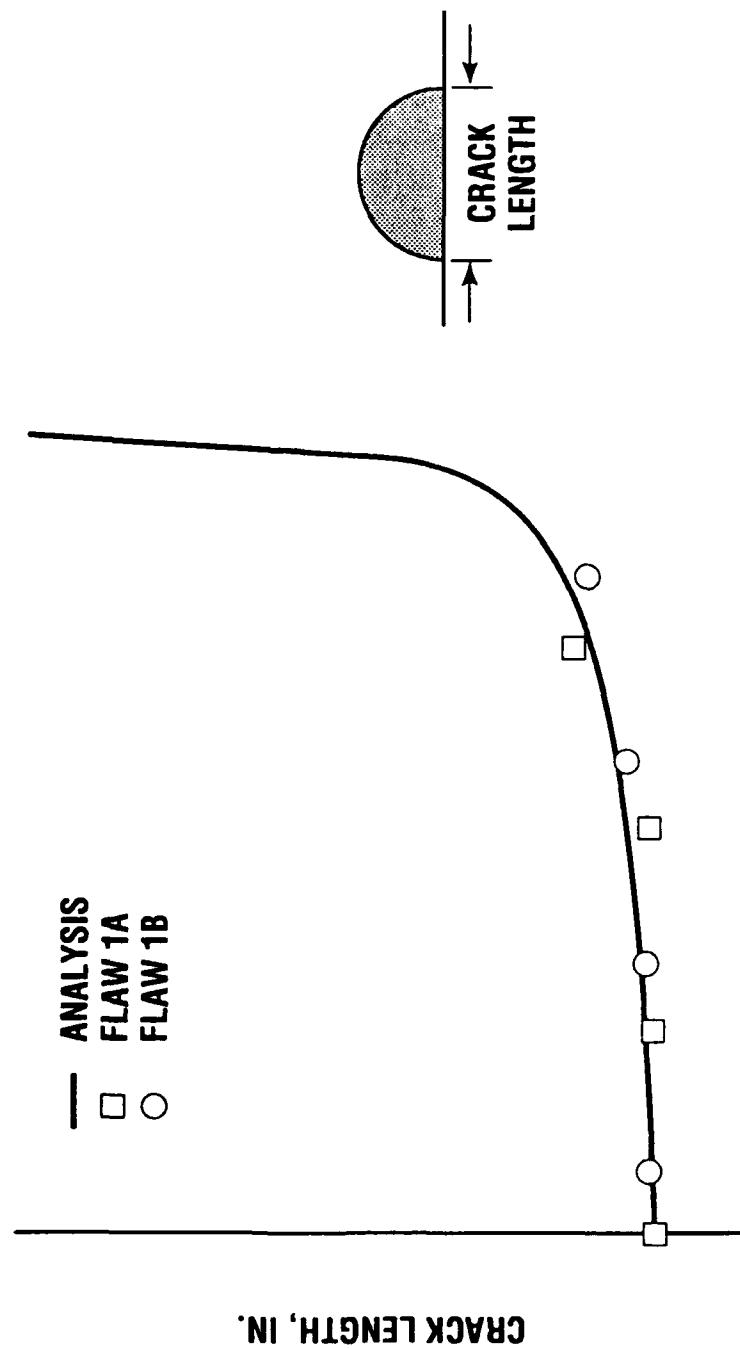


NO CRACK GROWTH OBSERVED AT SEVERAL LOCATIONS

- LOCATION 2--FORWARD BORE CORNER
 - LOCATION 3--AFT WEB
 - LOCATION 5--AFT FLANGE OUTER
 - LOCATION 6--SLOT BOTTOM
 - LOCATION 7--DISK POST
-
- SUSPECT CAUSES FOR LOCATIONS WITH NO CRACK GROWTH:
 - LACK OF CRACK INITIATION DUE TO STATISTICAL VARIATION (NOT ENOUGH FLAW SITES)
 - CONSTANT TEMPERATURE IN SPIN PIT--NO THERMAL GRADIENTS

HIGH PRESSURE TURBINE DISK BORE CRACK GROWTH HAS DIRECT CORRELATION TO ANALYSIS

FLAW LOCATION 1--DISK BORE



GM57-26

WHIRLPIT CYCLES

Allied-Signal Aerospace Company

Garrett Engine Division



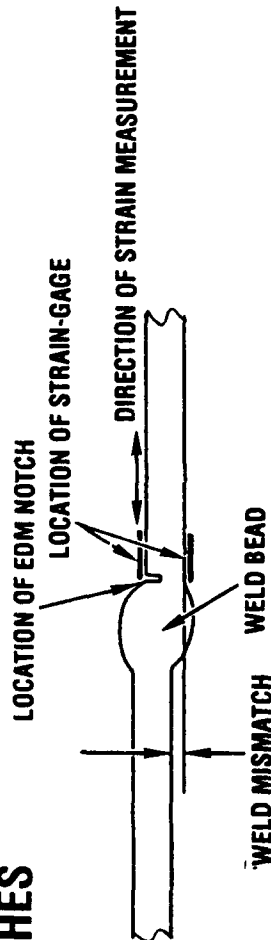
AGENDA

- TFE1042/F125 PROGRAM BACKGROUND
- TFE1042 DAMAGE TOLERANCE AND LOW CYCLE FATIGUE VERIFICATION
- SECOND-STAGE COMPRESSOR DISK DAMAGE TOLERANCE RESULTS
- HIGH PRESSURE TURBINE DISK DAMAGE TOLERANCE RESULTS
- **COMBUSTOR CASE DAMAGE TOLERANCE RESULTS**
- CONCLUSIONS

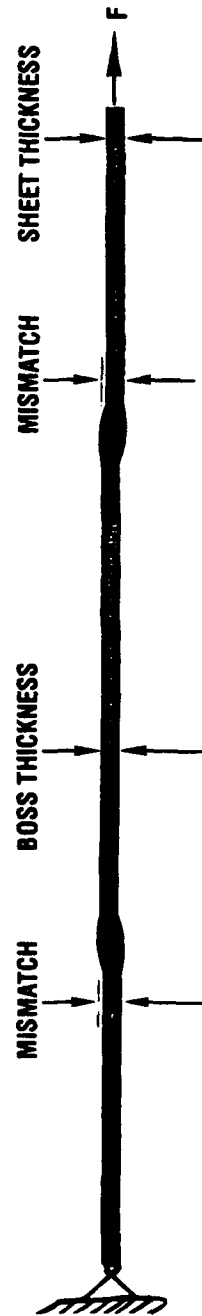
MEASURED STRAIN VALUES WERE REQUIRED TO CORRELATE STRESS ANALYSIS

- STRAIN-GAGE LOCATIONS WERE BASED UPON THE GEOMETRY:

BOSS THICKNESS
SHEET STOCK THICKNESS
WELD MISMATCHES

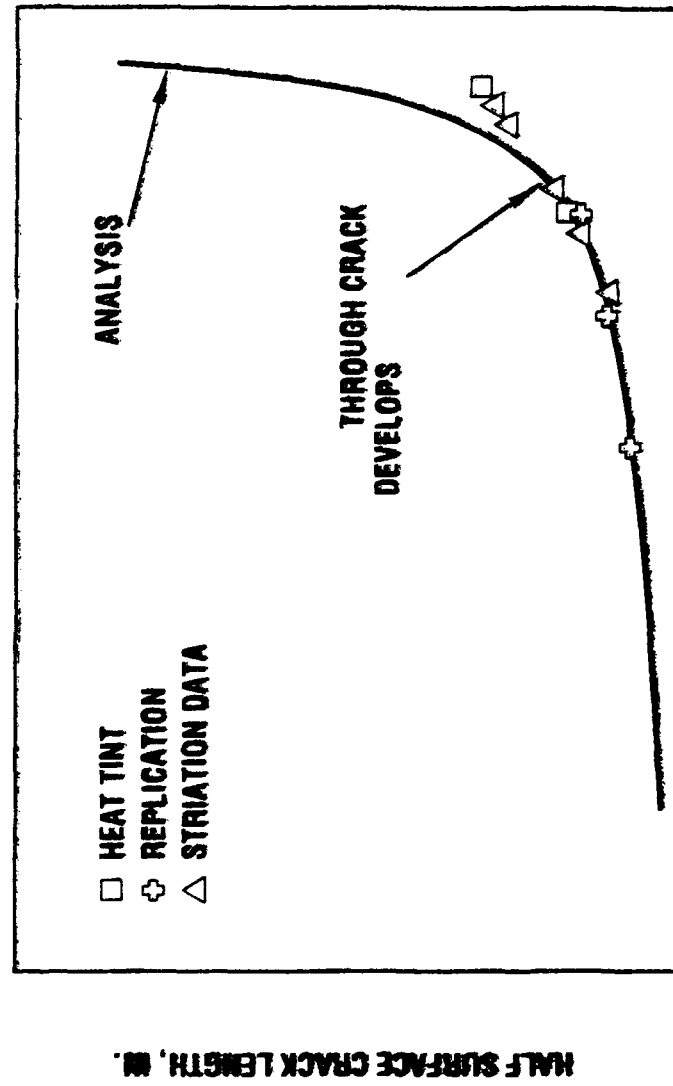


- ONCE STRAINS WERE CORRELATED TO THE STRESS ANALYSIS (FEA) AND THE DAMAGE TOLERANCE TESTS PERFORMED, THE DAMAGE TOLERANCE TEST ANALYSIS WAS COMPARED TO THE TEST RESULTS



COMBUSTOR CASE DAMAGE TOLERANCE TEST RESULTS SHOWS GOOD CORRELATION TO DAMAGE TOLERANCE ANALYSIS

REPRESENTS TYPICAL DATA FOR BOSS WELD CRACK



400457-32

Allied-Signal Aerospace Company

Garrett Engine Division



AGENDA

- TFE1042/F125 PROGRAM BACKGROUND
- TFE1042 DAMAGE TOLERANCE AND LOW CYCLE FATIGUE VERIFICATION
- SECOND-STAGE COMPRESSOR DISK DAMAGE TOLERANCE RESULTS
- HIGH PRESSURE TURBINE DISK DAMAGE TOLERANCE RESULTS
- COMBUSTOR CASE DAMAGE TOLERANCE RESULTS

• CONCLUSIONS

DAMAGE TOLERANCE TEST RESULTS SUMMARY

- DAMAGE TOLERANCE TEST EXPERIENCE HAS SHOWN EXCELLENT CORRELATION TO ANALYSIS, ONCE STRESS DIFFERENCE BETWEEN TEST CONDITIONS AND ANALYSIS ARE KNOWN
- A COST EFFECTIVE APPROACH TO ASSESSING DAMAGE TOLERANCE IS TO PLACE MORE EMPHASIS ON CORRELATING THE STRESS ANALYSIS
- SPINPIT TEST RESULTS VERIFY EFFECT OF ACTUAL COMPONENT GEOMETRY

**DAMAGE TOLERANCE PROGRAM HAS VERIFIED
CRACK GROWTH RATE CALCULATION PROCEDURE**



GE Aircraft Engines

Competition in Probabilistic Life Analysis

**1990 USAF Structural Integrity
Program Conference**

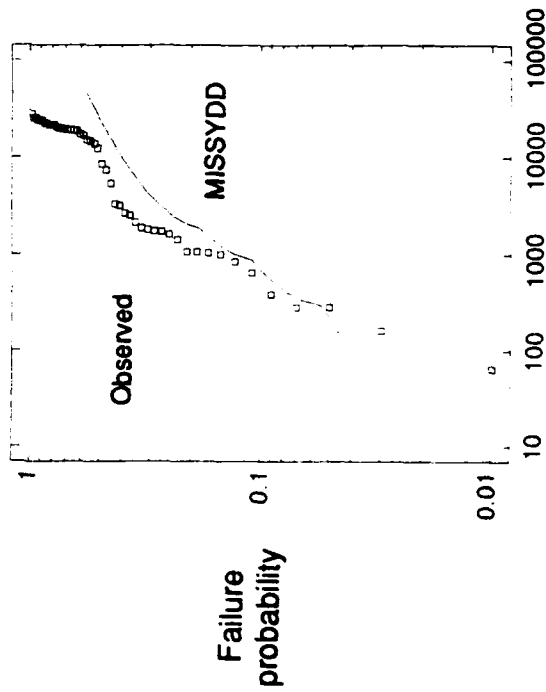
December 13, 1990

P.G. Roth

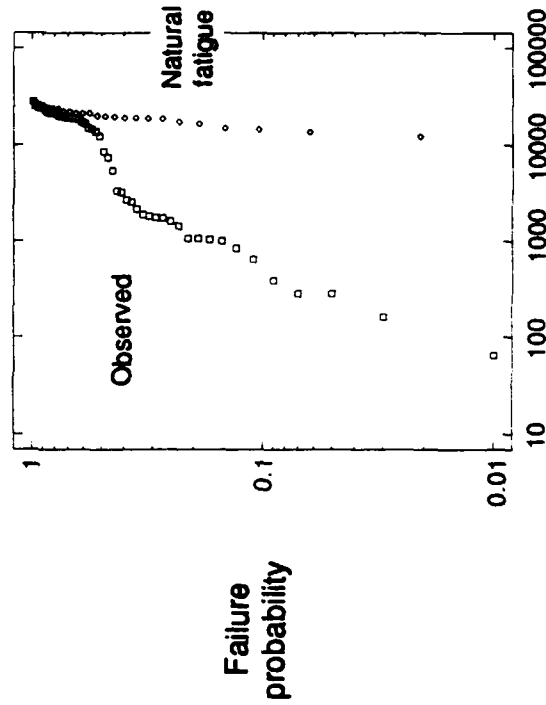
Competition in Probabilistic Life Analysis

- Traditional design practices are often in question
 - Some feel they are conservative, some non-conservative
- Probabilistic alternatives have been developing for a number of years
 - Initiatives by industry and government (USAF, NASA, JPL)
- Care is required
 - Probabilistic approaches always appear more quantitative but they can mislead
- A few relevant studies will be presented and future directions suggested

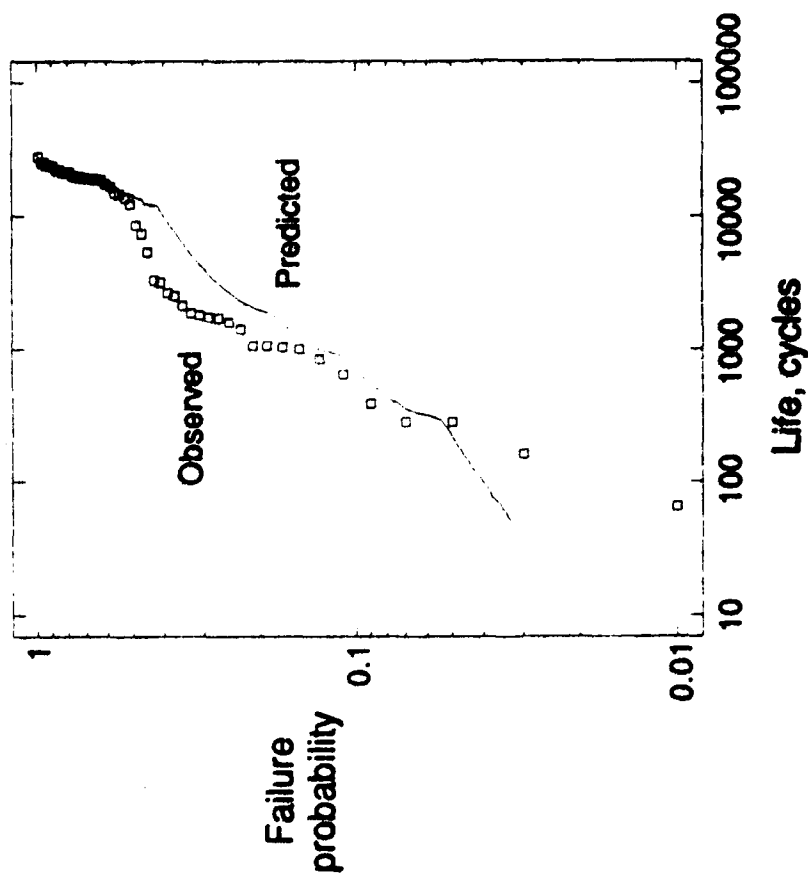
- A central premise of risk analysis is that risks compete . . . that probabilities must be combined
 - $P_{\text{survival of whole}} = \prod P_{\text{survival of parts}}$
- Demonstrated: hourglass specimens manufactured from seeded as-HIP PM René 95 and fatigue tested
 - Seeded defects are in direct competition with natural failure mechanisms



Predicted defect failure distribution compared to data



Fatigue distribution compared to data

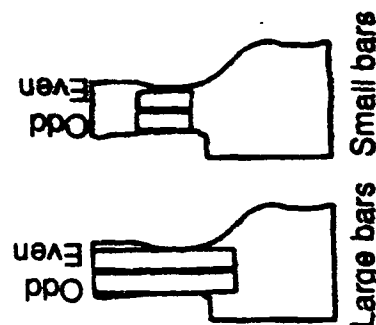
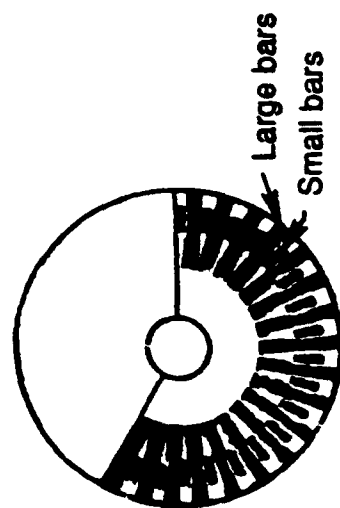


- Predicted defect failure distribution combined with fatigue distribution and compared to data

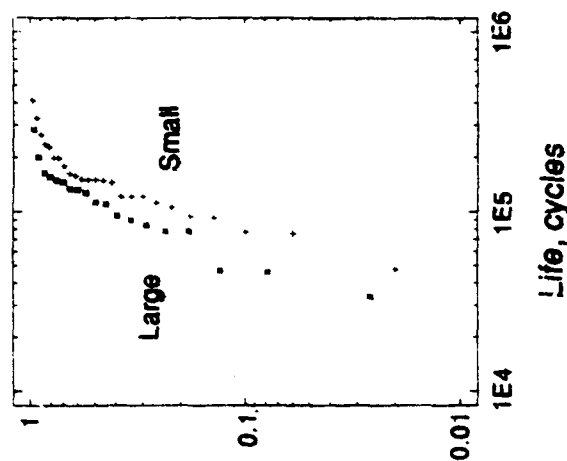
$$- P_{\text{failure}} = 1 - (1 - P_{\text{defect failure}}) \times (1 - P_{\text{fatigue failure}})$$

-
- The premise of competition (if blindly applied) can yield unrealistically low survival probabilities
 - Unbounded pessimism is as useless as unbounded optimism is bad
 - Volumetric impact on properties recognized by Leonardo DaVinci
 - Observed that the strength of wires decreased with increasing length
 - A statistical interpretation was eventually developed
 - Weibull an important contributor
 - GEAE first experienced a statistical size effect in powder alloys
 - Fatigue life is controlled by defects (ceramic inclusions, porosity)
 - The likelihood of defect occurrence is volumetric
 - MISSYDD (MISSion SYntesis given Defect DIstribution) developed to evaluate failure probabilities

- Whenever there is scatter, there is potentially a size effect
- We learned a few things in checking this out
- LCF size effect study #1
 - Compared large and small specimens from a single wrought Inconel 718 forging
 - All shotpeened to force internal initiations
 - Simple cycle mission at room temperature

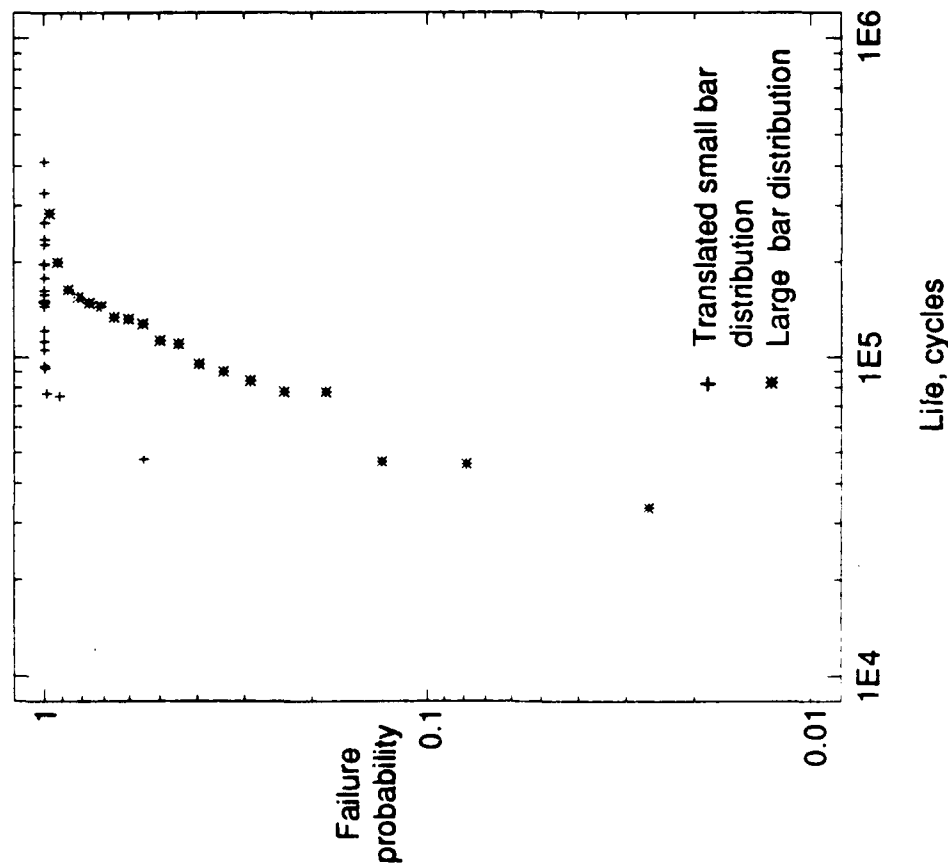


Failure probability

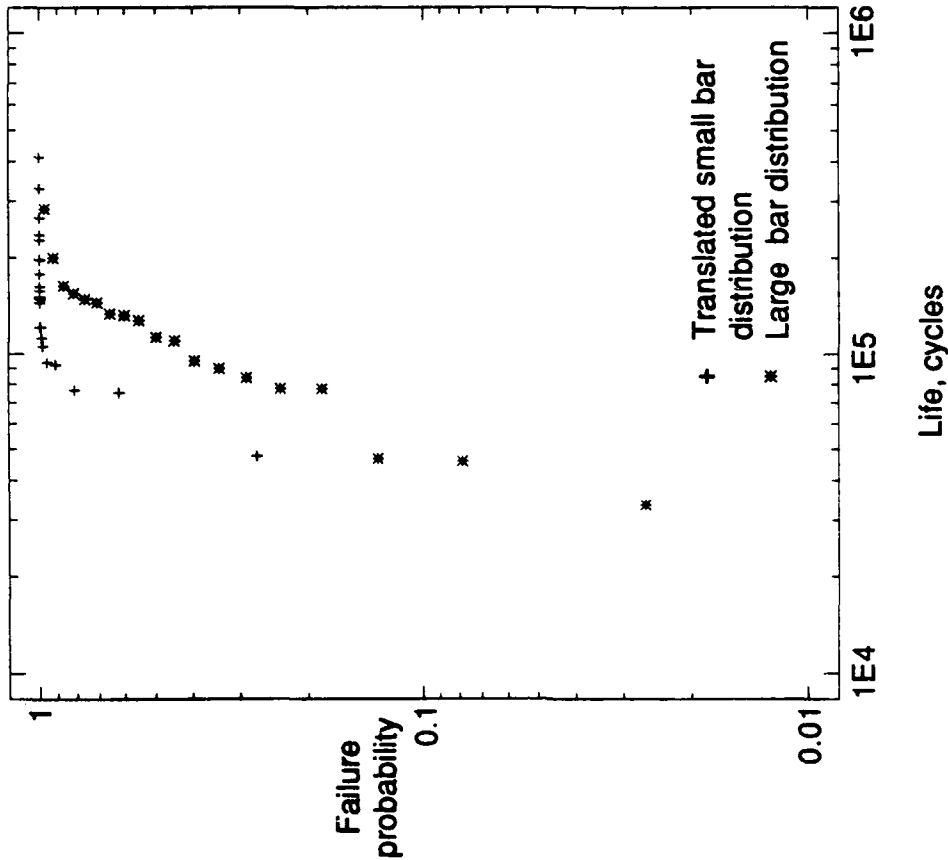


Cutup plan

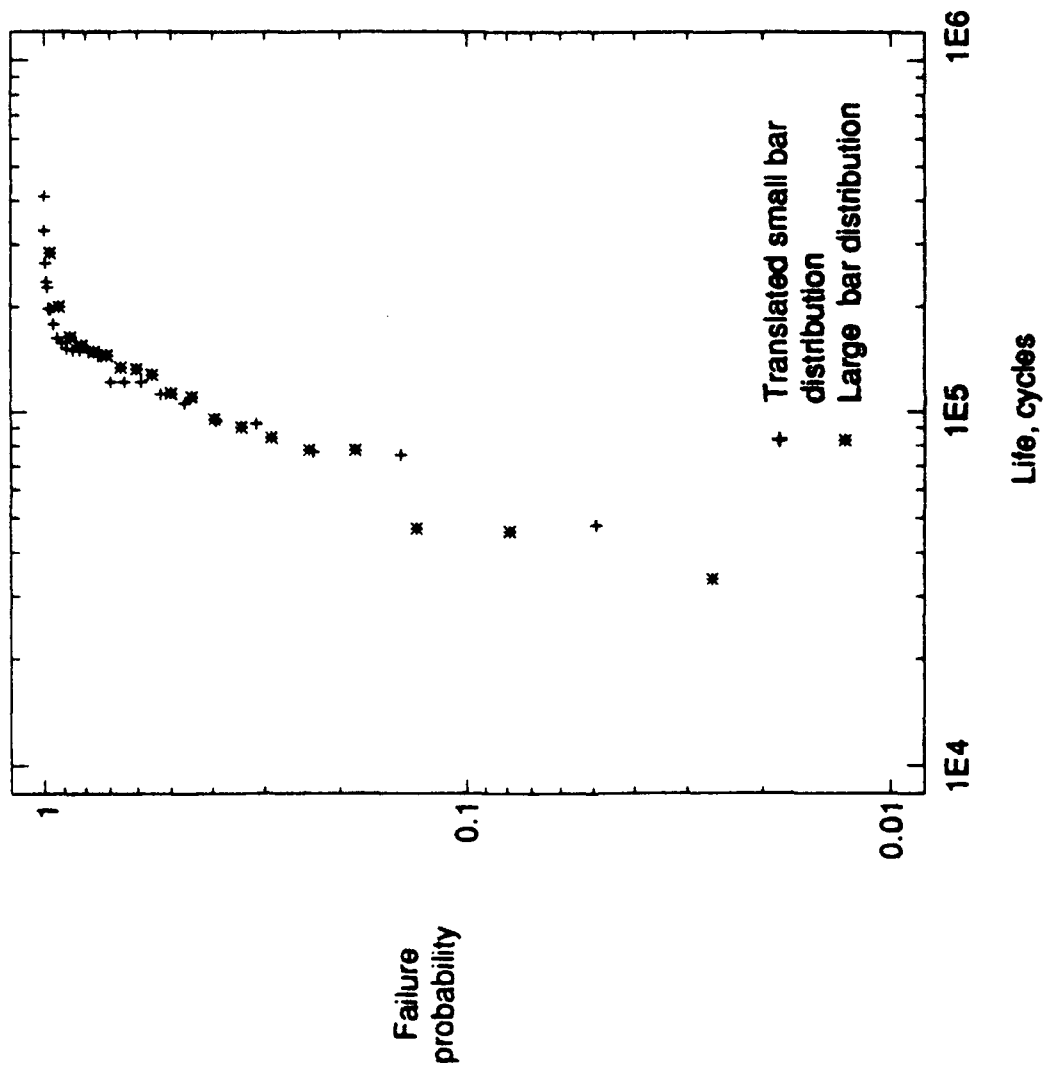
Fatigue distributions



- Despite shotpeening, most bars initiated at surface
- Volumetric scaling did not work

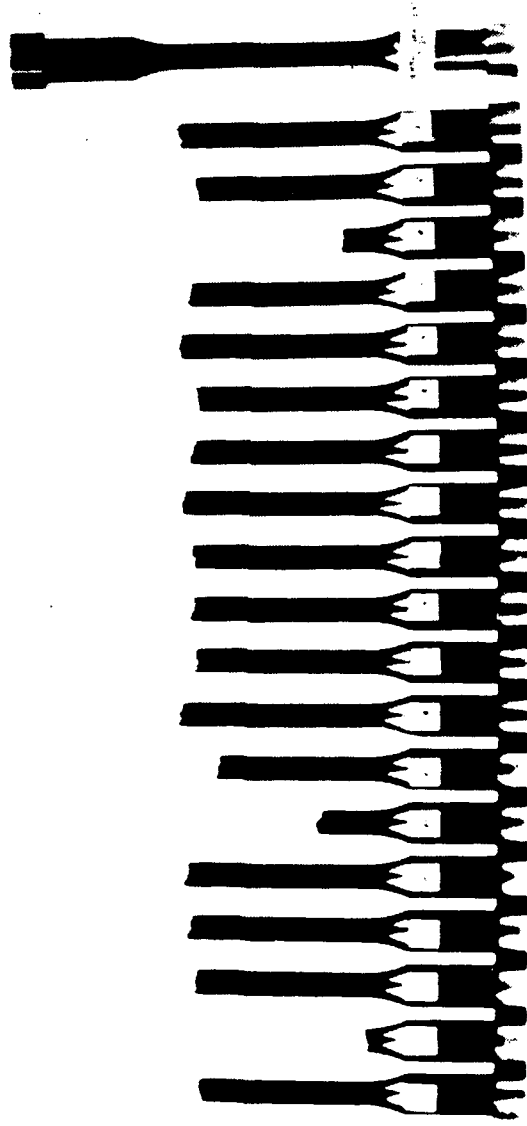


- Despite only modest stress concentration (3%) most bars initiated near radius transition
- Areametric scaling did not work



Diametric scaling proved sensible

Closer Consideration of the Failure Locations Led to the Correct Interpretation

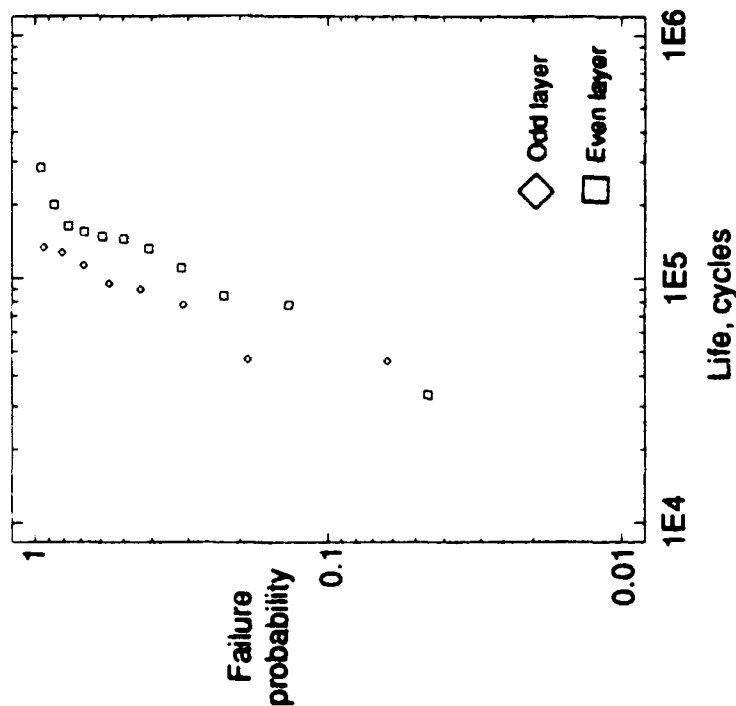


Failed large specimens, rim ends down

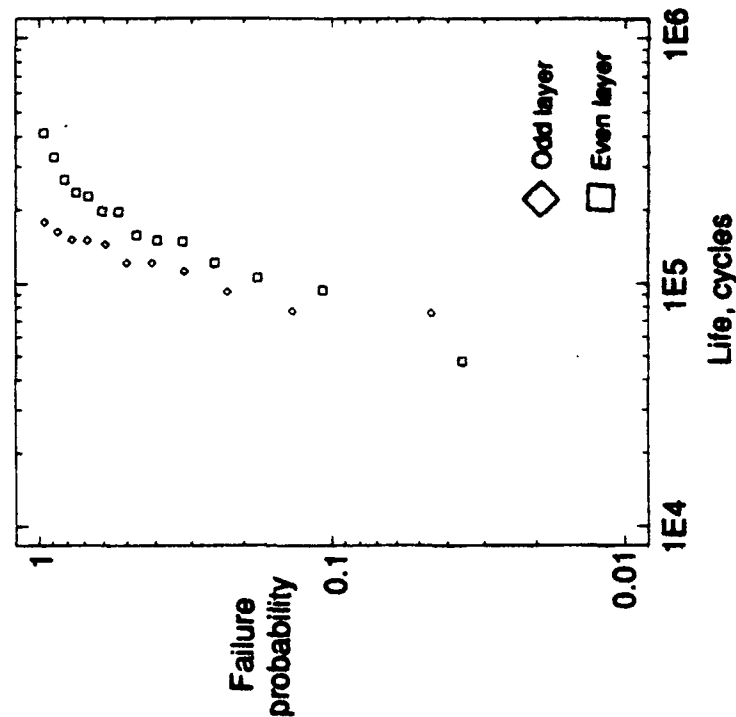
- There is apparently a gradient in fatigue capability along the 3.8 inch parallel section of the specimen

- Comparison of even and odd specimens (adjacent layers) confirmed fatigue stratification

- Small but statistically uniform differences were detectable between samples of material in close (1 inch) proximity



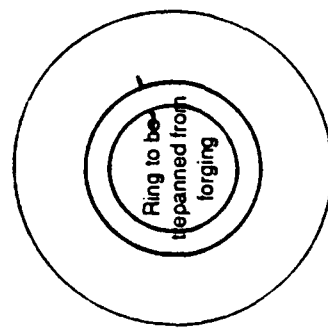
Large even vs. odd



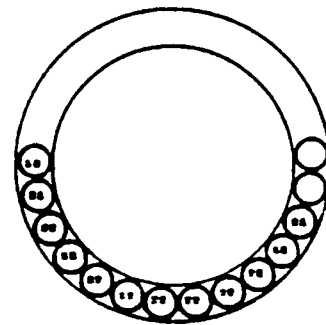
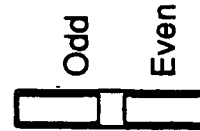
Small even vs. odd

- Another example with E+F -150 mesh PM René 95 under more realistic conditions

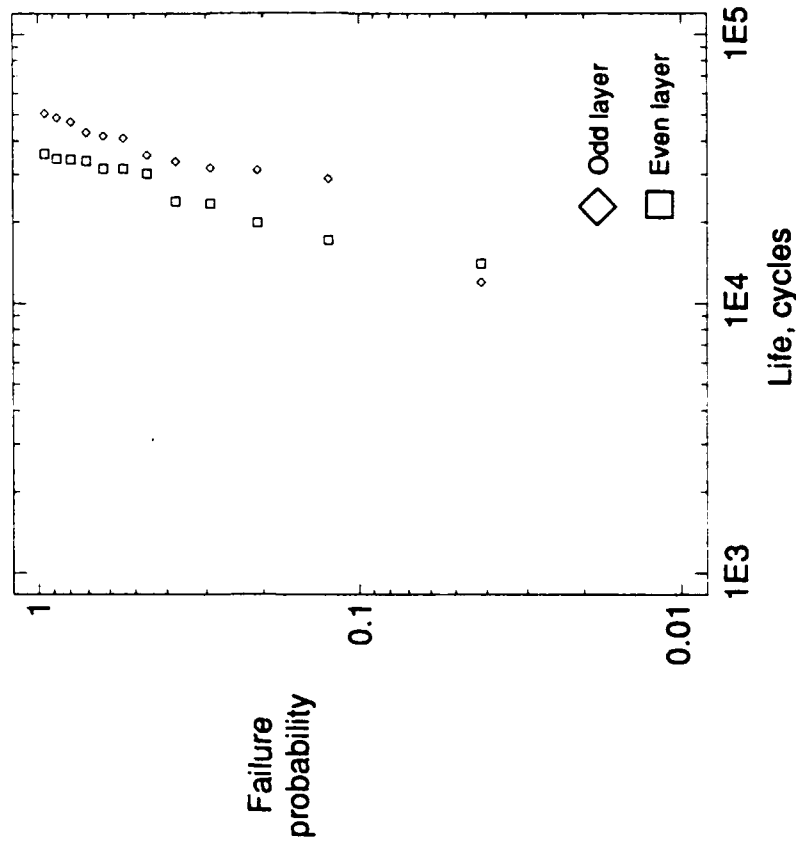
- Specimens again cut from a single forging
- Tested at 750°F ... complex mission



Ring dimensions: ID – 5 inches
 OD – 6.5 inches
 Depth – 4 inches
 (OD of forging is about 13 inches)



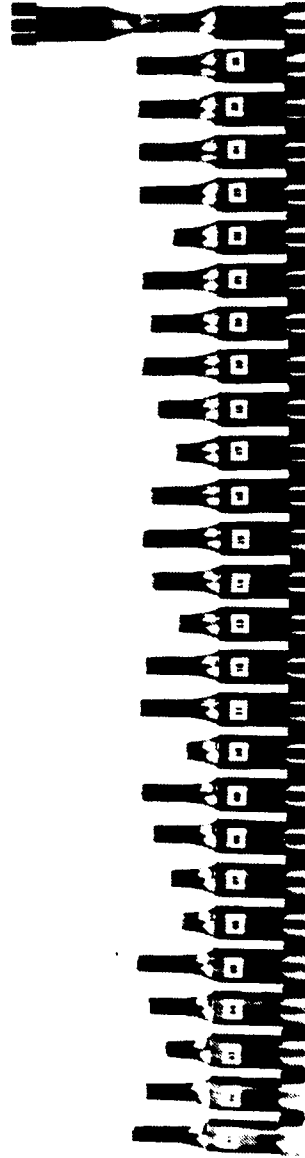
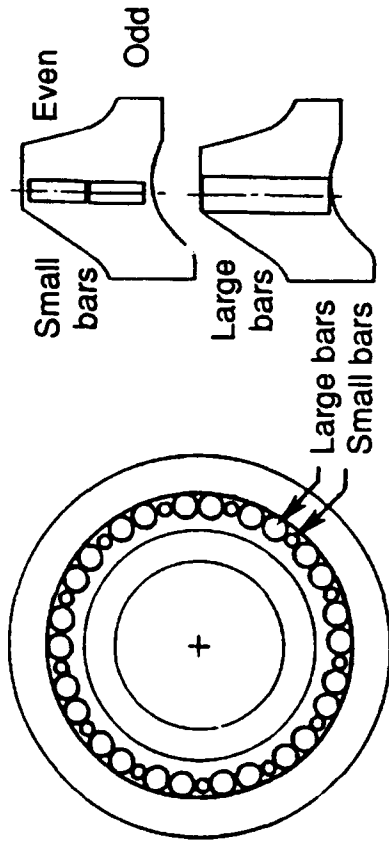
Cutup plan



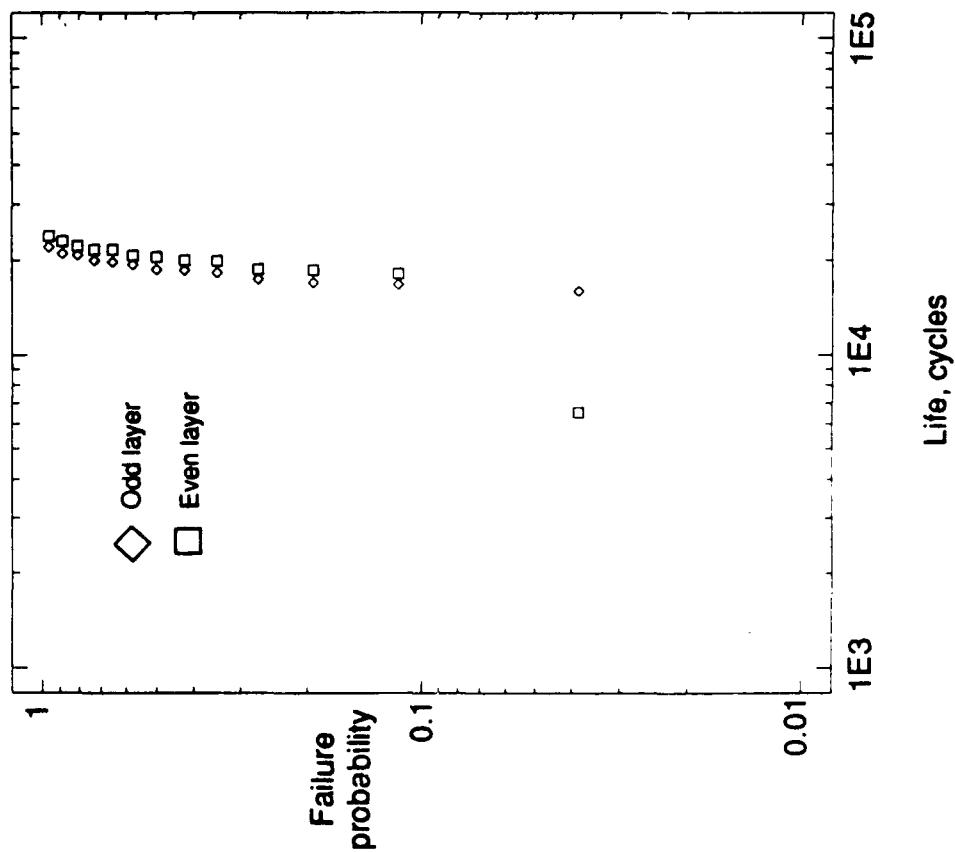
Failure distributions

- LCF size effect study No. 2

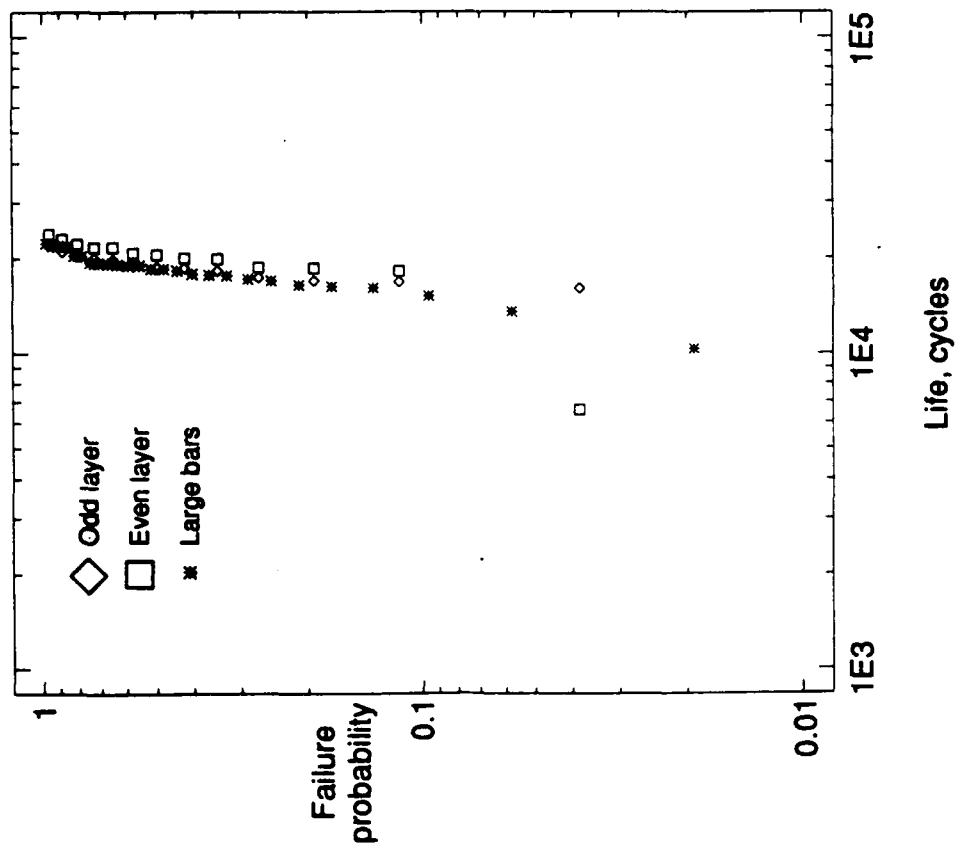
- Got smarter with cutup plan
- Simple cycle mission at room temperature
- Competition demonstrated and validated



Failed large specimens, even ends down

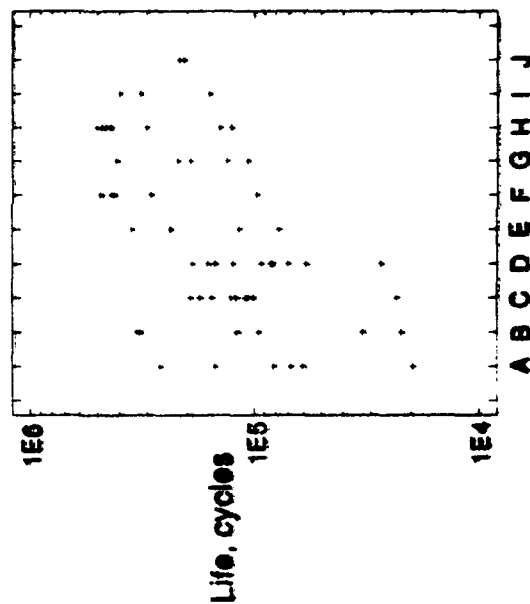


Even and odd
layers compared



Large specimen failure
distribution coincides with small
odd distribution

- Implication for statistical analysis of data
 - In the systems tested, data from standard cutup plans reflect sampling variability rather than statistical material variability
- Principal component of material variability appears to be part-to-part
 - Production forging data
(fixed temperature and strain range)



VSE data ranges compared from forging to forging

- Ignoring stratification:

- $P_{\text{survival of whole}} = \Pi P_{\text{survival of parts}}$

- Recognizing stratification:

- $P_{\text{survival of whole}} = \text{minimum}(P_{\text{survival of parts}})$

- $\Pi P_{\text{survival of parts}} \leq \text{minimum}(P_{\text{survival of parts}})$

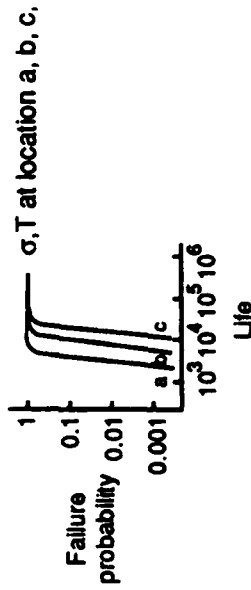
- To ignore it is conservative

- Reality lies between these extremes

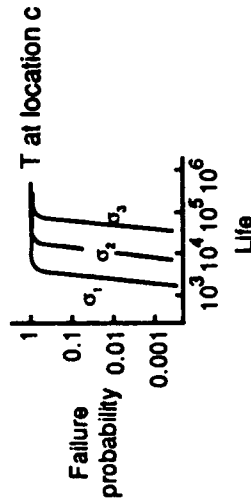
-
- The above data suggests that machining and testing can be reasonably controlled for the type of specimens considered
 - Other data, however, shows large discrepancies between machine shops (consistent with measured surface residual stresses)
 - Process in control during a single operation . . . less control from operation to operation
 - This suggests that more attention be focused on realistically configured and produced specimens
 - Given controlled machining and testing, material cutup plans should be approached differently

LCF Data Generation

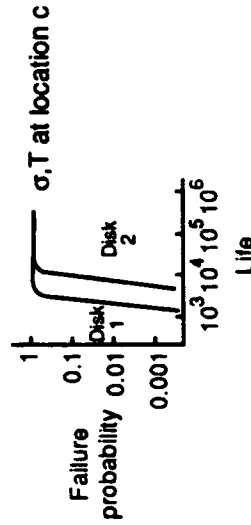
1) Extensive cutups of a few parts to statistically map properties



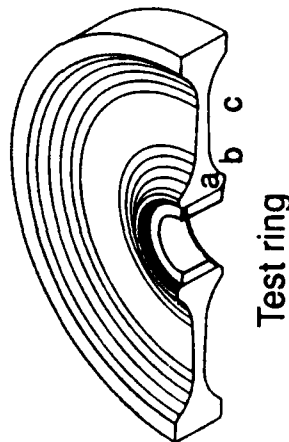
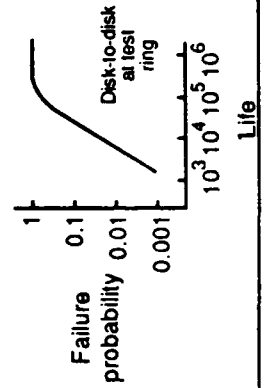
2) Characterize correlations between conditions



3) Characterize correlations between parts



4) Production evaluation of test material



Data Application

- For disks:
 - 1 Individual features evaluated separately (features separated into distinct production operations ... e.g. turned bodies, milled boltholes, broached dovetail slots)
 - 2) Component subdivided into zones identified by material evaluation
 - 3) Same part distributions scaled to zone size and integrated
 - 4) Part-to-part variability introduced to yield predicted population failure distribution
- Important mechanistic factors remain to be addressed (e.g. damage accumulation during complex missions, stress field multiaxiality)
- Other failure mechanisms factored in as necessary (e.g. defects)

Summary

- The above studies indicate the role of competition in controlled systems
- Development of precise statistical estimates requires recognition of data stratification
 - Must tighten focus on material evaluation
- Initial studies only . . . but the messages are useful

**Preliminary Damage Tolerance Evaluation of
Selected F412-GE-400 Engine Components**

**1990 USAF Structural Integrity Conference
December 11-13, 1990
San Antonio, Texas**

R.E. Kehl

GE Aircraft Engines

Outline

- **USAF F412 ERR2 Background**
- **USN / USAF Mission Comparison**
- **Turbomachinery Components and Preliminary Results**
- **Assessment Summary**

USAF F412 Early Risk Reduction (ERR2) Assessment Background

GE Aircraft Engines

3

F412-GE-400 Program

- GEAE is under contract to design, develop, and qualify the F412 engine for the USN application.
- The F412 engine is derived from the F404 and F110 engine designs.
- GEAE designed F412 engine turbomachinery to meet USN durability criteria.

GEAE is meeting USN needs and design requirements.

GE Aircraft Engines

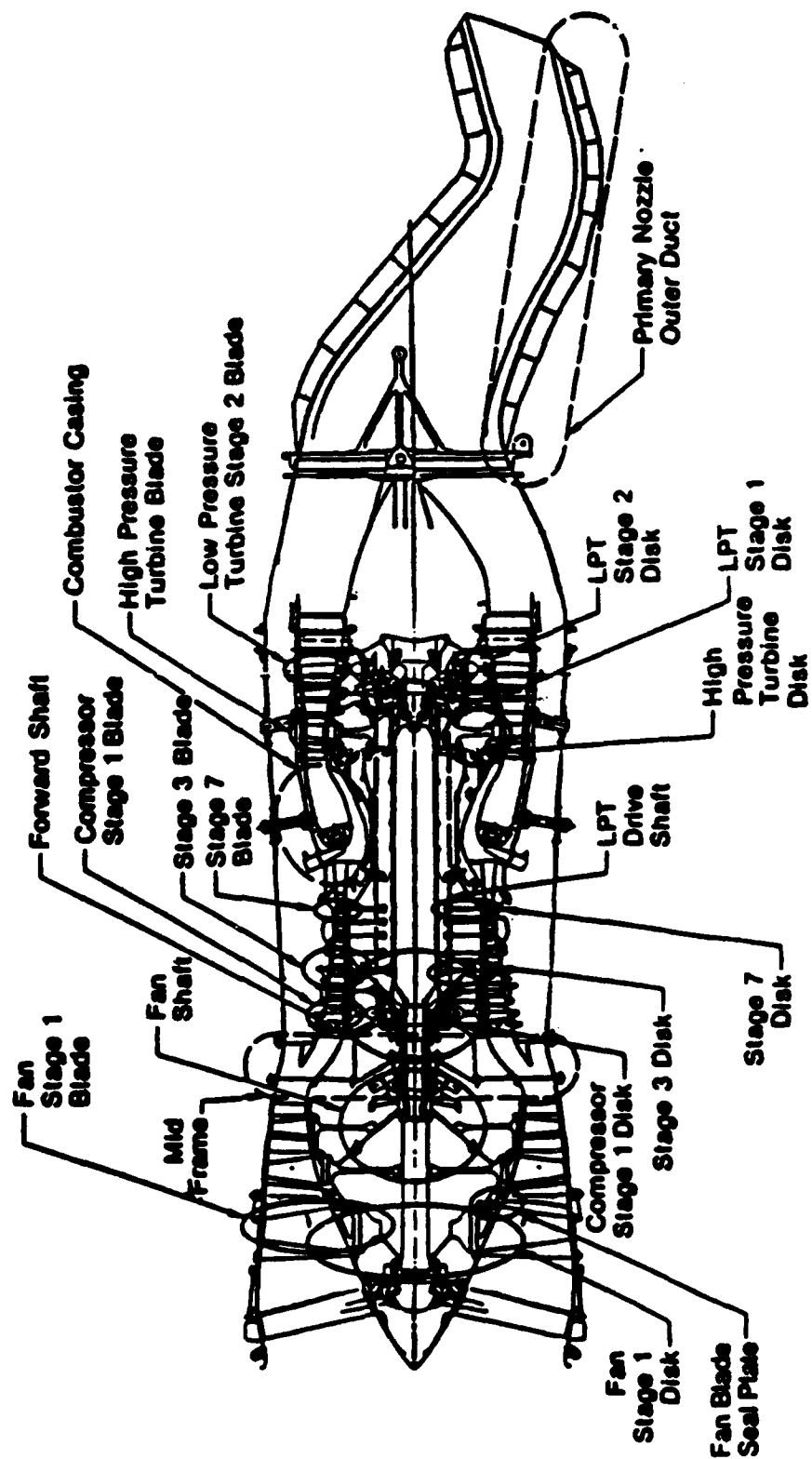
USAF ERR2 Assessment

- The "Early Risk Reduction" assessment evaluates potential changes to airframe and engine due to differences in USAF usage and integrity criteria.
- GEAE's ERR2 assessment evaluates selected engine components throughout the engine, characterizing the entire F412 engine.
- F412 engine turbomachinery is evaluated for USAF goals.

Through ERR2 GEAE responds to USAF.

GE Aircraft Engines

USAF ERR2 Selected Engine Components

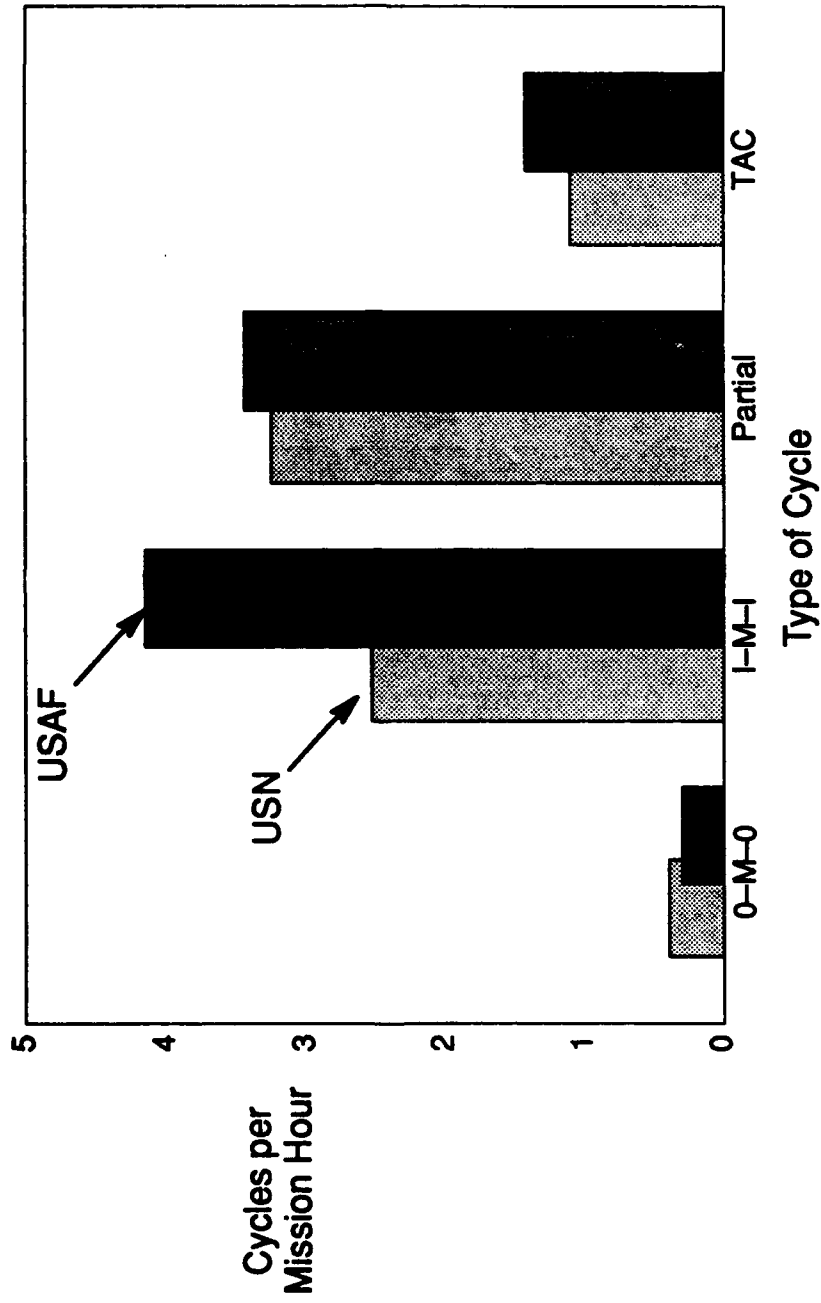


GE Aircraft Engines

USN / USAF Mission Comparison

GE Aircraft Engines

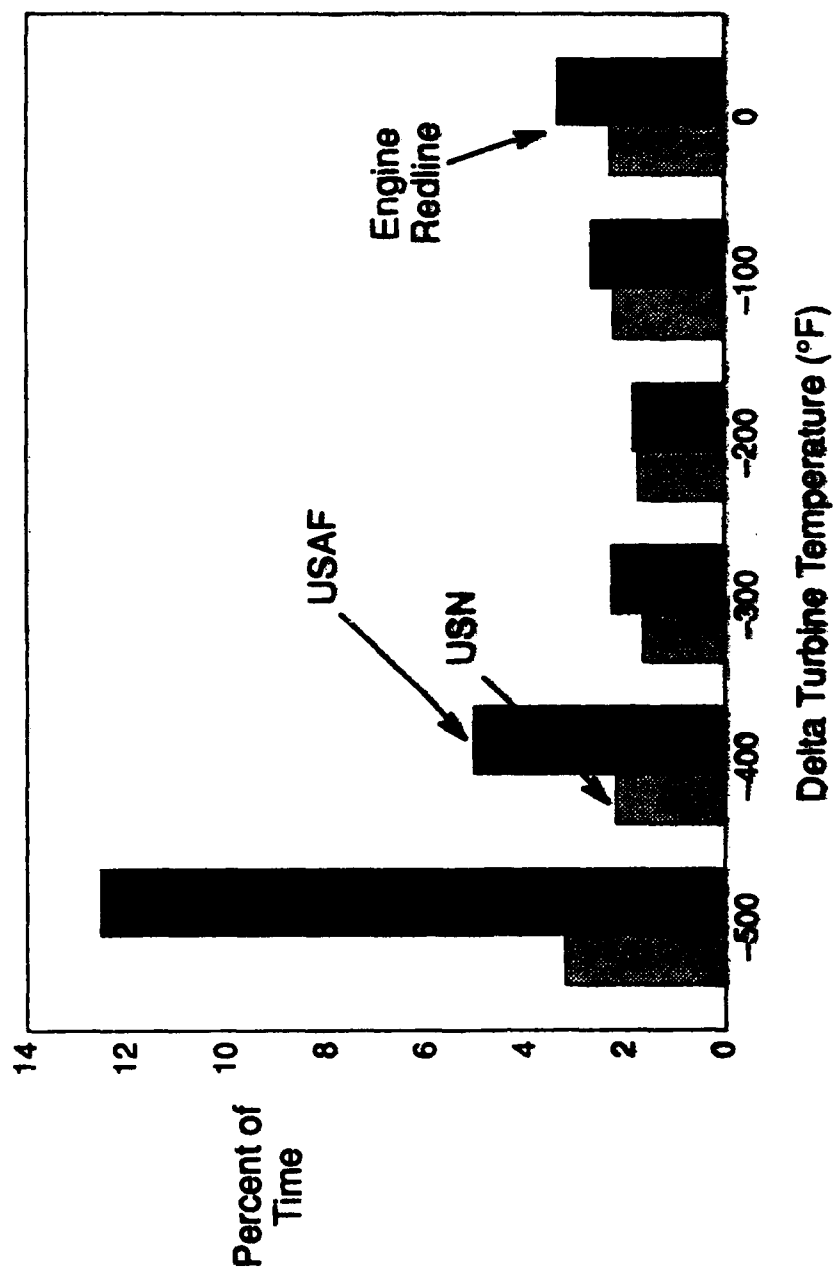
USN / USAF Cyclic Content Comparison



Air Force application has significantly more I-M-I cycles.

GE Aircraft Engines

USN / USAF Turbine Temperature Comparison



Air Force application has significantly higher turbine temperatures.

GE Aircraft Engines

Turbomachinery Components and Preliminary Results

GE Aircraft Engines

Fan Selected Locations

Label	Location	Assessment Complete
-------	----------	------------------------

Stage 1 Disk

F1D1, 2	Disk Bore	✓
F1D3	Disk Cone-Web Junction	✓
F1D4	Disk Dovetail	✓

Air Seal Plate

FSP1	Seal Plate Bolthole	✓
FSP2	Seal Plate Scallop	✓

Stage 3 Disk

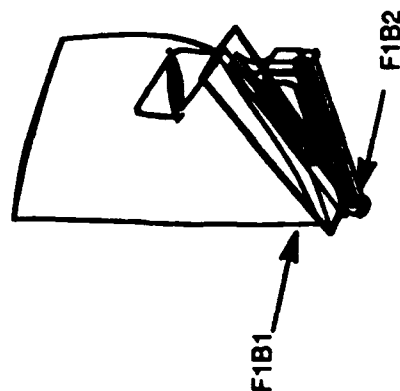
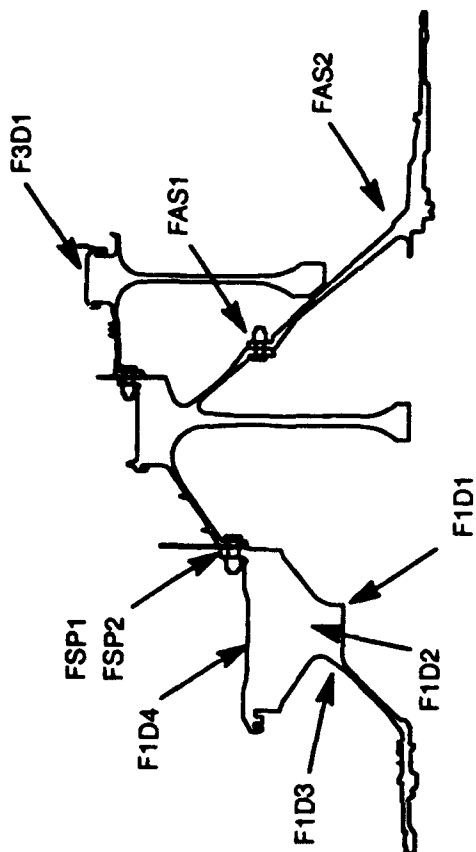
F3D1	Disk Dovetail	✓
------	---------------	---

Aft Shaft

FAS1	Shaft Bolthole	✓
FAS2	Shaft B Sump Hole	•

Stage 1 Blade

F1B1	Blade Dovetail	•
F1B2	Blade Airfoil Root	•

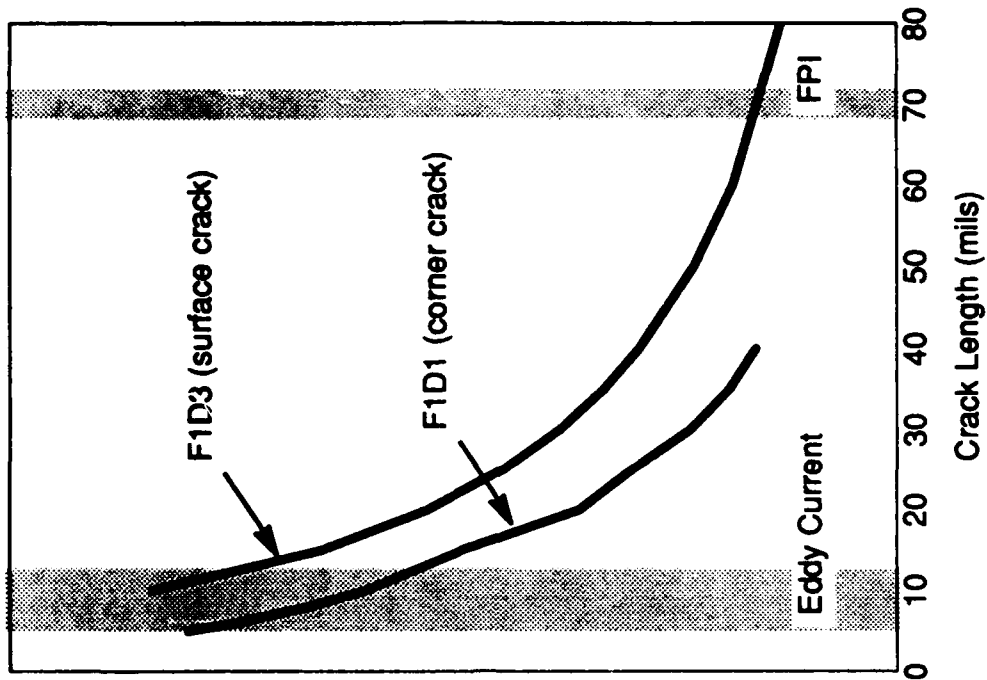
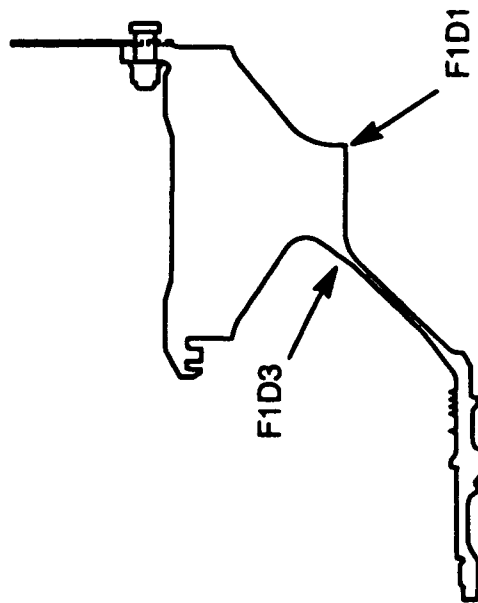


Selected locations characterize Fan.

GE Aircraft Engines

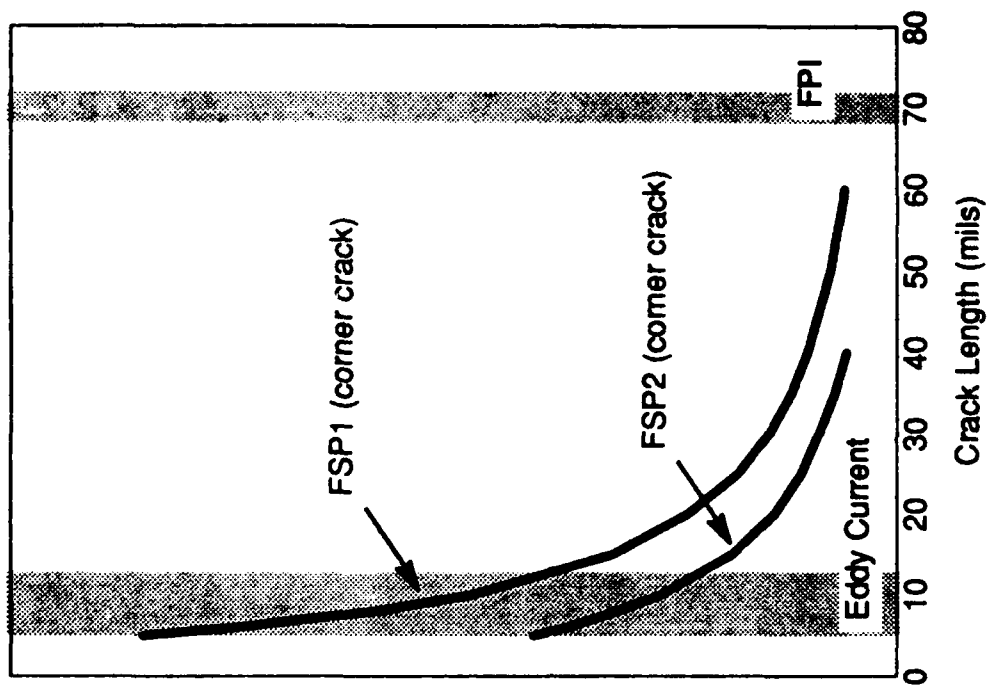
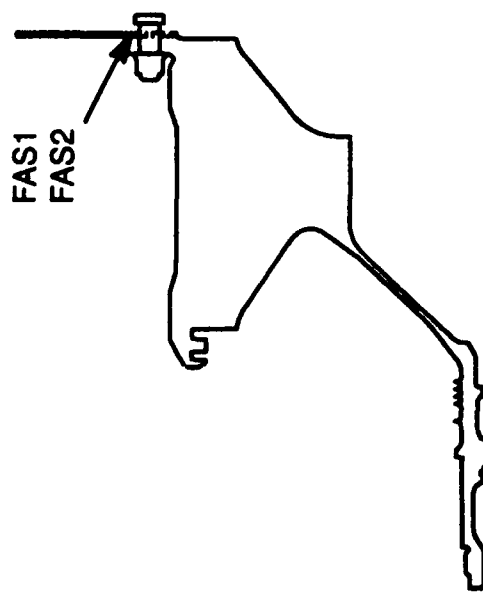
Fan Stage 1 Disk Fracture Mechanics Life

Label	Location
F1D1	Disk Bore (Surface)
F1D3	Disk Cone-Web Junction



Fan Stage 1 Air Seal Plate Fracture Mechanics Life

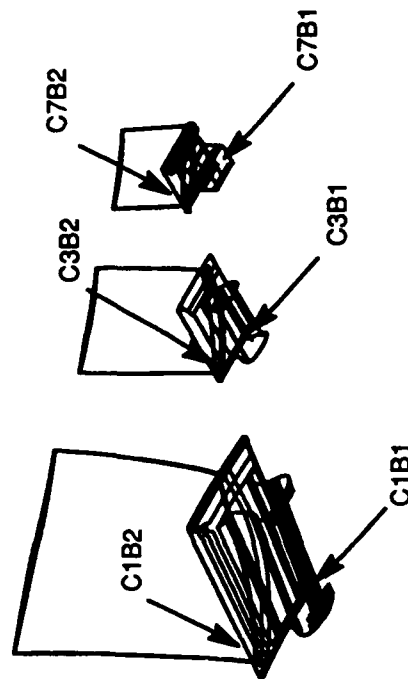
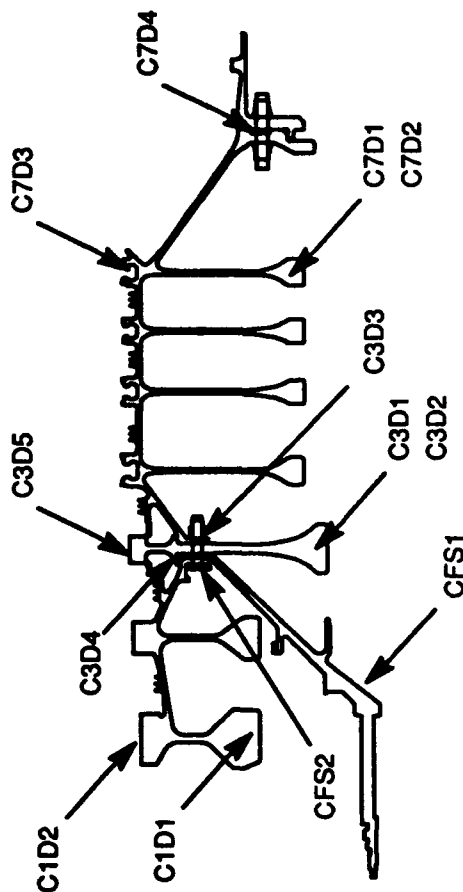
Label	Location
FSP1	Seal Plate Bolthole
FSP2	Seal Plate Scallop



GE Aircraft Engines

Compressor Selected Locations

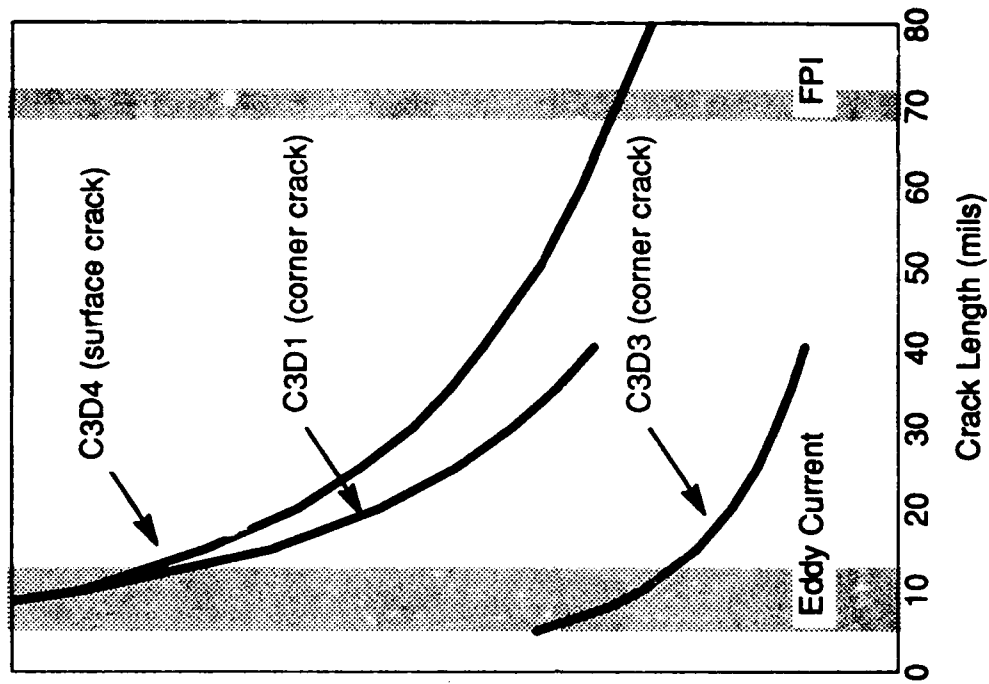
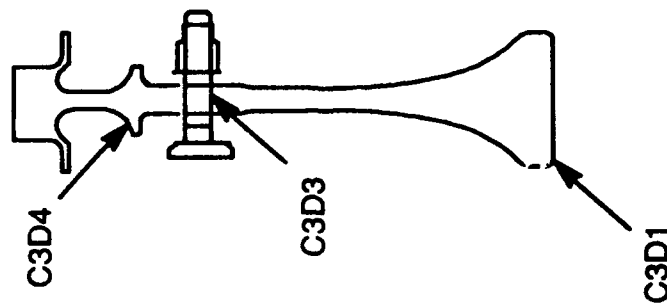
Label	Location	Assessment
Stage 1 & 2 Spool		
C1D1, 2	Stage 1 Disk Bore	✓
C1D2	Stage 1 Disk Dovetail	✓
Stage 1 Blade		
C1B1	Blade Dovetail	•
C1B2	Blade Airfoil Root	•
Forward Shaft		
CFS1	Shaft Bolthole	✓
CFS2	Shaft Venthole	✓
Stage 3 Disk		
C3D1, 2	Disk Bore	✓
C3D3	Disk Bolthole	✓
C3D4	Disk Forward Rabbet Fillet	✓
C3D5	Disk Dovetail	✓
Stage 3 Blade		
C3B1	Blade Dovetail	•
C3B2	Blade Airfoil Root	•
Stage 4 to 7 Spool		
C7D1, 2	Stage 7 Disk Bore	✓
C7D3	Stage 7 Disk Dovetail LL Slot	✓
C7D4	Stage 7 Disk Bolthole	✓
Stage 7 Blade		
C7B1	Blade Dovetail	•
C7B2	Blade Airfoil Root	•



Selected locations characterize Compressor.

Compressor Stage 3 Disk Fracture Mechanics Life

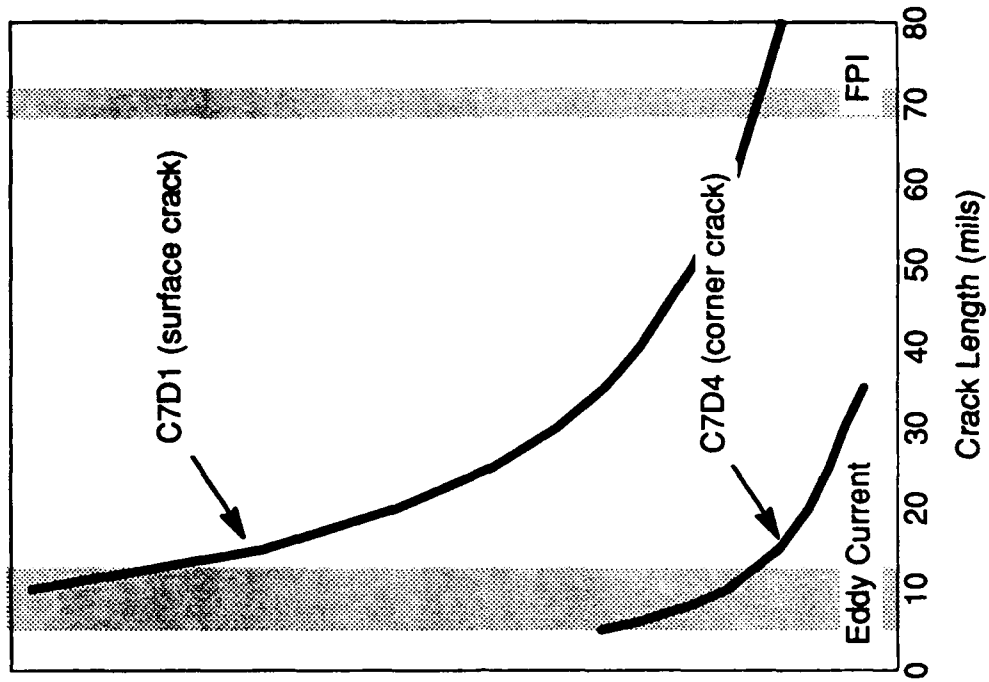
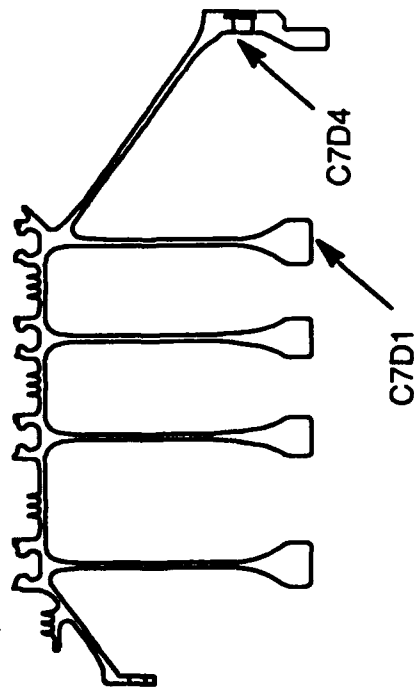
Label	Location
C3D1	Disk Bore (Surface)
C3D3	Disk Bolthole
C3D4	Disk Forward Rabbet Fillet



GE Aircraft Engines

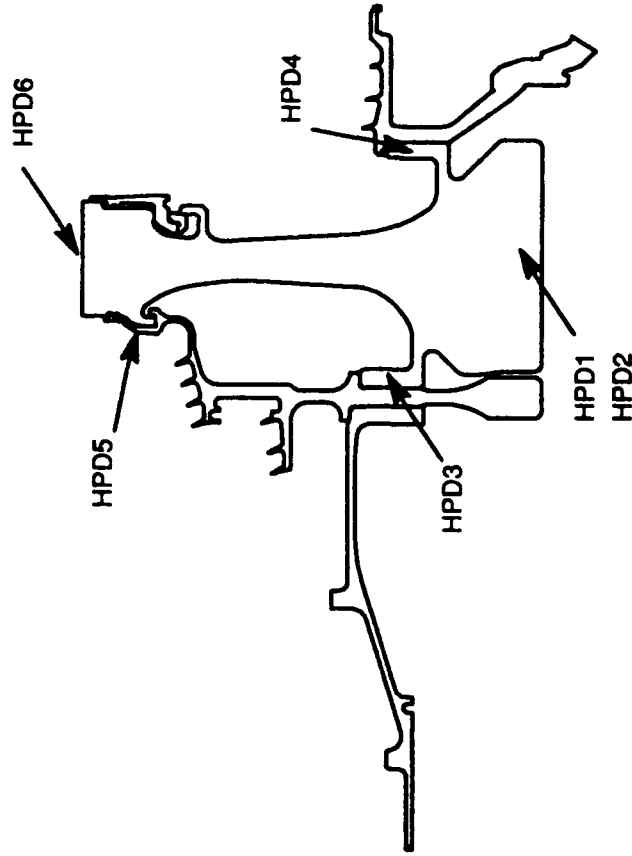
Compressor Stage 4 to 7 Spool Fracture Mechanics Life

Label	Location
C7D1	Stage 7 Disk Bore (Surface)
C7D4	Stage 7 Disk Bolthole



HP Turbine Selected Locations

<u>Label</u>	<u>Location</u>	<u>Assessment</u> <u>Complete</u>
Disk		
HPD1, 2	Disk Bore	•
HPD3	Disk Forward Bolthole	•
HPD4	Disk Aft Bolthole	•
HPD5	Disk Forward Fillet	•
HPD6	Disk Post	•
Blade		
HPB1	Blade Dovetail	•
HPB2	Blade Airfoil Root	•



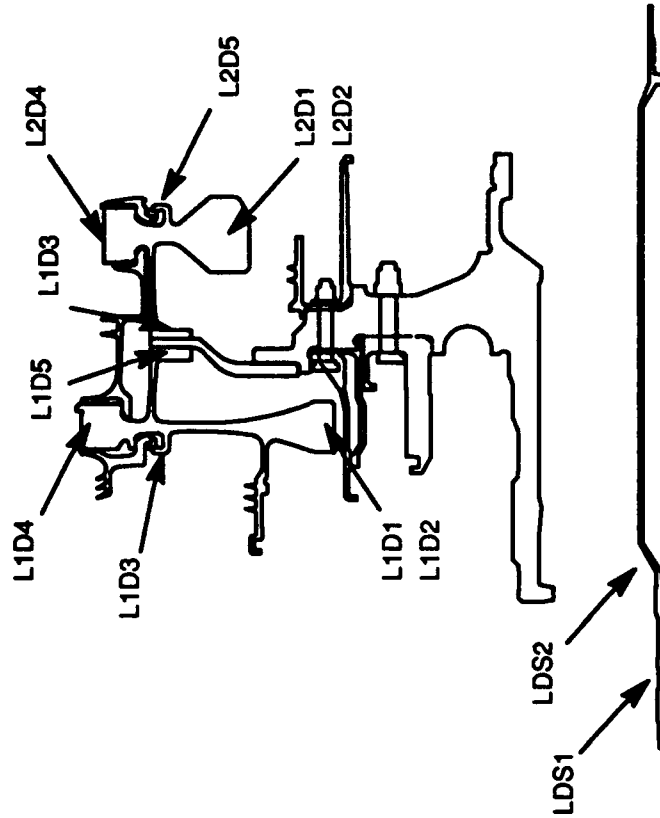
Selected locations characterize HP Turbine.

GE Aircraft Engines

LP Turbine Selected Locations

<u>Label</u>	<u>Location</u>	<u>Assessment</u>
Stage 1 Disk		
L1D1, 2	Disk Bore	.
L1D3	Disk Forward Fillet	.
L1D4	Disk Post	.
L1D5	Disk Bolthole	.
Stage 2 Disk		
L1D1, 2	Disk Bore	.
L1D3	Disk Bolthole	.
L1D4	Disk Post	.
L1D5	Disk Aft Fillet	.
Stage 2 Blade		
L1B1	Blade Dovetail	.
L1B2	Blade Airfoil Root	.
Driveshaft		
LDS1	Shaft Spline	.
LDS2	Shaft Venthole	.

Complete



Selected locations characterize LP Turbine.

Assessment Summary

GE Aircraft Engines

Summary

- USAF ERR2 assessment has been completed for F412 fan and compressor rotors. Work is continuing on the blades, turbines and static structures. Selected components throughout the F412 engine characterize the entire engine.
- The potential USAF usage is more severe than the USN mission both in terms cyclic content and turbine temperatures.
- Sophisticated inspection techniques like Eddy current may be required.

Words to be used with presentation:

Title: Preliminary Damage Tolerance Evaluation of Selected F412-GE-400 Engine Components
R. E. Kehl

Title Pg: (Title page and marketing photograph of F412 engine side by side) GE Aircraft Engines is performing a structural integrity assessment of selected components of the F412 engine currently being designed and qualified for the Navy A12 application, as part of an Air Force Early Risk Reduction (ERR) study; a study to evaluate the proposed Air Force ATA application. This presentation is a short synopsis of the objectives of the study, some preliminary engine turbomachinery fracture mechanics results and conclusions.

Chart 2: (Title page and chart 2 side by side) Here's an outline of the topics that I'll be discussing. I'll start with some background on the F412 engine in the Navy A12 application and move on to the Air Force Early Risk Reduction effort. The ERR study starts with a comparison of the engine usage in the Navy application versus that of the proposed Air Force ATA application. I'll present the engine turbomachinery components chosen for the study and some preliminary damage tolerance assessment results for the fan and compressor rotors. Finally, I'll summarize our status and draw some conclusions based on the preliminary results.

Chart 3: (Chart 3 and chart 4 side by side) Let's start with a discussion of the F412 engine, its Navy application, and its potential Air Force application.

Chart 4: GE Aircraft Engines is designing, developing and qualifying the F412 engine for the Navy A12 application.

The F412 engine is a fixed nozzle medium bypass turbofan engine derived from the F404 engine used by the Navy in the F/A-18 aircraft, and from the F110 engine used by the Navy in the F14 and by the Air Force in F15 and F16 aircraft.

The airframe companies, McDonnell Douglas Aircraft and General Dynamics-Fort Worth, provided GE with a detailed Navy mission definition.

The F412 engine is designed to meet Navy durability criteria. There is no Navy requirement to establish maintenance intervals based on fracture mechanics life criteria. With the F412 engine, GE is meeting the Navy's needs and design requirements.

Chart 5: (Replace chart 4) The objective of the "Early Risk Reduction" contract is to provide the Air Force with a preliminary look at the kinds of changes the airframe and engines may need to meet Air Force usage and integrity requirements.

As with the Navy mission, the airframe companies provided GE with a detailed mission definition of the proposed Air Force usage to evaluate engine components.

The ERR damage tolerance assessment evaluates selected components throughout the engine, characterizing the integrity of the engine as a whole.

The F412 engine is assessed relative to potential USAF goals. There are no defined USAF ATA requirements. Preliminary goals are ambitious: 10000 MH durability, and 5000 MH for inspection or maintenance intervals. Through the ERR study GE is responding to Air Force needs.

Chart 6: (Replace chart 5) These are the F412 engine components that are being evaluated by the

ERR assessment. The F412 engine consists of a three stage fan driven by a two stage low pressure turbine and a seven stage compressor driven by a single stage high pressure turbine. Note the turbomachinery components being evaluated: the fan stage 1 rotor, blade and air seal, the fan aft shaft, three stages to characterize the compressor, stages 1, 3, and 7, turbine turbomachinery, the high-pressure turbine rotor and blade, both low pressure turbine rotors, and the low pressure turbine stage 2 blade. Some static structural components including the midframe, and a pressure case, the combustor casing are also included. This variety of components is distributed to provide a picture of the F412 engine as a whole.

Chart 7: (Chart 7 and chart 8 side by side) My next topic is a comparison of the Navy usage with the proposed Air Force usage. Differences in the missions include the weight of the aircraft, the mix of the types of missions flown, and the expected life capability.

Chart 9: (Replace chart 8) The different usage together with the increased weight of the ATA version of the aircraft results in higher engine turbine temperatures. Turbine temperature can be taken as representative of the severity of engine cycle conditions. The proposed Air Force application spends more time at higher temperatures. The proposed Air Force ATA application is more severe than the Navy A12 application in terms of both cycles and turbine temperature.

Chart 10: (Chart 10 and chart 11 side by side) My next topic is a review of the F412 turbomachinery components being evaluated in the Early Risk Reduction effort, our current status and some preliminary results.

Chart 11: This is the axisymmetric finite-element model of the fan rotor, and the three-dimensional finite-element model of the stage 1 fan blade. In the fan, we are evaluating the stage 1 rotor, blade and air seal plate, and the fan aft shaft. The stage 3 disk dovetail is also included. We've finished our assessment of most fan rotor locations. Work is continuing on one shaft location and the stage 1 blade. The choice of components characterizes the fan as a whole.

Chart 12: (Replace chart 11) These are the results of a fracture mechanics assessment of two locations on the fan stage 1 rotor. The first assessment assumes a corner crack in the rotor bore, the second, a surface crack at the cone-web junction. Typical florescent-penetrant-inspection capability (FPI) is finding a 35 by 70 mil surface crack, indicated by the shaded region to the right of the graph. Typical Eddy current inspection capability is somewhat smaller than a 10 by 20 mil surface crack, or a 10 by 10 mil corner crack, indicated by the shaded region to the left of the graph. Using more sophisticated techniques such as Eddy Current, the fracture mechanics life increases significantly.

Chart 13: (Replace chart 12) These are the results of a fracture mechanics assessment of two locations on the fan stage 1 air seal. The air seal is a thin plate structure bolted to the rear of the stage 1 disk. Corner cracks in the bolthole and in the scallop between boltholes are evaluated. Again we can see that the fracture mechanics life is increased significantly when Eddy Current inspection is used.

Chart 14: (Replace chart 13) This is the axisymmetric finite-element model of the compressor rotor, and the three-dimensional finite-element models of the stage 1, 3, and 7 compressor blades. In the compressor, we're evaluating stage 1, 3, and 7 rotors, blades, and the compressor forward shaft.

We've finished our assessment of the compressor rotor locations. Work is continuing on the blades. The choice of components is made to characterize the compressor as a whole.

Chart 15: (Replace chart 14) These are the results of a fracture mechanics assessment of three locations on the compressor stage 1 disk. Corner cracks in the disk bore and bolthole, and a surface crack in the forward rabbit fillet are evaluated. Using more sophisticated inspection techniques, that fracture mechanics life increases significantly.

Chart 16: (Replace chart 15) These are the results of a fracture mechanics assessment of two locations on the compressor stage 4 to stage 7 spool. We're looking primarily toward the aft end of the spool, the stage 7. A surface crack in the stage 7 disk bore, and a corner crack in the stage 7 bolthole are evaluated. The fracture mechanics capability can be increased if more sophisticated inspection techniques are used.

Chart 17: (Replace chart 16) This is the axisymmetric finite-element model of the high pressure turbine rotor. In the high pressure turbine, we're evaluating the rotor and the serpentine cooled blade. We've finished stress analysis of the rotor and are currently evaluating the durability life capability. The choice of components is made to characterize the high pressure turbine as a whole.

Chart 18: (Replace chart 17) This is the axisymmetric finite-element model of the low pressure turbine rotor. In the low pressure turbine, we're evaluating both stage 1 and stage 2 rotors, the uncooled shrouded stage 2 blade, and the fan driveshaft. As with the high pressure turbine, we've finished stress analysis of the rotor and are currently evaluating the durability life capability. The choice of components is made to characterize the low pressure turbine as a whole.

The ERR assessment also includes other components; specifically, the midframe, characterizing a structural static component, and the combustor case, characterizing a pressure case.

Chart 19: (Chart 19 and chart 20 side by side) Finally, I'll try to summarize the objectives of this assessment of the F412 engine, our current status and the preliminary results to date.

Chart 20: The damage tolerance assessment has been completed on the F412 fan and compressor rotors. Work continues on blades, turbines and static structures. These components are selected to characterize the life capability of the F412 engine as a whole.

The proposed Air Force ATA usage differs from the baseline Navy A12 design usage. The proposed Air Force usage is more severe than the Navy both in terms of cyclic damage, and in terms of turbine temperatures.

Preliminary results of fan and compressor rotor components indicate that some locations may require more sophisticated inspection techniques, such as Eddy current inspections used for some F110 components, to achieve potential Air Force maintenance goals.

In the Early Risk Reduction evaluation, GE has taken the opportunity to respond to Air Force needs.

Thankyou

SPATE
(Stress Pattern Analysis by Thermal Emission)
AND
GAS TURBINE ENGINE STRUCTURAL INTEGRITY

D.H. Nethaway
T.E. Purcell
Pratt & Whitney
W. Palm Beach, Florida



1990 USAF Engine Structural Integrity Program Conference
December 11-13, 1990

SPATE AND ENGINE STRUCTURAL INTEGRITY

Outline

- Background
- Component Applications
- Dynamic Environment NDE
- Summary

BACKGROUND

TSA (Thermographic Stress Analysis)

- Non-Contacting
- Full Field
- Analysis of Structures Under Cyclic Loading
- Broad Frequency Range (2 Hz to > 30 KHz)
- High Spatial Resolution (20 Mil Dia.)

BACKGROUND

Thermoelastic Relationship for Isotropic Materials at Adiabatic Conditions

$$\Delta T = - \frac{\alpha T}{\rho C_{\sigma}} \Delta \sigma$$

Where:

α

Coefficient of Expansion

ρ

Density

T

Mean Temperature

C_{σ}

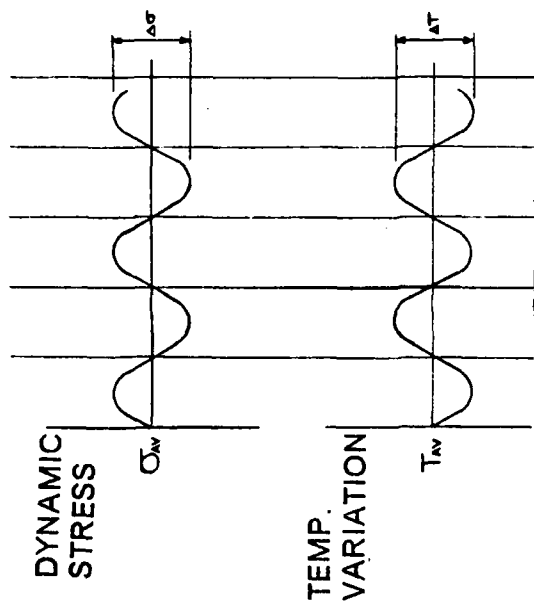
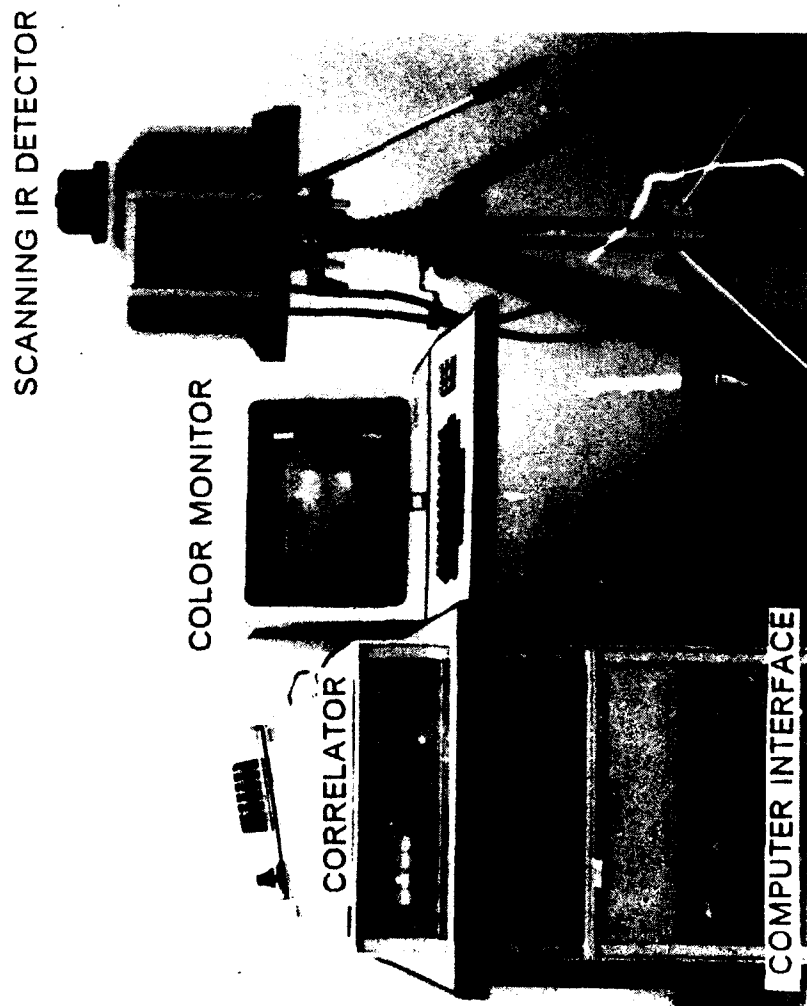
Specific Heat

$\Delta \sigma$

Peak to Peak Amplitude of the
Periodic Change in the Sum of
the Principal Stresses

BACKGROUND

SPATE 9000 System



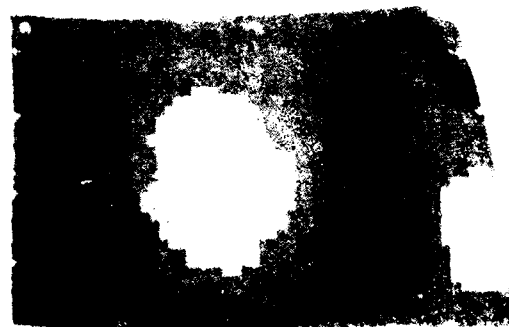
System detects instantaneous infra-red flux emitted from each point as a result of minute temp. fluctuations of a structure subjected to dynamic stress changes.

BACKGROUND

Typical Thermoelastic Stress Patterns



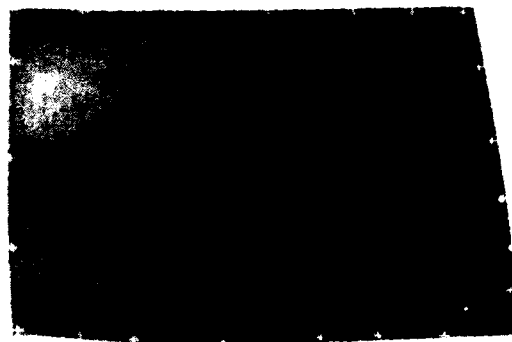
FIRST BENDING



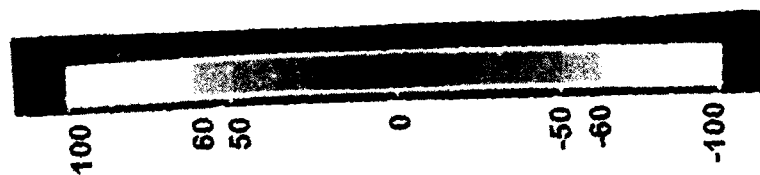
SECOND BENDING



FIRST TORSION



SECOND CHORDWISE BENDING



PERCENT OF
MAXIMUM
DYNAMIC
STRESS (%)

APPLICATIONS

Cold Section / Hot Section Components

- Compressor Vane
 - Analytical Analysis Verification
- Compressor Blade
 - Instrumentation Optimization
- Turbine Blade
 - Component Modification

APPLICATIONS - COMPRESSOR VANE

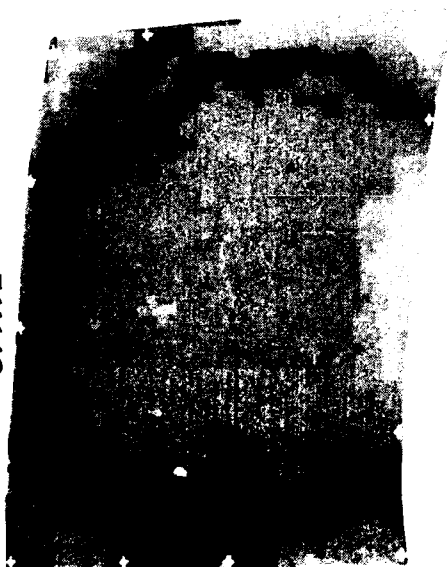
Verification of Analytical Structural Analysis

- Vibratory Stress Distributions
- Critical Stress Locations - Goodman Limits
- Define FOD Boundaries

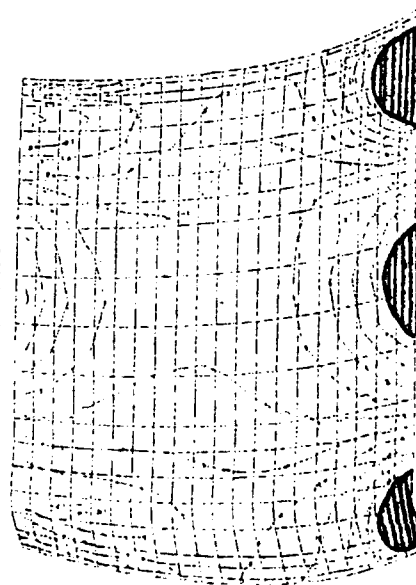
APPLICATIONS - COMPRESSOR VANE

SPATE Patterns Confirm NASTRAN Analytical Calculations

SPATE

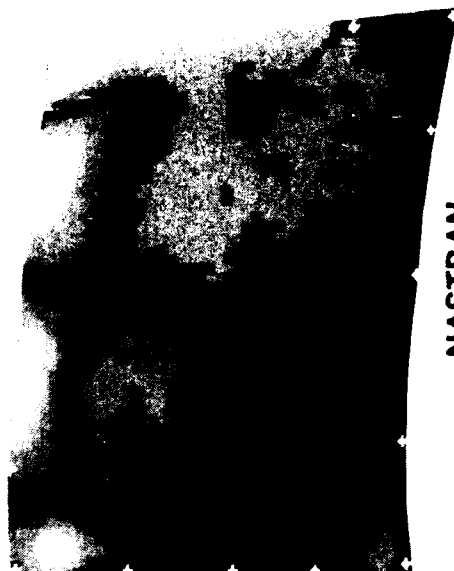


NASTRAN

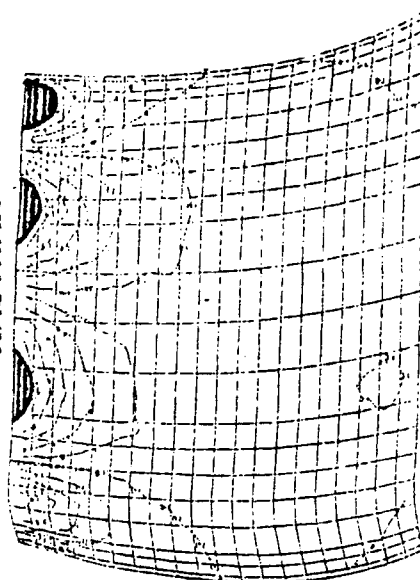


FIRST BENDING
(4400 HZ)

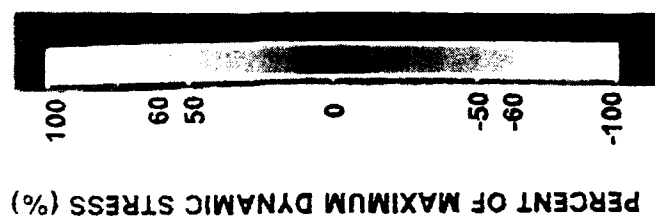
SPATE



NASTRAN



SECOND BENDING
(7100 HZ)

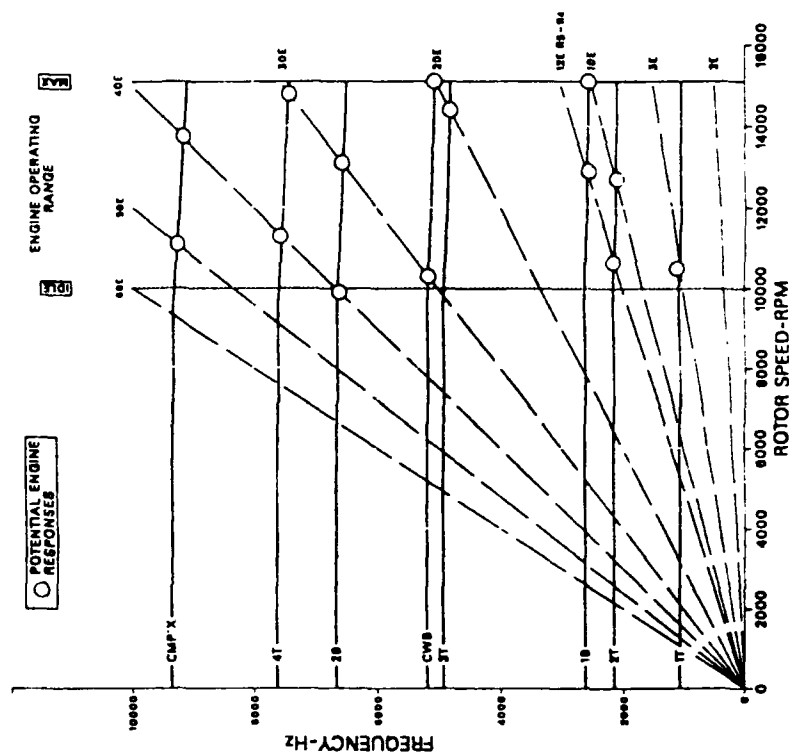


APPLICATIONS - COMPRESSOR BLADE

Engine Test Strain Gage Optimization

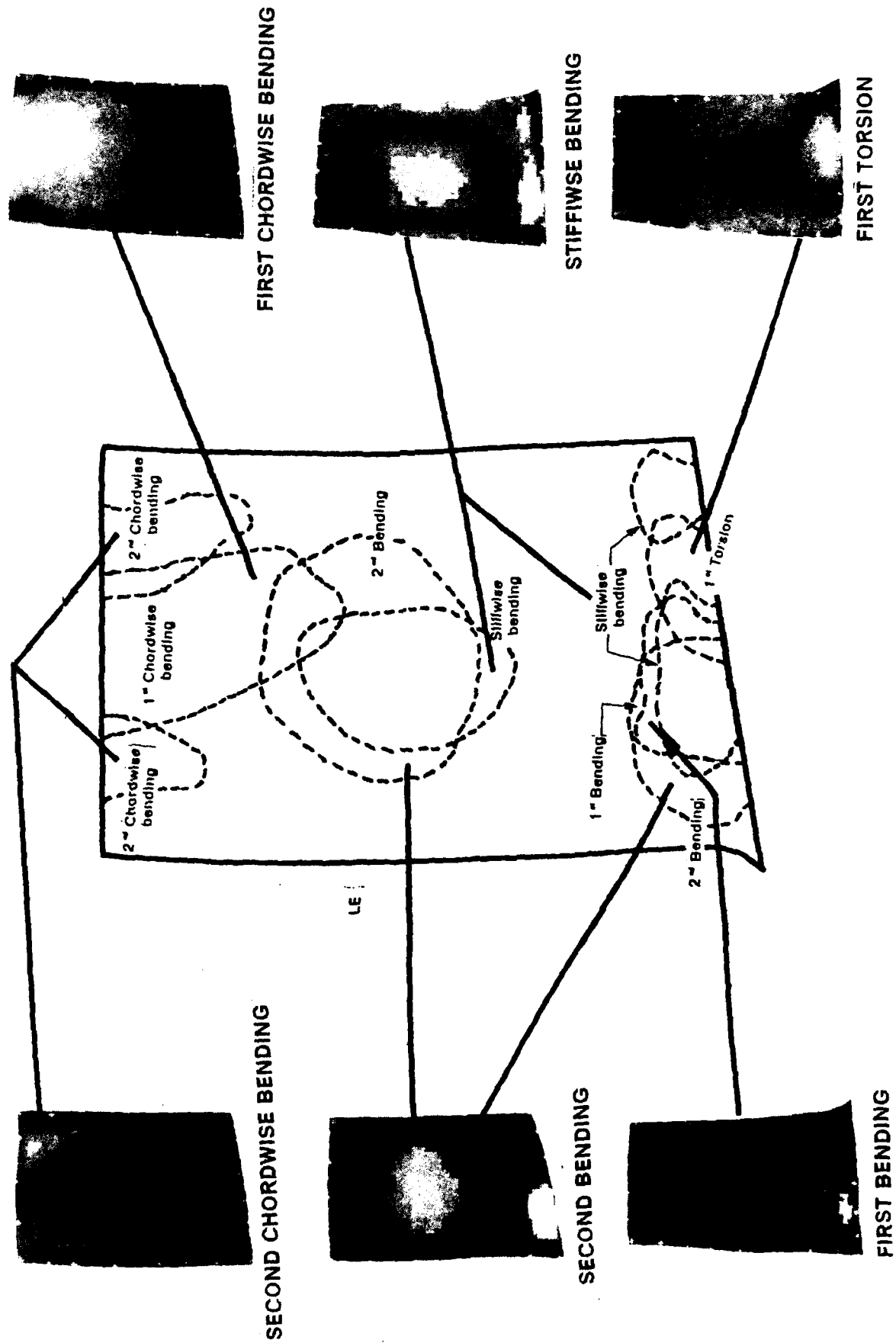
- Reduce Cost of Engine Test
- Maximize Vibratory Response Coverage

COMPONENT CAMPBELL DIAGRAM



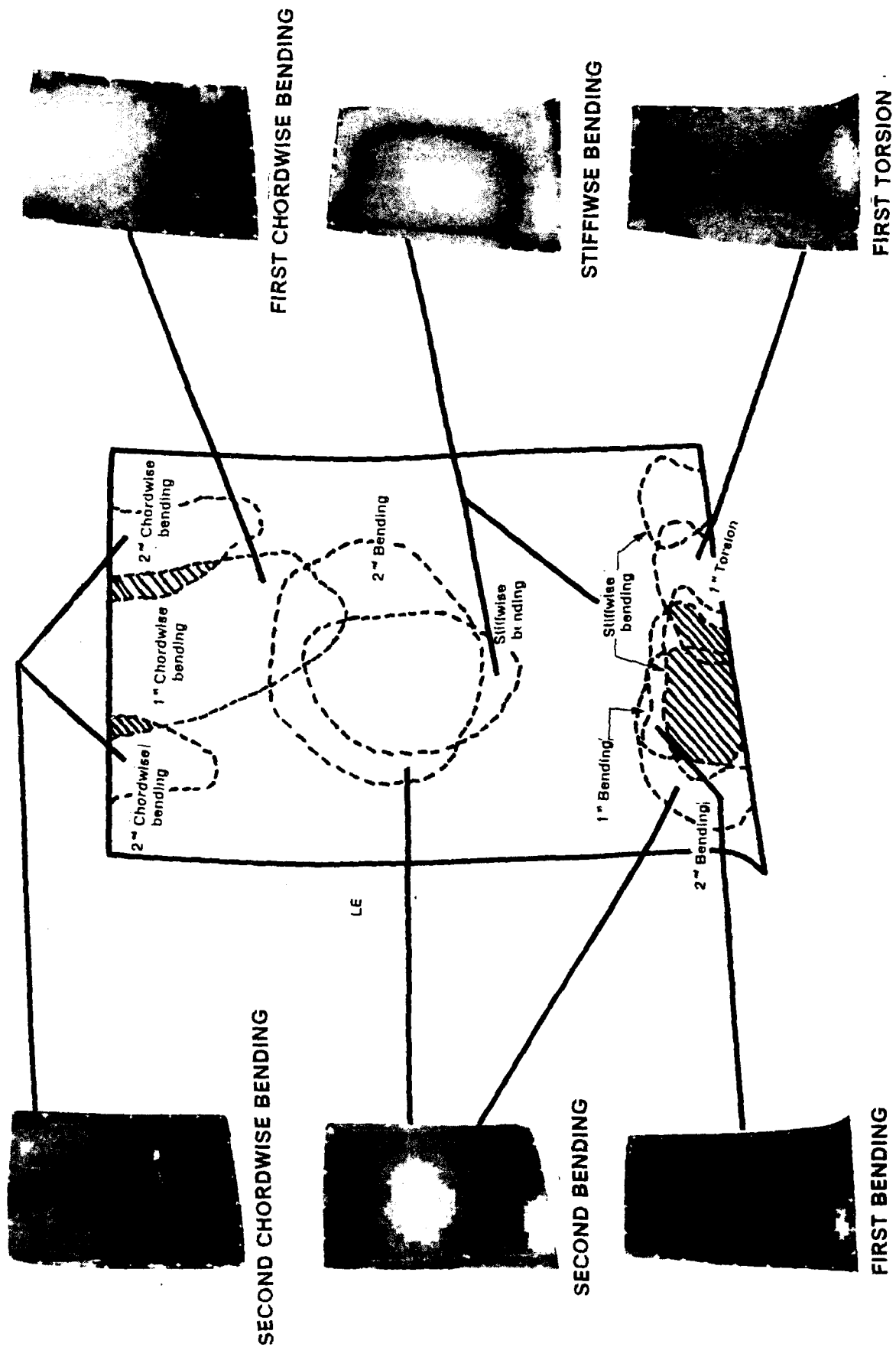
INSTRUMENTATION OPTIMIZATION - COMPRESSOR BLADE

Multiple Modes Monitored With Reduced Strain Gage Coverage



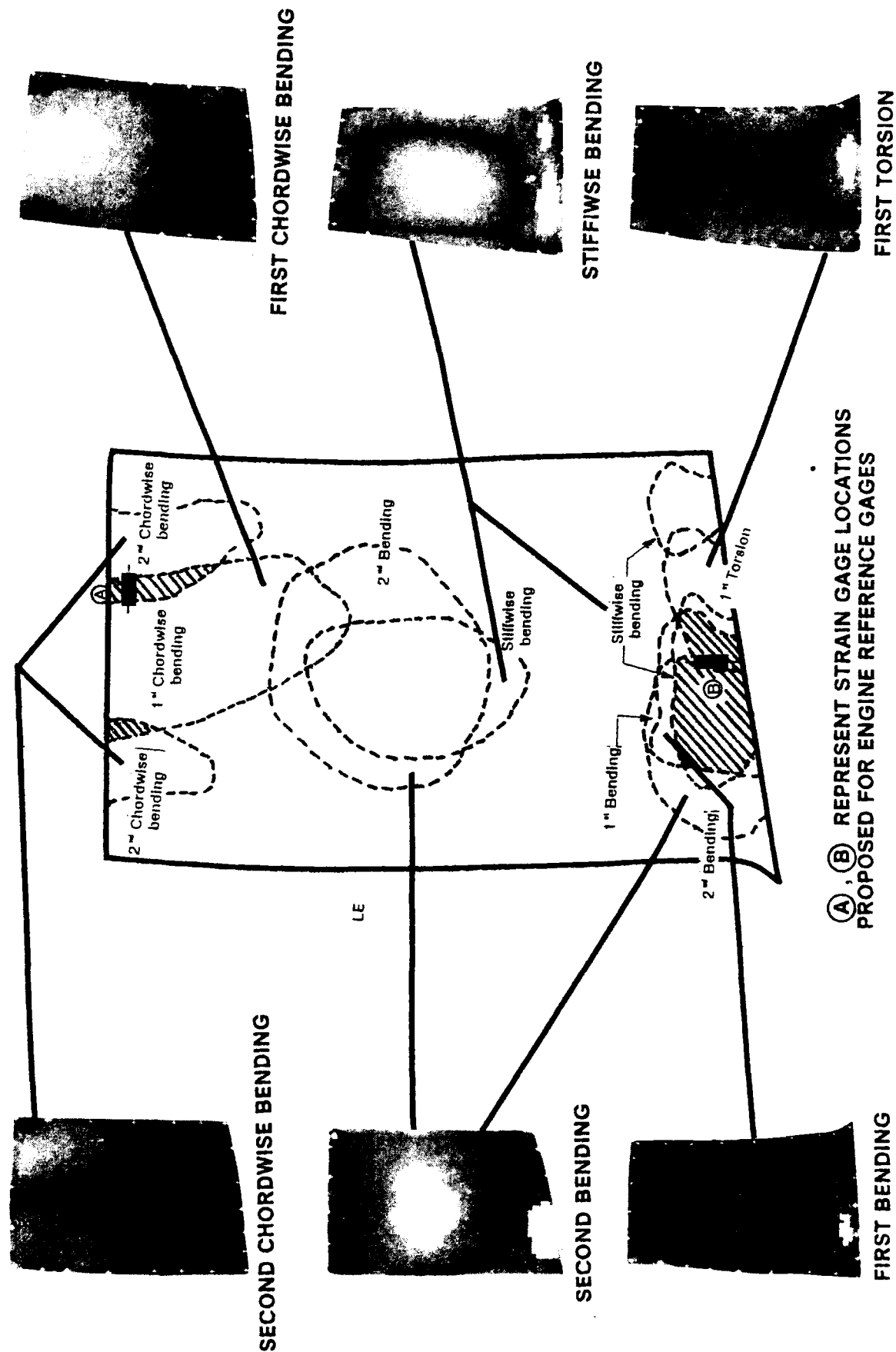
INSTRUMENTATION OPTIMIZATION - COMPRESSOR BLADE

Multiple Modes Monitored With Reduced Strain Gage Coverage



INSTRUMENTATION OPTIMIZATION - COMPRESSOR BLADE

Multiple Modes Monitored With Reduced Strain Gage Coverage



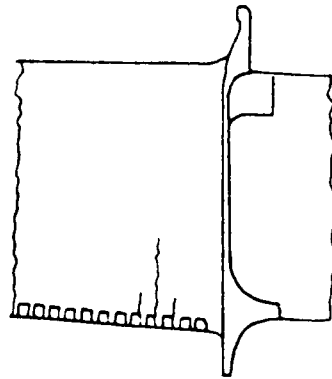
APPLICATIONS - TURBINE BLADE

Structural Assessment of Blade Modifications

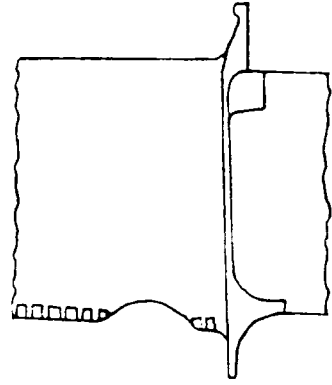
- Quick Assessment - Non Intrusive
- Non-Destructive
- Good Correlation with Component Endurance Capability

APPLICATIONS - TURBINE BLADE

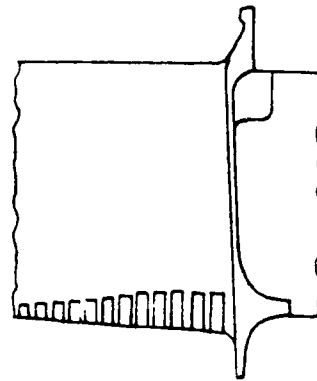
Cooling Slot Modifications



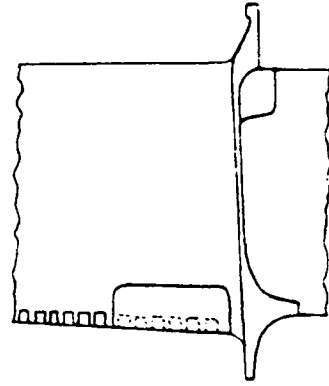
Engine Distress
Baseline



Modified
Cutback TE



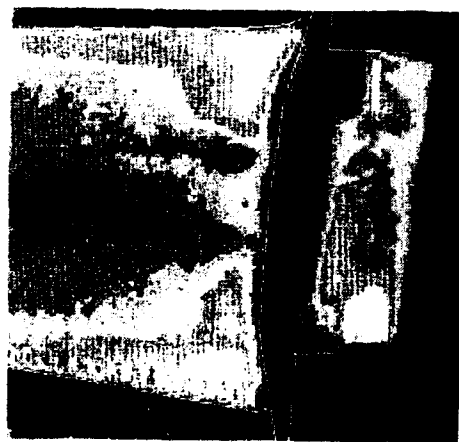
Modified
Elongated Cooling Slots



Modified
*Pressure Side TE Pocket
Cutback*

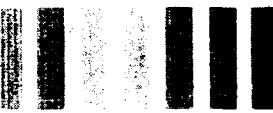
APPLICATIONS - TURBINE BLADE

Structural Assessment Using Component Dynamic Environment



Baseline

First Bending Mode



% σ_{\max}

Cutback TE



Elongated TE Slots



*Pressure Side TE Pocket
Cutback*

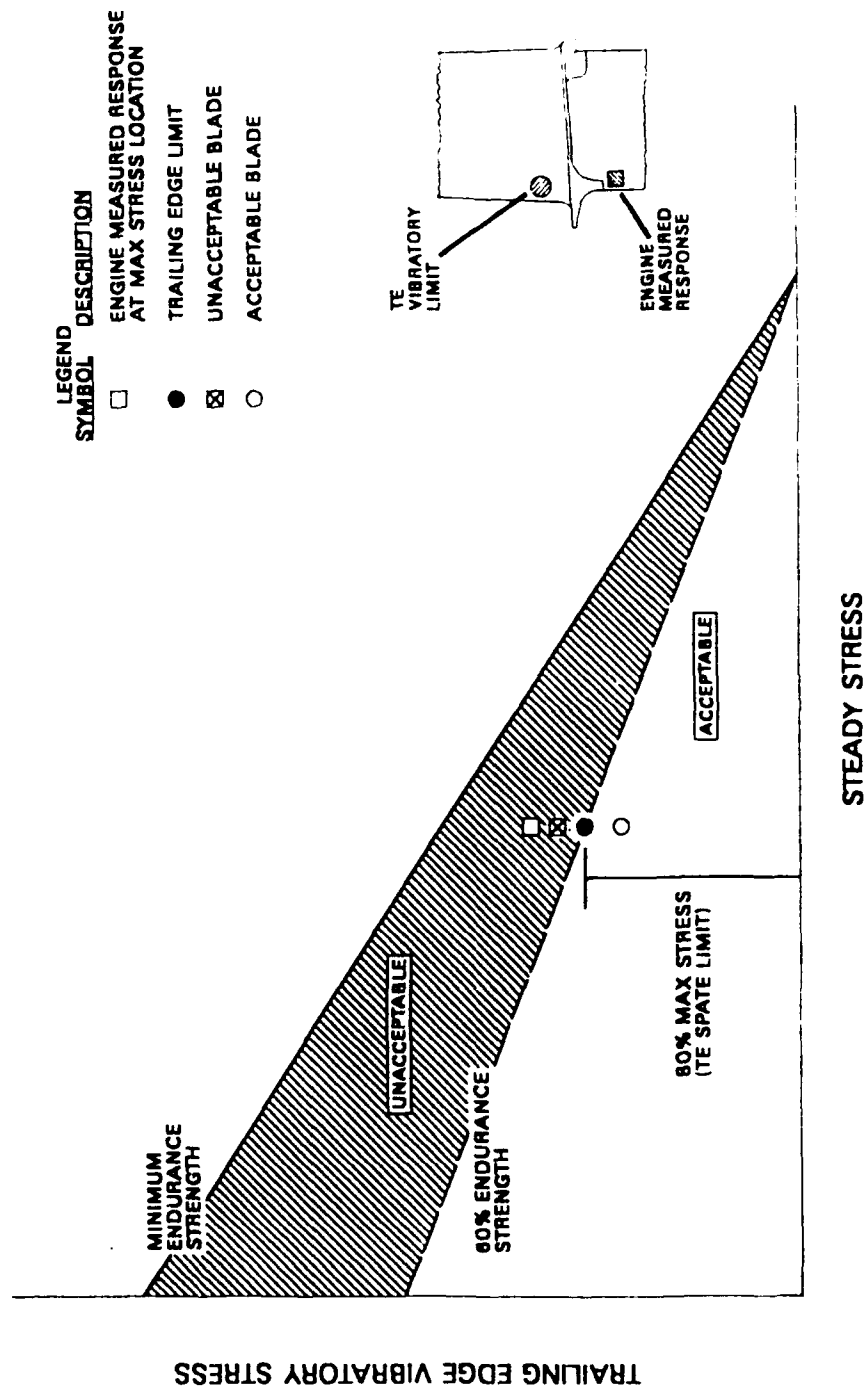
DYNAMIC ENVIRONMENT NDE

- Inspect Components Using Realistic Dynamic Load Conditions
- Not Subject to Operator Interpretation (I.E. Not a Visual Inspection)
- Individual Inspection Results Normalized to Common Reference Point

DYNAMIC ENVIRONMENT NDE

Screening Of Turbine Blades Using Engine Dynamic Load Conditions

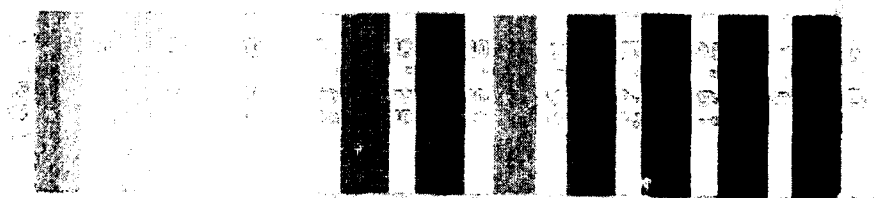
MODIFIED TURBINE BLADE AIRFOIL GOODMAN DIAGRAM (TRAILING EDGE)



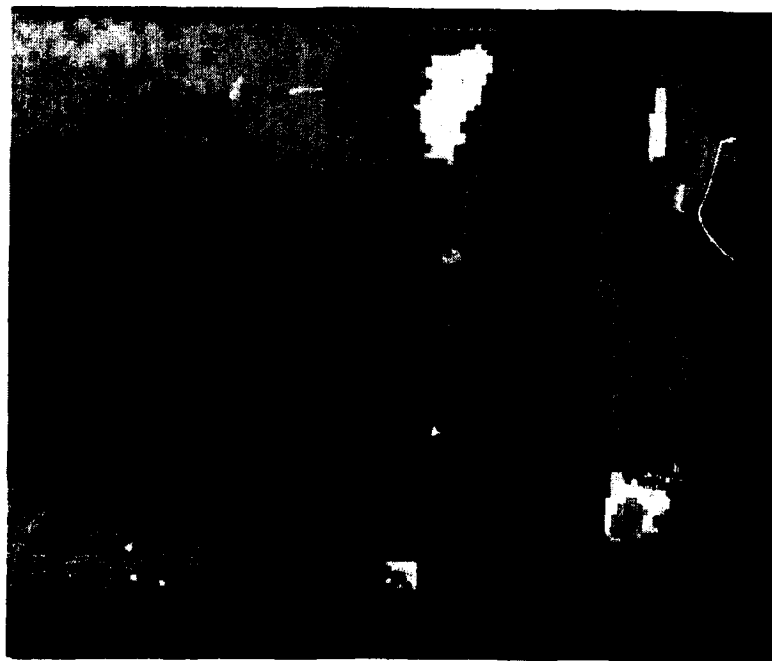
DYNAMIC ENVIRONMENT NDE

Screening Of Turbine Blades With Reworked Cooling Slots

1st Bending Mode



% σ_{\max}



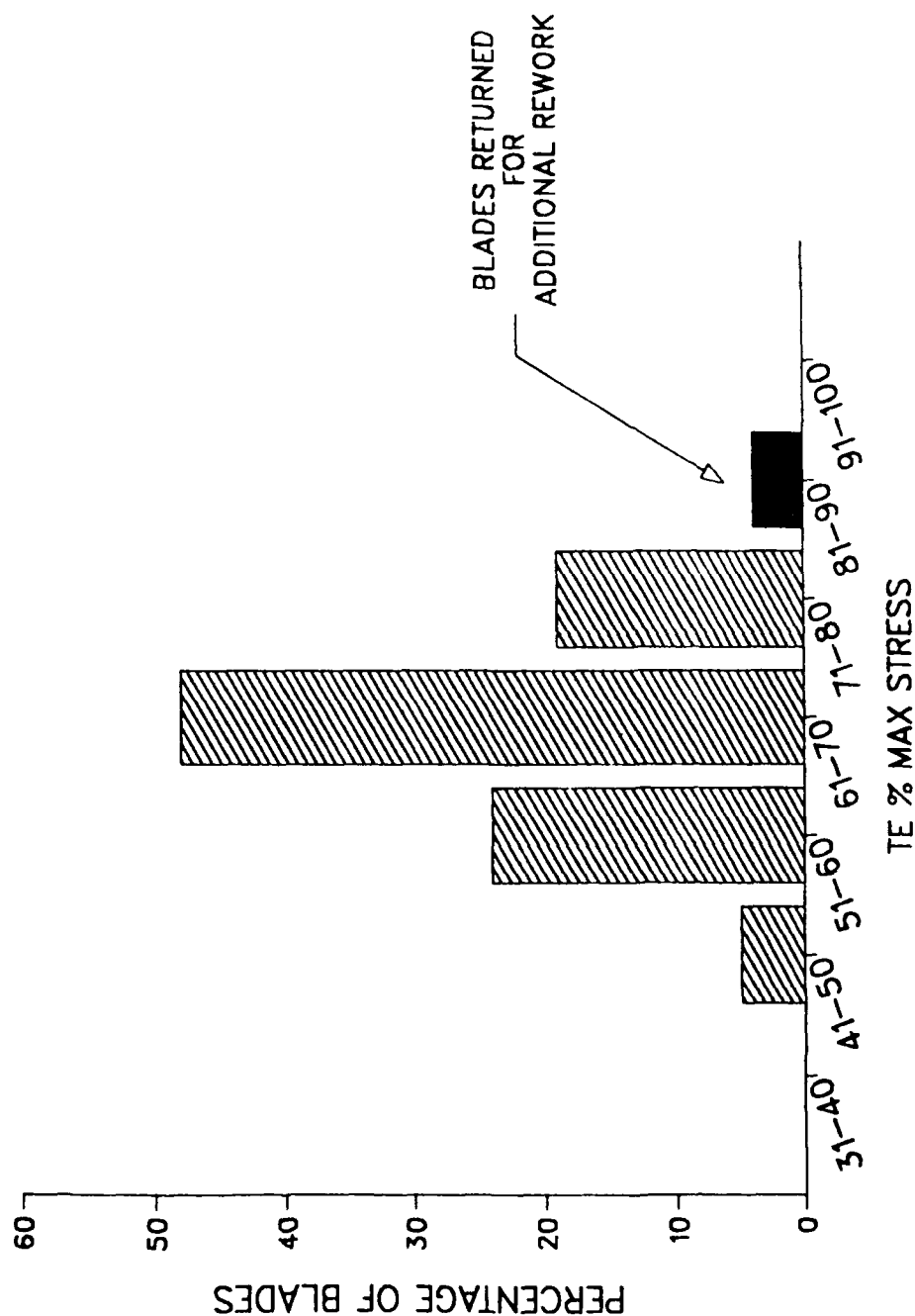
Acceptable
($TE < 80\% \sigma_{\max}$)



Unacceptable
($TE > 80\% \sigma_{\max}$)

DYNAMIC ENVIRONMENT NDE

*SPATE Screens Blades With Unacceptable Trailing Edge Stress Levels
For Additional Rework*



SUMMARY

- Non-Contacting - No Effect on Dynamic Response
- Applicable to a Wide Variety of Components and Frequency Range
- Good Correlation With Conventional Experimental (Strain Gage) and Analytical Techniques
- Cost Effective Method to Conduct "Full-Field" Stress Analysis as Compared to Other Experimental Techniques
- Efficient Method for Optimizing Engine Test Strain Gage Instrumentation
- NDE Technique for Structural Assessment of Engine Components Using Realistic Dynamic Environments

USAF Structural Integrity Program Conference

San Antonio, Texas

11-13 December 1990

IMPACT OF AIR FORCE DAMAGE TOLERANCE REQUIREMENTS ON THE WEIGHT OF AN ADVANCED TECHNOLOGY ENGINE NOZZLE

798

James A. Long, Jr
Senior Project Engineer

Norman A. Ducharme, Jr
Project Engineer

Robert E. Delaneuville
Project Engineer



AVP381401 900811

Abstract

A detailed analysis was conducted to assess the potential impact of the Air Force's damage tolerance requirements on the weight of a two-dimensional/convergent-divergent nozzle for an advanced technology military turbofan engine. Initial assessments, using fracture mechanics techniques which are traditionally applied to typical engine structures, indicated that a considerable increase in the weight of the nozzle system would be required to meet Air Force inspection interval requirements of 2000 engine flight hours (EFH) with a crack propagation margin (safety factor) of 2.0. This conclusion conflicted with the requirement for light weight and was considered pessimistic since the nozzle design incorporated many geometric features which tend to retard crack growth but are not given credit in traditional analysis of engine structures.

A rigorous analysis was conducted to define a more realistic nozzle weight impact. Selected components were initially optimized to achieve strength, vibration, and durability requirements. Fracture mechanics was employed to assess crack growth life at key locations on the structure. The analysis utilized a modified Willenborg model in conjunction with mission loading spectra to account for crack retardation due to overload effects. Life from an initial flaw size was calculated as a function of thickness, until the thickness required to control crack growth throughout the operational service life was defined. By comparing the thickness required to achieve full life damage tolerance to the initial thickness, the associated weight impact was identified. Where appropriate, load redistribution benefits were utilized to minimize weight. The study indicated that the weight increase was considerably lower than the weight increase predicted by the traditional analysis. Material specimen testing was accomplished to verify the results of the rigorous analysis.

NOZZLE DAMAGE TOLERANCE IMPACT

Preview

- Background
- Fracture mechanics study
 - Groundrules
 - Methodology
 - Results
- Weight impact projection
- Summary

Nozzle Configuration

Pratt & Whitney envisions that the next generation high performance military fighter engine will be a twin spool, counter-rotating, augmented turbofan. Its design will feature a low bypass ratio, moderate overall pressure ratio, and state-of-the-art rotor speeds and rotor inlet temperatures. The size, cycle, and configuration of the engine will be tailored to provide a balance between maximum augmented thrust at transonic flight conditions and nonaugmented thrust during supersonic cruise.

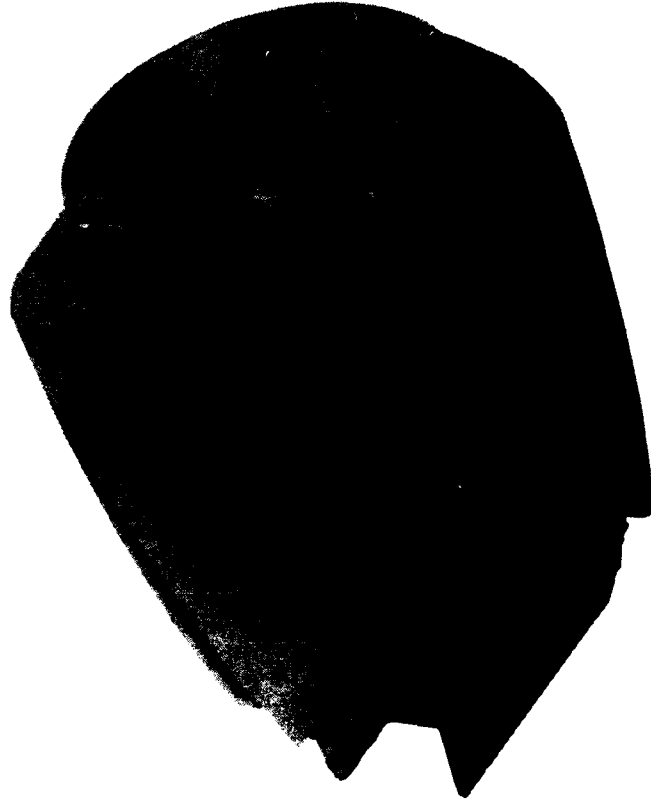
The engine will include an advanced technology rectangular (two-dimensional) nozzle which makes extensive use of burn-resistant titanium to minimize weight and maximize safety and durability. A reinforced sheet and stringer box structure will accommodate operating loads. Advanced cooling techniques will control temperatures. Independent actuation of convergent and divergent flaps will provide independent control of the throat and exit areas, as well as vectoring capability.

Thrust vectoring will improve aircraft short take-off and landing (STOL) characteristics and will permit unique flight maneuvering during air combat. The two-dimensional nozzle will also result in a reduced radar cross-section, enhancing the aircraft's survivability to the missile threat.

Such nozzles are operating today. Indeed, two-dimensional nozzles developed by Pratt & Whitney, including the STOL/Maneuver Technology Demonstrator (MTD) nozzle currently being tested on an F-15 aircraft, have demonstrated excellent performance and structural durability during over 2500 hours of intensive ground testing and 100 hours of flight tests.

ADVANCED TECHNOLOGY NOZZLE

Rectangular nozzle improves aircraft STOL and air combat maneuvering capabilities



- Two-dimensional
- Variable throat and exit areas
- Advanced titanium structure
- Vectoring capability
- Reduced radar cross-section

Nozzle Component Classification

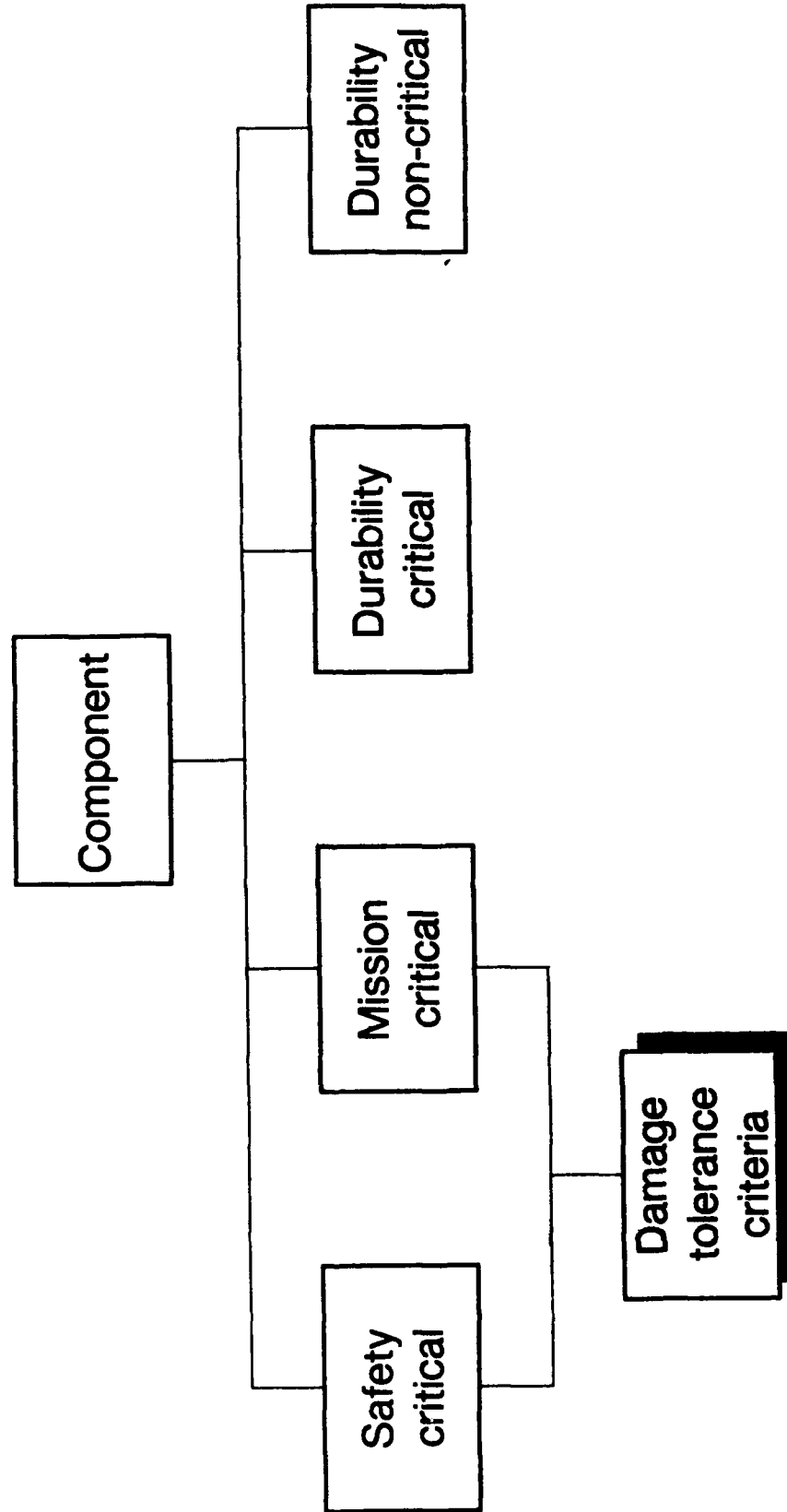
Components of an advanced two-dimensional nozzle were placed in one of four primary categories according to their structural/functional criticality. The categories are:

- *Safety critical* — Failure results in probable loss of aircraft or hazard to personnel
- *Mission critical* — Failure significantly degrades mission capability such as non-recoverable in-flight shutdown
 - Indirect safety impact
 - Handling qualities inadequate to complete mission flight phase
- *Durability critical* — Failure generates a significant economic impact but does not impair flight safety or mission capability
- *Durability non-critical* — Failure causes a minor economic impact and may initiate unscheduled maintenance

Current design philosophy requires safety or mission critical components to be damage tolerant, i.e., provide continued functional operation in the presence of flaws, cracks, or other damage introduced during manufacturing or incurred during operation.

NOZZLE COMPONENT CLASSIFICATION

Safety/mission critical parts require damage tolerance



Damage Tolerance Design Process

A systematic evaluation process was used to assess the damage tolerance capability of safety and mission critical nozzle components. A failure modes effects and critically analysis (FMECA) provided identification of operating hazards and potentially damaging modes. If the damage mechanism was controllable by classical fracture mechanics criteria, a fracture screening analysis was completed to assess the potential for crack growth during the design service life.

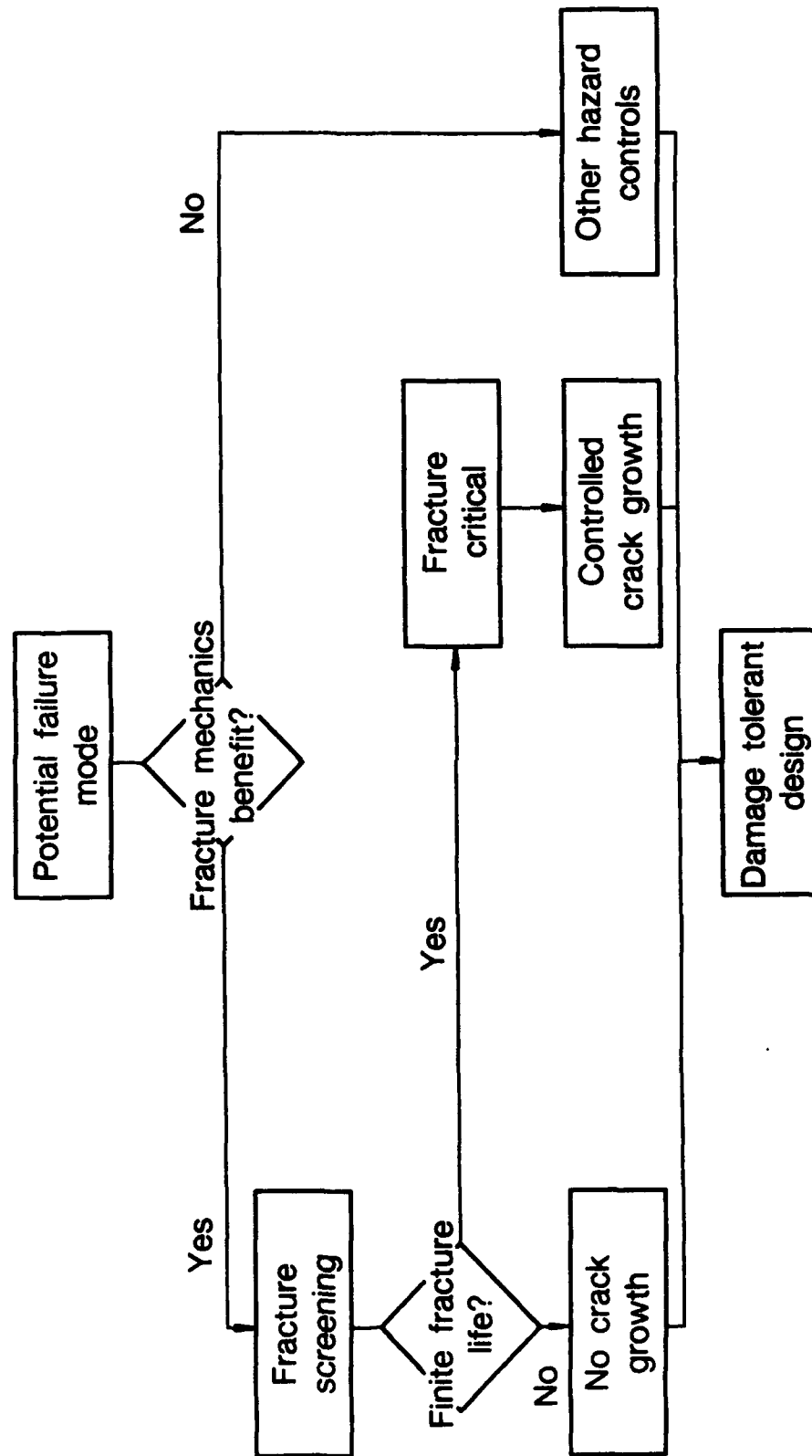
Nozzle components were considered to be damage tolerant if the screening analysis confirmed that operating stresses were low enough so that the largest flaw size, which will pass the non-destructive inspection recommended for the component, will not propagate.

If crack growth within the design service life was predicted, the component was classified as fracture critical and control of crack growth was required to achieve damage tolerance. For fracture critical components, a fracture mechanics analysis must confirm that typical initial flaw sizes will not reach critical dimensions and cause part rupture during a specified maintenance free operating period.

If fracture mechanics design principles did not influence the damage mechanism, other hazard controls such as frequency margin and thermal cooling were applied to nozzle components. Often these special controls were sufficient to render the design damage tolerant.

DAMAGE TOLERANCE DESIGN PROCESS

Design actions are dictated by potential failure mode



AVP381405 900911

Critical Nozzle Components

The initial assessment of the structural/functional critically of the nozzle components concluded the following:

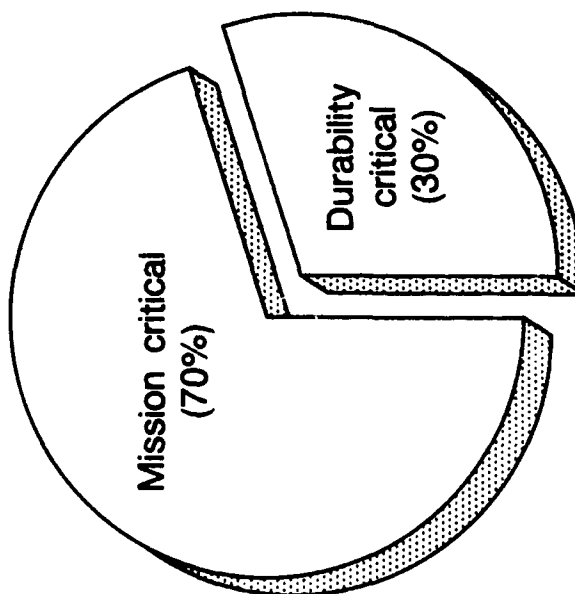
- No safety critical nozzle components were identified
- Most nozzle components are mission critical
- Many components require fracture screening to assess their damage tolerance capability
- The nozzle components which are subject to fracture screening account for 50% of the nozzle weight

The requirement for damage tolerance has a potentially significant impact on the weight of the nozzle.

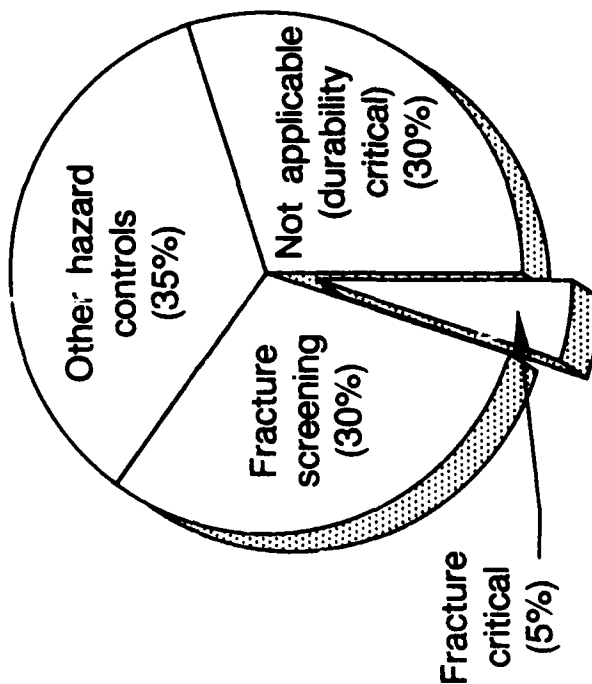
CRITICAL NOZZLE COMPONENTS

Many mission critical nozzle components require fracture screening analysis to assess their damage tolerance

Criticality classification



Damage tolerance action



- **Components subject to fracture screening account for 50% of the nozzle weight**

Initial Fracture Screening Evaluation

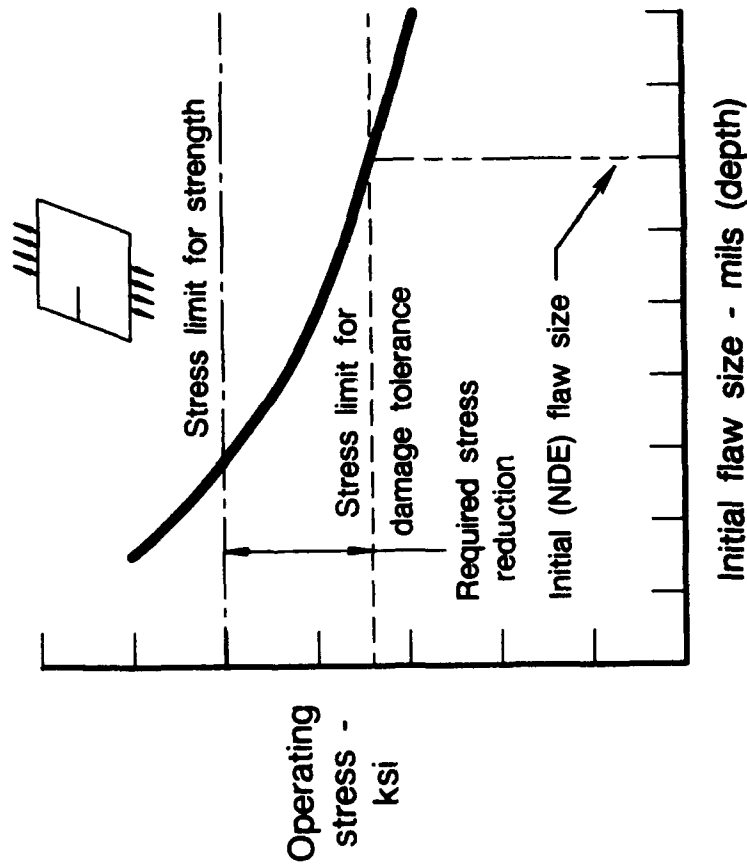
A fracture screening assessment was initially conducted using a conservative analysis which was based on simplified flat plate fracture models of thru-thickness cracks subject to a constant amplitude mission spectrum. Miner's rule, which treats each loading cycle independently, was used to accumulate the effects of damage. The potentially beneficial effects of load redistribution during crack growth were not credited. However, increases in the stress field as the crack progressed towards instability were accounted for in the stress intensity solution. The effects of cyclic damage occurring throughout the design service life were reduced to a single point equivalent mission related to the maximum operating stress.

Design curves were prepared which plotted stress as a function of flaw size for a constant fracture life of 4000 engine flight hours (EFH). This value is twice the Air Force's planned inspection interval of 2000 EFH, or approximately eight years of peacetime operational service. An initial flaw depth was used in conjunction with the design curve to define the stress limit for achieving full life damage tolerance. A 2:1 crack length to depth ratio was assumed. The initial flaw size was selected to be easily detectable to a 90 percent normal probability of detection reliability using conventional non-destructive inspection techniques such as fluorescent penetrant inspection (FPI).

Comparison of the resulting damage tolerance stress limit with the strength limit, which is a function of the material's yield strength, revealed that increased thickness was necessary to control crack growth during the design service life. Preliminary estimates indicated that the weight of the nozzle could be increased by as much as 107 lbs or approximately 3 percent of the total weight of a typical (3500 lb) military fighter engine.

INITIAL FRACTURE SCREENING EVALUATION

Stress reduction established by conservative design curves indicates a potentially significant increase in nozzle weight



- Flat plate fracture model
- Thru-crack subject to tensile load
- Constant amplitude spectrum
- Miner's rule damage accumulation
- No load redistribution effects
- Single point equivalent mission

Fracture Mechanics Study — Groundrules

Although a weight increase of only 3 percent of the total engine weight may, at first glance, seem minor, engine flight weight is diligently scrutinized and any potential increase is aggressively challenged. A rule of thumb within the aircraft industry is that the impact of damage tolerance is about 1 percent of the total airframe structural weight. Because of the similarity between the sheet and stringer construction of the rectangular nozzle and airframe structure, the initial analysis results were considered pessimistic.

A rigorous crack growth analysis of selected components representative of the nozzle structure, was initiated to provide a more accurate assessment of the weight increase required for a damage tolerant nozzle. The intent of the detailed analysis was to eliminate much of the conservatism inherent in the initial fracture screening evaluation. Groundrules for the study were established.

FRACTURE STUDY - GROUND RULES

A detailed crack growth analysis was initiated to better evaluate the potential increase in nozzle weight

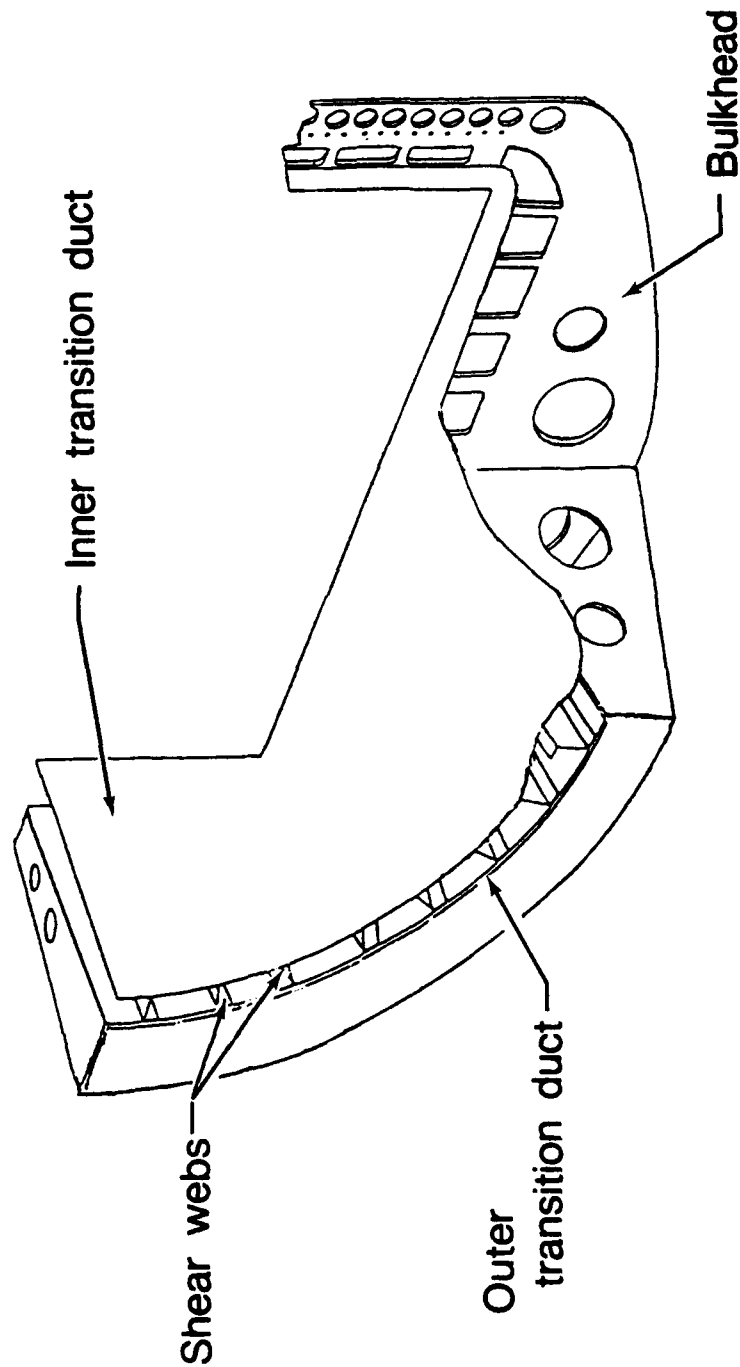
- Optimize baseline configuration to achieve USAF strength/vibration/durability requirements
- Use modified Willenborg crack retardation model
- Simulate load redistribution during crack growth
- Use burn resistant beta titanium in hot areas for improved safety margin
- Fracture life must exceed design service life
- Design flaw size: Easily detectable to a 90% normal probability of detection

Components Selected For Detailed Study

Components of the nozzle bulkhead and transition duct were selected for the detailed fracture life analysis and parametric study. The structural design of these components is typical of the sheet and stringer construction used in a rectangular nozzle.

COMPONENTS SELECTED FOR ANALYSIS

Detailed fracture analysis was performed on components representative of the nozzle structure



AVE381409 901611

Material Considerations

A very important consideration in the design of these nozzle components was the use of a highly alloyed, burn resistant beta titanium material developed by Pratt & Whitney.

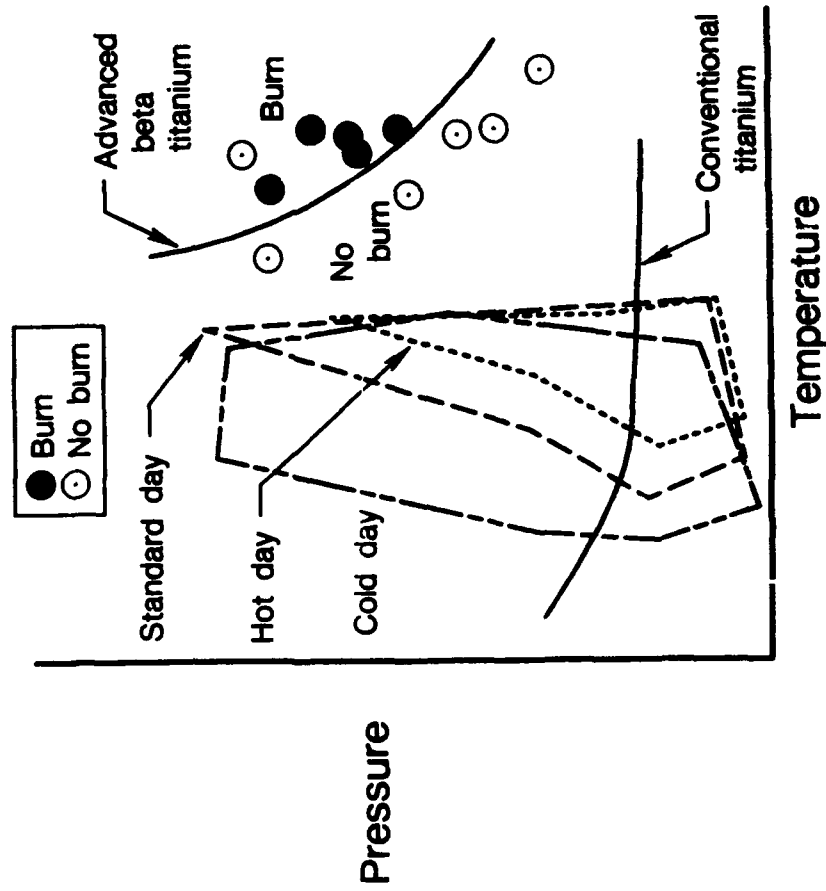
This advanced alloy was selected over conventional titanium alloys to provide an increased safety margin relative to the possibility of a titanium fire. Nozzle operating pressures and temperatures are such that self-sustained burning is possible over a significant portion of the flight envelope if conventional titaniums are used. Advanced Beta Titanium will not burn anywhere within the flight envelope.

Over 500 mechanical and physical property tests have been conducted on this alloy. Relative to conventional titaniums, such as Ti-6-4 and Ti-6-2-4-2, Advanced Beta Titanium provides significantly higher burn resistance, improved creep resistance, improved high temperature strength, and improved high cycle fatigue resistance. The material is also easier to weld.

Although at room temperature the crack growth rate of Advanced Beta Titanium is equivalent to that of conventional titanium, at elevated temperatures crack growth is slightly faster. This characteristic must be considered when components made from this material are designed for damage tolerance.

MATERIAL CONSIDERATIONS

Use of advanced beta titanium alloy required for superior burn resistance



Relative to conventional titanium advanced beta titanium exhibits:

- No self sustained burning within the flight envelope
- +100°F improved creep resistance
- +10% improved specific strength
- +40% improved tensile strength
- +50% improved HCF resistance
- Slightly faster crack growth rate

Effects of Mission Loading Spectra

Detailed stress analysis of the selected nozzle components reflected the effects of the mission loading spectra.

Stresses in the nozzle are produced by differential pressure loadings and by thermal gradients. To a great extent, the influence of thermal gradients can be controlled by the use of advanced cooling techniques and by design features which accommodate thermal growth. Pressure loading is a function of flight condition.

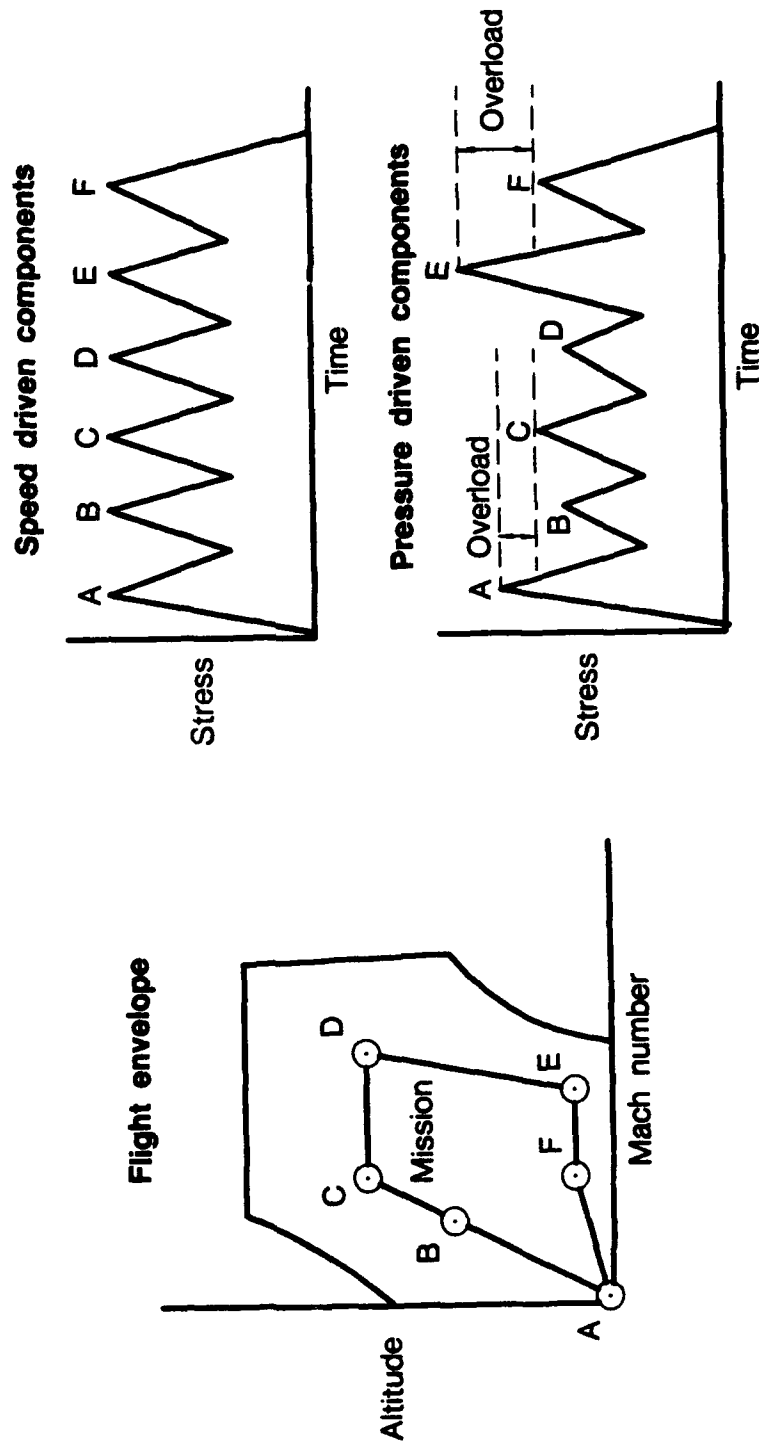
During a mission, as the aircraft operates at different altitudes and at different Mach numbers within the flight envelope, operating pressures in the nozzle vary considerably even though engine rotor speed excursions at these conditions may be nearly identical.

For a given rotor speed, rotating components, such as turbine disks, whose stresses are direct functions of the rotational speed, will experience nearly the same stress regardless of flight condition.

This is not the case for pressure driven components. For these components, an analysis of the stress time history resulting from the mission loading spectra reveals a direct correlation between operating stress level and the magnitude of the pressure load. At high pressure flight conditions, these components periodically experience overload cycles which exceed the stress levels experienced at other flight conditions. The overload cycle significantly influences the crack growth rate during subsequent subcycles.

EFFECTS OF MISSION LOADING SPECTRA

Mission spectrum analysis reflects the effects of overload cycles typically associated with pressure driven components



AVP381411 901611

Willenborg Crack Growth Model

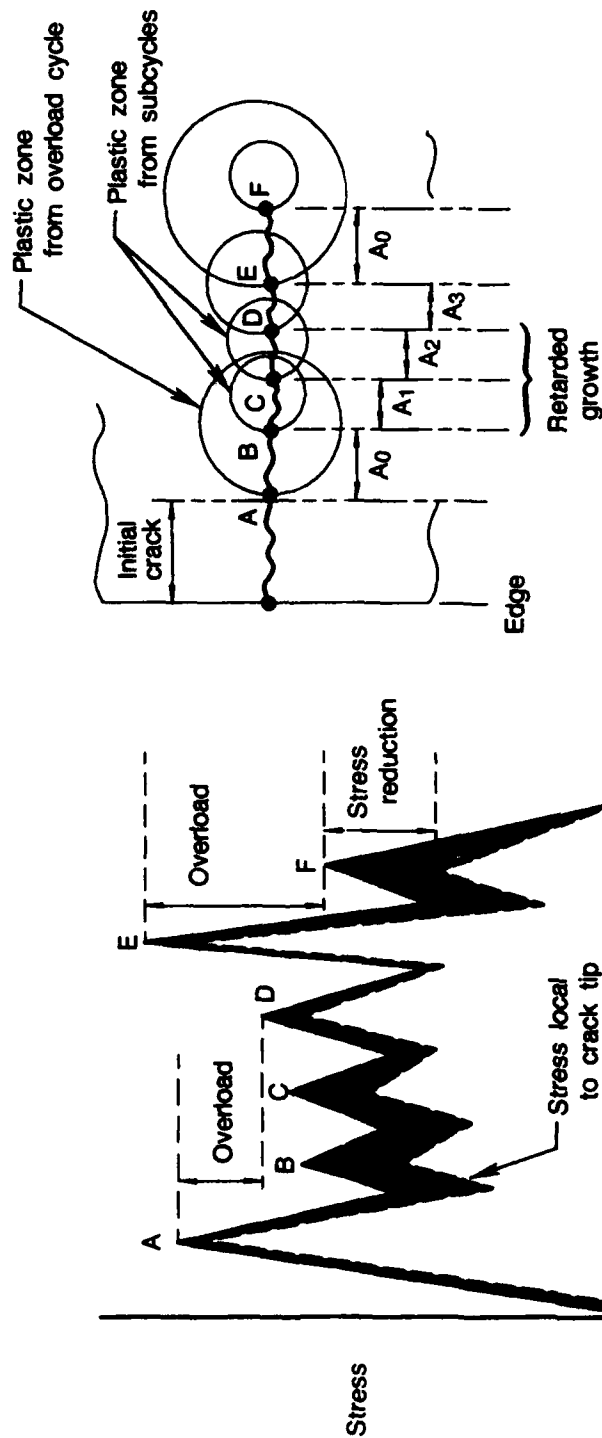
The fracture life of the selected nozzle components was calculated using a modified Willenborg crack growth model. The Willenborg model recognizes the retardation in subcycle crack growth as the crack progresses through the plastic zone produced during the overload cycle.

At overload a significant stress field is produced at the crack tip. During the unloading portion of the cycle, a residual compressive stress field is produced which affects the subsequent subcycles which are less than the overload. Effective stress at the crack tip is reduced because of the residual compressive stress and, as a result, crack growth rate decreases. As the crack progresses beyond the influence of the previous overload cycle, the rate of crack growth returns to that normally expected if the subcycle is treated independently. If other overload cycles occur, the crack growth during subsequent subcycles is retarded until the effects of the overload die out.

The Willenborg model superimposes a compressive stress field to reduce the effective stress intensity at the crack tip and, consequently, to decrease the rate of crack growth.

WILLENBORG CRACK GROWTH MODEL

Model recognizes retardation in subcycle crack growth produced by the overload cycle



- Stress at the crack tip is reduced because of the compression in the plastic zone produced during overload

Comparative Crack Growth Data

Specimen testing was performed to permit the comparison of analysis results with actual crack growth data.

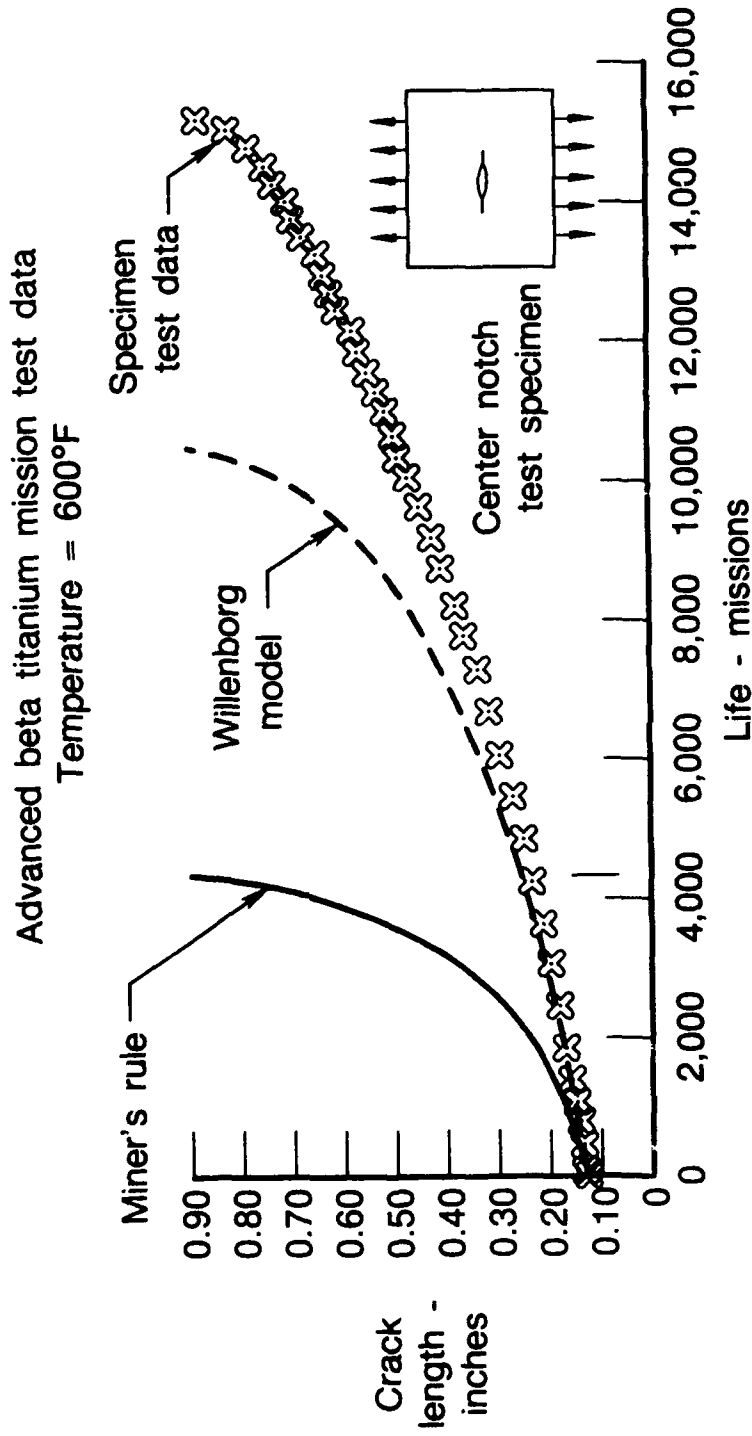
For example, crack length versus mission life was plotted from data obtained during testing of a 16 mil (0.016 inch) thick, center notch specimen made from Advanced Beta Titanium material. During the test the temperature was held constant at 600°F and the specimen was subjected to load cycles simulating the nozzle mission spectra.

A review of the test results revealed the following conclusions:

- A Miner's Rule accumulation of the effects of cyclic damage, where each cycle is treated independently, is very conservative. Calculated life using this technique is significantly below the actual data.
- Results using the Willenborg retardation model, which permits the overload cycles to influence the crack growth rate during subsequent subcycles, clearly demonstrated improved correlation with the actual data. However, some conservatism is still apparent.

COMPARATIVE CRACK GROWTH DATA

Specimen testing confirms improved correlation using Willenborg model



• Willenborg model reduces analysis conservatism

AVP381413 901611

Fracture Analysis of Bulkhead

Typical of the parametric fracture analyses conducted on the selected nozzle components, is the analysis of the nozzle bulkhead.

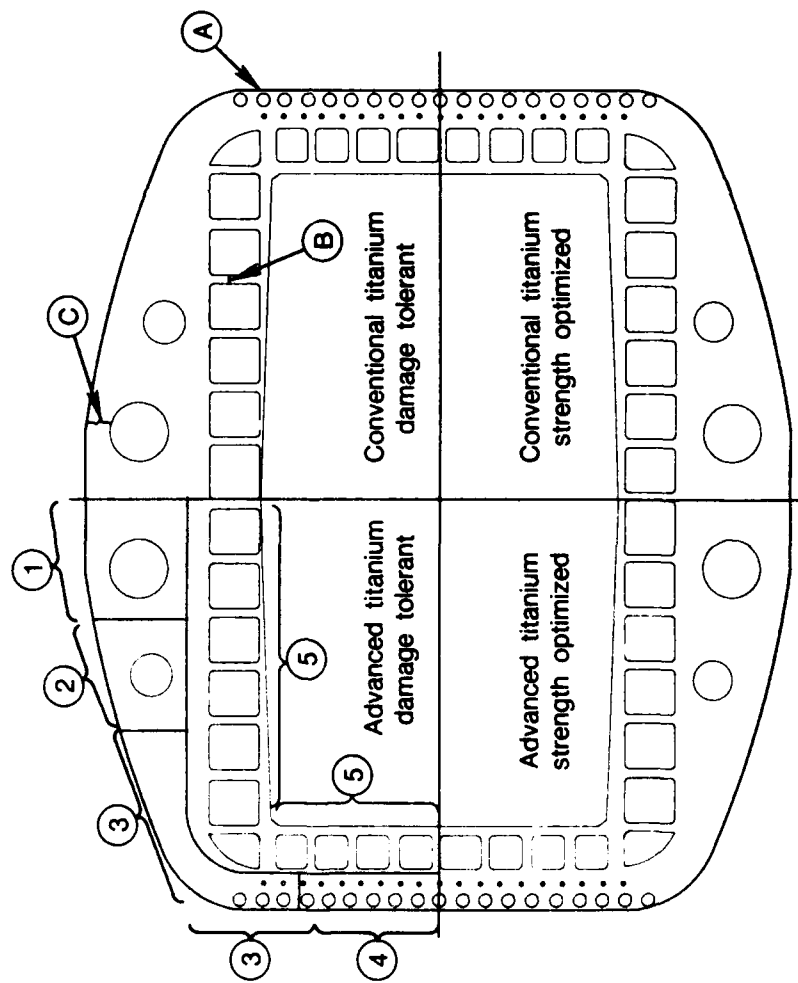
Using both the Miner's rule analysis and the Willenborg model, crack growth life was calculated at key structural locations on the bulkhead. The areas selected for analysis were characterized by high stress and represented fracture limited and strength limited regions. Some locations were selected where the application of load redistribution was justified. Likewise, areas of no load redistribution were also analyzed.

A NASTRAN finite element model was used to calculate the stress distribution. The model was constructed to permit tailoring of the thickness throughout the structure.

Analyses were conducted to facilitate comparison of the thickness required in each area of the structure for a design that was optimized for strength versus one which also meets damage tolerance requirements. The crack growth behavior of conventional titanium versus Advanced Beta Titanium was also investigated.

FRACTURE ANALYSIS OF BULKHEAD

Parametric study of bulkhead typified the crack growth analysis conducted on the selected nozzle components



- High stress areas analyzed
- (A) Load redistribution
- (B) No load redistribution
- (C) Strength limited
- Tailored thickness (zones 1-5)
- Strength optimized vs damage tolerant design
- Conventional vs advanced titanium material

AVP381414 901711

Load Redistribution Considerations

If justified by the load carrying capability of the structural design, the beneficial effects of load redistribution were included in the life calculation. The following summarizes the different approaches for no load redistribution versus load redistribution.

No Load Redistribution

- Fracture life at each initiation location evaluated separately

- Crack initiated at A ; no crack at C

$$\text{Crack A} = a_i \rightarrow B \mid N_{AB}$$

- Crack initiated at C ; no crack at A

$$\text{Crack C} = a_i \rightarrow E \mid N_{CE}$$

- Reduction in effective cross section considered in stress intensity solution

- Total life is the lesser of the crack growth life from A \rightarrow B or the crack growth life from C \rightarrow E

Load Redistribution

- Analyses adheres to guidelines in USAF Damage Tolerance Handbook (AFWAL TR 82-3073)

- Cracks initiated simultaneously at A & C

$$\left. \begin{array}{l} \text{Crack A} = a_i \rightarrow B \\ \text{Crack C} = 0.005 \text{ in.} \rightarrow D \\ (a_i > 0.005 \text{ in.}) \end{array} \right\} N_{AB} = N_{CD}$$

- Reduction in effective cross section considered in stress intensity solution

- Modeling elements released to simulate crack A - B, C - D

- Growth restarted at D under higher stress resulting from cracks A - B, C - D

$$\text{Crack D} = a_x \rightarrow E \mid N_{DE}$$

$$(a_x > 0.005 \text{ in.})$$

- Modeling elements released to simulate crack A - E

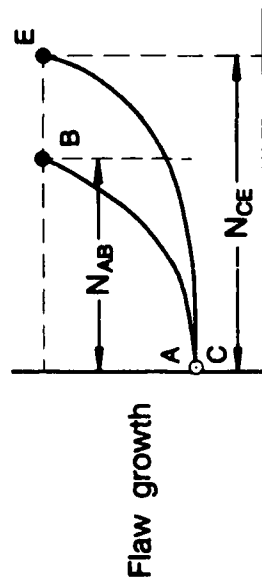
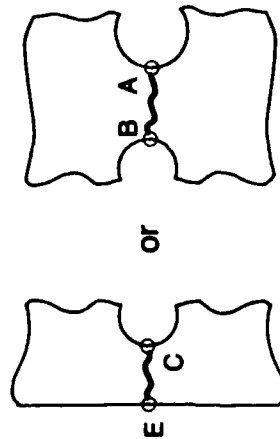
- Redistributed stress at F evaluated to assure adequate strength at limit loads

- Total life is the sum of the crack growth life from A \rightarrow B plus the crack growth life from D \rightarrow E

LOAD REDISTRIBUTION CONSIDERATIONS

Load redistribution benefits were included if justified by the structural design

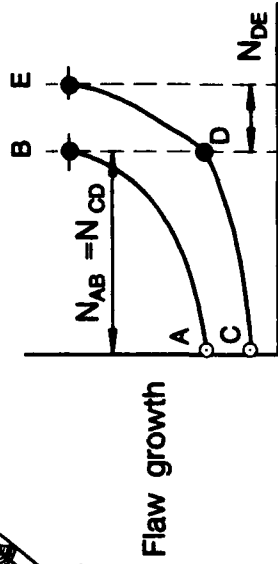
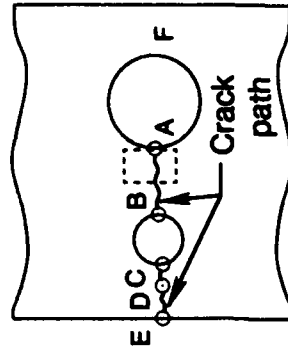
No load redistribution



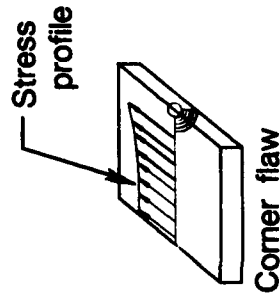
$$\text{Life} = N_{AB} \text{ or } N_{CE}$$

(Whichever is less)

Load redistribution



$$\text{Life} = N_{AB} + N_{DE}$$



Weight Impact for Damage Tolerance

A step-by-step process was followed to evaluate the weight impact associated with making each of the selected components damage tolerant.

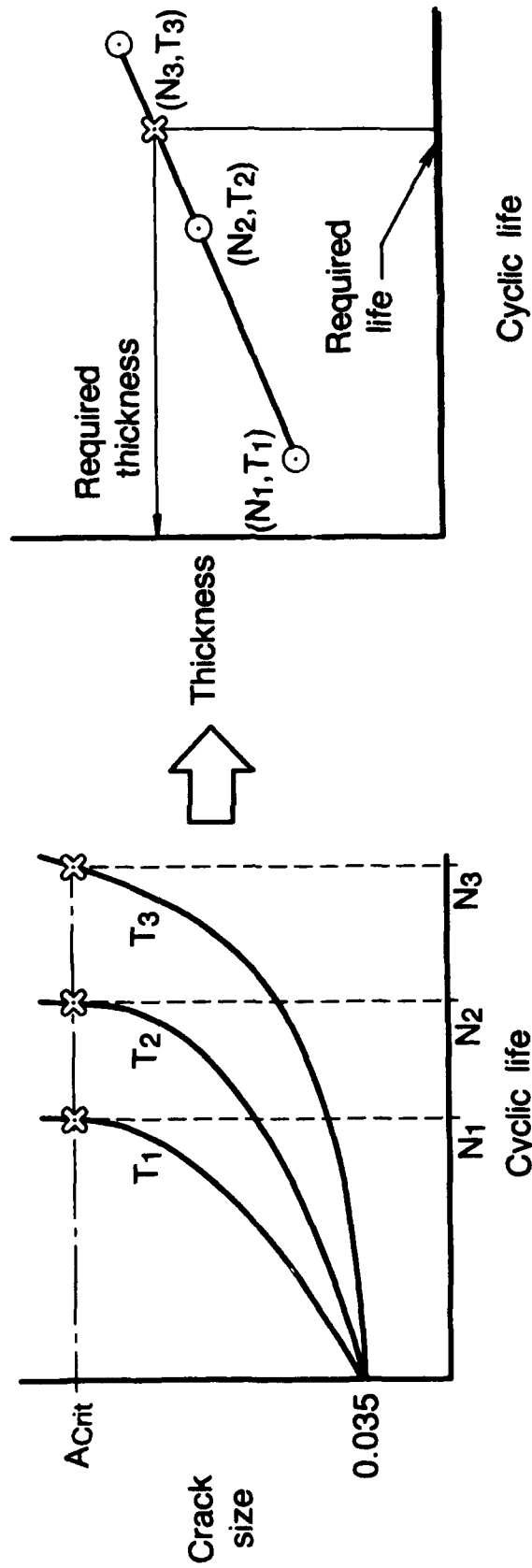
Stress distributions were computed for a variety of thicknesses. Crack behavior as a consequence of the resulting stress field was calculated so that crack size versus cyclic life could be plotted as a function of thickness.

The life required for the initial assumed flaw size to propagate to the critical size producing part rupture was plotted as a function of thickness. Using this plot the thickness required to achieve the specified fracture (safety limit) life was determined.

The weight impact associated with the damage tolerance requirement was calculated from the thickness increase over a strength optimized design.

WEIGHT IMPACT OF DAMAGE TOLERANCE

Weight impact determined by increase in thickness required to achieve full life damage tolerance



$$\Delta \text{ weight} = \sum_{i=1}^{\eta} \rho [(\tau_{\text{req'd}} - \tau_0) A]$$

Fracture Mechanics Study Results

The detail analysis using the Willenborg retardation model, realistic nozzle mission spectra with overload effects, and load redistribution as applicable, indicated that the weight impact for damage tolerance was significantly less than predicted by the initial fracture screening assessment (Miner's rule).

The conclusion, based on these results for the selected nozzle components, is that a damage tolerant rectangular nozzle design is feasible.

FRACTURE MECHANICS STUDY RESULTS

A damage tolerant nozzle design is feasible

Component ¹	Weight increase (lbs) ²	
	Miner's rule	Willenborg model
• Bulkhead	+21.6	+1.8
• Inner transition duct	+1.3	+1.0
• Outer transition duct	+5.5	+4.2
• Shear web	+4.8	+0.4
	+33.2	+7.4

1) Assumes the use of advanced beta titanium material

2) Weight is relative to a strength optimized baseline configuration

AVP381417 901611

Typical Weight Factors

Since the selected nozzle components were typical of the rest of the nozzle structure, weight factors were derived from the detailed fracture mechanics study which were used to project the total weight increase required for damage tolerance. Weight factors were determined with and without load redistribution for both advanced and conventional titanium material.

TYPICAL WEIGHT FACTORS

Factors derived from fracture mechanics study were used to project the weight impact on remaining nozzle structure

$$W_{DT} = W_{BASE} \times F_w$$

Configuration	Weight factor (Fw)	
	Advanced titanium	Conventional titanium
• Sheet and stringer		
- No load redistribution	1.20	1.02
- Load redistribution	1.06	1.005
• Unique structures	1.12	1.006

Damage Tolerance Design Impact

Using the weight factors to project the total nozzle weight impact required for damage tolerance, a modest weight increase of approximately 29 lbs was derived. This is less than 1 percent of the weight of a typical military fighter engine. Based on aircraft industry experience, this is considered a reasonable value.

DAMAGE TOLERANCE DESIGN IMPACT

A small nozzle weight increase is required for damage tolerance

Component	Weight increase (lbs)	
	Damage tolerant design	
• Transition duct and bulkhead		+8.6
• Sidewalls		+5.7
• Actuation system		+0.6
• Convergent flap		+5.1
• Divergent/external flaps		+8.8
Δ weight for damage tolerance		+28.8 lbs

Summary

Based on this assessment, the design of a damage tolerant rectangular nozzle for an advanced augmented military turbofan engine with a useful fracture life of 4000 engine flight hours from a conservative initial flaw size is achievable.

The nozzle weight impact is minor — less than 1 percent of the total weight of a typical military fighter engine.

An efficient structural design, incorporating geometric features which resist crack growth, is necessary. So is the proper selection of material, which considers crack growth behavior in addition to burn resistance and strength, vibration, and durability requirements.

Fracture mechanics techniques exist to analyze such designs. These techniques are being used today in the airframe industry to assess the capability of sheet and stringer type structures.

Experimental data confirms that these analytical methods provide a less conservative means of predicting fatigue crack growth behavior for engine nozzle structures.

NOZZLE DAMAGE TOLERANCE IMPACT

Summary

- A damage tolerant nozzle is feasible
- Nozzle weight impact is minor
- Conclusion is based on improved fracture analysis
- Specimen testing has confirmed analysis results

1990 USAF Structural Integrity Program Conference

San Antonio, Texas
11-13 December 1990

ENVIRONMENTAL CHARACTERIZATION OF EXTERNAL COMPONENTS FOR AN ADVANCED SUBORBITAL ENGINE



Project Engineer

Bobbie R. Vincent
Project Engineer

Elliot B. Smith
Senior Analytical Engineer



AVP381421 900312

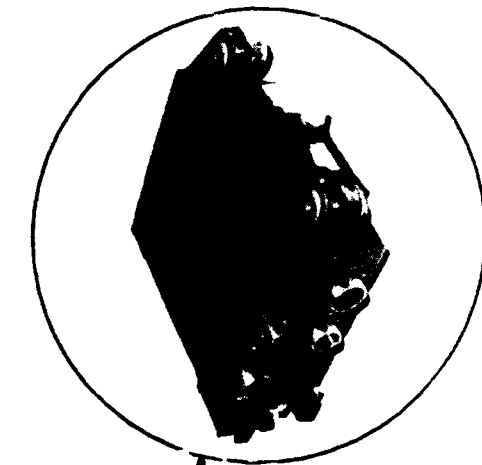
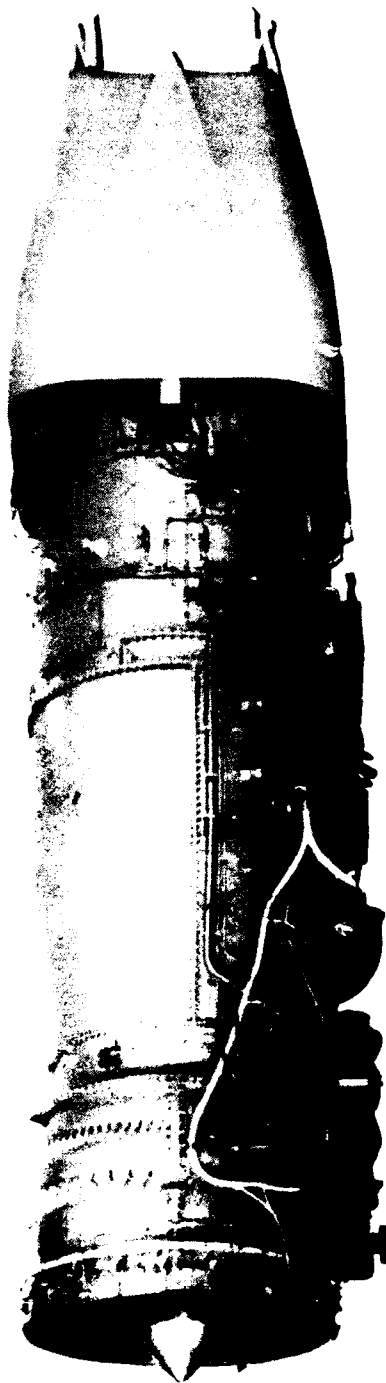
ENVIRONMENTAL CHARACTERIZATION

Presentation overview

- Background
- Environment types
- Environmental parameter definition for an external component

APPLICATION

- Advanced turbofan engine
- All external components and hardware

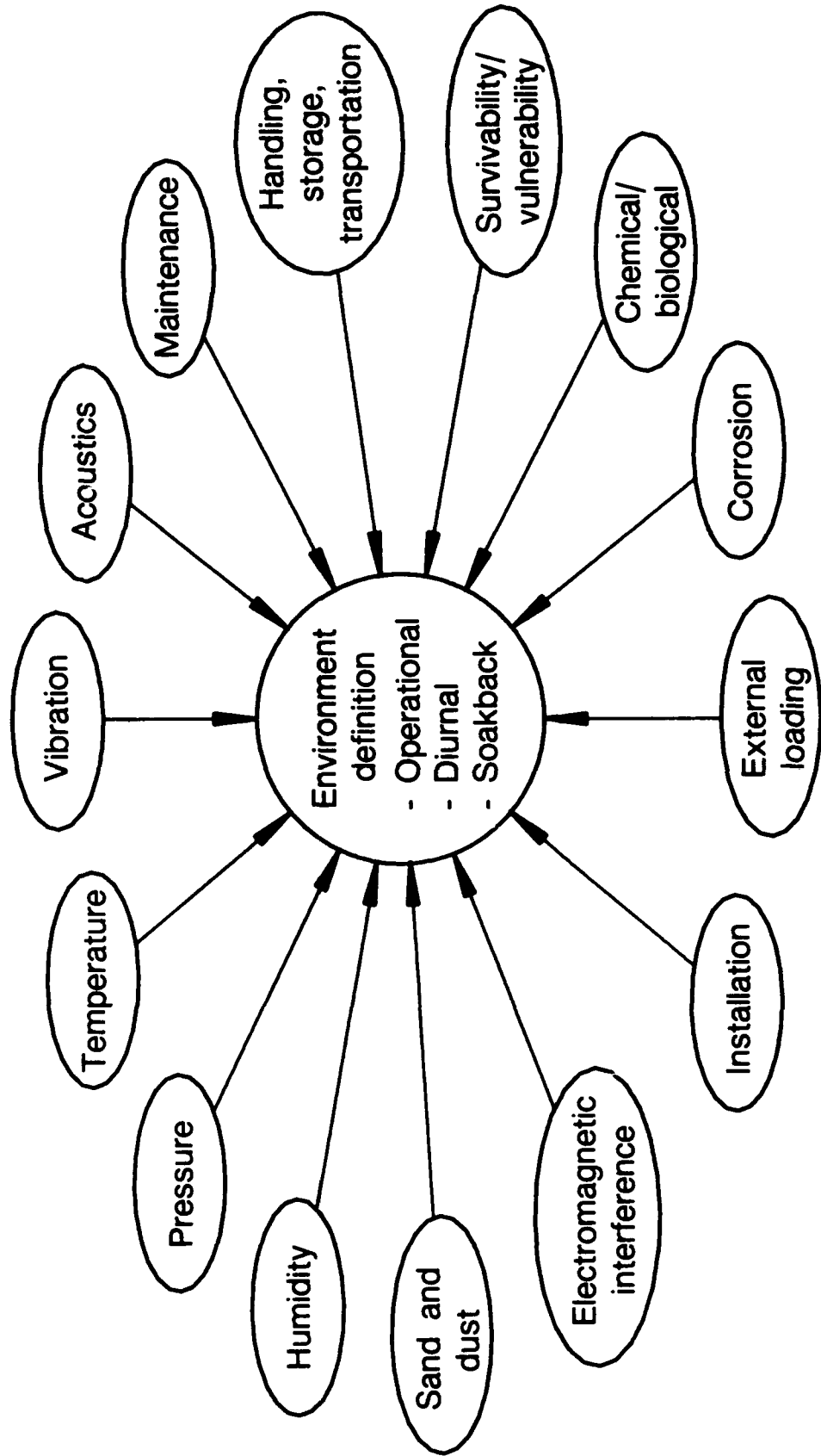


FADEC - Full Authority
Digital Electronic
Control

AVB381423 900312

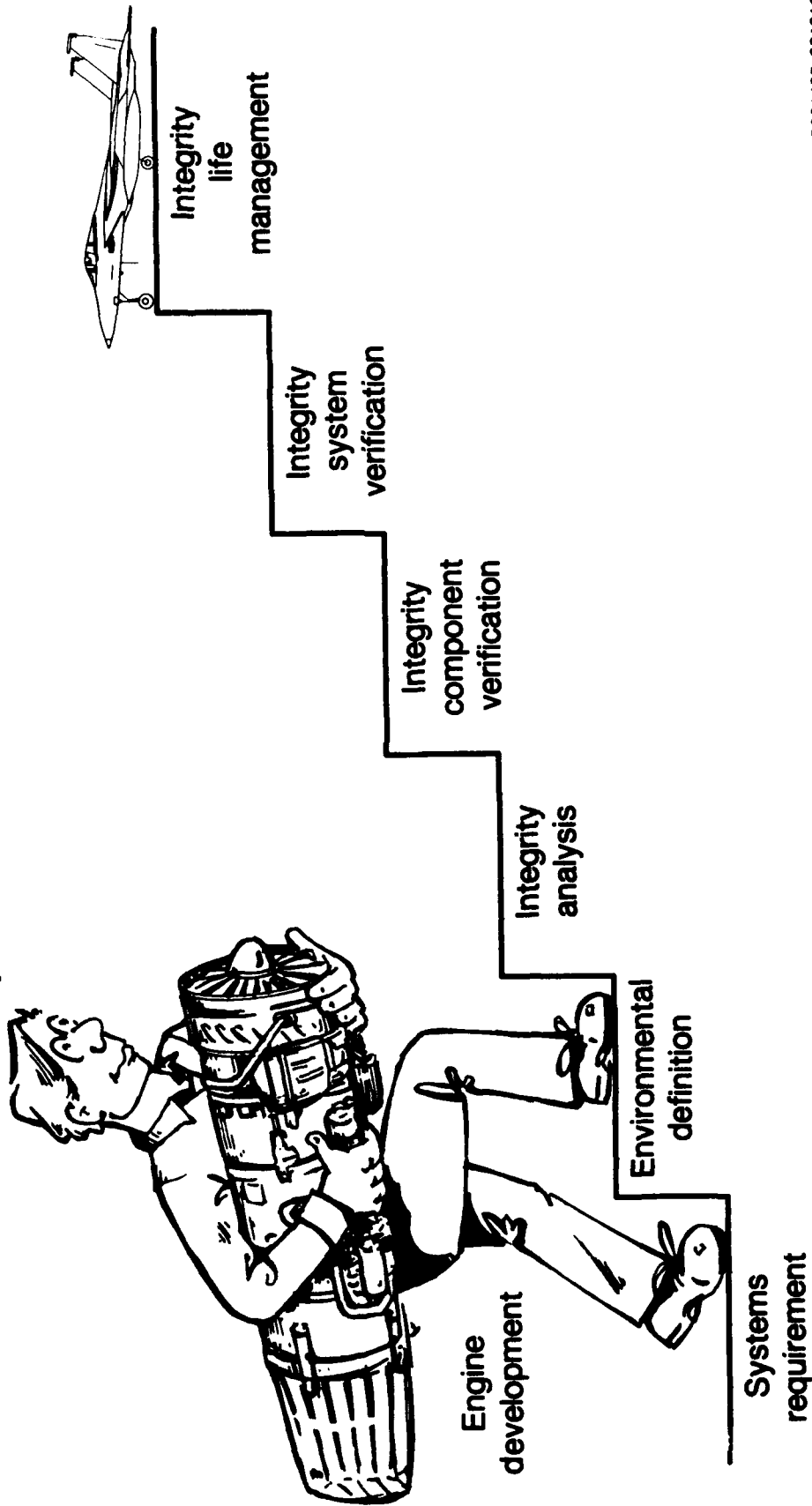
EXTERNAL ENVIRONMENTS

Multiple environmental categories



IMPORTANCE OF ENVIRONMENTS

Definition - First step in development process



AVP381425 901211

CA&E ENVIRONMENT

Define the environment throughout the operational lifetime

- Shipping, handling, transportation and storage
 - Preservation mediums
 - Temperature, humidity
 - Vibration, shock
- On-equipment usage
 - Temperature, pressure
 - Humidity, sand and dust, corrosion, EMI
 - External loading, vibration, acoustics
 - Chemical/biological, survivability/vulnerability
- Off-equipment usage
 - Temperature, pressure
 - Vibration, acoustics

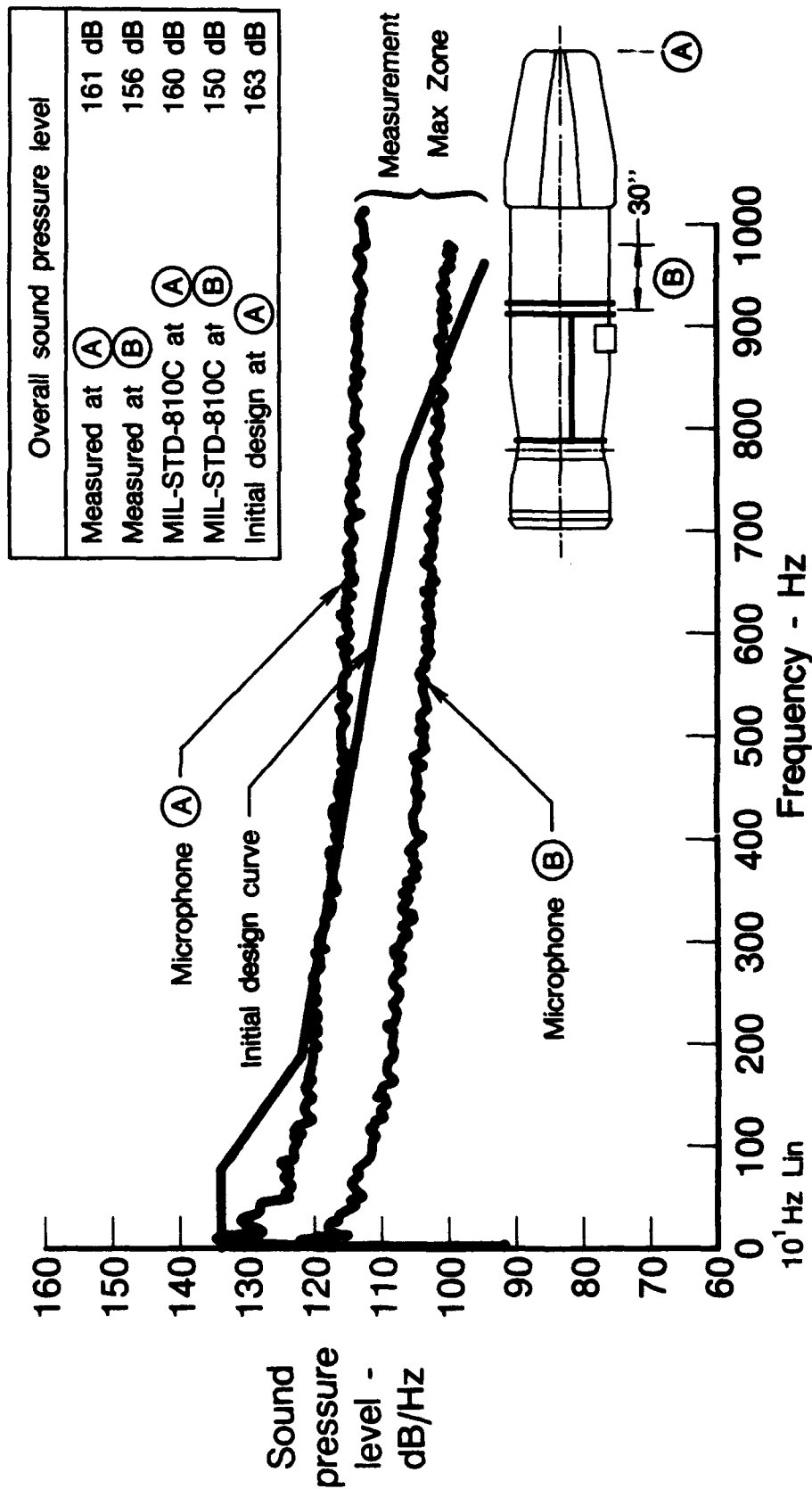
ACOUSTIC ENVIRONMENT

Application environment adjusted

- Dual engine application
 - Doubles SPL = +3.0 dB
- Airflow/nozzle pressure ratio differences
 - +0.8 dB
- Includes effect of nozzle vectoring
- No adjustment for effect of nacelle shielding

EXTERNAL ACOUSTIC ENVIRONMENT

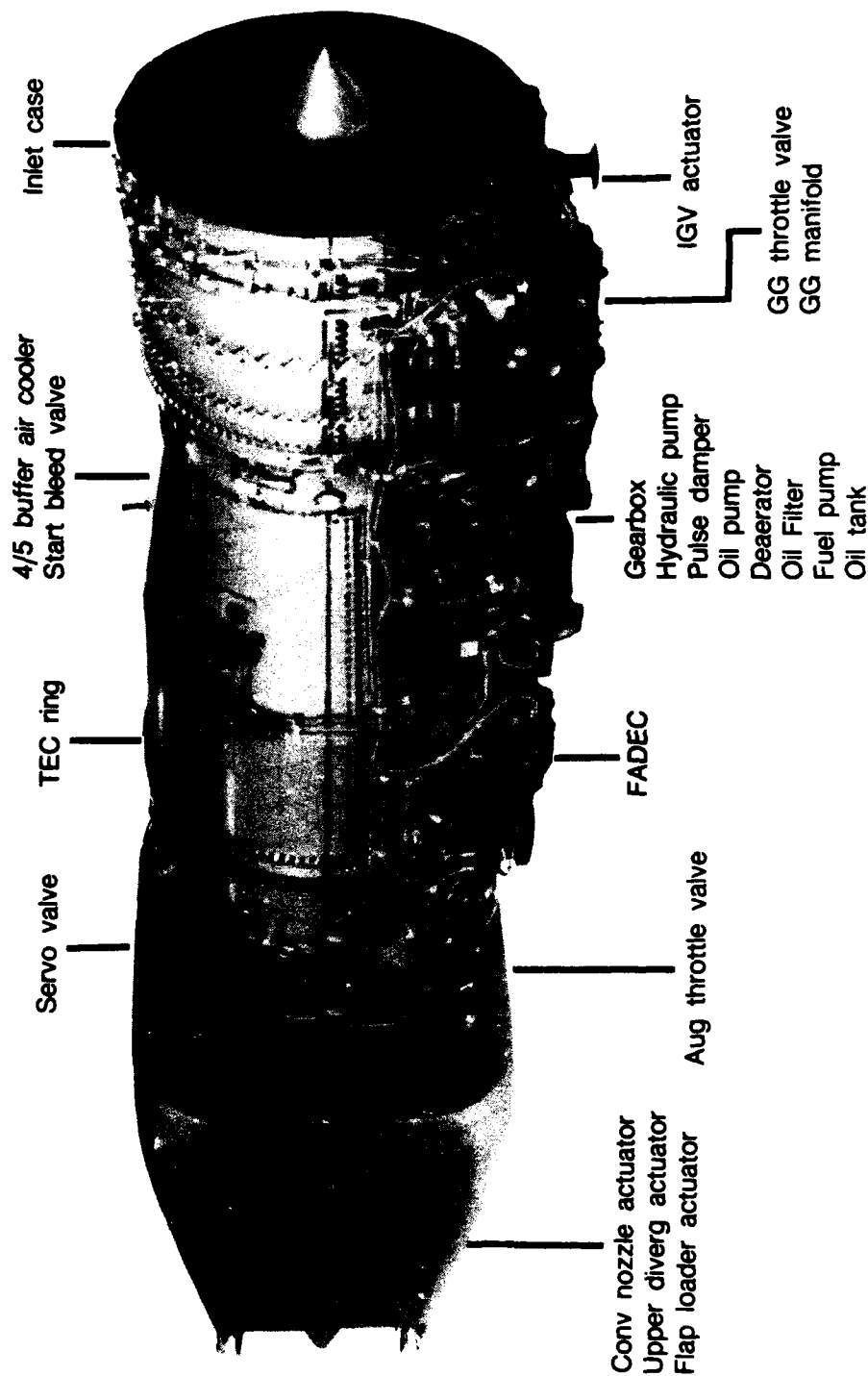
Engine measurements confirm design levels



AVP381428 900312

VIBRATION ENVIRONMENT

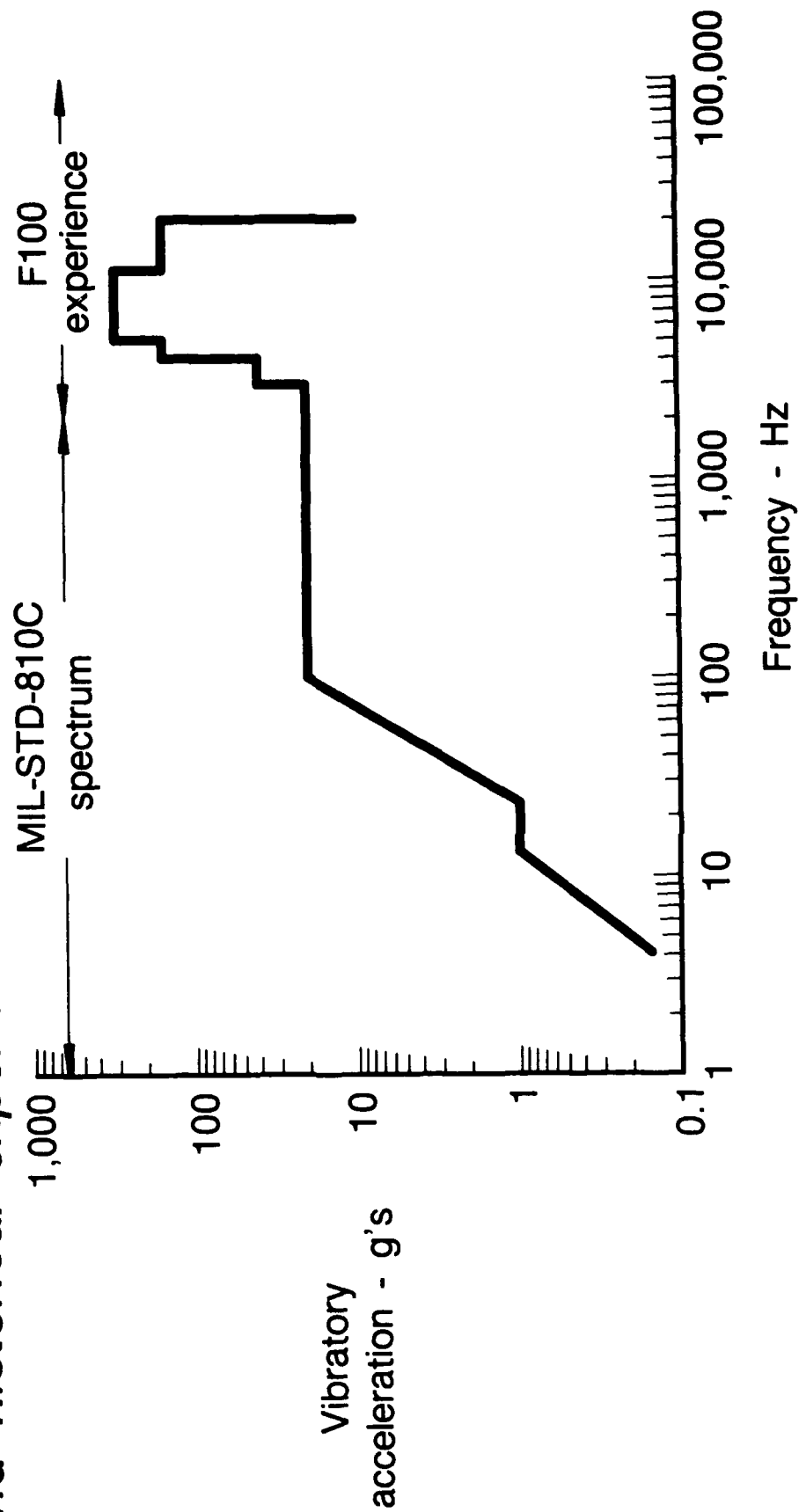
Over 180 accelerometer locations provide survey of engine vibration levels



AVB381430 901211

VIBRATION ENVIRONMENT

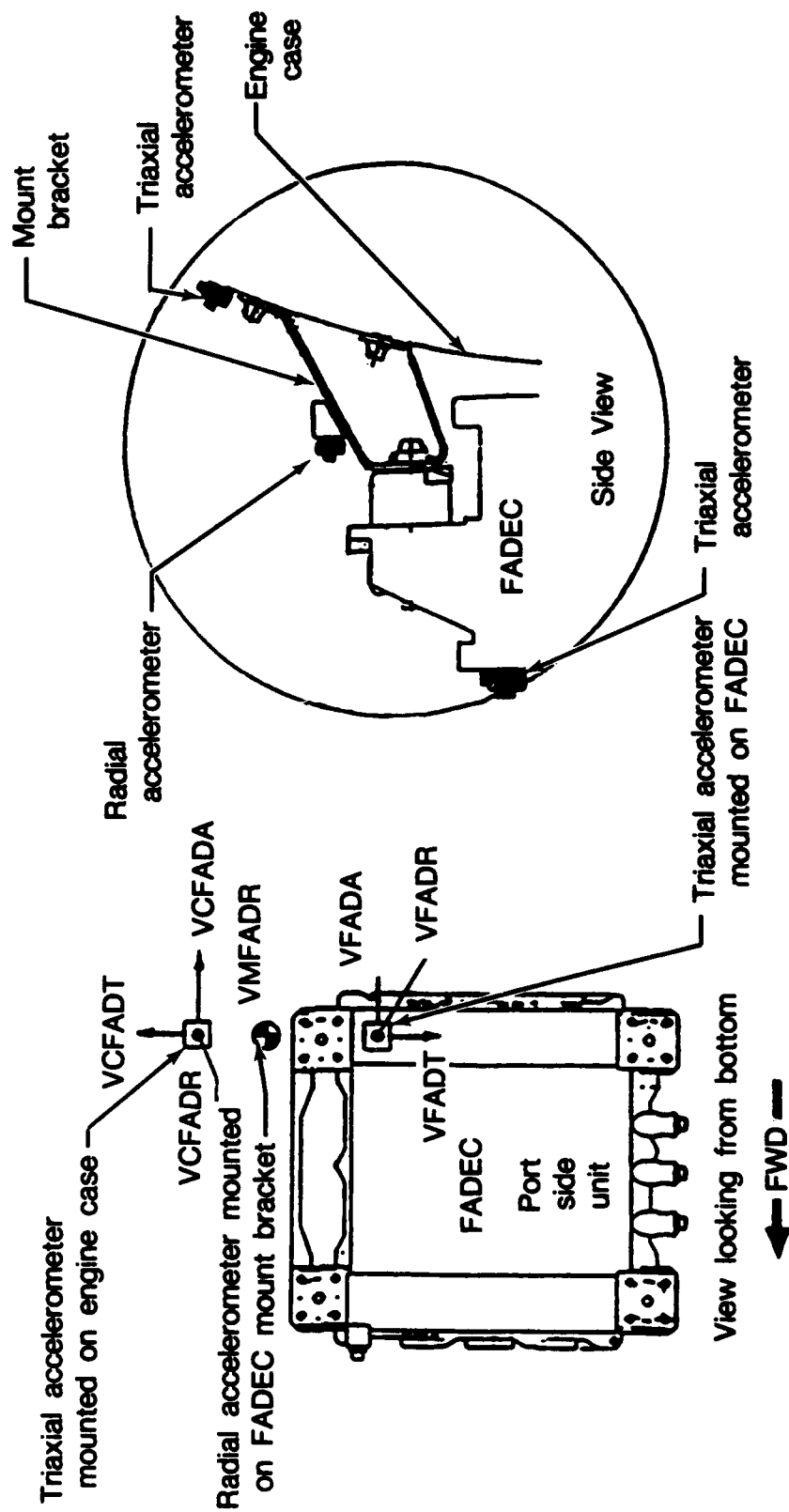
Initial assumed environment based on MIL-STD-810C and historical experience



AVP381431 902111

VIBRATION ENVIRONMENT

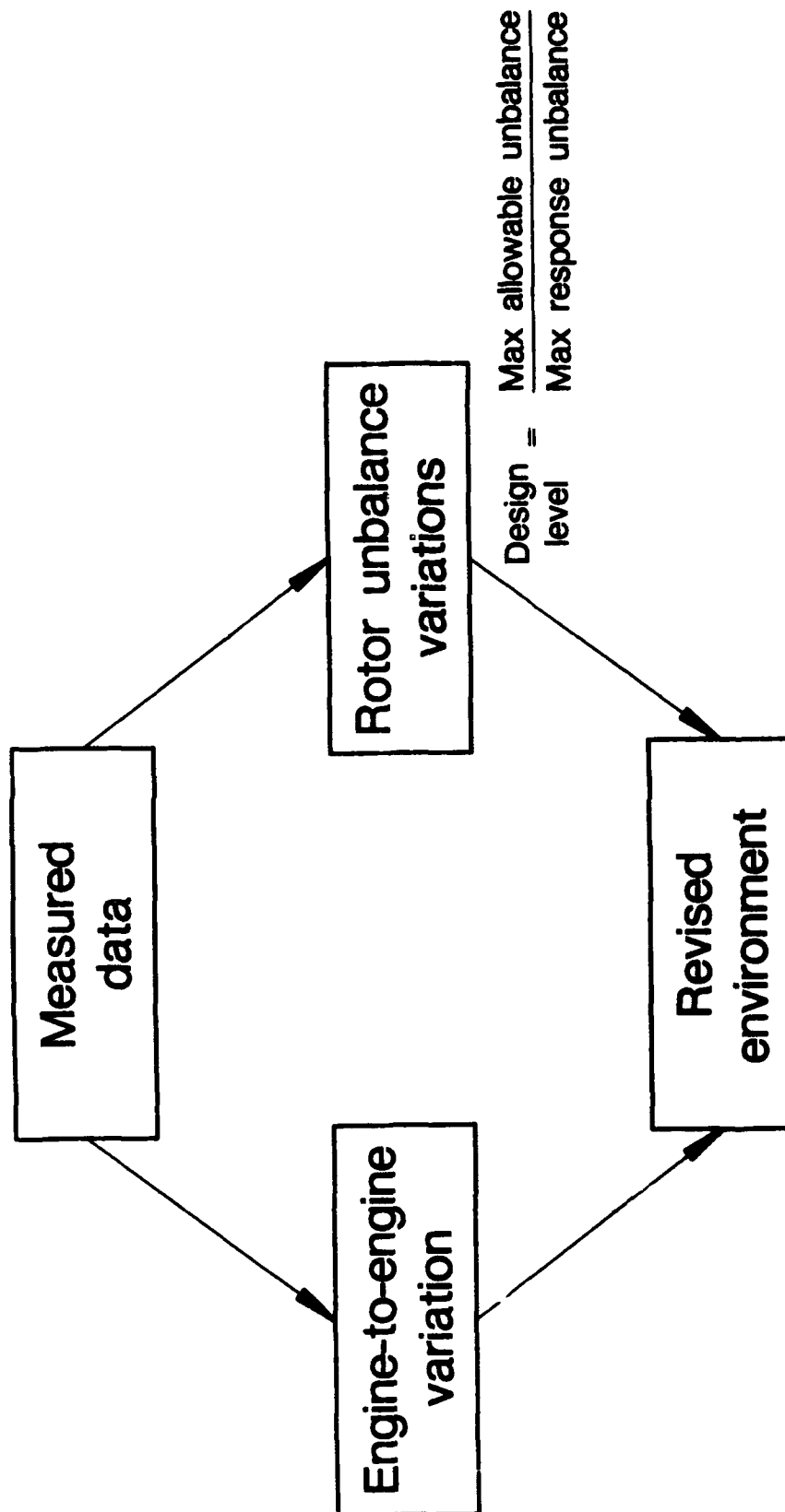
FADEC accelerometer locations



AVB381432 902011

VIBRATION ENVIRONMENT

Application environment adjusted



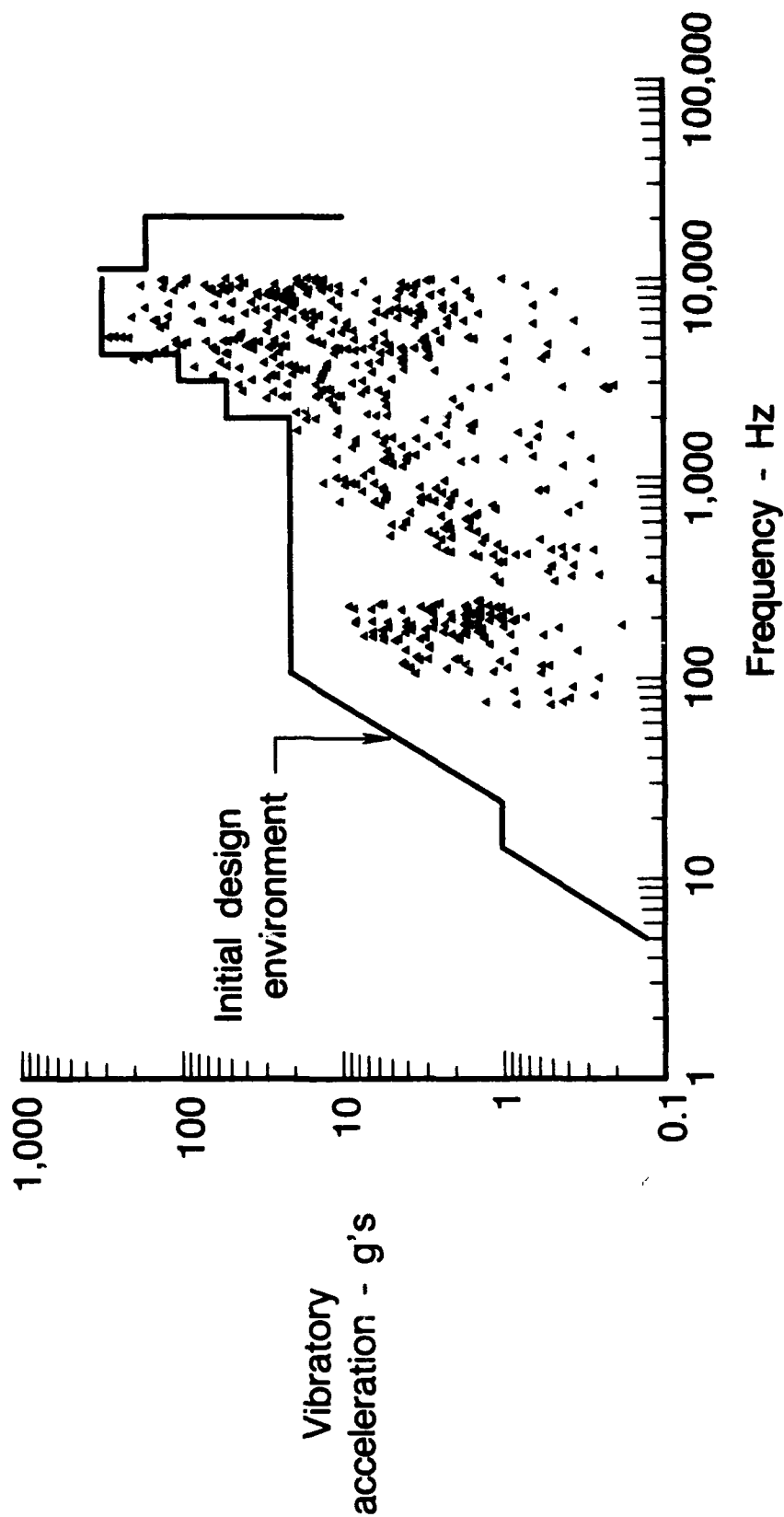
AVP381433 900911

Maximum acceleration vs. frequency for FADEC



ENGINE TEST DATA

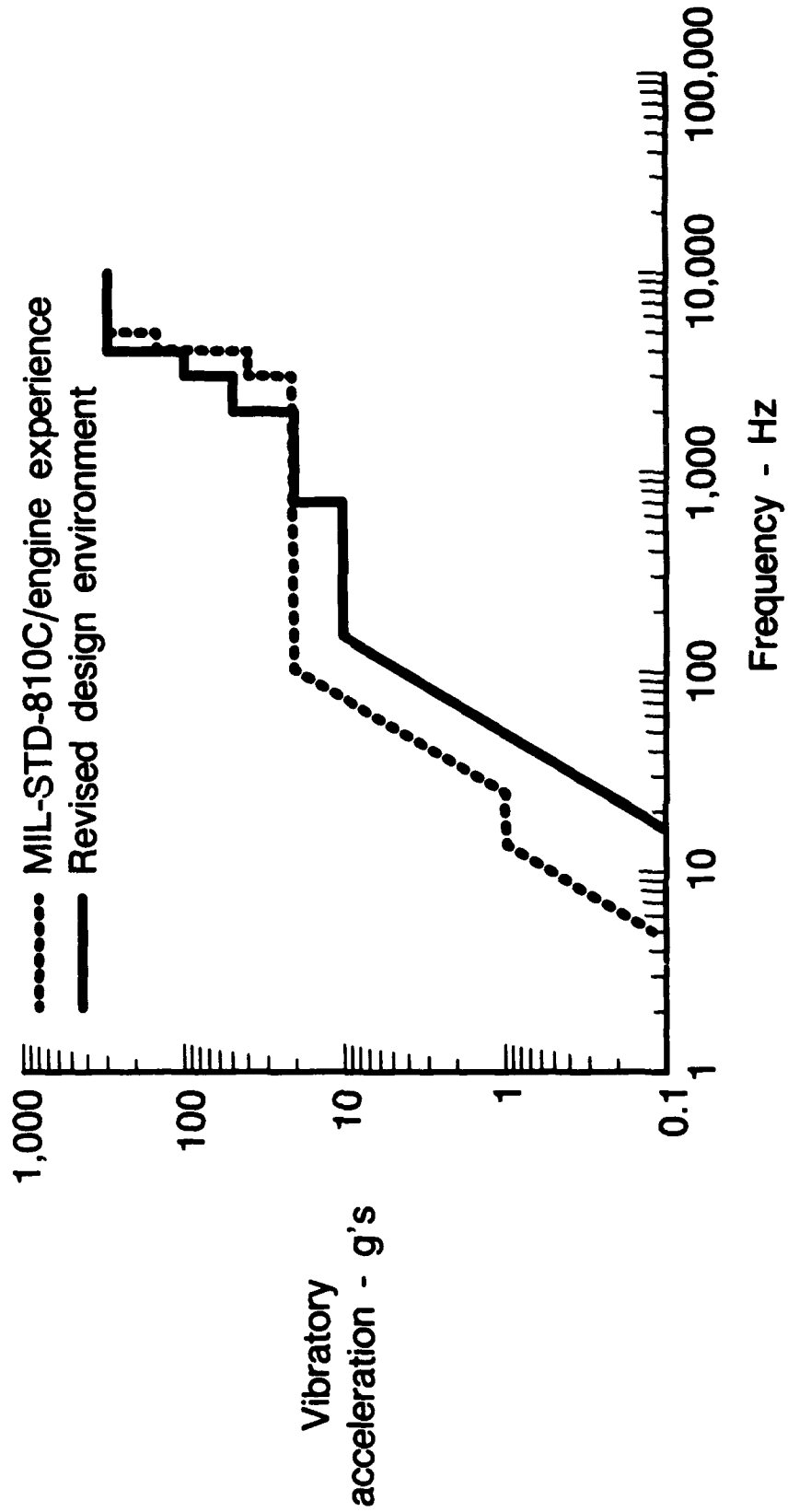
Maximum acceleration vs frequency - All locations



AVP381435 900312

VIBRATION ENVIRONMENT

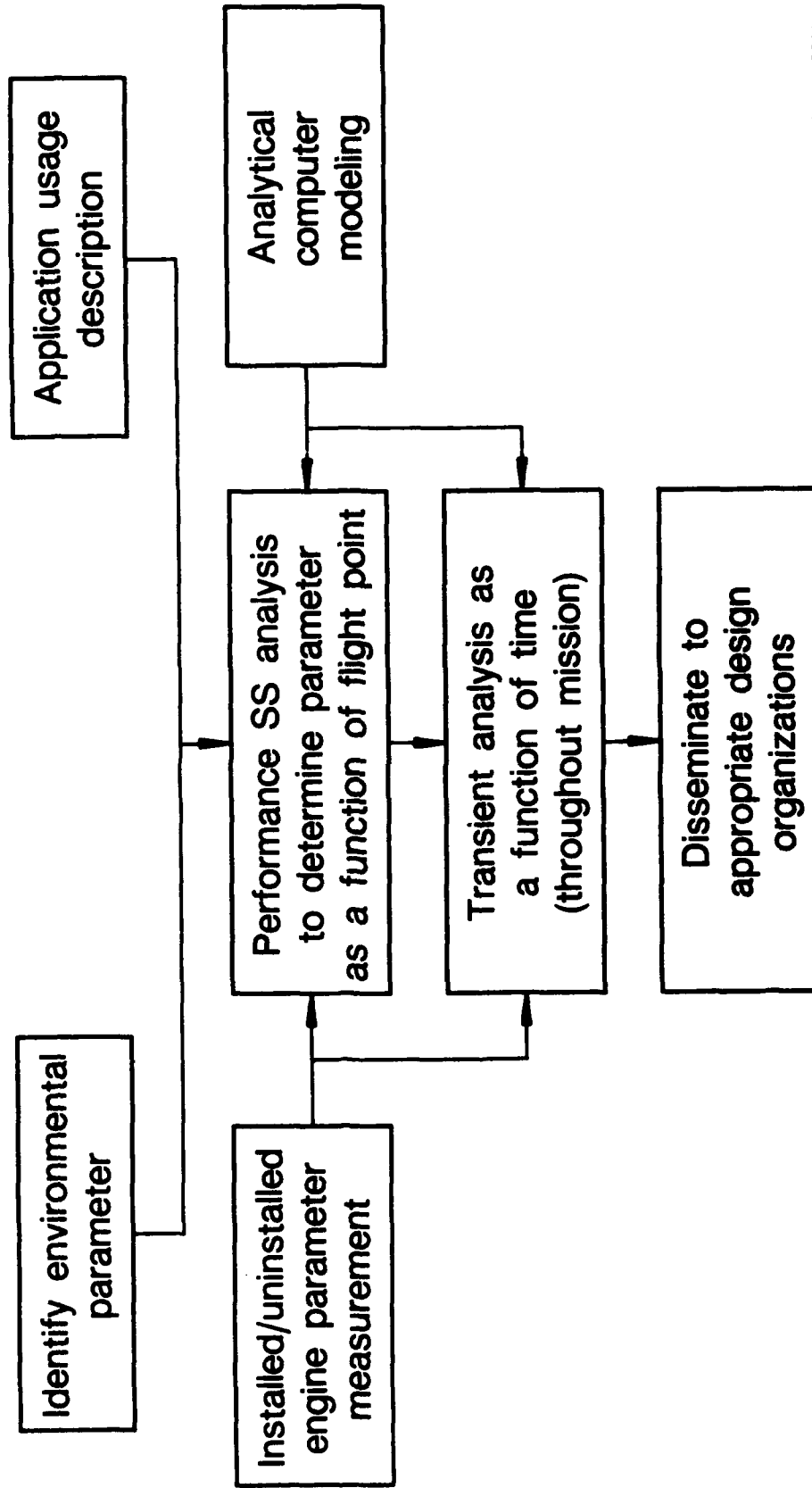
Comparison of actual data to historical environment



AVP381436 902011

COMPONENT LOCAL ENVIRONMENT

Parameter definition approach

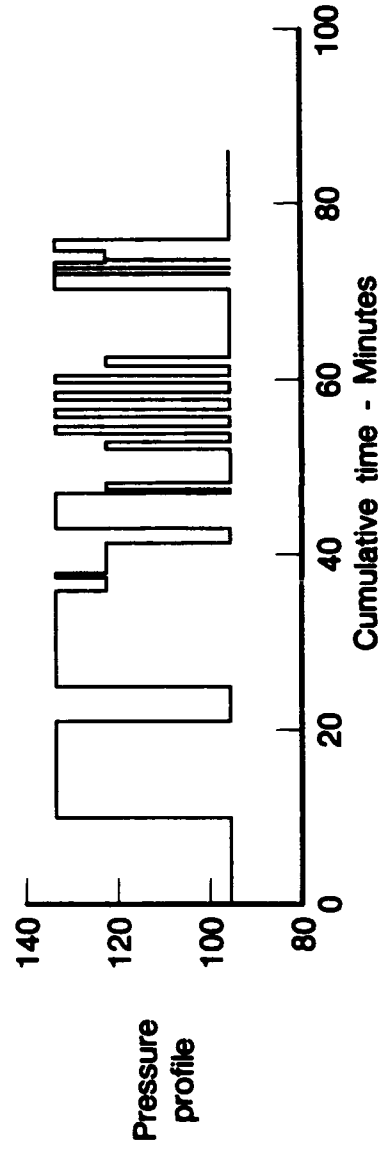


AVP381437 900911

LOCAL ENVIRONMENT

Primary use for durability/damage tolerance evaluations

- Durability analysis
 - Low cycle fatigue wear
- Damage tolerance analysis
 - Crack growth analysis
 - Residual strength
- Durability/damage tolerance test profiles



AVP381438 900312

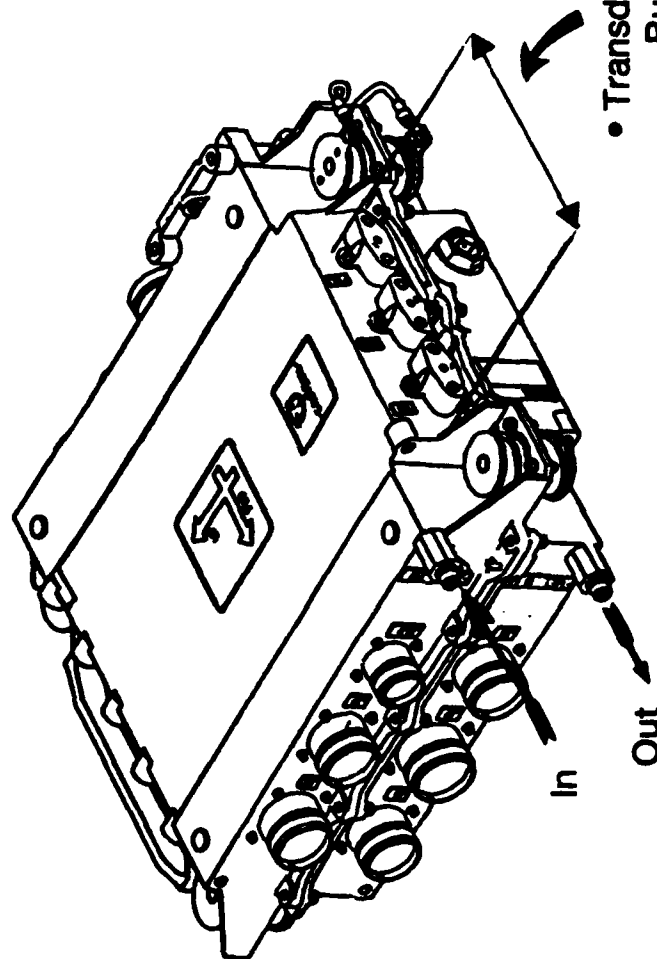
COMPONENT LOCAL ENVIRONMENT

FADEC input parameters

- Nacelle air
 - Pressure
 - Temperature
 - Velocity



Engine case temperature



- Fuel cooling
 - Pressure
 - Temperature
 - Flow

- Transducer input
 - Burner pressure
 - Inlet pressure
 - Turbine cooling pressure
 - Nozzle pressure

AVB381438 901211

COMPONENT LOCAL ENVIRONMENT

Typical parameter definition table

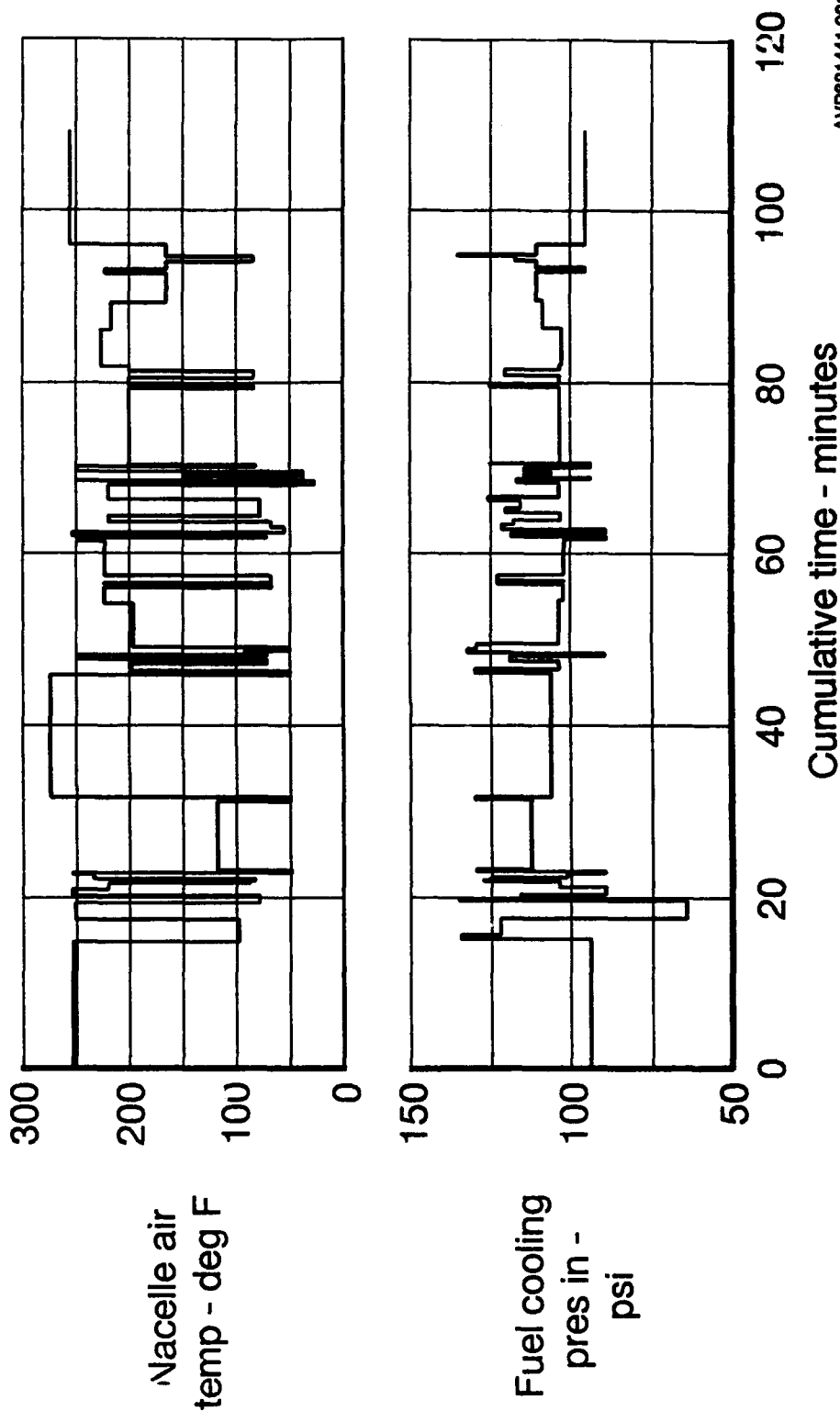
Time		Engine		Nacelle air		Transducers				Fuel cooling				
Delta (sec)	Cum (min)	Case (deg F)	Temp (deg F)	Press. (psi)	Velocity (ft/sec)	PB (psi)	PS2 (psi)	PS6 (psi)	PS13 (psi)	Temp (deg F)	Press. (psi)	Press. (psi)	Flow (PPH)	Power (watts)
CONDUCT NORMAL START-UP SEQUENCE														
900.0	15.000	150.	255.	15.	2.	60.03	14.48	15.43	20.34	60.	95.2	90.2	280.	(TBD)
30.0	15.500	375.	100.	15.	3.	370.93	14.95	62.41	69.86	60.	134.9	129.9	280.	
120.0	17.500	330.	100.	13.	5.	251.37	15.35	42.23	53.41	60.	123.5	118.5	280.	
120.0	19.500	160.	252.	13.	5.	57.83	15.56	13.76	21.56	60.	65.4	60.4	280.	
10.0	19.667	410.	110.	13.	5.	408.39	16.46	68.75	76.95	60.	135.3	130.3	280.	
45.0	20.417	290.	80.	9.	5.	195.17	11.30	31.45	41.42	60.	117.0	112.0	280.	
45.0	21.167	145.	255.	9.	5.	52.23	11.48	10.52	17.87	60.	90.6	85.6	280.	
45.0	21.917	225.	222.	9.	5.	110.12	11.42	20.08	26.93	60.	105.0	100.0	280.	
15.0	22.167	370.	90.	9.	6.	304.32	12.27	51.16	57.35	60.	128.5	123.5	280.	
15.0	22.417	355.	85.	7.	6.	274.93	11.08	46.21	51.82	60.	126.0	121.0	280.	
30.0	22.917	230.	235.	5.	6.	93.96	7.30	15.46	21.88	60.	102.5	97.5	280.	
10.0	23.083	155.	255.	5.	6.	49.19	7.35	9.31	13.73	60.	90.5	85.5	280.	
20.0	23.417	300.	50.	5.	6.	196.84	7.10	33.48	36.15	60.	131.0	126.0	280.	
490.0	31.583	270.	120.	5.	6.	136.07	7.23	20.92	28.72	60.	113.5	108.5	280.	
15.0	31.833	300.	50.	5.	6.	196.84	7.10	33.48	36.15	60.	131.0	126.0	280.	
840.0	46.167	250.	275.	4.	6.	83.80	4.51	12.40	18.10	60.	107.0	102.0	280.	
15.0	46.417	300.	50.	5.	6.	196.84	7.10	33.48	36.15	60.	131.0	126.0	280.	
60.0	47.417	240.	200.	7.	6.	113.91	11.34	19.93	28.05	60.	105.0	100.0	280.	
30.0	47.917	350.	75.	7.	6.	248.54	9.90	44.95	46.60	60.	120.0	115.0	280.	
20.0	48.250	150.	250.	7.	6.	52.41	10.27	10.48	16.71	60.	90.6	85.6	280.	

60.0	47.417	240.	200.	7.	6.	113.91	11.34	19.93	28.05	60.	105.0	100.0	280.
30.0	47.917	350.	75.	7.	6.	268.54	9.90	44.95	46.60	60.	120.0	115.0	280.
20.0	48.250	150.	250.	7.	6.	52.41	10.27	10.48	16.71	60.	90.6	85.6	280.

AVB381440 900312

COMPONENT LOCAL ENVIRONMENT

Typical parameter profiles



AVP381441 901211

FUTURE PLANS

- **Define transient response**
- **Continue environment definition**
- **Flight test/installed test data**

SUMMARY

- Environment dictates component operational effectiveness
- Acoustic levels confirm MIL-STD assumptions
- Vibration levels measured lower than MIL-STD-810C
- Component durability and damage tolerance predicated upon environment variations

THE RESULTS OF USING A MICRO PROCESSOR BASED STRUCTURAL DATA RECORDER TO SUPPORT INDIVIDUAL AIRCRAFT TRACKING OF THE B-1B AIRCRAFT

A. G. Denyer

Senior Engineering Specialist - Rockwell International

ABSTRACT

As part of the USAF Aircraft Structural Integrity Program (ASIP), Rockwell International developed an Individual Aircraft Tracking (IAT) system for the B-1B aircraft. The IAT program accumulates and analyzes operational usage statistics and load spectra data from each aircraft in the fleet, in order to predict the current structural damage status at selected critical structural locations. The IAT analysis provides the data from which structural inspections, repairs and replacements are defined and scheduled.

INTRODUCTION

In 1972 the USAF instituted the Aircraft Structural Integrity Program (ASIP) Requirements (1) to which aircraft would be designed and maintained to ensure safety of flight and to provide an economic maintenance schedule. Included in these requirements is the Individual Aircraft Tracking (IAT) program which predicts potential flaw growth in critical areas of the structure on each individual aircraft in response to its unique operational usage. The purpose of such a program is to provide the USAF the information necessary to schedule specific structural inspection and maintenance tasks at proper intervals so as to ensure adequate strength, durability and damage tolerance of the structure of each aircraft throughout the required service life.

The B-1B was the first USAF aircraft to incorporate, as a design requirement, an ASIP dedicated, microprocessor based, Structural Data Collector (SDC) to record structural loads on every aircraft. This paper presents a description of, and sample output from, the B-1B IAT system which comprises, data acquisition, data collection and processing procedures, analysis programs and reporting procedures.

The damage computation within the IAT program utilizes the principles of linear elastic fracture mechanics. The crack growth equations, initial and final flaw assumptions are presented for a typical structural location as are the results of analyses for both the durability and damage tolerance regions of the crack growth curve. The accumulated structural damage is computed for the applied loads representing the service experience while the remaining life is based on the crack growth life from the current crack size to a defined allowable crack limit. The remaining life estimates are predicted assuming that future utilization of the aircraft is an extension of average squadron usage for the previous two years. The useful remaining life of the structure is a function of the durability analysis while the inspection requirements are based on the damage tolerance analysis.

Finally the paper will discuss the advantages of an IAT program based on a structural loads recorder and the procedures for incorporating the IAT program results into the Force Structural Maintenance Plan.

DATA ACQUISITION PROVISIONS

Structural Data Collector

The IAT analysis programs require a detailed definition of the operational environment. For the B-1B, the collecting of operational data is performed by a microprocessor based solid state data collection and storage device called the Structural Data Collector (SDC). One such instrument is installed on each B-1B aircraft. The SDC samples, processes and records data from six, ASIP dedicated, strain gages located at strategic points on the airframe, and a dedicated vertical accelerometer. The balance of the data required by the IAT system is extracted from non ASIP information available in the Central Integrated Test System (CITS).

The Central Integrated Test System provides on-aircraft capability for in-flight passive monitoring, data entry, fault isolation and active testing of most aircraft systems and subsystems. In support of its primary functions CITS monitors many of the parameters to be processed by the SDC recorder. This parameter monitoring capability is used to supply the SDC with parameters of interest via a dedicated high speed serial-digital CITS/SDC link.

The CITS data entry function is used to supply the SDC with necessary manual entry flight documentation via the CITS Control and Display Panel.

TABLE 1 provides the list of measured parameters and documentary items recorded by the SDC

Other Data Acquisition Requirements

The B-1B IAT software system requires data inputs from sources other than the SDC.

- 1) **Possession and Utilization Record Summary**
The USAF maintained AFR65-110/GO33 (2) system provides a summary of aircraft ownership, possession and utilization records, a sample of which is shown in TABLE 2. This data provides the current flight hour status of each aircraft.
- 2) **Aircraft Mission Records.**
The USAF maintained Core Automated Maintenance System (CAMS)(3) provides a record of each mission in terms of date of mission, mission type, flight length and landings. TABLE 3 reflects a sample of this data which is used as back up data in the situation that the SDC data is unavailable.
- 3) **Aircraft Maintenance Records**
The USAF maintained CAMS data base provides base level maintenance records of significance while depot level maintenance actions are recorded manually and converted to computer compatible form. The data includes inspections, repairs, part replacement and component interchanges which may affect the predicted structural damage status on a particular aircraft .

The USAF maintained data collection systems are the responsibility of the USAF Air Logistics Command which provides computer tapes of data on a monthly basis.

Parameter	Data Comp Meth	Sample Rate /sec	Data Source
Strain Gage - Stabilizer Left Hand	pv	40	ASIP
Strain Gage - Stabilizer Right Hand	pv	40	ASIP
Strain Gage - Stabilizer Support Fitting Side plate	pv	40	ASIP
Strain Gage - Wing Sweep Actuator	pv	40	ASIP
Strain Gage - Wing Lower Skin	pv	40	ASIP
Strain Gage - Forward Fuselage Dorsal Longeron	pv	40	ASIP
Vertical Acceleration (Nz)	pv	40	ASIP
Wing Sweep Angle	th	1	CITS
Flap Position	th	1	CITS
Gross Weight	th	1	CITS
Center of Gravity	hac1	1	CITS
Mach Number	th	1	CITS
Altitude (Pressure)	th	1	CITS
Altitude (Radar)	hac2	1	CITS
Weight on Wheels (on/off)	desc	1	CITS
Refuel Nozzle Latch (connect/unconnect)	desc	1	CITS
Structural Mode Control System (on/off)	desc	1	CITS
Terrain Following Radar Status (on/off)	desc	1	CITS
Terrain Following Radar Mode (manual/auto)	desc	1	CITS
Terrain Following Radar Ride (soft/medium/hard)	desc	1	CITS
Engine Number 1 Stop	desc	1	CITS
Engine Number 2 Stop	desc	1	CITS
Engine Number 3 Stop	desc	1	CITS
Engine Number 4 Stop	desc	1	CITS
DOCUMENTORY ITEMS	NOTES		
Aircraft Serial Number	1) ASIP - ASIP Dedicated Sensor		
Mission Date	2) CITS - Data from Central Integrated Test System		
Take Off Gross Weight	3) Desc - Discrete Parameter		
Stores Weight	4) pv - Peak-Valley Compression Algorithm		
Mission Type Code	5) th - Time History Compression Algorithm		
Base Code	6) hac1 - Recorded with Gross Weight		
	7) hac2 - Recorded with Pressure Altitude		

TABLE 1 - STRUCTURAL DATA COLLECTOR, RECORDED PARAMETERS, DATA COMPRESSION METHODS, SAMPLE RATES AND DATA SOURCES

Aircraft Possession and Utilization Records - May 1980	
Aircraft Serial Number	B1B XXXX
Date of Record	88152
Owning Organization	SAC
Possessing Organization	0096BHVWG
Base Code	FNWZ
Accumulated Flight Hours	273.3 hours
TABLE 2 - SAMPLE DATA FROM USAF AFR65-110/GO33 SYSTEM	

Mission Records for May 1988			Aircraft No. B1B XXXX	
Mission	Date	Mission Code	Flight Length	Landings
1	881	T2	4.5	3
2	88133	T3	3.7	2
3	88133	T3	0.9	6
4	88134	T2	7.1	5
5	88134	T2	0.9	9
TABLE 3 - SAMPLE DATA FROM USAF CAMS DATA BASE				

DATA COLLECTION AND PROCESSING PROCEDURES

SDC Data Collection and Processing

The main function of the SDC is parameter monitoring. TABLE 1 defines the list of parameters, their source, monitored sample rate and data compression method. The SDC software performs the five sub-tasks as follows:-

- 1) Each parameter is sampled at the time interval defined by its sample rate shown in TABLE 1.
- 2) Each sampled parameter value is validated so as to protect the archival memory from erroneous data. The tests include maximum and minimum range tests, maximum rate of change tests and excessive recording of a parameter in the archival memory.
- 3) Each parameter is processed through one of two data compression algorithms. These algorithms significantly increase the number of flight hours of data that can be stored in the archival memory by systematically eliminating insignificant or redundant information. Parameters that are cyclic in nature, such as strain records, are compressed using a peak-valley search routine. The routine locates and saves only significant local maximas and minimas in the parameter time history. All intervening points are discarded. Smoothly varying parameters, such as altitude, are compressed by a moving window technique called time history compression. This algorithm saves a parameter value whenever its current value has changed by more than a prescribed amount from the previously saved value.
- 4) Each validated and compressed parameter value is stored in highly compacted variable format storage records. Each record contains a

parameter identifier, the relative time tag to its previous record, the parameter data value and the values of associated time hack parameters. The basic assumption is only to include those data that changed from the previous record.

- 5) The final task is to record the data in the SDC archival memory. Records are archived sequentially into Electronically Erasable Programmable Read Only Memory (EEPROM). Two techniques are used to minimize the impact of EEPROM hardware failure. First a read after write ensures that the information is stored properly. Secondly the memory is logically divided into 1K blocks. Data within blocks are formatted and stored allowing retrieval from any one block independently of all other blocks.

Data Extraction Procedures

At scheduled intervals, or when maintenance indicates that the SDC memory is filled to capacity, the stored flight information is extracted from the SDC memory by a hand portable, battery powered ground support device called the Structural Data Extractor (SDE). The SDE is a micro-processor controlled solid state memory device designed for flight-line usage. The SDE is capable of extracting the contents of the SDC memory module into its own solid state memory and maintaining these data until such time as its memory contents can be transferred on to convenient computer compatible 8 inch flexible disks by the CITS ground processor.

Data Collection and Processing Programs

A software package, shown in FIGURE 1 performs the task of accumulating the flight loads data received from the field and generating computer tapes of flight loads history suitable for batch processing through the IAT analysis system.

The software package comprises two(2) separate computer programs. One program is the Transcription Micro-computer Program which provides the micro-computer to main frame interface. This program was developed by the USAF at the Aircraft Structural Integrity Management Information Systems (ASIMIS) facility and was specifically tailored to the USAF hardware/software environment. The other program is the Raw Data Reduction (RADAR) program which is a main frame computer program for accumulating, validating and editing data and generating analysis data tapes. The functions and inter-relationships of these programs are described below.

Transcription Micro-computer Program

A micro-computer program copies the SDC 8 inch flexible disks as received from the field onto mainframe compatible storage media (disk files or magnetic tape). The data contained therein is copied byte by byte without reformatting onto a mainframe accessible storage device. The output file provides the input to the accumulation and validation mainframe software.

Raw Data Reduction (RADAR) Program

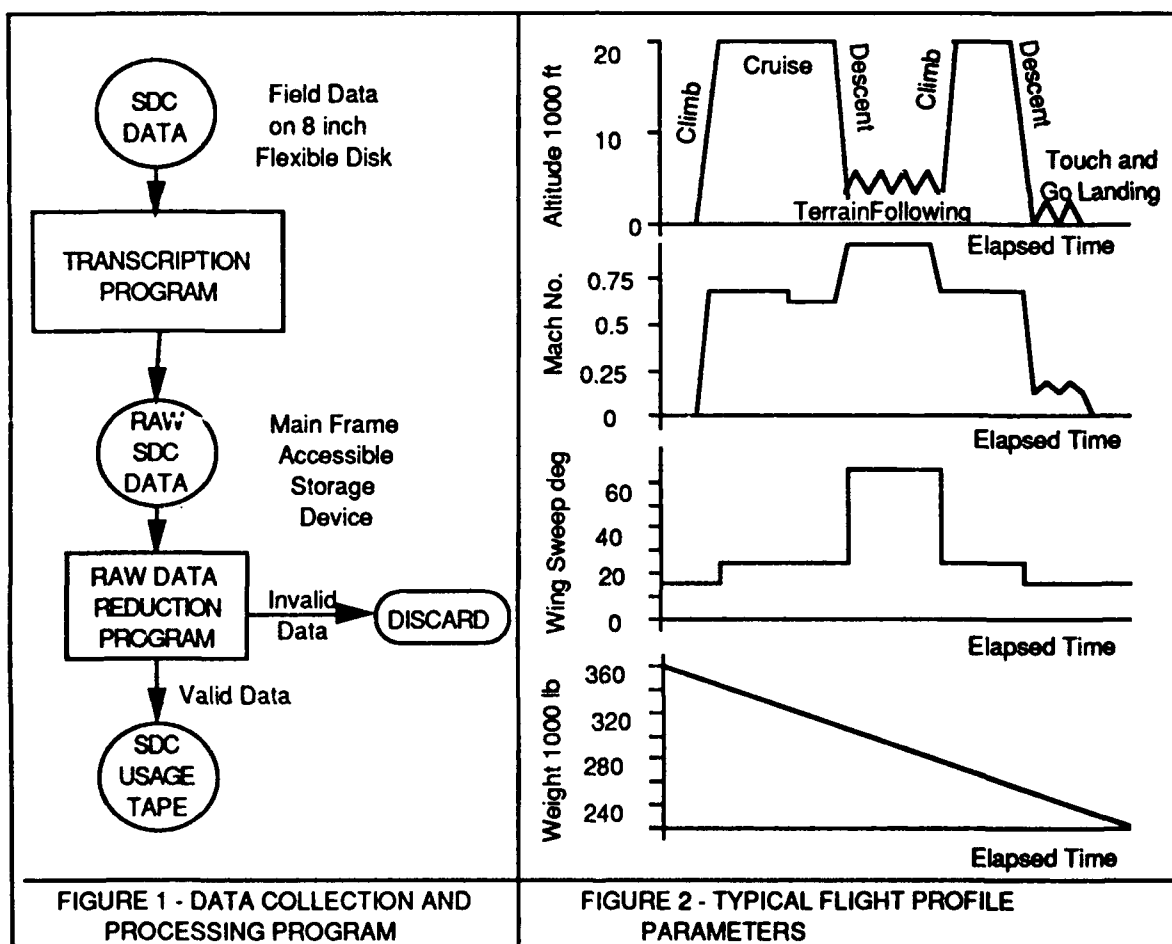
The RADAR program converts the as recorded SDC information into sequenced time histories of each recorded parameter in engineering units. The output of the program is the SDC USAGE TAPES suitable for batch processing through the IAT analysis programs. The program is equipped with sort routines to

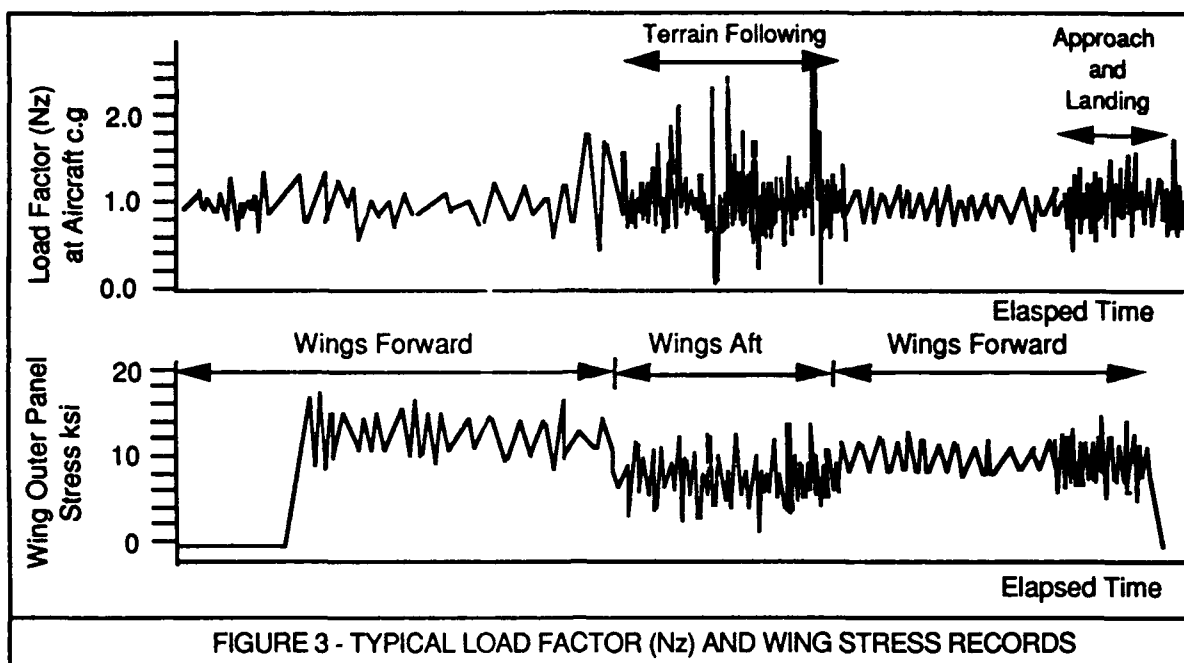
separate the data by aircraft and sort in date sequence, based on the dates provided in the SDC documentary data.

A 'VALIDATION' module evaluates the SDC records for validity and suitability for further processing. If key aspects are missing, clearly invalid or inconsistent with other data, an entire flight may be declared invalid. Flights are declared invalid, for example, if the aircraft serial number identification has been omitted from all documentary records on a particular data extraction from the SDC. Another cause of invalid data are those flights for which the data is incomplete (flights appear to end in the air) due to saturation of the SDC memory or loss of communication between the SDC and CITS. Individual parameters are also evaluated and may be declared invalid. Validity checks include monitoring coincident values of various parameters such as Mach number and altitude for combinations outside the aircraft envelope. A not infrequent occurrence is 'drop out' where a parameter records an extreme value and returns to normal. These can be detected and removed. Extensive printed diagnostics allow the analyst to monitor automated validation decisions made by the program.

An 'EDIT' module is provided wherein individual parameters, flights or an entire SDC record may have validity flags reset.

Sample parameter time histories are shown in plot form in FIGURES 2 and 3





INDIVIDUAL AIRCRAFT TRACKING (IAT) ANALYSIS PROGRAMS

The IAT program has three (3) purposes :-

- 1) To provide for each aircraft, the rate at which the fatigue capability is being used and an estimate of the remaining life
- 2) To provide usage statistics for each aircraft, for each squadron, and force wide to aid USAF using command in force use planning.
- 3) To provide for each aircraft, the intervals at which specified critical structural locations must be inspected in order to maintain structural integrity.

The IAT analysis is implemented using a package of computer programs developed specifically for these tasks. The input to the tracking system are the flight and maintenance records of each aircraft. Its output, supplied in periodic reports, consists of usage statistics, accumulated structural damage estimates, remaining life estimates and structural inspection intervals.

The primary source of flight data are the SDC USAGE TAPES produced by the RADAR program. The back-up source of flight data is the usage records maintained within the CAMS database and input to the IAT program via USAF supplied data tapes.

The usage statistics accumulated by the IAT program are indexed and maintained for individual aircraft defined by serial number, by USAF squadron number and as a force wide accumulation. Damage records are indexed and maintained by structural location on appropriate individual components which are defined by title and component serial number. The definition of components are those items which are considered interchangeable between aircraft or from spares. Serialized components include wing panels, stabilizers, nacelles and wing sweep

actuators. The non-interchangeable components, wing center box and fuselage are identified by the aircraft serial number. All reporting of usage data and damage values is by aircraft serial number. The IAT program maintains a MAINTENANCE RECORDS MASTER FILE to correlate specific component serial numbers to appropriate aircraft.

The number of structural details monitored by the IAT program is limited to a small number of control locations, such that the critical areas of each major component is covered. Typically one location per component will be tracked although multiple points are necessary for some components where the load response to the flight parameters vary between locations. The list and location of the B-1B tracked airframe locations are shown in TABLE 4.

ID	Structural Location	Crack Length Limits (ins)			
		Durability		Dam .Tol	
		Ai	Af	Af	Ai
1	Wing Lower Outboard Pivot Lug Plate	0.01	0.07	0.03	0.19
2	Wing Lower Cover at Rear Spar Attachment	0.01	0.10	0.05	0.79
3	Wing Center Section Lower Skin at Front Spar	0.01	0.20	0.05	1.23
4	Wing Center Section Lower Skin at Mid Spar	0.01	0.18	0.05	5.92
5	Wing Sweep Actuator at Ball Race	0.05	0.22	0.05	0.22
6	Forward Fuselage Dorsal Longeron	0.01	0.58	0.05	0.58
7	Aft Intermediate Fuselage Shoulder Longeron	0.01	0.40	0.05	0.40
8	Aft Intermediate Fuselage Outboard Longeron	0.01	0.20	0.05	1.93
9	Nacelle Support Beam	0.01	0.18	0.05	0.25
10	Stabilizer Support Beam	0.01	0.35	0.05	0.35
11	Horizontal Stabilizer Bearing Support Fitting	0.01	0.10	0.05	0.19
12	Vertical Stabilizer Skin	0.01	0.12	0.05	1.24
13	Nacelle Forward Attachment Fitting	0.01	0.44	0.05	0.44
14	Nacelle Aft Connecting Link	0.01	0.71	0.05	0.70
TABLE 4 - TRACKING CONTROL POINTS AND CRACK LENGTH LIMITS					

Damage computations within IAT are performed for both the durability and damage tolerance regions of the analytic crack growth curve as defined in FIGURE 4 with pre-selected initial flaw sizes given in TABLE 4. The crack growth calculation consists of two phases; the analytical estimate of the crack growth due to the load cycles to which the part has been subjected, and the estimate of the remaining life from the current crack size to the limiting crack length. The limiting crack sizes shown in TABLE 4 are defined as follows:-

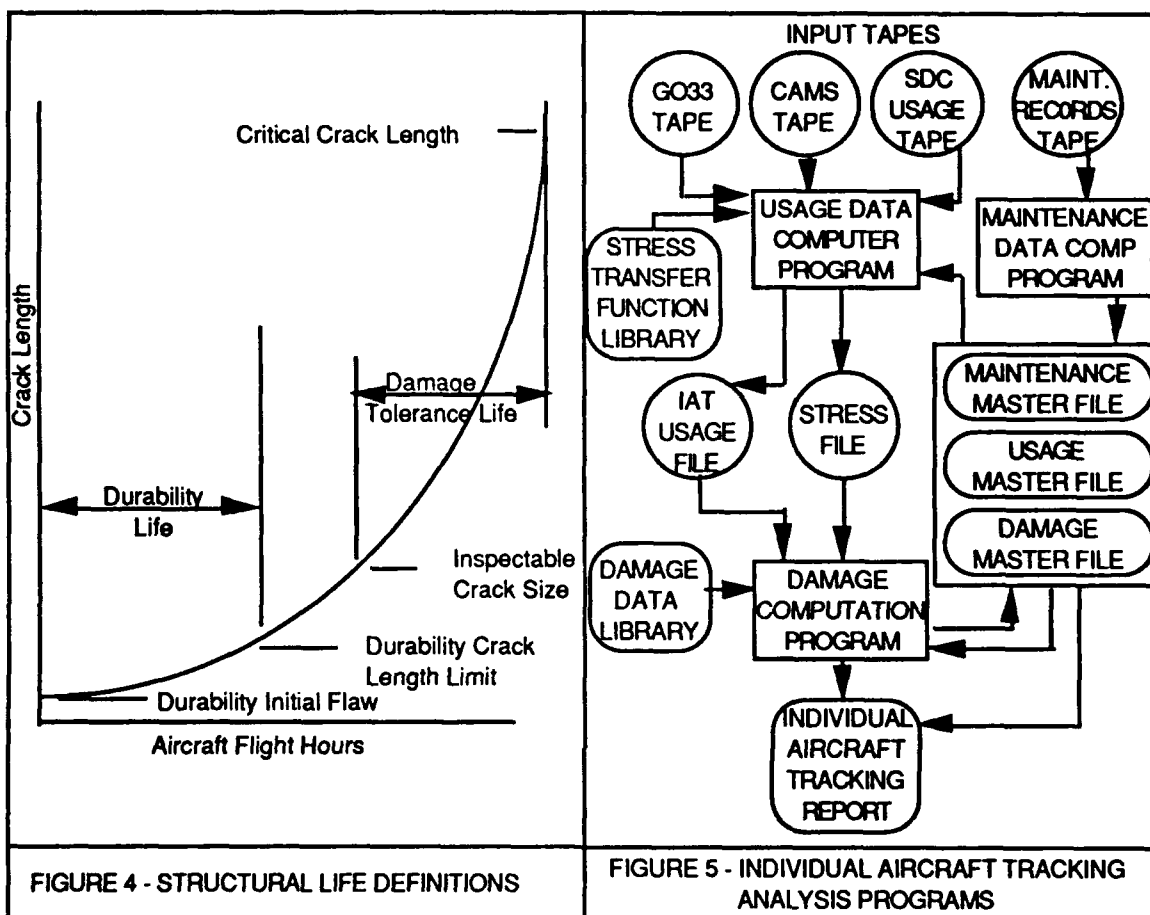
The durability crack limit is the smaller of the economic repair limit and the functional impairment limit.

The economic repair limit is the largest crack that can be repaired without a prohibitively expensive modification to the structure.

The functional impairment limit is the largest crack size that can exist in the structure without impairing the functional capability.

The damage tolerance crack limit is the crack length at which rapid unstable crack growth commences if the structure is subjected to design limit load.

The functions and inter-relationships of the four (4) computer programs and three (3) associated master files within the IAT system package are defined in FIGURE 5 and described below



Maintenance Records Master File

Contains the configuration status and maintenance records of each tracked component on each aircraft. The configuration status is indexed by aircraft serial number and maintains the current allocation of each major component by name and component serial number to that aircraft serial number. The maintenance records are indexed by structural location and component serial number. In addition the configuration status maintains the design modification status to reflect significant design changes during the production or by in-service modifications.

Usage Records Master File

Contains the flight records of each aircraft. The file is indexed by aircraft serial number for the individual aircraft records, by squadron for data accumulated for all aircraft operating within the squadron and by force for the records of force wide usage. A record of the B-1B design usage is also kept.

Damage Records Master File

Contains the accumulated damage records for each tracked location on each component. The records which include the accumulated flight hours on the component and the damage accumulation records stored as crack growth curves. These are indexed by structural location and component serial number. The crack sizes are initialized to the durability and damage tolerance initial flaw sizes defined in TABLE 4.

Usage Data Computer Program (UDCP)

The Usage Data Computer Program has three primary functions:-

- 1) Establishment of the aircraft current accumulated flight hours.
- 2) The compilation of individual aircraft usage information in flight-by-flight sequence for a specific calendar period. The output is a sequential file of usage data organized by aircraft serial number.
- 3) Compilation of stress spectra at each tracked location to represent that usage.

The primary requirement of a tracking program is that all flight hours of each aircraft be included in the damage computation estimates. To ensure this goal the program first establishes the accumulated flight hours at the period end date from the AFR 65-110/GO33 data, a sample of which is shown in TABLE 2.

The second task is to create a flight-by-flight usage file for each aircraft from the SDC records, CAMS utilization records (TABLE 3) or statistically from the historical records in the USAGE RECORDS MASTER FILE. The program is priority driven to use SDC data if valid, CAMS data or finally, if no mission data is available, to use the statistical records of the appropriate squadron. The software code has extensive validation and correction criteria. Typical of the corrections imposed is that of mission type if the SDC documentary data is in violation with the recorded SDC information. The correlation between the SDC and CAMS records is established by comparing the SDC data of, date, flight length, mission type and number of landings with the corresponding CAMS information. The data included in the created usage file is shown in TABLE 5. Of significance is the keys denoting the availability of strain gage records and load factor (Nz) and the time histories for selected parameters.

The third task is to compile a stress spectra file for each tracked structural location from the SDC records using appropriate stress transfer equations which are stored in the STRESS TRANSFER FUNCTION LIBRARY and accessed by the UDCP.

The transfer equation for the tracking control point 2 (TABLE 4) on the wing outer panel is as follows:-

Ground Stress is $16.0 + (0.828 * SG5)$ psi

Flight Stress is $882.0 + (0.734 * SG5) - (9.3 * flap) - (4.7 * wing)$ psi

where

SG5 is Wing strain gage reading

flap is flap angle

wing is wing angle

Ground Stress is defined in the SDC by the weight on wheels parameter..

The equations were developed using a least squares fit regression analysis technique applied to the structural stresses computed for the fatigue design conditions of the airplane. Each tracking point has a unique stress transfer function. For some locations, remote from a strain gage, the transfer function relates the stress to the flight parameters including vertical load factor (Nz), gross weight, Mach number, altitude and airplane geometry. Some tracking control points have different transfer functions on selected aircraft due to design changes during production. The modification status of each aircraft is maintained in the MAINTENANCE RECORDS MASTER FILE.

Data Item	Value	Notes
Date	88125	1
Data Source Key	SDC	1
Spectrum Availability Nz	yes	2
Flight Parameters	yes	2
Wing Strain Gage	yes	2
Wing Actuator Gage	yes	2
Fuselage Gage	yes	2
Stabilizer Gages (3)	yes	2
Mission Code	1	1
Flight Length	4.5	1
Squadron Number		1
Base Location	FNWZ	1
Total Landings	3	1
Take Off Gross Weight	360.0	
Take Off Fuel Weight	170.0	
Landing Gross Weight	220	
Terrain Following Radar (on/off)	off	
Terrain Following Mode (auto/manual)	Manual	
Terrain Following Hours	1.0	
Terrain Following Mach Number	0.85	
Terrain Following Altitude	2000.0	
Terrain Following Wing Angle	65.0	
Terrain Following Gross Weight	300.0	
Refuel Hours	0	
Number of Refuel Operations	0	
Hours above Mach 1.0	0	
Hours < 2000 ft and Mach No. < 0.5	0.5	
Hours with Flaps Down	0.4	
Number of Flap Operations	5	
Number of Wing Sweeps	1	
Pre-Flight Hours	251.3	1
Notes		
1) Data available from CAMS utilization records		
2) Denotes Spectrum Availability for this Flight		
TABLE 5 - IAT USAGE FILE - Typical Mission - Aircraft No. XXXX		

Maintenance Data Computer Program (MDCP)

The task of the MDCP is to maintain the configuration status and maintenance records of each aircraft in the MAINTENANCE RECORDS MASTER FILE.

The configuration status consists of two types of data:-

- 1) The assignment of serialized numbered components to each aircraft.
- 2) The assignment of modification status of each tracking location of each component. The modification status refers to the design of the parts assigned to each aircraft.

The initial assignment of components to specific aircraft serial numbers and the incorporation of design changes was established by the production criteria and stored accordingly in the MAINTENANCE RECORDS MASTER FILE. Changes to the configuration status are conveyed to the IAT system by USAF supplied tapes which reflect maintenance actions by the USAF. The MDCP interrogates the maintenance tapes for items of significance to the IAT, evaluates the data and updates the master file if necessary.

The maintenance actions which affect the damage calculations and inspection requirements must be identified and stored for use by the Damage Computation Program. Typical of such actions are the replacement and/or repair of specified critical parts and the results of structural inspections.

Damage Computation Computer Program (DCCP)

The processing core of the IAT system is the DCCP which performs four primary tasks:-

- 1) Updating the USAGE MASTER FILE with newly processed usage statistics.
- 2) Updating the DAMAGE RECORDS MASTER FILE as a result maintenance actions.
- 3) Computing the analytical structural damage due to the application of the recorded loads, where available, or from the recorded usage. The program updates the DAMAGE RECORDS MASTER FILE to reflect the current damage accumulated at each structural location on each aircraft.
- 4) Computing the remaining available life based on the assumption that future usage is an extrapolation of recent past usage and updating the DAMAGE RECORDS MASTER FILE.

The usage file generated by the UDCP is used to update the USAGE MASTER FILE for appropriate aircraft and squadron as well the force wide records. The master file is maintained to make available usage statistics for last two years, in periods of six months, in addition to the life-time usage. The usage statistics include the distribution of mission types and the number of flight hours and landings for each mission type. Additional data such as the average conditions of take off gross weight, number of wing sweeps, number of flap operations, number of refuelling segments, maximum Mach number and altitude during the flight are kept for each mission type. For mission types which include terrain following the statistics include the time spent in various terrain following modes.

The DAMAGE RECORDS MASTER FILE may be updated as a result of maintenance actions. The DCCP will, on request, interrogate the MAINTENANCE RECORDS MASTER FILE for unincorporated maintenance actions and update the

DAMAGE RECORDS MASTER FILE as appropriate. The prime changes to the file is the reset of durability and/or damage tolerance crack sizes as a result of part replacement, repair or confirmed inspection.

The analytical structural damage is accumulated in terms of increasing crack lengths due to the structural loading caused by the aircraft usage. When stress spectra are available from the SDC records as defined by keys in the USAGE FILE the program utilizes cycle-by-cycle crack growth methodology. The principles of linear elastic fracture mechanics (LEFM) coded into the crack growth program CRKGRO (4) is duplicated in the IAT program. Based on the LEFM concept, the stress state surrounding the crack tip can be characterized by a single parameter, the stress intensity factor K. Furthermore the subcritical flaw growth can be characterized as a function of the cyclic range of the stress intensity factor. The crack growth is computed per cycle (da/dN) using a crack growth rate equation fitted to material property subcritical flaw growth rate data and an integration procedure to obtain the complete crack growth curve.

Fatigue Crack Growth Rate Equation (Walker Equation)

$$\frac{da}{dN} = C[(1-R)^{m-1} \times \Delta K]^n \quad \text{if } R > 0$$

$$\frac{da}{dN} = C[(1-R)^q \times K_{\max}]^n \quad \text{if } R < 0$$

where C, m, n, q are material properties

R is Ratio of applied stress $\sigma_{\min}/\sigma_{\max}$

K_{\max} is Stress Intensity Factor due to applied stress σ_{\max}

K_{\min} is Stress Intensity Factor due to applied stress σ_{\min}

$$\Delta K = K_{\max} - K_{\min}$$

The stress intensity factor equations used in the IAT program depend on the local geometry of the structure and the flaw and were selected from (4). The crack growth integration routine includes a tensile overload retardation model and a compressive load acceleration model also defined in (4).

The current crack size in the DAMAGE RECORDS MASTER FILE is the initial crack size for analysis which computes the change in crack length due to the stress spectrum. The crack growth material properties, local part geometry and crack models are stored in the DAMAGE DATA LIBRARY.

After the accumulated crack growth has been determined for the entire stress spectrum available for the period considered, the USAGE FILE is scanned for any flights for which stress spectra are unavailable. For each of these missions the crack growth is estimated from pre-generated crack growth curves representing various mission profiles. The pre-generated crack growth curves represent specified typical missions covering the expected B-1B usage and are stored in the DAMAGE DATA LIBRARY. The curves were generated analytically using B-1B design loads for four (4) groups of missions.

- 1) Training Missions with a low altitude/high speed (terrain following) segment
- 2) Training Mission without a low altitude/high speed segment.
- 3) Missions representing flight test activities.
- 4) Missions representing predominantly touch and go landing practice.

Within group '1', curves were created for a range of flight lengths, take off gross weights, terrain following time and terrain following criteria of Mach number.

Within groups '2' through '4', curves were created for a range flight lengths and take off gross weights.

Based on the mission type, an algorithm relates the mission to one of the above groups of the pre-compiled crack growth curves. Knowing the current crack length, the change in crack length due to the mission is found for each curve by a graphical integration procedure defined in (5). The final 'delta a' for the mission is found by linear interpolation based on the actual flight parameters of flight length, take off gross weight and terrain following statistics as compared to the parameter values in the pre-generated curves. The accumulated crack size is then 'a current' plus the final 'delta a'. The above analysis is performed for all additional missions using both the durability and damage tolerance regions of the curves. The updated crack sizes are returned to the DAMAGE RECORDS MASTER FILE.

To compute the remaining available structural life, a usage model is constructed. In general, this model is compiled from the historic database kept in the USAGE RECORDS MASTER FILE. The preferred base is the two year history of the appropriate operational squadron. If the accumulated data under this criteria is less than 200 flight hours the database is defined as follows in preferred order: two years operational data force wide, life time force wide or design usage. A composite usage file is thus created in a format identical to that used to define the actual usage. The crack growth is computed using the graphical integration routine defined above, commencing with the current crack size and repeatedly applying the composite usage file until the limiting crack sizes is reached.

REPORTING PROCEDURES

The tracking report program assembles the usage and damage statistics into highly stylized formats suitable for direct inclusion into the periodic IAT and inspection requirement reports. The reports are both tabular and graphical in nature. The usage, maintenance, and damage records are provided for each aircraft, and force wide comparisons are provided for selected usage and damage statistics.

Usage

TABLE 6 presents the usage records for the high-time, median and low-time aircraft while TABLE 7 provides a sample of mission statistics comparing the records from three squadrons with the design usage. TABLE 8 gives a representation of usage statistics for a single aircraft.

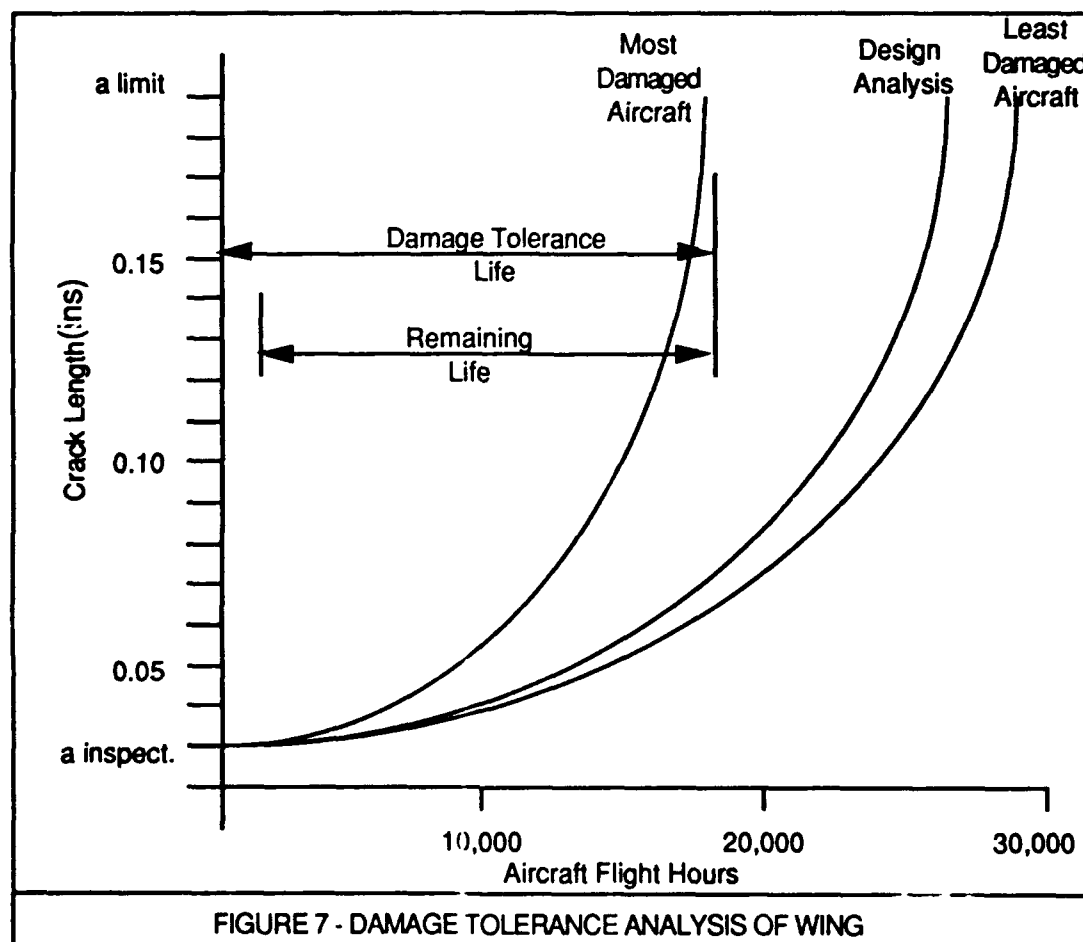
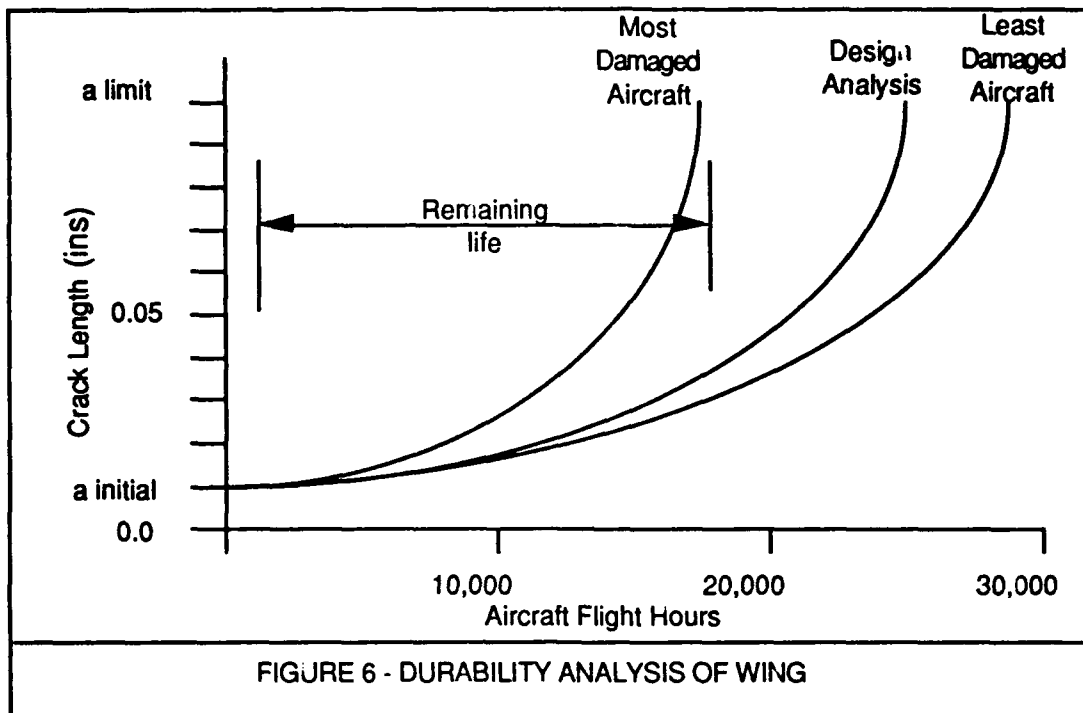
Parameter	Force Leader		Force Median		Force Trailer	
	Value	ASN	Value	ASN	Value	ASN
Flight Hours	740.3	850072	222.1	850067	4.3	860135
Missions	155	850064	55	850063	1	860135
Total Landings	1194	850062	320	860010	7	860135
Terrain Following Hrs	175.3	850064	51.8	860113	1.1	860135
TABLE 6 - FORCE UTILIZATION SUMMARY AS OF 30 JUNE 1988						

Squadron	Mission Type								
	1A	1B	1C	1D	2A	2B	3	4	5
0000AFTCE								99	1
0096BHVWG	64		23	8	3	1			
0344BHVWG	50		24	7	13	2	2		
Design	5	80				15			
Mission Types 1A Training Mission with Terrain Follow, Take off Wt. >300 kips, Mach No. during TF > 0.8 1B Training Mission with Terrain Follow, Take off Wt. <300 kips, Mach No. during TF > 0.8 1C Training Mission with Terrain Follow, Take off Wt. >300 kips, Mach No. during TF < 0.8 1D Training Mission with Terrain Follow, Take off Wt. <300 kips, Mach No. during TF < 0.8 2A Training Mission without Terrain Follow, Take off Wt. >300 kips 2B Training Mission without Terrain Follow, Take off Wt. >300 kips 3 Ferry Flight 4 Flight Test 5 Direct Test Support									
TABLE 7 - MISSION TYPE DISTRIBUTION (percentage) AS OF JUNE 1988									

Damage

The damage records are presented for each tracked location . The type of data available is represented in TABLE 8. An indication of the variation of structural life within the force is shown by curves of the form shown in FIGURES 6 and 7. These curves present the durability and damage tolerance lives from initial flaw to final crack size for the most and least potentially damaged aircraft compared to the design curves.

AIRCRAFT IDENTIFICATION			
AIRCRAFT B1B XXXX AS OF DATE 30 JUNE 1988 COMMAND SAC SQUADRON 0096BHVWG HOME BASE DYESS AFB			
USAGE STATISTICS		MISSION TYPE DISTRIBUTION	
Flight Hours	601.8	Type	Percent
Missions	43	1	95.7
Landings	162	2	3.2
Terrain Following Hrs.	33.4	3	1.1
Average Flight Length	3.6	4	
Average Take Off Gross Wt.	328.0	5	
Average Landing Gross Wt.	231.0		
DAMAGE RECORDS - LEFT HAND WING			
Data Component Serial No. Location	Wing Location 1 Wing L12020010610006 Lower Outboard Lug	Wing Location 2 Wing L12020010610006 Lower Skin	
Component Flight Hours	601.8	601.8	
Hours Since Inspection	601.8	601.8	
Durability Crack Length (ins)	.010023	.010706	
Durability Crack Limit (ins)	.07	.1	
Durability Life (Hours)	>100000	25307	
Remaining Durability Life (Hours)	>100000	24705	
Damage Tolerance Crack Length (ins)	.030793	.056344	
Damage Tolerance Crack Limit (ins)	.19	.79	
Damage Tolerance Life (Hours)	20635	41165	
Remaining Damage Tolerance Life (Hrs)	20033	40564	
TABLE 8 - SAMPLE OF INDIVIDUAL AIRCRAFT RECORDS			



Maintenance Requirements

The inspection interval is a function of the damage tolerance life; namely the damage tolerance life divided by 2.0. Thus for an aircraft with a damage tolerance life of 10000 flight hours, measured as shown in FIGURE 7, the inspection interval is $10000/2 = 5000$ flight hours.

In order to convert the inspection intervals to calendar time the IAT utilization statistics are used. The IAT USAGE MASTER FILE maintains flight hour records for the previous two years in six month blocks. The utilization rate is assumed to be the maximum rate from any block.

For Aircraft XXXX the utilization rates are for example:-

January 1987 - June 1987	92 hours
July 1987 - December 1987	107 hours
January 1988 - June 1988	140 hours
July 1988 - December 1988	200 hours

Thus inspection interval is $5000 / (2 * 200) = 12$ years

For those inspection locations which do not correspond to a tracking control point the following procedure is followed:-

Based on the damage tolerance analysis performed during the design of the aircraft a ratio is obtained between the damage tolerance life of the inspection location and the damage tolerance life of the closest tracking control point. This ratio is then applied to the above inspection interval computation

The durability analyses, a sample of which is shown in figure 6 is monitored so that the necessary maintenance can be scheduled in a timely manner to minimize cost and prevent functional impairment.

IAT DATA PROCESSING COST COMPARISON

The B-1B was the first aircraft fleet to be equipped with an onboard data collector for the purpose of IAT. Most previous IAT programs were based on data collected by means of pilot logs compiled manually during or after the flight. TABLE 9 provides a data processing cost comparison of the pilot log system as compared to the micro-processor recording system. Each primary data processing task is listed with costs distributed to give unity for the entire pilot log system. For comparison the recording system data processing costs are given for usage data collecting only (weight, Mach number altitude and aircraft geometry etc) and for a system which monitors usage data, load factor data and strain gage data. These costs are based only on computing time. Engineering review time is assumed to be comparable for the various systems. The economics of using an electronic recorder for IAT should however consider the software development and hardware costs and the ease of the data collection tasks at the operating bases and the transfer of data between the field and the processing station.

The relative quantity of data to support IAT analysis is also shown in TABLE 9 for the various systems. The SDC provides significantly more data than is available through a pilot reporting system both in terms of time histories of

significant parameters and data on those parameters which cannot be defined by the pilot such as structural load.

Task	Pilot Card Reporting	Usage Recording	Usage & Strain Recording
GO33/CAMS Data Processing	0.01	0.01	0.01
SDC Raw Data Extraction		3.60	3.60
SDC Raw Data Validation		7.34	7.95
Flight Usage Data Compilation		0.01	0.01
Flight Stresses Compilation			3.04
Aircraft Usage Compilation	0.19	0.10	0.10
Damage Compilation (Stress)			1.15
Damage Compilation (Usage)	0.14	0.14	
Remaining Life Estimates	0.65	0.65	0.65
IAT Report	0.15	0.15	0.15
Total Cost Comparison	1.0	11.85	16.52
Data Quantity Comparison	1.0	120.0	600.0
TABLE 9 - IAT DATA PROCESSING COST COMPARISON			

LESSONS LEARNED

The B-1B ASIP loads data collecting system took advantage of the CITS system which monitored many of the parameters required by the IAT program by directly linking the SDC with CITS. This had the advantage of reduced hardware costs for flight parameter measuring sensors and ensuring that these sensors are maintained as required to support other aircraft systems. The disadvantage of the system however was that required changes for ASIP could only be implemented in conjunction with a CITS update. Further changes made in CITS to support other systems sometimes affect the ASIP program.

Any automated data collecting system must have provision and procedures for recording minimal documentary data such as aircraft serial number, mission date, mission type and accumulated flight hours. This data is crucial for defining if data is missing due to failure of the SDC or due to flying without a SDC and for correlating the flight records with other USAF systems such as the CAMS and AFR 65-110/GO33 data. Data without aircraft identification has to be discarded.

The SDC records approximately 50000 bytes of data per flight and each piece of data must be verified as valid or invalid or as changed by the program based on the evidence of other parameters. Approximately 50% of the ground software program is dedicated to validation of the data. Among the prime reasons for data validation requirements is data drop out wherein a parameter providing a normal recording will show an off scale reading and return to normal. The parameters recorded as discrete records (On/Off) (1/0) are subject to bit jitter. A significant improvement could be obtained if off scale data would be recorded differently from legitimate data. This would require 3 bits for recording each discrete parameter. Currently the discrete parameters are checked against other parameters: for example the weight on wheels record is checked against the

altitude and Mach number records. The strain gages were not calibrated prior to service operation consequently the strain gage records corrected by the IAT program. The correction is based on the comparison of the ground static analytically computed loads and the SDC recorded snapshot immediately after the SDC power up. Validation criteria includes acceptable range, standard deviation, rate of change and cyclic frequency for individual parameters and correlation with other parameters.

CONCLUSIONS

Maintenance schedules based on an IAT program allow for immediate inspections to be performed on those aircraft subjected to severe usage thus maintaining the safety of flight. The less severely used aircraft can be scheduled for maintenance over an appropriate period to minimize the impact of out of service aircraft and work load on the maintenance facilities. In addition the correlation of usage statistics with damage rates allows the USAF to rotate aircraft through the squadrons in order to maximize the lifetime capability of the fleet. Finally the utilization plans can be tailored to some degree to minimize the structural damage.

The B-1B is the first USAF aircraft force wherein each aircraft is equipped with a loads monitoring device recording a significant number of flight parameters. Individual aircraft tracking is thus achieved without the use of pilot reporting forms. The variation and complexity of the B-1B flight profiles (high and low altitude mission segments) combined with a variable sweep wing makes the loads measurement a necessity for the IAT program. A very large quantity of data is collected necessitating a highly automated program with minimal manual interaction. The SDC records however, collected from 30 remote sensors and flight crew keyed in data is not 100% perfect. It was necessary therefore to write a sophisticated program capable of verifying, making intelligent assessments and correcting if possible the 'real world' data. After initial teething problems with the SDC and the SDC/CITS interface, the ground software program is operating with a high return of actual flight data. The net result should be to support the B-1B Force Structural Maintenance Plan with significantly enhanced data leading to reduced maintenance costs and improved structural integrity.

REFERENCES

- 1) MIL STD 1530A Military Standard - Aircraft Structural Integrity Program Requirements, December 1979.
- 2) AFR 65-110 Airforce Regulation - Aerospace Vehicle and Equipment Inventory, Status and Utilization Reporting System, April 1980.
- 3) HAF-683-604 Core Automated Maintenance System Functional Description .
- 4) NA-78-491-5 Improved Methods for Predicting Spectrum Loading Effect Fifth Quarterly Report, 30 September 1979.
- 5) Denyer, A.G. Fracture Mechanics Technology Applied to Individual Aircraft Tracking - American Society of Testing and Materials, Proceedings of the Thirteenth National Symposium of Fracture Mechanics.



144-A Mayhew Way, Walnut Creek, California 94596, USA • (415) 947-0400

"Flight Loads Recorder Installation

in

Tutor Jet Trainer"

By:

Jack Reichel and Ali Ghannadan

ESPRIT Technology Inc.

Presented at:

1990 ASIP Conference

San Antonio, Texas

December 12, 1990



144-A Mayhew Way, Walnut Creek, California 94596, USA • (415) 947-0400

"Flight Loads Recorder Installation"

in

Tutor Jet Trainer"

Introduction -

The Canadian Forces has adopted the ASIP philosophy to maintain its fleet of aircraft. In furtherance of this effort, a microprocessor Flight Loads Data Recording (FLDR) system was installed in a Tutor jet trainer and evaluated over a one-year period. The system provides an accurate record of all significant structural loads, on a "point in the sky" basis; i.e. the precise reading of each load peak and its time of occurrence, as well as the plane's altitude and airspeed, and the instantaneous reading of all other sensors.

This paper reviews the details of the eight-channel system and its installation, including recorder characteristics, transducers used, strain gauge locations, data compression algorithms and ground transcription.

Flight test results under controlled conditions are given and the benefits of the system for standard ASIP spectrum development are shown. Data will also be presented from two flights in which the test pilot flew first normally and then intentionally more aggressively. The effect of pilot input on strain levels is thus identified by comparing data from these flights that were identical except for the differing amounts of control input aggressiveness.

Also shown is how parameter correlation can be verified to establish a streamlined set of parameters for IAT tracking.

Finally, we show how the system's capability to graph a flight immediately after landing is used for pilot training and ASIP flight profile evaluation.

**This paper presents each slide on the right pages
and the speaker's accompanying narrative
on the facing left page.**

TOPICS

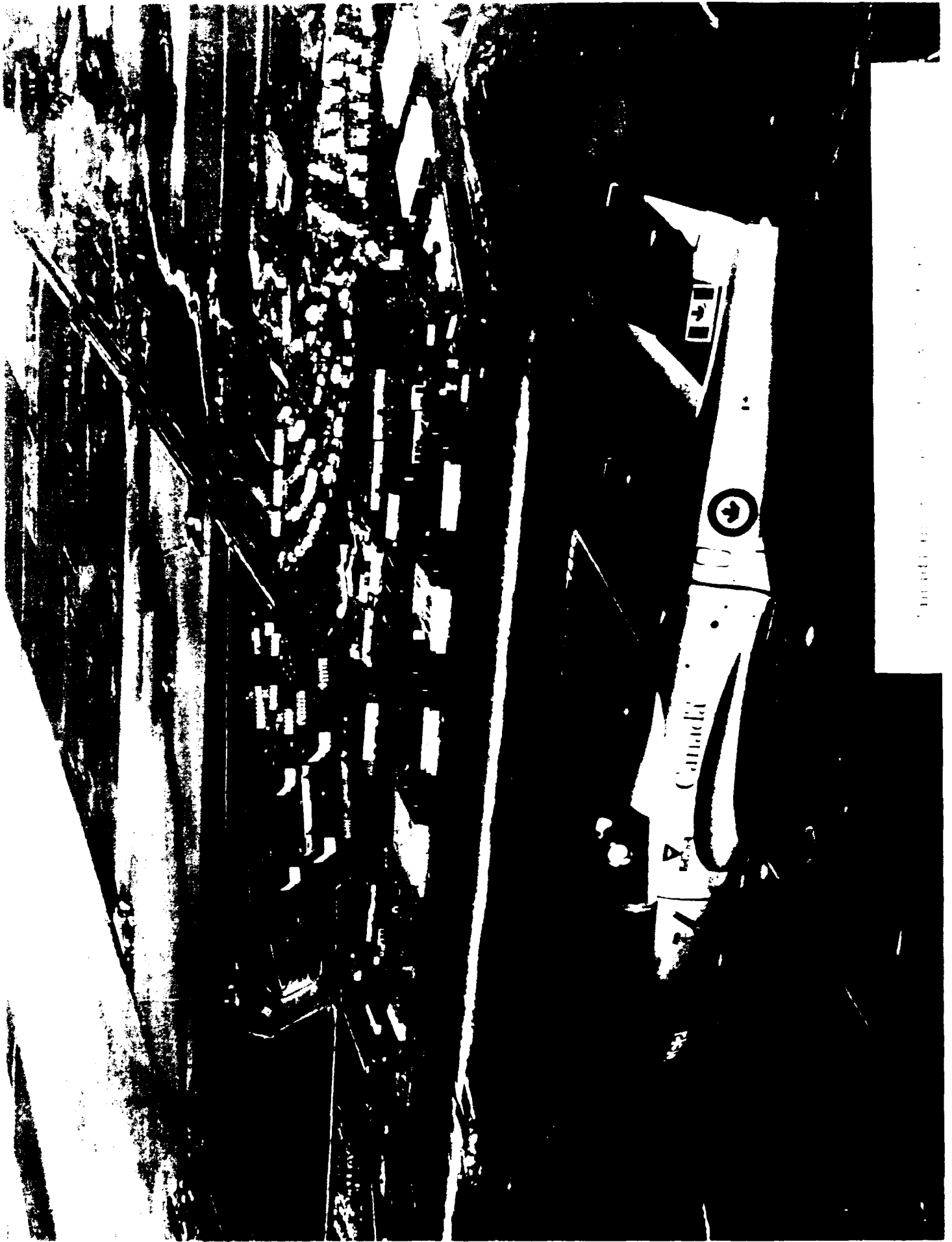
- * REVIEW OF FLDR INSTALLATION
- * STANDARD USAGE AND SPECTRUM DATA
- * LOADS EFFECT OF CONTROL SYSTEM INPUTS
- * PARAMETER CORRELATION
- * PILOT DE-BRIEFING

Aircraft Description -

The CT-114 Tutor was designed and built in Canada in the early 1960's by Canadair of Montreal, now Bombardier, and has been used since that time as the basic jet trainer of the Canadian Armed Forces.

The Tutor features side-by-side seating, similar to the USAF T-37 trainer. Its "G" limits are +7.33 and -3, the same as the F-5.

The Tutor is also used by the Snowbirds, Canada's world-renowned precision aerobatic team.



Canadian military aircraft in flight over a snowy mountain range.

Recording System Configuration

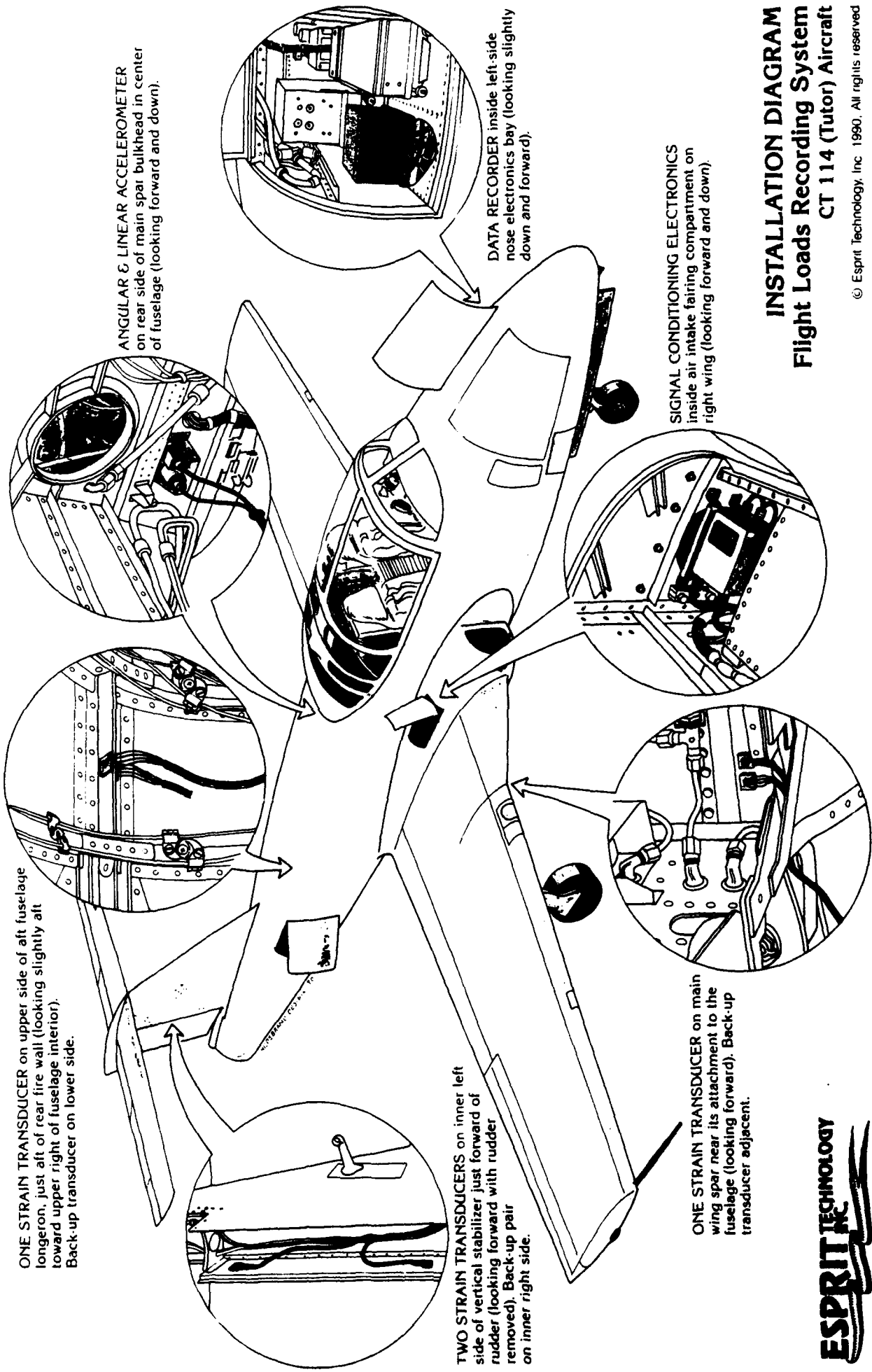
Data recorder - ELAPS IIA (8 channels) with Real-Time Clock

SCE module - provides signal conditioning for the strain gauges as well as altitude & airspeed signals (since the Tutor is not fitted with a CADC).

Accelerometer module - provides normal acceleration (Nz) and roll acceleration signals.

Strain Sensors - temperature-compensated, full-bridge modules located on:

- wing spar
- aft fuselage longeron
- vertical stabilizer tip
- vertical stabilizer base



ONE STRAIN TRANSDUCER on upper side of aft fuselage longeron, just aft of rear fire wall (looking slightly aft toward upper right of fuselage interior). Back-up transducer on lower side.

ANGULAR & LINEAR ACCELEROMETER on rear side of main spar bulkhead in center of fuselage (looking forward and down).

TWO STRAIN TRANSDUCERS on inner left side of vertical stabilizer just forward of rudder (looking forward with rudder removed). Back-up pair on inner right side.

DATA RECORDER inside left-side nose electronics bay (looking slightly down and forward).

SIGNAL CONDITIONING ELECTRONICS inside air intake fairing compartment on right wing (looking forward and down).

ONE STRAIN TRANSDUCER on main wing spar near its attachment to the fuselage (looking forward). Back-up transducer adjacent.

INSTALLATION DIAGRAM **Flight Loads Recording System** **CT 114 (Tutor) Aircraft**

© Esprit Technology, Inc. 1990. All rights reserved



Data Compression Algorithm -

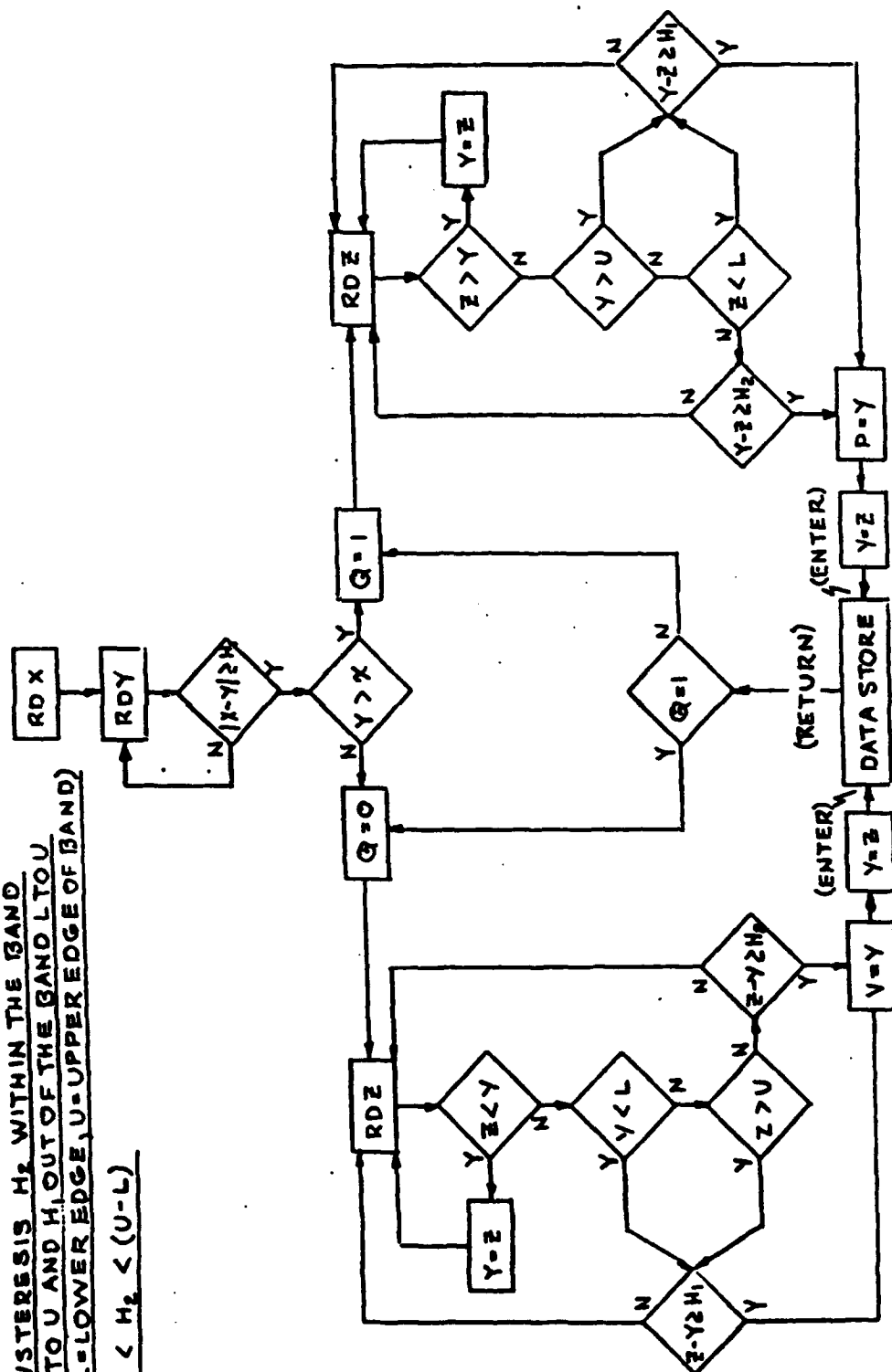
For on-board data compression of the Event recording, a Sequential Peak Valley (SPV) algorithm was provided in the recorder's embedded software.

This algorithm can also be provided in a variation (shown) which establishes two separate hysteresis levels. This permits use of a larger hysteresis level in the region close to zero, thereby streamlining the recording by reducing data "chatter".

Sequential Peak Valley (SPV) Algorithm (with Dual Hysteresis)

SEQUENTIAL PEAK VALLEY DETECTION ALGORITHM
WITH DUAL HYSTERESIS H_1 AND H_2 :

HYSTERESIS H_2 WITHIN THE BAND
L TO U AND H_1 OUT OF THE BAND L TO U
(L=LOWER EDGE, U=UPPER EDGE OF BAND)
 $H_1 < H_2 < (U-L)$

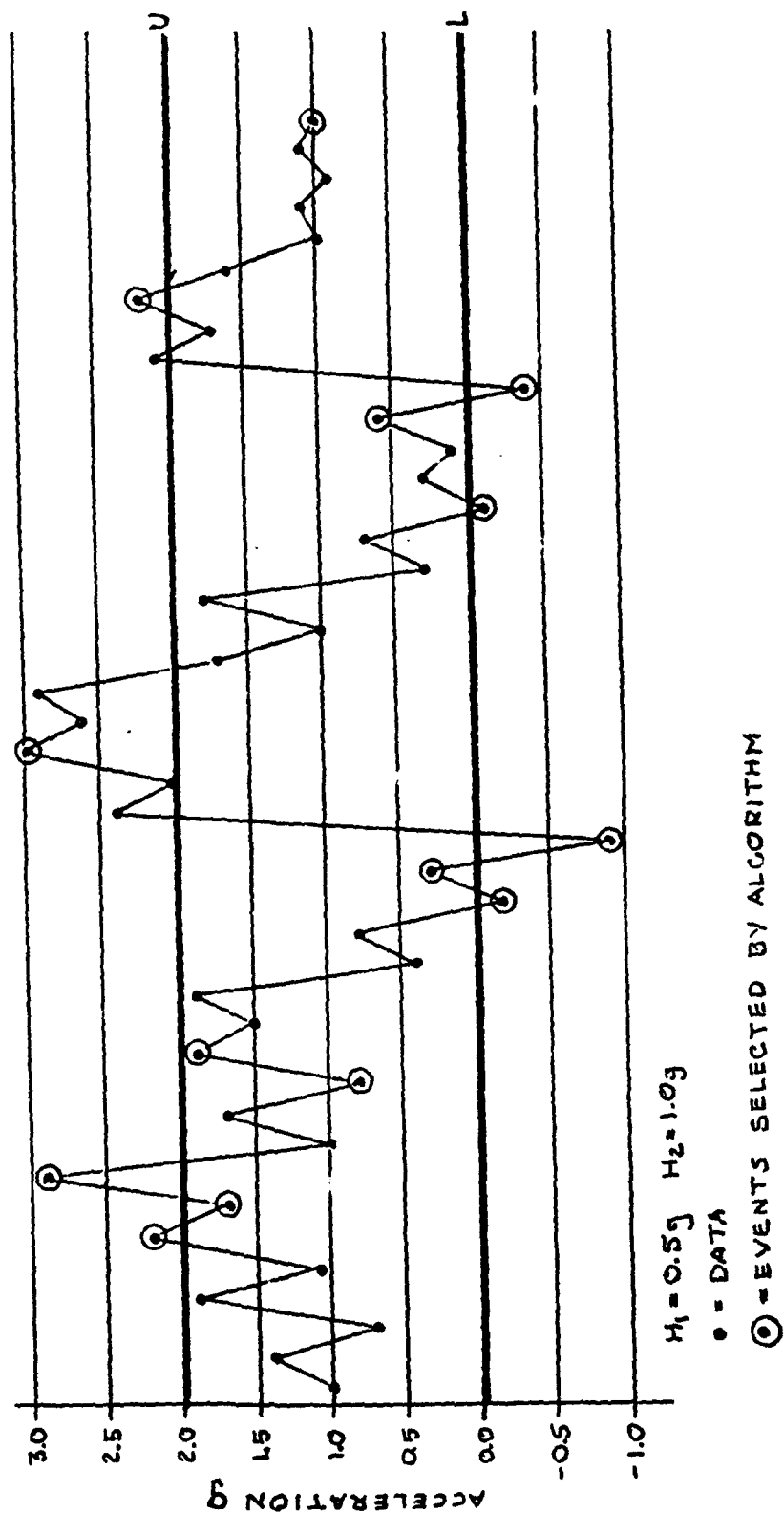


Typical Load Factor (Nz) Curve -

This slide illustrates how Nz peaks and valleys are qualified, and recorded in memory on the Event file.

The same procedure is used for each of the five other signals that were set up to be trigger variables.

Sample Nz Event Detection using SPV



System Characteristics -

- Data separated by flight and coded by Takeoff date time
- Four files recorded for each flight:
 - Events (for each signal designated as a SPV trigger)
 - Time history of all 8 inputs at 60-second intervals
 - System Health and Built-In Test report
 - Mission Summary (takeoff/landing times, touch & goes)
- System parameters can be changed *as-installed*:
 - Algorithm settings (SPV gates and hysteresis)
 - sampling rate of each trigger channel
 - time slice sampling interval
- Up to 6 inputs can be selected as independent triggers
(It is important to note that activating or deactivating a trigger has no effect on the other parameters or settings)
- High sample rate (≤ 400 s/sec per channel, or 3200 s/sec total) measures Event peaks accurately. Note that a 1% peak accuracy requires sample rate of $22 \times$ bandwidth
- Sufficient memory for 80 flights between downloads
- Flight results are graphed in color at landing

System Characteristics

- All Data time-coded in GMT
- Multiple recorded files
- Recorder program settings easily changed
- Multiple Triggers -- easily activated
- High sample rate to capture Event peaks
- Long Data Retrieval Intervals
- Graph data immediately upon landing

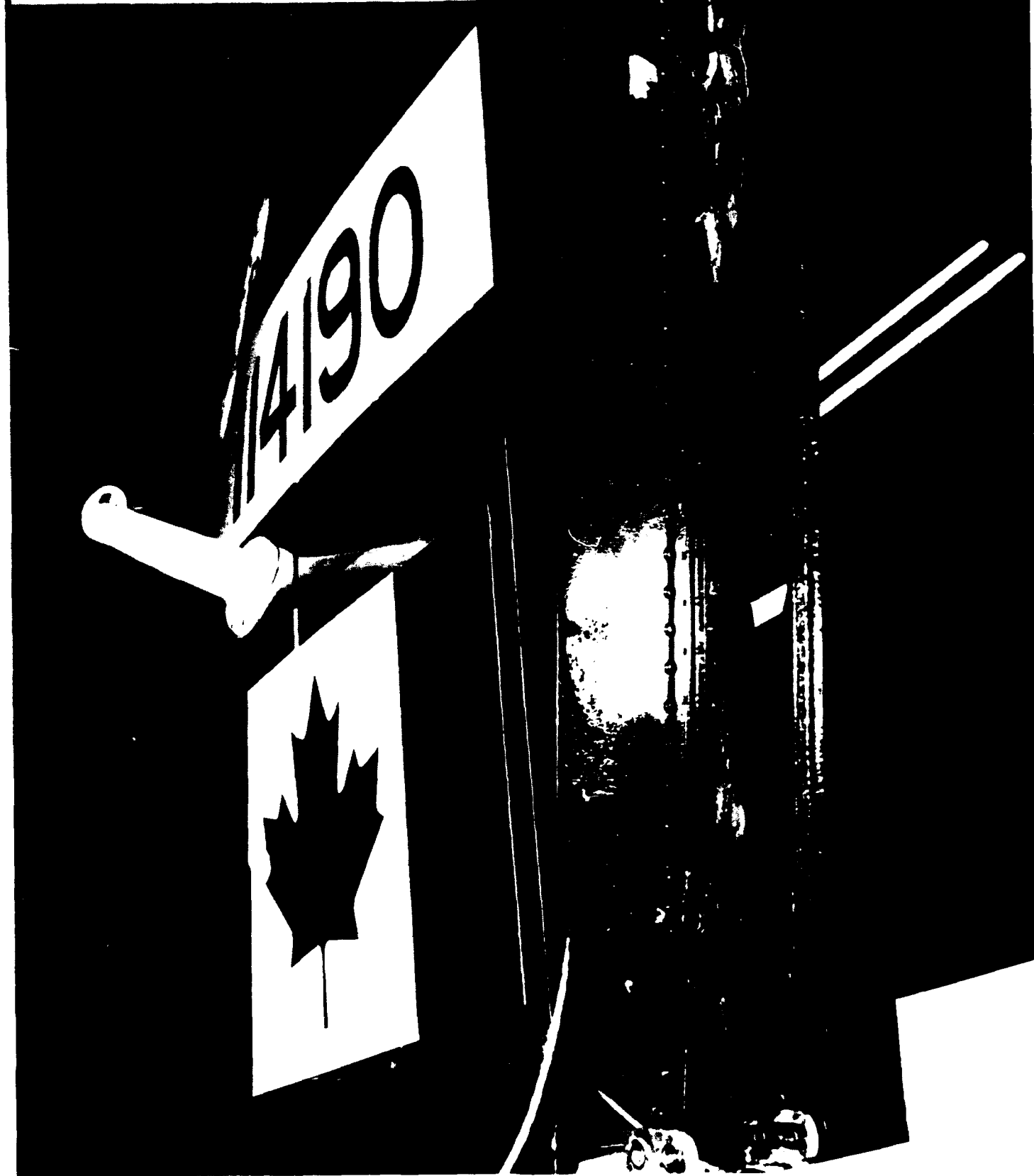
System Installation -

Photos were presented, showing details of the installation:

- Recorder installation in LH Elex bay - Nose
- Signal Conditioning Electronics installed in wing root
- Accelerometer module installed on main spar bulkhead
- Strain gauge on RH wing lower spar cap
- Strain gauge on aft fuselage longeron
- Strain gauges on Vertical Stabilizer base and tip (shown)

Note: in each of the four strain gauge locations, backup gauges were installed alongside the primary gauges.

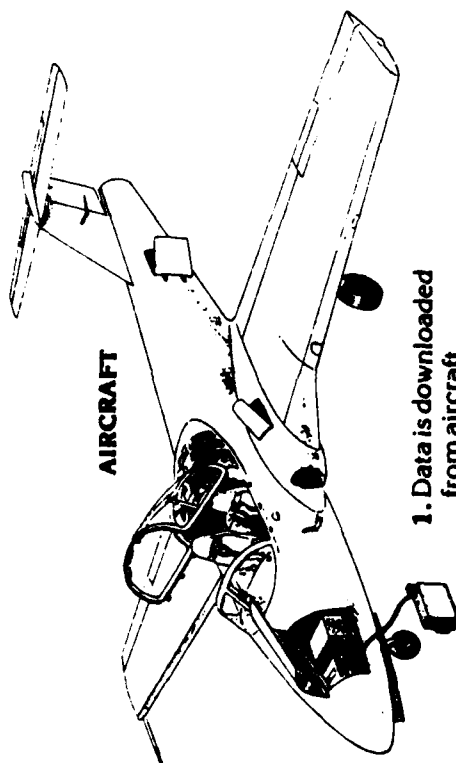
Strain Gauge Installation
Vertical Stabilizer



Data Retrieval and Transcription -

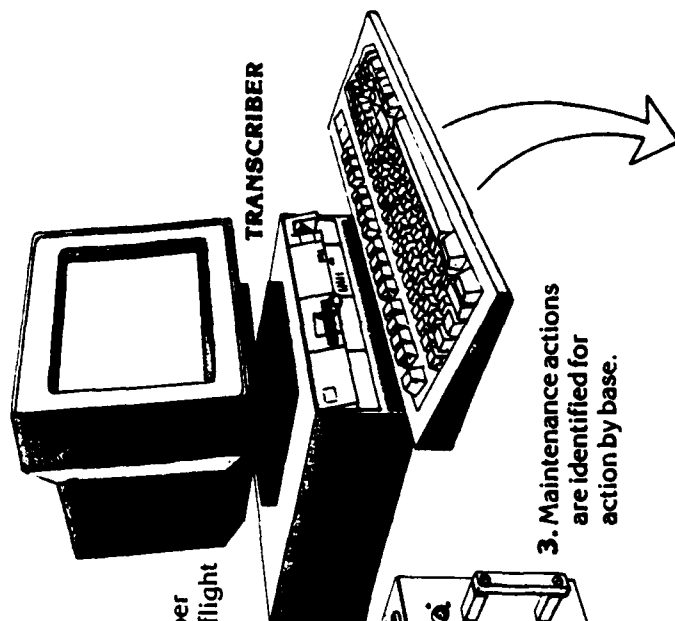
- System downloaded monthly
- Output on disk; sent to the ASIP engineers for analysis
- Built-in test faults corrected at base level.
Can also verify pilot over-stress reports
- Each flight can be graphed in color/zoom on Transcriber
for debriefing and flight review

FLIGHT LINE



1. Data is downloaded from aircraft once a month.

MAINTENANCE OFFICE

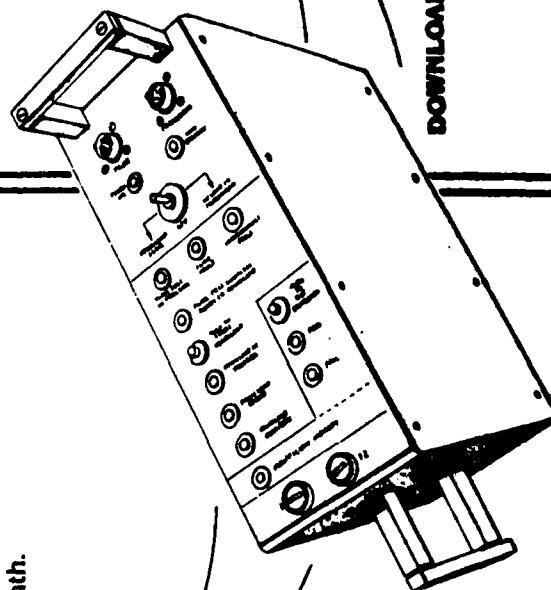


2. Data is transferred to transcriber where it is decoded, sorted by flight and stored on disk.

3. Maintenance actions are identified for action by base.

DISK

4. Data disk is sent to analysis group.



DOWNLOADER*

ESPRITE TECHNOLOGY

DATA RETRIEVAL DIAGRAM
Flight Loads Monitoring System
CT 114 (Tutor) Aircraft

*NOTE: Interrogator unit can also be used for downloading and transfer of data to disk.

© Esprit Technology, Inc. 1990. All rights reserved

Printout of Time History File

I mentioned earlier that there are a number of files recorded for each flight.

This slide shows a printout of a typical Time-History file. It is a snapshot of all 8 inputs, recorded every 60 seconds after liftoff. As noted earlier this time interval can easily be reprogrammed by the user.

By graphing this file, the separation of a flight into its various segments can be determined readily.

Printout of Event file

This slide shows a typical Event file printout -- in this case the events that were triggered by Nz exceedences.

A similar Event file is recorded for each additional input selected by the user as a trigger.

This data is used directly to determine usage severity by mission, and to calculate load factor spectra.

EVENT FILE

FLIGHT DATE: 8/11/88 AIRCRAFT TAIL NUMBER: 164101

Altitude	Time	Wz	Altitude	a-Wing	a-Fuselage	Roll-Accel	Airspeed	a-VStab-Base	a-VStab-Tip
10770.00	077.000	2.81	10770.00	550.00	-136.00	0.00	251.81	-156.00	-125.00
10770.00	077.000	-0.00	10770.00	-507.00	-488.00	0.00	256.66	-24.00	160.00
10770.00	077.000	0.85	10770.00	390.00	-224.00	0.00	261.31	-144.00	-119.00
10770.00	077.000	0.54	10770.00	31.00	-416.00	0.00	93.26	-34.00	-85.00
10770.00	077.000	0.04	10770.00	507.00	42.00	0.00	307.20	-108.00	17.00
10770.00	077.000	0.59	10770.00	21.00	-482.00	-0.57	76.54	-108.00	51.00
10770.00	077.000	1.73	10770.00	100.00	-490.00	-0.57	93.26	-336.00	-340.00
10770.00	077.000	0.00	10770.00	0.00	-599.00	-1.00	126.04	-192.00	-170.00
10770.00	077.000	0.04	10770.00	575.00	-259.00	0.00	211.77	-190.00	-137.00
10770.00	077.000	0.15	10770.00	26.00	-259.00	0.00	126.97	-60.00	-51.00
10770.00	077.000	0.15	10770.00	393.00	-147.00	0.00	186.93	-84.00	-58.00
10770.00	077.000	0.85	10770.00	155.00	-28.00	0.00	266.52	24.00	85.00
10770.00	077.000	0.15	10770.00	440.00	-35.00	0.00	298.38	-132.00	-58.00
10770.00	077.000	0.73	10770.00	117.00	-140.00	0.00	268.69	-120.00	-58.00
10770.00	077.000	0.15	10770.00	623.00	-7.00	0.00	288.99	-168.00	-170.00
10770.00	077.000	0.66	10770.00	699.00	-21.00	0.00	286.52	-180.00	-170.00
10770.00	077.000	-0.15	10770.00	356.00	21.00	0.00	286.52	-204.00	-187.00
10770.00	077.000	0.58	10770.00	65.00	-147.00	0.00	291.58	-144.00	-102.00
10770.00	077.000	3.15	10770.00	1376.00	77.00	0.00	291.46	-168.00	-170.00
10770.00	077.000	3.46	10770.00	702.00	-7.00	0.32	284.05	-192.00	-187.00
10770.00	077.000	5.92	10770.00	1355.00	31.00	0.00	279.11	-228.00	-238.00
10770.00	077.000	4.88	10770.00	1157.00	56.00	0.00	276.64	-204.00	-204.00
10770.00	077.000	5.95	10770.00	1379.00	70.00	0.00	274.15	-190.00	-187.00
10770.00	077.000	0.77	10770.00	104.00	-168.00	0.00	291.58	-192.00	-102.00
10770.00	077.000	3.00	10770.00	524.00	-84.00	0.00	279.11	-190.00	-170.00
10770.00	077.000	1.98	10770.00	416.00	-105.00	0.00	276.64	-180.00	-170.00
10770.00	077.000	3.08	10770.00	537.00	-91.00	0.00	274.15	-180.00	-187.00
10770.00	077.000	0.46	10770.00	13.00	-259.00	0.00	256.66	-122.00	-65.00
10770.00	077.000	2.15	10770.00	390.00	-147.00	0.00	291.46	-153.00	-170.00
10770.00	077.000	0.69	10770.00	78.00	-210.00	0.00	288.99	-108.00	-68.00
10770.00	077.000	5.08	10770.00	1131.00	-7.00	0.00	279.11	-228.00	-272.00
10770.00	077.000	0.42	10770.00	26.00	-264.00	0.00	236.91	-108.00	-51.00
10770.00	077.000	1.92	10770.00	351.00	-135.00	0.00	254.39	-180.00	-170.00
10770.00	077.000	0.65	10770.00	104.00	-77.00	0.00	303.12	-60.00	-34.00
10770.00	077.000	2.96	10770.00	595.00	-55.00	0.00	276.64	-156.00	-136.00
10770.00	077.000	1.62	10770.00	286.00	-203.00	0.00	225.19	-144.00	-85.00
10770.00	077.000	3.15	10770.00	524.00	-49.00	0.00	307.20	-204.00	-153.00
10770.00	077.000	0.54	10770.00	39.00	-147.00	0.00	296.41	-108.00	-68.00
10770.00	077.000	2.46	10770.00	442.00	-93.00	0.00	238.99	-192.00	-153.00
10770.00	077.000	-0.06	10770.00	-104.00	-175.00	0.67	286.52	-396.00	-493.00
10770.00	077.000	2.46	10770.00	429.00	-203.00	0.00	225.19	-190.00	-153.00
10770.00	077.000	0.69	10770.00	65.00	-63.00	0.00	284.05	-84.00	-68.00
10770.00	077.000	2.91	10770.00	553.00	31.00	0.00	311.29	-108.00	-59.00
10770.00	077.000	0.61	10770.00	52.00	-42.00	0.67	298.88	-132.00	-68.00

We have shown how data from the Flight Loads recording system is used for load factor spectrum development, in conjunction with a Load/Environment Spectrum Survey (LESS) program.

Now, let's look at some side benefits of such a recording system.

In one particular case, it was decided to see if the system was sensitive enough to measure the difference in recorded loads between a test flight flown with normal control inputs, and one using aggressive control forces.

This slide shows the flight syllabus of various aerobatic maneuvers that was established. Many of the maneuvers were from the Snowbird routine.

FLIGHT DATA - COMPARISON OF RECORDED LOADS,
NORMAL CONTROL INPUTS
VS.
AGGRESSIVE INPUTS

Flight Syllabus for test flight on 7 Feb. 1990:

<u>Item</u>	<u>Maneuver</u>
1.	Spin (left)
2.	Spin (right)
3.	Loop
4.	Clover Leaf
5.	Cuban 8
6.	Hesitation Roll
7.	Roll (off the top)
8.	Half Roll Pull Through
9.	Barrel Roll
10.	Roll In/Out
11.	Mini/Maxi
12.	Vertical Roll
13.	Vertical 8
14.	Slow Roll
15.	Spin (left)
16.	Closed Pattern
17.	Landing

The first test flight -- the one using normal control inputs -- was flown on 7 Feb 90 at 20:00 hours Zulu.

This slide shows the data from the Health file, including the BIT results.

Data from Health File -- Test with Smooth Inputs

Flight Date: 2: 7: 90 Aircraft Tail Number: 114190

19:48:06 Power on

FLDR Built-In Test results:

Master: Number of Satellites = 2

Real Time Clock Test: Pass

Dual Port RAM Test: Pass

Program Checksum Test: Pass

Satellite #1:

Static ram test: Pass

Dual Port ram test: Pass

Program Checksum Test: Pass

Offset test, channels 1,2,3,4: Pass

Load test, channels 1,2,3,4: Pass

Satellite #2:

Static ram test: Pass

Dual Port ram test: Pass

Program Checksum Test: Pass

Offset test, channels 5,6,7,8: Pass

Load test, channels 5,6,7,8: Pass

Average Starting Values:

Nz.....78.00

Altitude.....225.00

:

:

e - Vstab Tip.....130.60

The Health file also records all ground and flight times,
including Touch and Goes.

Health File (continued).....

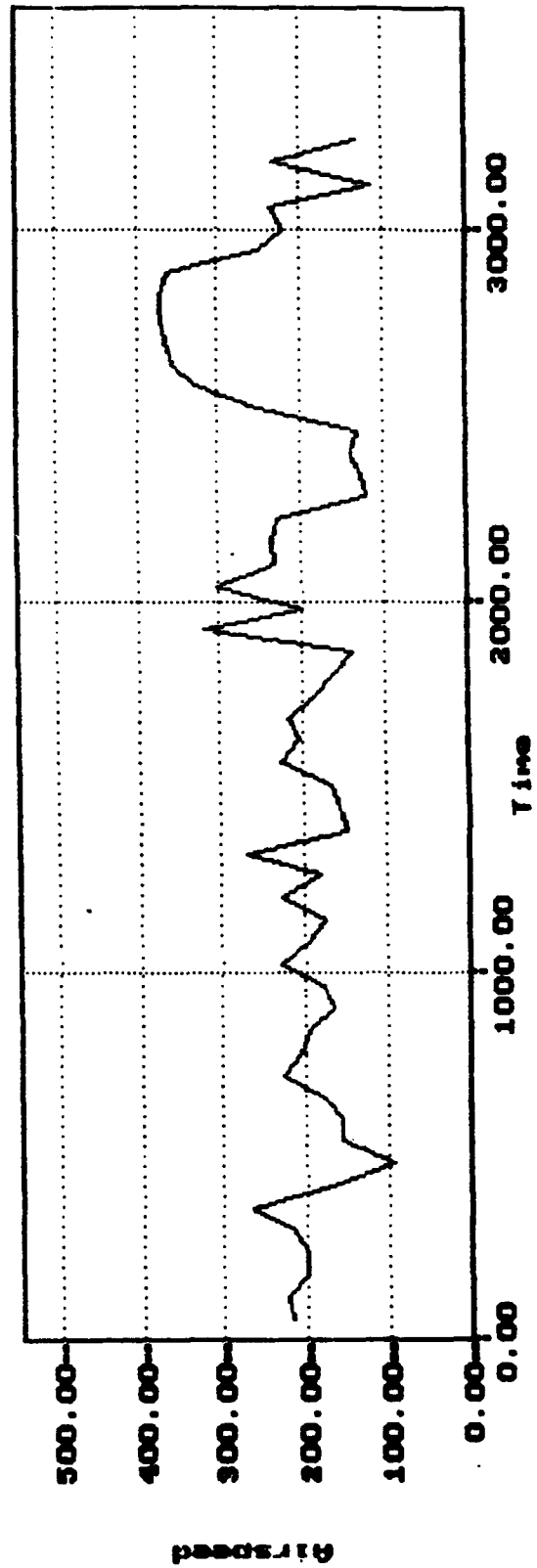
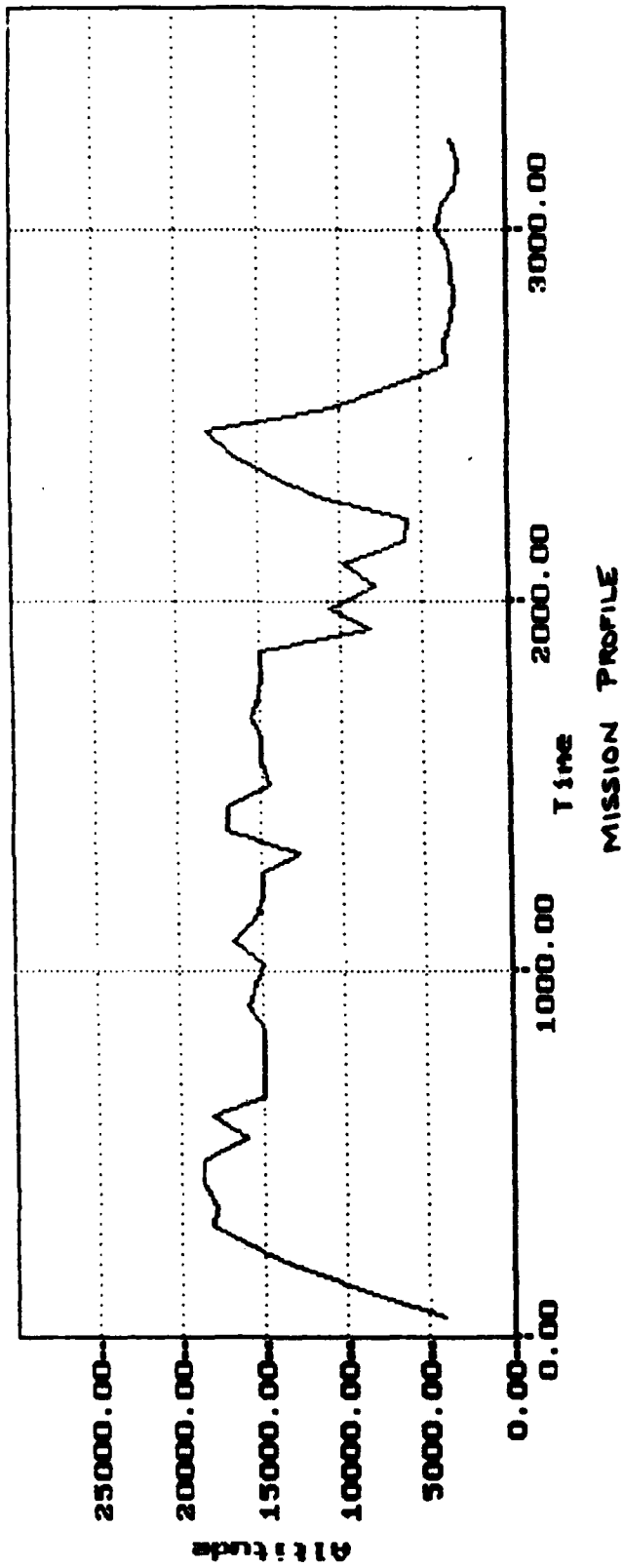
Ground Preflight <u>720</u> seconds before Flight 1		
20:00:06	Takeoff Flight 1	
20:54:47	Land Flight 1	
	Duration of Flight was <u>3281</u> seconds	} CAUSED BY FIRM LANDING
	Ground Time 0 seconds before Flight 2	
20:54:47	Takeoff Flight 2	
20:54:48	Land Flight 2	
	Duration of Flight 2 was <u>1</u> second	
	Ground Time 0 seconds before Flight 3	
20:54:48	Takeoff Flight 3	
20:54:49	Land Flight 3	
	Duration of Flight was <u>1</u> seconds	
	Ground Time 1 seconds before Flight 4	
20:54:50	Takeoff Flight 4	
20:54:50	Land Flight 4	
	Duration of Flight was <u>4</u> seconds	

Mission Information

Mission Code = Test Flight - aerobatic manoeuvres, normal
Configuration Code = Clean
Gross Weight at Takeoff = 7434 lbs.
Gross Weight at landing = 5941 lbs.
Fuel Weight at Takeoff = 1173 litres (1945.3 lbs.)
Fuel Weight at Landing = 273 litres (452.7 lbs.)

This slide shows the graph of the resultant Time History file of the test flight with normal control inputs.

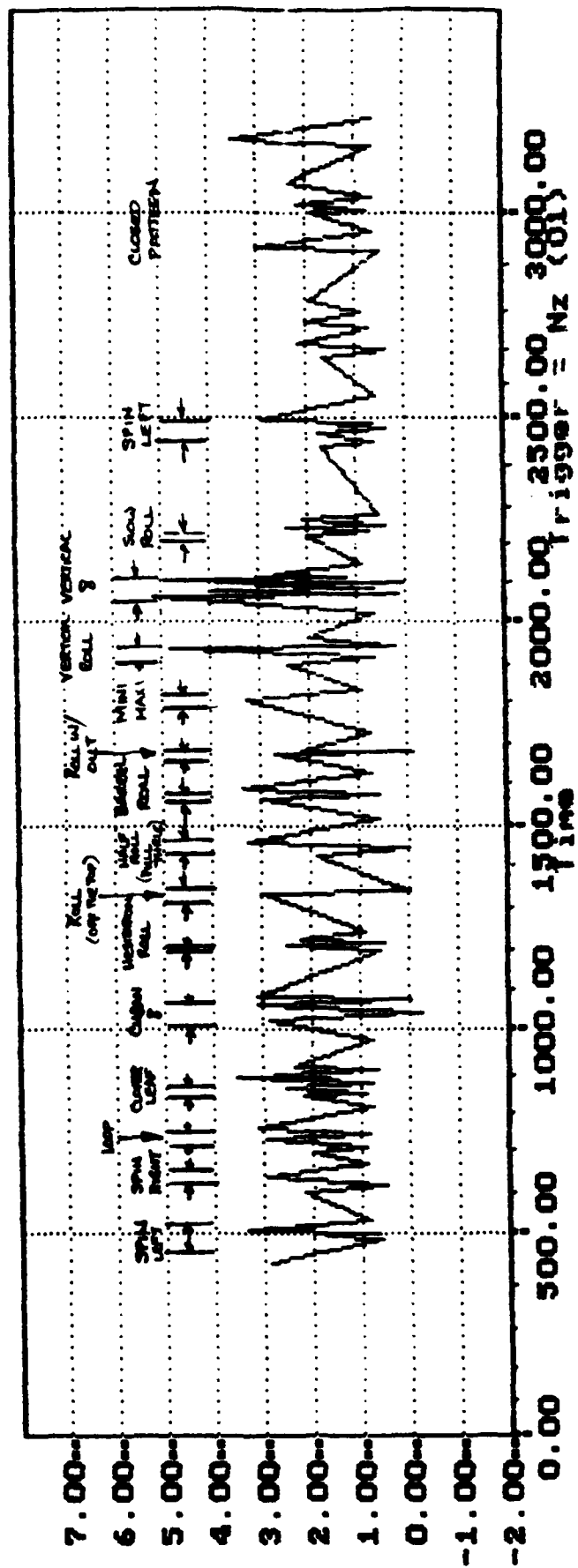
This curve provided the ASIP engineers with a general overview of the mission profile.



This slide shows the graph of one of the Event files of this same flight.

This file is of the events triggered by Nz.

Each of the maneuvers can be readily identified on the flight graph.



Using the flight syllabus as a guide, we can now establish the time duration, altitude and airspeed conditions for each maneuver in the flight test.

Note the rudder vibration reported by the pilot during snap roll entry to the left spins. Remember this because we will examine the condition in more detail later.

Flight Test Results

Including comments from test pilot

Feb. 7 '90 test flight (smooth inputs)

<u>Item</u>	<u>Maneuver</u>	<u>Time (sec)</u>	<u>Alt (ft)</u>	<u>Airspd (KIAS)</u>
1. *	Spin (left)	480 - 510	18 - 15K	115 (entry) - 80
2. #	Spin (right)	615 - 645	18 - 14.5	115 (entry) - 80
3.	Loop	730 - 765	15K	300
4.	Clover Leaf	855 - 885	14.5K	300
5.	Cuban 8	1020 - 1087	14.7K	250
6.	Hesitation Roll	1200 - 1215	15K	250
7. §	Roll(off the top)	1320 - 1350	13K	300
8.	½ Roll Pull Thru	1440 - 1465	17 - 13.5K	250
9.	Barrel Roll	1500 - 1595	14.5K	250
10.	Roll In/Out	1675 - 1690	15K	300
11.	Mini/Maxi	1800 - 1830	15K	300
12.	Vertical Roll	1930 - 1950	7K	300
13.	Vertical 8	2000 - 2010	7K	300
14.	Slow Roll	2220 - 2232	6K	250
15. ¶	Spin (left)	2470 - 2500	18 - 15K	115(entry) - 100
16.	Closed Pattern			
17.	Landing (Firm)			

Notes: * - unusual spin - snap roll entry; rudder vibration noted

- normal spin

§ - numerous banking between manoeuvres to stay in area

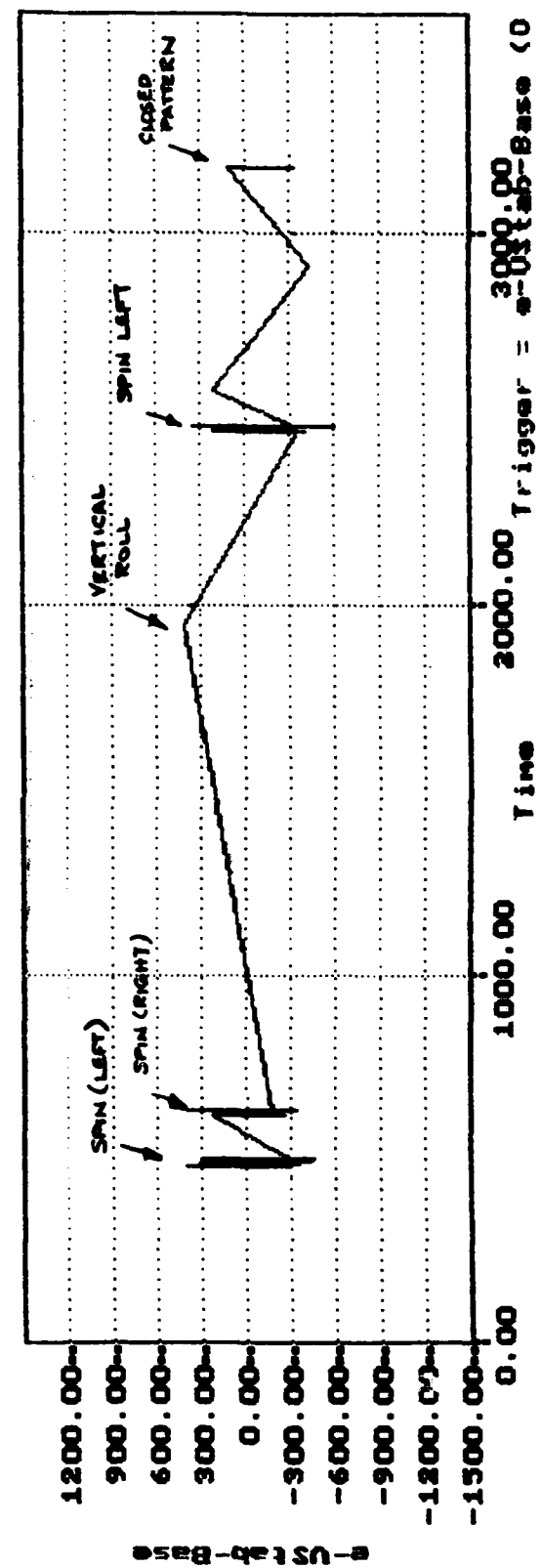
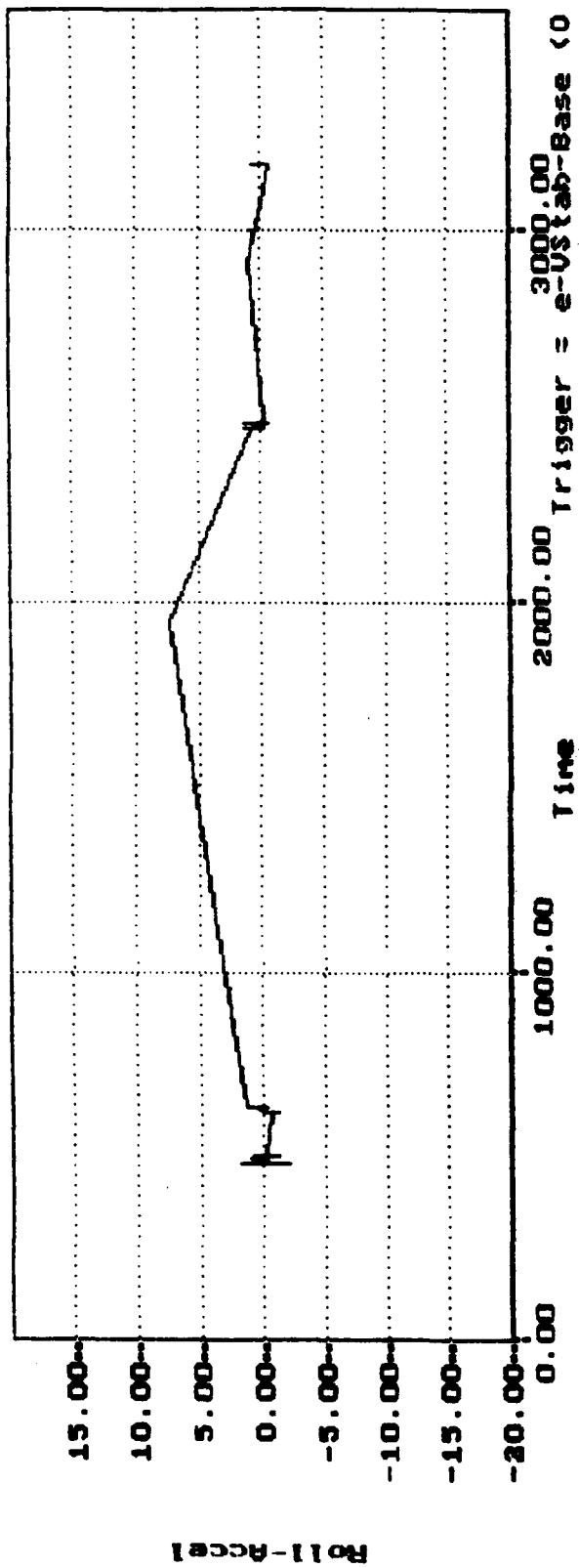
¶ - unusual spin as before. See note under Item 1.

I'm going to digress for a minute and describe the graphing and zooming capability of the system's Transcriber:

Shown here is the graph of the events recorded on one of the trigger sensors -- in this case, the strain gauge at the base of the vertical stabilizer (VSTAB base).

The lower curve shows the peak loads recorded by the VSTAB base strain gauge, and the upper curve shows the reading of the roll acceleration sensor at the instant of each VSTAB base strain measurement.

This illustrates how an associated variable of interest -- in this case the roll acceleration -- can be graphed on the same scale as the VSTAB base, so as to identify any correlation.



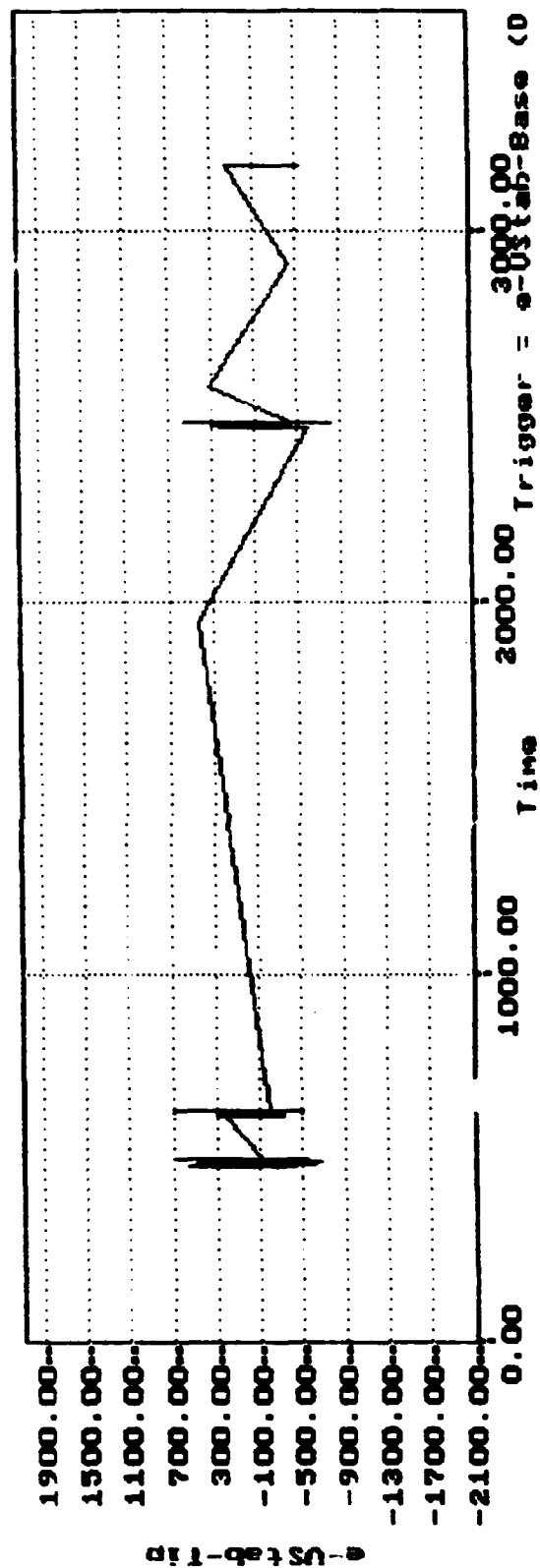
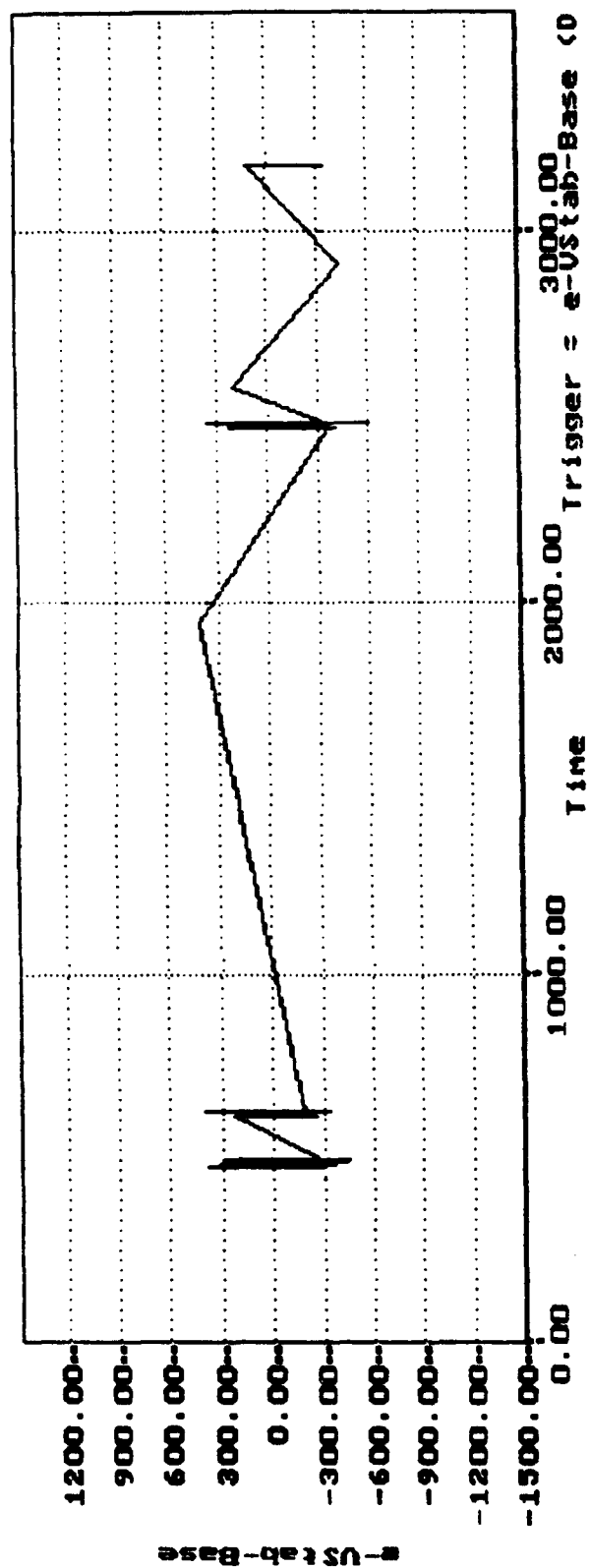
In fact, any trigger variable can be co-graphed with any of the other sensors. Shown is the VSTAB base peak loads, along with the simultaneous readings of the Vstab tip strain gauge.

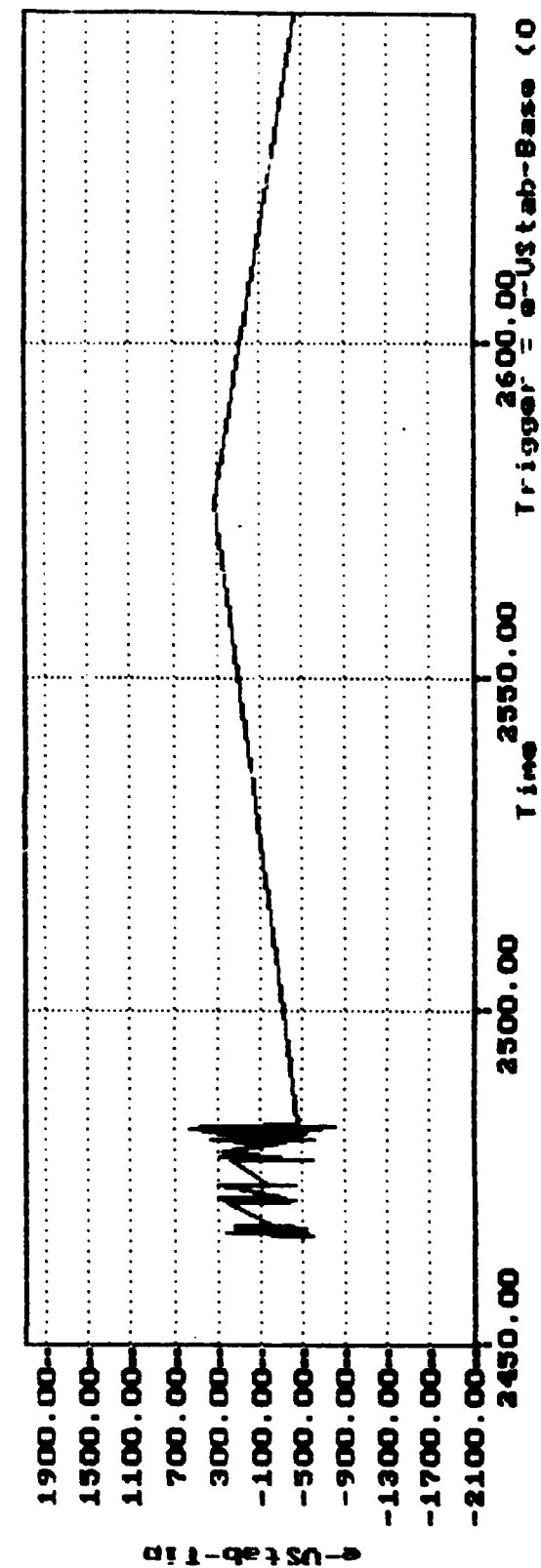
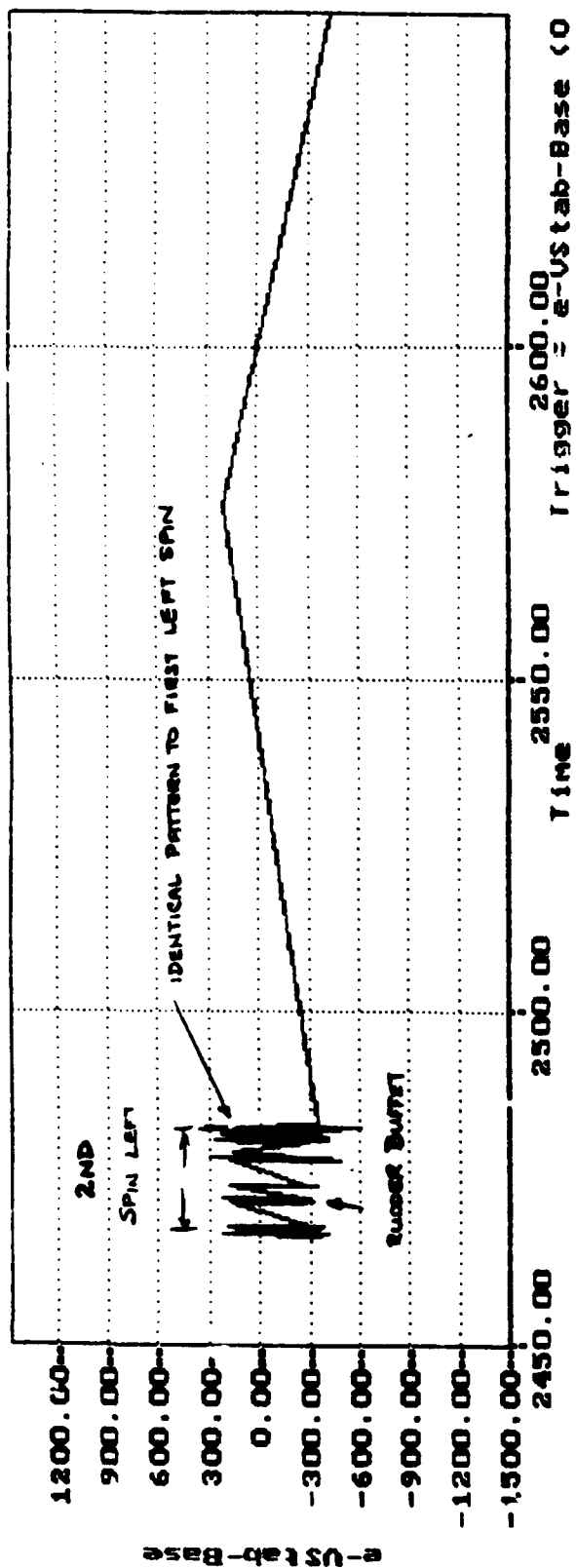
Since an Event file covers the entire flight, it is sometimes desirable to zoom in on a particular segment for better resolution.

Shown is how the second Spin Left maneuver was examined, by zooming to a 20-time enlargement of the time segment of interest.

This magnification permitted identification of strain cycling due to a high-frequency rudder buffet. This was the vibration condition noted by the test pilot during the left spin entries.

As can be seen, these graphing and zooming features are quite valuable for post flight evaluations.

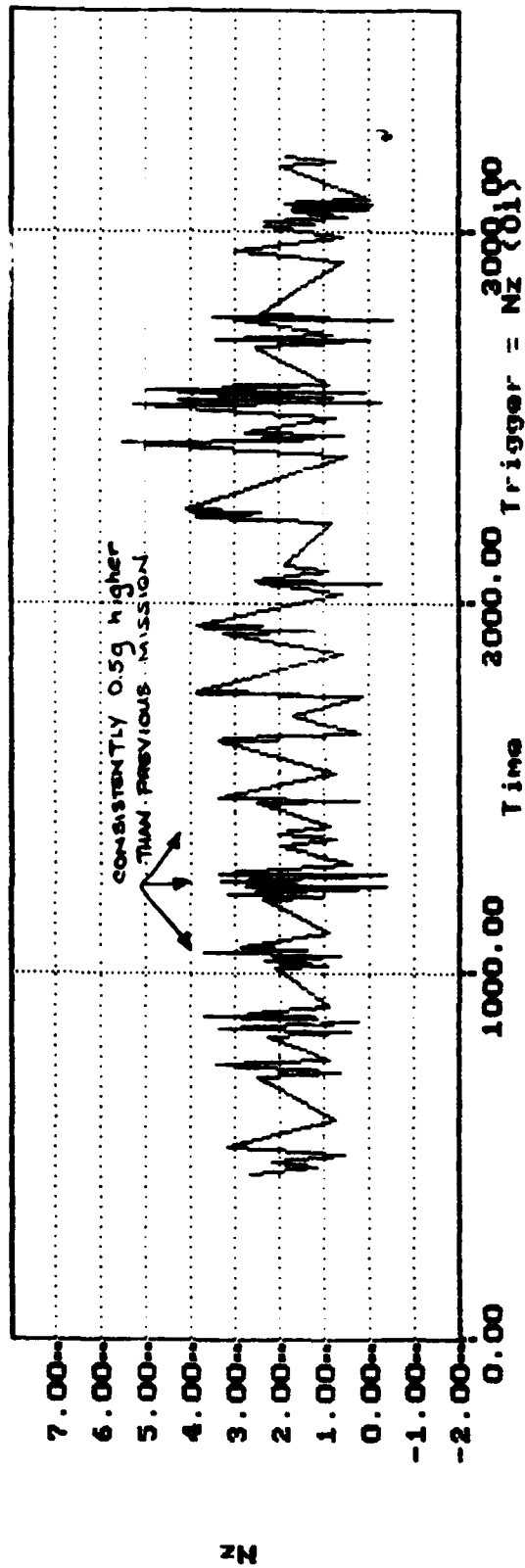




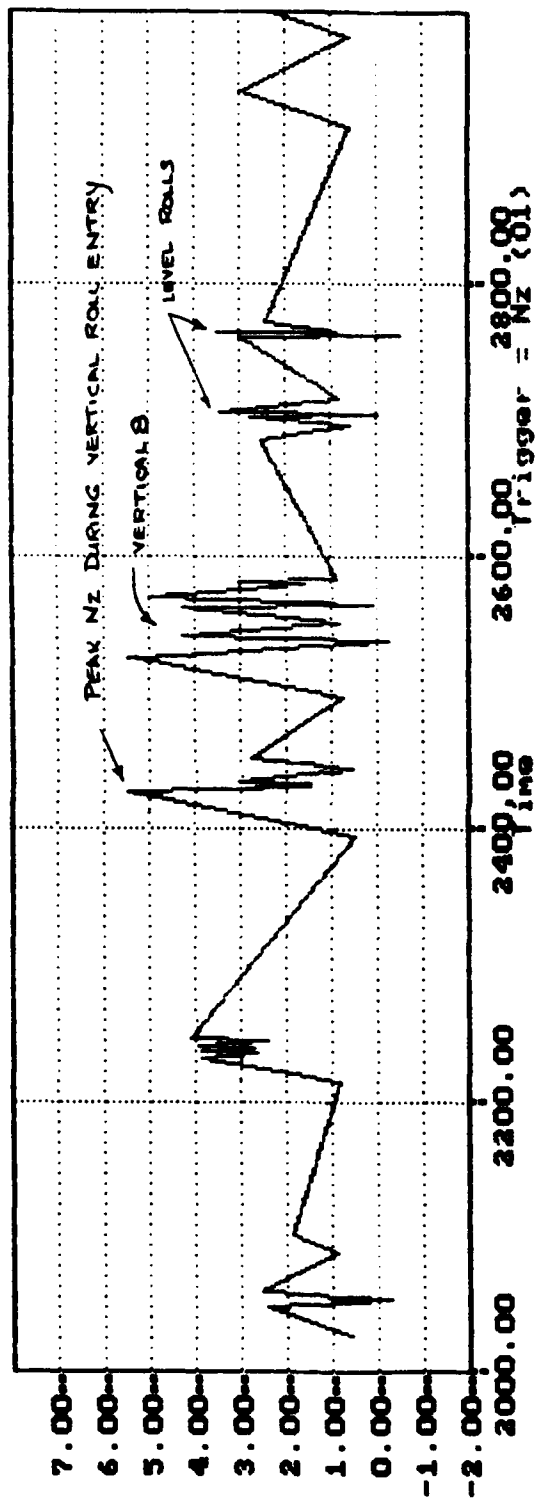
Now that we've looked at the graphing capability, let's return to the flight test comparison of handling qualities.

In order to assess the effects on structural loads from aggressive control inputs, the test flight was repeated on 19 February 90. The flight syllabus was the same except that the second spin maneuver was eliminated. In this test the pilot intentionally applied heavy-handed control inputs.

This slide is the graph of the resultant file of Load Factor peaks. A comparison with the earlier test (see page 31) shows vividly that the test flight with aggressive control forces resulted in normal load factor readings that were consistently 0.5g higher than the flight with normal control inputs.



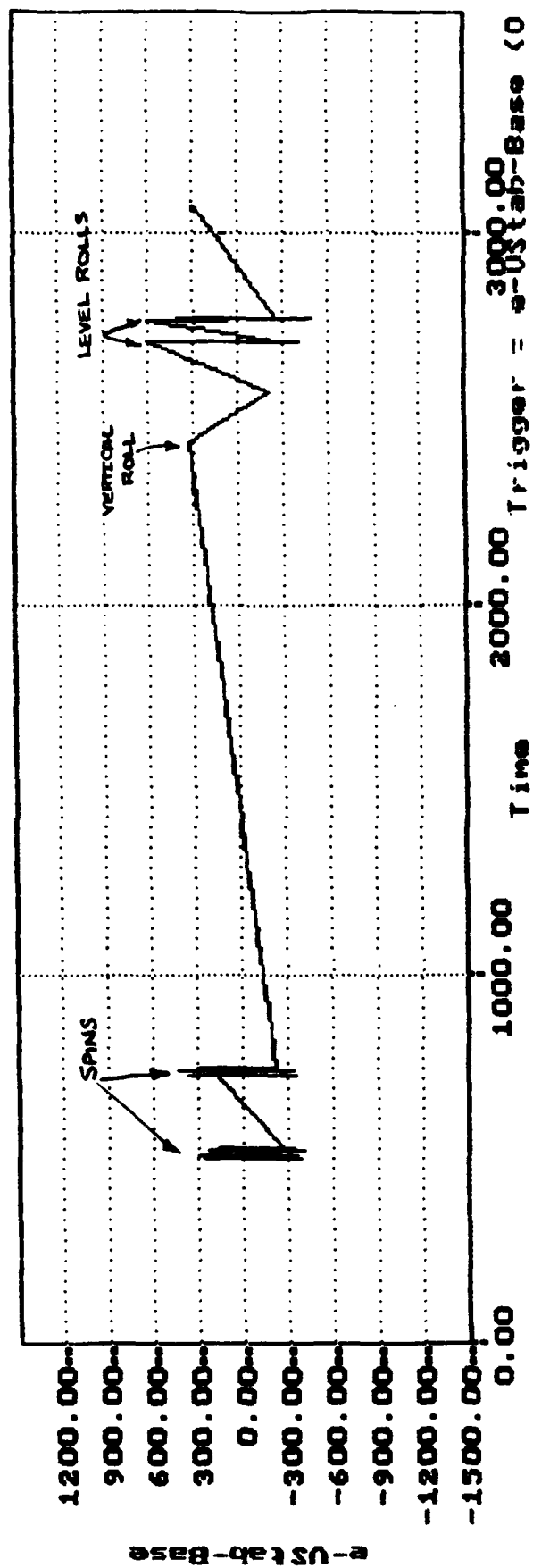
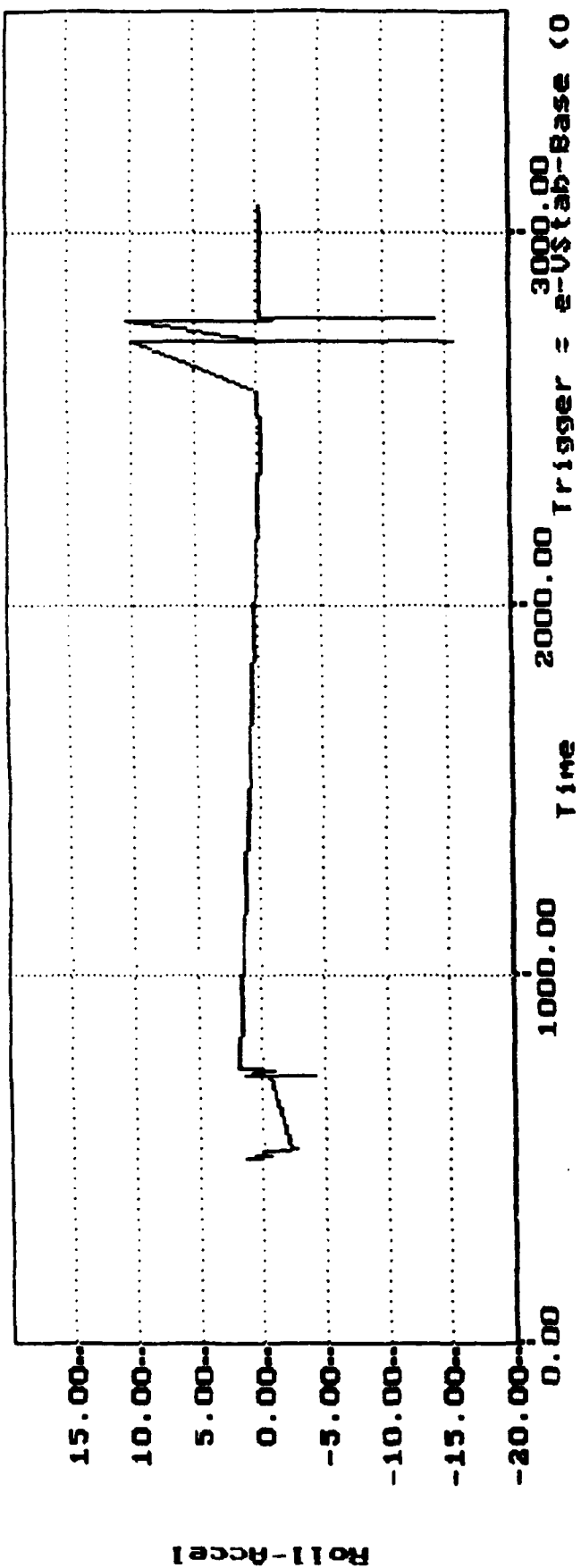
The magnitude of this increased loading can be examined in detail by zooming into particular maneuvers. This slide shows a magnification of the high-g peak region, in the time span between 2000 and 3000 seconds.



NZ

Likewise, looking at the file from the VSTAB base strain gauge trigger, the effect of the stronger control inputs on roll acceleration and VSTAB base strain can be clearly seen.

In summary, these tests showed how the effect on structural loads resulting from a difference in control inputs can be quantified accurately.



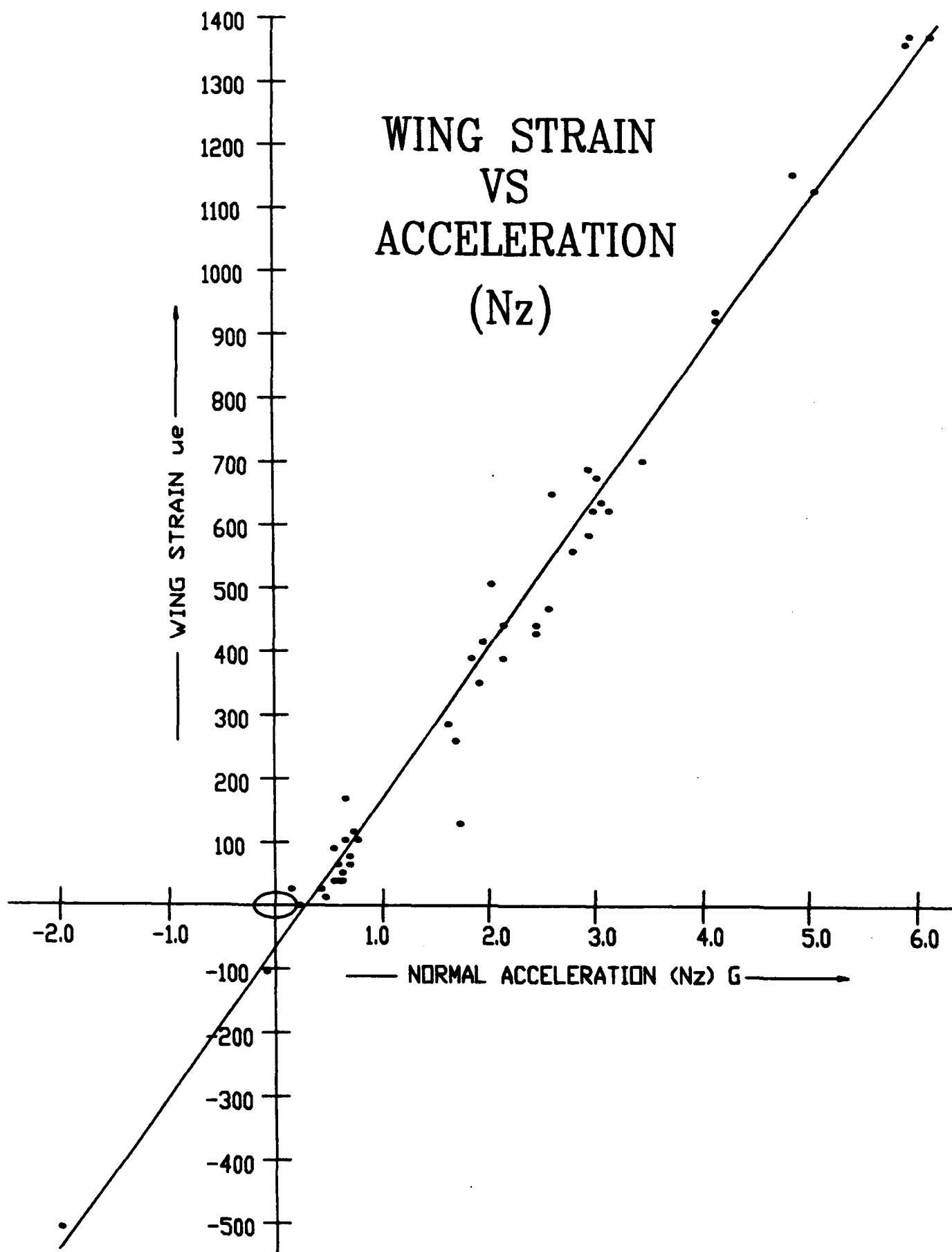
Now, let's look at another application of the recording system.

Correlation of Loads -

One of the purposes of an LESS survey is to determine which load parameters are correlated, so that in a later fleetwide Individual Aircraft Tracking (IAT) program, the recording and associated analysis requirements can be simplified.

As an example, this slide shows the relationship between N_z peaks and valleys and the simultaneous reading of the wing strain gauge at the instant of each N_z trigger. If one were certain that the wing strain peaks and valleys tracked the N_z peaks and valleys, then the N_z loads could be used as an analogue of the wing strain, in accordance with this relationship.

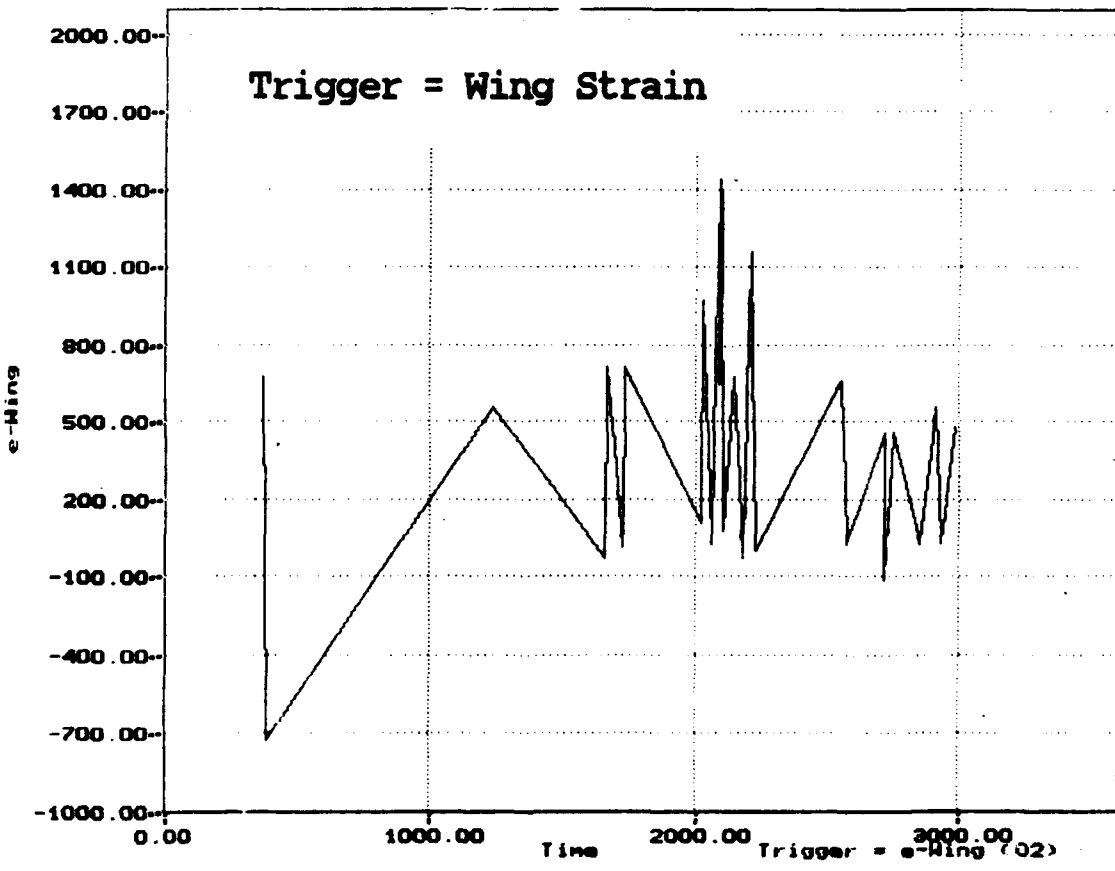
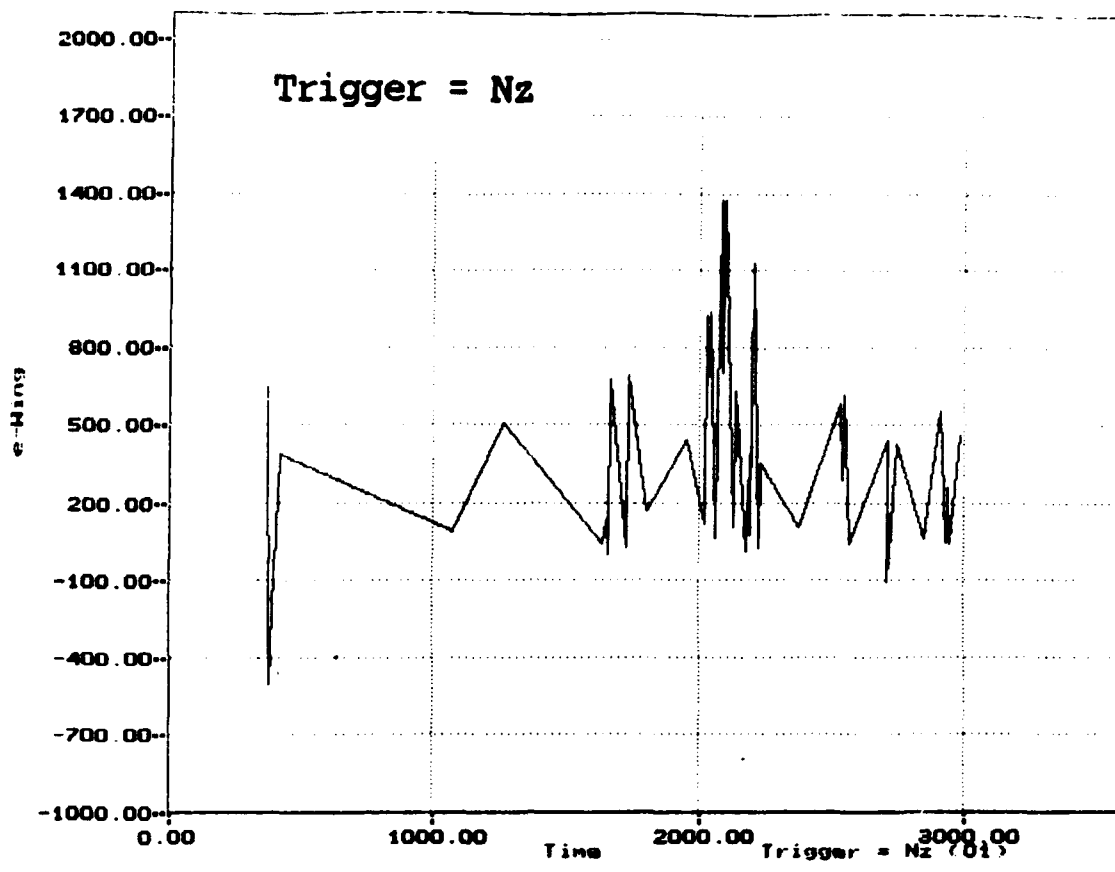
To show how the system can be used to determine such a correlation, we will examine the wing strain peaks and valleys as recorded at the instant of N_z events, and then again as determined by the file which triggered on the wing strain loads directly, as determined by the gauge's own output.



Load Correlation (cont.)

The top graph on this slide shows the wing strain peak loads as measured at the instant of N_z maxima and minima. The bottom graph in turn shows the wing strain peak loads as triggered by the wing strain gauge itself. As can be seen there is a very close correlation, leading to the conclusion that the wing spar strain loads could be derived fairly closely from N_z measurements.

This same analysis can be performed on other parameters, to see if they are likewise analogous. For example, by turning on the VSTAB base strain gauge as an independent trigger, it can be determined whether its peaking is simultaneous with the peak loading of the roll acceleration, or possible even N_z .



Finally, the system's graphing capability has been found to be valuable for pilot debriefing immediately after a flight. Being able to illustrate a particular point to a student in only a few minutes after landing, is vastly superior to showing him a graph a few days later and trying to get him to recall a particular incident.

In teaching, there is no substitute for immediate reinforcement.



Project Results -

The project proved that it is possible to identify certain types of aircraft maneuvers from their characteristic patterns in the recordings. Spins, for example, produce an unmistakable strain pattern in the vertical stabilizer. Rolls can be identified by the pattern produced in the roll accelerometer. The direction of the roll, its duration and the rate of onset can also be clearly defined.

In test flights when the pilot was asked to fly identical missions but with differing control input aggressiveness, the effect of pilot input on strain levels was determined accurately. Use of this data can facilitate the establishment of a fatigue life tracking system, either based on a trend or an Individual Aircraft Tracking basis.

A wide range of secondary applications are also possible, including: post incident and perhaps post accident information; identification of maneuvers through pattern recognition; and use of the graphing capability for pilot training.

Project Results

- **Determined maneuver loads accurately**
- **Measured difference in control inputs**
- **Correlated time phasing of loads**
- **Established parameters for IAT program**
- **Flight Graphing useful for pilot training**

Summary -

In addition to its conventional use for such structural analysis applications as load spectrum development and fatigue life cracking, a loads monitoring system has many secondary benefits. This paper has shown how a Flight Loads Data Recording system can be used to determine the correlation of various load parameters during a given maneuver. It can be used as well to evaluate the structural effects of such operating variables as pilot handling qualities (smooth control inputs vs. aggressive handling). It also demonstrates how the recording system's graphing capability is used by structural engineers and flight instructors to provide an on-the-spot review of the mission results and associated structural effects, immediately after landing.

Acknowledgement -

The authors hereby acknowledge and express appreciation for the professional assistance extended by the Canadian Forces personnel with whom we had the pleasure to work on this project.

A particular note of thanks is extended to: Lt. Col. Guimond, Major Zgela, and Captains Peetsma and LeGuellec of National Defense Headquarters in Ottawa; and Major Leversedge and Captain Craig of the BAMEO at Canadian Forces Base Moose Jaw.



144-A Mayhew Way, Walnut Creek, California 94596, USA
(415) 947-0400

From Theory to Practice: Evolution of the Standard Flight Data Recorder

**F. Saggio, K. Todoroff, T. Conquest
Smiths Industries
Aerospace & Defense Systems, Inc.
Grand Rapids, Michigan**

**Presented at the
1990 USAF Structural Integrity Program Conference
San Antonio, Texas
11 - 13 December 1990**

CLEARED FOR UNLIMITED DISTRIBUTION

From Theory to Practice: Evolution of the Standard Flight Data Recorder

F. Saggio, K. Todoroff, T. Conquest
Smiths' Industries
Aerospace & Defense Systems, Inc.
4141 Eastern S.E.
Grand Rapids, MI 49518-8727

Abstract

Since the inception of the Aircraft Structural Integrity Program (ASIP), the U.S. Air Force has acquired a large inventory of flight data recorders to fulfill the need of providing on-board flight data collection. A recent addition to the Air Force recording equipment inventory is the Standard Flight Data Recorder (SFDR), which represents a new generation solid state data recorder system presently applicable to 16 different USAF and USN aircraft. The basic SFDR design principles and features are given in a previous paper [1] and are not emphasized here. Rather, the purpose of this paper is to discuss the evolution of the SFDR system - from the design state, to the present configuration, and finally to look at the future capabilities and growth potential. The onboard microprocessor computing power allows additional opportunities for system growth via extended recorder use. Some areas for designated growth potential include maintenance diagnostics, vibration analysis, enhanced tracking capabilities, and training programs. The future trend is towards moving more computer processing from the ground facility to inflight by relying on improved onboard data reasonableness techniques presently available [2]. Comments are applicable to ASIP recorders in general.

1 Introduction

Since the late 1950's, the United States Air Force, through the Aircraft Structural Integrity Program, has procured and utilized a large collection of flight data recorders to monitor aircraft usage through the dynamic collection of key flight parameters. At first, some of the recorder systems were designed specifically for each individual aircraft. Furthermore, these recorders were used almost exclusively for data acquisition since they relied heavily on post flight data processing to perform the indepth analysis functions.

To the credit of the ASIP concept, these early flight recording devices have produced valuable data for fleetwide structural analysis. However, constrained by the then current technological limitations, they also possess some inherent drawbacks. Most notably:

- Large quantities of non-pertinent data are recorded. This entails extensive ground processing support to perform such tasks as data reformatting/transcribing, editing and validity checks.

- Data sample rates are non-programmable. Structural analysis personnel are unable to easily alter the sample rates when empirical data dictates a change.
- Inconvenient recording media are employed. Commonly used media are foil cartridges, tape cartridges, handfilled flight logs, punch cards, and records. This burdens the personnel at both the base level and ASIMIS.
- Mechanical and electro-mechanical devices are prone to high failure rates in the dynamic environment of military aircraft.
- Airborne equipment costs are high. The typical costs of electro-mechanical systems grow quickly due to the rugged design requirements imposed by the operating environment, the costs of frequent maintenance, and the associated costs of supplemental aircraft equipment (converter-multiplexers, strain gage amplifiers, pulse rate integrators).
- Limited duty applications. Multiple recorders are required for tasks such as mishap reconstruction, IAT, L/ESS, and ENSIP.

The Standard Flight Data Recorder (SFDR) was designed in the 1980's with the potential and capabilities to overcome many of the limitations of the previous generation of recording systems. The SFDR is a microprocessor-based, software controlled solid state flight recorder which processes and compresses selected aircraft data inflight, to reduce both the volume of recorded data and the subsequent amount of data editing performed during ground processing. An important design feature of the SFDR is its flexibility in hardware and software. It is anticipated that as technological innovation continues into the 1990's, other improvements are possible within the SFDR framework.

Given a broader perspective, it is noted that from the beginning of the ASIP initiative and continuing to the present day, three areas of technological advancement are creating evolutionary changes in flight data recorder systems. These advancements, depicted in Figure 1, are in the interrelated areas of Engineering Models, Hardware, and Software.

The remainder of this paper is organized as follows. Highlights of the present SFDR system including an application example are provided in the next two sections. This is followed by a brief introduction to the technology changes that have influenced ASIP recording. Through an appreciation of the current technical trends and needs, comments are offered concerning the next possible evolutionary events in flight data recording. Finally, the paper closes with summary remarks.

2 SFDR - Present Capabilities

The SFDR is a fully solid state airborne data recording system with no moving parts and which requires no alignment or calibration [1]. The system is much smaller than the tape recording systems it replaces, and is designed to record several types of data (e.g., Mishap, Tracking, Loads/Environment Spectra Survey, and Engine). The SFDR acquires raw data from the various aircraft sensors and the MIL-STD-1553B MUX bus, performs data reasonableness tests

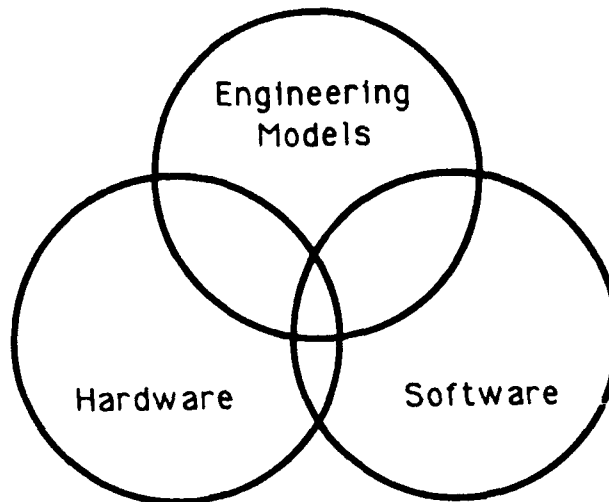


Figure 1: Areas for ASIP Technology Advancement

on the acquired data, and compresses this data using various data compression techniques unique to the type of recorded data. This approach presents a more reliable and cost effective alternative for collecting information than early flight recorder systems, which are limited by conservative sample rates and employ electro-mechanical counters, or a magnetic tape recording medium which is often prone to failure in severe operating environments.

The key feature of the SFDR is its flexibility, both in hardware and software. The software flexibility revolves around an Operational Flight Program (OFP) which programs a 1750A microprocessor. Each aircraft application possesses a unique OFP which controls the entire operation of the SFDR, including: parameter acquisition (with sampling rates), data reasonableness checks, data compression, data storage, and built in test. This software flexibility allows common hardware to be utilized across many applications by simply loading the specific OFP.

The major advantage of the SFDR over the earlier generation electro-mechanical tape recording systems is in data compression. While tape recording systems record a tremendous quantity of data, the data which is recorded is raw and uncompressed. Time consuming data reasonableness checks and data compression must then be performed at the ground processing facilities. The SFDR, on the other hand, performs data reasonableness checks and data compression during flight, in real time, and only records the pertinent information

necessary for further data analysis. This enables the use of solid state memory, thus lowering the acquisition and maintenance costs in comparison to tape recording systems. Recording compressed data also requires less ground data processing to produce the final engineering results. That is, real time analysis and processing creates no additional time delays to degrade the data reduction and analysis processes. Data compression techniques are tailored to each individual aircraft application, and thus support many different structural recording philosophies.

In general, data compression algorithms are primarily employed to reduce the volume of recorded data. This is accomplished by identifying and retaining the pertinent signal features and eliminating the unnecessary elements. Besides this, compression methods tend to reduce: mass memory size and costs; the level of ground processing; and the amount of corrupted data, when used in conjunction with data reasonableness checking. Key data compression techniques useful for ASIP purposes are: compressed time histories, occurrence histograms, peak-valley time histories. Once the compressed data is downloaded onto a floppy disk, it is ready to be decompressed via a ground-based computer.

With regards to the recording function, data reasonableness checking refers to interrogating the output from sensors and/or aircraft subsystems in order to determine the validity of the information. Reasonableness testing tends to improve the overall quality of the recorded data by the increased detection of sensor failures, and by the enhanced ability of maintenance personnel to identify and correct problems in a timely fashion. The SFDR may perform a variety of reasonableness tests, several of which are: BIT Flag Test, Limit Test, Activity Test, Rate of Change Test, and Chatter Test. As a minimum, for reasonableness testing to be useful, the results of the tests are recorded and made available to the appropriate systems and personnel. Further details are provided in References [1] and [2].

The next section presents an example of the onboard data processing and analysis for the C-130 SFDR system application.

3 C-130 Application Example

The Lockheed C-130 application of the SFDR provides an ideal example of the transition from ground based L/ESS processing to the airborne environment. The C-130 is one of the first operational platforms to utilize the SFDR based system, and as such, has provided considerable insight into the potential gains realized by shifting key processing tasks, previously relegated to large ground based systems, to the real time flight environment onboard the aircraft. Such an ambitious endeavor proved not only feasible, but necessary to preserve the fidelity of both the raw L/ESS data and the processed outputs of these data.

3.1 MXU-553/A Based System

For background information, the current C-130 Life History Recording Program (LHRP) system consists of two elements: a basic airborne data acquisition and recording system (MXU-553/A) and an extensive post flight ground based processing system. The onboard recording

components interface directly with both the dedicated sensors which are installed on the aircraft exclusively for the benefit of the flight recorder, and the existing sensors which serve to interface with other aircraft systems and subsystems. The onboard recording components acquire and record raw sensor data without performing data manipulation or processing. The ground based LHRP components accept the flight data (from the flight recording medium) and perform an extensive array of data processing (editing; data filtering and reasonableness checking; computing; mission segmenting and mean level determination; to name but a few) to generate the final product. The structure of this L/ESS recording program, and the limitations of the flight hardware, necessarily requires that the burden of data processing resides with the ground based elements of the system.

The inflight functions of the existing LHRP system are limited to signal acquisition and recording. The airborne recorder, the MXU-553/A, acquires raw data direct from the aircraft instrumentation, and records these data on a multi-track mylar magnetic tape. The recording system does not provide data reasonableness checking, data validity checking, or data filtering. Furthermore, the system incorporates only a basic Built-In Test (BIT) capability into the design of the flight recorder, yet contains no BIT of the supporting aircraft sensors. The tasks of data reasonableness checking, data validity checking, and data filtering are relegated to the ground based LHRP equipment. The task of detecting aircraft instrumentation malfunctions is a byproduct of the ground based data checking process. Consequently, the fidelity of the acquired raw data is held suspect. Additionally, the process of editing data for reasonableness and validity post flight allows for considerable error given the limitations of the current data review and reconstruction methods.

The MXU-553/A records the data in a continuous time history fashion such that the propensity of data retention on the magnetic tape is not pertinent, thus requiring further filtering and processing via the ground based LHRP equipment. This technique precludes the accurate generation of *computed* parameter (ie. bending moments, shear loads, etc.) maximum excursions from the baseline or nominal static value. Thus, the L/ESS analysis of these data must be accomplished with a modicum of caution.

3.2 SFDR Based System

The SFDR based LHRP system consists of two elements: the airborne data acquisition, processing, and recording system and a post flight ground based processing system. The SFDR interfaces directly with aircraft instrumentation in a manner similar to that of the previous system. Four primary functions are performed within the SFDR airborne system.

1. Data acquisition is responsible for collecting the electrical signals from the aircraft sensors, and performing electrical filtering.
2. Built-In Test determines the health of the SFDR system and of the sensors which provide the data input. The evaluation of sensor health is performed through the analysis of the parameter reasonableness checking routines.

3. Parameter reasonableness testing ensures that the acquired data is of sufficient fidelity to warrant further data processing
4. Data processing consists of data sampling, peak-valley screening, mission segmenting, breakpoint and mean level determination.

The third and fourth SFDR functions listed above were previously performed by the ground based post-processing system. The SFDR ground based LHRP components include base level and ASIMIS level data management. The base level component acquires the SFDR BIT and compressed time history data for subsequent analysis on a personal computer for generation of a health data printout. The ASIMIS level component acquires the compressed time history data for subsequent analysis on the L/ESS network.

From a top level perspective, the data acquisition function possesses only one significant difference from the previous recording system. The SFDR data acquisition function is controlled and mechanized through software. This provides the advantage of tailorability for each weapon system as well as tailorability within each weapon system type. The SFDR is targeted for use on all versions of C-130, which are as diverse as the missions they support. Subtle differences exist within the C-130 fleet relative to LHRP aircraft instrumentation. The SFDR accommodates these hardware differences and the resultant data processing differences with relative ease by identifying the C-130 aircraft type during recorder operation, and then implementing the required data processing that is unique to the sensor configuration.

The recorder Built-In Test determines the operational integrity of the SFDR system while providing a central facility for accumulating status. The BIT consists of Power-Up BIT, Continuous BIT, and Initiated BIT (initiated by either the ground support equipment, the flight crew, or by the MIL-STD-1553 bus controller). The BIT isolates failures to the Line Replaceable Unit and Shop Replaceable Unit level. The SFDR utilizes the results of the testing to generate a BIT summary, which is stored in non-volatile memory. The BIT summary consists of filtered BIT and Self-Test BIT records. The filtered BIT information is accumulated only when multiple samples fail the test. Failed tests which subsequently return to a full operational state prior to the acquisition of the n th failed sample are not reported as failures. Tests which fail the n th sample, increment the BIT history record stored in NVM. The C-130 BIT reporting and usage procedure allows for base level analysis of system faults and failures utilizing existing personal computers in the maintenance organization. This procedure is accomplished via Ground Readout Equipment on a periodic basis. (Those weapon systems which utilize the MIL-STD-1553 data bus, can collect the BIT data via the bus, thus providing the flight crew and maintenance personnel with real time system status on a per flight basis, thus further reducing the time interval between failure and repair.) This affords base maintenance personnel the ability to examine real time recorder system health, and the opportunity to take the appropriate maintenance action without delay. Consequently, the data lost to failed recorder or sensor components is reduced by upwards of two orders of magnitude.

As stated previously, the evaluation of sensor health is performed through the analysis of parameter reasonableness checking routines, and reported via Built-In Test. Of the nine different types of algorithms which are available for parameter reasonableness testing [2], the C-130 employs four methods.

Activity Test This verifies that sensors are articulated at minimum reasonable levels of activity. This test identifies frozen sensors.

Range Test This verifies that the sensors are articulated within reasonable upper and lower boundaries. This test identifies un-calibrated or out of tolerance sensors.

Chatter Test This verifies that the sensor activity is stable and normal (free of noise or abnormally high activity). This test identifies loose, broken, or unserviceable sensors. This test also prevents memory storage saturation with unusable data.

Rate of Change Test This verifies that the sensor activity does not exceed the physical capability of the aircraft. This test identifies loose, broken, or noisy sensors.

The SFDR uses the parameter reasonableness testing results for both BIT and data processing purposes. The sensor BIT data usage was discussed previously. When one or more of the four C-130 tests determines that the fidelity of the acquired data is questionable, the SFDR records the data as received but flags the erroneous portions for subsequent evaluation during post-flight analysis. Various other options have been requested by the managers of several weapon systems. A second option is to record the last valid sample of data (with a flag indicating a data anomaly) in lieu of the erroneous data. A third option is to halt recording only the erroneous data, while another technique is to halt all recording until the data subsequently meets the reasonableness criteria. Thus, onboard parameter reasonableness evaluation reduces the magnitude of post-flight data editing while preserving or enhancing the fidelity of the recorded data.

The most noteworthy aspect of transitioning data processing from the post-flight environment to onboard the aircraft is computing flight loads, generating aircraft performance data relative to Spectra Survey analysis, and data reduction via parameter peak-valley search methods [3]. The C-130 employs peak-valley examination of vertical acceleration, stress, and control surface deflection; mean level determination for these response parameters; peak counting/gust-maneuver separation for these response parameters. The peak-valley examination eliminates data which is either not pertinent for L/ESS analysis, is redundant, or whose changes in magnitude are insignificant. The C-130 L/ESS methods require a mean average (dynamic) for each of the response parameter's peaks and valleys. The SFDR calculates the mean average of each response parameter while saving the previous peak and valley values in a buffer in order to determine the next peak or valley. Given the changes in the flight profile, the mean average calculation is reinitialized as the aircraft changes state to the next subsequent mission segment. This requires the SFDR to constantly determine the present mission segment based on the logic of key flight parameters.

The range existing between the threshold levels represents a deadband. Parameter peaks and valleys which fall within a pre-defined deadband around the current parameter mean are discarded. Subsequently, the remaining response parameter peaks or valleys are then recorded along with their respective dynamic mean average value. The C-130 L/ESS methods also require that each peak or valley excursion be classified as a maneuver (pilot) induced load or a gust induced load. Each peak or valley is compared to a threshold level on either side of the mean average level. Response parameter excursions outside the dead band of less than two seconds are classified as gusts while excursions outside the dead band of greater than two seconds are classified as maneuvers. Each of the processing techniques described here require significant buffer usage which necessitates efficient algorithm and software development.

The onboard data processing is significant given the large amounts of memory previously available to ground based computers that are required for long term buffer storage during the mean-level and gust-maneuver separation calculation. Innovative computational techniques were devised to transfer the heavy burden of processing from the post-flight environment (which is not constrained by the size, weight, cooling, and subsequent memory limitations onboard an aircraft) to the onboard environment with its reduced memory and throughput capacity.

4 ASIP Technology Evolution

It is the function of fleet management to schedule maintenance, inspections, and aircraft retirement based on damage inspections (from the ASIP recording/tracking system). In order to assess the aircraft damage using a simple data tracking system, conservative assumptions may be required in order to account for all potential variables which may affect loading and fatigue damage. In effect, the simpler the tracking system, the more conservative the service life estimate. This implies that aircraft may be overhauled or retired earlier than necessary, which in turn represents unnecessary expense in terms of manpower and dollars.

As stated earlier, ASIP flight data recorders have evolved over the years due to technological advancements in analysis tools/models, hardware and software. It is therefore not surprising that with the trend for more mileage from older aircraft, the implication is for better analysis tools and models to make use of this improved data.

Table 1 provides a comparison of some factors in the evolution of ASIP flight data recorders. The following subsections present a brief outline of technology innovations that are influencing the evolution of ASIP recording.

4.1 Engineering Models

During the more recent years, we have seen a transition from safe life to damage tolerance analysis for ASIP, with the shift towards crack growth or fail safe methodologies. In this regard, there have been advancements in the analysis tools and corresponding engineering models, although as yet very little standardization. Data interpretation improvements have also been

Table 1: Evolution Comparison Factors

Factors	1970's Recorder	1990's Recorder
Technology	analog	digital
No. Parameters	tens	hundreds
Functionality	acquisition only	acquisition and analysis
Memory Type	tape	solid state (or optical disk)
Complexity	simple	sophisticated
Relative Reliability	1.0	5.0
Relative Power Consumption	1.0	0.20
Relative Size	1.0	0.25
Relative Weight	1.0	0.45
Relative Cost	1.0	0.25

made, with the programming of simple judgement/decision making into the computer via a rule-based software approach.

As engineering models have diversified, ASIP recorders have also changed. For comparison, the MXU tape based recorder systems are founded upon fatigue tracking principles, whereas fracture mechanics forms the basis for the SFDR solid state systems.

As a final comment, there is still need for innovations in

- vibration analysis
- maintenance diagnostics
- more elaborate tracking
- training applications

to complement the advancements in structural modeling and analysis which have already been realized.

4.2 Hardware

Recent innovations in sensor and recorder technology have improved the overall structures recording process. ASIP sensors, such as accelerometers and strain gages, have become increasingly more accurate and reliable with notable improvements in the areas of noise immunity and temperature stability. In addition, the transducer data required by multiple aircraft

subsystems can now be transmitted over a multiplex data bus (e.g., MIL-STD-1553B) permitting the recording of data from many more sensors than was previously available when transducers were dedicated to their own specific aircraft subsystem.

Continuing evolution in sensor technology has lead to the development of *smart sensors*. These transducers with their built-in integrated electronics may offer increased accuracy by automatically monitoring drift caused by varying environmental conditions, and may correct for this drift before the data is transmitted to the appropriate electronic subsystem. Also, strain gages may become more reliable by utilizing fiber optics in place of wire bridge legs, and new type fuse sensors that directly track the structural fatigue should enhance traditional Individual Aircraft Tracking systems.

Solid state structural recorders using advanced data compression techniques can now record the same information on board the aircraft as previous tape based recording systems with hundreds of megabytes of tape memory. This is due in part to the advancements in memory technology, with the capability to employ a megaword or more of Electrically Erasable Programmable Read Only Memory (EEPROM) or battery backed Random Access Memory (RAM) into a small amount of volume at relatively low cost.

Future structural recording systems will continue to expand the amount of solid state memory. This memory may also be complemented with optical disk systems which can record many megawords of data. Smarter analog acquisition subsystems will emerge which will sample data at higher rates and which will have greater digital signal processing capabilities to filter the data to aircraft specific requirements. Thirty two bit microprocessors may be utilized to handle the increased amount of data and thereby permit the use of more throughput and memory intensive data compression techniques.

4.3 Software

General advances in both mainframe and microcomputer equipment since ASIP's beginnings have made possible the use of more sophisticated engineering analysis models. During the last decade alone, there has been tremendous improvements in microprocessor capabilities, data reduction, and data compression algorithms. A direction implication is that more processing and analysis can be located onboard (spectra, histograms, crack growth inflight), to provide quicker results. Supporting this move is the data reasonableness testing which validates the data prior to processing. That is, data reasonableness helps determine if the data is suitable for further processing.

In essence, the key to future growth and evolution for ASIP recorders is in maintaining a sufficient amount of software flexibility. This is aided by:

1. expanded software control
2. processing decisions dictated by software
3. increased confidence in on-board processing results

Software flexibility is essential since standardization is difficult to achieve in ASIP recorders. Finally, it may be possible to incorporate principles of artificial intelligence and knowledge

representations into onboard ASIP software to offset some of the routine decision-making tasks of the human operator.

4.4 General Comments

To provide the required amount of structural recording coverage per aircraft, specific loads at strategic airframe locations needs to be simultaneously monitored. The ideal method is to install individual sensors at each location. Strain gages are the most common sensors for this purpose and can be easily monitored by the SFDR to detect the peaks and valleys necessary to build the appropriate aircraft load spectra.

While strain gages provide the most straightforward method of acquiring load data, the rigorous environment of the fighter aircraft typically produce component deformation that is hostile to strain gauge sensors. Component movements of this magnitude can easily induce permanent sensor failure or sensor mounting adhesive failure. Fortunately, if a particular aircraft type has a sufficient data base of its various loads based on previously conducted flight testing using direct load instrumentation, a method of onboard computed loads provide an attractive alternative. Common computed loads are fuselage bending moment, wing pivot bending moment, inner wing bending moment, outer wing torsion, and vertical/horizontal stabilizer shear to name a few. The loads equations typically contain from ten to thirty inputs, and utilize parameter look-up tables based on flight state. Each load can be subjected to peak-valley search processing, or other types of common or aircraft unique data processing algorithms.

A logical evolutionary step for the SFDR might be with onboard cycle-by-cycle crack growth analysis. Crack growth analysis commences with the acquisition of desired parameters and a peak/valley search (presently performed by SFDR). The remaining onboard processes involve: the computation of stress and stress intensity factor, the computation of retardation, and crack growth rate, and finally the accumulation of crack growth.

As a final comment, it is important to provide the data analyst with adequate data visibility in order to verify the quality and trends of recorded data. As expected, this places a constraint on how far data reduction/compression techniques may go.

5 Summary

The trend in ASIP recording is towards acquiring more parameters and performing more signal processing onboard to quickly provide detailed maintenance information to fleet management personnel. This is due to a desire to extend the service life of an aging aircraft inventory. Fortunately, steady improvements in engineering models, hardware and software over the past few years make this possible.

It appears that no two airframes (applications) have functionally identical ASIP recorder systems due to differences in usage, analysis techniques, subsystems, engines, and the like. Since pure standardization is difficult to achieve, flexibility in recorder design is imperative. A degree of commonality is expected for both recorder hardware and software, with hardware achieving the highest level of similarity for the SFDR. But variations in functions performed

and details in implementing these functions will continue. Thus the flexibility is expected to be achieved via software.

Finally, as ASIP recorders are broadening in purpose, there is a growing realization that the high quality of data from these recorder systems makes them valuable as a maintenance/diagnostics and tracking tool, as well as being equally valuable for test and debug functions. New opportunities will continue to evolve for ASIP recorders such as the SFDR as subsequent technological advances are made in hardware, software and ASIP engineering models.

References

1. Conquest, T., Saggio, F., Todoroff, K., "ASIP Concepts for the Standard Flight Data Recorder," USAF Structural Integrity Conference, San Antonio, TX, 29 November - 1 December, 1988.
2. Mayhan, T., "Improvements in Structural Integrity Data Validity Utilizing Airborne Parameter Reasonableness Techniques," USAF Structural Integrity Conference, San Antonio, TX, 4 - 7 December, 1989.
3. Bell, T. and Greenhaw, O., "C-130 LESS - Transition to the Standard Flight Data Recorder System," USAF Structural Integrity Conference, San Antonio, TX, 4 - 7 December, 1989.

A-10

**A-10A INDIVIDUAL AIRCRAFT TRACKING PROGRAM
(IATP)
VALIDATION OF CRACK GROWTH METHODOLOGY FOR
CHANGING FLIGHT SPECTRA**

PRESENTED AT

**1990 USAF STRUCTURAL INTEGRITY
PROGRAM CONFERENCE**

**11-13 DECEMBER 1990
SAN ANTONIO, TEXAS**

PRESENTED BY

**HERMAN AXELROD
KENNETH GRUBE
GRUMMAN CORPORATION**

**KENT MCPHAUL
SM-ALC/LASEC**



The A-10A is a close air support single-place, low wing, low tail configuration with two engines installed in nacelles that are mounted on pylons extending from the fuselage just aft of and above the wing. Twin vertical tails are located at the outboard tips of the horizontal tail. The A-10A is capable of delivery of up to 16,000 pounds of expendable ordnance from eleven wing pylon stations. A 30mm Gatling gun with a capacity of 1100 rounds is installed in the forward fuselage. A total of 713 aircraft were produced between 1975 and 1984. A-10 aircraft are actively deployed world wide and are assigned to the Air Force Tactical Air Command, Air National Guard and Reserves. Figure 1 presents the major topics of discussion of this paper. The overall dimensions of the A-10A aircraft are presented in Figure 2.

The methodology utilized in tracking the A-10 was presented in detail at the 1989 USAF Structural Integrity Program Conference and is included in the printed proceeding, WRDC-TR-90-4051. Figure 3 outlines the salient features of the tracking program. Briefly, the airplane tracking is based on fracture mechanics analysis. As part of an earlier damage tolerance assessment, 63 critical areas of the A-10 airframe were analyzed. Evaluations of the analyses indicated that the airplane could be tracked by 10 key control points - 4 wing, 3 fuselage, 1 nacelle and 2 empennage points. Damage coefficients defined as the average crack growth per N_2 occurrence were calculated. The coefficient for each point accounted for stress spectrum, geometry and material properties which exist at each location.

The A-10A is monitored through the implementation of the Individual Aircraft Tracking Program (IATP). The IATP consists of counting accelerometers which are installed on every airplane and record the normal load factor (N_2) exceedances for six N_2 levels. Also, approximately 84 aircraft contain multi-channel life history recorders which record other key loads/environment parameters. Recorded data is also used to monitor changes in usage which would affect crack growth monitoring.

Early in the program it was determined that all aircraft do not fly to the same spectrum. Cumulative probability curves of the number of aircraft attaining a specific N_2 exceedance rate at a give N_2 were generated from counting accelerometer usage data. Meetings with USAF concluded that all aircraft flying in the lower 15% of the probability curve would be considered flying a mild spectrum and those in the upper 15% flying a severe spectrum. Between 15% and 85%, the aircraft were considered flying in an average spectrum. The midpoint of each zone,

that is the 75%, 50.0% and 92.5% percentile points, were selected at each N_2 level and used to develop the tracking spectra shown in Figure 4.

As previously stated, damage coefficients are a function of stress spectrum loading. Therefore, coefficients were computed for mild average and severe spectra for each control point. The selection of which spectrum and therefore which set of damage coefficients to use for each component was made by comparison of data in the counting accelerometer windows. This is done automatically by the tracking software routines used by the Air Force.

The airplanes are individually tracked by components. Thus a wing, tail or nacelle could be removed from one airplane and installed on another and still be constantly monitored. In addition, major structural changes, i.e. block changes, are accommodated by calculating a new set of coefficients, installing them and making minor software changes to the program.

Software has been written and installed in computers at the Tinker Air Force Base at Oklahoma City. It accepts the previously mentioned damage tolerance coefficients for determining crack growth, Flight logs, counting accelerometer data, N_2 occurrences, usage and tail numbers, and any TCTO compliance repairs or design changes. This data is processed as depicted in Figure 5 and results in printed reports of spectrum hours used, spectrum hours remaining, TCTO compliance, etc.

Currently, the airplane is being tracked by spectra based on 3000 hours of multi-channel data along with 155500 hours of counting accelerator data. These spectra were based on early flight data gathered prior to the delivery of all production aircraft. Currently there is approximately 20,000 hours of multi-channel data and 2017000 hours of counting accelerometer data available. Data is collected in 6000 hour multi-channel database groups. The fleet is mature and the current database, 2nd 6000 hours, represents usage expected for the remainder of the useful life of the airplane provided there are no changes or mixes in mission profiles. It is comprised of 411594 hours of counting accelerometer and 5895 hours of multi-channel data. Additionally the current usage is more severe and significant changes in gross weight distributions have occurred. Figure 7 is a comparison of the 2nd 6000 hour database vs. the 3000 hour update and clearly shows the 2nd 6000 hour usage as more severe.

As a result two questions surface. First, should the tracking program be updated? And second, if so how? This paper assumes that the answers to the first question is yes. The answer to the second question is more complex.

The method of updating must consider basic issues as shown in Figure 8. Obviously, the paramount issue is prediction accuracy. This determines inspection intervals and thus presents a major impact on Life Cycle costs. Too conservative predictions result in unnecessary fleet inspections. Unconservative predictions cannot be tolerated because of impacts on pilot and aircraft safety. Additionally, the method should be sufficiently flexible to accommodate changes in aircraft usage without considerable testing.

Three evaluations were undertaken:

- (1) Develop new coefficients using the Wheeler retardation model; then verify by test for continued validity of the current methodology
- (2) Analytic models, then verify by test
 - (a) AFFDL-TR-74-129 closure model
 - (b) NASA TM 81890 Multi-Parameter Yield Zone (MPYZ) Model

A limited test and evaluation program was implemented as summarized in Figure 9. Because of program constraints, only two control points were selected. Wing Control points were selected because the wing is primarily N_2W critical. Thus the investigation eliminated the effects of evaluating combinations of parameters.

As shown in Figure 10, the 2nd 6000 hour database representing 411594 hours of counting accelerometer and 5895 hours of multichannel data was selected for this evaluation. A statistical maneuver spectrum was developed and normalized to 1000 hours. Exceedance curves were generated for each of the four zone boundaries, 0%, 15%, 85% and 100%. The boundaries of each zone were then rotated clockwise and counterclockwise and by linear interpolation 10 spectra were generated. Figure 11 indicates these spectra and defines them for future use. The fleet was examined and the aircraft sorted according to use within each zone and further sorted according to spectra within each zone of severity is as shown in Figure 12. The exceedance curve rotations statistically represented individual aircraft usage.

A major task of this evaluation was to assess the current method of tracking

the fleet while evaluating analytical methods. For each of the 10 spectra, coefficients and Wheeler constants were to be determined empirically and crack curves generated and compared to the test results. In order to evaluate the analytical methods, material constants were determined by test and used in their respective equations to generate crack curves to be compared with the actual test curves. To assist in the fractographic examination and construction of the test crack growth curves, marker bands were inserted into each test spectrum. Figure 14 indicates the frequency of marker band insertions.

All testing was accomplished utilizing automatic load application equipment as shown in Figure 15. Figures 16 and 17 respectively define the coupon geometry and material of wing control points 1 and 2. Wing control point 1 is representative of a low load transfer hole while control point 2 is of an open hole. All specimens were pre-cracked only on one side of the hole followed by constant amplitude cycling prior to random spectrum load testing. Figure 18 shows a typical fracture. It is of interest to note that while the specimen was pre-cracked on one side of the hole, fatigue cracks existed on both sides at failure.

Three specimens were tested to each of the 10 spectra for each control point. Thus a total of 60 coupons were tested to failure. Figures 19 and 20 display the pertinent data for each specimen. A crack geometry sketch relates the column headings to the crack propagation of any coupon.

Both analytical models, Crack Growth Closure and MPYZ, basically utilize the Paris equation modified by interaction material constants generated by test. The constant for the Paris equation is derived from constant amplitude da/dn testing. The interaction material constants were determined by controlled spectrum testing. Figure 22 defines the specimen geometry used to generate material constants. A controlled spectrum of loading was applied to each of three coupons, i.e. constant amplitude with multiple overloads, constant amplitude with single overload and constant amplitude with completely reversed overload. Figure 23 provides number of cycles and magnitude of stresses for each test.

Figures 24 and 25 are typical sections of the generated crack curves. The curve shown is only a portion of the total. The left curve is non-interactive. The dots are a portion of the actual test. The overload in any spectrum provides a plastic zone. As can be seen, the crack growth is retarded until the crack

propagates through the zone. It then grows as a non interactive crack. At this time the overload is again introduced thus providing several test curves prior to failure. The other two curves are examples of the evaluation of constants to be used in the two analytical models.

Random flight by flight spectra were applied to the analytical models and crack curves were generated. The objective was to attempt to generate an equation that could predict crack growth without the necessity of further testing.

Figures 26 thru 31 present the results of the coupon testing, Forman/Wheeler and Closure equations. The MPYZ equation was used to calculate crack curves in the severe zones for control point 1 and 2 but was found too conservative. Use of the MPYZ equation was therefore discontinued. A possible reason for this could be the lack of sufficient testing to determine material constants. The Closure model was very conservative in all zones for control point 1. Some reasons for this were uncertainties in definitizing the load transfer stress intensity solution due to friction effects and effects of tolerance variations in fastener holes both during installation and as the crack opens. However, in evaluating control point 2, the closure model yielded better results for the severe upper and mild upper tests but was unconservative with respect to the average upper tests. In all instances the Forman/Wheeler generated curves yielded good results.

As a further method of validation, weighted spectra, mild, average and severe, were generated based on the distribution of aircraft in each of the respective zones. These spectra were then compared to the 3000 hour spectra. As can be seen by the comparison on Figure 32 the spectra in each zone were almost identical.

An attempt was then made to compare crack growth curves based on weighted average coefficients or weighted average Wheeler constants followed by a comparison to a test weighted average exceedance curve in the same zone. Control point 2 severe zone was selected for this test. This eliminated the variables of friction and hole size tolerance. Three coupons were tested to failure. The cracks generated by these tests are plotted in Figure 33. Crack curves were calculated based on average coefficients and average Wheeler constants. Both curves indicated good results with the average Wheeler curve more conservative when compared to all test coupons.

In conclusion, the analytical predictive methods (closure/MPYZ) are inadequate for individual aircraft tracking use. Both models are much too conservative for load transfer hole geometries because of the variation in loaded hole stress intensity solutions. The Closure model was not conservative for all zones. Additional testing must be performed to adequately characterize material constants.

The current method of calculating A-10 crack growth for tracking remains satisfactory. The current method has been validated and most accurately predicts crack growth. This ability allows the aircraft to be operational longer between inspection intervals thus reducing life cycle costs.

Weighted average Wheeler constants, coefficients and spectrum within zone shows great promise for ease of accurately predicting useful life and accounting for changes in usage without the necessity for extensive testing. However this must be validated for all zones and all control points.

- Current Method of Monitoring
- Effects of Changing Spectrum
- Options
 - AFFDL-TR-74-129 crack growth analysis for arbitrary spectrum loading
 - NASA TM 81890 multi-parameter yield zone model for predicting spectrum growth
 - Empirical
- Test Program
- Results/Conclusions

FIGURE 1 AGENDA

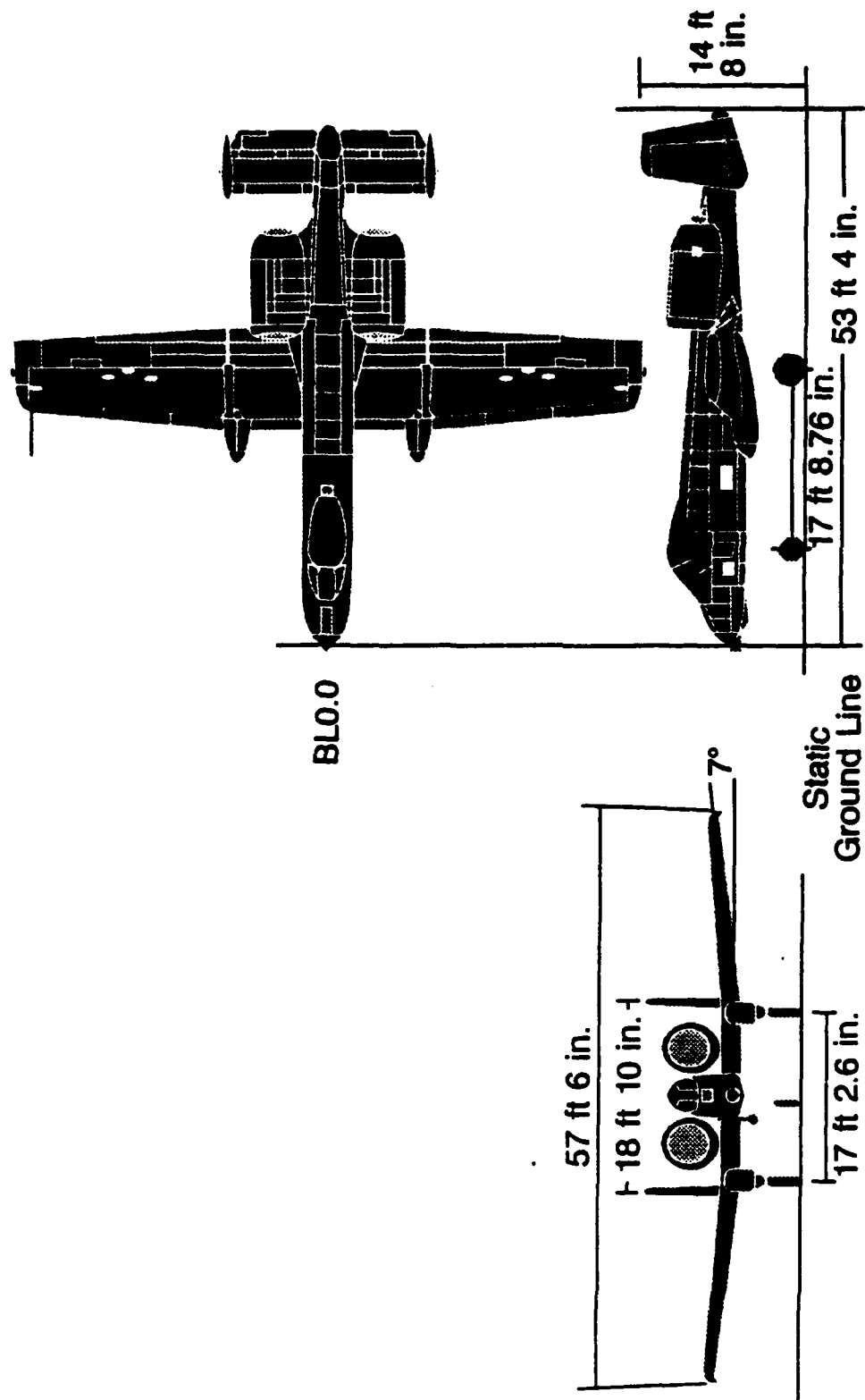


FIGURE 2 A-10A DIMENSION

Methodology

- Based on fracture analysis
- Damage coefficients in terms of crack extension per vertical load factor occurrence for ten control points
- Three usage spectra
 - Mild
 - Average
 - Severe
- Track by Components
- Automatic update by TCTO incorporation

FIGURE 3 INDIVIDUAL A/C COMPONENT TRACKING PROGRAM METHODOLOGY

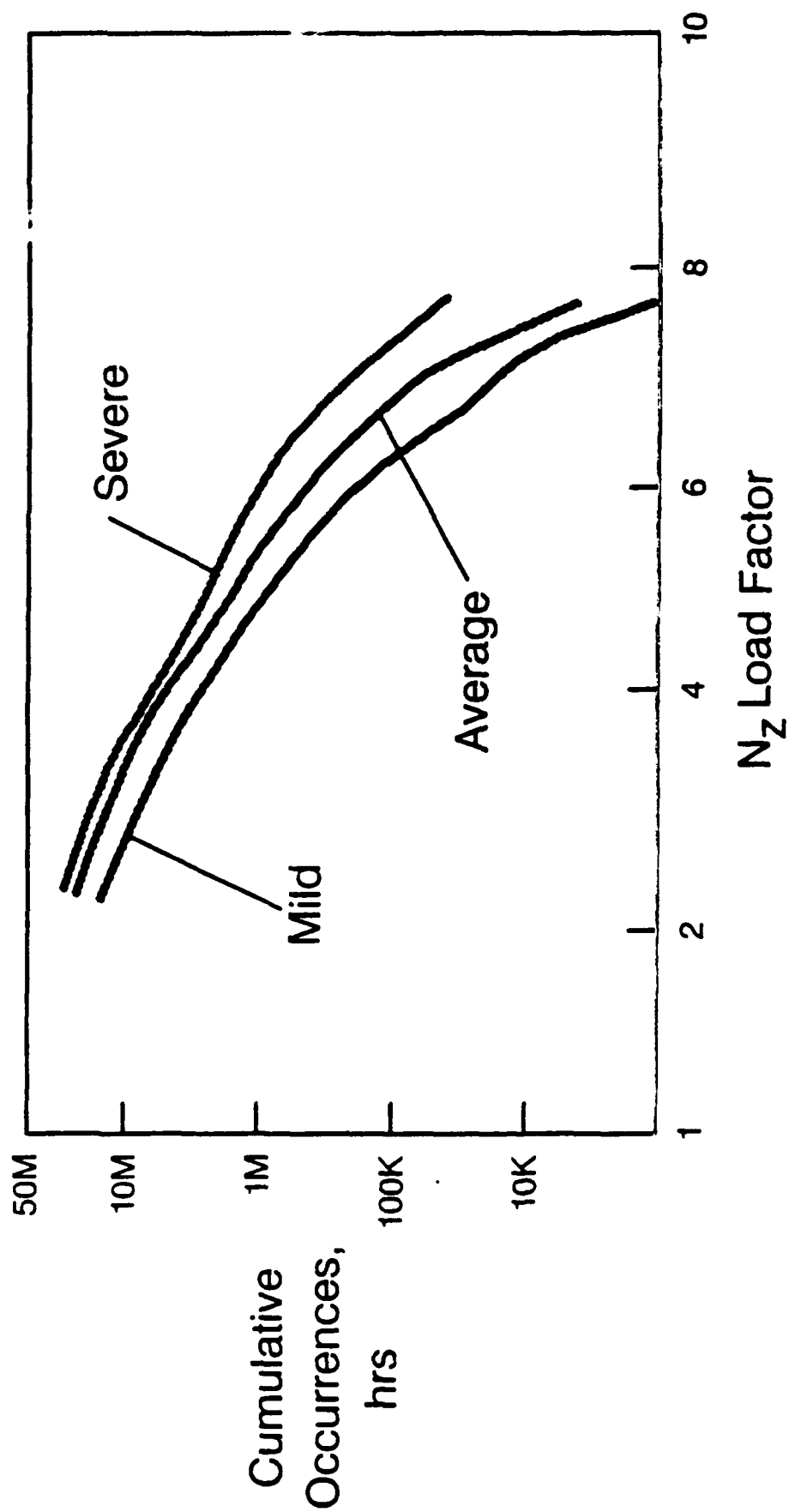


FIGURE 4 TRACKING SPECTRUM

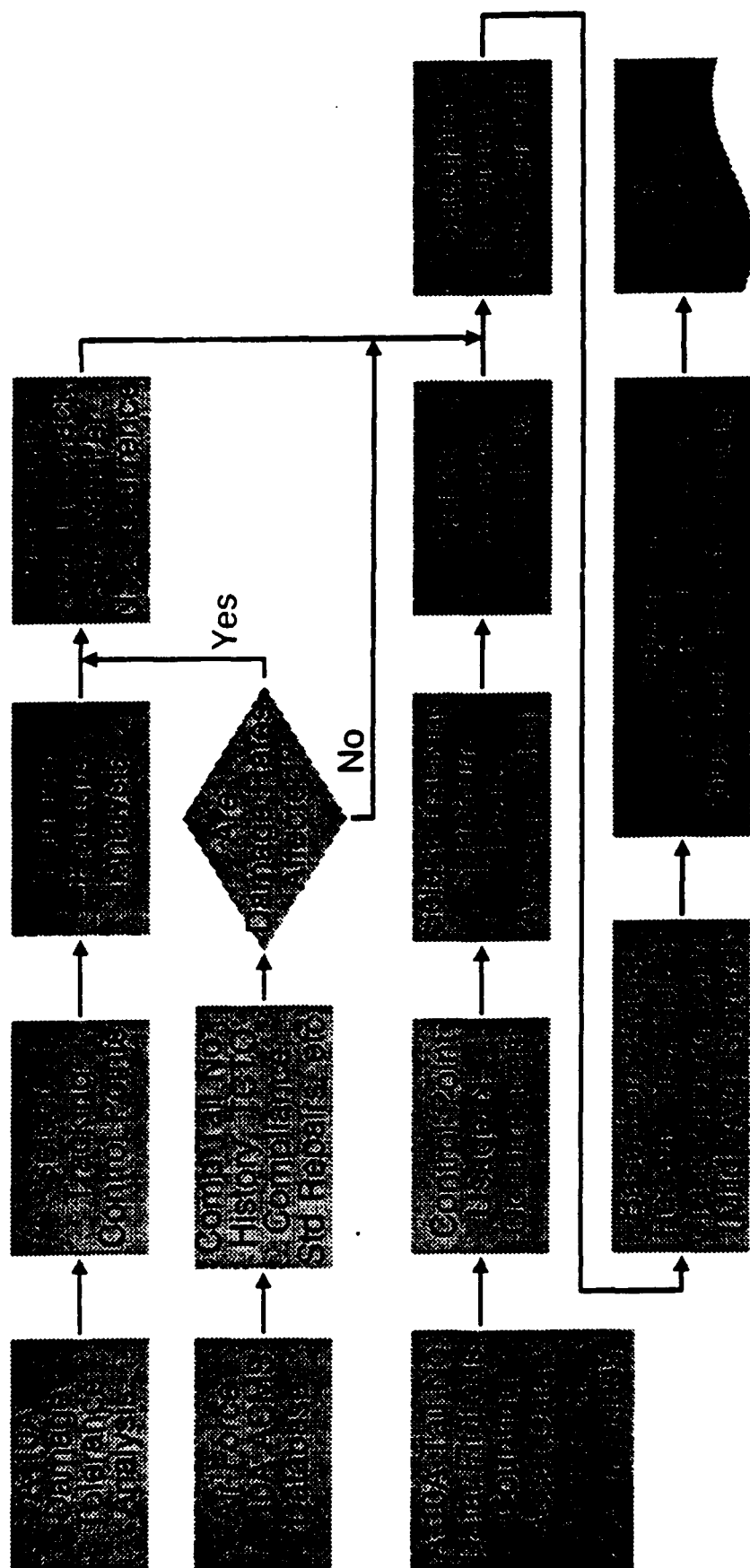


FIGURE 5 A-10A INDIVIDUAL A/C COMPONENT TRACKING PROGRAM UTILIZING FRACTURE ANALYSIS

- Last Update
 - Occurred in 1980
 - Based on 3000 hours MXU data
- More recent data available
 - 1st & 2nd 6000 hours MXU data available
 - Weapon system now mature
 - Usage more serve
 - Significant changes in gross weight distributions

FIGURE 6 IATP CURRENT TRACKING SPECTRUM

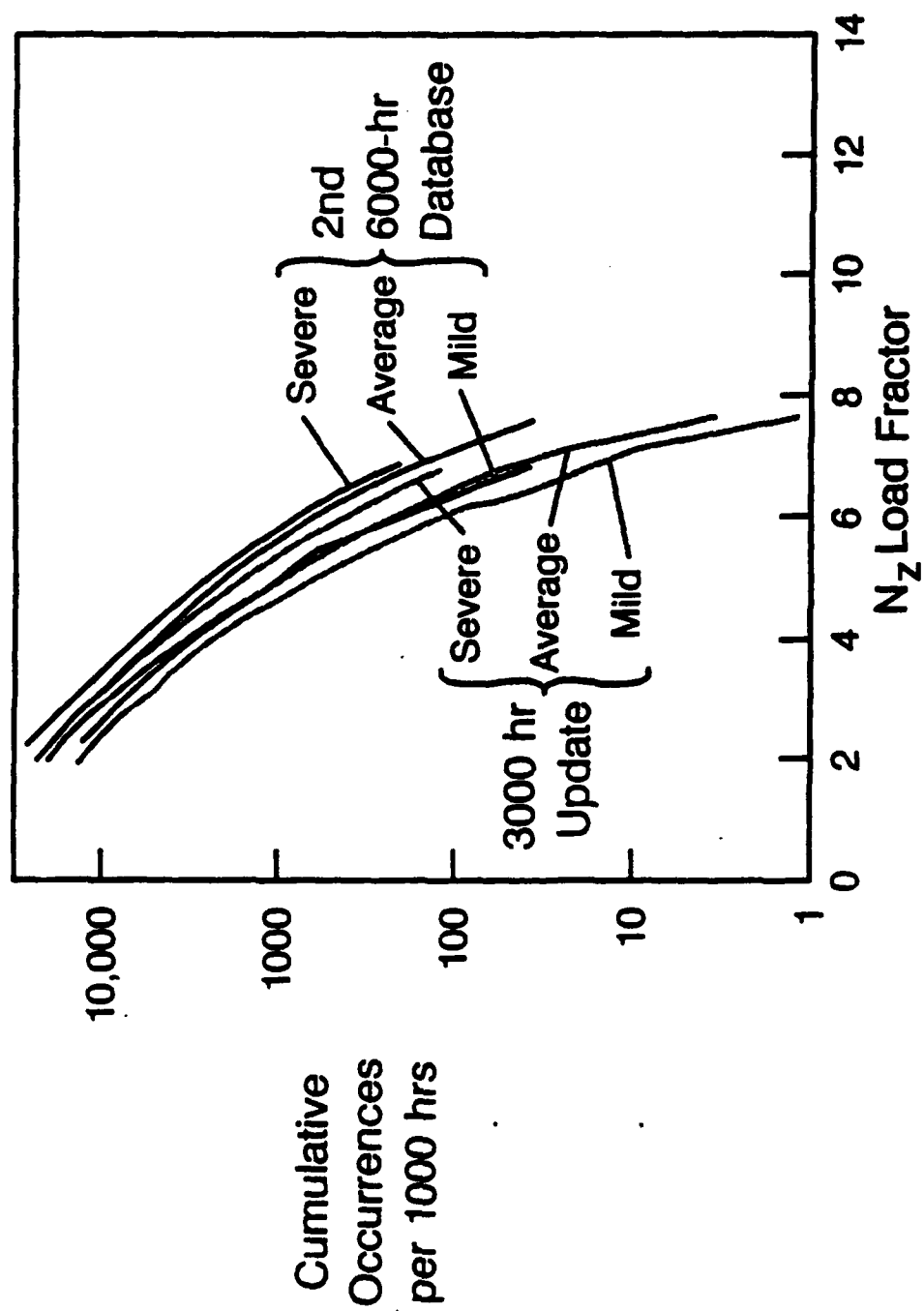


FIGURE 7 COMPARISON OF 2ND 6000-HR DATABASE WITH 3000-HR UPDATE

- **Issues**
 - Material & spectrum-sensitive
 - Individual aircraft vs group average
 - Prediction accuracy
 - Inspection schedule & methods
 - Universality for future changes
- **Alternatives**
 - Develop new coefficients; Verify by test
 - Wheeler retardation model
 - Analytic models; Verify by test
 - AFFDL-TR-74-129 Closure model
 - NASA TM 81890 MPYZ model

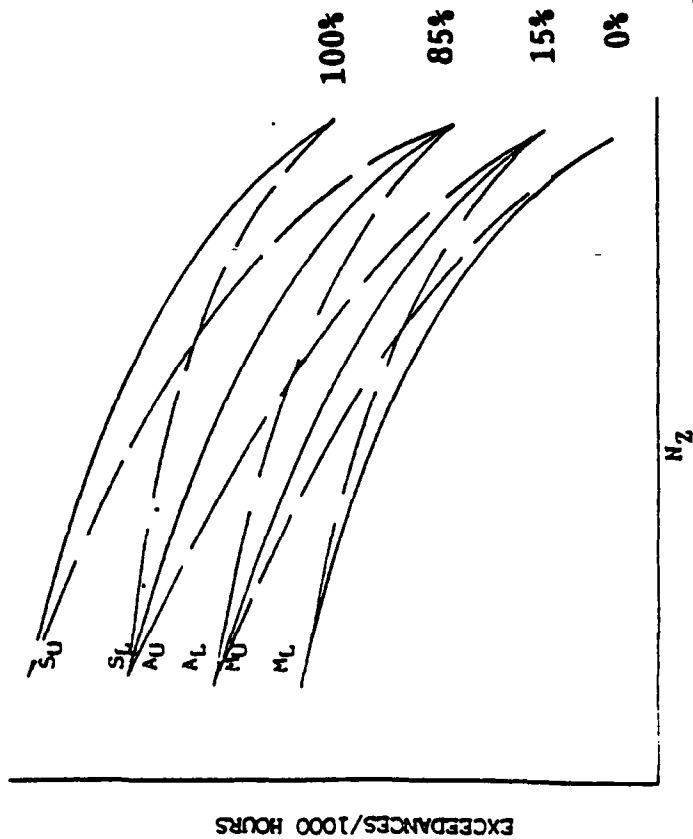
FIGURE 8 CURRENT METHODOLOGY VALIDATION FOR SPECTRUM CHANGE

- Utilize 2nd 6000-hr database to generate statistical exceedance curves
- Select two wing control Points (N_Z W-sensitive)
- Develop 10 spectra
- Perform representative coupon tests
 - Determine Wheeler retardation constants for each spectra
- Generate crack growth curves
 - AFFDL-TR-74-129 (Closure model)
 - NASA TM 81890 (MPYZ model)
- Evaluate the effects of spectrum variation on empirical & predictive crack growth methods

FIGURE 9 TEST AND ANALYSIS PROGRAM

- 2nd 6000-hr database
 - 411594 IAT flight hours
 - 5895 L/ESS hours
- Statistical Maneuver Spectrum Envelope
 - Normalized to 1000 hours
 - Sorted via increasing exceedances per 1000 hours
 - Developed table of cumulative percent of A/C vs exceedances per 1000 hours
 - 4 spectra boundaries (0, 15%, 85%, 100%)
 - Establish mild, average & severe & upper/lower rotational spectra via linear interpolation of spectra boundaries

FIGURE 10 SPECTRA DEVELOPMENT



3 MAJOR ZONES OF SEVERITY
 0 MILD
 0 AVERAGE
 0 SEVERE

SPECTRA		
NUMBER	DEFINITION	ROTATION
1	100% SPECTRUM	NONE
2	SU -SEVERE UPPER SPECTRUM	POSITIVE
3	SL -SEVERE LOWER SPECTRUM	NEGATIVE
4	85% SPECTRUM	NONE
5	AU -AVERAGE UPPER SPECTRUM	POSITIVE
6	AL -AVERAGE LOWER SPECTRUM	NEGATIVE
7	15% SPECTRUM	NONE
8	MU -MILD UPPER SPECTRUM	POSITIVE
9	ML -MILD LOWER SPECTRUM	NEGATIVE
10	0% SPECTRUM	NONE

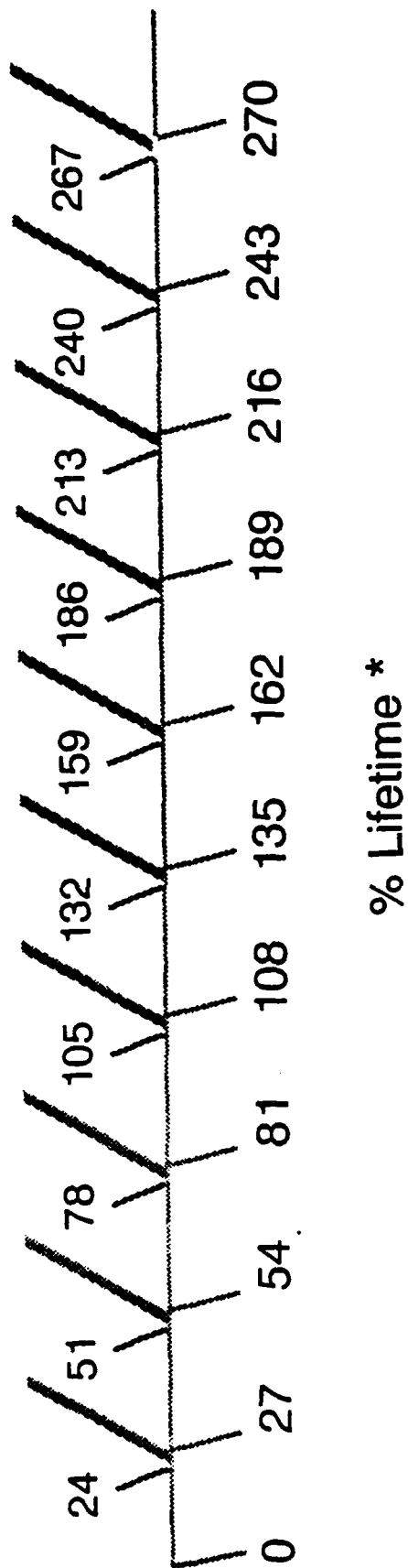
FIGURE 11 SPECTRA NUMBERING SYSTEM AND DEFINITION

MILD SPECTRUM		
<u>SPECTRUM</u>	<u>AIRCRAFT</u>	<u>PERCENT</u>
0%	5	7.25
LOWER	31	44.93
UPPER	9	13.04
15%	24	34.78
AVERAGE SPECTRUM		
<u>SPECTRUM</u>	<u>AIRCRAFT</u>	<u>PERCENT</u>
15%	134	27.46
LOWER	96	19.67
UPPER	142	29.10
85%	116	23.77
SEVERE SPECTRUM		
<u>SPECTRUM</u>	<u>AIRCRAFT</u>	<u>PERCENT</u>
85%	54	59.34
LOWER	19	20.88
UPPER	18	19.78
100%	0	0.00
TOTAL AIRCRAFT IN MILD ZONE	=	69
TOTAL AIRCRAFT IN AVERAGE ZONE	=	488
TOTAL AIRCRAFT IN SEVERE ZONE	=	91
TOTAL AIRCRAFT	= 648	

FIGURE 12 NUMBER OF AIRCRAFT WITHIN ZONES OF SEVERITY

- Empirical
 - For each zone calculate:
 - Average coefficients & average Wheeler constant based on No. of aircraft flying to each spectra
 - Generate crack growth curves based on average coefficients, average Wheeler & current methodology
- Analytical
 - Closure/MPYZ determine material constants based on test
 - Generate crack ground curves based on closure & MPYZ models

FIGURE 13 ASSESS VALIDITY OF CURRENT IATP METHODOLOGY



* One Lifetime = 8000 hrs

FIGURE 14 FRACTOGRAPHY ENHANCED BY USE OF MARKER BANDS

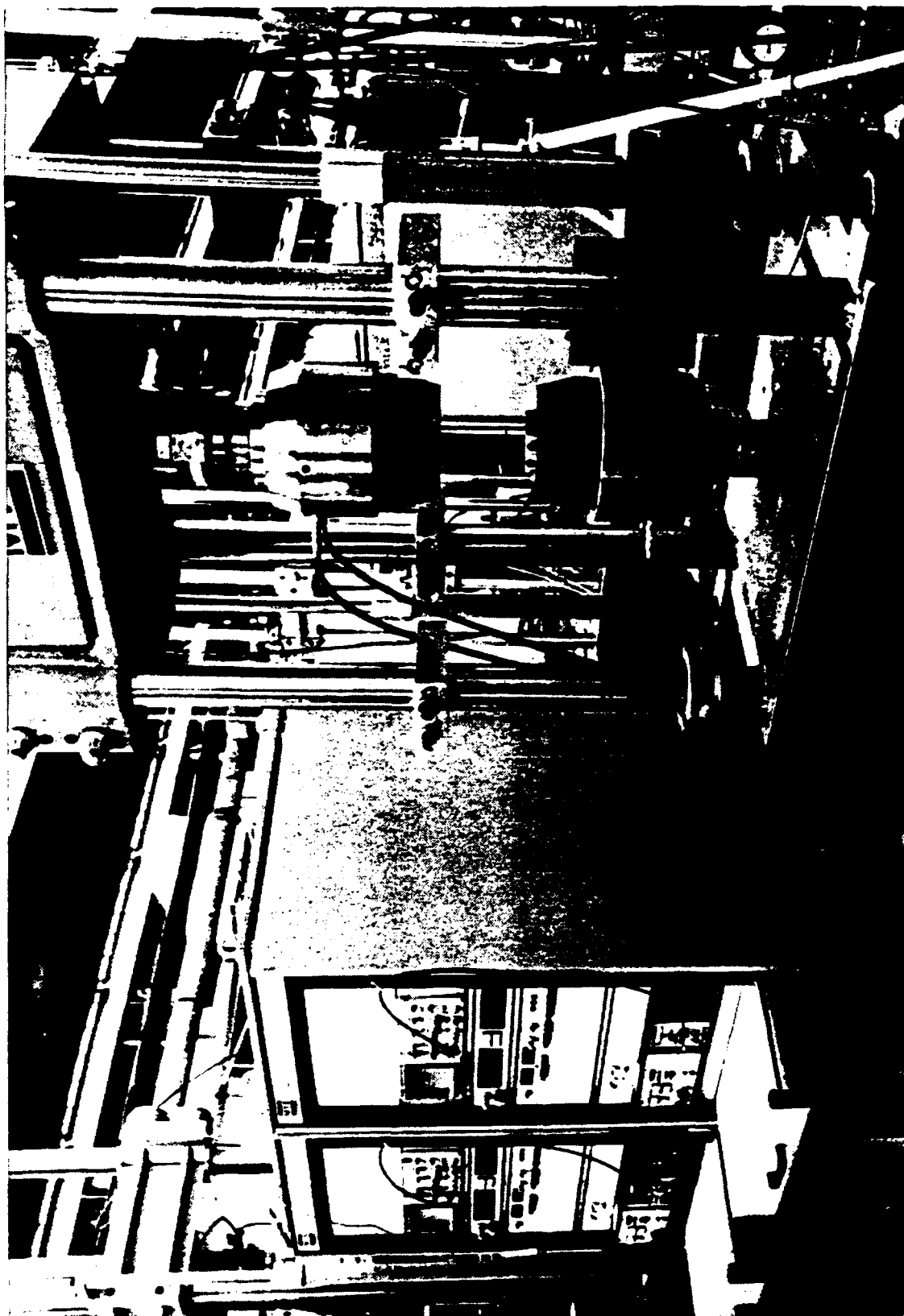


FIGURE 15 TYPICAL LABORATORY SET-UP

Lower Wing Skin/Rear Spar

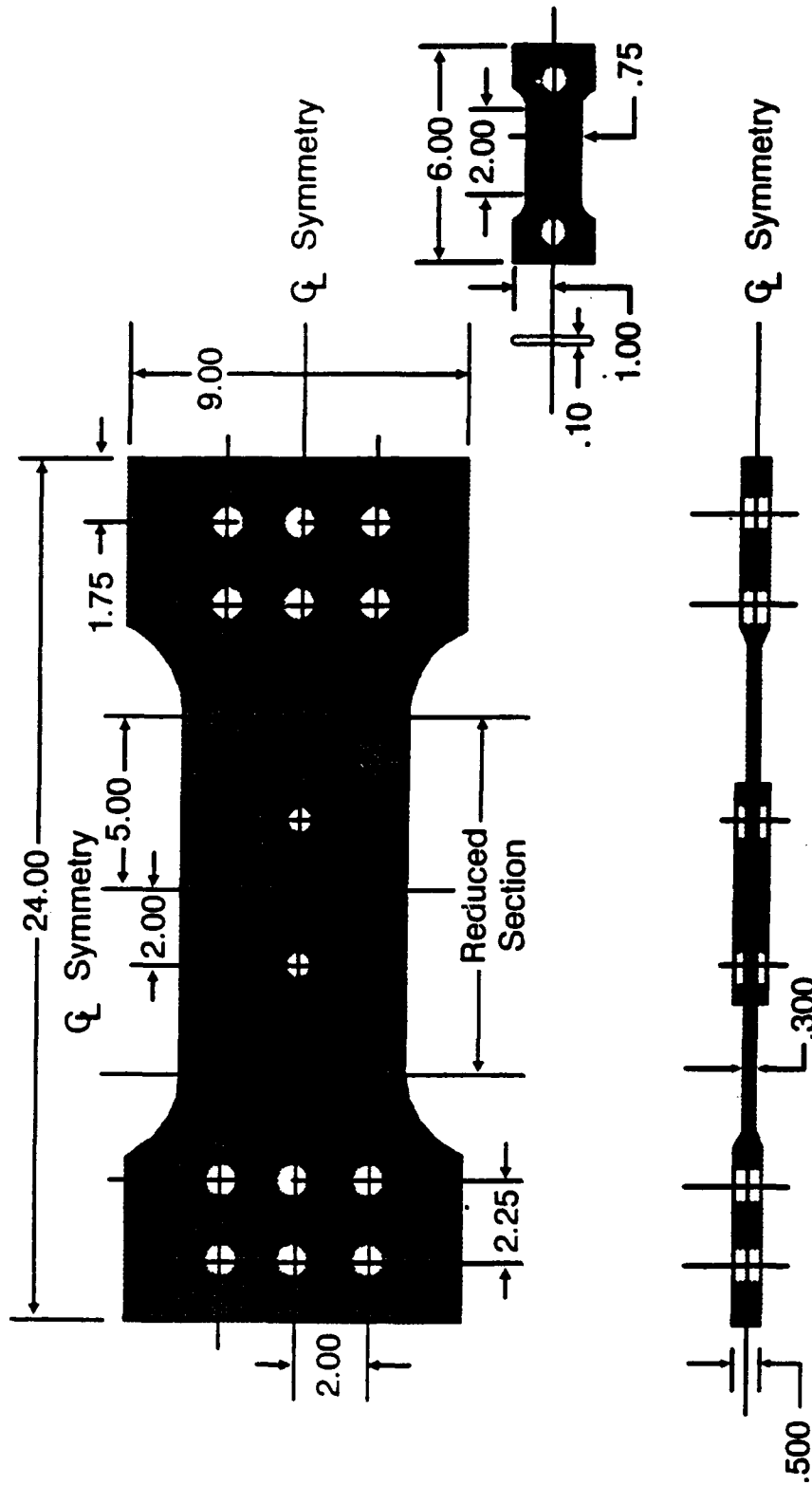
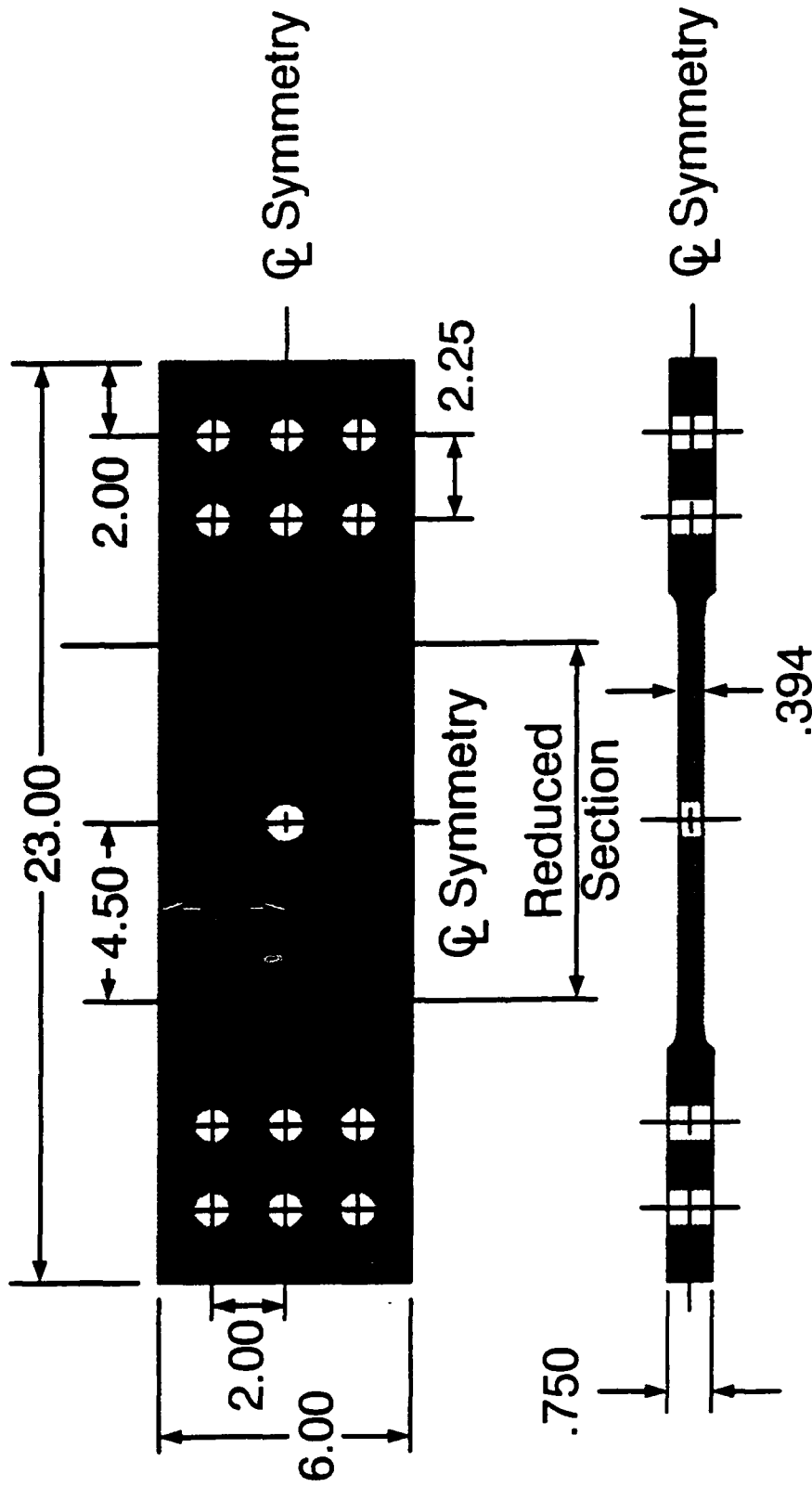


FIGURE 16 WING CONTROL POINT NO. 1

Wing Skin Plank: Fuel Transfer Hole



Material 2024-T3511 Extrusion

FIGURE 17 WING CONTROL POINT NO.2

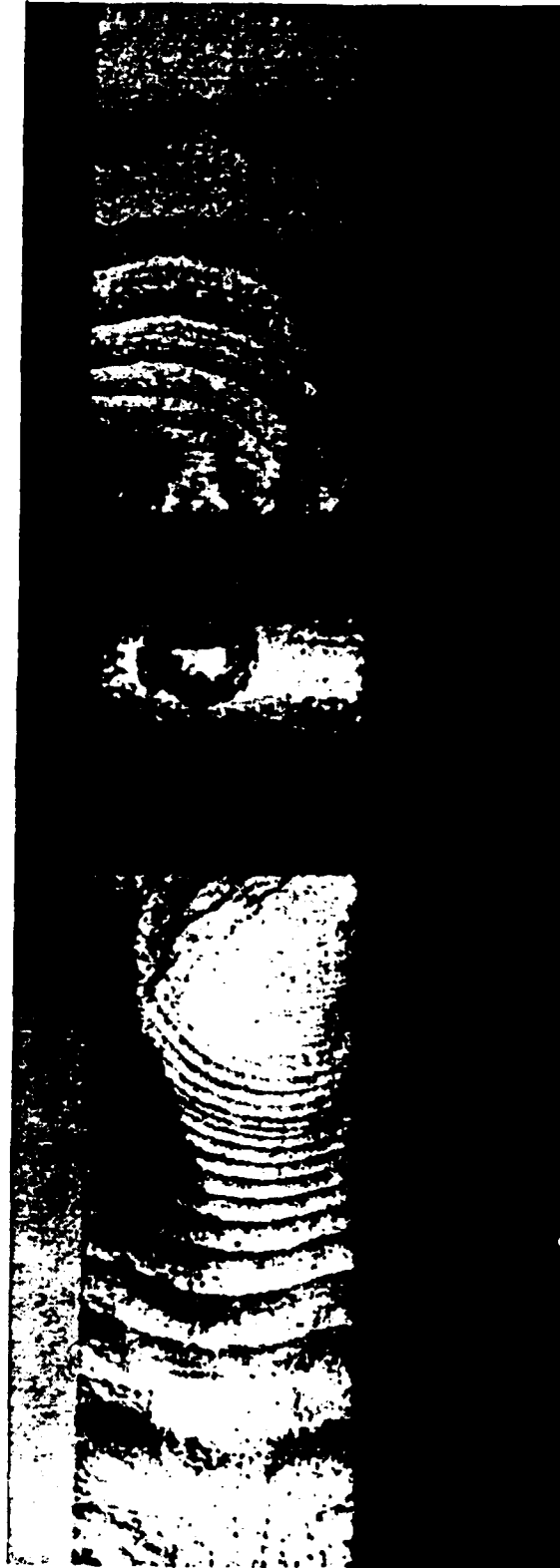
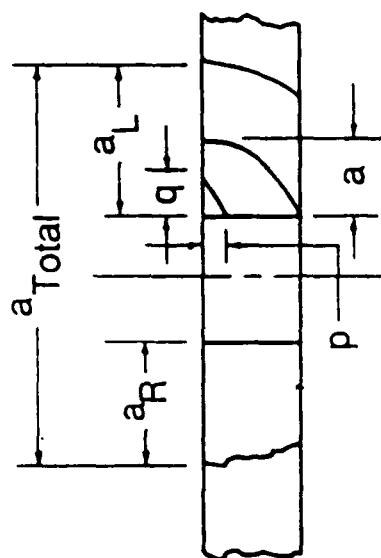


FIGURE 18 TYPICAL FRACTURE

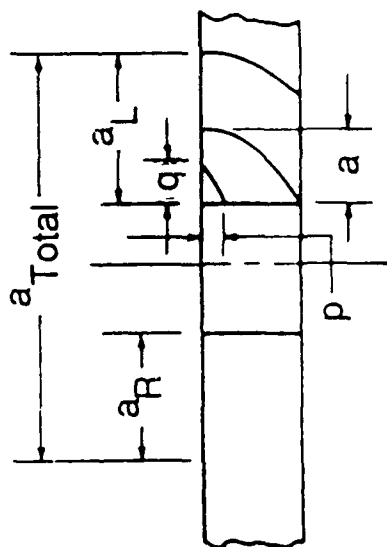
SPECTRUM	S/N	Max. Spec. Life Stress	Fail Life (hrs)	Init. Flaw q (in)	Init. Flow p (in)	Break Thru a (in)	Final Crack (L) (in)	Final Crack (R) (in)	Total Crack a (in)
100%	10	40.40	7840	0.044	none	none	0.719	0.530	1.749
	13	6747	6747	0.042	0.071	0.145	0.627	0.570	1.697
	27	7192	7192	0.000	none	0.054	0.560	0.580	1.640
Sev Upper	7	38.25	4603	0.039	0.075	0.136	0.845	0.650	1.995
	12	4653	4653	0.038	0.072	0.128	0.840	0.660	2.000
	36	5434	5434	0.031	0.059	0.155	0.749	0.550	1.799
Sev Lower	28	41.40	16338	0.000	none	0.040	0.659	0.600	1.759
	9	6535	6535	0.066	0.096	0.152	0.662	0.400	1.562
	18	6966	6966	0.060	0.094	0.143	0.691	0.500	1.691
65%	4	41.70	7831	0.066	none	none	0.950	0.680	2.130
	29	9837	9837	0.000	none	none	0.857	0.430	1.787
	31	4997	4997	0.062	none	none	0.545	0.400	1.445
Ave Upper	1	36.00	11257	0.029	0.052	0.127	0.878	0.650	2.028
	15	10747	10747	0.041	0.076	0.126	0.855	0.680	2.035
	21	15014	15014	0.000	none	0.122	0.803	0.770	2.073
Ave Lower	3	44.30	5993	0.045	0.072	0.163	0.429	0.350	1.279
	17	8153	8153	0.043	0.076	0.175	0.655	0.570	1.725
	33	8905	8905	0.034	0.066	0.124	0.465	0.330	1.295
15%	20	39.10	10583	0.036	0.074	0.143	0.594	0.480	1.574
	14	6407	6407	0.098	0.129	0.185	0.748	0.500	1.748
	34	8494	8494	0.041	0.068	0.139	0.655	0.500	1.655
Mld Upper	C	40.60	15251	0.065	none	0.065	0.618	0.520	1.638
	22	19790	19790	0.033	0.058	0.156	0.555	0.450	1.505
	B	17647	17647	0.033	0.036	0.145	0.485	0.400	1.385
Mld Lower	26	33.80	12637	0.036	0.067	0.152	0.594	0.540	1.634
	19	10694	10694	0.036	0.065	0.222	1.450	0.480	2.430
	A	17515	17515	0.023	0.044	0.180	0.885	0.900	2.285
0%	30	38.40	20768	0.000	none	0.108	0.652	0.550	1.702
	24	29224	29224	0.039	none	0.039	0.772	0.800	2.072
	25	26792	26792	0.000	none	0.067	0.633	0.500	1.633



Crack Geometry

FIGURE 19 TEST DATA WING CONTROL POINT 1

SPECTRUM	S/N	Max. Spec. Life Stress	Fail Life (hrs)	Init. Flaw q	Init. Flaw p	Break Thru a	Final Crack (L)	Final Crack (R)	Total Crack a	Avg. Crack a
		(ksi)	(hrs)	(in)	(in)	(in)	(in)	(in)	(in)	(in)
100%	3	37.60	6950	0.034	0.073	0.315	1.200	0.730	2.430	2.397
	21	5877	5877	0.046	0.070	0.248	1.080	0.720	2.300	
	4	6950	6950	0.026	0.045	0.300	1.130	0.830	2.460	
Sev Upper	6	35.60	4999	0.042	0.074	0.300	1.430	0.800	2.730	2.667
	8	6043	6043	0.044	0.088	0.272	1.400	0.960	2.860	
	10	6414	6414	0.027	0.056	0.311	1.160	0.750	2.410	
Sev Lower	20	38.40	9371	0.031	0.057	0.240	0.990	0.600	2.090	2.307
	24	10069	10069	0.041	0.073	0.278	1.420	0.740	2.660	
	27	7455	7455	0.040	0.076	0.328	1.130	0.540	2.170	
85%	30	38.70	8537	0.058	0.082	0.261	0.910	0.850	2.260	2.423
	26	9693	9693	0.035	0.076	0.245	1.470	0.990	2.960	
	29	7889	7889	0.036	0.068	0.277	1.050	0.500	2.050	
Ave Upper	13	33.40	6609	0.039	0.072	0.28	1.540	0.930	2.970	2.690
	18	6938	6938	0.042	0.074	0.289	1.410	0.730	2.640	
	1	6377	6377	0.046	0.072	0.318	1.140	0.820	2.460	
Ave Lower	16	41.10	11034	0.034	0.073	0.262	0.980	0.600	2.080	2.260
	7	13459	13459	0.027	0.062	0.292	0.910	0.600	2.010	
	31	10896	10896	0.040	0.076	0.249	1.270	0.920	2.690	
15%	5	36.30	8664	0.043	0.058	0.250	0.960	0.700	2.160	2.360
	15	13264	13264	0.000	0.000	0.600	1.240	1.020	2.260	
	22	9317	9317	0.039	0.075	0.255	1.260	0.900	2.660	
Mld Upper	23	38.20	12824	0.047	0.075	0.304	1.130	0.600	2.230	2.303
	11	16430	16430	0.038	0.070	0.360	1.080	0.560	2.140	
	25	14489	14489	0.035	0.078	0.258	1.200	0.840	2.540	
Mld Lower	14	31.30	8425	0.036	0.050	0.393	1.240	0.490	2.230	2.320
	9	8533	8533	0.028	0.057	0.303	1.200	0.530	2.230	
	19	7703	7703	0.036	0.055	0.421	1.430	0.570	2.500	
0%	12	35.70	17070	0.036	0.072	0.291	1.330	0.530	2.360	2.390
	17	19231	19231	0.022	0.049	0.274	1.120	0.880	2.500	
	28	17177	17177	0.035	0.079	0.313	1.180	0.630	2.310	



Crack Geometry

FIGURE 20 TEST DATA WING CONTROL POINT 2

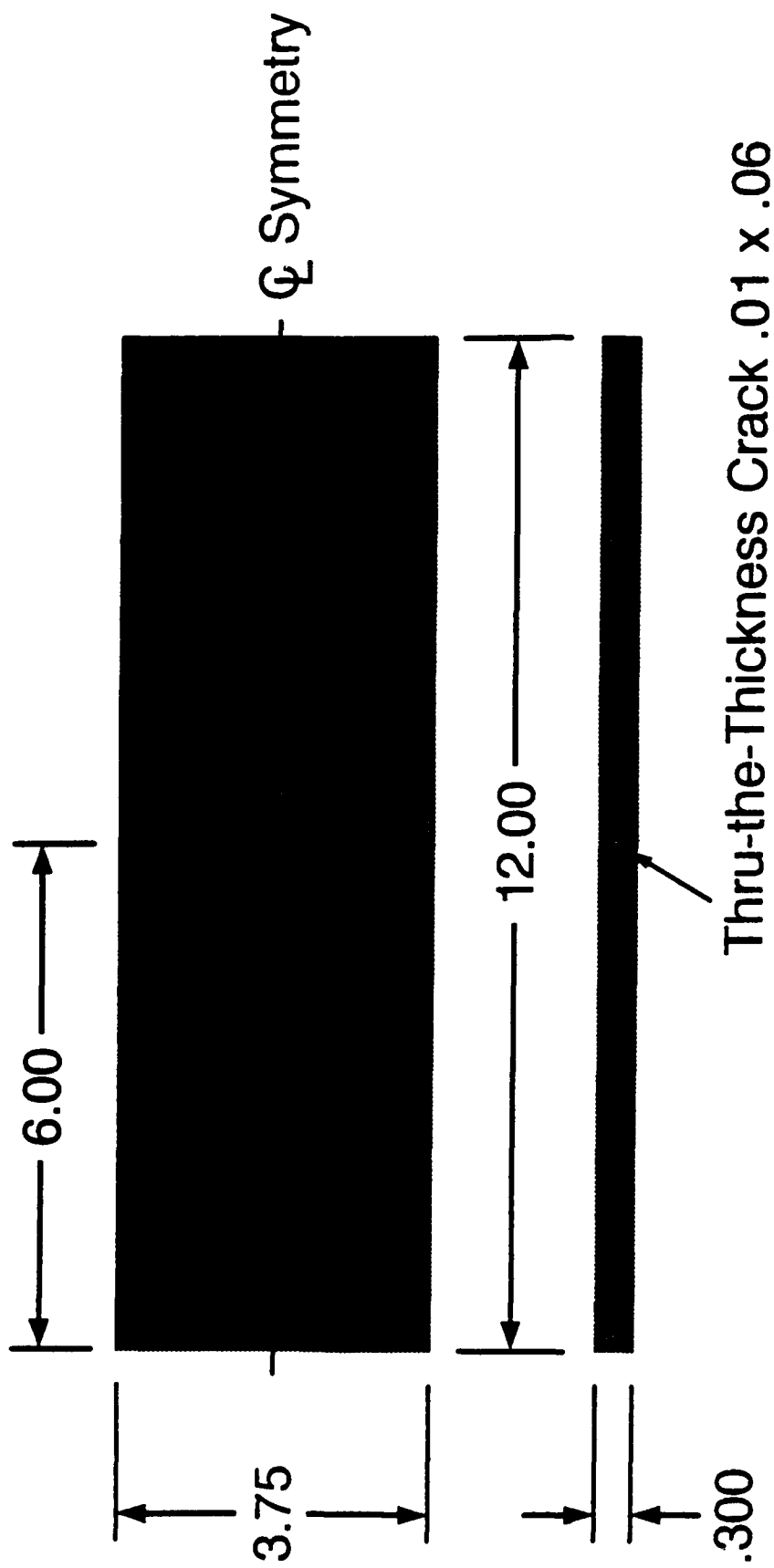
Crack Growth Closure Model/MPYZ Model

- Basic Paris equation
- Constants determined by da/dn testing
- Interaction material constants generated by test
- Define geometrical model for control point configuration
- Apply random flight by flight spectrum & generate crack growth curve
- Validation by limited coupon testing

Objective:

Apply to all critical locations without further testing

FIGURE 21 ANALYTICAL CRACK GROWTH MODELS

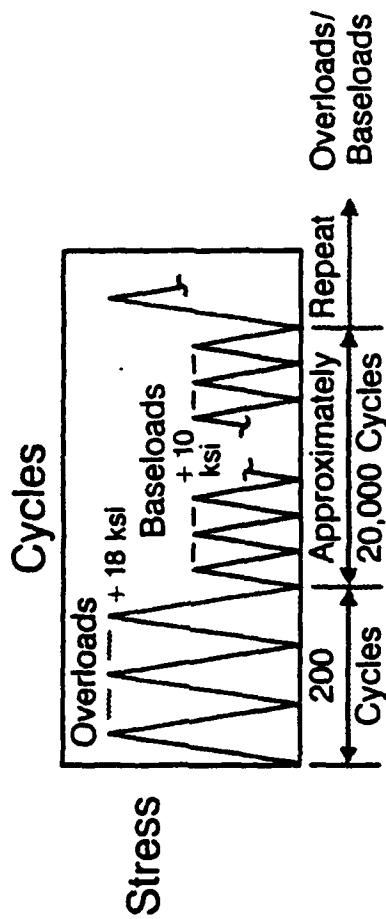


Material 2024-T351 Aluminum Plate

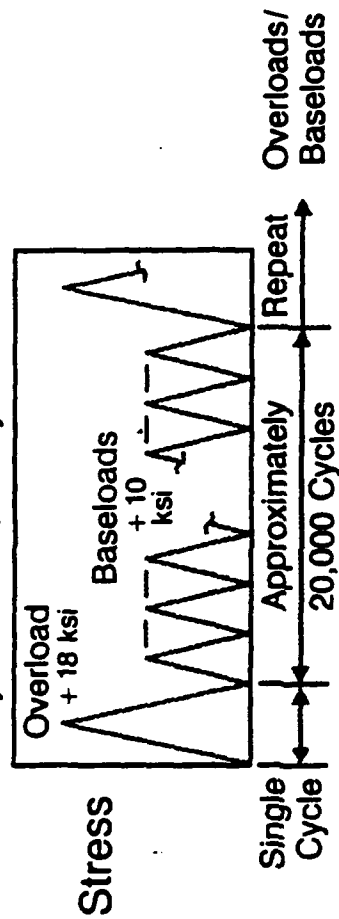
FIGURE 22 TEST SPECIMEN FOR MATERIAL CONSTANTS CLOSURE/MPYZ

● Spectra

Test 1 - Constant Amplitude with Multiple Overloads



Test 2 - Constant Amplitude with Single Overload



Test 3 - Constant Amplitude with Single Completely Reversed Overload

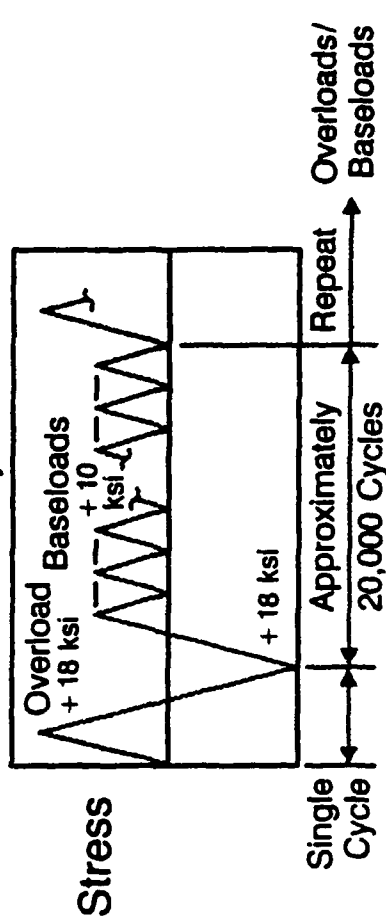


FIGURE 23 CLOSURE/MPYZ TEST PROGRAM FOR 2024-T351 MATERIAL CONSTANTS

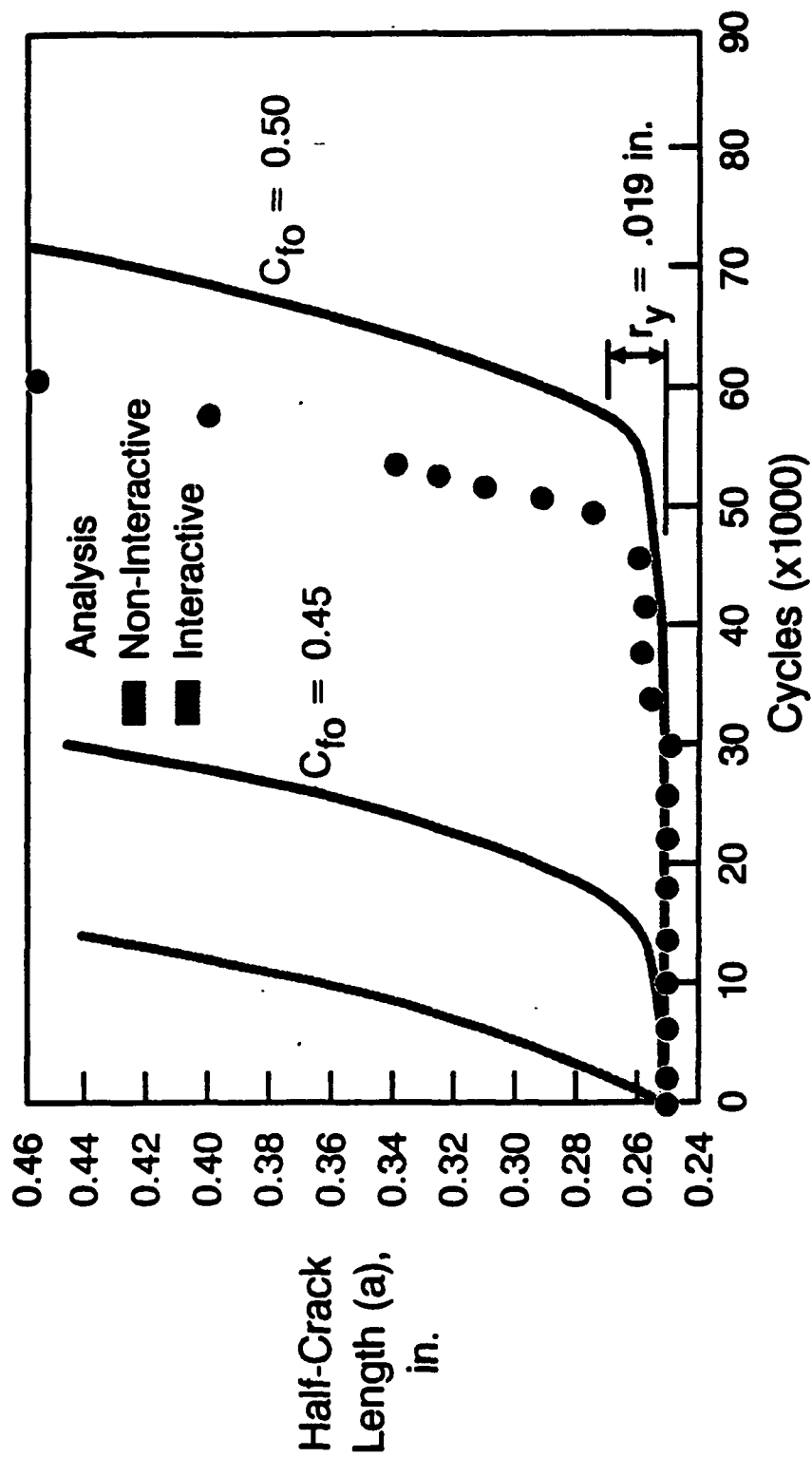


FIGURE 24 CRACK GROWTH FOLLOWING MULTIPLE OVERLOADS; 2024-T351 PLATE; CLOSURE MODEL

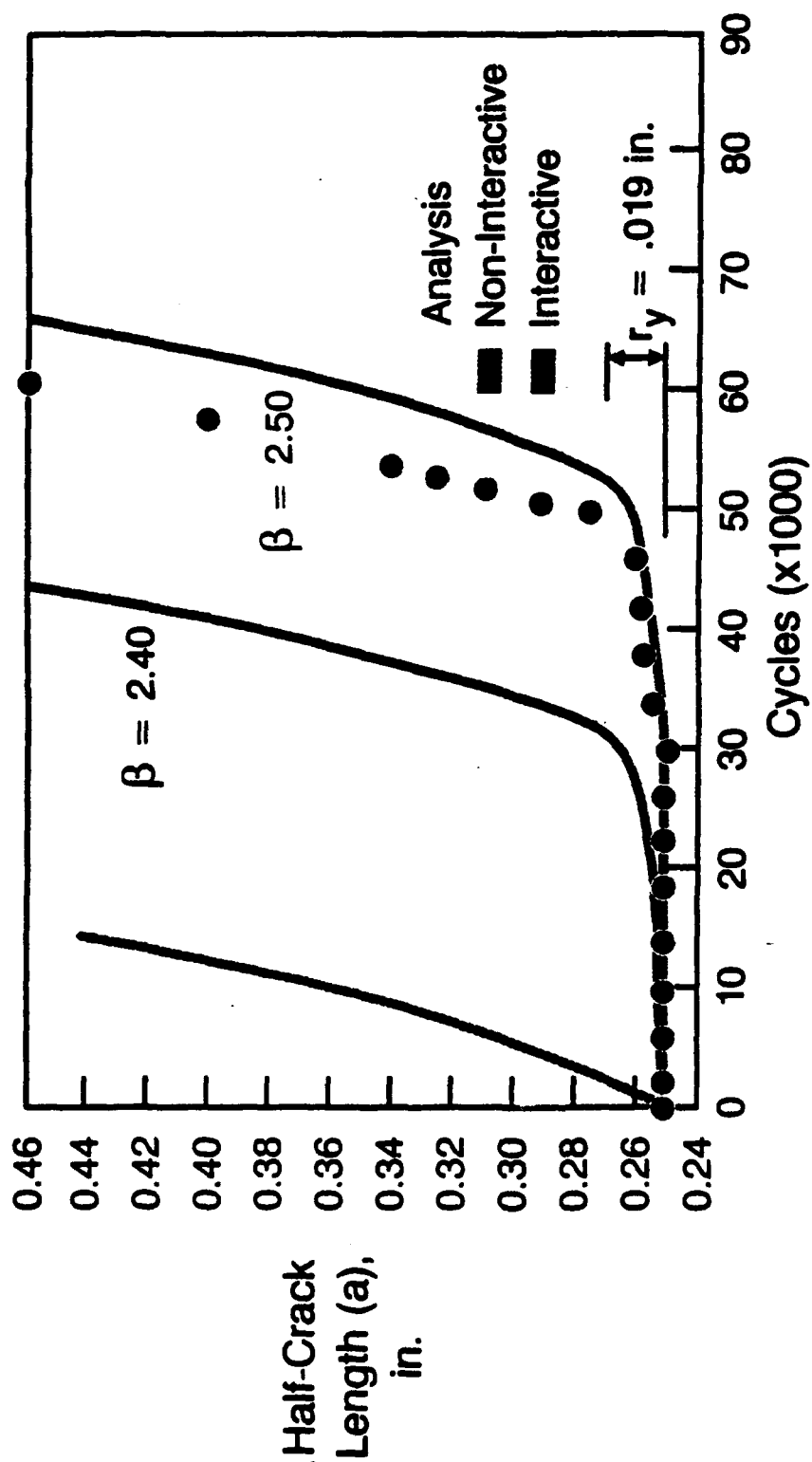


FIGURE 25 CRACK GROWTH FOLLOWING MULTIPLE OVERLOADS; 2024-T351 PLATE; MPYZ MODEL

2024-T351 Plate

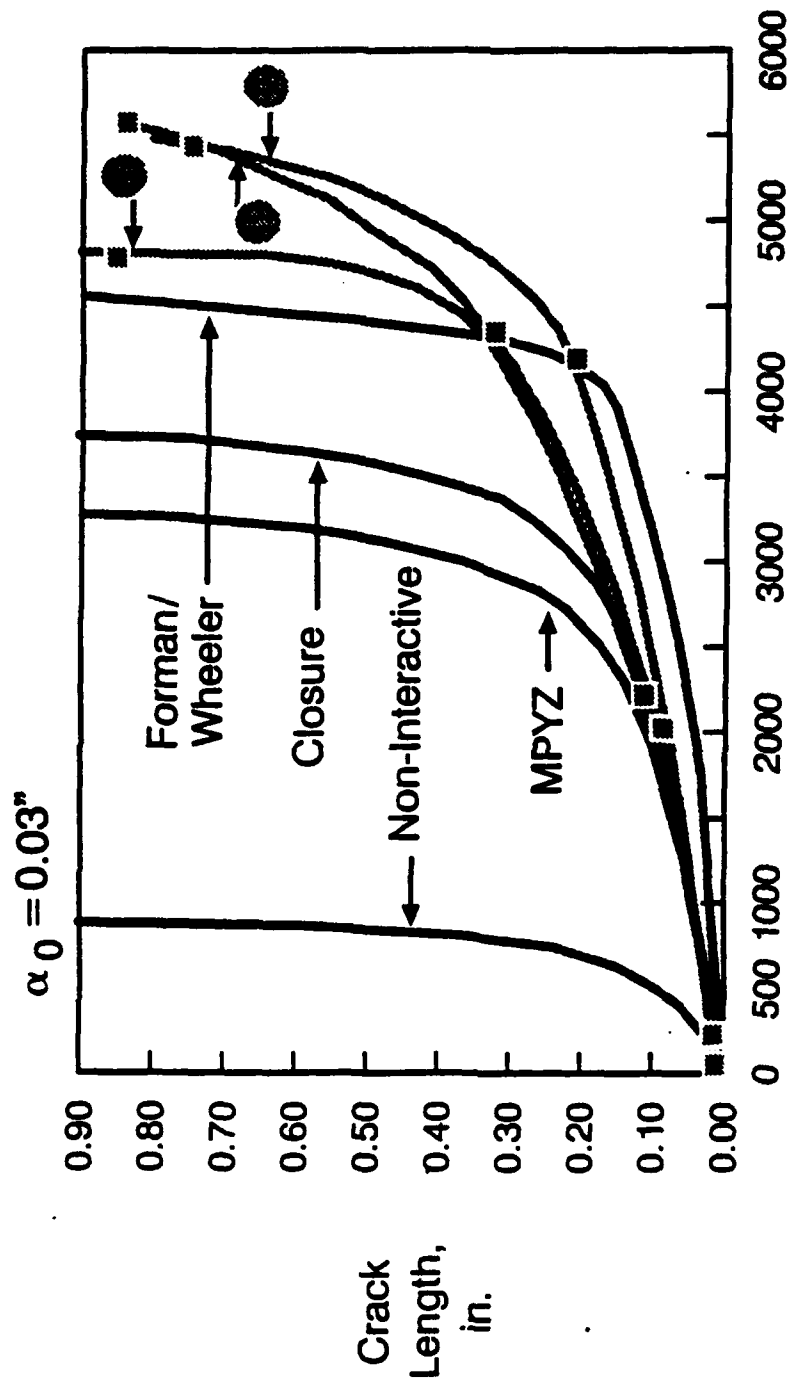


FIGURE 26 A-10A SEVERE UPPER SPECTRUM (CP1, NO. 7,12,36)

2024-T351 Plate

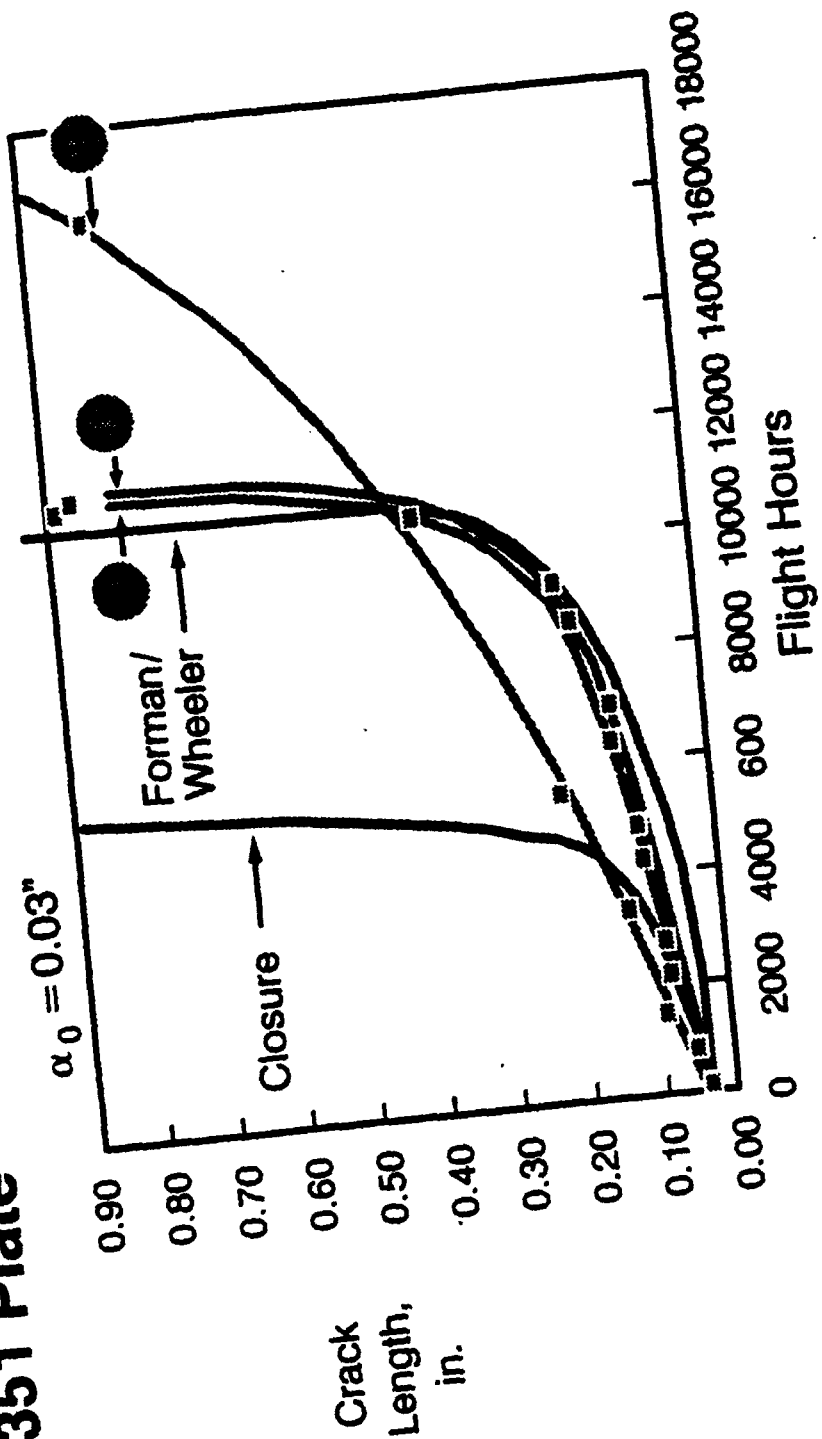


FIGURE 27 A-10A AVERAGE UPPER SPECTRUM (CP1, NO. 1,15,21)

2024-T351 Plate

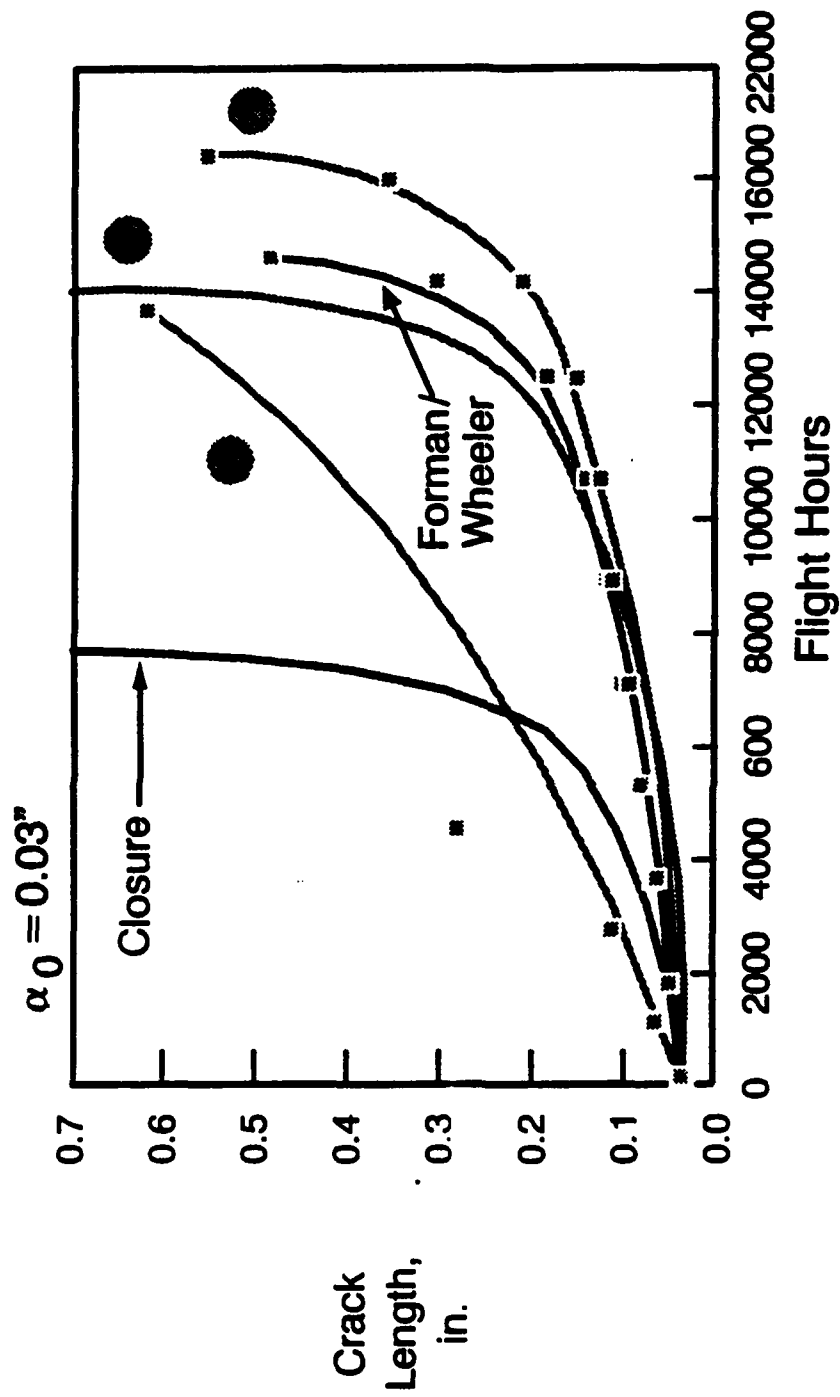


FIGURE 28 A-10A MILD UPPER SPECTRUM (CP1, NO. B, C, 22)

2024-T3511 Extrusion

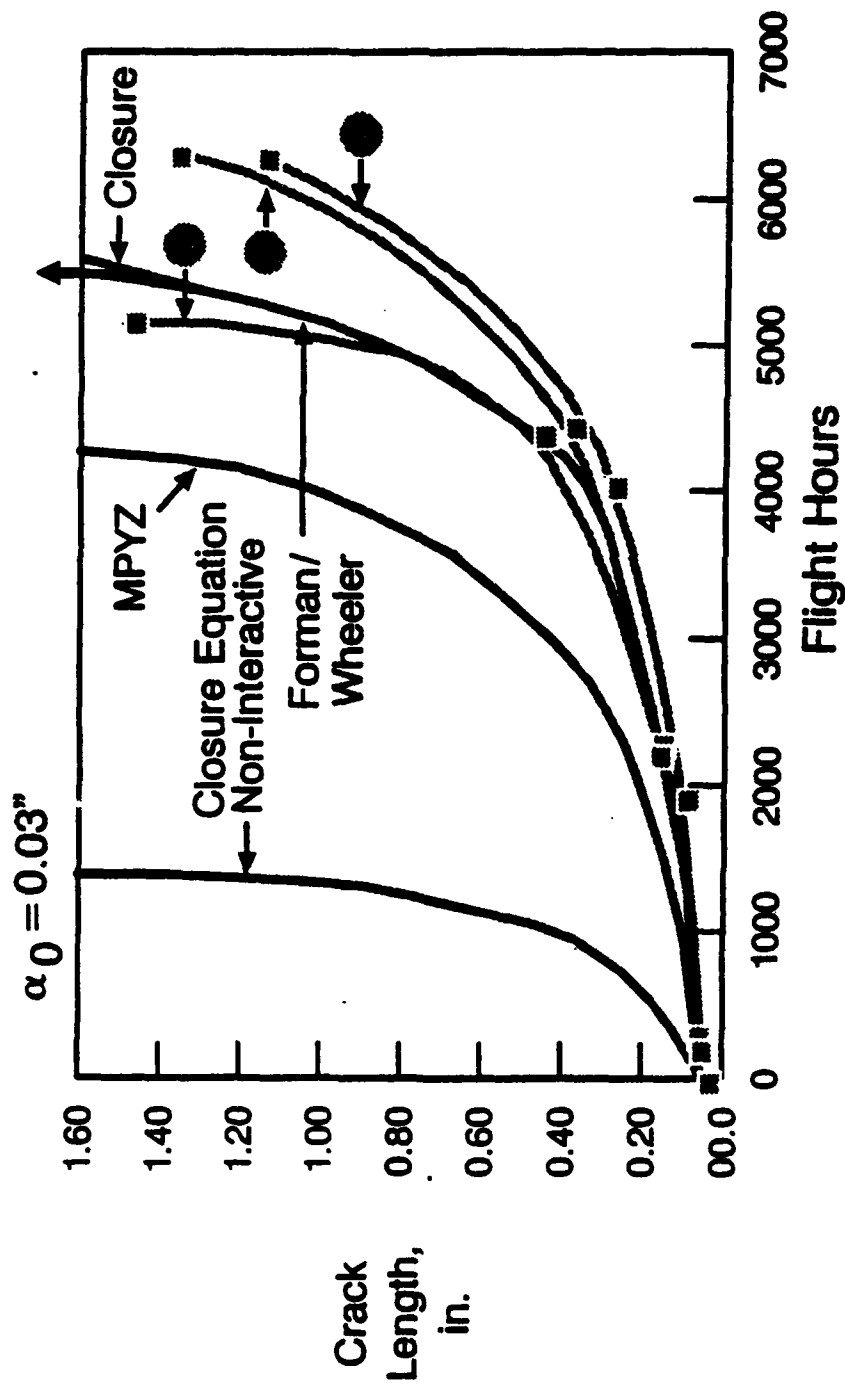


FIGURE 29 A-10A SEVERE UPPER SPECTRUM (CP2, NO. 6,8,10)

2024-T3511 Extrusion

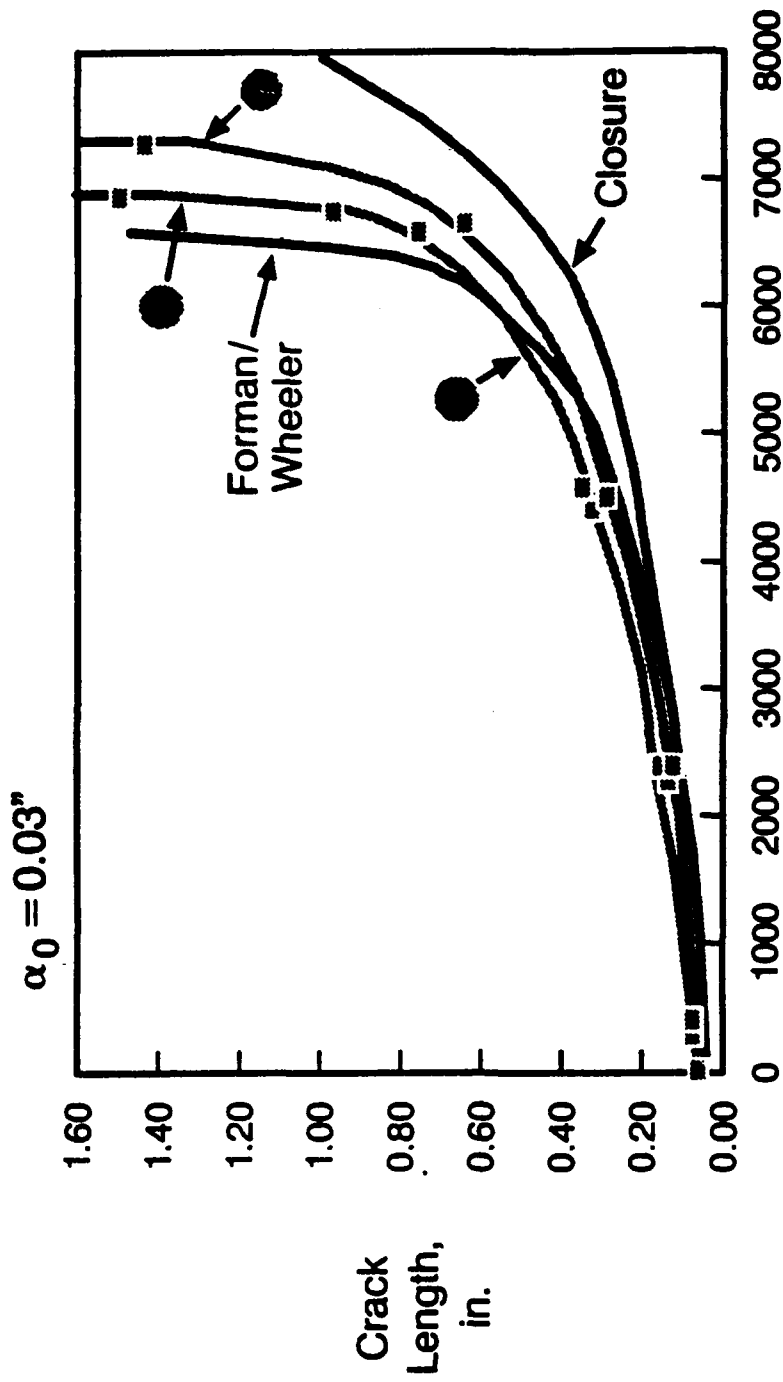


FIGURE 30 A-10A AVERAGE UPPER SPECTRUM (CP2, NO. 1,13,18)

2024-T3511 Extrusion

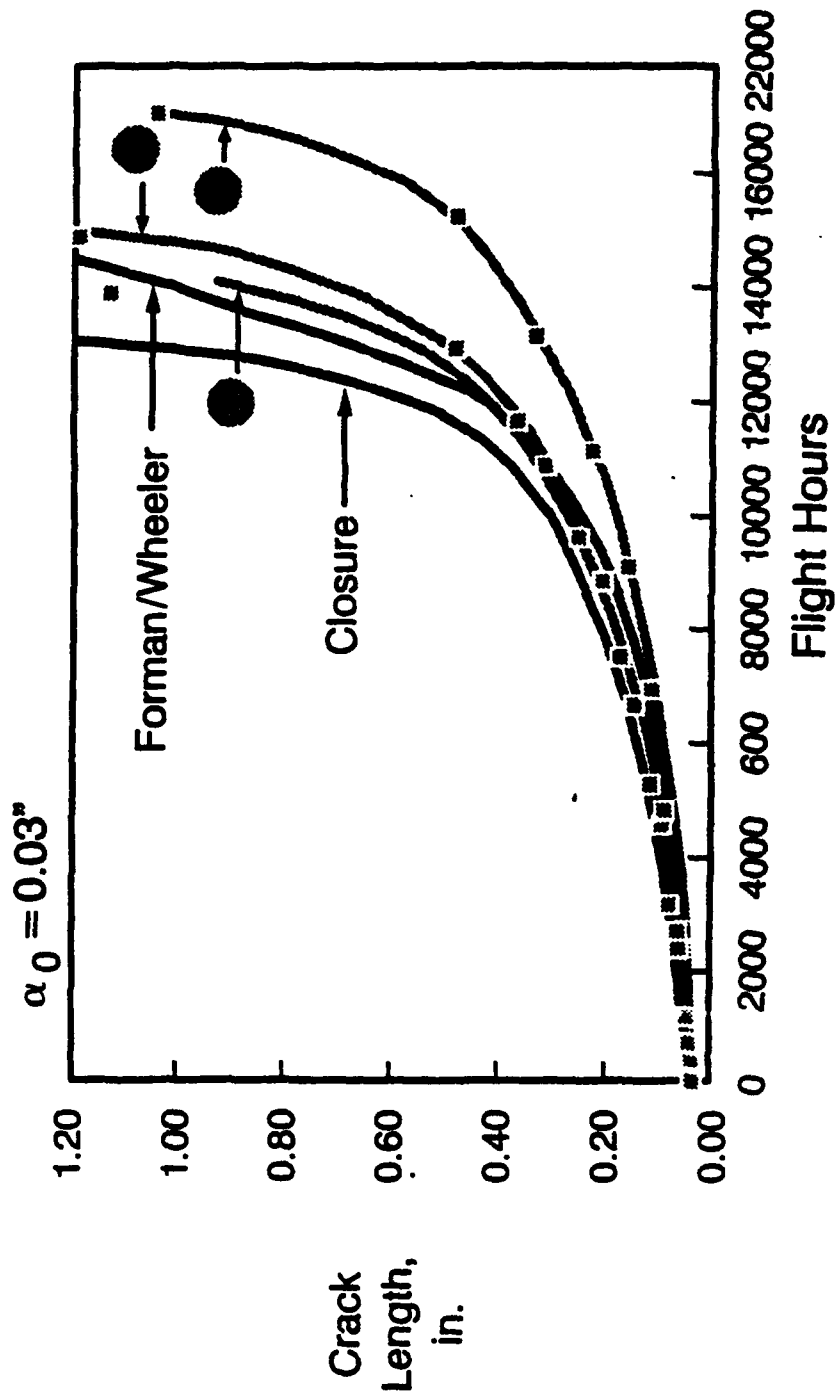


FIGURE 31 A-10A MILD UPPER SPECTRUM (CP2, NO. 11,23,25)

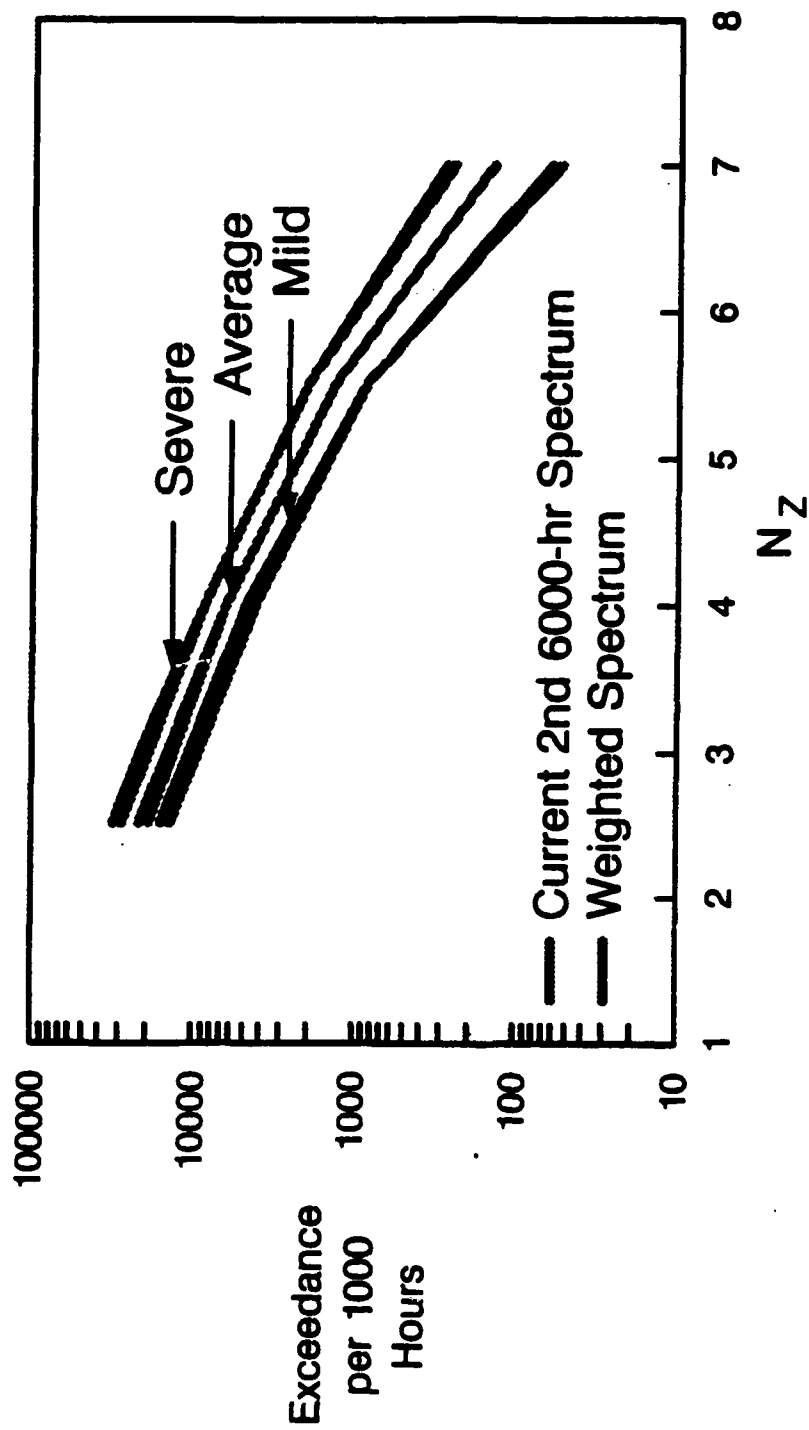


FIGURE 32 SPECTRA COMPARISON

CP2 2024-T3511 Extrusion

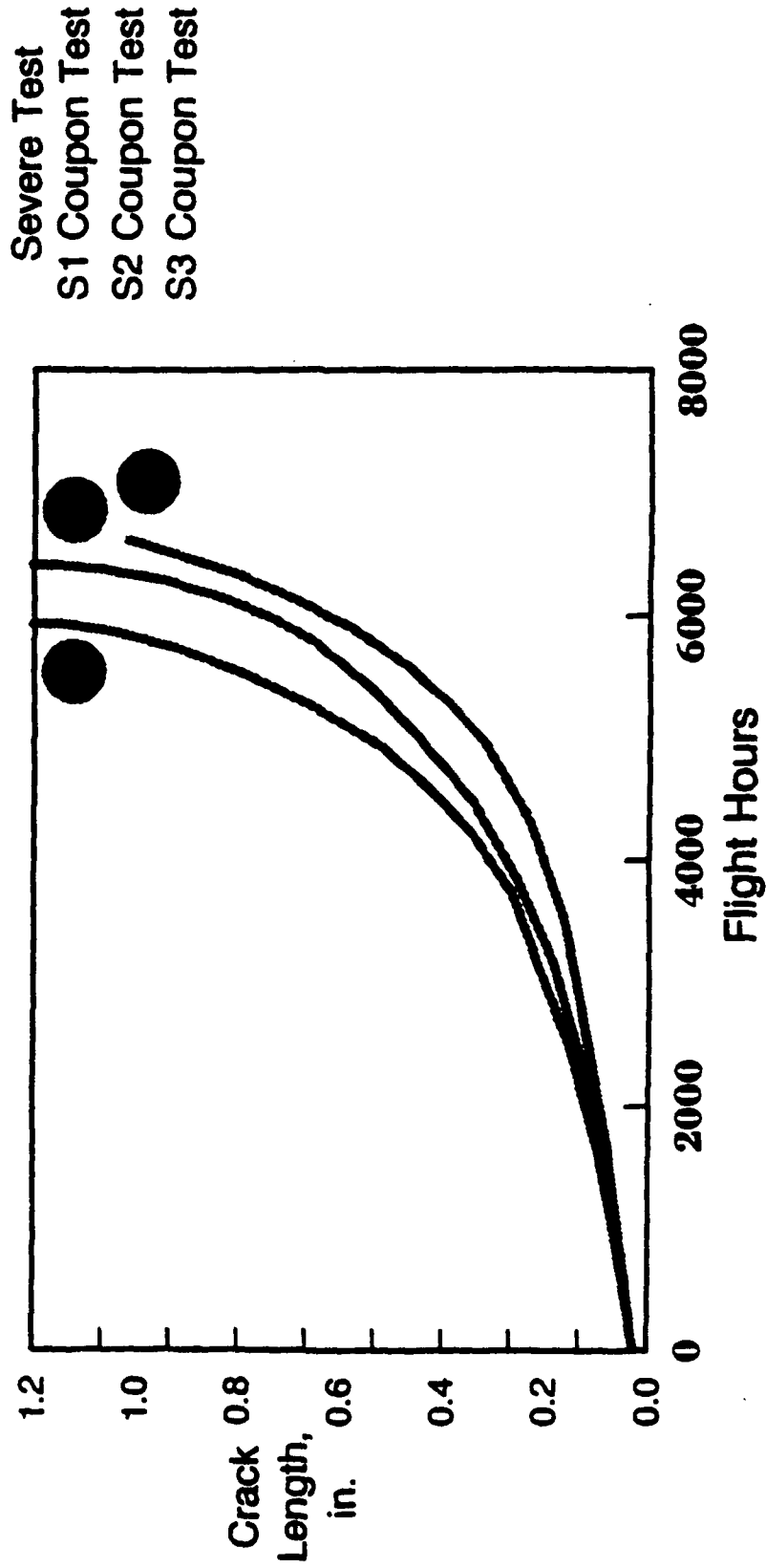


FIGURE 33 A-10A WEIGHTED SPECTRUM TEST RESULTS CP2

CP2 2024-T3511 Extrusion

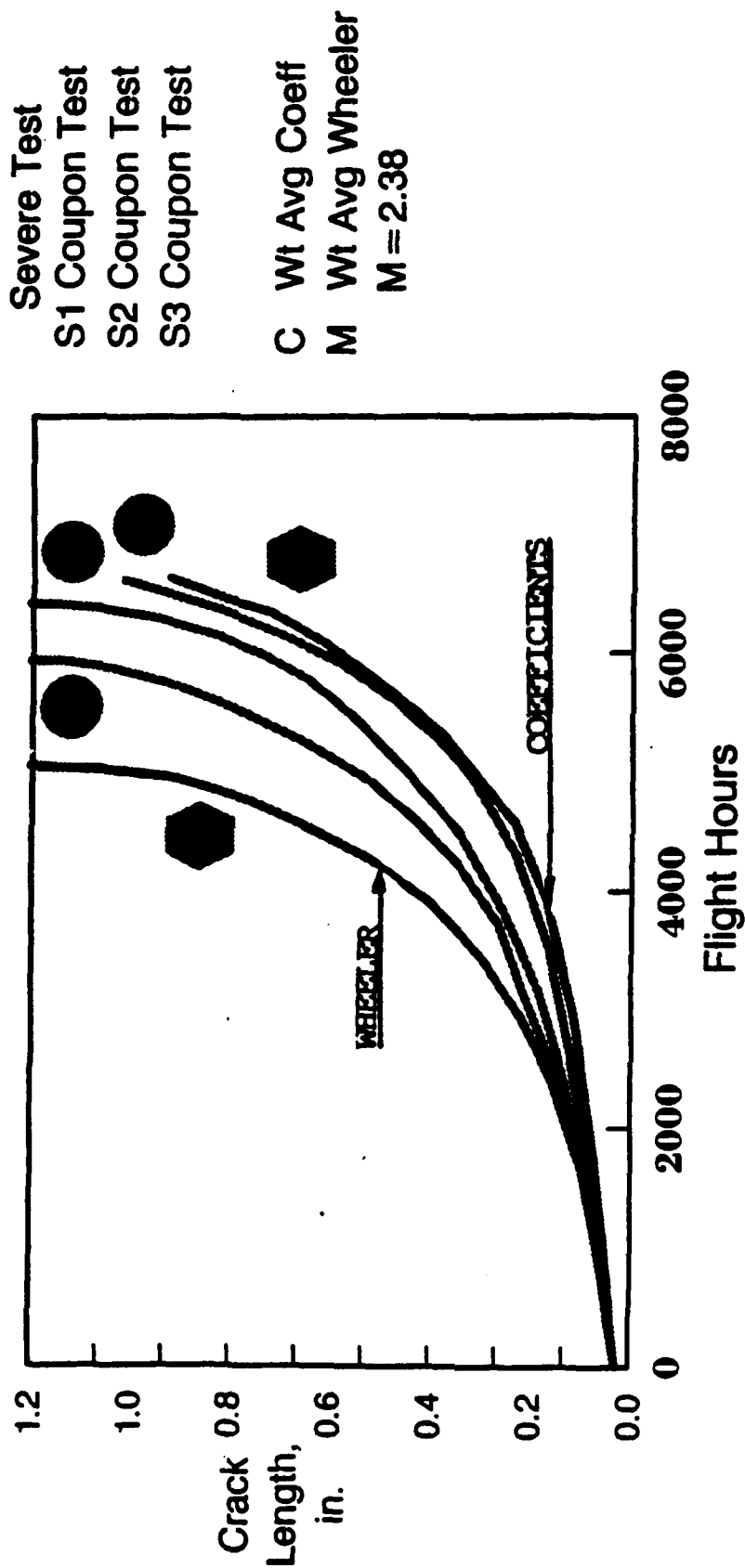


FIGURE 34 A-10 WEIGHTED SPECTRUM TEST RESULTS CP2 COMPARISON WITH WEIGHTED WHEELER & COEFFICIENT

Analytic Predictive Methods (Closure/MPYZ) are Inadequate for IATP Use

- Both models too conservative for load transfer holes significantly affected by variations in loaded holes stress intensity solutions
- Closure model not consistently conservative for open holes
- MPYZ model too conservative
 - Additional test data required for 2024 material constants
- All data based on N_Z W critical spectra & must be validated for combined load factors & speeds
- Spectrum changes would require limited testing to validate results

FIGURE 35 CONCLUSIONS ANALYTIC PREDICTIVE METHODS (CLOSURE/MPYZ)

Current Method of Calculating A-10 Crack Growth (IATP) Remain Satisfactory

- Current method validated
- Most accurately predicts crack growth
- Allows aircraft to be operational longer between inspections
- Least expensive when considering Life Cycle Costs
- Weighting of coefficients/Wheeler exponent within each zone shows great promise for ease in accurately accounting for spectra changes without extensive testing
- Capability available to track individual aircraft
- Has been validated for combination of load factors & speed

FIGURE 36 CONCLUSIONS CURRENT METHOD OF CALCULATING A-10 CRACK GROWTH

**AUTOMATIC CALCULATION OF AN AIRCRAFT'S SINK SPEED,
HORIZONTAL VELOCITY, PITCH ANGLE AND PITCH RATE, AND
ROLL ANGLE AND ROLL RATE AT TOUCHDOWN AND THEIR
APPLICATION TO STRUCTURAL INTEGRITY**

by:

John CICERO and Jamshid MOHAMMADI

**Systems & Electronics, Inc.
190 Gordon Street
Elk Grove Village, IL 60007**

**1990 USAF Structural Integrity Program Conference
11-13 December, 1990
San Antonio, Texas**

1.0 INTRODUCTION

Systems & Electronics, Inc. (SEI) has developed a system that will automatically calculate an aircraft's sink speed, horizontal velocity, pitch angle, pitch rate, roll angle, and roll rate at touchdown. These quantities can then be plotted as a function of approach distance at touchdown. Also, these quantities are entered into a database so that statistical results can be obtained. The results can then be input into a structural analysis program that evaluates the structural integrity of the aircraft and its landing gears.

Commercially available cameras are used to observe the aircraft at touchdown. One camera is placed perpendicular to the path of the runway and the other is placed parallel to the path of the runway. The first camera is used to obtain sink speed, horizontal velocity, pitch angle and pitch rate. The second camera is used to obtain the roll angle and roll rate.

The recorded images are then played back into a computer and digitized. The computer examines the images on a frame-by-frame basis to determine the position of the aircraft as a function of time. Once this information is known, the quantities described above can be automatically calculated. These quantities can be processed and presented in the form of time histories or power spectral density (PSD) functions. Structural dynamic analyses can then be conducted using the time histories or PSD's as the input to the analysis. The results are then used to evaluate the internal stresses developed in the critical structural components and the potential damage to these components at touchdown. These findings are then incorporated in the evaluation of the integrity of the aircraft.

2.0 DATA ACQUISITION TECHNIQUES

2.1 Equipment Requirements

Equipment selection depends upon the data acquisition method. In Method I, high quality camcorders mounted on tripods are used to record the aircraft at touchdown. The recorded images are then sent to the laboratory where they are processed as described later. In Method II, high quality cameras connected directly to computers are used to record the images. The images are instantaneously processed and the results are immediately available. While Method I has easily manageable equipment requirements, Method II represents a completely automated system. For either method, the cameras must be equipped with both a high-speed shutter to eliminate blurring and a zoom lens to properly set the field of view.

The recorded images must be digitized by a high-speed digitizer capable of on-the-fly digitization. This is particularly important in Method II because these images must be processed in real time. The digitizer should be located in a computer with at least the

power of a 80386 class machine and an 80387 math coprocessor.

2.2 Camera Placement and Field of View

Two cameras are required to obtain all the desired parameters. The images from the first camera are used to calculate pitch angle, sink speed, and horizontal velocity, while the images from the second camera are used to calculate roll angle. The first camera is placed so that the line-of-sight of the camera eye is perpendicular to the path of the runway. The second camera is placed so that the line-of-sight of the camera eye is identical to the path of the runway.

The proper field of view must be determined for each camera so that the aircraft can be observed for several frames prior to (and including) the touchdown. There are several things to consider when attempting to determine the correct field of view:

- Average horizontal velocity at touchdown.
- Average sink speed.
- The range of distance in which the aircraft will touch down on the runway.
- Height of a vertical reference line on the aircraft.
- Length of a horizontal reference line on the aircraft.

The minimum error occurs when the distance fallen by the aircraft is identical to the vertical reference of the object. For example, T-44's had typical sink speeds of 7 ft/sec, and the vertical stabilizer (vertical reference) had a height of 5.46 feet. From this information it can be determined that the aircraft should be in the field of view for 5.46 feet / 7 feet/second = 0.78 seconds (or about 24 30-second frames).

Next assume that the typical glide slope is 3.25 degrees. Then, the horizontal velocity is 7 feet/second / $\tan(3.25^\circ)$ = 123.3 feet/sec. At this velocity the initial field of view is $123.3 * 0.78 = 96$ feet wide.

2.3 Error Analysis

Given that the total field of view is 96 feet wide and that the field of view for the video system is approximately square, the height of the field of view is also 96 feet. Assume that there are 440 vertical lines of resolution. Each line corresponds to approximately $96/440 = 0.2182$ feet. Recall that the vertical stabilizer is 5.46 feet or 25 pixels. Therefore, a one pixel error corresponds to a four percent error.

2.4 Digitizing Procedure

After the images are recorded by the camera or camcorder, they are sent to the

computer and digitized. The computer examines the touchdown on a frame-by-frame basis. An aircraft position identification algorithm is used to determine the exact location of each aircraft within a frame. The algorithm begins by using background extraction to remove the background from each of the images with an aircraft in the field of view. After this procedure, only the aircraft remains in each image (i.e., the background has been removed). Next, a Monte Carlo technique is used to place a long but narrow box on the aircraft. The dimensions of the box are carefully selected so that the box will only fit in a very specific region of the aircraft. From this small box, a larger box is constructed. The dimensions of the larger box are chosen so that it always contains the main landing wheels. The program examines the larger box for the lowest point on the aircraft. This point always corresponds to the bottom of the main landing wheels. Next, a third box is constructed. The coordinates of this box are selected so that the box always contains the nose wheels but not the main landing wheels. Finally, the algorithm examines the third box for the lowest point on the aircraft. This point always corresponds to the bottom of the nose landing wheels. Once these points are found in each frame, the calculations described below can be performed and the desired parameters determined.

To obtain the necessary results, the aircraft must be observed for at least two frames. Additional frames are desirable because it enables the program to calculate all the desired parameters as a function of approach distance. However, if the frame at which the aircraft first enters the field of view and the frame at which the aircraft touches down are known, the following sets of coordinates can be obtained (Note that Frame 1 occurs before Frame 2):

<u>Description</u>	<u>Abbreviation</u>
Nose wheel (Frame 1)	(nwx ₁ ,nwy ₁)
Main wheels (Frame 1)	(mwx ₁ ,mwy ₁)
Frames between Frame 1 and Frame 2	f
Nose wheel (Frame 2)	(nwx ₂ ,nwy ₂)
Main wheels (Frame 2)	(mwx ₂ ,mwy ₂)
Left wing tip (Frame 2)	(lwx ₂ ,lwy ₂)
Right wing tip (Frame 2)	(rwx ₂ ,rwy ₂)

3.0 DATA ANALYSIS

3.1 Calculation of Landing Parameters

Once the coordinates from the previous section are obtained, the following

calculations can be performed:

- Feet per pixel, Scale,
$$\text{Scale} = \frac{\text{Distance from the main wheels to the nose wheel (feet)}}{[(mwx_2 + nwx_2)^2 + (mwy_2 + nwy_2)^2]^{1/2}}.$$
- Horizontal Velocity (feet/second) = $30 / f * \text{Scale} * |(mwx_1 - mwx_2)|.$
- Sink Speed (feet/second) = $30 / f * \text{Scale} * (mwy_2 - mwy_1).$
- Pitch Angle = $\tan^{-1}[|(mwy_2 - nwy_2)|/|(mwx_2 - nwx_2)|].$
- Roll Angle = $\tan^{-1}[(lwy_2 - rwy_2)/(lwx_2 - rwx_2)].$

3.2 Sample Results

Some of the statistical results obtained for 150 T-34 aircraft at touchdown are presented in Figures 1 through 3. Figure 1 presents a frequency distribution of the horizontal velocity in knots. Figure 2 presents a frequency distribution of the sink speed in feet/sec. Figure 3 presents a frequency distribution of the pitch angle in degrees.

4.0 APPLICATION TO STRUCTURAL INTEGRITY EVALUATION

One practical application of the collected dynamic parameters of the aircraft at the time of landing is in the area of structural integrity analysis of the aircraft in general and the landing gears in particular. The images obtained and processed can easily be converted into time history and/or power spectral density (PSD) functions. These functions can then be utilized as input to structural analysis of the aircraft and/or landing gears for the calculation of internal forces and the evaluation of system integrity. Depending on the type of data collected, two types of structural analyses can be conducted. These are:

- Dynamic analysis of the structure idealized as a system of lumped masses, springs and dashpots. In this analysis, the time history of the recorded parameters (i.e., velocities, pitch, roll, etc.) are needed and can be obtained using an appropriate shutter speed for the cameras.
- Analysis of the structure using the PSD functions of the recorded parameters. The cameras' positions and shutter speed should be properly designed if the objective is to develop PSD data for the recorded parameters.

In the following sections these structural analyses schemes, their requirements, limitations and advantages are explained. The discussion presented here covers a general

concept. Depending on the type of data collected, these methods can be simplified and specially geared to specific objectives. In the case of the SEI collected data, for example, the collected data can be used to determine an input acceleration (in the form of an impulse) for the landing gear structure at the time of impact with the ground. This simplifies the structural analysis process substantially while providing useful information on the status of internal forces in the structure at the time of landing.

4.1 Structural Analysis Using Time Histories

In this analysis, it is assumed that the cameras are properly designed and installed to record an appropriate number of frames as the aircraft approaches the ground and lands. The processed images can then be used to determine the time histories for different degrees of freedom of the structure. When the force in a landing gear is required, the data on the sink speed (vertical velocity) is perhaps the most important parameter and can be used to develop the time history data of the acceleration during landing. Idealizing the landing gear as a multi-degree-of-freedom dynamic system, one can write:

$$M\ddot{U} + C\dot{U} + KU = -M\ddot{Y} \quad (1)$$

In which the vector U contains the degrees of freedom of the structure, dot designates the time derivative, M is the matrix of masses and mass moments of inertia, C and K are damping and stiffness matrix, respectively, and \ddot{Y} contains the acceleration components of input motion. In a simplified case, the input motion consists of the vertical acceleration only; and Eq. 1 becomes that of motion of a single degree of freedom. Equation 1 can then be solved using a numerical analysis to obtain the response U of the individual spring elements of the landing gear. Once U are obtained, the forces in these elements can be obtained from the following matrix equation.

$$F = KU \quad (2)$$

in which F contains the forces in the spring elements.

The advantage of this method is that it uses a dynamic analysis of the landing gear structure. Using the method of mode superposition (Ref. 1) it is possible to obtain the maximum response (maximum force in individual spring members) and the corresponding contribution of the individual modes of vibration. As indicated earlier, the vertical acceleration at the time of impact is expected to contribute to the response predominantly. The disadvantage of the analysis is that Eq. 1 requires a numerical integration technique.

This may impose a somewhat larger error in calculation than what is expected in a numerical analysis. This is because the input data for the dynamic analysis is from images recorded by the cameras and processed by a computer. The accuracy of the time histories generated to a great extent depends on the elapsed time intervals between the frames recorded by the cameras. The limitations in the field of view and in the number of frames that can be recorded by the cameras may impose some approximation in the time histories calculated. This approximation is further augmented by the error associated with the numerical integration of Eq. 1.

4.2 Structural Analysis Using the PSD Functions

In this method the analysis is done in frequency domain. The dynamic analysis however can become complicated due to the fact that cross correlations between different degrees of freedom and their derivatives will be involved in the analysis. A complete description of the dynamic method can be found in Ref. 2. Alternatively, a static method can be used considering the fact that the PSD data for different degrees of freedom of the structure are available. These data are approximated as the actual recorded response of the system. Using Eq. 2, the force F_i in the i th spring element can be written as:

$$F_i = \sum_{j=1}^{j=r} k_{ij} u_j \quad (3)$$

in which r is the total degrees of freedom, u_j is the j th degree of freedom and k_{ij} are the stiffness coefficients. In terms of PSD functions, Eq. 3 can be written as:

$$\phi_{F_i}(\omega) = \sum_{j=1}^{j=r} \sum_{l=1}^{l=r} k_{ij} k_{il} \phi_{u_l}(\omega) \quad (4)$$

in which ϕ describes the power spectral density function. In terms of acceleration

\ddot{u} Eq. 4 can be written as:

$$\phi_{F_i}(\omega) = \sum_{j=1}^{j=r} \sum_{l=1}^{l=r} \frac{\phi_{\ddot{u}_l}(\omega)}{\omega^4} \quad (5)$$

In which \ddot{u}_j is the j th acceleration component and ω is the frequency. If the vertical velocity is taken as the most important dynamic parameter during the landing, the corresponding acceleration (and its PSD function) is used as the sole input to Eq. 5. This

simplifies the process substantially. Once the PSD of the force component F_i is found, the statistics associated with the exceedance of the force over specific threshold levels can be obtained and used in the evaluation of damage in the structural components and the corresponding probabilities of failure (Ref. 2).

The advantage of this method is that it can directly be used to determine the statistics associated with the force exceedance in the landing gear. The input PSD combines the results of all sample data collected at different times. Compared with a comprehensive dynamic analysis, the computation effort is less especially if the vertical acceleration is used as the only input motion component. The method has successfully been used in the evaluation of the internal force statistics for other types of structures (Refs. 3,4).

4.3 Input Data from Digitization of Recorded Landing Parameters

As described earlier, depending on the type of analysis selected, the camera system can be designed specifically to record the number of frames needed to be recorded and the type of data to be acquired. The experience with T-34 data reveals that the sink speed (vertical velocity) is relatively constant before landing. After impact with the ground, the velocity drops to nearly zero. The drop in the velocity occurs over a very short period of time Δt when the landing gear collapses (see Fig.4). The sudden drop in velocity appears as an impulse describing a peak in the acceleration. The impulse can be used as the input motion to Eq. 1. This simplifies the solution of Eq. 1 and eliminates the need for numerical integration.

In terms of the PSD function, the impulse can conveniently be presented as a *limited-band white noise* (Ref. 5). This is because of the special form of the acceleration function that appears as a sudden peak. Thus with a series of collected landing accelerations at the time of impact, the auto-correlation function of the acceleration can be idealized as the limited-band white noise shown in Fig. 5(a) which can be considered to be independent of the time lag τ for practical purposes. The corresponding power spectral density function appears in the form of Fig. 5(b). The PSD's constant value S_0 can be obtained using the mean square estimates of the acceleration. Denoting the mean square acceleration as $E(Y)$ the parameter S_0 will be

$$S_0 = \frac{E(\ddot{Y})}{2(\omega_1 - \omega_2)} \quad (6)$$

The limiting frequencies ω_1 and ω_2 of the band can be selected arbitrarily; however, the band should contain the natural frequency of the system. As it can be found out from Eq. 5, these limiting frequencies will also appear as the limits of the ϕ_{F_i} function. It is

noted that the final outcome of the analysis is the statistics of the exceedance of the force F_i and these statistics require the calculation of the area under the ϕ_{F_i} function between the frequencies ω_1 and ω_2 . A change in ω_1 and ω_2 will cause a proportional change in the ϕ_{F_i} function. However, the total area under the ϕ_{F_i} function will not be affected. This means that the analysis will not be grossly affected by the selection of ω_1 and ω_2 . However, as described earlier, it is important that ω_1 and ω_2 contain the natural frequency of the structural system.

5.0 SUMMARY AND CONCLUSIONS

SEI has developed a technique that can be used to automatically measure an aircraft's landing parameters. These parameters can then be used in the evaluation of the structural integrity of the landing gears and the aircraft. The evaluation technique provides several options which are summarized below.

Data gathering can be semi-automated (i.e., recording the images with camcorders, then processing the images in the laboratory) or fully automated (i.e., recording the images with cameras and processing the images on-the-fly). The fully automated technique requires more on-site equipment but does not require a technician.

Determining the correct field-of-view is critical in obtaining accurate results. The field-of-view is determined by many factors. The primary determining factors are aircraft type, pilot experience and landing objectives. SEI observed T-34's and T-44's piloted by students. This configuration generated a very gradual rate of decent and a very wide field-of-view. A more experienced pilot practicing aircraft carrier landings would generate a very narrow field-of-view. The smaller the field-of-view, the more accurate the results because the cameras can be set to obtain more images in a shorter period of time which in turn provides more data for the structural analysis techniques.

Depending on the type of data recorded and processed, two different types of structural analyses can be conducted for the calculation of internal forces in the landing gears and evaluation of their structural integrity. With a narrow field-of-view, where more images of the landing process can be recorded, a fairly accurate time history of the landing parameters including the vertical velocity can be obtained. In such a case, a structural dynamic analysis using the time histories can be conducted to obtain the response of the landing gears and the corresponding internal forces developed in them. However, with a very wide field of view, since the number of images taken is limited, the time histories of the landing parameters can not be reliably calculated. In this case, the sudden drop in the velocity at the time of impact can be used as an input into the structural analysis of the landing gears. As it is described in the paper, the PSD of the acceleration in the form of

a limited-band white noise can be used in the analysis. The analysis can be a dynamic random vibration or a static analysis which is simpler and can provide useful results with enough accuracy.

6.0 REFERENCES

1. Craig, R. R., *Structural dynamics, an application to computer methods*, John Wiley and Sons, New York, NY, 1981.
2. Lin, Y. K., *Probabilistic theory of structural dynamics*, R. E. Kreiger Publishing Co., Hunting, NY, 1976.
3. Mohammadi, J., "Application of field data to fatigue life evaluation," *Structures Congress*, American Society of Civil Engineers, New York, NY, 1991.
4. Mohammadi, J., Garg, V. K. and Subei, N., "Data-based evaluation of fatigue reliability of railroad cars," *Paper #84-WA/DE-11*, American Society of Mechanical Engineers, New York, NY, 1984.
5. Crandall, S. H. and Mark, W. D., *Random vibration in mechanical systems*, Academic Press, New York, NY, 1963.

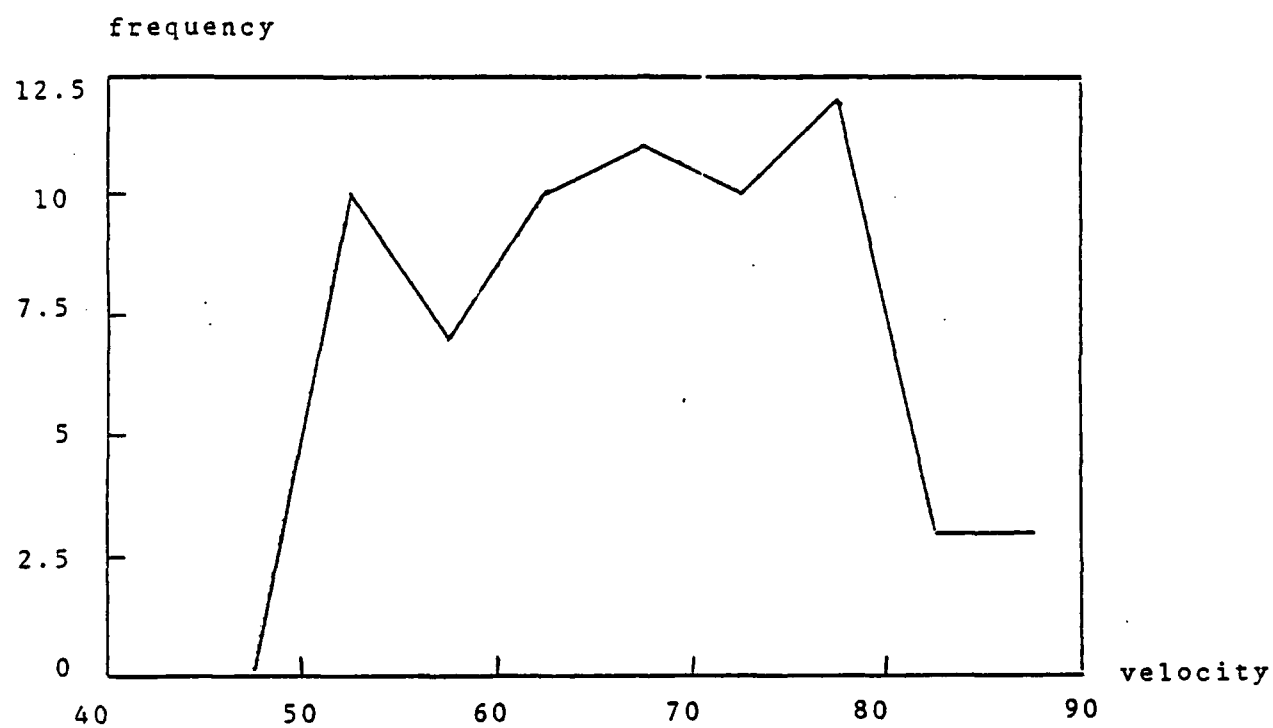


Fig. 1 A Frequency Distribution for the Horizontal Velocity in Knots for T-34 Aircraft

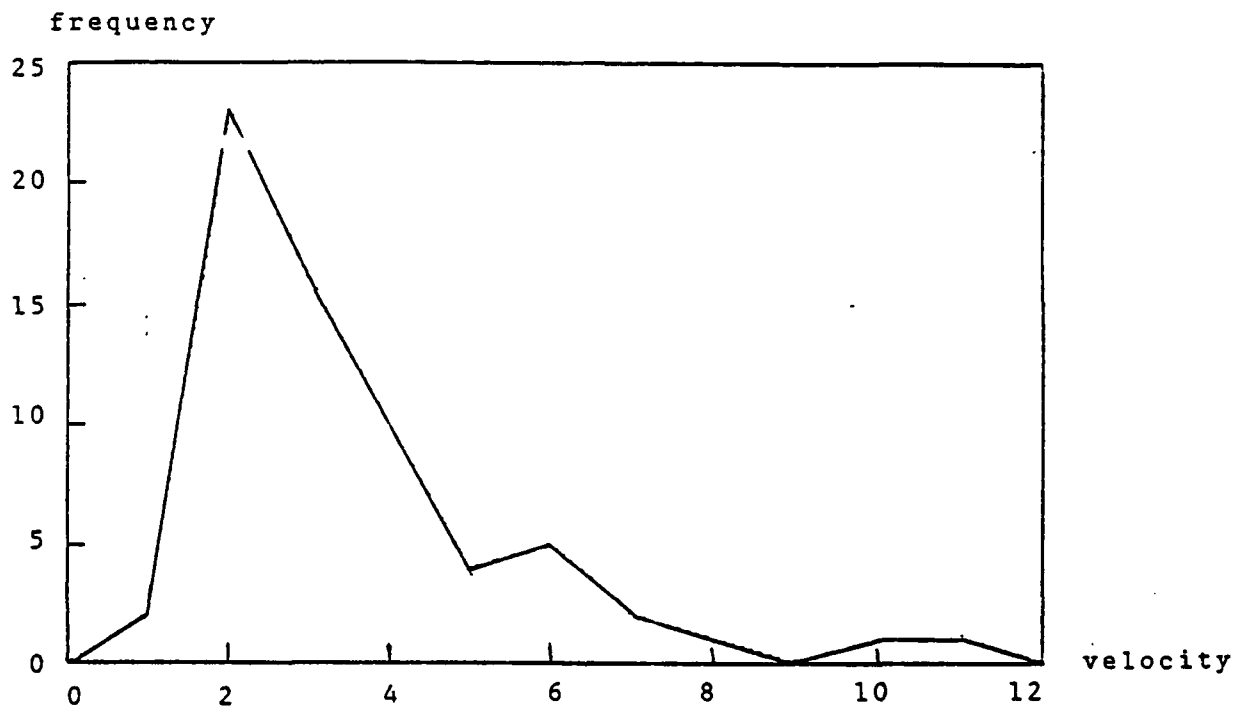


Fig. 2 A Frequency Distribution of the Sink Speed in Feet/second for T-34 Aircraft

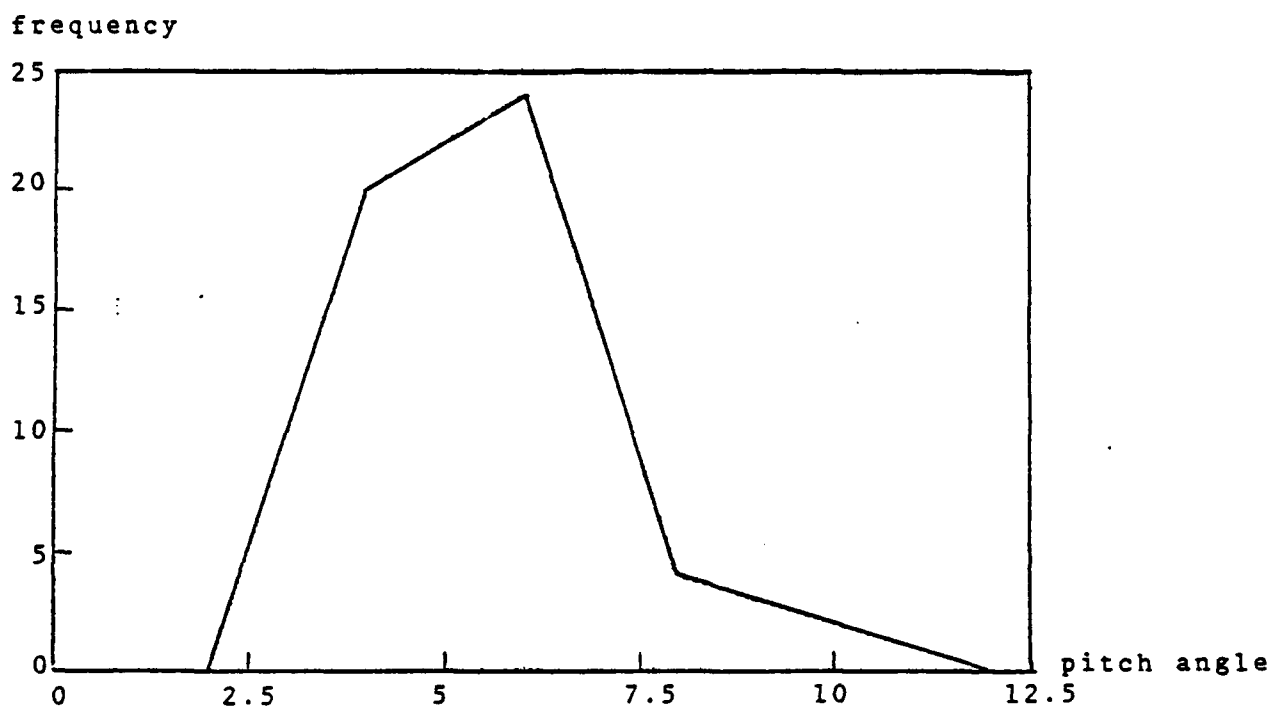
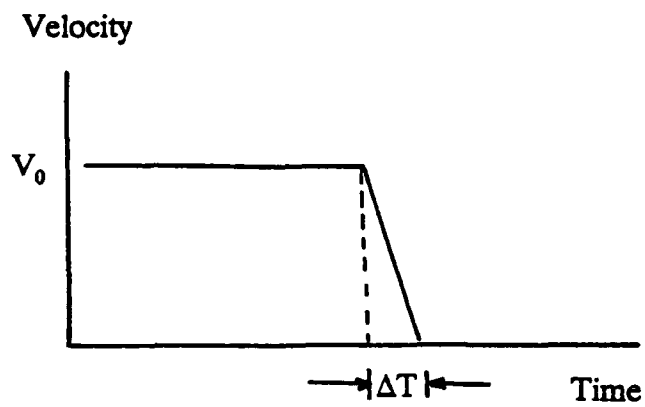
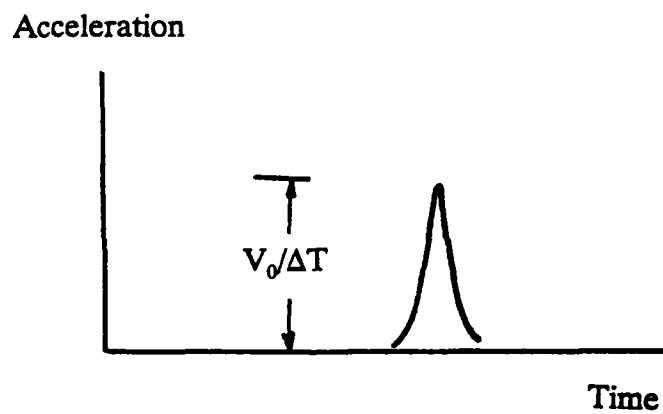


Fig. 3 A Frequency Distribution of the Pitch Angle in Degrees for T-34 Aircraft



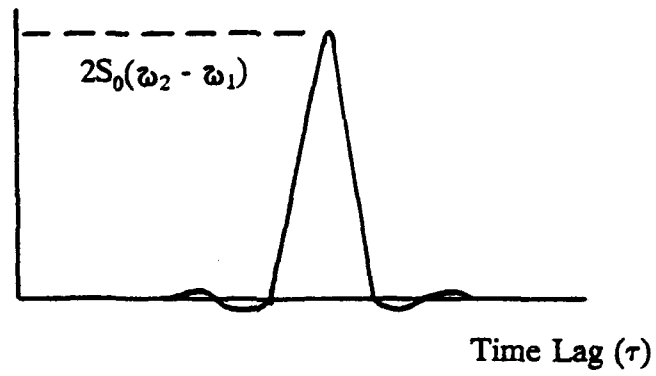
(a)



(b)

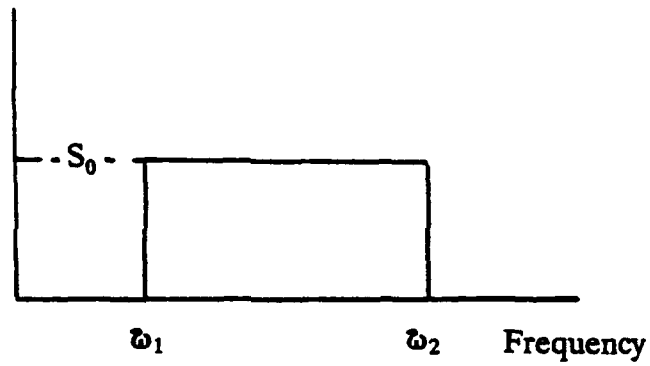
Fig. 4 Acceleration Function at Landing

Auto-correlation



(a)

PSD



(b)

Fig. 5 Band-Limited White Noise Representation of Acceleration

HEALTH AND USAGE MONITORING SYSTEMS IN AIRBORNE APPLICATIONS

I.T. Robertson
SIADS Basingstoke

ABSTRACT

This paper discusses the use of Integrated Health and Usage Monitoring Systems (IHUMS) in fixed and rotary wing aircraft. The prime function of IHUMS is to provide information to operators and associated support organisations which will enable them to promote on-condition maintenance of the aircraft.

The IHUMS comprises a complete system, enabling the user to capture, process and store data in real time on the aircraft, copy/transfer data between the aircraft and the ground-based elements of the system and present data for maintenance, analysis and management functions in a ground-station.

The information produced by the IHUMS may be related to the condition of the airframe structure or to other components e.g. engines and gearboxes. A variety of algorithms may be implemented in order to provide the real-time processing functions e.g. Low Cycle Fatigue (LCF) algorithms may be used for lifing critical parts both of the engine and of the airframe.

As well as being implemented as a stand-alone system the IHUMS may also be integrated with other on-board systems. In particular integration with a Standard Flight Data Recorder (SFDR) offers significant benefits in terms of extending the capability and cost effectiveness of the current generation SFDR.

This paper describes which IHUMS functions may be implemented with technology now available and attempts to identify where further work is required before the technology may be considered mature.

1. SYSTEM OVERVIEW

The general system described in this paper is an Integrated Health and Usage Monitoring System (IHUMS) whose functions are applicable to current and future aircraft, although the implementation in specific cases will be "special-to-type". The prime function of the IHUMS is to provide information to operators and associated support organisations which will enable them to promote on-condition maintenance of the aircraft. The IHUMS described here is relevant to both helicopter and fixed-wing applications, although not all the features apply to both cases.

The IHUMS comprises a complete system, enabling the user to capture, process and store data in real time on the aircraft, copy/transfer data between the aircraft and the ground-based elements of the system and present data for maintenance, analysis and management functions in a ground-station, which may be configured as a commercial p.c.

Due to the variety of possible Customer needs a major requirement of the IHUMS is for extreme modularity in design and implementation, in order to facilitate configuration of hardware and software to meet these needs. This applies in particular to airborne processing and I/O elements (see para. 3.1.2) which are best realised as a series of stand-alone modules each with some degree of intelligence. This allows such modules to be integrated with other equipments (e.g. with a Standard Flight Data Recorder), combined together to produce 1 or more stand-alone Line Replaceable Units (LRU's), or to be incorporated within Customer systems as Line Replaceable Modules (LRM's). Such an architecture also provides the flexibility to expand the system as additional modules become available.

2. FUNCTIONS PERFORMED BY IHUMS

An overall list of functions is given below (with no order of importance implied).

- Engine Monitoring
- Gearbox and Transmission Monitoring
- Rotor Track and Balance
- Aircraft/Airframe Monitoring
- Status Monitoring

3 IHUMS INSTALLATION REQUIREMENTS

To perform a specific installation 3 types of IHUMS elements are in general required, the elements implemented in a particular case being application-dependent. The types of elements are as follows:-

3.1 On-Board Elements

3.1.1 Sensors of all kinds (i.e. from standard transducers to stand-alone sensors with intelligence).

3.1.2 Embedded I/O and processing elements. These may be Line Replaceable Units (LRU's) or Line Replaceable Modules (LRM's).

3.1.3 Aircrew interfaces (i.e. controls and displays, including "alert" warnings)

3.1.4 Maintenance interfaces (e.g. for download of data by ground-crew)

3.1.5 Interfaces with other aircraft systems e.g. ACARS.

3.2 Data Copy/Transfer Elements

3.2.1 Hand-held Data Transfer Unit (DTU) purely for upload/download of maintenance data.

3.2.2 Front-end Interface Processor (FIP) with DTU functionality plus processing capability.

3.2.3 "Detachable" elements (e.g. data cassettes or 'smart' cards)

3.3 Data Manipulation and Presentation Elements

Stand-alone Personal Computer (PC) or more powerful derivative implementing a maintenance data-base for data upload/download to the on-board elements and a user interface for viewing/entering data.

In addition functionality may be included to permit a wide range of Maintenance activities (Trending, generation of rotor track and balance corrections, Maintenance Management, network to other computer system(s))

In a typical Maintenance Analysis implementation updated records are kept of the "on-condition" expired lives of aircraft (engine) components, based on lifing algorithms performed in real time in the aircraft. This may be expanded to embrace a Maintenance Management function which allows individual aircraft parts to be "tracked" in order to implement a fleet-wide Maintenance programme.

3.4 Airborne Versus Ground Analysis of Data

In the implementation of an IHUMS the relative amount of data processing and analysis performed in the air and on the ground must be considered. In general the efficiency of the airborne computer is increased by decreasing the amount of such data stored. The technology is available to filter and compress the data and to perform Health and Usage algorithms in real time, and it should be used. In particular, for usage calculations where only the end result is of interest (e.g. Low Cycle Fatigue - see 4.1.2.4 below) there is little point in downloading the corresponding unprocessed data or intermediate results.

However, in certain applications there may be a range of alternative processing techniques which may be used on the raw data and here it may be beneficial to download raw data (or intermediate calculations) and perform such analysis on the ground. For instance in Gearbox Vibration Analysis (see 4.2.1.2 below) the real-time signal averages may be downloaded so that a range of damage indicators may be performed and compared on the ground computer. In addition practical design considerations may dictate the use of a single standard of airborne hardware (and software) over a number of aircraft types. In this case all type-specific calculations must be performed at the ground station.

4 FUNCTIONAL DESCRIPTION

The functions listed in para 2 are now described in more detail.

4.1 Engine Monitoring

4.1.1 Engine Health, including the following :-

4.1.1.1 Power monitoring i.e. calculation of the discrepancy between theoretical power output at specified conditions and the actual mechanical power delivered, based on measurement of torque output from the engine. This automates an otherwise tedious (and potentially unreliable) area of pilot work-load as the implementation algorithm ensures that all the required data inputs remain in-range throughout the sampling period and also performs initial averaging and filtering of the raw data.

4.1.1.2 Thermal Efficiency monitoring i.e. calculation of the excess of a derived hot-end temperature (e.g. Turbine Entry Temperature based on shaft speed) over a measured value.

4.1.1.3 Recording of "snapshots" of input data to allow off-line monitoring of the condition of the engine. The recording may be initiated directly by the pilot or automatically when predefined conditions occur i.e. on take-off or at cruise. In addition a sequence of snapshots may be recorded when a preset condition (e.g. an exceedance or operation of a manual select) occurs. The resultant Incident Recording will normally cover a period from a fixed time before to a fixed time after the occurrence of the condition. Both snapshot and incident recording are currently used in Civil applications. The former gives an automatic data input to Engine Condition Trend Monitoring and similar programs; the latter is used by Operators to identify potential serious fault conditions quickly.

4.1.1.4 Engine to Engine Divergence monitoring. In 2 or more-engined aircraft the measured values of engine parameters from all engines is used to evaluate their relative performance at specified conditions.

4.1.1.5 Measurement of engine spool-up and spool-down times.

4.1.2 Engine Usage, including the following :-

4.1.2.1 Total Operating Time for the engine using a measured shaft speed as a threshold. Operating Times above other thresholds (e.g. above maximum compressor speed) may also be measured.

4.1.2.2 Number of starts based on accelerations through a shaft speed threshold. The start acceleration times may also be monitored.

4.1.2.3 Measurement and logging of exceedances of specified input parameters. The logged data may include time above an exceedance level, the maximum level attained and the number of exceedances which have occurred. This type of monitoring is currently used by Civil Operators both to track faults and to record where the engine has been misused (i.e. a "spy-in-the-cabin" facility!). In addition specified input parameters may be banded i.e. the time spent between a series of threshold values may be recorded.

4.1.2.4 Low Cycle Fatigue (LCF) calculation of critical parts based on measured shaft speeds, including in some cases incorporation of a thermal modifier using a hot-end temperature measurement. The technique requires accurate tracking of stress maxima and minima, identification of major and minor stress cycles and conversion of these cycles into fatigue usage. Manual LCF counting is currently commonly used as a means of lifing critical engine parts, based on a "cyclic exchange rate" i.e. a conversion factor between an airframe-related parameter such as the number of flights and the number of damage cycles accumulated by each component. Automating the measurement allows actual rather than notional LCF to be calculated and therefore the progressive usage to be accurately tracked as a function of actual engine conditions. This is of particular importance in the Military sphere, where the flight profile and resulting engine fatigue of individual aircraft will in general vary significantly from a mean value calculated at, say, squadron level. In addition certain "hot-end" engine components (e.g. turbine blades) may be lifed on thermal creep or thermal fatigue. Thermal creep is a function of stress on the component (calculated from measured rotational speed), component temperature and time. Thermal fatigue expresses the damage resulting from temperature-related stress variations; the stress cycles measured are converted to fatigue usage in the same way as for Low Cycle Fatigue.

4.2 Gearbox and Transmission Monitoring

4.2.1 Gearbox and Transmission Health Monitoring, including the following:

4.2.1.1 Oil Debris Monitoring - This involves the logging of particle counts from debris monitor(s) mounted integral with the gearbox lubrication system. Several systems are commercially available but experience in the field indicates that there remain technical problems with these devices. Due to their means of operation (insertion in the oil line) they are more suitable for incorporation in new aircraft than for retrofit.

4.2.1.2 Gearbox Vibration Monitoring - Certain types of localised gearbox damage (e.g. cracks in gear teeth) give rise to mechanical vibrations indicative of the damage. These damage-related vibrations may be captured by accelerometers mounted in suitable locations (e.g. on the gearbox casing) and the input signals sampled and processed in order to quantify the damage which has occurred.

The sampling of the accelerometers is in each case held in phase with a synchronising signal derived from the gearbox. This enables the sampling of each accelerometer to be phase-locked to the rotational frequency of a related gearbox shaft (sampling is in fact performed at a multiple of the gear-tooth meshing frequency). This in turn allows the "sample-sets" from successive rotations of the shaft to be added together in real time to form a "signal-average" from which the effects of noise and non-synchronous components are progressively eliminated. Each signal average is converted to the frequency domain using a Fast Fourier Transform (FFT) algorithm and then processed in order to generate a range of damage indicators derived from the shaft rotation and tooth-meshing spectrum.

The fundamental basis of this technique - the successful acquisition of the real-time signal-averages as described above - has been successfully demonstrated in recent Flight Trials in the UK instigated by the Civil Aviation Authority (CAA). Due to the comparatively rare occurrence of the faults being monitored these Trials have not demonstrated a strong correlation between actual faults logged and measured damage indicators. However evidence does exist from ground tests where faults were seeded in gearboxes as well as from a wide range of non-aerospace applications. The next phase of CAA-sponsored research work in the UK will expand this data-base, with particular emphasis on seeded faults, to enable a range of indicators to be established.

4.2.1.3 Bearing Vibration Monitoring - The output of accelerometers mounted near bearings may be used to give an indication of bearing distress. Although superficially similar to the gearbox vibration monitoring technique described above the monitoring technique is in fact fundamentally different. This is because the vibration generated by a damaged rolling element bearing is dominated by high-frequency resonances in the bearing races and the surrounding structure caused by successive damage-related impacts of the bearing. The repetition frequency of these impacts is asynchronous due to the motion of the cage and so it is not possible to apply the real-time signal averaging technique described above in this case. Instead the resonant signal is demodulated and the resultant signal amplitude and repetition frequency used to generate indicators of bearing damage. Although there have been successes in this area of analysis (ref.1) further work is required to demonstrate suitability in an airborne HUMS.

4.2.1.4 Bearing Temperature Monitoring using thermocouples fitted to bearing housings in order to detect heat build-up prior to bearing failure. This is a viable technique in that reliable data can be obtained but further work is required in order to develop criteria for inspection and removal of bearings.

4.2.2 Gearbox and Transmission Usage Monitoring - this is based on measured or calculated torque values. It includes damage to gear wheels as a function of measured torque and damage to splines and planet wheels based on the number of major torque cycles recorded.

Successful incorporation of this in an airborne HUMS has been demonstrated but application of the technique requires initiatives from gearbox manufacturers.

4.3 Rotor Track and Balance (RTB)

This involves measurement of accelerometer outputs and optical tracker data to give diagnostic information on rotor track errors which give rise to airframe vibration.

This is a well-established Maintenance technique with equipment available from several manufacturers. In its present form it is implemented as "carry-on" rather than permanently fitted equipment but there is considerable benefit to be gained by integrating it with airborne HUMS. By this means 24-hour RTB functionality may be obtained and the following functions provided -

4.3.1 Track - Collection and storage of averaged track data when the aircraft is in one of a number of predetermined steady-state flight conditions. In addition monitoring of track data on a rev by rev basis and storage of statistical information. This allows diagnostic assessment of rotor control system faults to be made e.g:

- Rotor RPM - detection of the effectiveness of the engine governor systems and recording of exceedances in terms of magnitude and duration.
- Blade Height - detection of excessive variations, leading to the detection of worn pitch link bearing and/or swash plate defects.
- Inter-Blade Timing - detection of excessive variations, leading to the detection of worn damper attachments or defective damper performance.
- Rotor Run-Up and Run-Down - recording of resonant behaviour of the rotor-to-tyres/skids behaviour of the aircraft, leading to the detection of worn undercarriage attachments, defective oleo struts, incorrectly inflated tyres and worn skid mountings.

- Raw Track Data - storage of limited amounts of raw track data for later analysis in order to detect and analyze transient fault conditions that would not be apparent in the averaged data.

4.3.2 Balance - Sampling of a minimum of 4 balance channels (accelerometers) synchronised in each case to a once-per-rev (OPR) input signal which is also used to derive the sampling frequency. This enables out-of-balance amplitude and phase data to be derived as follows -

- Main Rotor Lateral and Vertical Accelerometers - Lack of consistency of balance or lack of correlation with airspeed may be used to diagnose brinelled or fouled bearings.

- Tail Rotor Radial and Axial Accelerometers - Lack of correlation with airspeed may be used to diagnose worn/damaged stack bearings and/or brinelled feathering hinge bearings.

4.4 Aircraft/Airframe Monitoring

4.4.1 Airframe Vibration Monitoring - Measurement of accelerometer outputs and storage of selected spectra. The balance data acquired as described in 4.3.2 above may be used to provide a baseline set of airframe vibration data as harmonic signatures. Additional airframe vibration information may be collected as required, normally up to 5KHz.

4.4.2 Logging of aircraft flying hours.

4.4.3 Measurement of airframe structural fatigue, either by direct measurement of strain or indirectly by measurement of related parameters (e.g. g-level). There is currently a Programme in the UK (Harrier GR5) where an airborne computer is being introduced which monitors airframe-mounted strain-gauges and calculates fatigue usage of individual components in real time. Once operational this should give a much more satisfactory means of assessing airframe life than the currently-used fatigue meter which relies on a single g-measurement.

4.4.4 Control loads monitoring and analysis - Strain-gauges may also be used to monitor control loads so as to detect excessive values resulting from failures in control systems. To implement this monitoring technique in a meaningful fashion requires the involvement of the manufacturer with regard to the definition of normal and abnormal strain levels.

4.5 Status Monitoring

With the introduction of on-board computers and Electronic Instrument Systems this monitoring can be more comprehensive than on previous generations of aircraft. Typically the parameters monitored are exceedances of various kinds (e.g. turbine overspeeds) and other undesirable conditions. The outputs are various categories of alarm, some of which are maintenance actions and not directly indicated to the pilot.

5. FUTURE DEVELOPMENTS

As well as the areas indicated above where further work is required it is useful to consider future application of certain areas of current state-of-the-art technology. All of the techniques described above may be classed as analytical and discrete; together they comprise a series of separate algorithms each of which gives information on a limited set of components. In order to combine the various types of information in a meaningful way a higher level of processing may be utilised to diagnose the various "symptoms" and produce an overall, integrated assessment of aircraft condition. In this context 2 main approaches may be considered. The first of these is Expert Systems where all the available relevant expertise is implemented in a software program which provides the integrated diagnostic functions required. While such systems are now widespread in many applications their use in an IHUMS presents difficulties largely due to the complexity of the system being monitored and the lack of definitive diagnostic rules. Nonetheless work has been done in this area (e.g. ref.2) but concentrating on ground analysis rather than in an airborne processing role.

An alternative approach to Expert Systems is that of Neural Networks. This represents a radical departure from conventional ideas in that a system utilising this approach has no human-programmed fault condition symptoms with which to compare actual sensor data but rather "learns" from its own experience and builds its own internal model of its environment purely by exposure to it. Subsequently, on encountering an unusual, and so potentially abnormal, condition the system can signal an appropriate degree of concern depending on the improbability that the observed input is a member of the "normal" or familiar set. A diagnostic database can then be built up over time and the prospect exists for more general diagnostic capabilities than can be realised by triggering on known fault symptoms. Research is currently in progress in the UK in this area whereby aircraft test data is input to an Experimental Development System containing a neural network encoder and an intelligent monitor (ref.3).

6. REFERENCES

1. Condition Monitoring of rolling element bearings by vibration analysis. P.D.McFadden. Institution of Mechanical Engineers Seminar held in London on 9th January 1990.
2. The use of expert systems in advanced condition monitoring. D.W.Bridson, R.M. Atkinson and J. Woollons. Institution of Mechanical Engineers Seminar held in London on 9th January 1990.
3. Monitoring of helicopter transmission noise and vibration for fault diagnosis. I.T. Robertson, R.C. Witcomb and P.J.C. Skitt. First International Conference on Gearbox Noise and Vibration. 9-11 April 1990. Churchill College Cambridge, UK.

7. ACKNOWLEDGEMENT

W. Allan Clearwaters, Technical Director Helitune Limited for provision of data on Rotor Track and Balance applications.

HEALTH AND USAGE MONITORING SYSTEMS IN AIRBORNE APPLICATIONS

Iain Robertson,
Deputy Manager-HUMS
Engineering Group,
Smiths Industries Aerospace
& Defence Systems,
Basingstoke
England



SMITHS INDUSTRIES

BASINGSTOKE

OVERVIEW OF HUMS FUNCTIONS

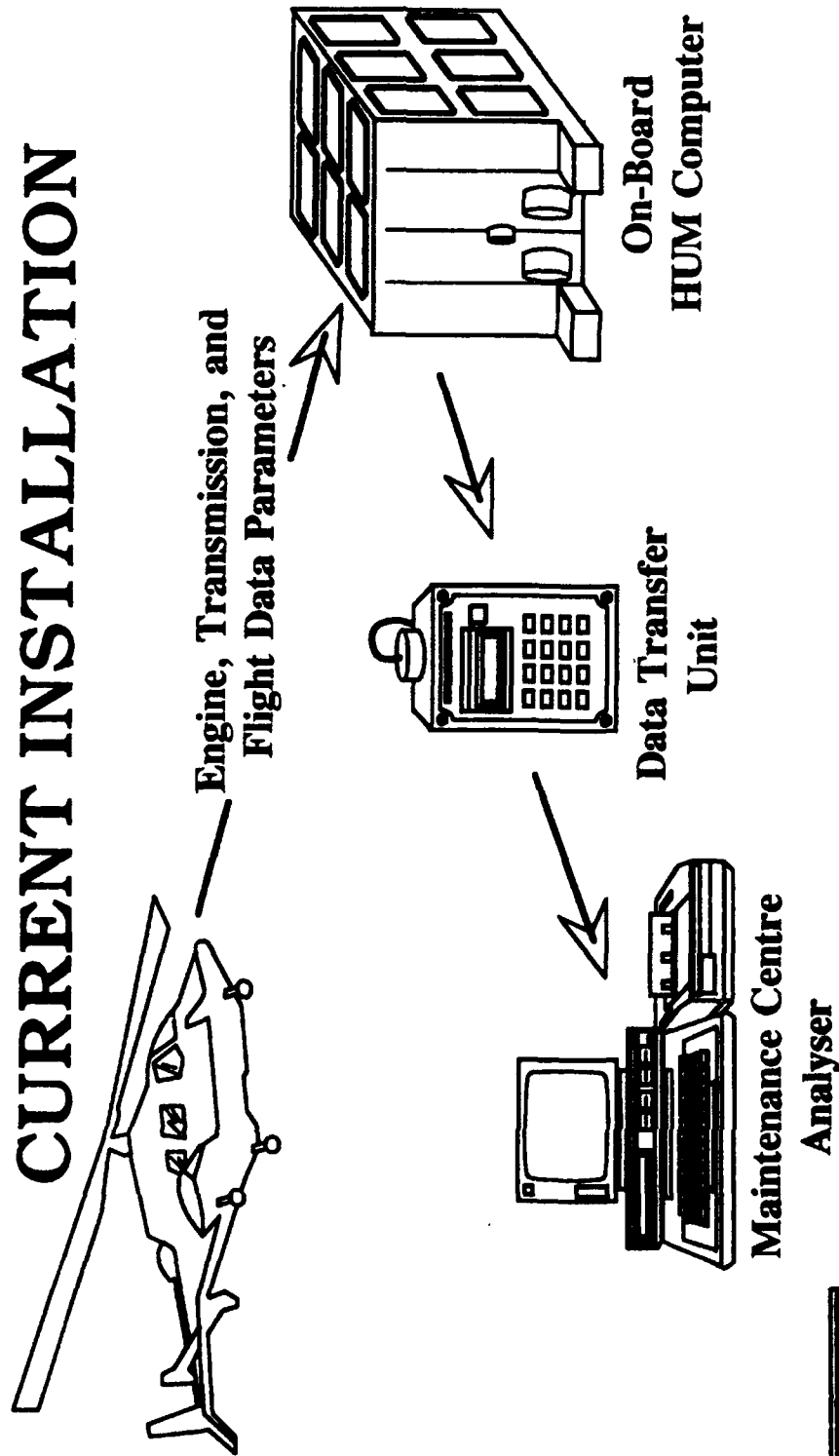
- 1 Engine monitoring
- 2 Gearbox and transmission monitoring
- 3 Rotor track and balance
- 4 Aircraft / Airframe monitoring
- 5 Status monitoring



SMITHS INDUSTRIES

BASINGSTOKE

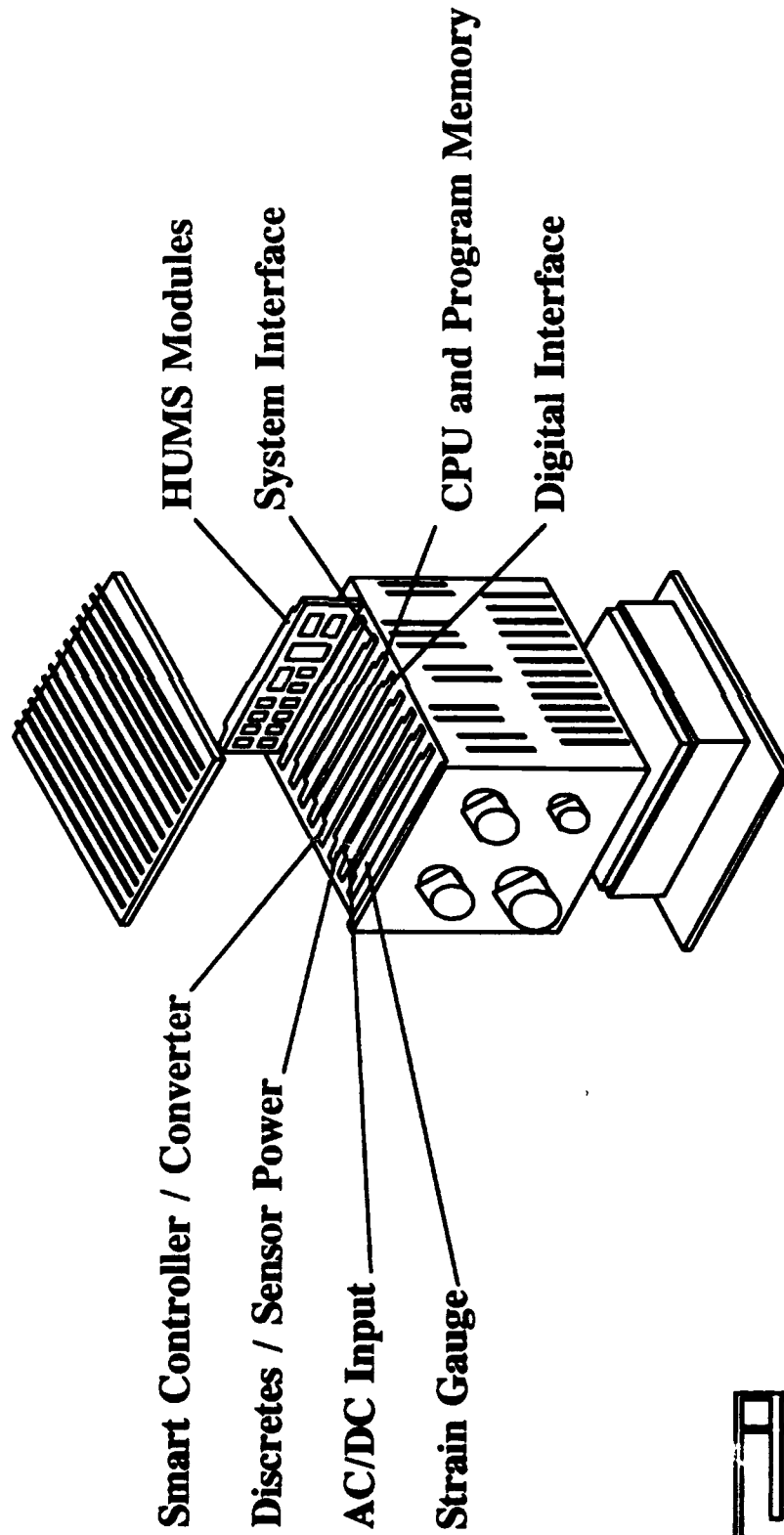
AIRBORNE HUMS - TYPICAL CURRENT INSTALLATION



SMITHS INDUSTRIES

BASINGSTOKE

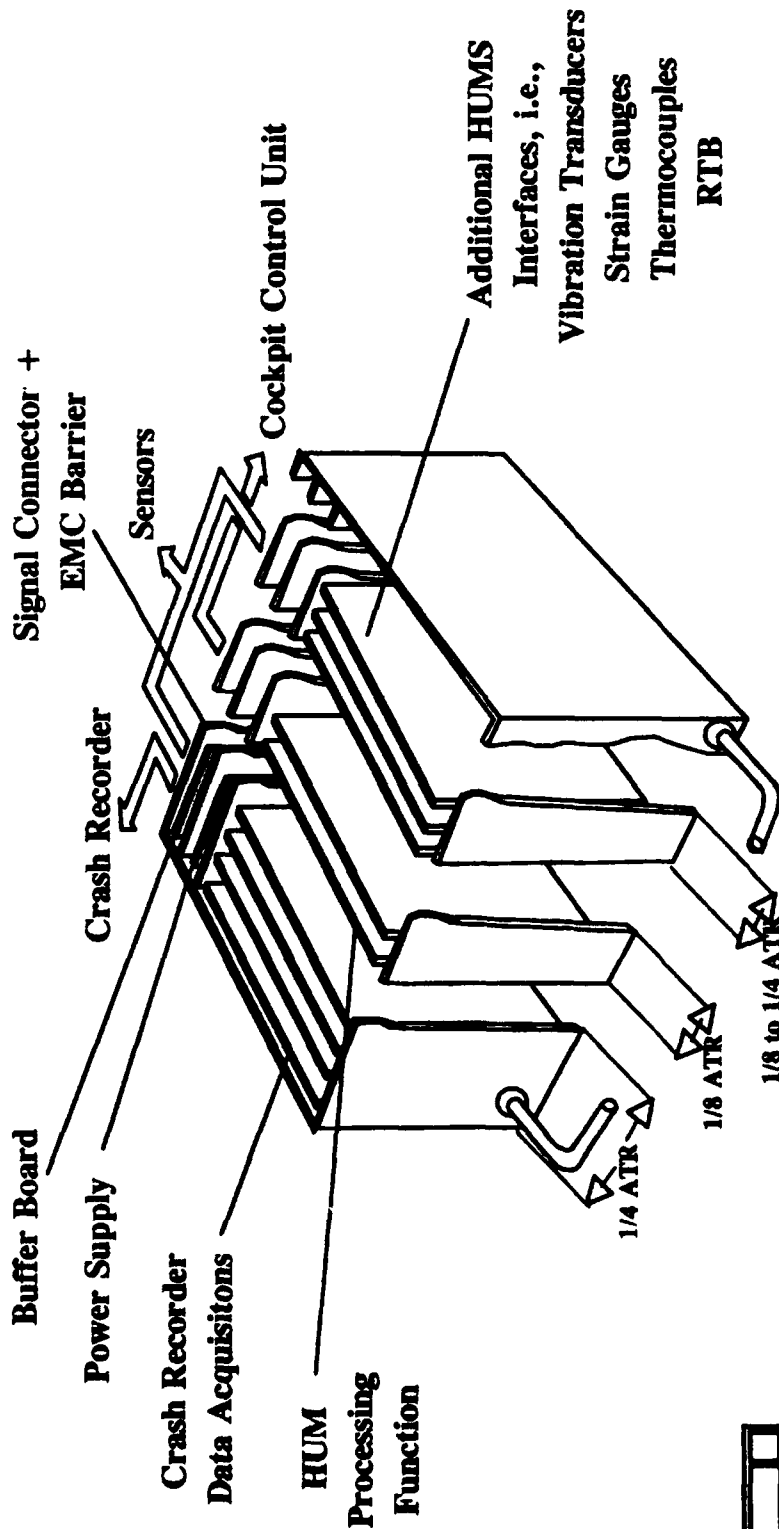
INTEGRATED HUMS AND CRASH RECORDER ACQUISITION UNIT



SMITHS INDUSTRIES

BASINGSTOKE

MODULAR HUMS COMPUTER SCHEMATIC

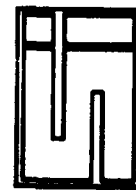
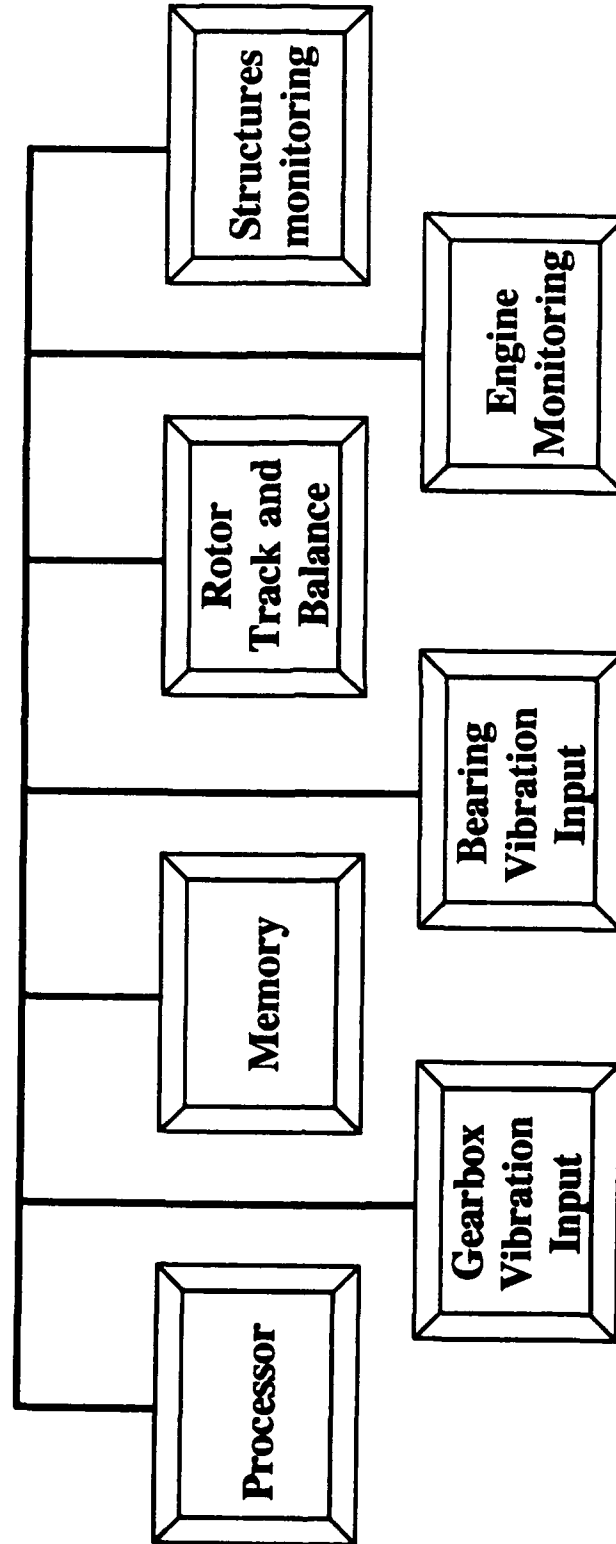


SMITHS INDUSTRIES

BASINGSTOKE

INTEGRATED HUMS SCHEMATIC

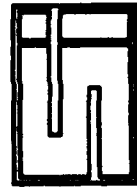
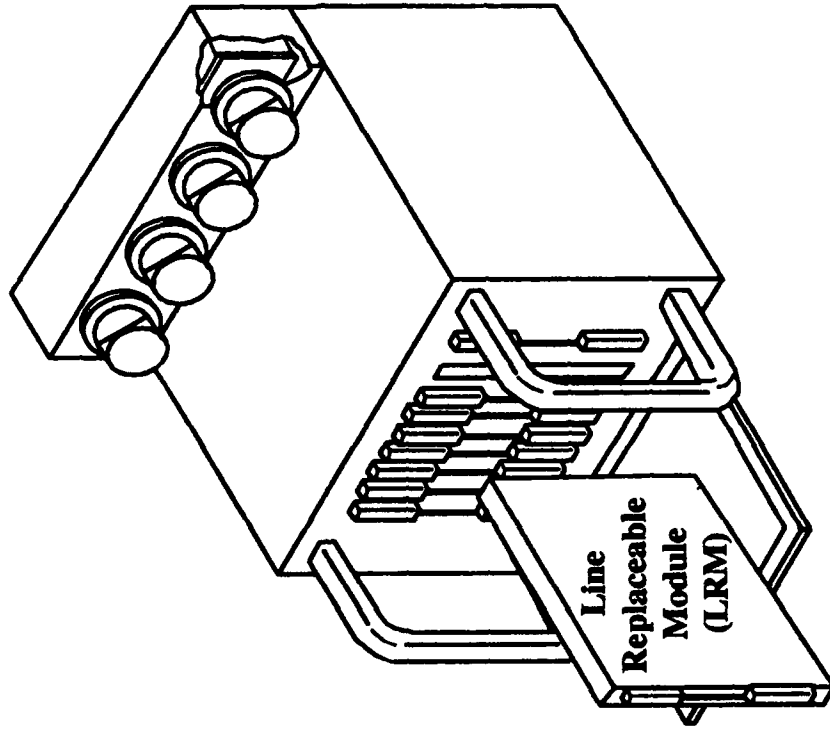
Internal bus on motherboard



SMITHS INDUSTRIES

BASINGSTOKE

HUMS IMPLEMENTATION IN MODULAR AVIONICS RACK



SMITHS INDUSTRIES

BASINGSTOKE

ENGINE MONITORING

1 Engine Health

- Performance monitoring
- Snapshots (for trending)
- Divergence monitoring
- etc

2 Engine Usage

- Low-cycle fatigue of critical parts
- Exceedance / Banding measurement
- Thermal creep / fatigue
- Engine start up data

3 Sensors Used

- Tachometer
- Pulse probes
- 0-5V sensors
- Thermocouples



SMITHS INDUSTRIES

BASINGSTOKE

GEARBOX AND TRANSMISSION MONITORING

1 Gearbox and Transmission Health

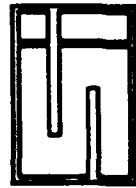
- Oil debris monitoring
- Gearbox vibration monitoring
- Bearing vibration monitoring

2 Gearbox and Transmission Usage

- Damage to rotating components
based on torque
- Damage to rotating components
based on torque cycles

3 Sensors Used

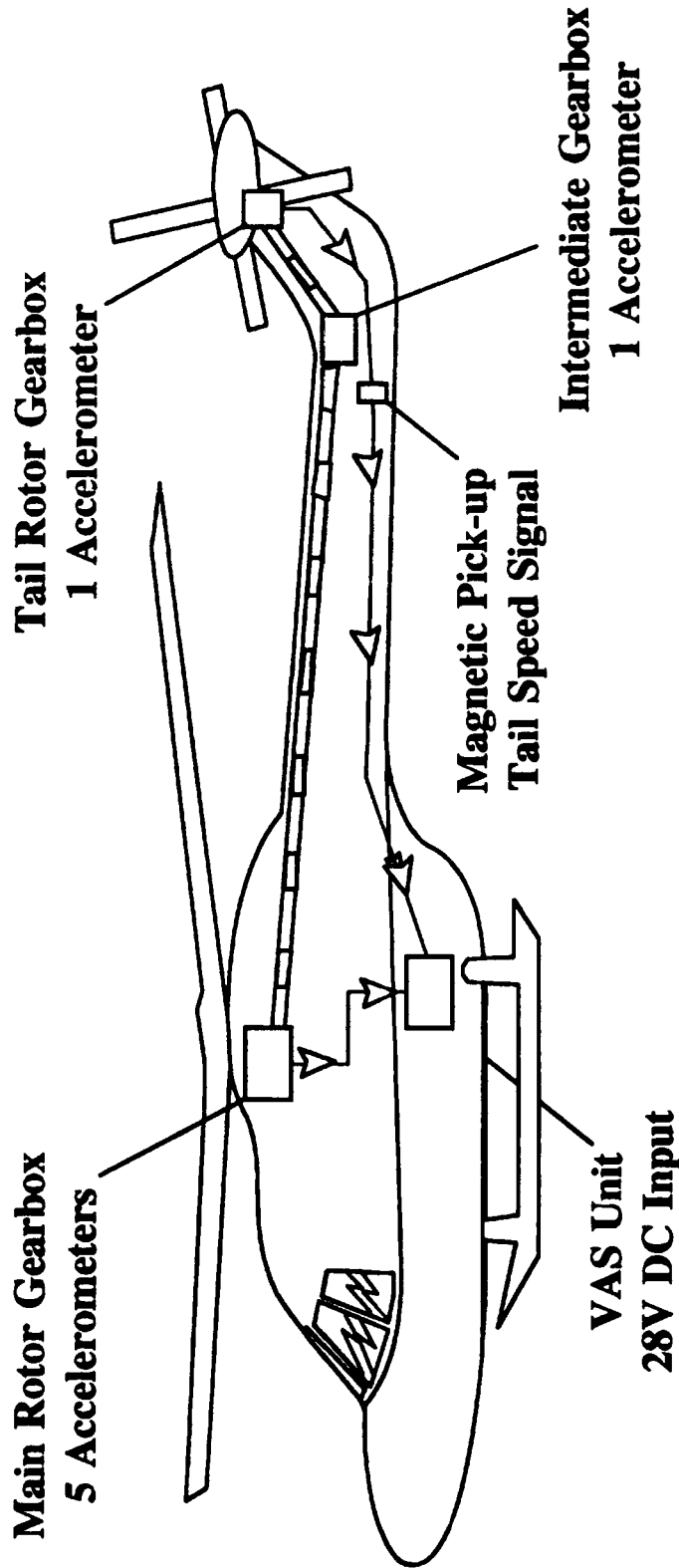
- Accelerometers
- In-line debris monitor
- Torquemeter



SMITHS INDUSTRIES

BASINGSTOKE

GEARBOX VIBRATION MONITORING - TRIALS INSTALLATION

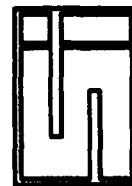
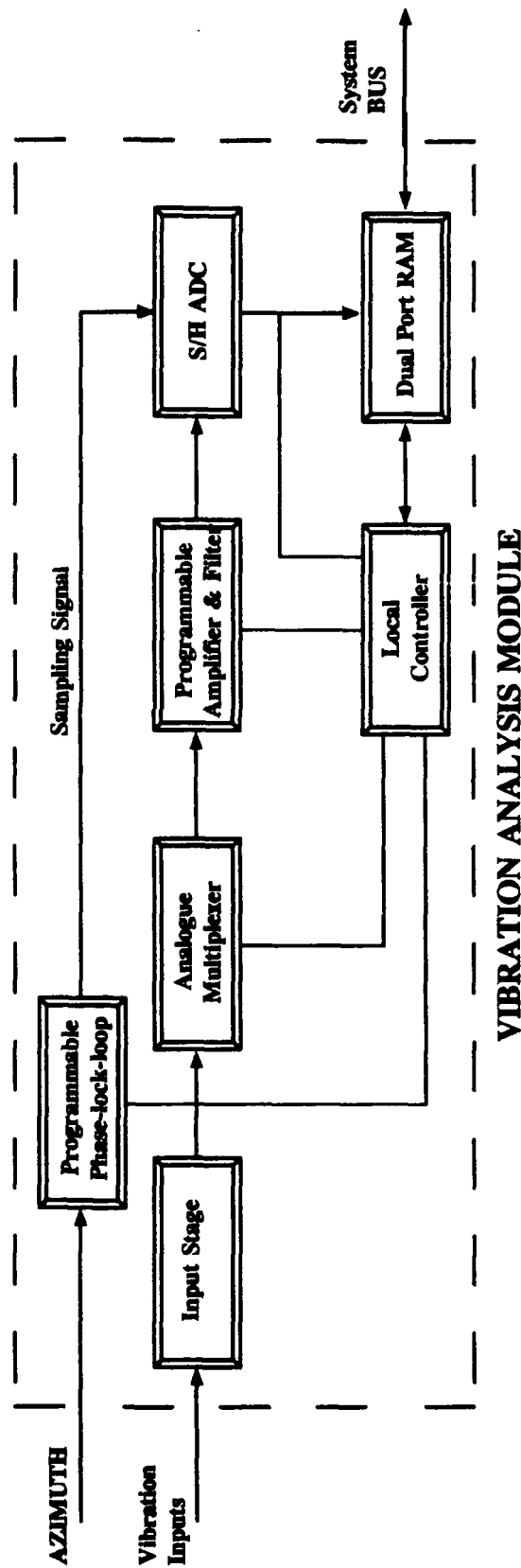


SMITHS INDUSTRIES

BASINGSTOKE

GEARBOX MONITORING DETECTION OF FAULTS IN ROTATING COMPONENTS

HARDWARE IMPLEMENTATION

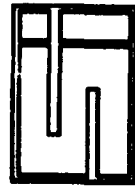


SMITHS INDUSTRIES

BASINGSTOKE

AIRCRAFT / AIRFRAME MONITORING

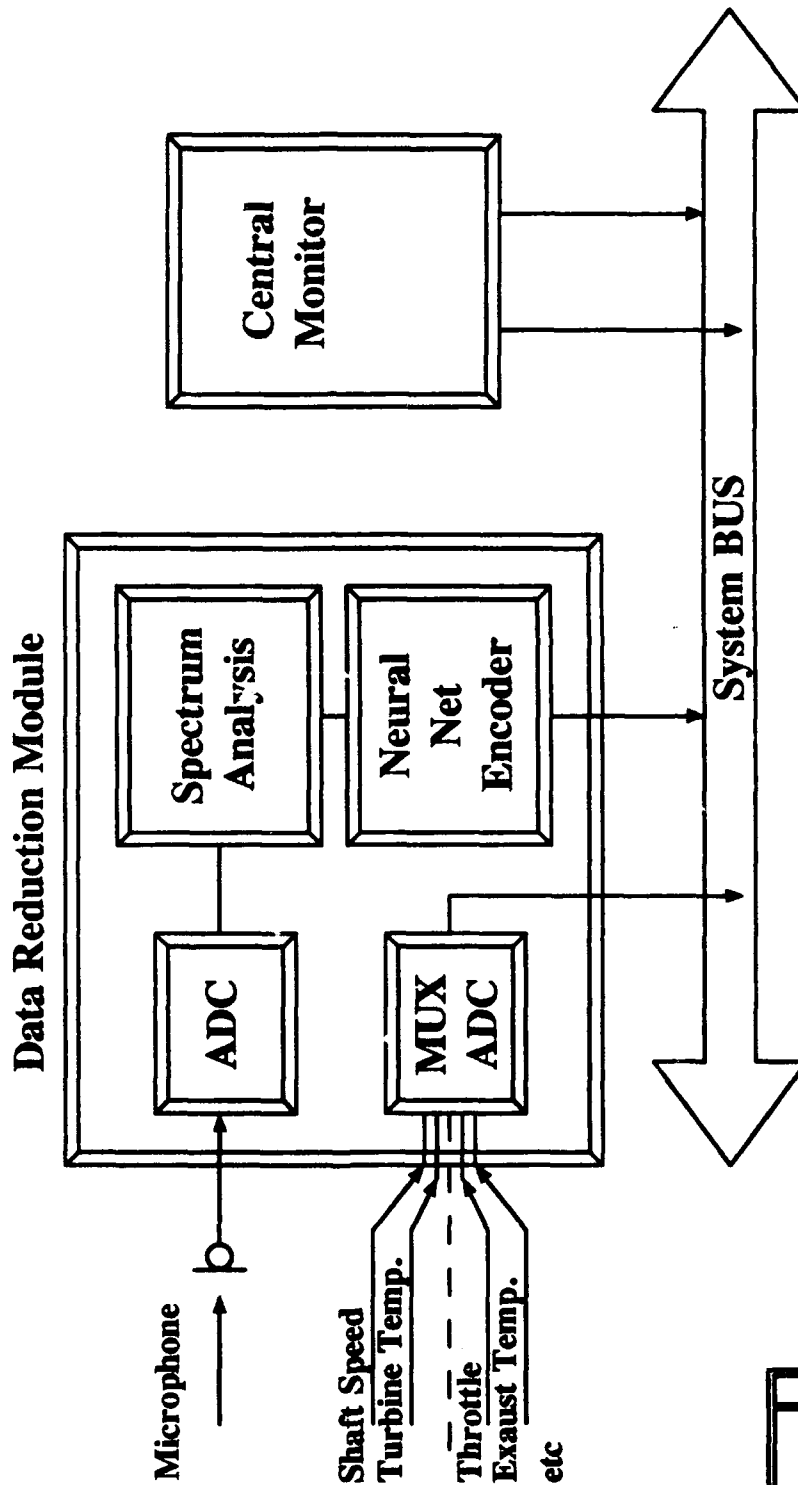
- 1 Logging of flying hours
- 2 Measurement of airframe structural fatigue
- 3 Monitoring of control loads
- 4 Monitoring of other aircraft systems
e.g., measurement of undercarriage life cycles



SMITHS INDUSTRIES

BASINGSTOKE

NEURAL NETWORK IMPLEMENTATION SCHEMATIC



SMITHS INDUSTRIES

BASINGSTOKE



"SHOT PEENING CAN REDUCE EFFECTS OF AGING ON AIRFRAME AND ENGINES"

J. S. Eckersley and
T. J. Meister
Metal Improvement Company
Paramus, NJ, USA

ABSTRACT

Metal Fatigue, Corrosion Fatigue and Stress Corrosion Cracking are the catastrophic modes of metal failure that can be significantly controlled or even avoided by the use of Controlled Shot Peening. This processes is often applied to new airframe, engine and landing gear components but it is being increasingly used at overhaul to restore compression to metal surfaces that have been subjected to high cycles and/or stresses, corrosion, wear, fretting, etc.

There are some cautions to be observed relating to ensuring correct intensity, coverage and choice of media, particularly when parts are to be peening on previously fatigued specimens. Computer Monitored Shot Peening, on site and off, will also be discussed.

DISCUSSION

Shot peening is a well-recognized method of preventing or greatly retarding metal failures from fatigue, stress corrosion cracking and corrosion fatigue (Fig. 1).^{1,2} Most aircraft structural parts are shot peened during manufacture to offset the life-debitting effects of machining, grinding, welding, anodizing, etc. (Figs. 2&3) Shot peening introduces known, high magnitude residual compressive stresses.^{3,4} As long as these compressive stresses remain in the surface of the

part, there is little danger of crack initiation. Over time, though, there are factors that can dissipate the protective effect of the shot peening. The subject of this paper is to outline some applications where peening has been used as a rejuvenation process but it is useful, first, to consider the dissipation factors.

* Heat, of course, will relieve the compressive stress. Structural components are not usually subject to high heat (more than 250°F for aluminum and 800°F for titanium) in service. However grinding or welding a shot peened surface will not only relieve the beneficial compressive stresses, but will replace them by detrimental tensile stresses.

* Service stresses, particularly peak load stresses, will eventually cause localized yielding of the peened surface, after many, many cycles. Peening the surface again, before cracks appear, will restore the compressive stresses to the original value of at least 50% of the ultimate tensile strength of the material. (Fig. 4)

* Physical removal of the surface layers, by general or pitting corrosion or exfoliation can cause eventual penetration of the compressive layer. In this category falls also the mechanical dressing of the surface to remove the corroded layers, which will also remove the shot peened layer. To further weaken the component, the dressing of the surface will reduce the effective cross section and in many cases, the dressing can introduce tensile stresses.⁵ Under these circumstances, re-peening of the dressed surface is mandatory.

SHOT PEENING FOR REJUVENATION

The same parameters and specifications should be adhered to when peening an aged component as were employed during manufacturing.⁶ The one recommended change is to use ceramic shot rather than cast steel. Cast steel will leave an iron deposit on the surface of aluminum. During manufacturing, the iron is removed prior to the application of the anodic coating but it is better to avoid it altogether when peening a structural component that is attached to the aircraft.⁷

Maintaining Almen intensities is critical, particularly in thin areas (Fig. 5). Coverage is especially critical when the problem is associated with stress corrosion and the use of a fluorescent tracer is recommended (Fig. 6).^{8,9} Where peening on the original part might have been desirable, now re-peening of a reworked part becomes essential since even with the re-peening, the aged part is not as resistant to fatigue and SSC as when it was new. For this reason, automatic or even computer controlled shot peening is to be preferred and available.^{10,11} Peening using hand-held nozzles or flapper wheels is not recommended and should be avoided (Fig. 7).

With a clearer understanding of the process, applications can be described where shot peening has been used to increase or restore the resistance to SCC & CF on aging aircraft.

a) As far back as the early 1970's, SCC was found on DC9 main landing gear attach fittings (aluminum). McDonnell Douglas required that all DC9s in service at that time be shot peened on site in the critical areas of the attach fittings. The

paint and anodic coating were removed in the critical areas and energy absorbent tape applied to mask off adjacent surfaces. The general area was enclosed in plastic sheet. The shot was contained by the differential pressure peening nozzle and returned to the pressure generators for recirculation. After peening, the anodic coating and paint were reapplied. It would appear that no further evidence of cracking in these areas has been found, after the shot peening was performed.

b) In an paper entitled "Maintenance of Concorde into the 21st Century," Mr. M. J. Phillips, Senior Engineer, British Airways plc., states the following: "The power flying control unit (PFCU) cradles have caused problems in the past... The rudder PFCU cradles were reshaped using a clamp-on profile jig as a guide, and then the cradle was shot peened in situ, to improve its structural reliability" (Fig 11).¹²

c) Drawings relating to Boeing 747, "corroded lower web, wing ctr. section, stn. 1000" carry the following "Repair Procedure" (abbreviated):

"1. To inspect lower web for corrosion hidden by lower chord, refer to Boeing S.B. 747-53-2064.

2. Blend out corrosion in web...

3. Remove fasteners shown...

4. Shot peen corroded area per BAC 5730 all over blended area.

Use 230-280 grade shot, .004"-.008" A-2 intensity - see ref. drg. 65B 10276 note 6 and Boeing Overhaul Manual Chapter 20-10-03 for information.

5. Alodine and paint whole of repaired area...

6. Apply sealant... to all faying surfaces.

7. ..replace removed section of chord along with splice plates and fixings."

d) There is a current Boeing specified retrofit process on all attachment lugs for the B-737-200 tail fin assemblies. The rework calls for reaming the lug bores to an oversize dimension, shot peening of the bores, followed by installing new bushings to fit. Due to the proximity of the lugs, a special tool has been manufactured to allow on-site peening of the lugs so that the fittings do not need to be disassembled from the aircraft or the fins. Sophisticated mask tooling is required to contain the shot.

The above examples are only typical of many applications of shot peening used on aging aircraft to prevent or greatly retard SCC, CF and metal fatigue. The process is applicable not only to the aluminum alloys (including aluminum lithium) but also to steels (landing gears, for instance), titanium and the super alloys used in jet engines. Jet engine components, incidentally, are shot peened several times for restoration of compressive stresses at periodic overhaul, usually as a protection against fretting fatigue (Fig. 8).¹³

EXFOLIATION CORROSION

Exfoliation Corrosion, a more severe form of Intergranular Corrosion, occurs along aluminum grain boundaries, which in sheet and plate are oriented parallel to the surface of the material, due to the rolling process. It is characterized by delamination of thin layers of aluminum, with white corrosion products between the layers. It is often found next to fasteners where the electrically insulating sealant or a cadmium plating, for in-

stance, has broken down, permitting a galvanic action between the dissimilar metals. Where fasteners are involved, the corrosion extends outward from the fastener hole, either from the entire circumference of the hole, or in one direction from a segment of the hole. In severe cases, the surface bulges upward, but in less severe cases, there may be no telltale bulging, and the corrosion can only be detected by nondestructive inspection methods (Fig. 9&10).¹⁴ Controlled shot peening is of little value in preventing exfoliation corrosion but it can be very effective in the process of repairing the damage. Service manuals normally call for the removal of the fastener; and then for the use of rotary files to grind away the corroded material followed by blending the area and polishing out the tool marks. Aircraft engineers have used controlled peening after the polishing to increase the fatigue strength of the newly reduced cross-section. The action of the peening can cause the surface to bulge out again where deeper exfoliation has taken place. The surface can then be reground and repeened until no further bulging occurs. The shot peening provides excellent NDT of the exfoliated material. The action of the peening on the thin exfoliated layer is essentially the same as that employed in the process of peen forming, used to generate the aerodynamic curvatures in the wing panels of most commercial airliners (Fig. 11).^{15,16} Peening of corroded surfaces can be accomplished using special enclosures to contain the media (Fig. 12). It is essential to maintain extreme control on the intensity of the peening not to cause

bulging of the skin itself, rather than just the exfoliated layer, which would scrap out the entire panel.

PREP OF CORRODED SURFACES

Chronologically, this section should have preceded the other but it is necessary to understand the principles of controlled shot peening to properly appreciate how these principles can be applied to effective blasting for removal of paint and the products of corrosion.

Plastic Media Blasting for paint removal showed great initial promise but has fallen down in some important areas. Airframe manufactures, for instance, have limited, by specification, paint removal by PMB to one time only because of the danger of damage to the surface of aircraft skins.¹⁷ Most aircraft will require several paintings during their useful life so a better method is still to be found. Also, dust and disposal of paint contaminated PMB has become a major problem -- not on the magnitude of the disposal of paint solvent chemicals, but a problem nonetheless. The current application techniques for PMB have largely been developed by the manufactures of plastic media in conjunction with the manufactures of paint.

There is a process development under way to apply the controls of shot peening to the technique of paint removal which, together with non-toxic water soluble blasting media, shows considerable promise in reducing substrate damage, dust and disposal of paint chips. Blasting to remove the products of corrosion from aircraft surfaces is very cost effective but it requires great expertise. The most common products of corrosion on aircraft are iron oxides on fastener heads

and aluminum oxides on the skins and structural members. These oxides are very hard and removal is difficult unless a media of equal or greater hardness is used. Glass beads, for instance, may be too soft. Fine aluminum oxide grit works very well and has been used successfully on a DC8 to clean along the rivet lines of the wings and fuselage prior to repainting. The expertise comes in determining the energy level (intensity) and dwell time for a given area bearing in mind that it is quite easy to blast a hole right through the skin if the correct parameters are not observed. Of necessity, the DC8 was blast cleaned manually but automatic equipment is now being developed for this purpose.

There exists also a requirement for blast cleaning the corrosion, followed by shot peening, between the skins in the overlap joints. After the fasteners are removed, the skins can be separated sufficiently to allow insertion of specially designed, automated, differential pressure nozzles that will contain the media in addition to doing the blasting.

CONCLUSION

Well established techniques of controlled shot peening, as used on aircraft components at the manufacturing stage, are being applied to aging aircraft in the field to prevent or retard failures from fatigue, stress corrosion cracking, corrosion fatigue, fretting, etc., by the introduction of high magnitude compressive stresses. Peening is also being used to identify and combat the effects of exfoliation corrosion. Similarly, the controls of shot peening are being applied to blasting for

the removal of paint and the products of general corrosion.

REFERENCES:

1. W. P. Koster, et al, "Surface Integrity of Machined Structural Components"; Technical Report AFML-TR-70-11, March 1970.
2. J. H. Milo, "Shot Peening Prevents Stress Corrosion Cracking in Aircraft Equipment"; Materials Protection (NACE), September 1968.
3. W. J. Harris, "Metallic Fatigue"; Pergamon Press, p.61.
4. H. O. Fuchs, "Shot Peening Stress Profiles"; available from Metal Improvement Company.
5. H. W. Zoeller and B. Cohen, "Shot Peening for Resistance to Stress Corrosion Cracking", AMS Technical Report No. D5-20.1.
6. B. W. Lifka and D. O. Sprowls, "Shot Peening - A Stress Corrosion Cracking Preventive for High Strength Aluminum Alloys"; Paper 86, NACE 26th Annual Conference Proceedings.
7. J. E. Campbell, "Shot Peening for Improved Fatigue Properties and Stress Corrosion Resistance"; Metals and Ceramics Information Center, Report No. MCIC-71-02.
8. MIL-S-13165C, "Shot Peening of Metal Parts", U.S. Military Specification, June 1989.
9. P. O'Hara, "DYESCAN Tracers as a Quality Control Tool for Coverage Determination in Controlled Shot Peening"; SAE Technical Paper Series 850708, February 1985.
10. J. J. Daly and D. E. Johnson, "Computer-Enhanced Shot Peening"; Advanced Materials and Processes, May, 1990.
11. "Shot Peening Applications - Seventh Edition"; available from Metal Improvement Company.
12. M. J. Phillips, "Maintenance of Concorde into 21st Century"; British Airways plc.
13. S. S. Manson, "Metal Fatigue Damage -- Mechanism, Detection, Avoidance and Repair with Special Reference to Gas Turbine Components"; ASTM STP-495, 1971.
14. D. J. Hagemeier, "Exfoliation Corrosion"; Materials and Process Engineering, Douglas Service, Volume XXXVII, September/October 1980.
15. D. Finch, "Aging Aircraft"; Engineering, September 1989.
16. C. F. Barrett, "Peen Forming"; Tool and Manufacturing Engineers Handbook 1984, Special Forming Methods.
17. "Plastic Media Abrasive Striping of Organic Finishes"; Boeing Document DC-54705.



Figure 1- Photomicrograph of crack found in a 7079-T6 forging, 500X.

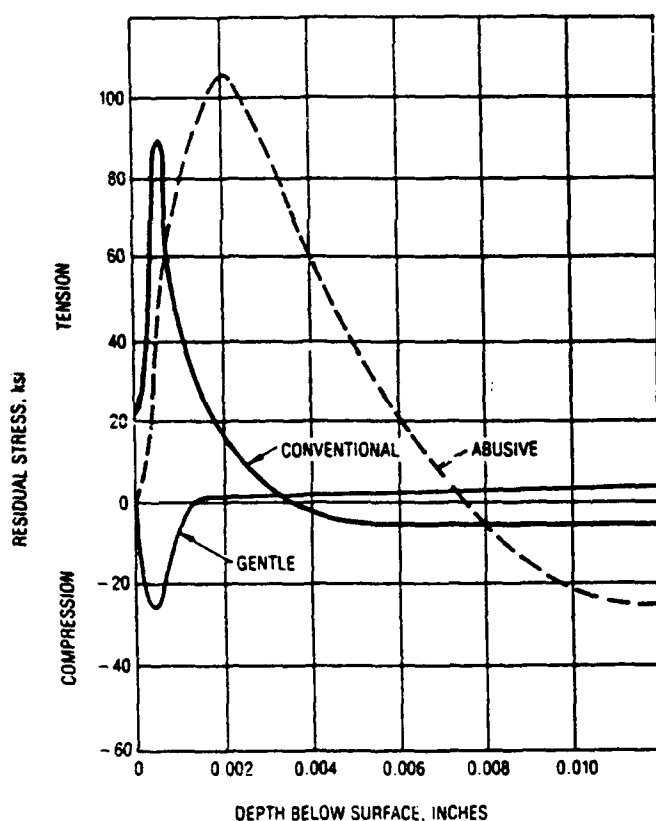


Figure 2- Residual stress in 4340 Steel (HRC 50) after surface grinding.

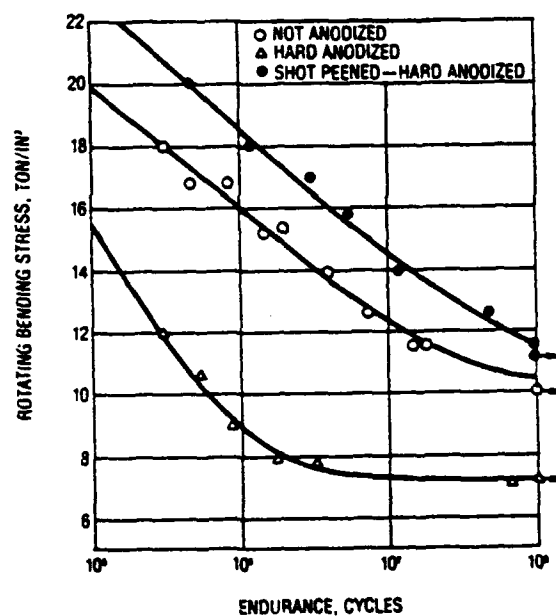


Figure 3- The influence of hard anodizing and shot peening on the failure strength of Duralumin (LI).

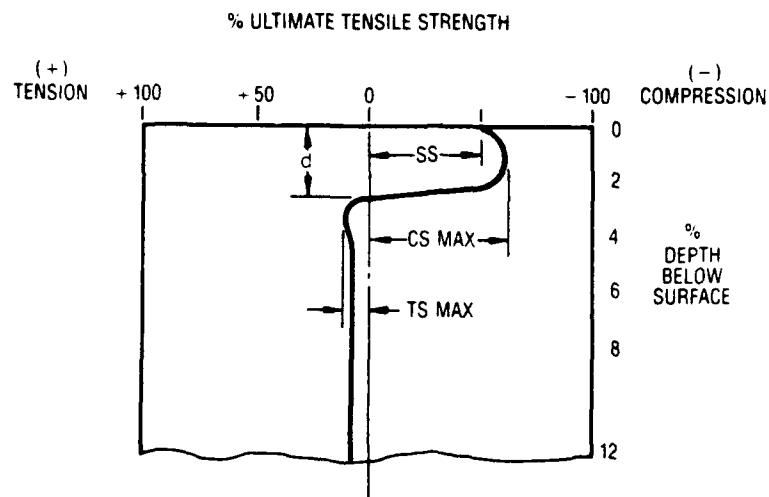


Figure 4- Example of Residual stress profile created by shot peening.

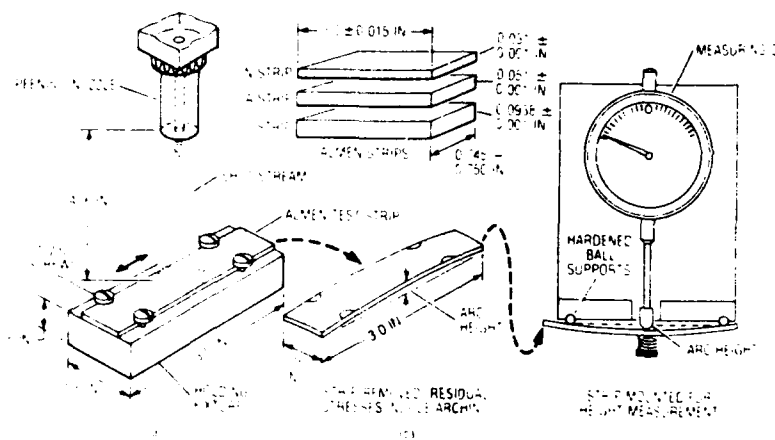


Figure 5- The Almen Intensity determination system.

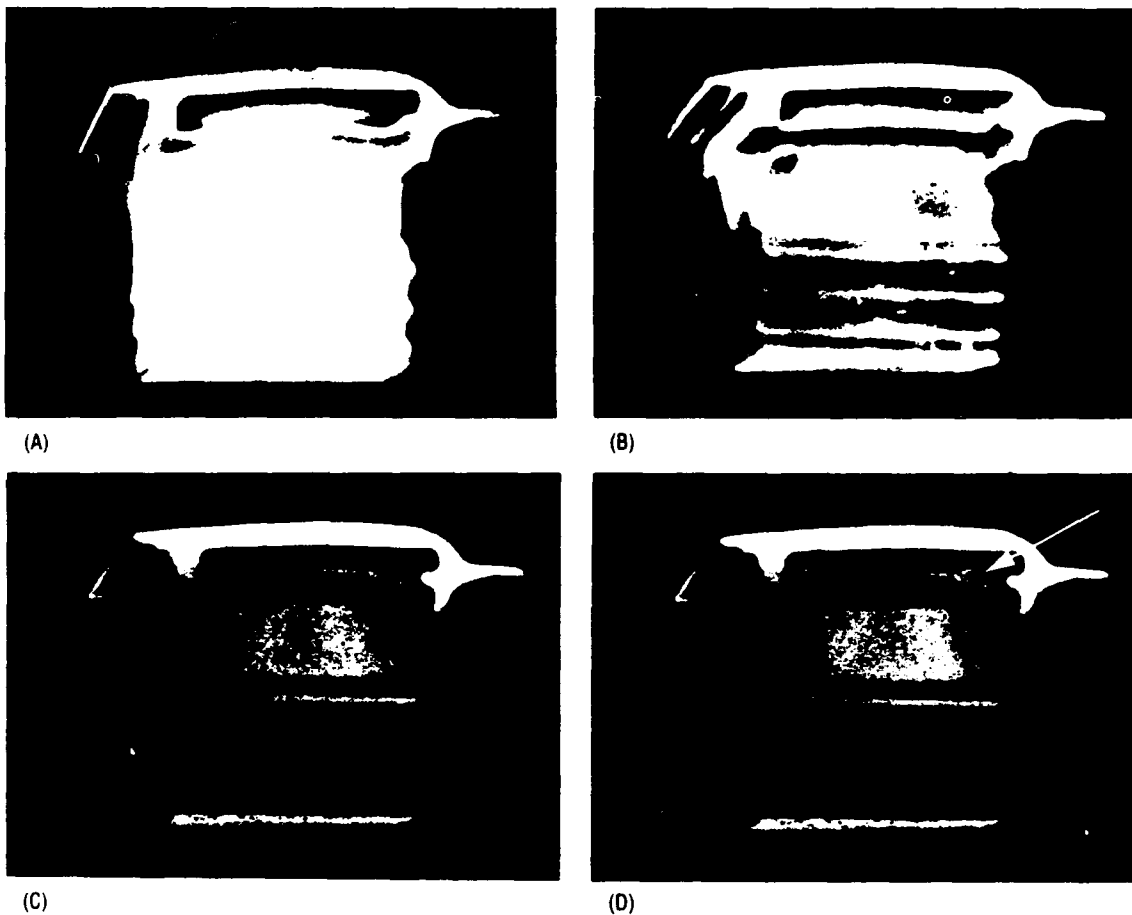


Figure 6- The Peenscan[®] System. (A) Coated, unpeened. (B) Peened 15 seconds, partial coverage. (C) Peened 60 seconds, improper nozzle angle in cavity (arrow).

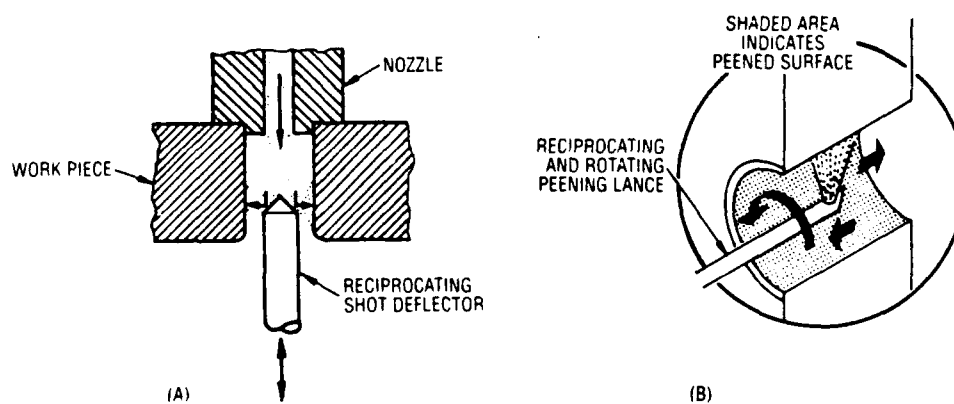


Figure 7- Shot peening of holes using deflector lance nozzle.

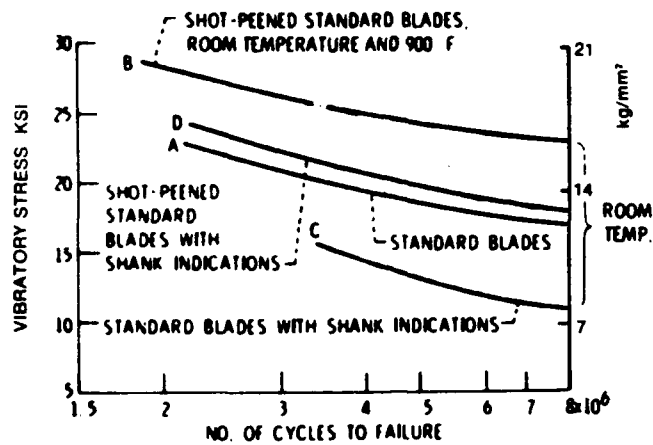


Figure 8- Suppression of fatigue damage of Inconel 713C turbine blades by shot peening.

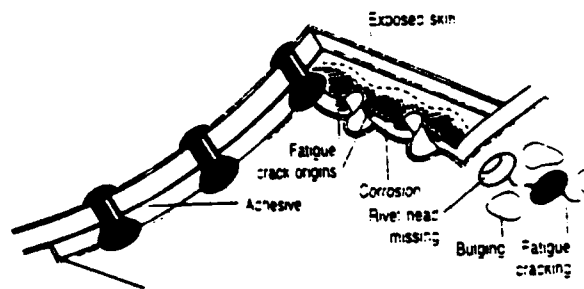


Figure 9- Exfoliation corrosion, which shows as bulges around rivet heads, can propagate into fatigue cracks.

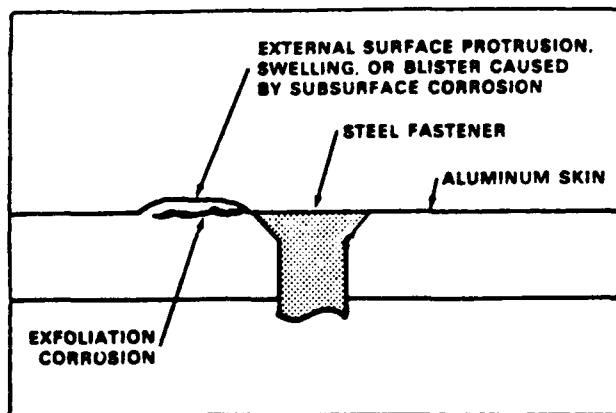


Figure 10- Section through typical exfoliation blister or protrusion.

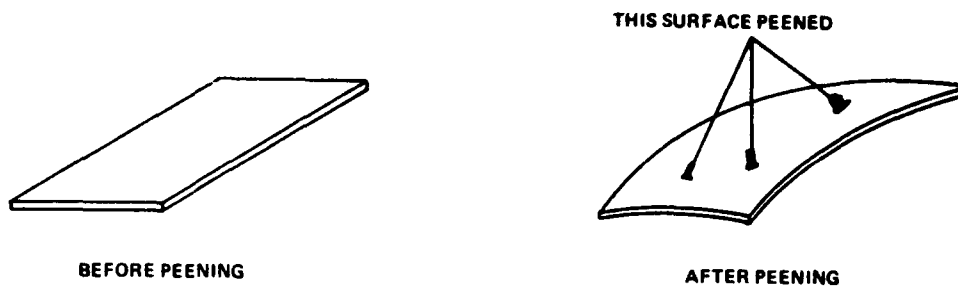


Figure 11- Compound curvature resulting from tri-axial forces induced by shot peening.

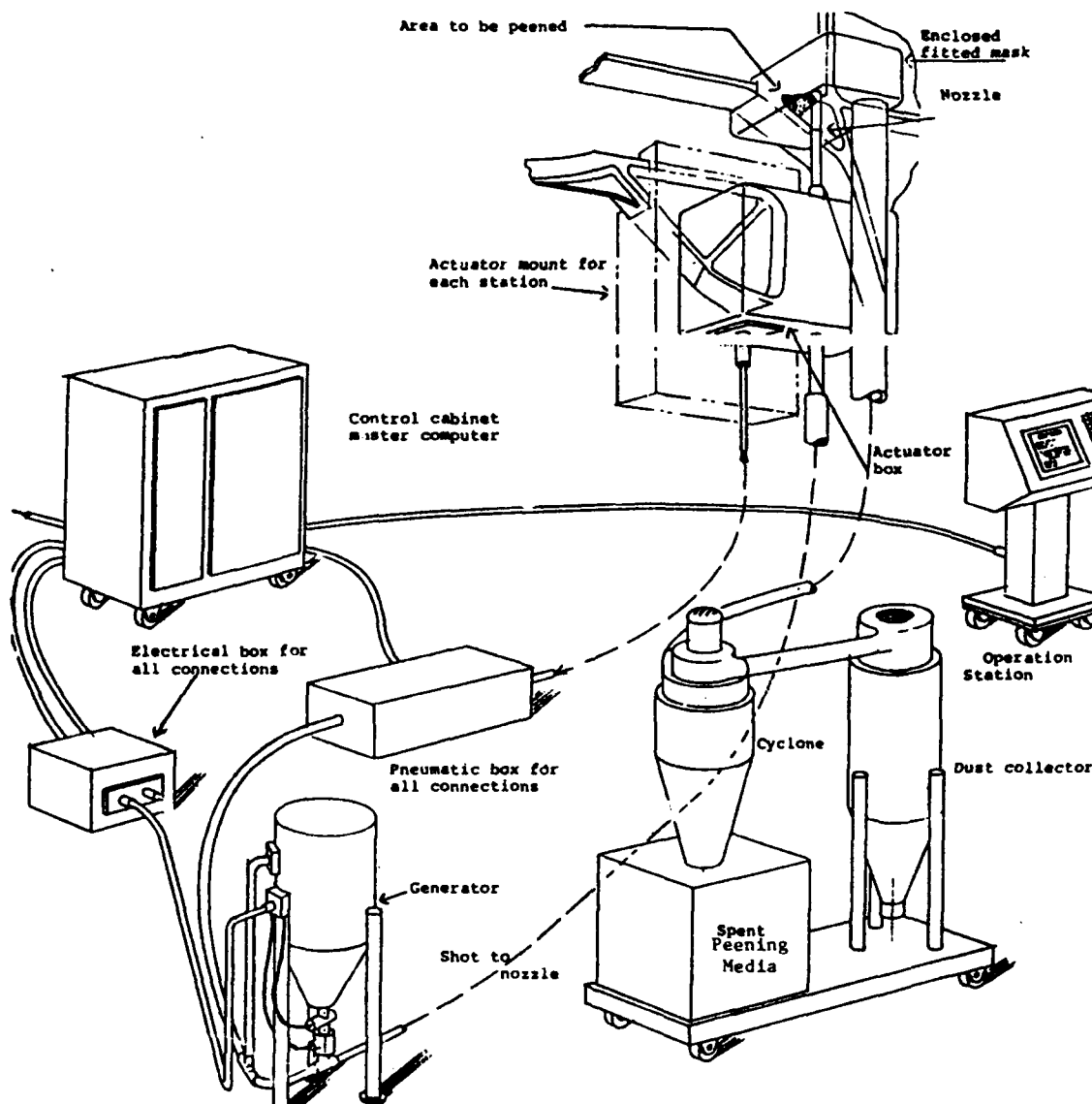


Figure 12- Schematic of computer controlled system for on-site shot peening of aging aircraft structures.

Model Sensitivity in Stress-Strength

Reliability Computations

**IS IT UTOPIAN TO DESIGN TO A VERY HIGH
STRUCTURAL RELIABILITY (0.999999) REQUIREMENT ?**

W. Matthews

D. Neal and M. Vangel

Army Materials Technology Laboratory

SLCMT-MSR, Watertown MA 02172-0001

STRUCTURAL RELIABILITY REGIME

* LIMITED DATA SETS: In Contrast To Data
From Numerous Inexpensive Components

* CATASTROPHIC FAILURE CONSEQUENCES

* SPECIALISTS OBSERVATIONS:

"The Irrationality Of The Reliability
Statistician Is In His Belief That
Figures On The Order Of .99, .999, .9999
Can Be Taken At Their Face Values With
Respect To Large Structures"

A.M.Freudenthal, Institute For The Study
Of Fatigue & Reliability, Report 2, 1963

* "All Models Are Wrong, But Some Are Useful "

G.E.P.Box, Robustness In Statistics, 1979

* "Point Estimates Are Virtually

Worthless In Reliability Engineering"

R.A.Evans, Technometrics, V 25, N 4, 1983

ISSUES INFLUENCING QUANTITATIVE STRUCTURAL RELIABILITY ESTIMATES

* SYSTEM COMPLEXITY

Many Components: Boundary Conditions
Interdependence Of Component Failure
Multiple Failure Sites- One Component
Multiaxial & Phased Combined Loading

* DATA LIMITATIONS- Infrequent Outliers

Loading Spectra
Material Properties
Structural Tests

* STRUCTURAL MODELING

Environmental Effects
Flaws
Surface Conditions

* STATISTICAL MODELING

MILITARY HELICOPTER REQUIREMENT

"The U.S.Army..Requires A Risk Level Less Than One Structural Failure In The Lifetime Of The Fleet..A Reliability Of .999999 Will Meet The Intent Of This Requirement"

R.Arden & F.Immen, American Helicopter Society Symposium, Williamsburg, VA, 1988

FIXED WING 1930's - 1990
UNMEASURED QUALIFICATION GOAL

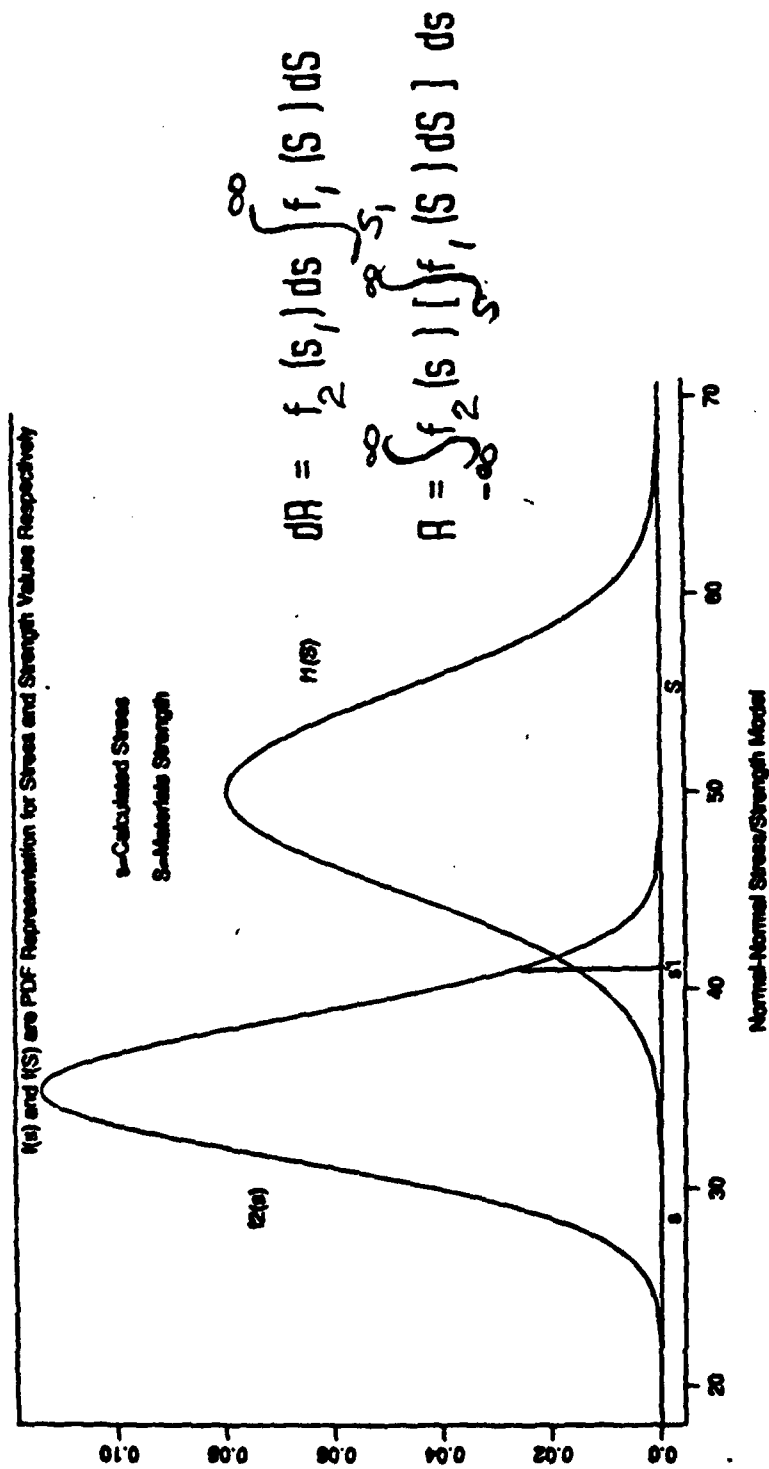
"It Is Found That The Structural Accident Rate Of Acceptable Military Aircraft Is In The Region Of Of 1 Per 10⁶ Flying Hours"

A.G.Pugsley

Aircraft Engineering, 1939

The Safety Of Structures, 1965

: Structural Reliability >999999/Flight



If S, s Are Normally Distributed

$$A = P(S - s > 0) = \Phi\left(\frac{\mu_s - \mu_s}{\sqrt{\sigma_s^2 + \sigma_s^2}}\right)$$

SENSITIVITY INVESTIGATION CONTAMINATED MODELS

$$N(m, SD^2) = (1-e)N(m, SD^2) + eN(K_2 m, K, SD^2)$$

- N - Normal PDF
- m, SD - Mean & Variance Uncontaminated
- K - Scaling Factor For Variance
- K - Scaling Factor For Mean
- 100e - Percent Contamination

Ref :

Reliability Computation:

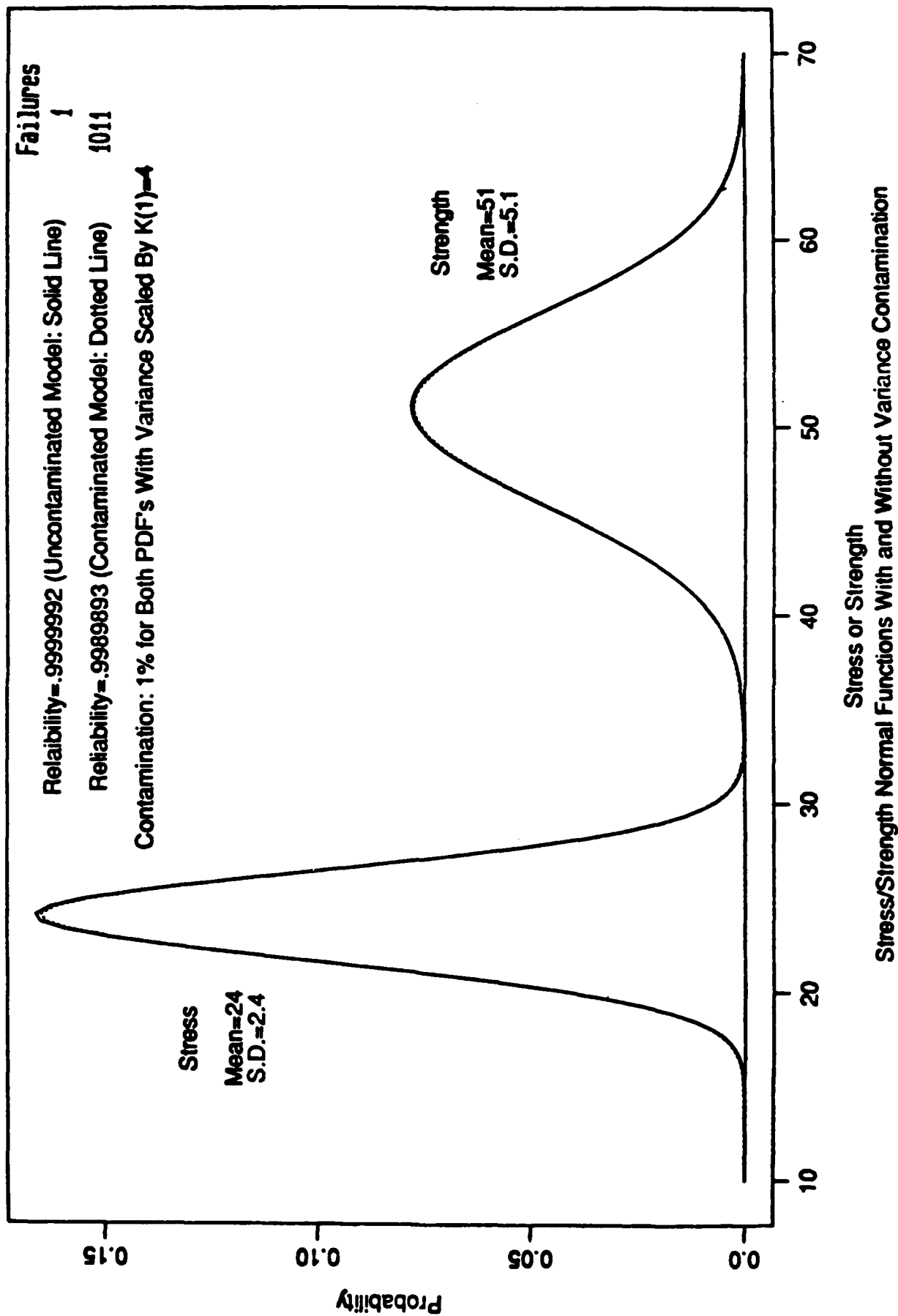
$$R = (1-e_1)(1-e_2)R(UC) + (1-e_2)R(C, S) + e_2(1-e_1)R(C, S) + e_1e_2R(C, Ss)$$

Example: Strength Variance Contamination

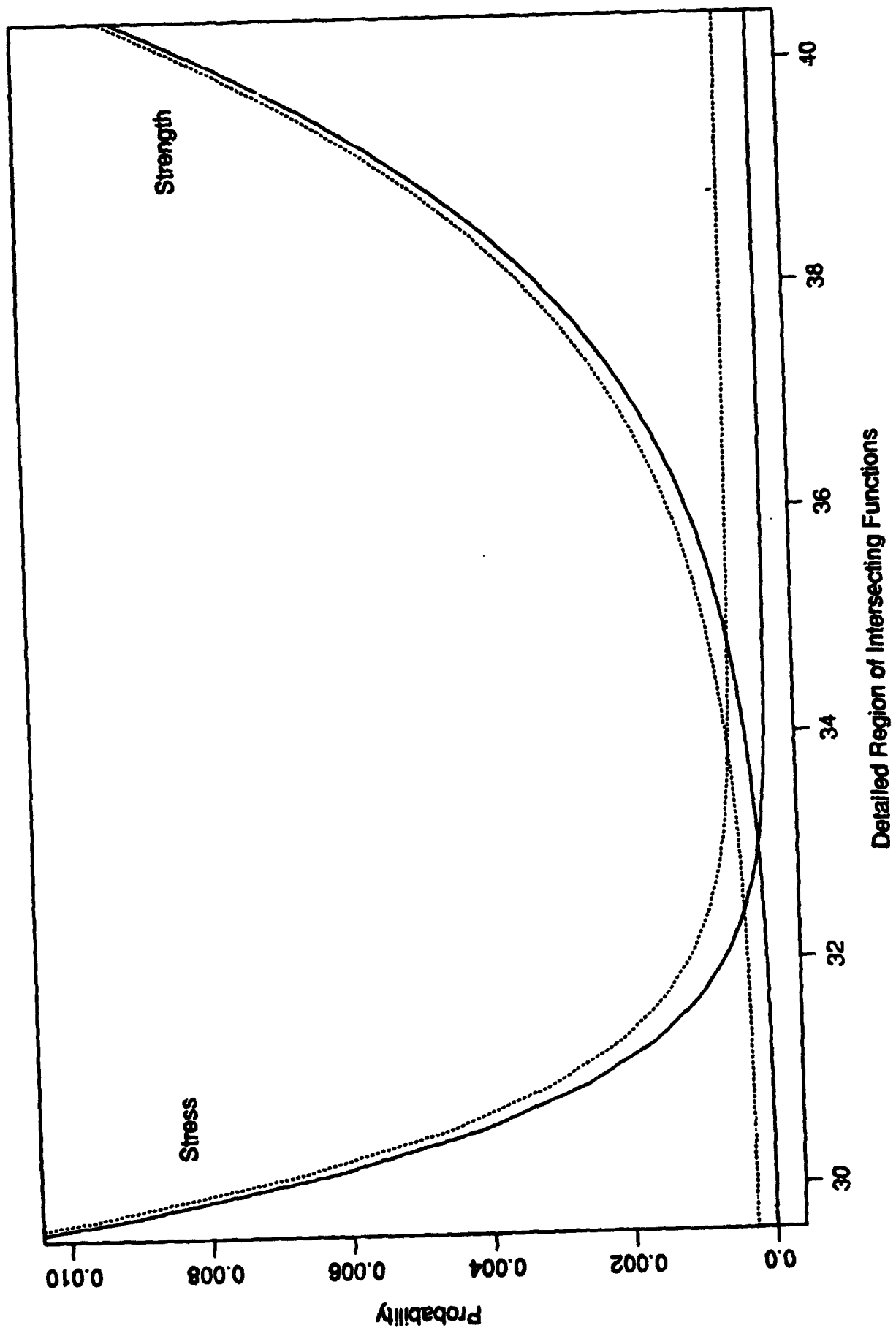
$$R = \Phi \left(\frac{m_s - m_s}{\sqrt{K, (SD)_s^2 + (SD)_s^2}} \right)$$

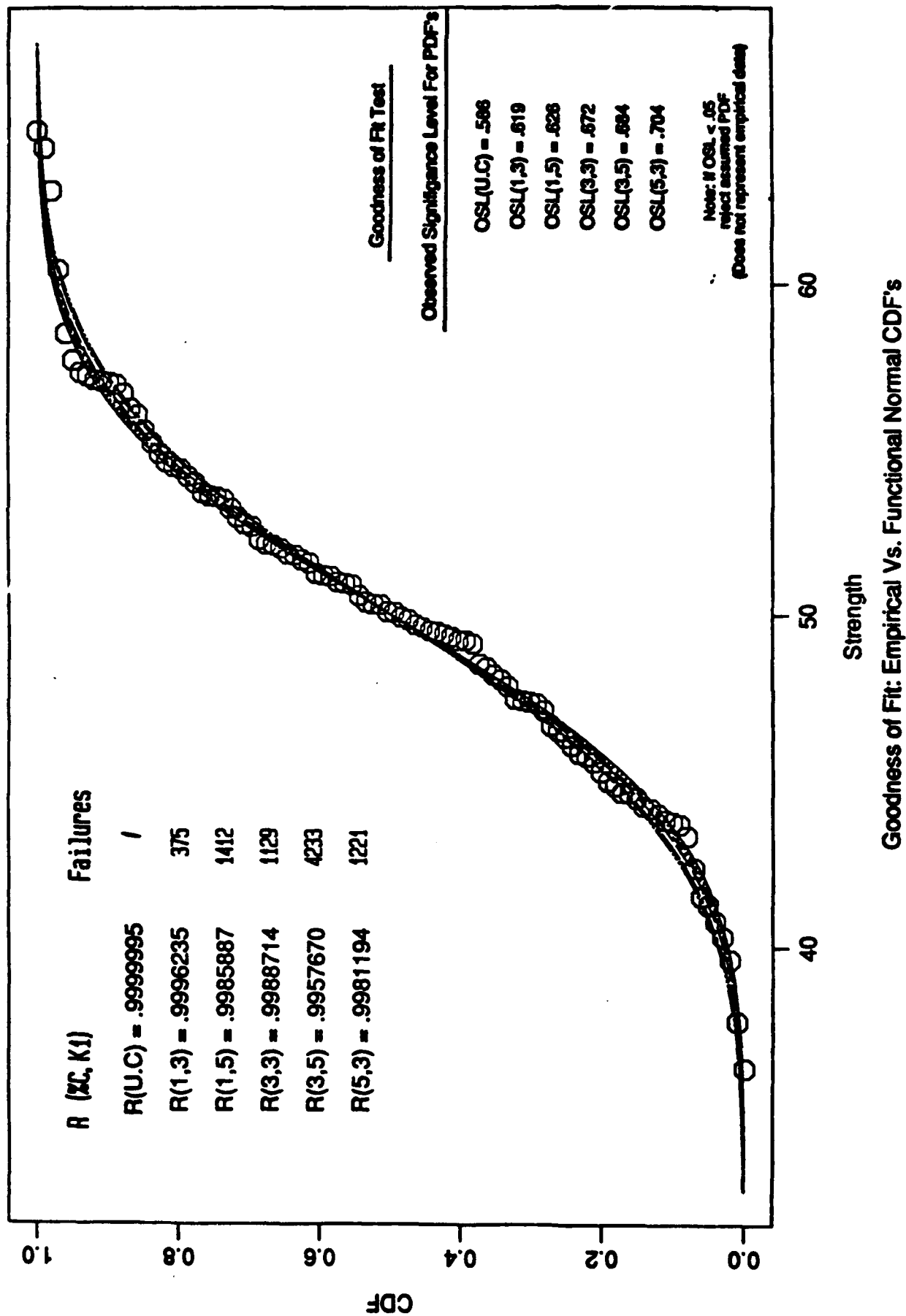
Donald M. Neal, William T. Matthews, and Mark G. Vangel
MODEL SENSITIVITY IN STRESS-STRENGTH
RELIABILITY COMPUTATIONS, MTL TR 91-3
U.S. Army Materials Technology Laboratory
Watertown, Massachusetts 02172-0001, January 1991

Normal Stress/Strength Models

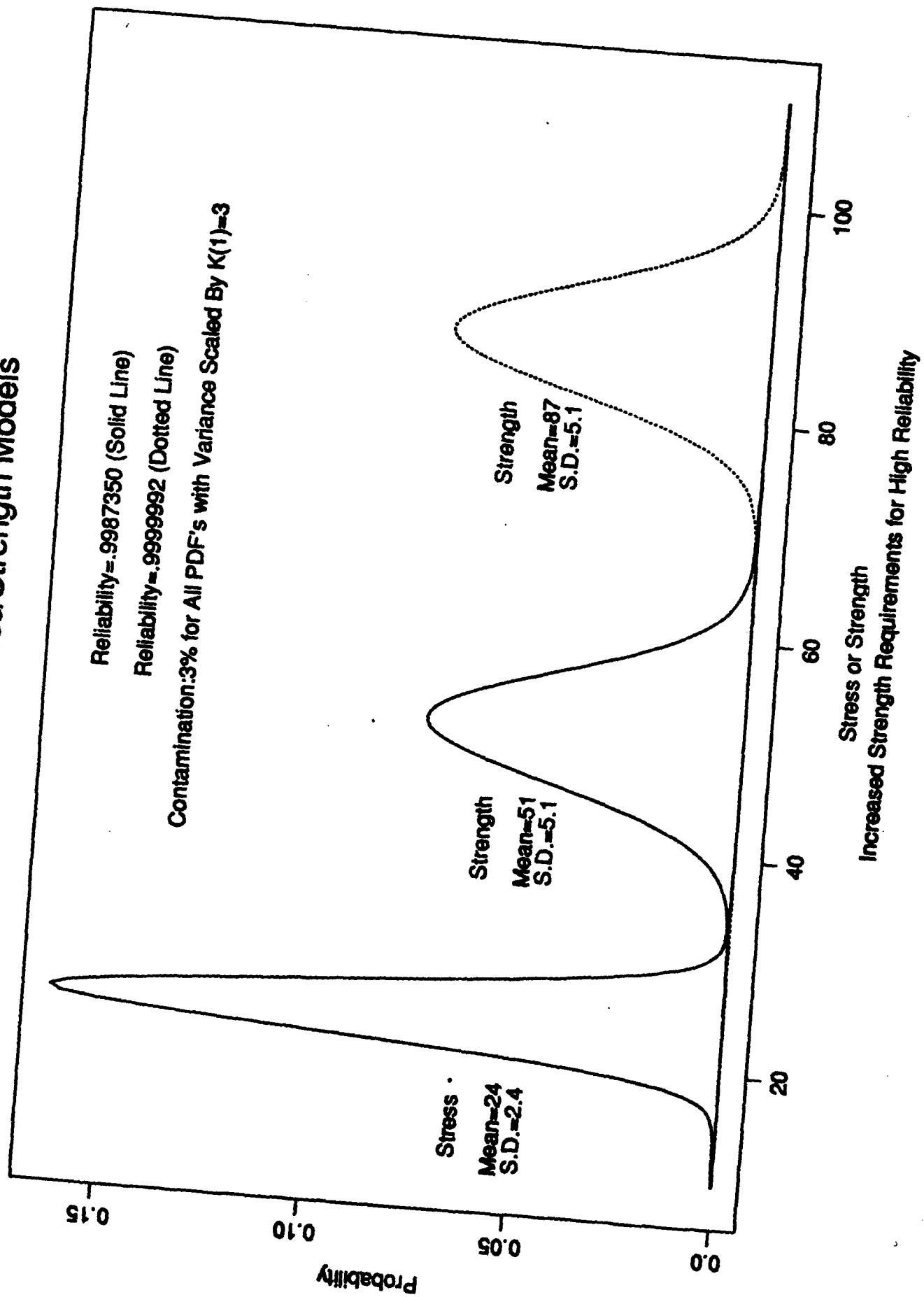


Normal Stress/Strength Models With Contamination





Normal Stress/Strength Models



RESULTS

- * ESTIMATES OF VERY HIGH RELIABILITY FROM STRESS-STRENGTH STRUCTURAL MODELS ARE VERY SENSITIVE TO SMALL CHANGES IN ASSUMED PDF
- * STRUCTURAL DESIGN BASED ON VARIABILITY OF CONTAMINATED MODELS IS VERY CONSERVATIVE

DISCUSSION

- * DETERMINATION OF CONFIDENCE LIMITS REQUIRES ASTRONOMICALLY LARGE DATA SETS: MODEL IDENTIFICATION, HIGH RELIABILITY
- * STRESS-STRENGTH PDF'S WITH SINGLE STATISTICAL MODE ARE:
VERY SIMPLISTIC RELATIVE TO STRUCTURES
MAY NEGLECT SUBSTANTIAL VARIABILITY
- * SENSITIVITY ANALYSES USING
CONTAMINATED MODELS MAY BE USEFUL -
BUT IDENTIFYING APPROPRIATE LEVEL OF
CONTAMINATION MAY BE DIFFICULT

CONCLUSIONS

*A POINT ESTIMATE OF HIGH RELIABILITY
FROM A STRESS-STRENGTH MODEL APPEARS
TO BE A VERY UNCERTAIN MEASURE OF
STRUCTURAL INTEGRITY

*LIGHTWEIGHT STRUCTURES BASED ON
OBTAINABLE RELIABILITY BOUNDS WOULD
SUFFER EXCESSIVE WEIGHT PENALTIES

*IN ADDITION TO BEING "WRONG",
STRESS- STRENGTH ESTIMATES APPEAR TO BE :
NOT TRULY USEFUL
A UTOPIAN IDEAL

* RESULTS SUPPORT OBSERVATION:

"The Probability Of Failure Of 10**-6
Has An Alice In Wonderland Flavor
And Should Be Banned From The
Technical Literature"
L. Breiman & C. Stone, to appear,
J. of Statistical Computation &
Simulation